NISTIR XXXX Draft

Face Recognition Technology Evaluation (FRTE)

Part 1: Verification

Patrick Grother
Mei Ngan
Kayee Hanaoka
Joyce C. Yang
Austin Hom

Information Access Division
Information Technology Laboratory

This publication is available free of charge from:
https://www.nist.gov/programs-projects/face-recognition-vendor-test-frvt-ongoing

2024/04/17

ACKNOWLEDGMENTS

The authors are grateful for the long-standing support and collaboration of the the Department of Homeland Security's Science & Technology Directorate (S&T) and the Office of Biometric Identity Management (OBIM).

Additionally, the authors are grateful to staff in the NIST Biometrics Research Laboratory for infrastructure supporting rapid evaluation of algorithms.

DISCLAIMER

Specific hardware and software products identified in this report were used in order to perform the evaluations described in this document. In no case does identification of any commercial product, trade name, or vendor, imply recommendation or endorsement by the National Institute of Standards and Technology, nor does it imply that the products and equipment identified are necessarily the best available for the purpose.

INSTITUTIONAL REVIEW BOARD

The National Institute of Standards and Technology's Research Protections Office reviewed the protocol for this project and determined it is not human subjects research as defined in Department of Commerce Regulations, 15 CFR 27, also known as the Common Rule for the Protection of Human Subjects (45 CFR 46, Subpart A).

FNMR(T) "False non-match rate"
FMR(T) "False match rate"

FRTE STATUS

This report is a draft NIST Interagency Report, and is open for comment. It is the thirty sixth edition of the report since the first was published in June 2017. Prior editions of this report are maintained on the FRTE website, and may contain useful information about older algorithms and datasets no longer used in FRTE.

FRTE remains open: All tracks of the FRTE are open to new algorithm submissions.

2024-04-17 changes since 2024-03-26:

- We have added results for first algorithms from four developers: Ovision, Vietnam National Cyber Security Technology Corporation, Vivotek, and Vocalize.
- We have added results for new algorithms from four returning developers: Intel Research Group, Kakao Bank, Luxand, and Turkcell Technology.
- We have retired results for nine algorithms per our policy to only list results for four algorithms per developer. Results for retired algorithms appear in prior versions of this report in the archive.

2024-03-26 changes since 2024-02-21:

- We have added results for first algorithms from six developers: FaceLocate, FPT Education, FPT Information System, Kogniza Technology, i2v Systems, and Seamfix.
- We have added results for new algorithms from eleven returning developers: AFR Engine, Aware, Beijing Hisign Technology, Cu-Face, Dactionable Technologies, First Credit Bureau Kazakhstan, Innovatrics, Nominder, Securif AI, Veridium, and Viettel Cyberspace Center.
- We have retired results for nine algorithms per our policy to only list results for two algorithms per developer. Results for retired algorithms appear in prior versions of this report in the archive.

2024-02-21 changes since 2024-01-22:

- We discontinued the visa-visa benchmark in FRTE since Feburary 14th 2024. For highly performing algorithms, the only remaining false negative error in that set were in babies and in a few greyscale poor quality half-tone scans of paper photos.
- We have added results for first algorithms from four developers: Online Mobile Services JSC, Openedge Technologies, TNI Technoology, and Yoti.
- We have added results for new algorithms from nine returning developers: CMC Institute of Science and Technology, City and County of Honolulu, Dermalog, Euronovate SA, Maxvision Technology, Megvii/Face++, Neurotechnology, Toshiba, useB, and Universidade de Coimbra.
- We have retired results for nine algorithms per our policy to only list results for two algorithms per developer. Results for retired algorithms appear in prior versions of this report in the archive.

2024-01-22 changes since 2023-12-15:

- We have added results for first algorithms from six developer: GPS Vietnam Trading, iCOMM Media & Tech, PAPIL11 S.R.O., QazSmartVision.AI, Sparsh CCTV, and VNIS Joint Stock.

- ▷ We have added results for new algorithms from eight returning developers: Cyberlink Corp, Intellivision, Hangzhuo AIlu Network Information Technology, Lebentech Biometrics, Momentum Digital, Regular Biometrics Solutions, ROC, and Via Technologies Inc.
- ▷ We have retired results for six algorithms per our policy to only list results for two algorithms per developer. Results for retired algorithms appear in prior versions of this report in the archive.

2023-12-15 changes since 2023-11-21:

- ▷ We have added results for first algorithms from five developer: CMC University, Element System Solutions Company, Fraud.com, Techainer, and Vietnam Payment Solutions.
- ▷ We have added results for new algorithms from thirteen returning developers: Accurascan, Adera Global, Alchera, Aware, Clearview AI, Cognitec Systems, Incode Technologies Inc, Inspur (Beijing) Electronic Information, IntelliVIX, ioNetworks, NHN Corp, PT Autentika Digital Indonesia, and Qnap Security.
- ▷ We have retired results for twelve algorithms per our policy to only list results for two algorithms per developer. Results for retired algorithms appear in prior versions of this report in the archive.

2023-11-21 changes since 2023-10-27:

- ▷ We have added results for new algorithms from ten returning developers: Coretech Knowledge Inc, Beijing DeepSense Technologies, General Interface Solutions Holding Ltd, Glory, Kakao Brain, Nominder, Smarvist Teknoloji, STCON LLC, Suprema AI Inc, and Yuan High-Tech Development
- ▷ We have retired results for eight algorithms per our policy to only list results for two algorithms per developer. Results for retired algorithms appear in prior versions of this report in the archive.

2023-10-27 changes since 2023-09-29:

- ▷ We have added results for first algorithms from two developer: Authme and Dactionable Technologies.
- ▷ We have added results for new algorithms from twelve returning developers: Intel Research Group, Guangzhou Pixel Solutions, Kasikorn Labs, Kakao Bank, Luxand, Megvii/Face++, Panasonic R+D Center Singapore, Private Identity LLC, Recognito, Seventh Sense Artificial Intelligence, UNICC-Solution Architecture Section, and Universidade de Coimbra.
- ▷ We have retired results for eight algorithms per our policy to only list results for two algorithms per developer. Results for retired algorithms appear in prior versions of this report in the archive.

2023-09-29 changes since 2023-09-09:

- ▷ We have added results for first algorithms from one developer: Intozi Tech.
- ▷ We have added results for new algorithms from seven returning developers: Euronovate, Maxvision Technology, Miaxis Biometrics, Mukh Technologies, Toshiba, University of Surrey-CVSSP, and useB.
- ▷ We have retired results for six algorithms per our policy to only list results for two algorithms per developer. Results for retired algorithms appear in prior versions of this report in the archive.

2023-09-09 changes since 2023-08-16:

- We have renamed and split FRVT into two sets of technology evaluations: The Face Recognition Technology Evaluation (FRTE) is the umbrella for the ongoing 1:1, 1:N and twins disambiguation tracks; the Face Analysis Technology Evaluation (FATE) holds the morph and attacked detection tracks, the quality assessment tracks, and the new age estimation tracks.
- We have added results for first algorithms from two developers: Facehawk and Regular Biometrics Solutions.
- We have added results for new algorithms from eight returning developers: CMC Institute of Science and Technology, Canon, Cu-Face, EI Networks, ICM Airport Technics, Securif AI, Securifai, Vietnam Posts and Telecommunications Group, and Vision Intelligence Center of Meituan
- We have retired results for six algorithms per our policy to only list results for two algorithms per developer. Results for retired algorithms appear in prior versions of this report in the archive.

2023-08-16 changes since 2023-07-21:

- We have added results for first algorithms from one developers: Facia.ai.
- We have added results for new algorithms from fifteen returning developers: Accurascan, Alchera, FOO, Hangzhuo AIlu Network Information Technology, HyperVerge, ioNetworks, Innovatrics, Nominder, Rank One Computing, Neurotechnology, Tech5, Tripleize, Unissey, UX Labs, and Verigram.
- We have retired results for ten algorithms per our policy to only list results for two algorithms per developer. Results for retired algorithms appear in prior versions of this report in the archive.

2023-07-21 changes since 2023-06-16:

- We have added results for first algorithms from five developers: DeCloak Intellegences, Innominds Software SEZ India, Trust Stamp, Vcortex Labs, and Viettel Cyberspace Center
- We have added results for new algorithms from fourteen returning developers: AFR Engine, Alice Biometrics, Euronovate SA, IMDS Software, Idemia, IntelliVIX, Intellivision, NHN, Pangiam, STCON, Samtech InfoNet, Veridium, VinBigData, and Vision-Box
- We have retired results for eleven algorithms per our policy to only list results for two algorithms per developer. Results for retired algorithms appear in prior versions of this report in the archive.
- We have stopped using wild images in FRVT since May 1st 2023. All results for that set have been removed from the website, and will be removed from future PDF reports.

2023-06-16 changes since 2023-04-20:

- We have added results for first algorithms from seven developers: EI Networks Private Ltd, General Interface Solutions Holding Ltd, Recognito, Serendipity Ltd, ST Engineering, and useB.
- We have added results for new algorithms from eighteen returning developers: Advance.AI, AYF Technology, Cyberlink Corp, Incode Technologies Inc, Intel Research Group, Intellibrain Technological Projects, Maxvision Technology, Megvii/Face++, Omnigarde Ltd, Paravision, Qnap Security, Seventh Sense Artificial Intelligence, Shanghai Jiao Tong University, Veridas Digital Authentication Solutions S.L., Universidade de Coimbra, Yuan High-Tech Development, UNICC-Solution Architecture Section, and Verihubs,verihubs-inteligensia.
- We have retired results for 15 algorithms per our policy to only list results for two algorithms per developer. Results for retired algorithms appear in prior versions of this report in the archive.

FNMR(T) "False non-match rate"
FMR(T) "False match rate"

2023-04-20 changes since 2023-04-04:

- ▷ We have added results for first algorithms from one developers: IDENTY.
- ▷ We have added results for new algorithms from three returning developers: Metsakuur, Autentika Digital Indonesia, and Verigram.
- ▷ FRVT will re-open 2023-05-01.
- ▷ We have retired results for 3 algorithms per our policy to only list results for two algorithms per developer. Results for retired algorithms appear in prior versions of this report in the archive.

2023-04-04 changes since 2023-03-09:

- ▷ We have added results for first algorithms from six developers: Aratek Biometrics City and County of Honolulu, FOO, Intelligent Control Technology NCS, and Swsam Solutions.
- ▷ We have added results for new algorithms from nine returning developers: Cubox, Glory, InsightFace AI, Miaxis Biometrics, Mukh Technologies, Turkcell Technology, Samsung S1, Via Technologies, and Vision Intelligence Center of Meituan
- ▷ We have retired results for 7 algorithms per our policy to only list results for two algorithms per developer. Results for retired algorithms appear in prior versions of this report in the archive.

2023-03-09 changes since 2023-02-01:

- ▷ We have added results for first algorithms from eight developers: Biometric LLC (biometric.vision) KZ, Candour Biometrics, Fast Enterprises, KakaoBank, Mitek Systems, Nominder, Private Identity, and UNICC-Solution Architecture Section.
- ▷ We have added results for new algorithms from 22 returning developers: AFR Engine, Biocube Matrics, CMC Institute of Science and Technology, Cloudwalk - Moontime Smart Technology, Cyberlink Corp, Beijing DeepSense Technologies, First Credit Bureau Kazakhstan, Enface, Hangzhuo AIlu Network Information Technology, Herta Security, IMDS Software, Inspur (Beijing) Electronic Information Industry Co, Intellivision, MicroFocus, Neurotechnology, Pangiam, NSENSE Corp, STCON LLC, Touchless ID, University of Surrey-CVSSP, Vision-Box, and YooniK.
- ▷ We have retired results for 14 algorithms per our policy to only list results for two algorithms per developer. Results for retired algorithms appear in prior versions of this report in the archive.
- ▷ We have introduced new set of non-frontal portrait to border comparisons. The new images are described in section 2.3 and their use in seciton 3.2.

2023-02-01 changes since 2022-12-15:

- ▷ We have added results for first algorithms from four developers: CU-Face, Korea ID, Onfido, and TrueID-VNG.
- ▷ We have added results for new algorithms from 21 returning developers: Alchera, Armatura, Cogent-Thales, Dermalog, Didi ChuXing Global Face, Gorilla, Hyperverge, Innovatrics, Intel Research, IntelliVIX, Intema-LGL, Kasikorn Labs, Paravision, Rank One Computing, Sensetime Group, Suprema AI, Tech5, Unissey, U. Coimbra Visteam, Vixvizion (Imagus), and Yuan High-Tech Development.

FNMR(T) "False non-match rate"
FMR(T) "False match rate"

- ▷ We have retired results for 20 algorithms per our policy to only list results for two algorithms per developer. Results for retired algorithms appear in prior versions of this report in the archive.
- ▷ We have introduced new set of non-frontal portrait to border comparisons. The new images are described in section 2.3 and their use in seciton 3.2.

2022-12-15 changes since 2022-11-06:

- ▷ We have added results for first algorithms from four developers: Miaxis Biometrics, PT Autentika Digital Indonesia, PT Qlue Performa Indonesia, and STCON.
- ▷ We have added results for new algorithms from 14 returning developers: Adera Global, Aiseemu Technology, Chunghwa Telecom,chtface, FRP, Griaule, Line Corporation, Maxvision Technology, Mukh Technologies, Papilon Savunma, Qnap Security, Realnetworks, Securif AI, SQIsoft, and Veridium.
- ▷ We have retired results for 10 algorithms per our policy to only list results for two algorithms per developer. Results for retired algorithms appear in prior versions of this report in the archive.

2022-11-06 changes since 2022-09-26:

- ▷ We have added results for first algorithms from six developers: AFR Engine, CMC Institute of Science and Technology, Saga Densan Center, Turkcell Technology, UXLabs, and Wise AI SDN BHD.
- ▷ We have added results for new algorithms from 14 returning developers: Coretech Knowledge, Cloudwalk - Moontime, Cloudmatrix, Deepglint, Guangzhou Pixel Solutions, Hangzhuo AIlu Network Information Technology, NEO Systems, One More Security, Palit Microsystems, Panasonic R+D Center Singapore, Samsung S1, Seventh Sense Artificial Intelligence, Touchless ID, and Veridas Digital Authentication Solutions S.L.
- ▷ We have retired results for 10 algorithms per our policy to only list results for two algorithms per developer. Results for retired algorithms appear in prior versions of this report in the archive.

2022-09-26 changes since 2022-08-30:

- ▷ We have added results for first algorithms from three developers: Codeline, First Credit Bureau Kazakhstan, and InfoCert.
- ▷ We have added results for new algorithms from 14 returning developers: Advancegroup, Armatura LLC, Beijing Hisign Technology, Cybercore, Cyberlink Corp, Herta Security, ICM Airport Technics, InsightFace AI, Metsakuur, NSENSE Corp, Samsung-SDS, Videmo Intelligente Videoanalyse, Vietnam Posts and Telecommunications Group, and Vision Intelligence Center of Meituan.
- ▷ We have retired results for 11 algorithms per our policy to only list results for two algorithms per developer. Results for retired algorithms appear in prior versions of this report in the archive.

2022-08-30 changes since 2022-07-29:

- ▷ We have added results for first algorithms from two developers: Aximetria, Intellibrain Technological Projects
- ▷ We have added results for new algorithms from twelve returning developers: Alchera Inc, Dermalog, Idemia, Incode Technologies Inc, Intellivision, Kasikorn Labs, Megvii/Face++, Techsign, TuringTech.vip, Universidade de Coimbra, Verijelais, Vixvizon

- We have retired results for six algorithms per our policy to only list results for two algorithms per developer. Results for retired algorithms appear in prior versions of this report in the archive.

2022-07-29 changes since 2022-06-27:

- We have added results for first algorithms from seven developers: FRP LLC (Hawaii), IMDS Software, Inspur (Beijing) Electronic Information Industry, Intema - LGL Group, PAPAGO, Qaz Biometric Systems, and VIDA-Digital Identity
- We have added results for new algorithms from nine returning developers: Cyberextruder, Glory, Maxvision Technology, Rank One Computing, Securif AI, Suprema AI, Suprema ID, Toshiba, and Yuan High-Tech Development.
- We have retired results for nine algorithms per our policy to only list results for two algorithms per developer. Results for retired algorithms appear in prior versions of this report in the archive.

2022-07-29 changes since 2022-06-27:

- We have added results for first algorithms from seven developers: FRP LLC (Hawaii), IMDS Software, Inspur (Beijing) Electronic Information Industry, Intema - LGL Group, PAPAGO, Qaz Biometric Systems, and VIDA-Digital Identity
- We have added results for new algorithms from nine returning developers: Cyberextruder, Glory, Maxvision Technology, Rank One Computing, Securif AI, Suprema AI, Suprema ID, Toshiba, and Yuan High-Tech Development.
- We have retired results for nine algorithms per our policy to only list results for two algorithms per developer. Results for retired algorithms appear in prior versions of this report in the archive.

2022-06-27 changes since 2022-06-03:

- We have added results for first algorithms from two developers: Krungthai Bank, and Smartbiometrik.
- We have added results for new algorithms from thirteen returning developers: Aiseemu, Corsight, Digidata, Griaule, Guangzhou Pixel Solutions, Hangzhuo AI Network Information Technology, Neurotechnology, Real Networks, Samsung S1, Sensetime Group, Smart Engines, Verihubs Inteligensia, and VinBigData.
- We have retired results for eight algorithms per our policy to only list results for two algorithms per developer. Results for retired algorithms appear in prior versions of this report in the archive.

2022-06-03 changes since 2022-05-05:

- We have added results for first algorithms from seven developers: Jaak IT, Metsakuur, Palit Microsystems, Smarvist Teknoloji, and Touchless ID.
- We have added results for new algorithms from sixteen returning developers: Cyberlink, FaceOnLive, Kakao Enterprise, Line Corporation (Line Clova), Multi-Modality Intelligence, NEO Systems, and Unissey
- We have retired results for four algorithms per our policy to only list results for two algorithms per developer. Results for retired algorithms appear in prior versions of this report in the archive.

- We have moved the results for the twenty human-difficult pairs used in the May 2018 paper *Face recognition accuracy of forensic examiners, superrecognizers, and face recognition algorithms* by Phillips et al. [1]. to the algorithm-specific report cards (example: PDF).
- Likewise, we have added figures showing impostor distribution shifts across demographics to the report card.

2022-05-05 changes since 2022-03-18:

- We have added results for first algorithms from seven developers: Accurascan, DICIO, FacePhi, Pangiam, University of Surrey-CVSSP, and Veridium.
- We have added results for new algorithms from sixteen returning developers: ACI Software, Canon Inc, Cloudwalk - Moontime Smart Technology, Cybercore,

2022-05-05 changes since 2022-03-18:

- We have added results for first algorithms from seven developers: Accurascan, DICIO, FacePhi, Pangiam, University of Surrey-CVSSP, and Veridium.
- We have added results for new algorithms from sixteen returning developers: ACI Software, Canon Inc, Cloudwalk - Moontime Smart Technology, Cybercore, Cyberextruder, Gemalto Cogent, HyperVerge Inc, KuKe3D Technology, Megvii/Face++, Mobbeel Solutions, Panasonic R+D Center Singapore, Qnap Security, Samsung-SDS, Vietnam Posts and Telecommunications Group, Viettel Group, and Vision Intelligence Center of Meituan.
- We have retired results for 12 algorithms per our policy to only list results for two algorithms per developer. Results for retired algorithms appear in prior versions of this report in the archive.

2022-03-18 changes since 2022-02-23:

- We have added support for the detection of multiple people in a single image (see Section 1.2). Specifically the API allows an algorithm to extract features from one or more faces it detects in an image. NIST scores such cases as a correct match when any detected face matches the reference photo, and as a false positive when either face matches a non-mated reference photo. The expected effect of doing this will be to improve reported false non-match rates, and to minimally elevate false match rates. This technique was only applied to images of type "border" and "kiosk".
- We have added results for first algorithms from four developers: IntelliVIX, Kasikorn Labs, Lebentech Biometrics, and Wicket.
- We have added results for new algorithms from 10 returning developers: Chunghwa Telecom, Cloudmatrix, Beijing DeepSense Technologies, FarBar Inc, Imagus Technology Pty, Intellivision, Maxvision Technology, NHN Corp, Seventh Sense Artificial Intelligence, and Verigram.
- We have retired results for 4 algorithms per our policy to only list results for two algorithms per developer. Results for retired algorithms appear in prior versions of this report in the archive.

2022-02-23 changes since 2022-01-24:

- We have added results for first algorithms from four developers: AFIS and Biometrics Consulting, Digidata, Graymatics, Hangzhuo AIlu Network Information Technology, KnowUTech LLC, Sukshi Technology Innovation, T4iSB, and TuringTech.vip

- We have added results for new algorithms from 18 returning developers: Cognitec Systems GmbH, GeoVision Inc, Glory, Herta Security, Intel Research Group, InsightFace AI, Kakao Enterprise, N-Tech Lab, Omnigarde Ltd, Papilon Savunma, Paravision, Realnetworks Inc, Reveal Media Ltd, Shenzhen Inst Adv Integrated Tech CAS, Suprema AI Inc, Toshiba, Universidade de Coimbra, and Yuan High-Tech Development
- We have retired results for 14 algorithms per our policy to only list results for two algorithms per developer. Results for retired algorithms appear in prior versions of this report in the archive.

2022-01-24 changes since 2022-01-20:

- We have added results for new algorithms from one returning developer: Vocord.

2022-01-20 changes since 2021-12-18:

- We have added results for first algorithms from four developers: Armatura, Beyne.AI, One More Security, and VinBigData
- We have added results for new algorithms from 19 returning developers: AuthenMetric, BOE Technology Group, Cybercore, Cyberlink, Dahua Technology, FaceTag Co, Innovatrics, Megvii, Mobbeel Solutions, Neurotechnology, Oz Forensics, Rank One Computing, Regula Forensics, Samsung S1, Securif AI, Sensetime Group, TigerIT Americas, Videmo Intelligente Videoanalyse, and YooniK.
- We have retired results for 14 algorithms per our policy to only list results for two algorithms per developer. Results for retired algorithms appear in prior versions of this report in the archive.

: **2021-12-16** changes since 2021-11-22:

- We have added results for first algorithms from five developers: Alfabeta, Cloudmatrix, Euronovate SA, FaceOnLive Inc, and Mobipin Technology.
- We have added results for new algorithms from ten returning developers: ACI Software, ITMO University, NEO Systems, Guangzhou Pixel Solutions, Panasonic R+D Center Singapore, Qnap Security, Scanovate, Tevian, Unissey, and Vietnam Posts and Telecommunications Group.
- We have retired results for eight algorithms per our policy to only list results for two algorithms per developer. Results for retired algorithms appear in prior versions of this report in the archive.
- We have revamped the figure showing performance on 20 pairs of open-source images. It now color-codes false negatives and postives against a default threshold value.

2021-11-22 changes since 2021-10-28:

- We have added results to the website for kiosk-collected images where the design and geometry configuration mean that many images have considerable downward pitch angle. In some images, the face is partially cropped. Some images have other background faces.
- We have stopped using child exploitation images in FRVT, as we lost access to the imagery. All results for that set have been removed from the website, and will be removed from future PDF reports.
- We have added results for first algorithms from seven new developers: CUDO Communication, Daon, KuKe3D Technology, Mantra Softech India, Maxvision Technology, Multi-Modality Intelligence, and Samsung-SDS.

- We have added results for new algorithms from seven returning developers: Acer Incorporated, Cloudwalk-Moontime Smart Technology, Gorilla Technology, ID3 Technology, Incode Technologies, NSENSE Corp., and SQIsoft.
- We have retired results for six algorithms per our policy to only list results for two algorithms per developer. Results for retired algorithms appear in prior versions of this report in the archive.

2021-10-28 changes since 2021-09-08:

- We have substantially revised the algorithm-specific report cards that are linked from the FRVT results page. (Example: HTML).
- We have added results for first algorithms from eight new developers: Beijing Mendaxia Technology, Beijing Hisign Technology, Biocube Matrics, Clearview AI, Reveal Media, Toppan ID Gate, Verigram, and Viettel High Technology.
- We have added results for new algorithms from thirty returning developers: 20Face, 3divi, Canon Inc Chunghwa Telecom, Corsight, Decatur Industries, Deepglint, Dermalog, FaceTag, Fiberhome Telecommunication Technologies, GeoVision, ICM Airport Technics, Imagus Technology, InsightFace AI, Kakao Enterprise, Kookmin University, Line Corporation, N-Tech Lab, NotionTag Technologies, Realnetworks, Suprema ID, Taiwan-Certificate Authority, Toshiba, Tripleize, Trueface.ai, Veridas Digital Authentication, Visidon, VisionLabs, YooniK, and Yuan High-Tech Development.
- We have retired results for twenty algorithms per our policy to only list results for two algorithms per developer. Results for retired algorithms appear in prior versions of this report in the archive.

2021-09-08 changes since 2021-08-02:

- We have added results for first algorithms from seven new developers: Griaule, SQIsoft, Qnap Security, Techsign, Smart Engines, Verihubs, and Wuhan Tianyu Information Industry.
- We have added results for new algorithms from sixteen returning developers: ADVANCE.AI, AuthenMetric, CloudSmart Consulting, Code Everest Pvt, Cognitec Systems, Thales Gemalto Cogent, Intel Research Group, Omnigarde, Oz Forensics, Rank One Computing, Samsung S1 Corp, Securif AI, Tevian, TigerIT Americas, Universidade de Coimbra, and Vigilant Solutions
- We have retired results for eleven algorithms per our policy to only list results for two algorithms per developer. Results for retired algorithms appear in prior versions of this report in the archive.

2021-08-02 changes since 2021-06-25:

- We have added results for first algorithms from eight new developers: Bee the Data, Closeli Inc, Coretech Knowledge Inc, Deepsense (France), ioNetworks Inc, Kakao Pay Corp, Seventh Sense Artificial Intelligence, and SK Telecom.
- We have added results for new algorithms from fifteen returning developers: Alchera Inc, Adera Global PTE, Aware, Bresee Technology, Cyberlink Corp, Expasoft LLC, Fujitsu Research and Development Center, Gorilla Technology, Idemia, Neurotechnology, NEO Systems, NHN Corp, Paravision, Panasonic R+D Center Singapore, and Shenzhen University-Macau University of Science and Technology.
- We have retired results for twelve algorithms per our policy to only list results for two algorithms per developer. Results for retired algorithms appear in prior versions of this report in the archive.

FNMR(T) "False non-match rate"
FMR(T) "False match rate"

2021-06-25 changes since 2021-05-21:

- ▷ We have added results for first algorithms from six new developers: Alice Biometrics, BOE Technology Group, Fincore, Neosecu, Sodec App, and Yuntu Data and Technology.
- ▷ We have added results for new algorithms from seven returning developers: Incode Technologies, HyperVerge, Mobbeel Solutions, Guangzhou Pixel Solutions, Remark Holdings, Sensetime, and Vietnam Posts and Telecommunications Group.
- ▷ We have retired results for four algorithms per our policy to only list results for two algorithms per developer. Results for retired algorithms appear in prior versions of this report in the archive.

2021-05-21 changes since 2021-04-26:

- ▷ We have added results for first algorithms from five new developers: Ekin Smart City Technologies, Suprema ID, Tripleize, Taiwan-Certificate Authority, and Vision Intelligence Center of Meituan.
- ▷ We have added results for new algorithms from eight returning developers: ID3 Technology, Imagus Technology, Momentum Digital, N-Tech Lab, NSENSE, Shanghai Jiao Tong University, Vision-Box, and Yuan High-Tech Development
- ▷ We have retired results for seven algorithms per our policy to only list results for two algorithms per developer. Results for retired algorithms appear in prior versions of this report in the archive.

2021-04-26 changes since 2021-04-16:

- ▷ We have added results for first algorithms from three new developers: Quantasoft, Rendip, and NEO Systems.
- ▷ We have added results for new algorithms from four returning developers: 3Divi, Realnetworks, Veridas Digital Authentication Solutions, and Universidade de Coimbra.
- ▷ We have retired results for three algorithms per our policy to only list results for two algorithms per developer. Results for retired algorithms appear in prior versions of this report in the archive.

2021-04-16 changes since 2021-03-19:

- ▷ We have added results for first algorithms from six new developers: 20Face, Beijing DeepSense Technologies, BitCenter UK, Enface, FaceTag, InsightFace AI, Line Corporation, Lema Labs, Nanjing Kiwi Network Technology, Omnigarde, Regula Forensics, and Suprema.
- ▷ We have added results for new algorithms from ten returning developers: CloudSmart Consulting, Dermalog, GeoVision, Neurotechnology, Panasonic R+D Center Singapore, Samsung S1, Securif AI, Trueface.ai, Vigilant Solutions, and Visidon.
- ▷ We have retired results for ten algorithms per our policy to only list results for two algorithms per developer. Results for retired algorithms appear in prior versions of this report in the archive.

2021-03-19 changes since 2021-03-05:

- ▷ We have added results for first algorithms from six new developers: Ajou University, AuthenMetric, Code Everest, Corsight, Papilon Savunma, and NHN Corp
- ▷ We have added results for new algorithms from seven returning developers: Alchera, Deepglint, Fiberhome Telecommunication Technologies, Kakao Enterprise, Kookmin University, Megvii/Face++, and NotionTag Technologies.
- ▷ We have updated many of the hyperlinked HTML report-cards to include seven figures on demographic dependence. Figures of this kind first appeared, and are documented in, the December 2019 document, NIST Interagency Report 8280 on demographic differentials in face recognition. The figures quantify false negative dependence on demographics using "visa-border" comparisons, and false positive dependence using comparisons of "application" photos that uniformly of quality and similar to visa photos.

2021-03-05 changes since 2021-01-19:

- ▷ We have added results for first algorithms from three new developers: IVA Cognitive, Mobbeel, and MoreDian Technology.
- ▷ We have added results for new algorithms from returning developers: Ability Enterprise - Andro Video, ACI Software, Adera Global, AnyVision, BioID Technologies, China Electronics Import-Export, Cognitec Systems, Fujitsu Research and Development Center, Glory, Guangzhou Pixel Solutions, Hengrui AI Technology, Incode Technologies, Intel Research, iQIYI, Mobai, Oz Forensics, Paravision, VisionLabs, and Xforward AI Technology.
- ▷ We have added a new "resources" tab to the main webpage. It includes sortable columns for data related to speed, model size, storage, and memory consumption.
- ▷ We have retired results for 13 algorithms per our policy to only list results for two algorithms per developer. Results for retired algorithms appear in prior versions of this report in the archive.

2021-01-19 changes since 2020-12-18:

- ▷ This report adds results for first algorithms from four developers: Herta Security, Irex AI, Shenzhen University-Macau University of Science and Technology, and Vietnam Posts and Telecommunications Group. See Table 9 for more information.
- ▷ The report also includes results for thirteen developers who have previously submitted algorithms: Bresee Technology, Canon (previously Canon Information Technology (Beijing)), Cyberlink, CSA IntelliCloud Technology, Dahua Technology, ID3 Technology, Imagus Technology (Vixvizion), Moontime Smart Technology, N-Tech Lab, Thales Cogent, Veridas Digital Authentication Solutions, Vocord, and Yuan High-Tech Development.
- ▷ We have retired results for ten algorithms per our policy to only list results for two algorithms per developer. Results for retired algorithms appear in prior versions of this report in the archive.

2020-12-18 changes since 2020-10-09:

- ▷ This report adds results for first algorithms from ten developers: BitCenter UK, CloudSmart Consulting, Cubox, Institute of Computing Technology, Naver Corp, Minivision, NSENSE Corp, Viettel Group, Visage Technologies, and Xiamen University. See Table 9 for more information.

FNMR(T) "False non-match rate"
FMR(T) "False match rate"

- The report also includes results for eighteen developers who have previously submitted algorithms: ADVANCE.AI, Awidit Systems, Chosun University, Dermalog, GeoVision, ICM Airport Technics, Idemia, Institute of Information Technologies, Kakao Enterprise, Neurotechnology, Panasonic R+D Center Singapore, Rank One Computing, Sensetime Group, Shanghai Jiao Tong University, TigerIT Americas LLC, Vigilant Solutions, Winsense, and YooniK
- We have retired results for twelve algorithms per our policy to only list results for two algorithms per developer. Results for retired algorithms appear in prior versions of this report in the archive.

Changes since September 18, 2020:

- This report adds results for first algorithms from five developers: Aigen, Cortica, Kookmin University, Securif AI and Vinai.
- The report also includes results for three developers who have previously submitted algorithms: Fujitsu Laboratories, Hengrui AI, and X-Forward AI.
- In the per-algorithm report-cards linked from tables and the main webpage, we have added a chart to showing reduction in error rates over the course of FRVT i.e. from 2017 onwards for all algorithms supplied by that developer. Similarly we have added a chart showing error rate reductions for our test of protective face mask verification.
- We plan to continue evaluating algorithms on various mask datasets. We hold that algorithms should be capable of detecting masks and verifying identity of all combinations of masked and unmasked faces. We have accordingly increased the amount to time allowed to extract those features from 1.0 to 1.5 seconds.

Changes since August 25, 2020:

- This report adds results for first algorithms from eight new developers. Akurat Satu Indonesia, Cybercore, Decatur Industries, Innef Labs, Satellite Innovation/Eocortex, Expasoft, and Mobai.
- The report includes results for seven developers who have previously submitted algorithms: 3Divi, BioID Technologies, Incode Technologies, Innovatrics, iSAP Solution, Synology, and Tevian.
- We have retired results for five algorithms per our policy to only list results for two algorithms per developer. Results for retired algorithms appear in prior versions of this report in the archive.

Changes since July 27, 2020:

- We have introduced per-algorithm report sheets. These are HTML documents linked from the accuracy tables in this report (i.e. Table 35) and on the FRVT 1:1 homepage. The sheets contain interactive graphics allowing, for example, mouseover exploration of FNMR(T) and FMR(T). Some of their content had previously appeared in this document.
- This report adds results for algorithms from six new developers. ACI Software, Bresee Technology, Fiberhome Telecommunication Technologies, Imageware Systems, Oz Forensics, and Pensees.
- The report includes results for thirteen developers who have previously submitted algorithms: Canon Information Technology (Beijing), Cyberlink, Dahua Technology, Gorilla Technology, ID3 Technology, Intel Research Group, iQIYI Inc, Momentum Digital, Netbridge Technology, Tech5 SA, Shenzhen AiMall Tech, Vigilant Solutions, and VisionLabs.
- We have retired results for nine algorithms per our policy to only list results for two algorithms per developer. Results for retired algorithms appear in prior versions of this report in the archive.

FNMR(T) "False non-match rate"
FMR(T) "False match rate"

Changes since May 18, 2020:

- The report is the first FRVT update since the pandemic closed it from March to June 2020.
- This report includes results for algorithms from nine new developers: GeoVision Inc, Su Zhou NaZhiTianDi Intelligent Technology, YooniK, AYF Technology, PXL Vision AG, Yuan High-Tech Development, Beihang University-ERCACAT, ICM Airport Technics, and Staqu Technologies
- This report includes results for algorithms from 15 returning developers Acer Incorporated, Antheus Technologia, Chosun University, Chunghwa Telecom, Idemia, Moontime Smart Technology, Neurotechnology, Guangzhou Pixel Solutions, Panasonic R+D Center Singapore, Rank One Computing, Scanovate, Shanghai Universiy - Shanghai Film Academy, Synesis, Trueface.ai, and Veridas Digital Authentication Solutions
- We have retired results for ten algorithms per our policy to only list results for two algorithms per developer. Results for retired algorithms appear in prior versions of this report in the archive.
- We separated timing and other resource consumption from the main participation table. The new Table 22 includes template generation durations for four kinds of images, not just mugshots.
- We have published a separate report, NIST Interagency Report 8311 on accuracy of pre-pandemic algorithms on subjects wearing face masks. We plan to track improvements in accuracy on masked images going forward. In particular, we invite submission of algorithms that can detect whether a person is wearing a mask, extract features from the full face or the exposed periocular region, and do appropriate comparison. We do not intend to evaluate algorithms that assume 100% of images will be of masked individuals.

Changes since March 25, 2020:

- The report is a maintenance release - it does not add any new algorithms, and FRVT has been closed to new algorithms since mid March 2020.
- We modified the primary accuracy summary, Table 35, as follows:
  - For visa images, the column for FNMR at FMR = 0.0001 has been removed. The visa images are so highly controlled that the error rates for the most accurate algorithms are dominated by false rejection of very young children and by the presence of a few noisy greyscale images. For now, two visa columns remain: FNMR at FMR= 10^{-6} and, for matched covariates, FNMR at FMR= 10^{-4}.
  - We have inserted a new column labelled "BORDER" giving accuracy for comparison of moderately poor webcam border-crossing photos that exhibit pose variations, poor compression, and low contrast due to strong background illumination. The accuracies are the worst from all cooperative image datasets used in FRVT.
- Accordingly, we updated the failure-to-template rates in Table 45.
- We withdrew a figure showing how false matches are concentrated in certain visa images used in cross-comparison, because it didn't attempt to include demographic information.

Changes since February 27, 2020:

- The report adds results algorithms from two new developers: Beijing Alleyes Technology, and the Chinese University of Hong Kong. Results for newly submitted algorithms from two other developers will appear in the next report.

FNMR(T) "False non-match rate"
FMR(T) "False match rate"

- The report adds results for algorithms from thirteen returning developers: ASUSTek Computer, Aware, Cyberlink Corp, Gorilla Technology, Innovative Technology, Kakao Enterprise, Lomonosov Moscow State University, Panasonic R+D Center Singapore, Shenzhen AiMall Technology, Shenzhen Intellifusion Technologies, Synology, Tech5 SA, and Via Technologies.
- Per policy to only list results for two algorithms per developer, we have dropped results for algorithms from Aware, Cyberlink, Gorilla Technology, Kakao Enterprise, Lomonosov Moscow State University, Panasonic R+D Center Singapore, and Tech5 SA.

Changes since January 20, 2020:

- The report adds results for five new developers: Ability Enterprise (Andro Video), Chosun University, Fujitsu Research and Development Center, University of Coimbra, and Xforward AI Technology.
- The report adds results for algorithms from six returning developers: AlphaSSTG, Incode Technologies, Kneron. Shanghai Jiao Tong University, Vocord, and X-Laboratory.
- We have corrected template comparison timing numbers for algorithms submitted September 2019 to January 2020. The values reported previously were slower due to a software bug.
- We have dropped results for algorithms from Vocord and Incode per policy to only list results for two algorithms per developer.
- The FRVT 1:1 homepage has been updated with latest accuracy results.
- The FRVT 1:N homepage now includes an update to the September 2019 NIST Interagency Report 8271. The new report adds results for one-to-many search algorithms submitted to NIST from June 2019 to January 2020.

Changes since January 6, 2020:

- Section 2 has been updated to better describe the Visa and Border images. The caption for Table 35 has been updated to better relate the accuracy values to particular image comparisons.
- The report adds results for five new developers: Acer, Advance.AI, Expasoft, Netbridge Technology, and Videmo Intelligente Videoanalyse.
- The report adds results for algorithms from 7 returning developers: China Electronics Import-Export Corp, Intel Research Group, ITMO University, Neurotechnology, N-Tech Lab, Rokid, and VisionLabs.
- We have dropped results from this edition of the report per policy to only list results for two algorithms per developer: N-Tech Lab, Neurotechnology, ITMO, Visionlabs, and CEIEC.
- The FRVT homepage has been updated with latest accuracy results.

Changes since November 11, 2019:

- Table 22 has been updated to include runtime memory usage. This is the first time such a quantity has been reported. The value is the peak size of the resident set size logged during enrollment of single images.
- We have migrated summary results table to a new platform that supports sortable tables: https://pages.nist.gov/frvt/html/frvt11.html
- The report adds results for four new developers: Antheus Technologia, BioID Technologies SA, Canon Information Tech. (Beijing), Samsung S1 (listed in the tables as S1), and Taiwan AI Labs.

FNMR(T) "False non-match rate"
FMR(T) "False match rate"

- The report adds results for algorithms from 13 returning developers: Anke Investments, Chunghwa Telecom, Deepglint, Institute of Information Technologies, iQIYI, Kneron, Ping An Technology, Paravision, KanKan Ai, Rokid Corporation, Shanghai Universiy - Shanghai Film Academy, Veridas Digital Authentication Solutions, and Videonetics Technology.
- We have dropped results from this edition of the report per policy to only list results for two algorithms per developer: remarkai-000, veridas-001, sensetime-001, iit-000, anke-003, and everai-002. Results for these are available in prior editions of this report linked from the FRVT page.
- We issued NIST Interagency Report 8280: FRVT Part 3: Demographics on 2019-12-19. It includes results for many of the algorithms covered by this report.

Changes since October 16, 2019:

- The report adds results for ten new developers: Ai-Union Technology, ASUSTek Computer, DiDi ChuXing Technology, Innovative Technology, Luxand, MVision, Pyramid Cyber Security + Forensic, Scanovate, Shenzhen AiMall Tech, and TUPU Technology.
- The report adds results for 12 returning developers: CTBC Bank Glory Gorilla Technology Guangzhou Pixel Solutions Imagus Technology Incode Technologies Lomonosov Moscow State University Rank One Computing Samtech InfoNet Shanghai Ulucu Electronics Technology Synesis, and Winsense.
- We have dropped results from this edition of the report per policy to only list results for two algorithms per developer: glory-000, gorilla-002, incode-003, rankone-006, and synesis-004.
- Results for five recently submitted algorithms will appear in the next report.

Changes since September 11, 2019:

- The report adds results for five new participants: Awidit Systems (Awiros), Momemtum Digital (Sertis), Trueface AI, Shanghai Jiao Tong University, and X-Laboratory.
- The reports adds results for five new algorithms from returning developers: Cyberlink, Hengrui AI Technology, Idemia, Panasonic R+D Singapore, and Tevian. This causes three algorithm, to be de-listed from the report per policy to list results for two algorithms per developer.

Changes since July 31 2019:

- The HTML table on the FRVT 1:1 homepage has been updated to include a column for cross-domain Visa-Border verification. Results for this new dataset appeared in the July 29 report under the name "CrossEV" - these are now renamed "Visa-Border".
- The FRVT 1:1 homepage lists algorithms according to lowest mean rank accuracy:
  Rank($\text{FNMR}_{\text{VISA}}$ at FMR = 0.000001) +
  Rank($\text{FNMR}_{\text{VISA-BORDER}}$ at FMR = 0.000001) +
  Rank($\text{FNMR}_{\text{MUGSHOT}}$ at FMR = 0.00001 after 14 years) +
  Rank($\text{FNMR}_{\text{WILD}}$ at FMR = 0.00001)
  This ordering rewards high accuracy across all datasets.
- The main results in Table 35 is now in landscape format to accomodate extra columns for the Visa-Border set, and mugshot comparisons after at least 12 years.
- The report adds results for nine new participants: Alpha SSTG, Intel Research, ULSee, Chungwa Telecon, iSAP Solution, Rokid, Shenzhen EI Networks, CSA Intellicloud, Shenzhen Intellifusion Technologies.

FNMR(T) "False non-match rate"
FMR(T) "False match rate"

- The reports adds results for six new algorithms from returning developers: Innovatrics, Dahua Technology, Tech5 SA, Intellivision, Nodeflux and Imperial College, London. One algorithm, from Imperial has been retired, per policy to list results for two algorithms per developer.
- The cross-country false match rate heatmaps have been replotted to reveal more structure by listing countries by region instead of alphabetically.
- The next version of this report will be posted around October 18, 2019.

Changes since July 3 2019:

- The HTML table on the FRVT 1:1 homepage has been updated to list the 20 most accurate developers rather than algorithms, choosing the most accurate algorithm from each developer based on visa and mugshot results. Also, the algorithms are ordered in terms of lowest mean rank across mugshot, visa and wild datasets, rewarding broad accuracy over a good result on one particular dataset.
- This report includes results for a new dataset - see the column labelled "visa-border" in Table 5. It compares a new set of high quality visa-like portraits with a set webcam border-crossing photos that exhibit moderately poor pose variations and background illumination. The two new sets are described in sections 2.2 and 2.4. The comparisons are "cross-domain" in that the algorithm must compare "visa" and "wild" images. Results for other algorithms will be added in future reports as they become available.
- This report adds results for algorithms from 9 developers submitted in early July 2019. These are from 3DiVi, Camvi, EverAI-Paravision, Facesoft, Farbar (F8), Institute of Information Technologies, Shanghai U. Film Academy, Via Technologies, and Ulucu Electronics Tech. Six of these are new participants.
- Several other algorithms have been submitted and are being evaluated. Results will be released in the next report, scheduled for September 5. That report will include results for new datasets.
- Older algorithms from Everai, Camvi and 3DiVi, have been retired, per the policy to list only two algorithms per developer.

Changes since June 20 2019:

- This report adds results for algorithms from 18 developers submitted in early June 2019. These are from CTBC Bank, Deep Glint, Thales Cogent, Ever AI Paravision, Gorilla Technology, Imagus, Incode, Kneron, N-Tech Lab, Neurotechnology, Notiontag Technologies, Star Hybrid, Videonetics, Vigilant Solutions, Winsense, Anke Investments, CEIEC, and DSK. Nine of these are new participants.
- Several other algorithms have been submitted and are being evaluated. Results will be released in the next report, scheduled for August 1.
- Older algorithms from Everai, Thales Cogent, Gorilla Technology, Incode, Neurotechnology, N-Tech Lab and Vigilant Solutions have been retired, per the policy to list only two algorithms per developer.

Changes since April 2019:

- This report adds results for nine algorithms from nine developers submitted in early June 2019. These are from Tencent Deepsea, Hengrui, Kedacom, Moontime, Guangzhou Pixel, Rank One Computing, Synesis, Sensetime and Vocord.
- Another 23 algorithms have been submitted and are being evaluated. Results will be released in the next report, scheduled for July 3.
- Older algorithms for Rank One, Synesis, and Vocord have been retired, per the policy to list only two algorithms per developer.

Changes since February 2019:

- This report adds results for 49 algorithms from 42 developers submitted in early March 2019.

FNMR(T) "False non-match rate"
FMR(T) "False match rate"

- This report omits results for algorithms that we retired. We retired for three reasons: 1. The developer submitted a new algorithm, and we only list two. 2. The algorithm needs a GPU, and we no longer allow GPU-based algorithms. 3. Inoperable algorithms.
- Previous results for retired algorithms are available in older editions of this report linked here.
- The mugshot database used from February 2017 to January 2019 has been replaced with an extract of the mugshot database documented in NIST Interagency Report 8238, November 2018. The new mugshot set is described in section 2.5 and is adopted because:
  - It has much better identity label integrity, so that false non-match rates are substantially lower than those reported in FRVT 1:1 reports to date - see Figure 135.
  - It includes images collected over a 17 year period such that ageing can be much better characterized - - see Figure 367.
- Using the new mugshot database, Figure 367 shows accuracy for four demographic groups identified in the biographic metadata that accompanies the data: black females, black males, white females and white males.
- The report added a figure (now moved to web) with results for the twenty human-difficult pairs used in the May 2018 paper *Face recognition accuracy of forensic examiners, superrecognizers, and face recognition algorithms* by Phillips et al. [1].
- The report uses an update to the wild image database that corrects some ground truth labels.
- Some results for the child exploitation database are not complete. They are typically updated less frequently than for other image sets.

FNMR(T) "False non-match rate"
FMR(T) "False match rate"

Contents

List of Tables

FNMR(T) "False non-match rate"
FMR(T) "False match rate"

List of Figures

FNMR(T) "False non-match rate"
FMR(T) "False match rate"

FNMR(T) "False non-match rate"
FMR(T) "False match rate"

FNMR(T) "False non-match rate"
FMR(T) "False match rate"

FNMR(T) "False non-match rate"
FMR(T) "False match rate"

FNMR(T) "False non-match rate"
FMR(T) "False match rate"

FNMR(T) "False non-match rate"
FMR(T) "False match rate"

FNMR(T) "False non-match rate"
FMR(T) "False match rate"

	Location	Developer Name	Short Name	Seq. Num.	Validation Date
1	NL	20Face	20face-000	000	2021-04-12
2	NL	20Face	20face-001	001	2021-09-29
3	US	3Divi	3divi-006	006	2021-04-14
4	US	3Divi	3divi-007	007	2021-09-27
5	TH	ACI Software	acisw-007	007	2021-11-15
6	TH	ACI Software	acisw-008	008	2022-03-22
7	US	AFIS and Biometrics Consulting	afisbiometrics-000	000	2022-01-27
8	US	AFR Engine	afrengine-002	002	2023-06-27
9	US	AFR Engine	afrengine-003	003	2024-03-15
10	TW	ASUSTek Computer Inc	asusaics-000	000	2019-10-24
11	TW	ASUSTek Computer Inc	asusaics-001	001	2020-02-25
12	CN	AYF Technology	ayftech-001	001	2020-07-06
13	CN	AYF Technology	ayftech-003	003	2023-05-15
14	TW	Ability Enterprise - Andro Video	androvideo-000	000	2021-01-25
15	IN	Accurascan	accurascan-002	002	2023-08-01
16	IN	Accurascan	accurascan-003	003	2023-12-06
17	TW	Acer Incorporated	acer-001	001	2020-06-30
18	TW	Acer Incorporated	acer-002	002	2021-11-10
19	SG	Adera Global PTE	adera-004	004	2022-11-14
20	SG	Adera Global PTE	adera-005	005	2023-11-17
21	SG	Advance.AI	advance-004	004	2022-09-06
22	SG	Advance.AI	advance-005	005	2023-05-25
23	TH	Ai First	aifirst-001	001	2019-11-21
24	TW	AiUnion Technology	aiunionface-000	000	2019-10-22
25	TH	Aigen	aigen-001	001	2020-10-06
26	TH	Aigen	aigen-002	002	2021-03-15
27	CN	Aiseemu Technology	aiseemu-001	001	2022-06-16
28	CN	Aiseemu Technology	aiseemu-002	002	2022-11-18
29	KR	Ajou University	ajou-001	001	2021-03-08
30	ID	Akurat Satu Indonesia	ptakuratsatu-000	000	2020-09-11
31	KR	Alchera Inc	alchera-006	006	2023-07-18
32	KR	Alchera Inc	alchera-007	007	2023-11-22
33	ID	Alfabeta	alfabeta-001	001	2021-12-02
34	ES	Alice Biometrics	alice-000	000	2021-06-15
35	ES	Alice Biometrics	alice-001	001	2023-07-05
36	RU	Alivia / Innovation Sys	isystems-001	001	2018-06-12
37	RU	Alivia / Innovation Sys	isystems-002	002	2018-10-18
38	IN	AllGoVision	allgovision-000	000	2019-03-01
39	CN	AlphaSSTG	alphaface-001	001	2019-09-03
40	CN	AlphaSSTG	alphaface-002	002	2020-02-20
41	GB	Amplified Group	amplifiedgroup-001	001	2019-03-01
42	CN	Anke Investments	anke-004	004	2019-06-27
43	CN	Anke Investments	anke-005	005	2019-11-21
44	BR	Antheus Technologia	antheus-000	000	2019-12-05
45	BR	Antheus Technologia	antheus-001	001	2020-06-25
46	GB	AnyVision	anyvision-004	004	2018-06-15
47	GB	AnyVision	anyvision-005	005	2021-02-03
48	CN	Aratek Biometrics Co Ltd	aratek-001	001	2023-03-27
49	US	Armatura LLC	armatura-001	001	2022-01-04
50	US	Armatura LLC	armatura-003	003	2023-01-13
51	CN	AuthenMetric	authenmetric-003	003	2021-08-09
52	CN	AuthenMetric	authenmetric-004	004	2022-01-03
53	TW	Authme	authme-001	001	2023-10-17
54	US	Aware	aware-007	007	2023-11-15
55	US	Aware	aware-008	008	2024-03-15
56	IN	Awidit Systems	awiros-001	001	2019-09-23
57	IN	Awidit Systems	awiros-002	002	2020-10-28
58	CH	Aximetria	aximetria-001	001	2022-08-10
59	JP	Ayonix	ayonix-000	000	2017-06-22
60	CN	BOE Technology Group	boetech-001	001	2021-06-22
61	CN	BOE Technology Group	boetech-002	002	2021-12-21
62	ES	Bee the Data	beethedata-000	000	2021-07-26
63	CN	Beihang University-ERCACAT	ercacat-001	001	2020-07-06
64	CN	Beijing Alleyes Technology	alleyes-000	000	2020-03-09
65	CN	Beijing DeepSense Technologies	deepsense-002	002	2023-02-22
66	CN	Beijing DeepSense Technologies	deepsense-003	003	2023-10-23
67	CN	Beijing Hisign Technology	hisign-002	002	2022-09-09
68	CN	Beijing Hisign Technology	hisign-003	003	2024-03-15
69	CN	Beijing Mendaxia Technology	mendaxiatech-000	000	2021-09-15
70	CN	Beijing Vion Technology Inc	vion-000	000	2018-10-19

Table 1: Summary of participant information included in this report.

FNMR(T) "False non-match rate"
FMR(T) "False match rate"

	Location	Developer Name	Short Name	Seq. Num.	Validation Date
71	KZ	Beyne.AI	beyneai-000	000	2022-01-03
72	CH	BioID Technologies SA	bioidtechswiss-001	001	2020-08-28
73	CH	BioID Technologies SA	bioidtechswiss-002	002	2021-02-17
74	IN	Biocube Matrics	biocube-001	001	2021-09-08
75	IN	Biocube Matrics	biocube-002	002	2023-02-09
76	KZ	Biometric LLC	biometric-vision-000	000	2023-01-25
77	UK	BitCenter UK	farfaces-001	001	2021-04-09
78	CN	Bitmain	bm-001	001	2018-10-17
79	CN	Bresee Technology	bresee-001	001	2020-12-30
80	CN	Bresee Technology	bresee-002	002	2021-06-30
81	VN	CMC Institute of Science and Technology	cist-003	003	2023-08-14
82	VN	CMC Institute of Science and Technology	cist-004	004	2024-02-15
83	VN	CMC Univerisity	cmcuni-001	001	2023-12-05
84	CN	CSA IntelliCloud Technology	intellicloudai-001	001	2019-08-13
85	CN	CSA IntelliCloud Technology	intellicloudai-002	002	2020-12-17
86	TW	CTBC Bank	ctbcbank-000	000	2019-06-28
87	TW	CTBC Bank	ctbcbank-001	001	2019-10-28
88	KR	CUDO Communication	cudocommunication-001	001	2021-10-20
89	US	Camvi Technologies	camvi-002	002	2018-10-19
90	US	Camvi Technologies	camvi-004	004	2019-07-12
91	FI	Candour Biometrics	candour-001	001	2023-02-10
92	JP	Canon Inc	canon-004	004	2022-04-25
93	JP	Canon Inc	canon-005	005	2023-09-05
94	CN	China Electronics Import-Export Corp	ceiec-003	003	2020-01-06
95	CN	China Electronics Import-Export Corp	ceiec-004	004	2021-01-18
96	CN	China University of Petroleum	upc-001	001	2019-06-05
97	CN	Chinese University of Hong Kong	cuhkee-001	001	2020-03-18
98	KR	Chosun University	chosun-001	001	2020-07-01
99	KR	Chosun University	chosun-002	002	2020-11-25
100	TW	Chunghwa Telecom	chtface-005	005	2022-03-09
101	TW	Chunghwa Telecom	chtface-006	006	2022-11-03
102	US	City and County of Honolulu	cchonolulu-000	000	2023-03-27
103	US	City and County of Honolulu	cchonolulu-001	001	2024-01-18
104	US	Clearview AI Inc	clearviewai-000	000	2021-09-22
105	US	Clearview AI Inc	clearviewai-001	001	2023-12-05
106	CN	Closeli Inc	closeli-001	001	2021-07-15
107	US	CloudSmart Consulting LLC	csc-002	002	2021-03-24
108	US	CloudSmart Consulting LLC	csc-003	003	2021-08-26
109	TW	Cloudmatrix	cloudmatrix-001	001	2022-02-16
110	TW	Cloudmatrix	cloudmatrix-002	002	2022-10-17
111	CN	Cloudwalk - Hengrui AI Technology	cloudwalk-hr-003	003	2020-09-25
112	CN	Cloudwalk - Hengrui AI Technology	cloudwalk-hr-004	004	2021-02-10
113	CN	Cloudwalk - Moontime Smart Technology	cloudwalk-mt-006	006	2022-10-20
114	CN	Cloudwalk - Moontime Smart Technology	cloudwalk-mt-007	007	2023-02-21
115	IN	Code Everest Pvt	facex-001	001	2021-03-08
116	IN	Code Everest Pvt	facex-002	002	2021-08-24
117	KR	Codeline	codeline-000	000	2022-09-13
118	DE	Cognitec Systems GmbH	cognitec-004	004	2022-02-10
119	DE	Cognitec Systems GmbH	cognitec-005	005	2023-12-01
120	TW	Coretech Knowledge Inc	coretech-001	001	2022-09-29
121	TW	Coretech Knowledge Inc	coretech-002	002	2023-11-02
122	IL	Corsight	corsight-002	002	2021-09-01
123	IL	Corsight	corsight-003	003	2022-06-09
124	IL	Cortica	cor-001	001	2020-09-24
125	TW	Cu-Face	cu-face-003	003	2023-08-28
126	TW	Cu-Face	cu-face-004	004	2024-03-13
127	KR	Cubox	cubox-002	002	2021-08-24
128	KR	Cubox	cubox-003	003	2023-03-07
129	JP	Cybercore	cybercore-002	002	2022-04-25
130	JP	Cybercore	cybercore-003	003	2022-08-31
131	US	Cyberextruder	cyberextruder-003	003	2022-03-16
132	US	Cyberextruder	cyberextruder-004	004	2022-07-20
133	TW	Cyberlink Corp	cyberlink-012	012	2023-06-02
134	TW	Cyberlink Corp	cyberlink-013	013	2023-12-15
135	MX	DICIO	dicio-001	001	2022-03-22
136	CN	DSK	dsk-000	000	2019-06-28
137	VN	Dactionable Technologies	datech-000	000	2023-10-16
138	VN	Dactionable Technologies	datech-001	001	2024-02-21
139	CN	Dahua Technology	dahua-006	006	2020-12-30
140	CN	Dahua Technology	dahua-007	007	2021-12-20

Table 2: Summary of participant information included in this report.

FNMR(T) "False non-match rate"
FMR(T) "False match rate"

	Location	Developer Name	Short Name	Seq. Num.	Validation Date
141	IE	Daon	daon-000	000	2021-11-03
142	TW	DeCloak Intellegences	decloakface-001	001	2023-06-13
143	US	Decatur Industries Inc	decatur-000	000	2020-08-18
144	US	Decatur Industries Inc	decatur-001	001	2021-09-27
145	CN	Deepglint	deepglint-004	004	2021-09-17
146	CN	Deepglint	deepglint-005	005	2022-10-17
147	FR	Deepsense	dps-000	000	2021-07-16
148	DE	Dermalog	dermalog-011	011	2022-12-12
149	DE	Dermalog	dermalog-012	012	2024-01-19
150	CN	DiDi ChuXing Technology	didiglobalface-001	001	2019-10-23
151	CN	DiDi ChuXing Technology	didiglobalface-002	002	2023-01-09
152	IN	Digidata	digidata-000	000	2022-01-27
153	IN	Digidata	digidata-001	001	2022-06-10
154	GB	Digital Barriers	digitalbarriers-002	002	2019-03-01
155	IN	EI Networks Private Ltd	einetworksindia-000	000	2023-05-03
156	IN	EI Networks Private Ltd	einetworksindia-001	001	2023-09-05
157	TR	Ekin Smart City Technologies	ekin-002	002	2021-05-04
158	TH	Element System Solutions Company Ltd	element-000	000	2023-11-14
159	AE	Enface	enface-001	001	2021-12-17
160	AE	Enface	enface-002	002	2023-02-27
161	CH	Euronovate SA	euronovate-003	003	2023-09-19
162	CH	Euronovate SA	euronovate-004	004	2024-01-19
163	RU	Expasoft LLC	expasoft-001	001	2020-09-03
164	RU	Expasoft LLC	expasoft-002	002	2021-07-26
165	LB	FOO	foomobi-001	001	2023-03-13
166	LB	FOO	foomobi-002	002	2023-08-07
167	VN	FPT Education	fedu-001	001	2024-03-15
168	VN	FPT Information System	fpt-000	000	2024-02-26
169	US	FRP LLC	frpkauai-001	001	2022-07-18
170	US	FRP LLC	frpkauai-002	002	2022-11-21
171	CA	FaceLocate	facelocate-001	001	2024-02-22
172	DE	FaceOnLive Inc	faceonlive-001	001	2021-11-23
173	DE	FaceOnLive Inc	faceonlive-002	002	2022-04-11
174	ES	FacePhi	facephi-000	000	2022-04-06
175	GB	FaceSoft	facesoft-000	000	2019-07-10
176	KR	FaceTag Co	facetag-000	000	2021-03-22
177	KR	FaceTag Co	facetag-002	002	2022-01-06
178	UK	Facehawk Ltd	facehawk-000	000	2023-08-22
179	UK	Facia.ai	facia-001	001	2023-07-21
180	TW	FarBar Inc	f8-001	001	2019-07-11
181	TW	FarBar Inc	f8-002	002	2022-03-02
182	US	Fast Enterprises	fastenterprises-000	000	2023-03-01
183	CN	Fiberhome Telecommunication Technologies	fiberhome-nanjing-003	003	2021-03-12
184	CN	Fiberhome Telecommunication Technologies	fiberhome-nanjing-004	004	2021-09-14
185	UK	Fincore Ltd	fincore-000	000	2021-06-07
186	KZ	First Credit Bureau Kazakhstan	firstcreditkz-002	002	2023-02-21
187	KZ	First Credit Bureau Kazakhstan	firstcreditkz-003	003	2024-02-20
188	UK	Fraud.com	fraudcom-000	000	2023-12-01
189	CN	Fujitsu Research and Development Center	fujitsulab-002	002	2021-02-24
190	CN	Fujitsu Research and Development Center	fujitsulab-003	003	2021-07-12
191	VN	GPS Vietnam Trading	gpstechvn-000	000	2024-01-02
192	US	Gemalto Cogent	cogent-007	007	2022-04-11
193	US	Gemalto Cogent	cogent-008	008	2023-01-03
194	TW	General Interface Solutions Holding Ltd	gistouch-000	000	2023-05-08
195	TW	General Interface Solutions Holding Ltd	gistouch-001	001	2023-11-09
196	TW	GeoVision Inc	geo-002	002	2021-04-01
197	TW	GeoVision Inc	geo-004	004	2022-02-10
198	JP	Glory	glory-006	006	2023-03-23
199	JP	Glory	glory-007	007	2023-11-10
200	TW	Gorilla Technology	gorilla-008	008	2021-11-08
201	TW	Gorilla Technology	gorilla-009	009	2022-12-14
202	US	Graymatics	graymatics-001	001	2022-01-13
203	US	Griaule	griaule-001	001	2022-05-31
204	US	Griaule	griaule-002	002	2022-12-02
205	CN	Guangzhou Pixel Solutions	pixelall-009	009	2022-10-26
206	CN	Guangzhou Pixel Solutions	pixelall-010	010	2023-10-18
207	CN	Hangzhuo AIlu Network Information Technology	hzailu-005	005	2023-08-10
208	CN	Hangzhuo AIlu Network Information Technology	hzailu-006	006	2023-12-28
209	ES	Herta Security	hertasecurity-002	002	2022-09-02
210	ES	Herta Security	hertasecurity-003	003	2023-01-27

Table 3: Summary of participant information included in this report.

FNMR(T) "False non-match rate"
FMR(T) "False match rate"

	Location	Developer Name	Short Name	Seq. Num.	Validation Date
211	CN	Hikvision Research Institute	hik-001	001	2019-03-01
212	IN	HyperVerge Inc	hyperverge-003	003	2022-04-11
213	IN	HyperVerge Inc	hyperverge-005	005	2023-08-08
214	AU	ICM Airport Technics	icm-004	004	2022-09-07
215	AU	ICM Airport Technics	icm-005	005	2023-09-05
216	FR	ID3 Technology	id3-006	006	2020-12-17
217	FR	ID3 Technology	id3-008	008	2021-11-10
218	UK	IDENTY	identy-000	000	2023-04-04
219	CA	IMDS Software	imds-software-002	002	2023-02-10
220	CA	IMDS Software	imds-software-003	003	2023-06-20
221	RU	ITMO University	itmo-007	007	2020-01-06
222	RU	ITMO University	itmo-008	008	2021-11-19
223	RU	IVA Cognitive	ivacognitive-001	001	2021-01-29
224	FR	Idemia	idemia-009	009	2022-07-27
225	FR	Idemia	idemia-010	010	2023-06-30
226	US	Imageware Systems	iws-000	000	2020-08-12
227	GB	Imperial College London	imperial-000	000	2019-03-01
228	GB	Imperial College London	imperial-002	002	2019-08-28
229	US	Incode Technologies Inc	incode-009	009	2021-06-22
230	US	Incode Technologies Inc	incode-013	013	2023-12-08
231	IT	InfoCert	infocert-001	001	2022-09-08
232	IN	Innef Labs	innefulabs-000	000	2020-09-04
233	IN	Innominds Software SEZ India Pvt	innominds-001	001	2023-06-23
234	GB	Innovative Technology	innovativetechnologyltd-001	001	2019-10-22
235	GB	Innovative Technology	innovativetechnologyltd-002	002	2020-02-26
236	SK	Innovatrics	innovatrics-010	010	2023-08-03
237	SK	Innovatrics	innovatrics-011	011	2024-03-08
238	CN	InsightFace AI	insightface-003	003	2022-08-23
239	CN	InsightFace AI	insightface-004	004	2023-03-31
240	CN	Inspur (Beijing) Electronic Information Industry Co	inspur-001	001	2023-02-24
241	CN	Inspur (Beijing) Electronic Information Industry Co	inspur-002	002	2023-12-08
242	CN	Institute of Computing Technology	icthtc-000	000	2020-11-29
243	RU	Institute of Information Technologies	iit-002	002	2019-12-04
244	RU	Institute of Information Technologies	iit-003	003	2020-12-01
245	IS	Intel Research Group	intelresearch-008	008	2023-10-03
246	IS	Intel Research Group	intelresearch-009	009	2024-03-26
247	KR	IntelliVIX	intellivix-004	004	2023-06-21
248	KR	IntelliVIX	intellivix-005	005	2023-11-14
249	AE	Intellibrain Technological Projects	g42-intellibrain-001	001	2022-07-27
250	AE	Intellibrain Technological Projects	g42-intellibrain-002	002	2023-05-10
251	CN	Intelligent Control Technology Co Ltd - IGearx	igearx-face-000	000	2023-03-28
252	US	Intellivision	intellivision-006	006	2023-07-14
253	US	Intellivision	intellivision-007	007	2023-12-19
254	LU	Intema-LGL Group	intema-000	000	2022-07-15
255	LU	Intema-LGL Group	intema-001	001	2023-01-11
256	IN	Intozi Tech Pvt Ltd	intozi-001	001	2023-09-25
257	US	IrexAI	irex-000	000	2020-12-17
258	IL	Is It You	isityou-000	000	2017-06-26
259	MX	Jaak IT	jaakit-001	001	2022-05-20
260	KR	Kakao Bank	kakaobank-001	001	2023-10-10
261	KR	Kakao Bank	kakaobank-002	002	2024-04-01
262	KR	Kakao Brain	kakao-008	008	2022-05-12
263	KR	Kakao Brain	kakao-009	009	2023-11-07
264	KR	Kakao Pay Corp	kakaopay-001	001	2021-07-06
265	TH	Kasikorn Labs	kasikornlabs-002	002	2022-12-13
266	TH	Kasikorn Labs	kasikornlabs-003	003	2023-10-05
267	SG	Kedacom International Pte	kedacom-000	000	2019-06-03
268	US	Kneron Inc	kneron-003	003	2019-07-01
269	US	Kneron Inc	kneron-005	005	2020-02-21
270	US	KnowUTech LLC	knowutech-000	000	2022-02-13
271	US	Kogniza Technology	kogniza-001	001	2024-03-01
272	KR	Kookmin University	kookmin-002	002	2021-03-05
273	KR	Korea Identification Inc	koreaid-001	001	2022-12-12
274	TH	Krungthai	krungthai-002	002	2022-06-21
275	CN	KuKe3D Technology	kuke3d-001	001	2021-10-28
276	CN	KuKe3D Technology	kuke3d-002	002	2022-04-14
277	MX	Lebentech Biometrics	lebentech-000	000	2022-02-16
278	MX	Lebentech Biometrics	lebentech-001	001	2023-12-12
279	IN	Lema Labs	lemalabs-001	001	2021-04-13
280	JP	Line Corporation	lineclova-002	002	2022-05-18

Table 4: Summary of participant information included in this report.

FNMR(T) "False non-match rate"
FMR(T) "False match rate"

	Location	Developer Name	Short Name	Seq. Num.	Validation Date
281	JP	Line Corporation	lineclova-003	003	2022-11-28
282	RU	Lomonosov Moscow State University	intsysmsu-001	001	2019-10-22
283	RU	Lomonosov Moscow State University	intsysmsu-002	002	2020-03-12
284	IN	Lookman Electroplast Industries	lookman-002	002	2018-06-13
285	IN	Lookman Electroplast Industries	lookman-004	004	2019-06-03
286	US	Luxand Inc	luxand-001	001	2023-10-17
287	US	Luxand Inc	luxand-003	003	2024-03-25
288	RU	MVision	mvision-001	001	2019-11-12
289	IN	Mantra Softech India	mantra-000	000	2021-10-28
290	CN	Maxvision Technology	maxvision-005	005	2023-09-21
291	CN	Maxvision Technology	maxvision-006	006	2024-01-19
292	CN	Megvii/Face++	megvii-008	008	2023-10-12
293	CN	Megvii/Face++	megvii-009	009	2024-02-12
294	KR	Metsakuur	metsakuurcompany-002	002	2022-09-14
295	KR	Metsakuur	metsakuurcompany-003	003	2023-04-04
296	CN	Miaxis Biometrics	miaxis-002	002	2023-03-22
297	CN	Miaxis Biometrics	miaxis-003	003	2023-09-19
298	GB	MicroFocus	microfocus-002	002	2018-10-17
299	GB	MicroFocus	microfocus-003	003	2023-02-23
300	CN	Minivision	minivision-000	000	2020-10-28
301	UK	Mitek Systems	mitek-000	000	2023-01-27
302	NO	Mobai	mobai-000	000	2020-08-26
303	NO	Mobai	mobai-001	001	2021-02-17
304	ES	Mobbeel Solutions	mobbl-001	001	2021-06-16
305	ES	Mobbeel Solutions	mobbl-003	003	2022-04-19
306	KR	Mobipin Technology	mobipintech-000	000	2021-11-23
307	TH	Momentum Digital	sertis-002	002	2021-05-13
308	TH	Momentum Digital	sertis-003	003	2023-12-27
309	CN	MoreDian Technology	moredian-000	000	2021-02-24
310	US	Mukh Technologies	mukh-003	003	2023-03-15
311	US	Mukh Technologies	mukh-004	004	2023-09-13
312	CN	Multi-Modality Intelligence	multimodality-000	000	2021-10-19
313	CN	Multi-Modality Intelligence	multimodality-001	001	2022-05-16
314	RU	N-Tech Lab	ntechlab-011	011	2021-09-13
315	RU	N-Tech Lab	ntechlab-012	012	2022-01-20
316	SG	NCS Pte Ltd	ncssg-001	001	2023-03-24
317	CA	NEO Systems	neosystems-004	004	2022-05-02
318	KR	NHN Corp	nhn-004	004	2023-06-26
319	KR	NHN Corp	nhn-005	005	2023-12-06
320	KR	NSENSE Corp	nsensecorp-004	004	2022-09-08
321	KR	NSENSE Corp	nsensecorp-005	005	2023-02-08
322	CN	Nanjing Kiwi Network Technology	kiwitech-000	000	2021-03-19
323	KR	Neosecu Co	openface-001	001	2021-06-15
324	TW	Netbridge Technology Incoporation	netbridgetech-001	001	2020-01-08
325	TW	Netbridge Technology Incoporation	netbridgetech-002	002	2020-08-11
326	LT	Neurotechnology	neurotechnology-017	017	2023-07-28
327	LT	Neurotechnology	neurotechnology-018	018	2024-02-09
328	ID	Nodeflux	nodeflux-002	002	2019-08-13
329	LT	Nominder	nominder-002	002	2023-11-04
330	LT	Nominder	nominder-003	003	2024-03-06
331	IN	NotionTag Technologies Private Limited	notiontag-001	001	2021-03-04
332	IN	NotionTag Technologies Private Limited	notiontag-002	002	2021-09-17
333	US	Omnigarde Ltd	omnigarde-002	002	2022-01-19
334	US	Omnigarde Ltd	omnigarde-003	003	2023-05-10
335	KR	One More Security	omface-000	000	2021-12-15
336	KR	One More Security	omface-001	001	2022-10-21
337	UK	Onfido	onfido-000	000	2022-12-13
338	VN	Online Mobile Services JSC	momovn-001	001	2024-01-26
339		Openedge Technologies Pvt	openedge-000	000	2024-01-29
340	AE	Ovision	ovisionllc-001	001	2024-04-03
341	RU	Oz Forensics LLC	oz-003	003	2021-08-09
342	RU	Oz Forensics LLC	oz-004	004	2021-12-13
343	TW	PAPAGO Inc	papago-001	001	2022-07-19
344	CZ	PAPIL11 S.R.O.	papil11-000	000	2024-01-04
345	ID	PT Autentika Digital Indonesia	autentika-001	001	2023-04-05
346	ID	PT Autentika Digital Indonesia	autentika-002	002	2023-11-21
347	ID	PT Qlue Performa Indonesia	qluevision-001	001	2022-11-15
348	CH	PXL Vision AG	pxl-001	001	2020-06-30
349	TW	Palit Microsystems	palit-000	000	2022-05-16
350	TW	Palit Microsystems	palit-001	001	2022-09-26

Table 5: Summary of participant information included in this report.

FNMR(T) "False non-match rate"
FMR(T) "False match rate"

	Location	Developer Name	Short Name	Seq. Num.	Validation Date
351	SG	Panasonic R+D Center Singapore	psl-011	011	2022-10-06
352	SG	Panasonic R+D Center Singapore	psl-012	012	2023-10-13
353	US	Pangiam	pangiam-001	001	2023-02-21
354	US	Pangiam	pangiam-002	002	2023-06-21
355	TR	Papilon Savunma	papsav1923-002	002	2022-01-20
356	TR	Papilon Savunma	papsav1923-003	003	2022-11-25
357	US	Paravision	paravision-013	013	2023-05-08
358	US	Paravision (EverAI)	paravision-011	011	2022-12-12
359	SG	Pensees Pte	pensees-001	001	2020-08-17
360	US	Private Identity LLC	privid-001	001	2023-02-06
361	US	Private Identity LLC	privid-002	002	2023-10-03
362	IN	Pyramid Cyber Security + Forensic (P)	pyramid-000	000	2019-11-04
363	KZ	Qaz Biometric Systems	qazbs-000	000	2022-06-22
364		QazSmartVision.AI	qazsmartvisionai-000	000	2024-01-11
365	TW	Qnap Security	qnap-004	004	2023-05-05
366	TW	Qnap Security	qnap-005	005	2023-11-16
367	CZ	Quantasoft	quantasoft-003	003	2021-04-19
368	US	ROC	rankone-015	015	2023-07-20
369	US	ROC	roc-016	016	2023-12-19
370	US	Realnetworks Inc	realnetworks-007	007	2022-06-14
371	US	Realnetworks Inc	realnetworks-008	008	2022-11-10
372	AE	Recognito	recognito-000	000	2023-05-24
373	AE	Recognito	recognito-001	001	2023-09-27
374	US	Regula Forensics	regula-000	000	2021-04-13
375	US	Regula Forensics	regula-001	001	2021-12-14
376	AM	Regular Biometrics Solutions	rebs-000	000	2023-08-22
377	AM	Regular Biometrics Solutions	rebs-001	001	2023-12-22
378	CN	Remark Holdings	remarkai-001	001	2019-03-01
379	CN	Remark Holdings	remarkai-003	003	2021-06-22
380	SG	Rendip	rendip-000	000	2021-04-19
381	UK	Reveal Media Ltd	revealmedia-005	005	2021-09-24
382	UK	Reveal Media Ltd	revealmedia-006	006	2022-01-26
383	CN	Rokid Corporation	rokid-000	000	2019-08-01
384	CN	Rokid Corporation	rokid-001	001	2019-12-13
385	KR	SK Telecom	sktelecom-000	000	2021-07-09
386	KR	SQIsoft	sqisoft-002	002	2021-11-03
387	KR	SQIsoft	sqisoft-003	003	2022-10-26
388	SG	ST Engineering	stengg-000	000	2023-06-06
389	SA	STCON LLC	stcon-002	002	2023-07-05
390	SA	STCON LLC	stcon-003	003	2023-11-07
391	DE	Saffe	saffe-001	001	2018-10-19
392	DE	Saffe	saffe-002	002	2019-03-01
393	JP	Saga Densan Center Co Ltd	sdc-000	000	2022-10-18
394	KR	Samsung S1 Corp	s1-005	005	2022-06-17
395	KR	Samsung S1 Corp	s1-007	007	2023-03-20
396	KR	Samsung-SDS	samsungsds-001	001	2022-04-18
397	KR	Samsung-SDS	samsungsds-002	002	2022-09-16
398	IN	Samtech InfoNet Limited	samtech-001	001	2019-10-15
399	IN	Samtech InfoNet Limited	samtech-002	002	2023-07-06
400	RU	Satellite Innovation/Eocortex	eocortex-000	000	2020-08-26
401	IL	Scanovate	scanovate-002	002	2020-06-26
402	IL	Scanovate	scanovate-003	003	2021-11-15
403	NG	Seamfix	seamfix-001	001	2024-03-08
404	RO	Securif AI	securifai-007	007	2023-08-17
405	RO	Securif AI	securifai-008	008	2024-02-26
406	CN	Sensetime Group	sensetime-007	007	2022-06-17
407	CN	Sensetime Group	sensetime-008	008	2023-01-04
408	UZ	Serendipity Ltd	serendipity-000	000	2023-05-31
409	SG	Seventh Sense Artificial Intelligence	seventhsense-003	003	2023-05-31
410	SG	Seventh Sense Artificial Intelligence	seventhsense-005	005	2023-10-05
411	US	Shaman Software	shaman-000	000	2017-12-05
412	US	Shaman Software	shaman-001	001	2018-01-13
413	CN	Shanghai Jiao Tong University	sjtu-004	004	2021-05-13
414	CN	Shanghai Jiao Tong University	sjtu-005	005	2023-05-05
415	CN	Shanghai Ulucu Electronics Technology	uluface-002	002	2019-07-10
416	CN	Shanghai Ulucu Electronics Technology	uluface-003	003	2019-11-12
417	CN	Shanghai University - Shanghai Film Academy	shu-002	002	2019-12-10
418	CN	Shanghai University - Shanghai Film Academy	shu-003	003	2020-06-24
419	CN	Shanghai Yitu Technology	yitu-003	003	2019-03-01
420	CN	Shenzhen AiMall Tech	aimall-002	002	2020-03-12

Table 6: Summary of participant information included in this report.

FNMR(T) "False non-match rate"
FMR(T) "False match rate"

	Location	Developer Name	Short Name	Seq. Num.	Validation Date
421	CN	Shenzhen AiMall Tech	aimall-003	003	2020-08-12
422	CN	Shenzhen EI Networks	einetworks-000	000	2019-08-13
423	CN	Shenzhen Inst Adv Integrated Tech CAS	siat-002	002	2018-06-13
424	CN	Shenzhen Inst Adv Integrated Tech CAS	siat-005	005	2022-02-08
425	CN	Shenzhen Intellifusion Technologies	intellifusion-001	001	2019-08-22
426	CN	Shenzhen Intellifusion Technologies	intellifusion-002	002	2020-03-18
427	CN	Shenzhen University-Macau University of Science and Technology	sztu-000	000	2020-12-17
428	CN	Shenzhen University-Macau University of Science and Technology	sztu-001	001	2021-07-13
429	RU	Smart Engines	smartengines-000	000	2021-08-25
430	RU	Smart Engines	smartengines-001	001	2022-05-31
431	ES	Smartbiometrik	smartbiometrik-001	001	2022-05-16
432	TR	Smarvist Teknoloji	smartvist-000	000	2022-05-10
433	TR	Smarvist Teknoloji	smartvist-001	001	2023-11-02
434	DE	Smilart	smilart-002	002	2018-02-06
435	DE	Smilart	smilart-003	003	2019-03-01
436	TR	Sodec App Inc	sodec-000	000	2021-06-02
437		Sparsh CCTV	sparsh-001	001	2024-01-02
438	IN	Staqu Technologies	staqu-000	000	2020-07-15
439	CN	Star Hybrid Limited	starhybrid-001	001	2019-06-19
440	CN	Su Zhou NaZhiTianDi intelligent technology	nazhiai-000	000	2020-06-25
441	IN	Sukshi Technology Innovation	sukshi-000	000	2022-02-13
442	KR	Suprema AI Inc	suprema-004	004	2023-01-09
443	KR	Suprema AI Inc	suprema-005	005	2023-10-25
444	KR	Suprema ID Inc	supremaid-001	001	2021-05-04
445	KR	Suprema ID Inc	supremaid-002	002	2022-06-24
446	UK	Swsam Solutions	swsam-001	001	2023-03-13
447	RU	Synesis	synesis-006	006	2019-10-10
448	RU	Synesis	synesis-007	007	2020-06-24
449	TW	Synology Inc	synology-000	000	2019-10-23
450	TW	Synology Inc	synology-002	002	2020-08-20
451	BR	T4iSB	t4isb-000	000	2022-01-28
452	VN	TNI Tech Co	tnitech-000	000	2024-02-05
453	CN	TUPU Technology	tuputech-000	000	2019-10-11
454	TW	Taiwan AI Labs	ailabs-001	001	2019-12-18
455	TW	Taiwan-Certificate Authority Incorporation	twface-000	000	2021-05-14
456	TW	Taiwan-Certificate Authority Incorporation	twface-001	001	2021-09-14
457	CH	Tech5 SA	tech5-007	007	2022-12-30
458	CH	Tech5 SA	tech5-008	008	2023-08-11
459	VN	Techainer	techainer-001	001	2023-11-30
460	TR	Techsign	techsign-000	000	2021-08-25
461	TR	Techsign	techsign-001	001	2022-07-01
462	CN	Tencent Deepsea Lab	deepsea-001	001	2019-06-03
463	RU	Tevian	tevian-007	007	2021-08-06
464	RU	Tevian	tevian-008	008	2021-12-06
465	US	TigerIT Americas LLC	tiger-005	005	2021-07-29
466	US	TigerIT Americas LLC	tiger-006	006	2021-12-13
467	RU	Tinkoff Bank	tinkoff-001	001	2021-05-13
468	CN	TongYi Transportation Technology	tongyi-005	005	2019-06-12
469	TW	Toppan ID Gate	toppanidgate-000	000	2021-09-28
470	JP	Toshiba	toshiba-007	007	2023-09-13
471	JP	Toshiba	toshiba-008	008	2024-02-01
472	ES	Touchless ID	touchlessid-002	002	2023-01-23
473	ES	Touchless ID	touchlessid-003	003	2023-07-12
474	JP	Tripleize	aize-002	002	2021-10-08
475	JP	Tripleize	aize-003	003	2023-08-10
476	VN	TrueID-VNG	trueidvng-001	001	2023-01-05
477	US	Trueface.ai	trueface-002	002	2021-03-29
478	US	Trueface.ai	trueface-003	003	2021-09-30
479	UK	Trust Stamp	truststamp-001	001	2023-07-14
480	CN	TuringTech.vip	turingtechvip-001	001	2022-02-03
481	CN	TuringTech.vip	turingtechvip-002	002	2022-07-27
482	TR	Turkcell Technology	turkcell-001	001	2023-03-15
483	TR	Turkcell Technology	turkcell-002	002	2024-03-18
484	CN	ULSee Inc	ulsee-001	001	2019-07-31
485	UN	UNICC-Solution Architecture Section	unicc-002	002	2023-06-07
486	UN	UNICC-Solution Architecture Section	unicc-003	003	2023-10-16
487	TW	UXLabs	uxlabs-001	001	2022-09-19
488	TW	UXLabs	uxlabs-003	003	2023-07-28
489	FR	Unissey	unissey-003	003	2022-12-19
490	FR	Unissey	unissey-004	004	2023-07-19

Table 7: Summary of participant information included in this report.

FNMR(T) "False non-match rate"
FMR(T) "False match rate"

	Location	Developer Name	Short Name	Seq. Num.	Validation Date
491	PT	Universidade de Coimbra	visteam-007	007	2023-10-18
492	PT	Universidade de Coimbra	visteam-008	008	2024-02-06
493	UK	University of Surrey-CVSSP	surrey-cvssp-002	002	2023-02-16
494	UK	University of Surrey-CVSSP	surrey-cvssp-003	003	2023-09-13
495	US	VCognition	vcog-002	002	2017-06-12
496	VN	VNIS Joint Stock	vnis-000	000	2024-01-08
497	US	Vcortex Labs	vcortex-001	001	2023-06-14
498	ES	Veridas Digital Authentication Solutions S.L.	veridas-008	008	2022-10-17
499	ES	Veridas Digital Authentication Solutions S.L.	veridas-009	009	2023-05-08
500	UK	Veridium	veridium-002	002	2023-06-30
501	UK	Veridium	veridium-003	003	2024-02-21
502	KZ	Verigram	verigram-001	001	2022-03-09
503	KZ	Verigram	verigram-003	003	2023-08-09
504	ID	Verihubs	verihubs-inteligensia-001	001	2022-06-16
505	ID	Verihubs	verihubs-inteligensia-002	002	2023-06-07
506	ID	Verijelas	verijelas-000	000	2022-08-01
507	TW	Via Technologies Inc	via-004	004	2023-02-23
508	TW	Via Technologies Inc	via-005	005	2023-12-26
509	AE	Viante.AI	viante-000	000	2023-06-09
510	DE	Videmo Intelligente Videoanalyse	videmo-001	001	2021-12-22
511	DE	Videmo Intelligente Videoanalyse	videmo-002	002	2022-08-31
512	IN	Videonetics Technology Pvt	videonetics-001	001	2019-06-19
513	IN	Videonetics Technology Pvt	videonetics-002	002	2019-11-21
514	VN	Vietnam National Cyber Security Technology Corporation	ncsgroup-000	000	2024-03-18
515	VN	Vietnam Payment Solution	vnpay-000	000	2023-12-05
516	VN	Vietnam Posts and Telecommunications Group	vnpt-005	005	2022-08-24
517	VN	Vietnam Posts and Telecommunications Group	vnpt-006	006	2023-08-18
518	VN	Viettel Cyberspace Center	vtcc-000	000	2023-06-26
519	VN	Viettel Cyberspace Center	vtcc-001	001	2023-11-20
520	VN	Viettel Group	vts-000	000	2020-11-04
521	VN	Viettel Group	vts-001	001	2022-04-20
522	VN	Viettel High Technology	viettelhightech-000	000	2021-08-04
523	US	Vigilant Solutions	vigilantsolutions-010	010	2021-04-07
524	US	Vigilant Solutions	vigilantsolutions-011	011	2021-08-07
525	VN	VinAI Research VietNam	vinai-000	000	2020-09-24
526	VN	VinBigData	vinbigdata-002	002	2022-06-07
527	VN	VinBigData	vinbigdata-003	003	2023-06-23
528	SE	Visage Technologies	visage-000	000	2020-12-09
529	FI	Visidon	vd-002	002	2021-04-12
530	FI	Visidon	vd-003	003	2021-10-12
531	CN	Vision Intelligence Center of Meituan	meituan-003	003	2023-03-06
532	CN	Vision Intelligence Center of Meituan	meituan-004	004	2023-08-16
533	PT	Vision-Box	visionbox-003	003	2023-02-01
534	PT	Vision-Box	visionbox-004	004	2023-06-30
535	RU	VisionLabs	visionlabs-010	010	2021-01-25
536	RU	VisionLabs	visionlabs-011	011	2021-10-13
537	TW	Vivotek	vivotek-001	001	2024-04-03
538	AU	Vixvizon	vixvizion-006	006	2022-08-11
539	AU	Vixvizon	vixvizion-007	007	2023-01-17
540	US	Vocalize	vocalize-001	001	2024-03-27
541	RU	Vocord	vocord-009	009	2020-12-28
542	RU	Vocord	vocord-010	010	2021-12-20
543	US	Wicket	wicket-000	000	2022-02-14
544	CN	Winsense	winsense-001	001	2019-10-16
545	CN	Winsense	winsense-002	002	2020-11-20
546	MY	Wise AI SDN BHD	wiseai-001	001	2022-10-25
547	CN	Wuhan Tianyu Information Industry	wuhantianyu-001	001	2021-08-05
548	CN	X-Laboratory	x-laboratory-000	000	2019-09-03
549	CN	X-Laboratory	x-laboratory-001	001	2020-01-21
550	CN	Xforward AI Technology	xforwardai-001	001	2020-09-25
551	CN	Xforward AI Technology	xforwardai-002	002	2021-02-10
552	CN	Xiamen Meiya Pico Information	meiya-001	001	2019-03-01
553	CN	Xiamen University	xm-000	000	2020-10-19
554	PT	YooniK	yoonik-003	003	2022-01-06
555	PT	YooniK	yoonik-004	004	2023-02-10
556	UK	Yoti	yoti-001	001	2024-02-13
557	TW	Yuan High-Tech Development	yuan-005	005	2022-06-22
558	TW	Yuan High-Tech Development	yuan-008	008	2023-11-06
559	CN	Yuntu Data and Technology	ytu-000	000	2021-06-16
560	CN	Zhuhai Yisheng Electronics Technology	yisheng-004	004	2018-06-12

Table 8: Summary of participant information included in this report.

FNMR(T) "False non-match rate"
FMR(T) "False match rate"

	Location	Developer Name	Short Name	Seq. Num.	Validation Date
561	IN	i2v Systems	i2v-001	001	2024-03-11
562	VN	iCOMM Media and Tech	icomm-000	000	2023-12-26
563	CN	iQIYI Inc	iqface-000	000	2019-06-04
564	CN	iQIYI Inc	iqface-003	003	2021-02-23
565	TW	iSAP Solution Corporation	isap-001	001	2019-08-07
566	TW	iSAP Solution Corporation	isap-002	002	2020-09-01
567	TW	ioNetworks Inc	ionetworks-001	001	2023-08-01
568	TW	ioNetworks Inc	ionetworks-002	002	2023-12-08
569	KR	useB	useb-001	001	2023-09-12
570	KR	useB	useb-002	002	2024-01-19

Table 9: Summary of participant information included in this report.

FNMR(T) "False non-match rate"
FMR(T) "False match rate"

	ALGORITHM	CONFIG	LIBRARY	TEMPLATE						COMPARISON[4]	
	NAME	DATA	DATA	MEMORY	SIZE	GENERATION TIME (ms)[4]				TIME (ns)[5]	
		(KB)[1]	(KB)[2]	(MB)[3]	(B)	MUGSHOT	480x720	960x1440	1600x2400	3000x4500	GENUINE	IMPOSTOR
1	20face-000	117155	324083	347 1417	150 2048 ± 0	60 232 ± 1	48 223 ± 1	43 226 ± 4	34 222 ± 1	21 224 ± 1	544 44880 ± 134	542 44462 ± 163
2	20face-001	226824	324119	360 1512	496 4096 ± 0	73 279 ± 2	57 266 ± 1	49 266 ± 1	44 267 ± 1	34 267 ± 0	412 5553 ± 54	409 5541 ± 65
3	3divi-006	273866	52656	315 1252	341 2048 ± 0	278 654 ± 1	248 651 ± 0	229 660 ± 1	210 678 ± 2	209 759 ± 13	130 775 ± 19	128 770 ± 22
4	3divi-007	483115	24723	323 1288	330 2048 ± 0	256 615 ± 1	223 616 ± 1	205 623 ± 1	192 644 ± 1	196 727 ± 5	118 707 ± 31	118 712 ± 25
5	accurascan-002	14057	24437	243 945	28 512 ± 0	34 173 ± 23	37 188 ± 14	33 191 ± 14	29 208 ± 16	39 317 ± 14	476 12255 ± 69	475 12231 ± 72
6	accurascan-003	998397	27018	424 1996	396 2048 ± 0	293 676 ± 1	263 677 ± 7	254 700 ± 8	246 751 ± 16	276 950 ± 47	56 540 ± 10	57 536 ± 10
7	acer-001	36650	66086	89 417	23 512 ± 0	52 199 ± 0	51 237 ± 28	44 229 ± 26	41 242 ± 37	30 259 ± 21	310 2453 ± 44	311 2461 ± 62
8	acer-002	43922	624858	49 192	250 2048 ± 0	42 184 ± 0	33 184 ± 0	27 185 ± 0	22 185 ± 0	16 186 ± 0	361 3370 ± 47	361 3350 ± 54
9	acisw-007	267619	36111	62 287	233 2048 ± 0	78 283 ± 0	69 293 ± 3	93 414 ± 0	85 404 ± 0	87 484 ± 1	194 1316 ± 22	193 1297 ± 23
10	acisw-008	171703	39359	284 1102	232 2048 ± 0	134 400 ± 1	91 362 ± 28	76 369 ± 9	52 300 ± 2	44 336 ± 5	195 1327 ± 19	196 1337 ± 32
11	adera-004	0	959123	396 1748	556 6144 ± 0	510 1246 ± 1	461 1204 ± 1	459 1230 ± 2	417 1207 ± 2	367 1254 ± 1	251 1840 ± 34	250 1828 ± 31
12	adera-005	0	959113	392 1734	553 6144 ± 0	401 914 ± 1	343 879 ± 3	324 880 ± 2	300 886 ± 2	264 910 ± 2	261 1896 ± 14	258 1874 ± 20
13	advance-004	803133	954494	164 681	145 2048 ± 0	470 1099 ± 20	436 1107 ± 15	418 1093 ± 21	380 1103 ± 21	340 1138 ± 21	266 1935 ± 35	267 1936 ± 32
14	advance-005	277607	126218	153 624	225 2048 ± 0	225 573 ± 1	201 574 ± 2	175 573 ± 2	154 574 ± 2	134 601 ± 2	220 1517 ± 16	220 1518 ± 26
15	afisbiometrics-000	545886	32882	278 1085	36 512 ± 0	501 1219 ± 1	444 1135 ± 1	432 1137 ± 2	394 1137 ± 1	342 1147 ± 1	202 1400 ± 29	198 1357 ± 32
16	afrengine-002	579618	239125	257 1018	394 2048 ± 0	379 851 ± 3	422 1065 ± 16	377 993 ± 7	287 855 ± 5	246 857 ± 9	186 1259 ± 13	190 1270 ± 23
17	afrengine-003	579563	239117	256 1017	167 2048 ± 0	466 1088 ± 1	357 911 ± 15	410 1067 ± 5	278 833 ± 3	289 989 ± 2	191 1294 ± 48	192 1284 ± 29
18	aifirst-001	224157	808777	107 485	116 2048 ± 0	234 587 ± 2	198 568 ± 2	184 584 ± 3	167 601 ± 6	207 755 ± 5	168 1099 ± 14	169 1087 ± 45
19	aigen-001	256958	595227	295 1154	267 2048 ± 0	557 1448 ± 9	527 1451 ± 8	533 1759 ± 6	527 2594 ± 4	517 5691 ± 44	378 3772 ± 57	378 3736 ± 56
20	aigen-002	205300	1316138	233 896	140 2048 ± 0	233 586 ± 24	207 582 ± 4	336 920 ± 4	511 1758 ± 5	516 5427 ± 17	375 3678 ± 44	374 3646 ± 48
21	ailabs-001	1054663	338989	314 1252	172 2048 ± 0	286 664 ± 4	304 774 ± 50	435 1145 ± 12	518 1972 ± 74	513 5205 ± 272	563 104034 ± 661	563 103415 ± 7722
22	aimall-002	370156	25210	372 1576	234 2048 ± 0	340 776 ± 4	368 927 ± 27	345 940 ± 21	324 955 ± 34	295 1003 ± 75	561 72811 ± 7399	558 71216 ± 6286
23	aimall-003	504324	171935	414 1913	88 1024 ± 0	283 662 ± 1	293 740 ± 51	273 752 ± 62	244 741 ± 46	226 807 ± 47	533 34565 ± 93	533 34598 ± 118
24	aiseemu-001	0	1005354	479 2701	497 4096 ± 0	437 1001 ± 1	404 1017 ± 0	388 1014 ± 5	355 1022 ± 2	316 1059 ± 4	401 4864 ± 25	400 4855 ± 32
25	aiseemu-002	0	1216980	510 3453	475 4096 ± 0	524 1298 ± 5	488 1303 ± 4	480 1313 ± 2	454 1329 ± 0	398 1348 ± 2	404 4917 ± 37	401 4916 ± 37
26	aiunionface-000	241642	840295	84 402	297 2048 ± 0	269 637 ± 13	299 754 ± 41	390 1025 ± 28	407 1179 ± 29	457 1639 ± 47	162 1072 ± 19	166 1080 ± 47
27	aize-002	257106	182517	138 586	174 2048 ± 0	167 467 ± 1	147 479 ± 1	276 756 ± 1	496 1477 ± 1	509 4617 ± 41	73 597 ± 16	79 598 ± 14
28	aize-003	257130	33045	130 546	328 2048 ± 0	45 187 ± 0	36 188 ± 0	25 182 ± 0	21 183 ± 0	18 195 ± 0	89 621 ± 37	72 592 ± 1
29	ajou-001	363257	31734	96 442	211 2048 ± 0	199 530 ± 0	177 536 ± 0	156 535 ± 0	143 549 ± 0	125 577 ± 0	72 597 ± 19	76 596 ± 13
30	alchera-006	1000967	493456	350 1426	133 2048 ± 0	194 522 ± 2	180 540 ± 3	163 544 ± 2	152 569 ± 3	200 739 ± 3	290 2233 ± 38	291 2253 ± 77
31	alchera-007	1000948	493456	352 1430	208 2048 ± 0	198 530 ± 2	191 556 ± 2	172 566 ± 2	156 581 ± 2	210 762 ± 4	285 2178 ± 35	285 2169 ± 44
32	alfabeta-001	128232	21780	13 74	25 512 ± 0	69 271 ± 0	63 276 ± 0	116 459 ± 2	299 886 ± 2	487 2547 ± 9	48 470 ± 25	49 458 ± 20
33	alice-000	1741293	19355	508 3329	501 4096 ± 0	418 950 ± 2	370 933 ± 1	351 949 ± 1	353 1011 ± 3	370 1264 ± 8	488 14975 ± 201	487 14890 ± 229
34	alice-001	1428001	17074	167 690	384 2048 ± 0	464 1080 ± 1	424 1075 ± 0	420 1095 ± 1	397 1143 ± 1	421 1435 ± 1	514 21885 ± 278	513 21921 ± 265
35	alleyes-000	507636	997090	224 857	397 2048 ± 0	343 784 ± 1	383 970 ± 61	362 974 ± 62	319 943 ± 69	314 1057 ± 23	192 1298 ± 34	195 1303 ± 51
36	allgovision-000	172509	155862	134 561	340 2048 ± 0	126 384 ± 8	107 395 ± 17	91 413 ± 14	109 471 ± 14	185 710 ± 21	528 29903 ± 406	527 29735 ± 194
37	alphaface-001	259849	81636	123 527	261 2048 ± 0	252 612 ± 1	219 613 ± 3	198 612 ± 1	178 619 ± 1	152 640 ± 2	154 1008 ± 10	154 1002 ± 19
38	alphaface-002	768995	70692	353 1434	242 2048 ± 0	263 628 ± 2	295 746 ± 19	271 751 ± 18	256 779 ± 22	234 828 ± 40	147 945 ± 25	148 935 ± 17
39	amplifiedgroup-001	0	47053	15 81	73 866 ± 2	16 93 ± 0	-	-	-	-	553 57803 ± 4210	551 56365 ± 1196
40	androvideo-000	174847	585063	86 405	207 2048 ± 0	71 277 ± 0	66 285 ± 0	59 314 ± 0	72 372 ± 1	141 620 ± 0	334 2860 ± 28	332 2847 ± 22
41	anke-004	349388	410776	170 706	440 2056 ± 0	262 625 ± 1	232 627 ± 2	216 635 ± 3	196 653 ± 2	286 982 ± 8	99 633 ± 22	99 632 ± 34
42	anke-005	328553	429160	291 1134	427 2056 ± 0	236 590 ± 2	212 594 ± 5	192 601 ± 3	189 638 ± 4	231 821 ± 24	111 685 ± 19	114 687 ± 26
43	antheus-000	119453	41994	24 116	58 520 ± 0	20 109 ± 1	35 187 ± 1	31 189 ± 1	25 195 ± 1	24 236 ± 2	434 6901 ± 268	433 6936 ± 103
44	antheus-001	119453	41962	25 118	57 520 ± 0	24 120 ± 1	56 265 ± 13	125 468 ± 22	422 1223 ± 27	489 2660 ± 87	426 6218 ± 47	423 6216 ± 45

Notes	
1	The configuration size does not capture static data included in libraries.
2	The library size is the combined total of all files provided in the submission lib folder. These libraries e.g. OpenCV may or may not be installed on any end user's platform natively and would not need to be installed with the algorithm. Some developers put neural network models in their libraries.
3	The memory usage is the peak resident set size reported by the ps system call during template generation.
4	The median template creation times are measured on Intel®Xeon®CPU E5-2630 v4 @ 2.20GHz processors.
5	The comparison durations, in nanoseconds, are estimated using std::chrono::high_resolution_clock which on the machine in (2) counts 1ns clock ticks. Precision is somewhat worse than that however. The ± value is the median absolute deviation times 1.48 for Normal consistency.

Table 10: Summary of algorithms and properties included in this report. The red superscripts give ranking for the quantity in that column.

	ALGORITHM	CONFIG	LIBRARY	TEMPLATE							COMPARISON[4]	
	NAME	DATA	DATA	MEMORY	SIZE	GENERATION TIME (ms)[4]					TIME (ns)[5]	
		(KB)[1]	(KB)[2]	(MB)[3]	(B)	MUGSHOT	480x720	960x1440	1600x2400	3000x4500	GENUINE	IMPOSTOR
45	anyvision-004	401001	630797	285 1102	87 1024 ± 0	106 355 ± 1	-	-	-	-	260 1891 ± 51	251 1829 ± 85
46	anyvision-005	190979	116595	267 1048	80 1024 ± 0	431 985 ± 1	397 997 ± 1	384 1004 ± 1	337 995 ± 1	291 995 ± 1	123 733 ± 14	123 733 ± 16
47	aratek-001	254521	15993	439 2135	298 2048 ± 0	65 251 ± 1	62 275 ± 0	48 252 ± 0	46 278 ± 0	37 286 ± 0	245 1776 ± 20	242 1744 ± 38
48	armatura-001	0	374608	514 3518	395 2048 ± 0	304 688 ± 1	270 689 ± 1	247 693 ± 1	229 708 ± 3	208 756 ± 13	29 270 ± 17	31 268 ± 11
49	armatura-003	0	836082	371 1572	555 6144 ± 0	452 1028 ± 1	411 1032 ± 1	392 1027 ± 0	358 1036 ± 1	306 1041 ± 3	552 51850 ± 56	550 51835 ± 48
50	asusaics-000	257418	245320	145 605	363 2048 ± 0	178 484 ± 13	165 506 ± 21	308 850 ± 26	514 1789 ± 61	518 6305 ± 188	410 5455 ± 78	408 5422 ± 112
51	asusaics-001	257418	245330	141 595	487 4096 ± 0	375 842 ± 17	402 1008 ± 20	499 1377 ± 28	525 2423 ± 90	522 7284 ± 277	451 8618 ± 42	450 8638 ± 136
52	autentika-001	0	3198534	380 1650	323 2048 ± 0	301 683 ± 2	358 912 ± 4	332 908 ± 3	309 919 ± 3	258 893 ± 4	559 71804 ± 600	557 70747 ± 582
53	autentika-002	0	3198136	384 1676	137 2048 ± 0	119 374 ± 1	167 511 ± 1	153 528 ± 1	133 534 ± 1	112 546 ± 1	547 46941 ± 1172	544 46351 ± 822
54	authenmetric-003	293599	39492	226 866	256 2048 ± 0	436 992 ± 1	401 1006 ± 1	383 1003 ± 2	344 1002 ± 1	305 1036 ± 1	243 1757 ± 19	243 1755 ± 19
55	authenmetric-004	381165	39492	309 1214	122 2048 ± 0	398 910 ± 1	356 909 ± 1	333 915 ± 1	310 921 ± 2	275 950 ± 1	238 1724 ± 14	236 1691 ± 29
56	authme-001	1015124	37791	435 2097	477 4096 ± 0	417 949 ± 1	381 969 ± 7	358 960 ± 6	326 961 ± 1	280 966 ± 4	330 2836 ± 34	330 2827 ± 54
57	aware-007	135312	18711	83 388	21 480 ± 0	320 713 ± 1	286 716 ± 1	264 731 ± 3	258 785 ± 8	292 999 ± 30	159 1058 ± 23	170 1091 ± 37
58	aware-008	135312	18715	82 387	20 480 ± 0	331 751 ± 1	292 737 ± 0	268 739 ± 3	277 825 ± 9	296 1007 ± 27	172 1120 ± 25	180 1152 ± 35
59	awiros-001	15499	87480	18 88	40 512 ± 0	17 97 ± 6	14 98 ± 4	18 138 ± 6	35 225 ± 7	120 556 ± 8	165 1079 ± 44	162 1050 ± 45
60	awiros-002	289016	203723	132 556	196 2048 ± 0	174 479 ± 0	161 500 ± 0	155 534 ± 0	177 618 ± 0	272 946 ± 1	269 1966 ± 31	269 1957 ± 25
61	aximetria-001	408902	487912	467 2539	295 2048 ± 0	446 1013 ± 1	406 1023 ± 21	394 1029 ± 5	340 999 ± 2	325 1091 ± 5	394 4401 ± 94	391 4490 ± 80
62	ayftech-001	195423	43580	184 731	24 512 ± 0	140 408 ± 23	145 476 ± 52	291 814 ± 108	516 1827 ± 384	515 5412 ± 1029	86 615 ± 16	142 885 ± 44
63	ayftech-003	526164	127257	377 1640	254 2048 ± 0	439 1003 ± 5	405 1017 ± 6	386 1006 ± 6	351 1009 ± 7	319 1063 ± 5	193 1301 ± 20	194 1300 ± 25
64	ayonix-000	58505	5252	10 69	97 1036 ± 0	2 18 ± 2	-	-	-	-	91 621 ± 23	94 620 ± 26
65	beethedata-000	227849	1087592	133 557	284 2048 ± 0	165 465 ± 0	144 467 ± 0	123 468 ± 0	107 467 ± 0	81 467 ± 0	279 2121 ± 34	280 2110 ± 38
66	beyneai-000	256958	591433	425 1998	358 2048 ± 0	158 451 ± 8	134 449 ± 1	278 767 ± 7	508 1603 ± 25	510 4669 ± 124	376 3730 ± 57	375 3668 ± 54
67	biocube-001	25030	6192987	100 457	478 4096 ± 0	77 282 ± 22	68 292 ± 24	151 521 ± 57	214 684 ± 59	377 1282 ± 68	513 21787 ± 96	512 21812 ± 109
68	biocube-002	69898	10651580	104 468	499 4096 ± 0	368 826 ± 4	324 838 ± 4	442 1175 ± 4	530 2933 ± 1074	525 9144 ± 1090	517 23074 ± 94	515 23036 ± 99
69	bioidtechswiss-001	1178769	120811	355 1455	49 512 ± 0	423 966 ± 4	477 1270 ± 270	472 1294 ± 96	478 1409 ± 157	469 1793 ± 79	318 2610 ± 25	318 2624 ± 32
70	bioidtechswiss-002	744786	114842	251 990	42 512 ± 0	405 917 ± 2	369 930 ± 2	352 952 ± 2	320 947 ± 3	315 1058 ± 11	284 2177 ± 29	286 2170 ± 31
71	biometric-vision-000	445487	72132	238 915	185 2048 ± 0	372 836 ± 3	323 831 ± 3	316 869 ± 5	323 955 ± 8	403 1370 ± 19	483 14437 ± 161	481 14325 ± 167
72	bm-001	287734	38076	35 148	1 64 ± 0	155 444 ± 88	-	-	-	-	259 1887 ± 31	259 1877 ± 26
73	boetech-001	261376	88710	517 3658	236 2048 ± 0	70 271 ± 1	58 268 ± 1	50 273 ± 0	47 286 ± 1	40 318 ± 1	557 68519 ± 1921	555 67648 ± 822
74	boetech-002	294347	88710	429 2057	125 2048 ± 0	90 305 ± 4	73 296 ± 1	53 302 ± 1	54 313 ± 1	49 348 ± 2	558 68921 ± 2137	556 69473 ± 2104
75	bresee-001	287880	23227	311 1223	266 2048 ± 0	502 1223 ± 3	466 1216 ± 1	483 1331 ± 1	424 1227 ± 1	401 1360 ± 1	537 37240 ± 655	536 37167 ± 584
76	bresee-002	313627	30902	418 1951	190 2048 ± 0	330 743 ± 4	446 1143 ± 2	436 1146 ± 2	398 1148 ± 2	351 1176 ± 2	246 1778 ± 22	246 1775 ± 23
77	camvi-002	236278	225285	186 737	85 1024 ± 0	295 677 ± 7	289 726 ± 36	315 869 ± 28	390 1129 ± 43	495 2785 ± 113	84 612 ± 26	83 603 ± 20
78	camvi-004	280733	615819	239 919	148 2048 ± 0	334 759 ± 10	334 861 ± 17	369 986 ± 34	438 1279 ± 51	497 2891 ± 158	148 948 ± 40	149 963 ± 31
79	candour-001	150086	97632	106 477	287 2048 ± 0	548 1400 ± 1	512 1396 ± 1	509 1408 ± 1	477 1407 ± 1	429 1464 ± 1	467 10725 ± 133	466 10712 ± 127
80	canon-004	2399160	114188	555 7037	557 6200 ± 0	416 948 ± 4	378 955 ± 3	357 959 ± 3	330 977 ± 3	320 1064 ± 2	438 7172 ± 63	436 7169 ± 51
81	canon-005	2521818	80309	552 6700	540 4148 ± 0	503 1223 ± 21	469 1221 ± 2	458 1230 ± 4	425 1234 ± 5	395 1329 ± 3	425 6142 ± 99	424 6226 ± 146
82	cchonolulu-000	727461	37284	88 416	33 512 ± 0	26 123 ± 13	20 126 ± 10	17 129 ± 10	16 134 ± 10	20 223 ± 10	239 1726 ± 35	237 1697 ± 35
83	cchonolulu-001	733744	37284	92 426	143 2048 ± 0	30 162 ± 21	40 197 ± 23	146 513 ± 96	383 1118 ± 267	478 2142 ± 584	395 4418 ± 37	389 4361 ± 35
84	ceiec-003	260371	88707	93 430	392 2048 ± 0	360 817 ± 4	346 883 ± 57	325 897 ± 60	304 899 ± 72	271 944 ± 72	292 2256 ± 38	290 2241 ± 54
85	ceiec-004	263476	67011	87 408	249 2048 ± 0	450 1024 ± 1	408 1027 ± 1	393 1027 ± 1	357 1030 ± 1	311 1055 ± 1	253 1844 ± 26	253 1836 ± 20
86	chosun-001	765615	707	111 491	301 2048 ± 0	341 783 ± 2	319 826 ± 4	532 1662 ± 13	533 3679 ± 67	531 11694 ± 243	151 998 ± 25	160 1035 ± 11
87	chosun-002	234001	31875	98 451	175 2048 ± 0	64 248 ± 3	61 273 ± 3	529 1495 ± 14	536 7920 ± 90	535 80302 ± 1349	92 623 ± 17	100 634 ± 13
88	chtface-005	408364	311100	345 1415	258 2048 ± 0	97 322 ± 0	77 316 ± 1	63 325 ± 2	60 324 ± 1	66 411 ± 2	263 1907 ± 19	260 1898 ± 23

Notes	
1	The configuration size does not capture static data included in libraries.
2	The library size is the combined total of all files provided in the submission lib folder. These libraries e.g. OpenCV may or may not be installed on any end user's platform natively and would not need to be installed with the algorithm. Some developers put neural network models in their libraries.
3	The memory usage is the peak resident set size reported by the ps system call during template generation.
4	The median template creation times are measured on Intel®Xeon®CPU E5-2630 v4 @ 2.20GHz processors.
5	The comparison durations, in nanoseconds, are estimated using std::chrono::high_resolution_clock which on the machine in (2) counts 1ns clock ticks. Precision is somewhat worse than that however. The ± value is the median absolute deviation times 1.48 for Normal consistency.

Table 11: Summary of algorithms and properties included in this report. The red superscripts give ranking for the quantity in that column.

	ALGORITHM	CONFIG	LIBRARY	TEMPLATE							COMPARISON[4]	
	NAME	DATA	DATA	MEMORY	SIZE	GENERATION TIME (ms)[4]					TIME (ns)[5]	
		(KB)[1]	(KB)[2]	(MB)[3]	(B)	MUGSHOT	480x720	960x1440	1600x2400	3000x4500	GENUINE	IMPOSTOR
89	chtface-006	733645	610439	457 2424	241 2048 ± 0	195 522 ± 1	169 514 ± 1	157 536 ± 2	147 561 ± 1	178 693 ± 2	274 2034 ± 41	276 2049 ± 29
90	cist-003	0	1267350	480 2706	550 5248 ± 0	521 1291 ± 1	487 1300 ± 1	492 1352 ± 3	441 1287 ± 2	386 1313 ± 1	443 7838 ± 63	442 7823 ± 40
91	cist-004	0	1603990	468 2563	551 5248 ± 0	507 1243 ± 1	478 1271 ± 1	464 1264 ± 3	429 1252 ± 1	378 1287 ± 1	357 3216 ± 25	357 3220 ± 32
92	clearviewai-000	342491	211852	484 2745	206 2048 ± 0	549 1402 ± 1	514 1403 ± 1	511 1412 ± 1	481 1420 ± 1	413 1418 ± 1	223 1592 ± 37	223 1561 ± 37
93	clearviewai-001	613532	511807	336 1353	119 2048 ± 0	268 635 ± 2	243 642 ± 1	228 659 ± 1	200 664 ± 1	169 674 ± 1	137 827 ± 10	137 829 ± 20
94	closeli-001	420342	9851	196 773	498 4096 ± 0	374 839 ± 1	326 843 ± 1	304 841 ± 1	282 845 ± 1	249 865 ± 1	409 5404 ± 17	407 5400 ± 25
95	cloudmatrix-001	10390	542121	54 249	364 2048 ± 0	22 114 ± 1	17 117 ± 0	15 118 ± 0	14 123 ± 1	13 169 ± 1	550 50263 ± 212	548 50243 ± 237
96	cloudmatrix-002	256635	693318	265 1036	294 2048 ± 0	130 395 ± 1	110 398 ± 1	87 399 ± 1	82 402 ± 1	73 437 ± 20	549 49578 ± 120	547 49602 ± 180
97	cloudwalk-hr-003	383739	144263	248 983	450 2057 ± 0	247 606 ± 0	209 588 ± 0	188 594 ± 0	171 612 ± 1	113 547 ± 2	435 6982 ± 80	434 6972 ± 84
98	cloudwalk-hr-004	502916	520169	343 1399	401 2049 ± 0	387 873 ± 1	342 877 ± 1	321 876 ± 1	294 879 ± 1	263 902 ± 3	473 11652 ± 127	472 11608 ± 123
99	cloudwalk-mt-006	563322	480071	512 3499	334 2048 ± 0	541 1385 ± 0	510 1392 ± 1	504 1398 ± 1	473 1397 ± 4	424 1444 ± 2	360 3364 ± 96	359 3324 ± 83
100	cloudwalk-mt-007	563322	480071	513 3499	311 2048 ± 0	539 1379 ± 2	520 1425 ± 7	514 1427 ± 6	480 1417 ± 2	423 1443 ± 7	346 3000 ± 68	342 2971 ± 74
101	cmcuni-001	0	604227	299 1177	357 2048 ± 0	483 1161 ± 1	458 1187 ± 1	448 1194 ± 5	415 1200 ± 1	357 1207 ± 1	355 3153 ± 22	354 3158 ± 26
102	codeline-000	361659	138388	306 1194	112 2048 ± 0	558 1453 ± 0	529 1456 ± 2	523 1456 ± 0	489 1457 ± 0	435 1483 ± 1	282 2171 ± 69	287 2194 ± 84
103	cogent-007	621565	72316	412 1888	66 550 ± 0	532 1329 ± 2	500 1333 ± 5	487 1337 ± 4	458 1353 ± 5	408 1390 ± 4	38 355 ± 8	39 367 ± 14
104	cogent-008	856817	73587	443 2176	67 550 ± 0	552 1412 ± 1	519 1419 ± 2	513 1426 ± 3	484 1437 ± 3	433 1476 ± 1	44 436 ± 14	45 441 ± 23
105	cognitec-004	705645	62678	136 580	416 2052 ± 0	163 463 ± 9	157 497 ± 9	140 504 ± 10	128 521 ± 10	145 631 ± 12	349 3028 ± 197	349 3059 ± 238
106	cognitec-005	326804	198231	209 819	419 2052 ± 0	92 311 ± 10	92 364 ± 12	77 370 ± 10	74 390 ± 10	94 498 ± 16	299 2332 ± 48	301 2330 ± 40
107	cor-001	1194948	11240	313 1249	452 2060 ± 0	316 699 ± 3	335 863 ± 76	314 865 ± 80	290 872 ± 89	277 952 ± 39	566 270145 ± 2259	566 282686 ± 11788
108	coretech-001	235361	305490	361 1523	222 2048 ± 0	305 688 ± 7	275 695 ± 7	317 870 ± 17	295 879 ± 15	254 877 ± 15	93 625 ± 25	105 641 ± 25
109	coretech-002	339881	296194	506 3300	147 2048 ± 0	161 459 ± 1	136 451 ± 1	309 851 ± 1	291 875 ± 2	285 980 ± 2	309 2443 ± 17	307 2436 ± 13
110	corsight-002	1474921	32093	413 1892	455 2080 ± 0	520 1290 ± 1	483 1287 ± 1	470 1290 ± 1	443 1307 ± 2	407 1388 ± 4	520 24953 ± 637	517 24263 ± 578
111	corsight-003	1413063	32198	378 1642	457 2080 ± 0	496 1202 ± 2	460 1190 ± 5	451 1199 ± 3	427 1236 ± 3	399 1349 ± 7	527 28754 ± 434	526 28279 ± 446
112	csc-002	0	519768	3 30	62 544 ± 0	171 473 ± 0	156 494 ± 0	129 481 ± 1	116 490 ± 1	100 514 ± 5	41 367 ± 11	40 371 ± 10
113	csc-003	0	400435	4 31	63 544 ± 0	184 499 ± 0	159 500 ± 1	139 502 ± 0	125 508 ± 1	109 535 ± 4	43 393 ± 8	42 397 ± 7
114	ctbcbank-000	257208	599238	135 570	289 2048 ± 0	220 568 ± 43	216 606 ± 38	246 690 ± 53	230 711 ± 50	236 831 ± 51	369 3551 ± 87	397 4805 ± 209
115	ctbcbank-001	275511	599238	142 603	166 2048 ± 0	275 652 ± 35	306 781 ± 30	320 875 ± 43	303 898 ± 51	303 1030 ± 47	382 3926 ± 45	381 3924 ± 56
116	cu-face-003	1015124	37791	436 2116	523 4096 ± 0	415 945 ± 1	377 955 ± 3	355 957 ± 2	322 949 ± 3	278 963 ± 2	325 2769 ± 19	326 2782 ± 41
117	cu-face-004	1016682	37791	431 2083	515 4096 ± 0	448 1022 ± 1	410 1031 ± 1	380 998 ± 3	370 1070 ± 1	300 1021 ± 2	335 2884 ± 38	335 2864 ± 48
118	cubox-002	542254	90975	421 1966	130 2048 ± 0	406 921 ± 1	363 921 ± 1	338 922 ± 1	314 933 ± 1	294 1003 ± 1	272 2008 ± 72	271 1969 ± 57
119	cubox-003	1694397	209684	511 3491	356 2048 ± 0	488 1179 ± 0	459 1189 ± 0	450 1198 ± 0	418 1208 ± 0	371 1264 ± 1	296 2289 ± 112	296 2297 ± 68
120	cudocommunication-001	385258	341277	277 1080	158 2048 ± 0	408 925 ± 1	365 923 ± 1	343 928 ± 1	313 932 ± 0	279 964 ± 1	315 2534 ± 20	317 2537 ± 20
121	cuhkee-001	787853	74917	466 2515	410 2052 ± 0	428 977 ± 31	-	-	-	-	321 2719 ± 60	327 2783 ± 56
122	cybercore-002	166096	7374	469 2565	163 2048 ± 0	180 489 ± 1	160 500 ± 4	138 500 ± 1	121 499 ± 2	106 528 ± 1	477 12389 ± 123	476 12352 ± 112
123	cybercore-003	289176	7969	531 4311	504 4096 ± 0	376 844 ± 2	331 855 ± 4	313 864 ± 4	289 862 ± 4	256 878 ± 2	417 5744 ± 41	417 5737 ± 31
124	cyberextruder-003	253300	12354	97 444	32 512 ± 0	129 390 ± 1	104 388 ± 1	86 393 ± 1	80 399 ± 1	70 435 ± 1	19 198 ± 4	18 189 ± 8
125	cyberextruder-004	169301	12354	67 302	3 128 ± 0	54 206 ± 0	44 208 ± 0	37 209 ± 0	38 229 ± 0	29 249 ± 1	9 145 ± 14	11 155 ± 14
126	cyberlink-012	1200318	102281	488 2789	559 6212 ± 0	243 601 ± 1	226 621 ± 5	197 610 ± 2	173 614 ± 2	158 649 ± 5	302 2343 ± 26	303 2377 ± 34
127	cyberlink-013	893519	102285	419 1964	558 6212 ± 0	245 603 ± 1	214 602 ± 2	195 606 ± 2	172 613 ± 2	154 642 ± 1	34 307 ± 7	34 306 ± 5
128	dahua-006	831641	119261	539 5068	277 2048 ± 0	547 1398 ± 2	513 1397 ± 1	508 1404 ± 1	474 1402 ± 1	410 1402 ± 1	27 249 ± 13	28 250 ± 11
129	dahua-007	1578737	119418	557 7237	493 4096 ± 0	546 1393 ± 2	506 1373 ± 1	500 1378 ± 1	467 1378 ± 1	405 1379 ± 2	40 367 ± 102	43 434 ± 108
130	daon-000	280726	2307	427 2010	453 2065 ± 0	217 562 ± 3	205 581 ± 5	280 791 ± 9	279 838 ± 15	310 1055 ± 32	497 16052 ± 88	496 16041 ± 85
131	datech-000	617605	139575	544 5599	520 4096 ± 0	224 573 ± 32	208 583 ± 44	187 593 ± 37	538 14123 ± 9564	533 15514 ± 2343	444 7857 ± 29	443 7852 ± 25
132	datech-001	835404	139615	556 7179	488 4096 ± 0	447 1017 ± 83	417 1057 ± 65	407 1062 ± 88	381 1109 ± 81	382 1299 ± 92	445 7944 ± 31	444 7981 ± 56

Notes	
1	The configuration size does not capture static data included in libraries.
2	The library size is the combined total of all files provided in the submission lib folder. These libraries e.g. OpenCV may or may not be installed on any end user's platform natively and would not need to be installed with the algorithm. Some developers put neural network models in their libraries.
3	The memory usage is the peak resident set size reported by the ps system call during template generation.
4	The median template creation times are measured on Intel®Xeon®CPU E5-2630 v4 @ 2.20GHz processors.
5	The comparison durations, in nanoseconds, are estimated using std::chrono::high_resolution_clock which on the machine in (2) counts 1ns clock ticks. Precision is somewhat worse than that however. The ± value is the median absolute deviation times 1.48 for Normal consistency.

Table 12: Summary of algorithms and properties included in this report. The red superscripts give ranking for the quantity in that column.

	ALGORITHM	CONFIG	LIBRARY	TEMPLATE						COMPARISON[4]	
	NAME	DATA	DATA	MEMORY	SIZE	GENERATION TIME (ms)[4]				TIME (ns)[5]	
		(KB)[1]	(KB)[2]	(MB)[3]	(B)	MUGSHOT	480x720	960x1440	1600x2400	3000x4500	GENUINE	IMPOSTOR
133	decatur-000	350495	171271	235 907	530 4100 ± 0	449 1024 ± 2	-	-	-	-	471 11439 ± 80	470 11418 ± 112
134	decatur-001	342866	253734	359 1508	404 2052 ± 0	471 1103 ± 2	421 1064 ± 2	408 1063 ± 2	367 1067 ± 2	322 1084 ± 2	82 610 ± 19	82 602 ± 8
135	decloakface-001	29693	170719	79 368	187 2048 ± 0	49 196 ± 58	41 201 ± 52	45 229 ± 53	51 298 ± 60	107 532 ± 61	398 4638 ± 19	395 4646 ± 22
136	deepglint-004	1073382	261571	502 3116	161 2048 ± 0	561 1470 ± 1	533 1474 ± 1	528 1485 ± 1	494 1474 ± 1	439 1492 ± 2	423 5961 ± 34	422 5955 ± 29
137	deepglint-005	960326	213877	498 2991	154 2048 ± 0	551 1408 ± 1	522 1431 ± 2	512 1424 ± 3	482 1424 ± 3	426 1446 ± 2	432 6765 ± 38	430 6765 ± 40
138	deepsea-001	147497	336250	76 358	82 1024 ± 0	264 630 ± 7	298 752 ± 37	269 746 ± 30	237 727 ± 32	229 820 ± 32	204 1401 ± 37	212 1467 ± 50
139	deepsense-002	73173	1266131	540 5280	74 896 ± 0	535 1350 ± 1	486 1299 ± 8	481 1324 ± 0	457 1348 ± 0	432 1474 ± 4	367 3505 ± 32	369 3515 ± 40
140	deepsense-003	73173	1359497	549 6555	76 901 ± 0	370 832 ± 2	371 940 ± 2	306 845 ± 4	333 983 ± 1	284 976 ± 7	248 1797 ± 25	248 1795 ± 19
141	dermalog-011	0	278395	175 716	2 128 ± 0	104 343 ± 0	86 345 ± 0	68 347 ± 0	65 351 ± 0	54 363 ± 0	32 299 ± 19	29 253 ± 14
142	dermalog-012	0	293431	177 723	4 128 ± 0	40 181 ± 0	28 179 ± 0	24 182 ± 0	23 186 ± 0	28 242 ± 0	11 163 ± 10	20 196 ± 16
143	dicio-001	61751	119517	17 84	59 520 ± 0	205 538 ± 0	195 563 ± 10	334 915 ± 3	515 1800 ± 7	514 5286 ± 30	327 2818 ± 20	328 2807 ± 31
144	didiglobalface-001	259849	70680	122 527	155 2048 ± 0	253 612 ± 1	240 633 ± 3	215 634 ± 3	194 650 ± 15	166 666 ± 4	149 973 ± 20	151 988 ± 20
145	didiglobalface-002	260054	161508	206 812	314 2048 ± 0	259 622 ± 1	239 633 ± 1	222 642 ± 2	198 659 ± 4	195 726 ± 15	61 560 ± 10	65 567 ± 13
146	digidata-000	133370	30249	57 259	367 2048 ± 0	112 361 ± 0	89 360 ± 0	73 361 ± 0	68 363 ± 0	57 380 ± 0	278 2084 ± 37	274 2039 ± 42
147	digidata-001	254564	33036	77 367	218 2048 ± 0	214 559 ± 1	193 561 ± 1	170 562 ± 1	149 564 ± 1	135 602 ± 1	465 10308 ± 102	464 10301 ± 121
148	digitalbarriers-002	83002	598577	416 1930	449 2056 ± 0	55 209 ± 11	53 250 ± 19	90 411 ± 37	265 808 ± 72	479 2236 ± 123	479 13409 ± 228	478 13267 ± 206
149	dps-000	0	2211812	344 1405	503 4096 ± 0	384 868 ± 2	349 893 ± 6	520 1445 ± 9	529 2910 ± 38	526 9345 ± 17	213 1473 ± 37	214 1479 ± 37
150	dsk-000	11967	782905	56 252	31 512 ± 0	88 304 ± 47	80 317 ± 33	381 1001 ± 96	528 2660 ± 170	529 10451 ± 832	437 7152 ± 115	435 7134 ± 111
151	einetworks-000	372608	219883	228 880	443 2056 ± 0	273 645 ± 3	-	-	-	-	402 4876 ± 66	403 5156 ± 77
152	einetworksindia-000	372375	479472	332 1322	448 2056 ± 0	121 378 ± 1	100 382 ± 1	82 383 ± 1	79 397 ± 0	78 456 ± 3	493 15171 ± 41	491 15138 ± 62
153	einetworksindia-001	562398	481792	402 1808	444 2056 ± 0	172 479 ± 0	150 481 ± 1	131 485 ± 1	119 494 ± 1	111 541 ± 1	491 15147 ± 63	490 15134 ± 74
154	ekin-002	51434	278	30 139	469 3072 ± 0	492 1186 ± 13	455 1180 ± 12	445 1181 ± 11	413 1191 ± 11	356 1207 ± 8	391 4294 ± 80	411 5569 ± 112
155	element-000	721679	24895	321 1287	322 2048 ± 0	133 399 ± 1	118 417 ± 1	101 428 ± 9	111 478 ± 14	174 688 ± 45	67 583 ± 10	68 585 ± 13
156	enface-001	370710	173609	162 669	89 1024 ± 0	211 550 ± 4	190 555 ± 3	234 668 ± 7	331 981 ± 15	484 2416 ± 59	431 6734 ± 68	431 6766 ± 69
157	enface-002	858356	98741	560 9004	84 1024 ± 0	451 1026 ± 1	414 1038 ± 3	404 1057 ± 7	386 1123 ± 4	396 1338 ± 8	222 1529 ± 23	222 1530 ± 35
158	eocortex-000	255937	59432	51 224	326 2048 ± 0	89 305 ± 22	85 341 ± 25	108 440 ± 47	106 464 ± 45	99 513 ± 44	146 923 ± 11	147 918 ± 11
159	ercacat-001	811623	58012	490 2816	414 2052 ± 0	457 1052 ± 3	-	-	-	-	316 2551 ± 62	314 2501 ± 81
160	euronovate-003	0	5637394	305 1193	462 2201 ± 0	87 300 ± 0	75 300 ± 0	54 303 ± 0	53 310 ± 0	46 340 ± 0	538 37908 ± 968	537 38285 ± 938
161	euronovate-004	0	1335993	268 1049	463 2201 ± 0	79 290 ± 0	70 294 ± 0	51 294 ± 0	49 295 ± 0	38 294 ± 0	545 46290 ± 490	543 46199 ± 484
162	expasoft-001	39057	983064	32 142	251 2048 ± 0	12 70 ± 0	10 74 ± 0	9 77 ± 0	8 73 ± 0	7 74 ± 0	232 1660 ± 35	233 1676 ± 48
163	expasoft-002	38760	59825	41 170	281 2048 ± 0	7 34 ± 0	5 34 ± 0	5 34 ± 0	4 34 ± 0	2 34 ± 0	453 8870 ± 78	452 8838 ± 77
164	f8-001	272977	19668	319 1276	191 2048 ± 0	366 822 ± 39	-	-	-	-	496 15262 ± 139	495 15277 ± 212
165	f8-002	28278	215616	16 84	317 2048 ± 0	9 39 ± 0	7 41 ± 0	8 75 ± 0	28 197 ± 1	180 702 ± 1	487 14765 ± 131	486 14790 ± 133
166	facehawk-000	120009	7737	28 129	72 776 ± 1	132 399 ± 0	112 402 ± 0	92 414 ± 1	77 391 ± 2	74 440 ± 3	469 10931 ± 155	468 10915 ± 149
167	facelocate-001	4739	11106	463 2449	5 168 ± 0	8 34 ± 1	6 38 ± 0	11 84 ± 1	12 112 ± 4	19 206 ± 13	457 9565 ± 91	458 9629 ± 131
168	faceonlive-001	0	71529	66 300	446 2056 ± 0	38 179 ± 0	29 179 ± 0	32 190 ± 0	32 217 ± 0	47 343 ± 1	160 1064 ± 37	159 1033 ± 35
169	faceonlive-002	155220	141019	252 997	229 2048 ± 0	342 783 ± 1	311 797 ± 2	284 794 ± 2	260 809 ± 3	262 901 ± 2	480 13798 ± 197	479 13743 ± 127
170	facephi-000	148904	5219	565 20248	253 2048 ± 0	385 871 ± 2	344 881 ± 3	323 880 ± 4	302 888 ± 4	274 949 ± 12	386 4067 ± 53	386 4047 ± 53
171	facesoft-000	370120	10612	202 796	389 2048 ± 0	291 675 ± 18	254 669 ± 3	242 686 ± 3	207 675 ± 5	172 687 ± 2	291 2239 ± 28	294 2277 ± 96
172	facetag-000	1232331	4022	244 965	70 684 ± 0	107 355 ± 17	96 369 ± 8	373 989 ± 33	524 2408 ± 91	523 7930 ± 316	560 72003 ± 625	559 71912 ± 612
173	facetag-002	819806	4021	171 706	324 2048 ± 0	207 544 ± 1	185 544 ± 0	161 542 ± 0	141 545 ± 0	118 554 ± 0	240 1730 ± 25	239 1733 ± 25
174	facex-001	305074	930372	509 3336	371 2048 ± 0	146 422 ± 4	128 434 ± 4	150 520 ± 7	243 737 ± 13	460 1670 ± 27	257 1871 ± 23	255 1846 ± 29
175	facex-002	305074	928334	499 3011	212 2048 ± 0	147 426 ± 5	125 429 ± 4	147 516 ± 8	240 730 ± 12	466 1738 ± 36	96 631 ± 25	92 614 ± 19
176	facia-001	296496	745403	231 889	247 2048 ± 0	468 1099 ± 1	438 1109 ± 0	427 1113 ± 0	387 1125 ± 3	365 1250 ± 1	556 62245 ± 397	554 62249 ± 496

Notes	
1	The configuration size does not capture static data included in libraries.
2	The library size is the combined total of all files provided in the submission lib folder. These libraries e.g. OpenCV may or may not be installed on any end user's platform natively and would not need to be installed with the algorithm. Some developers put neural network models in their libraries.
3	The memory usage is the peak resident set size reported by the ps system call during template generation.
4	The median template creation times are measured on Intel®Xeon®CPU E5-2630 v4 @ 2.20GHz processors.
5	The comparison durations, in nanoseconds, are estimated using std::chrono::high_resolution_clock which on the machine in (2) counts 1ns clock ticks. Precision is somewhat worse than that however. The ± value is the median absolute deviation times 1.48 for Normal consistency.

Table 13: Summary of algorithms and properties included in this report. The red superscripts give ranking for the quantity in that column.

	ALGORITHM	CONFIG	LIBRARY	TEMPLATE						COMPARISON[4]	
	NAME	DATA	DATA	MEMORY	SIZE	GENERATION TIME (ms)[4]				TIME (ns)[5]	
		(KB)[1]	(KB)[2]	(MB)[3]	(B)	MUGSHOT	480x720	960x1440	1600x2400	3000x4500	GENUINE	IMPOSTOR
177	farfaces-001	346494	44581	58 262	29 512 ± 0	489 1179 ± 1	456 1180 ± 1	444 1180 ± 0	409 1185 ± 1	359 1209 ± 2	140 855 ± 25	139 860 ± 31
178	fastenterprises-000	273365	235899	259 1030	386 2048 ± 0	282 662 ± 1	256 671 ± 0	232 664 ± 0	206 673 ± 3	173 688 ± 5	379 3806 ± 96	531 32064 ± 185
179	fedu-001	466605	496375	368 1557	296 2048 ± 0	238 592 ± 1	227 623 ± 1	206 624 ± 0	181 623 ± 0	155 647 ± 0	303 2362 ± 13	302 2361 ± 22
180	fiberhome-nanjing-003	352895	1482309	225 859	257 2048 ± 0	479 1136 ± 7	443 1134 ± 4	430 1132 ± 3	395 1139 ± 3	344 1154 ± 5	167 1097 ± 38	167 1083 ± 42
181	fiberhome-nanjing-004	443779	1482313	275 1077	474 4096 ± 0	529 1321 ± 5	489 1304 ± 3	478 1307 ± 2	444 1308 ± 3	393 1326 ± 5	189 1276 ± 40	189 1265 ± 38
182	fincore-000	256615	19409	127 536	162 2048 ± 0	190 508 ± 3	164 505 ± 0	142 508 ± 1	127 513 ± 2	108 535 ± 1	244 1765 ± 31	244 1763 ± 22
183	firstcreditkz-002	977538	24879	417 1951	135 2048 ± 0	513 1265 ± 1	480 1275 ± 4	476 1299 ± 7	456 1341 ± 17	443 1515 ± 40	128 761 ± 28	129 774 ± 32
184	firstcreditkz-003	1145884	24907	441 2144	318 2048 ± 0	494 1188 ± 79	535 1492 ± 77	536 2566 ± 293	535 4939 ± 888	532 14753 ± 3518	87 616 ± 10	91 613 ± 16
185	foomobi-001	0	219961	45 189	227 2048 ± 0	109 357 ± 0	103 388 ± 2	433 1138 ± 1	531 2974 ± 10	527 10101 ± 10	548 47409 ± 453	546 47413 ± 421
186	foomobi-002	0	219961	44 189	210 2048 ± 0	86 299 ± 0	81 323 ± 0	356 957 ± 1	526 2496 ± 2	524 8549 ± 7	529 30257 ± 724	528 30010 ± 320
187	fpt-000	19013	170633	50 219	134 2048 ± 0	23 118 ± 0	19 122 ± 1	16 122 ± 0	13 120 ± 0	15 178 ± 2	381 3871 ± 31	380 3883 ± 29
188	fraudcom-000	354020	561861	245 966	405 2052 ± 0	216 561 ± 2	179 539 ± 2	159 541 ± 1	145 557 ± 5	129 594 ± 6	293 2258 ± 10	292 2256 ± 29
189	frpkauai-001	507771	24807	529 4143	182 2048 ± 0	309 689 ± 1	273 691 ± 0	251 697 ± 2	234 714 ± 6	218 775 ± 31	126 752 ± 29	127 764 ± 23
190	frpkauai-002	519141	24803	287 1113	176 2048 ± 0	352 799 ± 0	393 987 ± 0	401 1046 ± 1	402 1163 ± 2	468 1769 ± 4	143 907 ± 20	143 886 ± 28
191	fujitsulab-002	0	1088887	385 1685	536 4104 ± 0	505 1237 ± 2	470 1222 ± 2	460 1236 ± 1	428 1251 ± 2	394 1327 ± 2	329 2836 ± 25	329 2809 ± 44
192	fujitsulab-003	662263	318209	551 6691	534 4104 ± 0	420 951 ± 20	372 941 ± 19	353 952 ± 19	328 971 ± 20	307 1045 ± 21	333 2855 ± 16	333 2849 ± 19
193	g42-intellibrain-001	1031335	235521	568 25154	14 269 ± 0	427 976 ± 6	384 975 ± 1	379 997 ± 2	369 1068 ± 3	402 1362 ± 8	420 5878 ± 96	420 5865 ± 71
194	g42-intellibrain-002	1043920	132389	564 19747	13 269 ± 0	402 915 ± 2	361 920 ± 2	349 946 ± 2	339 998 ± 4	362 1224 ± 8	485 14703 ± 56	485 14658 ± 97
195	geo-002	369903	98667	258 1021	117 2048 ± 0	346 791 ± 1	309 793 ± 0	283 794 ± 0	261 795 ± 1	223 803 ± 1	364 3407 ± 45	365 3422 ± 65
196	geo-004	168980	107714	322 1287	320 2048 ± 0	514 1268 ± 1	481 1279 ± 1	466 1274 ± 0	433 1259 ± 1	381 1296 ± 1	156 1023 ± 20	157 1028 ± 22
197	gistouch-000	155338	444582	129 541	346 2048 ± 0	99 325 ± 1	83 326 ± 1	67 337 ± 1	66 354 ± 1	93 495 ± 1	456 9505 ± 604	453 9443 ± 388
198	gistouch-001	426635	444545	381 1651	252 2048 ± 0	410 930 ± 3	360 919 ± 3	344 937 ± 4	327 966 ± 2	332 1113 ± 1	449 8475 ± 133	448 8460 ± 173
199	glory-006	0	1004784	460 2438	542 4182 ± 0	317 704 ± 1	303 774 ± 0	361 968 ± 2	522 2286 ± 18	528 10381 ± 151	419 5853 ± 77	419 5819 ± 74
200	glory-007	0	1004846	461 2442	541 4182 ± 0	128 385 ± 0	126 431 ± 0	178 575 ± 14	492 1464 ± 24	519 6782 ± 62	368 3506 ± 51	368 3489 ± 66
201	gorilla-008	450175	707000	404 1812	566 8338 ± 0	241 595 ± 1	210 590 ± 0	191 600 ± 1	180 621 ± 2	192 720 ± 9	397 4530 ± 44	393 4524 ± 38
202	gorilla-009	329584	297395	329 1304	544 4242 ± 0	396 899 ± 2	364 922 ± 1	328 901 ± 3	311 924 ± 4	304 1032 ± 12	298 2294 ± 74	298 2301 ± 66
203	gpstechvn-000	108365	345975	473 2646	375 2048 ± 0	84 296 ± 1	74 297 ± 1	55 304 ± 0	55 316 ± 0	58 382 ± 0	308 2442 ± 11	308 2440 ± 16
204	graymatics-001	13095	70406	26 128	482 4096 ± 0	46 191 ± 1	42 203 ± 1	186 592 ± 5	510 1698 ± 9	521 7150 ± 34	541 39874 ± 309	539 39762 ± 295
205	griaule-001	0	412061	318 1271	402 2052 ± 0	484 1164 ± 1	434 1096 ± 5	423 1099 ± 4	393 1136 ± 2	441 1509 ± 2	383 3948 ± 23	384 3957 ± 32
206	griaule-002	0	1320474	410 1870	418 2052 ± 0	365 822 ± 1	366 924 ± 4	330 907 ± 1	361 1038 ± 21	417 1430 ± 9	385 4005 ± 32	385 4012 ± 31
207	hertasecurity-002	0	944582	301 1182	39 512 ± 0	177 484 ± 7	146 478 ± 3	127 480 ± 3	120 495 ± 3	104 520 ± 3	295 2289 ± 40	293 2267 ± 48
208	hertasecurity-003	0	944583	300 1181	26 512 ± 0	183 495 ± 7	148 480 ± 3	132 486 ± 3	117 491 ± 3	103 520 ± 4	441 7619 ± 65	440 7597 ± 94
209	hik-001	667866	9290	550 6597	103 1408 ± 0	274 651 ± 0	253 667 ± 8	236 677 ± 16	215 686 ± 13	199 737 ± 12	51 488 ± 19	52 477 ± 22
210	hisign-002	1014906	102652	438 2131	458 2080 ± 0	350 797 ± 0	312 800 ± 5	286 800 ± 0	262 801 ± 0	224 803 ± 1	26 232 ± 11	22 207 ± 11
211	hisign-003	2232829	156367	374 1599	456 2080 ± 0	455 1040 ± 5	426 1083 ± 4	413 1085 ± 4	377 1088 ± 4	326 1093 ± 4	12 167 ± 8	10 150 ± 10
212	hyperverge-003	1167779	282156	476 2687	79 1024 ± 0	563 1477 ± 2	536 1503 ± 3	530 1520 ± 3	504 1525 ± 4	452 1565 ± 3	63 566 ± 11	63 561 ± 8
213	hyperverge-005	3413303	284050	475 2686	91 1024 ± 0	306 689 ± 0	271 690 ± 0	248 693 ± 0	226 702 ± 6	205 752 ± 5	47 465 ± 2	50 464 ± 10
214	hzailu-005	1573726	275643	505 3292	549 5128 ± 0	303 684 ± 10	258 673 ± 7	204 622 ± 1	212 682 ± 6	188 715 ± 2	255 1853 ± 51	252 1829 ± 34
215	hzailu-006	2996729	275643	548 6070	560 7176 ± 0	569 1498 ± 11	534 1483 ± 15	515 1439 ± 8	486 1441 ± 10	451 1564 ± 40	306 2434 ± 19	309 2452 ± 32
216	i2v-001	276820	26600	208 815	226 2048 ± 0	324 721 ± 0	291 729 ± 0	265 731 ± 0	241 731 ± 0	212 764 ± 0	472 11523 ± 176	471 11533 ± 142
217	icm-004	2012129	1089	269 1052	244 2048 ± 0	145 419 ± 6	114 407 ± 6	114 454 ± 15	168 603 ± 51	446 1527 ± 235	486 14730 ± 154	484 14521 ± 152
218	icm-005	877530	1097	288 1116	265 2048 ± 0	43 185 ± 3	31 181 ± 3	36 208 ± 9	58 321 ± 36	298 1014 ± 185	463 10245 ± 65	463 10245 ± 69
219	icomm-000	807818	139431	553 6728	510 4096 ± 0	246 605 ± 26	218 610 ± 30	194 605 ± 27	169 610 ± 23	153 641 ± 32	450 8507 ± 25	449 8516 ± 26
220	icthtc-000	172459	1471004	297 1165	128 2048 ± 0	103 338 ± 11	84 338 ± 9	104 437 ± 16	227 705 ± 24	465 1719 ± 44	408 5284 ± 63	406 5290 ± 54

Notes	
1	The configuration size does not capture static data included in libraries.
2	The library size is the combined total of all files provided in the submission lib folder. These libraries e.g. OpenCV may or may not be installed on any end user's platform natively and would not need to be installed with the algorithm. Some developers put neural network models in their libraries.
3	The memory usage is the peak resident set size reported by the ps system call during template generation.
4	The median template creation times are measured on Intel®Xeon®CPU E5-2630 v4 @ 2.20GHz processors.
5	The comparison durations, in nanoseconds, are estimated using std::chrono::high_resolution_clock which on the machine in (2) counts 1ns clock ticks. Precision is somewhat worse than that however. The ± value is the median absolute deviation times 1.48 for Normal consistency.

Table 14: Summary of algorithms and properties included in this report. The red superscripts give ranking for the quantity in that column.

	ALGORITHM	CONFIG	LIBRARY	TEMPLATE						COMPARISON[4]	
	NAME	DATA	DATA	MEMORY	SIZE	GENERATION TIME (ms)[4]				TIME (ns)[5]	
		(KB)[1]	(KB)[2]	(MB)[3]	(B)	MUGSHOT	480x720	960x1440	1600x2400	3000x4500	GENUINE	IMPOSTOR
221	id3-006	210116	7706	249 984	60 520 ± 0	300 683 ± 0	428 1088 ± 1	447 1192 ± 1	419 1209 ± 1	373 1270 ± 1	411 5547 ± 34	410 5563 ± 34
222	id3-008	242416	8151	270 1059	12 264 ± 0	362 819 ± 0	463 1209 ± 2	475 1297 ± 2	453 1329 ± 1	419 1433 ± 1	415 5658 ± 44	415 5624 ± 40
223	idemia-009	1066728	70572	478 2700	69 636 ± 0	497 1207 ± 1	467 1218 ± 1	457 1222 ± 2	421 1222 ± 3	375 1280 ± 10	416 5664 ± 84	413 5597 ± 90
224	idemia-010	996690	66244	452 2306	19 412 ± 0	242 596 ± 1	237 632 ± 22	207 624 ± 18	185 633 ± 7	190 719 ± 5	236 1699 ± 37	238 1703 ± 38
225	identy-000	271397	14217	105 474	160 2048 ± 0	308 689 ± 0	279 702 ± 0	257 712 ± 3	248 757 ± 0	282 970 ± 1	105 655 ± 25	103 637 ± 23
226	igearx-face-000	665623	298245	230 885	149 2048 ± 0	382 860 ± 1	333 855 ± 4	305 844 ± 0	296 881 ± 0	269 924 ± 3	227 1628 ± 45	231 1657 ± 41
227	iit-002	259579	52070	183 731	260 2048 ± 0	192 514 ± 1	173 531 ± 2	165 547 ± 1	158 583 ± 1	197 733 ± 2	155 1023 ± 7	155 1011 ± 66
228	iit-003	261288	53791	211 821	338 2048 ± 0	175 482 ± 0	154 493 ± 0	143 509 ± 0	138 541 ± 0	162 661 ± 0	35 324 ± 17	36 326 ± 8
229	imds-software-002	373632	352627	214 833	300 2048 ± 0	169 469 ± 1	376 954 ± 2	419 1094 ± 5	366 1064 ± 4	343 1153 ± 4	470 11100 ± 155	469 11090 ± 145
230	imds-software-003	373648	352628	194 769	270 2048 ± 0	95 317 ± 5	249 654 ± 4	281 793 ± 6	253 770 ± 4	245 848 ± 2	430 6624 ± 66	429 6603 ± 77
231	imperial-000	370120	10623	203 796	189 2048 ± 0	287 669 ± 1	261 675 ± 3	240 683 ± 17	209 676 ± 2	175 689 ± 2	280 2130 ± 32	277 2052 ± 100
232	imperial-002	472327	16134	405 1826	344 2048 ± 0	221 569 ± 1	206 581 ± 15	177 575 ± 5	155 576 ± 2	127 588 ± 3	294 2278 ± 90	281 2131 ± 44
233	incode-009	266103	21014	-	302 2048 ± 0	186 503 ± 0	153 490 ± 1	136 498 ± 0	124 505 ± 0	110 537 ± 0	169 1102 ± 28	172 1113 ± 29
234	incode-013	483720	41434	379 1647	259 2048 ± 0	202 535 ± 1	189 548 ± 1	168 555 ± 4	140 545 ± 1	140 618 ± 1	180 1152 ± 37	182 1154 ± 41
235	infocert-001	1204340	38972	358 1490	181 2048 ± 0	389 874 ± 1	347 891 ± 1	402 1050 ± 5	493 1473 ± 2	502 3174 ± 8	405 5055 ± 108	402 5008 ± 100
236	innefulabs-000	370588	162172	95 439	282 2048 ± 0	442 1006 ± 3	407 1025 ± 3	395 1030 ± 4	363 1041 ± 2	339 1135 ± 3	418 5782 ± 41	418 5741 ± 45
237	innominds-001	102207	777689	289 1124	121 2048 ± 0	102 333 ± 21	87 350 ± 19	66 335 ± 16	63 339 ± 17	48 346 ± 18	313 2482 ± 23	313 2491 ± 29
238	innovativetechnologyltd-001	177232	335757	73 341	138 2048 ± 0	151 433 ± 7	133 446 ± 8	106 439 ± 4	96 452 ± 4	88 485 ± 7	258 1877 ± 42	264 1924 ± 97
239	innovativetechnologyltd-002	173939	372324	236 912	373 2048 ± 0	281 661 ± 2	290 726 ± 4	366 981 ± 27	338 997 ± 40	213 766 ± 3	252 1841 ± 50	256 1857 ± 59
240	innovatrics-010	604731	111234	388 1715	538 4136 ± 0	250 611 ± 3	238 632 ± 2	261 723 ± 1	239 730 ± 1	214 768 ± 6	387 4077 ± 42	379 3857 ± 65
241	innovatrics-011	643997	50017	394 1745	543 4184 ± 0	333 754 ± 2	300 767 ± 3	277 765 ± 3	257 783 ± 4	250 867 ± 3	388 4135 ± 57	382 3937 ± 91
242	insightface-003	1016917	26668	367 1550	355 2048 ± 0	463 1073 ± 0	430 1092 ± 2	411 1070 ± 1	376 1082 ± 1	328 1101 ± 1	70 597 ± 16	75 595 ± 17
243	insightface-004	928816	26668	400 1800	286 2048 ± 0	523 1298 ± 1	501 1356 ± 2	479 1313 ± 1	446 1311 ± 0	400 1349 ± 1	62 565 ± 7	62 559 ± 5
244	inspur-001	364862	91934	215 833	124 2048 ± 0	542 1385 ± 1	503 1361 ± 4	506 1401 ± 2	501 1495 ± 1	472 1891 ± 1	414 5641 ± 42	414 5622 ± 40
245	inspur-002	447948	91934	255 1009	339 2048 ± 0	459 1056 ± 5	416 1056 ± 7	422 1096 ± 7	513 1776 ± 23	425 1444 ± 12	396 4504 ± 32	392 4515 ± 35
246	intellicloudai-001	220831	868246	159 655	308 2048 ± 0	168 468 ± 2	139 456 ± 1	121 466 ± 3	118 492 ± 1	146 632 ± 2	158 1056 ± 4	163 1051 ± 72
247	intellicloudai-002	259047	58559	515 3585	525 4100 ± 0	377 847 ± 1	328 847 ± 2	307 849 ± 1	284 853 ± 1	255 878 ± 4	136 822 ± 28	135 818 ± 23
248	intellifusion-001	271872	289387	192 762	276 2048 ± 0	335 764 ± 38	302 774 ± 39	285 797 ± 42	263 803 ± 34	225 805 ± 33	170 1112 ± 28	173 1128 ± 41
249	intellifusion-002	762731	385841	242 941	512 4096 ± 0	419 950 ± 2	433 1096 ± 42	415 1088 ± 33	404 1168 ± 31	348 1171 ± 10	237 1713 ± 57	232 1665 ± 87
250	intellivision-006	287736	262742	176 723	431 2056 ± 0	57 214 ± 0	46 214 ± 0	41 221 ± 0	45 272 ± 0	50 357 ± 1	492 15153 ± 32	492 15142 ± 38
251	intellivision-007	192454	262742	90 419	439 2056 ± 0	28 148 ± 0	23 157 ± 0	22 166 ± 0	20 180 ± 0	33 265 ± 0	489 15100 ± 50	488 15095 ± 45
252	intellivix-004	361668	128097	304 1189	127 2048 ± 0	148 427 ± 0	130 437 ± 0	110 444 ± 0	101 461 ± 0	122 565 ± 2	218 1498 ± 37	213 1478 ± 16
253	intellivix-005	774405	128093	519 3692	183 2048 ± 0	289 673 ± 1	245 643 ± 3	226 654 ± 3	204 666 ± 3	216 769 ± 5	215 1481 ± 65	211 1451 ± 26
254	intelresearch-008	523218	101214	307 1196	120 2048 ± 0	267 634 ± 1	233 630 ± 1	212 632 ± 1	186 635 ± 2	186 711 ± 4	374 3661 ± 34	373 3641 ± 44
255	intelresearch-009	290599	120716	366 1535	129 2048 ± 0	215 560 ± 1	252 664 ± 3	218 638 ± 3	211 678 ± 13	177 692 ± 4	380 3829 ± 207	376 3679 ± 71
256	intema-000	1532392	19488	280 1088	52 513 ± 0	445 1010 ± 0	398 1001 ± 4	378 994 ± 0	336 993 ± 5	313 1056 ± 1	144 910 ± 29	145 906 ± 32
257	intema-001	1122562	19536	356 1458	51 513 ± 0	530 1354 ± 1	494 1318 ± 5	486 1336 ± 4	452 1328 ± 2	404 1375 ± 0	150 977 ± 31	150 980 ± 31
258	intozi-001	21863	74210	31 140	345 2048 ± 0	14 85 ± 0	13 86 ± 0	13 86 ± 0	10 87 ± 0	8 87 ± 0	458 9579 ± 252	455 9530 ± 167
259	intsysmsu-001	384409	172480	200 789	243 2048 ± 0	255 614 ± 2	222 615 ± 2	223 642 ± 2	245 750 ± 3	346 1159 ± 4	90 621 ± 8	88 611 ± 31
260	intsysmsu-002	765921	172298	199 786	81 1024 ± 0	240 593 ± 1	310 793 ± 2	297 827 ± 1	292 875 ± 104	380 1293 ± 3	57 549 ± 25	60 548 ± 29
261	ionetworks-001	39860	333205	64 298	303 2048 ± 0	153 439 ± 2	127 433 ± 2	118 461 ± 2	97 454 ± 2	90 488 ± 2	427 6335 ± 103	426 6358 ± 91
262	ionetworks-002	337801	73038	395 1746	351 2048 ± 0	307 689 ± 1	257 672 ± 5	233 665 ± 3	205 669 ± 3	163 664 ± 6	433 6884 ± 154	432 6808 ± 102
263	iqface-000	268819	596337	169 704	547 4750 ± 32	206 538 ± 26	155 494 ± 2	162 543 ± 3	242 734 ± 4	409 1393 ± 4	569 636433 ± 38446	569 632654 ± 85615
264	iqface-003	370803	963398	212 821	548 4763 ± 37	196 529 ± 1	175 532 ± 2	190 599 ± 8	283 850 ± 2	461 1694 ± 2	568 575924 ± 2601	568 576653 ± 2051

Notes	
1	The configuration size does not capture static data included in libraries.
2	The library size is the combined total of all files provided in the submission lib folder. These libraries e.g. OpenCV may or may not be installed on any end user's platform natively and would not need to be installed with the algorithm. Some developers put neural network models in their libraries.
3	The memory usage is the peak resident set size reported by the ps system call during template generation.
4	The median template creation times are measured on Intel®Xeon®CPU E5-2630 v4 @ 2.20GHz processors.
5	The comparison durations, in nanoseconds, are estimated using std::chrono::high_resolution_clock which on the machine in (2) counts 1ns clock ticks. Precision is somewhat worse than that however. The ± value is the median absolute deviation times 1.48 for Normal consistency.

Table 15: Summary of algorithms and properties included in this report. The red superscripts give ranking for the quantity in that column.

	ALGORITHM	CONFIG	LIBRARY	TEMPLATE						COMPARISON[4]	
	NAME	DATA	DATA	MEMORY	SIZE	GENERATION TIME (ms)[4]				TIME (ns)[5]	
		(KB)[1]	(KB)[2]	(MB)[3]	(B)	MUGSHOT	480x720	960x1440	1600x2400	3000x4500	GENUINE	IMPOSTOR
265	irex-000	741899	47419	433 2090	471 3080 ± 0	380 852 ± 2	330 850 ± 1	319 874 ± 2	318 939 ± 1	364 1249 ± 5	21 201 ± 11	24 208 ± 8
266	isap-001	99049	204201	1 18	500 4096 ± 0	1 0 ± 0	-	-	-	-	46 459 ± 17	47 456 ± 11
267	isap-002	256765	49931	63 288	343 2048 ± 0	338 769 ± 3	409 1027 ± 2	322 877 ± 2	250 761 ± 1	265 912 ± 2	350 3045 ± 94	344 2973 ± 66
268	isityou-000	48010	36621	21 110	567 19200 ± 0	21 113 ± 5	-	-	-	-	565 237517 ± 1318	565 237374 ± 1279
269	isystems-001	274621	639268	283 1091	387 2048 ± 0	80 291 ± 9	-	-	-	-	59 557 ± 16	64 564 ± 22
270	isystems-002	358984	803389	373 1595	292 2048 ± 0	364 822 ± 8	-	-	-	-	125 749 ± 31	98 632 ± 28
271	itmo-007	415979	245376	447 2199	170 2048 ± 0	329 741 ± 2	-	-	-	-	317 2551 ± 50	316 2529 ± 80
272	itmo-008	726866	318238	341 1376	514 4096 ± 0	461 1060 ± 1	418 1058 ± 1	405 1059 ± 1	372 1072 ± 4	330 1104 ± 1	371 3578 ± 25	372 3580 ± 28
273	ivacognitive-001	256958	62791	246 975	184 2048 ± 0	522 1292 ± 3	484 1289 ± 4	471 1292 ± 4	442 1292 ± 3	390 1321 ± 4	389 4228 ± 41	387 4226 ± 41
274	iws-000	30875	3063	14 77	30 512 ± 0	72 277 ± 5	65 283 ± 1	135 494 ± 3	334 984 ± 3	498 2987 ± 39	152 999 ± 40	152 992 ± 22
275	jaakit-001	99024	24754	55 251	47 512 ± 0	13 76 ± 0	11 77 ± 0	10 79 ± 0	9 81 ± 0	10 93 ± 0	311 2466 ± 57	312 2465 ± 66
276	kakao-008	734583	104820	524 3879	197 2048 ± 0	478 1135 ± 3	448 1148 ± 3	437 1150 ± 3	399 1156 ± 1	350 1175 ± 1	124 736 ± 23	121 727 ± 22
277	kakao-009	766989	104820	528 4042	272 2048 ± 0	239 593 ± 1	215 603 ± 4	200 613 ± 2	176 617 ± 2	150 636 ± 4	45 457 ± 20	46 448 ± 17
278	kakaobank-001	780621	98829	446 2189	264 2048 ± 0	230 584 ± 0	217 608 ± 1	196 607 ± 5	213 684 ± 1	268 922 ± 2	526 27092 ± 174	525 27065 ± 158
279	kakaobank-002	780621	98833	464 2459	331 2048 ± 0	441 1004 ± 1	403 1010 ± 0	391 1025 ± 5	374 1078 ± 1	387 1313 ± 1	525 26972 ± 118	524 27022 ± 139
280	kakaopay-001	397864	179869	166 685	508 4096 ± 0	156 448 ± 0	181 542 ± 0	160 542 ± 0	139 542 ± 0	116 553 ± 0	97 633 ± 22	96 630 ± 22
281	kasikornlabs-002	256431	61063	148 613	291 2048 ± 0	404 917 ± 35	355 907 ± 13	359 963 ± 13	448 1320 ± 45	488 2629 ± 178	530 31025 ± 180	529 31054 ± 186
282	kasikornlabs-003	256442	61063	189 751	230 2048 ± 0	276 652 ± 5	250 656 ± 5	275 755 ± 11	349 1007 ± 27	480 2240 ± 168	519 24022 ± 121	516 23998 ± 97
283	kedacom-000	245292	37401	567 23574	17 292 ± 0	188 506 ± 3	188 547 ± 10	203 614 ± 9	162 588 ± 10	164 665 ± 24	109 684 ± 14	110 682 ± 16
284	kiwitech-000	369711	21375	217 841	354 2048 ± 0	237 591 ± 0	211 594 ± 0	189 595 ± 1	165 596 ± 0	136 609 ± 0	242 1755 ± 20	240 1734 ± 16
285	kneron-003	58366	1747	43 188	213 2048 ± 0	75 281 ± 3	64 280 ± 1	60 315 ± 13	70 365 ± 7	363 1224 ± 30	407 5237 ± 63	405 5274 ± 99
286	kneron-005	375374	13633	101 457	198 2048 ± 0	193 518 ± 2	171 522 ± 4	169 556 ± 5	249 757 ± 19	467 1760 ± 25	265 1922 ± 11	265 1926 ± 20
287	knowutech-000	808045	32886	330 1312	104 1536 ± 0	554 1419 ± 2	505 1372 ± 1	498 1377 ± 1	468 1382 ± 2	406 1386 ± 2	377 3743 ± 31	377 3693 ± 38
288	kogniza-001	0	394421	324 1288	105 1536 ± 0	519 1285 ± 2	490 1304 ± 4	469 1280 ± 2	437 1278 ± 2	392 1326 ± 2	343 2968 ± 37	343 2971 ± 20
289	kookmin-002	371771	30734	213 827	378 2048 ± 0	454 1038 ± 2	415 1047 ± 1	400 1045 ± 1	365 1061 ± 1	333 1116 ± 1	103 638 ± 19	101 636 ± 20
290	koreaid-001	256261	20152	403 1810	240 2048 ± 0	127 384 ± 2	105 390 ± 1	111 444 ± 2	144 556 ± 6	222 795 ± 5	101 636 ± 11	102 636 ± 10
291	krungthai-002	2360957	15033	302 1185	245 2048 ± 0	91 308 ± 0	76 314 ± 5	57 309 ± 0	57 319 ± 0	53 362 ± 0	347 3014 ± 20	345 2980 ± 22
292	kuke3d-001	403462	68786	125 530	494 4096 ± 0	359 814 ± 2	314 811 ± 2	292 814 ± 2	267 814 ± 1	240 834 ± 1	428 6412 ± 57	427 6413 ± 51
293	kuke3d-002	270544	1227855	210 820	123 2048 ± 0	187 504 ± 3	163 504 ± 1	144 511 ± 1	130 523 ± 2	126 585 ± 1	342 2943 ± 22	341 2966 ± 38
294	lebentech-000	0	10360	22 110	34 512 ± 0	3 22 ± 0	1 22 ± 0	1 22 ± 0	1 23 ± 0	1 23 ± 0	134 801 ± 42	136 825 ± 51
295	lebentech-001	0	144456	369 1567	353 2048 ± 0	35 174 ± 0	26 175 ± 0	34 200 ± 1	37 227 ± 9	64 397 ± 20	50 485 ± 17	51 473 ± 28
296	lemalabs-001	748400	198794	485 2745	157 2048 ± 0	356 810 ± 0	316 812 ± 0	290 813 ± 0	271 819 ± 0	244 844 ± 1	475 11930 ± 35	474 11913 ± 37
297	lineclova-002	475779	406756	334 1352	368 2048 ± 0	517 1284 ± 1	479 1275 ± 2	467 1275 ± 1	436 1273 ± 2	376 1281 ± 2	324 2765 ± 10	323 2767 ± 31
298	lineclova-003	585149	410482	390 1725	360 2048 ± 0	556 1444 ± 1	524 1438 ± 1	516 1439 ± 2	485 1440 ± 1	427 1446 ± 2	337 2890 ± 23	337 2899 ± 29
299	lookman-002	138200	25410	563 16518	65 548 ± 0	33 173 ± 1	-	-	-	-	83 610 ± 19	89 612 ± 22
300	lookman-004	244775	37401	566 23548	64 548 ± 0	189 507 ± 5	186 545 ± 12	202 613 ± 12	164 590 ± 11	160 656 ± 16	141 871 ± 29	141 878 ± 29
301	luxand-001	85194	72189	155 636	173 2048 ± 0	150 431 ± 0	132 443 ± 0	109 443 ± 2	95 448 ± 0	102 519 ± 0	207 1433 ± 16	209 1433 ± 16
302	luxand-003	127425	72189	221 847	111 2048 ± 0	318 706 ± 4	276 697 ± 1	252 698 ± 3	220 694 ± 0	219 782 ± 3	210 1443 ± 17	208 1431 ± 17
303	mantra-000	471458	62566	188 749	411 2052 ± 0	142 413 ± 18	152 487 ± 19	134 494 ± 18	126 511 ± 18	131 598 ± 19	353 3151 ± 51	352 3127 ± 63
304	maxvision-005	309326	61739	440 2138	309 2048 ± 0	444 1007 ± 1	473 1245 ± 5	389 1017 ± 1	362 1040 ± 4	383 1299 ± 3	268 1950 ± 38	268 1948 ± 34
305	maxvision-006	315987	61739	504 3172	263 2048 ± 0	511 1247 ± 3	462 1208 ± 3	455 1211 ± 5	420 1215 ± 1	372 1268 ± 4	267 1938 ± 17	266 1929 ± 35
306	megvii-008	1644071	44035	432 2086	399 2049 ± 0	528 1313 ± 1	516 1404 ± 4	494 1363 ± 2	461 1362 ± 3	414 1420 ± 2	509 20059 ± 1598	510 20448 ± 1633
307	megvii-009	1644071	44039	451 2294	400 2049 ± 0	530 1322 ± 1	499 1328 ± 1	488 1339 ± 3	521 2075 ± 3	411 1404 ± 4	510 20081 ± 1621	509 20260 ± 1577
308	meituan-003	860010	244091	487 2772	479 4096 ± 0	567 1487 ± 1	537 1518 ± 0	526 1469 ± 6	497 1478 ± 0	431 1471 ± 7	171 1112 ± 16	171 1097 ± 20

Notes	
1	The configuration size does not capture static data included in libraries.
2	The library size is the combined total of all files provided in the submission lib folder. These libraries e.g. OpenCV may or may not be installed on any end user's platform natively and would not need to be installed with the algorithm. Some developers put neural network models in their libraries.
3	The memory usage is the peak resident set size reported by the ps system call during template generation.
4	The median template creation times are measured on Intel®Xeon®CPU E5-2630 v4 @ 2.20GHz processors.
5	The comparison durations, in nanoseconds, are estimated using std::chrono::high_resolution_clock which on the machine in (2) counts 1ns clock ticks. Precision is somewhat worse than that however. The ± value is the median absolute deviation times 1.48 for Normal consistency.

Table 16: Summary of algorithms and properties included in this report. The red superscripts give ranking for the quantity in that column.

	ALGORITHM	CONFIG	LIBRARY	TEMPLATE						COMPARISON[4]	
	NAME	DATA	DATA	MEMORY	SIZE	GENERATION TIME (ms)[4]				TIME (ns)[5]	
		(KB)[1]	(KB)[2]	(MB)[3]	(B)	MUGSHOT	480x720	960x1440	1600x2400	3000x4500	GENUINE	IMPOSTOR
309	meituan-004	850507	244091	486 2759	476 4096 ± 0	349 796 ± 1	318 822 ± 0	295 820 ± 11	268 815 ± 11	232 824 ± 0	175 1149 ± 10	178 1148 ± 5
310	meiya-001	280055	264913	116 507	398 2049 ± 0	260 622 ± 12	-	-	-	-	447 8356 ± 615	446 8134 ± 97
311	mendaxiatech-000	1941475	45484	534 4397	524 4097 ± 0	508 1243 ± 2	475 1255 ± 1	496 1373 ± 2	507 1598 ± 3	490 2689 ± 8	546 46906 ± 275	545 46872 ± 217
312	metsakuurcompany-002	0	957558	247 980	433 2056 ± 0	430 980 ± 1	388 978 ± 1	363 976 ± 2	347 1005 ± 1	329 1103 ± 2	452 8766 ± 326	451 8786 ± 324
313	metsakuurcompany-003	0	957562	254 1004	438 2056 ± 0	421 965 ± 2	382 970 ± 5	406 1060 ± 12	346 1005 ± 6	336 1121 ± 1	446 8234 ± 145	445 8111 ± 280
314	miaxis-002	0	216484	70 328	48 512 ± 0	81 292 ± 0	67 290 ± 1	52 297 ± 0	50 298 ± 0	51 359 ± 1	161 1065 ± 48	161 1040 ± 54
315	miaxis-003	0	439726	143 604	342 2048 ± 0	266 634 ± 0	228 624 ± 2	201 613 ± 0	131 524 ± 0	165 665 ± 0	276 2053 ± 20	275 2048 ± 28
316	microfocus-002	96288	27362	42 176	6 256 ± 0	67 259 ± 18	-	-	-	-	36 337 ± 34	27 230 ± 25
317	microfocus-003	169603	27689	117 507	8 256 ± 0	181 490 ± 19	170 517 ± 30	272 752 ± 55	388 1126 ± 121	491 2713 ± 345	7 121 ± 5	7 117 ± 5
318	minivision-000	836697	16597	530 4263	511 4096 ± 0	453 1035 ± 1	413 1033 ± 2	397 1035 ± 1	359 1037 ± 1	317 1059 ± 2	312 2466 ± 26	310 2460 ± 25
319	mitek-000	105584	44643	60 277	92 1024 ± 0	66 256 ± 21	55 265 ± 10	78 375 ± 24	142 545 ± 42	327 1098 ± 124	331 2846 ± 88	324 2777 ± 74
320	mobai-000	365451	80573	198 786	554 6144 ± 0	336 766 ± 8	338 869 ± 6	453 1205 ± 31	517 1867 ± 45	506 3549 ± 190	498 16458 ± 333	497 16423 ± 1473
321	mobai-001	265297	60164	126 534	159 2048 ± 0	254 612 ± 3	221 614 ± 3	243 687 ± 9	301 886 ± 31	463 1707 ± 103	199 1386 ± 25	201 1377 ± 26
322	mobbl-001	231160	58706	52 226	205 2048 ± 0	41 183 ± 32	34 184 ± 25	72 354 ± 76	274 823 ± 396	494 2781 ± 1166	474 11832 ± 109	473 11851 ± 88
323	mobbl-003	172248	60960	61 282	215 2048 ± 0	285 664 ± 6	251 661 ± 5	231 663 ± 5	203 665 ± 6	176 691 ± 5	478 12506 ± 111	477 12509 ± 100
324	mobipintech-000	370514	303291	298 1173	383 2048 ± 0	509 1245 ± 1	471 1234 ± 1	465 1264 ± 1	459 1360 ± 1	464 1707 ± 1	484 14506 ± 214	483 14433 ± 197
325	momovn-001	246938	1013076	195 769	209 2048 ± 0	61 237 ± 1	59 268 ± 7	56 308 ± 10	48 293 ± 5	60 390 ± 3	209 1438 ± 13	210 1443 ± 13
326	moredian-000	525259	21374	264 1035	255 2048 ± 0	313 694 ± 0	277 698 ± 0	253 699 ± 0	224 700 ± 0	187 713 ± 1	249 1803 ± 11	247 1779 ± 23
327	mukh-003	556405	180996	408 1853	131 2048 ± 0	570 1896 ± 3	538 1948 ± 1	535 2003 ± 0	519 1981 ± 0	474 2016 ± 0	71 597 ± 13	85 604 ± 16
328	mukh-004	405118	181085	335 1353	141 2048 ± 0	213 558 ± 1	197 567 ± 1	173 569 ± 1	151 569 ± 3	128 593 ± 1	117 704 ± 1	116 703 ± 2
329	multimodality-000	0	503924	346 1417	132 2048 ± 0	144 416 ± 0	121 420 ± 0	99 423 ± 0	91 427 ± 0	80 463 ± 0	139 848 ± 25	133 800 ± 28
330	multimodality-001	185719	545045	342 1390	518 4096 ± 0	495 1190 ± 2	450 1169 ± 2	440 1165 ± 2	403 1167 ± 2	352 1177 ± 2	206 1424 ± 35	203 1384 ± 42
331	mvision-001	227502	149531	178 723	44 512 ± 0	310 691 ± 21	278 702 ± 19	250 697 ± 24	228 708 ± 29	183 710 ± 27	173 1123 ± 40	181 1154 ± 38
332	nazhiai-000	547484	16141	481 2716	307 2048 ± 0	299 683 ± 3	269 687 ± 2	302 835 ± 27	281 840 ± 31	241 834 ± 34	288 2230 ± 34	282 2133 ± 81
333	ncsgroup-000	95110	345861	266 1041	313 2048 ± 0	29 157 ± 0	21 153 ± 0	20 151 ± 0	17 157 ± 0	22 231 ± 0	305 2407 ± 16	305 2411 ± 22
334	ncssg-001	148743	490151	220 847	352 2048 ± 0	411 936 ± 2	375 946 ± 3	348 944 ± 2	317 938 ± 5	283 972 ± 2	372 3579 ± 50	366 3459 ± 34
335	neosystems-004	243546	352623	124 529	152 2048 ± 0	98 324 ± 0	284 711 ± 3	296 827 ± 7	285 854 ± 2	266 916 ± 2	482 14437 ± 176	482 14355 ± 173
336	netbridgetech-001	133108	205875	118 508	484 4096 ± 0	15 85 ± 1	12 83 ± 0	12 84 ± 0	11 92 ± 0	11 113 ± 4	454 9280 ± 74	454 9446 ± 512
337	netbridgetech-002	257687	49931	65 299	220 2048 ± 0	373 838 ± 6	325 838 ± 2	303 839 ± 1	280 839 ± 3	247 859 ± 3	338 2893 ± 65	348 3050 ± 123
338	neurotechnology-017	371650	98242	455 2385	7 256 ± 0	191 508 ± 2	168 513 ± 0	149 519 ± 1	132 533 ± 1	142 622 ± 15	1 80 ± 1	1 79 ± 1
339	neurotechnology-018	698669	98271	532 4367	54 515 ± 0	326 725 ± 1	296 747 ± 1	270 747 ± 4	252 769 ± 2	239 833 ± 22	2 85 ± 2	3 87 ± 7
340	nhn-004	931648	432753	493 2864	509 4096 ± 0	251 612 ± 0	236 632 ± 0	217 636 ± 0	208 676 ± 6	230 820 ± 0	500 17323 ± 99	499 17334 ± 133
341	nhn-005	1278729	432776	494 2890	522 4096 ± 0	357 811 ± 0	255 671 ± 13	225 652 ± 0	236 726 ± 12	257 890 ± 3	501 18123 ± 400	501 18214 ± 250
342	nodeflux-002	774668	690213	103 466	171 2048 ± 0	319 708 ± 4	283 709 ± 4	258 716 ± 5	235 716 ± 7	198 736 ± 3	366 3475 ± 62	364 3408 ± 143
343	nominder-002	249049	116931	407 1852	9 258 ± 0	137 405 ± 1	122 425 ± 2	100 424 ± 1	94 434 ± 0	96 505 ± 0	4 101 ± 11	4 102 ± 14
344	nominder-003	249964	116931	456 2417	10 258 ± 0	292 675 ± 2	268 683 ± 5	238 677 ± 2	225 701 ± 3	217 775 ± 3	3 87 ± 4	2 84 ± 4
345	notiontag-001	92753	427967	157 642	68 584 ± 0	409 929 ± 35	431 1092 ± 39	537 3709 ± 81	537 10233 ± 180	534 31181 ± 521	542 43636 ± 286	540 43724 ± 330
346	notiontag-002	271987	967207	497 2965	461 2120 ± 0	159 453 ± 2	137 453 ± 3	113 453 ± 3	99 458 ± 2	82 471 ± 3	511 20278 ± 194	508 20195 ± 186
347	nsensecorp-004	513276	139178	383 1675	278 2048 ± 0	555 1433 ± 0	525 1445 ± 7	522 1450 ± 3	500 1487 ± 5	-	304 2388 ± 42	304 2385 ± 63
348	nsensecorp-005	411845	138437	312 1240	365 2048 ± 0	559 1455 ± 0	528 1453 ± 0	521 1449 ± 0	488 1457 ± 2	438 1490 ± 4	281 2131 ± 51	284 2165 ± 66
349	ntechlab-011	786933	209458	554 6867	102 1280 ± 0	481 1148 ± 2	445 1142 ± 1	439 1159 ± 1	408 1185 ± 1	379 1290 ± 3	13 179 ± 11	15 173 ± 11
350	ntechlab-012	570796	212350	541 5450	466 2560 ± 0	527 1309 ± 1	497 1323 ± 1	484 1331 ± 1	460 1360 ± 1	428 1460 ± 3	24 211 ± 8	25 211 ± 7
351	omface-000	45945	844976	36 154	77 1024 ± 0	44 185 ± 1	43 206 ± 2	35 203 ± 1	24 195 ± 1	17 193 ± 1	49 481 ± 42	48 456 ± 20
352	omface-001	146370	1799745	34 145	86 1024 ± 0	47 194 ± 2	47 222 ± 2	38 209 ± 0	31 216 ± 1	23 233 ± 1	504 18369 ± 19	503 18366 ± 32

Notes	
1	The configuration size does not capture static data included in libraries.
2	The library size is the combined total of all files provided in the submission lib folder. These libraries e.g. OpenCV may or may not be installed on any end user's platform natively and would not need to be installed with the algorithm. Some developers put neural network models in their libraries.
3	The memory usage is the peak resident set size reported by the ps system call during template generation.
4	The median template creation times are measured on Intel®Xeon®CPU E5-2630 v4 @ 2.20GHz processors.
5	The comparison durations, in nanoseconds, are estimated using std::chrono::high_resolution_clock which on the machine in (2) counts 1ns clock ticks. Precision is somewhat worse than that however. The ± value is the median absolute deviation times 1.48 for Normal consistency.

Table 17: Summary of algorithms and properties included in this report. The red superscripts give ranking for the quantity in that column.

	ALGORITHM	CONFIG	LIBRARY	TEMPLATE						COMPARISON[4]	
	NAME	DATA	DATA	MEMORY	SIZE	GENERATION TIME (ms)[4]				TIME (ns)[5]	
		(KB)[1]	(KB)[2]	(MB)[3]	(B)	MUGSHOT	480x720	960x1440	1600x2400	3000x4500	GENUINE	IMPOSTOR
353	omnigarde-002	368860	32882	191 760	78 1024 ± 0	525 1303 ± 1	474 1246 ± 1	462 1249 ± 1	431 1253 ± 1	369 1261 ± 1	323 2727 ± 34	321 2686 ± 32
354	omnigarde-003	427751	35153	190 756	56 517 ± 0	288 673 ± 0	234 631 ± 1	214 633 ± 1	188 637 ± 1	156 647 ± 1	187 1259 ± 22	187 1244 ± 16
355	onfido-000	273478	959781	237 914	275 2048 ± 0	160 459 ± 17	135 451 ± 15	112 451 ± 14	103 462 ± 15	98 505 ± 18	226 1617 ± 50	227 1637 ± 53
356	openedge-000	447048	272235	340 1376	447 2056 ± 0	115 367 ± 0	113 404 ± 1	69 352 ± 1	64 350 ± 0	59 385 ± 0	490 15122 ± 41	489 15110 ± 48
357	openface-001	0	40111	20 100	315 2048 ± 0	27 148 ± 1	22 154 ± 0	74 365 ± 3	87 409 ± 9	138 616 ± 31	80 608 ± 14	84 604 ± 13
358	ovisionllc-001	192059	252531	273 1066	90 1024 ± 0	36 175 ± 0	27 175 ± 0	26 183 ± 0	27 196 ± 0	27 241 ± 0	336 2889 ± 38	339 2901 ± 47
359	oz-003	484147	519652	562 11575	423 2053 ± 0	538 1375 ± 12	507 1388 ± 3	534 1773 ± 16	520 2039 ± 6	503 3209 ± 5	562 73905 ± 456	561 73892 ± 444
360	oz-004	373982	1075452	558 7845	422 2053 ± 0	371 832 ± 7	340 871 ± 6	327 899 ± 10	375 1078 ± 12	455 1608 ± 10	555 61654 ± 418	553 61749 ± 450
361	palit-000	428754	144958	338 1360	516 4096 ± 0	223 570 ± 1	203 578 ± 1	179 576 ± 3	159 583 ± 1	137 614 ± 1	287 2227 ± 16	289 2226 ± 16
362	palit-001	173886	145564	139 587	316 2048 ± 0	58 227 ± 0	49 224 ± 1	42 224 ± 1	39 229 ± 3	32 262 ± 2	176 1150 ± 16	174 1135 ± 23
363	pangiam-001	1015455	37259	370 1569	319 2048 ± 0	425 972 ± 1	390 982 ± 3	365 981 ± 2	335 990 ± 7	309 1052 ± 2	8 136 ± 11	8 139 ± 13
364	pangiam-002	486035	39834	308 1205	337 2048 ± 0	94 316 ± 0	78 316 ± 0	61 317 ± 0	56 319 ± 1	41 326 ± 2	6 111 ± 13	5 103 ± 2
365	papago-001	669274	52817	453 2341	379 2048 ± 0	515 1272 ± 6	485 1296 ± 7	474 1295 ± 6	439 1281 ± 3	397 1345 ± 3	495 15236 ± 169	493 15184 ± 142
366	papil11-000	1146378	24895	445 2184	359 2048 ± 0	412 942 ± 3	437 1108 ± 2	452 1204 ± 6	465 1369 ± 10	475 2033 ± 35	85 612 ± 7	90 613 ± 11
367	papsav1923-002	491185	24727	292 1139	421 2052 ± 0	347 792 ± 1	387 978 ± 1	398 1042 ± 1	400 1158 ± 1	458 1641 ± 19	183 1209 ± 29	185 1206 ± 38
368	papsav1923-003	515576	24803	286 1113	321 2048 ± 0	351 797 ± 0	392 987 ± 1	399 1043 ± 1	406 1178 ± 1	470 1809 ± 7	142 903 ± 26	144 905 ± 34
369	paravision-011	781138	95589	458 2424	527 4100 ± 0	381 852 ± 0	339 871 ± 1	312 858 ± 1	286 854 ± 0	253 873 ± 1	225 1608 ± 35	225 1625 ± 32
370	paravision-013	1537125	95602	537 4648	531 4100 ± 0	434 991 ± 9	395 993 ± 5	374 992 ± 4	345 1002 ± 5	293 1002 ± 7	214 1481 ± 26	217 1490 ± 25
371	pensees-001	1619431	408932	415 1922	564 8200 ± 0	473 1108 ± 3	526 1448 ± 17	517 1439 ± 10	491 1464 ± 5	449 1546 ± 9	354 3151 ± 34	353 3143 ± 25
372	pixelall-009	0	1009114	391 1732	561 8192 ± 0	566 1484 ± 3	511 1395 ± 3	505 1400 ± 4	471 1391 ± 3	418 1433 ± 3	254 1848 ± 13	254 1842 ± 19
373	pixelall-010	0	1469903	477 2693	563 8192 ± 0	482 1153 ± 3	427 1084 ± 4	425 1103 ± 4	378 1093 ± 3	335 1118 ± 4	262 1906 ± 13	261 1898 ± 29
374	privid-001	0	76008	33 143	568 30720 ± 0	157 450 ± 0	138 454 ± 0	122 467 ± 1	110 472 ± 1	95 504 ± 1	499 17041 ± 74	498 17053 ± 100
375	privid-002	0	219733	261 1031	214 2048 ± 0	512 1261 ± 3	449 1156 ± 4	438 1155 ± 2	401 1162 ± 3	385 1302 ± 4	112 686 ± 22	109 680 ± 20
376	psl-011	814579	606050	538 4959	565 8248 ± 0	531 1324 ± 2	495 1323 ± 8	482 1326 ± 8	450 1324 ± 8	391 1322 ± 4	234 1680 ± 37	235 1688 ± 40
377	psl-012	1318147	622004	536 4535	539 4144 ± 0	475 1111 ± 2	441 1122 ± 2	426 1104 ± 2	384 1119 ± 1	334 1117 ± 1	66 583 ± 17	69 589 ± 17
378	ptakuratsatu-000	0	585434	333 1347	61 538 ± 0	390 875 ± 3	336 863 ± 48	342 928 ± 9	325 958 ± 17	321 1066 ± 26	422 5900 ± 103	416 5687 ± 167
379	pxl-001	110116	78231	38 168	41 512 ± 0	19 101 ± 5	16 104 ± 5	30 189 ± 12	86 408 ± 27	430 1470 ± 144	413 5598 ± 45	412 5590 ± 68
380	pyramid-000	372608	219883	204 804	429 2056 ± 0	228 583 ± 2	-	-	-	-	436 7147 ± 59	439 7586 ± 425
381	qazbs-000	362015	805258	262 1034	388 2048 ± 0	526 1307 ± 1	472 1243 ± 0	461 1248 ± 9	430 1253 ± 1	374 1270 ± 0	406 5181 ± 62	404 5167 ± 93
382	qazsmartvisionai-000	560570	99515	454 2371	35 512 ± 0	314 694 ± 1	282 708 ± 7	259 717 ± 5	231 711 ± 5	194 723 ± 7	133 795 ± 29	130 781 ± 34
383	qluevision-001	173605	205230	80 376	562 8192 ± 0	59 229 ± 1	50 230 ± 1	46 231 ± 1	40 233 ± 1	26 239 ± 1	362 3374 ± 38	362 3365 ± 41
384	qnap-004	371274	61422	253 1002	179 2048 ± 0	113 365 ± 0	93 365 ± 1	75 367 ± 0	71 368 ± 0	56 375 ± 3	107 681 ± 7	111 682 ± 13
385	qnap-005	977818	61429	491 2828	285 2048 ± 0	424 969 ± 5	394 988 ± 8	375 992 ± 6	342 1000 ± 7	297 1008 ± 6	98 633 ± 1	97 632 ± 13
386	quantasoft-003	370518	211354	271 1063	283 2048 ± 0	265 632 ± 2	242 634 ± 0	211 632 ± 0	183 631 ± 1	148 634 ± 0	20 201 ± 7	21 203 ± 8
387	rankone-015	0	289078	46 190	11 261 ± 0	209 547 ± 5	183 543 ± 6	181 578 ± 2	182 629 ± 7	259 894 ± 9	22 201 ± 19	14 172 ± 16
388	realnetworks-007	570797	101527	503 3145	430 2056 ± 0	534 1348 ± 2	502 1358 ± 11	493 1363 ± 10	469 1386 ± 9	444 1517 ± 6	60 559 ± 31	58 539 ± 35
389	realnetworks-008	73346	75421	85 402	437 2056 ± 0	85 296 ± 3	71 294 ± 3	71 353 ± 4	67 361 ± 5	89 485 ± 5	55 539 ± 31	59 543 ± 29
390	rebs-000	1375350	62664	496 2934	492 4096 ± 0	261 623 ± 0	241 633 ± 10	210 626 ± 10	175 616 ± 1	139 617 ± 0	177 1150 ± 1	179 1150 ± 2
391	rebs-001	2038561	62673	471 2582	532 4100 ± 0	353 802 ± 1	315 812 ± 8	299 829 ± 1	264 807 ± 2	227 811 ± 4	178 1151 ± 8	177 1145 ± 4
392	recognito-000	549308	247223	546 5903	468 2564 ± 0	465 1086 ± 2	435 1096 ± 1	424 1102 ± 2	396 1142 ± 3	360 1219 ± 7	16 193 ± 8	19 190 ± 16
393	recognito-001	517547	62334	521 3833	467 2564 ± 0	462 1072 ± 1	429 1089 ± 1	421 1095 ± 4	382 1112 ± 2	355 1205 ± 4	14 183 ± 10	16 183 ± 7
394	regula-000	262444	29384	147 610	188 2048 ± 0	493 1187 ± 1	442 1126 ± 1	429 1129 ± 0	392 1132 ± 1	347 1159 ± 1	53 491 ± 16	54 500 ± 22
395	regula-001	256075	25980	250 987	139 2048 ± 0	518 1284 ± 1	468 1220 ± 1	456 1222 ± 1	423 1226 ± 1	368 1255 ± 1	39 361 ± 10	37 342 ± 25
396	remarkai-001	241857	868314	181 730	407 2052 ± 0	369 831 ± 6	329 849 ± 18	403 1055 ± 25	414 1198 ± 34	445 1519 ± 38	185 1229 ± 20	134 805 ± 56

Notes	
1	The configuration size does not capture static data included in libraries.
2	The library size is the combined total of all files provided in the submission lib folder. These libraries e.g. OpenCV may or may not be installed on any end user's platform natively and would not need to be installed with the algorithm. Some developers put neural network models in their libraries.
3	The memory usage is the peak resident set size reported by the ps system call during template generation.
4	The median template creation times are measured on Intel®Xeon®CPU E5-2630 v4 @ 2.20GHz processors.
5	The comparison durations, in nanoseconds, are estimated using std::chrono::high_resolution_clock which on the machine in (2) counts 1ns clock ticks. Precision is somewhat worse than that however. The ± value is the median absolute deviation times 1.48 for Normal consistency.

Table 18: Summary of algorithms and properties included in this report. The red superscripts give ranking for the quantity in that column.

	ALGORITHM	CONFIG	LIBRARY	TEMPLATE							COMPARISON[4]	
	NAME	DATA	DATA	MEMORY	SIZE	GENERATION TIME (ms)[4]					TIME (ns)[5]	
		(KB)[1]	(KB)[2]	(MB)[3]	(B)	MUGSHOT	480x720	960x1440	1600x2400	3000x4500	GENUINE	IMPOSTOR
397	remarkai-003	280516	58559	525 3909	526 4100 ± 0	432 986 ± 1	396 993 ± 1	376 992 ± 1	341 999 ± 3	299 1019 ± 2	132 787 ± 20	131 793 ± 22
398	rendip-000	0	437653	185 735	126 2048 ± 0	164 464 ± 2	140 458 ± 0	126 473 ± 0	113 483 ± 1	119 556 ± 4	64 576 ± 13	66 573 ± 11
399	revealmedia-005	293933	202465	193 767	528 4100 ± 0	149 428 ± 0	124 428 ± 0	103 430 ± 0	93 433 ± 0	75 442 ± 0	273 2023 ± 38	272 2009 ± 26
400	revealmedia-006	293933	200912	187 745	412 2052 ± 0	123 381 ± 0	99 381 ± 0	81 382 ± 0	73 384 ± 0	62 394 ± 0	94 626 ± 35	80 600 ± 2
401	roc-016	0	674869	47 191	18 392 ± 0	218 562 ± 1	184 543 ± 2	167 553 ± 2	148 564 ± 2	143 626 ± 2	17 194 ± 8	12 161 ± 26
402	rokid-000	258612	396624	310 1218	435 2056 ± 0	208 546 ± 3	182 542 ± 2	164 545 ± 1	129 522 ± 3	121 563 ± 4	365 3457 ± 62	367 3463 ± 77
403	rokid-001	641223	413733	274 1071	451 2060 ± 0	399 911 ± 2	352 901 ± 5	326 899 ± 2	305 900 ± 3	261 901 ± 3	359 3345 ± 50	360 3346 ± 149
404	s1-005	482369	95685	294 1146	228 2048 ± 0	438 1001 ± 0	400 1002 ± 0	385 1004 ± 0	350 1008 ± 0	302 1029 ± 2	95 626 ± 74	70 589 ± 14
405	s1-007	482385	59657	293 1144	377 2048 ± 0	433 988 ± 1	379 965 ± 0	360 966 ± 0	329 972 ± 0	290 991 ± 0	104 648 ± 26	107 658 ± 25
406	saffe-001	85973	62488	39 168	101 1280 ± 0	74 281 ± 1	-	-	-	-	188 1274 ± 19	191 1277 ± 26
407	saffe-002	260622	28285	223 855	217 2048 ± 0	361 817 ± 11	313 805 ± 15	289 809 ± 19	269 815 ± 29	228 813 ± 23	120 717 ± 7	120 714 ± 29
408	samsungsds-001	1189592	147444	527 3922	480 4096 ± 0	480 1140 ± 3	447 1145 ± 4	489 1344 ± 5	463 1366 ± 5	442 1514 ± 7	551 51559 ± 773	549 51721 ± 1003
409	samsungsds-002	1040732	147475	507 3321	445 2056 ± 0	476 1118 ± 1	452 1175 ± 12	495 1372 ± 6	451 1324 ± 2	437 1489 ± 4	535 35803 ± 266	535 36181 ± 674
410	samtech-001	288082	219883	144 605	442 2056 ± 0	82 294 ± 3	-	-	-	-	442 7694 ± 59	441 7678 ± 91
411	samtech-002	192220	474779	174 714	426 2056 ± 0	56 212 ± 0	45 212 ± 0	40 215 ± 0	36 225 ± 0	36 285 ± 1	494 15231 ± 50	494 15215 ± 59
412	scanovate-002	256986	457227	222 850	310 2048 ± 0	315 696 ± 32	285 713 ± 33	267 738 ± 28	255 779 ± 32	349 1172 ± 53	348 3021 ± 38	351 3120 ± 163
413	scanovate-003	135585	89469	205 805	370 2048 ± 0	231 585 ± 1	220 613 ± 12	185 591 ± 1	170 610 ± 2	170 684 ± 1	341 2926 ± 22	340 2925 ± 20
414	sdc-000	256814	481583	197 784	271 2048 ± 0	400 913 ± 14	354 906 ± 9	434 1142 ± 19	512 1774 ± 45	511 4719 ± 222	532 32645 ± 93	532 32653 ± 112
415	seamfix-001	429267	86391	69 320	118 2048 ± 0	323 718 ± 8	281 707 ± 25	350 947 ± 18	502 1521 ± 55	507 4179 ± 226	421 5897 ± 118	421 5867 ± 123
416	securifai-007	94589	88169	137 583	231 2048 ± 0	185 500 ± 0	166 506 ± 0	137 499 ± 1	122 501 ± 1	97 505 ± 1	216 1484 ± 11	215 1483 ± 13
417	securifai-008	111759	84658	172 711	385 2048 ± 0	271 641 ± 4	246 647 ± 3	230 663 ± 3	193 645 ± 3	159 649 ± 1	217 1498 ± 11	216 1487 ± 13
418	sensetime-007	765353	37533	547 5950	93 1028 ± 0	543 1386 ± 41	496 1323 ± 2	491 1347 ± 2	464 1366 ± 2	454 1593 ± 8	211 1460 ± 29	207 1425 ± 26
419	sensetime-008	1176483	60067	545 5882	94 1028 ± 0	565 1479 ± 31	523 1436 ± 4	527 1482 ± 4	503 1525 ± 5	459 1669 ± 2	190 1283 ± 51	186 1240 ± 47
420	serendipity-000	0	346443	102 462	136 2048 ± 0	397 900 ± 8	351 901 ± 3	339 922 ± 2	316 936 ± 1	288 987 ± 2	79 602 ± 1	86 607 ± 10
421	sertis-002	460790	68929	161 660	235 2048 ± 0	491 1181 ± 1	453 1178 ± 0	446 1183 ± 0	411 1187 ± 0	361 1221 ± 0	166 1086 ± 32	164 1076 ± 31
422	sertis-003	0	451507	420 1965	327 2048 ± 0	154 441 ± 0	129 436 ± 2	119 461 ± 2	104 463 ± 1	85 473 ± 4	145 915 ± 10	146 917 ± 8
423	seventhsense-003	603091	453847	282 1090	417 2052 ± 0	440 1003 ± 2	386 977 ± 0	298 828 ± 1	270 817 ± 1	233 826 ± 2	221 1523 ± 25	221 1530 ± 22
424	seventhsense-005	4000865	453775	470 2581	533 4100 ± 0	477 1119 ± 1	440 1120 ± 1	431 1134 ± 4	391 1131 ± 2	341 1144 ± 1	326 2787 ± 28	325 2777 ± 22
425	shaman-000	0	120033	115 507	507 4096 ± 0	277 653 ± 16	-	-	-	-	42 380 ± 25	41 379 ± 31
426	shaman-001	0	174446	120 511	502 4096 ± 0	83 294 ± 2	-	-	-	-	100 635 ± 19	44 441 ± 25
427	shu-002	731250	148309	232 890	489 4096 ± 0	332 751 ± 2	301 769 ± 4	340 922 ± 4	483 1431 ± 9	505 3489 ± 47	570 2930763 ± 47355	570 2929759 ± 39149
428	shu-003	428774	146940	119 511	178 2048 ± 0	363 820 ± 6	322 828 ± 3	346 941 ± 9	445 1308 ± 15	499 3045 ± 44	314 2506 ± 26	315 2512 ± 38
429	siat-002	486842	7738	459 2434	409 2052 ± 0	226 579 ± 0	-	-	-	-	129 769 ± 13	125 750 ± 13
430	siat-005	380936	16935	327 1299	279 2048 ± 0	136 403 ± 0	111 400 ± 0	88 401 ± 0	84 403 ± 1	69 422 ± 7	65 577 ± 13	67 580 ± 17
431	sjtu-004	1953267	241108	483 2741	545 4608 ± 0	504 1236 ± 2	464 1209 ± 2	473 1294 ± 4	506 1554 ± 5	493 2738 ± 8	351 3057 ± 14	350 3070 ± 20
432	sjtu-005	1953267	241151	482 2734	546 4608 ± 0	244 601 ± 1	224 617 ± 1	262 724 ± 2	389 1127 ± 3	496 2855 ± 11	339 2898 ± 4	338 2900 ± 4
433	sktelecom-000	527132	298496	331 1321	106 1536 ± 0	474 1110 ± 1	439 1113 ± 1	428 1114 ± 1	385 1120 ± 1	345 1155 ± 1	524 26583 ± 128	520 26508 ± 126
434	smartbiometrik-001	30875	92620	11 72	37 512 ± 0	258 620 ± 7	231 625 ± 7	221 640 ± 4	238 728 ± 6	308 1047 ± 8	115 703 ± 31	117 710 ± 40
435	smartengines-000	1711	3025	8 50	15 288 ± 0	32 168 ± 7	30 180 ± 1	29 188 ± 3	33 217 ± 3	35 275 ± 1	18 197 ± 5	13 167 ± 11
436	smartengines-001	7095	4601	7 47	16 288 ± 0	100 333 ± 89	115 408 ± 1	97 423 ± 1	100 460 ± 2	117 553 ± 5	10 153 ± 11	9 143 ± 13
437	smartvist-000	5959	134084	40 169	46 512 ± 0	11 59 ± 0	9 56 ± 0	7 56 ± 0	6 58 ± 0	9 90 ± 1	208 1435 ± 31	206 1422 ± 48
438	smartvist-001	349219	25644	234 904	374 2048 ± 0	117 370 ± 0	97 374 ± 0	79 377 ± 1	89 422 ± 0	77 445 ± 0	328 2835 ± 99	331 2836 ± 80
439	smilart-002	111826	87805	59 263	83 1024 ± 0	37 176 ± 16	-	-	-	-	505 18784 ± 136	505 18795 ± 151
440	smilart-003	67339	91670	48 192	22 512 ± 0	39 180 ± 12	32 181 ± 10	58 313 ± 22	201 665 ± 49	481 2299 ± 196	200 1395 ± 74	156 1027 ± 66

Notes	
1	The configuration size does not capture static data included in libraries.
2	The library size is the combined total of all files provided in the submission lib folder. These libraries e.g. OpenCV may or may not be installed on any end user's platform natively and would not need to be installed with the algorithm. Some developers put neural network models in their libraries.
3	The memory usage is the peak resident set size reported by the ps system call during template generation.
4	The median template creation times are measured on Intel®Xeon®CPU E5-2630 v4 @ 2.20GHz processors.
5	The comparison durations, in nanoseconds, are estimated using std::chrono::high_resolution_clock which on the machine in (2) counts 1ns clock ticks. Precision is somewhat worse than that however. The ± value is the median absolute deviation times 1.48 for Normal consistency.

Table 19: Summary of algorithms and properties included in this report. The red superscripts give ranking for the quantity in that column.

	ALGORITHM	CONFIG	LIBRARY	TEMPLATE						COMPARISON[4]	
	NAME	DATA	DATA	MEMORY	SIZE	GENERATION TIME (ms)[4]				TIME (ns)[5]	
		(KB)[1]	(KB)[2]	(MB)[3]	(B)	MUGSHOT	480x720	960x1440	1600x2400	3000x4500	GENUINE	IMPOSTOR
441	sodec-000	836592	13142	495 2902	517 4096 ± 0	456 1041 ± 2	412 1032 ± 1	396 1035 ± 1	360 1037 ± 2	318 1061 ± 2	247 1794 ± 37	245 1775 ± 23
442	sparsh-001	0	366290	535 4525	237 2048 ± 0	297 680 ± 2	247 648 ± 1	219 638 ± 0	191 642 ± 0	189 717 ± 0	459 9600 ± 275	456 9601 ± 290
443	sqisoft-002	278039	386291	163 675	425 2056 ± 0	166 466 ± 8	143 466 ± 2	124 468 ± 11	102 461 ± 6	84 472 ± 4	127 758 ± 11	126 760 ± 23
444	sqisoft-003	362737	607964	207 812	434 2056 ± 0	270 638 ± 2	259 674 ± 7	260 718 ± 17	202 665 ± 6	191 720 ± 6	138 844 ± 11	138 844 ± 23
445	staqu-000	879661	624676	272 1064	481 4096 ± 0	358 813 ± 25	-	-	-	-	344 2979 ± 31	347 3007 ± 75
446	starhybrid-001	100509	289356	219 845	348 2048 ± 0	110 358 ± 82	88 355 ± 49	80 379 ± 58	81 401 ± 79	61 393 ± 67	164 1075 ± 51	165 1078 ± 53
447	stcon-002	1255490	62667	434 2095	505 4096 ± 0	227 583 ± 0	199 570 ± 2	176 574 ± 2	157 582 ± 1	144 630 ± 0	174 1143 ± 2	175 1142 ± 4
448	stcon-003	2119710	62673	522 3862	529 4100 ± 0	367 823 ± 0	317 821 ± 1	300 831 ± 3	273 823 ± 1	242 838 ± 2	179 1151 ± 5	183 1157 ± 5
449	stengg-000	361104	34674	179 724	299 2048 ± 0	355 809 ± 1	362 921 ± 2	382 1002 ± 1	260 794 ± 1	477 2130 ± 5	271 2005 ± 22	273 2011 ± 34
450	sukshi-000	94035	688738	81 382	569 32768 ± 0	138 407 ± 11	116 413 ± 8	141 504 ± 8	216 689 ± 11	453 1574 ± 28	461 9817 ± 50	459 9787 ± 62
451	suprema-004	1430475	116085	501 3096	513 4096 ± 0	564 1478 ± 2	531 1472 ± 2	525 1469 ± 1	495 1476 ± 1	440 1496 ± 1	356 3201 ± 14	356 3202 ± 22
452	suprema-005	1430177	116089	500 3093	521 4096 ± 0	348 794 ± 1	337 863 ± 1	288 808 ± 5	297 883 ± 1	235 830 ± 5	384 3950 ± 7	383 3948 ± 4
453	supremaid-001	258193	23479	128 541	268 2048 ± 0	173 479 ± 1	149 481 ± 0	128 481 ± 0	115 490 ± 0	105 522 ± 0	116 704 ± 19	106 652 ± 19
454	supremaid-002	256273	23899	72 334	361 2048 ± 0	176 483 ± 0	162 501 ± 0	133 488 ± 0	123 503 ± 0	123 565 ± 0	270 1990 ± 19	263 1923 ± 29
455	surrey-cvssp-002	903493	87776	389 1720	164 2048 ± 0	498 1213 ± 1	465 1211 ± 1	468 1279 ± 0	440 1282 ± 0	384 1300 ± 0	462 9906 ± 120	460 9911 ± 167
456	surrey-cvssp-003	1013099	109557	448 2208	369 2048 ± 0	344 789 ± 1	327 846 ± 1	311 854 ± 1	426 1234 ± 2	504 3283 ± 3	439 7358 ± 130	437 7336 ± 93
457	swsam-001	265887	95072	156 642	193 2048 ± 0	460 1058 ± 34	425 1079 ± 31	416 1091 ± 35	373 1076 ± 9	331 1109 ± 45	340 2902 ± 31	336 2892 ± 32
458	synesis-006	731941	21817	357 1472	535 4104 ± 0	210 549 ± 1	187 546 ± 1	166 552 ± 1	146 558 ± 2	151 639 ± 28	114 697 ± 32	115 688 ± 31
459	synesis-007	1442961	24145	462 2443	472 3080 ± 0	499 1215 ± 5	476 1268 ± 30	477 1306 ± 67	447 1311 ± 58	415 1423 ± 52	108 684 ± 32	113 686 ± 25
460	synology-000	221021	25809	99 453	144 2048 ± 0	139 407 ± 14	117 415 ± 14	249 694 ± 31	472 1396 ± 58	508 4568 ± 211	508 19720 ± 203	506 19767 ± 379
461	synology-002	256713	25943	110 488	219 2048 ± 0	395 886 ± 4	348 892 ± 3	337 920 ± 2	343 1000 ± 5	388 1317 ± 12	212 1466 ± 32	218 1496 ± 45
462	sztu-000	338637	15871	326 1298	290 2048 ± 0	200 531 ± 0	174 532 ± 0	154 533 ± 0	135 537 ± 0	114 548 ± 0	68 585 ± 11	74 592 ± 13
463	sztu-001	338650	15871	328 1299	224 2048 ± 0	203 535 ± 0	178 537 ± 0	158 538 ± 0	137 540 ± 0	115 553 ± 0	74 599 ± 10	78 598 ± 10
464	t4isb-000	234227	115237	75 345	146 2048 ± 0	443 1006 ± 5	399 1001 ± 1	387 1006 ± 1	352 1009 ± 1	301 1022 ± 2	373 3586 ± 34	370 3534 ± 34
465	tech5-007	0	340324	474 2647	45 512 ± 0	537 1360 ± 0	504 1366 ± 0	497 1376 ± 0	466 1373 ± 0	422 1438 ± 6	54 538 ± 19	55 516 ± 22
466	tech5-008	0	365877	543 5567	390 2048 ± 0	280 655 ± 3	229 624 ± 11	208 625 ± 11	184 631 ± 11	184 710 ± 12	440 7371 ± 81	438 7367 ± 99
467	techainer-001	198738	703687	423 1977	362 2048 ± 0	125 381 ± 9	106 391 ± 5	89 402 ± 5	78 391 ± 1	79 461 ± 5	468 10726 ± 189	467 10714 ± 243
468	techsign-000	0	1101622	422 1969	280 2048 ± 0	114 366 ± 1	109 398 ± 1	441 1172 ± 3	532 3065 ± 18	530 10460 ± 65	399 4758 ± 112	396 4789 ± 93
469	techsign-001	0	586983	411 1881	312 2048 ± 0	339 772 ± 35	308 788 ± 23	287 802 ± 42	321 949 ± 10	412 1409 ± 26	69 592 ± 11	73 592 ± 13
470	tevian-007	779934	19523	387 1712	95 1032 ± 0	229 583 ± 1	204 579 ± 0	183 580 ± 0	161 588 ± 1	149 636 ± 0	403 4894 ± 65	399 4841 ± 83
471	tevian-008	847177	19519	516 3610	96 1032 ± 0	393 884 ± 2	353 903 ± 1	329 903 ± 1	307 911 ± 1	273 946 ± 1	400 4828 ± 40	398 4811 ± 41
472	tiger-005	342866	253734	364 1532	408 2052 ± 0	467 1097 ± 2	423 1065 ± 2	409 1066 ± 2	368 1067 ± 3	324 1088 ± 3	88 620 ± 19	93 615 ± 16
473	tiger-006	421186	394688	173 714	413 2052 ± 0	545 1392 ± 16	518 1411 ± 10	519 1444 ± 10	505 1531 ± 11	471 1848 ± 10	250 1810 ± 20	249 1801 ± 13
474	tinkoff-001	274660	389272	150 616	293 2048 ± 0	486 1176 ± 3	454 1179 ± 3	443 1178 ± 3	405 1169 ± 2	353 1203 ± 3	393 4361 ± 74	390 4364 ± 75
475	tnitech-000	234032	13976	542 5471	216 2048 ± 0	143 415 ± 1	123 427 ± 1	96 419 ± 4	92 427 ± 3	71 436 ± 2	307 2438 ± 14	306 2436 ± 19
476	tongyi-005	1140701	138919	437 2121	460 2089 ± 0	31 165 ± 1	-	-	-	-	506 18924 ± 65	507 20158 ± 103
477	toppanidgate-000	671181	711850	399 1798	495 4096 ± 0	403 915 ± 1	359 916 ± 1	335 916 ± 1	308 917 ± 1	267 917 ± 1	521 25262 ± 84	518 25264 ± 97
478	toshiba-007	547545	76675	325 1297	424 2056 ± 0	325 722 ± 1	307 784 ± 0	279 777 ± 4	251 766 ± 2	237 832 ± 15	119 709 ± 22	119 712 ± 26
479	toshiba-008	707290	76687	398 1791	436 2056 ± 0	429 979 ± 1	385 976 ± 0	370 986 ± 3	348 1005 ± 2	312 1056 ± 14	106 674 ± 68	112 683 ± 71
480	touchlessid-002	255586	14284	78 367	194 2048 ± 0	118 371 ± 1	98 375 ± 1	105 438 ± 3	190 640 ± 10	450 1548 ± 57	264 1915 ± 41	257 1871 ± 38
481	touchlessid-003	271397	14226	121 512	142 2048 ± 0	141 410 ± 0	120 419 ± 0	102 429 ± 0	112 479 ± 1	171 685 ± 6	81 608 ± 17	77 596 ± 1
482	trueface-002	253947	123116	109 486	110 2000 ± 0	111 360 ± 0	90 361 ± 0	98 423 ± 0	163 590 ± 1	-	15 192 ± 14	17 186 ± 19
483	trueface-003	346530	24308	526 3916	335 2048 ± 0	472 1107 ± 22	262 677 ± 3	266 732 ± 7	306 905 ± 5	-	5 103 ± 11	6 112 ± 29
484	trueidvng-001	766071	37721	397 1781	552 6144 ± 0	426 975 ± 1	391 985 ± 1	372 989 ± 1	354 1016 ± 1	338 1128 ± 2	536 37129 ± 216	560 72067 ± 305

Notes	
1	The configuration size does not capture static data included in libraries.
2	The library size is the combined total of all files provided in the submission lib folder. These libraries e.g. OpenCV may or may not be installed on any end user's platform natively and would not need to be installed with the algorithm. Some developers put neural network models in their libraries.
3	The memory usage is the peak resident set size reported by the ps system call during template generation.
4	The median template creation times are measured on Intel®Xeon®CPU E5-2630 v4 @ 2.20GHz processors.
5	The comparison durations, in nanoseconds, are estimated using std::chrono::high_resolution_clock which on the machine in (2) counts 1ns clock ticks. Precision is somewhat worse than that however. The ± value is the median absolute deviation times 1.48 for Normal consistency.

Table 20: Summary of algorithms and properties included in this report. The red superscripts give ranking for the quantity in that column.

	ALGORITHM	CONFIG	LIBRARY	TEMPLATE						COMPARISON[4]	
	NAME	DATA	DATA	MEMORY	SIZE	GENERATION TIME (ms)[4]				TIME (ns)[5]	
		(KB)[1]	(KB)[2]	(MB)[3]	(B)	MUGSHOT	480x720	960x1440	1600x2400	3000x4500	GENUINE	IMPOSTOR
485	truststamp-001	1795742	275073	362 1524	71 768 ± 0	48 194 ± 0	38 191 ± 0	28 187 ± 0	30 210 ± 1	45 338 ± 8	448 8415 ± 66	447 8392 ± 71
486	tuputech-000	11476	17185	6 33	262 2048 ± 0	25 122 ± 4	18 120 ± 1	19 142 ± 2	26 196 ± 5	67 411 ± 14	518 23893 ± 406	519 25279 ± 406
487	turingtechvip-001	399874	54535	149 615	246 2048 ± 0	540 1384 ± 4	509 1391 ± 1	503 1393 ± 1	479 1411 ± 1	434 1476 ± 2	241 1733 ± 19	241 1734 ± 20
488	turingtechvip-002	167556	140995	227 877	306 2048 ± 0	568 1493 ± 2	491 1306 ± 1	501 1382 ± 1	455 1337 ± 1	416 1426 ± 3	481 13819 ± 103	480 13807 ± 137
489	turkcell-001	287616	133870	160 657	347 2048 ± 0	298 682 ± 0	274 695 ± 0	245 688 ± 1	218 692 ± 0	181 702 ± 0	392 4342 ± 71	388 4310 ± 72
490	turkcell-002	542178	139150	154 633	372 2048 ± 0	345 791 ± 1	192 559 ± 1	282 793 ± 3	259 793 ± 2	124 574 ± 0	358 3249 ± 65	358 3231 ± 53
491	twface-000	661735	11782	489 2796	195 2048 ± 0	386 871 ± 1	341 873 ± 1	318 873 ± 2	293 876 ± 2	260 898 ± 1	219 1504 ± 29	219 1510 ± 34
492	twface-001	671511	11782	492 2851	192 2048 ± 0	407 923 ± 1	367 925 ± 2	341 926 ± 1	312 929 ± 2	270 940 ± 2	203 1400 ± 32	204 1402 ± 37
493	ulsee-001	370519	57261	-	332 2048 ± 0	279 654 ± 2	-	-	-	-	424 6065 ± 94	425 6228 ± 77
494	uluface-002	0	480761	281 1088	115 2048 ± 0	388 873 ± 42	332 855 ± 9	364 978 ± 24	435 1271 ± 40	482 2333 ± 68	507 19207 ± 1114	504 18501 ± 274
495	uluface-003	97357	529422	317 1264	470 3072 ± 0	422 965 ± 11	380 968 ± 10	414 1087 ± 20	470 1387 ± 36	486 2469 ± 86	522 26057 ± 195	523 26865 ± 566
496	unicc-002	277015	1705310	382 1673	239 2048 ± 0	248 609 ± 1	225 620 ± 1	199 612 ± 0	199 660 ± 2	211 763 ± 3	297 2289 ± 13	295 2295 ± 22
497	unicc-003	361274	1737967	401 1806	274 2048 ± 0	533 1343 ± 3	498 1328 ± 1	490 1345 ± 1	462 1366 ± 1	436 1484 ± 6	301 2339 ± 74	300 2327 ± 29
498	unissey-003	0	814526	158 650	483 4096 ± 0	322 718 ± 1	294 744 ± 0	354 956 ± 1	476 1403 ± 1	500 3055 ± 2	224 1594 ± 20	224 1570 ± 44
499	unissey-004	1	1065839	260 1030	486 4096 ± 0	105 354 ± 2	94 366 ± 0	94 416 ± 0	88 417 ± 0	65 409 ± 0	390 4261 ± 124	394 4557 ± 480
500	upc-001	0	89914	276 1077	98 1052 ± 0	212 551 ± 15	280 703 ± 56	263 724 ± 51	247 751 ± 49	248 863 ± 33	352 3114 ± 44	355 3165 ± 97
501	useb-001	1000960	493816	351 1429	186 2048 ± 0	290 673 ± 4	202 577 ± 4	182 579 ± 8	166 596 ± 9	215 768 ± 2	289 2230 ± 65	297 2299 ± 90
502	useb-002	1000967	493456	349 1423	153 2048 ± 0	201 532 ± 2	305 778 ± 2	227 657 ± 4	197 657 ± 2	243 843 ± 3	300 2336 ± 47	299 2323 ± 60
503	uxlabs-001	291127	39378	168 700	490 4096 ± 0	131 395 ± 0	102 387 ± 0	84 388 ± 0	76 390 ± 0	63 396 ± 0	256 1863 ± 31	262 1921 ± 45
504	uxlabs-003	1051837	37767	376 1638	491 4096 ± 0	544 1390 ± 1	517 1410 ± 5	502 1391 ± 3	475 1402 ± 6	420 1435 ± 1	231 1645 ± 10	228 1641 ± 37
505	vcog-002	3229434	118946	518 3666	570 61504 ± 5	108 357 ± 25	-	-	-	-	567 296154 ± 3077	567 296436 ± 4183
506	vcortex-001	105305	55240	113 502	75 896 ± 0	53 201 ± 2	39 197 ± 0	39 209 ± 3	42 244 ± 6	55 371 ± 19	30 279 ± 4	32 277 ± 4
507	vd-002	254498	34389	5 31	55 516 ± 0	302 684 ± 5	265 679 ± 4	235 676 ± 5	219 693 ± 5	206 754 ± 5	33 300 ± 14	35 319 ± 32
508	vd-003	254505	44051	2 29	406 2052 ± 0	312 691 ± 5	272 690 ± 5	241 683 ± 4	217 691 ± 5	193 722 ± 5	153 1003 ± 11	153 1001 ± 7
509	veridas-008	1100495	1190915	559 8633	151 2048 ± 0	414 944 ± 12	374 945 ± 11	485 1334 ± 27	523 2382 ± 48	520 6959 ± 172	121 723 ± 14	122 731 ± 16
510	veridas-009	1100503	625120	561 9163	366 2048 ± 0	235 589 ± 6	196 565 ± 5	180 576 ± 5	160 583 ± 5	167 666 ± 6	102 638 ± 5	104 638 ± 16
511	veridium-002	0	52482	37 161	464 2486 ± 0	4 25 ± 0	3 25 ± 0	3 29 ± 0	3 30 ± 0	3 51 ± 0	543 43891 ± 177	541 43918 ± 167
512	veridium-003	0	25975	29 136	465 2490 ± 0	6 27 ± 0	2 25 ± 0	2 28 ± 0	2 30 ± 0	4 53 ± 0	534 34755 ± 140	534 34828 ± 177
513	verigram-001	282155	11773	472 2638	393 2048 ± 0	284 664 ± 2	260 675 ± 2	301 833 ± 4	416 1202 ± 7	492 2733 ± 32	233 1664 ± 60	229 1648 ± 56
514	verigram-003	1590775	20692	428 2052	485 4096 ± 0	311 691 ± 4	264 677 ± 1	237 677 ± 1	221 694 ± 1	204 746 ± 1	539 38843 ± 1140	538 38665 ± 1071
515	verihubs-inteligensia-001	216524	51916	94 437	329 2048 ± 0	219 564 ± 0	194 562 ± 0	171 566 ± 1	150 566 ± 0	132 600 ± 0	512 21770 ± 84	511 21735 ± 102
516	verihubs-inteligensia-002	361105	17045	180 727	203 2048 ± 0	170 471 ± 0	141 458 ± 0	117 459 ± 0	105 463 ± 1	83 471 ± 0	502 18131 ± 558	500 17851 ± 197
517	verijelas-000	254540	10322	393 1736	381 2048 ± 0	96 321 ± 0	82 325 ± 1	65 329 ± 0	62 335 ± 5	52 360 ± 0	464 10267 ± 143	462 10218 ± 109
518	via-004	530941	93634	339 1361	382 2048 ± 0	116 368 ± 0	108 397 ± 1	70 352 ± 1	69 364 ± 2	91 490 ± 1	28 255 ± 7	30 255 ± 8
519	via-005	510729	93629	450 2257	156 2048 ± 0	204 538 ± 0	172 528 ± 0	152 525 ± 1	134 535 ± 2	133 601 ± 1	25 223 ± 2	26 222 ± 7
520	viante-000	1244225	19718	365 1532	432 2056 ± 0	458 1054 ± 0	420 1059 ± 1	412 1075 ± 1	371 1070 ± 4	323 1087 ± 1	429 6461 ± 44	428 6424 ± 32
521	videmo-001	212051	95063	68 309	165 2048 ± 0	51 199 ± 0	24 164 ± 0	21 164 ± 0	18 164 ± 0	12 165 ± 0	31 296 ± 17	33 288 ± 16
522	videmo-002	212053	32963	71 333	333 2048 ± 0	50 199 ± 0	25 169 ± 0	23 169 ± 0	19 170 ± 0	14 170 ± 0	23 209 ± 7	23 208 ± 8
523	videonetics-001	30875	5963	9 61	27 512 ± 0	68 262 ± 3	60 273 ± 1	107 439 ± 3	272 820 ± 3	483 2393 ± 43	181 1153 ± 38	176 1142 ± 65
524	videonetics-002	121981	6289	23 115	415 2052 ± 0	76 282 ± 5	72 295 ± 1	145 513 ± 4	356 1029 ± 3	501 3151 ± 46	184 1219 ± 57	188 1262 ± 56
525	viettelhightech-000	259471	215557	91 421	177 2048 ± 0	162 461 ± 1	142 461 ± 2	120 461 ± 1	108 467 ± 2	92 494 ± 0	75 599 ± 11	71 591 ± 13
526	vigilantsolutions-010	348798	49973	216 841	108 1548 ± 0	257 615 ± 0	235 631 ± 0	213 632 ± 0	187 636 ± 0	161 659 ± 0	52 490 ± 13	53 488 ± 11
527	vigilantsolutions-011	255661	49973	140 591	107 1548 ± 0	135 402 ± 0	119 418 ± 0	95 418 ± 0	90 422 ± 0	76 445 ± 0	37 339 ± 20	38 366 ± 37
528	vinai-000	402391	866522	263 1034	376 2048 ± 0	469 1099 ± 1	432 1095 ± 1	417 1093 ± 1	379 1099 ± 1	337 1126 ± 1	345 2996 ± 20	346 2993 ± 26

Notes	
1	The configuration size does not capture static data included in libraries.
2	The library size is the combined total of all files provided in the submission lib folder. These libraries e.g. OpenCV may or may not be installed on any end user's platform natively and would not need to be installed with the algorithm. Some developers put neural network models in their libraries.
3	The memory usage is the peak resident set size reported by the ps system call during template generation.
4	The median template creation times are measured on Intel®Xeon®CPU E5-2630 v4 @ 2.20GHz processors.
5	The comparison durations, in nanoseconds, are estimated using std::chrono::high_resolution_clock which on the machine in (2) counts 1ns clock ticks. Precision is somewhat worse than that however. The ± value is the median absolute deviation times 1.48 for Normal consistency.

Table 21: Summary of algorithms and properties included in this report. The red superscripts give ranking for the quantity in that column.

	ALGORITHM	CONFIG	LIBRARY	TEMPLATE						COMPARISON[4]	
	NAME	DATA	DATA	MEMORY	SIZE	GENERATION TIME (ms)[4]				TIME (ns)[5]	
		(KB)[1]	(KB)[2]	(MB)[3]	(B)	MUGSHOT	480x720	960x1440	1600x2400	3000x4500	GENUINE	IMPOSTOR
529	vinbigdata-002	256322	138864	146 607	204 2048 ± 0	222 569 ± 2	200 572 ± 1	174 571 ± 1	153 572 ± 1	130 596 ± 1	283 2175 ± 44	283 2160 ± 53
530	vinbigdata-003	259968	183557	74 342	202 2048 ± 0	378 849 ± 6	492 1312 ± 1	310 853 ± 2	449 1321 ± 2	238 832 ± 2	163 1074 ± 37	168 1086 ± 40
531	vion-000	228219	7533	112 498	403 2052 ± 0	101 333 ± 1	-	-	-	-	540 39839 ± 3561	522 26830 ± 2241
532	visage-000	49218	70150	12 72	43 512 ± 0	5 27 ± 0	4 27 ± 0	4 31 ± 0	5 38 ± 0	6 63 ± 0	286 2220 ± 14	288 2218 ± 14
533	visionbox-003	259542	156891	316 1263	454 2068 ± 0	296 678 ± 2	266 682 ± 1	239 682 ± 2	222 695 ± 2	202 739 ± 5	230 1643 ± 56	230 1649 ± 66
534	visionbox-004	309730	154797	348 1422	537 4116 ± 0	120 378 ± 1	95 369 ± 0	85 389 ± 5	83 402 ± 2	72 437 ± 4	277 2071 ± 31	279 2076 ± 41
535	visionlabs-010	1067280	19357	229 883	50 513 ± 0	327 730 ± 0	288 717 ± 1	255 709 ± 0	232 713 ± 1	201 739 ± 0	78 600 ± 41	95 626 ± 35
536	visionlabs-011	1067280	19353	241 923	53 513 ± 0	328 731 ± 1	287 717 ± 1	256 710 ± 1	233 714 ± 1	203 741 ± 1	58 556 ± 26	61 559 ± 25
537	visteam-007	331673	264832	108 485	350 2048 ± 0	249 611 ± 1	230 625 ± 1	209 626 ± 1	174 615 ± 1	157 647 ± 0	320 2704 ± 38	322 2732 ± 54
538	visteam-008	582800	264832	182 731	248 2048 ± 0	487 1179 ± 1	451 1173 ± 1	454 1210 ± 1	412 1190 ± 3	358 1208 ± 1	319 2632 ± 28	319 2647 ± 42
539	vivotek-001	15240	247926	27 128	200 2048 ± 0	18 100 ± 0	15 101 ± 0	14 106 ± 0	15 134 ± 0	25 238 ± 1	523 26504 ± 57	521 26520 ± 69
540	vixvizion-006	594053	396294	337 1359	325 2048 ± 0	391 876 ± 9	320 828 ± 3	294 817 ± 1	275 825 ± 2	252 871 ± 1	76 600 ± 23	87 611 ± 25
541	vixvizion-007	594053	470119	354 1435	199 2048 ± 0	394 885 ± 35	321 828 ± 1	293 816 ± 1	276 825 ± 1	251 870 ± 1	77 600 ± 28	81 602 ± 34
542	vnis-000	285395	1404886	131 546	305 2048 ± 0	152 437 ± 1	131 443 ± 1	115 456 ± 2	98 458 ± 2	86 477 ± 2	198 1386 ± 10	202 1382 ± 16
543	vnpay-000	258919	1404844	114 504	269 2048 ± 0	62 239 ± 1	52 248 ± 0	47 252 ± 0	43 249 ± 0	31 260 ± 0	196 1353 ± 11	197 1353 ± 23
544	vnpt-005	560630	240888	296 1157	223 2048 ± 0	550 1403 ± 0	515 1404 ± 6	507 1403 ± 6	487 1456 ± 0	456 1630 ± 10	370 3562 ± 23	371 3554 ± 29
545	vnpt-006	1114807	360198	449 2245	168 2048 ± 0	516 1277 ± 2	508 1390 ± 19	510 1410 ± 14	498 1481 ± 30	462 1703 ± 69	363 3400 ± 20	363 3393 ± 22
546	vocalize-001	0	38841	19 96	38 512 ± 0	10 57 ± 0	8 55 ± 0	6 56 ± 0	7 60 ± 0	5 62 ± 0	201 1400 ± 59	199 1365 ± 26
547	vocord-009	1380132	201560	533 4372	109 1920 ± 0	562 1472 ± 2	532 1472 ± 1	531 1549 ± 1	509 1667 ± 2	476 2064 ± 2	275 2052 ± 50	278 2056 ± 39
548	vocord-010	902552	206873	523 3866	99 1088 ± 0	560 1459 ± 2	530 1459 ± 1	524 1463 ± 2	499 1484 ± 1	447 1535 ± 3	322 2724 ± 31	320 2653 ± 45
549	vtcc-000	284612	132031	151 619	336 2048 ± 0	93 315 ± 0	79 317 ± 0	62 321 ± 0	59 322 ± 0	43 334 ± 1	515 22074 ± 112	514 22173 ± 163
550	vtcc-001	528186	132058	303 1189	380 2048 ± 0	321 715 ± 1	-	-	-	-	516 22740 ± 167	562 86287 ± 1073
551	vts-000	256589	169760	386 1697	113 2048 ± 0	179 486 ± 1	151 481 ± 0	130 484 ± 0	114 485 ± 1	101 517 ± 0	564 124209 ± 352	564 123652 ± 358
552	vts-001	293000	475743	152 622	180 2048 ± 0	294 676 ± 1	267 683 ± 6	244 687 ± 3	223 695 ± 2	182 709 ± 2	460 9620 ± 44	457 9618 ± 54
553	wicket-000	826392	641802	430 2071	288 2048 ± 0	553 1419 ± 2	521 1429 ± 3	518 1444 ± 4	490 1460 ± 3	448 1537 ± 6	554 60976 ± 232	552 61096 ± 323
554	winsense-001	264428	32035	240 922	100 1280 ± 0	337 766 ± 7	419 1058 ± 47	367 983 ± 97	364 1053 ± 119	389 1320 ± 84	228 1631 ± 28	270 1964 ± 171
555	winsense-002	281379	25780	409 1855	221 2048 ± 0	182 494 ± 2	158 498 ± 1	148 519 ± 1	136 537 ± 1	147 634 ± 1	235 1683 ± 8	234 1685 ± 7
556	wiseai-001	189467	60781	53 245	201 2048 ± 0	63 240 ± 0	54 251 ± 0	64 328 ± 1	61 327 ± 0	42 332 ± 0	332 2850 ± 29	334 2852 ± 31
557	wuhantianyu-001	465118	66457	279 1086	238 2048 ± 0	272 642 ± 1	244 642 ± 1	224 644 ± 0	195 652 ± 0	179 697 ± 0	455 9502 ± 151	461 9920 ± 253
558	x-laboratory-000	520020	197310	363 1524	428 2056 ± 0	354 808 ± 7	350 897 ± 113	331 907 ± 103	298 886 ± 103	168 673 ± 39	122 725 ± 19	124 749 ± 34
559	x-laboratory-001	625140	398792	406 1844	441 2056 ± 0	232 586 ± 2	213 596 ± 5	193 603 ± 6	179 620 ± 7	221 793 ± 14	135 813 ± 28	140 872 ± 32
560	xforwardai-001	340100	51163	444 2176	349 2048 ± 0	490 1180 ± 2	457 1182 ± 1	449 1194 ± 1	410 1186 ± 2	354 1203 ± 1	131 779 ± 17	132 797 ± 13
561	xforwardai-002	707715	51163	426 2003	506 4096 ± 0	413 944 ± 1	373 942 ± 1	347 943 ± 4	315 935 ± 1	281 967 ± 1	205 1406 ± 8	205 1405 ± 13
562	xm-000	578041	148920	165 684	420 2052 ± 0	392 878 ± 2	345 882 ± 1	371 988 ± 2	432 1258 ± 3	485 2434 ± 7	229 1634 ± 17	226 1632 ± 20
563	yisheng-004	486351	38653	320 1279	473 3704 ± 0	122 378 ± 12	-	-	-	-	113 693 ± 137	56 526 ± 34
564	yitu-003	1525719	138919	520 3737	459 2082 ± 0	383 860 ± 0	-	-	-	-	503 18305 ± 71	502 18286 ± 62
565	yoonik-003	346691	265415	442 2161	169 2048 ± 0	435 991 ± 3	389 980 ± 1	368 984 ± 4	332 982 ± 1	287 983 ± 1	110 684 ± 45	108 678 ± 41
566	yoonik-004	469597	88673	201 792	273 2048 ± 0	500 1219 ± 1	482 1284 ± 1	463 1255 ± 1	434 1266 ± 0	366 1251 ± 1	157 1039 ± 42	158 1030 ± 40
567	yoti-001	267246	470114	290 1125	304 2048 ± 0	506 1238 ± 4	493 1316 ± 17	538 4099 ± 13	534 4160 ± 45	512 4774 ± 95	466 10352 ± 247	465 10364 ± 246
568	ytu-000	1477360	44032	465 2484	114 2048 ± 0	197 530 ± 0	176 533 ± 0	220 640 ± 0	288 861 ± 2	473 1949 ± 8	531 31797 ± 131	530 31794 ± 133
569	yuan-005	258312	145564	218 843	391 2048 ± 0	124 381 ± 0	101 386 ± 0	83 387 ± 2	75 390 ± 4	68 421 ± 3	182 1156 ± 8	184 1196 ± 26
570	yuan-008	620369	167833	375 1626	519 4096 ± 0	485 1169 ± 0	297 752 ± 0	274 752 ± 3	254 775 ± 4	220 782 ± 0	197 1362 ± 16	200 1377 ± 19

Notes	
1	The configuration size does not capture static data included in libraries.
2	The library size is the combined total of all files provided in the submission lib folder. These libraries e.g. OpenCV may or may not be installed on any end user's platform natively and would not need to be installed with the algorithm. Some developers put neural network models in their libraries.
3	The memory usage is the peak resident set size reported by the ps system call during template generation.
4	The median template creation times are measured on Intel®Xeon®CPU E5-2630 v4 @ 2.20GHz processors.
5	The comparison durations, in nanoseconds, are estimated using std::chrono::high_resolution_clock which on the machine in (2) counts 1ns clock ticks. Precision is somewhat worse than that however. The ± value is the median absolute deviation times 1.48 for Normal consistency.

Table 22: Summary of algorithms and properties included in this report. The red superscripts give ranking for the quantity in that column.

	Algorithm	FALSE NON-MATCH RATE (FNMR)															
		CONSTRAINED, COOPERATIVE														LESS CONSTRAINED, NON-COOP.	
	Name	VISAMC		VISA		MUGSHOT		MUGSHOT12+YRS		VISABORDER		BORDER		BORDER		KIOSKBORDER	
	FMR	0.0001		1E-06		1E-05		1E-05		1E-06		1E-06		1E-05		1E-06	
1	20face-000	0.1268	483	0.1828	481	0.1748	503	0.2768	503	0.1765	480	0.1864	342	0.0927	382	0.5943	241
2	20face-001	0.0521	458	0.0732	457	0.1414	501	0.2549	502	0.0769	454	0.1354	333	0.0419	337	0.8953	283
3	3divi-006	0.0064	264	0.0094	262	0.0047	255	0.0066	260	0.0091	266	0.0191	187	0.0113	205	0.2854	196
4	3divi-007	0.0024	100	0.0038	106	0.0028	121	0.0034	120	0.0046	167	0.0101	118	0.0082	143	0.2515	183
5	accurascan-002	0.4209	512	0.5213	512	0.5826	530	0.6642	526	0.6295	515	0.6937	423	0.3116	433	0.9162	287
6	accurascan-003	0.0017	57	0.0028	62	0.0024	46	0.0024	37	0.0029	82	0.0057	40	0.0048	57	0.0629	42
7	acer-001	0.0294	433	0.0504	437	0.0240	445	0.0463	451	0.0436	427	0.0622	294	0.0360	328	-	
8	acer-002	0.0169	400	0.0262	404	0.0103	380	0.0167	389	0.0182	365	0.0281	228	0.0159	251	0.1555	146
9	acisw-007	0.4276	514	0.5493	515	0.8425	550	0.9185	550	0.8424	531	0.9976	508	0.9930	528	0.9999	355
10	acisw-008	0.0100	334	0.0147	332	0.0094	373	0.0126	341	0.1740	479	0.6651	420	0.4545	454	0.9302	291
11	adera-004	0.0014	35	0.0022	36	0.0035	193	0.0050	201	0.0023	24	0.0212	198	0.0058	81	0.1469	142
12	adera-005	0.0017	52	0.0026	47	0.0027	107	0.0030	85	0.0024	28	0.0134	146	0.0049	58	0.1246	126
13	advance-004	0.0083	306	0.0101	278	0.0037	209	0.0054	217	0.0051	185	0.3555	385	0.1088	388	0.8285	267
14	advance-005	0.0059	252	0.0084	247	0.0043	239	0.0060	240	0.0065	223	0.9998	526	0.9993	539	1.0000	386
15	afisbiometrics-000	0.0051	217	0.0073	219	0.0030	145	0.0050	203	0.0044	160	0.0077	72	0.0057	78	0.0796	70
16	afrengine-002	0.0052	222	0.0071	214	0.0032	163	0.0043	178	0.0194	373	0.2125	351	0.0450	344	0.2330	177
17	afrengine-003	-		-		0.0028	127	0.0031	103	0.0116	309	0.0224	206	0.0208	289	0.0860	79
18	aifirst-001	0.0119	362	0.0170	351	0.0084	352	0.0127	345	0.0131	322	0.0212	197	0.0138	228	-	
19	aigen-001	0.0124	368	0.0219	384	0.0143	416	0.0217	411	0.0236	390	0.8960	462	0.3255	435	-	
20	aigen-002	0.0192	412	0.0343	415	0.0256	446	0.0402	442	0.0389	418	0.9196	466	0.3876	445	0.9994	344
21	ailabs-001	0.0158	396	0.0276	407	0.0192	432	0.0317	431	0.0352	411	0.0608	291	0.0434	340	-	
22	aimall-002	0.0119	363	0.0167	349	0.0224	441	0.0411	443	0.0233	388	0.0373	262	0.0235	301	-	
23	aimall-003	0.0033	143	0.0041	118	0.0033	185	0.0035	137	0.0056	204	0.0109	126	0.0087	159	-	
24	aiseemu-001	0.0021	75	0.0029	68	0.0027	105	0.0033	115	0.0038	134	0.0339	249	0.0057	79	0.4819	228
25	aiseemu-002	0.0023	93	0.0032	81	0.0026	85	0.0027	59	0.0036	125	0.0439	267	0.0057	77	0.4259	222
26	aiunionface-000	0.0104	341	0.0154	340	0.0082	348	0.0122	337	0.0141	329	0.0243	212	0.0169	257	-	
27	aize-002	0.0210	419	0.0327	412	0.0280	450	0.0489	455	0.0504	438	0.0692	302	0.0434	339	0.2657	191
28	aize-003	0.0086	311	0.0125	310	0.0072	330	0.0126	343	0.0516	441	0.6137	412	0.1038	387	0.9911	319
29	ajou-001	0.0093	324	0.0147	330	0.0071	329	0.0126	342	0.0173	360	0.0274	223	0.0186	271	-	
30	alchera-006	0.0028	119	0.0039	112	0.0026	84	0.0031	96	0.0025	45	0.0090	94	0.0042	32	0.0867	80
31	alchera-007	0.0034	157	0.0049	162	0.0026	83	0.0031	97	0.0026	55	0.0096	110	0.0044	40	0.0834	77
32	alfabeta-001	0.4867	522	0.5831	519	0.6855	536	0.8156	538	0.8253	530	0.7765	439	0.6416	474	0.9627	296
33	alice-000	0.0119	365	0.0192	370	0.0106	385	0.0170	390	0.0167	350	0.0265	220	0.0150	244	0.1824	161
34	alice-001	0.0034	158	0.0046	147	0.0032	161	0.0037	154	0.0030	93	0.3164	377	0.1088	389	0.8336	268
35	alleyes-000	0.0058	246	0.0090	256	0.0055	287	0.0087	308	0.0068	228	0.0105	123	0.0076	129	-	
36	allgovision-000	0.0346	446	0.0527	443	0.0232	442	0.0339	432	0.0372	415	0.0620	293	0.0443	343	-	
37	alphaface-001	0.0065	265	0.0097	271	0.0039	220	0.0063	252	0.0083	253	-		-		-	
38	alphaface-002	0.0052	223	0.0075	227	0.0030	138	0.0044	184	1.0000	560	0.0115	131	0.0084	153	-	
39	amplifiedgroup-001	0.5034	524	0.5848	520	0.6973	539	0.8316	539	0.7807	522	0.7724	436	0.6354	470	-	
40	androvideo-000	0.0243	425	0.0438	429	0.0239	444	0.0365	439	0.0483	434	0.1870	343	0.0635	364	-	
41	anke-004	0.0080	295	0.0154	339	0.0073	332	0.0112	329	0.0102	292	0.0178	179	0.0118	211	-	
42	anke-005	0.0070	272	0.0109	290	0.0059	297	0.0094	312	0.0105	294	0.0142	149	0.0102	186	-	
43	antheus-000	0.2564	499	0.3776	500	0.7240	540	0.8699	544	0.8899	539	0.9872	493	0.9483	513	-	
44	antheus-001	0.1311	484	0.2306	487	0.5113	525	0.6797	527	0.8748	538	0.9908	498	0.9649	521	-	

Table 23: FNMR is the proportion of mated comparisons below a threshold set to achieve the FMR given in the header on the fourth row. FMR is the proportion of impostor comparisons at or above that threshold. The light grey values give rank over all algorithms in that column. The pink columns use only same-sex impostors; others are selected regardless of demographics. The exception, in the green column, uses "matched-covariates" i.e. impostors of the same sex, age group, and country of birth. The second pink column includes effects of extended ageing. Missing entries for border, visa, mugshot and wild images generally mean the algorithm did not run to completion. The VISA *columns compare images described in section 2.1. The* MUGSHOT *columns compare images described in section 2.5. The* VISA-BORDER *column compare images described in section 2.2 with those of section 2.4. The* BORDER *column compares images described in section 2.4. The* KIOSK-BORDER *columns compare images described in section 2.6 with those of section 2.4.*

FNMR(T) "False non-match rate"
FMR(T) "False match rate"

		FALSE NON-MATCH RATE (FNMR)																	
	Algorithm	CONSTRAINED, COOPERATIVE																LESS CONSTRAINED, NON-COOP.	
	Name	VISAMC		VISA		MUGSHOT		MUGSHOT12+YRS		VISABORDER		BORDER		BORDER		KIOSKBORDER	
	FMR	0.0001		1E-06		1E-05		1E-05		1E-06		1E-06		1E-05		1E-06	
45	anyvision-004	0.0267	429	0.0385	423	0.0258	447	0.0487	454	0.0234	389	0.0301	232	0.0191	273	-	
46	anyvision-005	0.0023	92	0.0037	103	0.0027	119	0.0035	129	0.0049	179	0.0084	85	0.0069	110	-	
47	aratek-001	0.0033	148	0.0045	142	0.0028	126	0.0031	104	0.0043	154	0.0092	102	0.0069	112	0.0897	90
48	armatura-001	0.0033	144	0.0042	124	0.0031	152	0.0037	151	0.0056	203	0.0110	127	0.0092	168	0.4625	226
49	armatura-003	0.0020	73	0.0029	65	0.0026	94	0.0028	64	0.0025	50	0.0049	26	0.0043	36	0.0608	35
50	asusaics-000	0.0125	371	0.0209	380	0.0085	354	0.0134	354	0.0143	332	0.7189	427	0.0285	314	-	
51	asusaics-001	0.0125	372	0.0210	381	0.0085	356	0.0134	355	0.0143	333	0.7437	430	0.0289	317	-	
52	autentika-001	0.0444	454	0.0688	453	0.0987	493	0.1531	492	0.1547	474	1.0000	535	0.9997	543	1.0000	376
53	autentika-002	0.0536	462	0.0866	462	0.0657	486	0.1084	484	0.1548	475	0.9993	518	0.9939	529	1.0000	378
54	authenmetric-003	0.0036	173	0.0053	177	0.0039	225	0.0051	205	0.0095	276	0.9930	502	0.5932	465	1.0000	364
55	authenmetric-004	0.0027	114	0.0042	122	0.0033	179	0.0036	148	0.0083	256	0.9879	494	0.4058	448	1.0000	360
56	authme-001	0.0036	166	0.0049	160	0.0037	211	0.0040	164	0.0030	92	0.3075	373	0.1310	396	0.7046	256
57	aware-007	0.0101	338	0.0198	375	0.0060	303	0.0133	353	0.0224	385	0.5813	409	0.1673	410	0.8871	279
58	aware-008	-		-		0.0062	306	0.0143	368	0.0135	325	0.0332	244	0.0133	224	0.3622	208
59	awiros-001	0.4044	510	0.4622	506	0.5530	526	0.6518	524	0.2008	483	0.1994	346	0.1386	399	-	
60	awiros-002	0.1990	491	0.2561	489	0.3319	515	0.4411	514	0.3821	503	0.9938	503	0.2634	424	-	
61	aximetria-001	0.0111	352	0.0186	367	0.0110	391	0.0148	373	0.0170	355	0.3928	389	0.2090	416	0.7924	265
62	ayftech-001	0.0946	477	0.1941	482	0.2438	508	0.3625	508	0.1558	476	0.1589	336	0.0936	383	-	
63	ayftech-003	0.0023	95	0.0037	101	0.0026	99	0.0030	91	0.0072	236	0.5411	405	0.2515	421	0.8902	280
64	ayonix-000	0.4351	516	0.4872	508	0.6150	532	0.7510	532	0.6557	516	0.6361	415	0.4981	455	-	
65	beethedata-000	0.0127	375	0.0195	371	0.0092	365	0.0157	379	0.0171	357	0.0306	234	0.0204	285	0.1617	151
66	beyneai-000	0.0071	279	0.0107	286	0.0104	383	0.0131	351	0.0170	356	0.9837	491	0.6171	467	1.0000	356
67	biocube-001	0.5596	531	0.6834	529	0.7700	547	0.8712	545	0.8446	532	0.9661	484	0.7922	491	0.9846	313
68	biocube-002	0.0612	465	0.0856	461	0.2330	506	0.2972	505	0.2365	491	0.9327	473	0.6947	477	0.9989	337
69	bioidtechswiss-001	0.0054	228	0.0072	216	0.0069	322	0.0124	339	0.0060	211	0.0094	105	0.0065	99	-	
70	bioidtechswiss-002	0.0049	205	0.0067	203	0.0064	309	0.0116	332	0.0067	226	0.0117	132	0.0086	156	-	
71	biometric-vision-000	0.0023	90	0.0036	96	0.0028	128	0.0034	125	0.0028	81	0.3109	375	0.1504	403	0.6849	252
72	bm-001	0.7431	540	0.9494	542	0.9586	556	0.9843	556	0.9049	541	0.9021	464	0.8395	497	-	
73	boetech-001	0.0662	468	0.0802	460	0.0493	476	0.0791	474	0.0682	451	0.1074	321	0.0758	371	0.9951	326
74	boetech-002	0.0535	461	0.0565	446	0.0114	400	0.0136	357	0.0403	420	0.0650	296	0.0606	362	0.3470	206
75	bresee-001	0.0085	308	0.0143	326	0.0086	357	0.0153	376	0.0108	299	0.0168	171	0.0115	209	-	
76	bresee-002	0.0079	292	0.0101	275	0.0065	315	0.0079	290	0.0129	318	0.0263	219	0.0224	297	0.2137	174
77	camvi-002	0.0125	373	0.0221	386	0.0089	361	0.0145	371	0.0142	330	0.2650	365	0.0166	256	-	
78	camvi-004	0.0171	403	0.0316	411	0.0042	236	0.0049	199	0.0097	283	0.6636	419	0.0141	232	-	
79	candour-001	0.1048	481	0.3189	493	0.0130	411	0.0182	393	0.3879	505	0.9216	467	0.7071	482	0.9836	309
80	canon-004	0.0052	221	0.0091	259	0.0033	184	0.0058	232	0.0037	129	0.0770	308	0.0494	350	0.3192	203
81	canon-005	0.0024	98	0.0035	92	0.0025	70	0.0033	119	0.0052	189	0.0096	111	0.0090	163	0.0542	19
82	cchonolulu-000	0.7910	542	0.8611	538	0.9824	557	0.9926	557	0.9940	551	0.9861	492	0.9534	514	1.0000	358
83	cchonolulu-001	0.4202	511	0.4853	507	0.6298	533	0.7694	533	0.7402	519	0.9720	486	0.8870	505	0.9951	327
84	ceiec-003	0.0071	277	0.0107	285	0.0061	304	0.0079	293	0.0160	341	0.0316	237	0.0260	309	-	
85	ceiec-004	0.0038	179	0.0051	169	0.0045	248	0.0053	211	0.0062	217	0.3939	390	0.0104	193	-	
86	chosun-001	0.0525	459	0.0936	465	0.0742	489	0.1263	490	0.0978	467	1.0000	545	0.9354	510	-	
87	chosun-002	0.0390	449	0.0646	451	0.0339	462	0.0576	464	0.0455	432	0.6904	422	0.1746	411	-	
88	chtface-005	0.0033	146	0.0049	158	0.0029	135	0.0041	169	0.0044	159	0.0317	238	0.0066	100	0.1952	167

Table 24: FNMR is the proportion of mated comparisons below a threshold set to achieve the FMR given in the header on the fourth row. FMR is the proportion of impostor comparisons at or above that threshold. The light grey values give rank over all algorithms in that column. The pink columns use only same-sex impostors; others are selected regardless of demographics. The exception, in the green column, uses "matched-covariates" i.e. impostors of the same sex, age group, and country of birth. The second pink column includes effects of extended ageing. Missing entries for border, visa, mugshot and wild images generally mean the algorithm did not run to completion. The VISA *columns compare images described in section 2.1. The* MUGSHOT *columns compare images described in section 2.5. The* VISA-BORDER *column compare images described in section 2.2 with those of section 2.4. The* BORDER *column compares images described in section 2.4. The* KIOSK-BORDER *columns compare images described in section 2.6 with those of section 2.4.*

FNMR(T) "False non-match rate"
FMR(T) "False match rate"

		FALSE NON-MATCH RATE (FNMR)																	
	Algorithm	CONSTRAINED, COOPERATIVE																LESS CONSTRAINED, NON-COOP.	
	Name	VISAMC		VISA		MUGSHOT		MUGSHOT12+YRS		VISABORDER		BORDER		BORDER		KIOSKBORDER			
	FMR	0.0001		1E-06		1E-05		1E-05		1E-06		1E-06		1E-05		1E-06			
89	chtface-006	0.0029	124	0.0043	129	0.0026	101	0.0034	126	0.0040	140	0.2701	366	0.0065	98	0.4464	224		
90	cist-003	0.0065	266	0.0087	250	0.0046	251	0.0068	263	0.9993	554	0.9994	519	0.9993	540	0.9995	346		
91	cist-004	0.0043	190	0.0062	191	0.0031	151	0.0041	172	0.0031	98	0.0363	257	0.0069	113	0.2732	193		
92	clearviewai-000	0.0010	20	0.0019	29	0.0024	35	0.0028	67	0.0030	87	0.0058	42	0.0050	62	0.0604	33		
93	clearviewai-001	0.0015	44	0.0021	34	0.0024	39	0.0030	87	0.0022	21	0.0745	306	0.0194	278	0.2740	194		
94	closeli-001	0.0136	379	0.0163	344	0.0039	223	0.0054	216	0.0072	235	1.0000	536	0.0094	172	1.0000	380		
95	cloudmatrix-001	0.0668	469	0.1141	471	0.0539	479	0.0905	477	0.3509	500	0.9819	490	0.9010	507	0.9999	348		
96	cloudmatrix-002	0.0075	287	0.0113	297	0.0084	353	0.0120	334	0.9248	544	0.9997	523	0.9985	538	1.0000	384		
97	cloudwalk-hr-003	0.0026	112	0.0041	116	0.0040	229	0.0058	231	0.0060	213	0.9992	516	0.0094	170	-			
98	cloudwalk-hr-004	0.0009	13	0.0018	26	0.0034	186	0.0028	73	0.0052	187	0.9992	517	0.0093	169	-			
99	cloudwalk-mt-006	0.0006	8	0.0006	2	0.0023	21	0.0019	1	0.0016	3	0.0032	2	0.0030	5	0.0427	2		
100	cloudwalk-mt-007	0.0006	6	0.0007	3	0.0023	23	0.0019	2	0.0016	2	0.0032	1	0.0030	4	0.0419	1		
101	cmcuni-001	0.0025	108	0.0038	108	0.0025	66	0.0025	44	0.0022	19	0.0052	33	0.0034	11	0.0660	54		
102	codeline-000	0.0057	237	0.0079	235	0.0037	204	0.0053	215	0.2721	493	1.0000	537	0.9763	522	1.0000	387		
103	cogent-007	0.0022	89	0.0038	107	0.0028	130	0.0031	92	0.0040	141	0.0082	79	0.0067	102	0.1395	134		
104	cogent-008	0.0015	43	0.0027	57	0.0023	24	0.0025	42	0.0033	114	0.0063	54	0.0055	73	0.0884	85		
105	cognitec-004	0.0036	170	0.0053	175	0.0053	279	0.0056	223	0.0098	284	0.0202	195	0.0154	246	0.3436	205		
106	cognitec-005	0.0022	84	0.0030	72	0.0035	191	0.0041	166	0.0079	246	0.0480	277	0.0233	299	0.2134	173		
107	cor-001	0.0075	288	0.0113	296	0.0055	289	0.0084	300	0.0091	268	0.0148	154	0.0092	167	-			
108	coretech-001	0.0052	219	0.0067	205	0.0083	351	0.0092	310	0.0346	410	0.1363	334	0.0252	305	0.6210	245		
109	coretech-002	0.0020	68	0.0036	95	0.0064	313	0.0064	255	0.0118	310	0.0157	163	0.0110	200	0.3091	200		
110	corsight-002	0.0053	224	0.0068	207	0.0030	143	0.0041	171	0.0039	136	0.0079	75	0.0054	71	0.0747	65		
111	corsight-003	0.0026	110	0.0040	115	0.0028	122	0.0045	187	0.0035	123	0.0059	48	0.0046	46	0.0637	49		
112	csc-002	0.0099	331	0.0132	314	0.0077	337	0.0142	367	0.0126	316	0.0195	189	0.0146	239	-			
113	csc-003	0.0053	225	0.0065	196	0.0037	206	0.0047	191	0.0074	241	0.0124	139	0.0112	204	0.0928	100		
114	ctbcbank-000	0.0168	399	0.0250	397	0.0146	419	0.0224	412	0.0211	382	0.8964	463	0.3779	444	-			
115	ctbcbank-001	0.0155	393	0.0235	391	0.0148	424	0.0243	419	0.0207	377	0.9279	470	0.3469	439	-			
116	cu-face-003	0.0036	169	0.0049	163	0.0031	158	0.0037	153	0.0030	89	0.3075	372	0.1310	397	0.7046	257		
117	cu-face-004	-		-		0.0032	166	0.0035	132	0.0026	62	0.4284	394	0.2115	417	0.7861	264		
118	cubox-002	0.0034	159	0.0041	117	0.0025	62	0.0025	45	0.0033	113	0.0064	55	0.0058	82	0.0519	15		
119	cubox-003	0.0021	80	0.0028	61	0.0024	58	0.0026	50	0.0025	48	0.0046	16	0.0037	20	0.0495	12		
120	cudocommunication-001	0.4777	518	1.0000	555	0.4373	521	0.5360	519	1.0000	569	1.0000	563	1.0000	568	1.0000	455		
121	cuhkee-001	0.0036	172	0.0045	139	0.0031	159	0.0046	188	0.0051	186	0.0095	107	0.0079	133	-			
122	cybercore-002	0.0092	322	0.0119	300	0.0049	262	0.0072	271	0.9105	543	1.0000	544	1.0000	549	1.0000	385		
123	cybercore-003	0.0155	392	0.0164	345	0.0032	169	0.0033	118	0.0024	30	0.9719	485	0.8213	495	0.9993	341		
124	cyberextruder-003	0.0109	348	0.0169	350	0.0071	327	0.0112	330	0.0165	347	0.0410	266	0.0272	312	0.2308	176		
125	cyberextruder-004	0.0118	361	0.0181	364	0.0081	345	0.0133	352	0.0191	371	0.0329	241	0.0268	310	0.1904	164		
126	cyberlink-012	0.0010	21	0.0016	20	0.0036	197	0.0035	135	0.0047	172	0.0099	113	0.0074	125	0.1350	132		
127	cyberlink-013	0.0011	26	0.0017	21	0.0037	202	0.0036	142	0.0045	162	0.0090	96	0.0080	137	0.0924	98		
128	dahua-006	0.0027	113	0.0039	111	0.0031	156	0.0039	163	0.0039	135	0.0067	63	0.0058	80	-			
129	dahua-007	0.0017	51	0.0023	38	0.0026	92	0.0032	106	0.0033	109	0.0060	50	0.0054	70	0.0678	57		
130	daon-000	0.0095	326	0.0117	299	0.0068	319	0.0077	286	0.0092	271	0.0174	177	0.0137	227	0.1430	139		
131	datech-000	0.0020	74	0.0031	78	0.0031	154	0.0041	170	0.0033	112	0.1646	337	0.0667	366	0.4898	230		
132	datech-001	-		-		0.0028	124	0.0034	124	0.0026	67	0.2308	358	0.0818	375	0.5505	234		

Table 25: FNMR is the proportion of mated comparisons below a threshold set to achieve the FMR given in the header on the fourth row. FMR is the proportion of impostor comparisons at or above that threshold. The light grey values give rank over all algorithms in that column. The pink columns use only same-sex impostors; others are selected regardless of demographics. The exception, in the green column, uses "matched-covariates" i.e. impostors of the same sex, age group, and country of birth. The second pink column includes effects of extended ageing. Missing entries for border, visa, mugshot and wild images generally mean the algorithm did not run to completion. The VISA *columns compare images described in section 2.1. The* MUGSHOT *columns compare images described in section 2.5. The* VISA-BORDER *column compare images described in section 2.2 with those of section 2.4. The* BORDER *column compares images described in section 2.4. The* KIOSK-BORDER *columns compare images described in section 2.6 with those of section 2.4.*

FNMR(T) "False non-match rate"
FMR(T) "False match rate"

	Algorithm	FALSE NON-MATCH RATE (FNMR)															
		CONSTRAINED, COOPERATIVE														LESS CONSTRAINED, NON-COOP.	
	Name	VISAMC		VISA		MUGSHOT		MUGSHOT12+YRS		VISABORDER		BORDER		BORDER		KIOSKBORDER	
	FMR	0.0001		1E-06		1E-05		1E-05		1E-06		1E-06		1E-05		1E-06	
133	decatur-000	0.0714	470	0.1115	469	0.0608	484	0.1106	487	0.0866	459	1.0000	542	0.0714	369	-	
134	decatur-001	0.0424	452	0.0711	455	0.0237	443	0.0458	447	0.0447	430	1.0000	533	0.9969	536	1.0000	394
135	decloakface-001	0.0795	473	0.1131	470	0.3127	512	0.4259	512	0.2118	487	0.7926	443	0.6088	466	0.9589	295
136	deepglint-004	0.0025	104	0.0034	86	0.0039	224	0.0061	247	0.0050	182	0.0091	99	0.0082	142	0.1003	107
137	deepglint-005	0.0052	220	0.0059	188	0.0030	139	0.0031	93	0.0033	117	0.7620	435	0.1535	404	0.9912	320
138	deepsea-001	0.0136	380	0.0215	383	0.0142	415	0.0214	410	0.0163	345	0.0250	215	0.0192	275	-	
139	deepsense-002	0.0010	19	0.0016	19	0.0024	30	0.0023	22	0.0026	54	0.0052	34	0.0043	37	0.0781	69
140	deepsense-003	0.0009	18	0.0015	17	0.0025	71	0.0024	26	0.0023	26	0.0457	272	0.0097	176	0.2547	186
141	dermalog-011	0.0045	195	0.0062	193	0.0035	192	0.0059	236	0.0057	208	0.2242	353	0.0407	333	0.6329	246
142	dermalog-012	0.0080	297	0.0101	277	0.0037	208	0.0057	228	0.0055	198	0.0095	108	0.0068	108	0.0834	78
143	dicio-001	0.5486	529	0.6442	522	0.7516	542	0.8607	540	0.8678	537	0.8268	451	0.7034	480	0.9752	303
144	didiglobalface-001	0.0055	232	0.0092	261	0.0030	142	0.0045	186	0.0088	261	0.0119	135	0.0085	154	-	
145	didiglobalface-002	0.0033	151	0.0051	171	0.0026	93	0.0034	128	0.0033	111	0.0085	86	0.0047	52	0.1135	118
146	digidata-000	0.0967	478	0.1410	474	0.2596	509	0.3462	507	0.0293	403	0.0363	256	0.0212	291	0.1849	163
147	digidata-001	0.0224	422	0.0352	417	0.0330	459	0.0570	463	0.0109	301	0.0481	278	0.0123	219	0.3055	199
148	digitalbarriers-002	0.3360	506	0.3690	498	0.0877	491	0.1557	493	0.0971	466	0.0951	315	0.0497	351	-	
149	dps-000	0.0115	357	0.0176	361	0.0149	425	0.0185	398	0.0173	359	0.0275	225	0.0180	266	0.1757	157
150	dsk-000	0.1526	488	0.2169	485	0.3787	517	0.5426	520	0.3115	497	0.3089	374	0.1994	414	-	
151	einetworks-000	0.0099	332	0.0180	363	0.0088	360	0.0140	363	0.0130	320	0.0225	208	0.0147	241	-	
152	einetworksindia-000	0.0058	245	0.0074	224	0.0051	274	0.0061	248	0.0074	239	0.0193	188	0.0102	187	0.1819	160
153	einetworksindia-001	0.0042	187	0.0062	192	0.0048	256	0.0064	253	0.0057	206	0.0473	275	0.0092	166	0.3984	218
154	ekin-002	0.1168	482	0.2042	483	0.1530	502	0.2524	501	0.1777	481	0.2773	368	0.1347	398	0.8954	284
155	element-000	0.0023	94	0.0035	93	0.0024	51	0.0026	46	0.0029	83	0.0060	51	0.0048	54	0.0631	46
156	enface-001	0.0072	281	0.0107	284	0.0071	324	0.0138	359	0.0068	229	0.0515	281	0.0094	173	0.9942	324
157	enface-002	0.0033	150	0.0052	174	0.0038	217	0.0073	274	0.0026	66	0.9998	527	0.9995	542	1.0000	383
158	eocortex-000	0.3485	507	0.6943	530	0.1122	494	0.1574	494	0.2155	488	0.2257	357	0.1606	408	-	
159	ercacat-001	0.0036	171	0.0044	135	0.0033	178	0.0047	192	0.0106	295	0.0202	194	0.0184	269	-	
160	euronovate-003	0.0061	258	0.0088	253	0.0040	231	0.0060	241	0.0065	224	0.7815	441	0.5034	457	0.9823	307
161	euronovate-004	0.0082	301	0.0110	292	0.0050	270	0.0077	285	0.0074	240	0.6949	424	0.3354	437	0.9791	306
162	expasoft-001	0.0328	442	0.0488	434	0.0211	438	0.0342	434	0.0629	449	0.6483	417	0.2816	428	-	
163	expasoft-002	0.0170	401	0.0274	405	0.0787	490	0.0768	473	0.1629	477	0.9996	522	0.9631	520	1.0000	370
164	f8-001	0.0249	426	0.0336	413	0.0178	430	0.0232	415	0.0303	405	0.0615	292	0.0408	334	-	
165	f8-002	0.0340	444	0.0591	449	0.0213	439	0.0374	440	0.0452	431	0.0760	307	0.0502	352	0.2708	192
166	facehawk-000	1.0000	569	1.0000	561	1.0000	572	1.0000	567	1.0000	567	1.0000	564	1.0000	558	1.0000	521
167	facelocate-001	-		-		0.0664	487	0.1171	488	0.0950	465	0.9219	468	0.7041	481	0.9985	335
168	faceonlive-001	0.0269	431	0.0359	420	0.0387	467	0.0721	471	0.0246	395	0.0349	252	0.0220	294	0.2408	179
169	faceonlive-002	0.0121	366	0.0135	318	0.0033	181	0.0041	168	0.0037	131	0.9427	475	0.7927	492	0.9993	340
170	facephi-000	0.0044	192	0.0059	185	0.0047	252	0.0057	229	0.0088	262	1.0000	549	1.0000	552	1.0000	389
171	facesoft-000	0.0085	309	0.0112	293	0.0064	310	0.0107	325	0.0091	267	0.0171	173	0.0107	196	-	
172	facetag-000	0.2836	501	0.4081	503	0.2933	511	0.4303	513	0.3448	499	0.6312	414	0.3530	440	0.9753	304
173	facetag-002	0.0098	329	0.0147	331	0.0064	314	0.0110	327	0.0116	308	0.0190	186	0.0119	216	0.1334	130
174	facex-001	1.0000	570	1.0000	562	1.0000	565	1.0000	565	1.0000	566	1.0000	565	1.0000	556	-	
175	facex-002	0.0803	474	0.1404	473	0.1283	498	0.1979	499	0.1440	472	0.1952	345	0.1299	395	0.7427	258
176	facia-001	0.0083	305	0.0124	306	0.0064	312	0.0097	317	0.0098	285	0.9983	512	0.9849	523	1.0000	379

Table 26: FNMR is the proportion of mated comparisons below a threshold set to achieve the FMR given in the header on the fourth row. FMR is the proportion of impostor comparisons at or above that threshold. The light grey values give rank over all algorithms in that column. The pink columns use only same-sex impostors; others are selected regardless of demographics. The exception, in the green column, uses "matched-covariates" i.e. impostors of the same sex, age group, and country of birth. The second pink column includes effects of extended ageing. Missing entries for border, visa, mugshot and wild images generally mean the algorithm did not run to completion. The VISA *columns compare images described in section 2.1. The* MUGSHOT *columns compare images described in section 2.5. The* VISA-BORDER *column compare images described in section 2.2 with those of section 2.4. The* BORDER *column compares images described in section 2.4. The* KIOSK-BORDER *columns compare images described in section 2.6 with those of section 2.4.*

	Algorithm	FALSE NON-MATCH RATE (FNMR)															
		CONSTRAINED, COOPERATIVE														LESS CONSTRAINED, NON-COOP.	
	Name	VISAMC		VISA		MUGSHOT		MUGSHOT12+YRS		VISABORDER		BORDER		BORDER		KIOSKBORDER	
	FMR	0.0001		1E-06		1E-05		1E-05		1E-06		1E-06		1E-05		1E-06	
177	farfaces-001	0.4890	523	0.5860	521	0.5650	527	0.7268	530	0.8015	525	0.7511	431	0.5892	464	0.9536	294
178	fastenterprises-000	0.0093	323	0.0151	337	0.0098	375	0.0140	364	0.0209	379	0.2991	369	0.1608	409	0.6727	250
179	fedu-001	-		-		0.0033	173	0.0047	190	0.0128	317	0.9816	489	0.9216	509	0.9999	351
180	fiberhome-nanjing-003	0.0090	314	0.0139	322	0.0082	347	0.0144	369	0.0110	302	0.0174	175	0.0107	197	-	
181	fiberhome-nanjing-004	0.0037	177	0.0056	183	0.0031	153	0.0043	176	0.0043	156	0.0083	83	0.0061	93	-	
182	fincore-000	0.0309	439	0.0502	436	0.0281	451	0.0510	457	0.0521	442	0.0815	310	0.0522	353	0.3100	201
183	firstcreditkz-002	0.0018	60	0.0026	48	0.0024	45	0.0024	31	0.0029	86	0.0056	39	0.0049	59	0.0624	40
184	firstcreditkz-003	-		-		0.0023	26	0.0024	33	0.0026	59	0.0104	120	0.0047	50	0.0910	95
185	foomobi-001	0.4827	521	0.5795	517	0.6823	535	0.8132	536	0.8217	528	1.0000	558	1.0000	566	1.0000	439
186	foomobi-002	0.4827	520	0.5795	516	0.6823	534	0.8132	535	0.8217	527	1.0000	562	1.0000	569	1.0000	452
187	fpt-000	-		-		0.0213	440	0.0375	441	0.0364	413	0.9528	477	0.8729	502	0.9993	342
188	fraudcom-000	0.0110	350	0.0173	353	0.0083	349	0.0139	361	0.0166	348	0.0258	218	0.0177	262	0.1488	144
189	frpkauai-001	0.0023	91	0.0035	91	0.0026	79	0.0030	89	0.0040	143	0.0080	76	0.0072	119	0.0706	59
190	frpkauai-002	0.0024	101	0.0035	88	0.0024	53	0.0024	35	0.0033	116	0.0065	58	0.0058	83	0.0599	31
191	fujitsulab-002	0.0091	320	0.0124	307	0.0105	384	0.0156	377	0.0169	354	0.0345	251	0.0146	240	-	
192	fujitsulab-003	0.0045	196	0.0065	197	0.0057	293	0.0083	297	0.0080	248	0.0154	158	0.0101	184	0.5564	235
193	g42-intellibrain-001	0.0006	7	0.0009	8	0.0037	203	0.0044	179	0.0030	94	0.0059	46	0.0053	68	0.0750	66
194	g42-intellibrain-002	0.0006	9	0.0011	10	0.0029	134	0.0037	155	0.0028	73	0.0212	199	0.0091	164	0.1398	135
195	geo-002	0.0171	404	0.0187	368	0.0035	190	0.0051	207	0.0064	218	0.0117	133	0.0083	150	0.0938	101
196	geo-004	0.0030	126	0.0041	119	0.0025	72	0.0030	81	0.0035	122	0.0065	57	0.0053	67	0.0648	51
197	gistouch-000	0.0296	435	0.0518	440	0.0342	463	0.0609	466	0.0493	437	1.0000	550	1.0000	555	1.0000	395
198	gistouch-001	0.0176	407	0.0312	409	0.8931	552	0.9735	552	0.8625	533	1.0000	553	1.0000	571	1.0000	397
199	glory-006	0.0050	209	0.0068	206	0.0051	276	0.0070	268	0.0069	230	0.7869	442	0.5076	458	0.9719	299
200	glory-007	0.0050	214	0.0068	209	0.0050	269	0.0069	266	0.0068	227	0.0126	143	0.0083	149	0.1066	113
201	gorilla-008	0.0058	244	0.0091	258	0.0049	261	0.0079	292	0.0079	247	0.0126	142	0.0091	165	0.1217	124
202	gorilla-009	0.0049	204	0.0072	215	0.0038	215	0.0056	224	0.0065	222	0.0104	119	0.0070	114	0.1103	115
203	gpstechvn-000	0.0202	416	0.0355	419	0.0142	414	0.0248	420	0.0208	378	0.0495	280	0.0207	287	0.5098	232
204	graymatics-001	0.1039	479	0.1620	479	0.1344	500	0.1917	498	0.1648	478	0.5160	401	0.2689	425	0.9194	289
205	griaule-001	0.0057	240	0.0078	234	0.0045	247	0.0065	258	0.0070	231	0.7515	432	0.5106	459	0.9747	301
206	griaule-002	0.0021	82	0.0032	80	0.0025	76	0.0027	61	0.0034	120	0.0996	319	0.0201	283	0.3978	216
207	hertasecurity-002	0.0206	417	0.0315	410	0.0060	298	0.0078	288	0.0253	397	0.0696	304	0.0457	345	0.4565	225
208	hertasecurity-003	0.0079	294	0.0104	280	0.0060	299	0.0078	287	0.0255	398	0.0732	305	0.0460	346	0.4731	227
209	hik-001	0.0096	328	0.0125	309	0.0093	371	0.0164	387	0.0108	300	0.0937	313	0.0127	220	-	
210	hisign-002	0.0029	122	0.0044	134	0.0027	115	0.0032	112	0.0028	80	0.0409	265	0.0132	223	0.2016	169
211	hisign-003	-		-		0.0030	140	0.0036	141	0.0036	126	0.0582	286	0.0201	284	0.2584	187
212	hyperverge-003	0.0019	66	0.0030	69	0.0025	64	0.0029	78	0.0027	68	0.0049	30	0.0042	34	0.0576	25
213	hyperverge-005	0.0026	111	0.0039	114	0.0027	103	0.0031	102	0.0036	128	0.0066	60	0.0055	72	0.0658	53
214	hzailu-005	0.0172	405	0.0197	374	0.0028	129	0.0036	145	0.0032	107	0.0058	43	0.0048	55	0.0751	67
215	hzailu-006	0.0161	397	0.0174	355	0.0024	48	0.0027	52	0.0026	60	0.0049	29	0.0044	43	0.0654	52
216	i2v-001	-		-		0.0946	492	0.1369	491	0.3989	507	0.9998	525	0.9966	534	1.0000	371
217	icm-004	0.0079	293	0.0120	301	0.0074	334	0.0107	324	0.0091	269	0.0281	229	0.0128	221	0.2778	195
218	icm-005	0.0100	333	0.0140	323	0.0091	362	0.0108	326	0.0169	353	0.0319	239	0.0290	318	0.1775	159
219	icomm-000	0.0019	65	0.0033	83	0.0033	180	0.0044	180	0.0031	102	0.1350	332	0.0552	358	0.4196	221
220	icthtc-000	0.0260	428	0.0396	425	0.0207	437	0.0339	433	0.0291	402	0.0474	276	0.0346	325	-	

Table 27: FNMR is the proportion of mated comparisons below a threshold set to achieve the FMR given in the header on the fourth row. FMR is the proportion of impostor comparisons at or above that threshold. The light grey values give rank over all algorithms in that column. The pink columns use only same-sex impostors; others are selected regardless of demographics. The exception, in the green column, uses "matched-covariates" i.e. impostors of the same sex, age group, and country of birth. The second pink column includes effects of extended ageing. Missing entries for border, visa, mugshot and wild images generally mean the algorithm did not run to completion. The VISA *columns compare images described in section 2.1. The* MUGSHOT *columns compare images described in section 2.5. The* VISA-BORDER *column compare images described in section 2.2 with those of section 2.4. The* BORDER *column compares images described in section 2.4. The* KIOSK-BORDER *columns compare images described in section 2.6 with those of section 2.4.*

	Algorithm	FALSE NON-MATCH RATE (FNMR)															
		CONSTRAINED, COOPERATIVE														LESS CONSTRAINED, NON-COOP.	
	Name	VISAMC		VISA		MUGSHOT		MUGSHOT12+YRS		VISABORDER		BORDER		BORDER		KIOSKBORDER	
	FMR	0.0001		1E-06		1E-05		1E-05		1E-06		1E-06		1E-05		1E-06	
221	id3-006	0.0072	282	0.0103	279	0.0049	263	0.0074	277	0.0095	275	0.0165	169	0.0119	215	-	
222	id3-008	0.0039	181	0.0055	180	0.0032	167	0.0042	174	0.0081	250	0.0155	160	0.0134	225	0.1186	119
223	idemia-009	0.0022	88	0.0030	74	0.0022	13	0.0023	24	0.0023	23	0.0046	17	0.0039	24	0.0533	16
224	idemia-010	0.0015	45	0.0026	46	0.0022	14	0.0020	5	0.0020	13	0.0040	10	0.0033	9	0.0465	6
225	identy-000	0.0073	284	0.0095	266	0.0050	266	0.0067	261	0.0071	234	0.8257	450	0.4310	450	0.9839	310
226	igearx-face-000	0.0091	317	0.0146	329	0.0163	428	0.0362	438	0.0399	419	0.6436	416	0.3305	436	0.7832	263
227	iit-002	0.0111	355	0.0177	362	0.0085	355	0.0140	362	0.0193	372	0.0332	246	0.0260	307	-	
228	iit-003	0.0082	302	0.0151	336	0.0053	281	0.0084	301	0.0122	313	0.0199	192	0.0137	226	-	
229	imds-software-002	0.0048	202	0.0072	218	0.0036	199	0.0052	210	0.0047	170	0.9981	510	0.0078	131	1.0000	373
230	imds-software-003	0.0032	137	0.0047	152	0.0028	120	0.0036	147	0.0036	127	0.9987	513	0.0063	95	1.0000	368
231	imperial-000	0.0067	269	0.0108	288	0.0080	343	0.0134	356	0.0087	259	0.0581	285	0.0102	188	-	
232	imperial-002	0.0058	247	0.0081	240	0.0055	288	0.0085	304	0.0083	254	0.0157	161	0.0103	189	-	
233	incode-009	0.0044	191	0.0067	204	0.0034	187	0.0051	204	0.0049	180	0.0091	98	0.0067	103	0.0892	88
234	incode-013	0.0035	163	0.0049	159	0.0032	162	0.0039	162	0.0051	184	0.0094	104	0.0081	141	0.0768	68
235	infocert-001	0.0105	345	0.0172	352	0.0078	339	0.0125	340	0.0159	339	0.1573	335	0.0565	359	0.5716	238
236	innefulabs-000	0.0122	367	0.0199	376	0.0112	398	0.0197	404	0.0222	384	0.0372	261	0.0271	311	-	
237	innominds-001	0.5569	530	0.6541	525	0.7642	546	0.8665	543	0.7629	520	0.8200	447	0.6359	471	0.9841	312
238	innovativetechnologyltd-001	0.0578	464	0.0938	466	0.0501	477	0.0981	479	0.0592	447	0.0779	309	0.0422	338	-	
239	innovativetechnologyltd-002	0.0451	455	0.0716	456	0.0541	480	0.1009	482	0.0506	439	0.0682	300	0.0371	329	-	
240	innovatrics-010	0.0017	58	0.0031	79	0.0027	113	0.0028	65	0.0041	147	0.0078	73	0.0066	101	0.0744	64
241	innovatrics-011	-		-		0.0026	98	0.0027	55	0.0032	105	0.0060	49	0.0044	41	0.0615	38
242	insightface-003	0.0015	40	0.0021	33	0.0045	246	0.0034	127	0.1298	468	1.0000	559	0.9407	511	1.0000	438
243	insightface-004	0.0015	41	0.0023	39	0.0052	278	0.0036	146	0.1403	471	0.9923	501	0.9128	508	0.9989	336
244	inspur-001	0.0035	162	0.0049	157	0.0025	67	0.0030	86	0.0029	85	0.9951	504	0.9592	517	1.0000	362
245	inspur-002	0.0025	105	0.0039	113	0.0024	32	0.0027	54	0.0031	97	0.0062	53	0.0047	51	0.1112	117
246	intellicloudai-001	0.0142	385	0.0234	390	0.0092	367	0.0145	370	0.0162	343	0.0371	260	0.0171	259	-	
247	intellicloudai-002	0.0059	251	0.0085	249	0.0060	300	0.0069	267	0.0108	298	0.2477	364	0.0171	258	-	
248	intellifusion-001	0.0072	280	0.0094	264	0.0056	292	0.0085	305	0.0111	304	0.0212	200	0.0143	234	-	
249	intellifusion-002	0.0059	250	0.0077	233	0.0040	228	0.0074	276	0.0085	257	0.5352	404	0.0104	194	-	
250	intellivision-006	0.0111	354	0.0174	356	0.0110	392	0.0162	384	0.0181	363	0.0313	235	0.0191	274	0.2416	180
251	intellivision-007	0.0086	310	0.0128	313	0.0098	376	0.0159	382	0.0133	323	0.0218	204	0.0154	247	0.1751	156
252	intellivix-004	0.0032	139	0.0045	143	0.0025	74	0.0031	101	0.0040	139	0.0074	68	0.0063	96	0.0662	55
253	intellivix-005	0.0034	161	0.0048	154	0.0024	36	0.0027	60	0.0035	121	0.0067	62	0.0059	91	0.0609	36
254	intelresearch-008	0.0009	15	0.0013	11	0.0025	65	0.0025	38	0.0028	77	0.0304	233	0.0048	56	0.2375	178
255	intelresearch-009	-		-		0.0024	60	0.0025	40	0.0028	79	0.0058	44	0.0046	47	0.0665	56
256	intema-000	0.0012	29	0.0017	23	0.0023	15	0.0022	16	0.0022	20	0.0172	174	0.0061	92	0.0996	106
257	intema-001	0.0010	23	0.0014	14	0.0021	5	0.0020	8	0.0019	11	0.0037	7	0.0030	6	0.0457	5
258	intozi-001	0.9982	545	0.9998	545	0.9998	563	1.0000	566	1.0000	558	1.0000	546	1.0000	554	1.0000	427
259	intsysmsu-001	0.9543	544	0.9888	544	0.9923	558	0.9948	558	0.9977	552	0.9955	505	0.9892	526	-	
260	intsysmsu-002	0.0130	376	0.0254	399	0.0137	412	0.0267	426	0.0160	340	0.0267	222	0.0145	238	-	
261	ionetworks-001	0.0254	427	0.0388	424	0.0435	473	0.0662	468	0.0426	424	0.8936	461	0.7391	488	0.9964	331
262	ionetworks-002	0.0045	193	0.0066	198	0.0033	177	0.0047	193	0.0544	443	0.9648	482	0.8765	504	0.9994	343
263	iqface-000	0.0091	319	0.0143	324	0.0075	336	0.0110	328	0.0171	358	0.2234	352	0.0359	327	-	
264	iqface-003	0.0058	248	0.0079	236	0.0051	275	0.0058	234	0.0104	293	0.0200	193	0.0193	276	-	

Table 28: FNMR is the proportion of mated comparisons below a threshold set to achieve the FMR given in the header on the fourth row. FMR is the proportion of impostor comparisons at or above that threshold. The light grey values give rank over all algorithms in that column. The pink columns use only same-sex impostors; others are selected regardless of demographics. The exception, in the green column, uses "matched-covariates" i.e. impostors of the same sex, age group, and country of birth. The second pink column includes effects of extended ageing. Missing entries for border, visa, mugshot and wild images generally mean the algorithm did not run to completion. The VISA *columns compare images described in section 2.1. The* MUGSHOT *columns compare images described in section 2.5. The* VISA-BORDER *column compare images described in section 2.2 with those of section 2.4. The* BORDER *column compares images described in section 2.4. The* KIOSK-BORDER *columns compare images described in section 2.6 with those of section 2.4.*

2024/04/17 08:45:50

FNMR(T) "False non-match rate"
FMR(T) "False match rate"

	Algorithm	FALSE NON-MATCH RATE (FNMR)															
		CONSTRAINED, COOPERATIVE														LESS CONSTRAINED, NON-COOP.	
	Name	VISAMC		VISA		MUGSHOT		MUGSHOT12+YRS		VISABORDER		BORDER		BORDER		KIOSKBORDER	
	FMR	0.0001		1E-06		1E-05		1E-05		1E-06		1E-06		1E-05		1E-06	
265	irex-000	0.0052	218	0.0099	272	0.0056	291	0.0083	298	0.0137	327	0.0163	167	0.0078	130	-	
266	isap-001	0.5092	525	0.6588	526	0.6899	538	0.7978	534	0.7200	517	0.7253	428	0.5373	462	-	
267	isap-002	0.0114	356	0.0186	366	0.0087	358	0.0151	375	0.0156	338	0.5134	400	0.0333	321	-	
268	isityou-000	0.5682	532	0.7033	532	1.0000	571	0.9999	563	1.0000	564	1.0000	567	1.0000	560	-	
269	isystems-001	0.0149	389	0.0245	395	0.0138	413	0.0210	408	0.0209	381	0.0332	245	0.0223	296	-	
270	isystems-002	0.0118	360	0.0182	365	0.0111	395	0.0162	385	0.0166	349	0.0284	230	0.0195	279	-	
271	itmo-007	0.0080	296	0.0125	308	0.0107	386	0.0185	396	0.0167	351	0.0222	205	0.0144	237	-	
272	itmo-008	0.0090	315	0.0150	334	0.0058	294	0.0059	238	0.0187	367	0.0355	253	0.0339	322	0.1758	158
273	ivacognitive-001	0.0189	410	0.0351	416	0.0123	406	0.0235	416	0.0198	375	0.0274	224	0.0155	248	-	
274	iws-000	0.4824	519	0.5801	518	0.6859	537	0.8155	537	0.8251	529	0.7756	438	0.6400	473	-	
275	jaakit-001	0.5830	533	0.7146	533	0.8173	549	0.8893	548	0.8950	540	0.8387	454	0.7091	483	0.9733	300
276	kakao-008	0.0011	24	0.0018	27	0.0023	17	0.0023	20	0.0021	18	0.0041	11	0.0035	13	0.0475	8
277	kakao-009	0.0009	16	0.0013	12	0.0023	19	0.0023	21	0.0020	14	0.0039	9	0.0034	10	0.0468	7
278	kakaobank-001	0.0030	127	0.0046	145	0.0032	170	0.0039	159	0.0049	178	0.9998	528	0.9994	541	1.0000	393
279	kakaobank-002	-		-		0.0026	90	0.0036	140	0.0038	132	0.3184	378	0.1174	392	0.6931	254
280	kakaopay-001	0.0152	391	0.0252	398	0.0145	418	0.0270	427	0.0232	387	0.0344	250	0.0194	277	0.2005	168
281	kasikornlabs-002	0.0069	271	0.0091	257	0.0048	257	0.0063	251	0.0076	243	0.0144	152	0.0110	201	0.1249	127
282	kasikornlabs-003	0.0057	235	0.0076	228	0.0042	237	0.0056	225	0.0059	210	0.0123	137	0.0098	177	0.1212	123
283	kedacom-000	0.0055	231	0.0081	242	0.0111	397	0.0120	335	0.0415	422	0.0966	317	0.0686	367	-	
284	kiwitech-000	0.0076	289	0.0105	282	0.0081	346	0.0128	347	0.0096	277	0.0163	166	0.0101	185	-	
285	kneron-003	0.0542	463	0.0902	463	0.0346	464	0.0562	461	0.0919	463	0.1251	328	0.0973	384	-	
286	kneron-005	0.0157	394	0.0259	401	0.0126	410	0.0212	409	0.0406	421	0.0693	303	0.0542	357	-	
287	knowutech-000	0.0039	182	0.0055	179	0.0028	133	0.0042	173	0.0042	150	0.0077	71	0.0059	87	0.0820	75
288	kogniza-001	-		-		0.0028	132	0.0031	105	0.0025	46	0.0048	23	0.0042	31	0.0557	21
289	kookmin-002	0.0054	229	0.0077	231	0.0043	240	0.0065	257	0.0123	314	0.7591	434	0.0198	282	-	
290	koreaid-001	0.0031	135	0.0045	141	0.0026	91	0.0032	108	0.0043	155	0.0083	80	0.0068	109	0.0743	63
291	krungthai-002	0.0105	344	0.0161	341	0.0091	364	0.0141	365	0.7350	518	0.9889	495	0.9605	518	0.9999	350
292	kuke3d-001	0.0058	242	0.0104	281	0.0083	350	0.0093	311	0.0270	400	0.9901	497	0.8341	496	1.0000	363
293	kuke3d-002	0.0077	290	0.0135	317	0.0069	321	0.0098	318	0.0111	303	1.0000	548	1.0000	553	1.0000	375
294	lebentech-000	0.5940	534	0.7032	531	0.8854	551	0.9511	551	0.9089	542	0.9970	507	0.9861	525	0.9999	353
295	lebentech-001	0.0304	438	0.9032	540	0.9998	564	1.0000	564	1.0000	559	1.0000	540	0.9999	548	1.0000	390
296	lemalabs-001	0.0111	353	0.0175	358	0.0088	359	0.0142	366	0.0143	331	0.0228	209	0.0140	230	0.1646	153
297	lineclova-002	0.0021	76	0.0035	89	0.0025	61	0.0027	57	0.0041	145	0.0086	89	0.0072	118	0.1595	148
298	lineclova-003	0.0018	63	0.0030	70	0.0028	131	0.0031	94	0.0041	146	0.0083	82	0.0075	128	0.1014	108
299	lookman-002	0.0297	436	0.0547	445	0.0339	461	0.0562	460	0.0614	448	0.0960	316	0.0790	372	-	
300	lookman-004	0.0074	286	0.0099	273	0.0124	408	0.0149	374	0.0430	426	0.0866	311	0.0694	368	-	
301	luxand-001	0.0116	358	0.0925	464	0.0144	417	0.0267	425	1.0000	563	1.0000	568	1.0000	561	1.0000	501
302	luxand-003	-		-		0.9938	559	0.9999	561	0.2905	496	0.2256	356	0.0849	378	0.4876	229
303	mantra-000	0.0037	175	0.0052	173	0.0054	285	0.0056	226	0.0097	282	0.0181	180	0.0151	245	-	
304	maxvision-005	0.0014	37	0.0026	51	0.0024	41	0.0024	27	0.0025	40	0.1216	326	0.0332	320	0.3922	215
305	maxvision-006	0.0016	49	0.0026	49	0.0024	44	0.0024	30	0.0024	38	0.4012	392	0.1799	412	0.7634	259
306	megvii-008	0.0003	1	0.0008	6	0.0023	27	0.0021	11	0.0024	39	0.0049	27	0.0047	53	0.0541	18
307	megvii-009	0.0003	2	0.0008	7	0.0023	28	0.0021	10	0.0018	6	0.0149	155	0.0036	15	0.1096	114
308	meituan-003	0.0017	50	0.0021	32	0.0024	38	0.0023	25	0.0024	34	0.0084	84	0.0046	45	0.0883	84

Table 29: FNMR is the proportion of mated comparisons below a threshold set to achieve the FMR given in the header on the fourth row. FMR is the proportion of impostor comparisons at or above that threshold. The light grey values give rank over all algorithms in that column. The pink columns use only same-sex impostors; others are selected regardless of demographics. The exception, in the green column, uses "matched-covariates" i.e. impostors of the same sex, age group, and country of birth. The second pink column includes effects of extended ageing. Missing entries for border, visa, mugshot and wild images generally mean the algorithm did not run to completion. The VISA *columns compare images described in section 2.1. The* MUGSHOT *columns compare images described in section 2.5. The* VISA-BORDER *column compare images described in section 2.2 with those of section 2.4. The* BORDER *column compares images described in section 2.4. The* KIOSK-BORDER *columns compare images described in section 2.6 with those of section 2.4.*

FNMR(T) "False non-match rate"
FMR(T) "False match rate"

		FALSE NON-MATCH RATE (FNMR)															
	Algorithm	CONSTRAINED, COOPERATIVE														LESS CONSTRAINED, NON-COOP.	
	Name	VISAMC		VISA		MUGSHOT		MUGSHOT12+YRS		VISABORDER		BORDER		BORDER		KIOSKBORDER	
	FMR	0.0001		1E-06		1E-05		1E-05		1E-06		1E-06		1E-05		1E-06	
309	meituan-004	0.0014	34	0.0021	31	0.0024	40	0.0024	34	0.0023	27	0.0070	64	0.0044	42	0.0813	74
310	meiya-001	0.0171	402	0.0275	406	0.0159	427	0.0261	424	0.0311	406	0.2250	355	0.0245	303	-	
311	mendaxiatech-000	0.0027	115	0.0036	94	0.0029	136	0.0036	149	0.0031	99	0.0057	41	0.0051	63	-	
312	metsakuurcompany-002	0.0048	203	0.0071	213	0.0030	144	0.0043	177	0.0032	106	0.2059	349	0.0665	365	0.5374	233
313	metsakuurcompany-003	0.0034	155	0.0051	168	0.0026	88	0.0036	139	0.0028	74	0.2418	362	0.1001	386	0.5866	240
314	miaxis-002	0.0745	471	0.0774	459	0.3215	513	0.4000	511	0.1485	473	0.2087	350	0.2058	415	0.3846	213
315	miaxis-003	0.0045	194	0.0067	202	0.0037	210	0.0050	202	0.0061	215	0.0139	148	0.0088	160	0.1322	128
316	microfocus-002	0.3605	508	0.5057	511	0.5783	529	0.7223	529	0.5909	513	0.5963	410	0.4160	449	-	
317	microfocus-003	0.0416	450	0.0607	450	0.0652	485	0.1025	483	0.0793	455	0.2248	354	0.0923	381	0.6153	243
318	minivision-000	0.0033	145	0.0048	155	0.0038	218	0.0049	196	0.0055	195	0.0094	106	0.0079	135	-	
319	mitek-000	0.6882	538	0.8192	537	0.9568	555	0.9788	555	0.9545	549	0.9437	476	0.8494	499	0.9931	322
320	mobai-000	0.0360	447	0.0439	430	0.0372	465	0.0700	469	0.0367	414	0.0939	314	0.0795	374	-	
321	mobai-001	0.0199	415	0.0219	385	0.0047	253	0.0061	244	0.0093	273	0.0174	176	0.0138	229	-	
322	mobbl-001	0.3208	502	0.4375	504	0.5680	528	0.7193	528	0.6282	514	0.5783	407	0.3984	446	0.8864	278
323	mobbl-003	0.0087	312	0.0134	316	0.0062	305	0.0087	307	0.0099	286	0.0197	190	0.0122	218	0.1618	152
324	mobipintech-000	0.0090	316	0.0149	333	0.0039	227	0.0057	227	0.0115	307	0.0465	273	0.0182	268	0.6443	247
325	momovn-001	0.1044	480	0.1694	480	0.3253	514	0.5244	517	0.3861	504	0.9995	521	0.9985	537	1.0000	382
326	moredian-000	0.3874	509	0.4912	509	0.9988	561	0.9999	562	0.9990	553	0.9999	531	0.9998	545	-	
327	mukh-003	0.0077	291	0.0113	295	0.0111	396	0.0224	413	0.0061	214	0.7813	440	0.4504	453	0.9899	317
328	mukh-004	0.0050	213	0.0069	211	0.0051	273	0.0099	319	0.0045	161	0.0083	81	0.0059	89	0.1030	110
329	multimodality-000	0.0034	156	0.0047	151	0.0036	200	0.0044	183	0.0077	244	0.9976	509	0.4456	452	1.0000	374
330	multimodality-001	0.0029	123	0.0042	121	0.0031	149	0.0035	131	0.0038	133	0.0071	66	0.0059	86	0.0732	61
331	mvision-001	0.0191	411	0.0233	388	0.0204	435	0.0356	436	0.0198	376	0.0337	248	0.0242	302	-	
332	nazhiai-000	0.0040	183	0.0059	187	0.0036	194	0.0048	195	0.0057	207	0.0125	140	0.0083	148	-	
333	ncsgroup-000	-		-		0.0126	409	0.0226	414	0.0179	362	0.1715	339	0.0287	315	0.6160	244
334	ncssg-001	0.0207	418	0.1540	476	0.0045	245	0.0067	262	0.0056	205	0.1180	325	0.0301	319	0.3908	214
335	neosystems-004	0.0279	432	0.0495	435	0.0289	455	0.0585	465	0.0439	429	0.9621	480	0.1296	394	0.9996	347
336	netbridgetech-001	0.4749	517	0.6599	527	0.4438	522	0.5676	521	0.4491	510	1.0000	534	0.9541	515	-	
337	netbridgetech-002	0.0101	336	0.0166	347	0.0077	338	0.0127	344	0.0133	324	0.8215	448	0.0523	354	-	
338	neurotechnology-017	0.0017	56	0.0031	75	0.0023	16	0.0025	43	0.0025	49	0.0047	22	0.0038	23	0.0612	37
339	neurotechnology-018	0.0020	69	0.0029	64	0.0022	11	0.0024	32	0.0024	36	0.0046	18	0.0037	19	0.0586	27
340	nhn-004	0.0030	125	0.0044	138	0.0025	73	0.0029	80	0.0030	95	0.0331	242	0.0113	206	0.1598	149
341	nhn-005	0.0028	116	0.0043	126	0.0023	25	0.0027	53	0.0025	41	0.0047	19	0.0038	22	0.0554	20
342	nodeflux-002	0.0186	409	0.0340	414	0.0261	448	0.0451	445	0.0548	444	1.0000	543	1.0000	551	-	
343	nominder-002	0.0025	107	0.0037	102	0.0033	175	0.0037	152	0.0026	65	0.5785	408	0.1435	401	0.8381	269
344	nominder-003	-		-		0.0031	148	0.0034	123	0.0026	53	0.7010	425	0.2159	418	0.8909	281
345	notiontag-001	0.6846	537	0.8006	536	0.3955	518	0.5247	518	0.8669	535	0.8313	453	0.6362	472	-	
346	notiontag-002	0.0066	268	0.0089	254	0.0045	244	0.0061	245	0.0077	245	0.0137	147	0.0104	192	0.1106	116
347	nsensecorp-004	0.1370	485	0.1397	472	0.0066	317	0.0094	313	1.0000	568	1.0000	566	1.0000	559	1.0000	527
348	nsensecorp-005	0.0055	234	0.0080	239	0.0039	222	0.0058	235	0.2723	494	0.9999	530	0.9949	530	1.0000	388
349	ntechlab-011	0.0012	28	0.0019	28	0.0024	49	0.0028	74	0.0029	84	0.0055	38	0.0047	49	0.0630	44
350	ntechlab-012	0.0011	25	0.0016	18	0.0023	29	0.0030	84	0.0026	56	0.0050	32	0.0043	35	0.0587	29
351	omface-000	0.2573	500	0.3835	501	0.3590	516	0.4903	515	0.3956	506	0.5003	398	0.2595	422	0.9137	286
352	omface-001	0.0137	382	0.0212	382	0.0114	401	0.0187	399	0.0174	361	1.0000	570	0.0214	293	1.0000	502

Table 30: FNMR is the proportion of mated comparisons below a threshold set to achieve the FMR given in the header on the fourth row. FMR is the proportion of impostor comparisons at or above that threshold. The light grey values give rank over all algorithms in that column. The pink columns use only same-sex impostors; others are selected regardless of demographics. The exception, in the green column, uses "matched-covariates" i.e. impostors of the same sex, age group, and country of birth. The second pink column includes effects of extended ageing. Missing entries for border, visa, mugshot and wild images generally mean the algorithm did not run to completion. The VISA *columns compare images described in section 2.1. The* MUGSHOT *columns compare images described in section 2.5. The* VISA-BORDER *column compare images described in section 2.2 with those of section 2.4. The* BORDER *column compares images described in section 2.4. The* KIOSK-BORDER *columns compare images described in section 2.6 with those of section 2.4.*

FNMR(T) "False non-match rate"
FMR(T) "False match rate"

	Algorithm	FALSE NON-MATCH RATE (FNMR)															
		CONSTRAINED, COOPERATIVE														LESS CONSTRAINED, NON-COOP.	
	Name	VISAMC		VISA		MUGSHOT		MUGSHOT12+YRS		VISABORDER		BORDER		BORDER		KIOSKBORDER	
	FMR	0.0001		1E-06		1E-05		1E-05		1E-06		1E-06		1E-05		1E-06	
353	omnigarde-002	0.0033	152	0.0046	149	0.0027	118	0.0039	160	0.0041	148	0.0076	70	0.0059	90	0.0806	72
354	omnigarde-003	0.0024	97	0.0038	105	0.0024	59	0.0029	77	0.0032	108	0.0059	47	0.0049	61	0.0706	60
355	onfido-000	0.1472	487	0.2881	491	0.0335	460	0.0731	472	0.0515	440	0.9915	500	0.9579	516	1.0000	357
356	openedge-000	0.0045	197	0.0062	194	0.0049	260	0.0069	265	0.0049	177	0.9889	496	0.7991	493	0.9999	352
357	openface-001	0.1804	489	0.2921	492	0.2878	510	0.3906	510	0.2054	485	0.2338	360	0.1549	405	0.6531	248
358	ovisionllc-001	-		-		0.0058	295	0.0081	294	0.8171	526	1.0000	547	1.0000	550	1.0000	372
359	oz-003	0.0095	327	0.0143	325	0.0054	286	0.0077	284	0.0096	280	0.0175	178	0.0118	212	0.1404	136
360	oz-004	0.0033	147	0.0049	161	0.0038	219	0.0055	219	0.0081	251	0.0163	168	0.0142	233	-	
361	palit-000	0.0062	260	0.0084	248	0.0039	221	0.0055	218	0.0055	197	0.4610	397	0.2468	420	0.8695	273
362	palit-001	0.0050	208	0.0068	210	0.0032	171	0.0047	194	0.0045	164	0.0110	128	0.0058	85	0.1446	140
363	pangiam-001	0.0031	133	0.0044	133	0.0029	137	0.0040	165	0.0028	78	0.0362	255	0.0056	76	0.1711	155
364	pangiam-002	0.0030	128	0.0042	123	0.0026	100	0.0031	98	0.0030	91	0.1772	340	0.0385	331	0.6076	242
365	papago-001	0.0067	270	0.0096	269	0.0051	277	0.0077	283	0.0071	232	0.0126	141	0.0086	157	0.1033	111
366	papil11-000	0.0021	81	0.0030	71	0.0024	31	0.0024	36	0.0025	51	0.0047	21	0.0040	29	0.0536	17
367	papsav1923-002	0.0021	83	0.0034	84	0.0026	81	0.0030	90	0.0048	174	0.0093	103	0.0086	155	0.0630	43
368	papsav1923-003	0.0025	106	0.0035	90	0.0024	55	0.0025	39	0.0034	118	0.0066	59	0.0058	84	0.0603	32
369	paravision-011	0.0008	11	0.0020	30	0.0021	8	0.0020	7	0.0026	57	0.0053	35	0.0049	60	0.0498	13
370	paravision-013	0.0010	22	0.0018	25	0.0021	6	0.0019	3	0.0019	12	0.0041	12	0.0036	17	0.0442	4
371	pensees-001	0.0087	313	0.0133	315	0.0071	326	0.0122	338	0.0145	334	0.0252	216	0.0195	280	-	
372	pixelall-009	0.0018	59	0.0025	44	0.0024	52	0.0026	48	0.0031	101	0.3475	382	0.0053	66	0.9006	285
373	pixelall-010	0.0020	70	0.0030	73	0.0025	69	0.0028	76	0.0031	100	0.3512	383	0.0054	69	0.8813	277
374	privid-001	0.3350	505	0.5013	510	0.4327	520	0.5880	522	0.9790	550	1.0000	539	0.9998	544	1.0000	391
375	privid-002	0.0460	456	0.0652	452	0.0524	478	0.0882	476	0.0671	450	0.9769	487	0.8960	506	0.9999	349
376	psl-011	0.0013	33	0.0026	52	0.0021	1	0.0021	9	0.0024	31	0.0047	20	0.0035	14	0.0565	24
377	psl-012	0.0017	53	0.0027	56	0.0021	9	0.0023	18	0.0021	15	0.0039	8	0.0032	7	0.0494	11
378	ptakuratsatu-000	0.0060	255	0.0089	255	0.0070	323	0.0104	322	0.0096	281	0.0152	156	0.0100	182	-	
379	pxl-001	0.0488	457	0.0752	458	0.0586	483	0.1087	485	0.0946	464	0.1065	320	0.0625	363	-	
380	pyramid-000	0.0136	378	0.0233	389	0.0117	403	0.0192	402	0.0185	366	0.0322	240	0.0206	286	-	
381	qazbs-000	0.0058	241	0.0083	246	0.0046	250	0.0072	270	0.0130	321	0.0244	213	0.0196	281	0.7784	262
382	qazsmartvisionai-000	0.0008	12	0.0011	9	0.0021	2	0.0022	12	0.0018	8	0.0035	5	0.0030	3	0.0441	3
383	qluevision-001	0.0223	421	0.0419	427	0.0205	436	0.0343	435	0.0327	409	0.8762	456	0.7413	489	0.9908	318
384	qnap-004	0.0046	199	0.0061	190	0.0038	214	0.0059	239	0.0042	152	0.9960	506	0.9442	512	1.0000	361
385	qnap-005	0.0033	153	0.0047	153	0.0068	320	0.0071	269	0.0096	279	0.0184	183	0.0163	253	0.0948	103
386	quantasoft-003	0.0081	300	0.0113	294	0.0056	290	0.0076	281	0.0091	270	0.0161	165	0.0107	198	0.1193	120
387	rankone-015	0.0009	14	0.0014	15	0.0024	37	0.0026	47	0.0024	37	0.0044	15	0.0037	18	0.0635	48
388	realnetworks-007	0.0031	134	0.0051	170	0.0028	125	0.0035	133	0.0048	175	0.0091	97	0.0074	124	0.0945	102
389	realnetworks-008	0.0022	86	0.0039	109	0.0038	213	0.0045	185	0.0055	193	0.0100	117	0.0080	140	0.0889	86
390	rebs-000	0.0030	129	0.0043	131	0.0024	43	0.0032	107	0.0024	29	0.3069	371	0.1170	391	0.7667	260
391	rebs-001	0.0037	174	0.0049	164	0.0024	56	0.0033	114	0.0025	42	0.0257	217	0.0096	175	0.1487	143
392	recognito-000	0.0004	4	0.0006	1	0.0021	7	0.0022	17	0.0016	4	0.0555	283	0.0207	288	0.1943	165
393	recognito-001	0.0003	3	0.0007	5	0.0021	4	0.0022	14	0.0016	1	0.0663	297	0.0257	306	0.1825	162
394	regula-000	0.0184	408	0.0376	422	0.0103	381	0.0185	395	0.0120	311	0.9983	511	0.0231	298	1.0000	377
395	regula-001	0.0072	283	0.0107	287	0.0102	379	0.0179	392	0.0123	315	0.0333	247	0.0174	260	0.3711	211
396	remarkai-001	0.0144	386	0.0256	400	0.0102	378	0.0159	383	0.0162	344	0.0582	287	0.0185	270	-	

Table 31: FNMR is the proportion of mated comparisons below a threshold set to achieve the FMR given in the header on the fourth row. FMR is the proportion of impostor comparisons at or above that threshold. The light grey values give rank over all algorithms in that column. The pink columns use only same-sex impostors; others are selected regardless of demographics. The exception, in the green column, uses "matched-covariates" i.e. impostors of the same sex, age group, and country of birth. The second pink column includes effects of extended ageing. Missing entries for border, visa, mugshot and wild images generally mean the algorithm did not run to completion. The VISA *columns compare images described in section 2.1. The* MUGSHOT *columns compare images described in section 2.5. The* VISA-BORDER *column compare images described in section 2.2 with those of section 2.4. The* BORDER *column compares images described in section 2.4. The* KIOSK-BORDER *columns compare images described in section 2.6 with those of section 2.4.*

	Algorithm	FALSE NON-MATCH RATE (FNMR)																	
		CONSTRAINED, COOPERATIVE																LESS CONSTRAINED, NON-COOP.	
	Name	VISAMC		VISA		MUGSHOT		MUGSHOT12+YRS		VISABORDER		BORDER		BORDER		KIOSKBORDER			
	FMR	0.0001		1E-06		1E-05		1E-05		1E-06		1E-06		1E-05		1E-06			
397	remarkai-003	0.0047	201	0.0063	195	0.0033	183	0.0049	197	0.0054	190	0.0100	116	0.0072	120	0.0908	93		
398	rendip-000	0.0055	233	0.0077	230	0.0048	259	0.0060	243	0.0080	249	0.0142	151	0.0110	202	0.1027	109		
399	revealmedia-005	0.0050	211	0.0074	223	0.0050	267	0.0068	264	0.0075	242	0.0124	138	0.0104	195	0.0895	89		
400	revealmedia-006	0.0040	184	0.0067	201	0.0041	234	0.0056	222	0.0056	200	0.0085	88	0.0068	106	0.0872	82		
401	roc-016	0.0009	17	0.0014	16	0.0023	20	0.0024	28	0.0024	32	0.0042	13	0.0035	12	0.0558	22		
402	rokid-000	0.0093	325	0.0145	327	0.0073	333	0.0102	321	0.0164	346	0.0280	227	0.0214	292	-			
403	rokid-001	0.0105	343	0.0162	342	0.0094	374	0.0163	386	0.0181	364	0.0276	226	0.0165	254	-			
404	s1-005	0.0024	103	0.0036	99	0.0025	75	0.0029	79	0.0026	63	0.0048	25	0.0038	21	0.0638	50		
405	s1-007	0.0023	96	0.0056	182	0.0024	33	0.0028	62	0.0025	47	0.0048	24	0.0039	25	0.0608	34		
406	saffe-001	0.4339	515	0.5261	513	0.7539	544	0.8736	546	0.7977	524	0.9810	488	0.7435	490	-			
407	saffe-002	0.0119	364	0.0206	377	0.0107	389	0.0177	391	0.0244	394	0.9998	524	0.2785	427	-			
408	samsungsds-001	0.0015	39	0.0026	50	0.0023	22	0.0023	23	0.0024	33	0.1660	338	0.0536	355	0.4995	231		
409	samsungsds-002	0.0017	55	0.0027	55	0.0023	18	0.0022	13	0.0021	17	0.0043	14	0.0036	16	0.0586	28		
410	samtech-001	0.0197	413	0.0365	421	0.0146	422	0.0241	418	0.0238	393	0.0394	263	0.0251	304	-			
411	samtech-002	0.0084	307	0.0127	312	0.0093	369	0.0158	380	0.0113	306	0.0442	269	0.0132	222	0.4110	220		
412	scanovate-002	0.0175	406	0.0355	418	0.0146	420	0.0286	428	0.0269	399	0.0301	231	0.0178	264	-			
413	scanovate-003	0.0054	227	0.0080	238	0.0054	282	0.0072	273	0.0312	407	0.0599	288	0.0568	360	-			
414	sdc-000	0.0303	437	0.0526	442	0.0572	482	0.1094	486	0.0867	460	0.6230	413	0.3682	443	0.8797	276		
415	seamfix-001	-		-		0.1973	504	0.2878	504	0.2613	492	0.3156	376	0.1976	413	0.8176	266		
416	securifai-007	0.0124	370	0.0175	359	0.0064	311	0.0105	323	0.0108	297	0.9999	529	0.9966	535	1.0000	381		
417	securifai-008	-		-		0.0060	302	0.0102	320	0.2096	486	0.9649	483	0.8757	503	0.9990	338		
418	sensetime-007	0.0012	32	0.0022	35	0.0021	10	0.0020	6	0.0018	7	0.0034	4	0.0029	2	0.0479	10		
419	sensetime-008	0.0008	10	0.0014	13	0.0021	3	0.0020	4	0.0018	9	0.0036	6	0.0033	8	0.0504	14		
420	serendipity-000	0.0046	198	0.0069	212	0.0042	238	0.0056	221	0.0073	238	0.9129	465	0.7189	486	0.9952	328		
421	sertis-002	0.0049	206	0.0061	189	0.0039	226	0.0061	249	0.0055	194	0.0099	114	0.0070	115	0.0921	97		
422	sertis-003	0.0049	207	0.0059	186	0.0037	205	0.0058	233	0.0055	199	0.0100	115	0.0072	121	0.0881	83		
423	seventhsense-003	0.0035	165	0.0046	146	0.0026	97	0.0033	113	0.0062	216	0.0448	270	0.0175	261	0.2594	188		
424	seventhsense-005	0.0031	136	0.0045	140	0.0028	123	0.0030	82	0.0028	76	0.0466	274	0.0165	255	0.1949	166		
425	shaman-000	0.9297	543	0.9774	543	0.9990	562	0.9997	560	0.9999	555	1.0000	538	0.9999	546	-			
426	shaman-001	0.3346	504	0.4616	505	0.2368	507	0.3723	509	0.3574	501	0.3527	384	0.2304	419	-			
427	shu-002	-		0.0079	237	0.0146	421	0.0308	429	1.0000	557	0.0183	181	0.0115	208	-			
428	shu-003	0.0028	118	0.0041	120	0.0050	265	0.0088	309	0.0081	252	0.0133	145	0.0094	171	-			
429	siat-002	0.0091	318	0.0126	311	0.0109	390	0.0190	401	0.0276	401	0.0516	282	0.0464	348	-			
430	siat-005	0.0021	77	0.0038	104	0.0059	296	0.0049	198	0.0742	452	0.9623	481	0.6801	475	0.9833	308		
431	sjtu-004	0.0014	36	0.0025	43	0.0027	106	0.0028	75	0.0046	165	0.0086	91	0.0073	122	0.0906	92		
432	sjtu-005	0.0029	121	0.0036	98	0.0025	77	0.0027	58	0.0044	157	0.0120	136	0.0072	117	0.1325	129		
433	sktelecom-000	0.0038	178	0.0054	178	0.0031	147	0.0051	206	0.0042	149	0.3418	380	0.0061	94	0.9499	293		
434	smartbiometrik-001	0.5485	528	0.6442	523	0.7550	545	0.8611	542	0.8677	536	0.8270	452	0.7030	479	0.9752	302		
435	smartengines-000	0.6240	535	0.7562	534	0.9552	554	0.9784	554	0.9515	548	0.9288	472	0.8200	494	0.9930	321		
436	smartengines-001	0.6434	536	0.7666	535	0.9446	553	0.9750	553	0.9387	546	0.9556	478	0.8647	501	0.9972	333		
437	smartvist-000	0.0912	475	0.1587	477	0.1163	496	0.1841	496	0.1397	470	0.9372	474	0.7107	484	0.9990	339		
438	smartvist-001	0.0137	381	0.0244	393	0.0099	377	0.0158	381	0.0151	335	0.1349	331	0.0419	336	0.5589	237		
439	smilart-002	0.2440	496	0.3532	497	-		-		0.3785	502	0.4145	393	0.2611	423	-			
440	smilart-003	0.6944	539	0.8836	539	0.0695	488	0.1193	489	0.0894	462	0.1221	327	0.0737	370	-			

Table 32: FNMR is the proportion of mated comparisons below a threshold set to achieve the FMR given in the header on the fourth row. FMR is the proportion of impostor comparisons at or above that threshold. The light grey values give rank over all algorithms in that column. The pink columns use only same-sex impostors; others are selected regardless of demographics. The exception, in the green column, uses "matched-covariates" i.e. impostors of the same sex, age group, and country of birth. The second pink column includes effects of extended ageing. Missing entries for border, visa, mugshot and wild images generally mean the algorithm did not run to completion. The VISA *columns compare images described in section 2.1. The* MUGSHOT *columns compare images described in section 2.5. The* VISA-BORDER *column compare images described in section 2.2 with those of section 2.4. The* BORDER *column compares images described in section 2.4. The* KIOSK-BORDER *columns compare images described in section 2.6 with those of section 2.4.*

FNMR(T) "False non-match rate"
FMR(T) "False match rate"

		FALSE NON-MATCH RATE (FNMR)															
	Algorithm	CONSTRAINED, COOPERATIVE														LESS CONSTRAINED, NON-COOP.	
	Name	VISAMC		VISA		MUGSHOT		MUGSHOT12+YRS		VISABORDER		BORDER		BORDER		KIOSKBORDER	
	FMR	0.0001		1E-06		1E-05		1E-05		1E-06		1E-06		1E-05		1E-06	
441	sodec-000	0.0033	149	0.0044	137	0.0040	230	0.0053	213	0.0054	191	0.0096	109	0.0080	136	0.0915	96
442	sparsh-001	0.0018	61	0.0029	66	0.0026	87	0.0028	71	0.0027	69	0.8806	457	0.6313	469	0.9963	329
443	sqisoft-002	0.0082	303	0.0124	304	0.0051	272	0.0086	306	0.0102	291	0.0183	182	0.0122	217	0.1498	145
444	sqisoft-003	0.0041	186	0.0055	181	0.0026	80	0.0032	111	0.0039	137	1.0000	572	1.0000	557	1.0000	546
445	staqu-000	0.0139	383	0.0208	379	0.0104	382	0.0145	372	0.0156	337	0.8063	446	0.1408	400	-	
446	starhybrid-001	0.0108	346	0.0138	320	0.0081	344	0.0113	331	0.0152	336	0.0265	221	0.0189	272	-	
447	stcon-002	0.0031	132	0.0043	128	0.0025	63	0.0034	122	0.0030	90	0.9988	514	0.9855	524	1.0000	365
448	stcon-003	0.0038	180	0.0050	166	0.0024	34	0.0032	110	0.0023	25	0.1082	322	0.0350	326	0.3982	217
449	stengg-000	0.0059	253	0.0082	245	0.0037	207	0.0060	242	0.0050	181	0.5065	399	0.0792	373	0.9348	292
450	sukshi-000	0.5409	526	0.6612	528	0.4556	523	0.6567	525	0.9296	545	0.8898	460	0.7384	487	0.9899	316
451	suprema-004	0.0024	99	0.0035	87	0.0032	165	0.0036	143	0.0028	71	0.0053	36	0.0045	44	0.0625	41
452	suprema-005	0.0022	85	0.0036	97	0.0034	189	0.0031	100	0.0026	64	0.0050	31	0.0044	39	0.0588	30
453	supremaid-001	0.0053	226	0.0073	222	0.0045	243	0.0066	259	0.0099	288	0.0186	184	0.0148	242	0.1040	112
454	supremaid-002	0.0063	263	0.0094	265	0.0044	241	0.0062	250	0.0072	237	0.0229	210	0.0095	174	0.2986	198
455	surrey-cvssp-002	0.0019	64	0.0028	60	0.0027	114	0.0028	66	0.0024	35	0.5978	411	0.1206	393	0.8488	271
456	surrey-cvssp-003	0.0016	48	0.0028	59	0.0022	12	0.0024	29	0.0022	22	0.3048	370	0.0539	356	0.5830	239
457	swsam-001	0.0268	430	0.0476	432	0.0271	449	0.0460	448	0.0584	446	0.7745	437	0.5013	456	0.9642	297
458	synesis-006	0.0070	274	0.0096	268	0.0107	387	0.0166	388	-		0.0128	144	0.0089	161	-	
459	synesis-007	0.0050	210	0.0073	221	0.0062	308	0.0076	280	-		0.0105	121	0.0080	138	-	
460	synology-000	0.0149	388	0.0238	392	0.0148	423	0.0261	422	0.0221	383	0.0331	243	0.0209	290	-	
461	synology-002	0.0104	342	0.0153	338	0.0107	388	0.0184	394	0.0189	369	0.2032	347	0.0180	265	-	
462	sztu-000	0.0092	321	0.0139	321	0.0091	363	0.0201	406	0.0136	326	0.0685	301	0.0118	214	-	
463	sztu-001	0.0031	131	0.0043	132	0.0025	68	0.0028	72	0.0051	183	0.0113	129	0.0089	162	0.9963	330
464	t4isb-000	0.0058	243	0.0087	251	0.0041	235	0.0064	256	0.0083	255	0.0157	162	0.0103	190	0.1196	121
465	tech5-007	0.0020	71	0.0029	63	0.0024	42	0.0028	63	0.0034	119	0.8622	455	0.5335	461	0.9867	314
466	tech5-008	0.0020	72	0.0031	77	0.0026	86	0.0028	69	0.0026	58	0.9238	469	0.7170	485	0.9984	334
467	techainer-001	0.0061	256	0.0092	260	0.0046	249	0.0073	275	0.0060	212	0.9575	479	0.8567	500	0.9995	345
468	techsign-000	0.0325	441	0.0511	438	0.0435	474	0.0710	470	0.0746	453	0.1104	323	0.0841	376	0.4288	223
469	techsign-001	0.0110	349	0.0196	373	0.0067	318	0.0120	336	0.0087	260	0.2475	363	0.0883	380	0.6767	251
470	tevian-007	0.0019	67	0.0027	54	0.0032	168	0.0041	167	0.0045	163	0.0086	90	0.0078	132	0.0925	99
471	tevian-008	0.0012	30	0.0017	24	0.0033	172	0.0042	175	0.0042	151	0.0081	77	0.0068	107	0.0909	94
472	tiger-005	0.0624	466	0.2450	488	0.0292	457	0.0556	459	0.0430	425	1.0000	532	0.9964	533	1.0000	366
473	tiger-006	0.0066	267	0.0101	276	0.0050	271	0.0075	279	0.0089	264	0.0158	164	0.0117	210	0.1466	141
474	tinkoff-001	0.0145	387	0.0244	394	0.0318	458	0.0636	467	0.0236	391	1.0000	555	0.0339	323	1.0000	407
475	tnitech-000	0.0025	109	0.0037	100	0.0033	176	0.0035	134	0.0025	44	0.8893	459	0.6283	468	0.9883	315
476	tongyi-005	0.0073	285	0.0146	328	0.0187	431	0.0421	444	0.0161	342	0.0215	201	0.0149	243	-	
477	toppanidgate-000	0.0021	79	0.0033	82	0.0026	82	0.0028	68	0.0039	138	0.0075	69	0.0068	104	0.0631	45
478	toshiba-007	0.0016	47	0.0023	41	0.0024	57	0.0023	19	0.0021	16	0.0629	295	0.0056	74	0.2301	175
479	toshiba-008	0.0012	27	0.0017	22	0.0024	47	0.0022	15	0.0019	10	0.0108	125	0.0039	27	0.0899	91
480	touchlessid-002	0.0070	273	0.0096	270	0.0407	469	0.0469	452	0.4234	509	0.9991	515	0.9953	532	1.0000	367
481	touchlessid-003	0.0061	257	0.0081	241	0.0040	232	0.0053	214	0.0056	202	0.0155	159	0.0082	144	0.1370	133
482	trueface-002	0.0060	254	0.0096	267	0.0048	258	0.0061	246	0.0112	305	0.0198	191	0.0155	249	-	
483	trueface-003	0.0070	275	0.0094	263	0.0053	280	0.0081	295	0.0122	312	0.0217	203	0.0159	252	0.1204	122
484	trueidvng-001	0.0063	261	0.0077	232	0.0033	182	0.0044	181	0.0046	166	0.0086	92	0.0069	111	0.0809	73

Table 33: FNMR is the proportion of mated comparisons below a threshold set to achieve the FMR given in the header on the fourth row. FMR is the proportion of impostor comparisons at or above that threshold. The light grey values give rank over all algorithms in that column. The pink columns use only same-sex impostors; others are selected regardless of demographics. The exception, in the green column, uses "matched-covariates" i.e. impostors of the same sex, age group, and country of birth. The second pink column includes effects of extended ageing. Missing entries for border, visa, mugshot and wild images generally mean the algorithm did not run to completion. The VISA *columns compare images described in section 2.1. The* MUGSHOT *columns compare images described in section 2.5. The* VISA-BORDER *column compare images described in section 2.2 with those of section 2.4. The* BORDER *column compares images described in section 2.4. The* KIOSK-BORDER *columns compare images described in section 2.6 with those of section 2.4.*

FNMR(T) "False non-match rate"
FMR(T) "False match rate"

	Algorithm	FALSE NON-MATCH RATE (FNMR)																	
		CONSTRAINED, COOPERATIVE																LESS CONSTRAINED, NON-COOP.	
	Name	VISAMC		VISA		MUGSHOT		MUGSHOT12+YRS		VISABORDER		BORDER		BORDER		KIOSKBORDER			
	FMR	0.0001		1E-06		1E-05		1E-05		1E-06		1E-06		1E-05		1E-06			
485	truststamp-001	0.0242	424	0.0484	433	0.0194	434	0.0359	437	0.0381	417	0.8808	458	0.6898	476	0.9948	325		
486	tuputech-000	0.3218	503	0.3696	499	-		-		0.3237	498	0.4304	395	0.2973	432	-			
487	turingtechvip-001	0.0330	443	0.0540	444	0.0458	475	0.1007	480	0.4715	511	0.9286	471	0.8448	498	0.9964	332		
488	turingtechvip-002	0.0126	374	0.0163	343	0.0092	368	0.0118	333	0.2264	490	1.0000	560	0.9925	527	0.9999	354		
489	turkcell-001	0.0043	189	0.0066	200	0.0037	212	0.0055	220	0.0043	153	0.0440	268	0.0082	145	0.3148	202		
490	turkcell-002	-		-		0.0036	198	0.0053	212	0.0044	158	0.0371	259	0.0075	126	0.2871	197		
491	twface-000	0.0051	215	0.0072	217	0.0041	233	0.0058	230	0.0071	233	0.0153	157	0.0100	179	0.1595	147		
492	twface-001	0.0036	167	0.0051	167	0.0031	157	0.0038	157	0.0049	176	0.0091	100	0.0075	127	0.0831	76		
493	ulsee-001	0.0151	390	0.0246	396	0.0113	399	0.0185	397	0.0187	368	0.6766	421	0.0181	267	-			
494	ultinous-000	0.2343	494	0.3484	496	-		-		-		-		-		-			
495	ultinous-001	0.2485	497	0.4003	502	-		-		-		-		-		-			
496	uluface-002	0.0081	298	0.0123	303	0.0071	325	0.0095	316	0.0107	296	1.0000	551	0.0140	231	-			
497	uluface-003	0.0100	335	0.0150	335	0.0079	340	0.0128	346	-		-		-		-			
498	unicc-002	0.2153	493	0.2190	486	0.0417	471	0.0526	458	0.0891	461	0.1321	330	0.1125	390	0.3813	212		
499	unicc-003	0.0217	420	0.0260	402	0.0093	372	0.0136	358	0.0129	319	0.0216	202	0.0143	235	0.2091	170		
500	unissey-003	0.0057	236	0.0082	244	0.0047	254	0.0082	296	0.0067	225	0.5179	402	0.2863	430	0.8684	272		
501	unissey-004	0.0043	188	0.0066	199	0.0037	201	0.0052	208	0.0048	173	0.5272	403	0.2903	431	0.8777	275		
502	upc-001	0.0234	423	0.0519	441	0.0291	456	0.0490	456	0.0294	404	0.2316	359	0.0389	332	-			
503	useb-001	0.0035	164	0.0053	176	0.0027	111	0.0033	117	0.0027	70	0.0085	87	0.0044	38	0.0806	71		
504	useb-002	0.0028	120	0.0039	110	0.0027	110	0.0031	99	0.0025	43	0.0090	95	0.0042	33	0.0867	81		
505	uxlabs-001	0.0534	460	0.0570	447	0.0118	404	0.0131	350	0.0237	392	0.0399	264	0.0288	316	0.2097	172		
506	uxlabs-003	0.2133	492	0.2143	484	0.0386	466	0.0457	446	0.0374	416	0.3343	379	0.1554	406	0.6941	255		
507	vcog-002	0.7522	541	0.9033	541	-		-		-		-		-		-			
508	vcortex-001	0.0131	377	0.0207	378	0.0192	433	0.0315	430	0.2238	489	0.3586	386	0.3536	441	0.3569	207		
509	vd-002	0.0429	453	0.0704	454	0.0569	481	0.0844	475	0.0801	456	0.0937	312	0.0577	361	-			
510	vd-003	0.0199	414	0.0222	387	0.0115	402	0.0130	349	0.0138	328	0.0239	211	0.0177	263	0.1647	154		
511	veridas-008	0.0032	140	0.0045	144	0.0030	141	0.0033	116	0.0085	258	0.0206	196	0.0143	236	0.1228	125		
512	veridas-009	0.0031	130	0.0043	125	0.0030	146	0.0035	130	0.0055	192	0.0106	124	0.0100	180	0.0959	104		
513	veridium-002	0.0343	445	0.0427	428	0.0283	453	0.0460	449	0.0489	435	0.0673	298	0.0464	347	0.3658	209		
514	veridium-003	-		-		0.0286	454	0.0462	450	0.0492	436	0.0679	299	0.0470	349	0.3672	210		
515	verigram-001	0.0032	141	0.0044	136	0.0027	108	0.0032	109	0.0030	88	0.9995	520	0.9953	531	1.0000	392		
516	verigram-003	0.0101	337	0.0109	289	0.0034	188	0.0039	161	0.0037	130	0.0070	65	0.0063	97	0.0559	23		
517	verihubs-inteligensia-001	0.0071	276	0.0114	298	0.0050	268	0.0076	282	0.0096	278	0.0165	170	0.0114	207	0.1409	138		
518	verihubs-inteligensia-002	0.0028	117	0.0043	130	0.0025	78	0.0030	83	0.0047	169	0.0092	101	0.0083	151	0.0983	105		
519	verijelas-000	0.2488	498	0.3431	495	0.4861	524	0.6004	523	0.0811	457	0.1148	324	0.0440	341	0.4077	219		
520	via-004	0.0099	330	0.0135	319	0.0031	160	0.0044	182	0.0055	196	0.4009	391	0.0080	139	0.9840	311		
521	via-005	0.0063	262	0.0082	243	0.0031	150	0.0037	156	0.0032	104	0.3659	388	0.0068	105	0.8709	274		
522	viante-000	0.0004	5	0.0007	4	0.0026	96	0.0026	51	0.0017	5	0.0033	3	0.0029	1	0.0475	9		
523	videmo-001	0.0295	434	0.0417	426	0.0164	429	0.0261	423	0.0355	412	0.0603	290	0.0442	342	0.2428	181		
524	videmo-002	0.0158	395	0.0288	408	0.0149	426	0.0249	421	0.0230	386	0.3429	381	0.1468	402	0.8393	270		
525	videonetics-001	0.5483	527	0.6446	524	0.7517	543	0.8607	541	0.8664	534	0.8255	449	0.6956	478	-			
526	videonetics-002	0.4274	513	0.5329	514	0.6081	531	0.7438	531	0.7775	521	0.7297	429	0.5756	463	-			
527	viettelhightech-000	0.0117	359	0.0166	348	0.0110	393	0.0198	405	0.0167	352	0.0249	214	0.0158	250	0.1604	150		
528	vigilantsolutions-010	0.0109	347	0.0164	346	0.0074	335	0.0095	315	0.0209	380	0.0365	258	0.0233	300	0.2465	182		

Table 34: FNMR is the proportion of mated comparisons below a threshold set to achieve the FMR given in the header on the fourth row. FMR is the proportion of impostor comparisons at or above that threshold. The light grey values give rank over all algorithms in that column. The pink columns use only same-sex impostors; others are selected regardless of demographics. The exception, in the green column, uses "matched-covariates" i.e. impostors of the same sex, age group, and country of birth. The second pink column includes effects of extended ageing. Missing entries for border, visa, mugshot and wild images generally mean the algorithm did not run to completion. The VISA *columns compare images described in section 2.1. The* MUGSHOT *columns compare images described in section 2.5. The* VISA-BORDER *column compare images described in section 2.2 with those of section 2.4. The* BORDER *column compares images described in section 2.4. The* KIOSK-BORDER *columns compare images described in section 2.6 with those of section 2.4.*

FNMR(T) "False non-match rate"
FMR(T) "False match rate"

		FALSE NON-MATCH RATE (FNMR)																	
	Algorithm	CONSTRAINED, COOPERATIVE																LESS CONSTRAINED, NON-COOP.	
	Name	VISAMC		VISA		MUGSHOT		MUGSHOT12+YRS		VISABORDER		BORDER		BORDER		KIOSKBORDER	
	FMR	0.0001		1E-06		1E-05		1E-05		1E-06		1E-06		1E-05		1E-06	
529	vigilantsolutions-011	0.0124	369	0.0176	360	0.0073	331	0.0095	314	0.0196	374	0.0360	254	0.0221	295	0.2633	190
530	vinai-000	0.0081	299	0.0124	305	0.0045	242	0.0072	272	0.0089	263	0.1814	341	0.0112	203	-	
531	vinbigdata-002	0.0102	339	0.0175	357	0.0071	328	0.0084	302	0.0090	265	0.8017	445	0.3134	434	0.9936	323
532	vinbigdata-003	0.0771	472	0.0992	468	0.1202	497	0.1756	495	0.2762	495	0.2369	361	0.0100	181	0.8914	282
533	vion-000	0.0419	451	0.0590	448	0.0422	472	0.0478	453	0.0581	445	0.0968	318	0.0847	377	-	
534	visage-000	0.0933	476	0.1441	475	0.1316	499	0.2416	500	0.1395	469	0.1920	344	0.1001	385	-	
535	visionbox-003	0.0057	238	0.0075	225	0.0062	307	0.0083	299	0.0100	289	0.9915	499	0.9625	519	1.0000	359
536	visionbox-004	0.0046	200	0.0075	226	0.0060	301	0.0075	278	0.0056	201	0.0316	236	0.0070	116	0.2528	184
537	visionlabs-010	0.0017	54	0.0024	42	0.0026	95	0.0030	88	0.0033	115	0.0061	52	0.0052	65	-	
538	visionlabs-011	0.0012	31	0.0022	37	0.0024	54	0.0026	49	0.0028	72	0.0053	37	0.0046	48	0.0635	47
539	visteam-007	0.0312	440	0.0448	431	0.0416	470	0.1008	481	0.0466	433	0.0602	289	0.0281	313	0.2601	189
540	visteam-008	0.0378	448	0.0515	439	0.0391	468	0.0937	478	0.0437	428	0.0567	284	0.0260	308	0.2533	185
541	vivotek-001	-		-		0.9982	560	0.9994	559	1.0000	556	1.0000	541	0.9999	547	1.0000	369
542	vixvizion-006	0.0082	304	0.0122	302	0.0093	370	0.0194	403	0.0099	287	0.0169	172	0.0108	199	0.1338	131
543	vixvizion-007	0.0110	351	0.0191	369	0.0080	342	0.0157	378	0.0101	290	0.0190	185	0.0118	213	0.1407	137
544	vnis-000	0.1397	486	0.1608	478	0.2184	505	0.2976	506	0.5277	512	0.3603	387	0.2714	426	0.6929	253
545	vnpay-000	0.2380	495	0.2614	490	0.4054	519	0.4968	516	0.3993	508	0.4389	396	0.4006	447	0.7693	261
546	vnpt-005	0.0036	168	0.0052	172	0.0027	109	0.0031	95	0.0036	124	0.0066	61	0.0056	75	0.0621	39
547	vnpt-006	0.0034	160	0.0050	165	0.0027	104	0.0035	138	0.0026	61	0.0049	28	0.0040	30	0.0585	26
548	vocalize-001	-		-		0.7356	541	0.8750	547	0.7830	523	0.7067	426	0.5268	460	0.9164	288
549	vocord-009	0.0022	87	0.0029	67	0.0036	195	0.0046	189	0.0052	188	0.0098	112	0.0086	158	-	
550	vocord-010	0.0024	102	0.0031	76	0.0036	196	0.0049	200	0.0025	52	0.0065	56	0.0040	28	0.0679	58
551	vtcc-000	0.0051	216	0.0068	208	0.0054	283	0.0064	254	0.9451	547	1.0000	554	1.0000	572	1.0000	400
552	vtcc-001	0.0054	230	0.0076	229	0.0049	264	0.0079	291	0.0064	220	0.0225	207	0.0083	147	1.0000	410
553	vts-000	0.0103	340	0.0174	354	0.0080	341	0.0129	348	0.0250	396	0.0450	271	0.0372	330	-	
554	vts-001	0.0033	142	0.0048	156	0.0027	112	0.0036	144	0.0032	103	0.6519	418	0.3563	442	0.9218	290
555	wicket-000	0.0018	62	0.0028	58	0.0024	50	0.0027	56	0.0031	96	0.7968	444	0.4340	451	0.9788	305
556	winsense-001	0.0062	259	0.0099	274	0.0092	366	0.0210	407	0.0093	272	0.0144	153	0.0098	178	-	
557	winsense-002	0.0050	212	0.0073	220	0.0038	216	0.0059	237	0.0064	219	0.0118	134	0.0084	152	-	
558	wiseai-001	0.0658	467	0.0964	467	0.7743	548	0.8956	549	0.1967	482	0.7526	433	0.3419	438	0.9695	298
559	wuhantianyu-001	0.0163	398	0.0262	403	0.0281	452	0.0569	462	0.0316	408	0.0486	279	0.0344	324	0.2097	171
560	x-laboratory-000	0.0071	278	0.0106	283	0.0123	407	0.0138	360	0.0419	423	0.5629	406	0.2852	429	-	
561	x-laboratory-001	0.0059	249	0.0110	291	0.0054	284	0.0078	289	0.0094	274	0.0142	150	0.0100	183	-	
562	xforwardai-001	0.0021	78	0.0034	85	0.0027	116	0.0028	70	0.0046	168	0.0088	93	0.0079	134	-	
563	xforwardai-002	0.0016	46	0.0023	40	0.0026	102	0.0025	41	0.0040	142	0.0081	78	0.0074	123	-	
564	xm-000	0.0015	38	0.0026	53	0.0031	155	0.0038	158	0.0058	209	0.0105	122	0.0082	146	-	
565	yisheng-004	0.1988	490	0.3329	494	0.1147	495	0.1849	497	0.2044	484	-		-		-	
566	yitu-003	0.0015	42	0.0026	45	0.0066	316	0.0085	303	0.0064	221	0.0114	130	0.0103	191	-	
567	yoonik-003	0.0034	154	0.0047	150	0.0032	164	0.0037	150	0.0816	458	0.2033	348	0.1601	407	0.3210	204
568	yoonik-004	0.0041	185	0.0059	184	0.0033	174	0.0052	209	0.0040	144	0.0071	67	0.0051	64	0.0732	62
569	yoti-001	0.0139	384	0.0195	372	0.0110	394	0.0187	400	0.0191	370	0.1255	329	0.0415	335	0.5578	236
570	ytu-000	0.0057	239	0.0087	252	0.0121	405	0.0238	417	0.0047	171	0.0078	74	0.0059	88	-	
571	yuan-005	0.0037	176	0.0046	148	0.0027	117	0.0035	136	0.0033	110	0.2706	367	0.0876	379	0.6695	249
572	yuan-008	0.0032	138	0.0043	127	0.0026	89	0.0034	121	0.0028	75	0.0059	45	0.0039	26	0.0891	87

Table 35: FNMR is the proportion of mated comparisons below a threshold set to achieve the FMR given in the header on the fourth row. FMR is the proportion of impostor comparisons at or above that threshold. The light grey values give rank over all algorithms in that column. The pink columns use only same-sex impostors; others are selected regardless of demographics. The exception, in the green column, uses "matched-covariates" i.e. impostors of the same sex, age group, and country of birth. The second pink column includes effects of extended ageing. Missing entries for border, visa, mugshot and wild images generally mean the algorithm did not run to completion. The VISA *columns compare images described in section 2.1. The* MUGSHOT *columns compare images described in section 2.5. The* VISA-BORDER *column compare images described in section 2.2 with those of section 2.4. The* BORDER *column compares images described in section 2.4. The* KIOSK-BORDER *columns compare images described in section 2.6 with those of section 2.4.*

FNMR(T) "False non-match rate"
FMR(T) "False match rate"

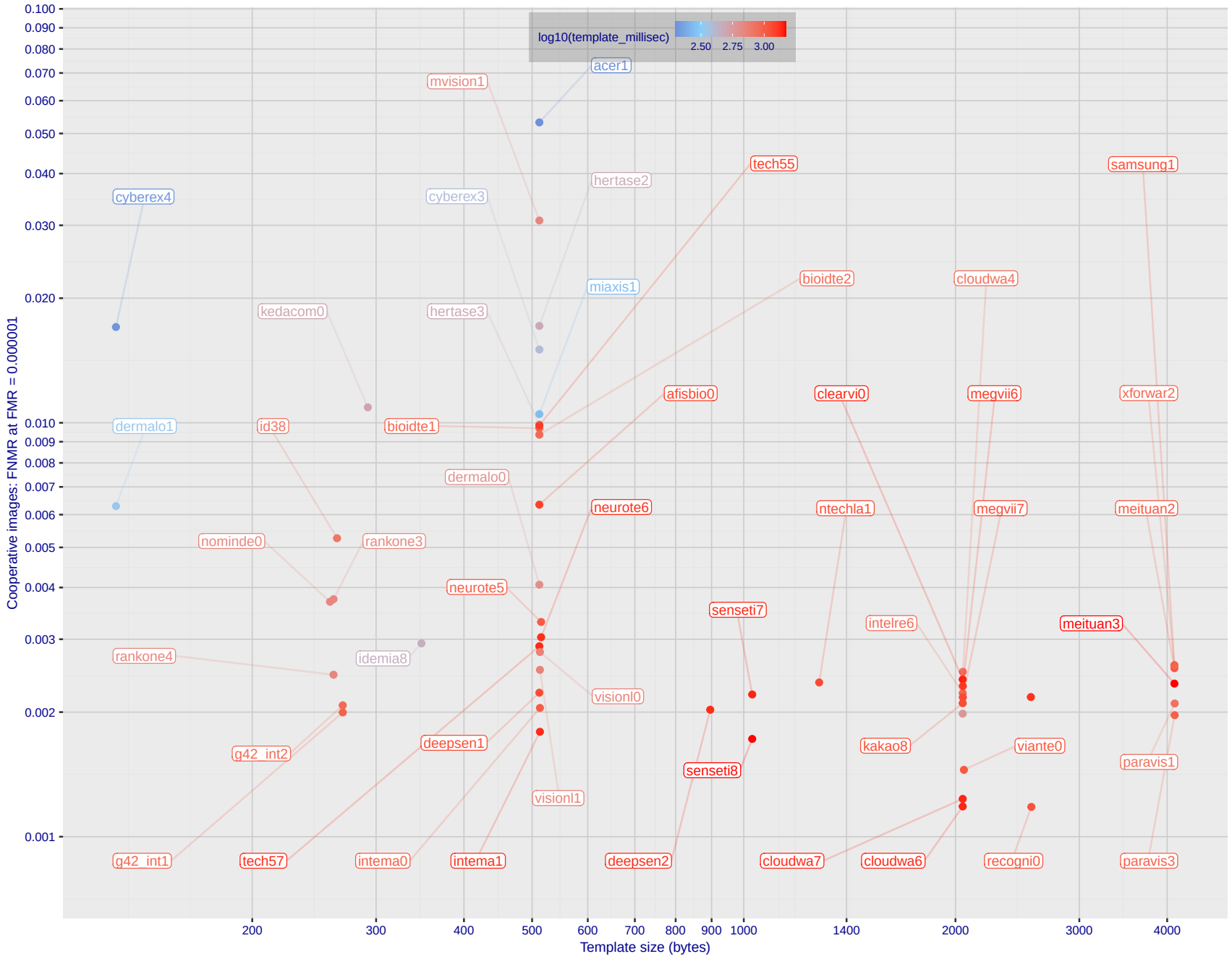

Figure 1: The points show false non-match rates (FNMR) versus the size of the encoded template. FNMR is the geometric mean of FNMR values for visa and mugshot images (from Figs. 106 and 135) at the false match rate (FMR) given in the y-axis label. The color of the points encodes template generation time - which spans at least one order of magnitude. Durations are measured on a single core of a c. 2016 Intel Xeon CPU E5-2630 v4 running at 2.20GHz. Algorithms with poor FNMR are omitted.

2024/04/17 08:45:50
FNMR(T) "False non-match rate"
FMR(T) "False match rate"

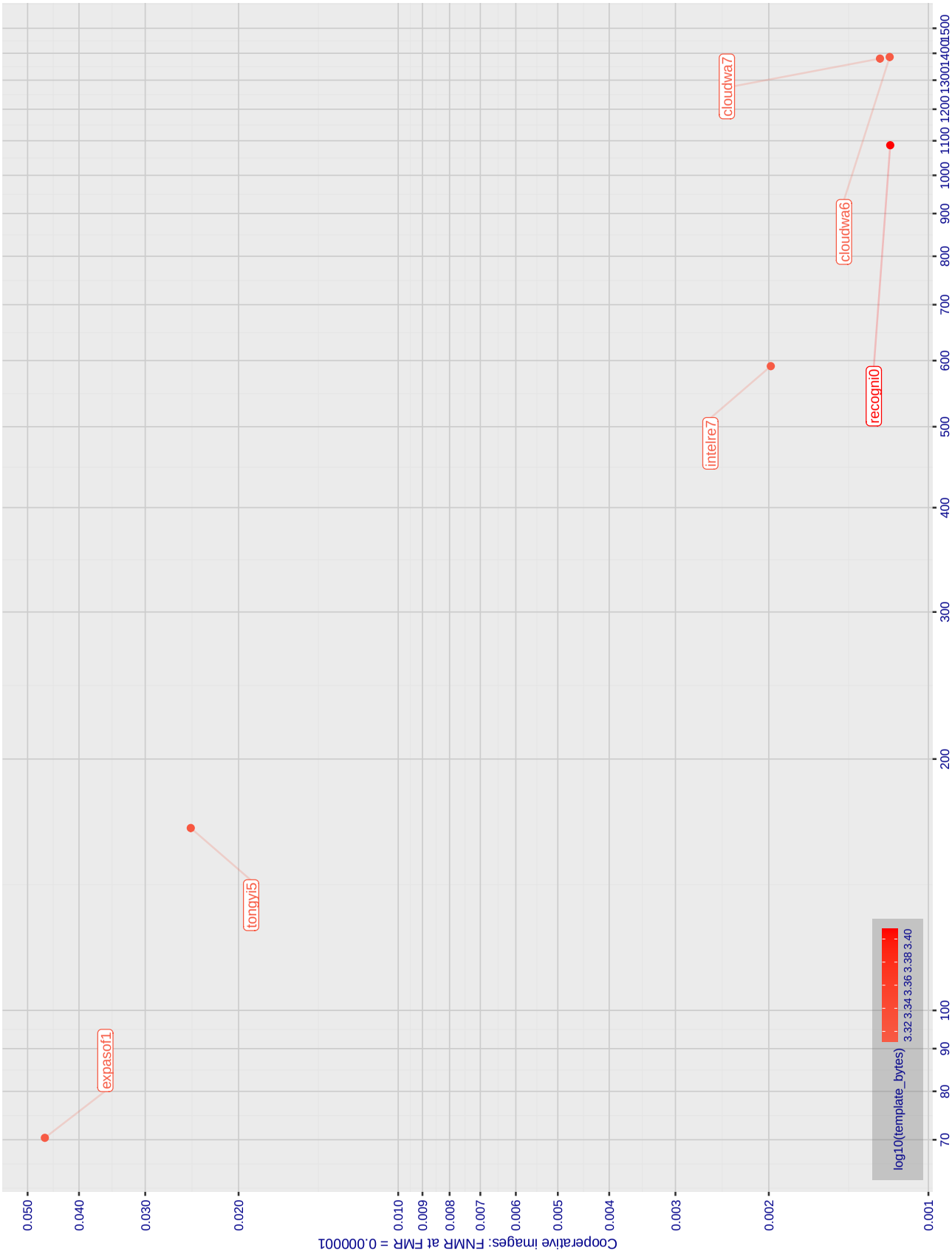

Figure 2: The points show false non-match rates (FNMR) versus the duration of the template generation operation. FNMR is the geometric mean of FNMR values for visa and mugshot images (from Figs. 106 and 135) at a false match rate (FMR) given in the y-axis label. Template generation time is a median estimated over 640 x 480 pixel portraits. It is measured on a single core of a c. 2016 Intel Xeon CPU E5-2630 v4 running at 2.20GHz. The color of the points encodes template size - which span two orders of magnitude. Algorithms with poor FNMR are omitted.

FNMR(T) "False non-match rate"
FMR(T) "False match rate"

1 Metrics

1.1 Core accuracy

Given a vector of N genuine scores, u, the false non-match rate (FNMR) is computed as the proportion below some threshold, T:

$$\text{FNMR}(T) = 1 - \frac{1}{N}\sum_{i=1}^{N} H(u_i - T) \tag{1}$$

where $H(x)$ is the unit step function, and $H(0)$ taken to be 1.

Similarly, given a vector of N impostor scores, v, the false match rate (FMR) is computed as the proportion above T:

$$\text{FMR}(T) = \frac{1}{N}\sum_{i=1}^{N} H(v_i - T) \tag{2}$$

The threshold, T, can take on any value. We typically generate a set of thresholds from quantiles of the observed impostor scores, v, as follows. Given some interesting false match rate range, $[\text{FMR}_L, \text{FMR}_U]$, we form a vector of K thresholds corresponding to FMR measurements evenly spaced on a logarithmic scale

$$T_k = Q_v(1 - \text{FMR}_k) \tag{3}$$

where Q is the quantile function, and FMR_k comes from

$$\log_{10}\text{FMR}_k = \log_{10}\text{FMR}_L + \frac{k}{K}\ [\log_{10}\text{FMR}_U - \log_{10}\text{FMR}_L] \tag{4}$$

Error tradeoff characteristics are plots of FNMR(T) vs. FMR(T). These are plotted with $\text{FMR}_U \to 1$ and FMR_L as low as is sustained by the number of impostor comparisons, N. This is somewhat higher than the "rule of three" limit $3/N$ because samples are not independent, due to re-use of images.

1.2 Multi-template scoring methodology

There are some scenarios when one or more people exist and are detected in an image, and some of the proposed test images include K $>$ 1 persons for some images and situations where the subject of interest may or may not be the foreground face (largest face in the image). The NIST FRTE 1:1 API supports this by allowing generation of multiple templates representing each person detected in an image. When this occurs, NIST will match all templates generated from the enrollment image with all templates generated from the verification image and use the **maximum** similarity score across all template comparisons. This scoring approach will be used in our calculation of FMR and FNMR (this applies to both genuine and imposter comparisons).

FNMR(T) "False non-match rate"
FMR(T) "False match rate"

2 Datasets

2.1 Visa images

- ▷ The number of images is on the order of 10^5.
- ▷ The number of subjects is on the order of 10^5.
- ▷ The number of subjects with two images is on the order of 10^4.
- ▷ The images have geometry in reasonable conformance with the ISO/IEC 19794-5 Full Frontal image type. Pose is generally excellent.
- ▷ The images are of size 252x300 pixels. The mean interocular distance (IOD) is 69 pixels.
- ▷ The images are of subjects from greater than 100 countries, with significant imbalance due to visa issuance patterns.
- ▷ The images are of subjects of all ages, including children, again with imbalance due to visa issuance demand.
- ▷ Many of the images are live capture. A substantial number of the images are photographs of paper photographs.
- ▷ When these images are input to the algorithm, they are labelled as being of type "ISO" - see Table 4 of the FRTE API.

2.2 Application images

- ▷ The number of images is on the order of 10^6.
- ▷ The number of subjects is on the order of 10^6.
- ▷ The number of subjects with two images is on the order of 10^6.
- ▷ The images have geometry in good conformance with the ISO/IEC 19794-5 Full Frontal image type. Pose is generally excellent.
- ▷ The images are of size 300x300 pixels. The mean interocular distance (IOD) is 61 pixels.
- ▷ The images are of subjects from greater than 100 countries, with significant imbalance due to population and immigration patterns.
- ▷ The images are of subjects of adults.
- ▷ All of the images are live capture.
- ▷ When these images are input to the algorithm, they are labelled as being of type "ISO" - see Table 4 of the FRTE API.

2.3 Application images with head yaw

- ▷ The number of images is on the order of 10^5.
- ▷ The number of subjects is on the order of 10^5.
- ▷ The number of subjects with two images is on the order of 10^5.
- ▷ The images have geometry in good conformance with the ISO/IEC 19794-5 Full Frontal image type *except* the yaw angle is between 25 and 85 degrees. Our pose estimates are approximate, with an angular error that increases with yaw. The angular estimates will be improved over time.
- ▷ The images are of size 300x300 pixels. The mean interocular distance (IOD), if frontal, would be about pixels, but reduces with cosine of yaw.
- ▷ The images are of subjects from greater than 100 countries, with significant imbalance due to population and immigration patterns.

FNMR(T) "False non-match rate"
FMR(T) "False match rate"

- ▷ The images are of subjects of adults.
- ▷ All of the images are live capture.
- ▷ When these images are input to the algorithm, they are labelled as being of type ”WILD” - see Table 4 of the FRTE API.

2.4 Border crossing images

- ▷ The number of images is on the order of 10^6.
- ▷ The number of subjects is on the order of 10^6.
- ▷ The number of subjects with two images is on the order of 10^6.
- ▷ The images are taken with at camera oriented by an attendant toward a cooperating subject. This is done under time constraints so there are role, pitch and yaw angle variations. Also background illumination is sometimes strong, so the face is under-exposed. There is some perspective distortion due to close range images. Some faces are partially cropped.
- ▷ The images have mean IOD of 38 pixels.
- ▷ The images are of subjects of adults and childen aged 12 or above.
- ▷ The images are of subjects from greater than 100 countries, with significant imbalance due to population and immigration patterns.
- ▷ The images are all live capture.
- ▷ When these images are input to the algorithm, they are labelled as being of type ”WILD” - see Table 4 of the FRTE API.

2.5 Mugshot images

- ▷ The number of images is on the order of 10^6.
- ▷ The number of subjects is on the order of 10^6.
- ▷ The number of subjects with two images is on the order of 10^6.
- ▷ The images have geometry in reasonable conformance with the ISO/IEC 19794-5 Full Frontal image type.
- ▷ The images are of variable sizes. The median IOD is 105 pixels. The mean IOD is 113 pixels. The 1-st, 5-th, 10-th, 25-th, 75-th, 90-th and 99-th percentiles are 34, 58, 70, 87, 121, 161 and 297 pixels.
- ▷ The images are of subjects from the United States.
- ▷ The images are of adults.
- ▷ The images are all live capture.
- ▷ When these images are input to the algorithm, they are labelled as being of type ”mugshot” - see Table 4 of the FRTE API.

2.6 Kiosk images

- ▷ The number of images is on the order of 10^6.
- ▷ The number of subjects is on the order of 10^5.
- ▷ The number of subjects with multiple images is the order of 10^5.

FNMR(T) “False non-match rate”
FMR(T) “False match rate”

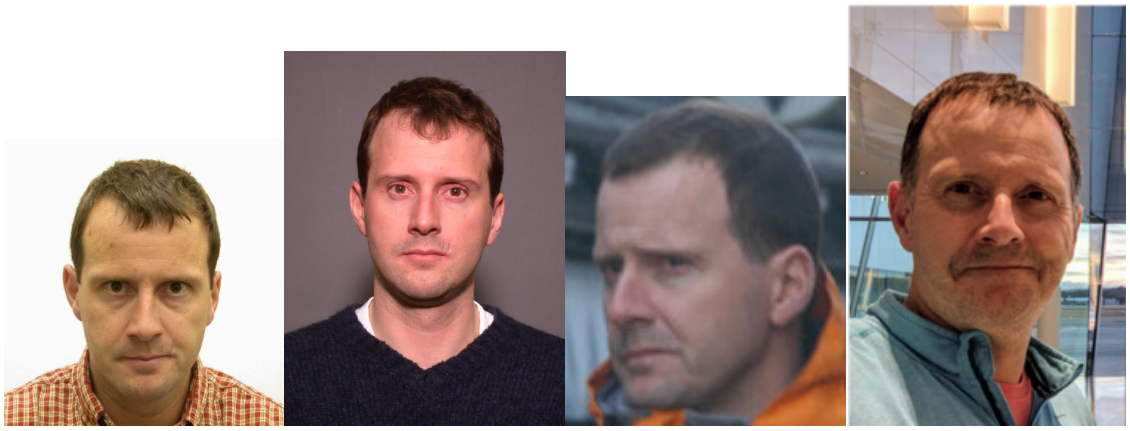

(a) Visa (b) Mugshot (c) Wild (d) Border

Figure 3: The figure gives simulated samples of image types used in this report.

- The images are taken at kiosk equipped with a camera intended to capture a centered face. However the images have specific quality defects arising from the camera triggering before the subject looks at it. These are downward pitch of the face relative to the optical axis; cropping of the forehead; and cropping of left or right part of the face. Partial cropping affects perhaps 10% of the images. Resolution does not vary widely.
- The images are of adults.
- The images have mean IOD of 44 pixels, with maximum below 75, and minimum when both eyes are present above 25 pixels.
- All of the images are live capture, none are scanned.
- When these images are input to the algorithm, they are labelled as being of type ”WILD” - see Table 4 of the FRTE API.

2.7 Wild images

- The number of images is on the order of 10^5.
- The number of subjects is on the order of 10^4.
- The number of subjects with two images on the order of 10^4.
- The images include many photojournalism-style images. Images are given to the algorithm using a variable but generally tight crop of the head. Resolution varies very widely. The images are very unconstrained, with wide yaw and pitch pose variation. Faces can be occluded, including hair and hands.
- The images are of adults.
- All of the images are live capture, none are scanned.
- When these images are input to the algorithm, they are labelled as being of type ”WILD” - see Table 4 of the FRTE API.

3 Results

3.1 Test goals

- To state absolute accuracy for different kinds of images, including those with and without subject cooperation.

FNMR(T) “False non-match rate”
FMR(T) “False match rate”

▷ To state comparative accuracy, across algorithms.

3.2 Test design

Method: For visa images:

▷ The comparisons are of visa photos against visa photos.
▷ The number of genuine comparisons is on the order of 10^4.
▷ The number of impostor comparisons is on the order of 10^{10}.
▷ The comparisons are fully zero-effort, meaning impostors are paired without attention to sex, age or other covariates. However, later analysis is conducted on subsets.
▷ The number of persons is on the order of 10^5.
▷ The number of images used to make a template is one.
▷ The number of templates used to make each comparison score is two corresponding to simple one-to-one verification.

Method: For mugshot images:

▷ The comparisons are of mugshot photos against mugshot photos.
▷ The number of genuine comparisons is on the order of 10^6.
▷ The number of impostor comparisons is on the order of 10^8.
▷ The impostors are paired by sex, but not by age or other covariates.
▷ The number of persons is on the order of 10^6.
▷ The number of images used to make a template is one.
▷ The number of templates used to make each comparison score is two, corresponding to simple one-to-one verification.

Method: For visa-border comparisons:

▷ The comparisons are of visa-like frontals against border crossing webcam photos.
▷ The number of genuine comparisons is on the order of 10^6.
▷ The number of impostor comparisons is on the order of 10^8.
▷ The impostors are paired by sex, but not by age or other covariates.
▷ The number of persons is on the order of 10^6.
▷ The number of images used to make a template is one.
▷ The number of templates used to make each comparison score is two, corresponding to simple one-to-one verification.

Method: For visa-border non-frontal yaw comparisons:

▷ The comparisons are of visa-like images with yaw 25 to 85 degrees against border crossing webcam photos.
▷ The number of genuine comparisons is on the order of 10^5.
▷ The number of impostor comparisons is on the order of 10^8.
▷ The impostors are paired by sex, but not by age or other covariates.

FNMR(T) "False non-match rate"
FMR(T) "False match rate"

- ▷ The number of persons is on the order of 10^5.
- ▷ The number of images used to make a template is one.
- ▷ The number of templates used to make each comparison score is two, corresponding to simple one-to-one verification.

Method: For kiosk-border comparisons:

- ▷ The comparisons are of visa-like frontals against kiosk-style photos.
- ▷ The number of genuine comparisons is on the order of 10^6.
- ▷ The number of impostor comparisons is on the order of 10^8.
- ▷ The impostors are paired by sex, but not by age or other covariates.
- ▷ The number of persons is on the order of 10^5.
- ▷ The number of images used to make a template is one.
- ▷ The number of templates used to make each comparison score is two, corresponding to simple one-to-one verification.

Method: For border-border comparisons:

- ▷ The comparisons are of border crossing webcam photos.
- ▷ The number of genuine comparisons is on the order of 10^6.
- ▷ The number of impostor comparisons is on the order of 10^8.
- ▷ The impostors are paired by sex, but not by age or other covariates.
- ▷ The number of persons is on the order of 10^6.
- ▷ The number of images used to make a template is one.
- ▷ The number of templates used to make each comparison score is two corresponding to simple one-to-one verification.

Method: For wild images:

- ▷ The comparisons are of wild photos against wild photos.
- ▷ The number of genuine comparisons is on the order of 10^6.
- ▷ The number of impostor comparisons is on the order of 10^8.
- ▷ The comparisons are fully zero-effort, meaning impostors are paired without attention to sex, age or other covariates.
- ▷ The number of persons is on the order of 10^4.
- ▷ The number of images used to make a template is one.
- ▷ The number of templates used to make each comparison score is two corresponding to simple one-to-one verification.

Method: For child exploitation images:

- ▷ The comparisons are of unconstrained child exploitation photos against others of the same type.
- ▷ The number of genuine comparisons is on the order of 10^4.
- ▷ The number of impostor comparisons is on the order of 10^7.

- ▷ The comparisons are fully zero-effort, meaning impostors are paired without attention to sex, age or other covariates.
- ▷ The number of persons is on the order of 10^3.
- ▷ The number of images used to make 1 template is 1.
- ▷ The number of templates used to make each comparison score is two corresponding to simple one-to-one verification.
- ▷ We produce two performance statements. First, is a DET as used for visa and mugshot images. The second is a cumulative match characteristic (CMC) summarizing a simulated one-to-many search process. This is done as follows.
  - We regard M enrollment templates as items in a gallery.
  - These M templates come from $M > N$ individuals, because multiple images of a subject are present in the gallery under separate identifiers.
  - We regard the verification templates as search templates.
  - For each search we compute the rank of the highest scoring mate.
  - This process should properly be conducted with a 1:N algorithm, such as those tested in NIST IR 8009. We use the 1:1 algorithms in a simulated 1:N mode here to a) better reflect what a child exploitation analyst does, and b) to show algorithm efficacy is better than that revealed in the verification DETs.

FNMR(T) "False non-match rate"
FMR(T) "False match rate"

3.3 Failure to enroll

FNMR(T) "False non-match rate"
FMR(T) "False match rate"

	Algorithm	Failure to Enrol Rate[1]									
	Name	APPLICATION		BORDER		KIOSK		MUGSHOT		VISA	
	Name	SEC. 2.2		SEC. 2.4		SEC. 2.6		SEC. 2.5		SEC. 2.1	
1	20face-000	0.0000	327	0.0008	290	0.0217	242	0.0000	157	0.0004	319
2	20face-001	0.0000	278	0.0008	289	0.0000	15	0.0000	163	0.0004	311
3	3divi-006	0.0000	365	0.0007	251	0.0214	239	0.0001	299	0.0002	145
4	3divi-007	0.0000	326	0.0007	250	0.0214	240	0.0001	298	0.0002	146
5	accurascan-002	0.0001	507	0.0060	511	0.0838	390	0.0006	477	0.0022	525
6	accurascan-003	0.0000	251	0.0009	326	0.0226	249	0.0000	201	0.0003	202
7	acer-001	0.0000	267	0.0011	358	-	425	0.0001	262	0.0004	328
8	acer-002	0.0000	466	0.0008	280	0.0191	210	0.0003	412	0.0004	339
9	acisw-007	0.0000	155	0.0000	67	0.0000	66	0.0000	14	0.0000	127
10	acisw-008	0.0000	347	0.0009	317	0.0173	191	0.0004	438	0.0004	224
11	adera-004	0.0000	259	0.0008	276	0.0202	220	0.0003	427	0.0004	286
12	adera-005	0.0000	257	0.0008	277	0.0202	219	0.0003	426	0.0004	285
13	advance-004	0.0001	511	0.0010	347	0.0157	174	0.0008	495	0.0006	461
14	advance-005	0.0000	324	0.0003	152	0.0074	106	0.0002	369	0.0003	149
15	afisbiometrics-000	0.0000	296	0.0008	268	0.0213	237	0.0000	162	0.0004	329
16	afrengine-002	0.0000	273	0.0007	260	0.0183	199	0.0005	453	0.0004	388
17	afrengine-003	0.0000	318	0.0099	525	0.0384	334	0.0005	452	-	571
18	aifirst-001	0.0000	37	0.0000	12	-	481	0.0000	82	0.0000	55
19	aigen-001	0.0000	62	0.0000	58	-	421	0.0000	133	0.0000	9
20	aigen-002	0.0000	128	0.0000	81	0.0000	56	0.0000	16	0.0000	96
21	ailabs-001	0.0000	264	0.0090	523	-	427	0.0007	488	0.0005	413
22	aimall-002	0.0000	444	0.0043	492	-	487	0.0012	512	0.0005	434
23	aimall-003	0.0000	413	0.0012	376	-	484	0.0004	431	0.0005	405
24	aiseemu-001	0.0000	214	0.0000	99	0.0000	48	0.0000	32	0.0000	81
25	aiseemu-002	0.0000	116	0.0000	90	0.0000	63	0.0000	25	0.0000	107
26	aiunionface-000	0.0000	149	0.0000	69	-	571	0.0000	7	0.0000	124
27	aize-002	0.0000	184	0.0014	397	0.0230	256	0.0005	469	0.0004	315
28	aize-003	0.0000	34	0.0000	130	0.0001	76	0.0000	86	0.0000	133
29	ajou-001	0.0000	239	0.0020	428	-	453	0.0001	306	0.0004	391
30	alchera-006	0.0000	262	0.0009	312	0.0228	253	0.0001	335	0.0004	263
31	alchera-007	0.0000	271	0.0009	314	0.0228	251	0.0001	337	0.0004	258
32	alfabeta-001	0.0005	537	0.0650	561	0.2142	406	0.0024	537	0.0018	519
33	alice-000	0.0000	21	0.0006	214	0.0133	154	0.0000	185	0.0004	244
34	alice-001	0.0000	91	0.0006	216	0.0133	153	0.0000	188	0.0004	243
35	alleyes-000	0.0000	346	0.0010	337	-	495	0.0002	351	0.0004	364
36	allgovision-000	0.0007	545	0.0062	512	-	457	0.0026	540	0.0052	536
37	alphaface-001	0.0000	302	0.0012	365	-	544	0.0000	248	0.0004	368
38	alphaface-002	0.0000	330	0.0012	364	-	562	0.0000	246	0.0004	369
39	amplifiedgroup-001	0.0114	562	0.1023	566	-	533	0.0189	564	0.0279	544
40	androvideo-000	0.0000	54	0.0000	1	-	471	0.0000	77	0.0000	50
41	anke-004	0.0000	288	0.0011	355	-	445	0.0001	316	0.0004	371
42	anke-005	0.0000	332	0.0012	367	-	556	0.0001	328	0.0004	387
43	antheus-000	0.0000	138	0.0000	76	-	532	0.0000	18	0.0000	101
44	antheus-001	0.0000	52	0.0000	5	-	468	0.0000	78	0.0000	47
45	anyvision-004	0.0000	431	0.0017	414	-	512	0.0001	329	0.0004	325
46	anyvision-005	0.0000	301	0.0013	381	-	543	0.0000	205	0.0004	253
47	aratek-001	0.0000	182	0.0000	115	0.0000	37	0.0000	56	0.0000	63
48	armatura-001	0.0000	453	0.0021	437	0.0257	278	0.0005	462	0.0005	414
49	armatura-003	0.0000	236	0.0012	369	0.0333	313	0.0004	434	0.0004	304
50	asusaics-000	0.0000	40	0.0000	11	-	482	0.0000	83	0.0000	56
51	asusaics-001	0.0000	17	0.0000	21	-	455	0.0000	91	0.0000	33
52	autentika-001	0.0000	81	0.0000	47	0.0000	2	0.0000	130	0.0000	5
53	autentika-002	0.0000	88	0.0000	41	0.0000	18	0.0000	115	0.0000	29
54	authenmetric-003	0.0000	55	0.0000	3	0.0000	25	0.0000	75	0.0000	48
55	authenmetric-004	0.0000	199	0.0000	106	0.0000	52	0.0000	45	0.0000	89
56	authme-001	0.0000	472	0.0009	324	0.0245	265	0.0003	424	0.0005	406
57	aware-007	0.0000	280	0.0012	370	0.0325	305	0.0000	221	0.0004	342
58	aware-008	0.0000	245	0.0012	373	0.0327	307	0.0000	218	-	554

Table 36: FTE is the proportion of failed template generation attempts. Failures can occur because the software throws an exception, or because the software electively refuses to process the input image. This would typically occur if a face is not detected. FTE is measured as the number of function calls that give EITHER a non-zero error code OR that give a "small" template. This is defined as one whose size is less than 0.3 times the median template size for that algorithm. This second rule is needed because some algorithms incorrectly fail to return a non-zero error code when template generation fails.
A hyphen "-" indicates the dataset was not produced. [1]*The effects of FTE are included in the accuracy results of this report by regarding any template comparison involving a failed template to produce a low similarity score. Thus higher FTE results in higher FNMR and lower FMR.*

FNMR(T) "False non-match rate"
FMR(T) "False match rate"

	Algorithm	Failure to Enrol Rate[1]									
	Name	APPLICATION		BORDER		KIOSK		MUGSHOT		VISA	
	Name	SEC. 2.2		SEC. 2.4		SEC. 2.6		SEC. 2.5		SEC. 2.1	
59	awiros-001	0.0039	551	0.0369	552	-	548	0.0386	566	0.0872	547
60	awiros-002	0.0000	468	0.0038	481	-	459	0.0007	486	0.0012	509
61	aximetria-001	0.0000	395	0.0010	348	0.0217	243	0.0001	349	0.0004	310
62	ayftech-001	0.0002	529	0.0046	497	-	431	0.0043	554	0.0011	488
63	ayftech-003	0.0000	86	0.0006	235	0.0123	147	0.0000	116	0.0000	24
64	ayonix-000	0.0053	554	0.0341	548	-	451	0.0113	562	0.0137	541
65	beethedata-000	0.0005	536	0.0042	490	0.0366	325	0.0002	366	0.0010	483
66	beyneai-000	0.0000	134	0.0000	78	0.0000	54	0.0000	21	0.0000	99
67	biocube-001	0.0006	540	0.0391	553	0.1207	394	0.0015	519	0.0020	522
68	biocube-002	0.0000	344	0.0046	500	0.0721	384	0.0008	494	0.0012	504
69	bioidtechswiss-001	0.0000	342	0.0007	246	-	500	0.0000	190	0.0004	353
70	bioidtechswiss-002	0.0000	279	0.0007	249	-	446	0.0000	196	0.0004	343
71	biometric-vision-000	0.0000	338	0.0005	190	0.0107	135	0.0002	397	0.0004	279
72	bm-001	0.0000	137	0.0000	74	-	536	0.0000	137	0.0000	103
73	boetech-001	0.0087	560	0.0272	543	0.2117	403	0.0032	547	0.0160	542
74	boetech-002	0.0087	559	0.0272	542	0.2117	404	0.0032	546	0.0160	543
75	bresee-001	0.0000	311	0.0010	343	-	541	0.0002	365	0.0003	184
76	bresee-002	0.0000	433	0.0020	432	0.0219	245	0.0008	489	0.0004	293
77	camvi-002	0.0000	222	0.0000	97	-	502	0.0000	38	0.0000	82
78	camvi-004	0.0000	195	0.0000	129	-	491	0.0000	60	0.0000	70
79	candour-001	0.0000	174	0.0000	117	0.0000	42	0.0000	70	0.0000	76
80	canon-004	0.0000	244	0.0008	267	0.0234	260	0.0000	239	0.0004	331
81	canon-005	0.0000	18	0.0044	494	0.0269	286	0.0000	191	0.0004	276
82	cchonolulu-000	0.0054	555	0.0395	555	0.2802	411	0.0036	549	0.0012	503
83	cchonolulu-001	0.0056	556	0.0414	556	0.2894	412	0.0038	552	0.0012	506
84	ceiec-003	0.0000	215	0.0013	392	-	517	0.0001	273	0.0004	354
85	ceiec-004	0.0000	161	0.0008	288	-	561	0.0000	197	0.0004	269
86	chosun-001	0.0000	133	0.0000	79	-	530	0.0000	19	0.0000	98
87	chosun-002	0.0000	24	0.0000	19	-	450	0.0000	93	0.0000	35
88	chtface-005	0.0000	6	0.0017	410	0.0320	301	0.0000	223	0.0004	361
89	chtface-006	0.0000	65	0.0017	411	0.0320	300	0.0000	224	0.0004	359
90	cist-003	0.0000	185	0.0011	353	0.0343	319	0.0000	54	0.0000	61
91	cist-004	0.0000	213	0.0005	192	0.0108	136	0.0000	35	0.0000	80
92	clearviewai-000	0.0000	316	0.0003	155	0.0081	114	0.0000	225	0.0003	161
93	clearviewai-001	0.0000	376	0.0006	225	0.0174	192	0.0001	254	0.0004	237
94	closeli-001	0.0000	120	0.0000	86	0.0000	57	0.0000	31	0.0000	113
95	cloudmatrix-001	0.0000	401	0.0028	454	0.0225	247	0.0001	263	0.0004	240
96	cloudmatrix-002	0.0000	385	0.0028	453	0.0225	246	0.0001	269	0.0004	236
97	cloudwalk-hr-003	0.0000	314	0.0008	291	-	566	0.0001	279	0.0004	257
98	cloudwalk-hr-004	0.0000	295	0.0011	361	-	430	0.0004	432	0.0003	209
99	cloudwalk-mt-006	0.0000	372	0.0006	221	0.0158	176	0.0002	378	0.0004	373
100	cloudwalk-mt-007	0.0000	292	0.0006	218	0.0158	175	0.0002	380	0.0004	370
101	cmcuni-001	0.0000	194	0.0005	200	0.0119	144	0.0000	59	0.0000	69
102	codeline-000	0.0000	84	0.0000	43	0.0000	16	0.0000	119	0.0000	27
103	cogent-007	0.0000	440	0.0000	126	0.0000	73	0.0000	206	0.0000	134
104	cogent-008	0.0000	13	0.0010	349	0.0304	295	0.0000	234	0.0004	221
105	cognitec-004	0.0001	500	0.0037	480	0.0580	358	0.0003	423	0.0005	416
106	cognitec-005	0.0000	460	0.0026	449	0.0550	356	0.0002	360	0.0005	412
107	cor-001	0.0000	341	0.0006	226	-	501	0.0002	399	0.0004	324
108	coretech-001	0.0000	492	0.0033	471	0.0677	372	0.0005	465	0.0011	497
109	coretech-002	0.0000	203	0.0013	393	0.0301	293	0.0000	159	0.0004	336
110	corsight-002	0.0000	312	0.0005	211	0.0152	167	0.0001	317	0.0004	306
111	corsight-003	0.0000	303	0.0006	234	0.0175	193	0.0001	308	0.0004	318
112	csc-002	0.0015	549	0.0033	468	-	570	0.0006	479	0.0006	464
113	csc-003	0.0015	550	0.0033	467	0.0445	348	0.0006	480	0.0006	465
114	ctbcbank-000	0.0001	503	0.0051	504	-	463	0.0011	509	0.0019	520
115	ctbcbank-001	0.0000	469	0.0036	479	-	477	0.0005	463	0.0010	482
116	cu-face-003	0.0000	439	0.0009	323	0.0245	266	0.0003	414	0.0004	376

Table 37: FTE is the proportion of failed template generation attempts. Failures can occur because the software throws an exception, or because the software electively refuses to process the input image. This would typically occur if a face is not detected. FTE is measured as the number of function calls that give EITHER a non-zero error code OR that give a "small" template. This is defined as one whose size is less than 0.3 times the median template size for that algorithm. This second rule is needed because some algorithms incorrectly fail to return a non-zero error code when template generation fails.
A hyphen "-" indicates the dataset was not produced. [1]*The effects of FTE are included in the accuracy results of this report by regarding any template comparison involving a failed template to produce a low similarity score. Thus higher FTE results in higher FNMR and lower FMR.*

FNMR(T) "False non-match rate"
FMR(T) "False match rate"

	Algorithm	Failure to Enrol Rate[1]									
	Name	APPLICATION		BORDER		KIOSK		MUGSHOT		VISA	
	Name	SEC. 2.2		SEC. 2.4		SEC. 2.6		SEC. 2.5		SEC. 2.1	
117	cu-face-004	0.0000	383	0.0007	261	0.0179	195	0.0001	327	-	553
118	cubox-002	0.0000	406	0.0006	230	0.0159	179	0.0002	398	0.0005	439
119	cubox-003	0.0000	165	0.0010	345	0.0210	233	0.0002	359	0.0004	357
120	cudocommunication-001	0.0000	79	0.0000	48	0.0000	1	0.0000	129	0.0000	4
121	cuhkee-001	0.0000	294	0.0011	360	-	435	0.0000	161	0.0004	298
122	cybercore-002	0.0000	447	0.0001	134	0.0014	79	0.0002	357	0.0002	139
123	cybercore-003	0.0000	261	0.0003	157	0.0060	94	0.0005	468	0.0003	165
124	cyberextruder-003	0.0000	446	0.0077	516	0.0887	391	0.0001	343	0.0006	459
125	cyberextruder-004	0.0000	443	0.0097	524	0.1025	392	0.0001	331	0.0007	466
126	cyberlink-012	0.0000	163	0.0004	184	0.0106	133	0.0000	144	0.0003	185
127	cyberlink-013	0.0000	59	0.0004	183	0.0106	132	0.0000	154	0.0003	182
128	dahua-006	0.0000	41	0.0000	123	-	483	0.0000	231	0.0003	210
129	dahua-007	0.0000	97	0.0000	124	0.0000	74	0.0000	235	0.0003	208
130	daon-000	0.0000	476	0.0028	457	0.0577	357	0.0014	516	0.0015	514
131	datech-000	0.0000	284	0.0004	168	0.0089	123	0.0000	207	0.0003	152
132	datech-001	0.0000	331	0.0004	169	0.0089	124	0.0000	204	-	569
133	decatur-000	0.0000	408	0.0020	427	-	527	0.0004	444	0.0005	407
134	decatur-001	0.0000	265	0.0009	319	0.0194	213	0.0001	284	0.0004	282
135	decloakface-001	0.0000	248	0.0016	406	0.0392	337	0.0001	311	0.0005	442
136	deepglint-004	0.0000	307	0.0005	187	0.0130	151	0.0002	394	0.0004	268
137	deepglint-005	0.0000	422	0.0019	421	0.0438	347	0.0006	475	0.0006	462
138	deepsea-001	0.0000	30	0.0000	13	-	480	0.0000	90	0.0000	54
139	deepsense-002	0.0000	164	0.0006	236	0.0191	209	0.0000	181	0.0004	229
140	deepsense-003	0.0000	61	0.0004	179	0.0110	138	0.0000	165	0.0003	164
141	dermalog-011	0.0000	487	0.0005	188	0.0116	141	0.0001	261	0.0003	162
142	dermalog-012	0.0000	370	0.0003	162	0.0068	102	0.0003	415	0.0005	445
143	dicio-001	0.0005	539	0.0649	559	0.2136	405	0.0024	535	0.0012	502
144	didiglobalface-001	0.0000	298	0.0012	366	-	550	0.0000	247	0.0004	366
145	didiglobalface-002	0.0000	249	0.0012	363	0.0247	267	0.0000	249	0.0004	363
146	digidata-000	0.0000	377	0.0023	443	0.0375	333	0.0004	447	0.0006	456
147	digidata-001	0.0000	343	0.0023	444	0.0375	332	0.0004	448	0.0006	455
148	digitalbarriers-002	0.0001	517	0.0045	495	-	454	0.0028	543	0.0027	529
149	dps-000	0.0000	64	0.0000	55	0.0000	8	0.0000	132	0.0000	12
150	dsk-000	0.0000	211	0.0000	101	-	511	0.0000	34	0.0000	79
151	einetworks-000	0.0000	470	0.0017	412	-	494	0.0002	385	0.0005	429
152	einetworksindia-000	0.0000	454	0.0018	418	0.0516	352	0.0002	405	0.0005	433
153	einetworksindia-001	0.0000	452	0.0018	416	0.0516	350	0.0002	408	0.0005	432
154	ekin-002	0.0000	29	0.0000	127	0.0004	77	0.0000	152	0.0000	132
155	element-000	0.0000	308	0.0008	296	0.0192	211	0.0000	199	0.0003	190
156	enface-001	0.0000	8	0.0012	374	0.0304	296	0.0000	193	0.0004	302
157	enface-002	0.0000	305	0.0004	173	0.0084	121	0.0000	172	0.0004	227
158	eocortex-000	0.0095	561	0.0602	558	-	522	0.0094	561	0.0059	537
159	ercacat-001	0.0000	196	0.0005	203	-	489	0.0000	217	0.0003	188
160	euronovate-003	0.0000	355	0.0006	223	0.0159	178	0.0002	381	0.0004	365
161	euronovate-004	0.0000	457	0.0016	405	0.0236	261	0.0015	520	0.0006	458
162	expasoft-001	0.0000	27	0.0000	16	-	488	0.0000	81	0.0000	52
163	expasoft-002	0.0000	103	0.0000	33	0.0000	12	0.0000	105	0.0000	19
164	f8-001	0.0003	532	0.0059	509	-	492	0.0035	548	0.0030	535
165	f8-002	0.0000	495	0.0150	534	0.0685	376	0.0005	451	0.0013	511
166	facehawk-000	0.0000	441	0.0357	549	0.0720	383	0.0021	531	0.0009	479
167	facelocate-001	0.0000	228	0.0019	423	0.0329	308	0.0000	226	-	561
168	faceonlive-001	0.0000	483	0.0029	462	0.0481	349	0.0013	514	0.0011	489
169	faceonlive-002	0.0002	527	0.0009	322	0.0075	109	0.0008	492	0.0008	478
170	facephi-000	0.0000	90	0.0004	170	0.0090	125	0.0001	319	0.0004	231
171	facesoft-000	0.0000	1	0.0000	29	-	466	0.0000	98	0.0000	37
172	facetag-000	0.0000	150	0.0000	71	0.0000	70	0.0000	6	0.0000	122
173	facetag-002	0.0000	98	0.0000	35	0.0000	11	0.0000	110	0.0000	17
174	facex-001	0.0001	523	0.0360	550	-	461	0.0047	557	0.0027	530

Table 38: FTE is the proportion of failed template generation attempts. Failures can occur because the software throws an exception, or because the software electively refuses to process the input image. This would typically occur if a face is not detected. FTE is measured as the number of function calls that give EITHER a non-zero error code OR that give a "small" template. This is defined as one whose size is less than 0.3 times the median template size for that algorithm. This second rule is needed because some algorithms incorrectly fail to return a non-zero error code when template generation fails.
A hyphen "-" indicates the dataset was not produced. [1]*The effects of FTE are included in the accuracy results of this report by regarding any template comparison involving a failed template to produce a low similarity score. Thus higher FTE results in higher FNMR and lower FMR.*

FNMR(T) "False non-match rate"
FMR(T) "False match rate"

	Algorithm	Failure to Enrol Rate[1]									
	Name	APPLICATION		BORDER		KIOSK		MUGSHOT		VISA	
	Name	SEC. 2.2		SEC. 2.4		SEC. 2.6		SEC. 2.5		SEC. 2.1	
175	facex-002	0.0001	524	0.0360	551	0.2663	409	0.0047	556	0.0027	531
176	facia-001	0.0000	131	0.0005	186	0.0122	146	0.0001	253	0.0004	252
177	farfaces-001	0.0000	465	0.0007	248	0.0061	96	0.0003	421	0.0003	173
178	fastenterprises-000	0.0000	317	0.0082	520	0.0169	188	0.0001	340	0.0003	186
179	fedu-001	0.0000	94	0.0000	38	0.0000	14	0.0000	121	-	552
180	fiberhome-nanjing-003	0.0000	207	0.0004	176	-	521	0.0000	47	0.0003	156
181	fiberhome-nanjing-004	0.0000	46	0.0004	175	-	472	0.0000	71	0.0003	155
182	fincore-000	0.0000	323	0.0008	293	0.0185	201	0.0001	256	0.0004	358
183	firstcreditkz-002	0.0000	233	0.0010	350	0.0232	259	0.0000	220	0.0004	261
184	firstcreditkz-003	0.0000	471	0.0010	346	0.0219	244	0.0000	210	-	572
185	foomobi-001	0.0007	542	0.0000	46	0.0000	3	0.0020	530	0.0011	490
186	foomobi-002	0.0007	541	0.0000	14	0.0000	29	0.0020	529	0.0011	491
187	fpt-000	0.0001	505	0.0007	252	0.0076	110	0.0006	481	-	568
188	fraudcom-000	0.0000	398	0.0055	508	0.0308	298	0.0002	387	0.0004	350
189	frpkauai-001	0.0000	416	0.0024	447	0.0360	324	0.0001	271	0.0004	379
190	frpkauai-002	0.0000	411	0.0019	425	0.0321	303	0.0000	243	0.0004	303
191	fujitsulab-002	0.0000	146	0.0009	305	-	567	0.0001	325	0.0003	157
192	fujitsulab-003	0.0000	227	0.0008	274	0.0166	184	0.0001	315	0.0001	137
193	g42-intellibrain-001	0.0000	212	0.0000	100	0.0000	47	0.0000	33	0.0000	78
194	g42-intellibrain-002	0.0000	89	0.0000	42	0.0000	17	0.0000	114	0.0000	28
195	geo-002	0.0000	334	0.0015	400	0.0332	311	0.0001	252	0.0004	386
196	geo-004	0.0000	291	0.0005	209	0.0138	157	0.0001	301	0.0004	275
197	gistouch-000	0.0000	493	0.0188	537	0.1345	397	0.0018	525	0.0007	467
198	gistouch-001	0.0000	135	0.0002	136	0.0027	82	0.0001	293	0.0003	160
199	glory-006	0.0000	382	0.0020	431	0.0345	320	0.0001	321	0.0004	380
200	glory-007	0.0000	415	0.0020	435	0.0403	342	0.0002	389	0.0005	404
201	gorilla-008	0.0000	358	0.0009	327	0.0259	279	0.0001	281	0.0004	355
202	gorilla-009	0.0000	299	0.0010	340	0.0276	287	0.0001	265	0.0004	338
203	gpstechvn-000	0.0000	42	0.0000	7	0.0000	27	0.0000	73	0.0000	45
204	graymatics-001	0.0000	140	0.0010	329	0.0210	230	0.0001	341	0.0004	291
205	griaule-001	0.0000	4	0.0012	375	0.0366	328	0.0000	179	0.0004	345
206	griaule-002	0.0000	102	0.0007	253	0.0209	224	0.0000	242	0.0004	292
207	hertasecurity-002	0.0000	122	0.0000	84	0.0000	59	0.0000	166	0.0000	130
208	hertasecurity-003	0.0000	25	0.0000	18	0.0000	33	0.0000	151	0.0000	129
209	hik-001	0.0000	44	0.0000	131	-	475	0.0000	72	0.0000	44
210	hisign-002	0.0000	405	0.0006	231	0.0150	163	0.0001	323	0.0003	203
211	hisign-003	0.0000	404	0.0008	294	0.0237	262	0.0001	322	-	560
212	hyperverge-003	0.0000	100	0.0008	272	0.0210	231	0.0002	403	0.0004	283
213	hyperverge-005	0.0000	35	0.0008	271	0.0210	232	0.0002	402	0.0004	287
214	hzailu-005	0.0000	258	0.0004	171	0.0081	115	0.0002	358	0.0003	194
215	hzailu-006	0.0000	304	0.0004	172	0.0081	116	0.0002	356	0.0003	198
216	i2v-001	0.0000	456	0.0018	420	0.0341	318	0.0001	294	-	562
217	icm-004	0.0000	477	0.0033	473	0.0698	378	0.0006	478	0.0010	487
218	icm-005	0.0002	526	0.0117	530	0.1223	395	0.0018	527	0.0014	513
219	icomm-000	0.0000	286	0.0004	178	0.0098	129	0.0000	227	0.0003	172
220	icthtc-000	0.0001	521	0.0047	501	-	456	0.0028	544	0.0029	532
221	id3-006	0.0000	421	0.0009	325	-	526	0.0004	437	0.0005	425
222	id3-008	0.0000	217	0.0006	233	0.0184	200	0.0001	339	0.0004	226
223	idemia-009	0.0000	77	0.0004	182	0.0077	111	0.0000	170	0.0003	191
224	idemia-010	0.0000	175	0.0004	167	0.0074	107	0.0000	68	0.0003	174
225	identy-000	0.0000	494	0.0020	433	0.0152	166	0.0012	511	0.0004	382
226	igearx-face-000	0.0000	241	0.0006	215	0.0153	169	0.0004	436	0.0004	344
227	iit-002	0.0000	475	0.0021	436	-	437	0.0009	501	0.0005	440
228	iit-003	0.0000	281	0.0008	292	-	448	0.0000	203	0.0004	232
229	imds-software-002	0.0000	110	0.0000	93	0.0000	61	0.0000	26	0.0000	105
230	imds-software-003	0.0000	33	0.0000	8	0.0000	32	0.0000	87	0.0000	58
231	imperial-000	0.0000	125	0.0000	83	-	537	0.0000	17	0.0000	94
232	imperial-002	0.0000	221	0.0000	95	-	506	0.0000	41	0.0000	84

Table 39: FTE is the proportion of failed template generation attempts. Failures can occur because the software throws an exception, or because the software electively refuses to process the input image. This would typically occur if a face is not detected. FTE is measured as the number of function calls that give EITHER a non-zero error code OR that give a "small" template. This is defined as one whose size is less than 0.3 times the median template size for that algorithm. This second rule is needed because some algorithms incorrectly fail to return a non-zero error code when template generation fails.
A hyphen "-" indicates the dataset was not produced. [1]*The effects of FTE are included in the accuracy results of this report by regarding any template comparison involving a failed template to produce a low similarity score. Thus higher FTE results in higher FNMR and lower FMR.*

FNMR(T) "False non-match rate"
FMR(T) "False match rate"

	Algorithm	Failure to Enrol Rate[1]									
	Name	APPLICATION		BORDER		KIOSK		MUGSHOT		VISA	
	Name	SEC. 2.2		SEC. 2.4		SEC. 2.6		SEC. 2.5		SEC. 2.1	
233	incode-009	0.0000	396	0.0009	311	0.0255	277	0.0002	368	0.0004	274
234	incode-013	0.0001	525	0.0012	371	0.0254	276	0.0005	461	0.0004	395
235	infocert-001	0.0000	428	0.0059	510	0.0424	344	0.0001	290	0.0006	446
236	innefulabs-000	0.0000	373	0.0024	446	-	516	0.0003	420	0.0005	421
237	innominds-001	0.0000	448	0.0030	465	0.0637	366	0.0010	507	0.0008	476
238	innovativetechnologyltd-001	0.0001	520	0.0050	503	-	465	0.0024	539	0.0025	528
239	innovativetechnologyltd-002	0.0000	417	0.0046	496	-	447	0.0057	559	0.0005	422
240	innovatrics-010	0.0000	325	0.0019	422	0.0393	338	0.0001	280	0.0004	228
241	innovatrics-011	0.0000	362	0.0001	133	0.0017	80	0.0000	148	-	565
242	insightface-003	0.0000	56	0.0000	4	0.0000	24	0.0000	76	0.0000	49
243	insightface-004	0.0000	206	0.0000	104	0.0000	49	0.0000	49	0.0000	91
244	inspur-001	0.0000	190	0.0000	109	0.0000	36	0.0000	62	0.0000	68
245	inspur-002	0.0000	82	0.0000	45	0.0000	4	0.0000	128	0.0000	8
246	intellicloudai-001	0.0000	118	0.0000	87	-	545	0.0000	30	0.0000	112
247	intellicloudai-002	0.0000	36	0.0008	283	-	485	0.0000	202	0.0004	223
248	intellifusion-001	0.0000	309	0.0005	205	-	539	0.0001	276	0.0003	204
249	intellifusion-002	0.0000	112	0.0000	128	-	552	0.0000	139	0.0000	109
250	intellivision-006	0.0001	514	0.0041	487	0.0528	354	0.0005	459	0.0007	470
251	intellivision-007	0.0001	515	0.0041	486	0.0528	355	0.0005	458	0.0007	471
252	intellivix-004	0.0000	183	0.0022	440	0.0333	315	0.0000	53	0.0000	60
253	intellivix-005	0.0000	101	0.0022	439	0.0333	314	0.0000	107	0.0000	20
254	intelresearch-008	0.0000	144	0.0006	237	0.0169	189	0.0000	146	0.0004	280
255	intelresearch-009	0.0000	73	0.0007	262	0.0232	258	0.0000	153	-	550
256	intema-000	0.0000	16	0.0005	193	0.0126	149	0.0000	232	0.0004	233
257	intema-001	0.0000	340	0.0004	181	0.0106	134	0.0000	149	0.0003	212
258	intozi-001	0.0000	269	0.0005	210	0.0126	148	0.0001	350	0.0004	217
259	intsysmsu-001	0.0000	124	0.0010	342	-	547	0.0001	303	0.0004	326
260	intsysmsu-002	0.0000	157	0.0010	341	-	560	0.0001	302	0.0004	327
261	ionetworks-001	0.0000	179	0.0081	518	0.0666	367	0.0000	55	0.0000	62
262	ionetworks-002	0.0000	87	0.0003	148	0.0048	87	0.0000	117	0.0000	25
263	iqface-000	0.0000	154	0.0000	66	-	564	0.0000	13	0.0000	126
264	iqface-003	0.0000	473	0.0076	515	-	514	0.0006	471	0.0005	444
265	irex-000	0.0000	426	0.0009	321	-	415	0.0000	228	0.0005	403
266	isap-001	0.0000	170	0.0000	121	-	496	0.0000	64	0.0000	71
267	isap-002	0.0000	10	0.0000	23	-	460	0.0000	104	0.0000	43
268	isityou-000	0.0068	558	0.0316	546	-	528	0.0023	534	0.0010	485
269	isystems-001	0.0000	481	0.0035	476	-	554	0.0010	504	0.0007	469
270	isystems-002	0.0000	482	0.0035	477	-	518	0.0010	505	0.0007	468
271	itmo-007	0.0000	80	0.0009	303	-	414	0.0003	428	0.0000	6
272	itmo-008	0.0000	113	0.0135	531	0.1239	396	0.0024	538	0.0000	110
273	ivacognitive-001	0.0000	389	0.0011	357	-	478	0.0001	268	0.0004	384
274	iws-000	0.0005	538	0.0650	562	-	439	0.0024	536	0.0012	505
275	jaakit-001	0.0008	547	0.0858	565	0.2713	410	0.0042	553	0.0021	524
276	kakao-008	0.0000	201	0.0009	308	0.0209	228	0.0001	296	0.0004	266
277	kakao-009	0.0000	57	0.0009	307	0.0209	227	0.0001	297	0.0004	262
278	kakaobank-001	0.0000	47	0.0006	222	0.0176	194	0.0000	168	0.0004	234
279	kakaobank-002	0.0000	235	0.0010	352	0.0303	294	0.0000	192	-	556
280	kakaopay-001	0.0000	399	0.0013	390	0.0322	304	0.0001	272	0.0004	389
281	kasikornlabs-002	0.0000	488	0.0033	470	0.0698	379	0.0004	441	0.0012	499
282	kasikornlabs-003	0.0000	486	0.0033	469	0.0698	380	0.0004	440	0.0012	500
283	kedacom-000	0.0000	220	0.0000	96	-	507	0.0000	40	0.0000	85
284	kiwitech-000	0.0000	337	0.0009	301	-	557	0.0004	439	0.0005	411
285	kneron-003	0.0239	565	0.0306	544	-	549	0.0044	555	0.0016	517
286	kneron-005	0.0000	485	0.0226	539	-	535	0.0006	470	0.0005	419
287	knowutech-000	0.0000	232	0.0008	270	0.0215	241	0.0000	214	0.0004	334
288	kogniza-001	0.0000	335	0.0012	378	0.0337	317	0.0003	425	-	570
289	kookmin-002	0.0000	176	0.0000	118	-	493	0.0000	69	0.0000	75
290	koreaid-001	0.0000	159	0.0023	445	0.0371	330	0.0000	238	0.0005	408

Table 40: FTE is the proportion of failed template generation attempts. Failures can occur because the software throws an exception, or because the software electively refuses to process the input image. This would typically occur if a face is not detected. FTE is measured as the number of function calls that give EITHER a non-zero error code OR that give a "small" template. This is defined as one whose size is less than 0.3 times the median template size for that algorithm. This second rule is needed because some algorithms incorrectly fail to return a non-zero error code when template generation fails.
A hyphen "-" indicates the dataset was not produced. [1]*The effects of FTE are included in the accuracy results of this report by regarding any template comparison involving a failed template to produce a low similarity score. Thus higher FTE results in higher FNMR and lower FMR.*

FNMR(T) "False non-match rate"
FMR(T) "False match rate"

	Algorithm	Failure to Enrol Rate[1]									
	Name	APPLICATION		BORDER		KIOSK		MUGSHOT		VISA	
	Name	SEC. 2.2		SEC. 2.4		SEC. 2.6		SEC. 2.5		SEC. 2.1	
291	krungthai-002	0.0000	348	0.0005	198	0.0111	140	0.0002	384	0.0003	211
292	kuke3d-001	0.0000	5	0.0000	27	0.0000	22	0.0000	95	0.0000	39
293	kuke3d-002	0.0000	111	0.0000	92	0.0000	60	0.0000	27	0.0000	104
294	lebentech-000	0.0042	552	0.0029	464	0.0252	274	0.0051	558	0.0066	538
295	lebentech-001	0.0000	497	0.0012	377	0.0317	299	0.0004	445	0.0005	428
296	lemalabs-001	0.0000	48	0.0005	208	0.0141	158	0.0002	379	0.0004	235
297	lineclova-002	0.0000	83	0.0007	240	0.0181	197	0.0000	127	0.0000	7
298	lineclova-003	0.0000	463	0.0023	441	0.0700	381	0.0002	404	0.0005	409
299	lookman-002	0.0000	132	0.0000	80	-	529	0.0000	20	0.0000	97
300	lookman-004	0.0000	70	0.0000	53	-	420	0.0000	135	0.0000	14
301	luxand-001	0.0000	429	0.0016	408	0.0366	326	0.0006	474	0.0005	426
302	luxand-003	0.0000	432	0.0016	409	0.0366	327	0.0006	473	-	564
303	mantra-000	0.0001	501	0.0041	489	0.0680	375	0.0003	419	0.0004	397
304	maxvision-005	0.0000	321	0.0009	299	0.0229	255	0.0002	354	0.0004	308
305	maxvision-006	0.0000	290	0.0007	264	0.0226	248	0.0002	363	0.0004	300
306	megvii-008	0.0000	247	0.0010	332	0.0206	222	0.0002	393	0.0004	360
307	megvii-009	0.0000	260	0.0010	331	0.0206	223	0.0002	392	0.0004	362
308	meituan-003	0.0000	283	0.0013	386	0.0251	271	0.0001	310	0.0004	330
309	meituan-004	0.0000	353	0.0013	387	0.0251	272	0.0001	309	0.0004	335
310	meiya-001	0.0000	479	0.0028	458	-	474	0.0004	446	0.0010	486
311	mendaxiatech-000	0.0000	300	0.0010	333	0.0206	221	0.0002	395	0.0004	367
312	metsakuurcompany-002	0.0000	177	0.0000	116	0.0000	43	0.0000	67	0.0000	77
313	metsakuurcompany-003	0.0000	114	0.0000	91	0.0000	62	0.0000	23	0.0000	106
314	miaxis-002	0.0448	569	0.1162	567	0.2565	408	0.2128	567	0.0347	545
315	miaxis-003	0.0000	359	0.0013	383	0.0262	282	0.0001	342	0.0003	167
316	microfocus-002	0.0001	518	0.0053	506	-	473	0.0008	493	0.0016	516
317	microfocus-003	0.0001	513	0.0049	502	0.0819	389	0.0007	487	0.0015	515
318	minivision-000	0.0000	20	0.0000	20	-	449	0.0000	94	0.0000	34
319	mitek-000	0.0000	425	0.0029	461	0.0521	353	0.0002	382	0.0003	176
320	mobai-000	0.0000	436	0.0114	528	-	422	0.0003	422	0.0012	508
321	mobai-001	0.0000	390	0.0040	483	-	476	0.0001	318	0.0012	507
322	mobbl-001	0.0000	474	0.0052	505	0.0678	373	0.0002	362	0.0005	427
323	mobbl-003	0.0000	484	0.0029	463	0.0633	365	0.0002	388	0.0009	480
324	mobipintech-000	0.0000	180	0.0000	114	0.0000	38	0.0000	58	0.0000	64
325	momovn-001	0.0015	548	0.0010	328	0.0103	130	0.0011	510	0.0008	474
326	moredian-000	0.0000	270	0.0009	300	-	419	0.0004	443	0.0005	410
327	mukh-003	0.0000	268	0.0003	145	0.0060	95	0.0001	348	0.0003	199
328	mukh-004	0.0000	282	0.0013	389	0.0327	306	0.0000	236	0.0004	218
329	multimodality-000	0.0000	158	0.0000	63	0.0000	65	0.0000	1	0.0000	116
330	multimodality-001	0.0000	32	0.0009	298	0.0259	280	0.0000	88	0.0000	59
331	mvision-001	0.0000	51	0.0000	6	-	467	0.0000	79	0.0000	46
332	nazhiai-000	0.0000	63	0.0000	56	-	426	0.0000	131	0.0000	11
333	ncsgroup-000	0.0000	186	0.0000	111	0.0000	41	0.0000	52	-	559
334	ncssg-001	0.0000	210	0.0000	103	0.0000	50	0.0000	46	0.0000	92
335	neosystems-004	0.0000	171	0.0000	122	0.0000	44	0.0000	65	0.0000	72
336	netbridgetech-001	0.0000	60	0.0000	57	-	424	0.0000	134	0.0000	10
337	netbridgetech-002	0.0000	72	0.0000	50	-	417	0.0000	126	0.0000	2
338	neurotechnology-017	0.0000	11	0.0003	164	0.0065	100	0.0000	100	0.0000	128
339	neurotechnology-018	0.0000	238	0.0003	166	0.0074	108	0.0000	186	0.0004	220
340	nhn-004	0.0000	420	0.0000	65	0.0000	67	0.0001	347	0.0004	348
341	nhn-005	0.0000	306	0.0000	85	0.0000	58	0.0000	215	0.0004	254
342	nodeflux-002	0.0000	339	0.0261	541	-	499	0.0008	491	0.0005	423
343	nominder-002	0.0000	310	0.0006	219	0.0119	142	0.0002	386	0.0003	205
344	nominder-003	0.0000	297	0.0005	199	0.0095	127	0.0002	364	-	567
345	notiontag-001	0.0000	136	0.0000	75	-	534	0.0027	542	0.0000	102
346	notiontag-002	0.0000	141	0.0000	72	0.0000	69	0.0000	12	0.0000	121
347	nsensecorp-004	0.0406	568	0.0035	475	0.0181	196	0.0016	522	0.0760	546
348	nsensecorp-005	0.0000	74	0.0000	52	0.0000	5	0.0000	125	0.0000	1

Table 41: FTE is the proportion of failed template generation attempts. Failures can occur because the software throws an exception, or because the software electively refuses to process the input image. This would typically occur if a face is not detected. FTE is measured as the number of function calls that give EITHER a non-zero error code OR that give a "small" template. This is defined as one whose size is less than 0.3 times the median template size for that algorithm. This second rule is needed because some algorithms incorrectly fail to return a non-zero error code when template generation fails.
A hyphen "-" indicates the dataset was not produced. [1]*The effects of FTE are included in the accuracy results of this report by regarding any template comparison involving a failed template to produce a low similarity score. Thus higher FTE results in higher FNMR and lower FMR.*

FNMR(T) "False non-match rate"
FMR(T) "False match rate"

	Algorithm	Failure to Enrol Rate[1]									
	Name	APPLICATION		BORDER		KIOSK		MUGSHOT		VISA	
	Name	SEC. 2.2		SEC. 2.4		SEC. 2.6		SEC. 2.5		SEC. 2.1	
349	ntechlab-011	0.0000	66	0.0003	143	0.0057	90	0.0000	237	0.0004	216
350	ntechlab-012	0.0000	15	0.0003	142	0.0057	91	0.0000	233	0.0004	219
351	omface-000	0.0000	191	0.0000	110	0.0000	35	0.0000	61	0.0000	67
352	omface-001	0.0000	9	0.0000	125	0.0000	75	0.0000	103	0.0000	42
353	omnigarde-002	0.0000	277	0.0008	266	0.0213	236	0.0000	194	0.0004	320
354	omnigarde-003	0.0000	151	0.0007	263	0.0212	235	0.0000	145	0.0004	270
355	onfido-000	0.0000	480	0.0040	482	0.0804	388	0.0004	429	0.0012	501
356	openedge-000	0.0000	237	0.0014	394	0.0212	234	0.0003	418	0.0004	352
357	openface-001	0.0000	449	0.0104	527	0.0668	368	0.0004	435	0.0006	463
358	ovisionllc-001	0.0000	58	0.0000	2	0.0000	26	0.0000	74	-	557
359	oz-003	0.0000	45	0.0002	138	0.0042	85	0.0000	150	0.0003	148
360	oz-004	0.0000	458	0.0003	151	0.0041	84	0.0000	164	0.0002	138
361	palit-000	0.0000	352	0.0005	202	0.0134	155	0.0002	372	0.0004	264
362	palit-001	0.0000	319	0.0007	265	0.0201	217	0.0002	370	0.0004	271
363	pangiam-001	0.0000	129	0.0005	207	0.0128	150	0.0002	409	0.0003	213
364	pangiam-002	0.0000	202	0.0003	161	0.0072	104	0.0000	184	0.0003	180
365	papago-001	0.0000	378	0.0008	273	0.0159	180	0.0002	407	0.0004	294
366	papil11-000	0.0000	272	0.0008	295	0.0192	212	0.0000	208	0.0003	207
367	papsav1923-002	0.0000	243	0.0018	419	0.0268	285	0.0000	219	0.0004	332
368	papsav1923-003	0.0000	414	0.0019	426	0.0321	302	0.0000	245	0.0004	297
369	paravision-011	0.0000	26	0.0010	335	0.0201	215	0.0001	289	0.0004	222
370	paravision-013	0.0000	178	0.0010	338	0.0201	216	0.0001	288	0.0004	225
371	pensees-001	0.0000	234	0.0000	24	-	458	0.0000	101	0.0000	41
372	pixelall-009	0.0000	197	0.0000	107	0.0000	51	0.0000	44	0.0000	88
373	pixelall-010	0.0000	168	0.0000	60	0.0000	64	0.0000	3	0.0000	118
374	privid-001	0.0001	522	0.0176	536	0.0598	362	0.0021	532	0.0021	523
375	privid-002	0.0198	563	0.0040	484	0.0386	336	0.0014	517	0.0011	493
376	psl-011	0.0000	275	0.0003	144	0.0063	98	0.0000	141	0.0003	192
377	psl-012	0.0000	289	0.0003	149	0.0067	101	0.0000	140	0.0003	193
378	ptakuratsatu-000	0.0000	361	0.0007	259	-	519	0.0001	255	0.0003	175
379	pxl-001	0.0000	499	0.0044	493	-	515	0.0005	460	0.0022	526
380	pyramid-000	0.0001	516	0.0041	488	-	513	0.0005	457	0.0007	472
381	qazbs-000	0.0000	43	0.0009	309	0.0265	284	0.0000	177	0.0004	284
382	qazsmartvisionai-000	0.0000	336	0.0003	165	0.0083	119	0.0000	143	0.0003	181
383	qluevision-001	0.0000	430	0.0008	279	0.0153	168	0.0008	490	0.0004	401
384	qnap-004	0.0000	216	0.0016	404	0.0402	341	0.0000	240	0.0001	135
385	qnap-005	0.0001	506	0.0078	517	0.0581	359	0.0010	506	0.0005	443
386	quantasoft-003	0.0000	438	0.0015	402	0.0355	322	0.0005	456	0.0006	457
387	rankone-015	0.0000	104	0.0000	34	0.0000	13	0.0000	106	0.0000	18
388	realnetworks-007	0.0000	368	0.0013	391	0.0425	345	0.0000	147	0.0004	305
389	realnetworks-008	0.0000	263	0.0002	140	0.0045	86	0.0000	142	0.0002	147
390	rebs-000	0.0000	71	0.0005	189	0.0130	152	0.0000	189	0.0004	242
391	rebs-001	0.0000	166	0.0005	197	0.0144	161	0.0000	198	0.0004	296
392	recognito-000	0.0000	366	0.0003	146	0.0056	89	0.0000	211	0.0003	197
393	recognito-001	0.0000	349	0.0003	147	0.0056	88	0.0000	213	0.0003	195
394	regula-000	0.0000	145	0.0000	73	0.0000	68	0.0000	10	0.0000	120
395	regula-001	0.0000	96	0.0000	36	0.0000	10	0.0000	109	0.0000	16
396	remarkai-001	0.0000	162	0.0000	62	-	553	0.0000	5	0.0000	117
397	remarkai-003	0.0000	374	0.0007	247	0.0187	202	0.0000	222	0.0004	249
398	rendip-000	0.0000	418	0.0016	407	0.0293	290	0.0002	367	0.0004	396
399	revealmedia-005	0.0000	424	0.0007	254	0.0189	205	0.0009	500	0.0004	399
400	revealmedia-006	0.0000	67	0.0009	318	0.0238	263	0.0001	313	0.0004	349
401	roc-016	0.0000	143	0.0000	132	0.0006	78	0.0000	11	0.0000	131
402	rokid-000	0.0000	223	0.0072	513	-	504	0.0001	295	0.0005	417
403	rokid-001	0.0000	123	0.0013	385	-	546	0.0000	28	0.0000	114
404	s1-005	0.0000	229	0.0004	177	0.0120	145	0.0001	266	0.0002	141
405	s1-007	0.0000	219	0.0006	220	0.0110	139	0.0001	267	0.0002	140
406	saffe-001	0.0000	147	0.0000	68	-	572	0.0000	9	0.0000	125

Table 42: FTE is the proportion of failed template generation attempts. Failures can occur because the software throws an exception, or because the software electively refuses to process the input image. This would typically occur if a face is not detected. FTE is measured as the number of function calls that give EITHER a non-zero error code OR that give a "small" template. This is defined as one whose size is less than 0.3 times the median template size for that algorithm. This second rule is needed because some algorithms incorrectly fail to return a non-zero error code when template generation fails.
A hyphen "-" indicates the dataset was not produced. [1]*The effects of FTE are included in the accuracy results of this report by regarding any template comparison involving a failed template to produce a low similarity score. Thus higher FTE results in higher FNMR and lower FMR.*

FNMR(T) "False non-match rate"
FMR(T) "False match rate"

	Algorithm	Failure to Enrol Rate[1]									
	Name	APPLICATION		BORDER		KIOSK		MUGSHOT		VISA	
	Name	SEC. 2.2		SEC. 2.4		SEC. 2.6		SEC. 2.5		SEC. 2.1	
407	saffe-002	0.0000	99	0.0000	37	-	432	0.0000	108	0.0000	15
408	samsungsds-001	0.0000	69	0.0005	204	0.0146	162	0.0001	291	0.0003	200
409	samsungsds-002	0.0000	218	0.0004	180	0.0119	143	0.0001	287	0.0003	189
410	samtech-001	0.0001	512	0.0032	466	-	436	0.0004	442	0.0008	473
411	samtech-002	0.0000	451	0.0018	417	0.0516	351	0.0002	406	0.0005	431
412	scanovate-002	0.0000	381	0.0018	415	-	462	0.0000	250	0.0004	392
413	scanovate-003	0.0000	410	0.0233	540	0.3371	413	0.0006	472	0.0004	402
414	sdc-000	0.0000	491	0.0035	474	0.0678	374	0.0005	466	0.0011	496
415	seamfix-001	0.0000	75	0.0000	51	0.0000	6	0.0000	124	-	549
416	securifai-007	0.0000	188	0.0000	112	0.0000	40	0.0000	51	0.0000	66
417	securifai-008	0.0000	39	0.0000	9	0.0000	31	0.0000	84	-	558
418	sensetime-007	0.0000	109	0.0004	174	0.0106	131	0.0000	195	0.0003	171
419	sensetime-008	0.0000	115	0.0007	258	0.0250	269	0.0000	138	0.0003	215
420	serendipity-000	0.0000	369	0.0008	275	0.0202	218	0.0001	345	0.0004	316
421	sertis-002	0.0000	78	0.0007	244	0.0152	165	0.0000	244	0.0004	273
422	sertis-003	0.0000	276	0.0008	285	0.0183	198	0.0000	209	0.0004	309
423	seventhsense-003	0.0000	266	0.0003	159	0.0083	120	0.0000	175	0.0002	144
424	seventhsense-005	0.0000	256	0.0002	141	0.0065	99	0.0000	178	0.0003	158
425	shaman-000	0.0000	167	0.0000	59	-	558	0.0000	4	0.0000	119
426	shaman-001	0.0000	95	0.0000	39	-	442	0.0000	120	0.0000	31
427	shu-002	0.0000	400	0.0010	344	-	565	0.0005	450	0.0004	383
428	shu-003	0.0000	142	0.0007	241	-	569	0.0001	259	0.0003	170
429	siat-002	0.0000	285	0.0012	372	-	438	0.0000	216	0.0004	299
430	siat-005	0.0000	85	0.0000	44	0.0000	72	0.0000	118	0.0000	26
431	sjtu-004	0.0000	181	0.0000	113	0.0000	39	0.0000	57	0.0003	159
432	sjtu-005	0.0000	496	0.0000	26	0.0000	23	0.0000	96	0.0006	453
433	sktelecom-000	0.0000	364	0.0008	286	0.0190	207	0.0000	229	0.0004	337
434	smartbiometrik-001	0.0005	535	0.0649	560	0.2147	407	0.0017	524	0.0008	477
435	smartengines-000	0.0066	557	0.0150	533	0.1656	400	0.0022	533	0.0013	510
436	smartengines-001	0.0003	531	0.0073	514	0.0714	382	0.0007	483	0.0005	424
437	smartvist-000	0.0000	23	0.0026	452	0.0357	323	0.0002	352	0.0011	495
438	smartvist-001	0.0000	250	0.0005	191	0.0069	103	0.0001	333	0.0003	183
439	smilart-002	0.0000	489	0.0036	478	-	486	-	570	0.0011	494
440	smilart-003	0.0003	530	0.0100	526	-	423	0.0014	515	0.0013	512
441	sodec-000	0.0000	68	0.0000	54	0.0000	7	0.0000	136	0.0000	13
442	sparsh-001	0.0000	160	0.0007	239	0.0168	186	0.0000	155	0.0004	255
443	sqisoft-002	0.0000	139	0.0003	156	0.0078	112	0.0000	171	0.0003	214
444	sqisoft-003	0.0000	225	0.0003	160	0.0078	113	0.0000	173	0.0003	179
445	staqu-000	0.0000	76	0.0000	49	-	418	0.0000	123	0.0000	3
446	starhybrid-001	0.0001	519	0.0033	472	-	470	0.0009	499	0.0023	527
447	stcon-002	0.0000	367	0.0011	354	0.0226	250	0.0000	183	0.0003	163
448	stcon-003	0.0000	126	0.0005	196	0.0142	160	0.0000	182	0.0004	251
449	stengg-000	0.0000	49	0.0013	388	0.0350	321	0.0000	200	0.0004	313
450	sukshi-000	0.0000	105	0.0000	32	0.0000	9	0.0000	112	0.0000	21
451	suprema-004	0.0000	246	0.0014	396	0.0299	291	0.0000	169	0.0004	277
452	suprema-005	0.0000	391	0.0014	395	0.0299	292	0.0005	455	0.0004	346
453	supremaid-001	0.0000	350	0.0020	430	0.0330	309	0.0001	305	0.0004	393
454	supremaid-002	0.0000	356	0.0020	429	0.0330	310	0.0001	304	0.0004	394
455	surrey-cvssp-002	0.0000	459	0.0006	224	0.0156	172	0.0001	283	0.0004	295
456	surrey-cvssp-003	0.0000	106	0.0009	304	0.0165	183	0.0000	111	0.0001	136
457	swsam-001	0.0000	187	0.0012	379	0.0263	283	0.0000	50	0.0000	65
458	synesis-006	0.0000	192	0.0003	163	-	490	0.0000	230	0.0003	154
459	synesis-007	0.0000	320	0.0013	384	-	563	0.0002	391	0.0004	307
460	synology-000	0.0000	117	0.0000	89	-	551	0.0000	24	0.0000	108
461	synology-002	0.0000	208	0.0000	102	-	524	0.0000	48	0.0000	93
462	sztu-000	0.0000	92	0.0000	40	-	440	0.0000	122	0.0000	30
463	sztu-001	0.0000	130	0.0000	77	0.0000	55	0.0000	22	0.0000	100
464	t4isb-000	0.0000	7	0.0000	25	0.0000	20	0.0000	102	0.0000	40

Table 43: FTE is the proportion of failed template generation attempts. Failures can occur because the software throws an exception, or because the software electively refuses to process the input image. This would typically occur if a face is not detected. FTE is measured as the number of function calls that give EITHER a non-zero error code OR that give a "small" template. This is defined as one whose size is less than 0.3 times the median template size for that algorithm. This second rule is needed because some algorithms incorrectly fail to return a non-zero error code when template generation fails.
A hyphen "-" indicates the dataset was not produced. [1]*The effects of FTE are included in the accuracy results of this report by regarding any template comparison involving a failed template to produce a low similarity score. Thus higher FTE results in higher FNMR and lower FMR.*

FNMR(T) "False non-match rate"
FMR(T) "False match rate"

	Algorithm	Failure to Enrol Rate[1]									
	Name	APPLICATION		BORDER		KIOSK		MUGSHOT		VISA	
	Name	SEC. 2.2		SEC. 2.4		SEC. 2.6		SEC. 2.5		SEC. 2.1	
465	tech5-007	0.0000	293	0.0014	398	0.0305	297	0.0000	180	0.0004	259
466	tech5-008	0.0000	12	0.0007	238	0.0168	185	0.0000	160	0.0004	245
467	techainer-001	0.0000	478	0.0004	185	0.0085	122	0.0005	454	0.0004	347
468	techsign-000	0.0007	543	0.0334	547	0.2093	402	0.0020	528	0.0011	492
469	techsign-001	0.0000	354	0.0008	297	0.0253	275	0.0002	374	0.0004	317
470	tevian-007	0.0000	322	0.0015	403	0.0429	346	0.0002	383	0.0004	340
471	tevian-008	0.0000	287	0.0006	217	0.0109	137	0.0000	187	0.0003	168
472	tiger-005	0.0000	360	0.0009	320	0.0194	214	0.0001	282	0.0004	290
473	tiger-006	0.0000	397	0.0011	359	0.0396	339	0.0001	338	0.0004	398
474	tinkoff-001	0.0000	407	0.0008	284	0.0171	190	0.0001	326	0.0004	288
475	tnitech-000	0.0000	357	0.0003	158	0.0060	93	0.0005	467	0.0003	166
476	tongyi-005	0.0000	169	0.0000	120	-	498	0.0000	66	0.0000	73
477	toppanidgate-000	0.0000	255	0.0008	278	0.0232	257	0.0004	430	0.0004	323
478	toshiba-007	0.0000	379	0.0005	195	0.0082	117	0.0002	401	0.0004	312
479	toshiba-008	0.0000	387	0.0005	194	0.0082	118	0.0002	400	0.0004	314
480	touchlessid-002	0.0000	108	0.0043	491	0.1087	393	0.0000	113	0.0000	23
481	touchlessid-003	0.0000	254	0.0010	339	0.0287	288	0.0002	353	0.0004	385
482	trueface-002	0.0000	392	0.0046	498	-	469	0.0003	410	0.0005	436
483	trueface-003	0.0000	386	0.0046	499	0.0397	340	0.0003	411	0.0005	438
484	trueidvng-001	0.0000	402	0.0020	434	0.0385	335	0.0002	377	0.0005	420
485	truststamp-001	0.0000	351	0.0010	336	0.0189	206	0.0000	174	0.0003	187
486	tuputech-000	0.0003	533	0.0116	529	-	428	-	571	0.0081	540
487	turingtechvip-001	0.0001	509	0.0007	256	0.0061	97	0.0007	482	0.0006	449
488	turingtechvip-002	0.0001	508	0.0017	413	0.0097	128	0.0007	484	0.0006	450
489	turkcell-001	0.0000	50	0.0002	139	0.0034	83	0.0001	292	0.0003	150
490	turkcell-002	0.0000	93	0.0002	137	0.0026	81	0.0001	258	-	551
491	twface-000	0.0000	226	0.0000	94	0.0000	46	0.0000	37	0.0000	86
492	twface-001	0.0000	38	0.0000	10	0.0000	30	0.0000	85	0.0000	57
493	ulsee-001	0.0000	3	0.0000	30	-	464	0.0000	97	0.0000	36
494	ultinous-000	-	572	-	571	-	510	-	568	0.0003	178
495	ultinous-001	-	571	-	572	-	497	-	569	0.0003	177
496	uluface-002	0.0000	121	0.0000	88	-	542	0.0000	29	0.0000	111
497	uluface-003	0.0000	204	0.0001	135	-	520	0.0002	355	0.0002	142
498	unicc-002	0.0316	567	0.0082	519	0.0188	203	0.0226	565	0.0936	548
499	unicc-003	0.0007	544	0.0022	438	0.0094	126	0.0026	541	0.0029	533
500	unissey-003	0.0000	152	0.0008	269	0.0191	208	0.0001	285	0.0004	272
501	unissey-004	0.0000	22	0.0009	310	0.0240	264	0.0001	314	0.0004	301
502	upc-001	0.0000	455	0.0003	153	-	508	0.0003	413	0.0003	196
503	useb-001	0.0000	345	0.0009	315	0.0228	254	0.0001	334	0.0004	265
504	useb-002	0.0000	231	0.0009	313	0.0228	252	0.0001	336	0.0004	260
505	uxlabs-001	0.0000	31	0.0000	15	0.0000	28	0.0000	89	0.0000	53
506	uxlabs-003	0.0000	148	0.0000	70	0.0000	71	0.0000	8	0.0000	123
507	vcog-002	-	570	-	570	-	441	-	572	0.0019	521
508	vcortex-001	0.0000	467	0.2295	568	0.0802	387	0.0017	523	0.0006	448
509	vd-002	0.0000	224	0.0000	98	1.0000	503	0.0000	39	0.0000	83
510	vd-003	0.0001	510	0.0041	485	0.0676	371	0.0030	545	0.0029	534
511	veridas-008	0.0000	450	0.0026	450	0.0595	360	0.0001	320	0.0005	415
512	veridas-009	0.0000	445	0.0026	451	0.0597	361	0.0001	286	0.0005	418
513	veridium-002	0.0000	498	0.0083	521	0.1591	398	0.0010	503	0.0005	435
514	veridium-003	0.0001	504	0.0087	522	0.1615	399	0.0014	518	-	566
515	verigram-001	0.0000	393	0.0003	154	0.0060	92	0.0002	390	0.0003	201
516	verigram-003	0.0000	490	0.0025	448	0.0288	289	0.0009	502	0.0008	475
517	verihubs-inteligensia-001	0.0000	242	0.0029	459	0.0669	369	0.0001	270	0.0004	351
518	verihubs-inteligensia-002	0.0000	333	0.0029	460	0.0669	370	0.0001	264	0.0004	356
519	verijelas-000	0.0000	252	0.0023	442	0.0375	331	0.0004	449	0.0006	454
520	via-004	0.0000	173	0.0000	119	0.0000	45	0.0000	63	0.0000	74
521	via-005	0.0000	200	0.0000	105	0.0000	53	0.0000	42	0.0000	90
522	viante-000	0.0000	380	0.0008	287	0.0168	187	0.0001	312	0.0004	400

Table 44: FTE is the proportion of failed template generation attempts. Failures can occur because the software throws an exception, or because the software electively refuses to process the input image. This would typically occur if a face is not detected. FTE is measured as the number of function calls that give EITHER a non-zero error code OR that give a "small" template. This is defined as one whose size is less than 0.3 times the median template size for that algorithm. This second rule is needed because some algorithms incorrectly fail to return a non-zero error code when template generation fails.
A hyphen "-" indicates the dataset was not produced. [1]*The effects of FTE are included in the accuracy results of this report by regarding any template comparison involving a failed template to produce a low similarity score. Thus higher FTE results in higher FNMR and lower FMR.*

FNMR(T) "False non-match rate"
FMR(T) "False match rate"

	Algorithm	Failure to Enrol Rate[1]									
	Name	APPLICATION		BORDER		KIOSK		MUGSHOT		VISA	
	Name	SEC. 2.2		SEC. 2.4		SEC. 2.6		SEC. 2.5		SEC. 2.1	
523	videmo-001	0.0000	435	0.0170	535	0.0332	312	0.0010	508	0.0011	498
524	videmo-002	0.0000	172	0.0006	232	0.0189	204	0.0001	300	0.0004	248
525	videonetics-001	0.0004	534	0.0309	545	-	444	0.0015	521	0.0010	484
526	videonetics-002	0.0000	423	0.0459	557	-	509	0.0006	476	0.0005	441
527	viettelhightech-000	0.0000	461	0.0019	424	0.0368	329	0.0007	485	0.0005	437
528	vigilantsolutions-010	0.0000	437	0.0028	455	0.0609	363	0.0001	275	0.0004	230
529	vigilantsolutions-011	0.0000	442	0.0028	456	0.0609	364	0.0001	274	0.0004	238
530	vinai-000	0.0000	127	0.0000	82	-	540	0.0000	15	0.0000	95
531	vinbigdata-002	0.0000	205	0.0015	401	0.0250	270	0.0000	212	0.0004	375
532	vinbigdata-003	0.0000	328	0.0007	243	0.0151	164	0.0000	251	0.0004	256
533	vion-000	0.0050	553	0.0392	554	-	538	0.0130	563	0.0078	539
534	visage-000	0.0000	462	0.0054	507	-	531	0.0009	497	0.0006	451
535	visionbox-003	0.0000	412	0.0010	330	0.0209	229	0.0001	307	0.0004	333
536	visionbox-004	0.0000	384	0.0013	380	0.0248	268	0.0001	330	0.0004	381
537	visionlabs-010	0.0000	427	0.0009	306	-	443	0.0001	332	0.0004	321
538	visionlabs-011	0.0000	189	0.0006	229	0.0156	173	0.0001	277	0.0004	247
539	visteam-007	0.0000	313	0.0008	282	0.0209	225	0.0000	158	0.0004	239
540	visteam-008	0.0000	329	0.0008	281	0.0209	226	0.0000	156	0.0004	241
541	vivotek-001	0.0000	230	0.0006	227	0.0161	181	0.0000	36	-	563
542	vixvizion-006	0.0000	28	0.0000	17	0.0000	34	0.0000	80	0.0000	51
543	vixvizion-007	0.0000	2	0.0000	28	0.0000	21	0.0000	99	0.0000	38
544	vnis-000	0.0007	546	0.0695	564	0.0756	385	0.0038	551	0.0009	481
545	vnpay-000	0.0000	434	0.0657	563	0.0693	377	0.0037	550	0.0006	447
546	vnpt-005	0.0000	193	0.0006	213	0.0154	170	0.0002	375	0.0004	278
547	vnpt-006	0.0000	153	0.0006	212	0.0154	171	0.0002	373	0.0004	281
548	vocalize-001	0.0216	564	0.0193	538	0.1691	401	0.0068	560	-	555
549	vocord-009	0.0000	253	0.0006	228	-	479	0.0001	344	0.0003	153
550	vocord-010	0.0000	403	0.0005	206	0.0141	159	0.0002	376	0.0003	206
551	vtcc-000	0.0000	14	0.0000	22	0.0000	19	0.0000	92	0.0000	32
552	vtcc-001	0.0000	409	0.0010	334	0.0161	182	0.0000	241	0.0004	250
553	vts-000	0.0000	419	0.0011	356	-	433	0.0001	346	0.0004	390
554	vts-001	0.0000	119	0.0003	150	0.0073	105	0.0000	167	0.0003	151
555	wicket-000	0.0000	371	0.0009	302	0.0260	281	0.0000	176	0.0004	289
556	winsense-001	0.0000	156	0.0000	64	-	559	0.0000	2	0.0000	115
557	winsense-002	0.0000	198	0.0000	108	-	525	0.0000	43	0.0000	87
558	wiseai-001	0.0001	502	0.0137	532	0.0768	386	0.0018	526	0.0018	518
559	wuhantianyu-001	0.0000	19	0.0007	245	0.0159	177	0.0001	257	0.0004	322
560	x-laboratory-000	0.0247	566	0.0000	61	-	555	0.0005	464	0.0002	143
561	x-laboratory-001	0.0000	274	0.0012	368	-	416	0.0001	324	0.0004	378
562	xforwardai-001	0.0000	240	0.0007	255	-	452	0.0003	417	0.0004	372
563	xforwardai-002	0.0000	315	0.0007	257	-	568	0.0003	416	0.0004	377
564	xm-000	0.0000	209	0.0007	242	-	523	0.0001	260	0.0003	169
565	yisheng-004	0.0002	528	-	569	-	434	0.0013	513	0.0006	460
566	yitu-003	0.0000	107	0.0000	31	-	429	0.0009	498	0.0000	22
567	yoonik-003	0.0000	394	0.0009	316	0.0214	238	0.0002	361	0.0004	341
568	yoonik-004	0.0000	53	0.0012	362	0.0251	273	0.0001	278	0.0004	246
569	yoti-001	0.0000	388	0.0014	399	0.0418	343	0.0008	496	0.0006	452
570	ytu-000	0.0000	375	0.0010	351	-	505	0.0002	396	0.0004	374
571	yuan-005	0.0000	363	0.0005	201	0.0134	156	0.0002	371	0.0004	267
572	yuan-008	0.0000	464	0.0013	382	0.0336	316	0.0004	433	0.0005	430

Table 45: FTE is the proportion of failed template generation attempts. Failures can occur because the software throws an exception, or because the software electively refuses to process the input image. This would typically occur if a face is not detected. FTE is measured as the number of function calls that give EITHER a non-zero error code OR that give a "small" template. This is defined as one whose size is less than 0.3 times the median template size for that algorithm. This second rule is needed because some algorithms incorrectly fail to return a non-zero error code when template generation fails.
A hyphen "-" indicates the dataset was not produced. [1]*The effects of FTE are included in the accuracy results of this report by regarding any template comparison involving a failed template to produce a low similarity score. Thus higher FTE results in higher FNMR and lower FMR.*

FNMR(T) "False non-match rate"
FMR(T) "False match rate"

3.4 Recognition accuracy

Core algorithm accuracy is stated via:

- ▷ **Cooperative subjects**
  - The summary table of Figure 35;
  - The visa image DETs of Figure 106;
  - The mugshot DETs of Figure 135;
  - The mugshot ageing profiles of Figure 367;
  - The human-difficult pairs of Figure 51
- ▷ **Non-cooperative subjects**
  - The photojournalism DET of Figure 152

Figure 285 shows dependence of false match rate on algorithm score threshold. This allows a deployer to set a threshold to target a particular false match rate appropriate to the security objectives of the application.

Figure 284 likewise shows FMR(T) but for mugshots, and specially four subsets of the population.

Note that in both the mugshot and visa sets false match rates vary with the ethnicity, age, and sex, of the enrollee and impostor. For example figure 181 summarizes FMR for impostors paired from four groups black females, black males, white females, white males.

FNMR(T) "False non-match rate"
FMR(T) "False match rate"

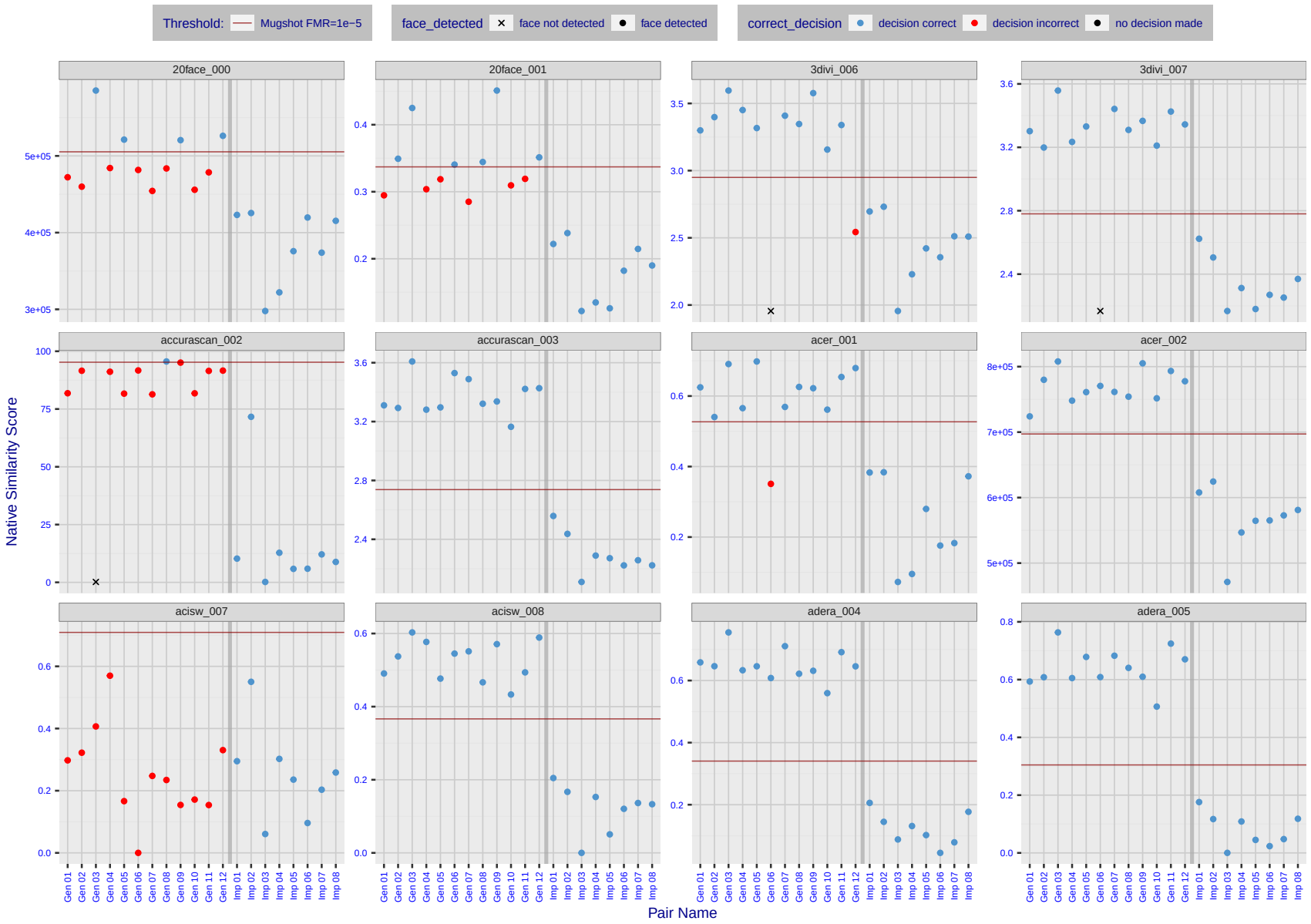

Figure 4: The figure shows algorithms' similarity scores for 12 genuine and 8 impostor image pairs used in a May 2018 paper by Phillips et al. ([1]). The threshold (red horizontal line) is a value calibrated to give FMR = 0.0001 on mugshot images. Points above the threshold correspond to pairs determined to be genuine, and points below the threshold correspond to pairs determined to be impostors. If the determined class (genuine or impostor) matches the real class, points will be blue; if not, red. An X represents face detection failure in either of the images in the pair. Note that the sample size (n=20) is small, and the figure may change substantially if larger or different sets are used. The images can be viewed on p. 13 of the Appendix, where Gen 01 corresponds to Same-Identity Pair 1, Gen 02 corresponds to Same-Identity Pair 2, and so on.

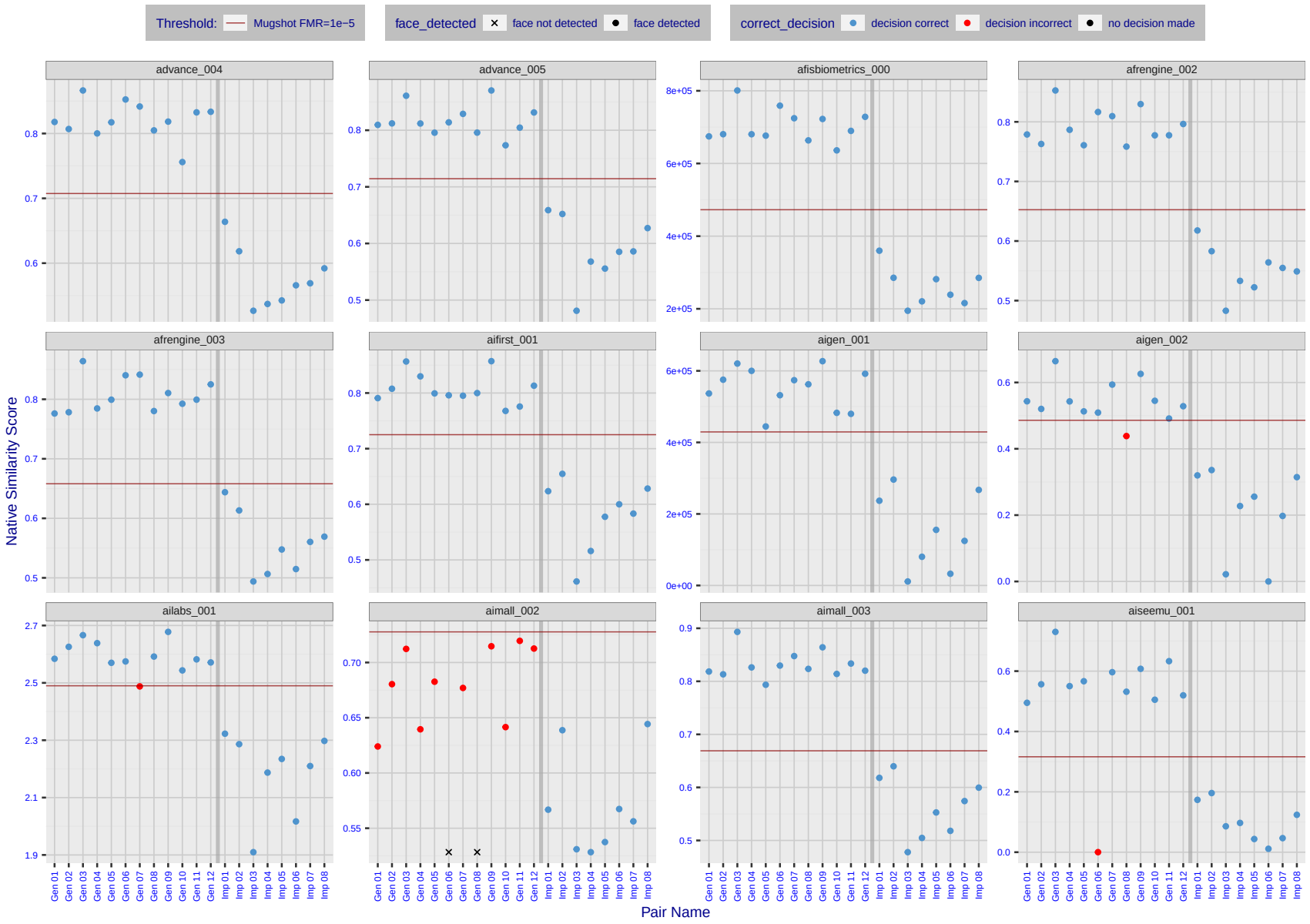

Figure 5: The figure shows algorithms' similarity scores for 12 genuine and 8 impostor image pairs used in a May 2018 paper by Phillips et al. ([1]). The threshold (red horizontal line) is a value calibrated to give FMR = 0.0001 on mugshot images. Points above the threshold correspond to pairs determined to be genuine, and points below the threshold correspond to pairs determined to be impostors. If the determined class (genuine or impostor) matches the real class, points will be blue; if not, red. An X represents face detection failure in either of the images in the pair. Note that the sample size (n=20) is small, and the figure may change substantially if larger or different sets are used. The images can be viewed on p. 13 of the Appendix, where Gen 01 corresponds to Same-Identity Pair 1, Gen 02 corresponds to Same-Identity Pair 2, and so on.

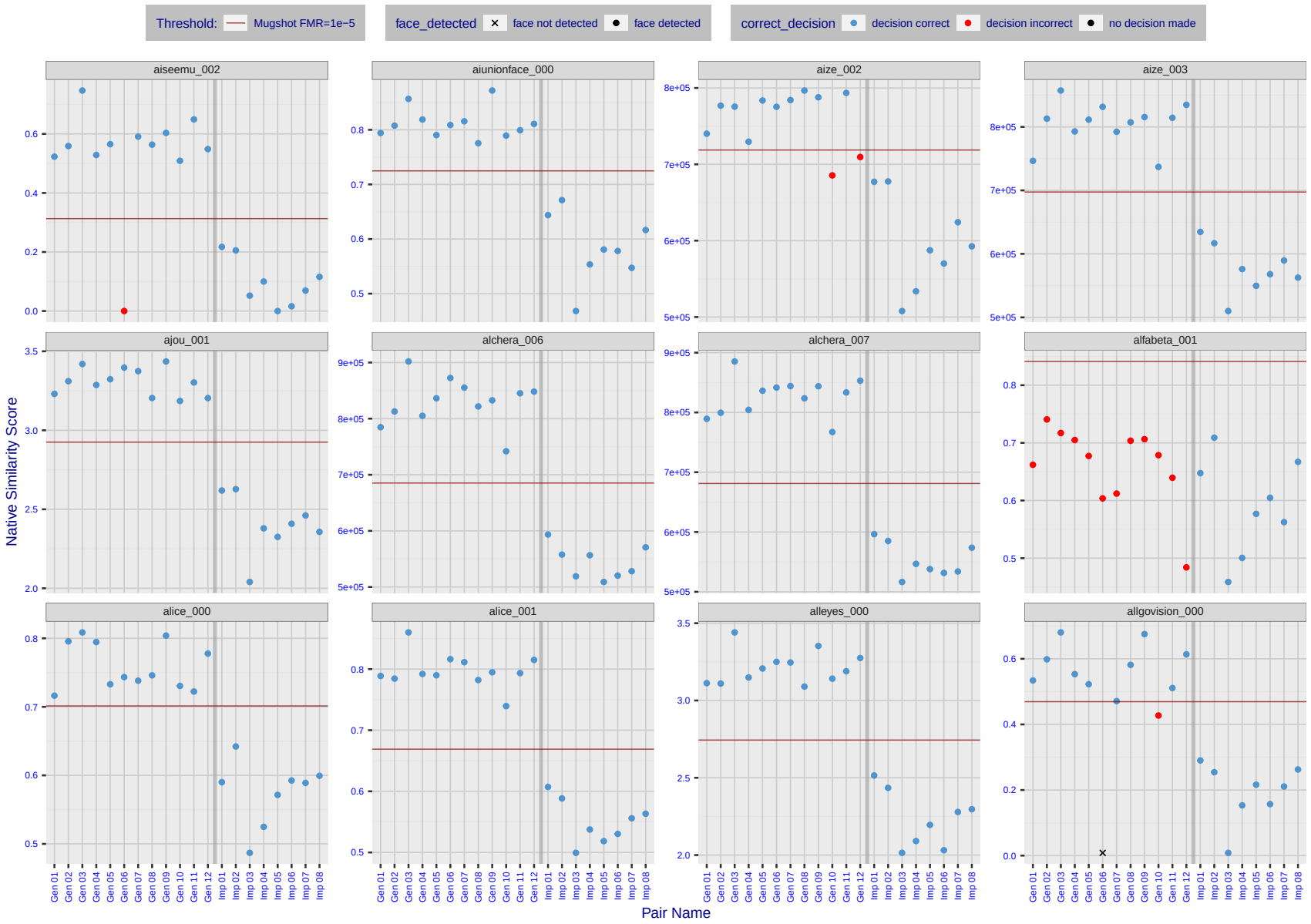

Figure 6: The figure shows algorithms' similarity scores for 12 genuine and 8 impostor image pairs used in a May 2018 paper by Phillips et al. ([1]). The threshold (red horizontal line) is a value calibrated to give FMR = 0.0001 on mugshot images. Points above the threshold correspond to pairs determined to be genuine, and points below the threshold correspond to pairs determined to be impostors. If the determined class (genuine or impostor) matches the real class, points will be blue; if not, red. An X represents face detection failure in either of the images in the pair. Note that the sample size (n=20) is small, and the figure may change substantially if larger or different sets are used. The images can be viewed on p. 13 of the Appendix, where Gen 01 corresponds to Same-Identity Pair 1, Gen 02 corresponds to Same-Identity Pair 2, and so on.

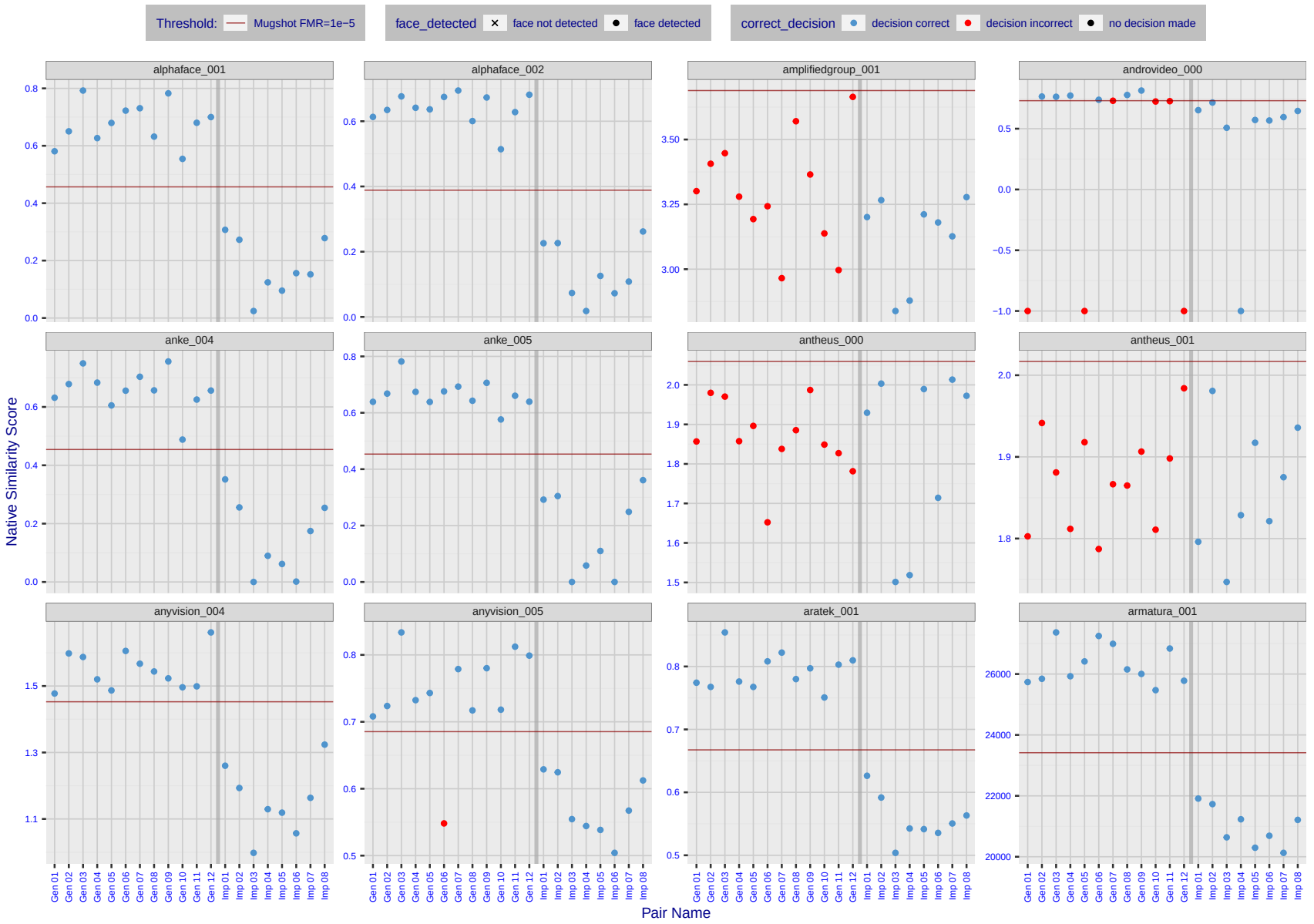

Figure 7: The figure shows algorithms' similarity scores for 12 genuine and 8 impostor image pairs used in a May 2018 paper by Phillips et al. ([1]). The threshold (red horizontal line) is a value calibrated to give FMR = 0.0001 on mugshot images. Points above the threshold correspond to pairs determined to be genuine, and points below the threshold correspond to pairs determined to be impostors. If the determined class (genuine or impostor) matches the real class, points will be blue; if not, red. An X represents face detection failure in either of the images in the pair. Note that the sample size (n=20) is small, and the figure may change substantially if larger or different sets are used. The images can be viewed on p. 13 of the Appendix, where Gen 01 corresponds to Same-Identity Pair 1, Gen 02 corresponds to Same-Identity Pair 2, and so on.

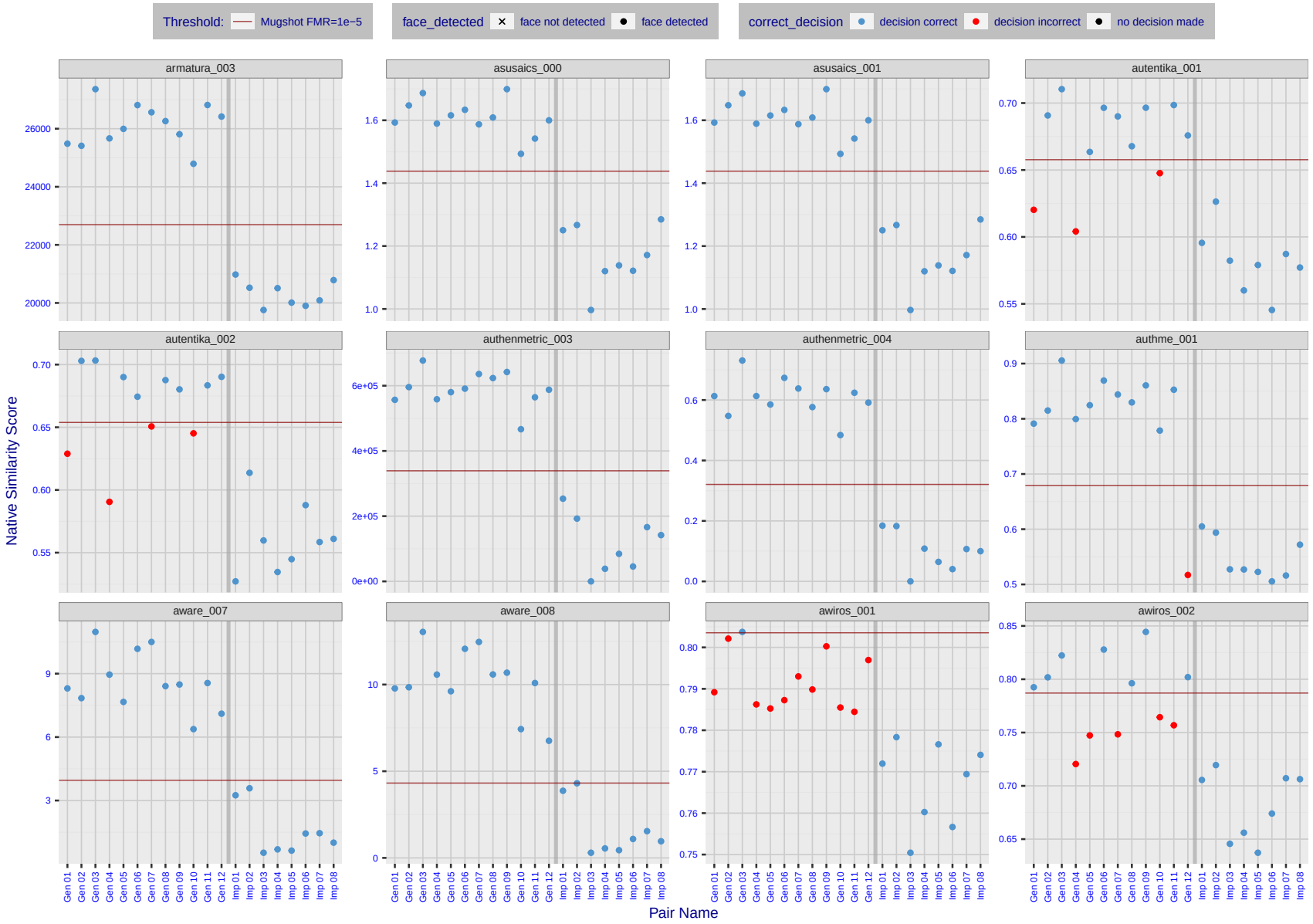

Figure 8: The figure shows algorithms' similarity scores for 12 genuine and 8 impostor image pairs used in a May 2018 paper by Phillips et al. ([1]). The threshold (red horizontal line) is a value calibrated to give FMR = 0.0001 on mugshot images. Points above the threshold correspond to pairs determined to be genuine, and points below the threshold correspond to pairs determined to be impostors. If the determined class (genuine or impostor) matches the real class, points will be blue; if not, red. An X represents face detection failure in either of the images in the pair. Note that the sample size (n=20) is small, and the figure may change substantially if larger or different sets are used. The images can be viewed on p. 13 of the Appendix, where Gen 01 corresponds to Same-Identity Pair 1, Gen 02 corresponds to Same-Identity Pair 2, and so on.

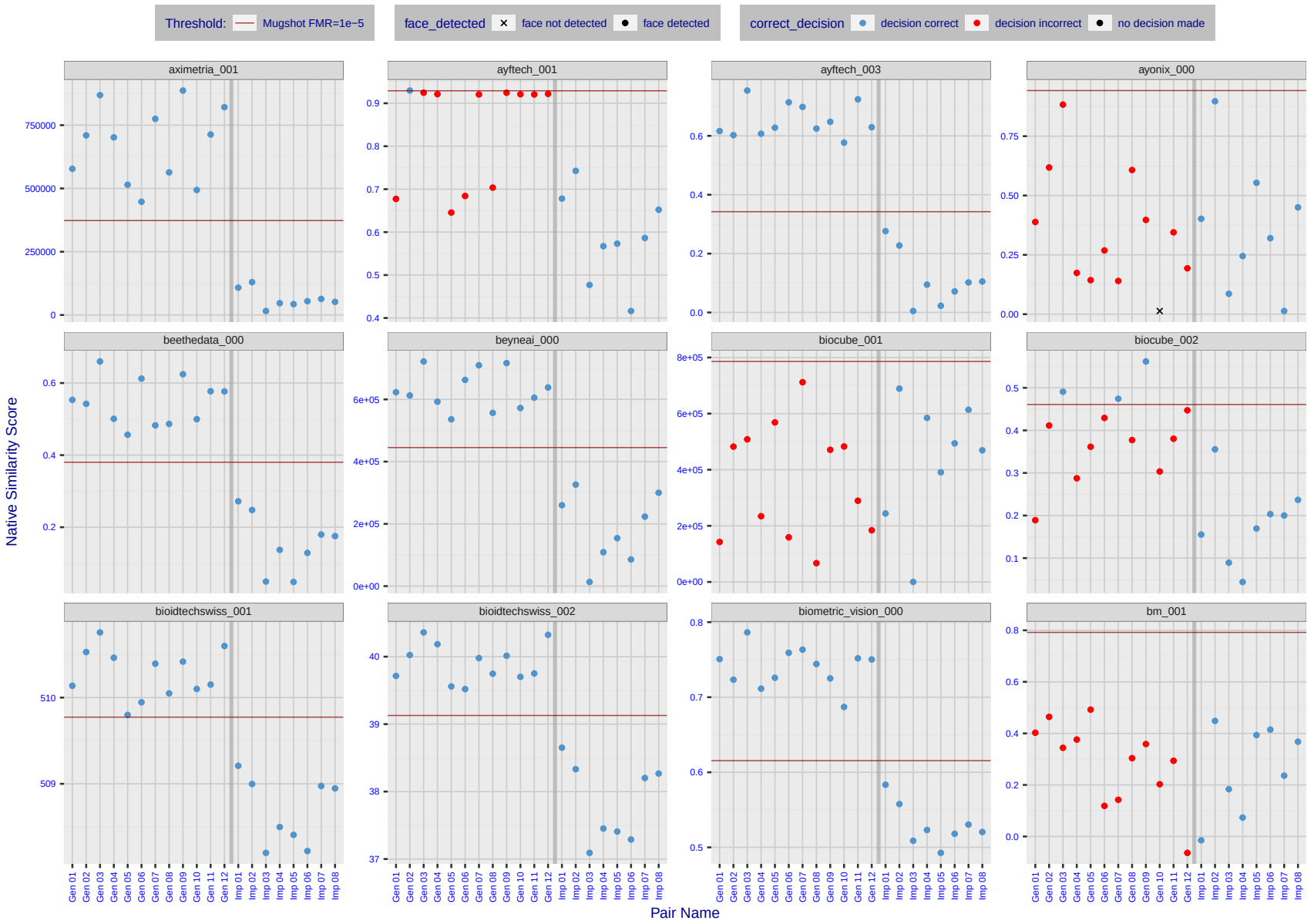

Figure 9: The figure shows algorithms' similarity scores for 12 genuine and 8 impostor image pairs used in a May 2018 paper by Phillips et al. ([1]). The threshold (red horizontal line) is a value calibrated to give FMR = 0.0001 on mugshot images. Points above the threshold correspond to pairs determined to be genuine, and points below the threshold correspond to pairs determined to be impostors. If the determined class (genuine or impostor) matches the real class, points will be blue; if not, red. An X represents face detection failure in either of the images in the pair. Note that the sample size (n=20) is small, and the figure may change substantially if larger or different sets are used. The images can be viewed on p. 13 of the Appendix, where Gen 01 corresponds to Same-Identity Pair 1, Gen 02 corresponds to Same-Identity Pair 2, and so on.

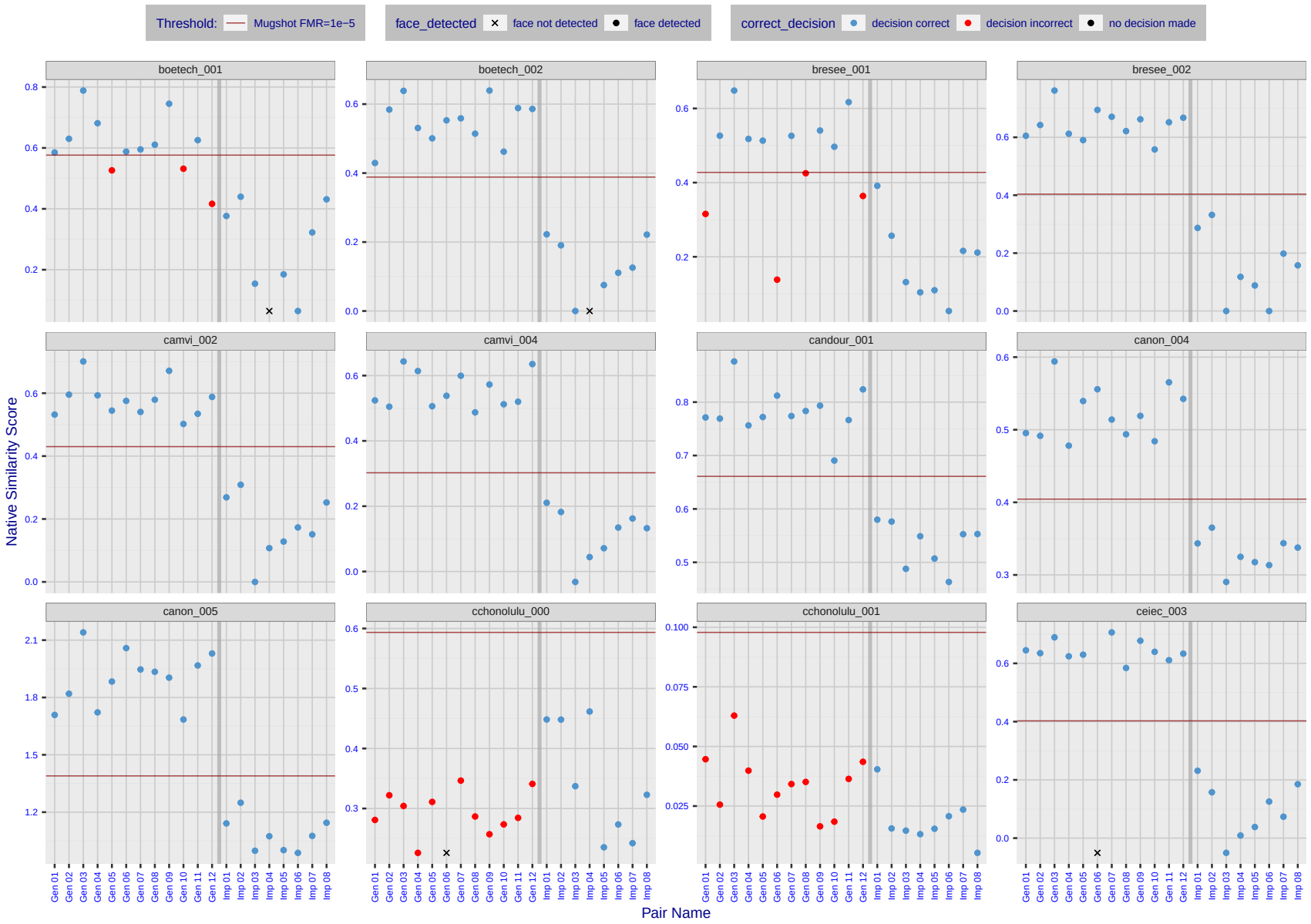

Figure 10: The figure shows algorithms' similarity scores for 12 genuine and 8 impostor image pairs used in a May 2018 paper by Phillips et al. ([1]). The threshold (red horizontal line) is a value calibrated to give FMR = 0.0001 on mugshot images. Points above the threshold correspond to pairs determined to be genuine, and points below the threshold correspond to pairs determined to be impostors. If the determined class (genuine or impostor) matches the real class, points will be blue; if not, red. An X represents face detection failure in either of the images in the pair. Note that the sample size (n=20) is small, and the figure may change substantially if larger or different sets are used. The images can be viewed on p. 13 of the Appendix, where Gen 01 corresponds to Same-Identity Pair 1, Gen 02 corresponds to Same-Identity Pair 2, and so on.

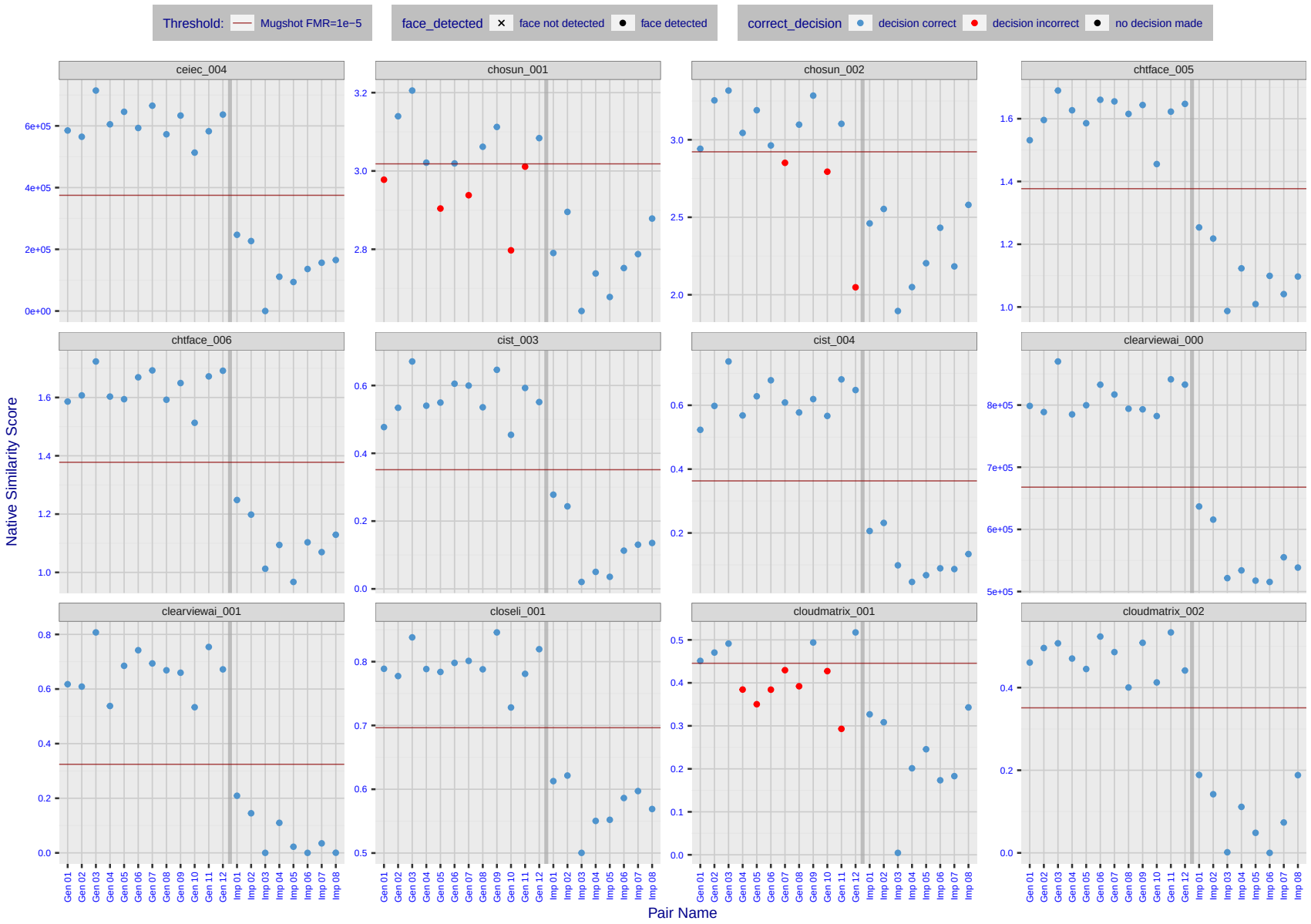

Figure 11: The figure shows algorithms' similarity scores for 12 genuine and 8 impostor image pairs used in a May 2018 paper by Phillips et al. ([1]). The threshold (red horizontal line) is a value calibrated to give FMR = 0.0001 on mugshot images. Points above the threshold correspond to pairs determined to be genuine, and points below the threshold correspond to pairs determined to be impostors. If the determined class (genuine or impostor) matches the real class, points will be blue; if not, red. An X represents face detection failure in either of the images in the pair. Note that the sample size (n=20) is small, and the figure may change substantially if larger or different sets are used. The images can be viewed on p. 13 of the Appendix, where Gen 01 corresponds to Same-Identity Pair 1, Gen 02 corresponds to Same-Identity Pair 2, and so on.

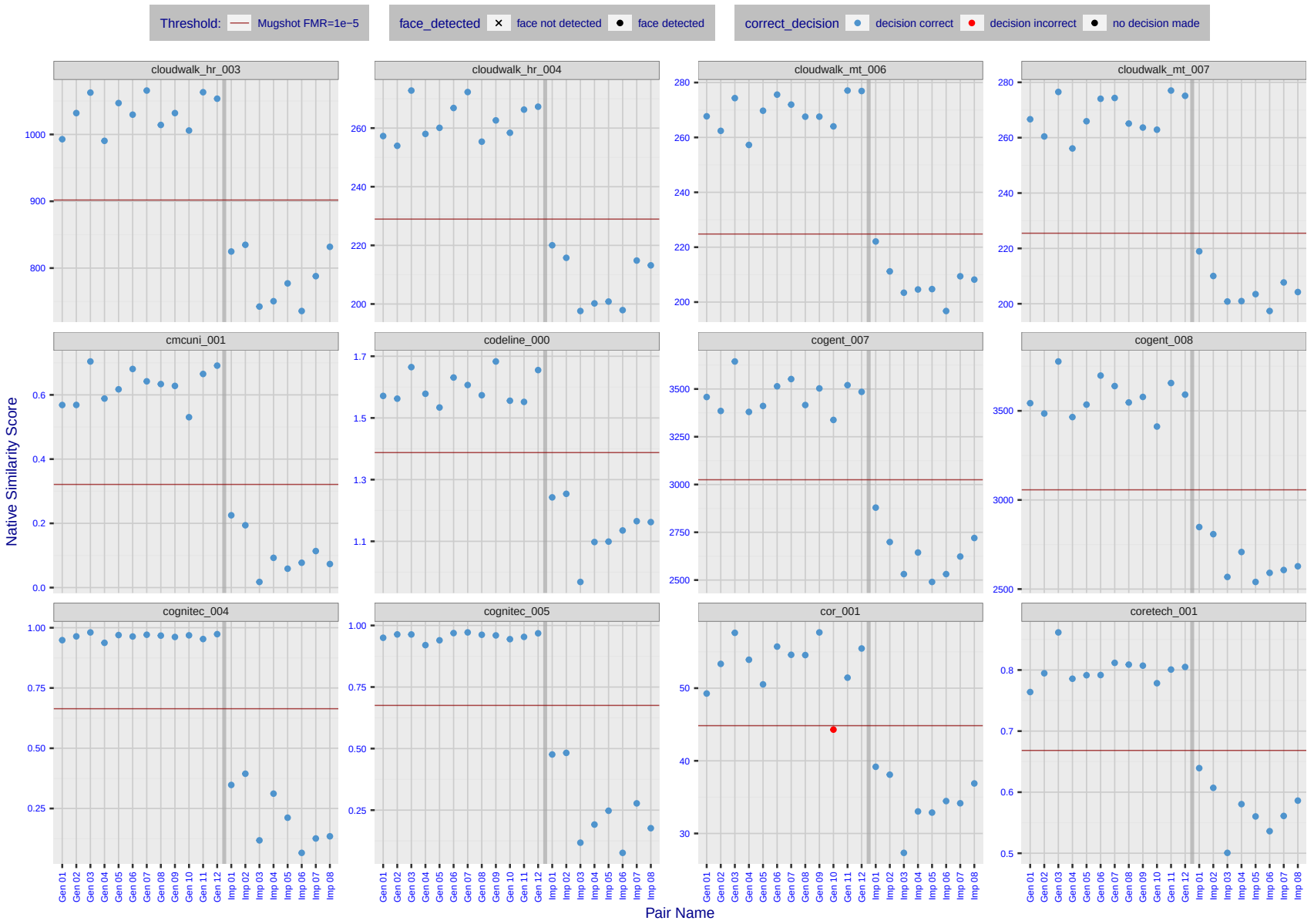

Figure 12: The figure shows algorithms' similarity scores for 12 genuine and 8 impostor image pairs used in a May 2018 paper by Phillips et al. ([1]). The threshold (red horizontal line) is a value calibrated to give FMR = 0.0001 on mugshot images. Points above the threshold correspond to pairs determined to be genuine, and points below the threshold correspond to pairs determined to be impostors. If the determined class (genuine or impostor) matches the real class, points will be blue; if not, red. An X represents face detection failure in either of the images in the pair. Note that the sample size (n=20) is small, and the figure may change substantially if larger or different sets are used. The images can be viewed on p. 13 of the Appendix, where Gen 01 corresponds to Same-Identity Pair 1, Gen 02 corresponds to Same-Identity Pair 2, and so on.

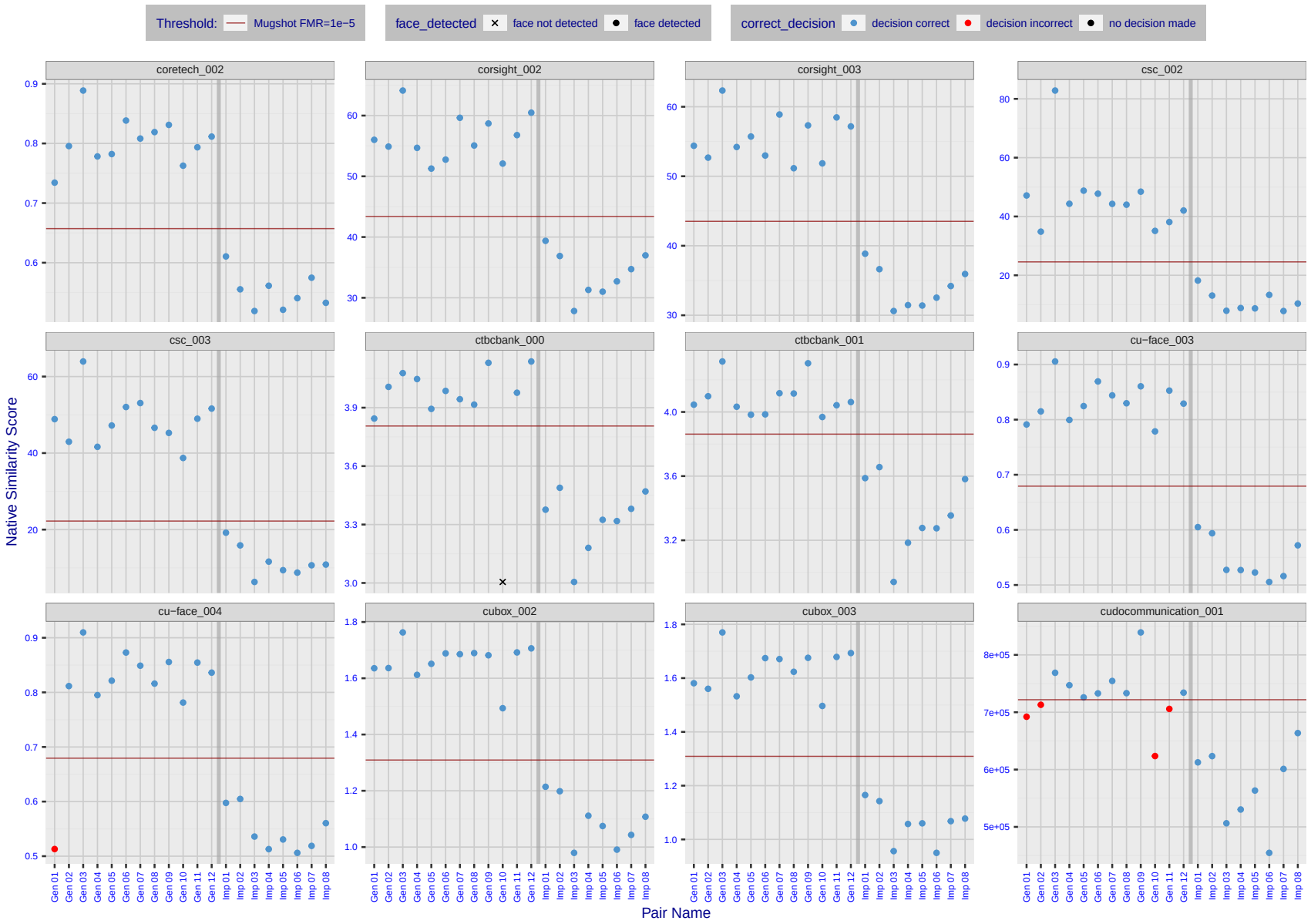

Figure 13: The figure shows algorithms' similarity scores for 12 genuine and 8 impostor image pairs used in a May 2018 paper by Phillips et al. ([1]). The threshold (red horizontal line) is a value calibrated to give FMR = 0.0001 on mugshot images. Points above the threshold correspond to pairs determined to be genuine, and points below the threshold correspond to pairs determined to be impostors. If the determined class (genuine or impostor) matches the real class, points will be blue; if not, red. An X represents face detection failure in either of the images in the pair. Note that the sample size (n=20) is small, and the figure may change substantially if larger or different sets are used. The images can be viewed on p. 13 of the Appendix, where Gen 01 corresponds to Same-Identity Pair 1, Gen 02 corresponds to Same-Identity Pair 2, and so on.

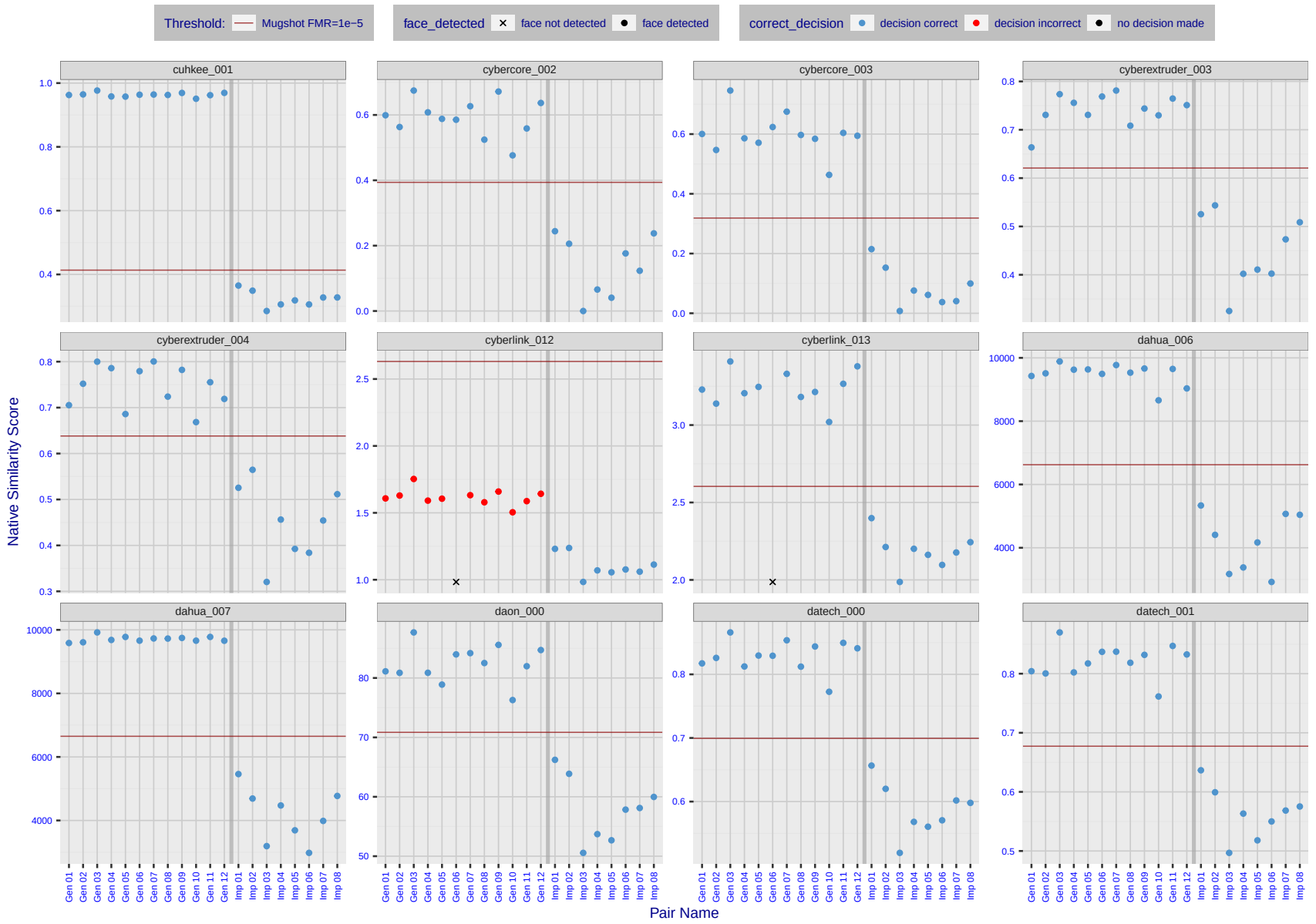

Figure 14: The figure shows algorithms' similarity scores for 12 genuine and 8 impostor image pairs used in a May 2018 paper by Phillips et al. ([1]). The threshold (red horizontal line) is a value calibrated to give FMR = 0.0001 on mugshot images. Points above the threshold correspond to pairs determined to be genuine, and points below the threshold correspond to pairs determined to be impostors. If the determined class (genuine or impostor) matches the real class, points will be blue; if not, red. An X represents face detection failure in either of the images in the pair. Note that the sample size (n=20) is small, and the figure may change substantially if larger or different sets are used. The images can be viewed on p. 13 of the Appendix, where Gen 01 corresponds to Same-Identity Pair 1, Gen 02 corresponds to Same-Identity Pair 2, and so on.

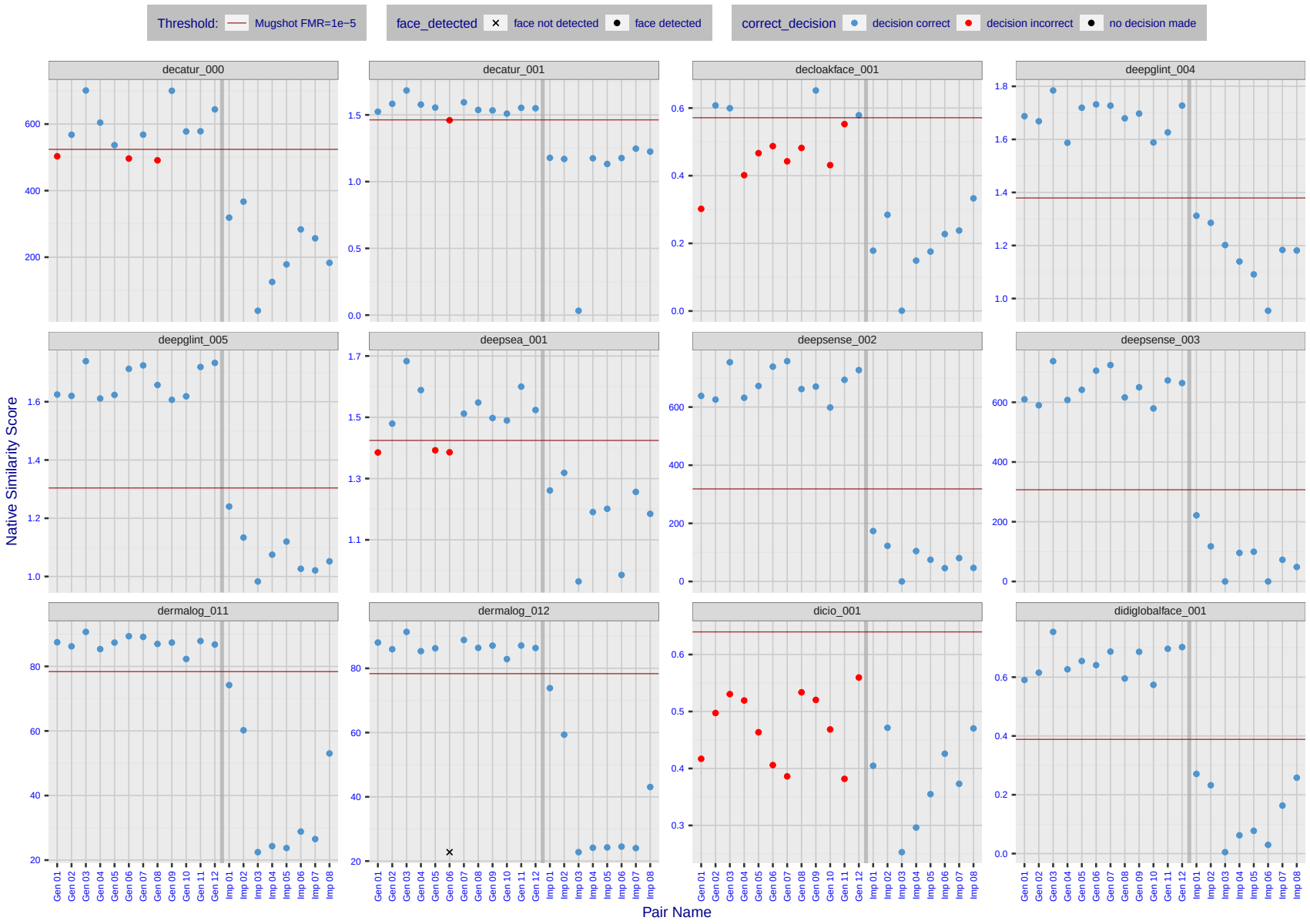

Figure 15: The figure shows algorithms' similarity scores for 12 genuine and 8 impostor image pairs used in a May 2018 paper by Phillips et al. ([1]). The threshold (red horizontal line) is a value calibrated to give FMR = 0.0001 on mugshot images. Points above the threshold correspond to pairs determined to be genuine, and points below the threshold correspond to pairs determined to be impostors. If the determined class (genuine or impostor) matches the real class, points will be blue; if not, red. An X represents face detection failure in either of the images in the pair. Note that the sample size (n=20) is small, and the figure may change substantially if larger or different sets are used. The images can be viewed on p. 13 of the Appendix, where Gen 01 corresponds to Same-Identity Pair 1, Gen 02 corresponds to Same-Identity Pair 2, and so on.

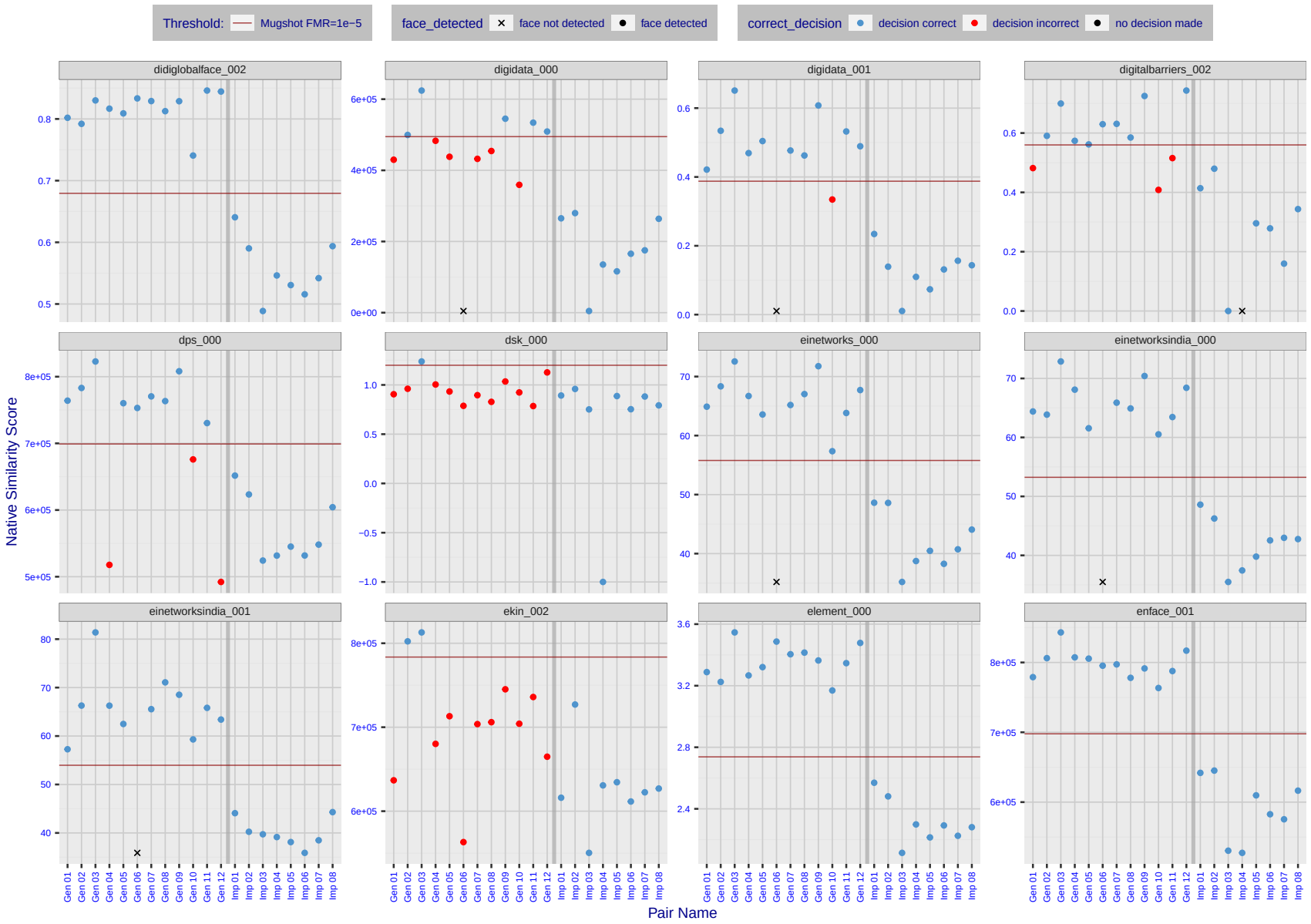

Figure 16: The figure shows algorithms' similarity scores for 12 genuine and 8 impostor image pairs used in a May 2018 paper by Phillips et al. ([1]). The threshold (red horizontal line) is a value calibrated to give FMR = 0.0001 on mugshot images. Points above the threshold correspond to pairs determined to be genuine, and points below the threshold correspond to pairs determined to be impostors. If the determined class (genuine or impostor) matches the real class, points will be blue; if not, red. An X represents face detection failure in either of the images in the pair. Note that the sample size (n=20) is small, and the figure may change substantially if larger or different sets are used. The images can be viewed on p. 13 of the Appendix, where Gen 01 corresponds to Same-Identity Pair 1, Gen 02 corresponds to Same-Identity Pair 2, and so on.

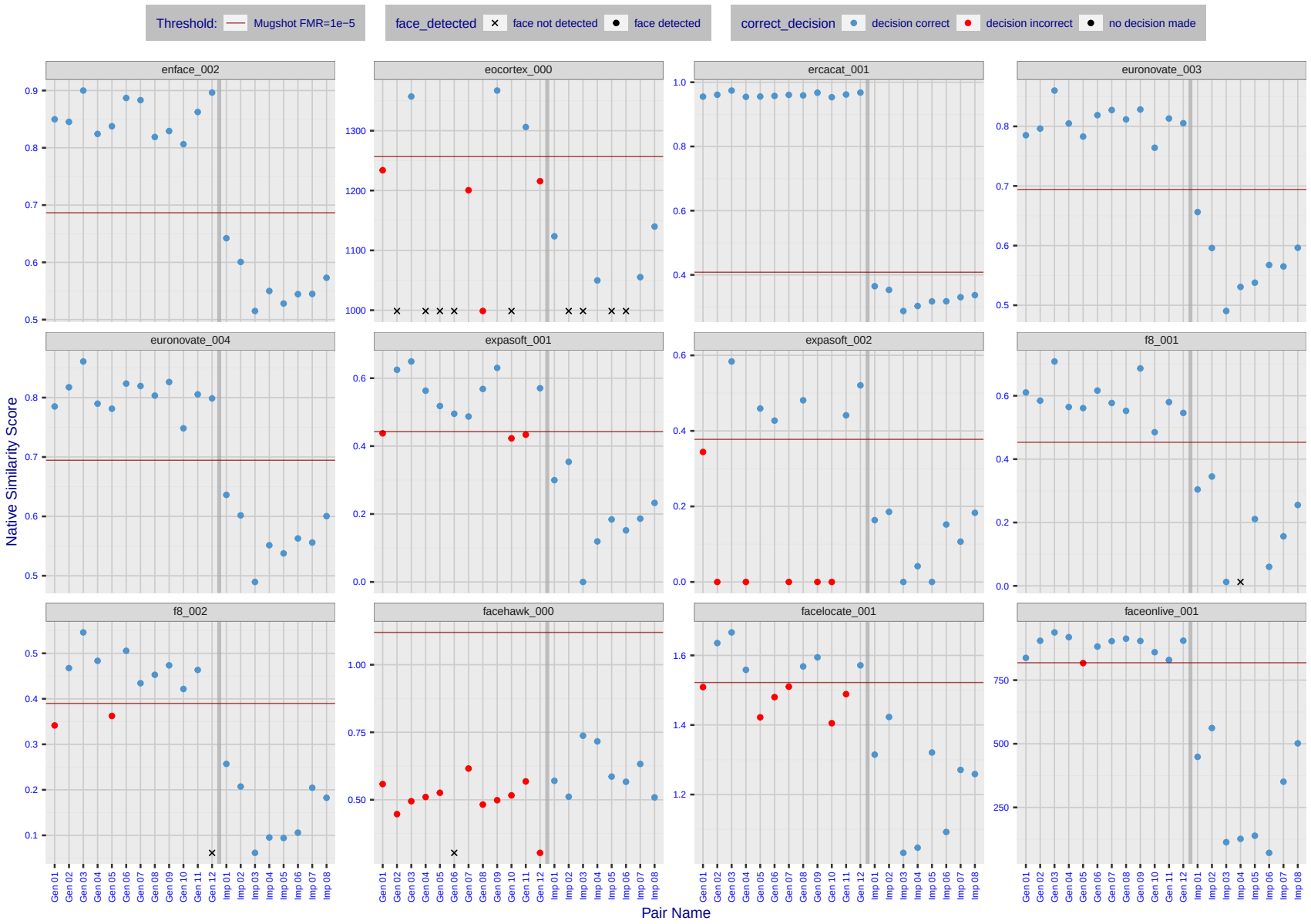

Figure 17: The figure shows algorithms' similarity scores for 12 genuine and 8 impostor image pairs used in a May 2018 paper by Phillips et al. ([1]). The threshold (red horizontal line) is a value calibrated to give FMR = 0.0001 on mugshot images. Points above the threshold correspond to pairs determined to be genuine, and points below the threshold correspond to pairs determined to be impostors. If the determined class (genuine or impostor) matches the real class, points will be blue; if not, red. An X represents face detection failure in either of the images in the pair. Note that the sample size (n=20) is small, and the figure may change substantially if larger or different sets are used. The images can be viewed on p. 13 of the Appendix, where Gen 01 corresponds to Same-Identity Pair 1, Gen 02 corresponds to Same-Identity Pair 2, and so on.

2024/04/17 08:45:50

FNMR(T) "False non-match rate"
FMR(T) "False match rate"

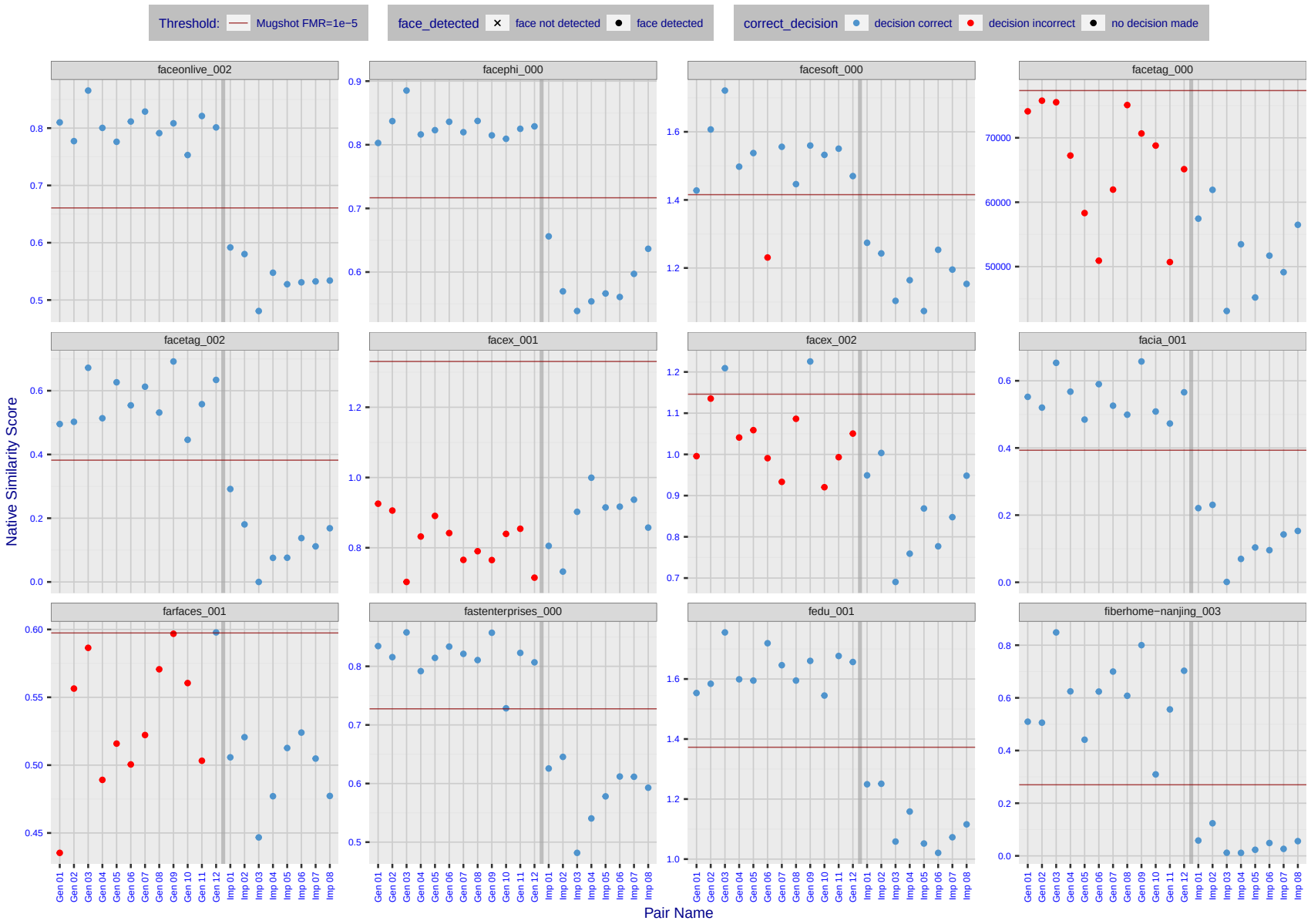

Figure 18: The figure shows algorithms' similarity scores for 12 genuine and 8 impostor image pairs used in a May 2018 paper by Phillips et al. ([1]). The threshold (red horizontal line) is a value calibrated to give FMR = 0.0001 on mugshot images. Points above the threshold correspond to pairs determined to be genuine, and points below the threshold correspond to pairs determined to be impostors. If the determined class (genuine or impostor) matches the real class, points will be blue; if not, red. An X represents face detection failure in either of the images in the pair. Note that the sample size (n=20) is small, and the figure may change substantially if larger or different sets are used. The images can be viewed on p. 13 of the Appendix, where Gen 01 corresponds to Same-Identity Pair 1, Gen 02 corresponds to Same-Identity Pair 2, and so on.

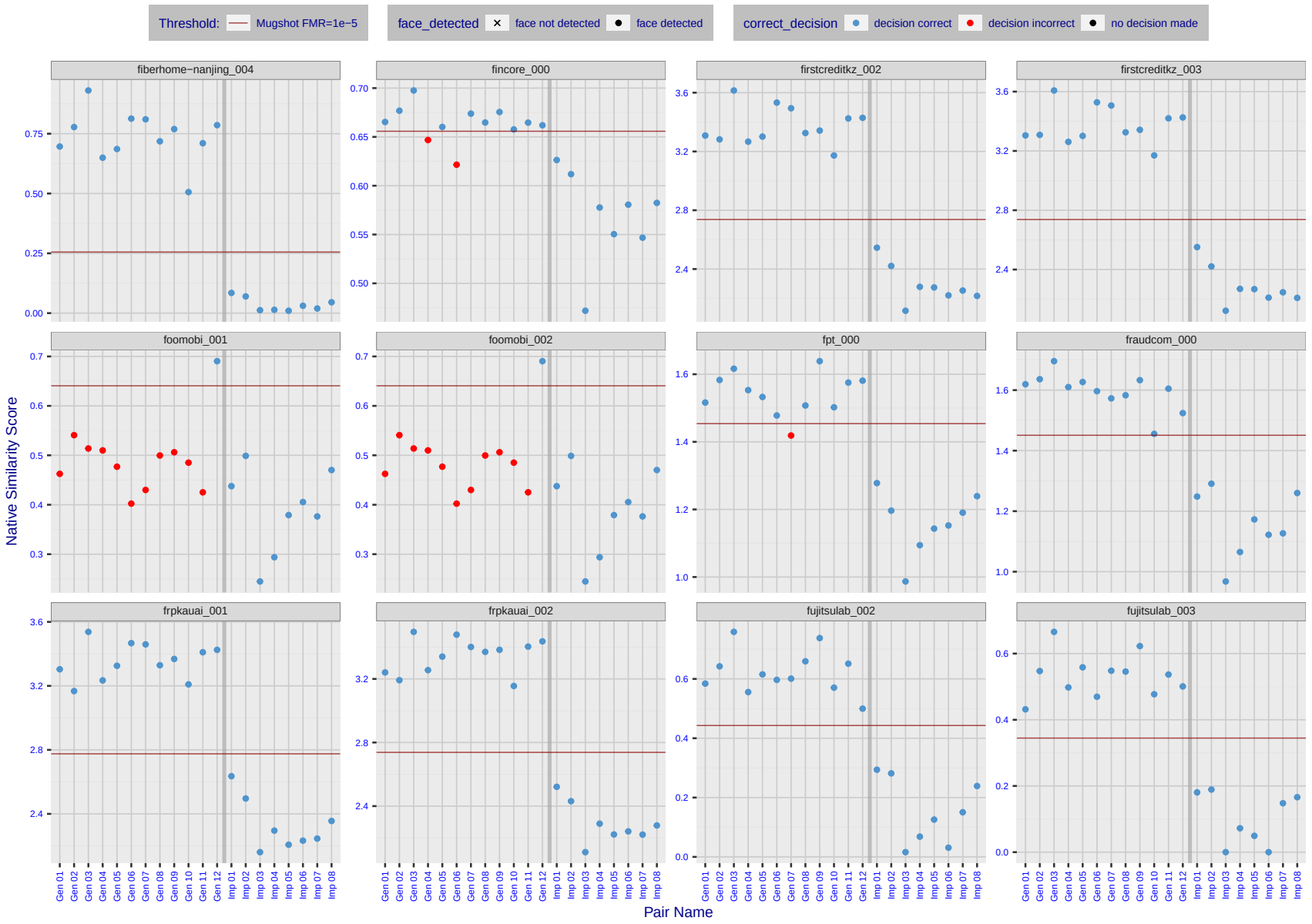

Figure 19: The figure shows algorithms' similarity scores for 12 genuine and 8 impostor image pairs used in a May 2018 paper by Phillips et al. ([1]). The threshold (red horizontal line) is a value calibrated to give FMR = 0.0001 on mugshot images. Points above the threshold correspond to pairs determined to be genuine, and points below the threshold correspond to pairs determined to be impostors. If the determined class (genuine or impostor) matches the real class, points will be blue; if not, red. An X represents face detection failure in either of the images in the pair. Note that the sample size (n=20) is small, and the figure may change substantially if larger or different sets are used. The images can be viewed on p. 13 of the Appendix, where Gen 01 corresponds to Same-Identity Pair 1, Gen 02 corresponds to Same-Identity Pair 2, and so on.

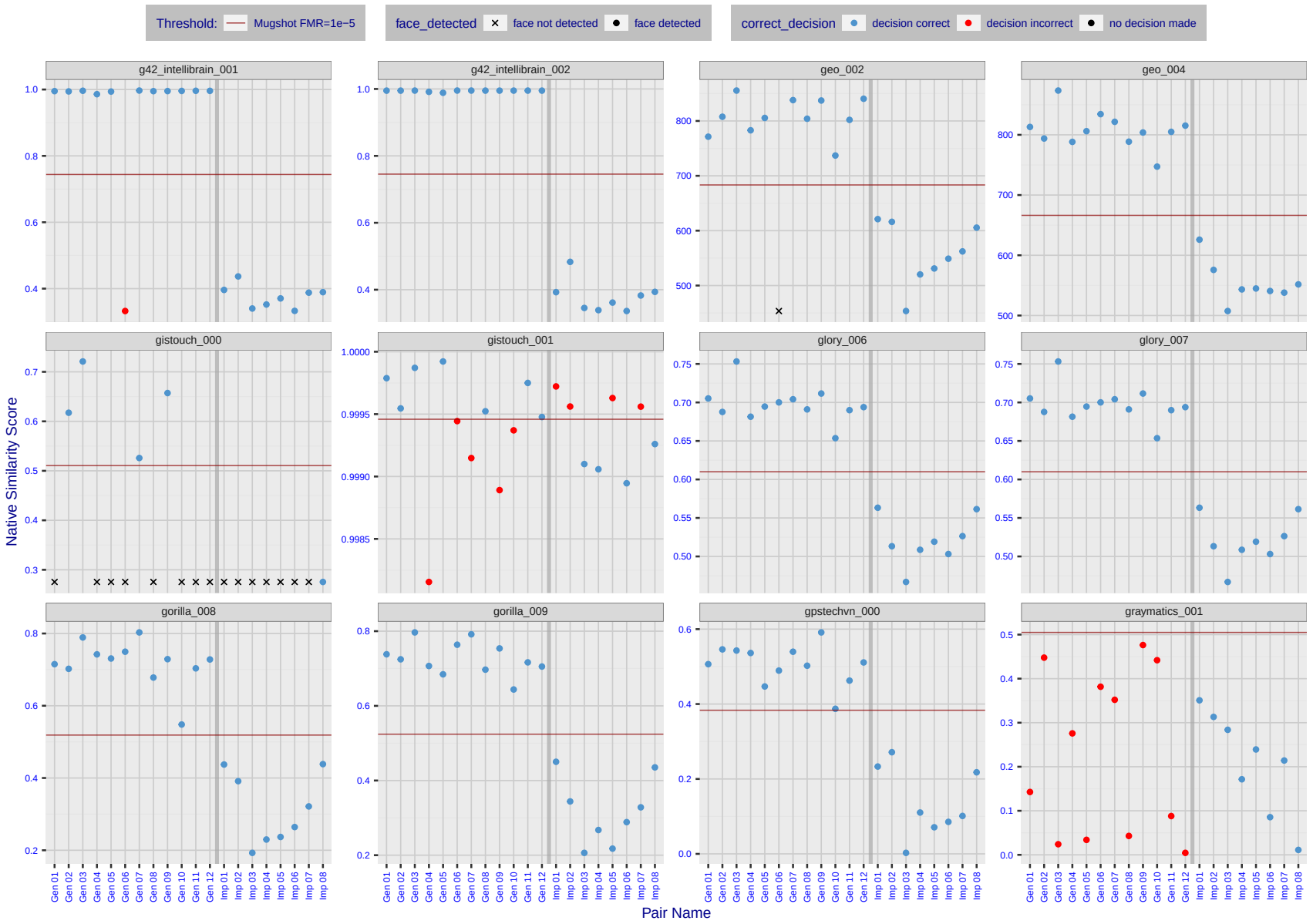

Figure 20: The figure shows algorithms' similarity scores for 12 genuine and 8 impostor image pairs used in a May 2018 paper by Phillips et al. ([1]). The threshold (red horizontal line) is a value calibrated to give FMR = 0.0001 on mugshot images. Points above the threshold correspond to pairs determined to be genuine, and points below the threshold correspond to pairs determined to be impostors. If the determined class (genuine or impostor) matches the real class, points will be blue; if not, red. An X represents face detection failure in either of the images in the pair. Note that the sample size (n=20) is small, and the figure may change substantially if larger or different sets are used. The images can be viewed on p. 13 of the Appendix, where Gen 01 corresponds to Same-Identity Pair 1, Gen 02 corresponds to Same-Identity Pair 2, and so on.

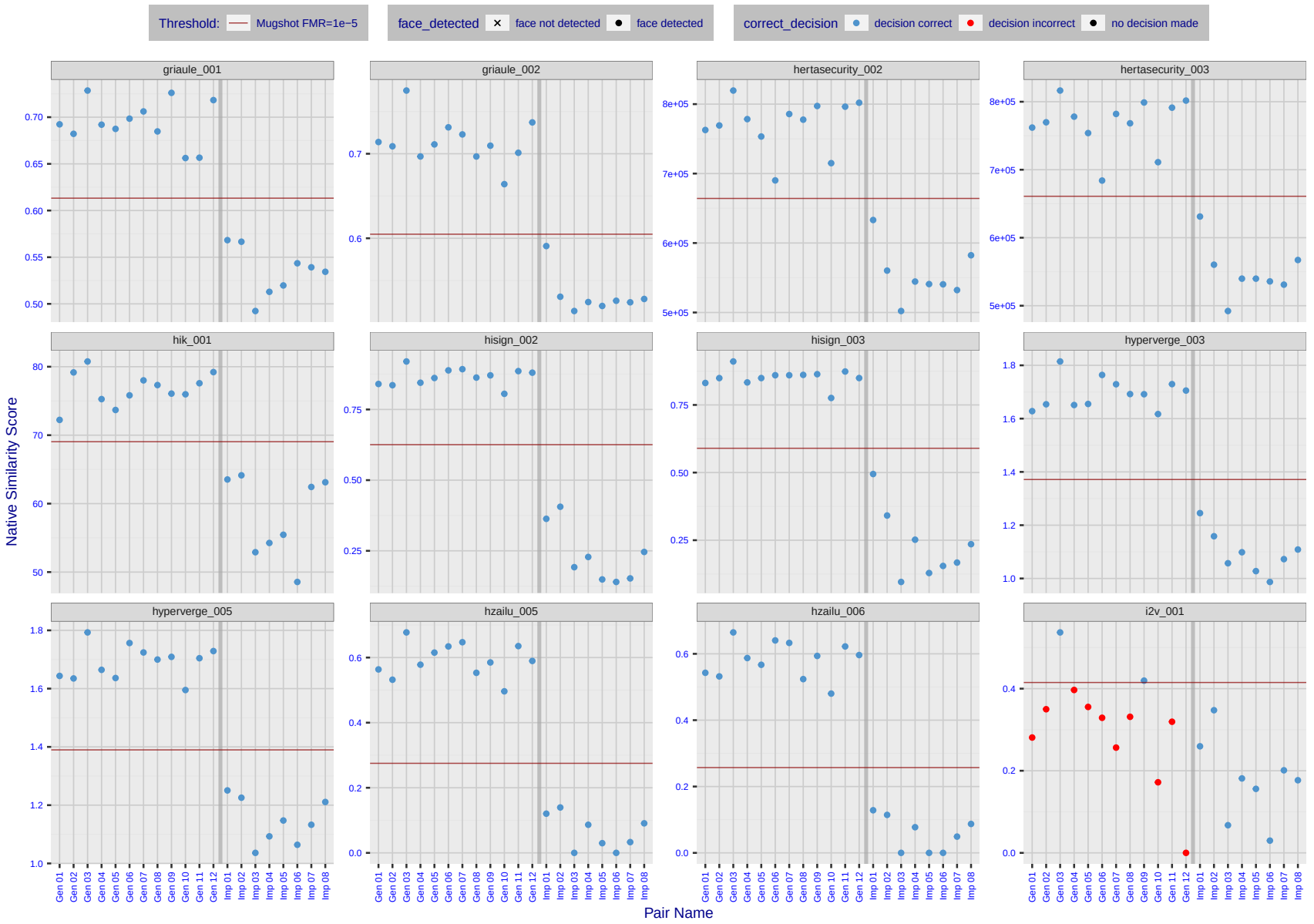

Figure 21: The figure shows algorithms' similarity scores for 12 genuine and 8 impostor image pairs used in a May 2018 paper by Phillips et al. ([1]). The threshold (red horizontal line) is a value calibrated to give FMR = 0.0001 on mugshot images. Points above the threshold correspond to pairs determined to be genuine, and points below the threshold correspond to pairs determined to be impostors. If the determined class (genuine or impostor) matches the real class, points will be blue; if not, red. An X represents face detection failure in either of the images in the pair. Note that the sample size (n=20) is small, and the figure may change substantially if larger or different sets are used. The images can be viewed on p. 13 of the Appendix, where Gen 01 corresponds to Same-Identity Pair 1, Gen 02 corresponds to Same-Identity Pair 2, and so on.

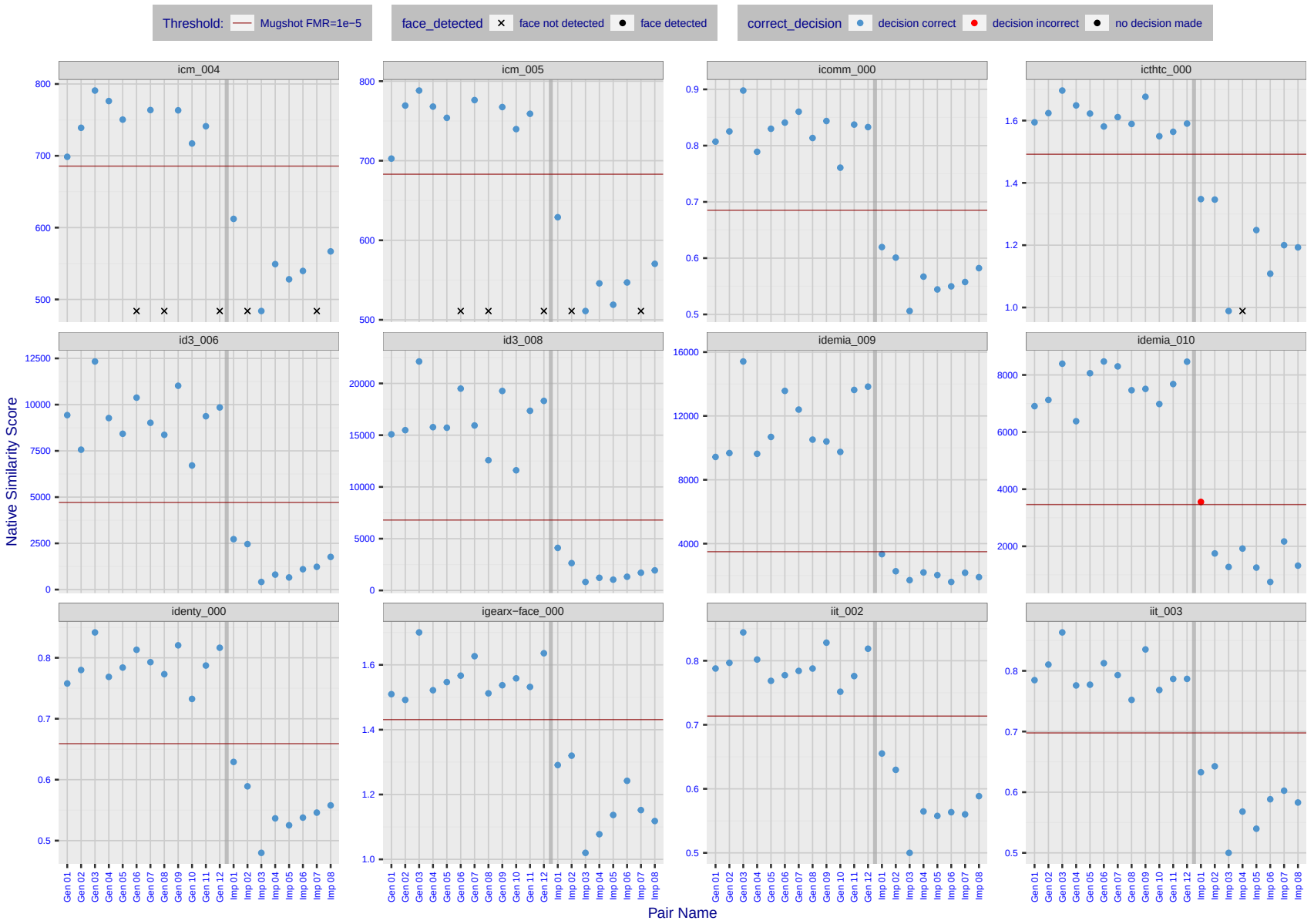

Figure 22: The figure shows algorithms' similarity scores for 12 genuine and 8 impostor image pairs used in a May 2018 paper by Phillips et al. ([1]). The threshold (red horizontal line) is a value calibrated to give FMR = 0.0001 on mugshot images. Points above the threshold correspond to pairs determined to be genuine, and points below the threshold correspond to pairs determined to be impostors. If the determined class (genuine or impostor) matches the real class, points will be blue; if not, red. An X represents face detection failure in either of the images in the pair. Note that the sample size (n=20) is small, and the figure may change substantially if larger or different sets are used. The images can be viewed on p. 13 of the Appendix, where Gen 01 corresponds to Same-Identity Pair 1, Gen 02 corresponds to Same-Identity Pair 2, and so on.

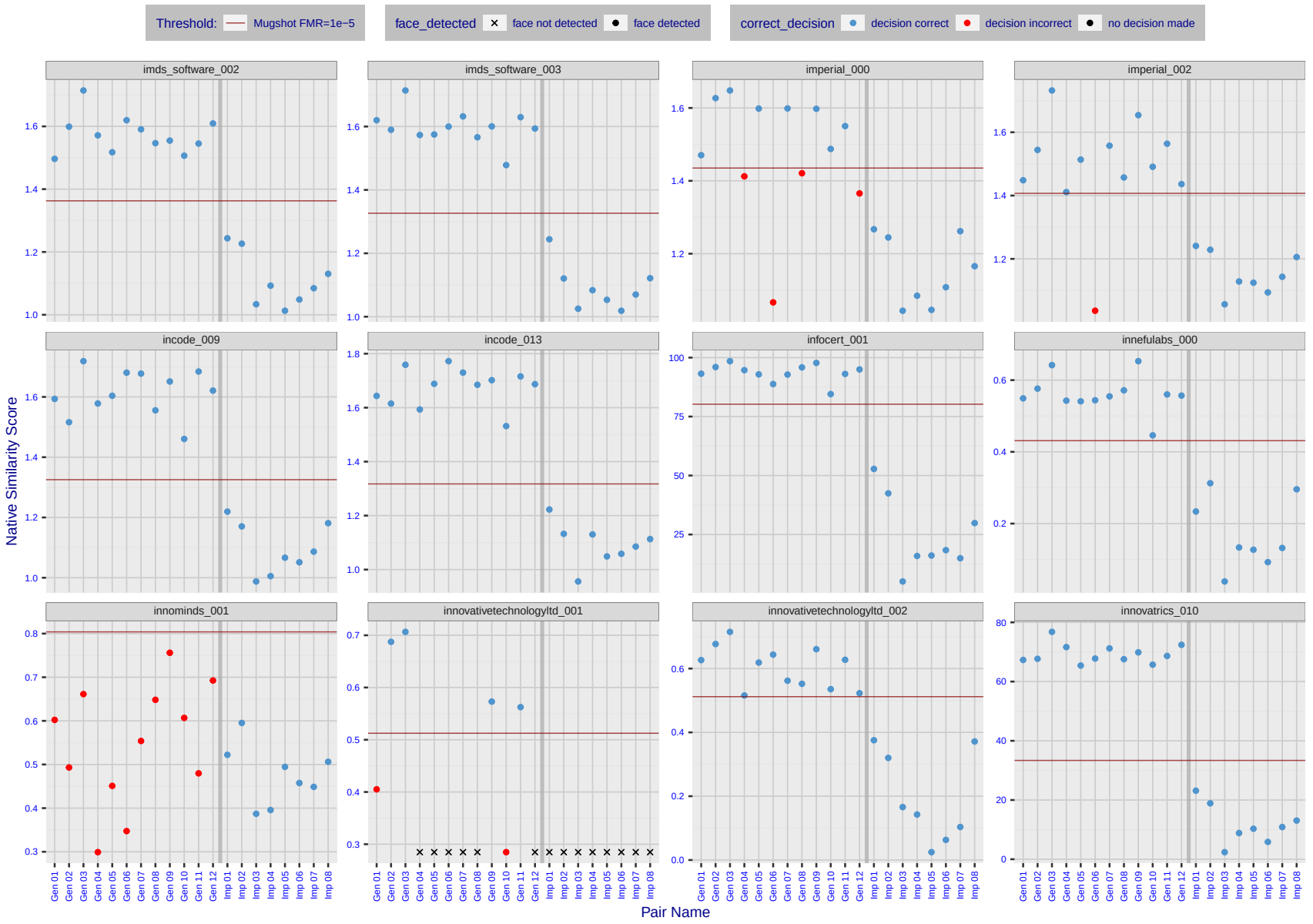

Figure 23: The figure shows algorithms' similarity scores for 12 genuine and 8 impostor image pairs used in a May 2018 paper by Phillips et al. ([1]). The threshold (red horizontal line) is a value calibrated to give FMR = 0.0001 on mugshot images. Points above the threshold correspond to pairs determined to be genuine, and points below the threshold correspond to pairs determined to be impostors. If the determined class (genuine or impostor) matches the real class, points will be blue; if not, red. An X represents face detection failure in either of the images in the pair. Note that the sample size (n=20) is small, and the figure may change substantially if larger or different sets are used. The images can be viewed on p. 13 of the Appendix, where Gen 01 corresponds to Same-Identity Pair 1, Gen 02 corresponds to Same-Identity Pair 2, and so on.

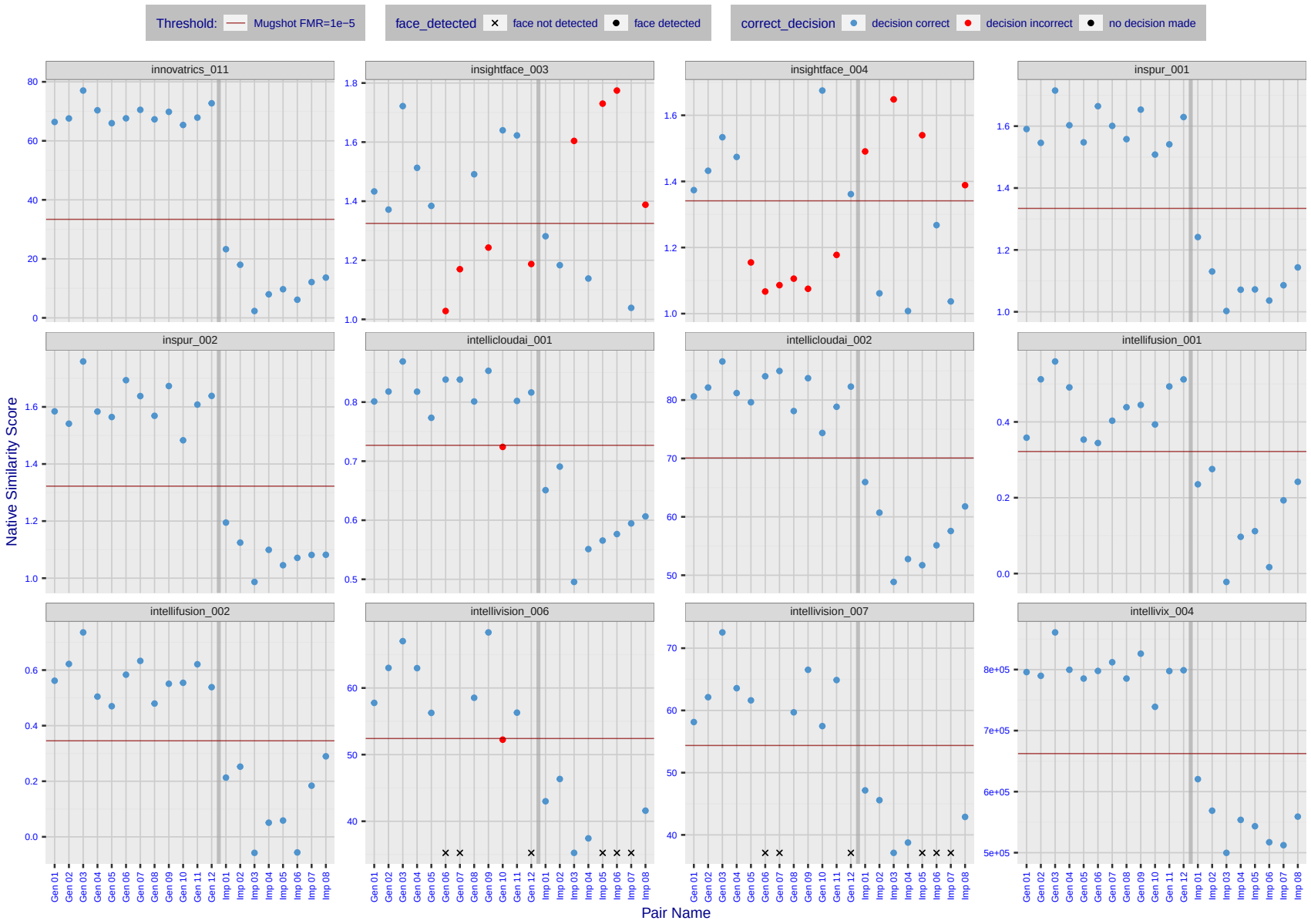

Figure 24: The figure shows algorithms' similarity scores for 12 genuine and 8 impostor image pairs used in a May 2018 paper by Phillips et al. ([1]). The threshold (red horizontal line) is a value calibrated to give FMR = 0.0001 on mugshot images. Points above the threshold correspond to pairs determined to be genuine, and points below the threshold correspond to pairs determined to be impostors. If the determined class (genuine or impostor) matches the real class, points will be blue; if not, red. An X represents face detection failure in either of the images in the pair. Note that the sample size (n=20) is small, and the figure may change substantially if larger or different sets are used. The images can be viewed on p. 13 of the Appendix, where Gen 01 corresponds to Same-Identity Pair 1, Gen 02 corresponds to Same-Identity Pair 2, and so on.

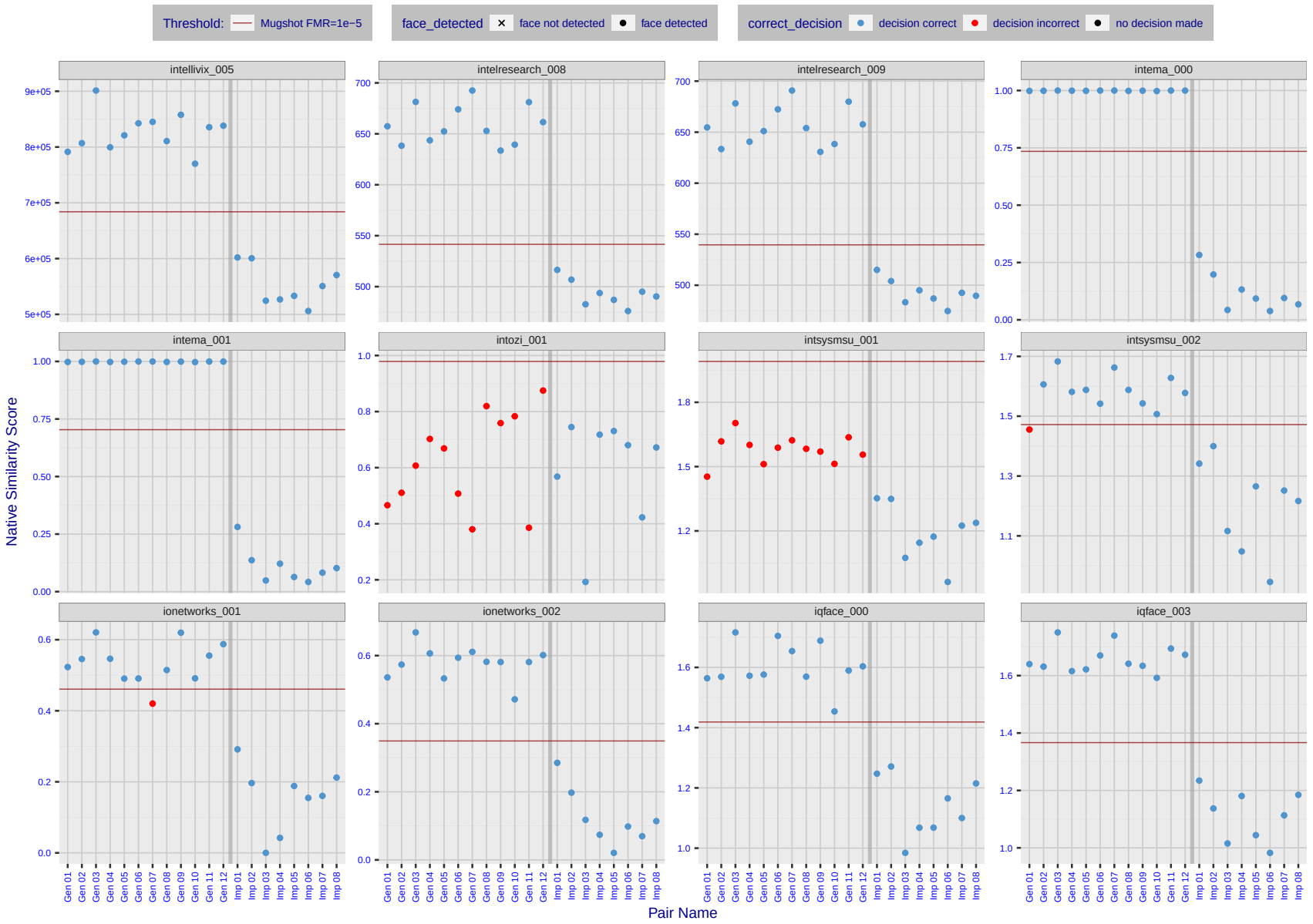

Figure 25: The figure shows algorithms' similarity scores for 12 genuine and 8 impostor image pairs used in a May 2018 paper by Phillips et al. ([1]). The threshold (red horizontal line) is a value calibrated to give FMR = 0.0001 on mugshot images. Points above the threshold correspond to pairs determined to be genuine, and points below the threshold correspond to pairs determined to be impostors. If the determined class (genuine or impostor) matches the real class, points will be blue; if not, red. An X represents face detection failure in either of the images in the pair. Note that the sample size (n=20) is small, and the figure may change substantially if larger or different sets are used. The images can be viewed on p. 13 of the Appendix, where Gen 01 corresponds to Same-Identity Pair 1, Gen 02 corresponds to Same-Identity Pair 2, and so on.

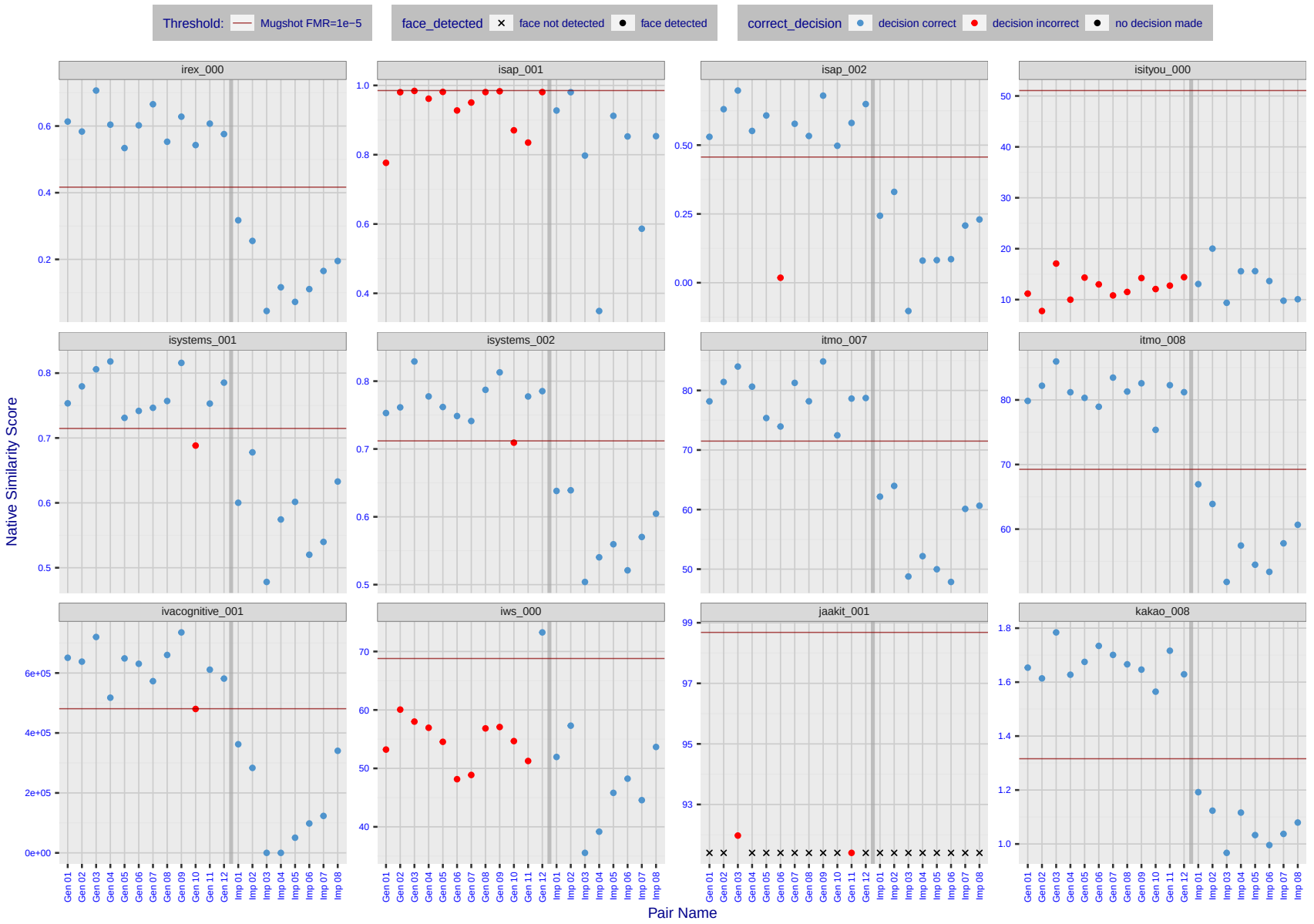

Figure 26: The figure shows algorithms' similarity scores for 12 genuine and 8 impostor image pairs used in a May 2018 paper by Phillips et al. ([1]). The threshold (red horizontal line) is a value calibrated to give FMR = 0.0001 on mugshot images. Points above the threshold correspond to pairs determined to be genuine, and points below the threshold correspond to pairs determined to be impostors. If the determined class (genuine or impostor) matches the real class, points will be blue; if not, red. An X represents face detection failure in either of the images in the pair. Note that the sample size (n=20) is small, and the figure may change substantially if larger or different sets are used. The images can be viewed on p. 13 of the Appendix, where Gen 01 corresponds to Same-Identity Pair 1, Gen 02 corresponds to Same-Identity Pair 2, and so on.

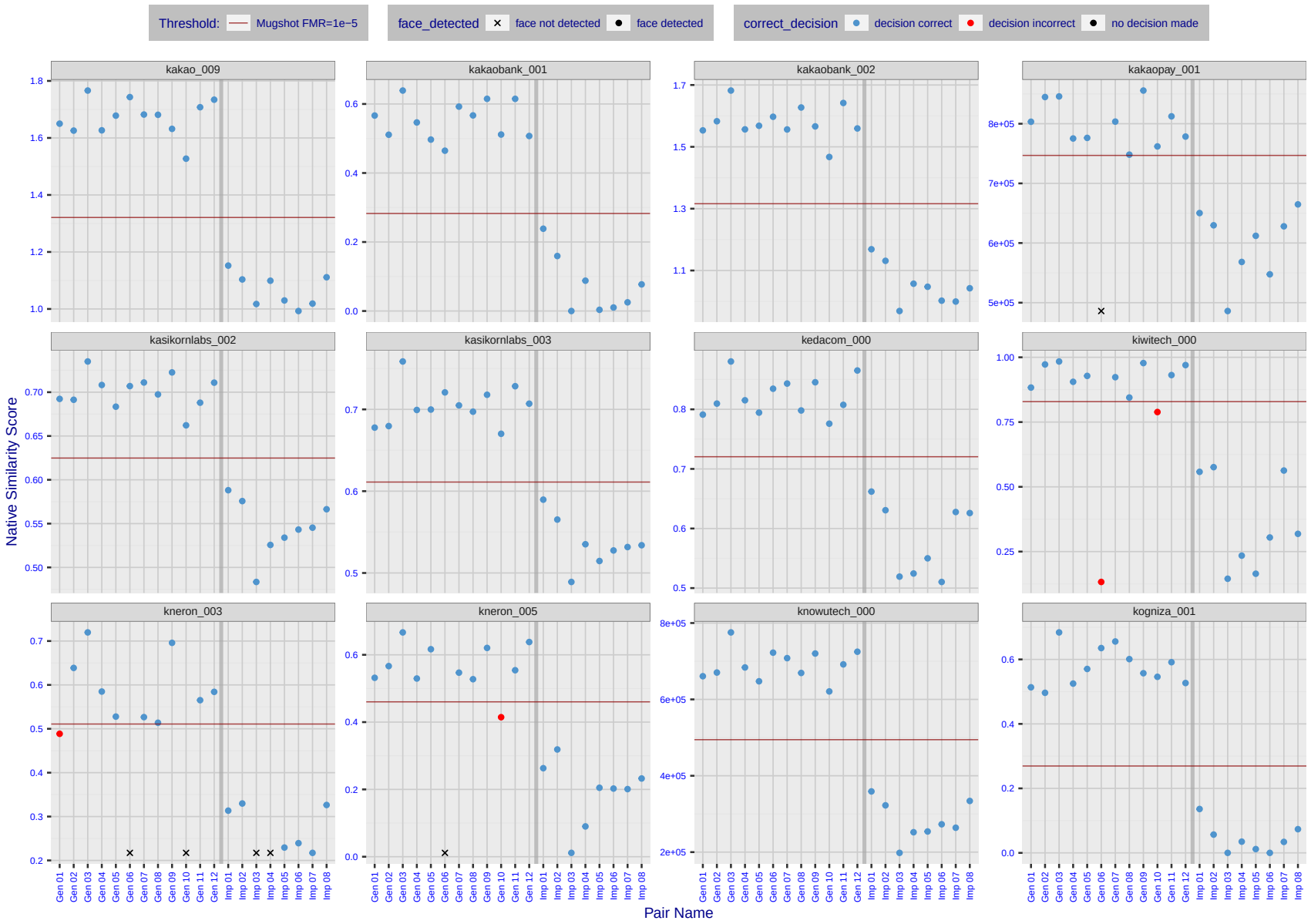

Figure 27: The figure shows algorithms' similarity scores for 12 genuine and 8 impostor image pairs used in a May 2018 paper by Phillips et al. ([1]). The threshold (red horizontal line) is a value calibrated to give FMR = 0.0001 on mugshot images. Points above the threshold correspond to pairs determined to be genuine, and points below the threshold correspond to pairs determined to be impostors. If the determined class (genuine or impostor) matches the real class, points will be blue; if not, red. An X represents face detection failure in either of the images in the pair. Note that the sample size (n=20) is small, and the figure may change substantially if larger or different sets are used. The images can be viewed on p. 13 of the Appendix, where Gen 01 corresponds to Same-Identity Pair 1, Gen 02 corresponds to Same-Identity Pair 2, and so on.

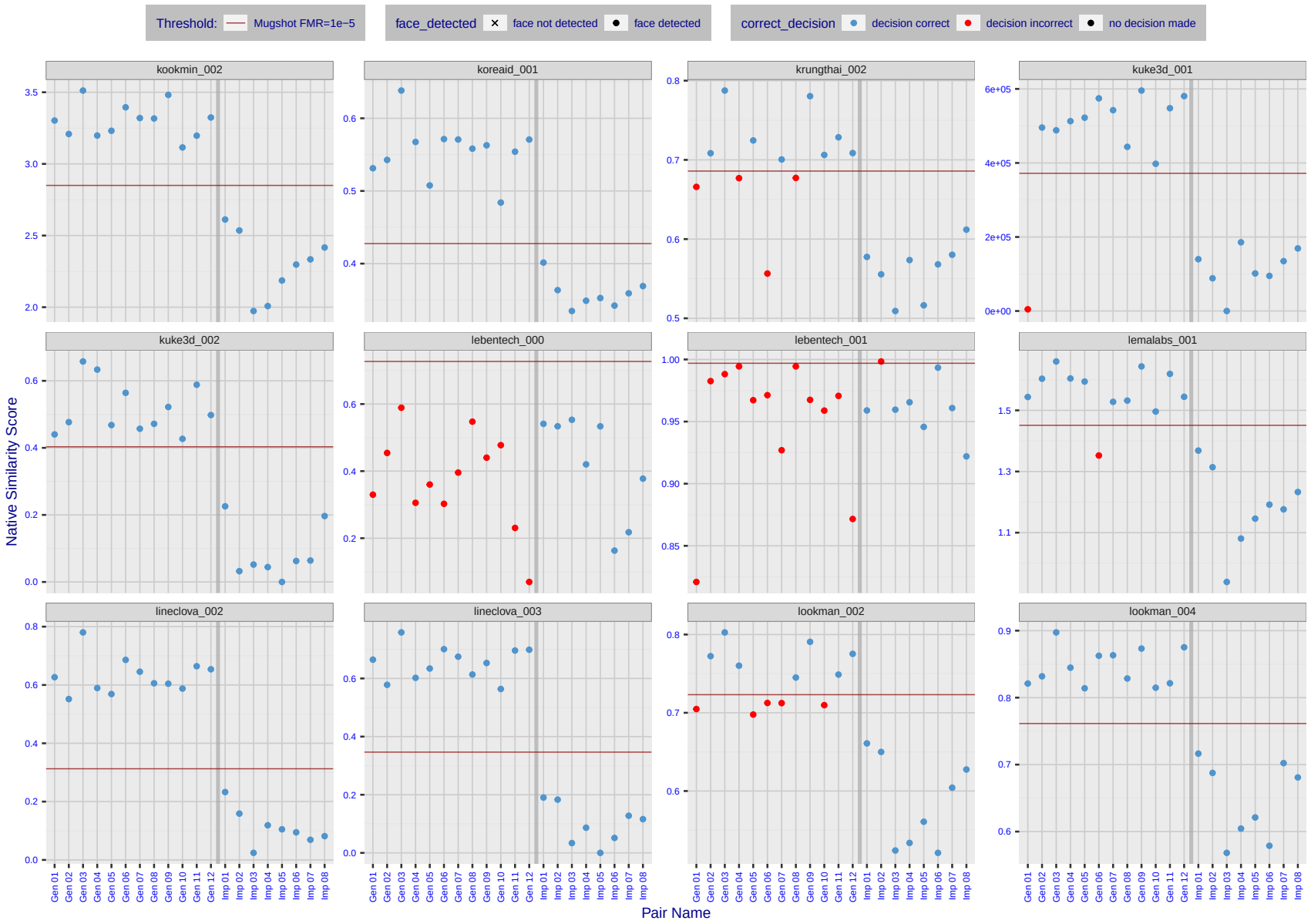

Figure 28: The figure shows algorithms' similarity scores for 12 genuine and 8 impostor image pairs used in a May 2018 paper by Phillips et al. ([1]). The threshold (red horizontal line) is a value calibrated to give FMR = 0.0001 on mugshot images. Points above the threshold correspond to pairs determined to be genuine, and points below the threshold correspond to pairs determined to be impostors. If the determined class (genuine or impostor) matches the real class, points will be blue; if not, red. An X represents face detection failure in either of the images in the pair. Note that the sample size (n=20) is small, and the figure may change substantially if larger or different sets are used. The images can be viewed on p. 13 of the Appendix, where Gen 01 corresponds to Same-Identity Pair 1, Gen 02 corresponds to Same-Identity Pair 2, and so on.

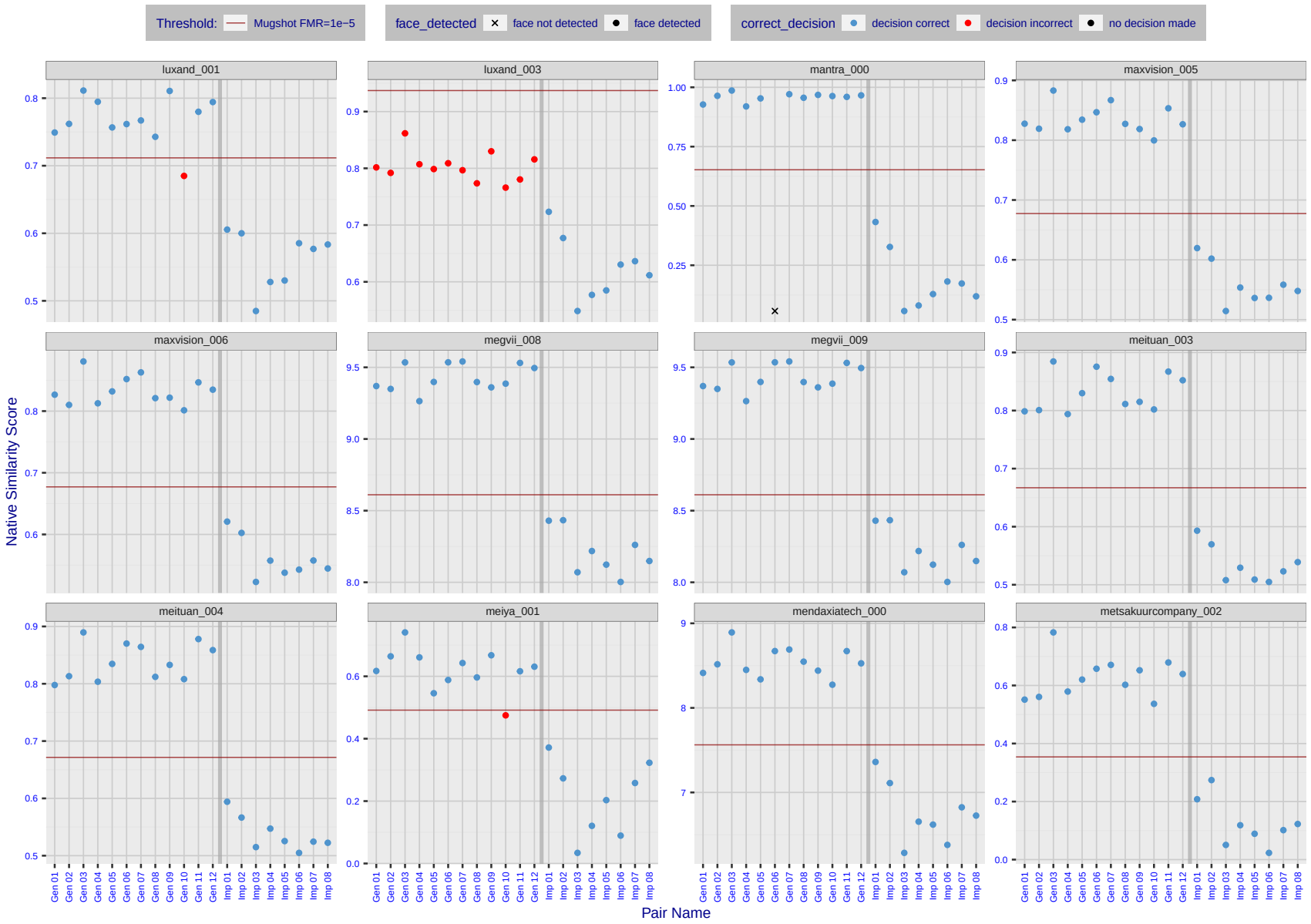

Figure 29: The figure shows algorithms' similarity scores for 12 genuine and 8 impostor image pairs used in a May 2018 paper by Phillips et al. ([1]). The threshold (red horizontal line) is a value calibrated to give FMR = 0.0001 on mugshot images. Points above the threshold correspond to pairs determined to be genuine, and points below the threshold correspond to pairs determined to be impostors. If the determined class (genuine or impostor) matches the real class, points will be blue; if not, red. An X represents face detection failure in either of the images in the pair. Note that the sample size (n=20) is small, and the figure may change substantially if larger or different sets are used. The images can be viewed on p. 13 of the Appendix, where Gen 01 corresponds to Same-Identity Pair 1, Gen 02 corresponds to Same-Identity Pair 2, and so on.

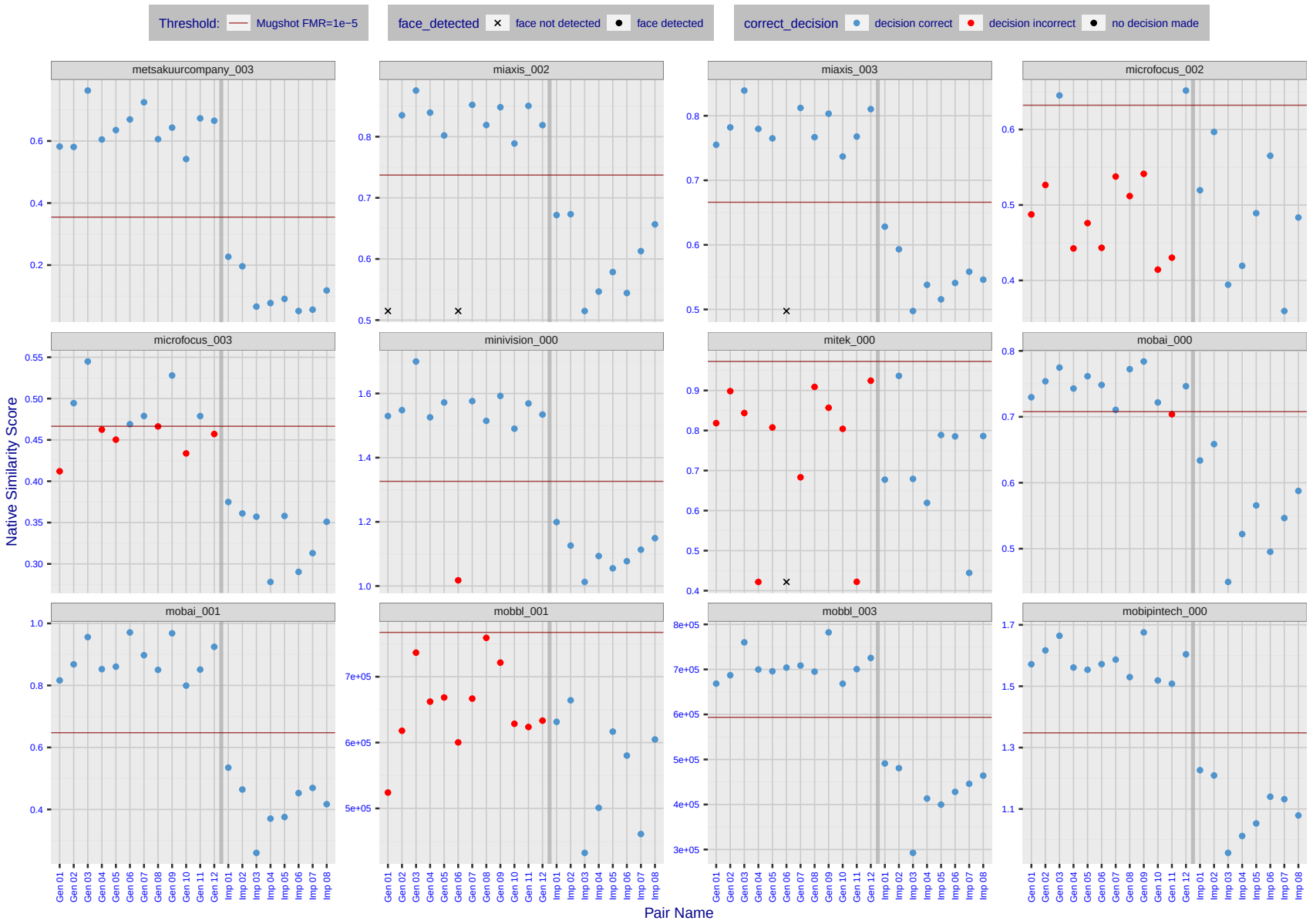

Figure 30: The figure shows algorithms' similarity scores for 12 genuine and 8 impostor image pairs used in a May 2018 paper by Phillips et al. ([1]). The threshold (red horizontal line) is a value calibrated to give FMR = 0.0001 on mugshot images. Points above the threshold correspond to pairs determined to be genuine, and points below the threshold correspond to pairs determined to be impostors. If the determined class (genuine or impostor) matches the real class, points will be blue; if not, red. An X represents face detection failure in either of the images in the pair. Note that the sample size (n=20) is small, and the figure may change substantially if larger or different sets are used. The images can be viewed on p. 13 of the Appendix, where Gen 01 corresponds to Same-Identity Pair 1, Gen 02 corresponds to Same-Identity Pair 2, and so on.

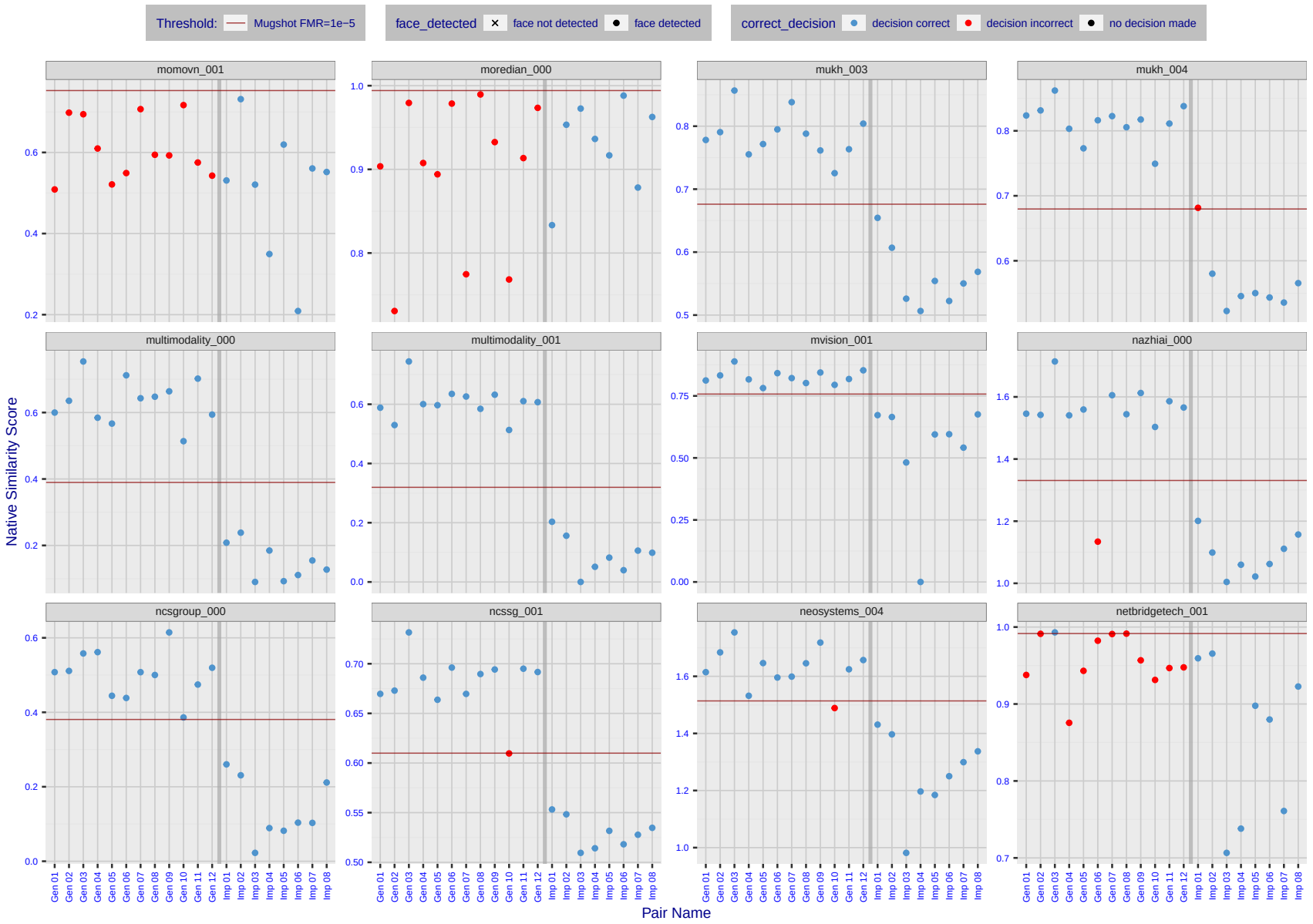

Figure 31: The figure shows algorithms' similarity scores for 12 genuine and 8 impostor image pairs used in a May 2018 paper by Phillips et al. ([1]). The threshold (red horizontal line) is a value calibrated to give FMR = 0.0001 on mugshot images. Points above the threshold correspond to pairs determined to be genuine, and points below the threshold correspond to pairs determined to be impostors. If the determined class (genuine or impostor) matches the real class, points will be blue; if not, red. An X represents face detection failure in either of the images in the pair. Note that the sample size (n=20) is small, and the figure may change substantially if larger or different sets are used. The images can be viewed on p. 13 of the Appendix, where Gen 01 corresponds to Same-Identity Pair 1, Gen 02 corresponds to Same-Identity Pair 2, and so on.

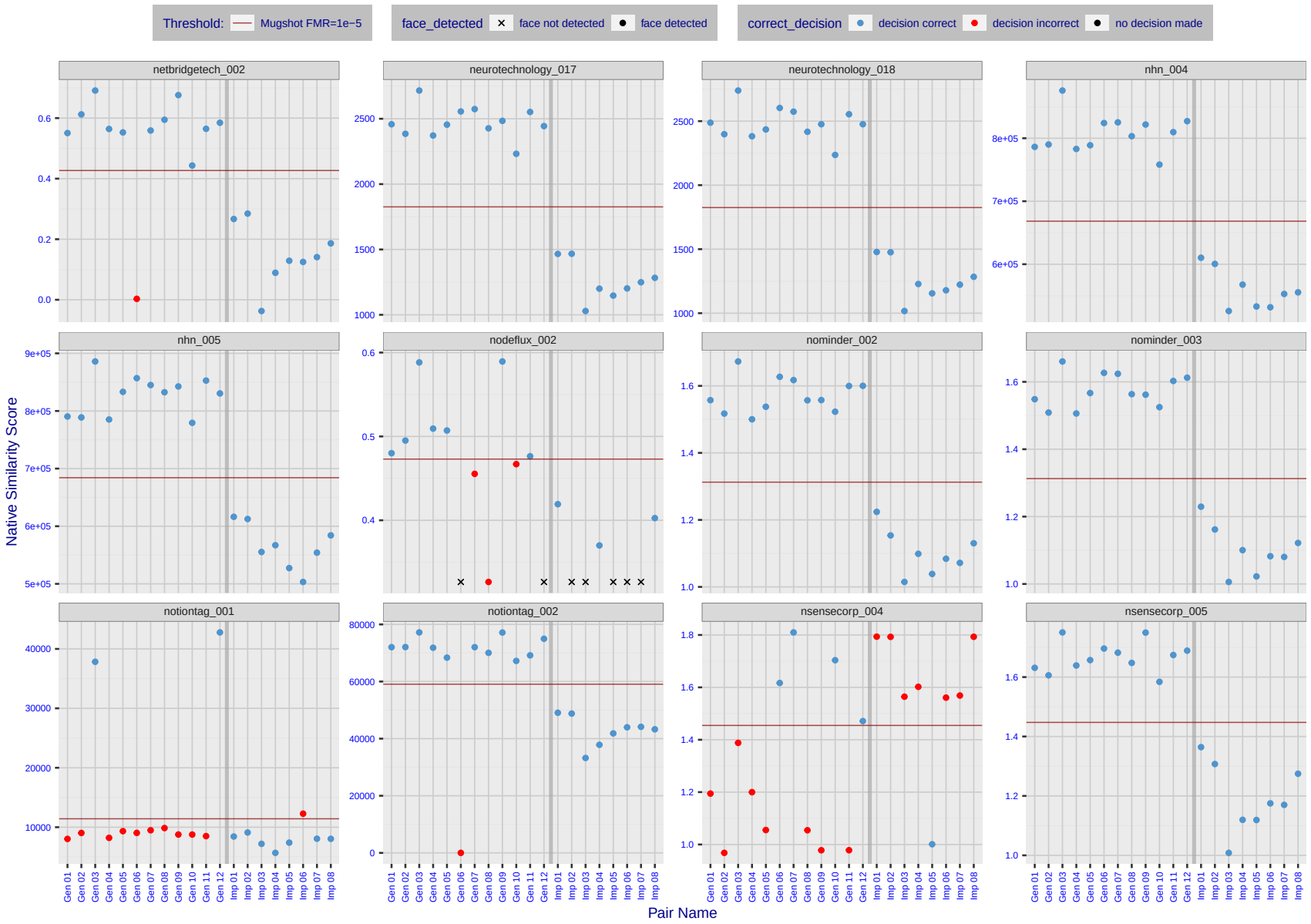

Figure 32: The figure shows algorithms' similarity scores for 12 genuine and 8 impostor image pairs used in a May 2018 paper by Phillips et al. ([1]). The threshold (red horizontal line) is a value calibrated to give FMR = 0.0001 on mugshot images. Points above the threshold correspond to pairs determined to be genuine, and points below the threshold correspond to pairs determined to be impostors. If the determined class (genuine or impostor) matches the real class, points will be blue; if not, red. An X represents face detection failure in either of the images in the pair. Note that the sample size (n=20) is small, and the figure may change substantially if larger or different sets are used. The images can be viewed on p. 13 of the Appendix, where Gen 01 corresponds to Same-Identity Pair 1, Gen 02 corresponds to Same-Identity Pair 2, and so on.

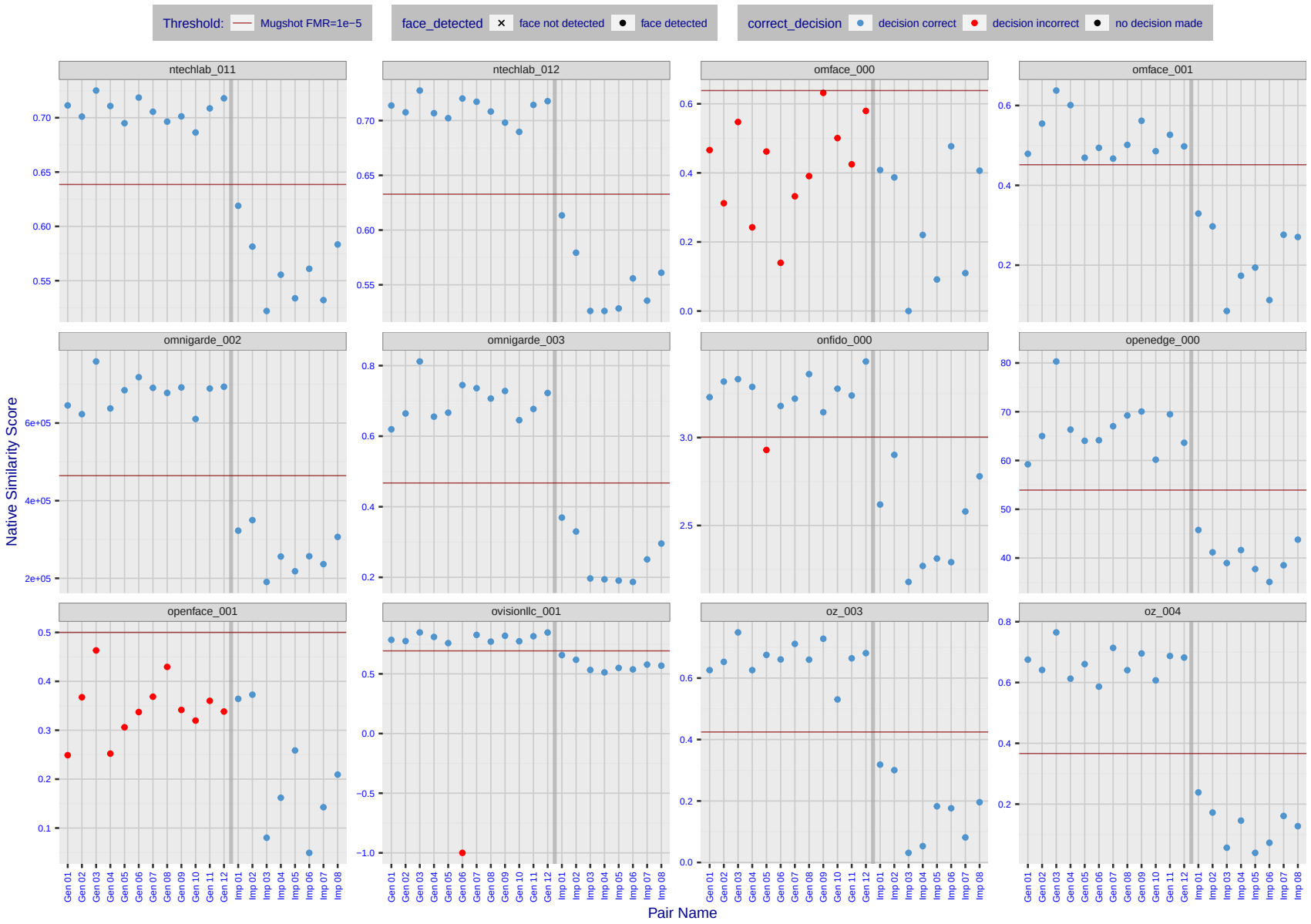

Figure 33: The figure shows algorithms' similarity scores for 12 genuine and 8 impostor image pairs used in a May 2018 paper by Phillips et al. ([1]). The threshold (red horizontal line) is a value calibrated to give FMR = 0.0001 on mugshot images. Points above the threshold correspond to pairs determined to be genuine, and points below the threshold correspond to pairs determined to be impostors. If the determined class (genuine or impostor) matches the real class, points will be blue; if not, red. An X represents face detection failure in either of the images in the pair. Note that the sample size (n=20) is small, and the figure may change substantially if larger or different sets are used. The images can be viewed on p. 13 of the Appendix, where Gen 01 corresponds to Same-Identity Pair 1, Gen 02 corresponds to Same-Identity Pair 2, and so on.

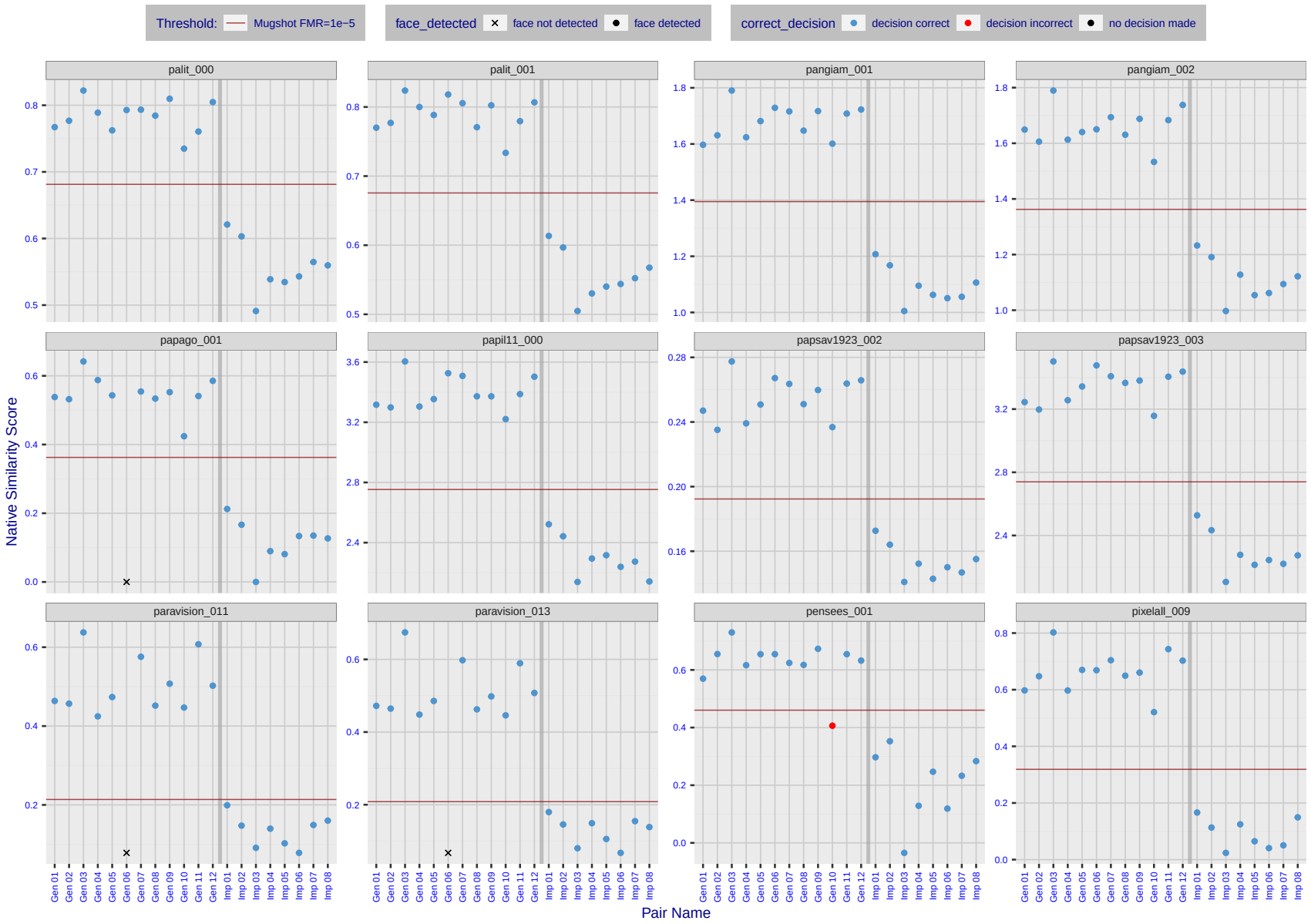

Figure 34: The figure shows algorithms' similarity scores for 12 genuine and 8 impostor image pairs used in a May 2018 paper by Phillips et al. ([1]). The threshold (red horizontal line) is a value calibrated to give FMR = 0.0001 on mugshot images. Points above the threshold correspond to pairs determined to be genuine, and points below the threshold correspond to pairs determined to be impostors. If the determined class (genuine or impostor) matches the real class, points will be blue; if not, red. An X represents face detection failure in either of the images in the pair. Note that the sample size (n=20) is small, and the figure may change substantially if larger or different sets are used. The images can be viewed on p. 13 of the Appendix, where Gen 01 corresponds to Same-Identity Pair 1, Gen 02 corresponds to Same-Identity Pair 2, and so on.

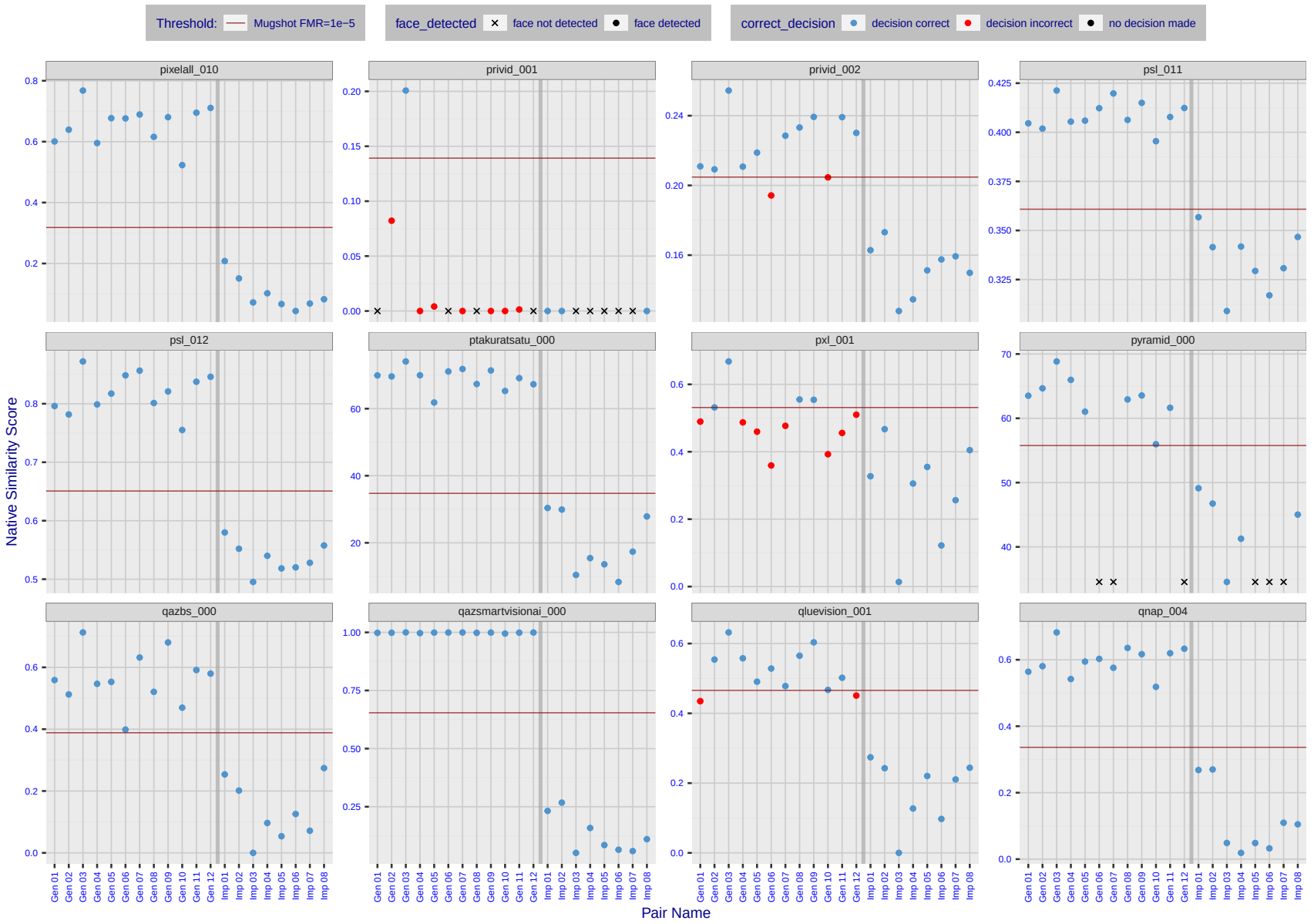

Figure 35: The figure shows algorithms' similarity scores for 12 genuine and 8 impostor image pairs used in a May 2018 paper by Phillips et al. ([1]). The threshold (red horizontal line) is a value calibrated to give FMR = 0.0001 on mugshot images. Points above the threshold correspond to pairs determined to be genuine, and points below the threshold correspond to pairs determined to be impostors. If the determined class (genuine or impostor) matches the real class, points will be blue; if not, red. An X represents face detection failure in either of the images in the pair. Note that the sample size (n=20) is small, and the figure may change substantially if larger or different sets are used. The images can be viewed on p. 13 of the Appendix, where Gen 01 corresponds to Same-Identity Pair 1, Gen 02 corresponds to Same-Identity Pair 2, and so on.

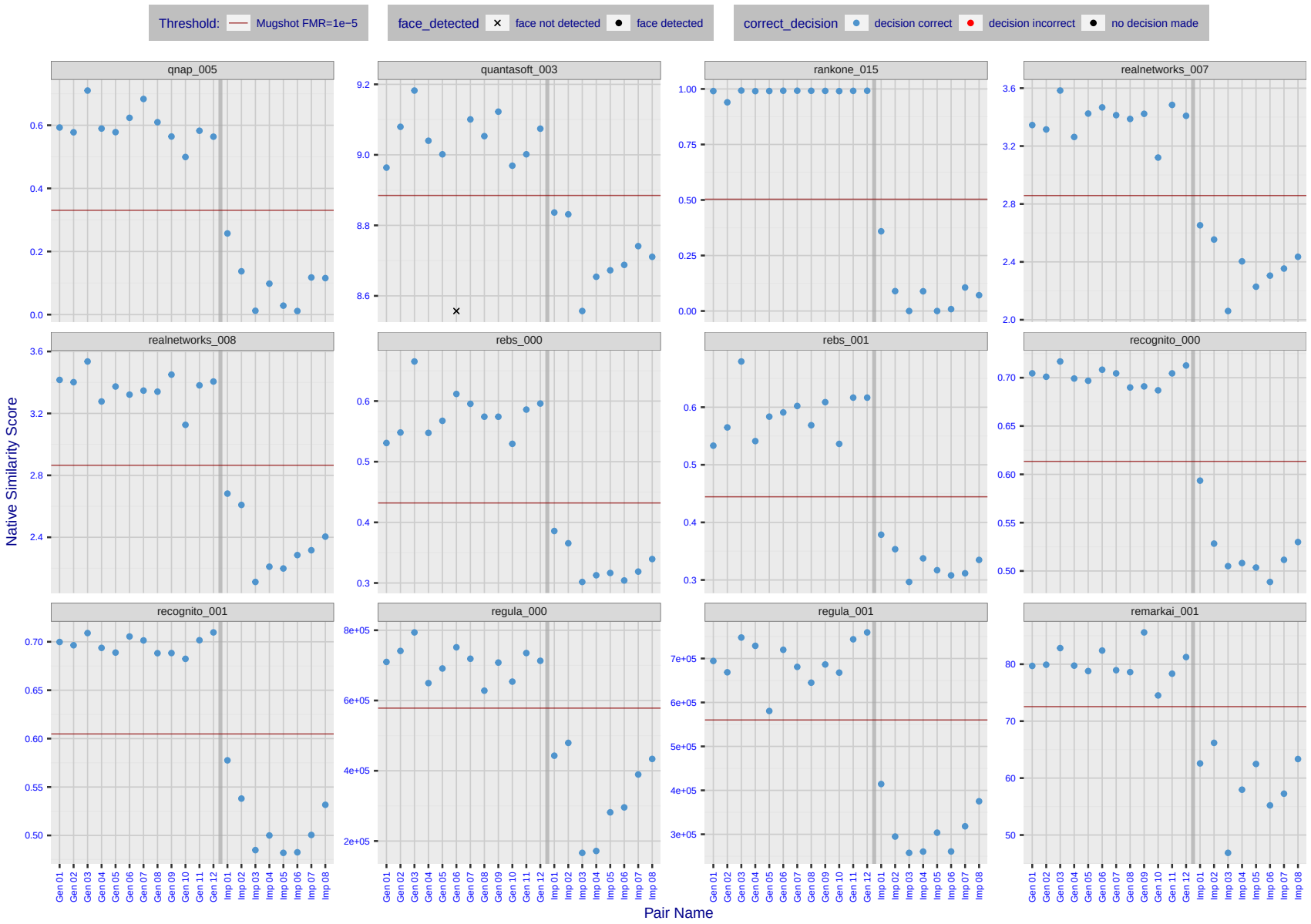

Figure 36: The figure shows algorithms' similarity scores for 12 genuine and 8 impostor image pairs used in a May 2018 paper by Phillips et al. ([1]). The threshold (red horizontal line) is a value calibrated to give FMR = 0.0001 on mugshot images. Points above the threshold correspond to pairs determined to be genuine, and points below the threshold correspond to pairs determined to be impostors. If the determined class (genuine or impostor) matches the real class, points will be blue; if not, red. An X represents face detection failure in either of the images in the pair. Note that the sample size (n=20) is small, and the figure may change substantially if larger or different sets are used. The images can be viewed on p. 13 of the Appendix, where Gen 01 corresponds to Same-Identity Pair 1, Gen 02 corresponds to Same-Identity Pair 2, and so on.

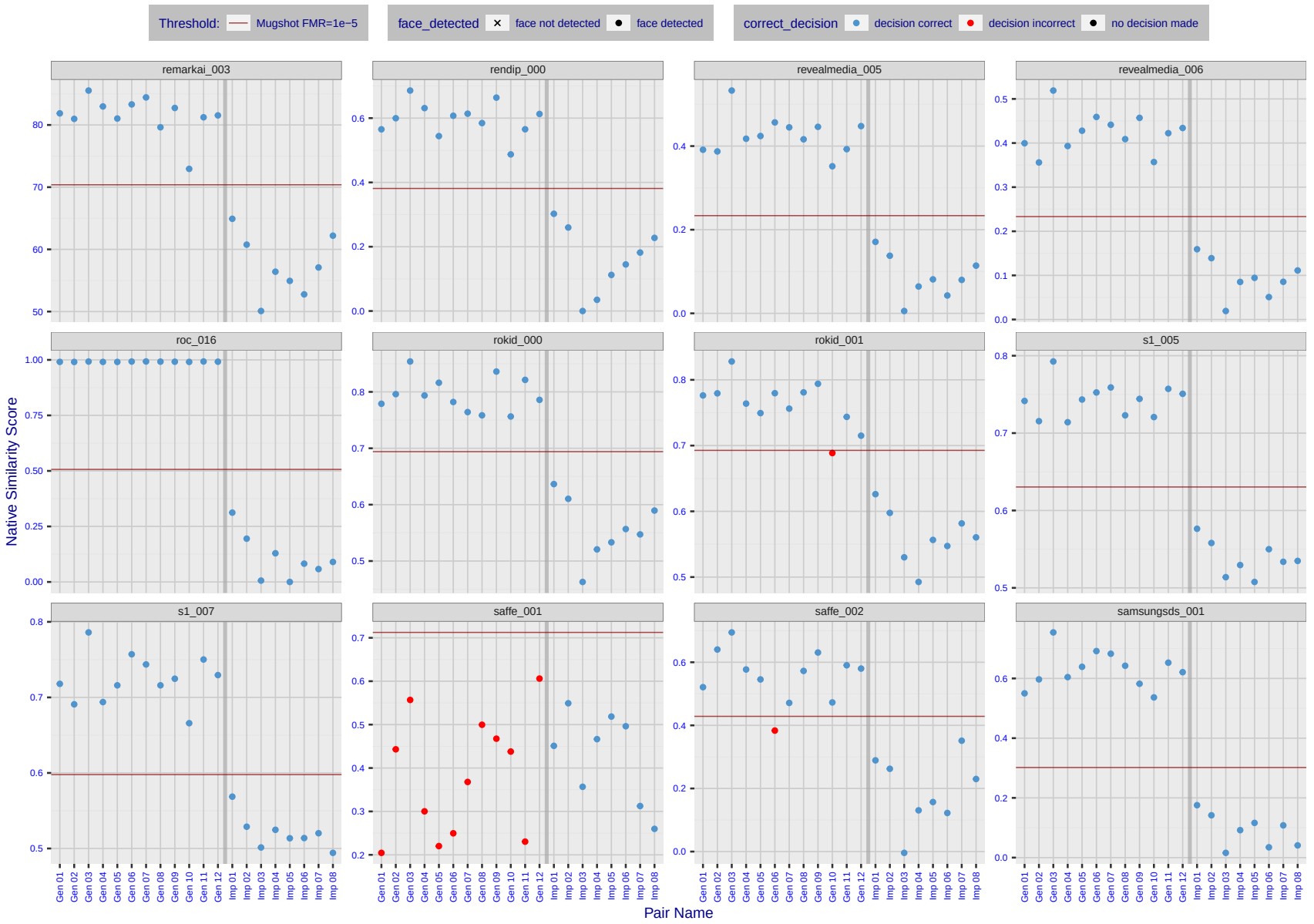

Figure 37: The figure shows algorithms' similarity scores for 12 genuine and 8 impostor image pairs used in a May 2018 paper by Phillips et al. ([1]). The threshold (red horizontal line) is a value calibrated to give FMR = 0.0001 on mugshot images. Points above the threshold correspond to pairs determined to be genuine, and points below the threshold correspond to pairs determined to be impostors. If the determined class (genuine or impostor) matches the real class, points will be blue; if not, red. An X represents face detection failure in either of the images in the pair. Note that the sample size (n=20) is small, and the figure may change substantially if larger or different sets are used. The images can be viewed on p. 13 of the Appendix, where Gen 01 corresponds to Same-Identity Pair 1, Gen 02 corresponds to Same-Identity Pair 2, and so on.

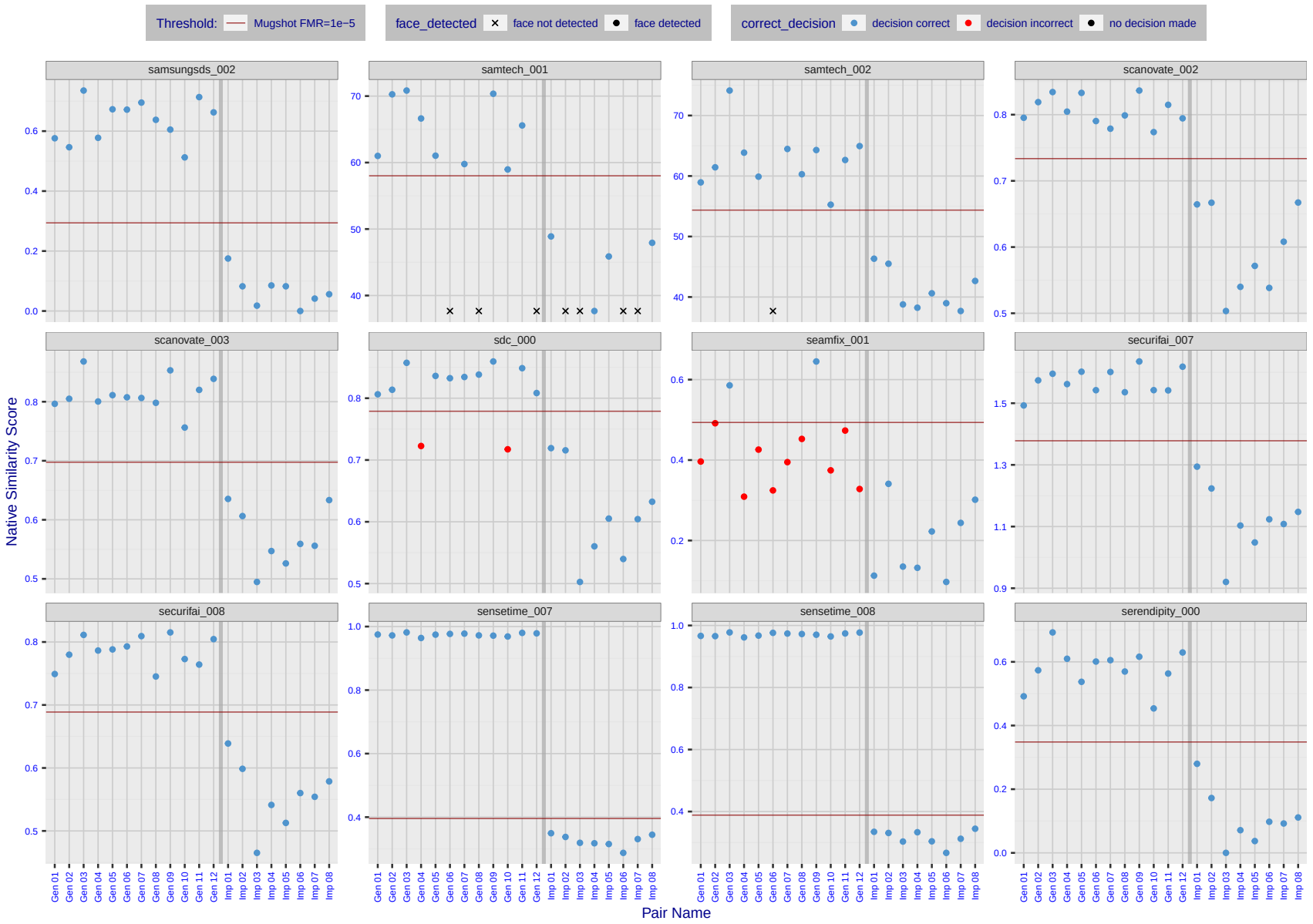

Figure 38: The figure shows algorithms' similarity scores for 12 genuine and 8 impostor image pairs used in a May 2018 paper by Phillips et al. ([1]). The threshold (red horizontal line) is a value calibrated to give FMR = 0.0001 on mugshot images. Points above the threshold correspond to pairs determined to be genuine, and points below the threshold correspond to pairs determined to be impostors. If the determined class (genuine or impostor) matches the real class, points will be blue; if not, red. An X represents face detection failure in either of the images in the pair. Note that the sample size (n=20) is small, and the figure may change substantially if larger or different sets are used. The images can be viewed on p. 13 of the Appendix, where Gen 01 corresponds to Same-Identity Pair 1, Gen 02 corresponds to Same-Identity Pair 2, and so on.

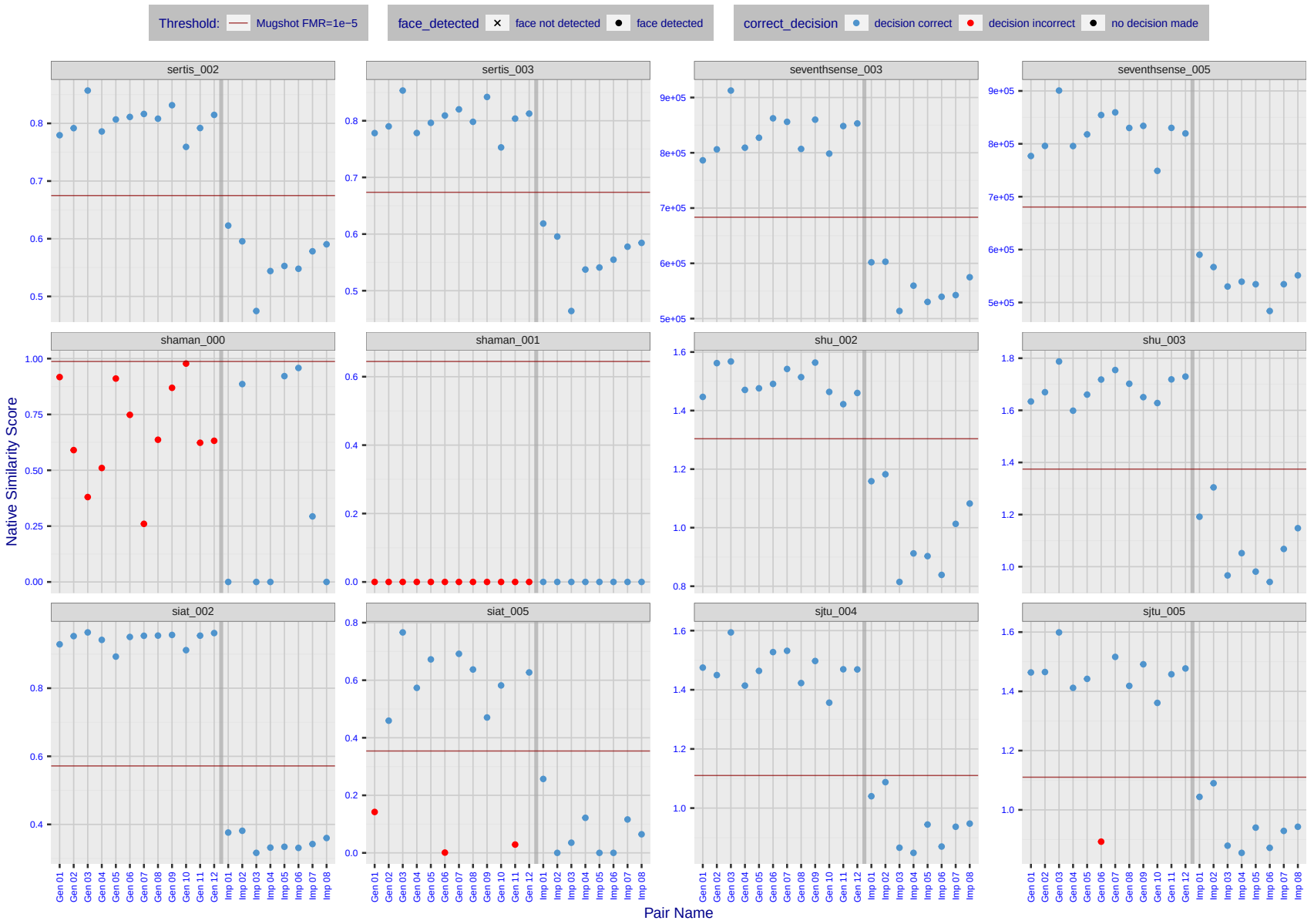

Figure 39: The figure shows algorithms' similarity scores for 12 genuine and 8 impostor image pairs used in a May 2018 paper by Phillips et al. ([1]). The threshold (red horizontal line) is a value calibrated to give FMR = 0.0001 on mugshot images. Points above the threshold correspond to pairs determined to be genuine, and points below the threshold correspond to pairs determined to be impostors. If the determined class (genuine or impostor) matches the real class, points will be blue; if not, red. An X represents face detection failure in either of the images in the pair. Note that the sample size (n=20) is small, and the figure may change substantially if larger or different sets are used. The images can be viewed on p. 13 of the Appendix, where Gen 01 corresponds to Same-Identity Pair 1, Gen 02 corresponds to Same-Identity Pair 2, and so on.

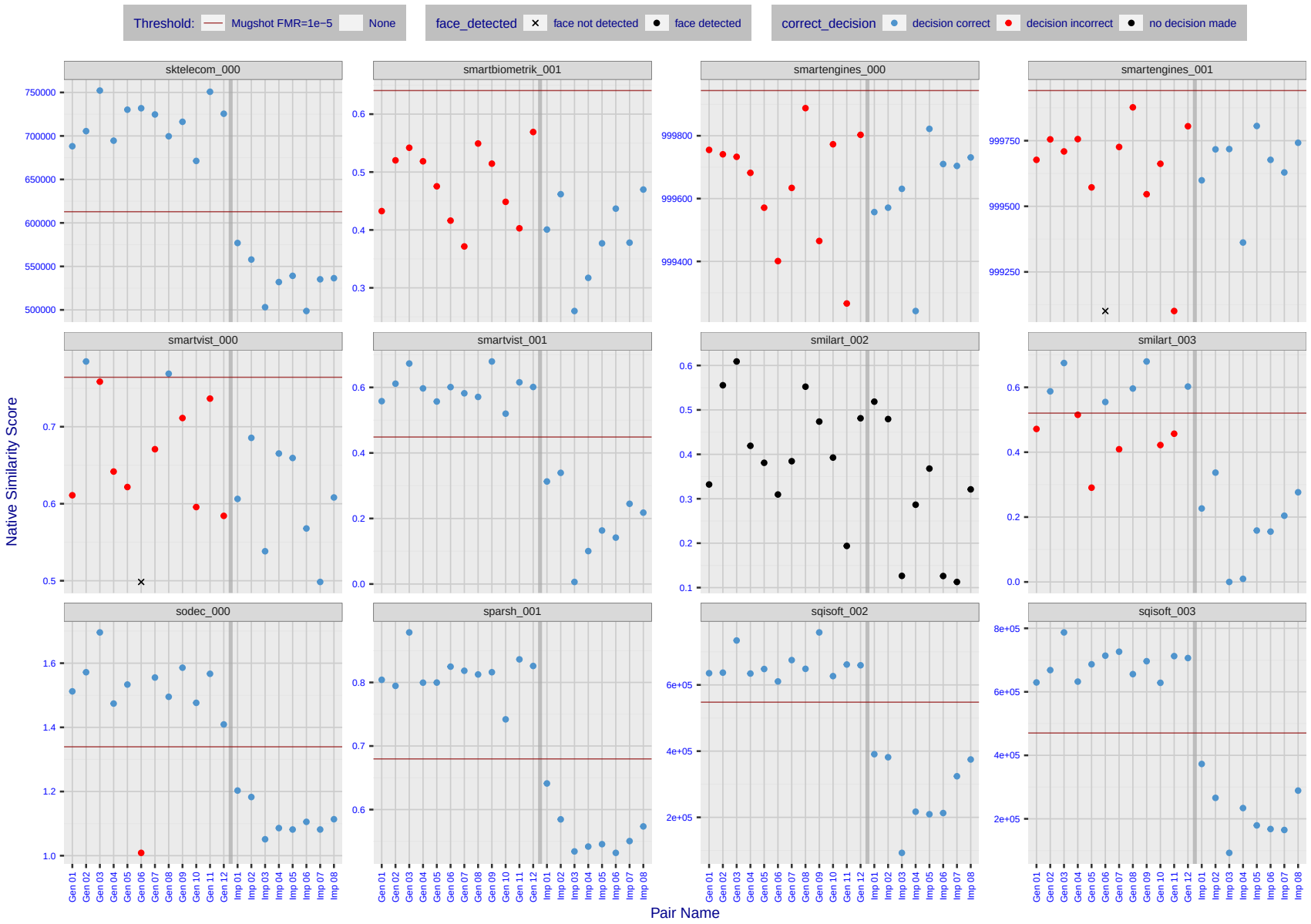

Figure 40: The figure shows algorithms' similarity scores for 12 genuine and 8 impostor image pairs used in a May 2018 paper by Phillips et al. ([1]). The threshold (red horizontal line) is a value calibrated to give FMR = 0.0001 on mugshot images. Points above the threshold correspond to pairs determined to be genuine, and points below the threshold correspond to pairs determined to be impostors. If the determined class (genuine or impostor) matches the real class, points will be blue; if not, red. An X represents face detection failure in either of the images in the pair. Note that the sample size (n=20) is small, and the figure may change substantially if larger or different sets are used. The images can be viewed on p. 13 of the Appendix, where Gen 01 corresponds to Same-Identity Pair 1, Gen 02 corresponds to Same-Identity Pair 2, and so on.

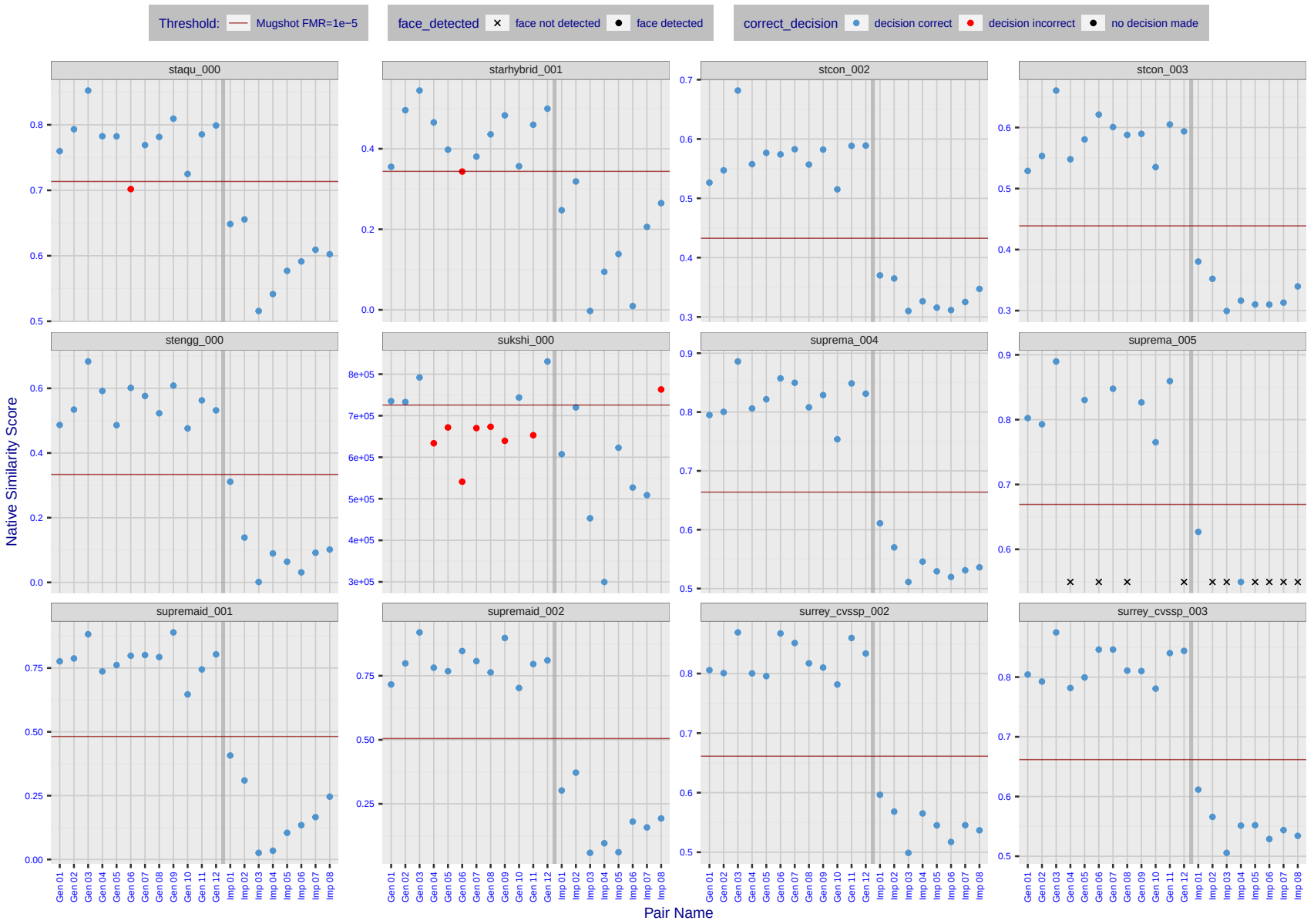

Figure 41: The figure shows algorithms' similarity scores for 12 genuine and 8 impostor image pairs used in a May 2018 paper by Phillips et al. ([1]). The threshold (red horizontal line) is a value calibrated to give FMR = 0.0001 on mugshot images. Points above the threshold correspond to pairs determined to be genuine, and points below the threshold correspond to pairs determined to be impostors. If the determined class (genuine or impostor) matches the real class, points will be blue; if not, red. An X represents face detection failure in either of the images in the pair. Note that the sample size (n=20) is small, and the figure may change substantially if larger or different sets are used. The images can be viewed on p. 13 of the Appendix, where Gen 01 corresponds to Same-Identity Pair 1, Gen 02 corresponds to Same-Identity Pair 2, and so on.

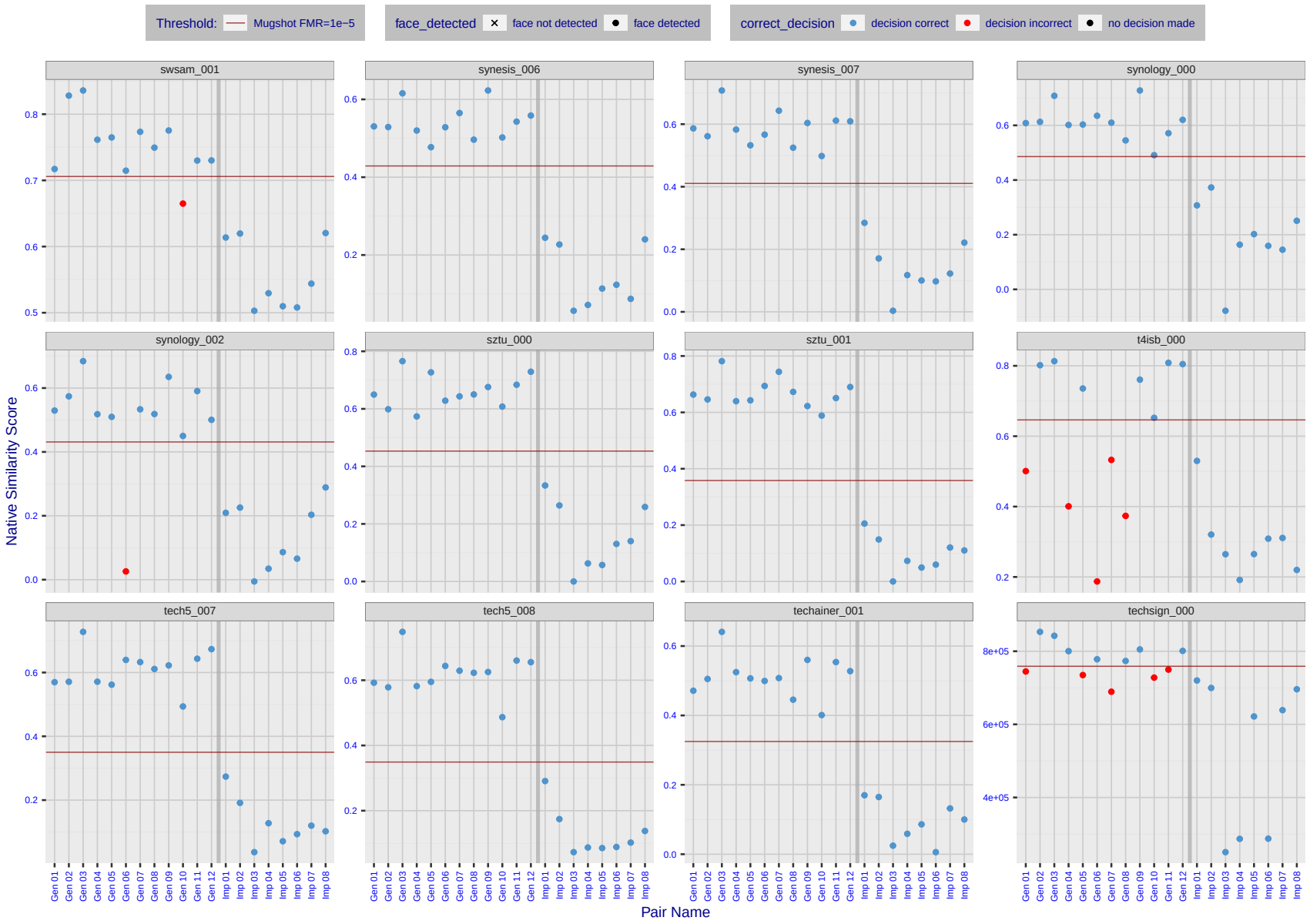

Figure 42: The figure shows algorithms' similarity scores for 12 genuine and 8 impostor image pairs used in a May 2018 paper by Phillips et al. ([1]). The threshold (red horizontal line) is a value calibrated to give FMR = 0.0001 on mugshot images. Points above the threshold correspond to pairs determined to be genuine, and points below the threshold correspond to pairs determined to be impostors. If the determined class (genuine or impostor) matches the real class, points will be blue; if not, red. An X represents face detection failure in either of the images in the pair. Note that the sample size (n=20) is small, and the figure may change substantially if larger or different sets are used. The images can be viewed on p. 13 of the Appendix, where Gen 01 corresponds to Same-Identity Pair 1, Gen 02 corresponds to Same-Identity Pair 2, and so on.

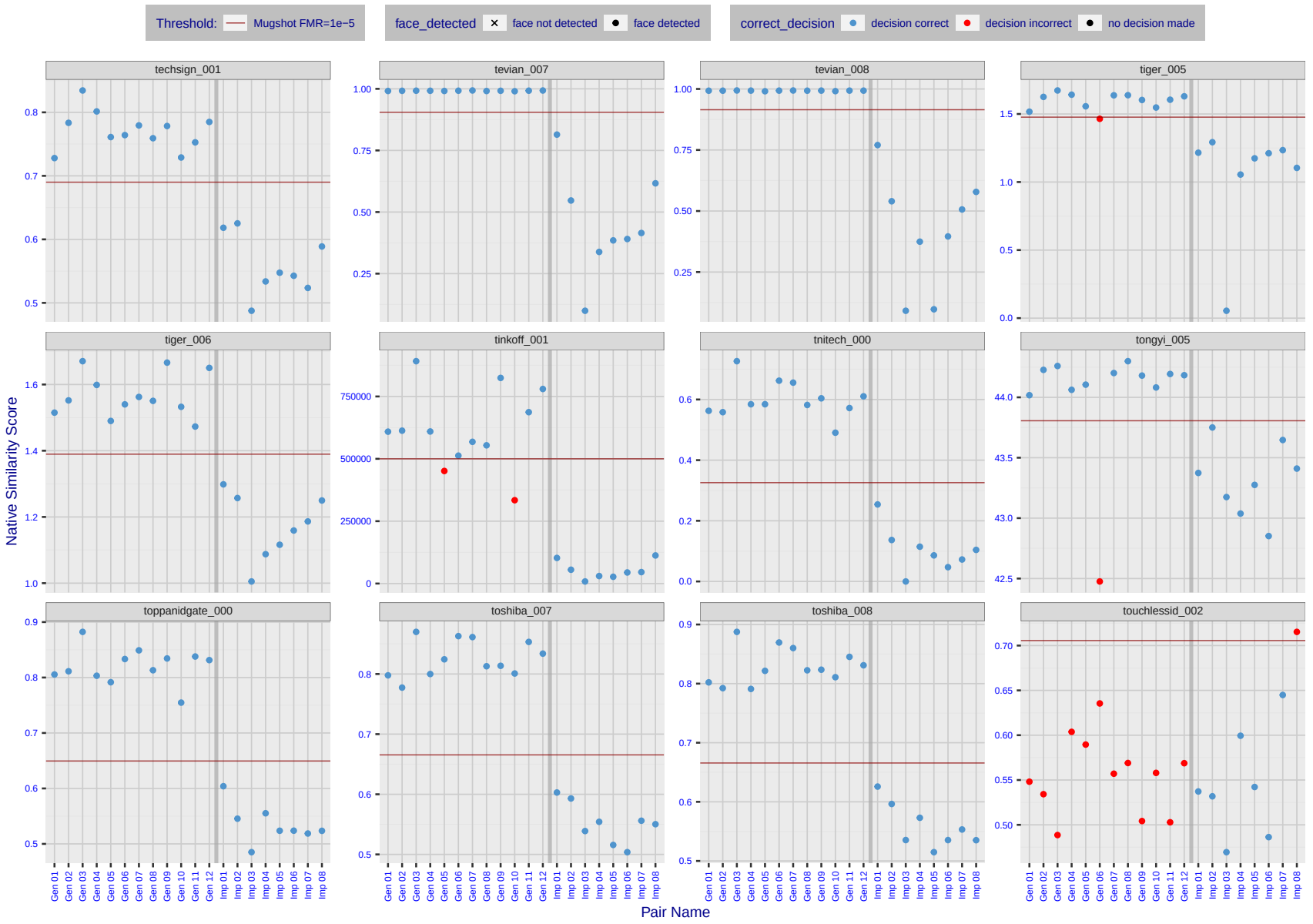

Figure 43: The figure shows algorithms' similarity scores for 12 genuine and 8 impostor image pairs used in a May 2018 paper by Phillips et al. ([1]). The threshold (red horizontal line) is a value calibrated to give FMR = 0.0001 on mugshot images. Points above the threshold correspond to pairs determined to be genuine, and points below the threshold correspond to pairs determined to be impostors. If the determined class (genuine or impostor) matches the real class, points will be blue; if not, red. An X represents face detection failure in either of the images in the pair. Note that the sample size (n=20) is small, and the figure may change substantially if larger or different sets are used. The images can be viewed on p. 13 of the Appendix, where Gen 01 corresponds to Same-Identity Pair 1, Gen 02 corresponds to Same-Identity Pair 2, and so on.

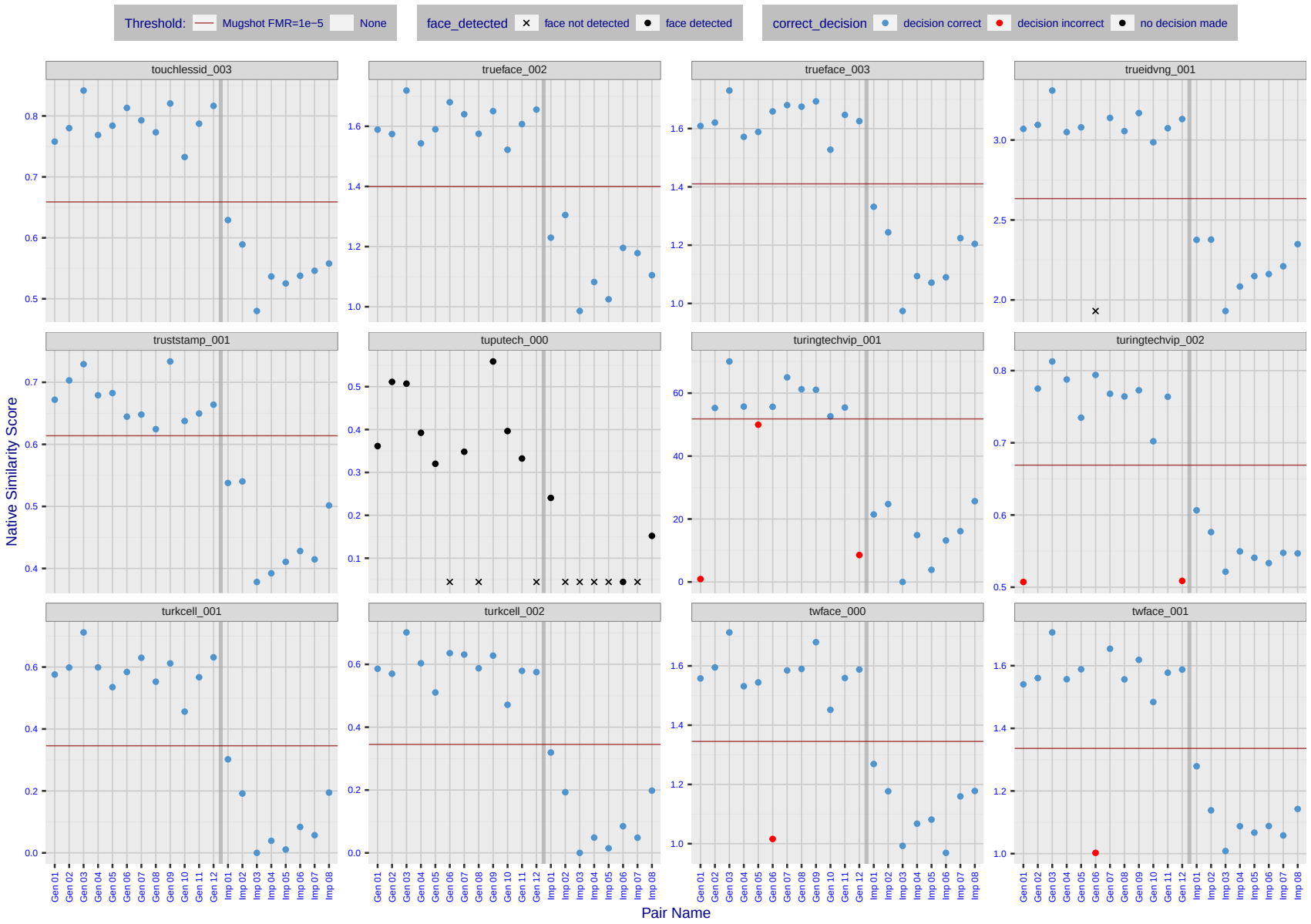

Figure 44: The figure shows algorithms' similarity scores for 12 genuine and 8 impostor image pairs used in a May 2018 paper by Phillips et al. ([1]). The threshold (red horizontal line) is a value calibrated to give FMR = 0.0001 on mugshot images. Points above the threshold correspond to pairs determined to be genuine, and points below the threshold correspond to pairs determined to be impostors. If the determined class (genuine or impostor) matches the real class, points will be blue; if not, red. An X represents face detection failure in either of the images in the pair. Note that the sample size (n=20) is small, and the figure may change substantially if larger or different sets are used. The images can be viewed on p. 13 of the Appendix, where Gen 01 corresponds to Same-Identity Pair 1, Gen 02 corresponds to Same-Identity Pair 2, and so on.

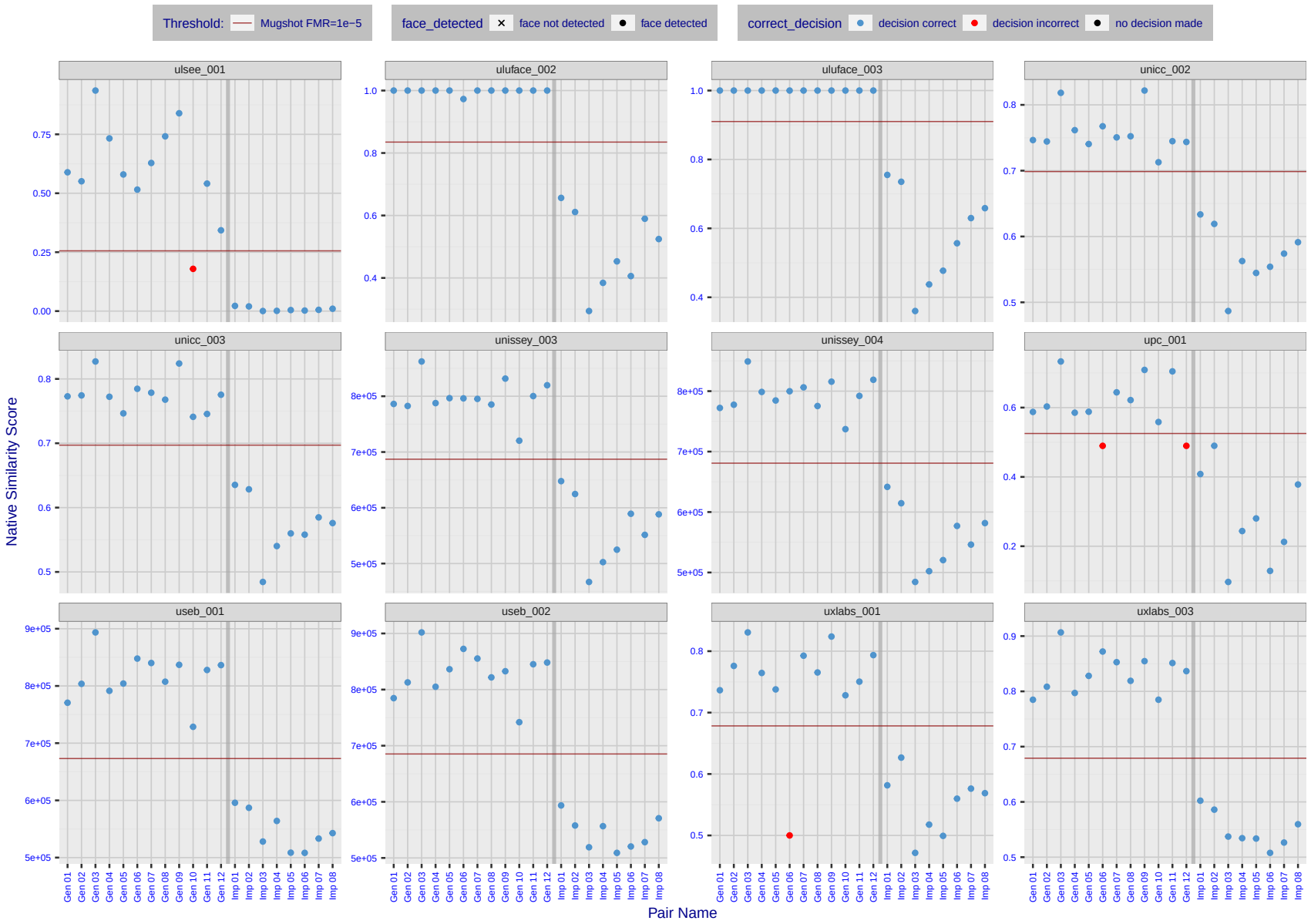

Figure 45: The figure shows algorithms' similarity scores for 12 genuine and 8 impostor image pairs used in a May 2018 paper by Phillips et al. ([1]). The threshold (red horizontal line) is a value calibrated to give FMR = 0.0001 on mugshot images. Points above the threshold correspond to pairs determined to be genuine, and points below the threshold correspond to pairs determined to be impostors. If the determined class (genuine or impostor) matches the real class, points will be blue; if not, red. An X represents face detection failure in either of the images in the pair. Note that the sample size (n=20) is small, and the figure may change substantially if larger or different sets are used. The images can be viewed on p. 13 of the Appendix, where Gen 01 corresponds to Same-Identity Pair 1, Gen 02 corresponds to Same-Identity Pair 2, and so on.

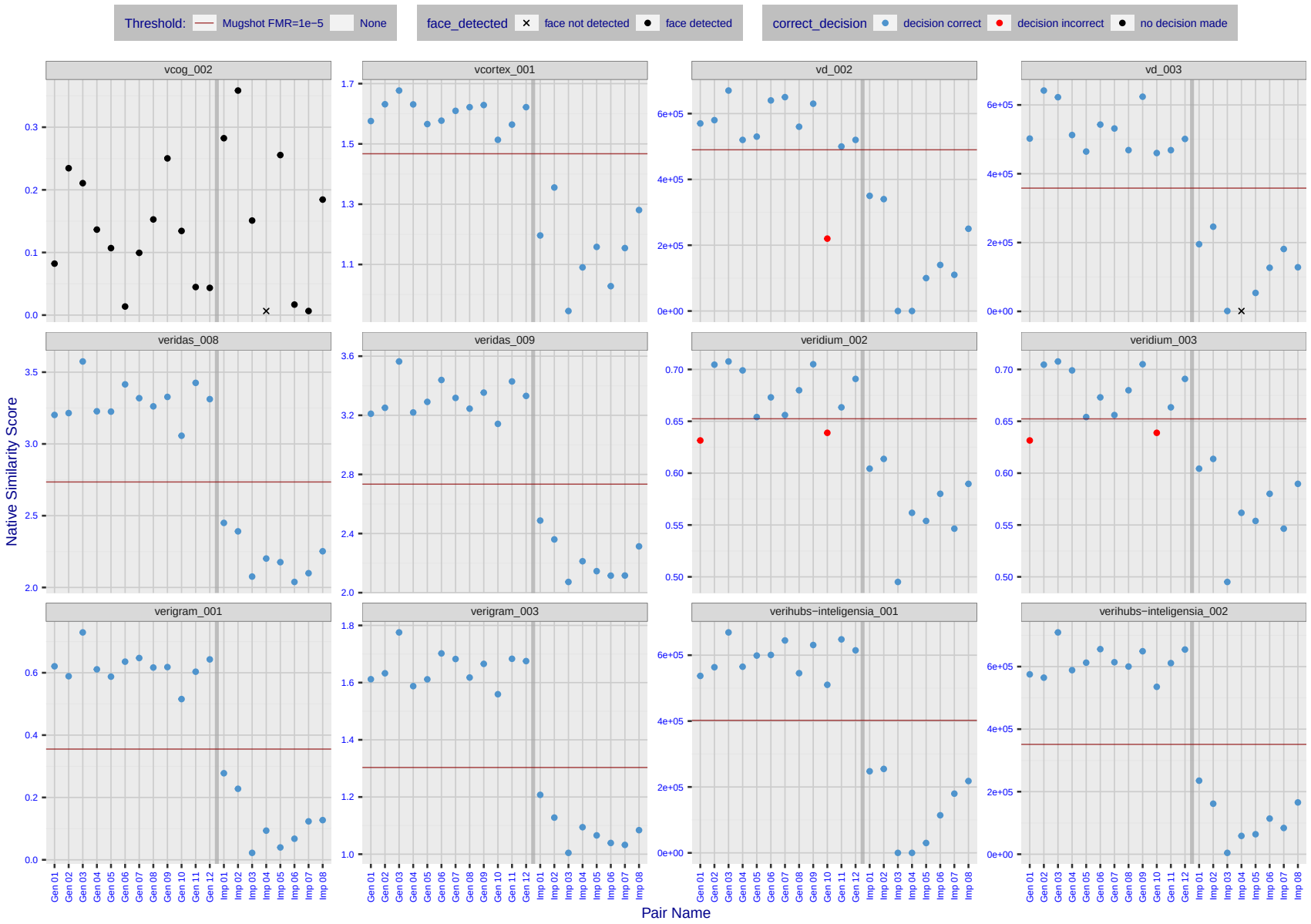

Figure 46: The figure shows algorithms' similarity scores for 12 genuine and 8 impostor image pairs used in a May 2018 paper by Phillips et al. ([1]). The threshold (red horizontal line) is a value calibrated to give FMR = 0.0001 on mugshot images. Points above the threshold correspond to pairs determined to be genuine, and points below the threshold correspond to pairs determined to be impostors. If the determined class (genuine or impostor) matches the real class, points will be blue; if not, red. An X represents face detection failure in either of the images in the pair. Note that the sample size (n=20) is small, and the figure may change substantially if larger or different sets are used. The images can be viewed on p. 13 of the Appendix, where Gen 01 corresponds to Same-Identity Pair 1, Gen 02 corresponds to Same-Identity Pair 2, and so on.

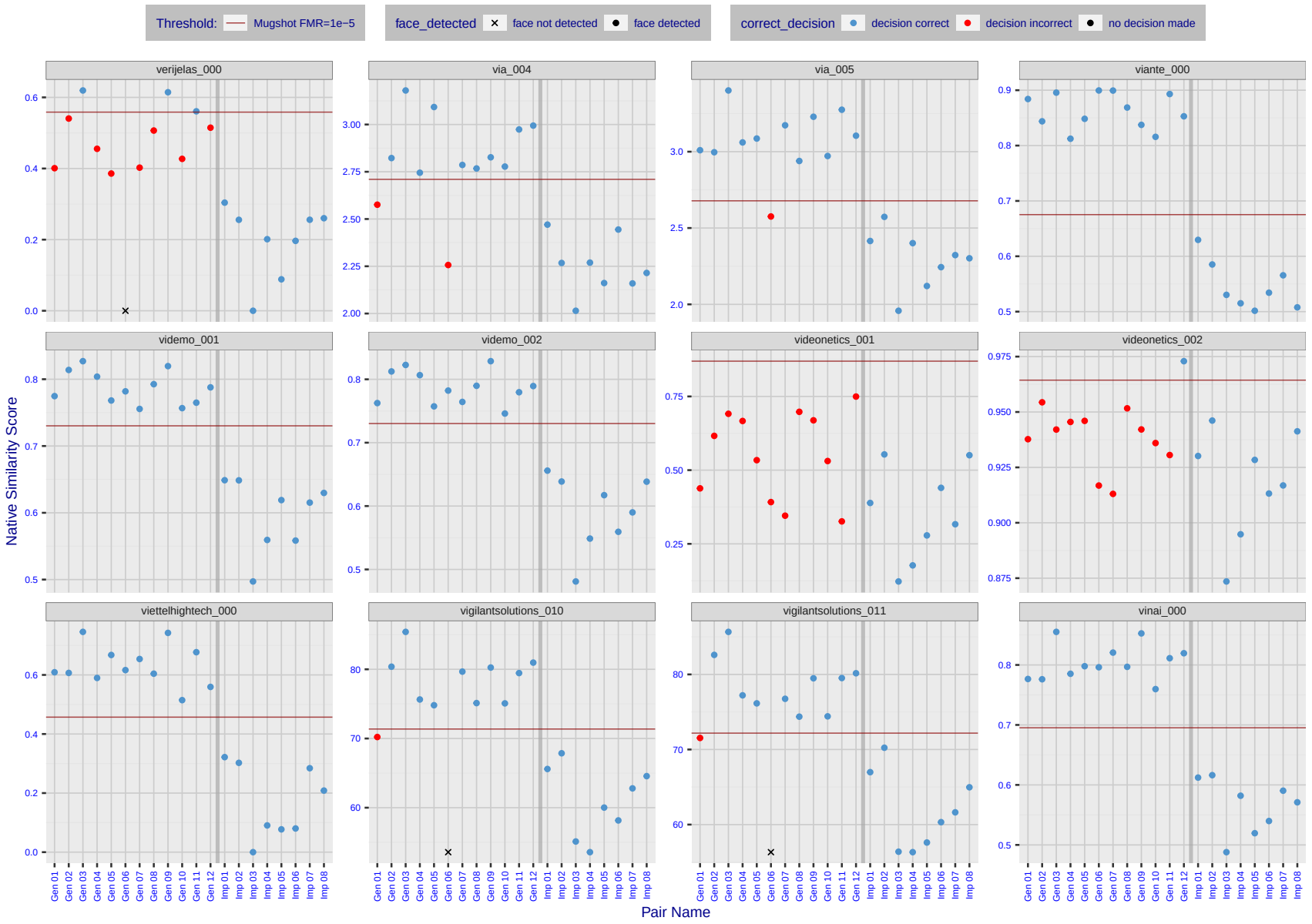

Figure 47: The figure shows algorithms' similarity scores for 12 genuine and 8 impostor image pairs used in a May 2018 paper by Phillips et al. ([1]). The threshold (red horizontal line) is a value calibrated to give FMR = 0.0001 on mugshot images. Points above the threshold correspond to pairs determined to be genuine, and points below the threshold correspond to pairs determined to be impostors. If the determined class (genuine or impostor) matches the real class, points will be blue; if not, red. An X represents face detection failure in either of the images in the pair. Note that the sample size (n=20) is small, and the figure may change substantially if larger or different sets are used. The images can be viewed on p. 13 of the Appendix, where Gen 01 corresponds to Same-Identity Pair 1, Gen 02 corresponds to Same-Identity Pair 2, and so on.

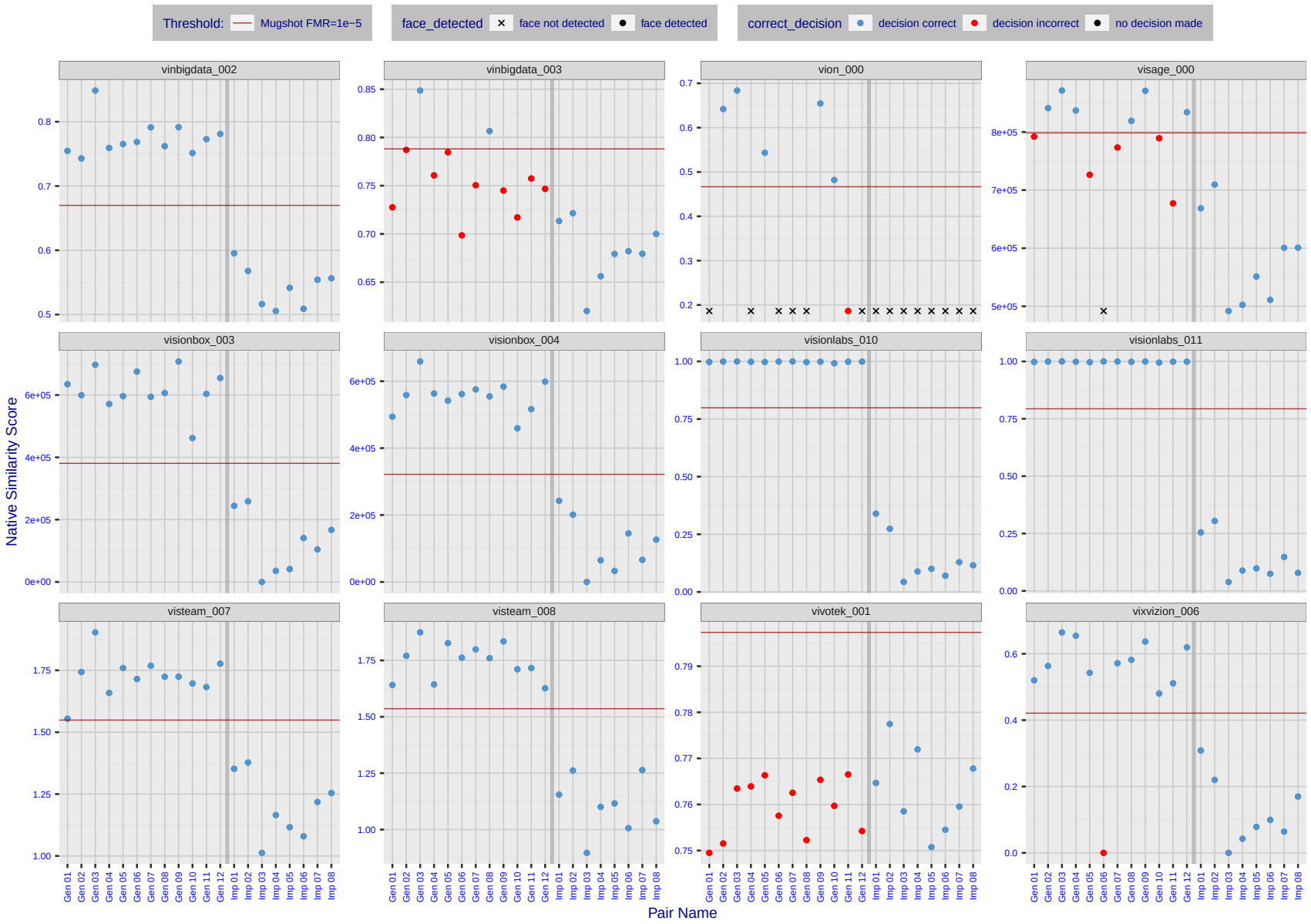

Figure 48: The figure shows algorithms' similarity scores for 12 genuine and 8 impostor image pairs used in a May 2018 paper by Phillips et al. ([1]). The threshold (red horizontal line) is a value calibrated to give FMR = 0.0001 on mugshot images. Points above the threshold correspond to pairs determined to be genuine, and points below the threshold correspond to pairs determined to be impostors. If the determined class (genuine or impostor) matches the real class, points will be blue; if not, red. An X represents face detection failure in either of the images in the pair. Note that the sample size (n=20) is small, and the figure may change substantially if larger or different sets are used. The images can be viewed on p. 13 of the Appendix, where Gen 01 corresponds to Same-Identity Pair 1, Gen 02 corresponds to Same-Identity Pair 2, and so on.

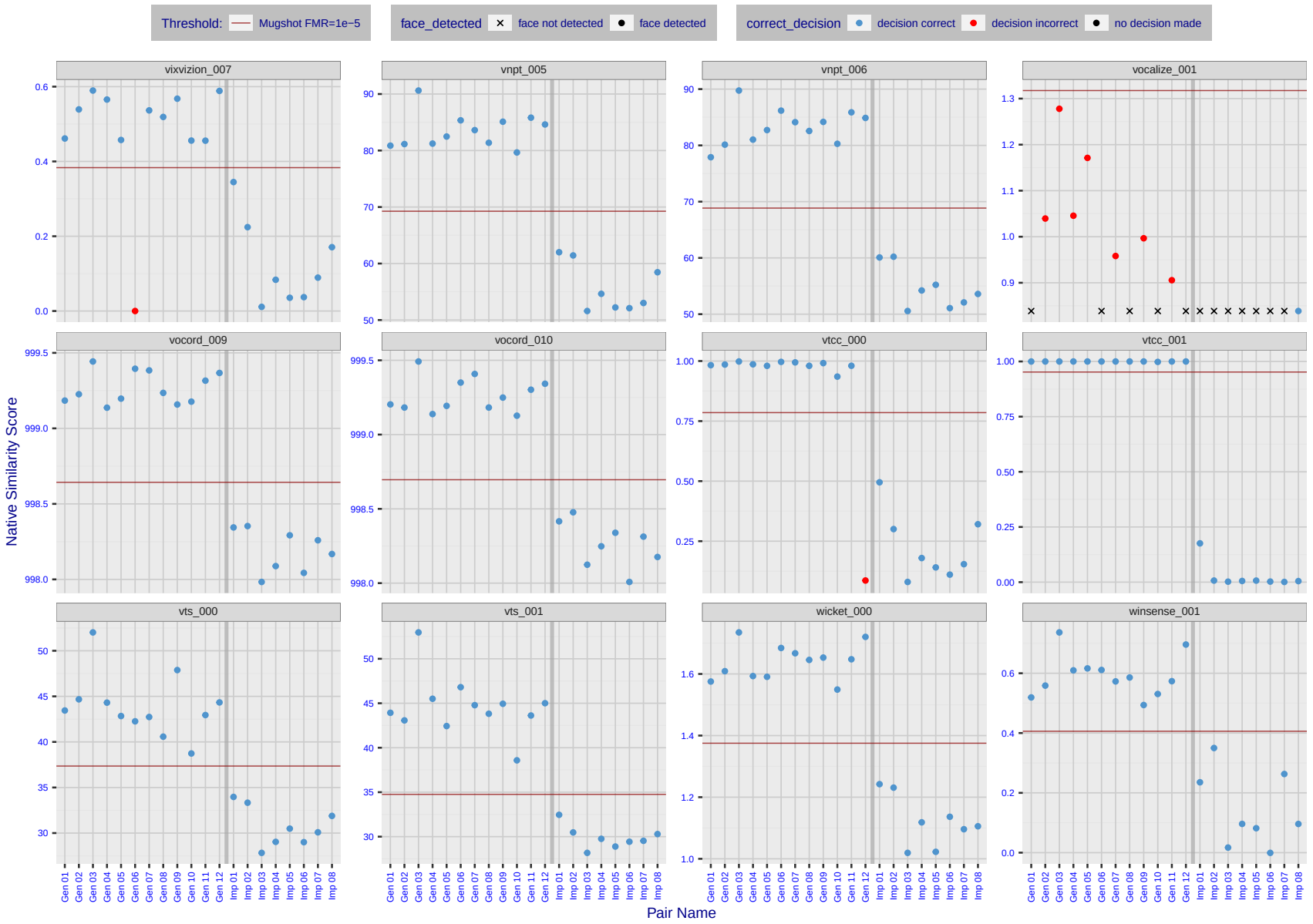

Figure 49: The figure shows algorithms' similarity scores for 12 genuine and 8 impostor image pairs used in a May 2018 paper by Phillips et al. ([1]). The threshold (red horizontal line) is a value calibrated to give FMR = 0.0001 on mugshot images. Points above the threshold correspond to pairs determined to be genuine, and points below the threshold correspond to pairs determined to be impostors. If the determined class (genuine or impostor) matches the real class, points will be blue; if not, red. An X represents face detection failure in either of the images in the pair. Note that the sample size (n=20) is small, and the figure may change substantially if larger or different sets are used. The images can be viewed on p. 13 of the Appendix, where Gen 01 corresponds to Same-Identity Pair 1, Gen 02 corresponds to Same-Identity Pair 2, and so on.

FNMR(T) "False non-match rate"
FMR(T) "False match rate"

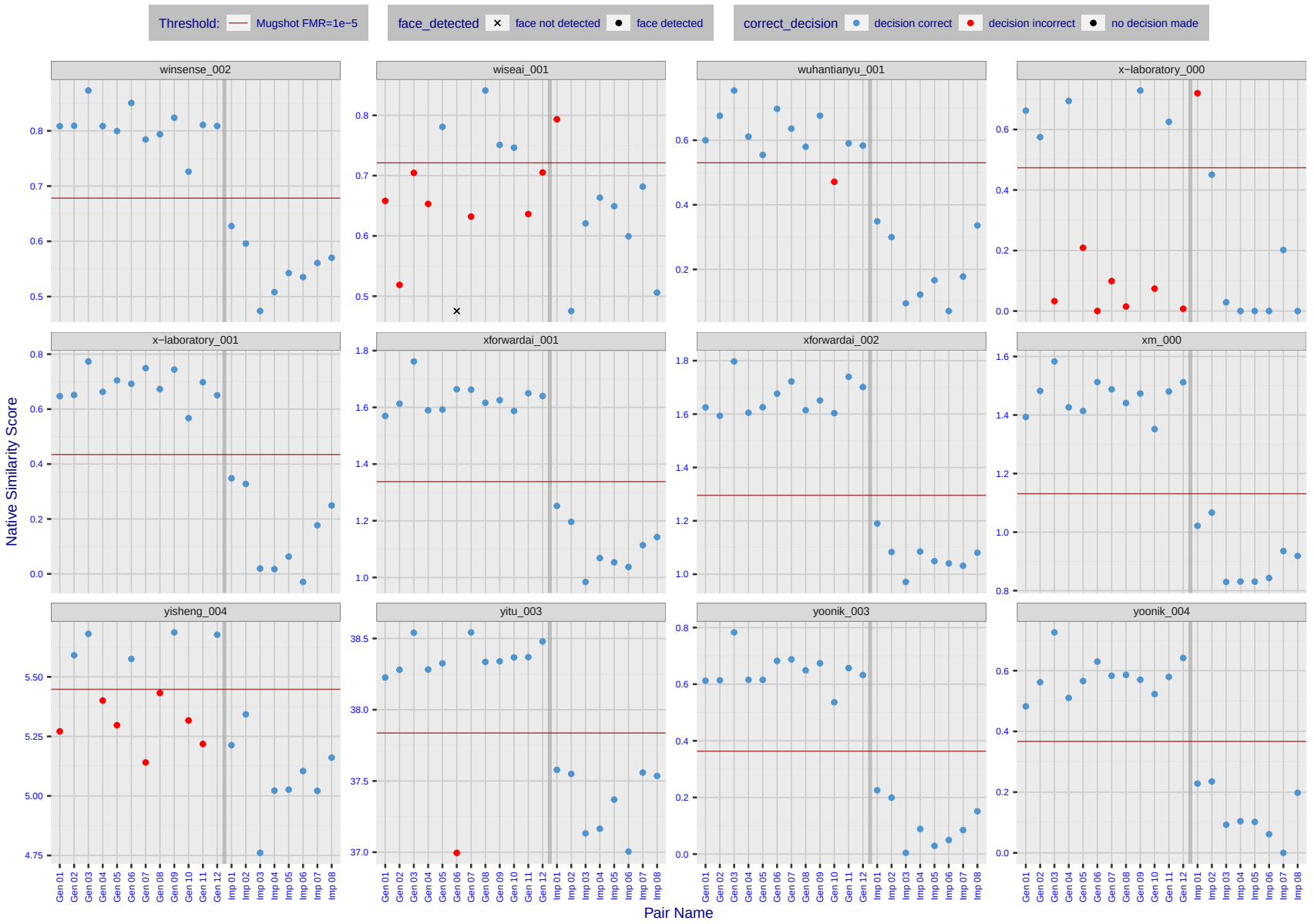

Figure 50: The figure shows algorithms' similarity scores for 12 genuine and 8 impostor image pairs used in a May 2018 paper by Phillips et al. ([1]). The threshold (red horizontal line) is a value calibrated to give FMR = 0.0001 on mugshot images. Points above the threshold correspond to pairs determined to be genuine, and points below the threshold correspond to pairs determined to be impostors. If the determined class (genuine or impostor) matches the real class, points will be blue; if not, red. An X represents face detection failure in either of the images in the pair. Note that the sample size (n=20) is small, and the figure may change substantially if larger or different sets are used. The images can be viewed on p. 13 of the Appendix, where Gen 01 corresponds to Same-Identity Pair 1, Gen 02 corresponds to Same-Identity Pair 2, and so on.

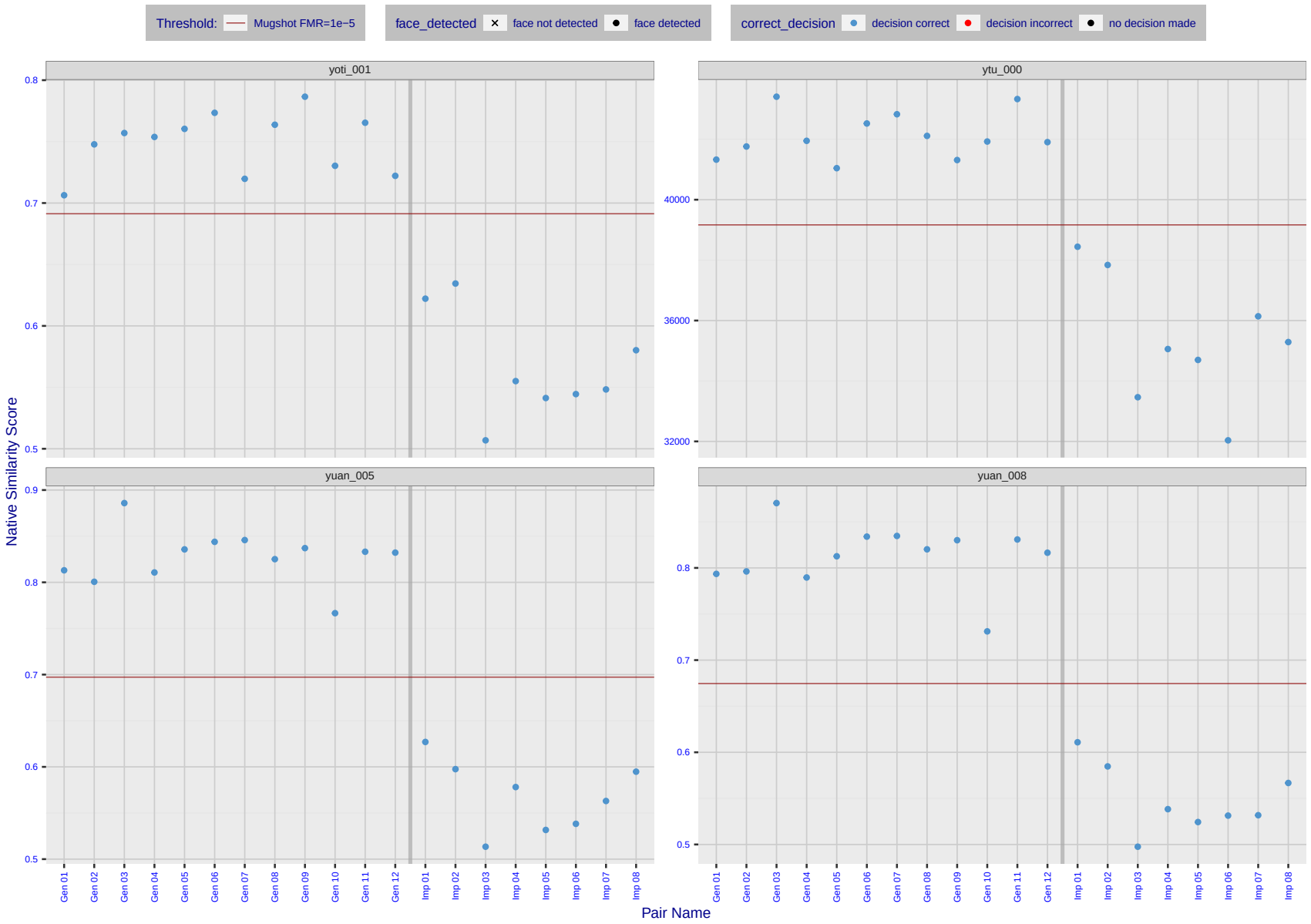

Figure 51: The figure shows algorithms' similarity scores for 12 genuine and 8 impostor image pairs used in a May 2018 paper by Phillips et al. ([1]). The threshold (red horizontal line) is a value calibrated to give FMR = 0.0001 on mugshot images. Points above the threshold correspond to pairs determined to be genuine, and points below the threshold correspond to pairs determined to be impostors. If the determined class (genuine or impostor) matches the real class, points will be blue; if not, red. An X represents face detection failure in either of the images in the pair. Note that the sample size (n=20) is small, and the figure may change substantially if larger or different sets are used. The images can be viewed on p. 13 of the Appendix, where Gen 01 corresponds to Same-Identity Pair 1, Gen 02 corresponds to Same-Identity Pair 2, and so on.

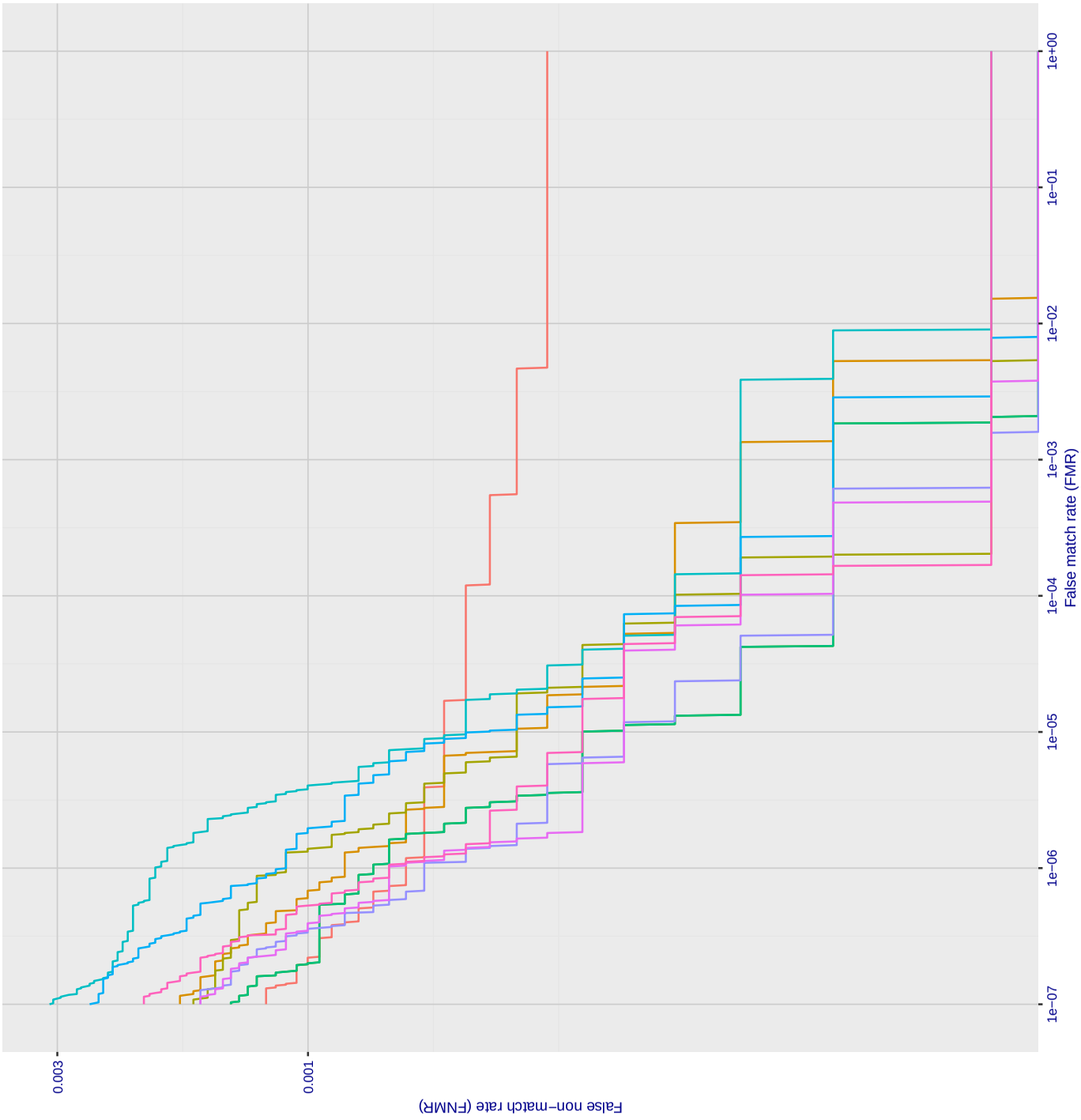

Figure 52: For the visa images, detection error tradeoff (DET) characteristics showing false non-match rate vs. false match rate plotted parametrically on threshold, T. The scales are logarithmic in order to show many decades of FMR.

FNMR(T) "False non-match rate"
FMR(T) "False match rate"

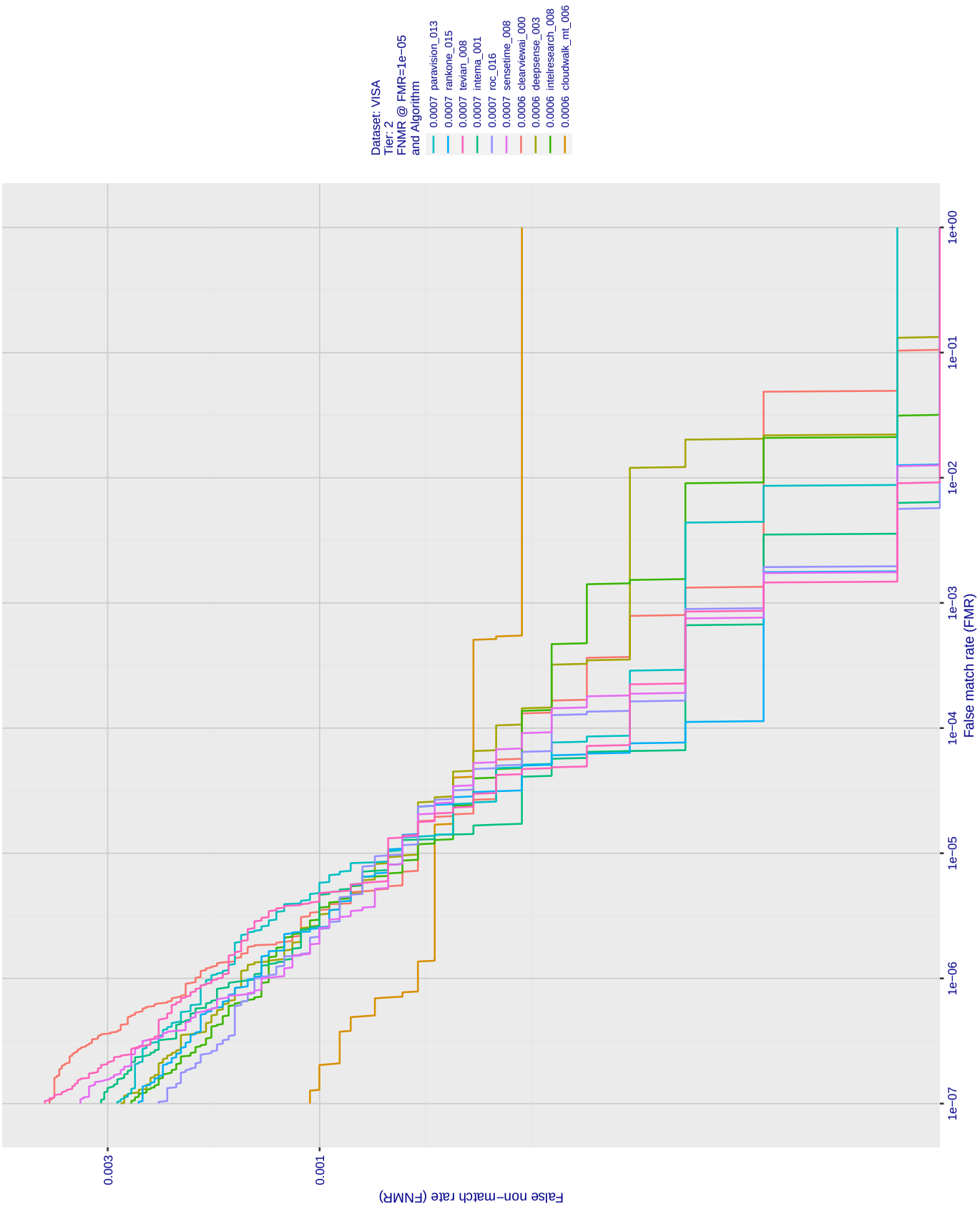

Figure 53: For the visa images, detection error tradeoff (DET) characteristics showing false non-match rate vs. false match rate plotted parametrically on threshold, T. The scales are logarithmic in order to show many decades of FMR.

FNMR(T) "False non-match rate"
FMR(T) "False match rate"

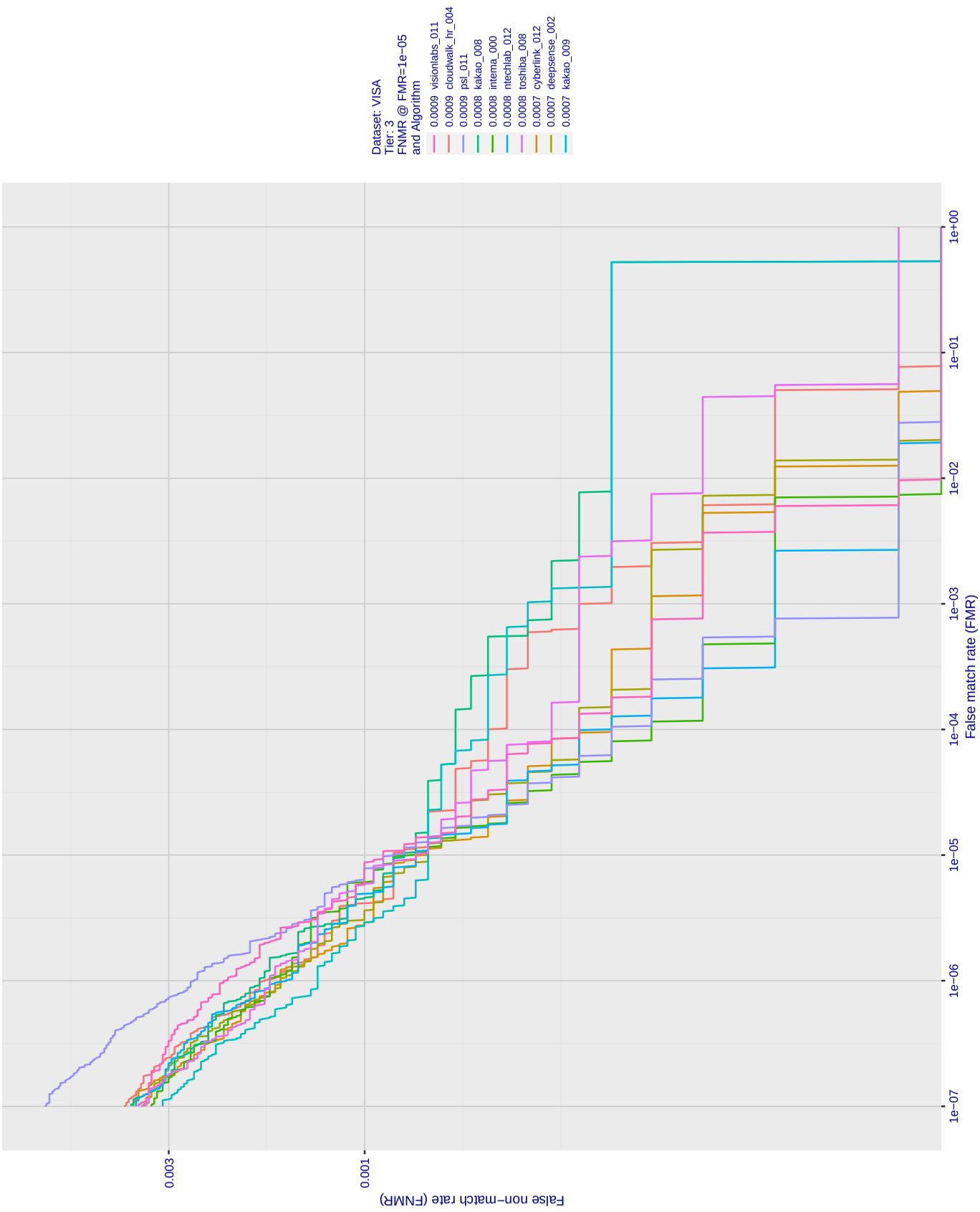

Figure 54: For the visa images, detection error tradeoff (DET) *characteristics showing false non-match rate vs. false match rate plotted parametrically on threshold, T. The scales are logarithmic in order to show many decades of* FMR.

FNMR(T) "False non-match rate"
FMR(T) "False match rate"

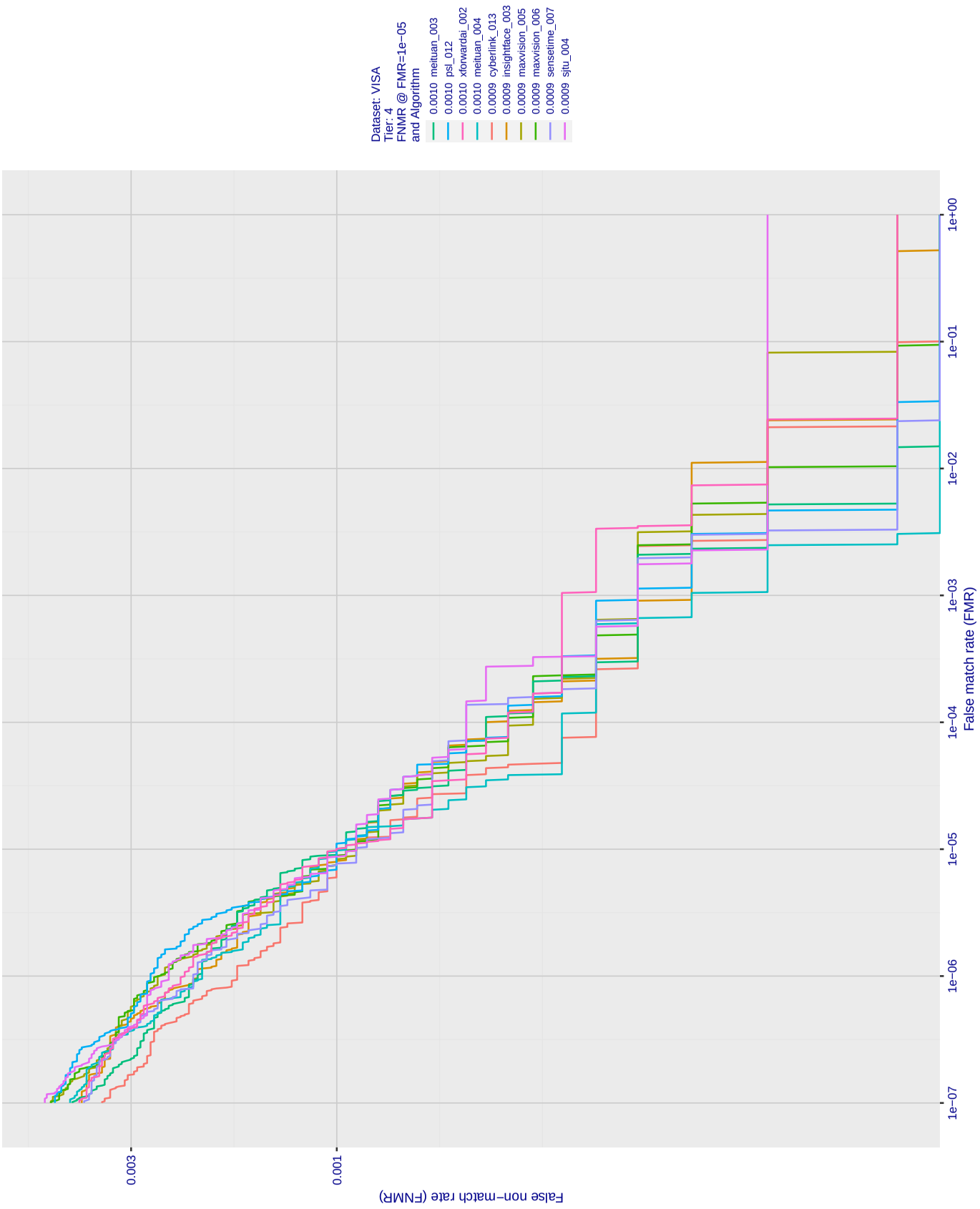

Figure 55: For the visa images, detection error tradeoff (DET) characteristics showing false non-match rate vs. false match rate plotted parametrically on threshold, T. The scales are logarithmic in order to show many decades of FMR.

FNMR(T) "False non-match rate"
FMR(T) "False match rate"

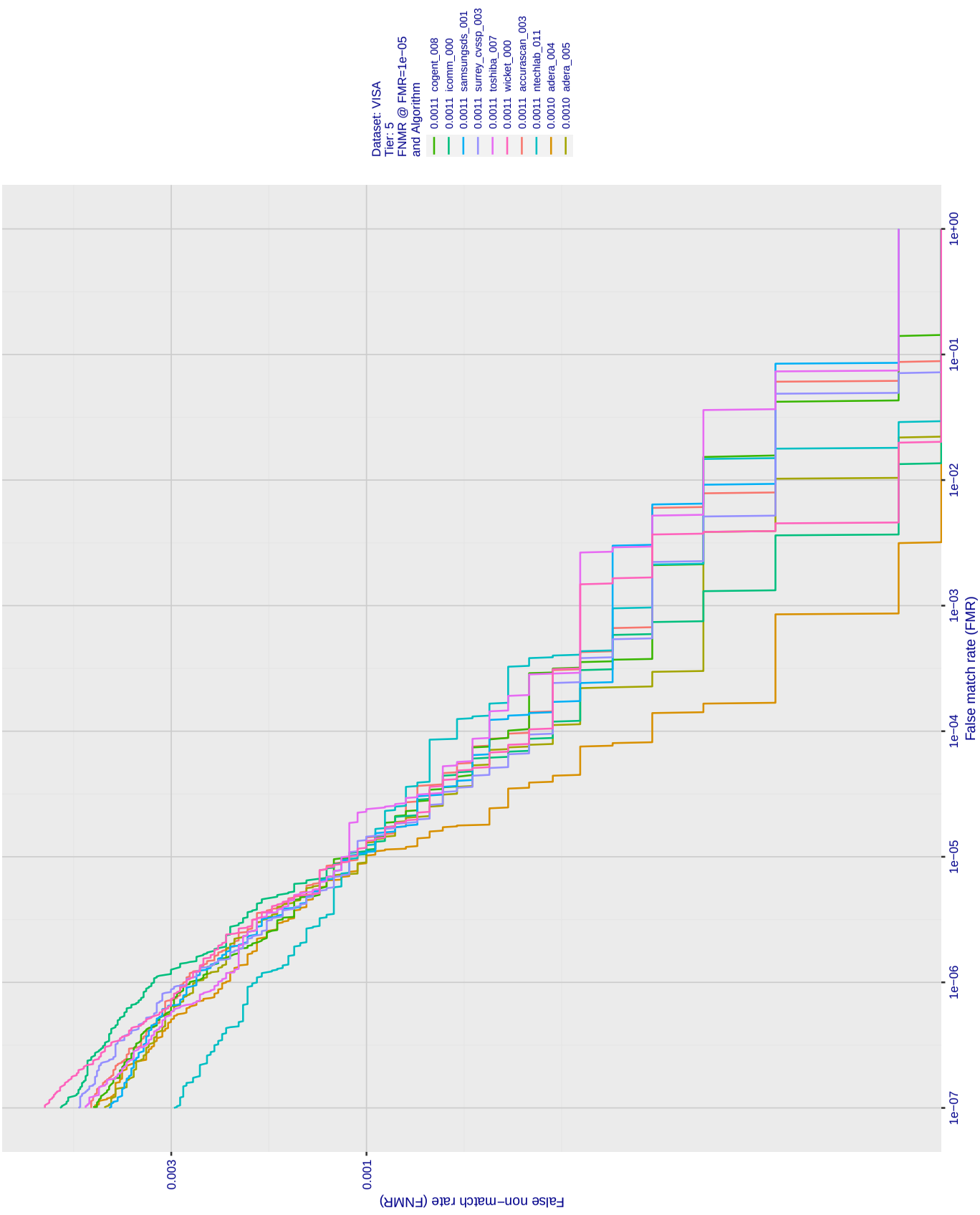

Figure 56: For the visa images, detection error tradeoff (DET) characteristics showing false non-match rate vs. false match rate plotted parametrically on threshold, T. The scales are logarithmic in order to show many decades of FMR.

FNMR(T) "False non-match rate"
FMR(T) "False match rate"

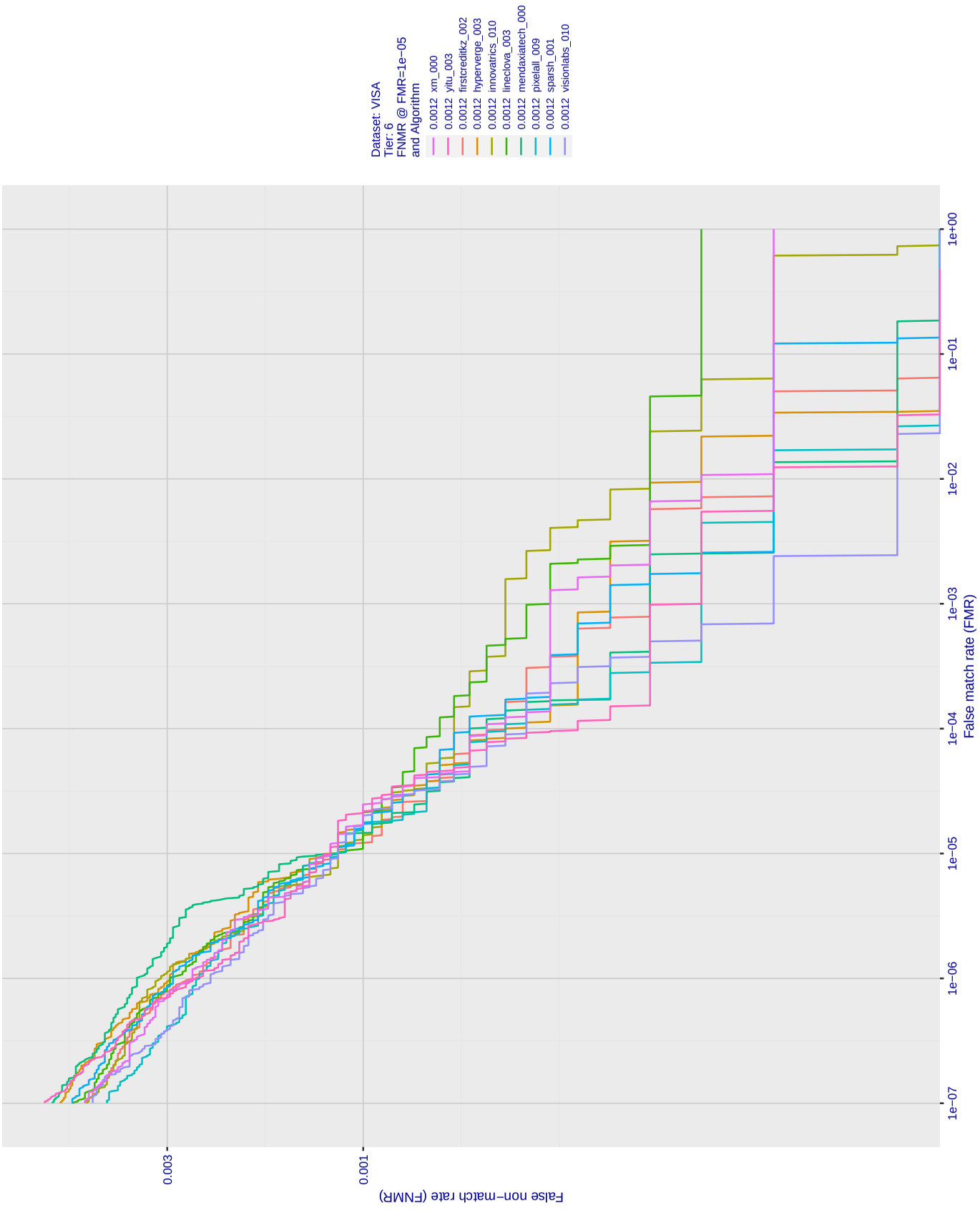

Figure 57: For the visa images, detection error tradeoff (DET) characteristics showing false non-match rate vs. false match rate plotted parametrically on threshold, T. The scales are logarithmic in order to show many decades of FMR.

FNMR(T) "False non-match rate"
FMR(T) "False match rate"

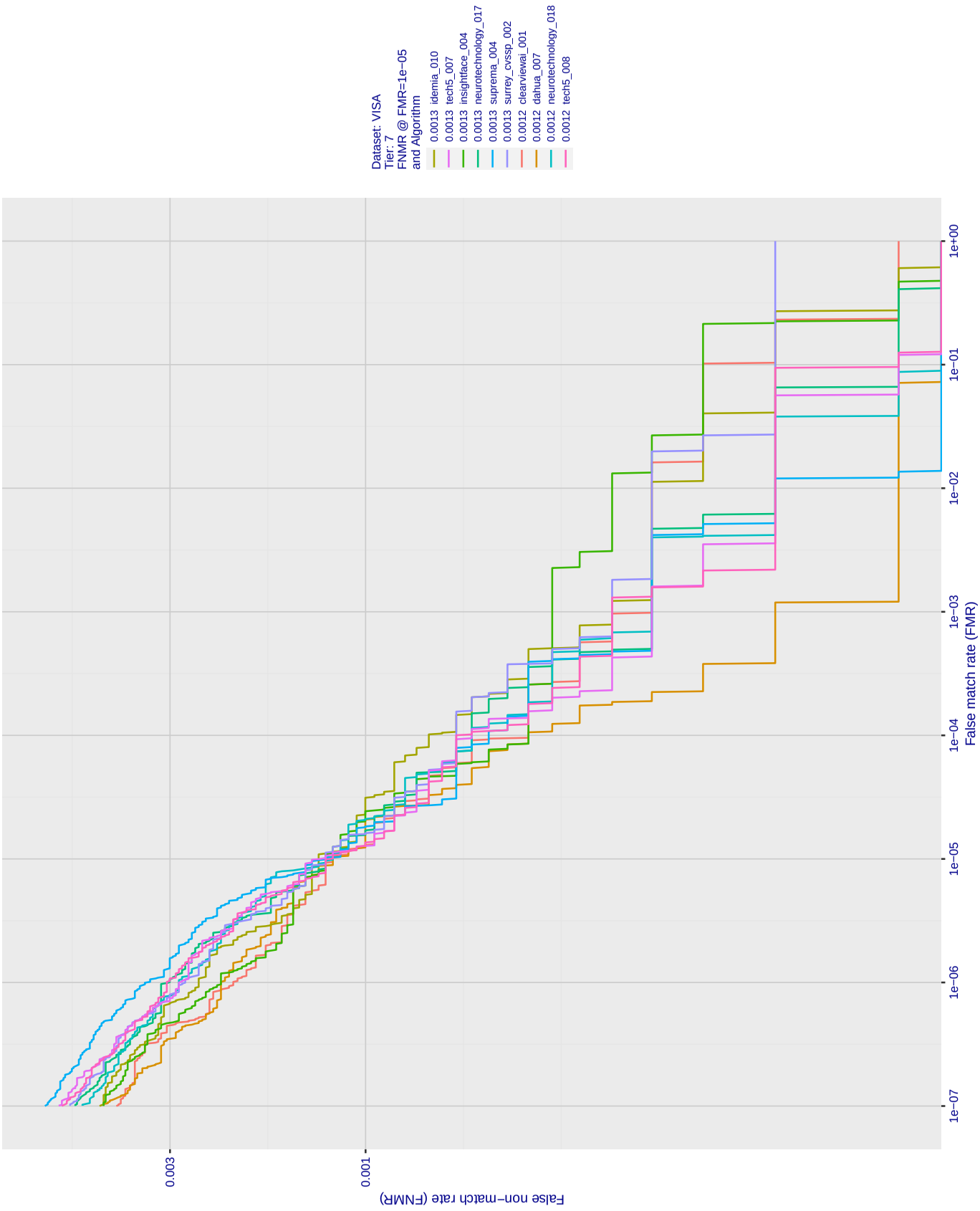

Figure 58: For the visa images, detection error tradeoff (DET) characteristics showing false non-match rate vs. false match rate plotted parametrically on threshold, T. The scales are logarithmic in order to show many decades of FMR.

FNMR(T) "False non-match rate"
FMR(T) "False match rate"

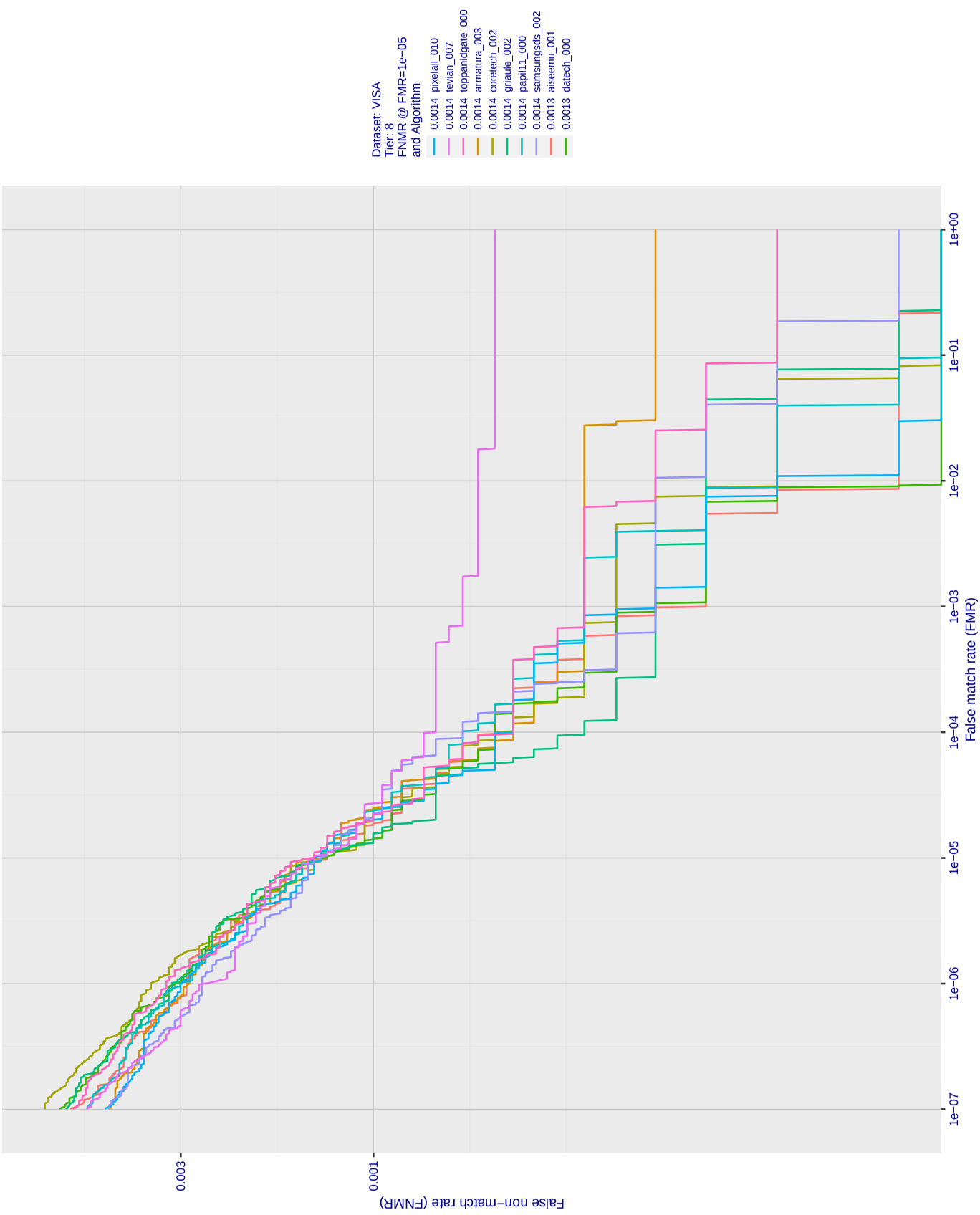

Figure 59: For the visa images, detection error tradeoff (DET) characteristics showing false non-match rate vs. false match rate plotted parametrically on threshold, T. The scales are logarithmic in order to show many decades of FMR.

FNMR(T) "False non-match rate"
FMR(T) "False match rate"

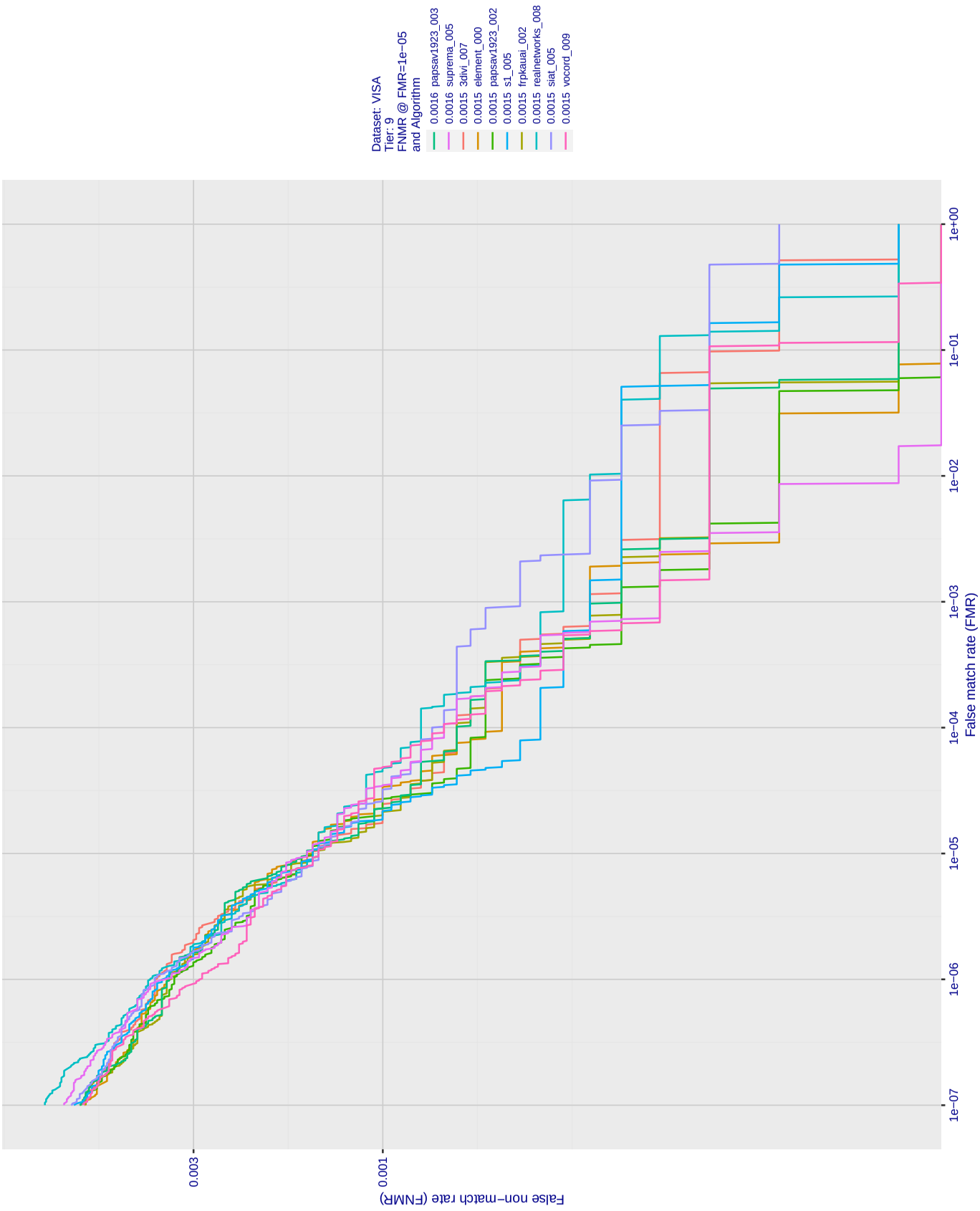

Figure 60: For the visa images, detection error tradeoff (DET) characteristics showing false non-match rate vs. false match rate plotted parametrically on threshold, T. The scales are logarithmic in order to show many decades of FMR.

FNMR(T) "False non-match rate"
FMR(T) "False match rate"

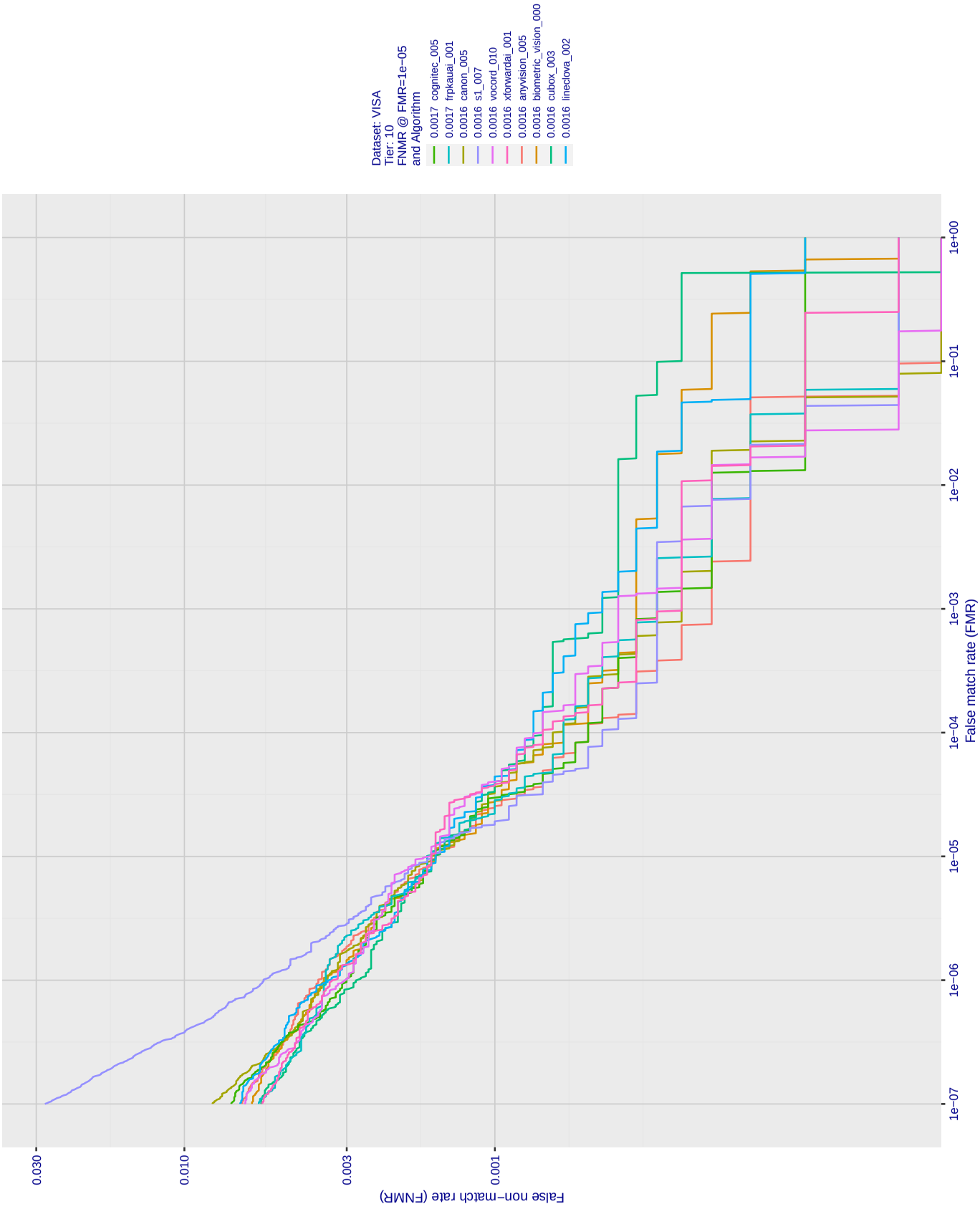

Figure 61: For the visa images, detection error tradeoff (DET) characteristics showing false non-match rate vs. false match rate plotted parametrically on threshold, T. The scales are logarithmic in order to show many decades of FMR.

FNMR(T) "False non-match rate"
FMR(T) "False match rate"

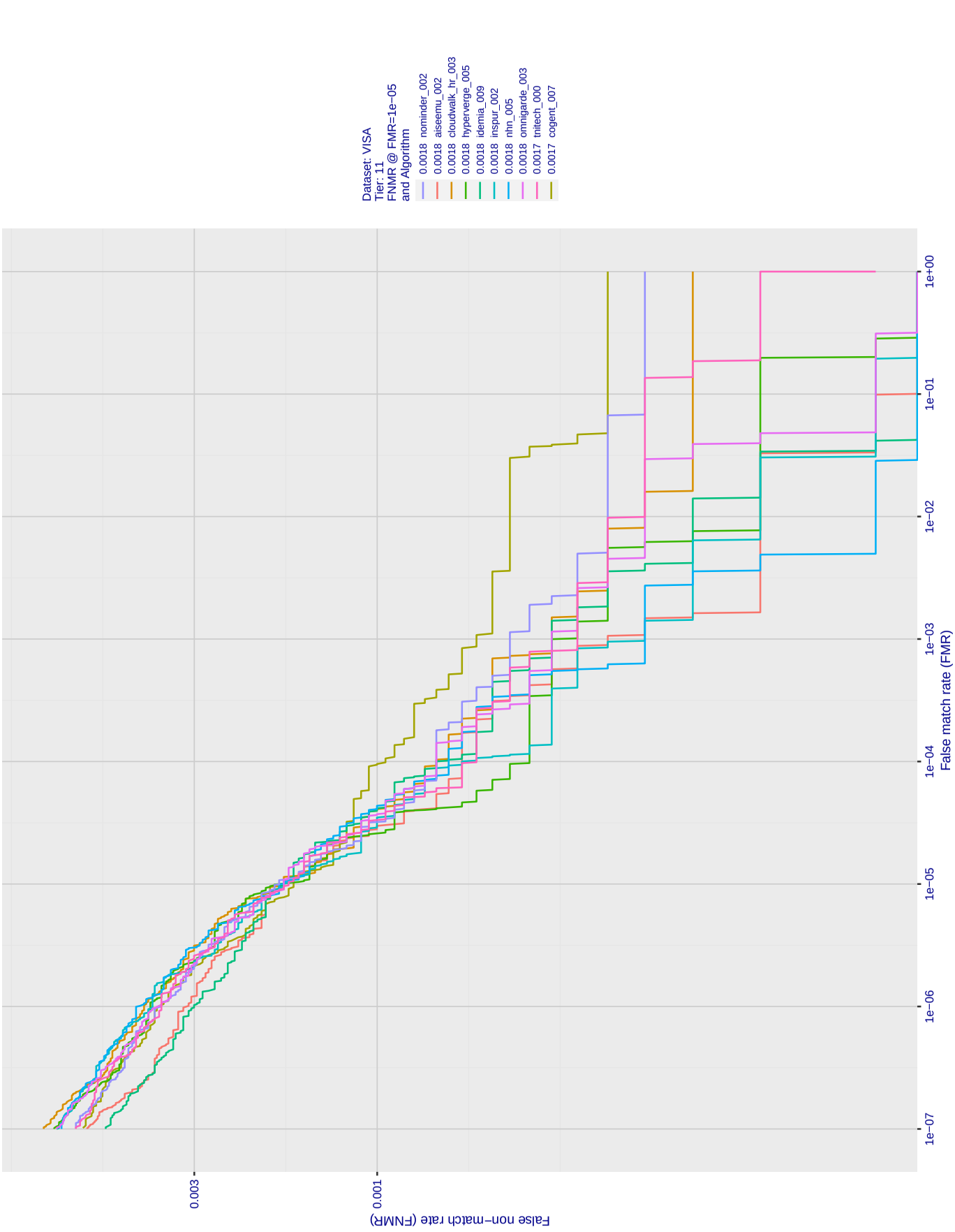

Figure 62: For the visa images, detection error tradeoff (DET) characteristics showing false non-match rate vs. false match rate plotted parametrically on threshold, T. The scales are logarithmic in order to show many decades of FMR.

FNMR(T) "False non-match rate"
FMR(T) "False match rate"

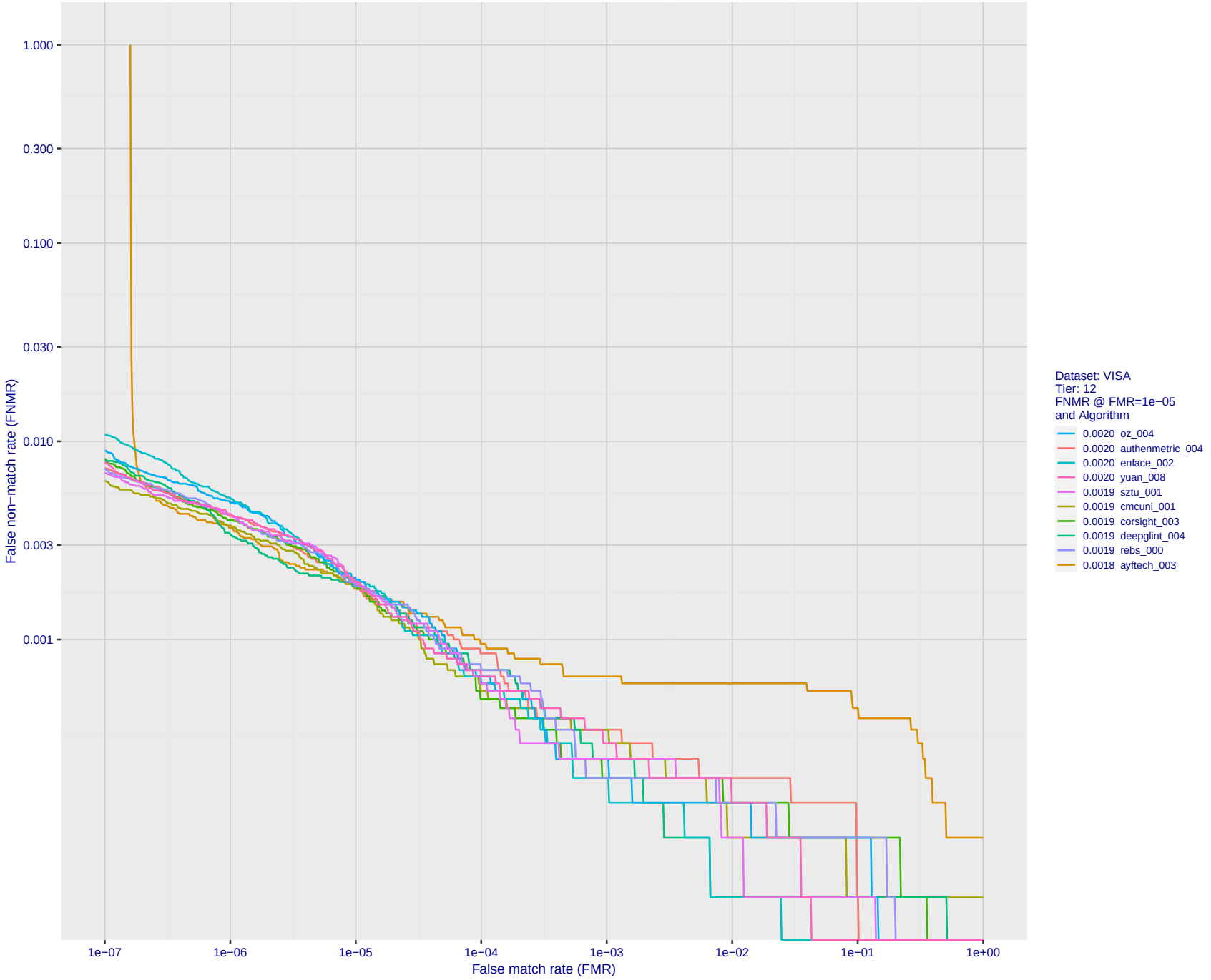

Figure 63: For the visa images, detection error tradeoff (DET) characteristics showing false non-match rate vs. false match rate plotted parametrically on threshold, T. The scales are logarithmic in order to show many decades of FMR.

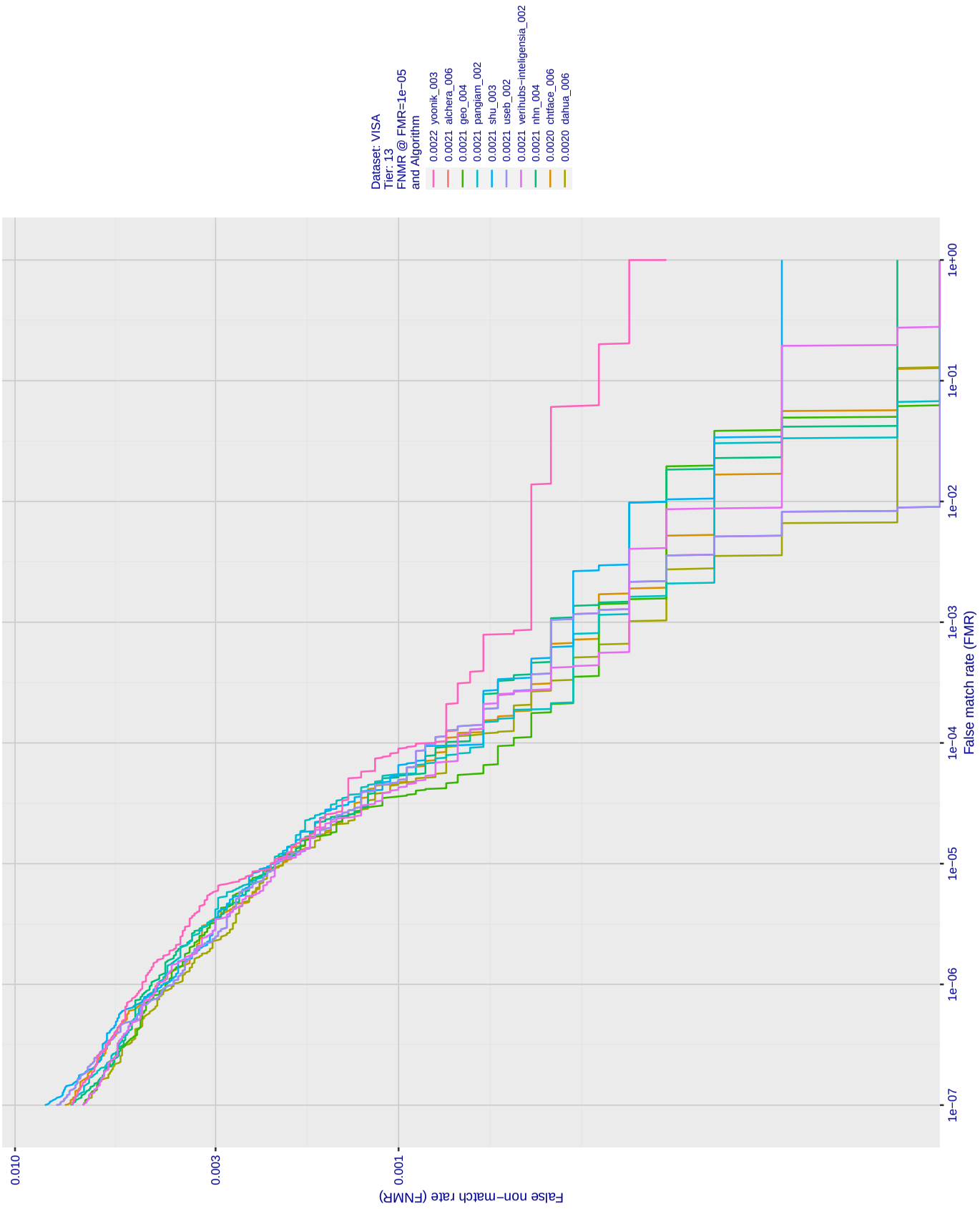

Figure 64: For the visa images, detection error tradeoff (DET) characteristics showing false non-match rate vs. false match rate plotted parametrically on threshold, T. The scales are logarithmic in order to show many decades of FMR.

FNMR(T) "False non-match rate"
FMR(T) "False match rate"

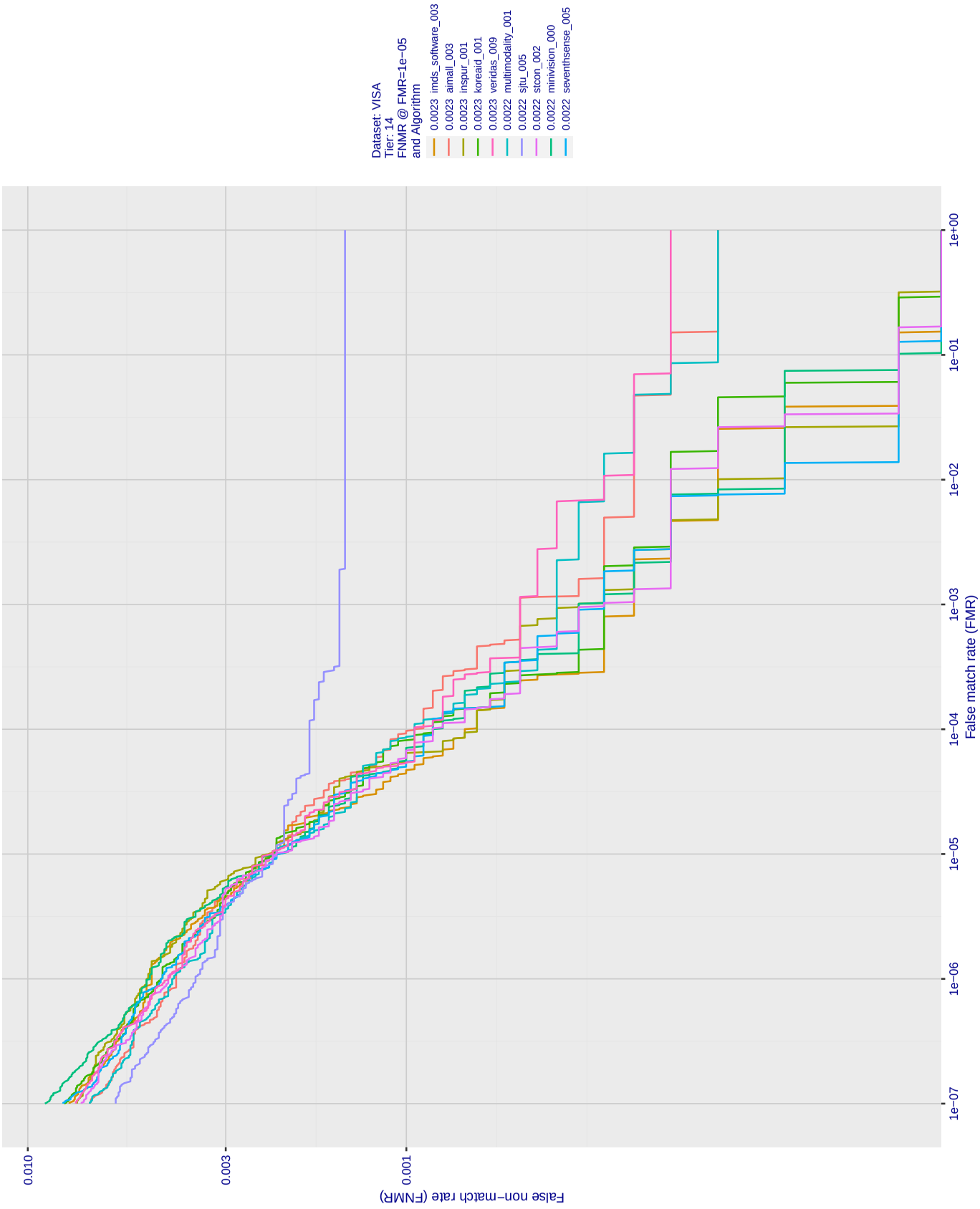

Figure 65: For the visa images, detection error tradeoff (DET) characteristics showing false non-match rate vs. false match rate plotted parametrically on threshold, T. The scales are logarithmic in order to show many decades of FMR.

FNMR(T) "False non-match rate"
FMR(T) "False match rate"

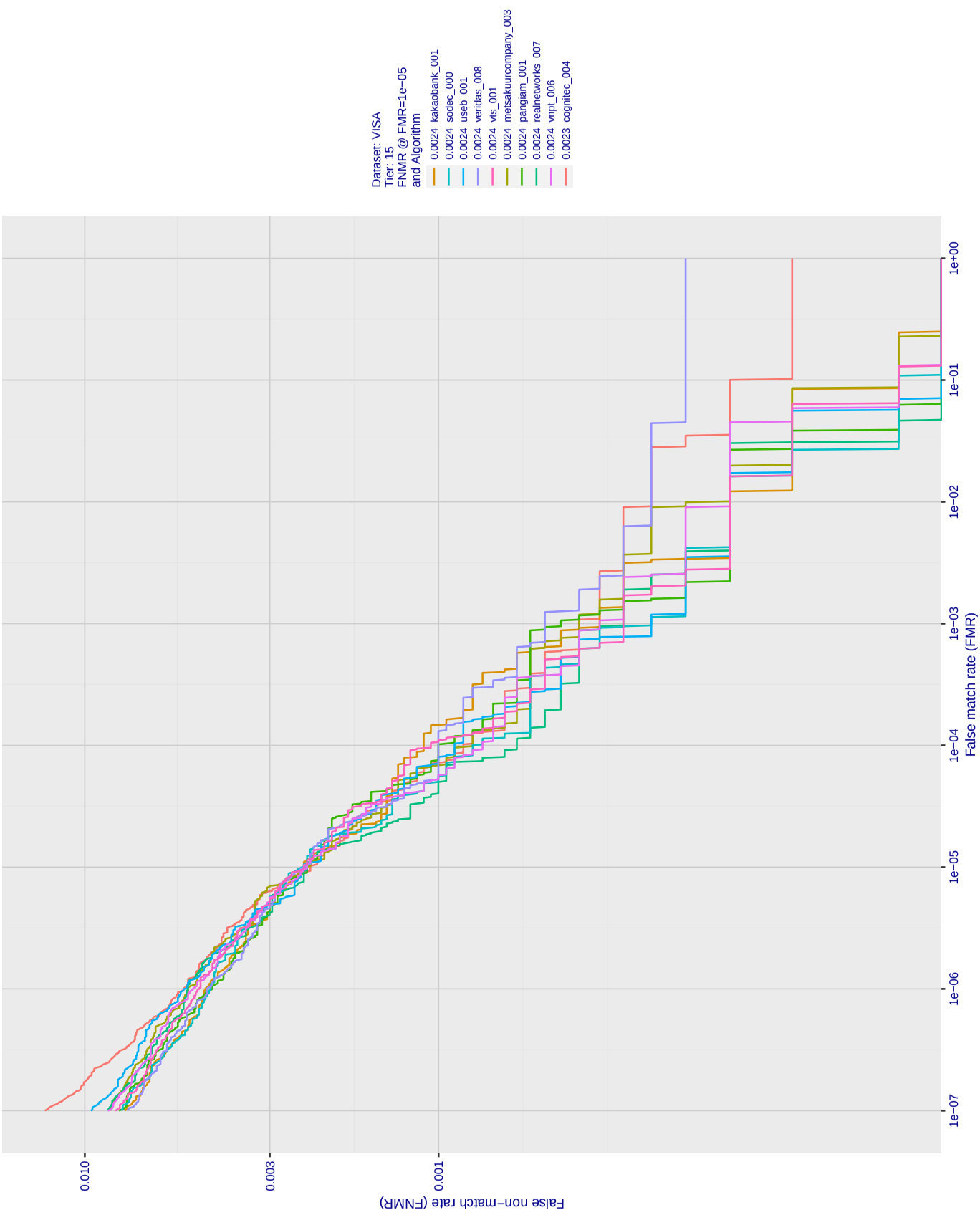

Figure 66: For the visa images, detection error tradeoff (DET) characteristics showing false non-match rate vs. false match rate plotted parametrically on threshold, T. The scales are logarithmic in order to show many decades of FMR.

FNMR(T) "False non-match rate"
FMR(T) "False match rate"

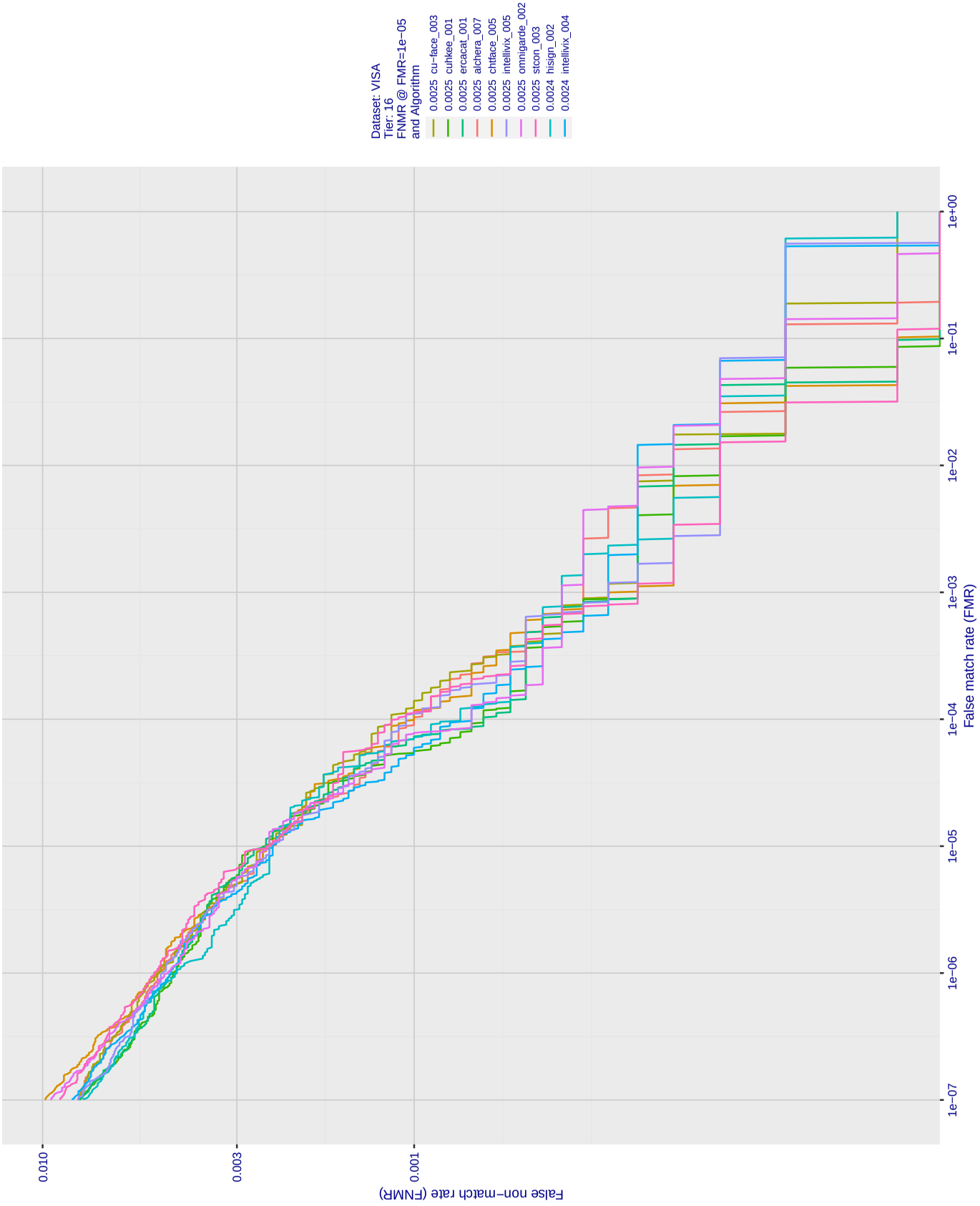

Figure 67: For the visa images, detection error tradeoff (DET) characteristics showing false non-match rate vs. false match rate plotted parametrically on threshold, T. The scales are logarithmic in order to show many decades of FMR.

FNMR(T) "False non-match rate"
FMR(T) "False match rate"

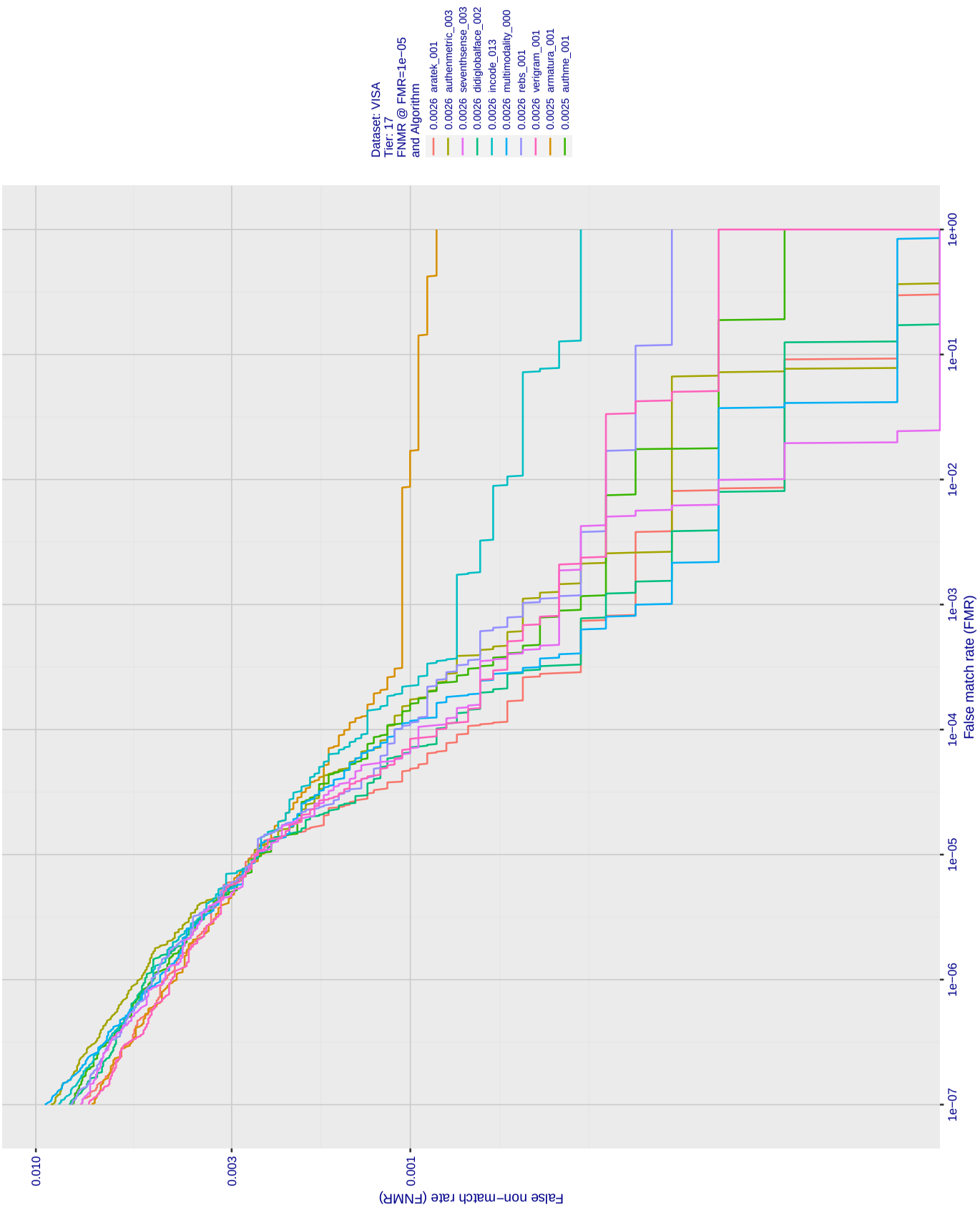

Figure 68: For the visa images, detection error tradeoff (DET) characteristics showing false non-match rate vs. false match rate plotted parametrically on threshold, T. The scales are logarithmic in order to show many decades of FMR.

FNMR(T) "False non-match rate"
FMR(T) "False match rate"

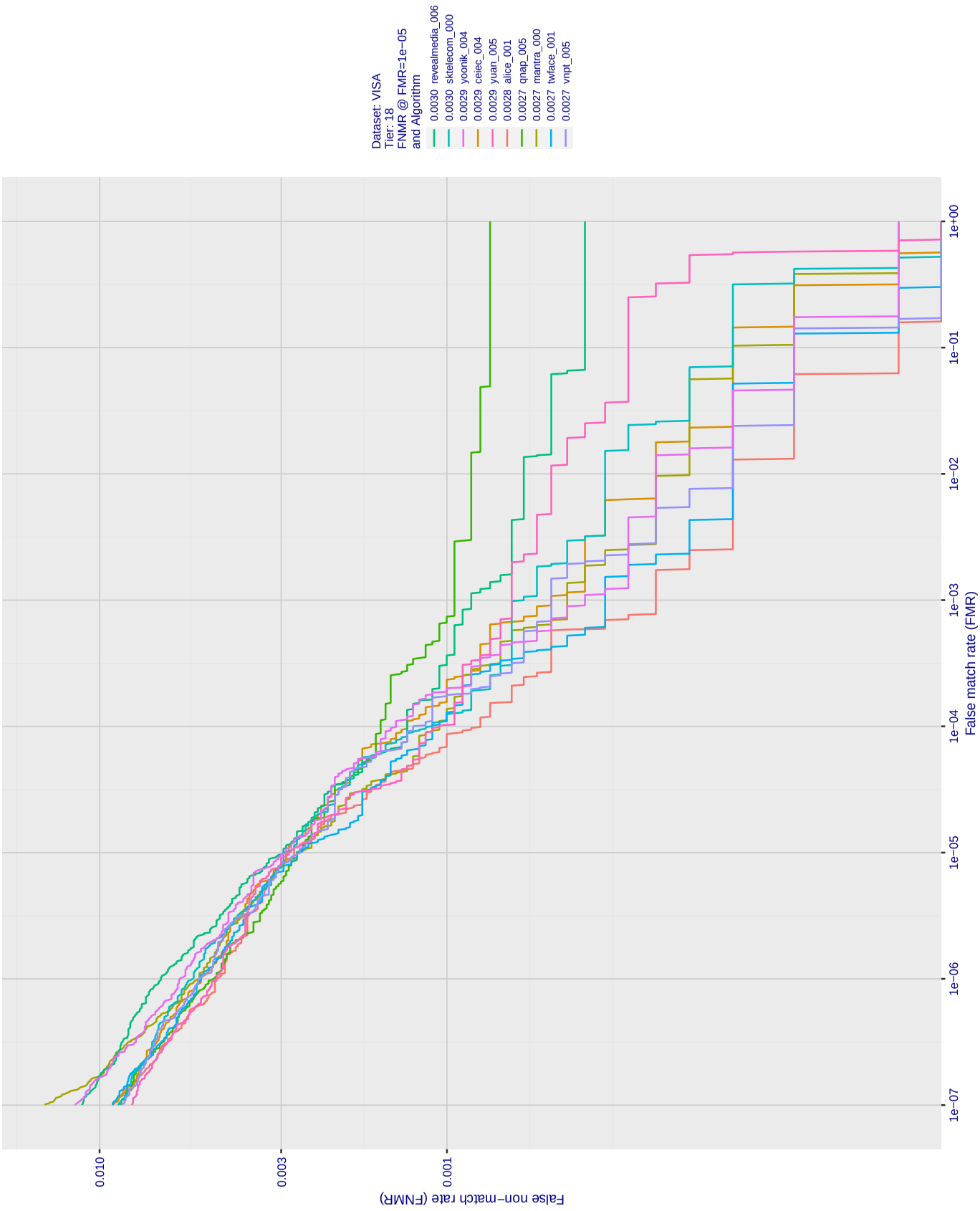

Figure 69: For the visa images, detection error tradeoff (DET) characteristics showing false non-match rate vs. false match rate plotted parametrically on threshold, T. The scales are logarithmic in order to show many decades of FMR.

FNMR(T) "False non-match rate"
FMR(T) "False match rate"

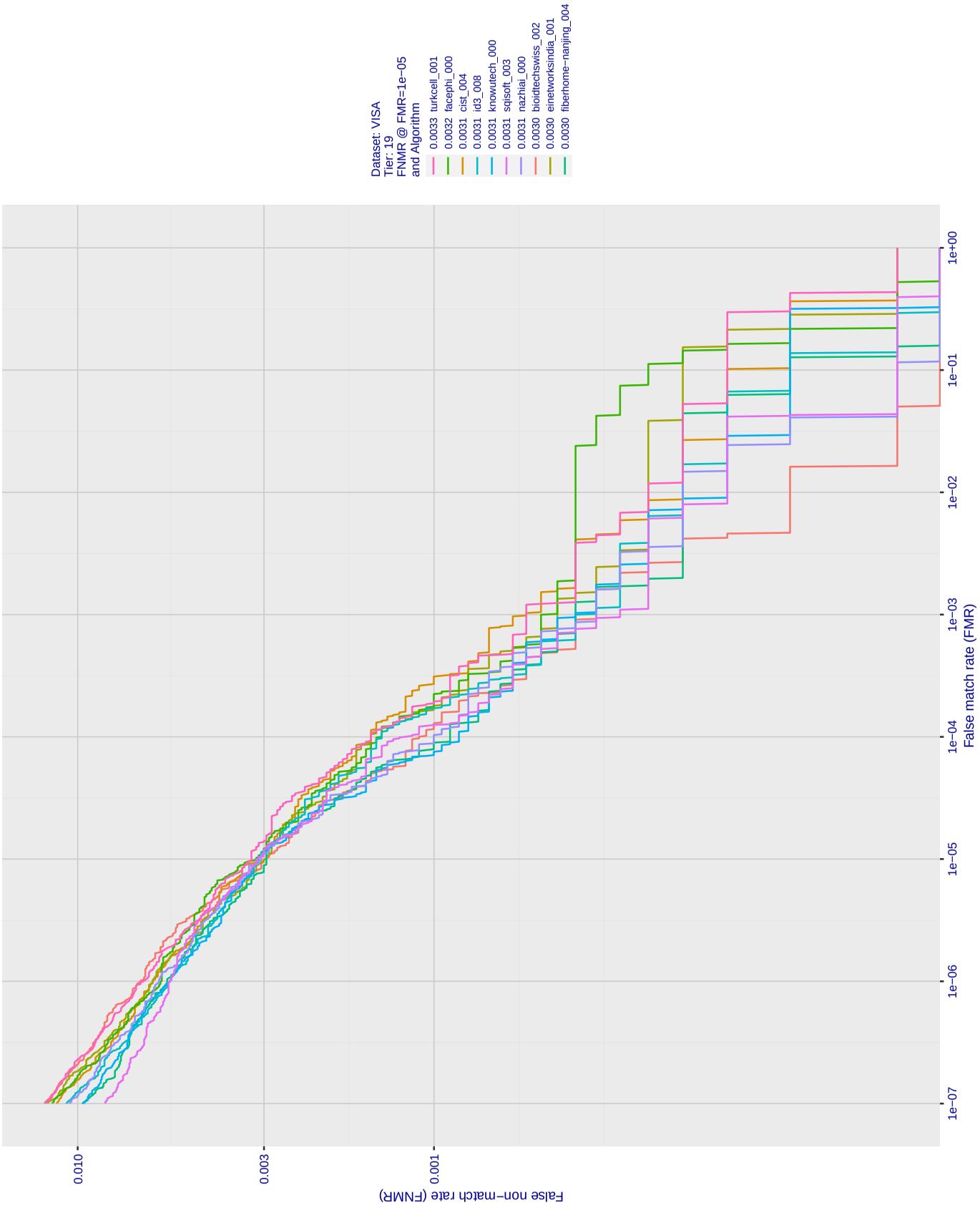

Figure 70: For the visa images, detection error tradeoff (DET) characteristics showing false non-match rate vs. false match rate plotted parametrically on threshold, T. The scales are logarithmic in order to show many decades of FMR.

FNMR(T) "False non-match rate"
FMR(T) "False match rate"

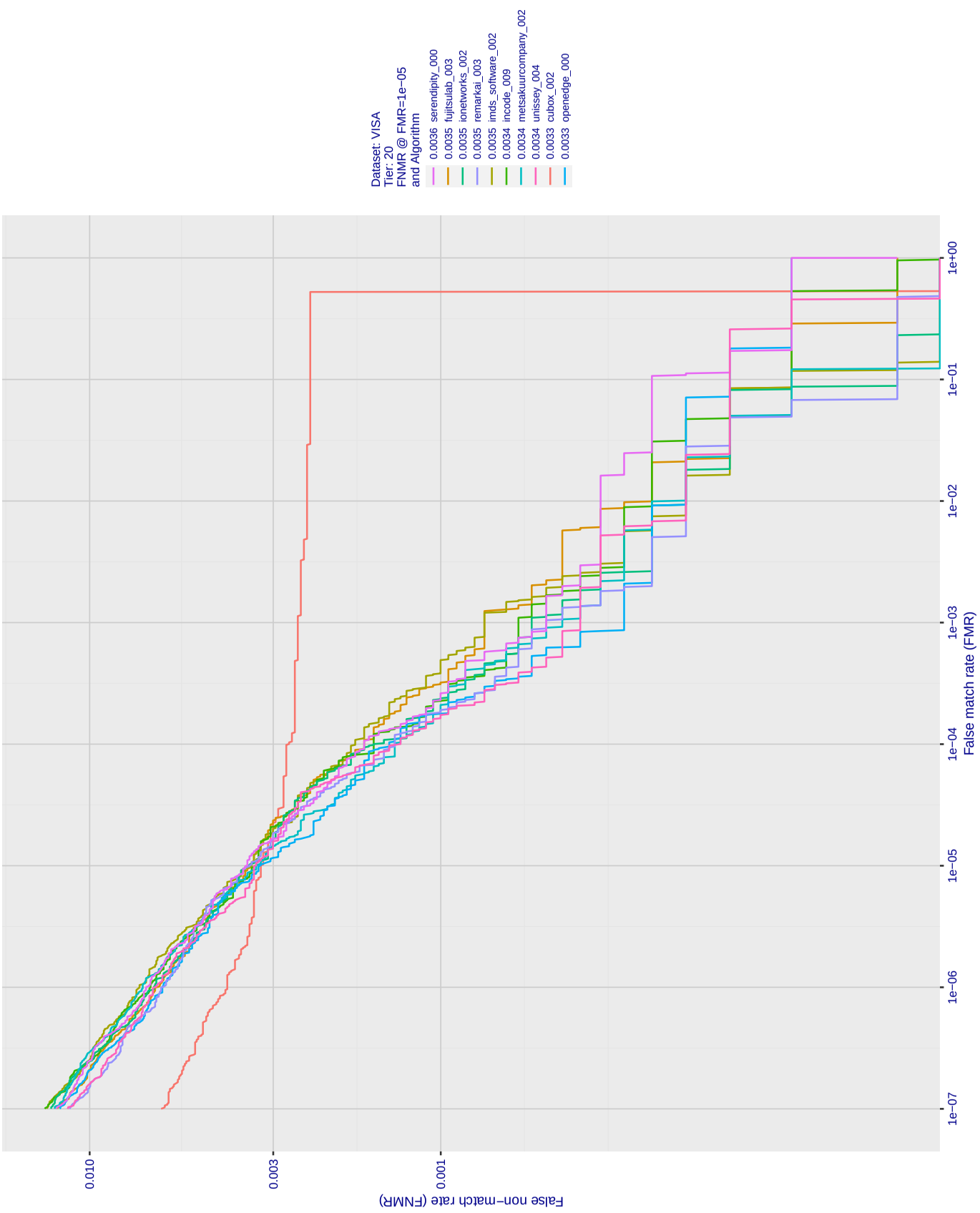

Figure 71: For the visa images, detection error tradeoff (DET) characteristics showing false non-match rate vs. false match rate plotted parametrically on threshold, T. The scales are logarithmic in order to show many decades of FMR.

FNMR(T) "False non-match rate"
FMR(T) "False match rate"

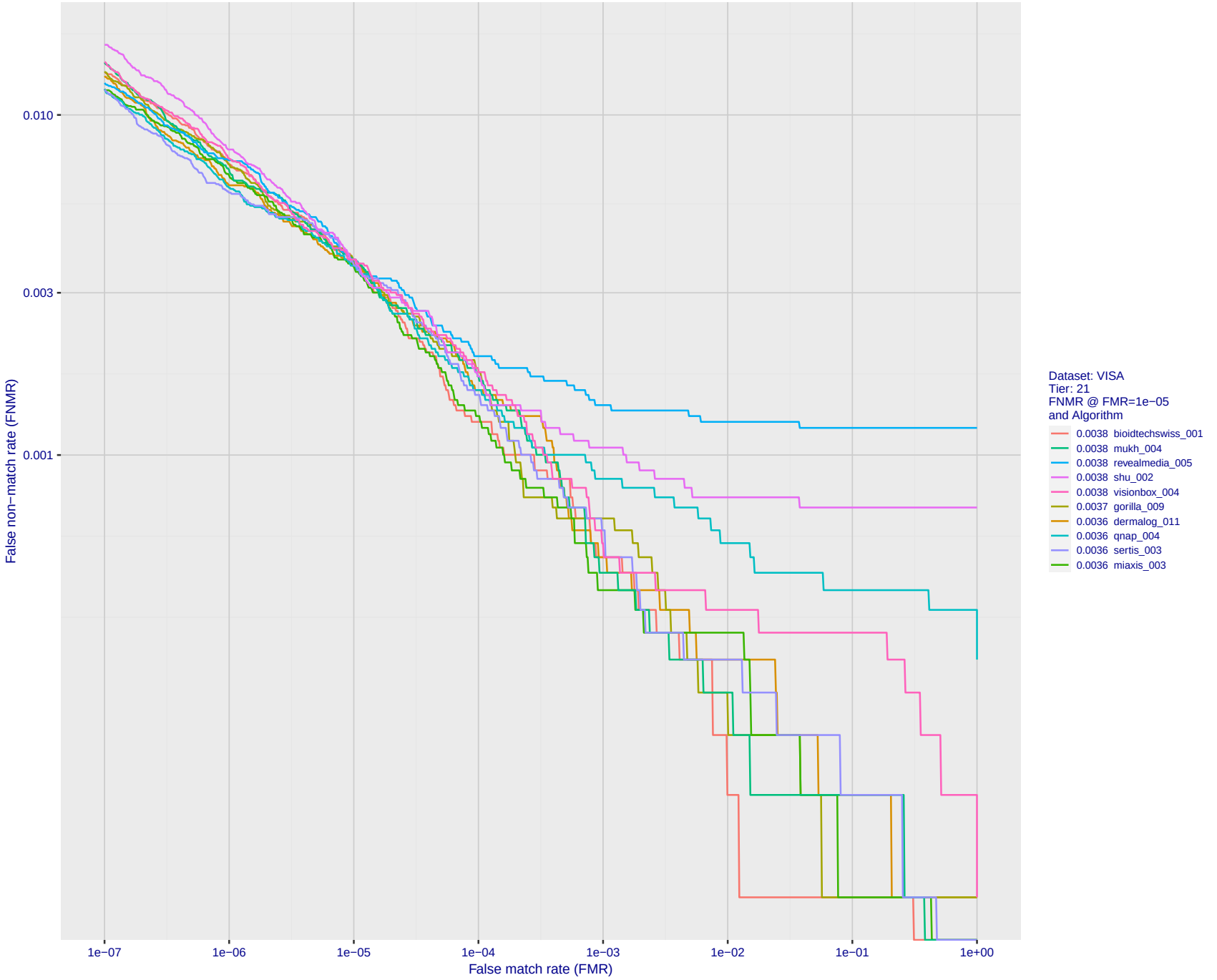

Figure 72: For the visa images, detection error tradeoff (DET) characteristics showing false non-match rate vs. false match rate plotted parametrically on threshold, T. The scales are logarithmic in order to show many decades of FMR.

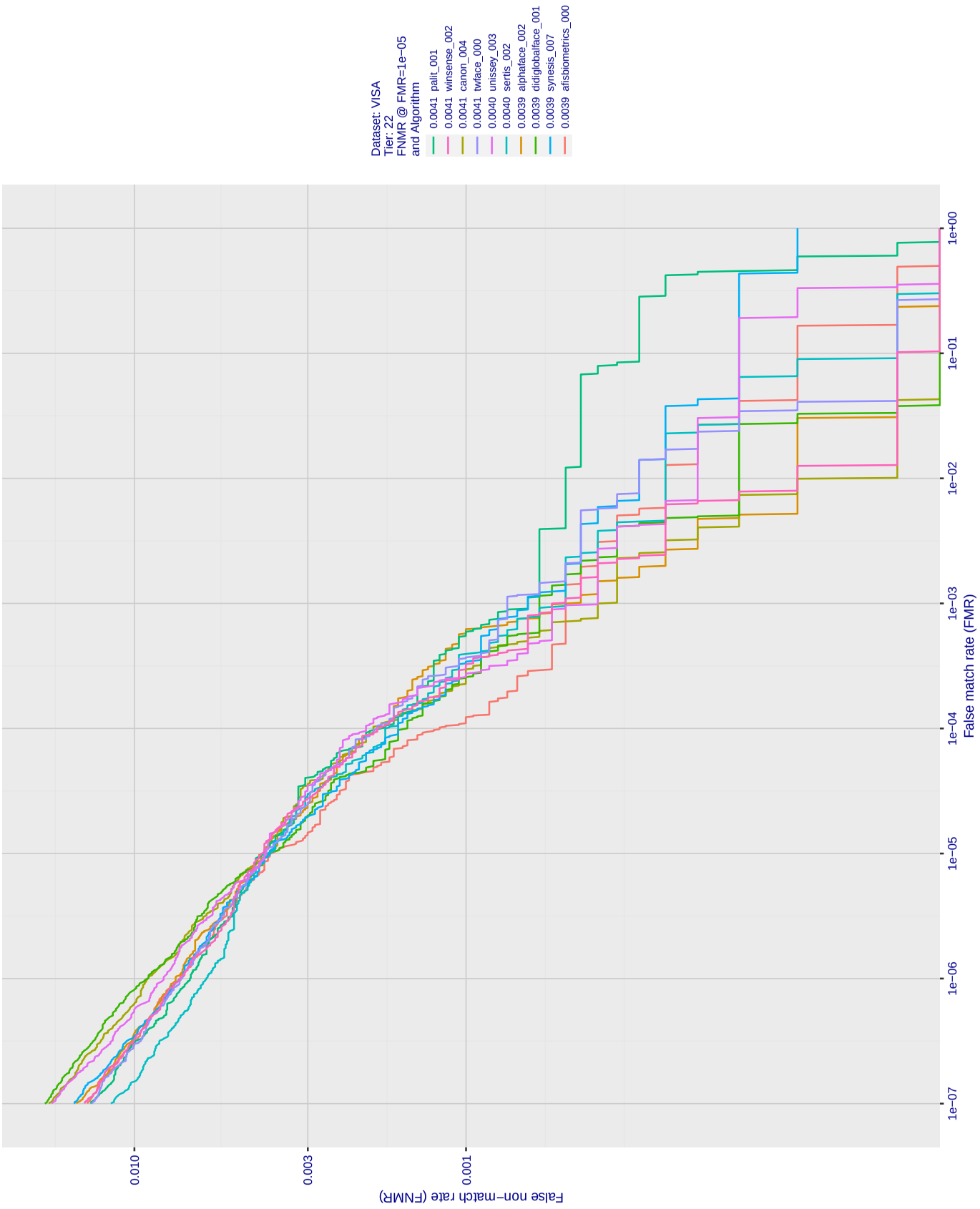

Figure 73: For the visa images, detection error tradeoff (DET) characteristics showing false non-match rate vs. false match rate plotted parametrically on threshold, T. The scales are logarithmic in order to show many decades of FMR.

FNMR(T) "False non-match rate"
FMR(T) "False match rate"

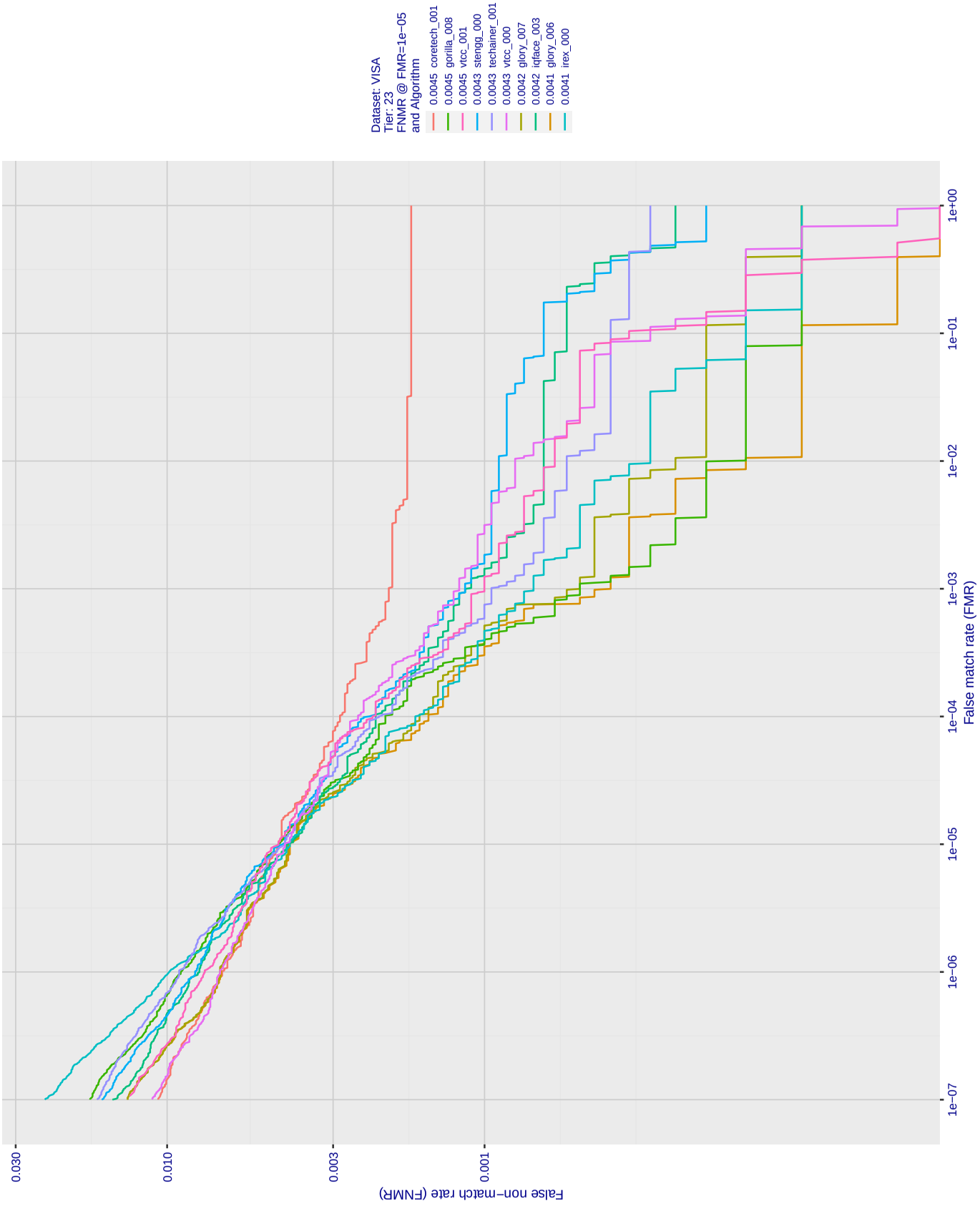

Figure 74: For the visa images, detection error tradeoff (DET) characteristics showing false non-match rate vs. false match rate plotted parametrically on threshold, T. The scales are logarithmic in order to show many decades of FMR.

FNMR(T) "False non-match rate"
FMR(T) "False match rate"

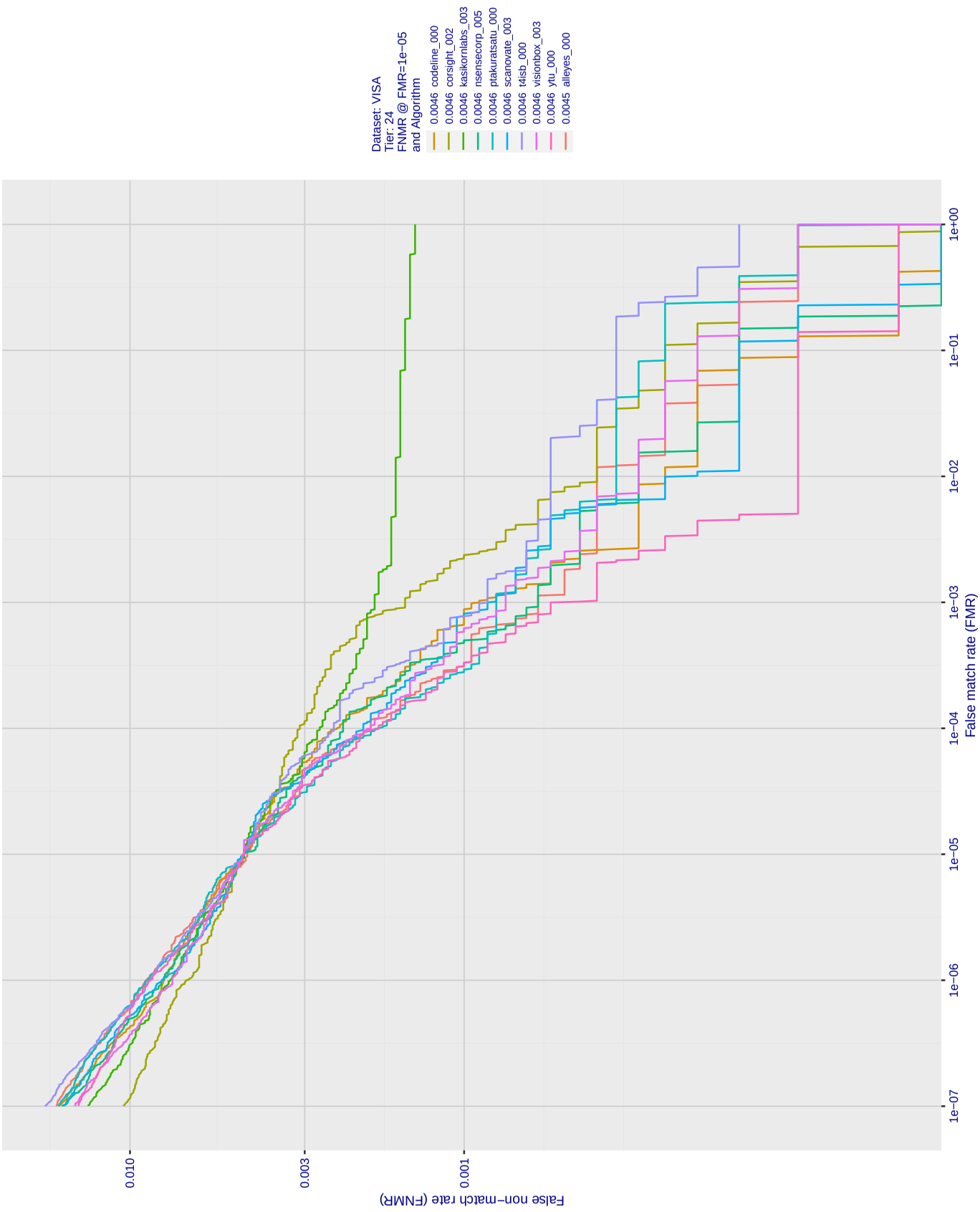

Figure 75: For the visa images, detection error tradeoff (DET) characteristics showing false non-match rate vs. false match rate plotted parametrically on threshold, T. The scales are logarithmic in order to show many decades of FMR.

FNMR(T) "False non-match rate"
FMR(T) "False match rate"

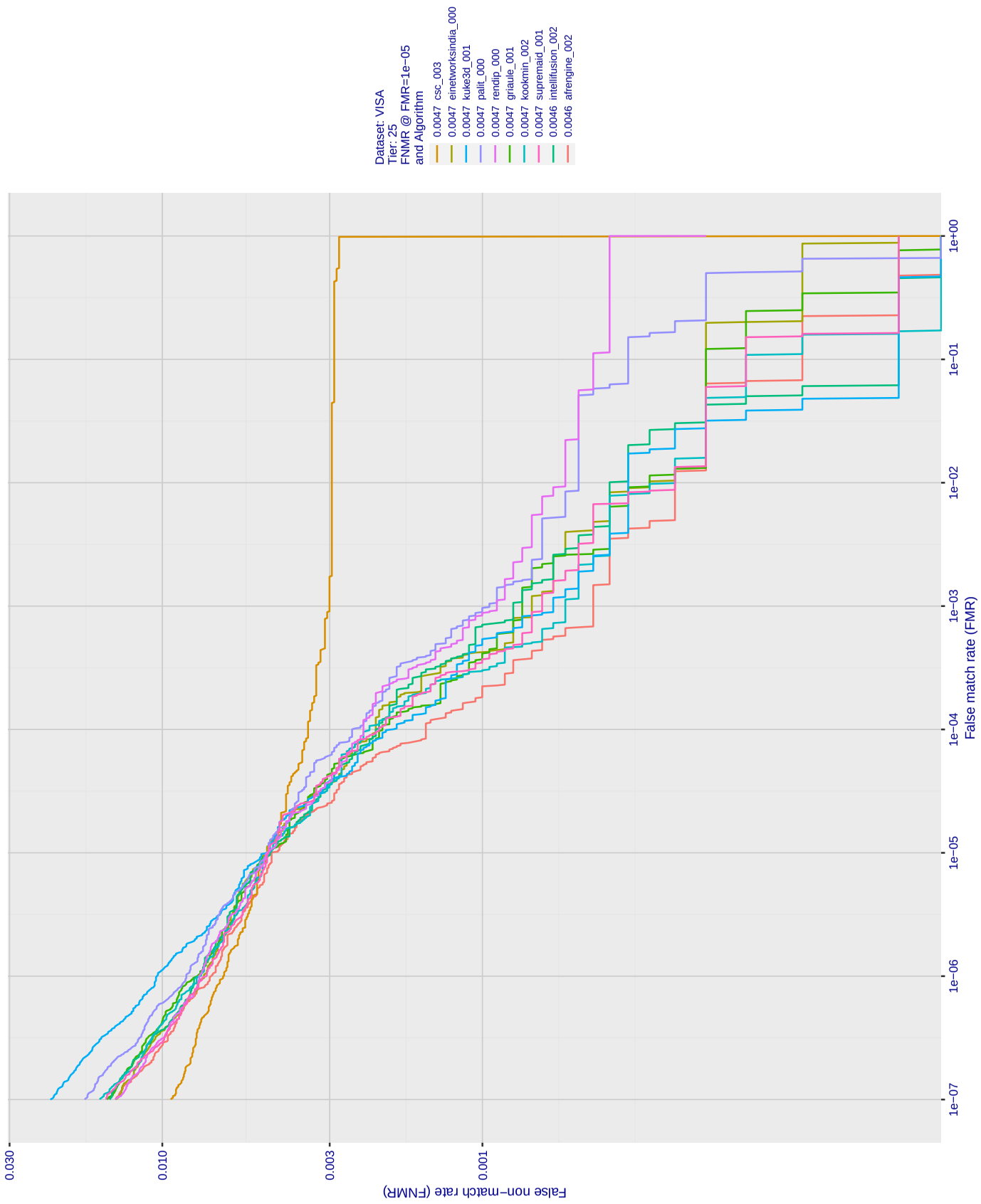

Figure 76: For the visa images, detection error tradeoff (DET) characteristics showing false non-match rate vs. false match rate plotted parametrically on threshold, T. The scales are logarithmic in order to show many decades of FMR.

FNMR(T) "False non-match rate"
FMR(T) "False match rate"

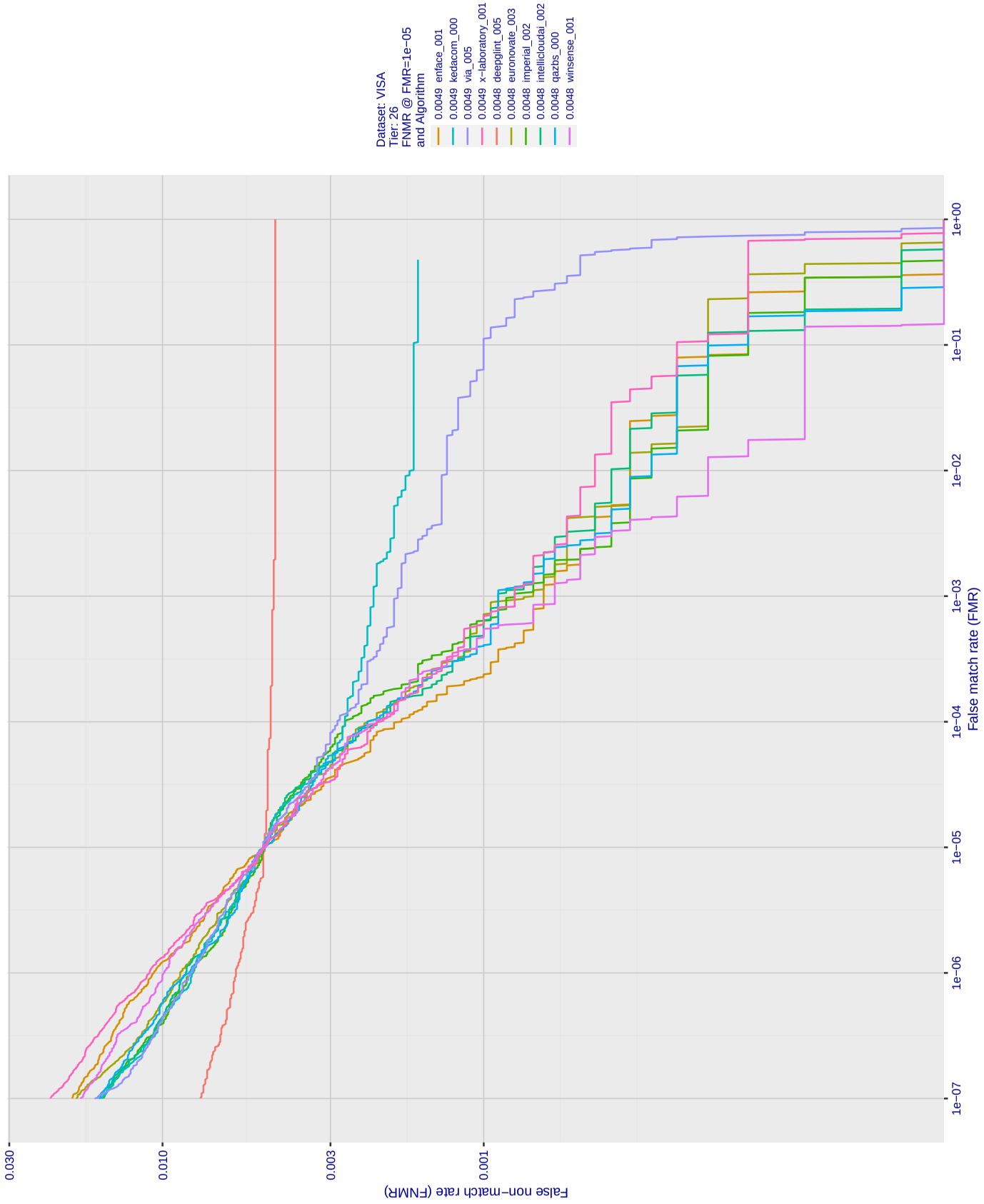

Figure 77: For the visa images, detection error tradeoff (DET) characteristics showing false non-match rate vs. false match rate plotted parametrically on threshold, T. The scales are logarithmic in order to show many decades of FMR.

FNMR(T) "False non-match rate"
FMR(T) "False match rate"

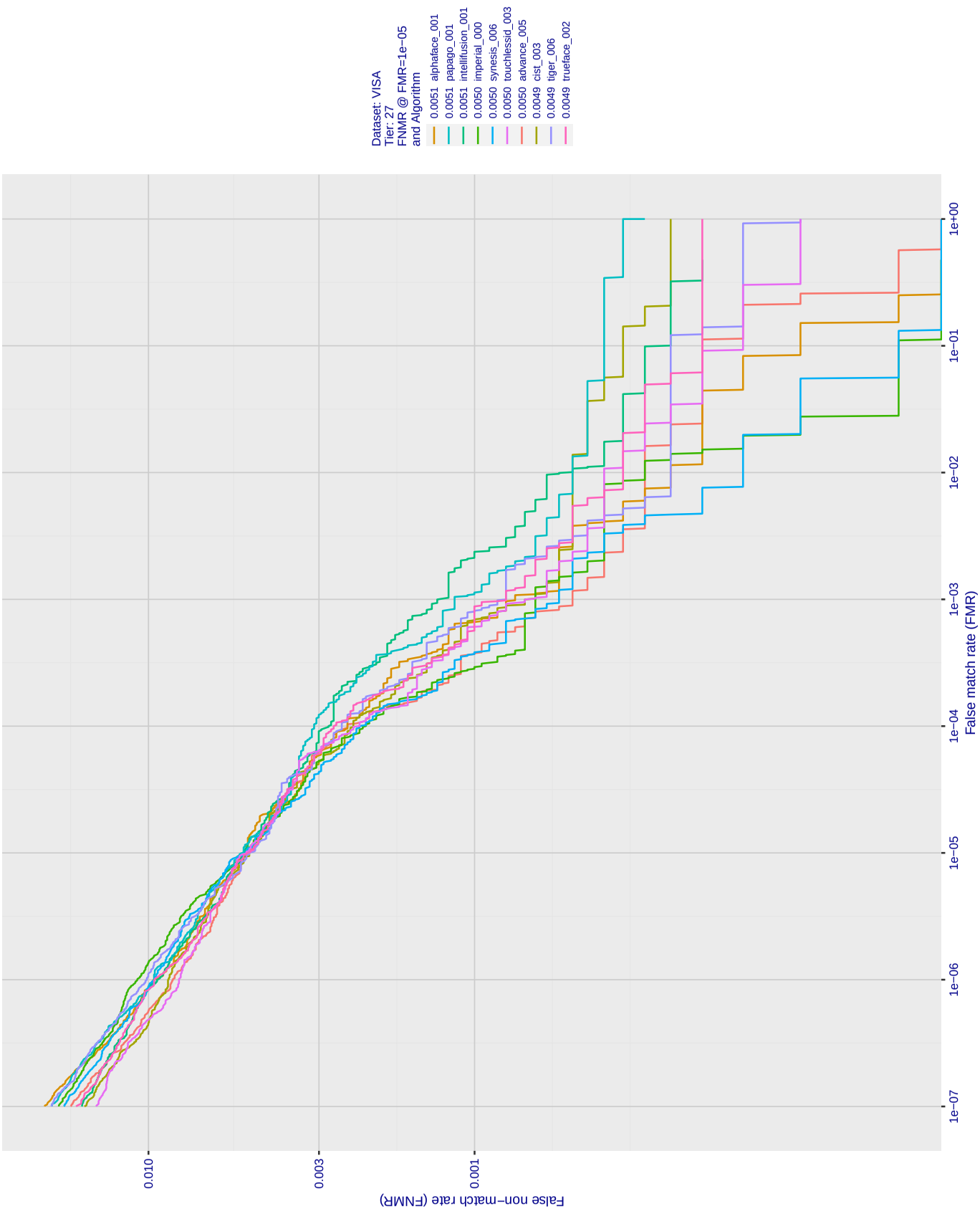

Figure 78: For the visa images, detection error tradeoff (DET) *characteristics showing false non-match rate vs. false match rate plotted parametrically on threshold, T. The scales are logarithmic in order to show many decades of* FMR.

FNMR(T) "False non-match rate"
FMR(T) "False match rate"

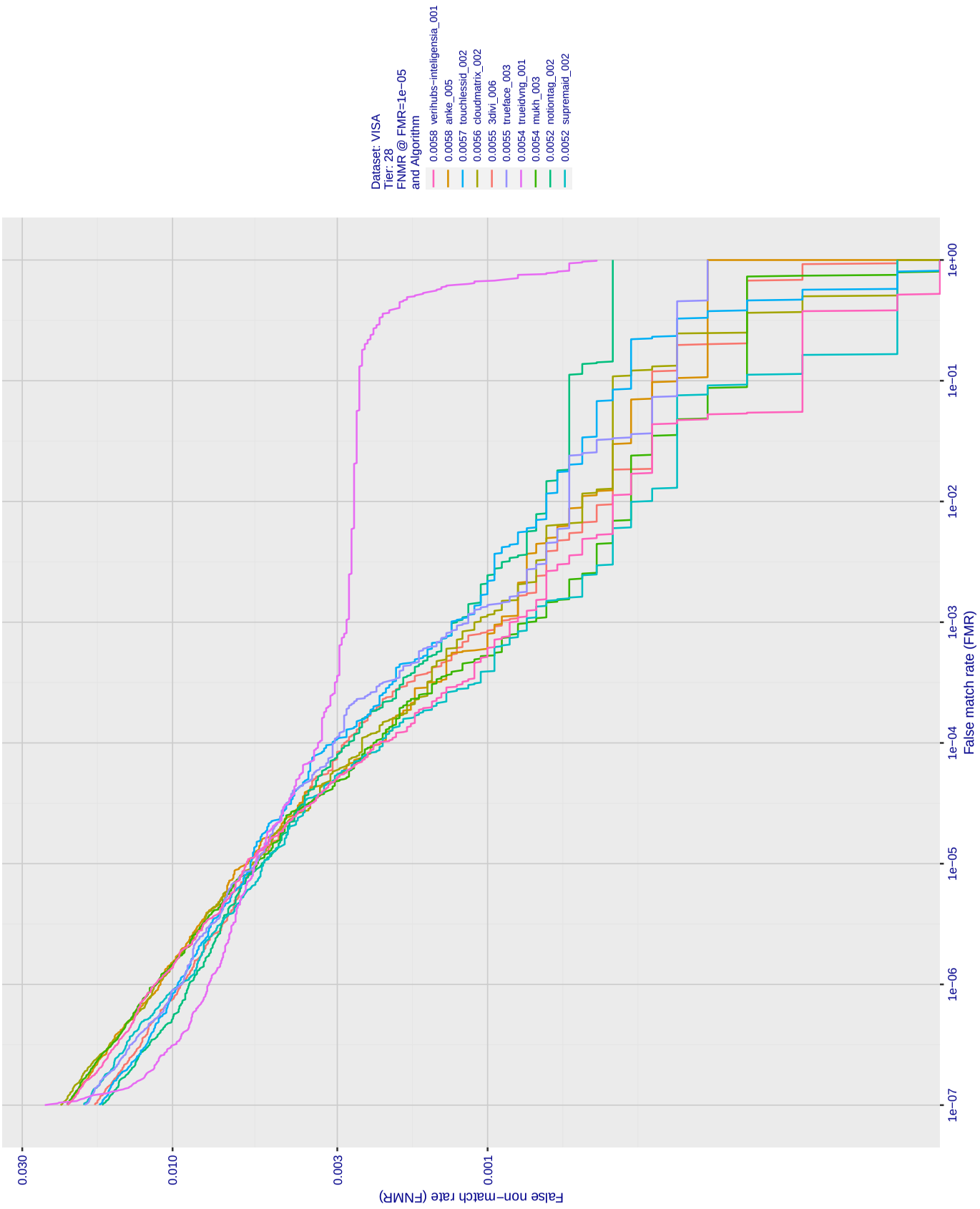

Figure 79: For the visa images, detection error tradeoff (DET) characteristics showing false non-match rate vs. false match rate plotted parametrically on threshold, T. The scales are logarithmic in order to show many decades of FMR.

FNMR(T) "False non-match rate"
FMR(T) "False match rate"

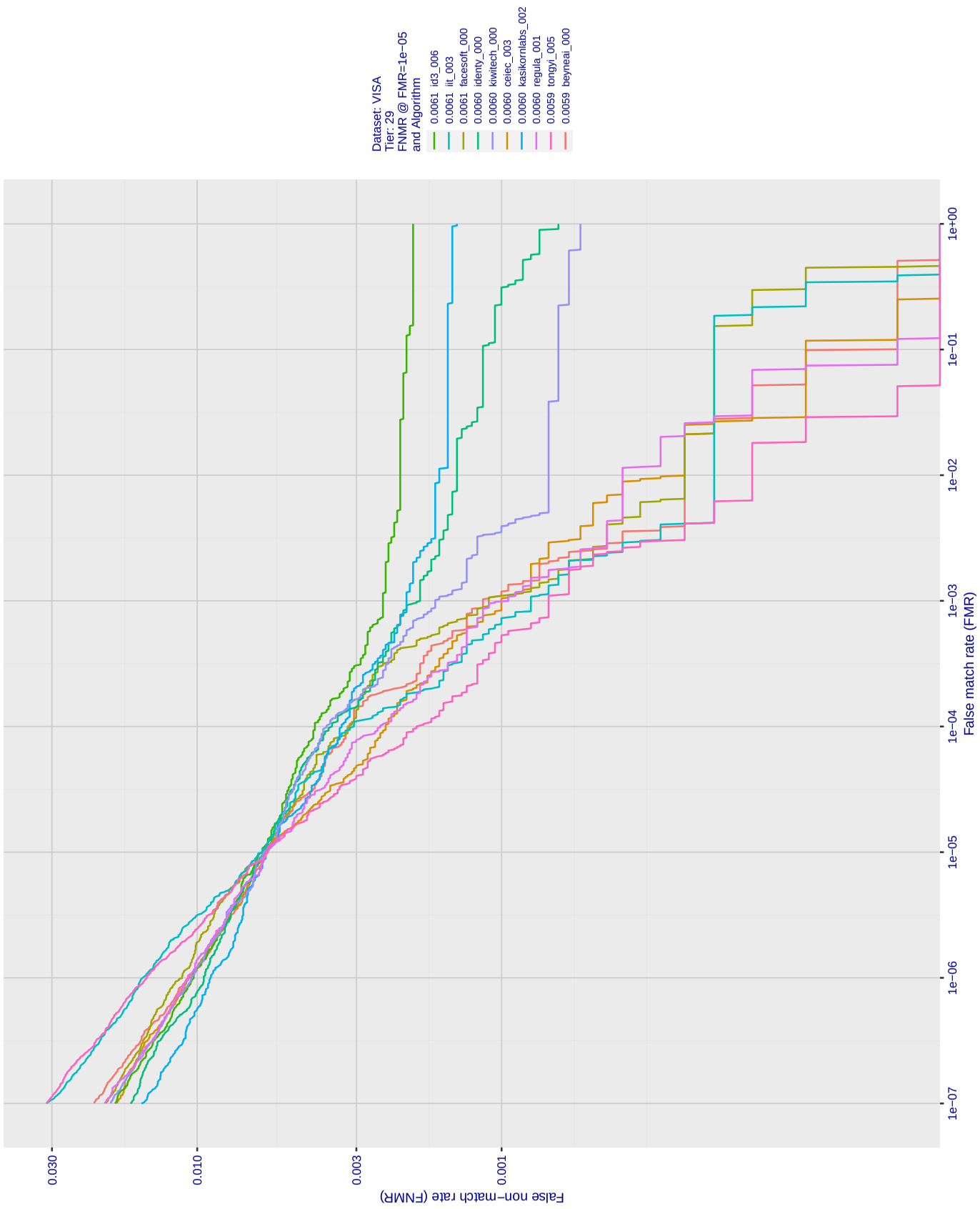

Figure 80: For the visa images, detection error tradeoff (DET) characteristics showing false non-match rate vs. false match rate plotted parametrically on threshold, T. The scales are logarithmic in order to show many decades of FMR.

FNMR(T) "False non-match rate"
FMR(T) "False match rate"

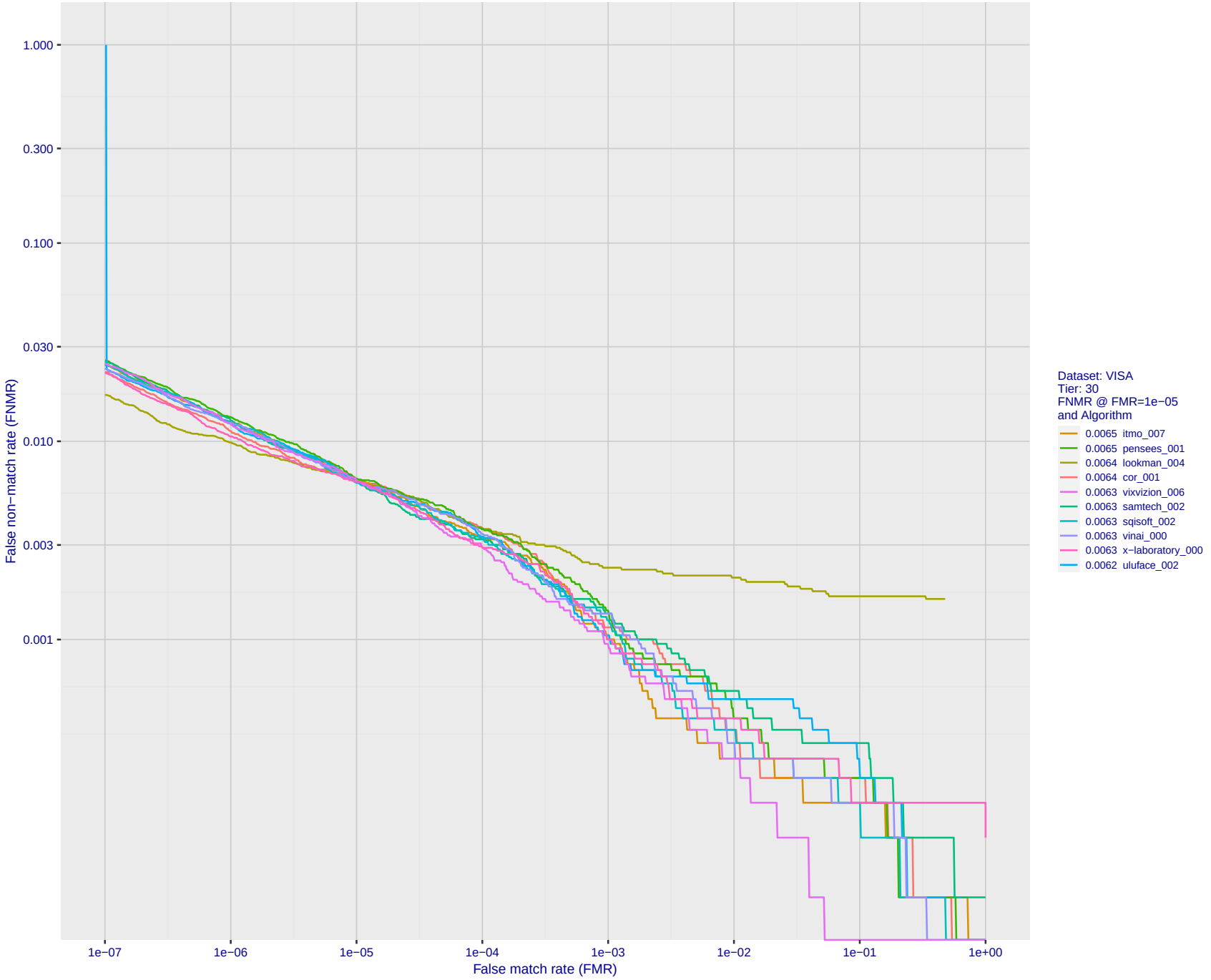

*Figure 81: For the visa images, detection error tradeoff (*DET*) characteristics showing false non-match rate vs. false match rate plotted parametrically on threshold, T. The scales are logarithmic in order to show many decades of* FMR*.*

2024/04/17 08:45:50 FNMR(T) "False non-match rate" FMR(T) "False match rate"

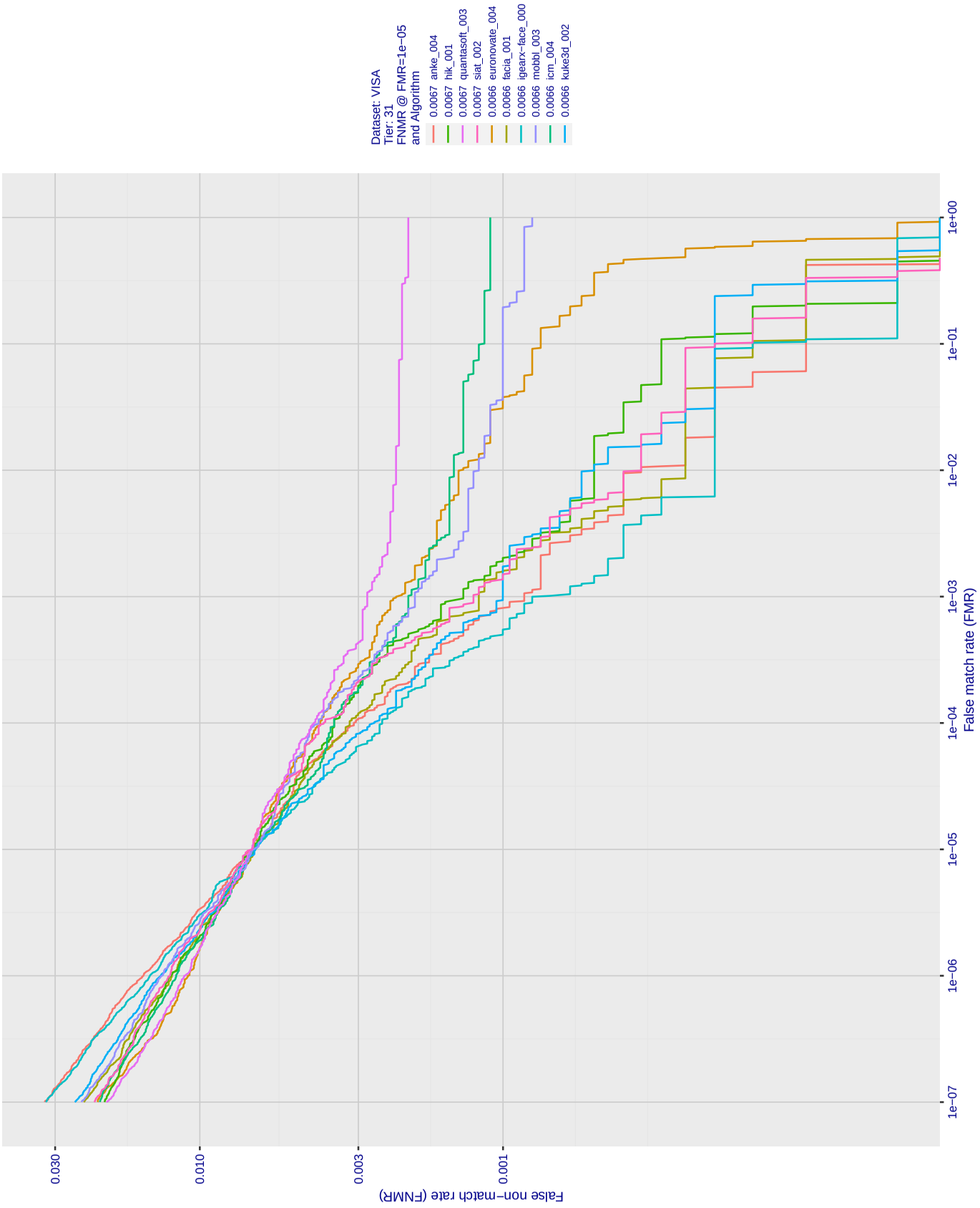

Figure 82: For the visa images, detection error tradeoff (DET) characteristics showing false non-match rate vs. false match rate plotted parametrically on threshold, T. The scales are logarithmic in order to show many decades of FMR.

FNMR(T) "False non-match rate"
FMR(T) "False match rate"

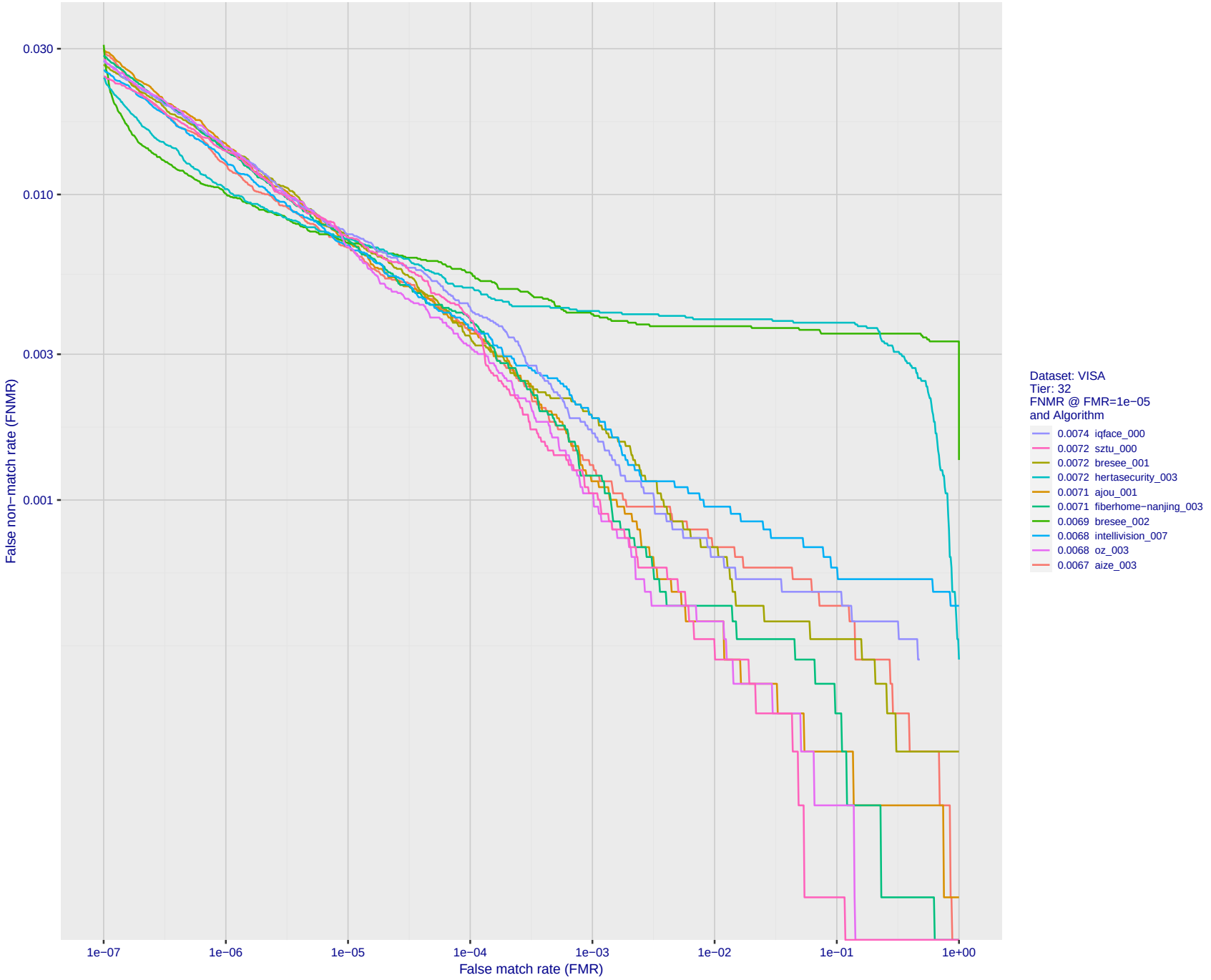

Figure 83: For the visa images, detection error tradeoff (DET) characteristics showing false non-match rate vs. false match rate plotted parametrically on threshold, T. The scales are logarithmic in order to show many decades of FMR.

FNMR(T) "False non-match rate"
FMR(T) "False match rate"

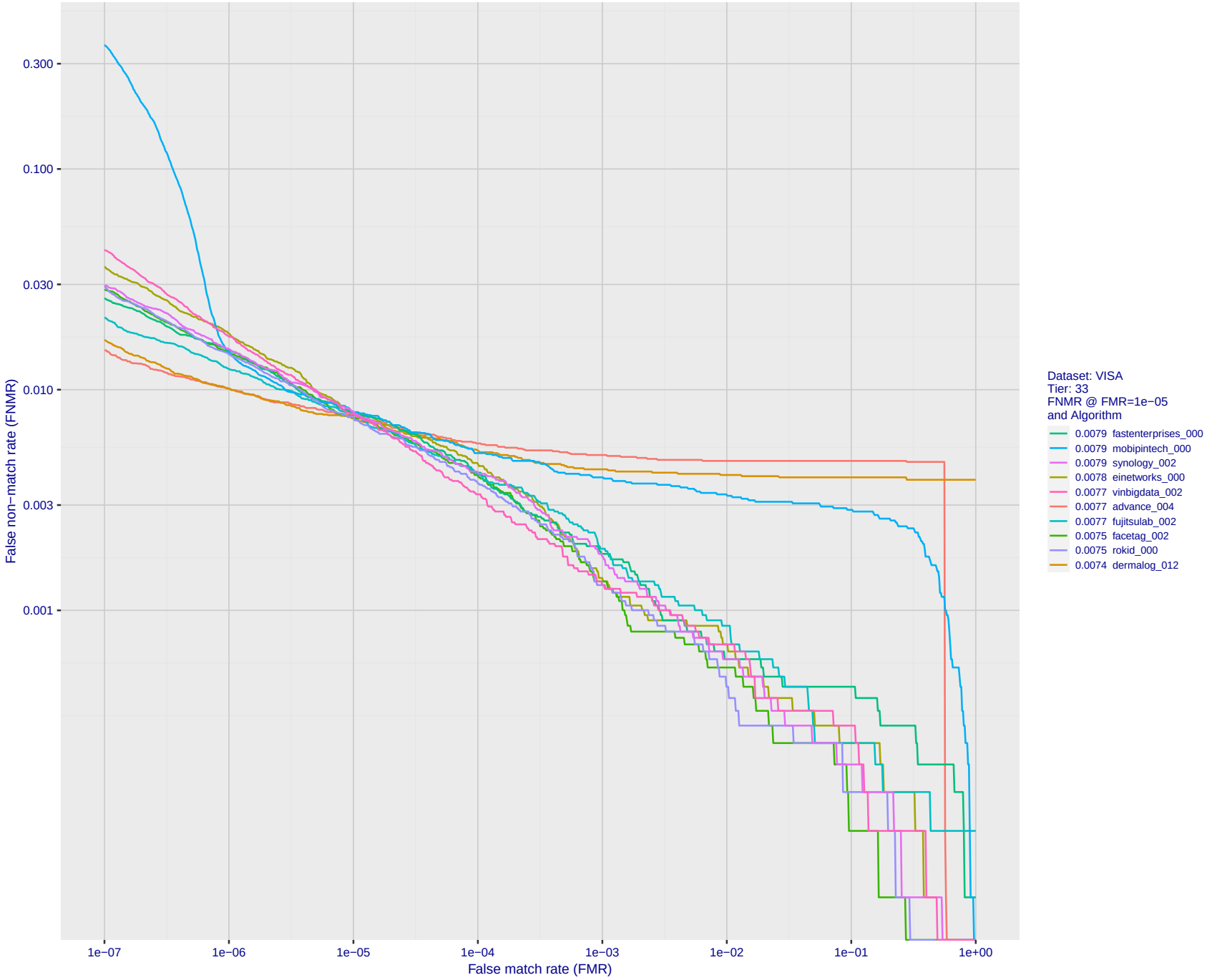

Figure 84: For the visa images, detection error tradeoff (DET) characteristics showing false non-match rate vs. false match rate plotted parametrically on threshold, T. The scales are logarithmic in order to show many decades of FMR.

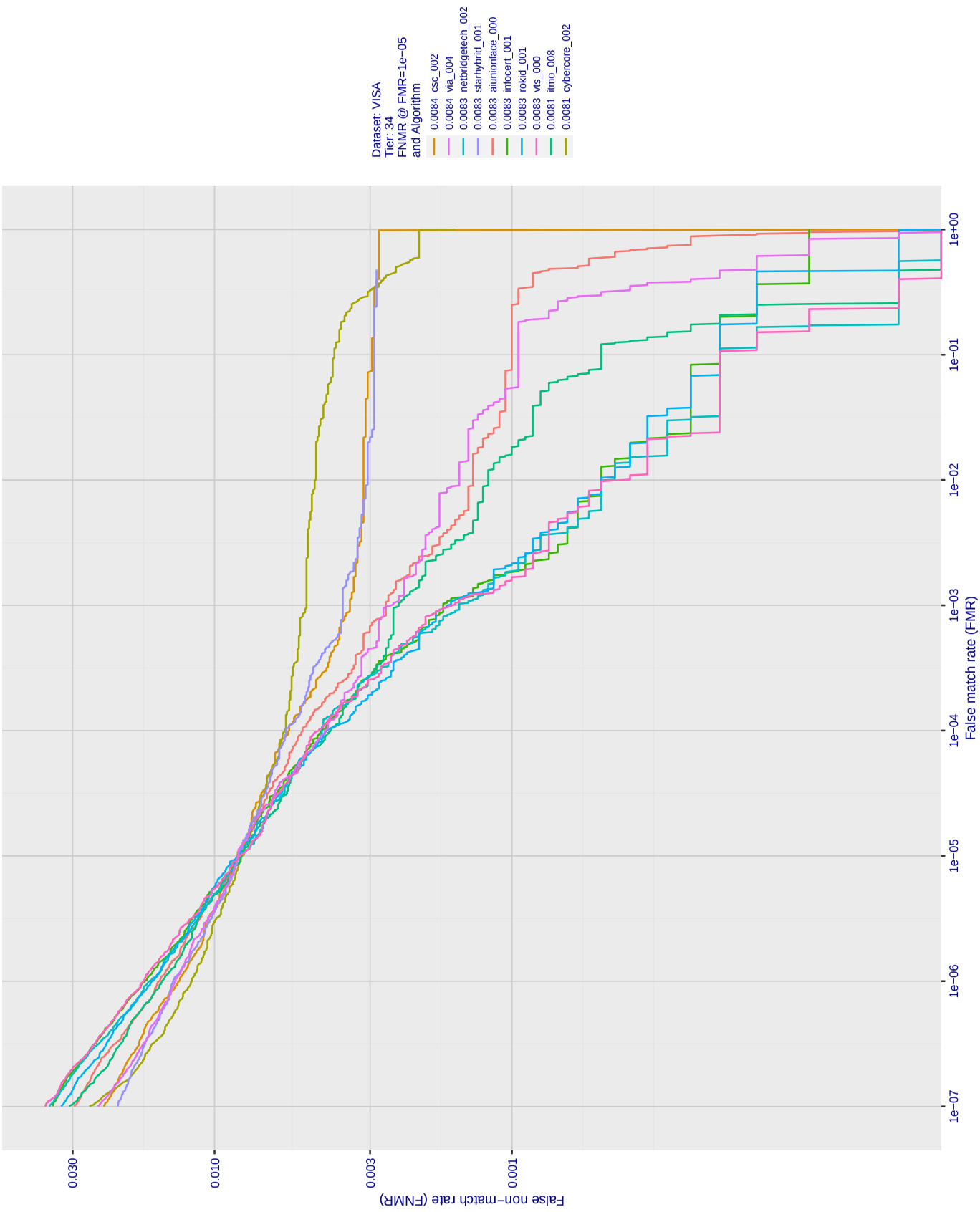

Figure 85: For the visa images, detection error tradeoff (DET) characteristics showing false non-match rate vs. false match rate plotted parametrically on threshold, T. The scales are logarithmic in order to show many decades of FMR.

FNMR(T) "False non-match rate"
FMR(T) "False match rate"

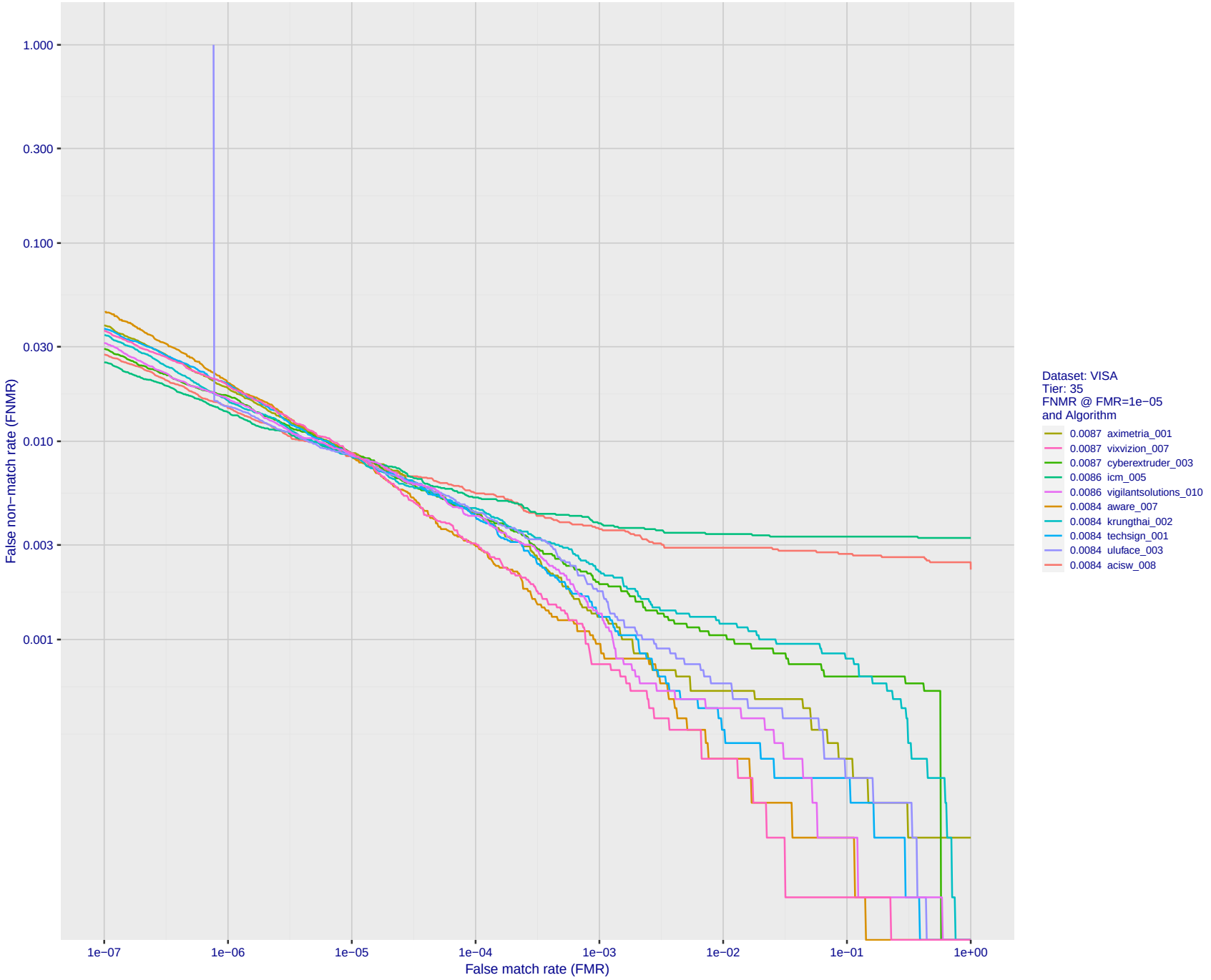

*Figure 86: For the visa images, detection error tradeoff (*DET*) characteristics showing false non-match rate vs. false match rate plotted parametrically on threshold, T. The scales are logarithmic in order to show many decades of* FMR*.*

2024/04/17 08:45:50
FNMR(T) "False non-match rate"
FMR(T) "False match rate"

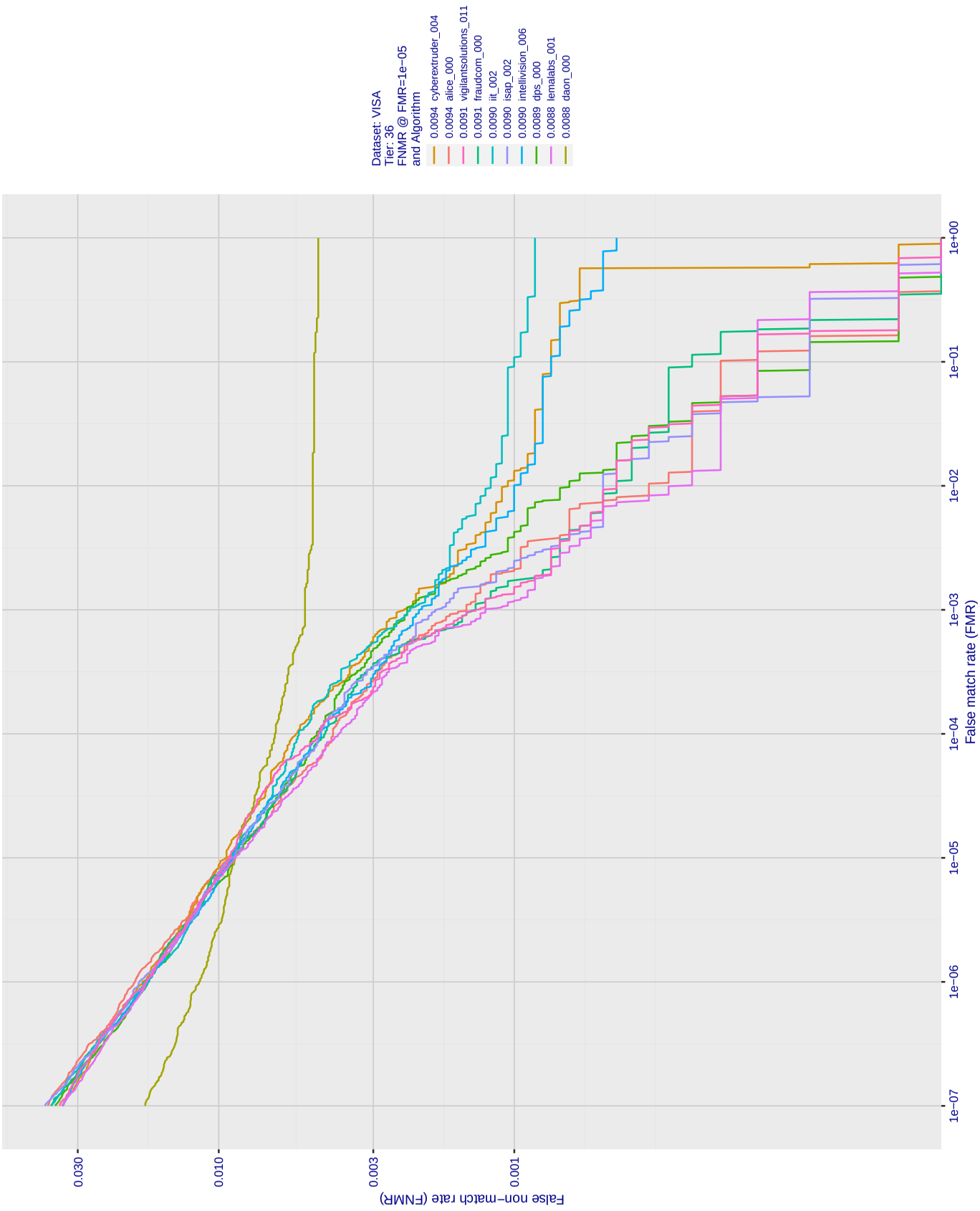

Figure 87: For the visa images, detection error tradeoff (DET) characteristics showing false non-match rate vs. false match rate plotted parametrically on threshold, T. The scales are logarithmic in order to show many decades of FMR.

FNMR(T) "False non-match rate"
FMR(T) "False match rate"

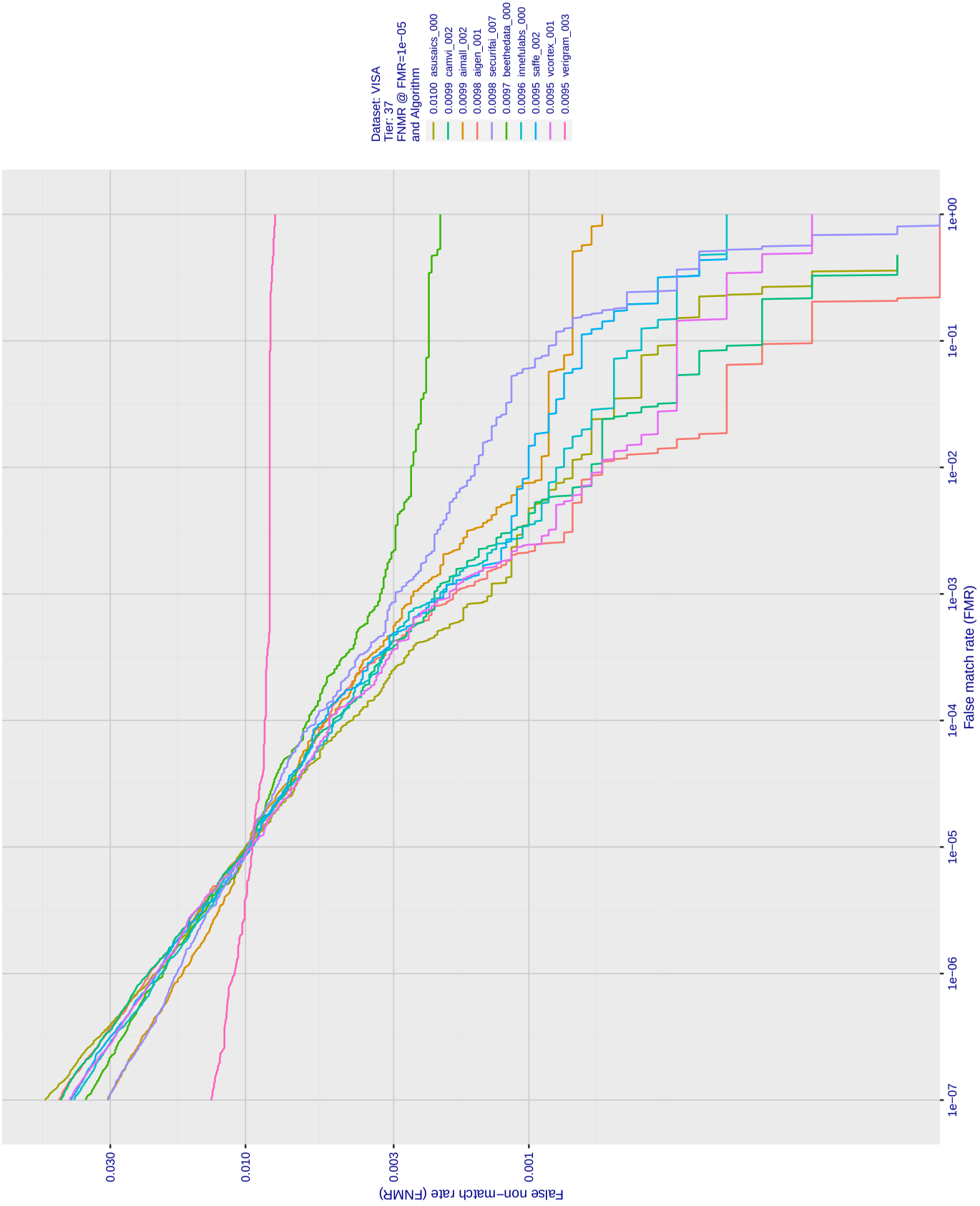

Figure 88: For the visa images, detection error tradeoff (DET) characteristics showing false non-match rate vs. false match rate plotted parametrically on threshold, T. The scales are logarithmic in order to show many decades of FMR.

FNMR(T) "False non-match rate"
FMR(T) "False match rate"

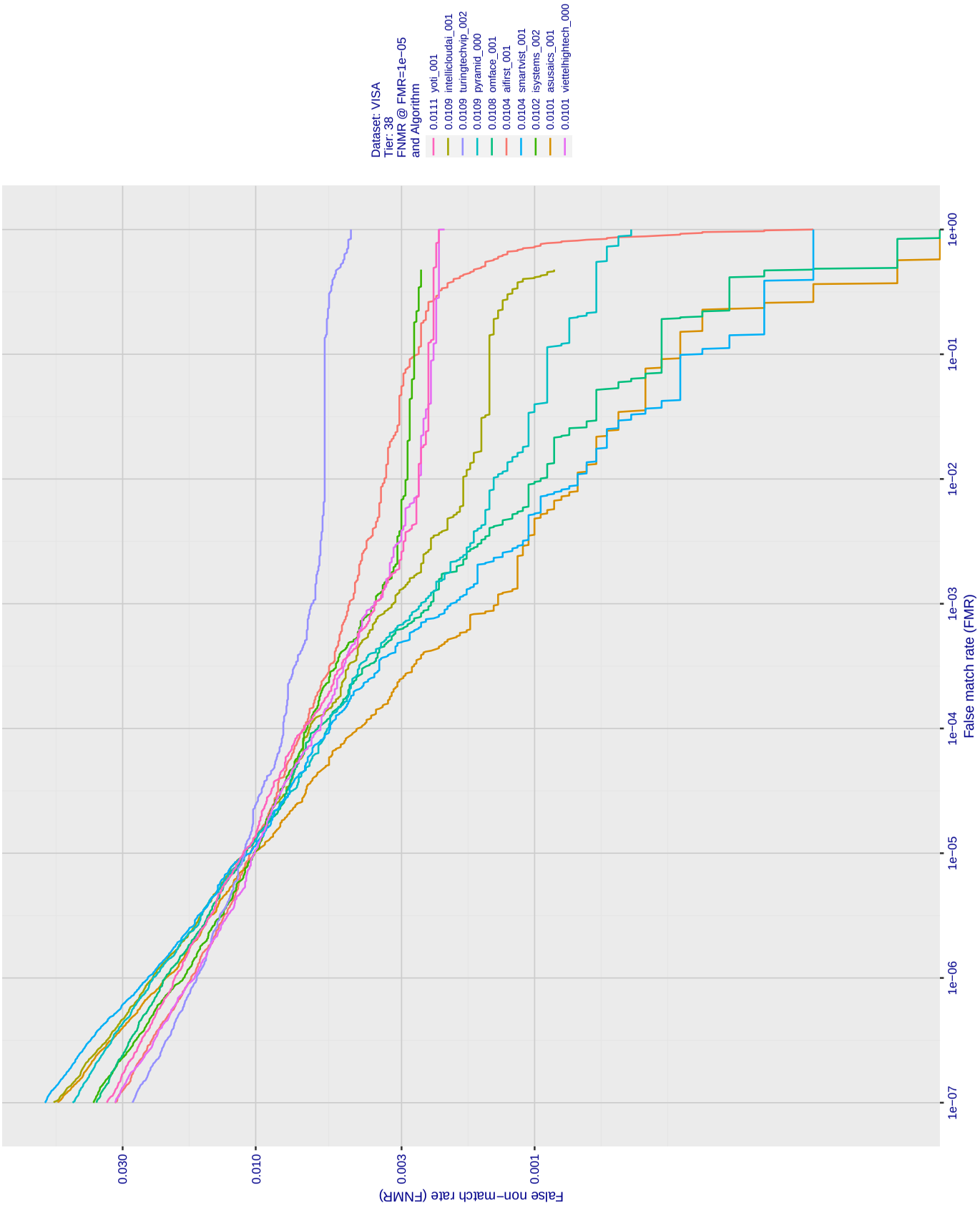

Figure 89: For the visa images, detection error tradeoff (DET) characteristics showing false non-match rate vs. false match rate plotted parametrically on threshold, T. The scales are logarithmic in order to show many decades of FMR.

FNMR(T) "False non-match rate"
FMR(T) "False match rate"

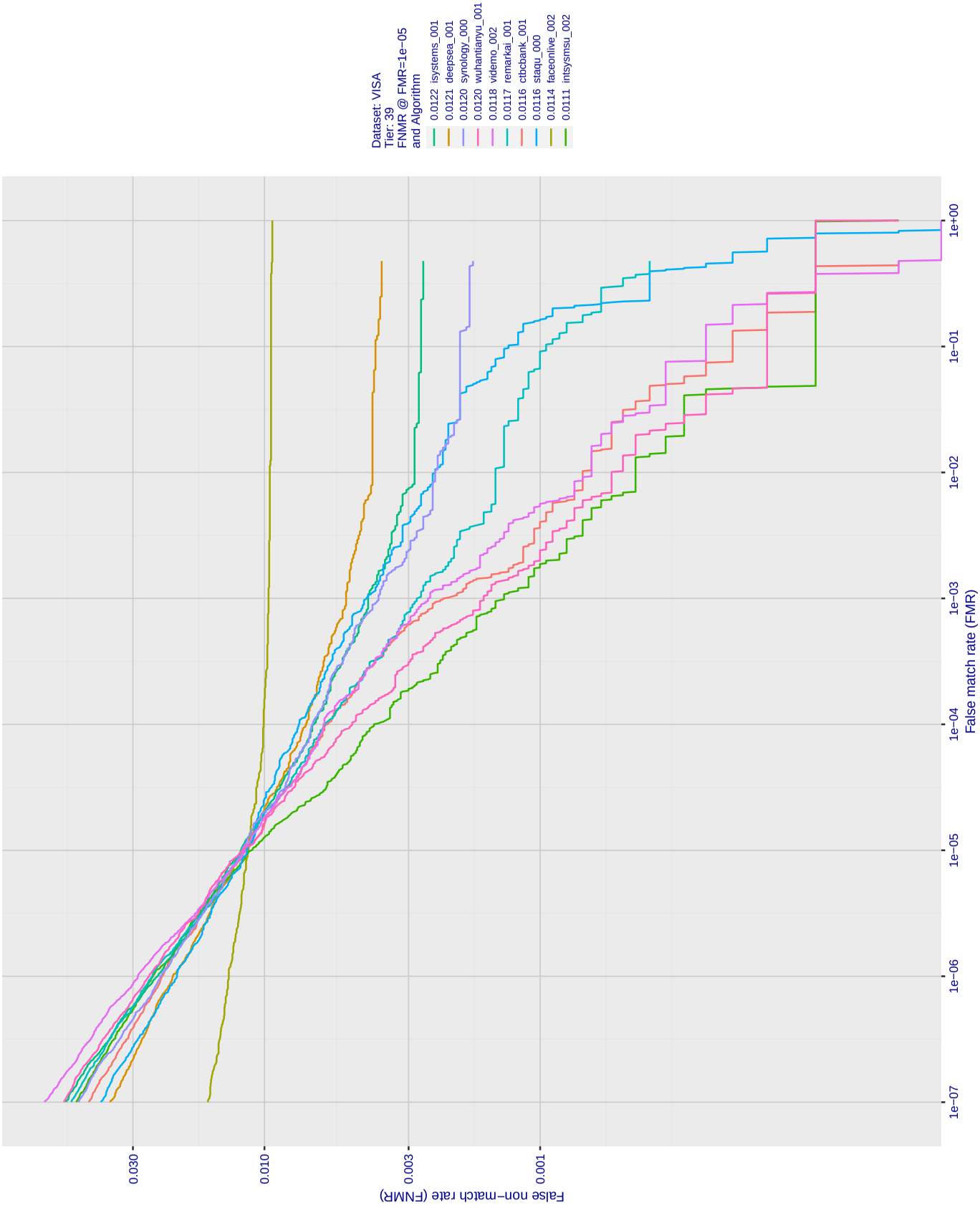

Figure 90: For the visa images, detection error tradeoff (DET) characteristics showing false non-match rate vs. false match rate plotted parametrically on threshold, T. The scales are logarithmic in order to show many decades of FMR.

FNMR(T) "False non-match rate"
FMR(T) "False match rate"

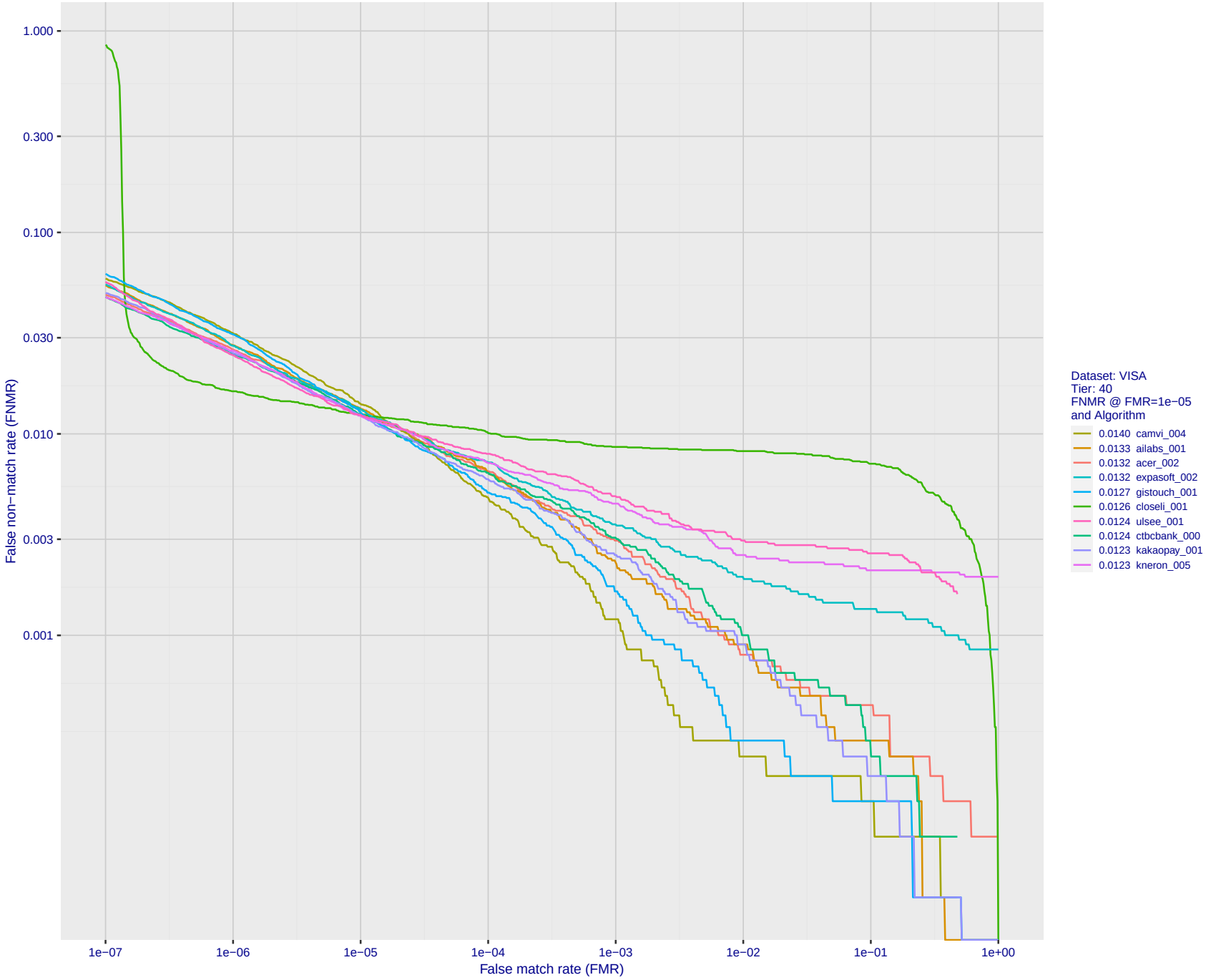

Figure 91: For the visa images, detection error tradeoff (DET) characteristics showing false non-match rate vs. false match rate plotted parametrically on threshold, T. The scales are logarithmic in order to show many decades of FMR.

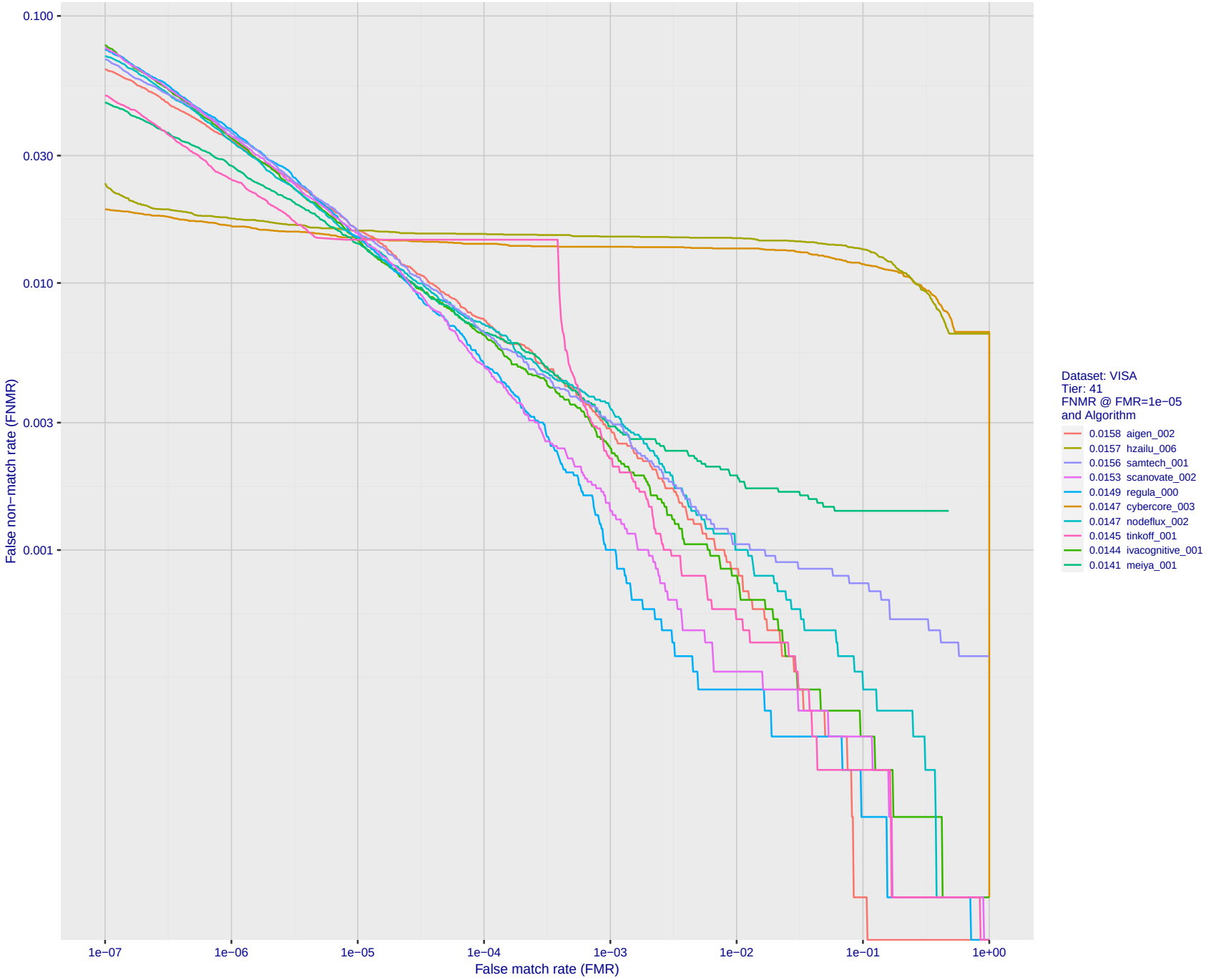

Figure 92: For the visa images, detection error tradeoff (DET) characteristics showing false non-match rate vs. false match rate plotted parametrically on threshold, T. The scales are logarithmic in order to show many decades of FMR.

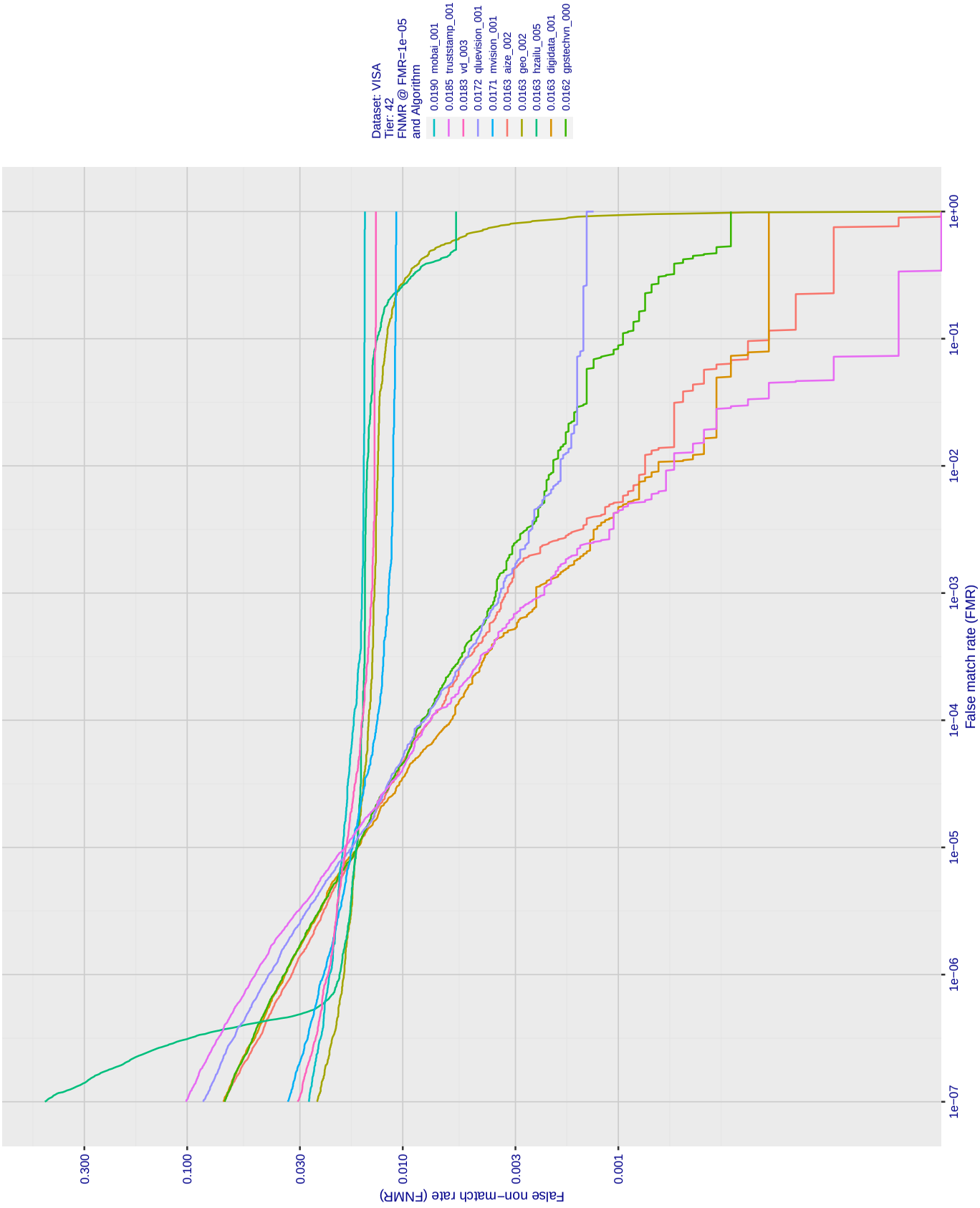

Figure 93: For the visa images, detection error tradeoff (DET) characteristics showing false non-match rate vs. false match rate plotted parametrically on threshold, T. The scales are logarithmic in order to show many decades of FMR.

FNMR(T) "False non-match rate"
FMR(T) "False match rate"

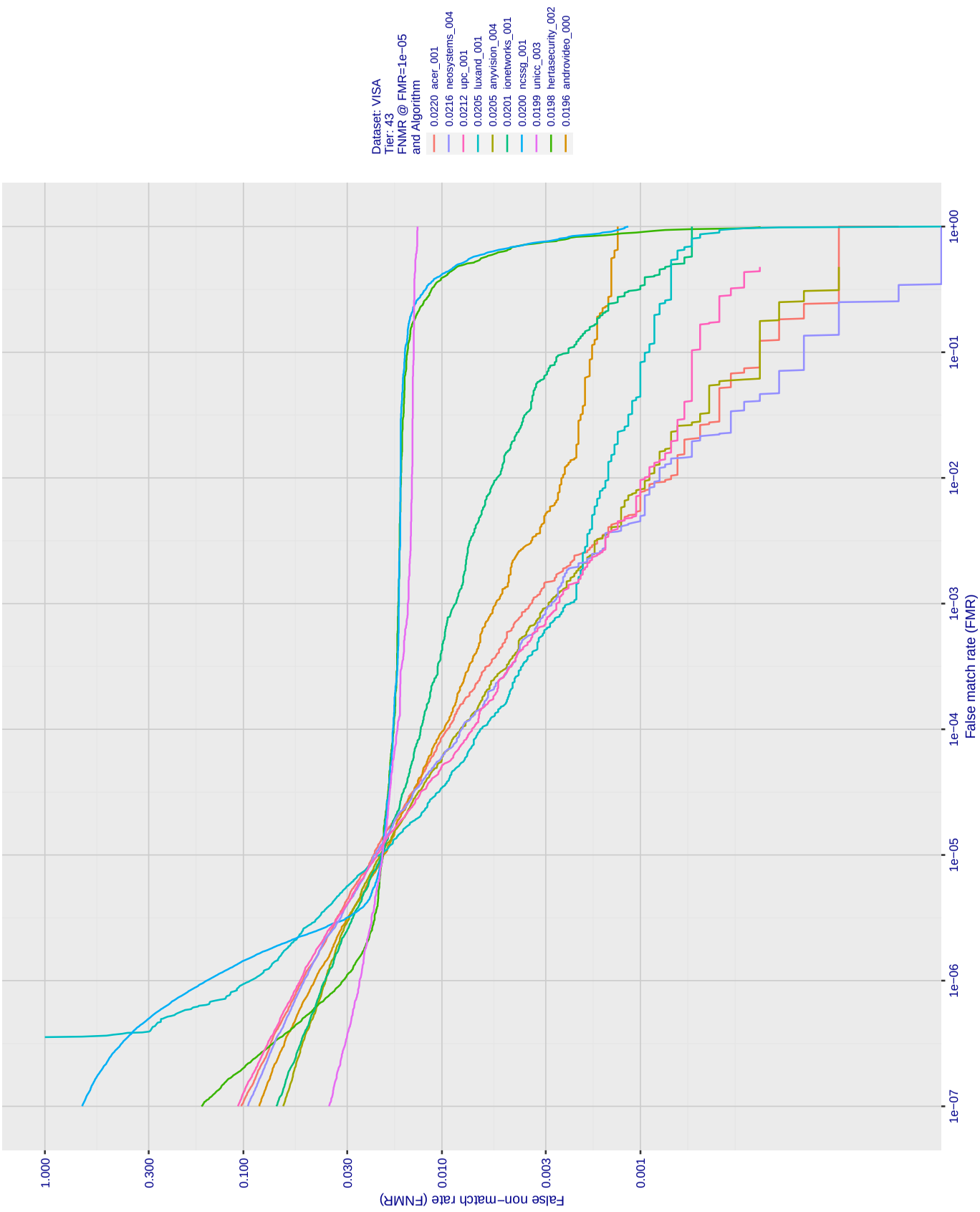

Figure 94: For the visa images, detection error tradeoff (DET) characteristics showing false non-match rate vs. false match rate plotted parametrically on threshold, T. The scales are logarithmic in order to show many decades of FMR.

FNMR(T) "False non-match rate"
FMR(T) "False match rate"

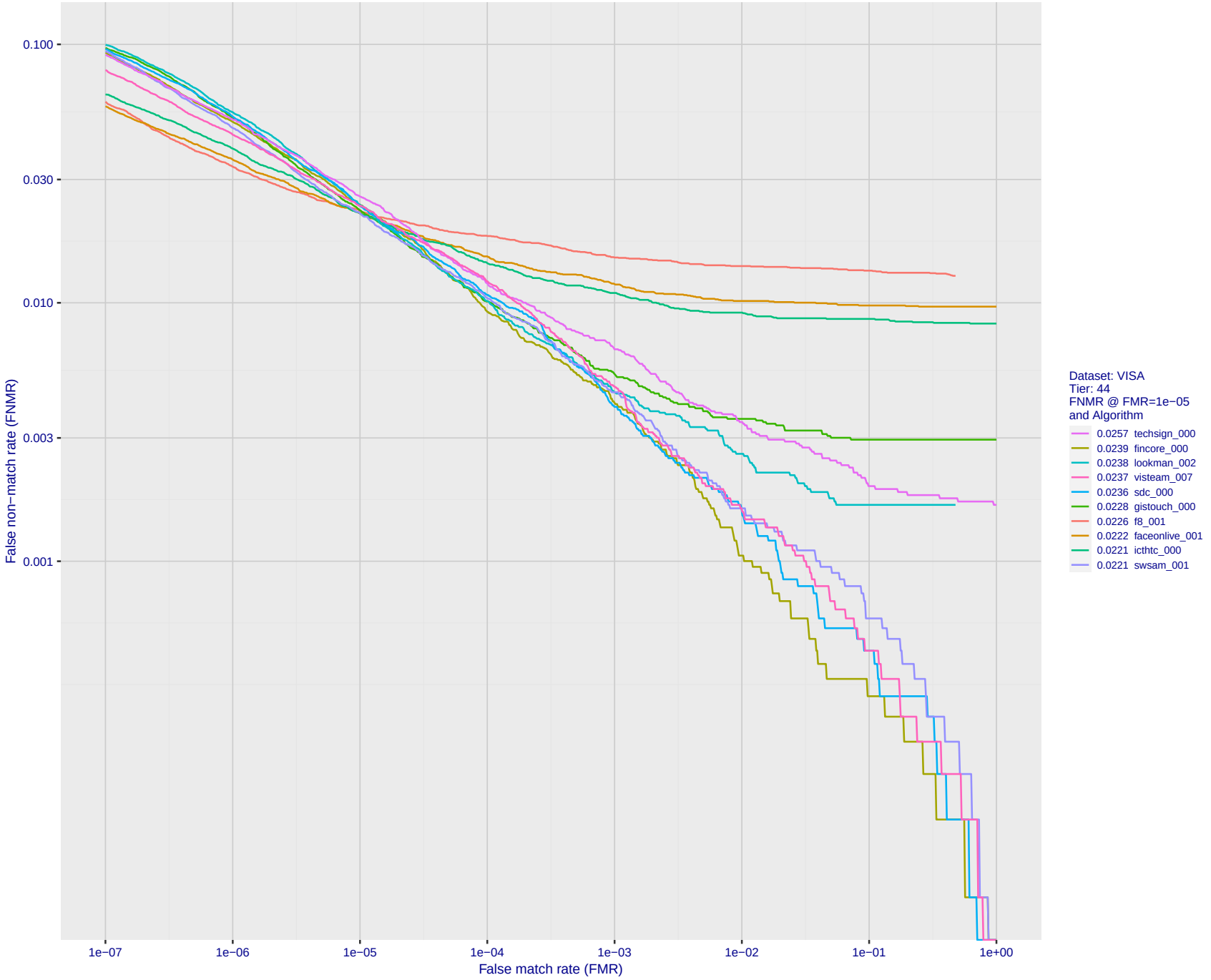

Figure 95: For the visa images, detection error tradeoff (DET) characteristics showing false non-match rate vs. false match rate plotted parametrically on threshold, T. The scales are logarithmic in order to show many decades of FMR.

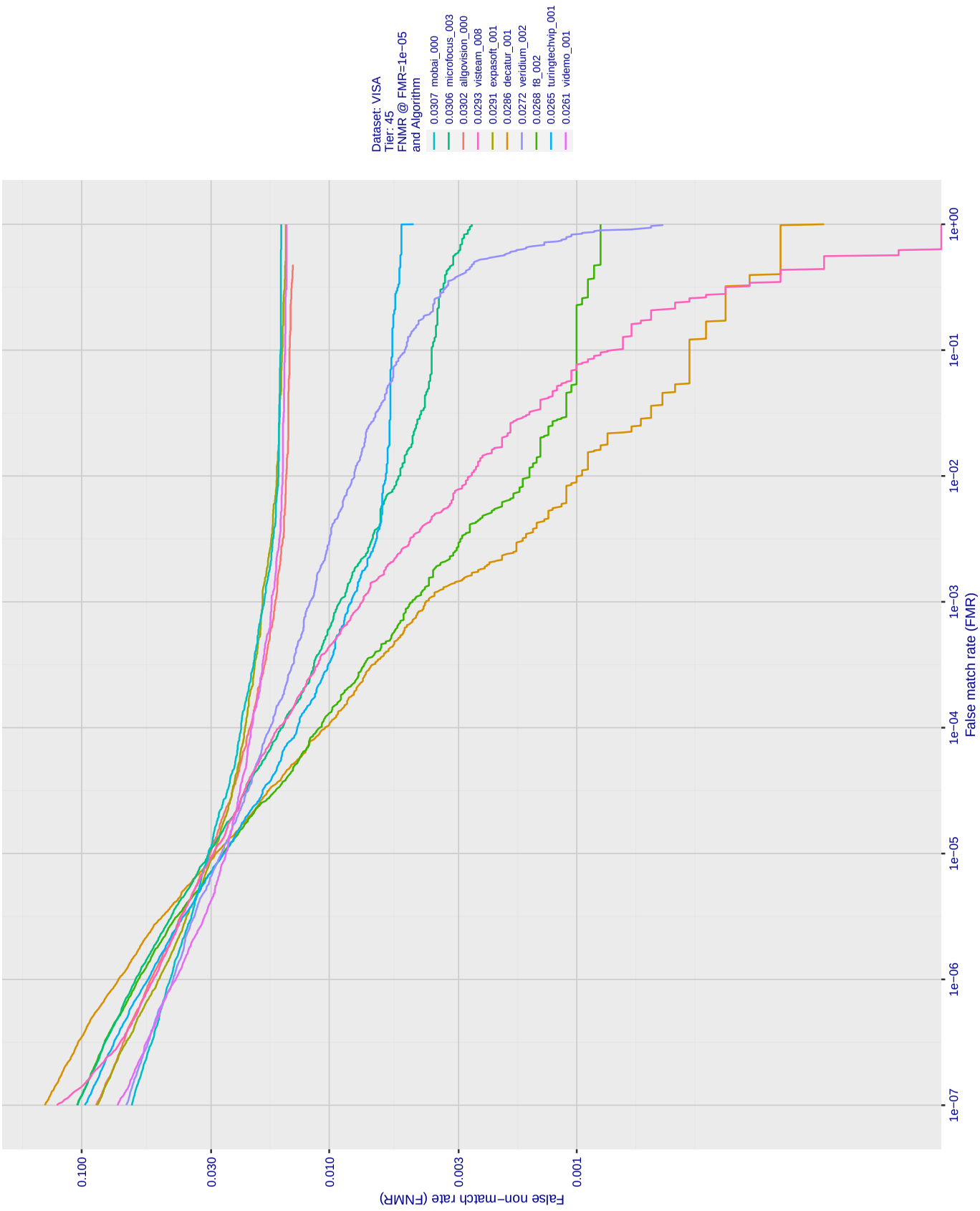

Figure 96: For the visa images, detection error tradeoff (DET) characteristics showing false non-match rate vs. false match rate plotted parametrically on threshold, T. The scales are logarithmic in order to show many decades of FMR.

FNMR(T) "False non-match rate"
FMR(T) "False match rate"

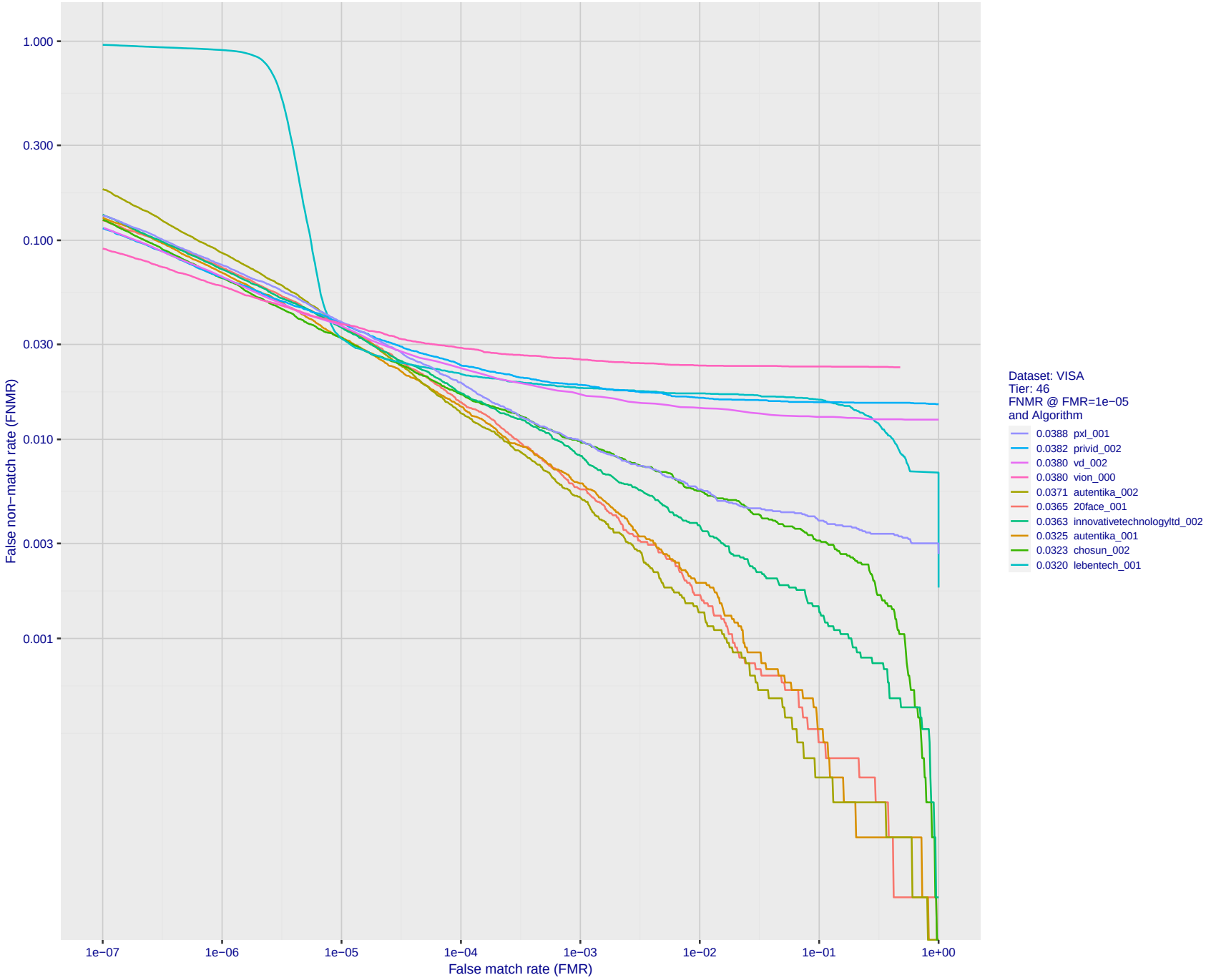

Figure 97: For the visa images, detection error tradeoff (DET) characteristics showing false non-match rate vs. false match rate plotted parametrically on threshold, T. The scales are logarithmic in order to show many decades of FMR.

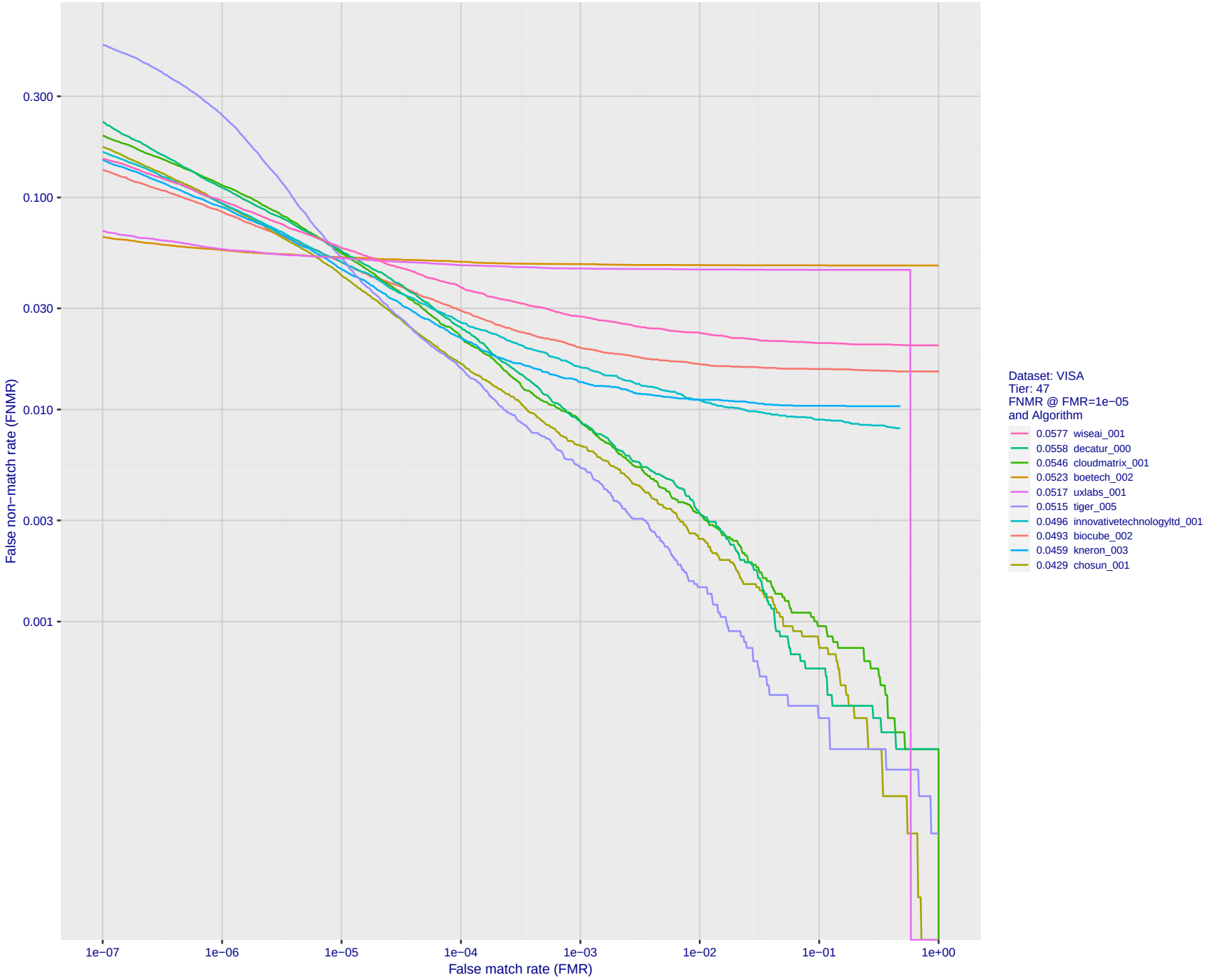

*Figure 98: For the visa images, detection error tradeoff (*DET*) characteristics showing false non-match rate vs. false match rate plotted parametrically on threshold, T. The scales are logarithmic in order to show many decades of* FMR*.*

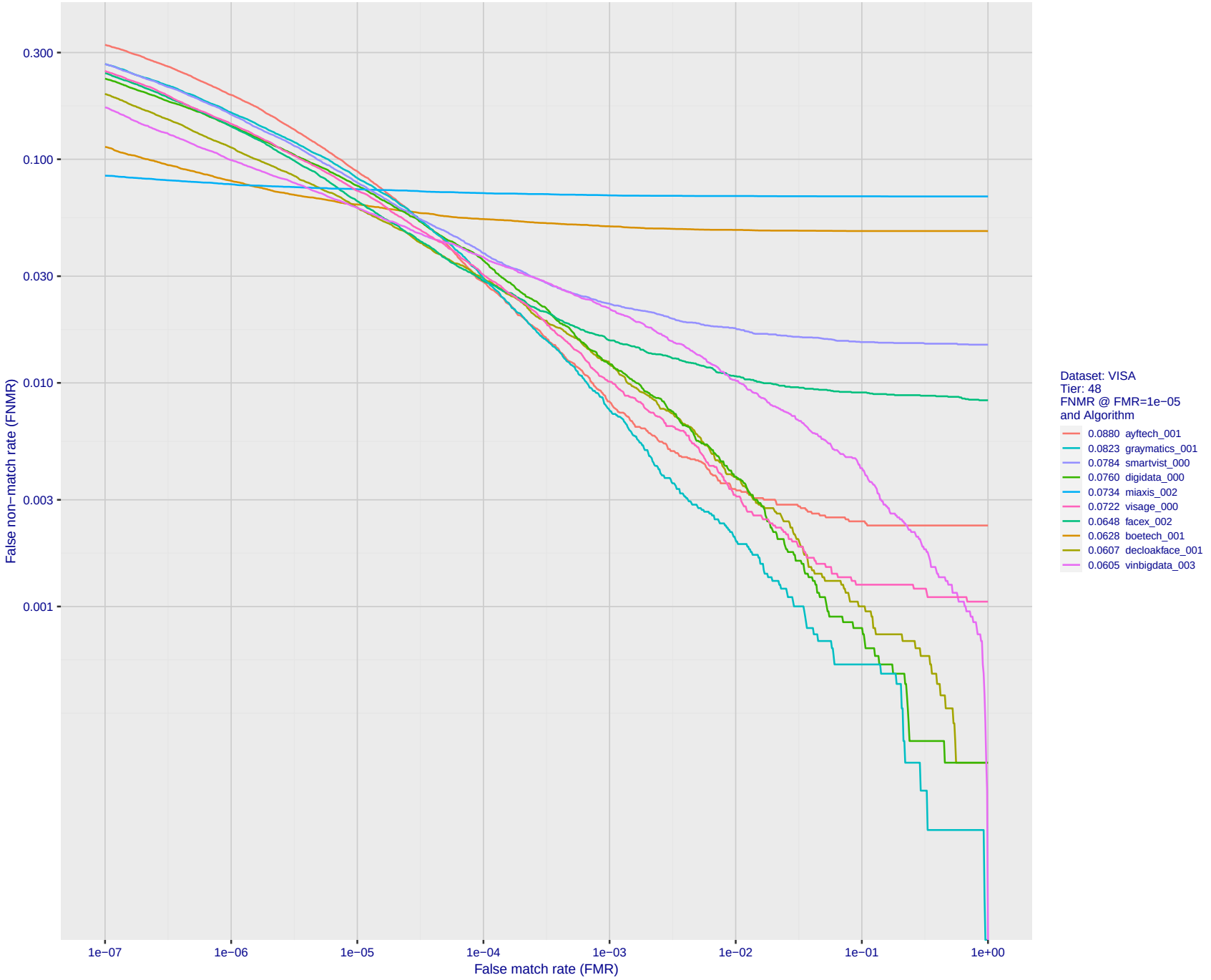

Figure 99: For the visa images, detection error tradeoff (DET) characteristics showing false non-match rate vs. false match rate plotted parametrically on threshold, T. The scales are logarithmic in order to show many decades of FMR.

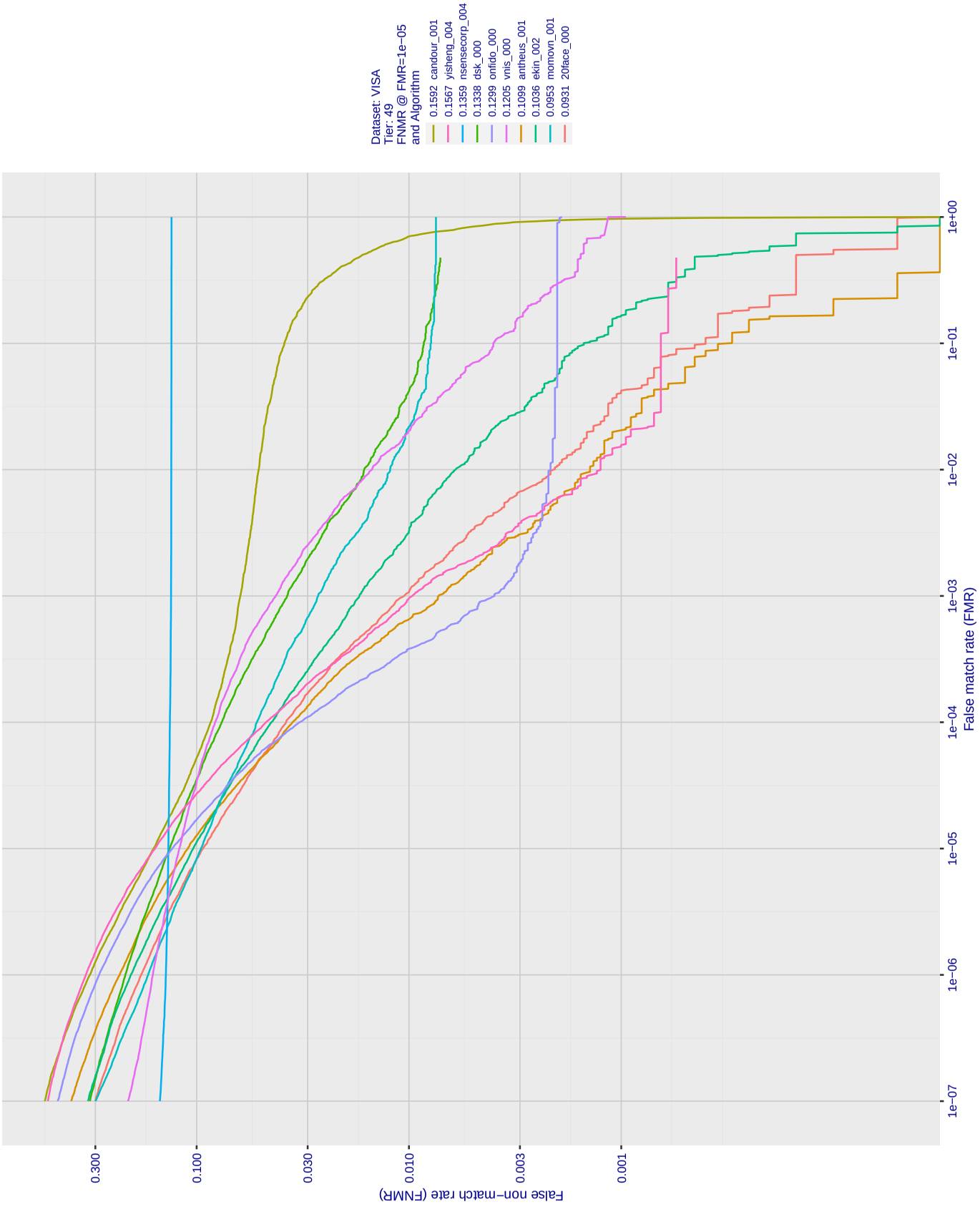

Figure 100: For the visa images, detection error tradeoff (DET) characteristics showing false non-match rate vs. false match rate plotted parametrically on threshold, T. The scales are logarithmic in order to show many decades of FMR.

FNMR(T) "False non-match rate"
FMR(T) "False match rate"

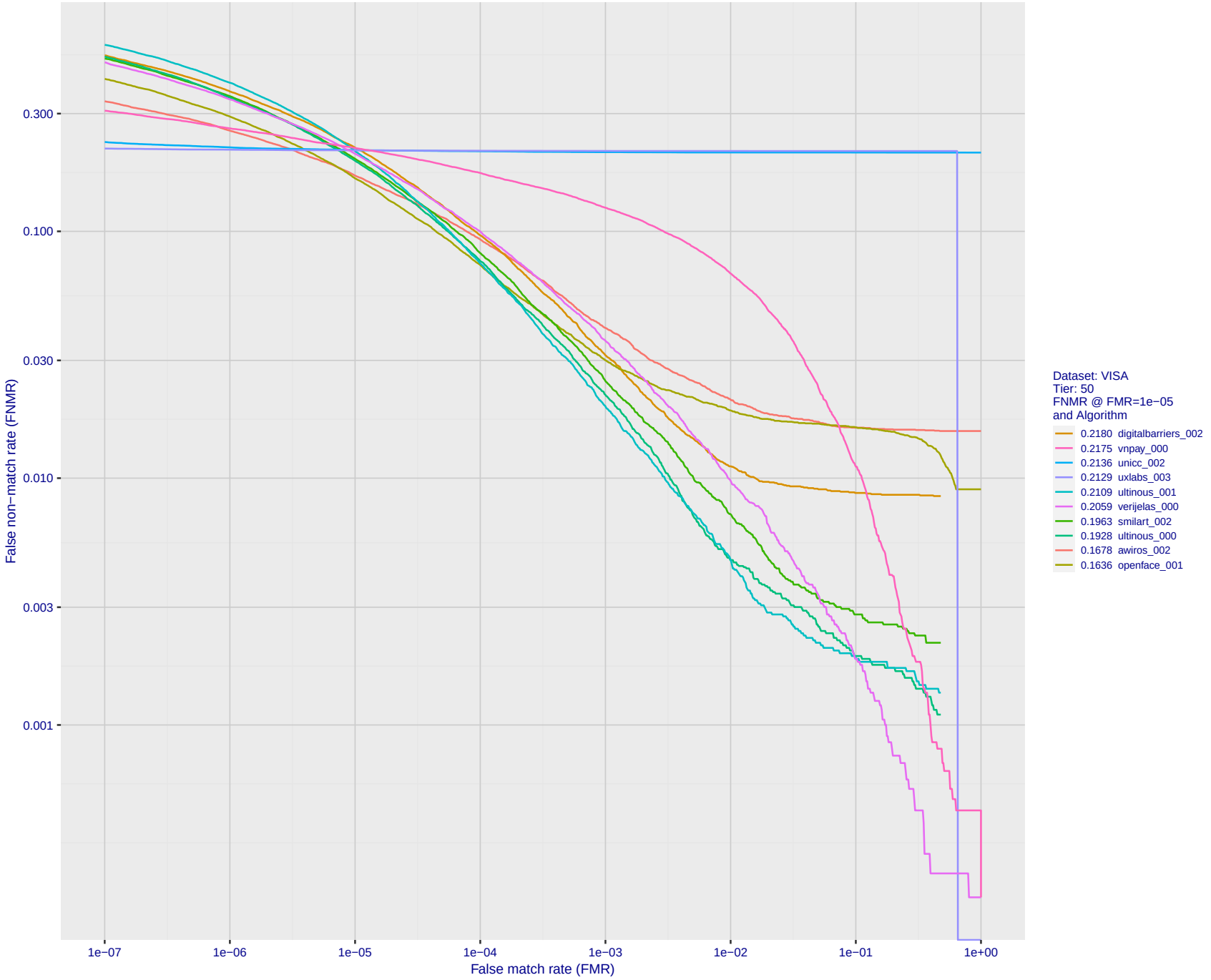

Figure 101: For the visa images, detection error tradeoff (DET) characteristics showing false non-match rate vs. false match rate plotted parametrically on threshold, T. The scales are logarithmic in order to show many decades of FMR.

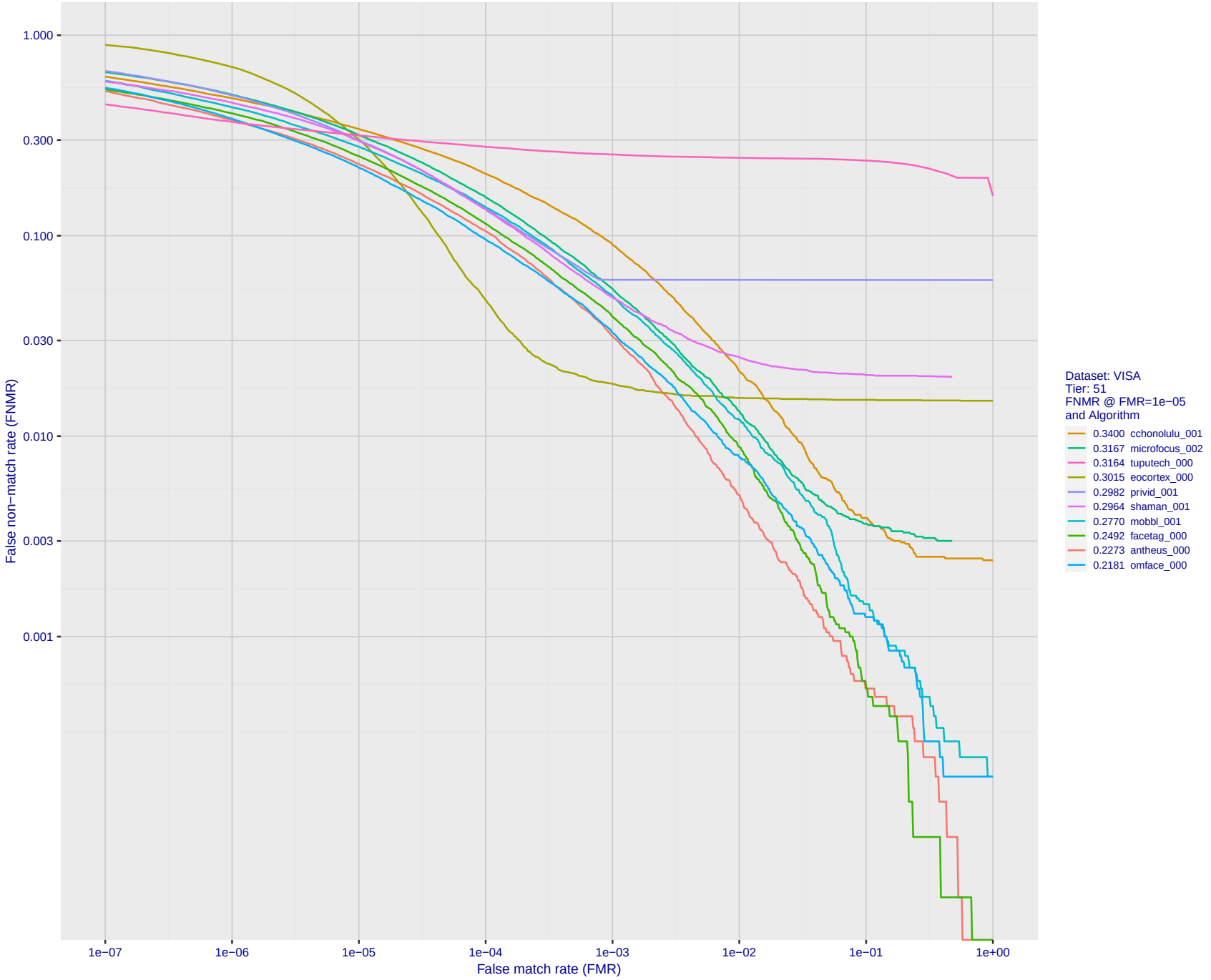

Figure 102: For the visa images, detection error tradeoff (DET) characteristics showing false non-match rate vs. false match rate plotted parametrically on threshold, T. The scales are logarithmic in order to show many decades of FMR.

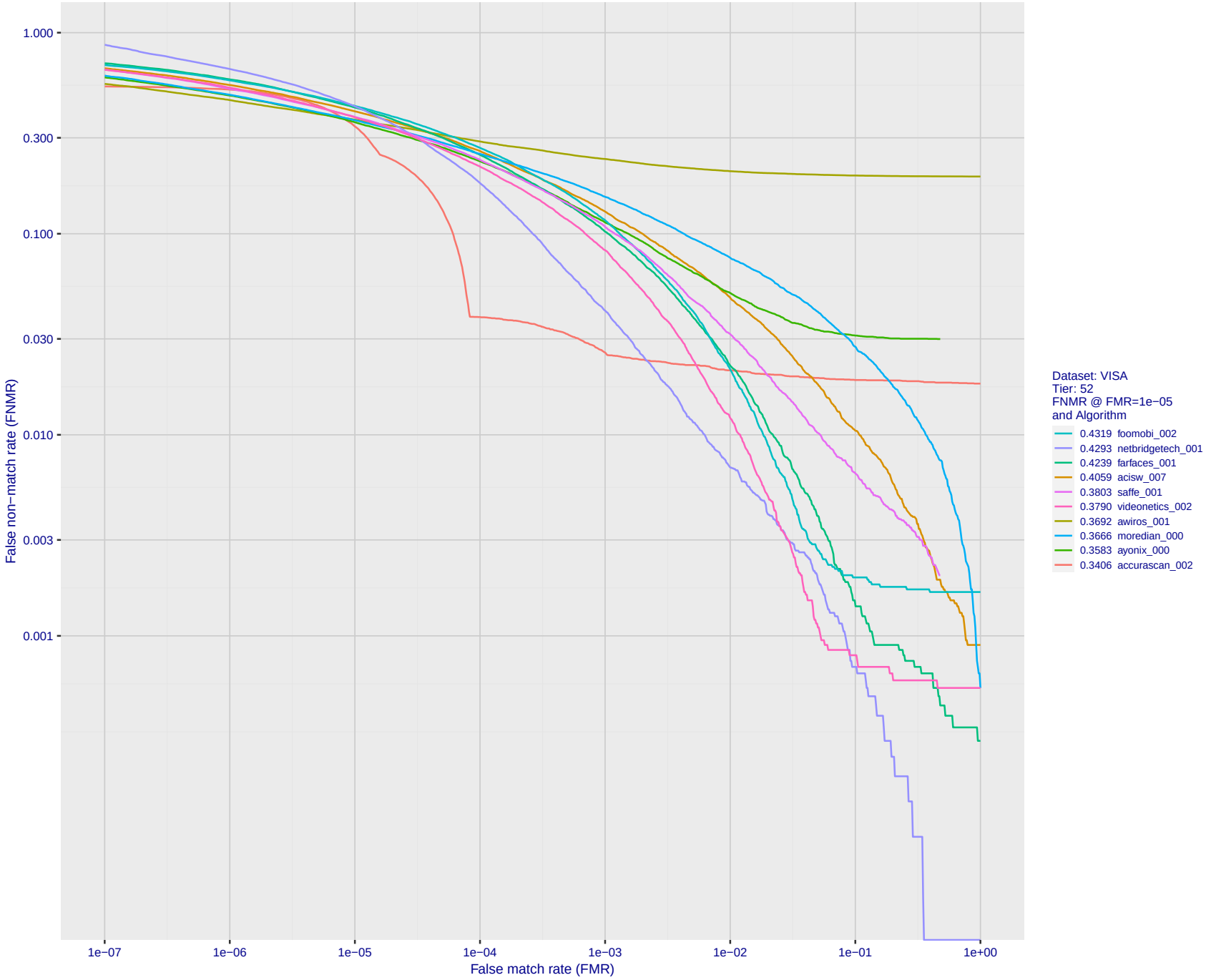

Figure 103: For the visa images, detection error tradeoff (DET) characteristics showing false non-match rate vs. false match rate plotted parametrically on threshold, T. The scales are logarithmic in order to show many decades of FMR.

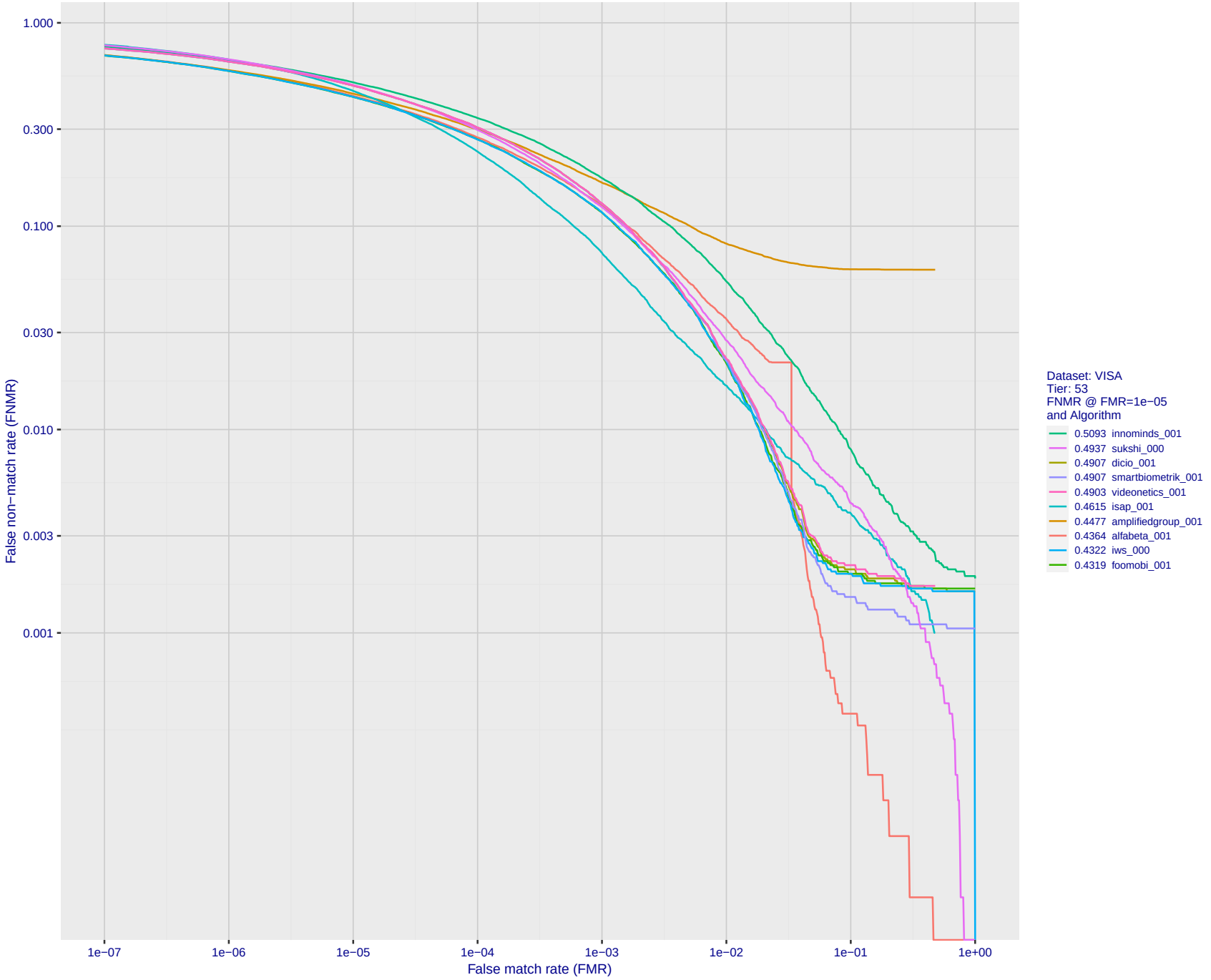

Figure 104: For the visa images, detection error tradeoff (DET) characteristics showing false non-match rate vs. false match rate plotted parametrically on threshold, T. The scales are logarithmic in order to show many decades of FMR.

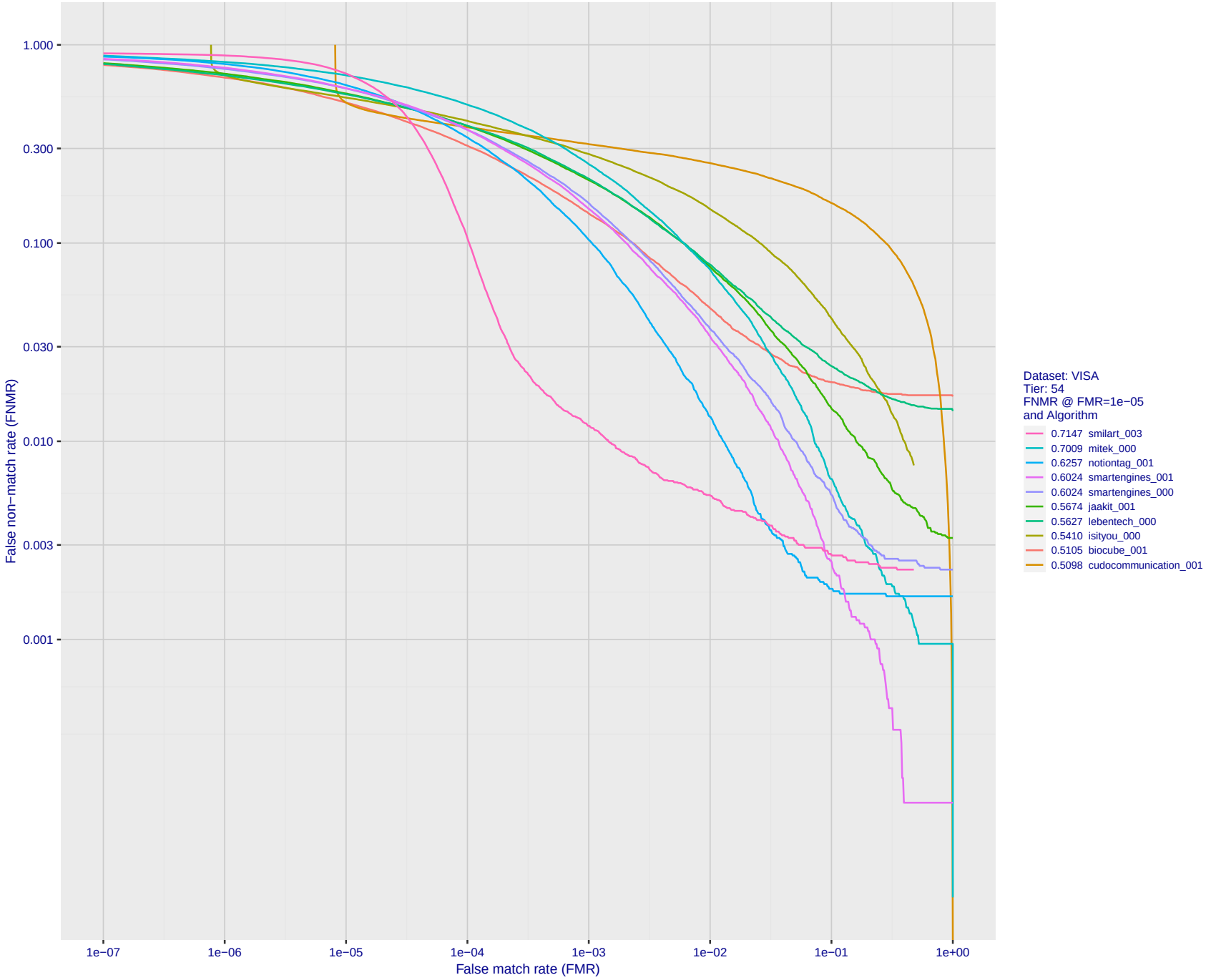

Figure 105: For the visa images, detection error tradeoff (DET) characteristics showing false non-match rate vs. false match rate plotted parametrically on threshold, T. The scales are logarithmic in order to show many decades of FMR.

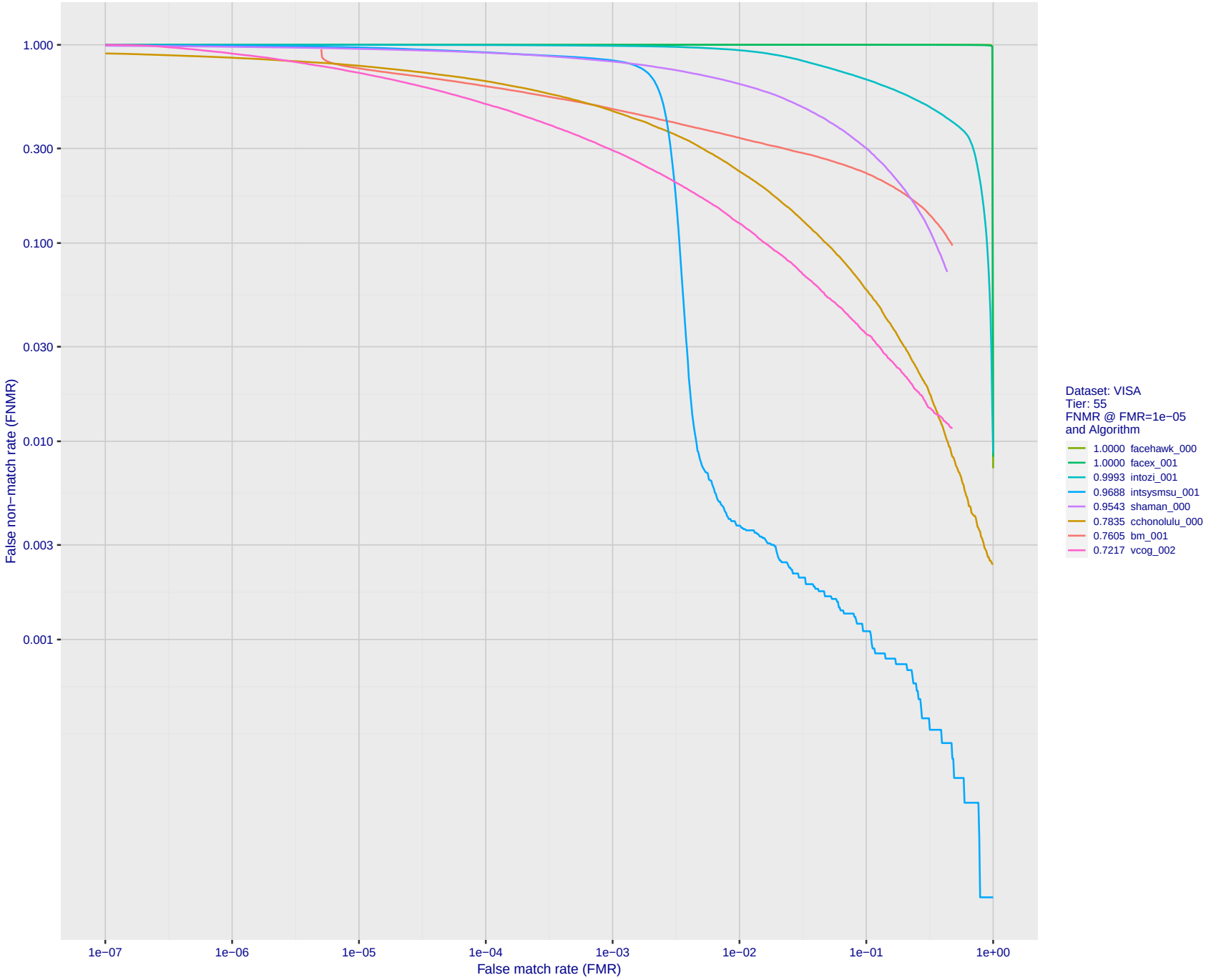

Figure 106: For the visa images, detection error tradeoff (DET) characteristics showing false non-match rate vs. false match rate plotted parametrically on threshold, T. The scales are logarithmic in order to show many decades of FMR.

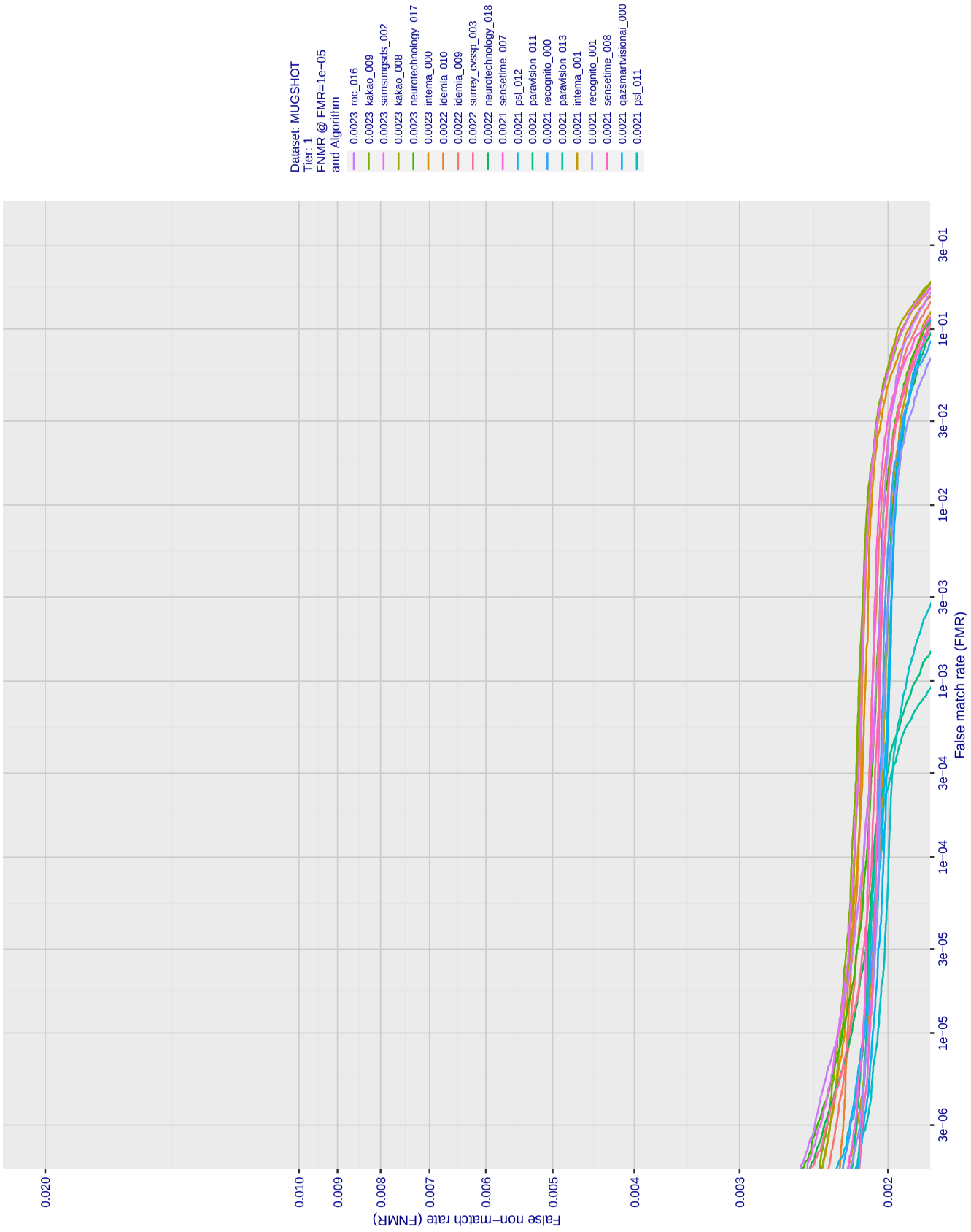

Figure 107: For the mugshot images, detection error tradeoff (DET) characteristics showing false non-match rate vs. false match rate plotted parametrically on threshold, T. The scales are logarithmic in order to show decades of FMR.

FNMR(T) "False non-match rate"
FMR(T) "False match rate"

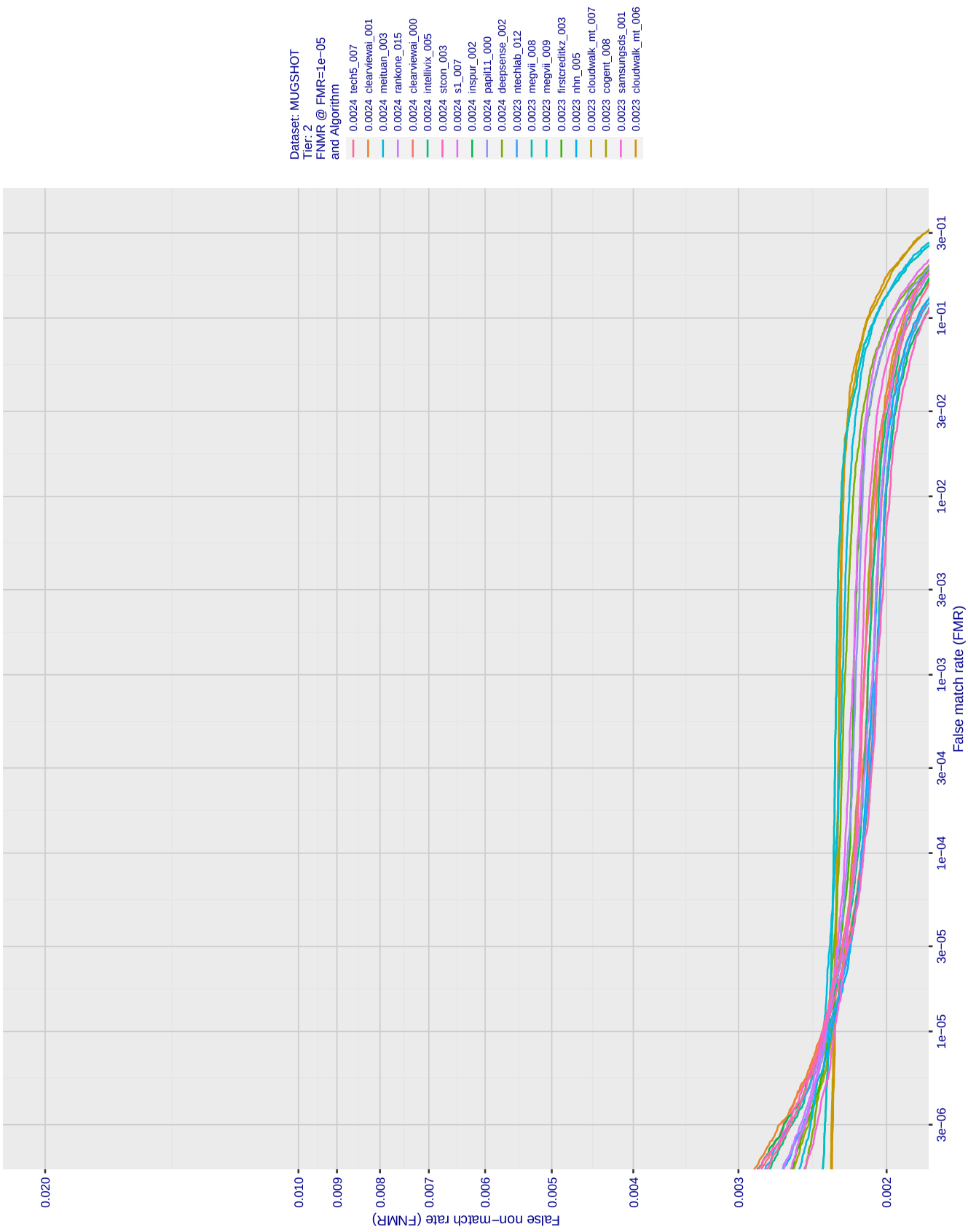

Figure 108: For the mugshot images, detection error tradeoff (DET) characteristics showing false non-match rate vs. false match rate plotted parametrically on threshold, T. The scales are logarithmic in order to show decades of FMR.

FNMR(T) "False non-match rate"
FMR(T) "False match rate"

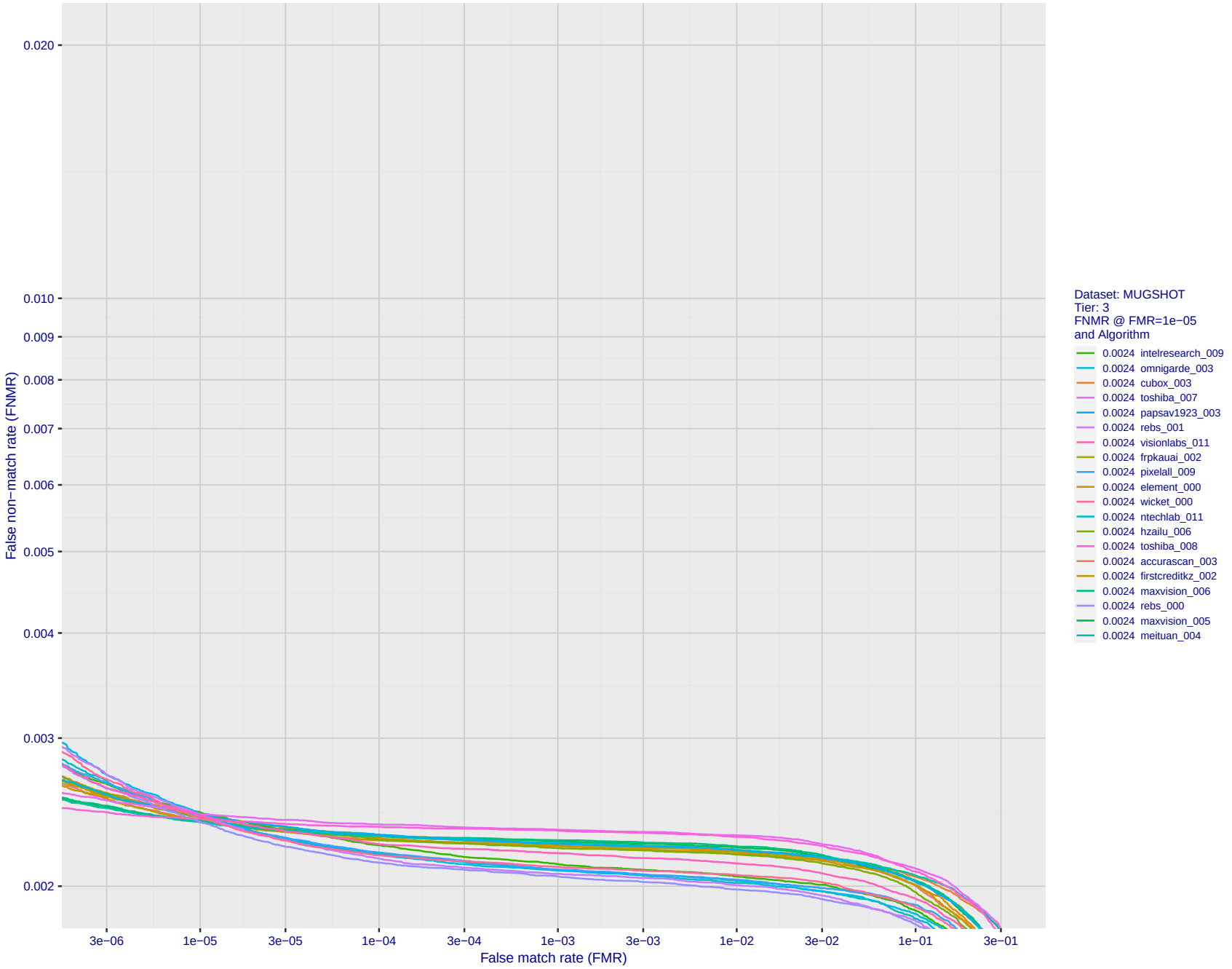

*Figure 109: For the mugshot images, detection error tradeoff (*DET*) characteristics showing false non-match rate vs. false match rate plotted parametrically on threshold, T. The scales are logarithmic in order to show decades of* FMR*.*

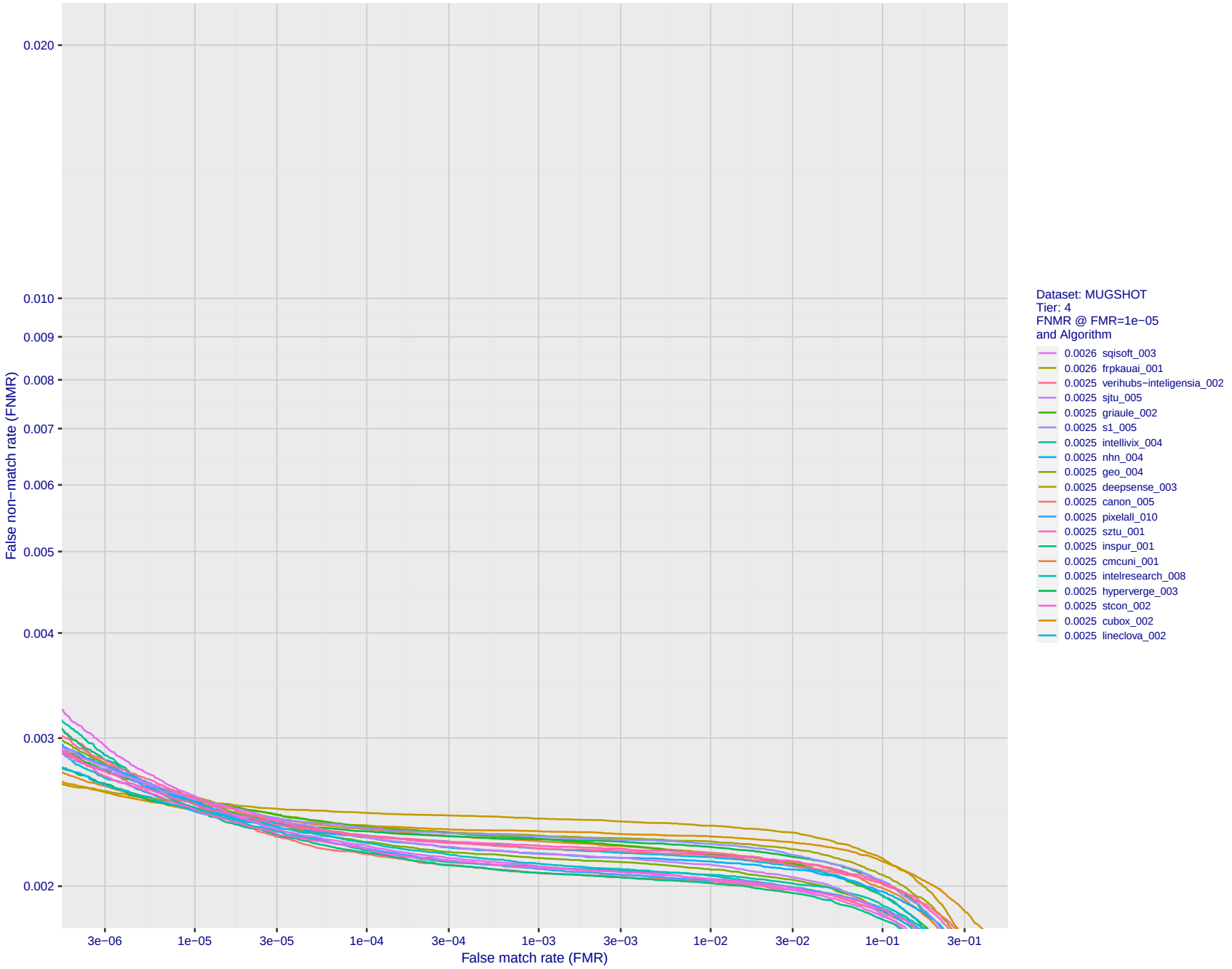

*Figure 110: For the mugshot images, detection error tradeoff (*DET*) characteristics showing false non-match rate vs. false match rate plotted parametrically on threshold, T. The scales are logarithmic in order to show decades of* FMR.

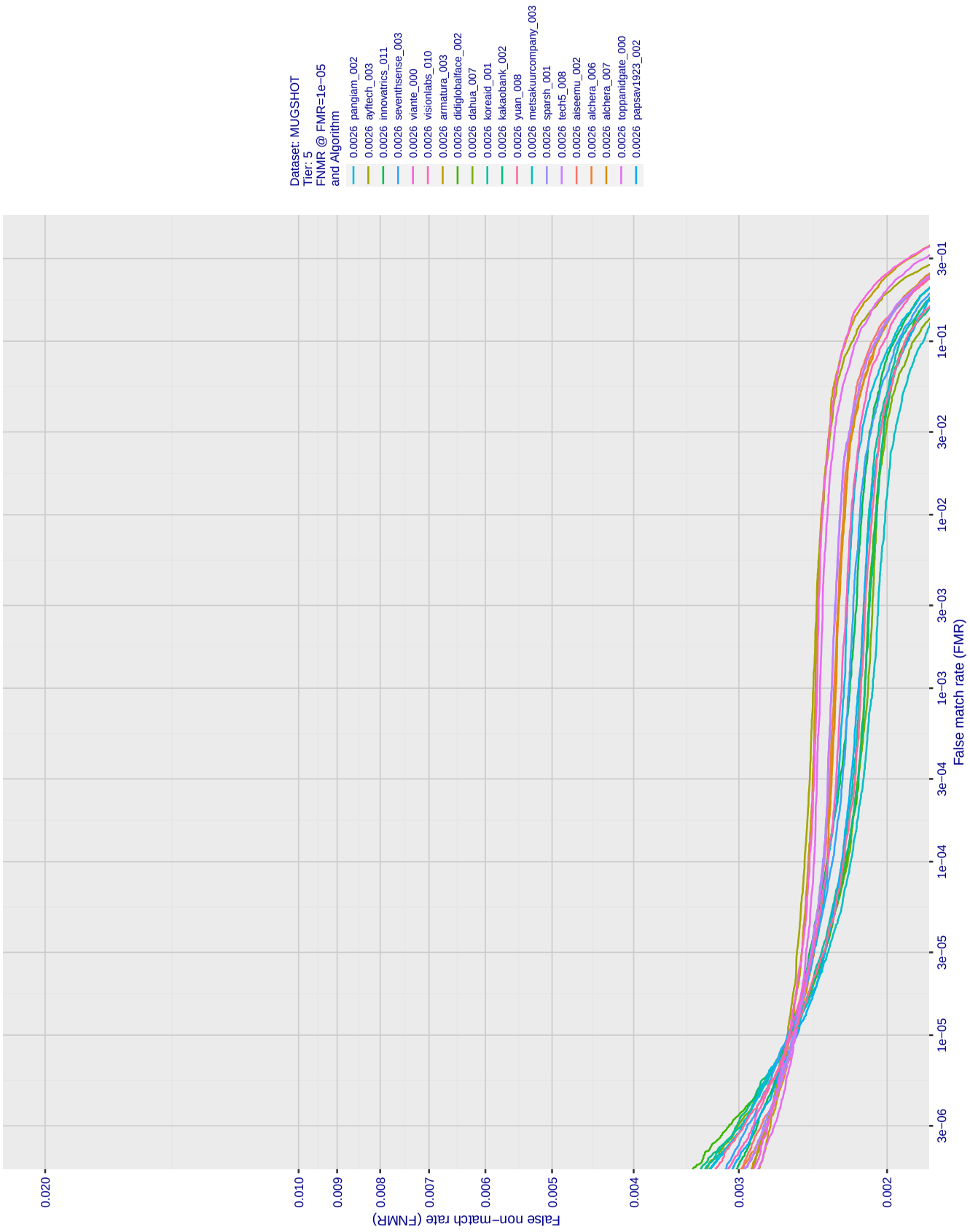

Figure 111: For the mugshot images, detection error tradeoff (DET) characteristics showing false non-match rate vs. false match rate plotted parametrically on threshold, T. The scales are logarithmic in order to show decades of FMR.

FNMR(T) "False non-match rate"
FMR(T) "False match rate"

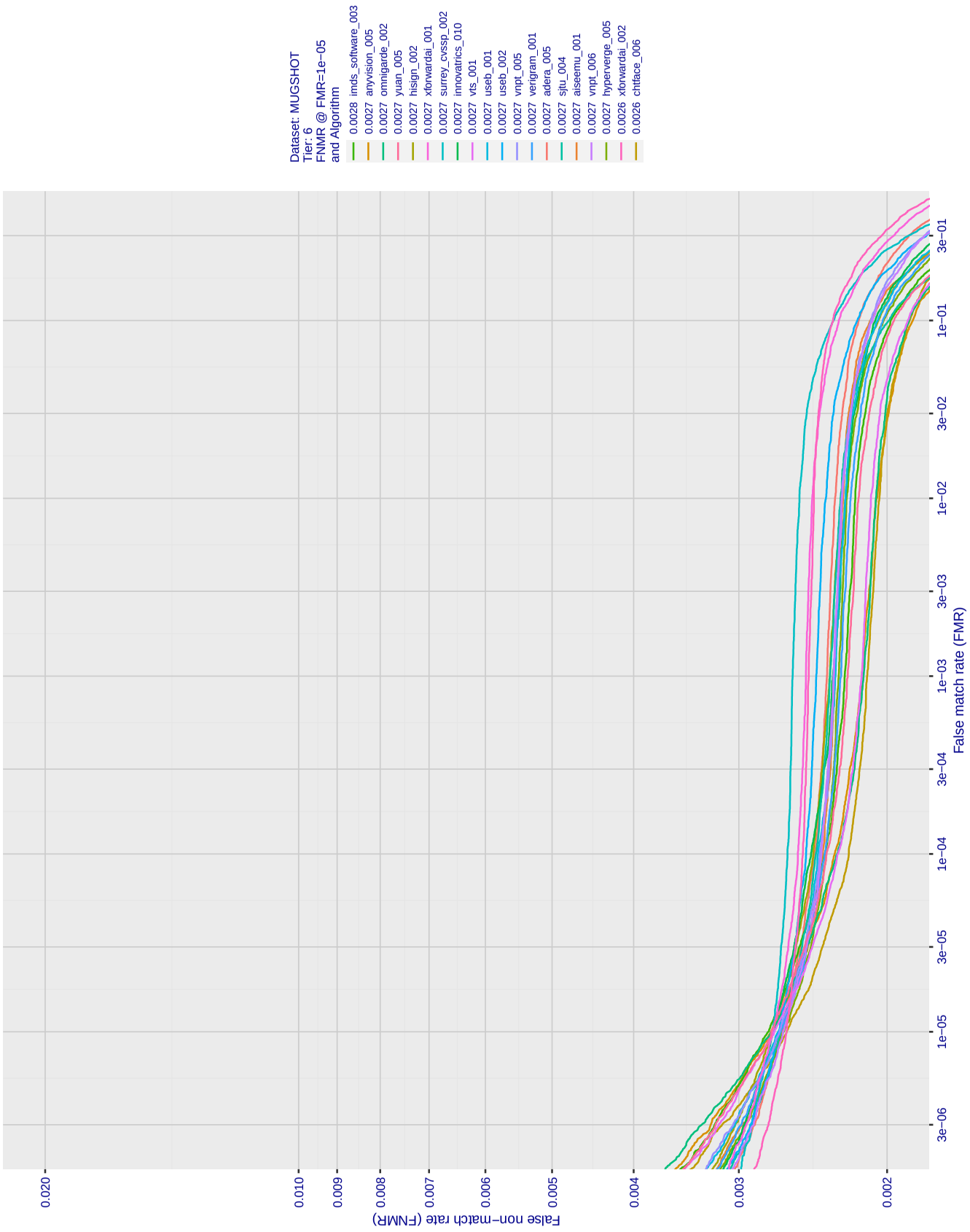

Figure 112: For the mugshot images, detection error tradeoff (DET) characteristics showing false non-match rate vs. false match rate plotted parametrically on threshold, T. The scales are logarithmic in order to show decades of FMR.

FNMR(T) "False non-match rate"
FMR(T) "False match rate"

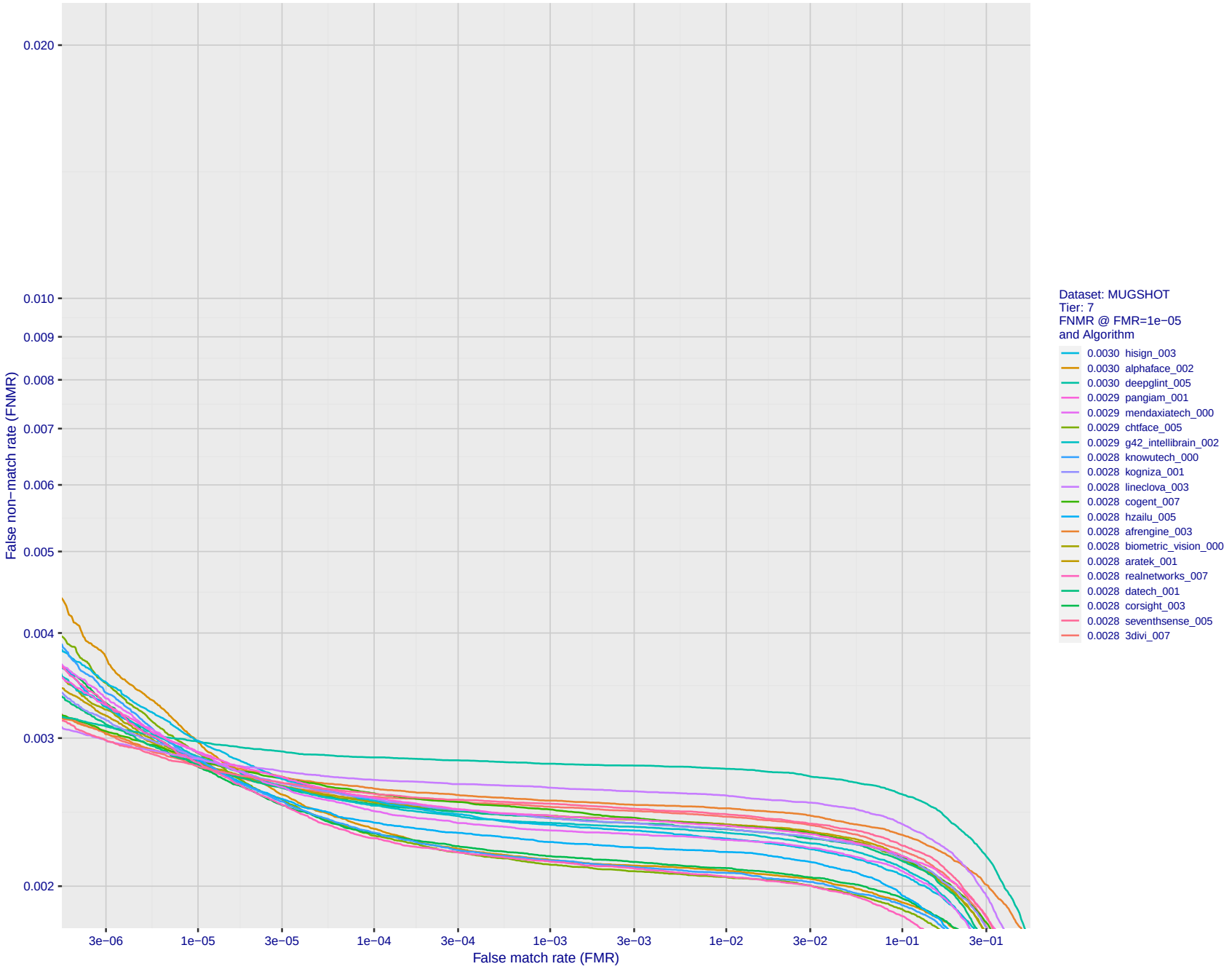

Figure 113: For the mugshot images, detection error tradeoff (DET) characteristics showing false non-match rate vs. false match rate plotted parametrically on threshold, T. The scales are logarithmic in order to show decades of FMR.

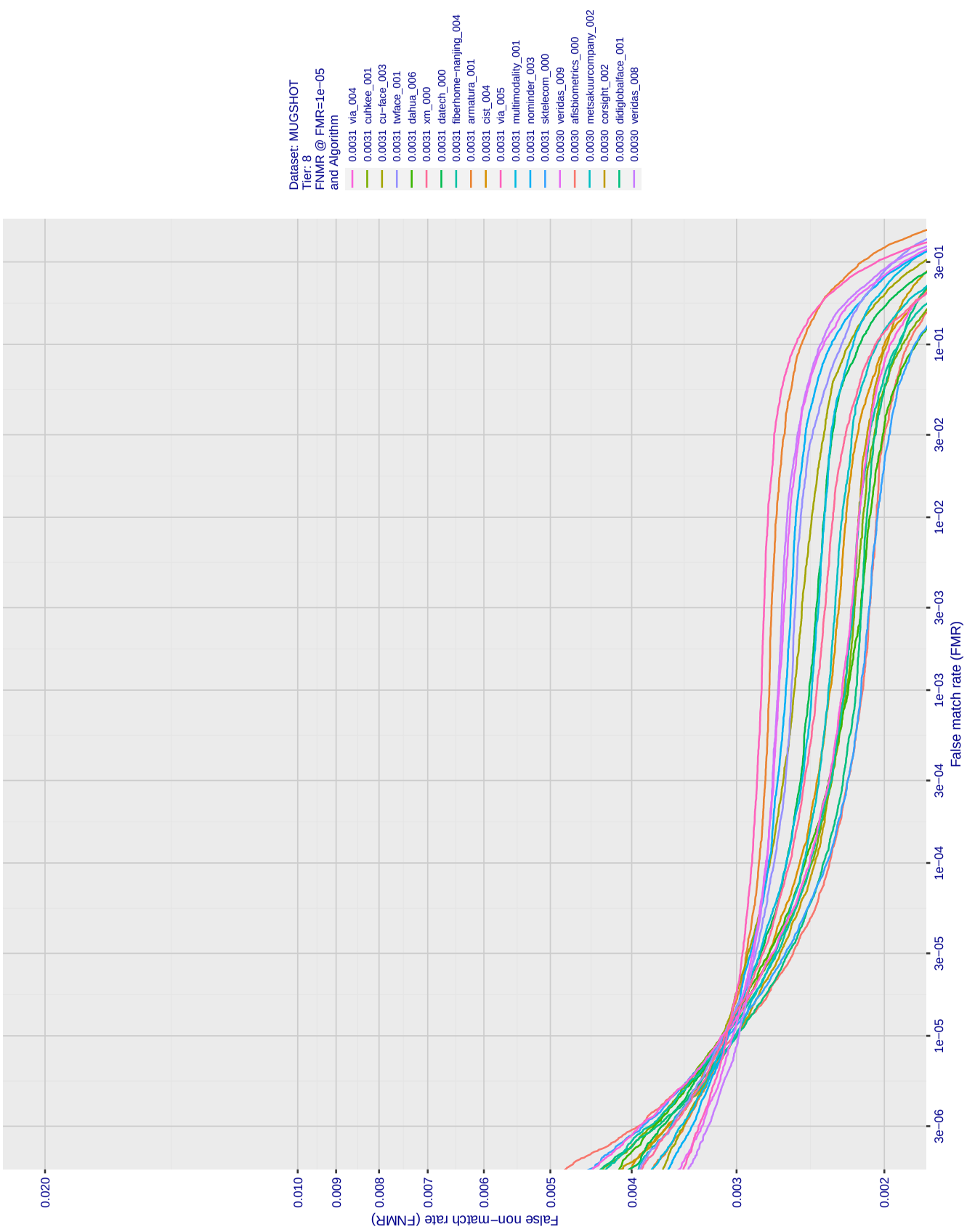

Figure 114: For the mugshot images, detection error tradeoff (DET) characteristics showing false non-match rate vs. false match rate plotted parametrically on threshold, T. The scales are logarithmic in order to show decades of FMR.

FNMR(T) "False non-match rate"
FMR(T) "False match rate"

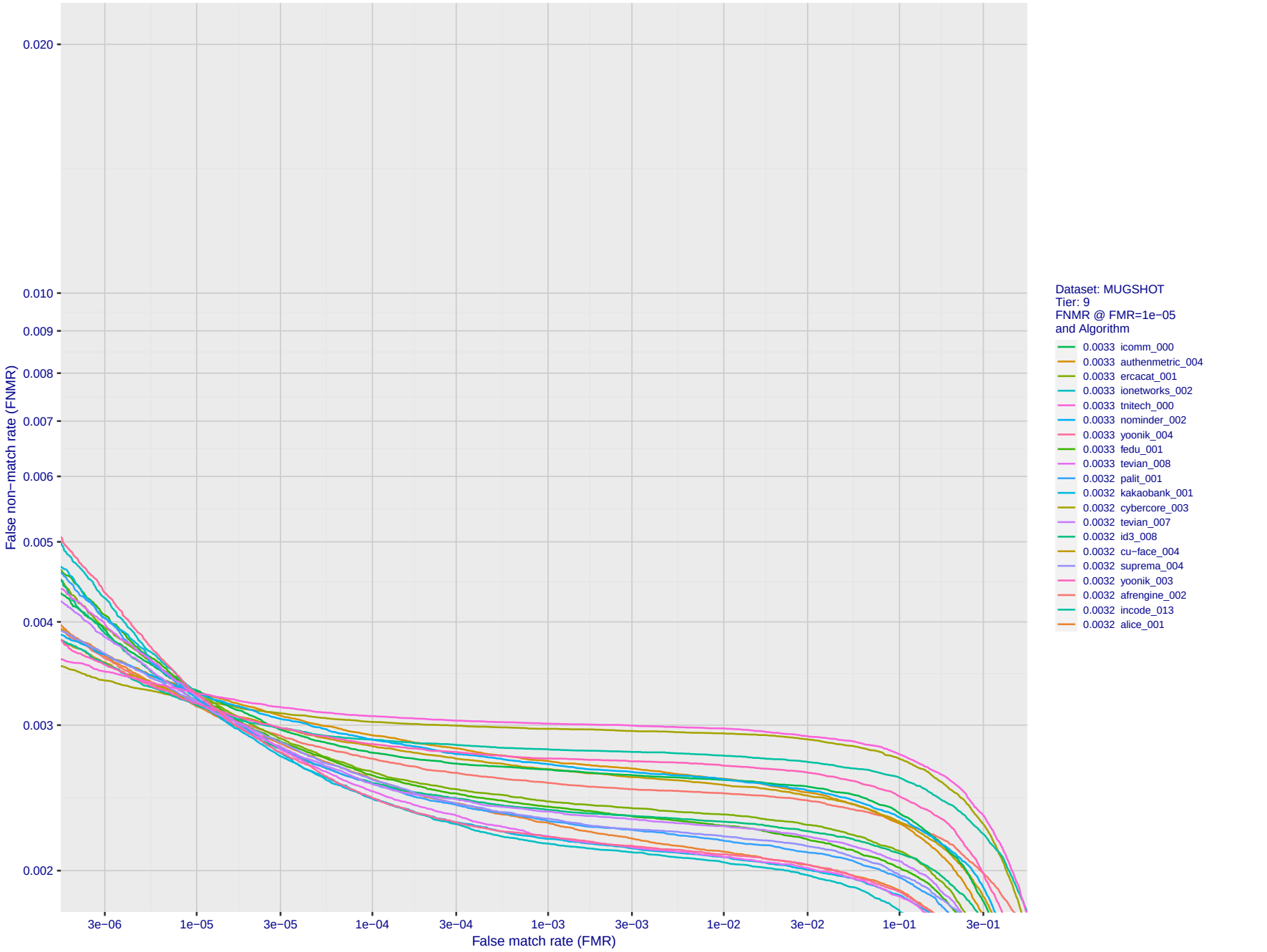

Figure 115: For the mugshot images, detection error tradeoff (DET) characteristics showing false non-match rate vs. false match rate plotted parametrically on threshold, T. The scales are logarithmic in order to show decades of FMR.

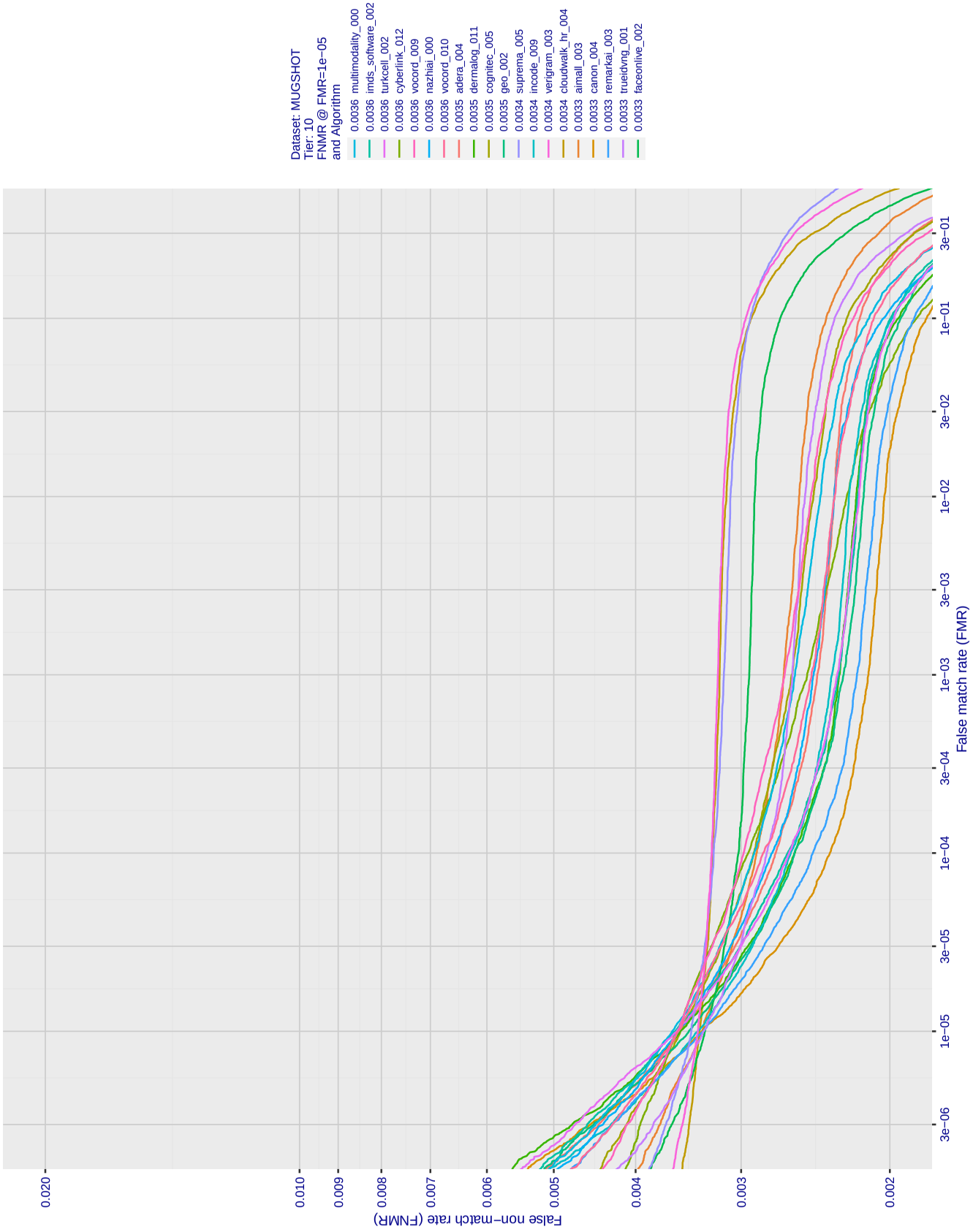

Figure 116: For the mugshot images, detection error tradeoff (DET) characteristics showing false non-match rate vs. false match rate plotted parametrically on threshold, T. The scales are logarithmic in order to show decades of FMR.

FNMR(T) "False non-match rate"
FMR(T) "False match rate"

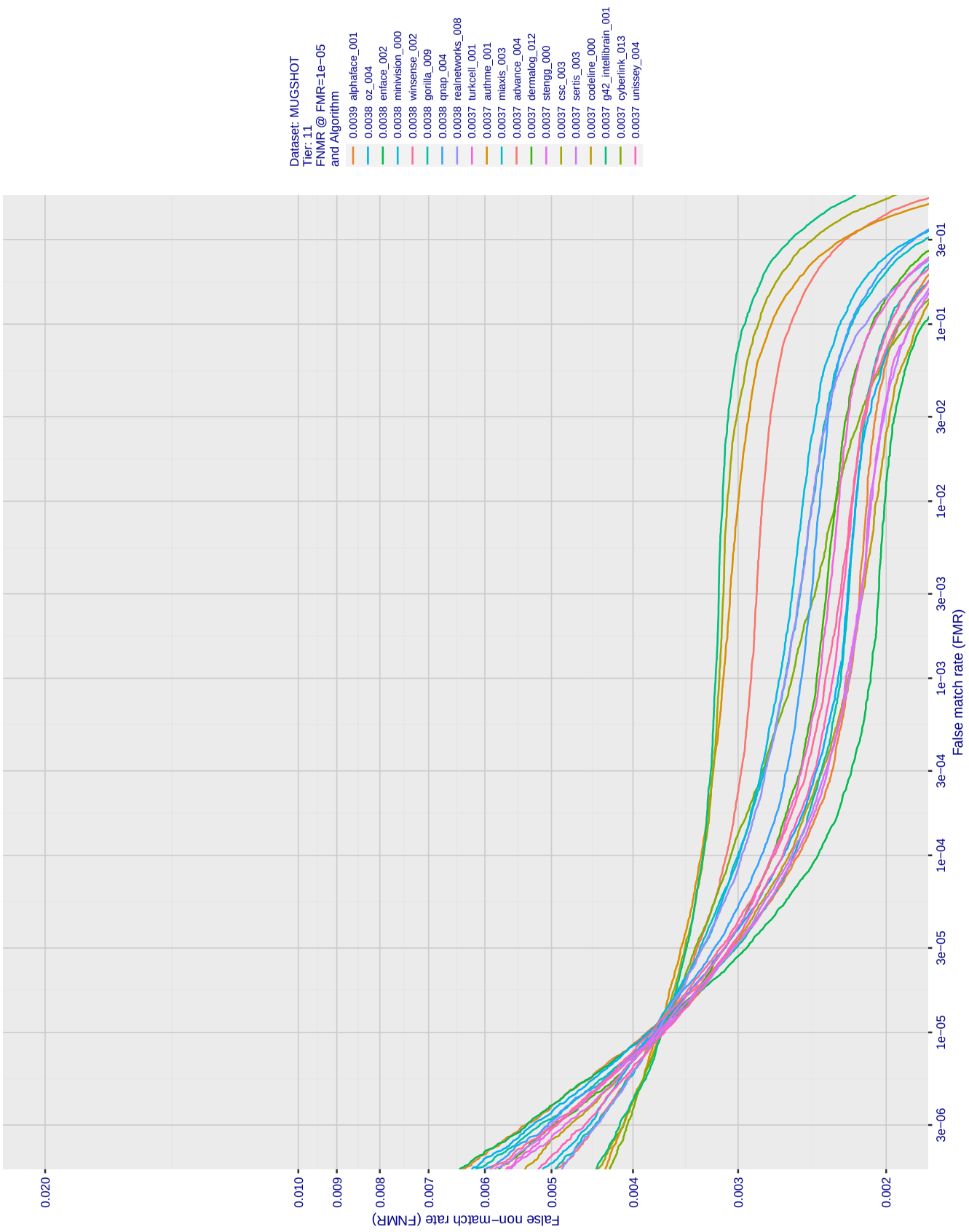

Figure 117: For the mugshot images, detection error tradeoff (DET) characteristics showing false non-match rate vs. false match rate plotted parametrically on threshold, T. The scales are logarithmic in order to show decades of FMR.

FNMR(T) "False non-match rate"
FMR(T) "False match rate"

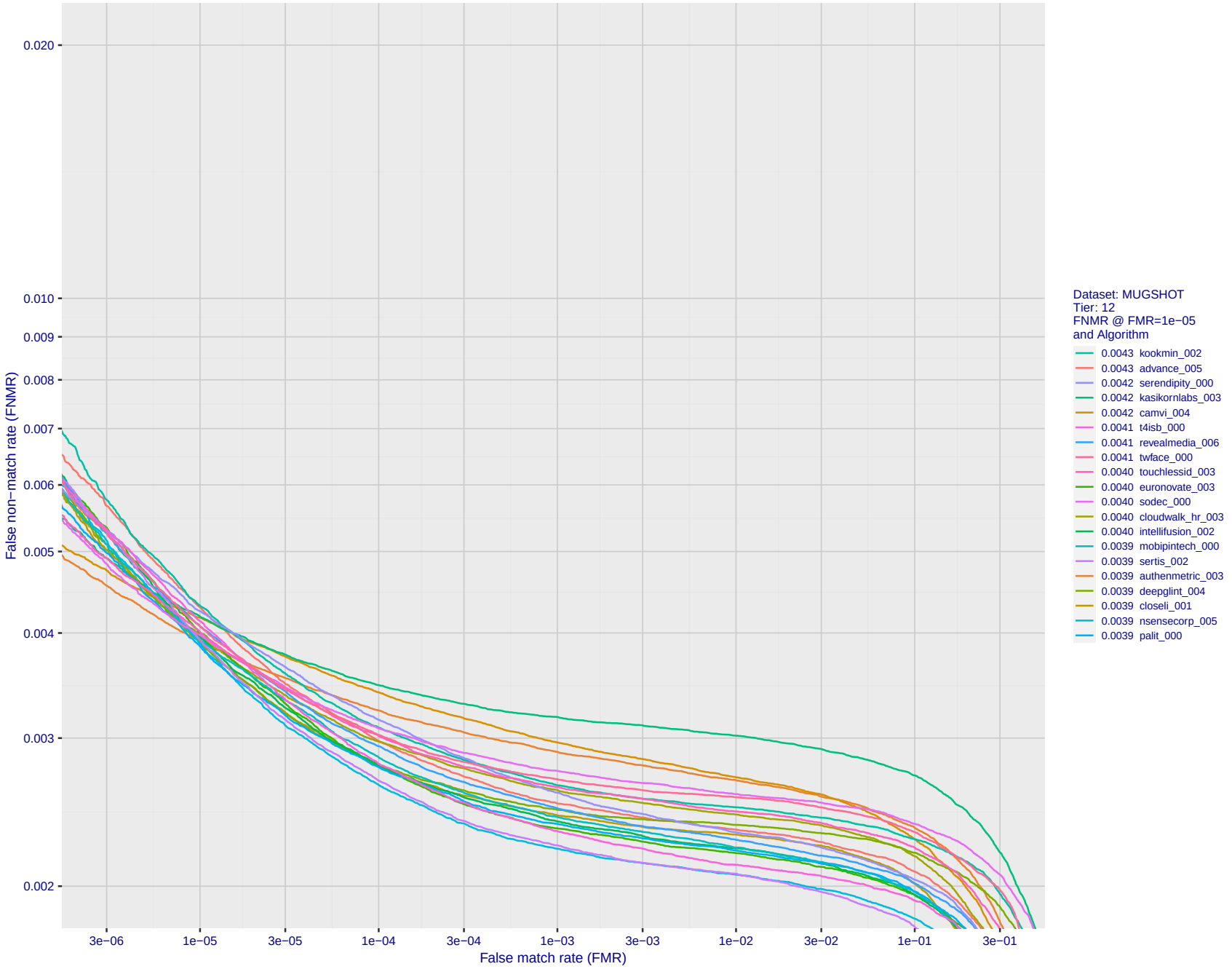

*Figure 118: For the mugshot images, detection error tradeoff (*DET*) characteristics showing false non-match rate vs. false match rate plotted parametrically on threshold, T. The scales are logarithmic in order to show decades of* FMR.

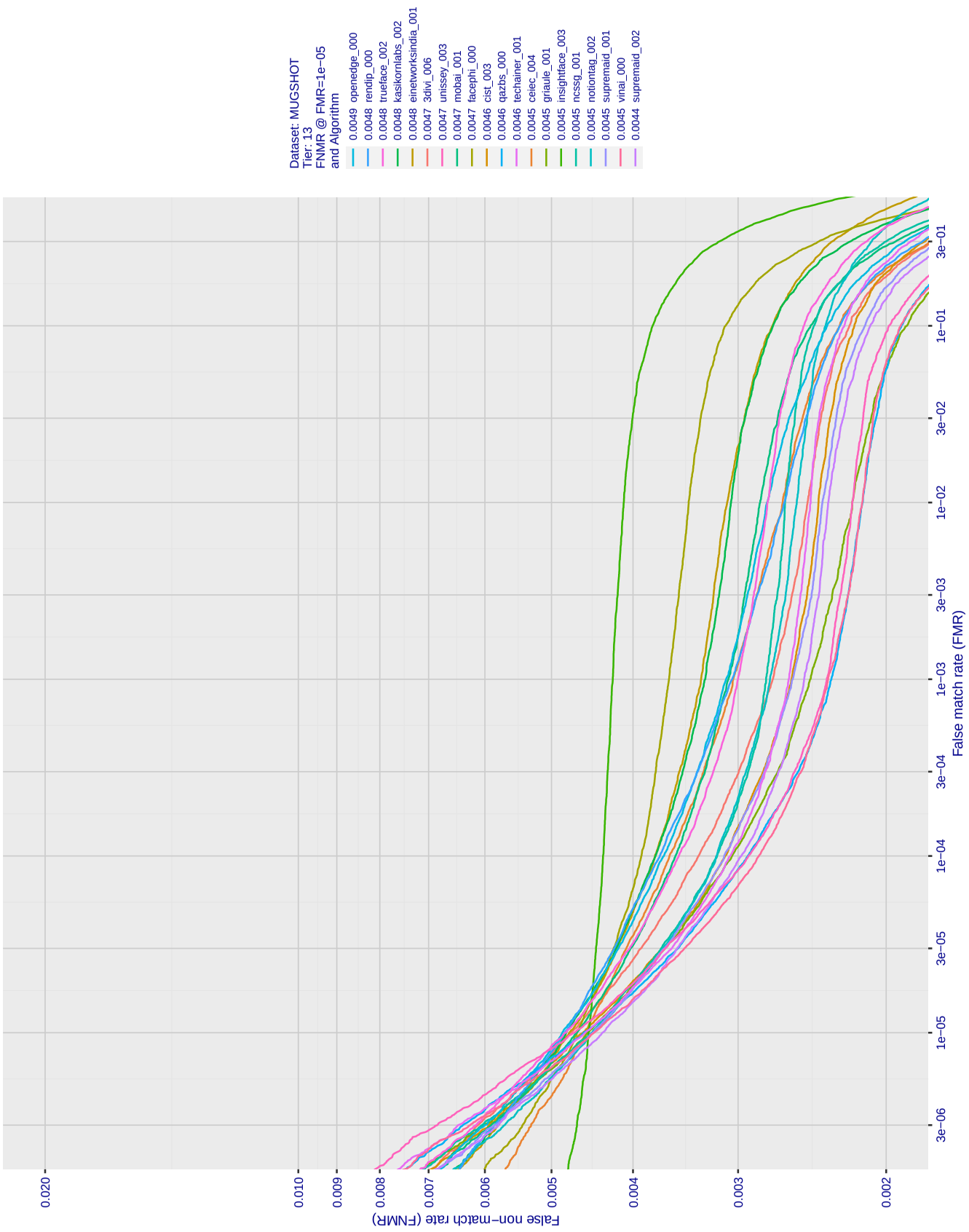

Figure 119: For the mugshot images, detection error tradeoff (DET) characteristics showing false non-match rate vs. false match rate plotted parametrically on threshold, T. The scales are logarithmic in order to show decades of FMR.

FNMR(T) "False non-match rate"
FMR(T) "False match rate"

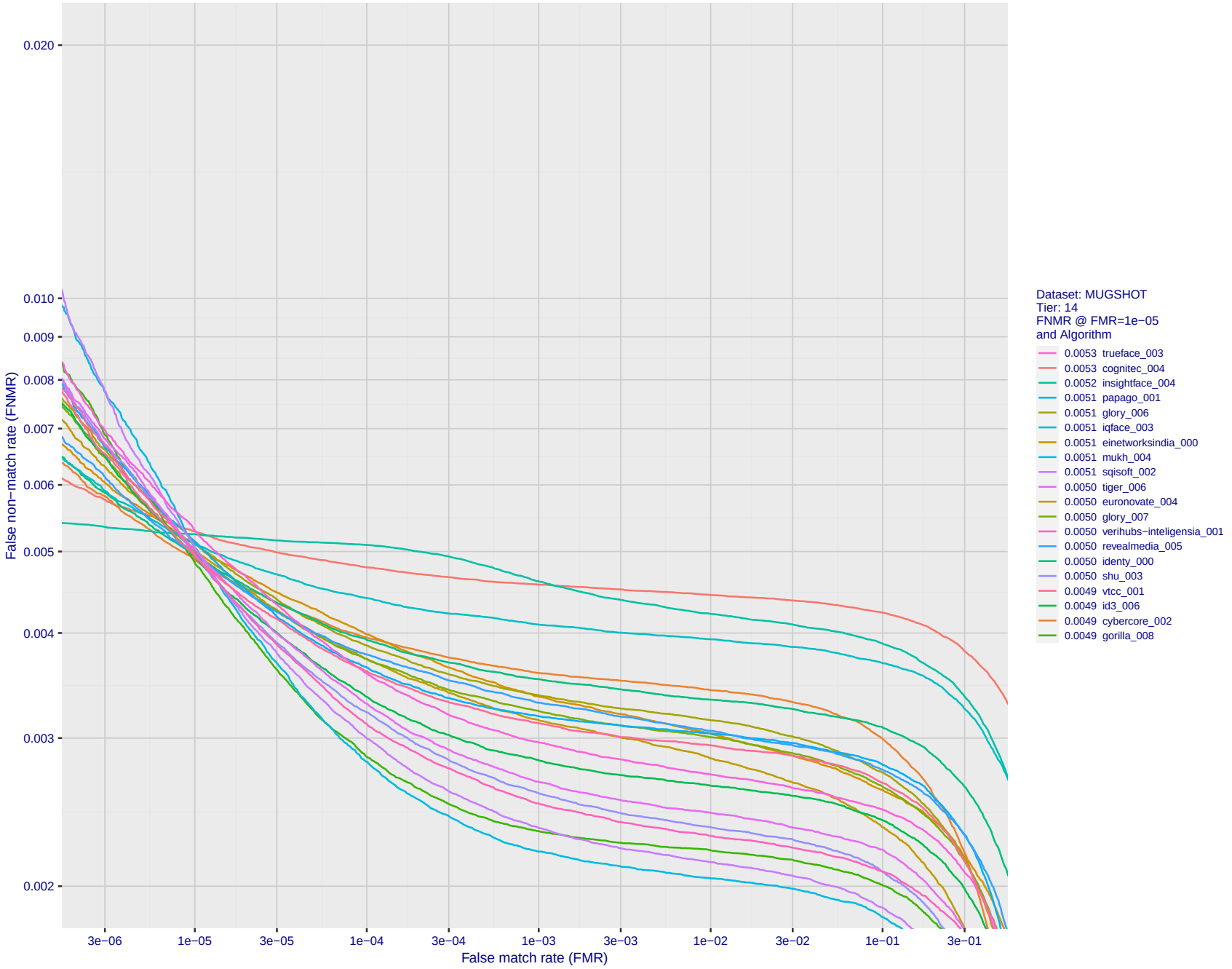

*Figure 120: For the mugshot images, detection error tradeoff (*DET*) characteristics showing false non-match rate vs. false match rate plotted parametrically on threshold, T. The scales are logarithmic in order to show decades of* FMR*.*

FNMR(T) "False non-match rate"
FMR(T) "False match rate"

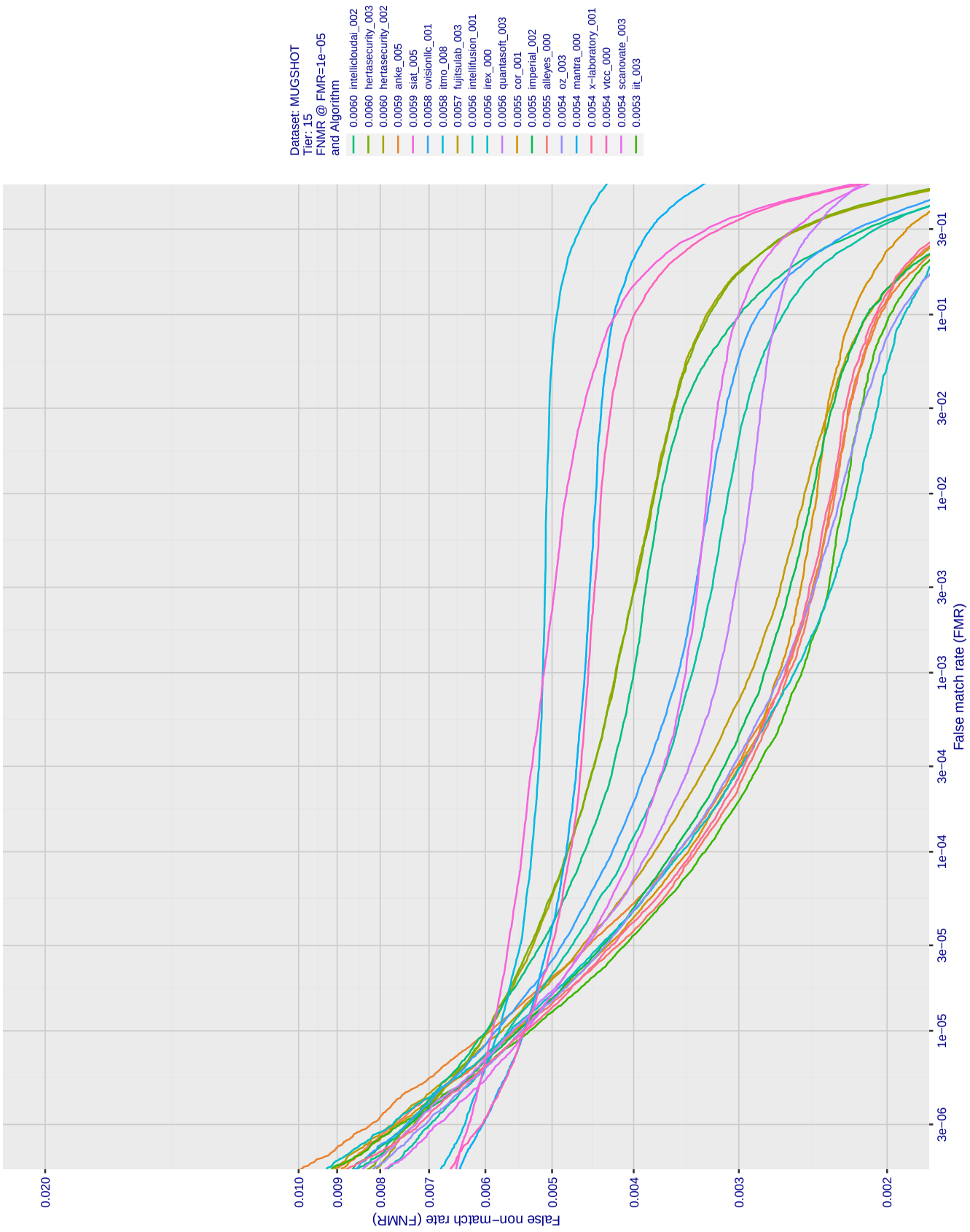

Figure 121: For the mugshot images, detection error tradeoff (DET) characteristics showing false non-match rate vs. false match rate plotted parametrically on threshold, T. The scales are logarithmic in order to show decades of FMR.

FNMR(T) "False non-match rate"
FMR(T) "False match rate"

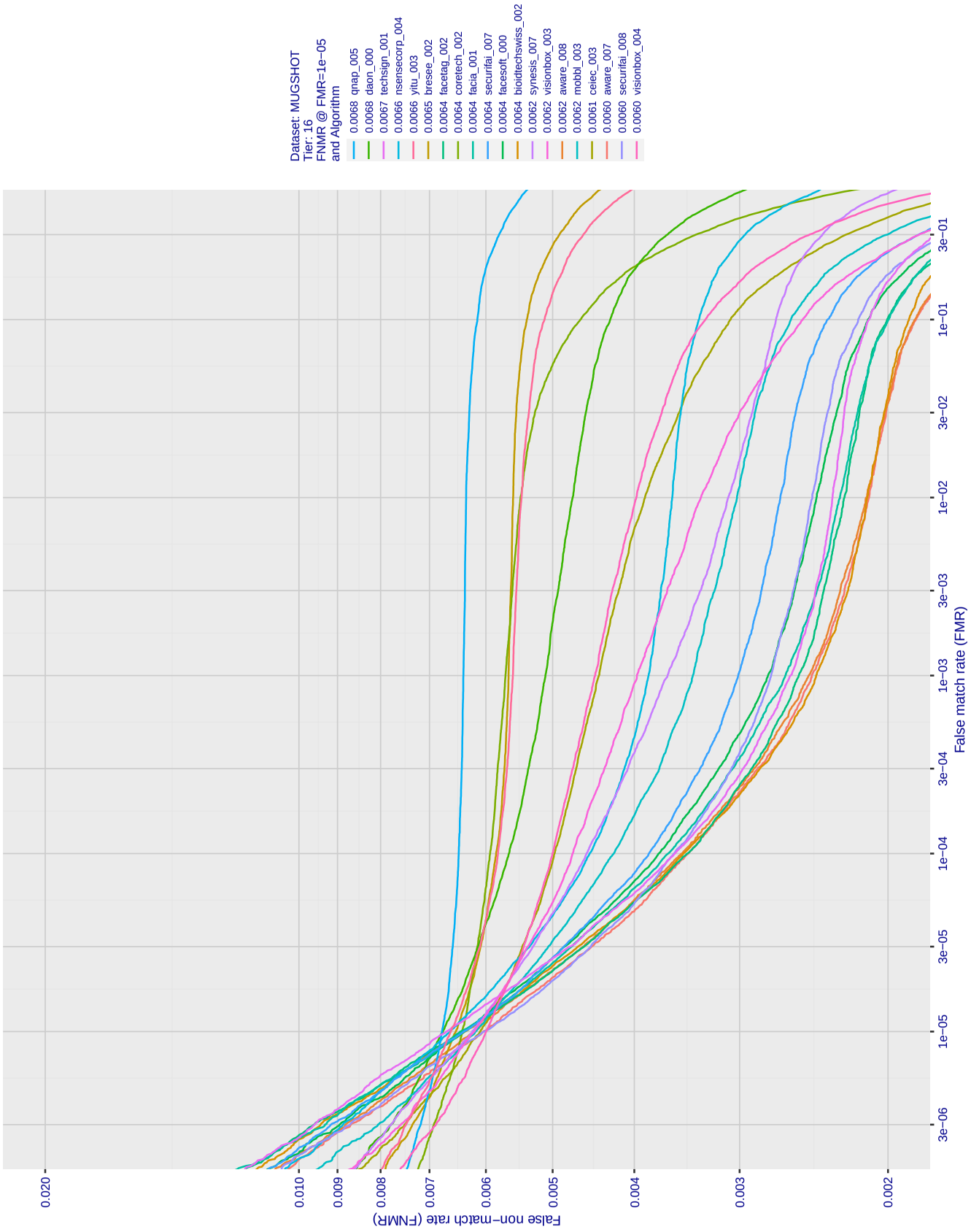

Figure 122: For the mugshot images, detection error tradeoff (DET) characteristics showing false non-match rate vs. false match rate plotted parametrically on threshold, T. The scales are logarithmic in order to show decades of FMR.

FNMR(T) "False non-match rate"
FMR(T) "False match rate"

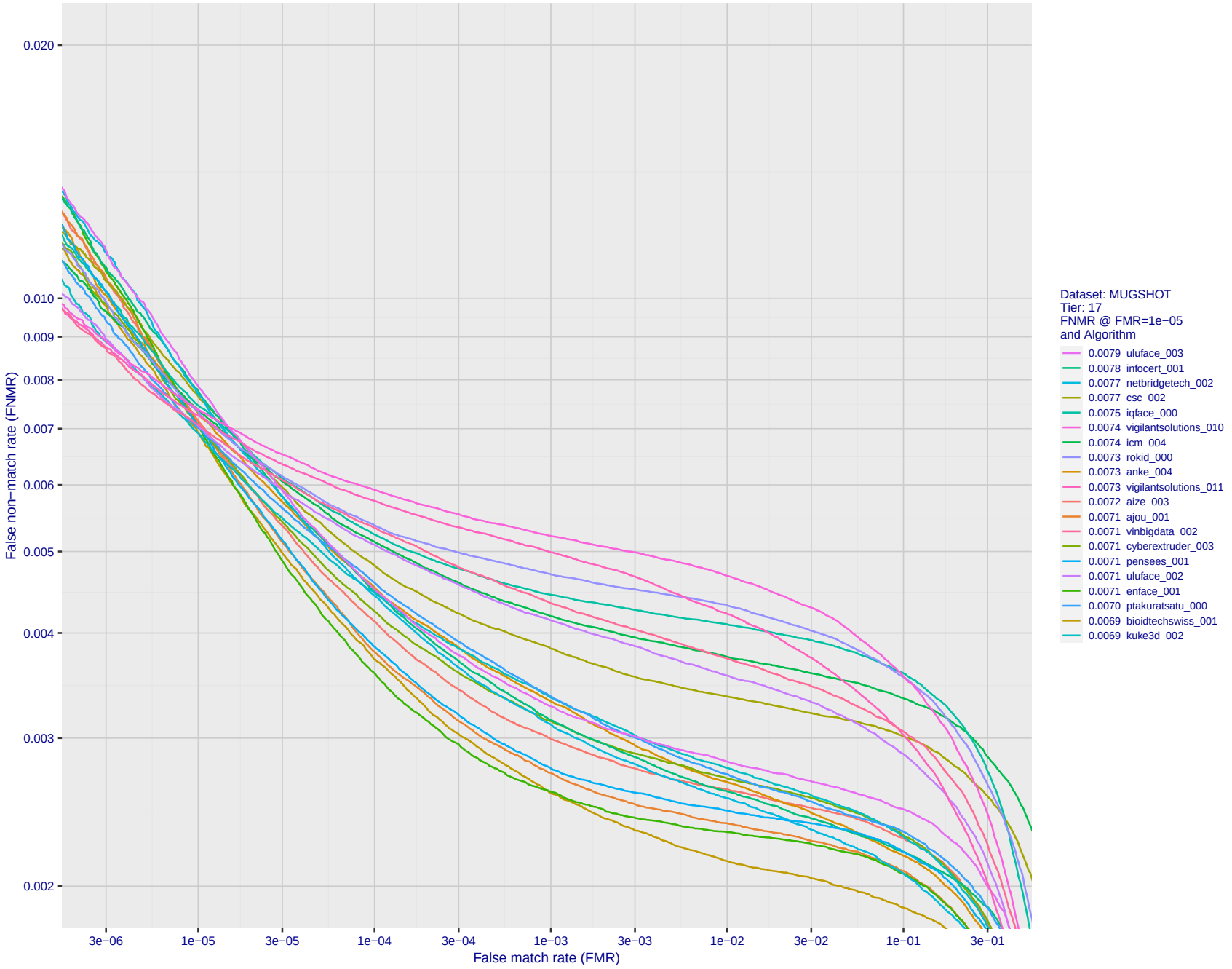

Figure 123: For the mugshot images, detection error tradeoff (DET) characteristics showing false non-match rate vs. false match rate plotted parametrically on threshold, T. The scales are logarithmic in order to show decades of FMR.

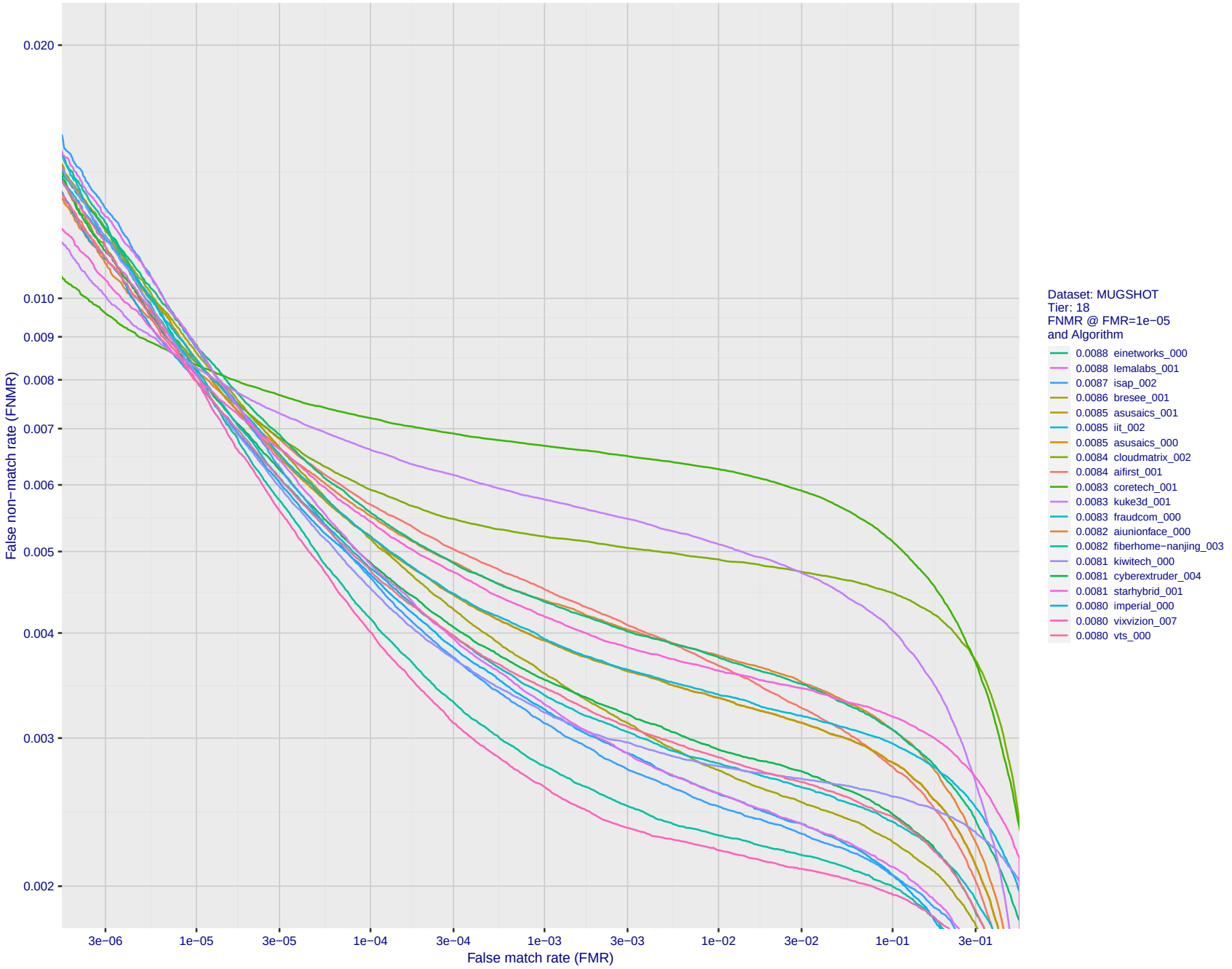

Figure 124: For the mugshot images, detection error tradeoff (DET) characteristics showing false non-match rate vs. false match rate plotted parametrically on threshold, T. The scales are logarithmic in order to show decades of FMR.

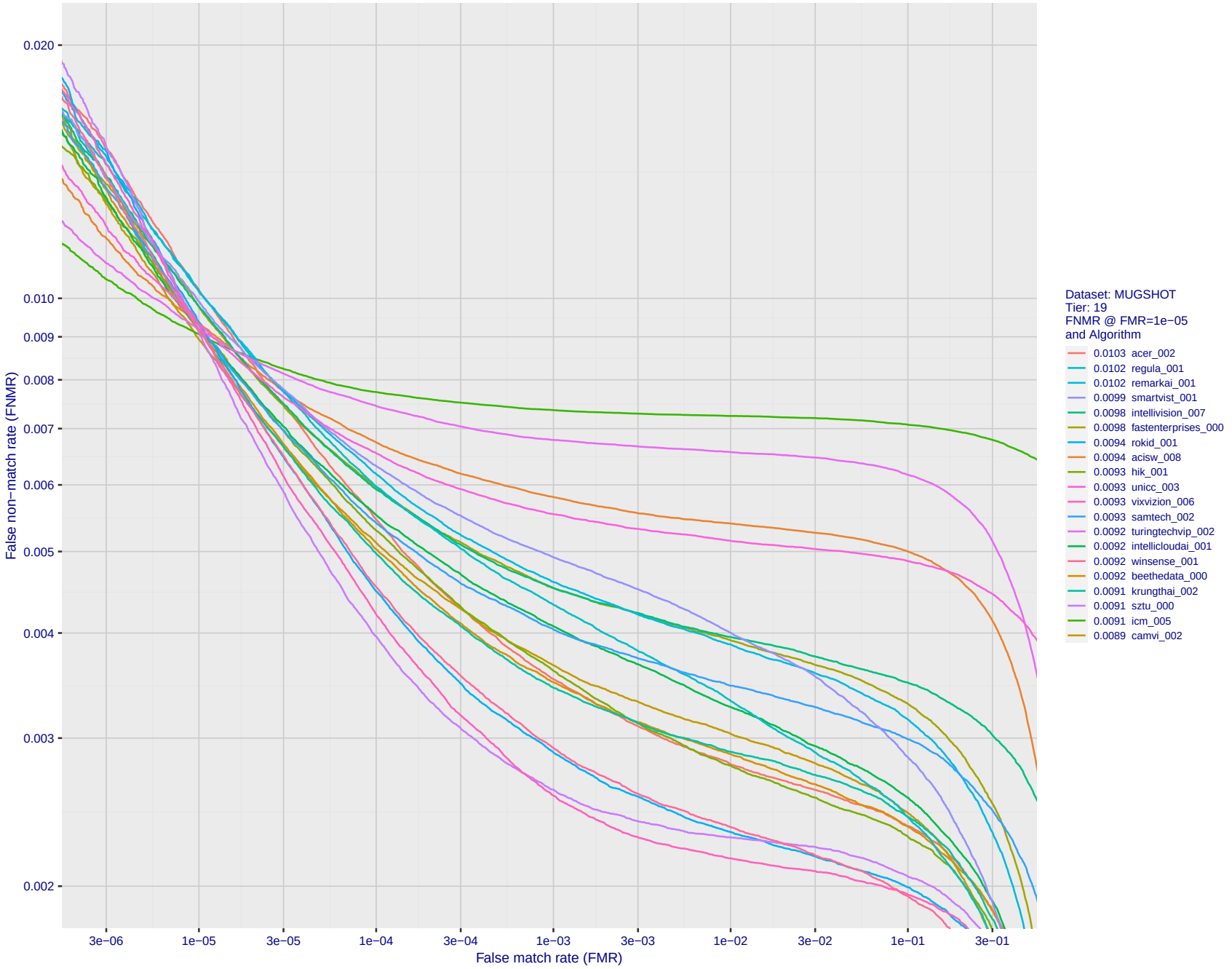

Figure 125: For the mugshot images, detection error tradeoff (DET) characteristics showing false non-match rate vs. false match rate plotted parametrically on threshold, T. The scales are logarithmic in order to show decades of FMR.

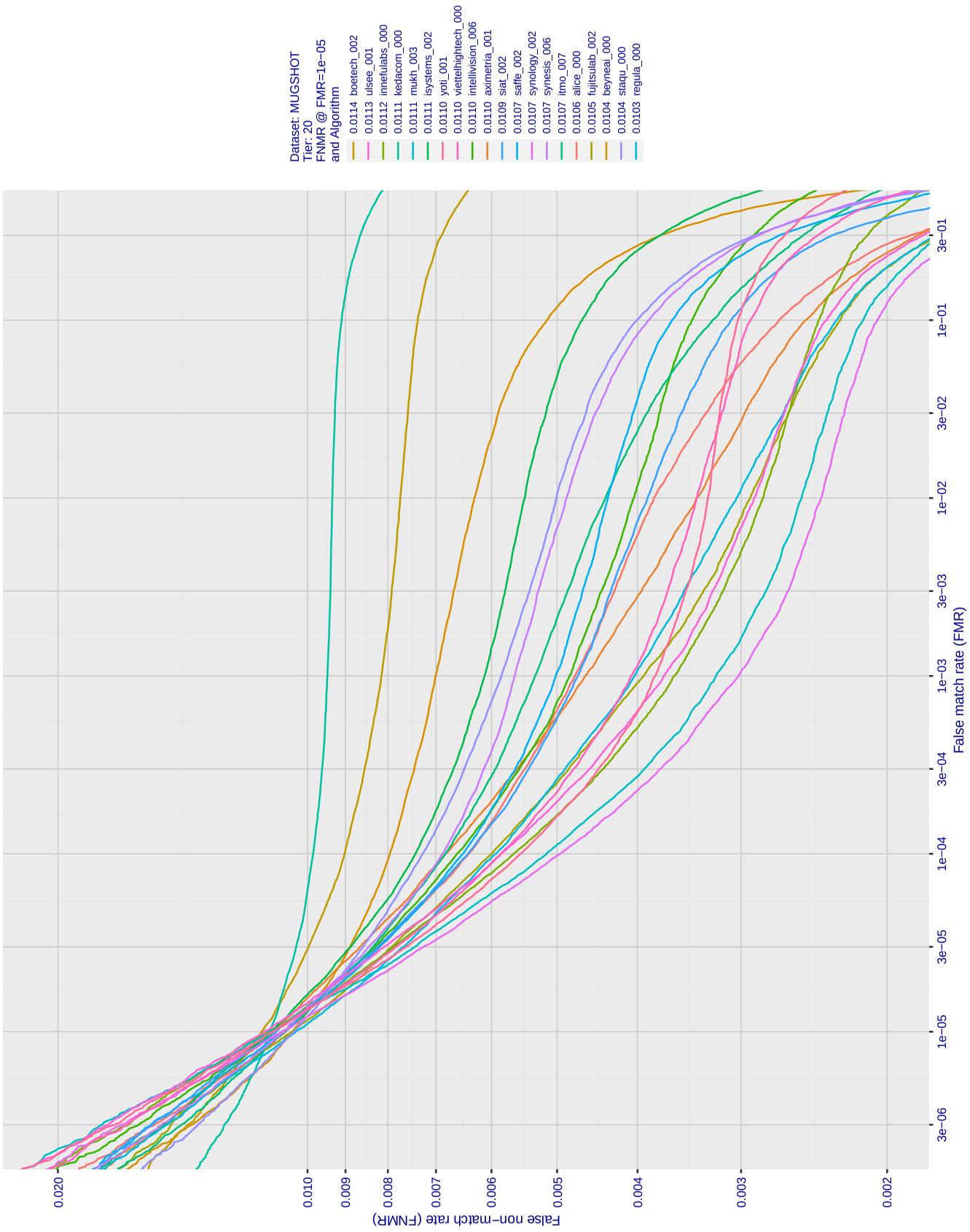

Figure 126: For the mugshot images, detection error tradeoff (DET) characteristics showing false non-match rate vs. false match rate plotted parametrically on threshold, T. The scales are logarithmic in order to show decades of FMR.

FNMR(T) "False non-match rate"
FMR(T) "False match rate"

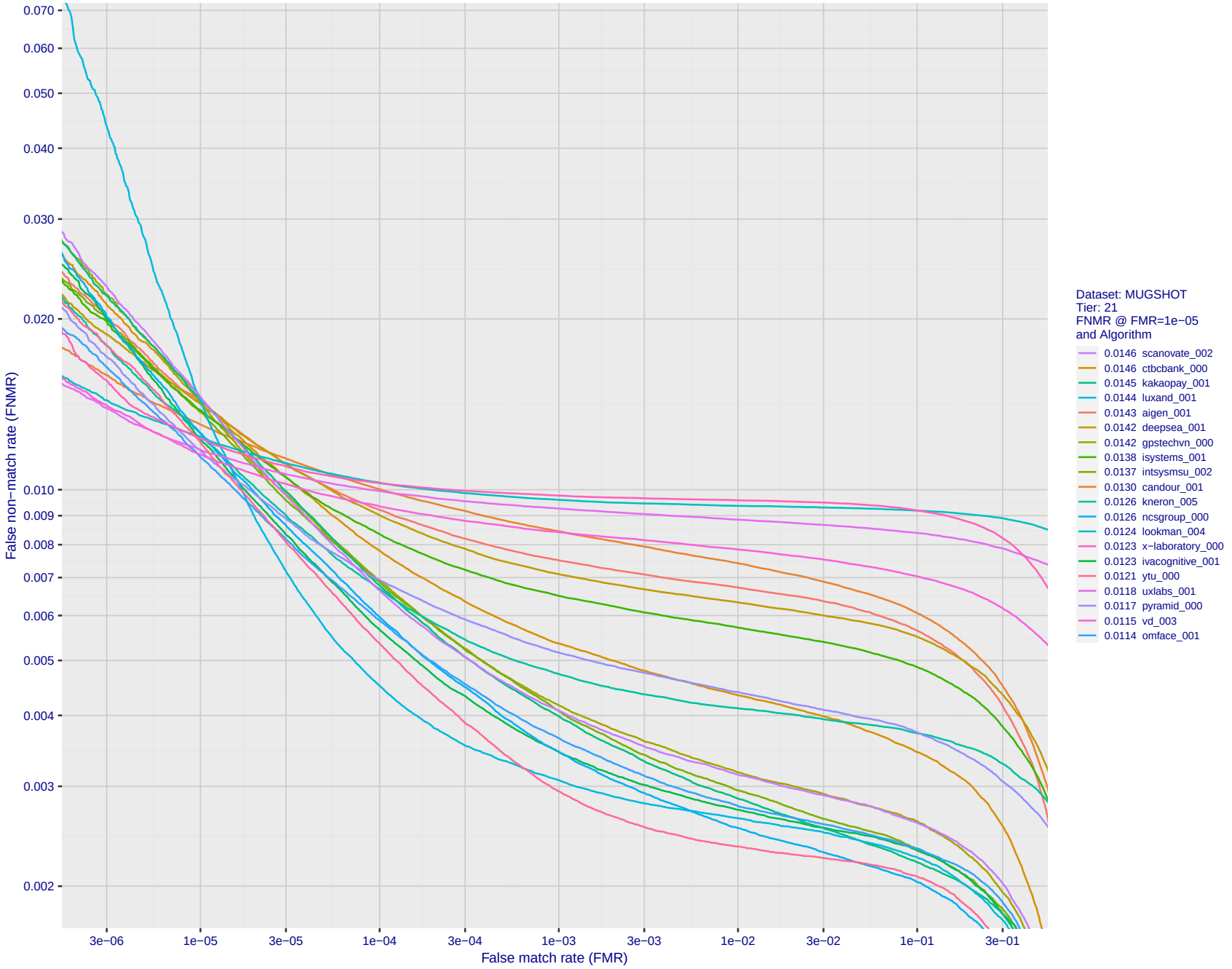

Figure 127: For the mugshot images, detection error tradeoff (DET) characteristics showing false non-match rate vs. false match rate plotted parametrically on threshold, T. The scales are logarithmic in order to show decades of FMR.

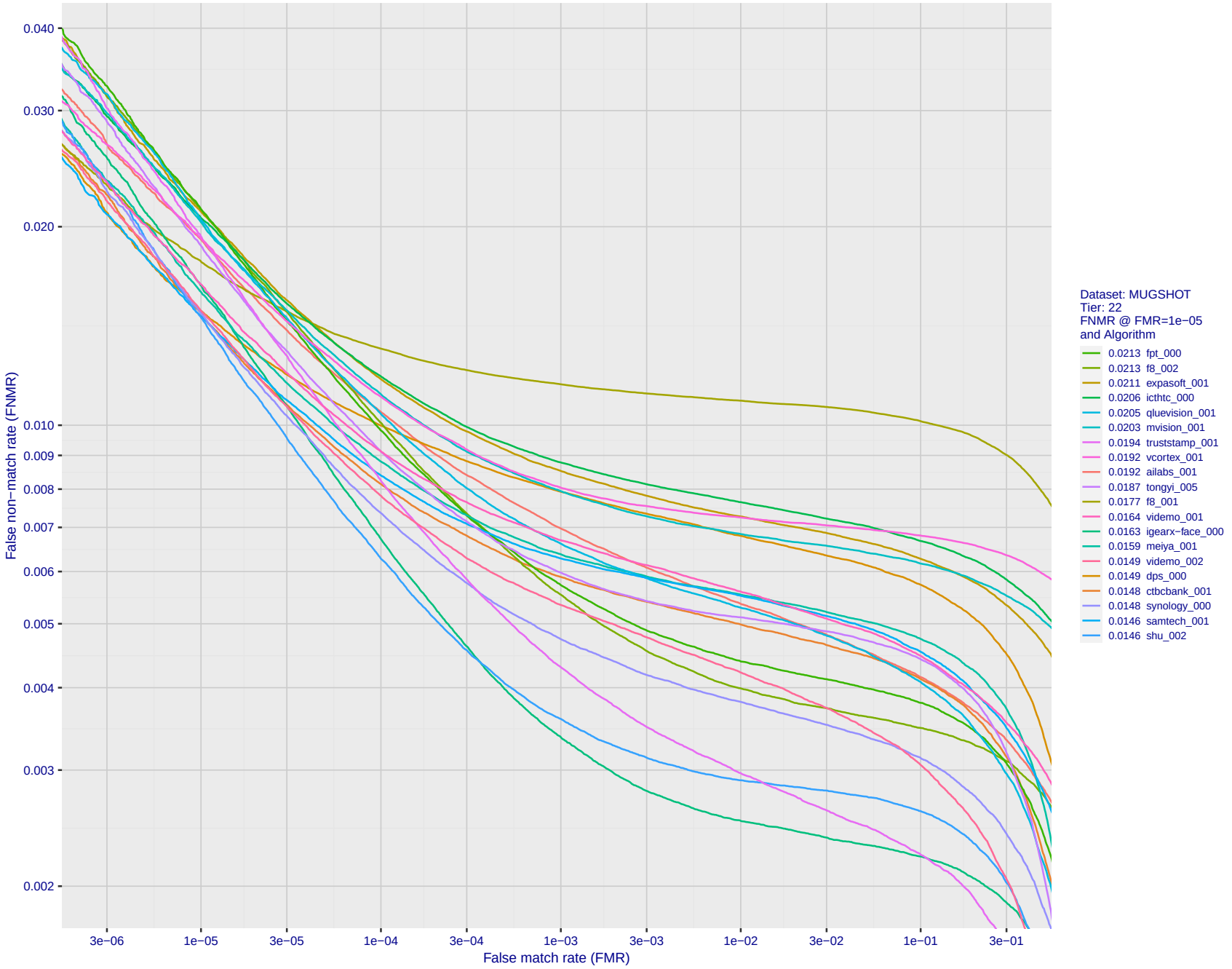

*Figure 128: For the mugshot images, detection error tradeoff (*DET*) characteristics showing false non-match rate vs. false match rate plotted parametrically on threshold, T. The scales are logarithmic in order to show decades of* FMR.

FNMR(T) "False non-match rate"
FMR(T) "False match rate"

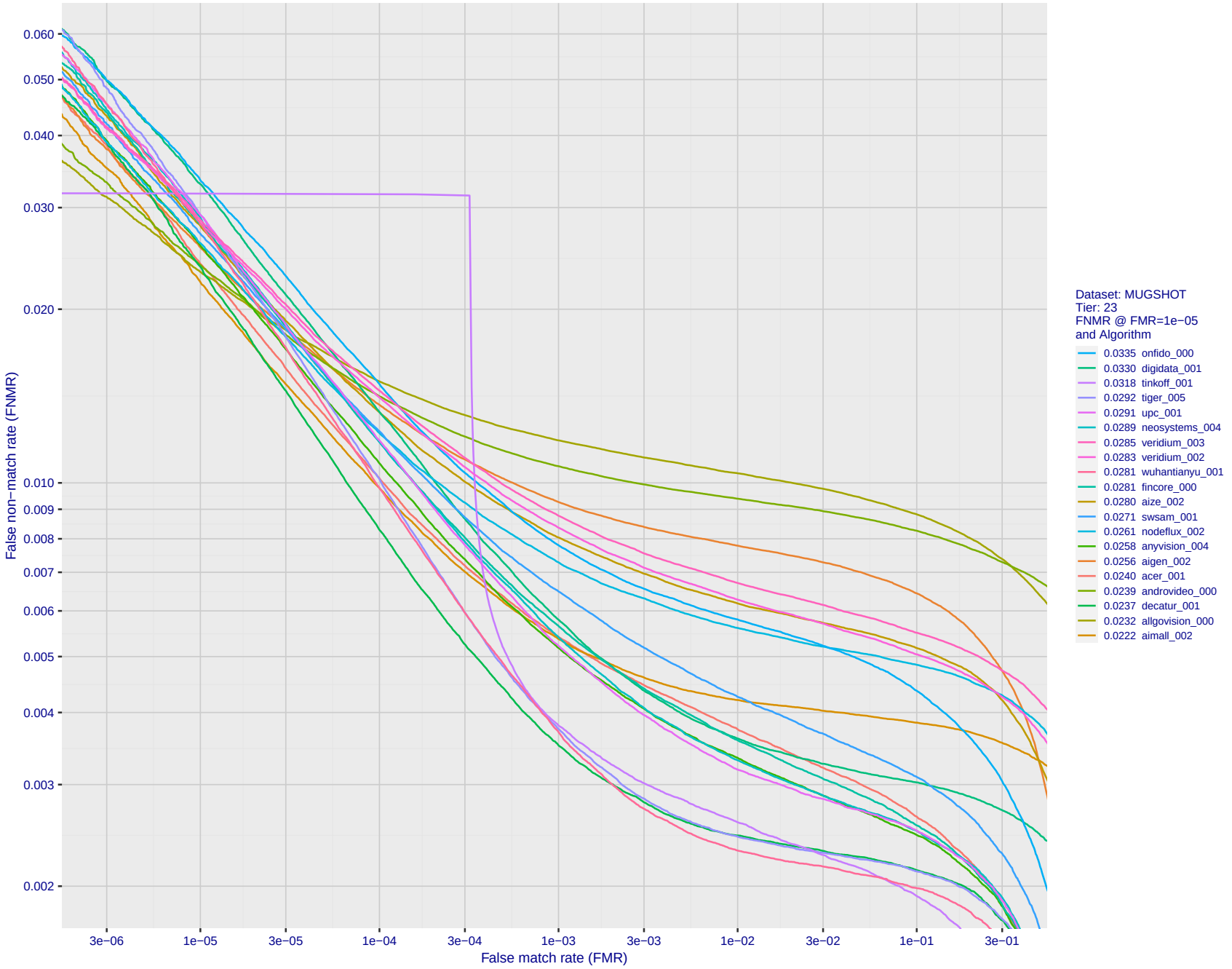

Figure 129: For the mugshot images, detection error tradeoff (DET) characteristics showing false non-match rate vs. false match rate plotted parametrically on threshold, T. The scales are logarithmic in order to show decades of FMR.

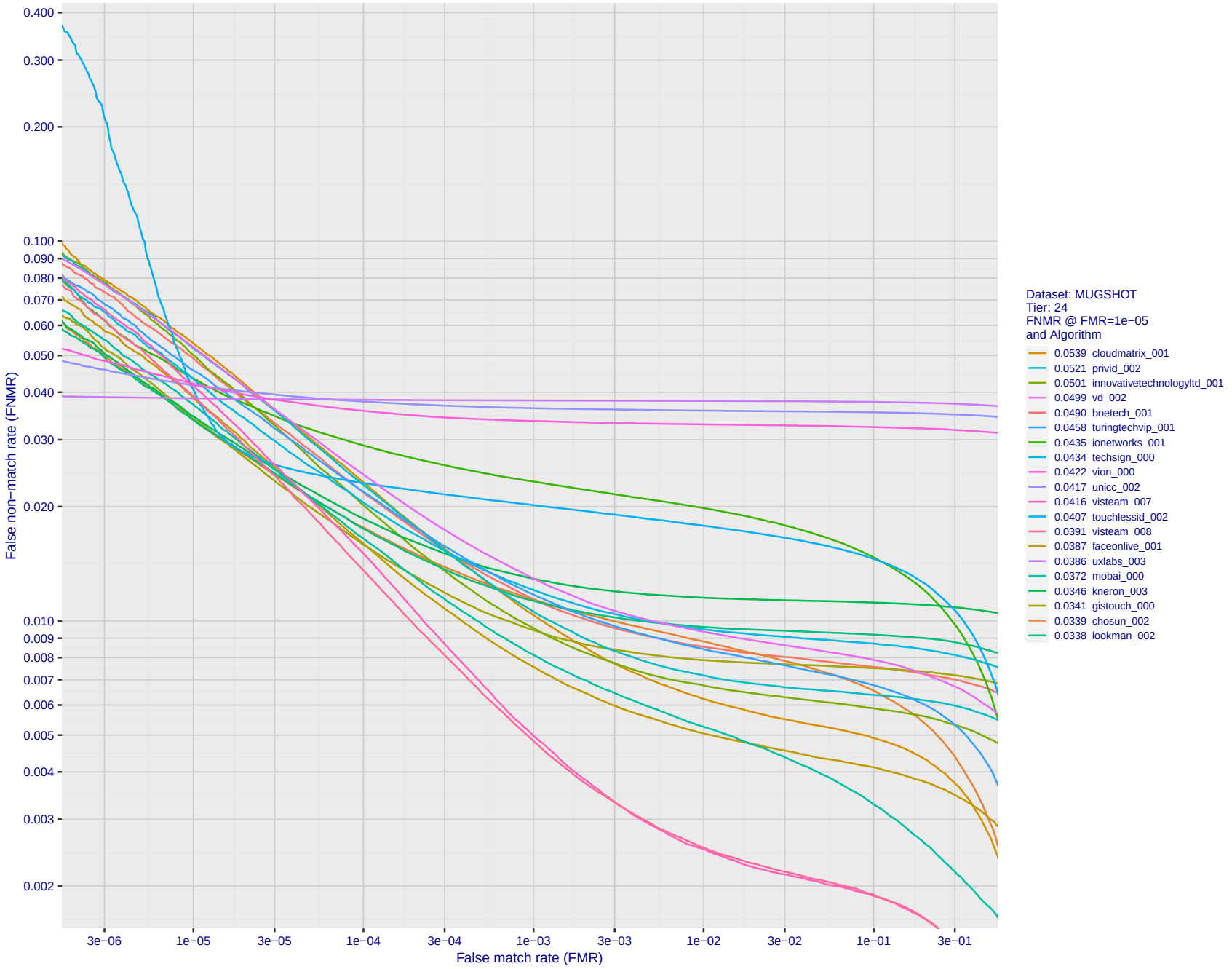

Figure 130: For the mugshot images, detection error tradeoff (DET) characteristics showing false non-match rate vs. false match rate plotted parametrically on threshold, T. The scales are logarithmic in order to show decades of FMR.

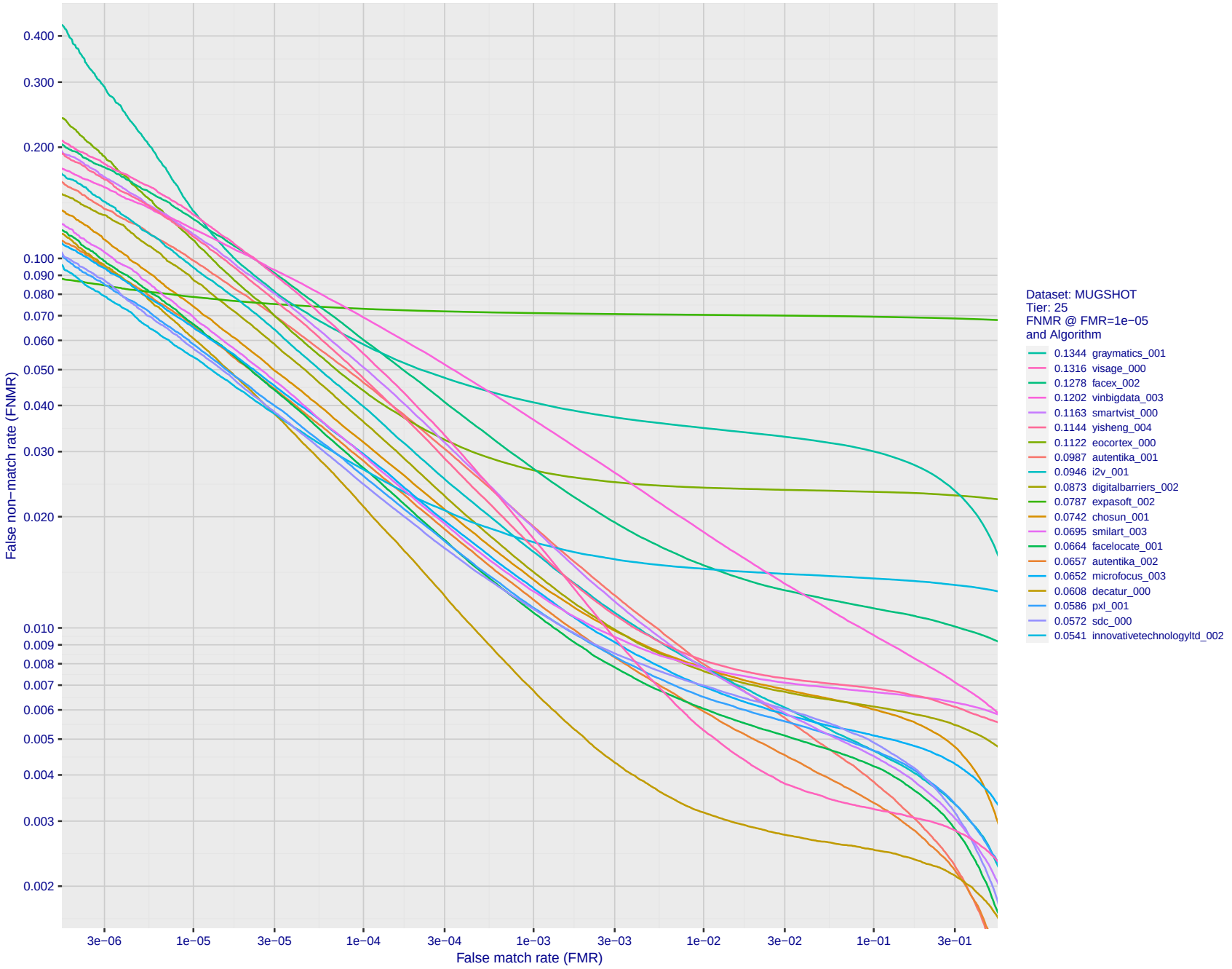

Figure 131: For the mugshot images, detection error tradeoff (DET) characteristics showing false non-match rate vs. false match rate plotted parametrically on threshold, T. The scales are logarithmic in order to show decades of FMR.

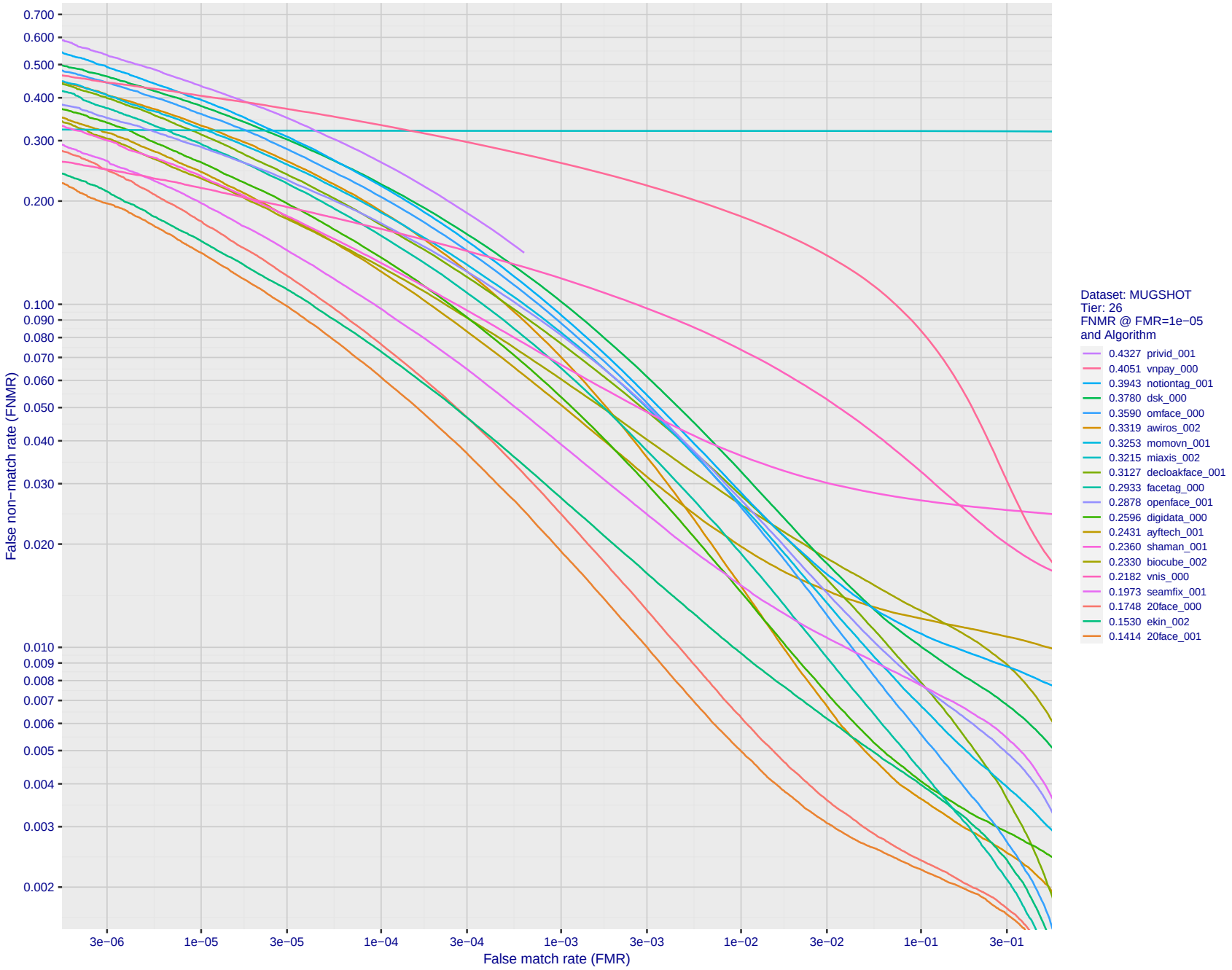

*Figure 132: For the mugshot images, detection error tradeoff (*DET*) characteristics showing false non-match rate vs. false match rate plotted parametrically on threshold, T. The scales are logarithmic in order to show decades of* FMR.

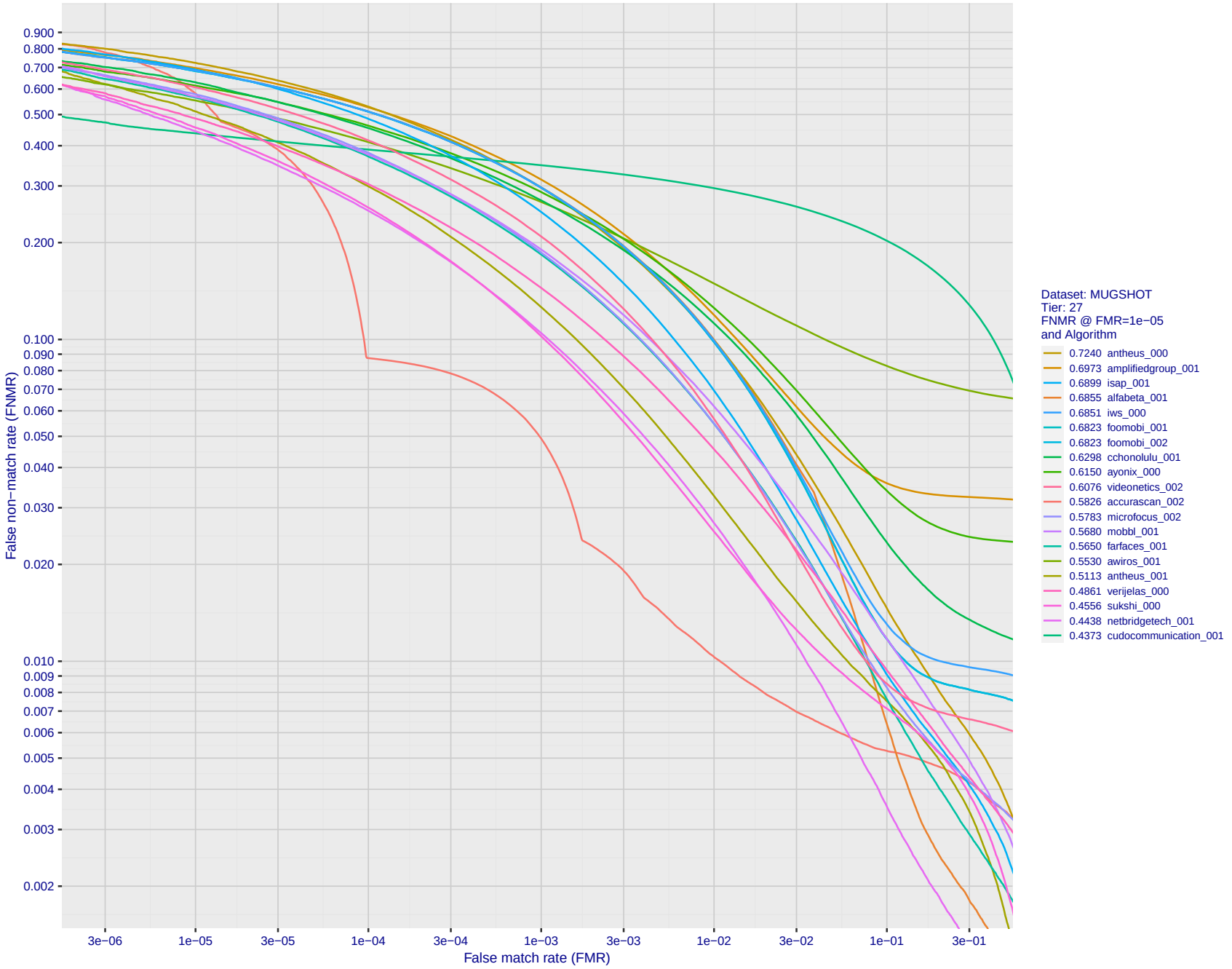

Figure 133: For the mugshot images, detection error tradeoff (DET) characteristics showing false non-match rate vs. false match rate plotted parametrically on threshold, T. The scales are logarithmic in order to show decades of FMR.

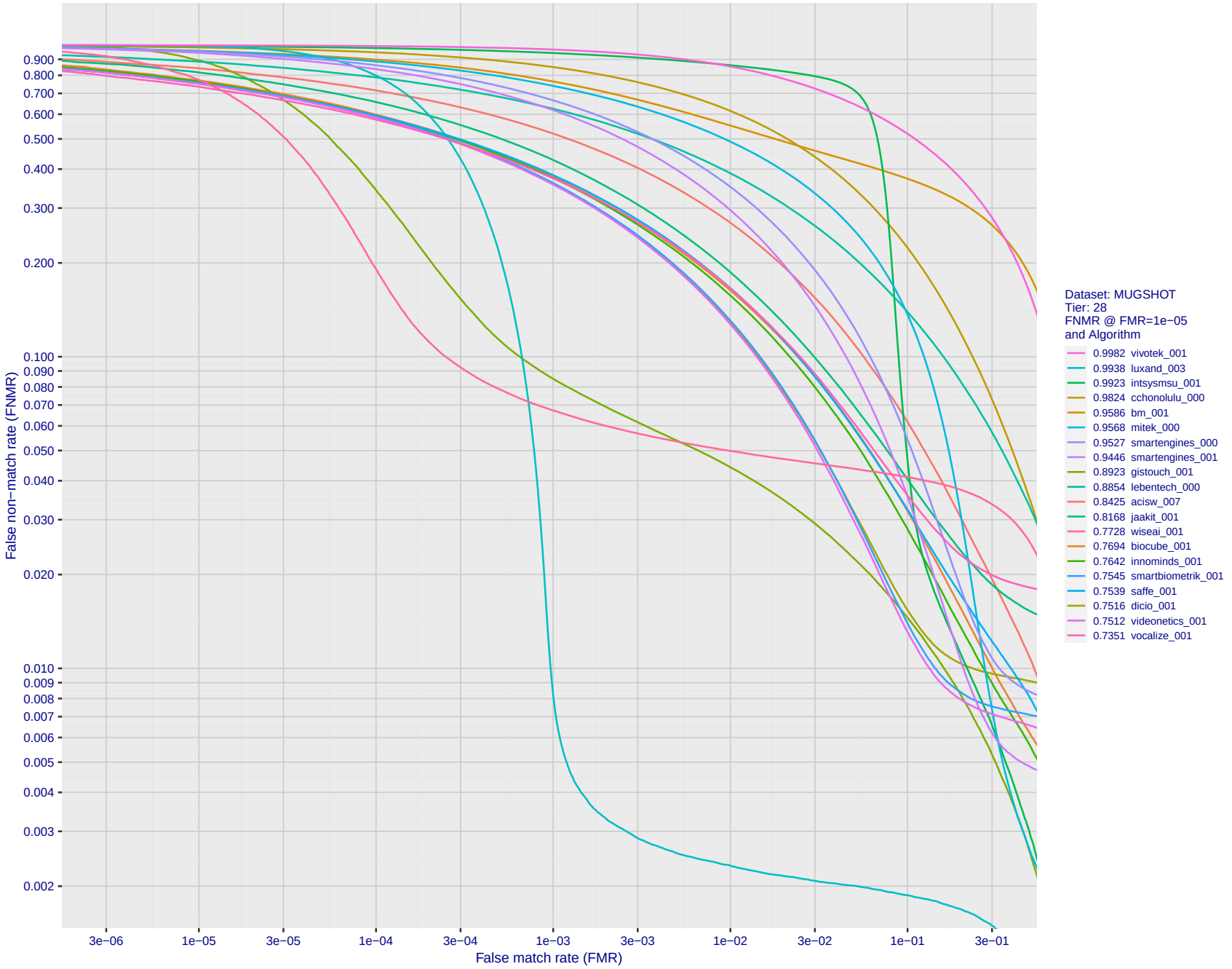

Figure 134: For the mugshot images, detection error tradeoff (DET) characteristics showing false non-match rate vs. false match rate plotted parametrically on threshold, T. The scales are logarithmic in order to show decades of FMR.

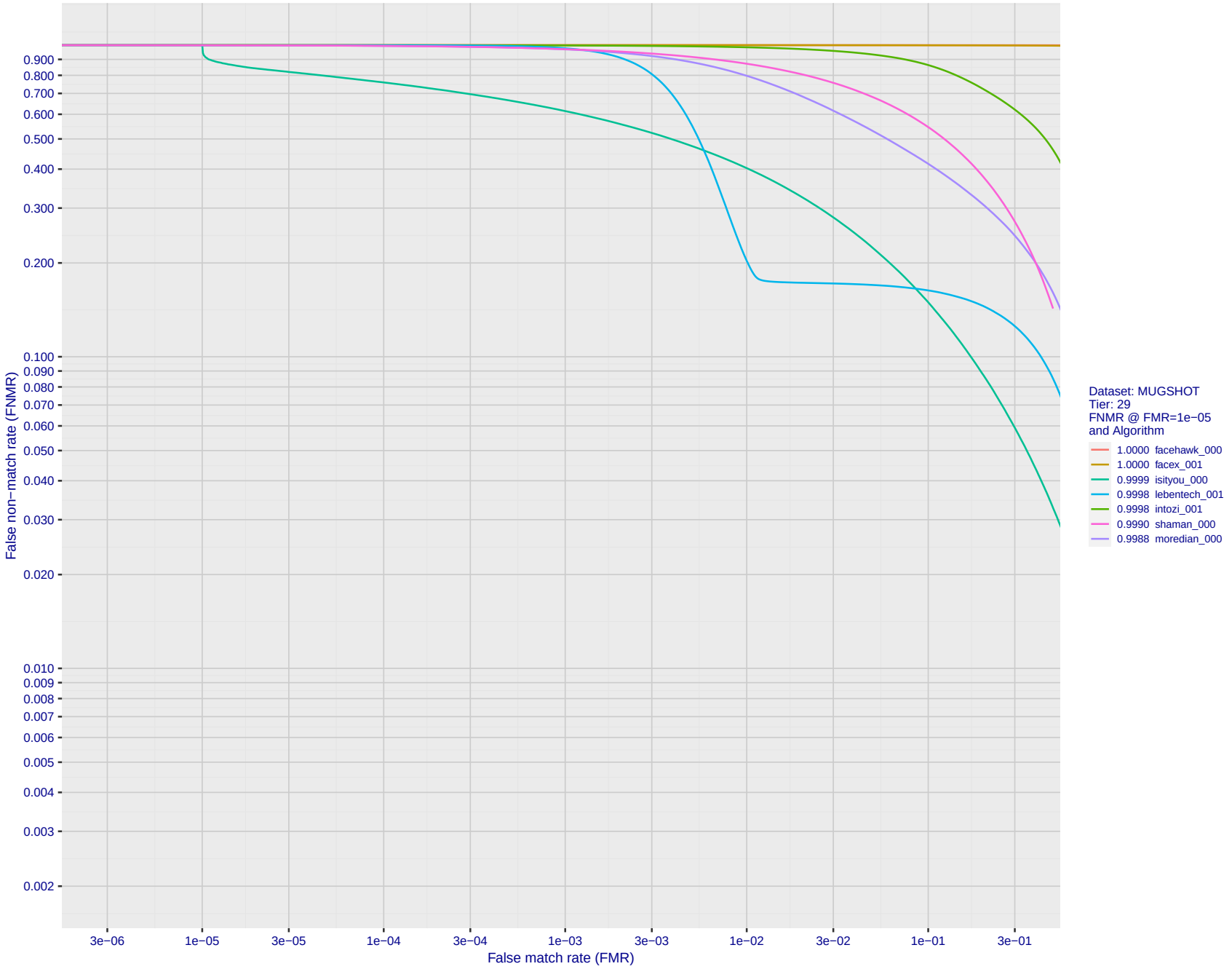

Figure 135: For the mugshot images, detection error tradeoff (DET) characteristics showing false non-match rate vs. false match rate plotted parametrically on threshold, T. The scales are logarithmic in order to show decades of FMR.

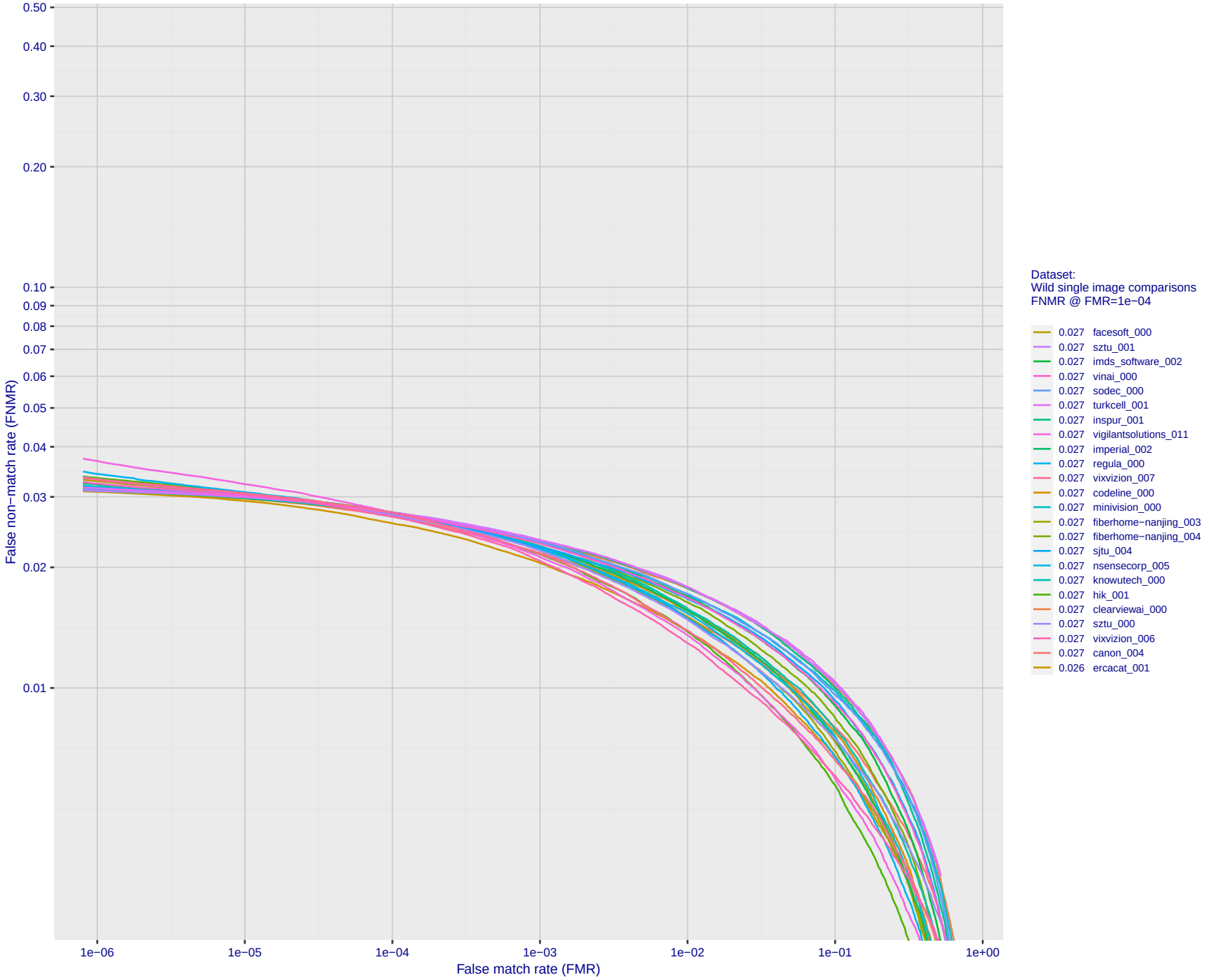

Figure 136: For the 2018 wild image comparisons, detection error tradeoff (DET) characteristics showing false non-match rate vs. false match rate plotted parametrically on threshold, T. The scales are logarithmic in order to show several decades of FMR.

2024/04/17 08:45:50 FNMR(T) "False non-match rate" FMR(T) "False match rate"

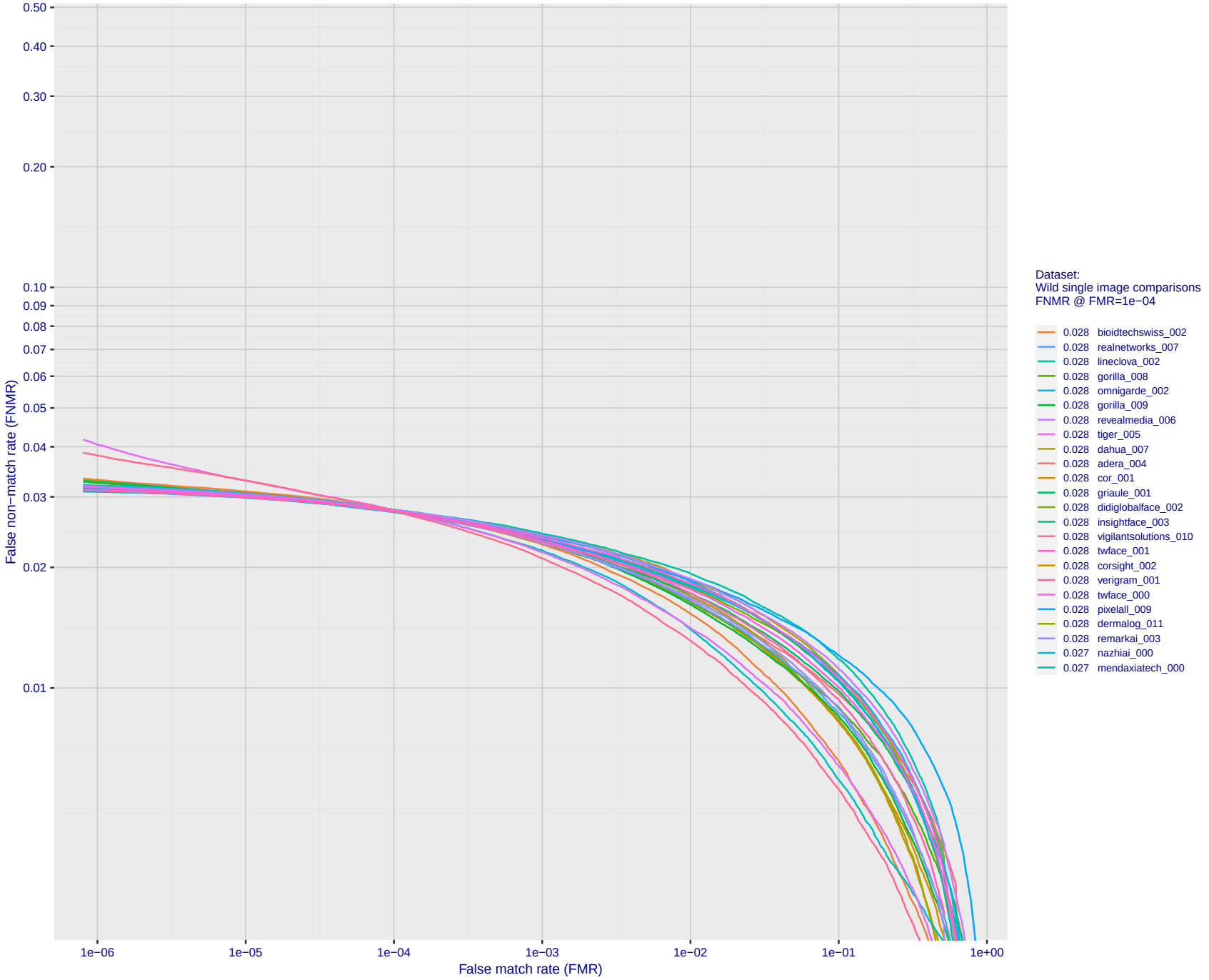

Figure 137: For the 2018 wild image comparisons, detection error tradeoff (DET) characteristics showing false non-match rate vs. false match rate plotted parametrically on threshold, T. The scales are logarithmic in order to show several decades of FMR.

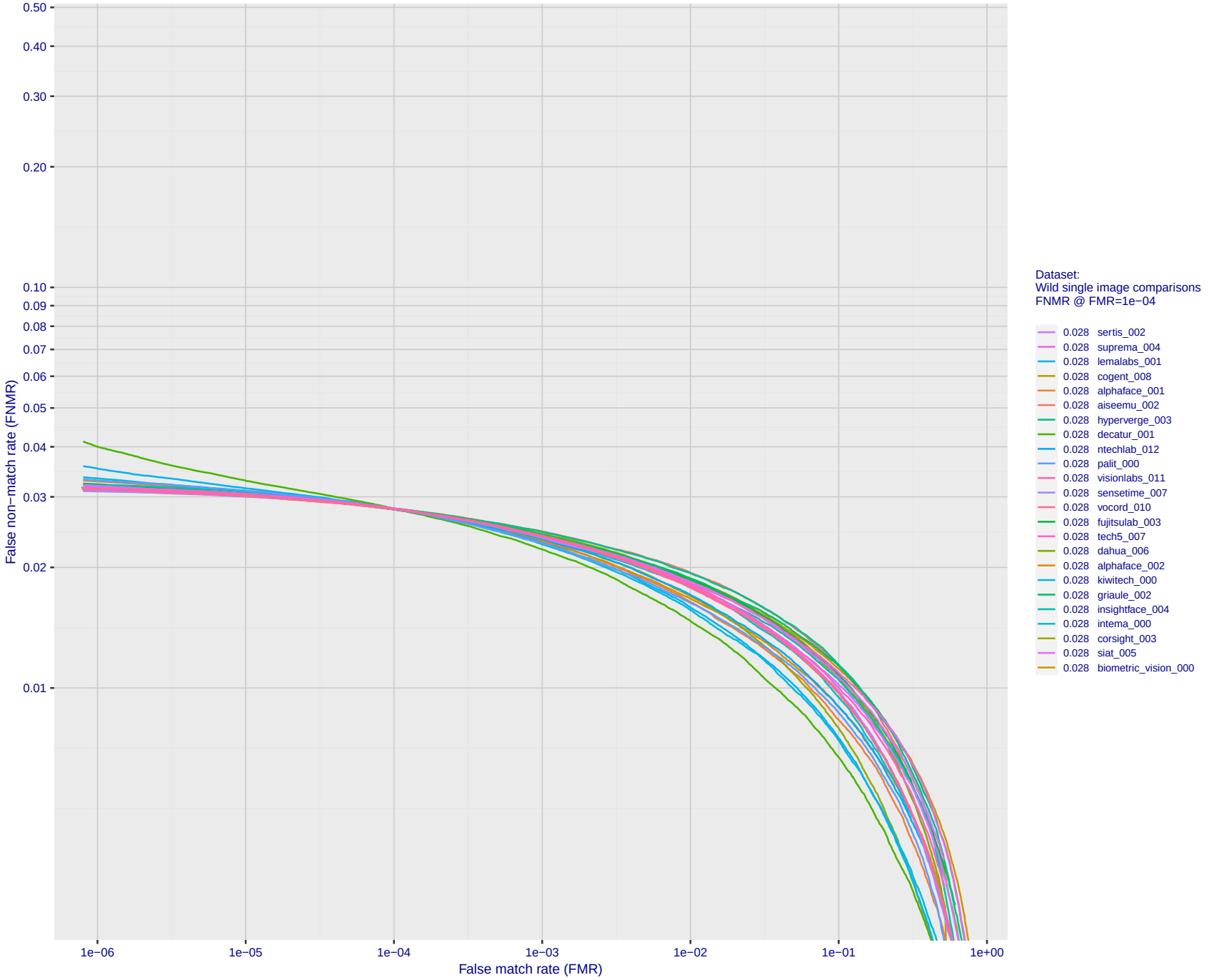

Figure 138: For the 2018 wild image comparisons, detection error tradeoff (DET) characteristics showing false non-match rate vs. false match rate plotted parametrically on threshold, T. The scales are logarithmic in order to show several decades of FMR.

FNMR(T) "False non-match rate"
FMR(T) "False match rate"

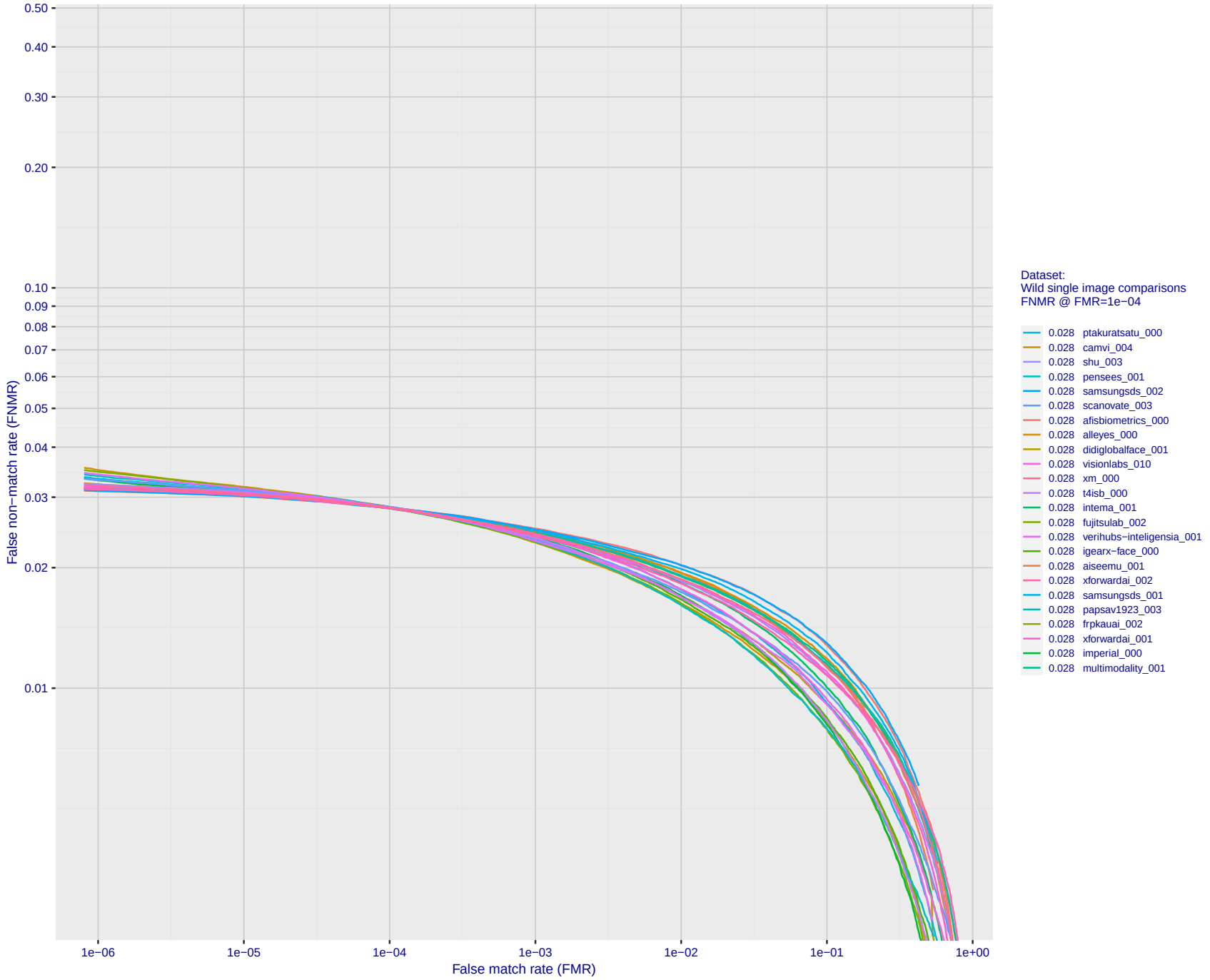

Figure 139: For the 2018 wild image comparisons, detection error tradeoff (DET) characteristics showing false non-match rate vs. false match rate plotted parametrically on threshold, T. The scales are logarithmic in order to show several decades of FMR.

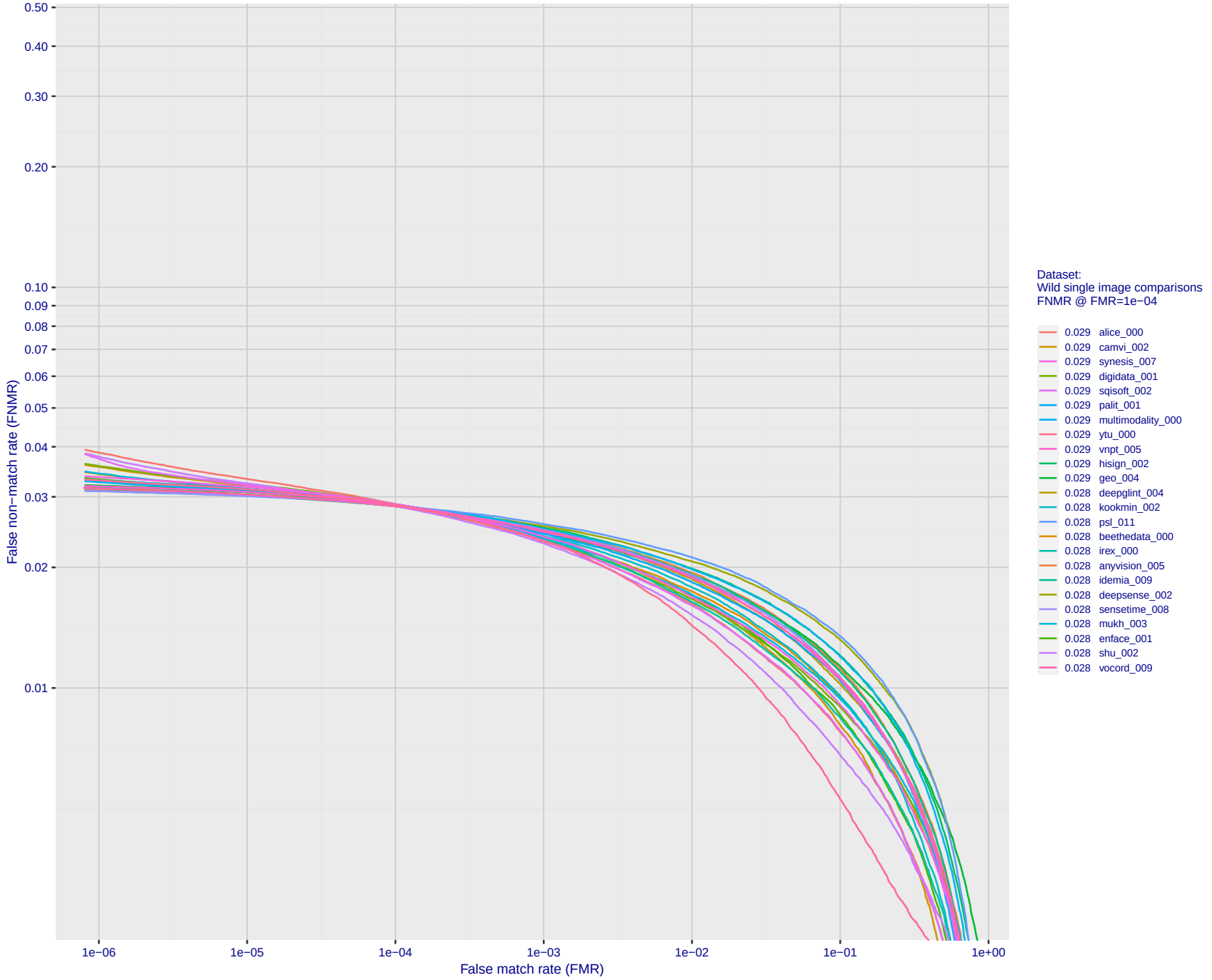

Figure 140: For the 2018 wild image comparisons, detection error tradeoff (DET) characteristics showing false non-match rate vs. false match rate plotted parametrically on threshold, T. The scales are logarithmic in order to show several decades of FMR.

2024/04/17 08:45:50 FNMR(T) "False non-match rate" FMR(T) "False match rate"

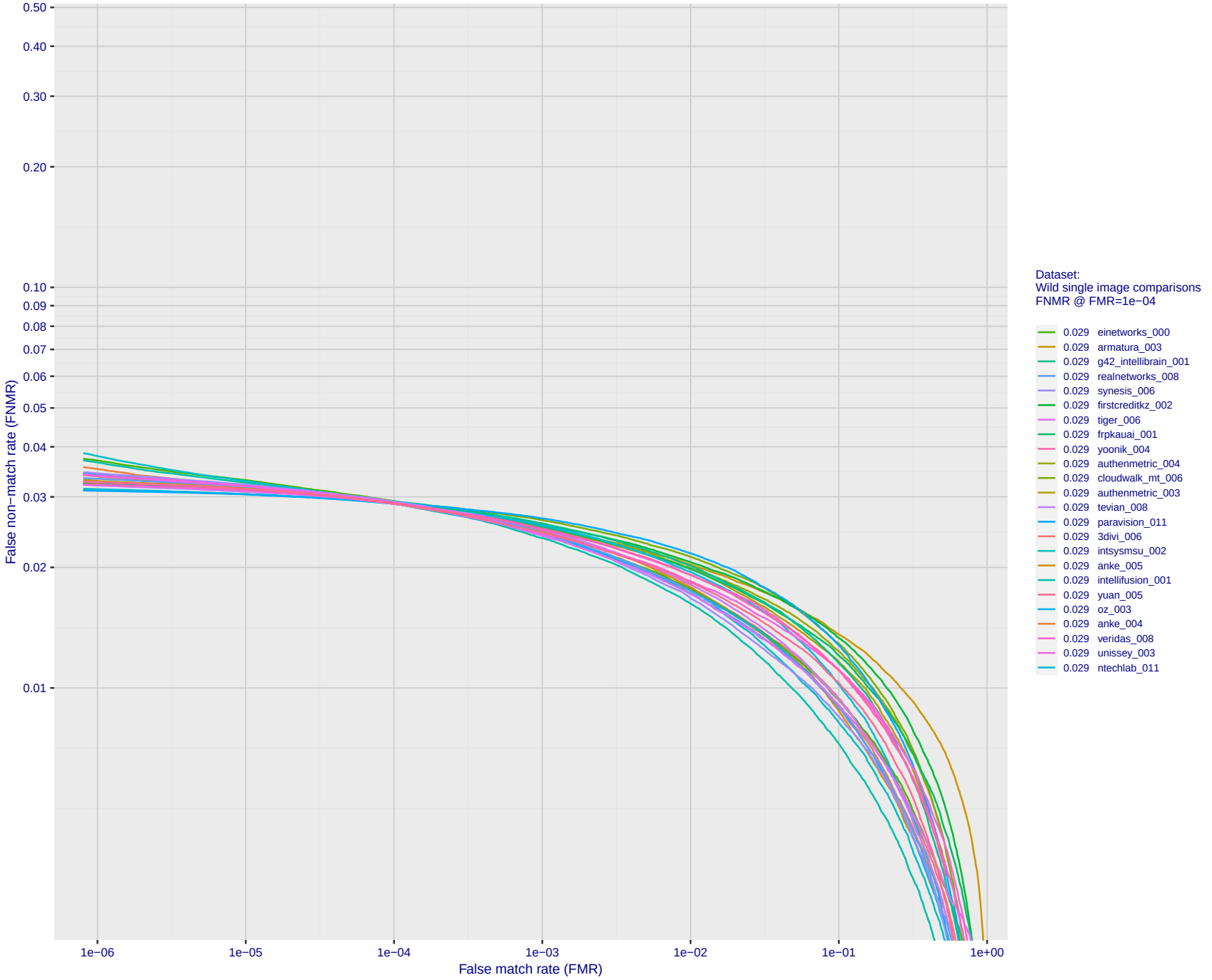

Figure 141: For the 2018 wild image comparisons, detection error tradeoff (DET) characteristics showing false non-match rate vs. false match rate plotted parametrically on threshold, T. The scales are logarithmic in order to show several decades of FMR.

2024/04/17 08:45:50 FNMR(T) "False non-match rate" FMR(T) "False match rate"

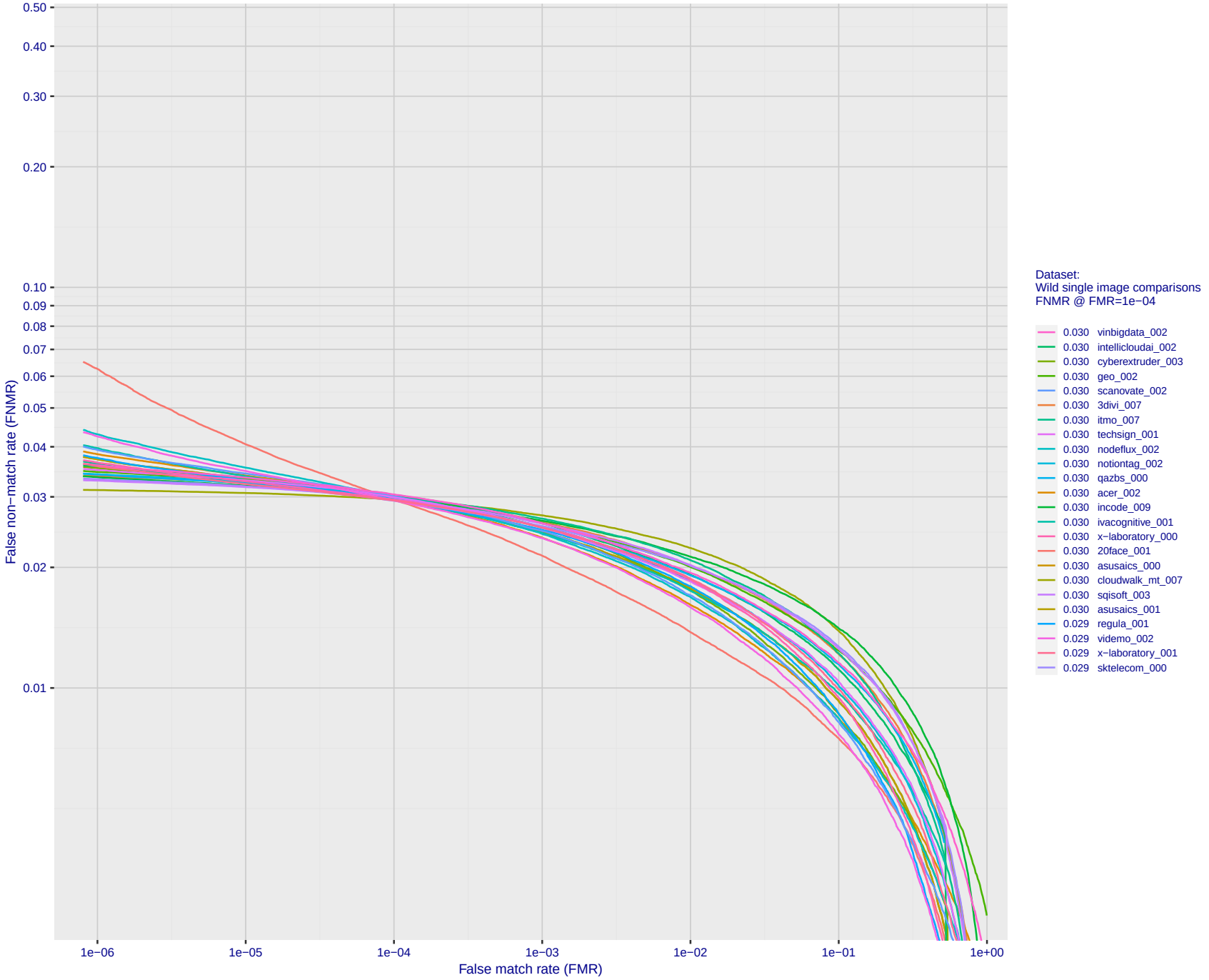

Figure 142: For the 2018 wild image comparisons, detection error tradeoff (DET) characteristics showing false non-match rate vs. false match rate plotted parametrically on threshold, T. The scales are logarithmic in order to show several decades of FMR.

FNMR(T) "False non-match rate"
FMR(T) "False match rate"

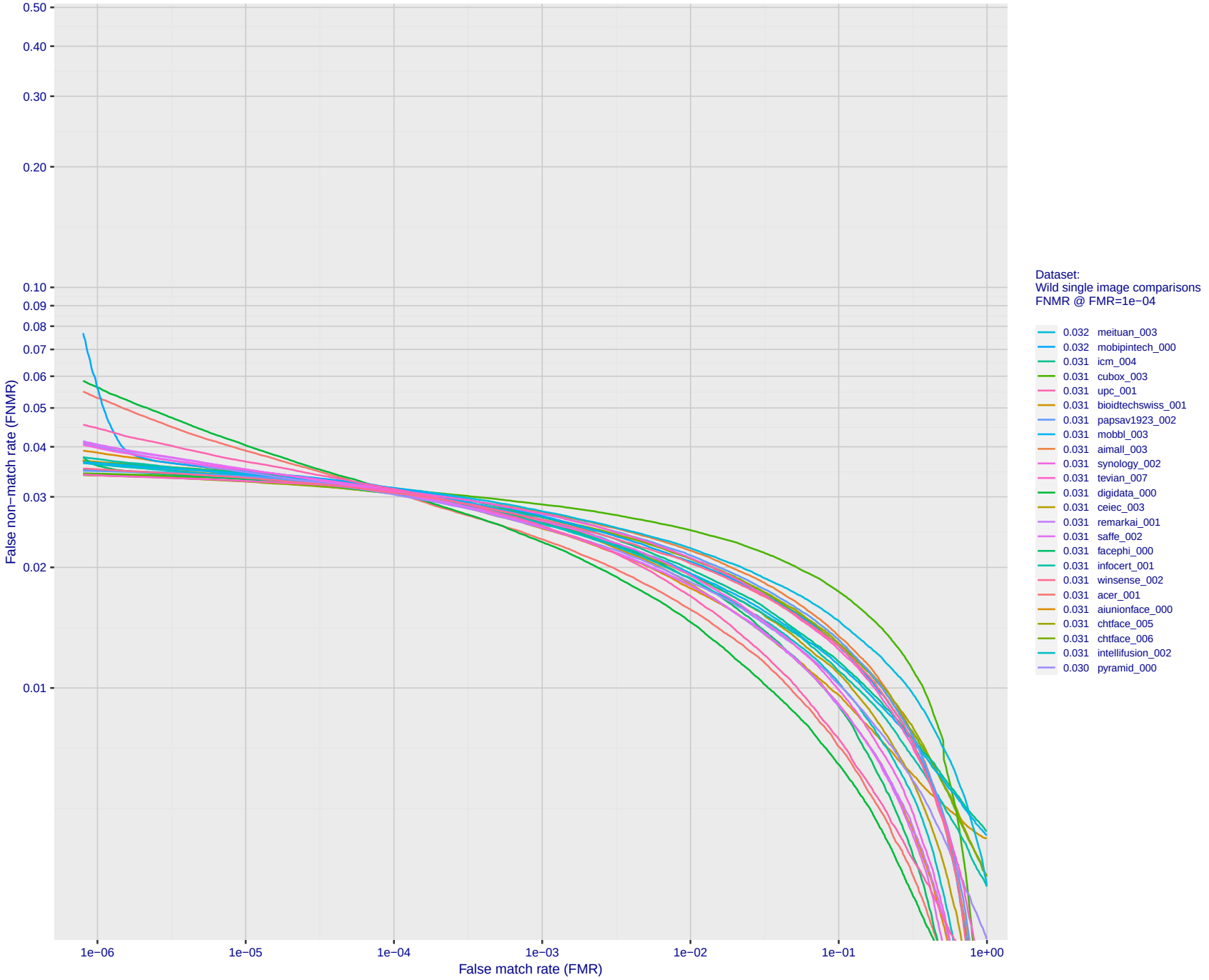

Figure 143: For the 2018 wild image comparisons, detection error tradeoff (DET) characteristics showing false non-match rate vs. false match rate plotted parametrically on threshold, T. The scales are logarithmic in order to show several decades of FMR.

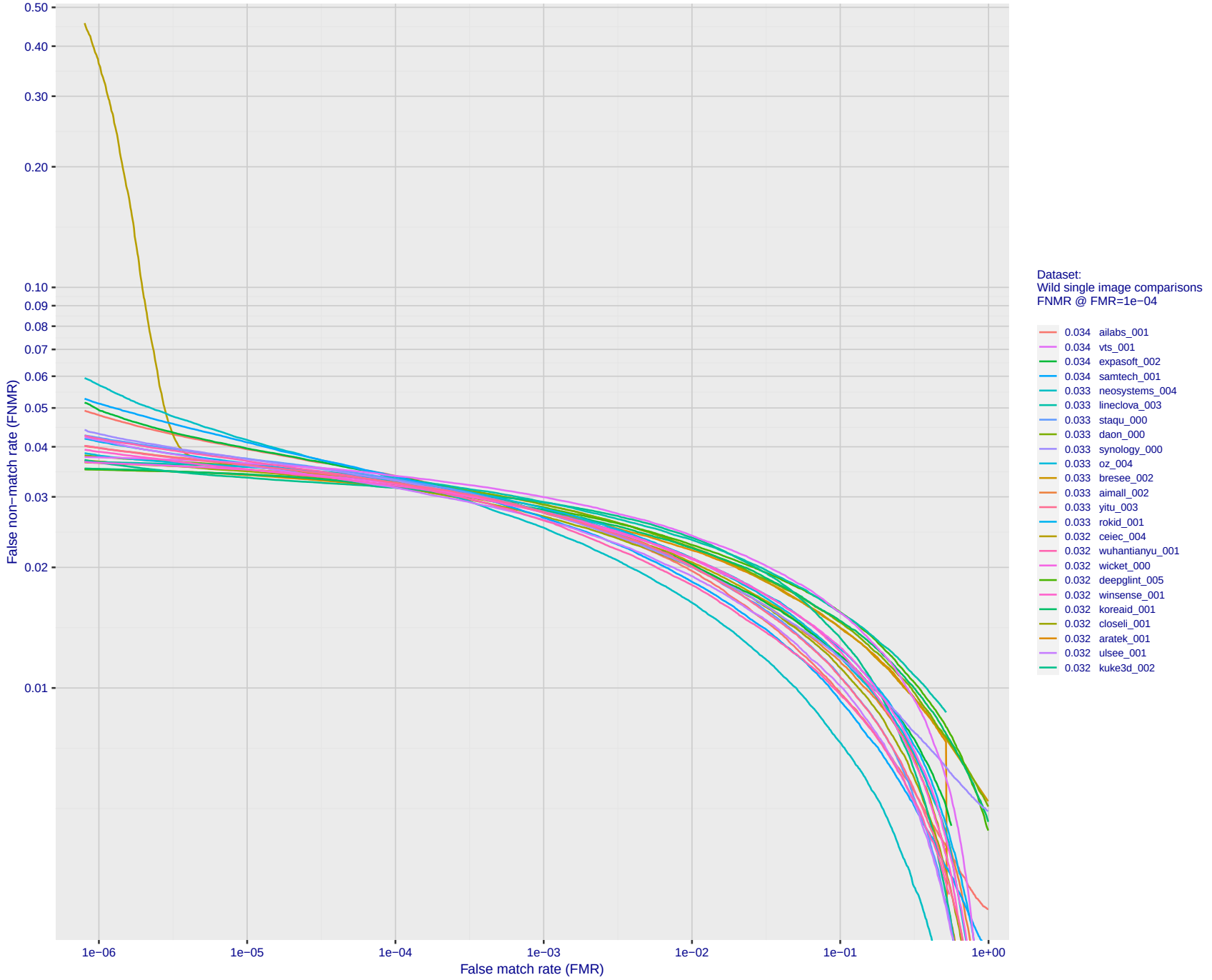

Figure 144: For the 2018 wild image comparisons, detection error tradeoff (DET) characteristics showing false non-match rate vs. false match rate plotted parametrically on threshold, T. The scales are logarithmic in order to show several decades of FMR.

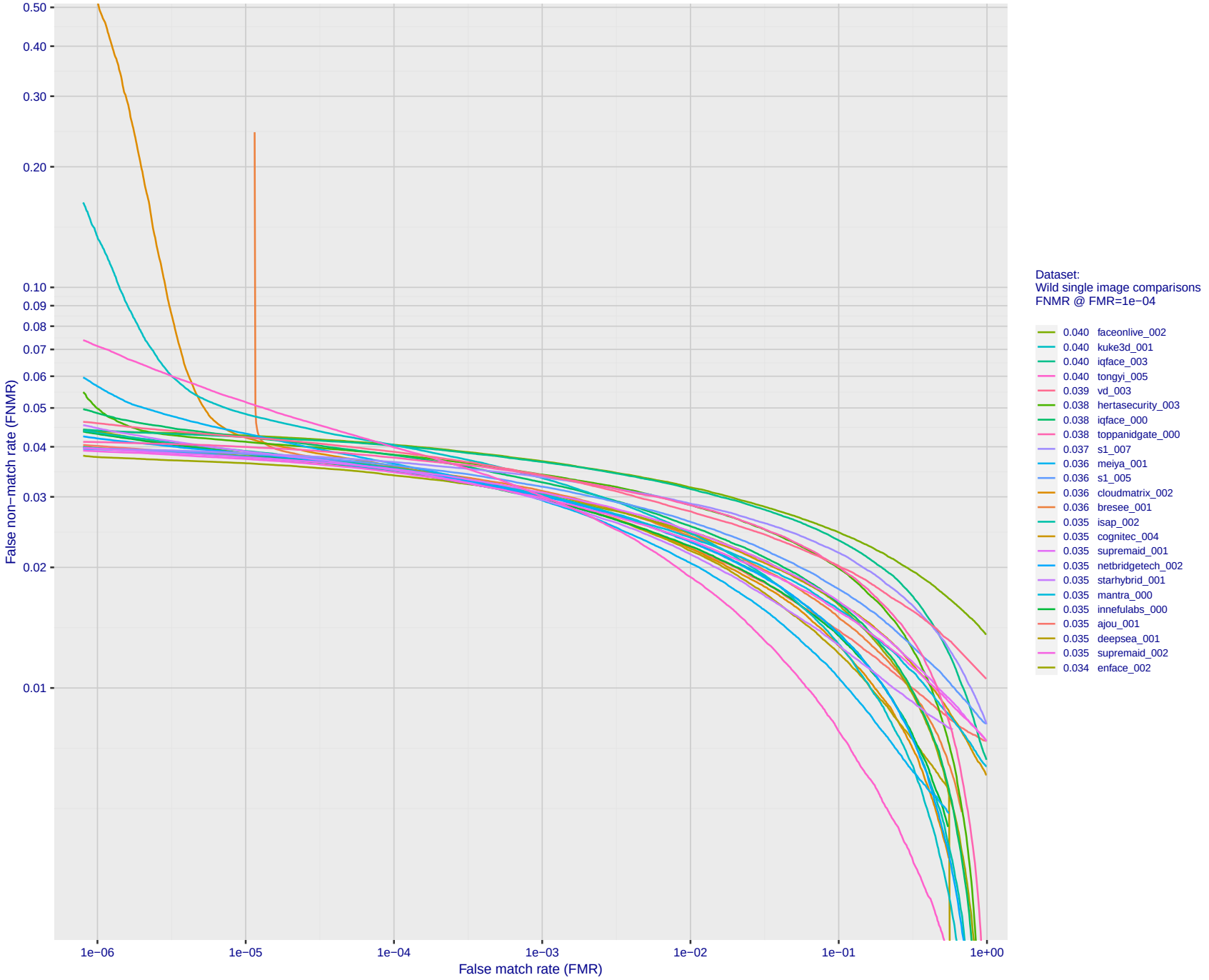

Figure 145: For the 2018 wild image comparisons, detection error tradeoff (DET) characteristics showing false non-match rate vs. false match rate plotted parametrically on threshold, T. The scales are logarithmic in order to show several decades of FMR.

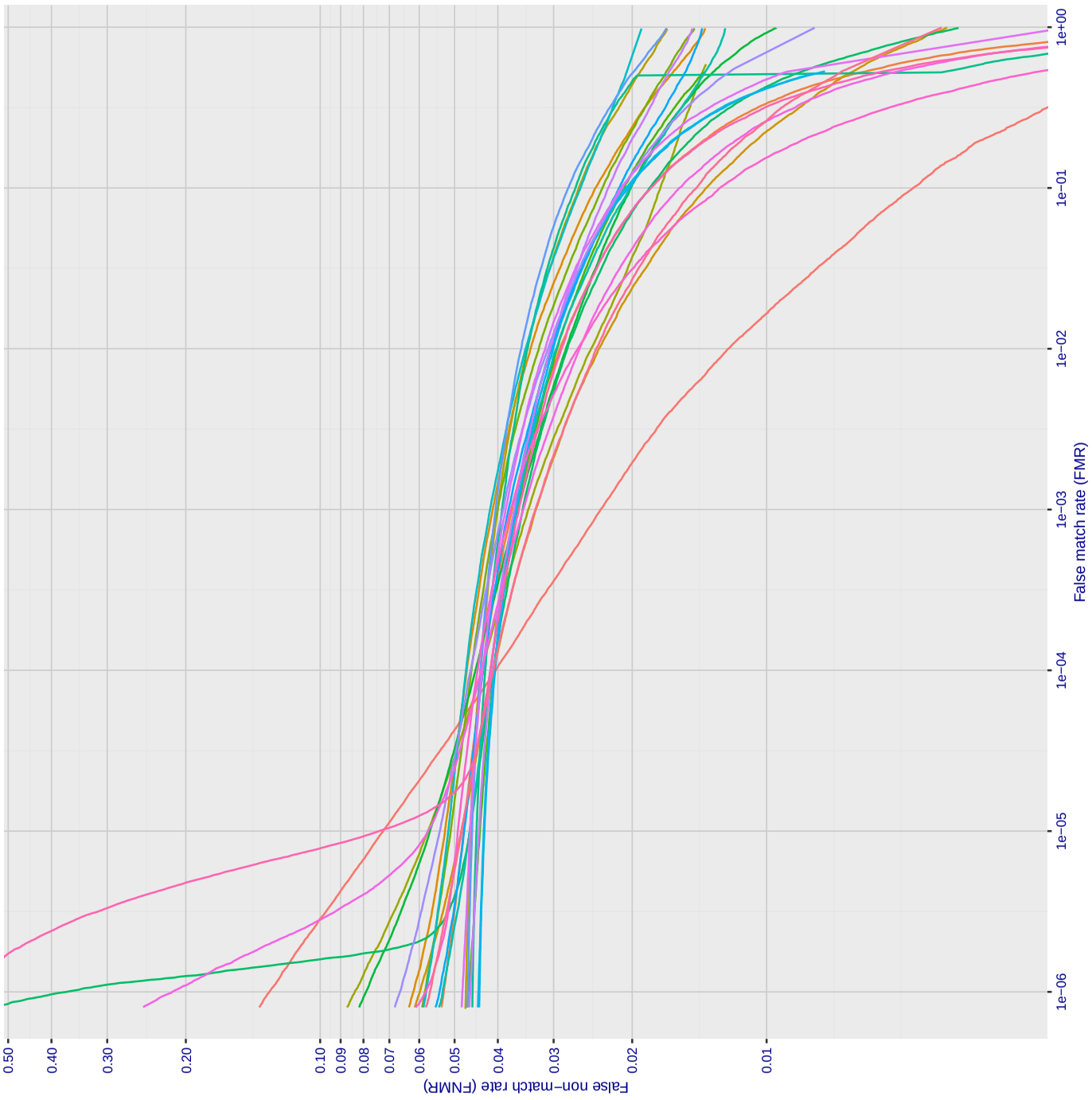

Figure 146: For the 2018 wild image comparisons, detection error tradeoff (DET) characteristics showing false non-match rate vs. false match rate plotted parametrically on threshold, T. The scales are logarithmic in order to show several decades of FMR.

FNMR(T) "False non-match rate"
FMR(T) "False match rate"

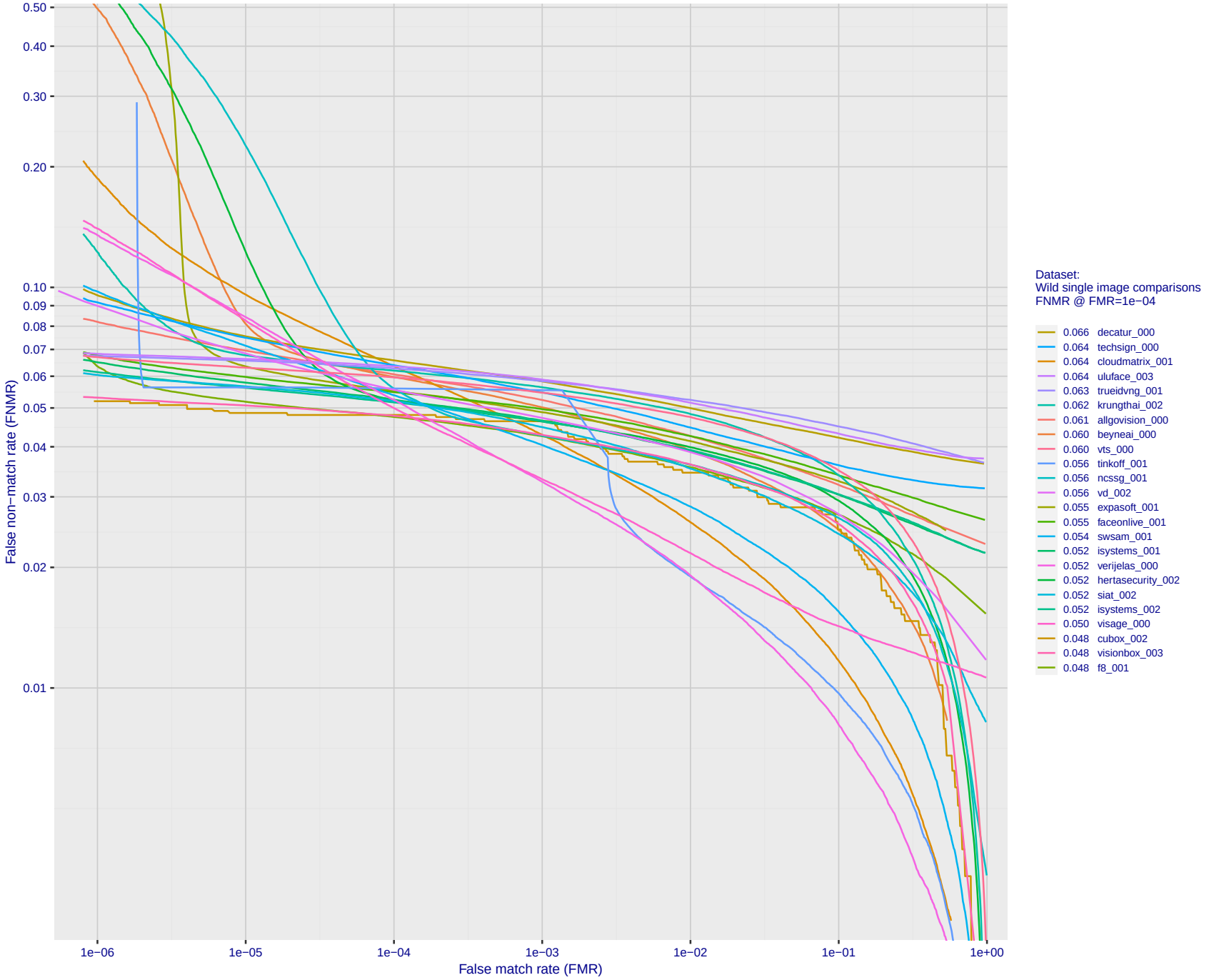

Figure 147: For the 2018 wild image comparisons, detection error tradeoff (DET) characteristics showing false non-match rate vs. false match rate plotted parametrically on threshold, T. The scales are logarithmic in order to show several decades of FMR.

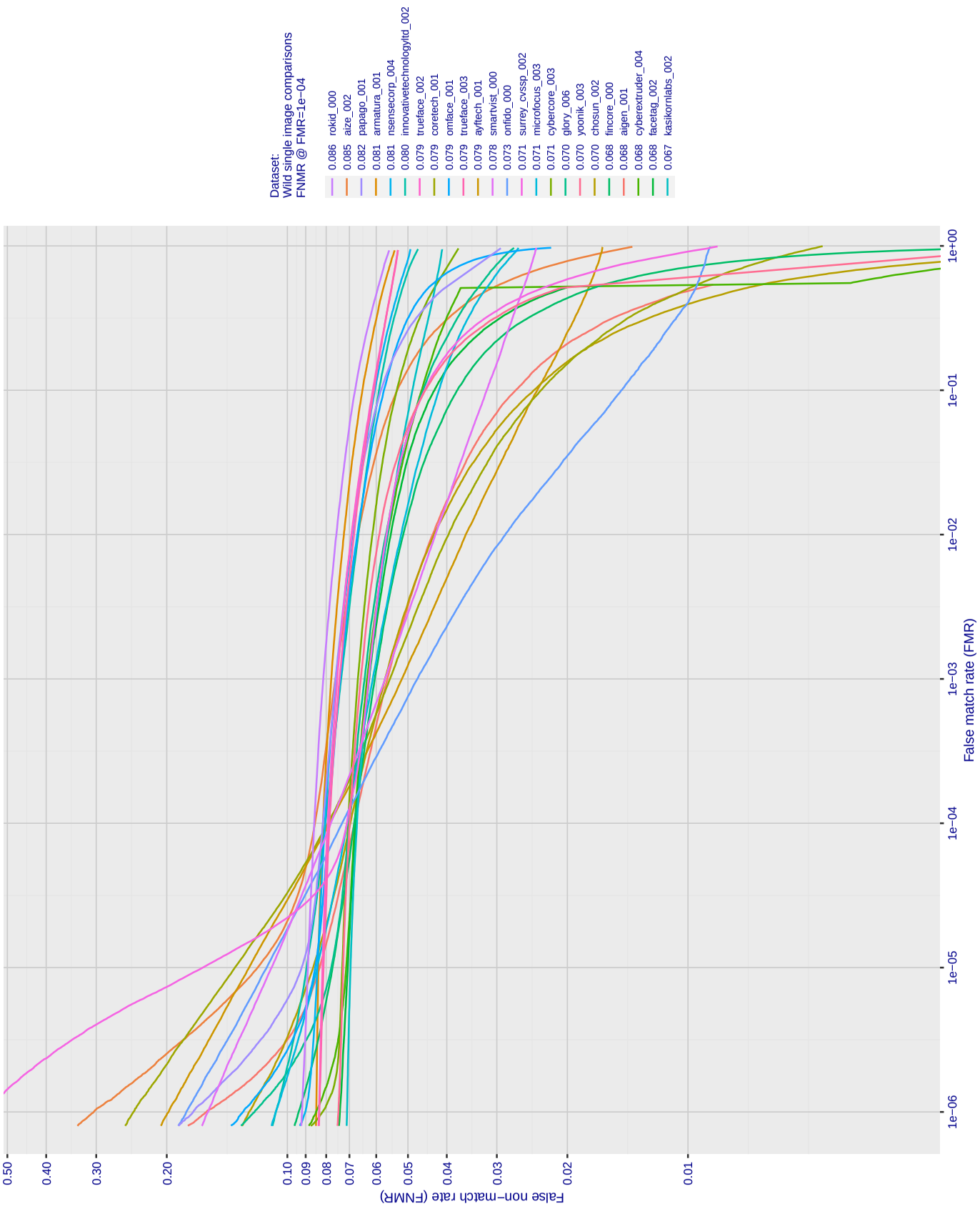

Figure 148: For the 2018 wild image comparisons, detection error tradeoff (DET) characteristics showing false non-match rate vs. false match rate plotted parametrically on threshold, T. The scales are logarithmic in order to show several decades of FMR.

FNMR(T) "False non-match rate"
FMR(T) "False match rate"

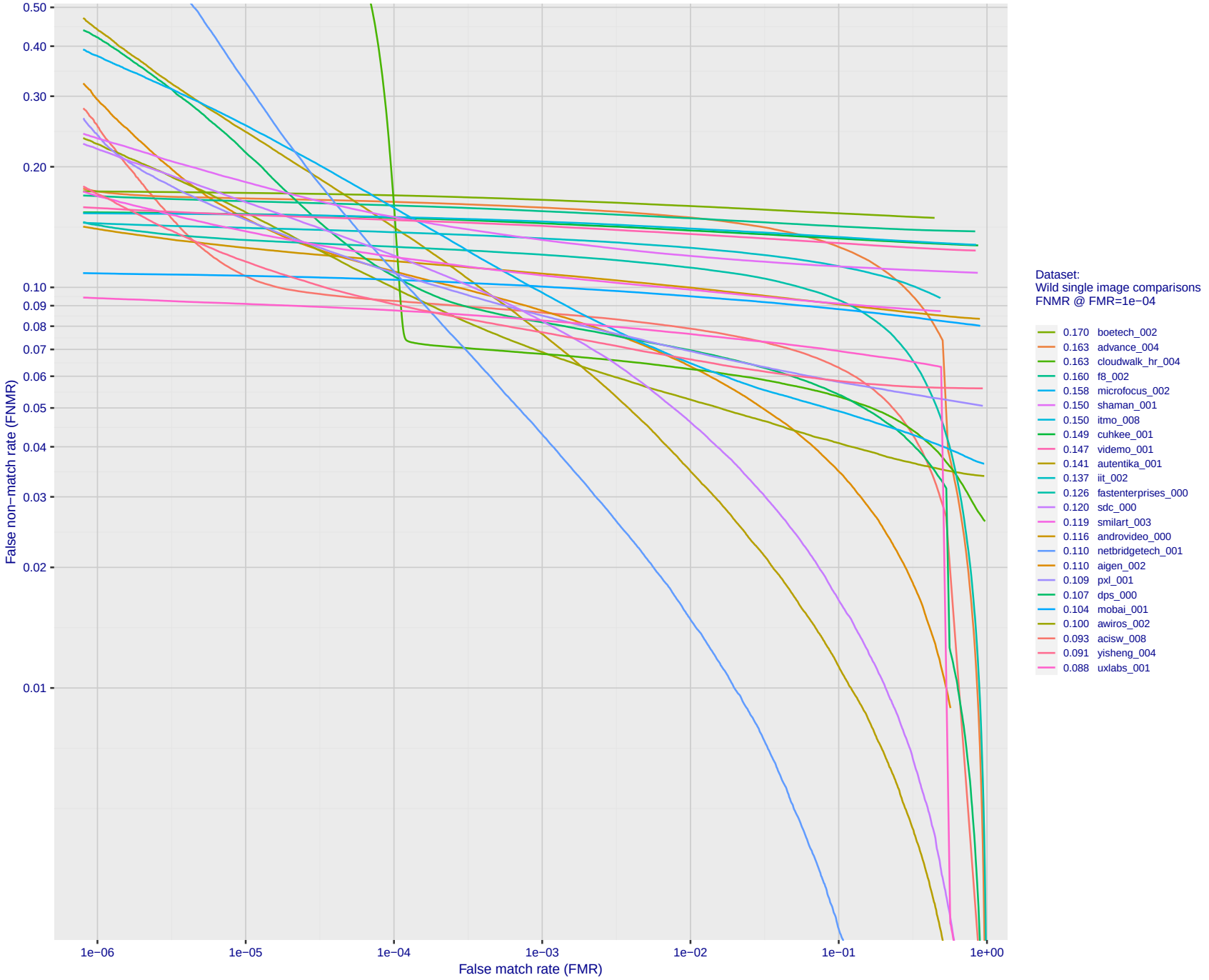

Figure 149: For the 2018 wild image comparisons, detection error tradeoff (DET) characteristics showing false non-match rate vs. false match rate plotted parametrically on threshold, T. The scales are logarithmic in order to show several decades of FMR.

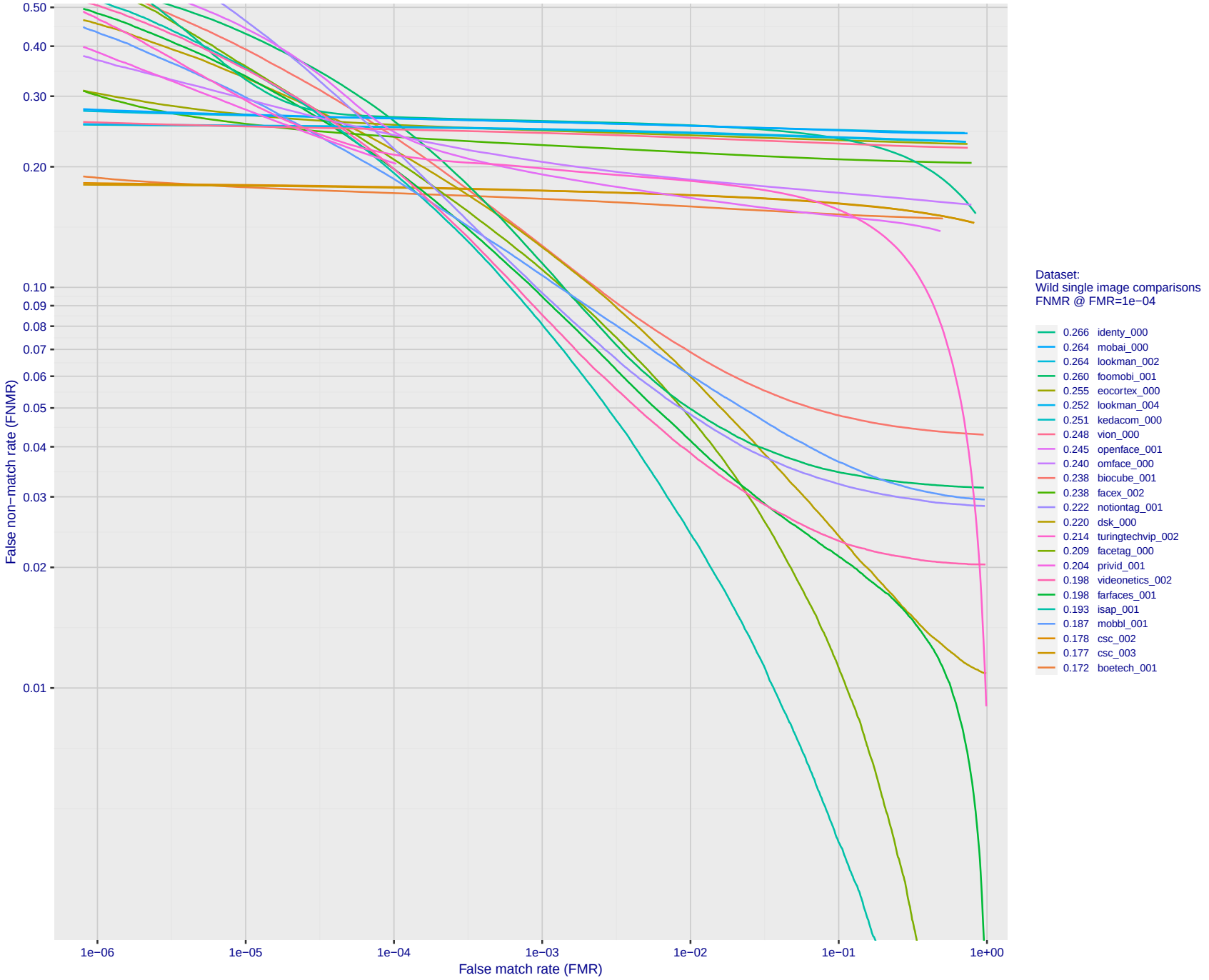

Figure 150: For the 2018 wild image comparisons, detection error tradeoff (DET) characteristics showing false non-match rate vs. false match rate plotted parametrically on threshold, T. The scales are logarithmic in order to show several decades of FMR.

FNMR(T) "False non-match rate"
FMR(T) "False match rate"

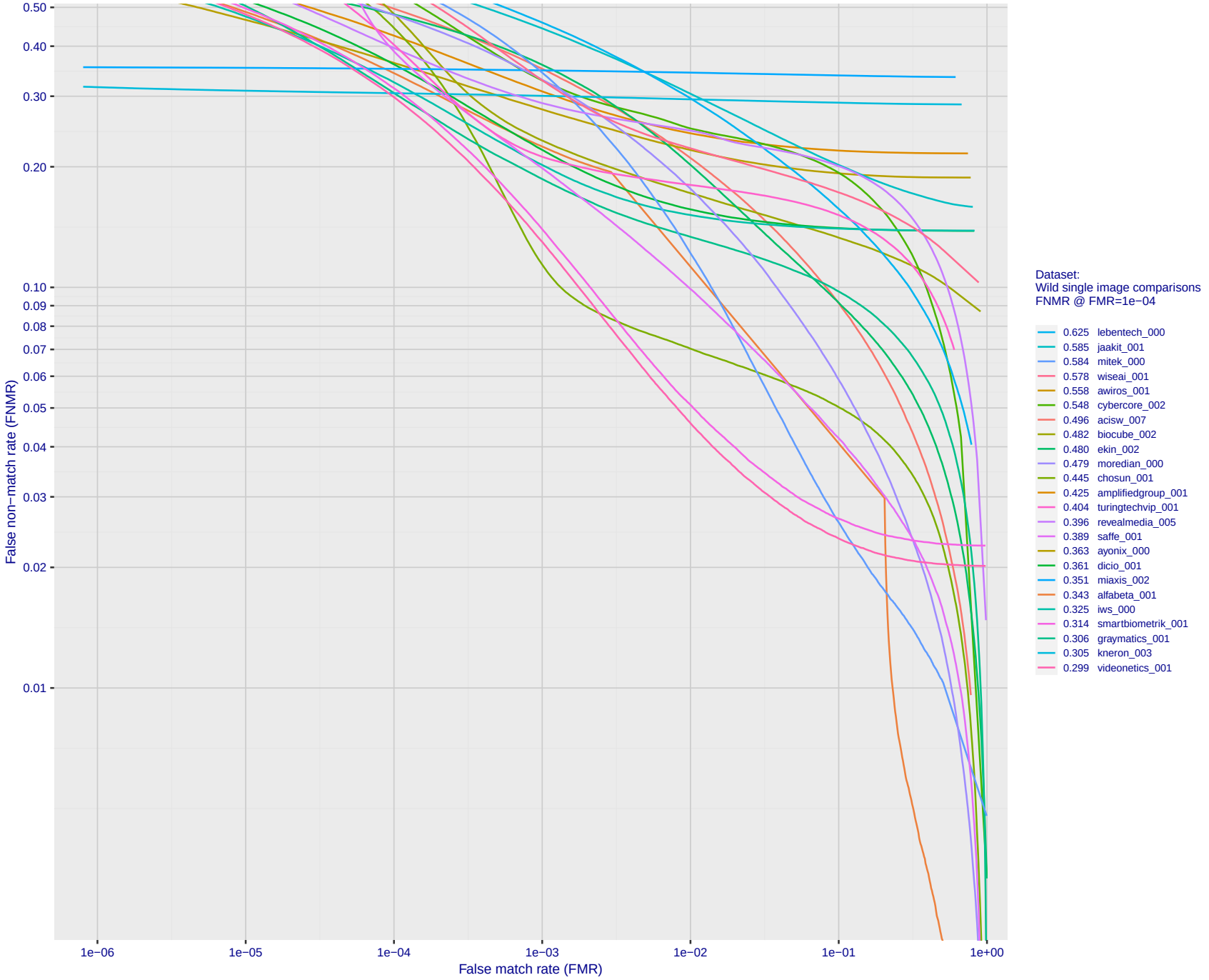

Figure 151: For the 2018 wild image comparisons, detection error tradeoff (DET) characteristics showing false non-match rate vs. false match rate plotted parametrically on threshold, T. The scales are logarithmic in order to show several decades of FMR.

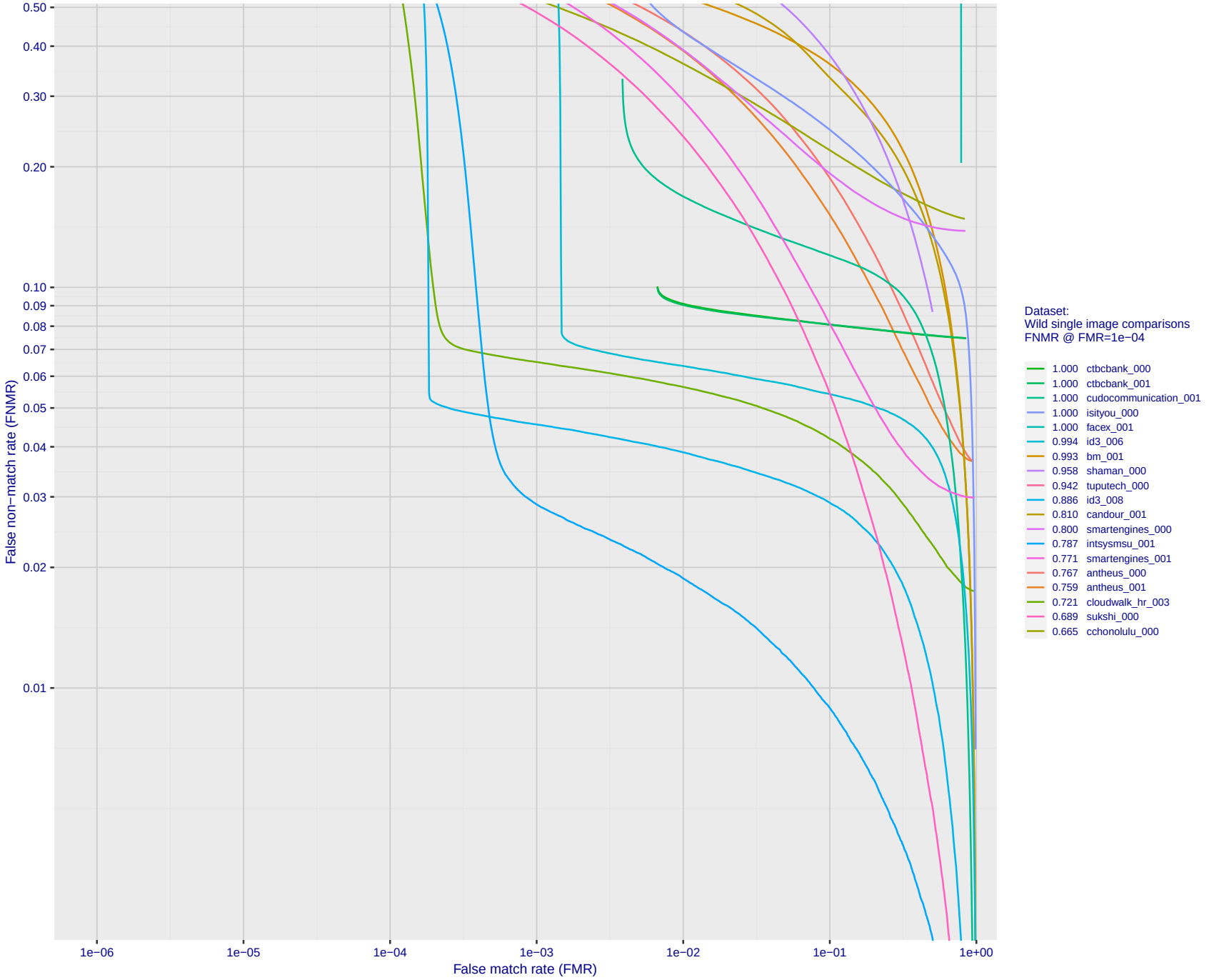

Figure 152: For the 2018 wild image comparisons, detection error tradeoff (DET) characteristics showing false non-match rate vs. false match rate plotted parametrically on threshold, T. The scales are logarithmic in order to show several decades of FMR.

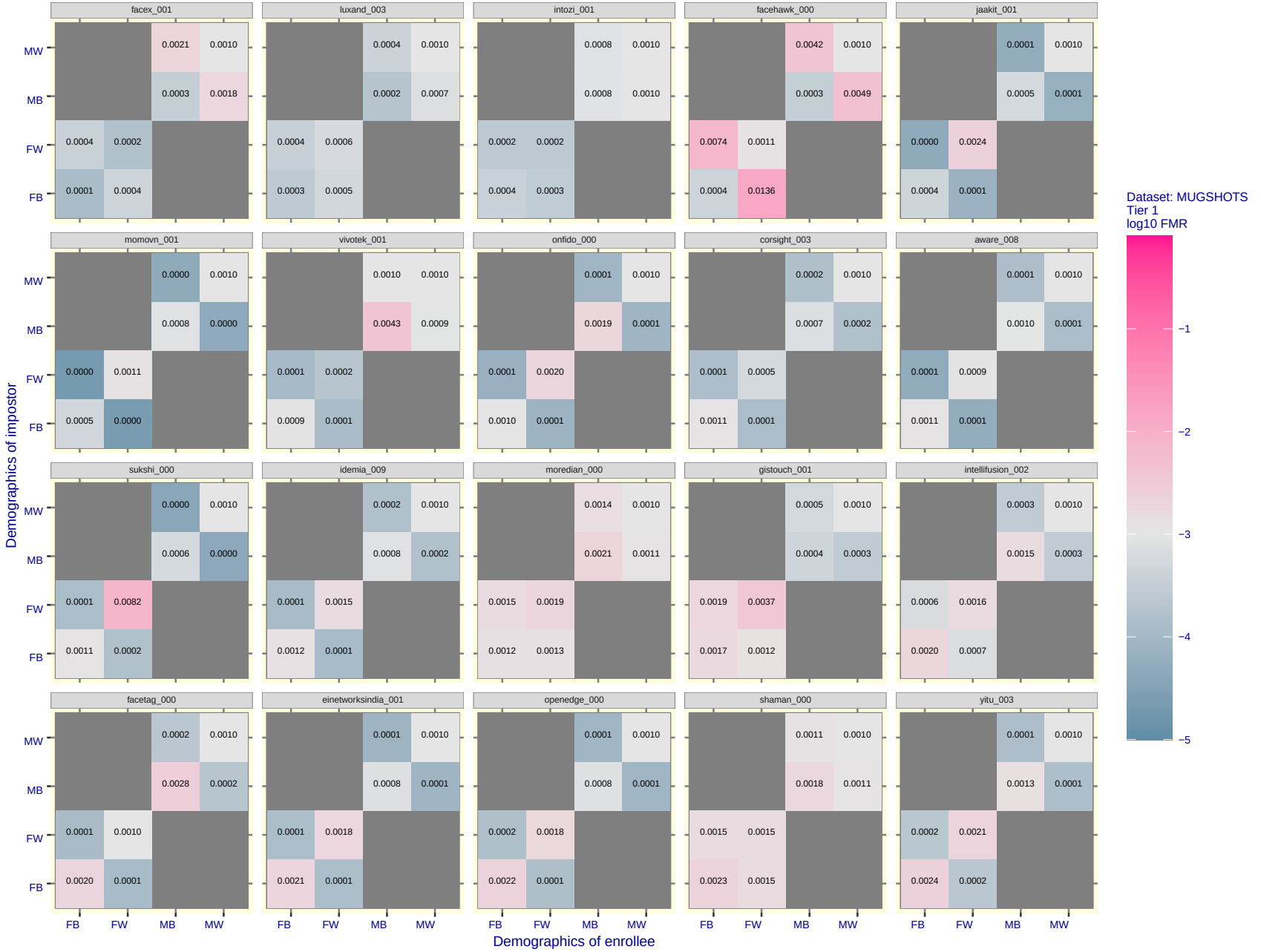

Figure 153: For the mugshot images, FMR *for same-sex impostor pairs of images annotated with codes for black female, black male, white female, white male. The threshold is set for each algorithm to give* FMR *= 0.001 for white males which is the demographic that usually gives the lowest* FMR*. This means the top right box is the same color in all panels. The panels are sorted over multiple pages in order of* FMR *on black females, which is the demographc that usually gives the highest* FMR*.*

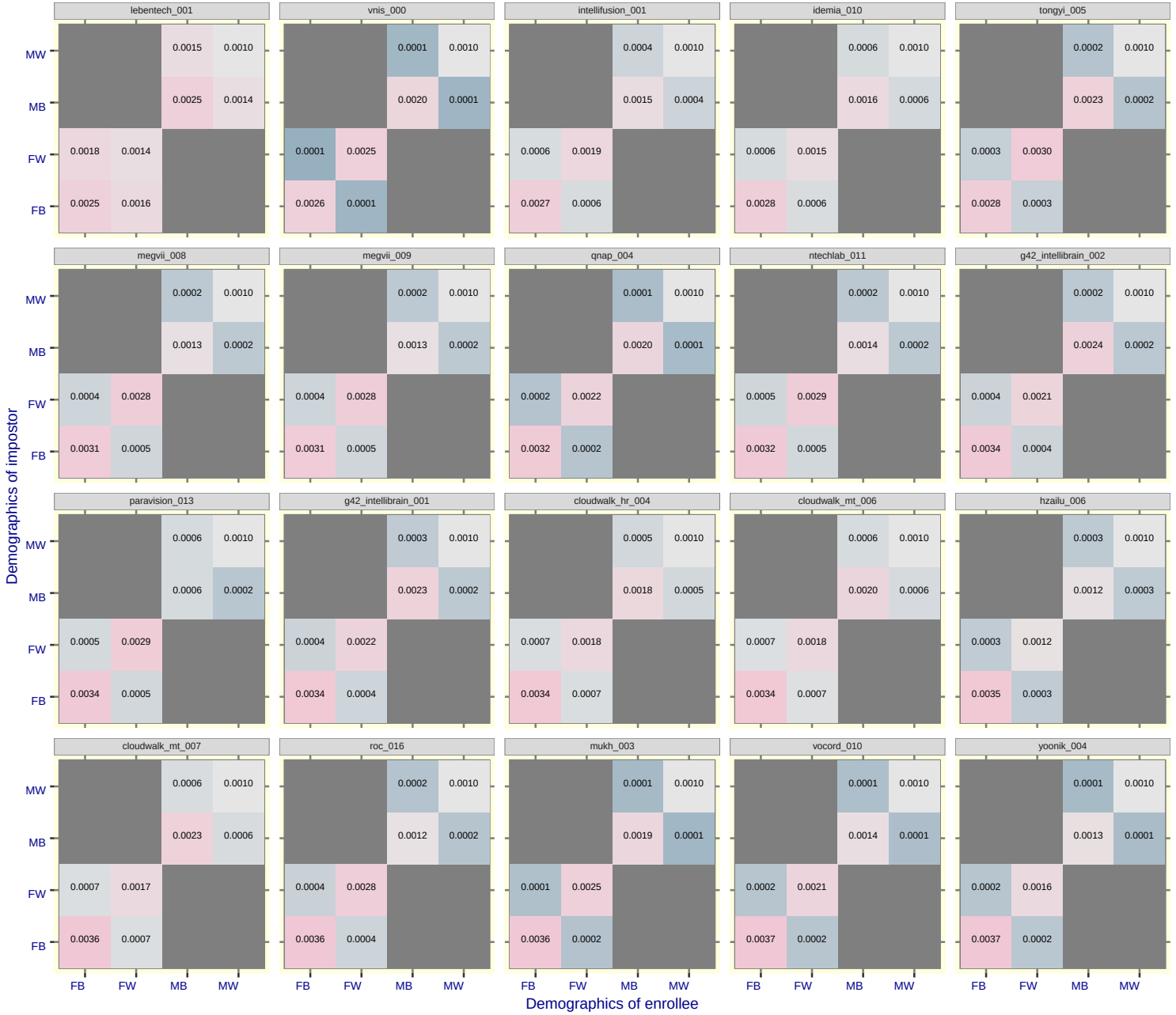

Figure 154: For the mugshot images, FMR *for same-sex impostor pairs of images annotated with codes for black female, black male, white female, white male. The threshold is set for each algorithm to give* FMR *= 0.001 for white males which is the demographic that usually gives the lowest* FMR*. This means the top right box is the same color in all panels. The panels are sorted over multiple pages in order of* FMR *on black females, which is the demographc that usually gives the highest* FMR*.*

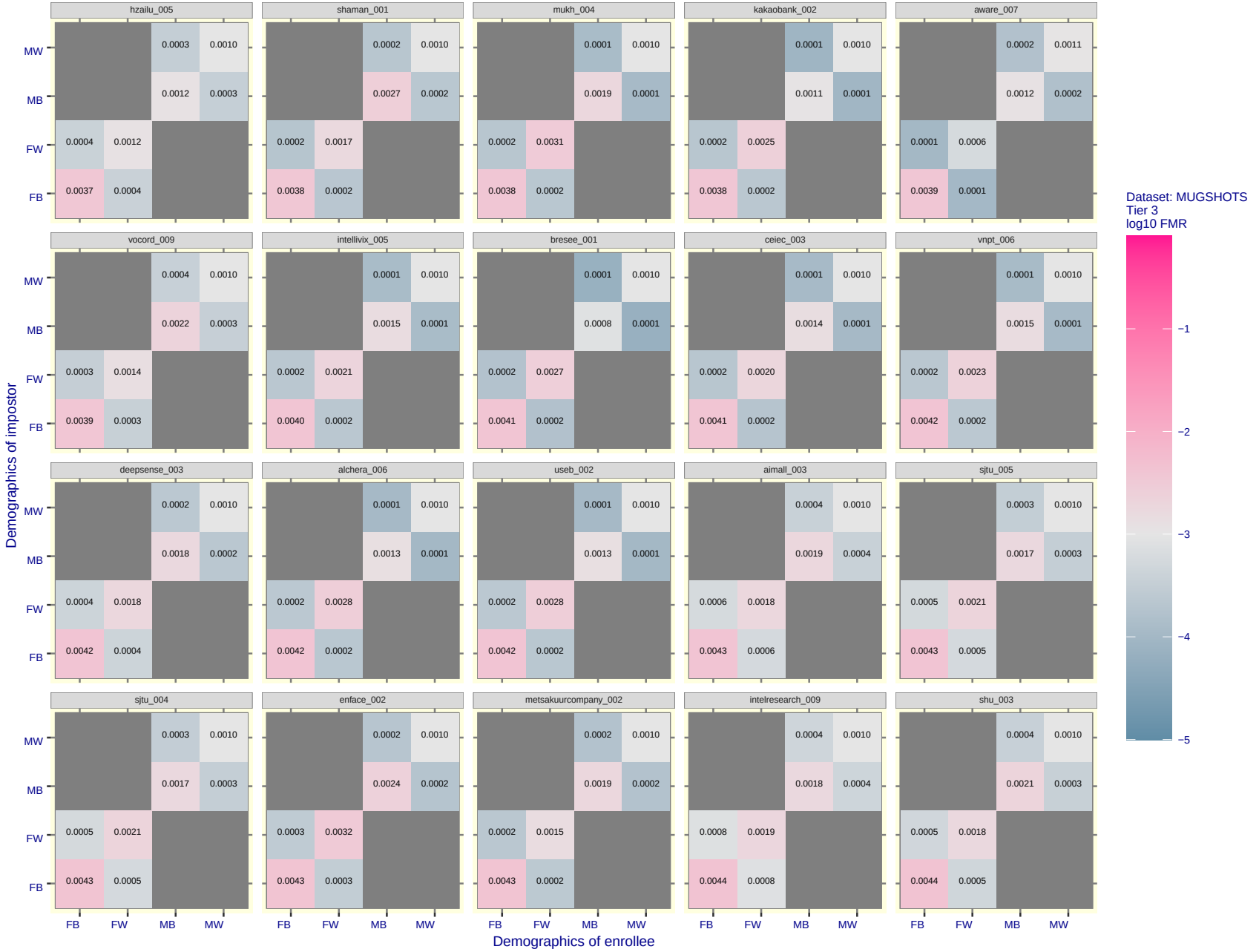

Figure 155: For the mugshot images, FMR *for same-sex impostor pairs of images annotated with codes for black female, black male, white female, white male. The threshold is set for each algorithm to give* FMR *= 0.001 for white males which is the demographic that usually gives the lowest* FMR*. This means the top right box is the same color in all panels. The panels are sorted over multiple pages in order of* FMR *on black females, which is the demographc that usually gives the highest* FMR*.*

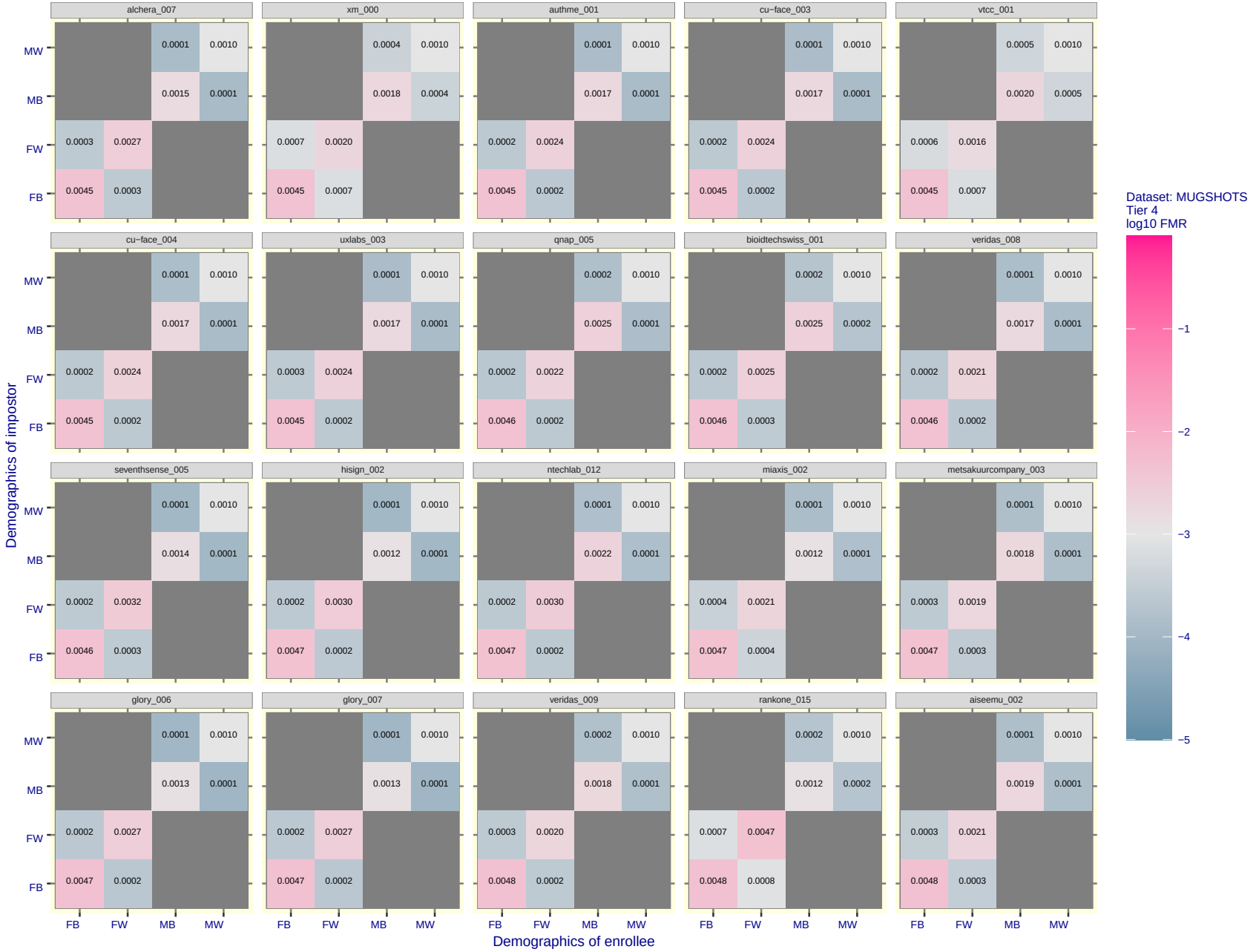

Figure 156: For the mugshot images, FMR *for same-sex impostor pairs of images annotated with codes for black female, black male, white female, white male. The threshold is set for each algorithm to give* FMR *= 0.001 for white males which is the demographic that usually gives the lowest* FMR*. This means the top right box is the same color in all panels. The panels are sorted over multiple pages in order of* FMR *on black females, which is the demographc that usually gives the highest* FMR*.*

2024/04/17 08:45:50
FNMR(T) "False non-match rate"
FMR(T) "False match rate"

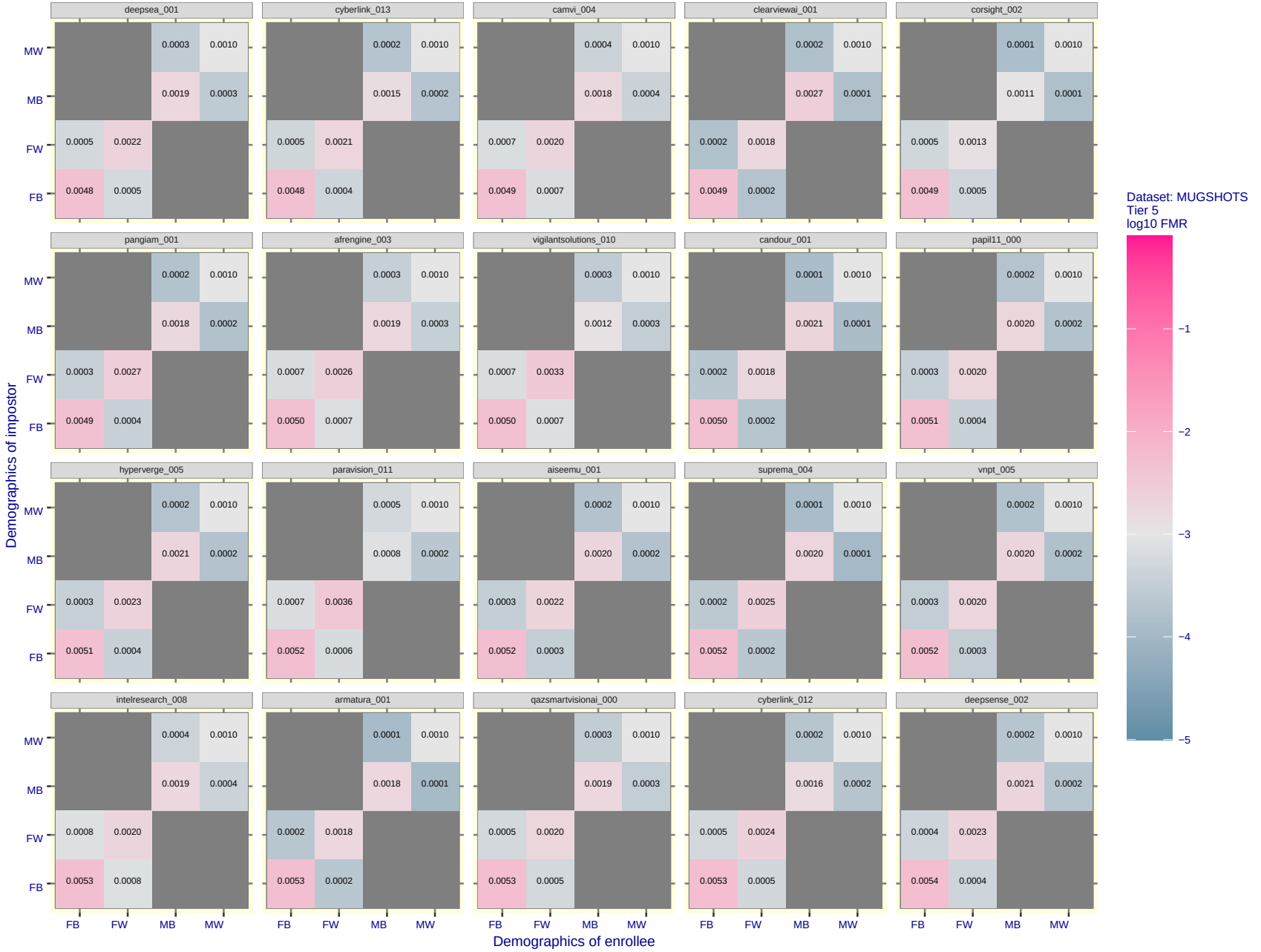

Figure 157: For the mugshot images, FMR *for same-sex impostor pairs of images annotated with codes for black female, black male, white female, white male. The threshold is set for each algorithm to give* FMR *= 0.001 for white males which is the demographic that usually gives the lowest* FMR*. This means the top right box is the same color in all panels. The panels are sorted over multiple pages in order of* FMR *on black females, which is the demographc that usually gives the highest* FMR*.*

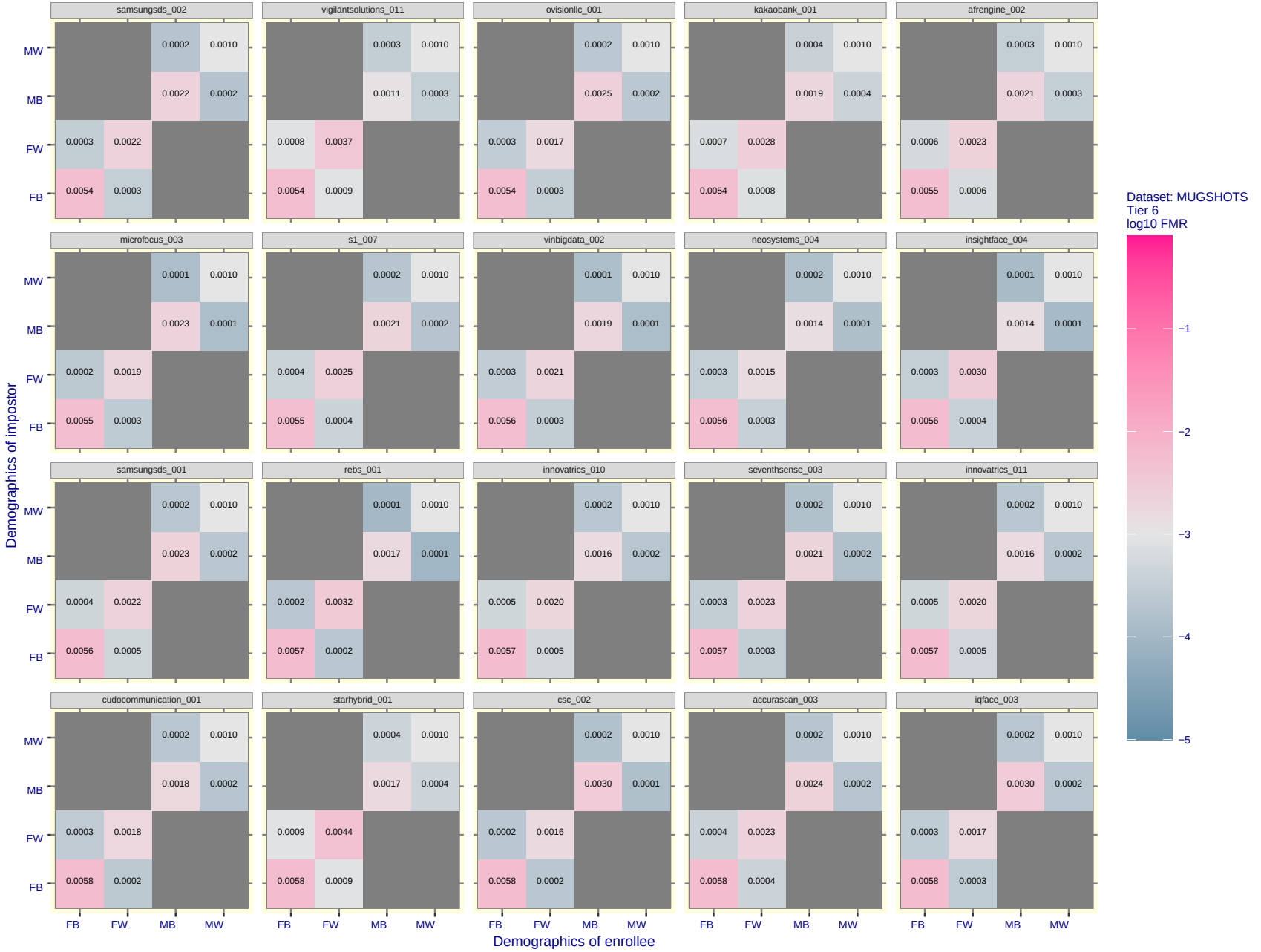

Figure 158: For the mugshot images, FMR *for same-sex impostor pairs of images annotated with codes for black female, black male, white female, white male. The threshold is set for each algorithm to give* FMR *= 0.001 for white males which is the demographic that usually gives the lowest* FMR*. This means the top right box is the same color in all panels. The panels are sorted over multiple pages in order of* FMR *on black females, which is the demographc that usually gives the highest* FMR*.*

2024/04/17 08:45:50
FNMR(T) "False non-match rate"
FMR(T) "False match rate"

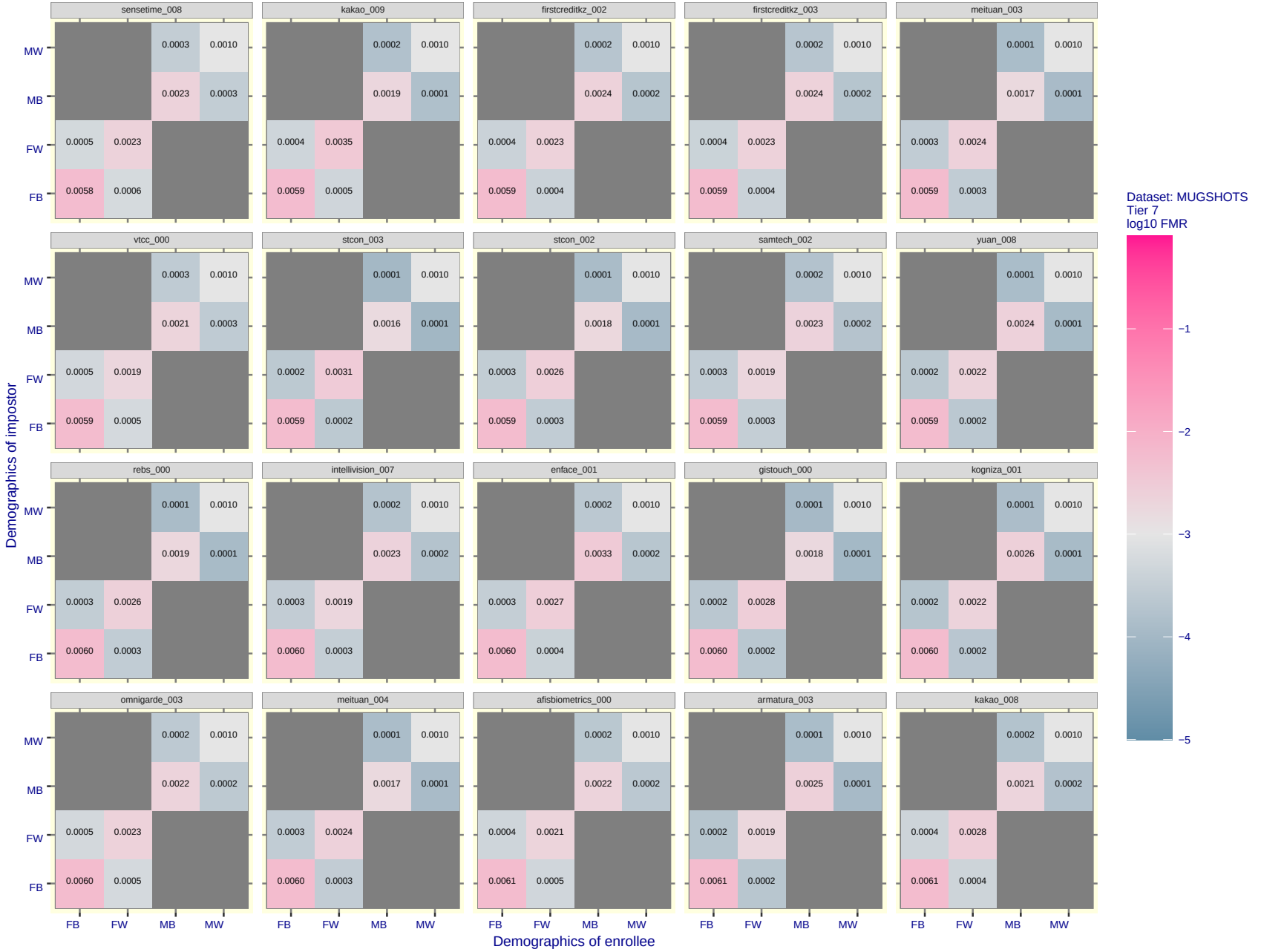

Figure 159: For the mugshot images, FMR *for same-sex impostor pairs of images annotated with codes for black female, black male, white female, white male. The threshold is set for each algorithm to give* FMR *= 0.001 for white males which is the demographic that usually gives the lowest* FMR*. This means the top right box is the same color in all panels. The panels are sorted over multiple pages in order of* FMR *on black females, which is the demographc that usually gives the highest* FMR*.*

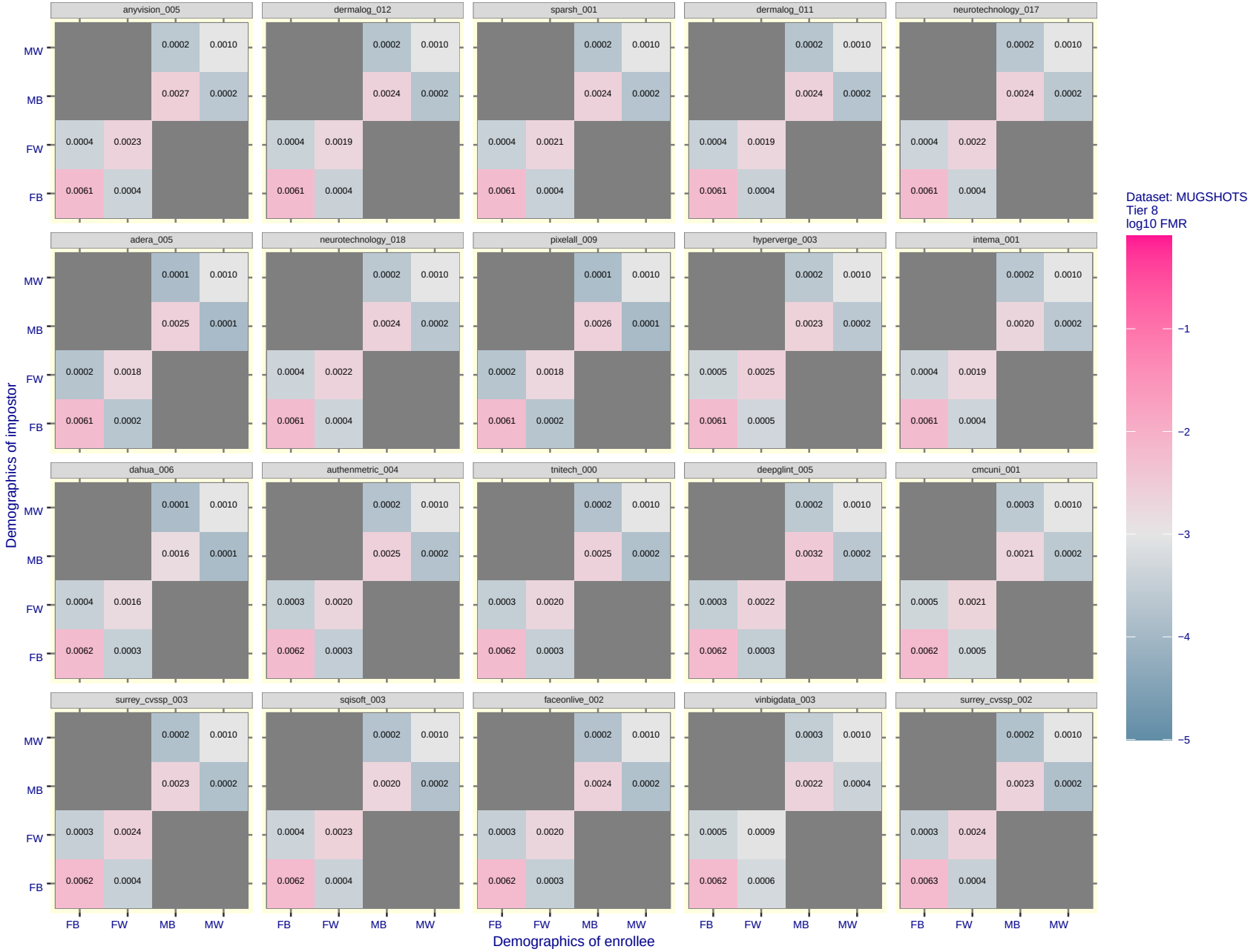

Figure 160: For the mugshot images, FMR *for same-sex impostor pairs of images annotated with codes for black female, black male, white female, white male. The threshold is set for each algorithm to give* FMR *= 0.001 for white males which is the demographic that usually gives the lowest* FMR*. This means the top right box is the same color in all panels. The panels are sorted over multiple pages in order of* FMR *on black females, which is the demographc that usually gives the highest* FMR*.*

2024/04/17 08:45:50
FNMR(T) "False non-match rate"
FMR(T) "False match rate"

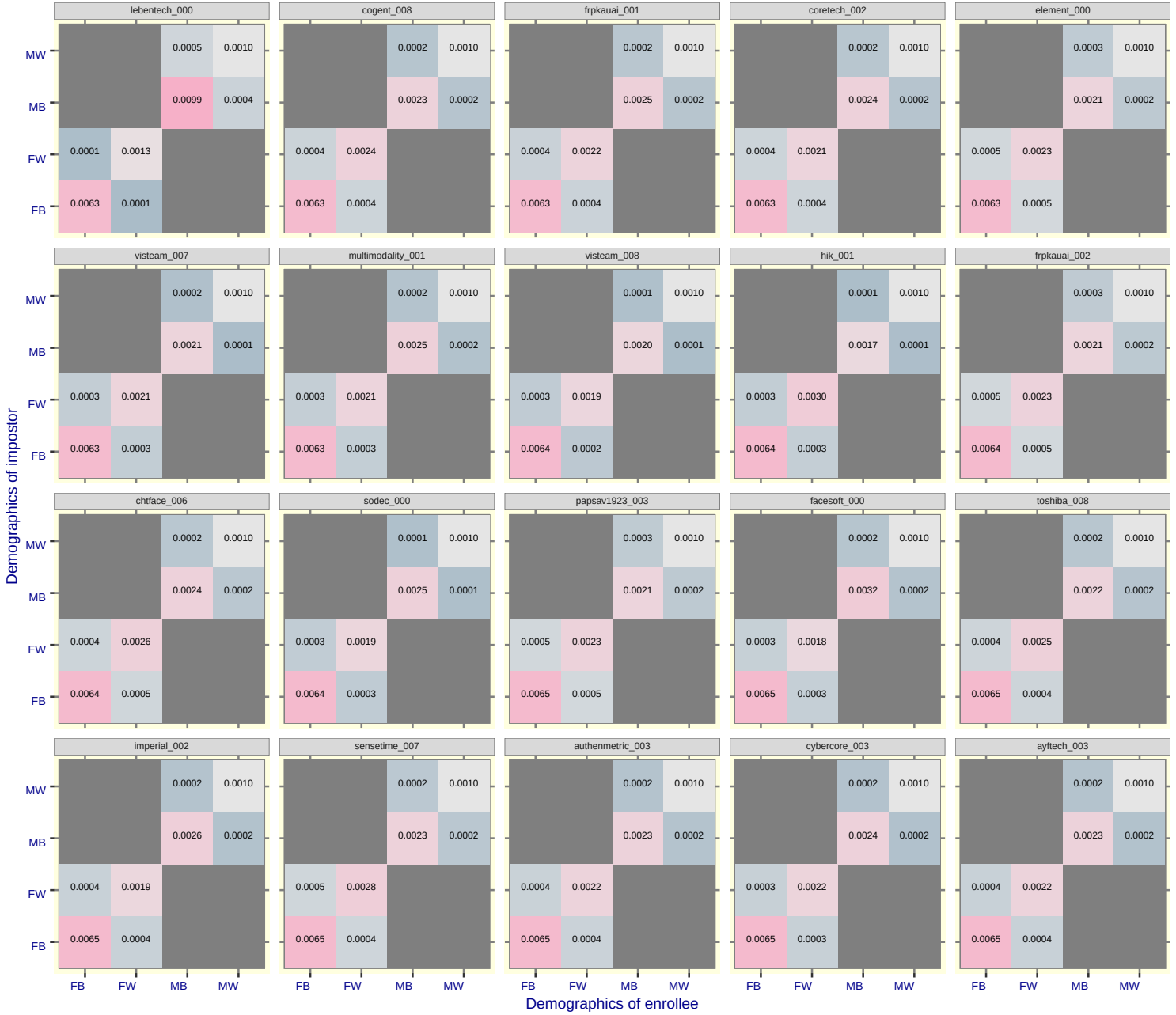

Figure 161: For the mugshot images, FMR *for same-sex impostor pairs of images annotated with codes for black female, black male, white female, white male. The threshold is set for each algorithm to give* FMR *= 0.001 for white males which is the demographic that usually gives the lowest* FMR*. This means the top right box is the same color in all panels. The panels are sorted over multiple pages in order of* FMR *on black females, which is the demographc that usually gives the highest* FMR*.*

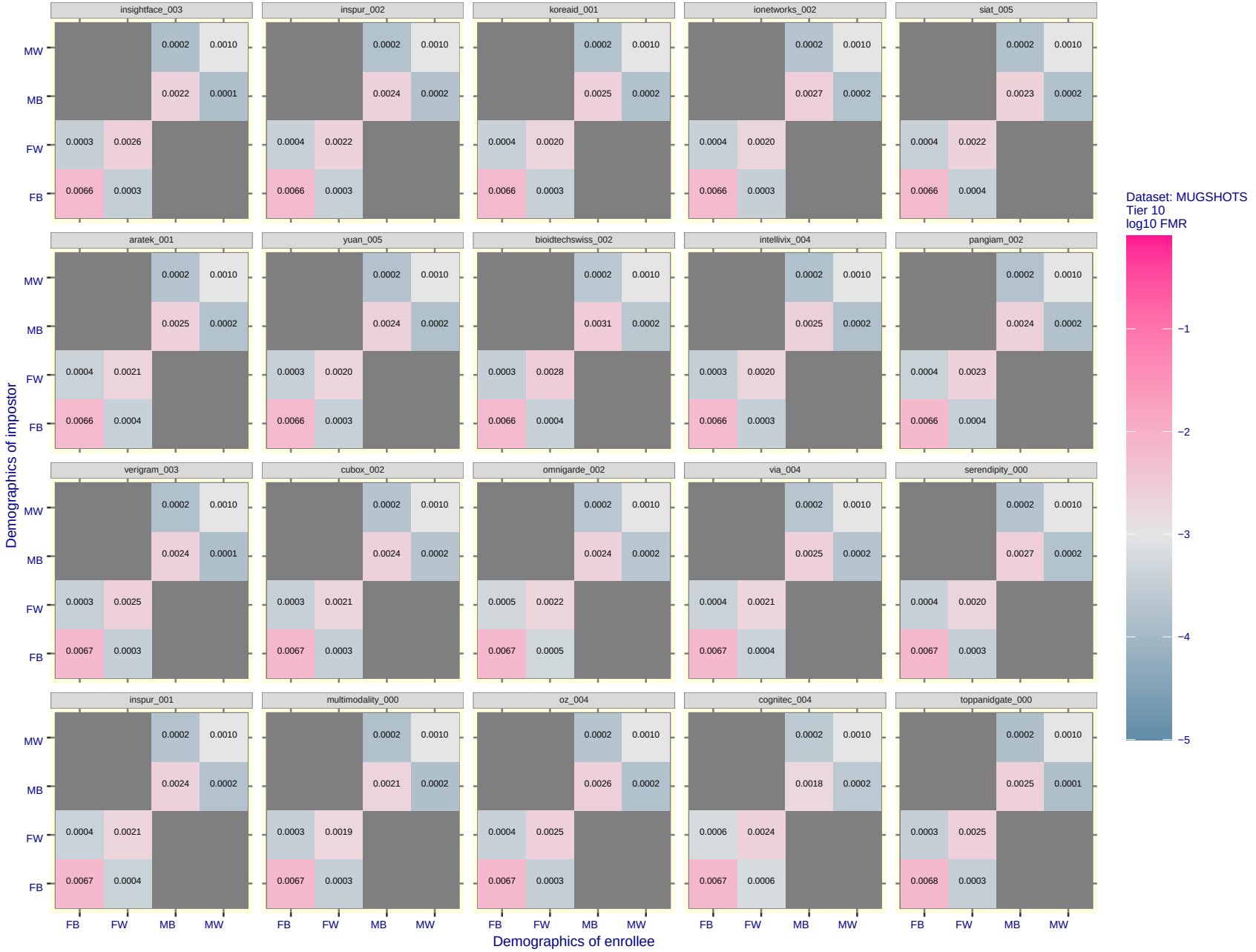

Figure 162: For the mugshot images, FMR *for same-sex impostor pairs of images annotated with codes for black female, black male, white female, white male. The threshold is set for each algorithm to give* FMR *= 0.001 for white males which is the demographic that usually gives the lowest* FMR*. This means the top right box is the same color in all panels. The panels are sorted over multiple pages in order of* FMR *on black females, which is the demographc that usually gives the highest* FMR*.*

2024/04/17 08:45:50
FNMR(T) "False non-match rate"
FMR(T) "False match rate"

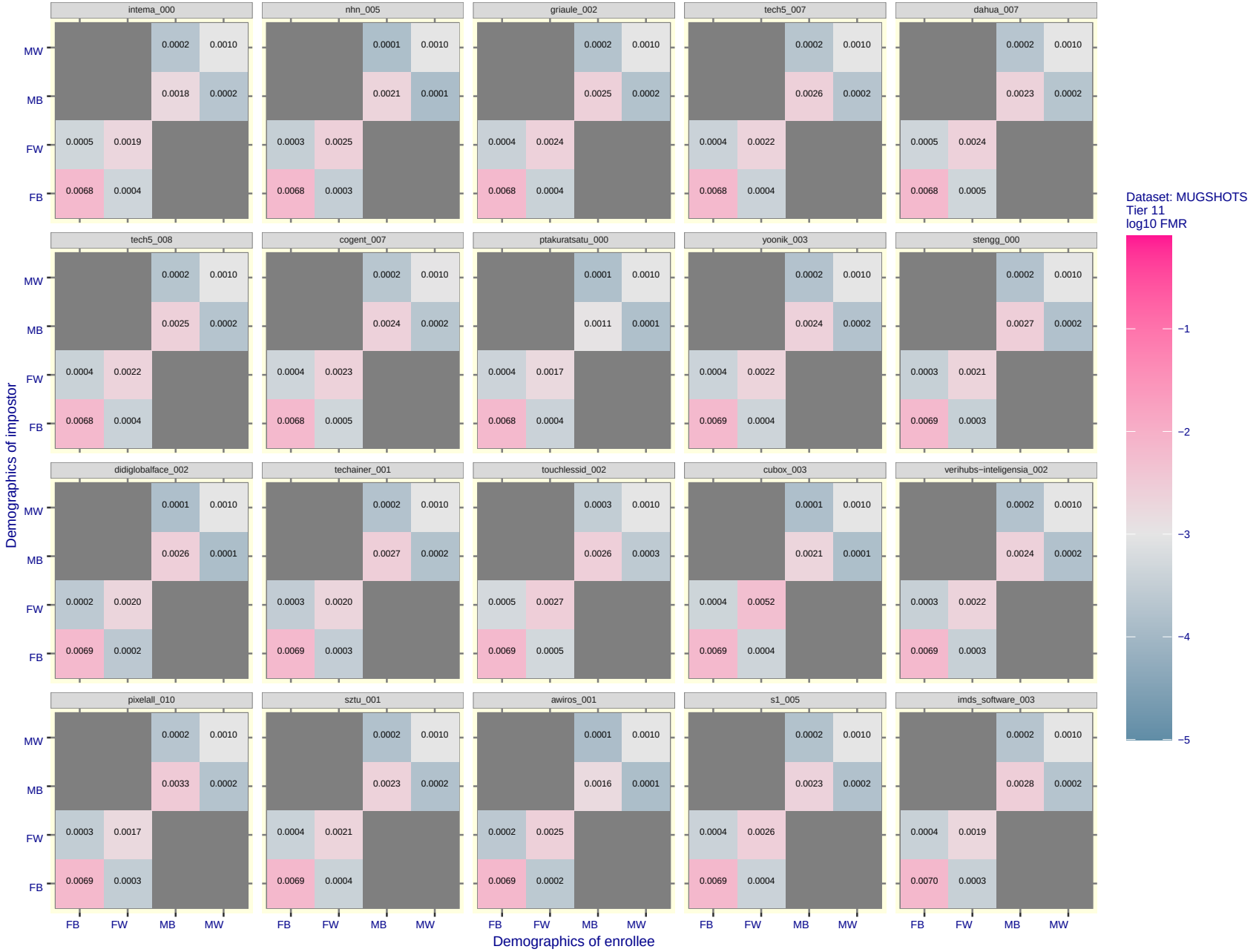

Figure 163: For the mugshot images, FMR *for same-sex impostor pairs of images annotated with codes for black female, black male, white female, white male. The threshold is set for each algorithm to give* FMR *= 0.001 for white males which is the demographic that usually gives the lowest* FMR*. This means the top right box is the same color in all panels. The panels are sorted over multiple pages in order of* FMR *on black females, which is the demographc that usually gives the highest* FMR*.*

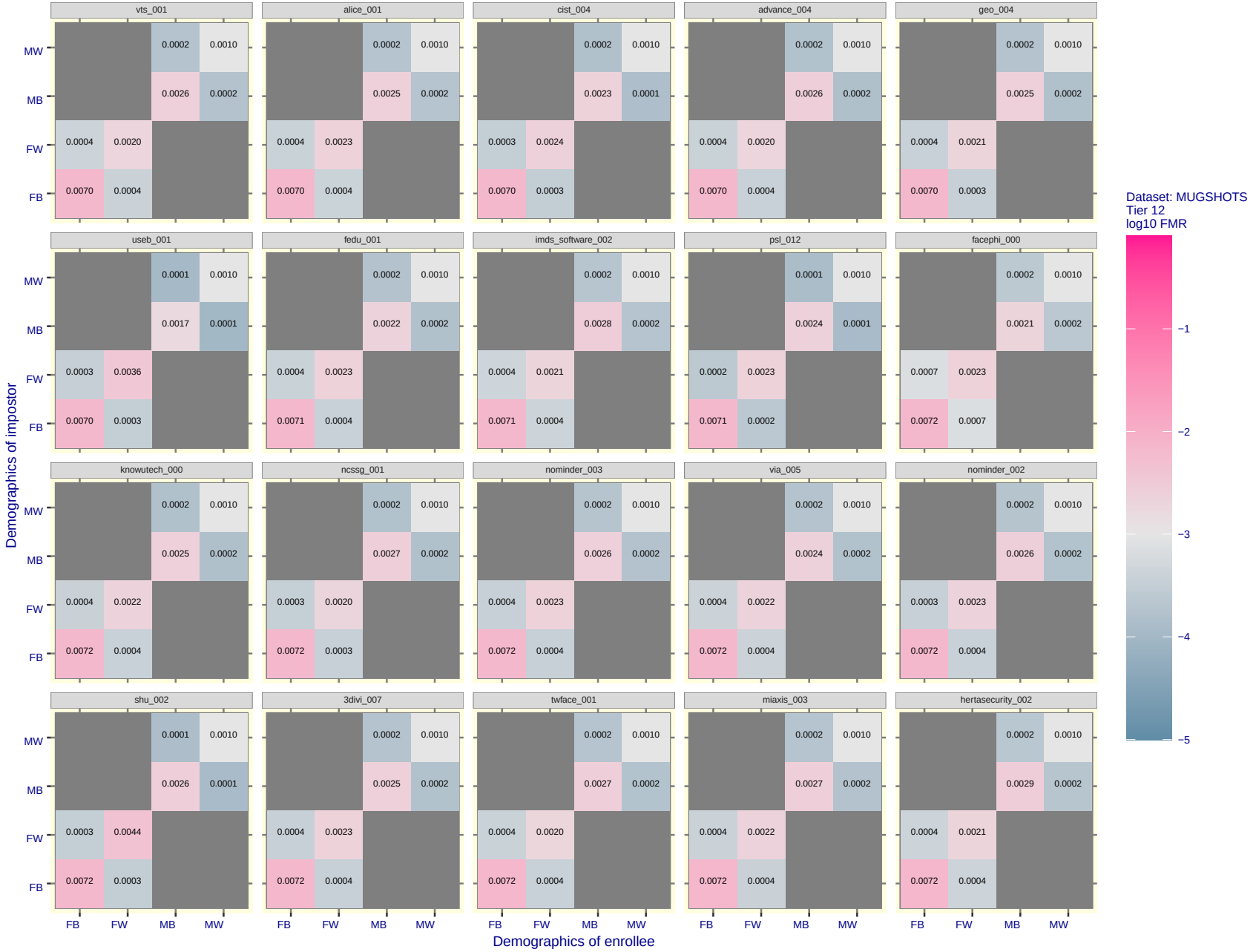

Figure 164: For the mugshot images, FMR *for same-sex impostor pairs of images annotated with codes for black female, black male, white female, white male. The threshold is set for each algorithm to give* FMR *= 0.001 for white males which is the demographic that usually gives the lowest* FMR*. This means the top right box is the same color in all panels. The panels are sorted over multiple pages in order of* FMR *on black females, which is the demographc that usually gives the highest* FMR*.*

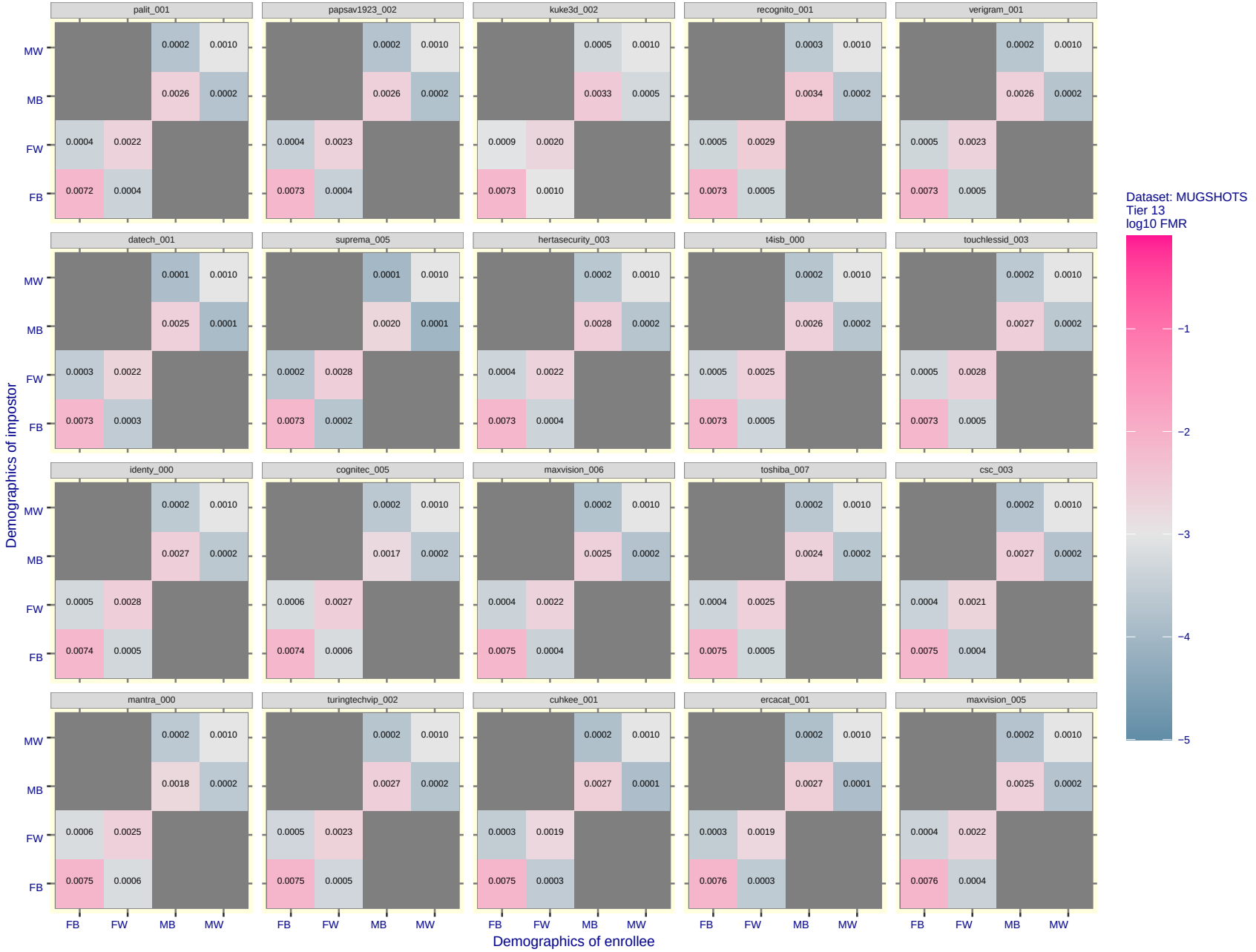

Figure 165: For the mugshot images, FMR *for same-sex impostor pairs of images annotated with codes for black female, black male, white female, white male. The threshold is set for each algorithm to give* FMR *= 0.001 for white males which is the demographic that usually gives the lowest* FMR*. This means the top right box is the same color in all panels. The panels are sorted over multiple pages in order of* FMR *on black females, which is the demographc that usually gives the highest* FMR*.*

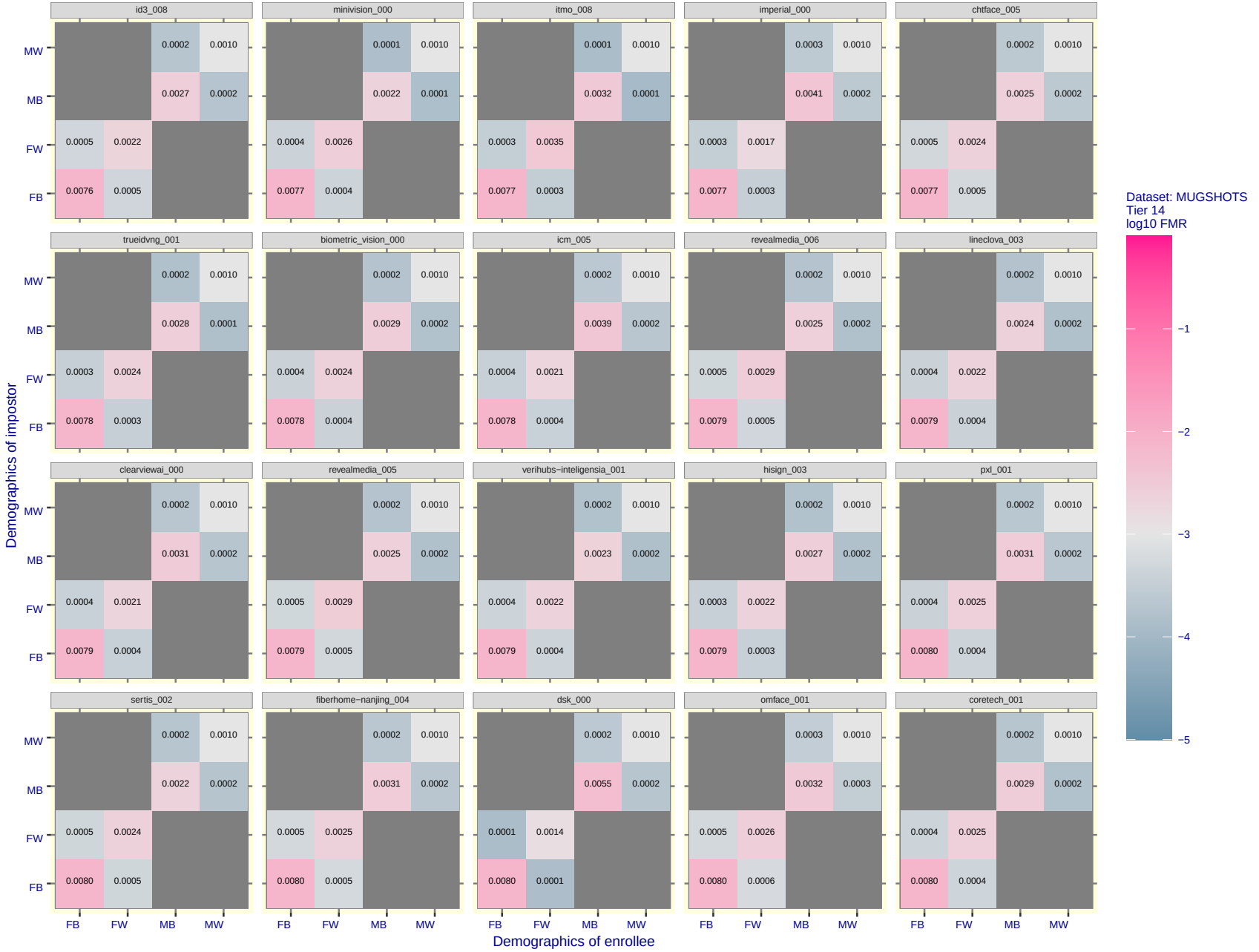

Figure 166: For the mugshot images, FMR *for same-sex impostor pairs of images annotated with codes for black female, black male, white female, white male. The threshold is set for each algorithm to give* FMR *= 0.001 for white males which is the demographic that usually gives the lowest* FMR*. This means the top right box is the same color in all panels. The panels are sorted over multiple pages in order of* FMR *on black females, which is the demographc that usually gives the highest* FMR*.*

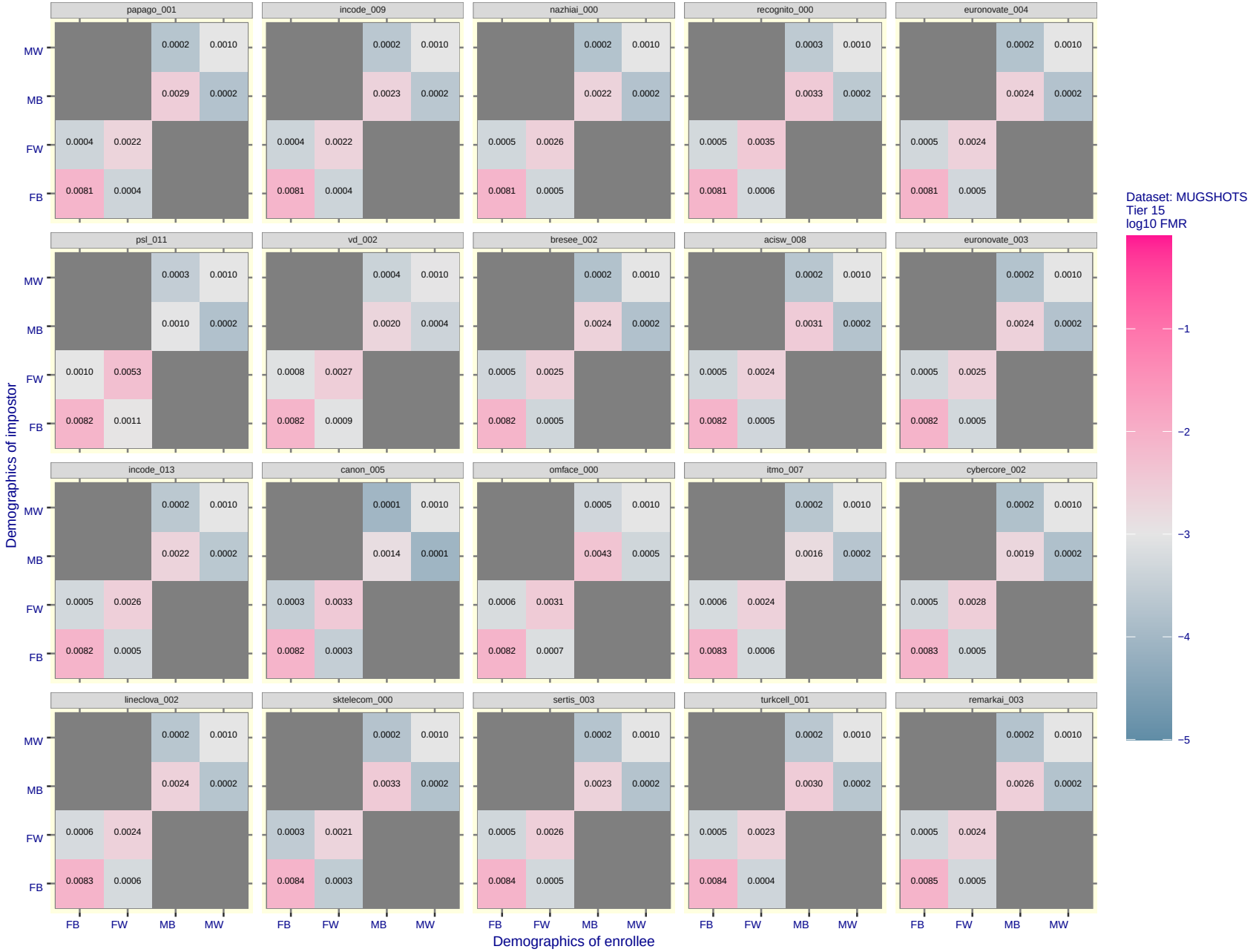

Figure 167: For the mugshot images, FMR *for same-sex impostor pairs of images annotated with codes for black female, black male, white female, white male. The threshold is set for each algorithm to give* FMR *= 0.001 for white males which is the demographic that usually gives the lowest* FMR*. This means the top right box is the same color in all panels. The panels are sorted over multiple pages in order of* FMR *on black females, which is the demographc that usually gives the highest* FMR*.*

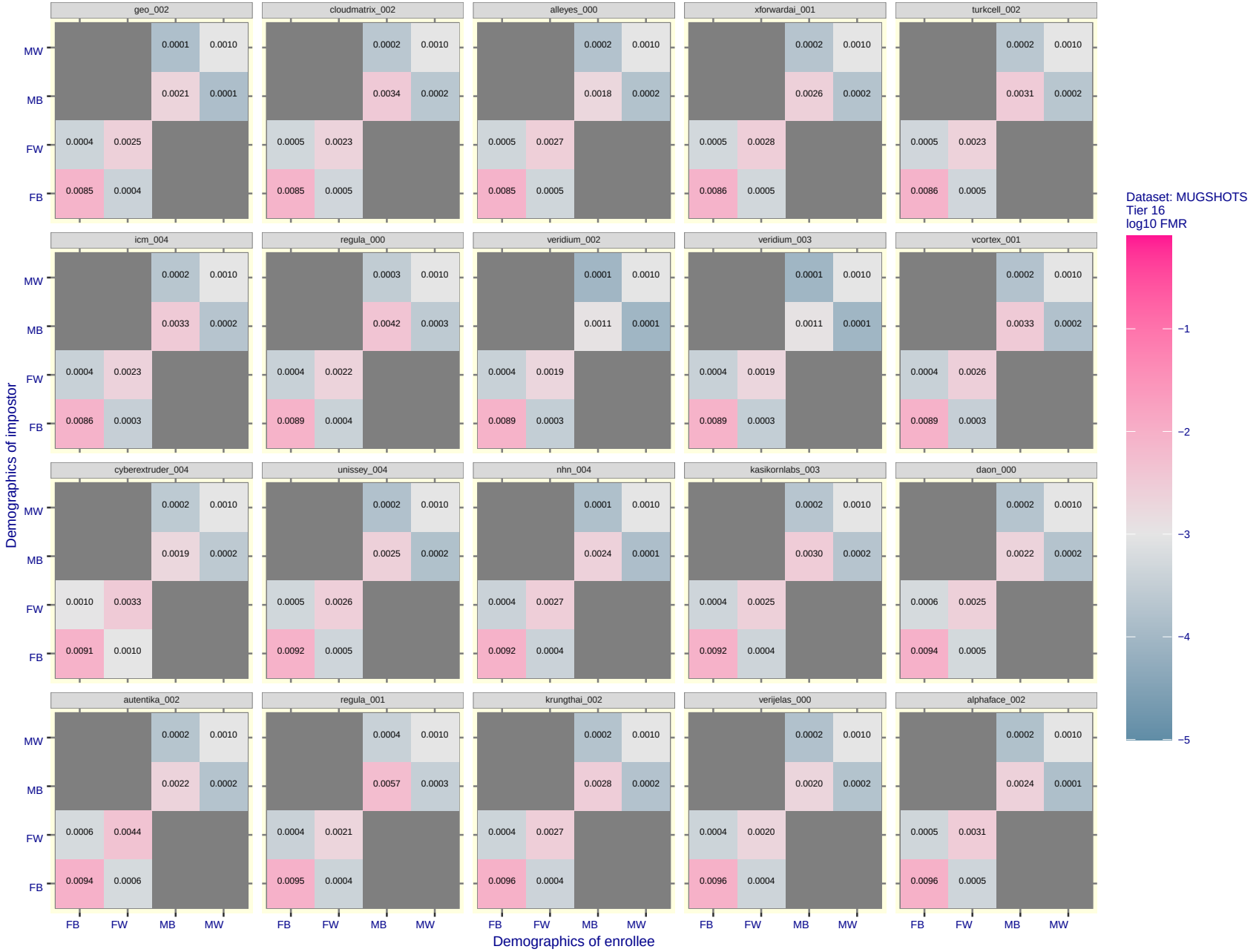

Figure 168: For the mugshot images, FMR *for same-sex impostor pairs of images annotated with codes for black female, black male, white female, white male. The threshold is set for each algorithm to give* FMR *= 0.001 for white males which is the demographic that usually gives the lowest* FMR*. This means the top right box is the same color in all panels. The panels are sorted over multiple pages in order of* FMR *on black females, which is the demographc that usually gives the highest* FMR*.*

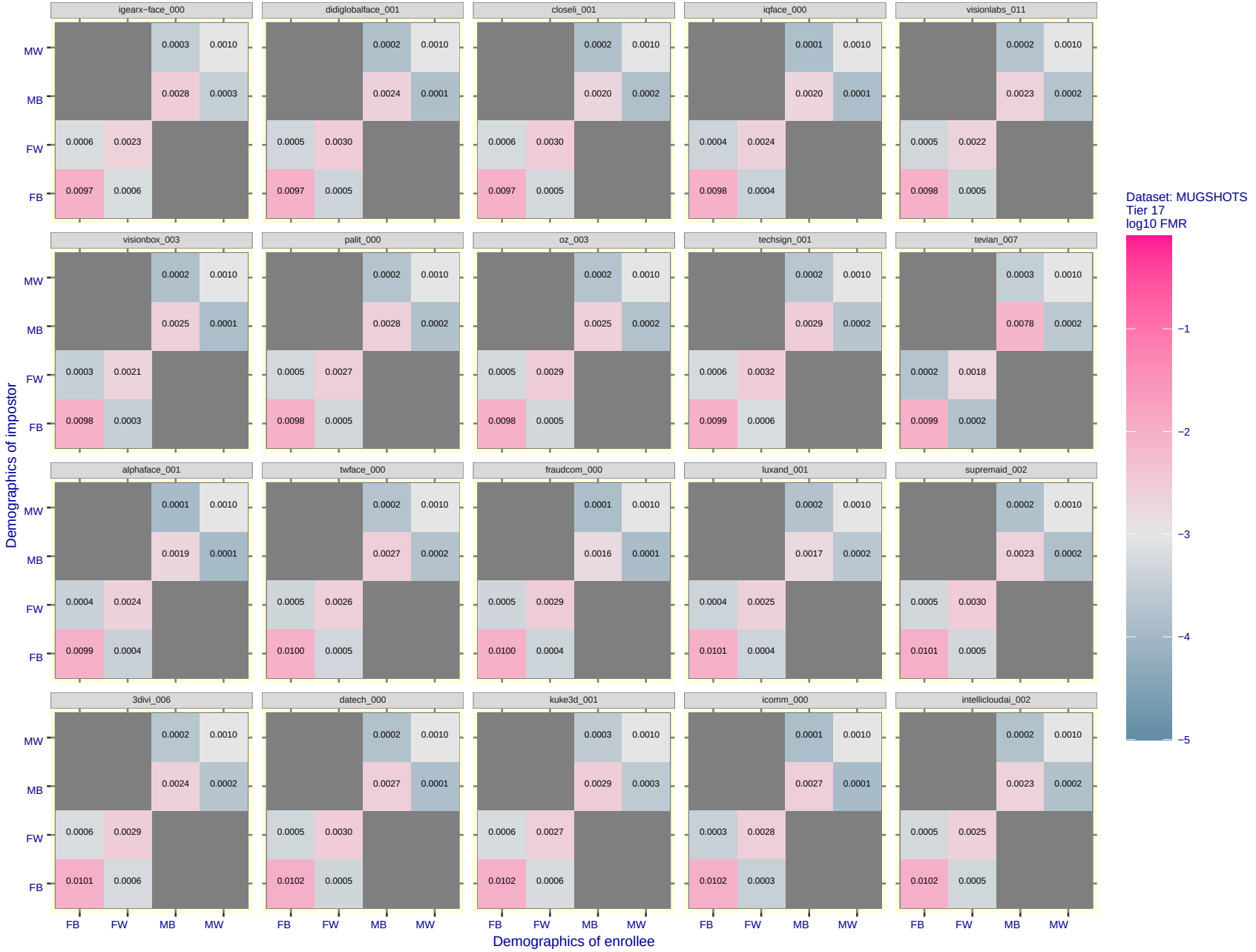

Figure 169: For the mugshot images, FMR *for same-sex impostor pairs of images annotated with codes for black female, black male, white female, white male. The threshold is set for each algorithm to give* FMR *= 0.001 for white males which is the demographic that usually gives the lowest* FMR*. This means the top right box is the same color in all panels. The panels are sorted over multiple pages in order of* FMR *on black females, which is the demographc that usually gives the highest* FMR*.*

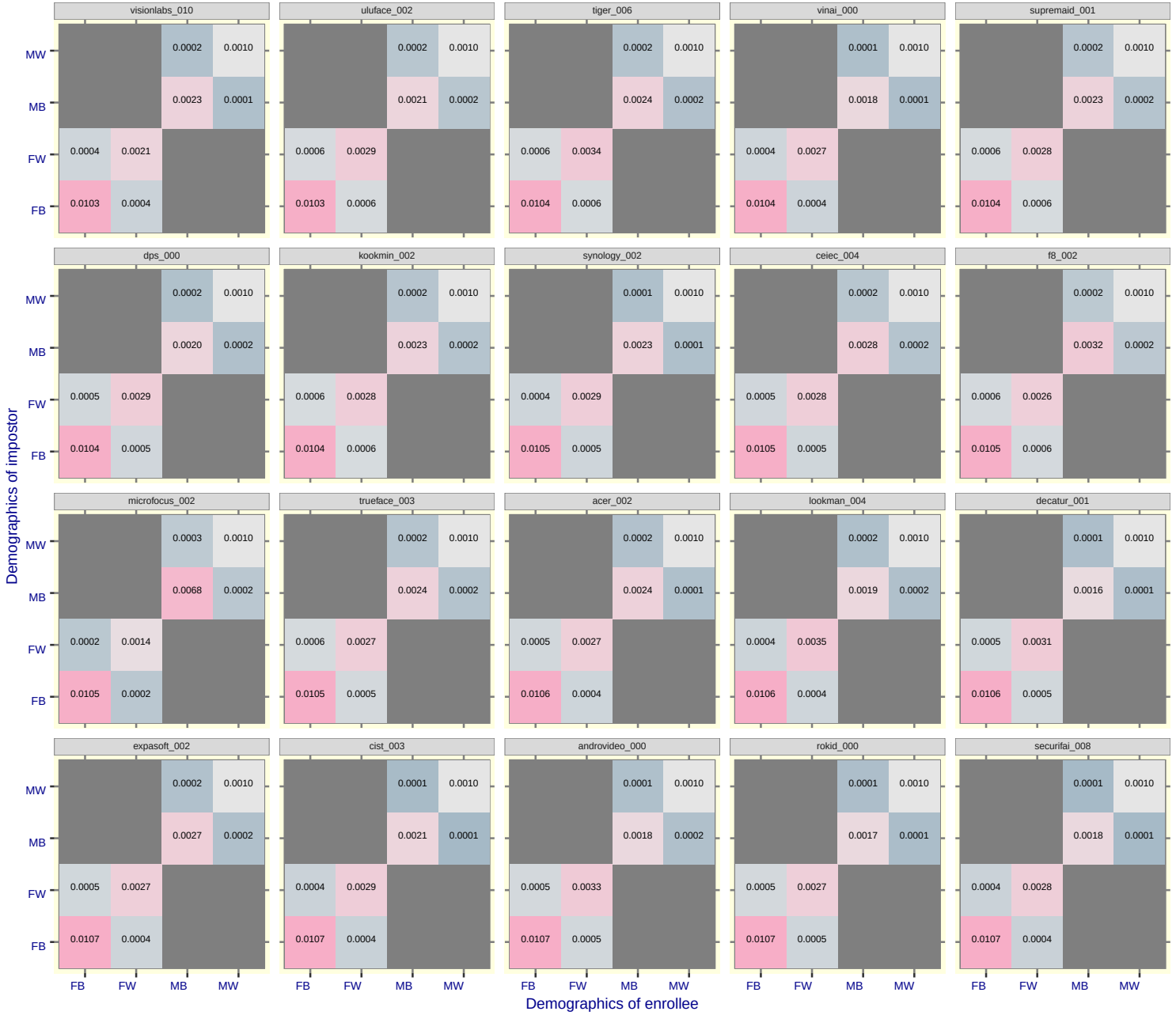

Figure 170: For the mugshot images, FMR *for same-sex impostor pairs of images annotated with codes for black female, black male, white female, white male. The threshold is set for each algorithm to give* FMR *= 0.001 for white males which is the demographic that usually gives the lowest* FMR*. This means the top right box is the same color in all panels. The panels are sorted over multiple pages in order of* FMR *on black females, which is the demographc that usually gives the highest* FMR*.*

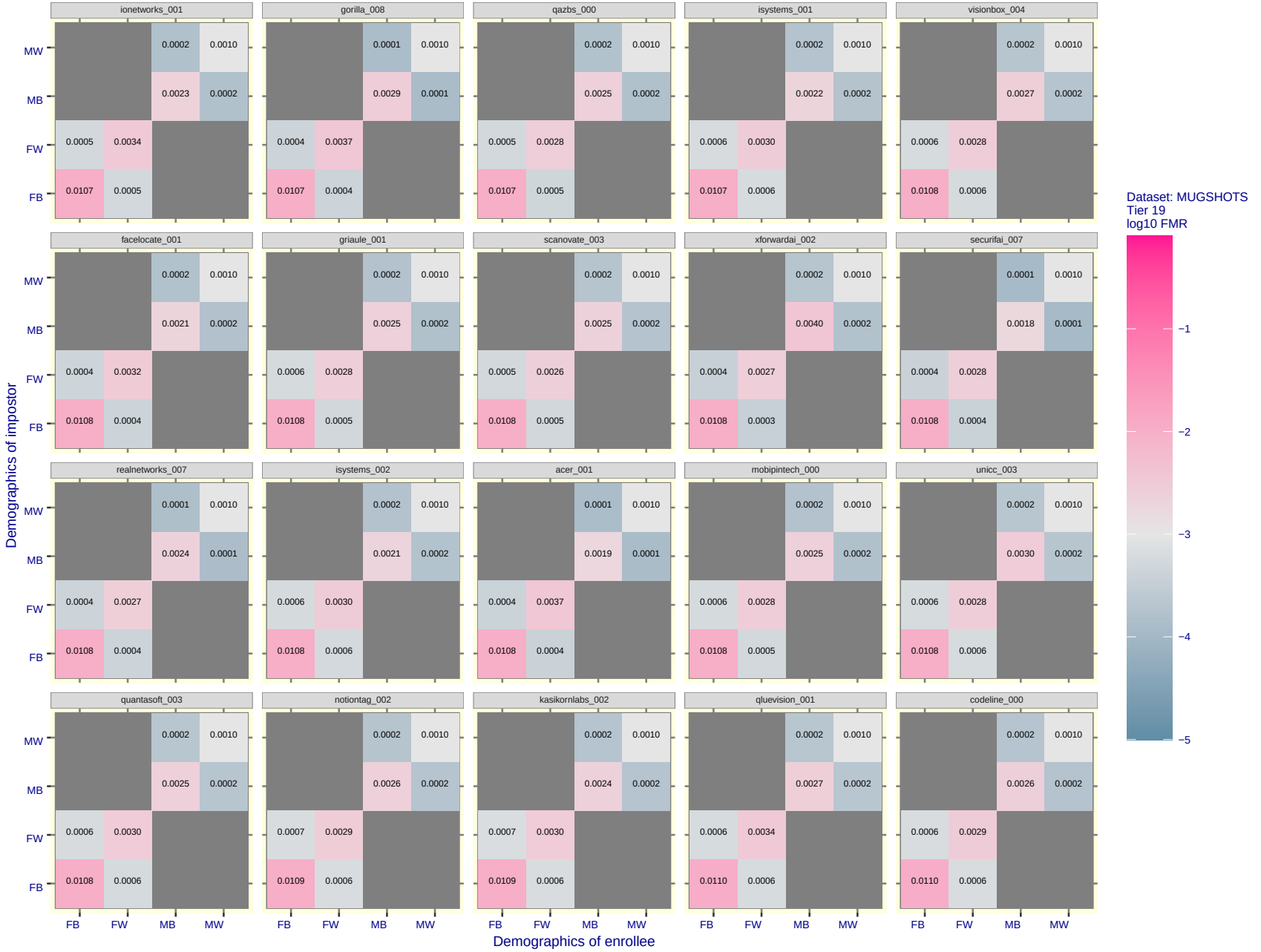

Figure 171: For the mugshot images, FMR *for same-sex impostor pairs of images annotated with codes for black female, black male, white female, white male. The threshold is set for each algorithm to give* FMR *= 0.001 for white males which is the demographic that usually gives the lowest* FMR*. This means the top right box is the same color in all panels. The panels are sorted over multiple pages in order of* FMR *on black females, which is the demographc that usually gives the highest* FMR*.*

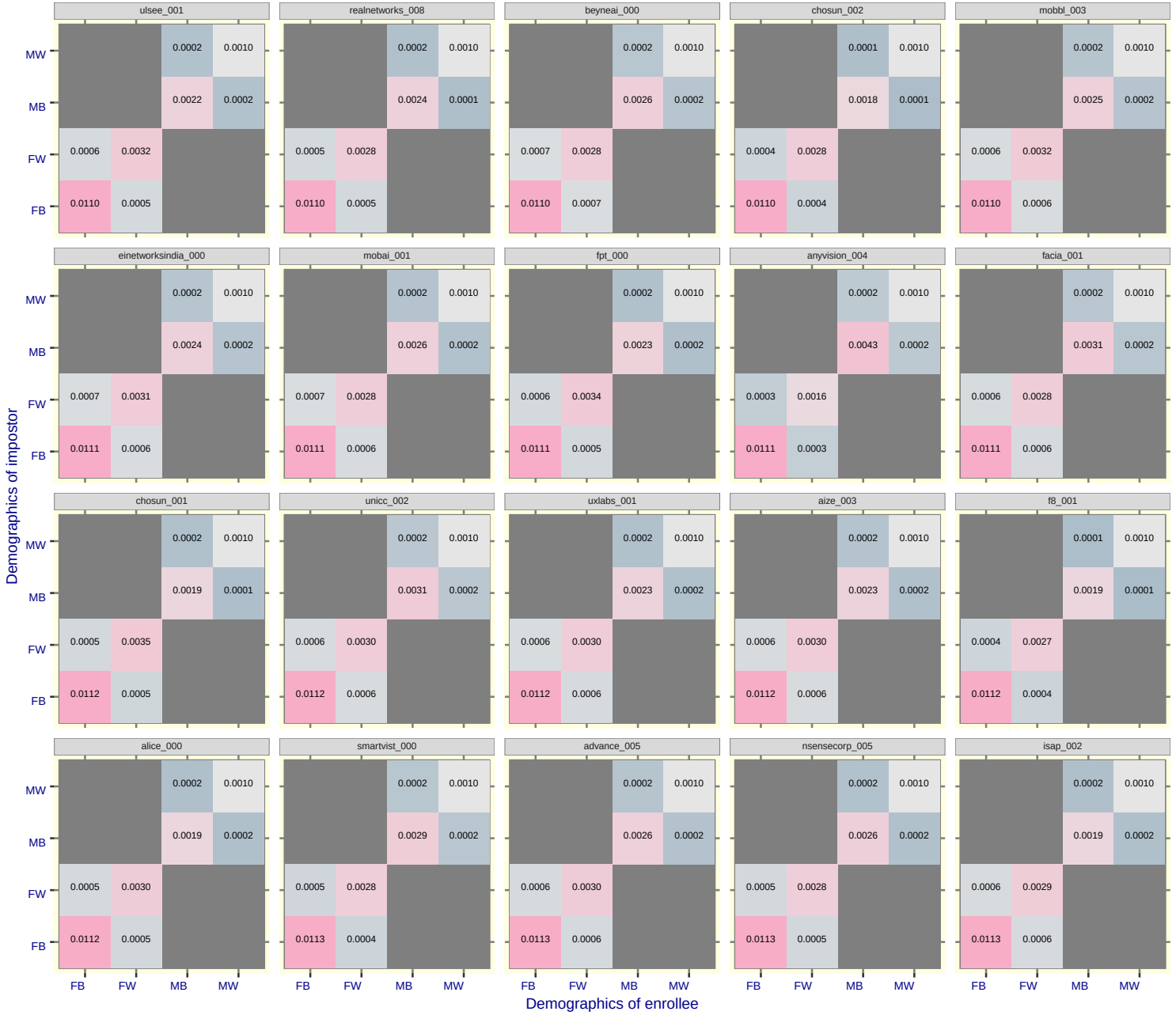

Figure 172: For the mugshot images, FMR *for same-sex impostor pairs of images annotated with codes for black female, black male, white female, white male. The threshold is set for each algorithm to give* FMR *= 0.001 for white males which is the demographic that usually gives the lowest* FMR*. This means the top right box is the same color in all panels. The panels are sorted over multiple pages in order of* FMR *on black females, which is the demographc that usually gives the highest* FMR*.*

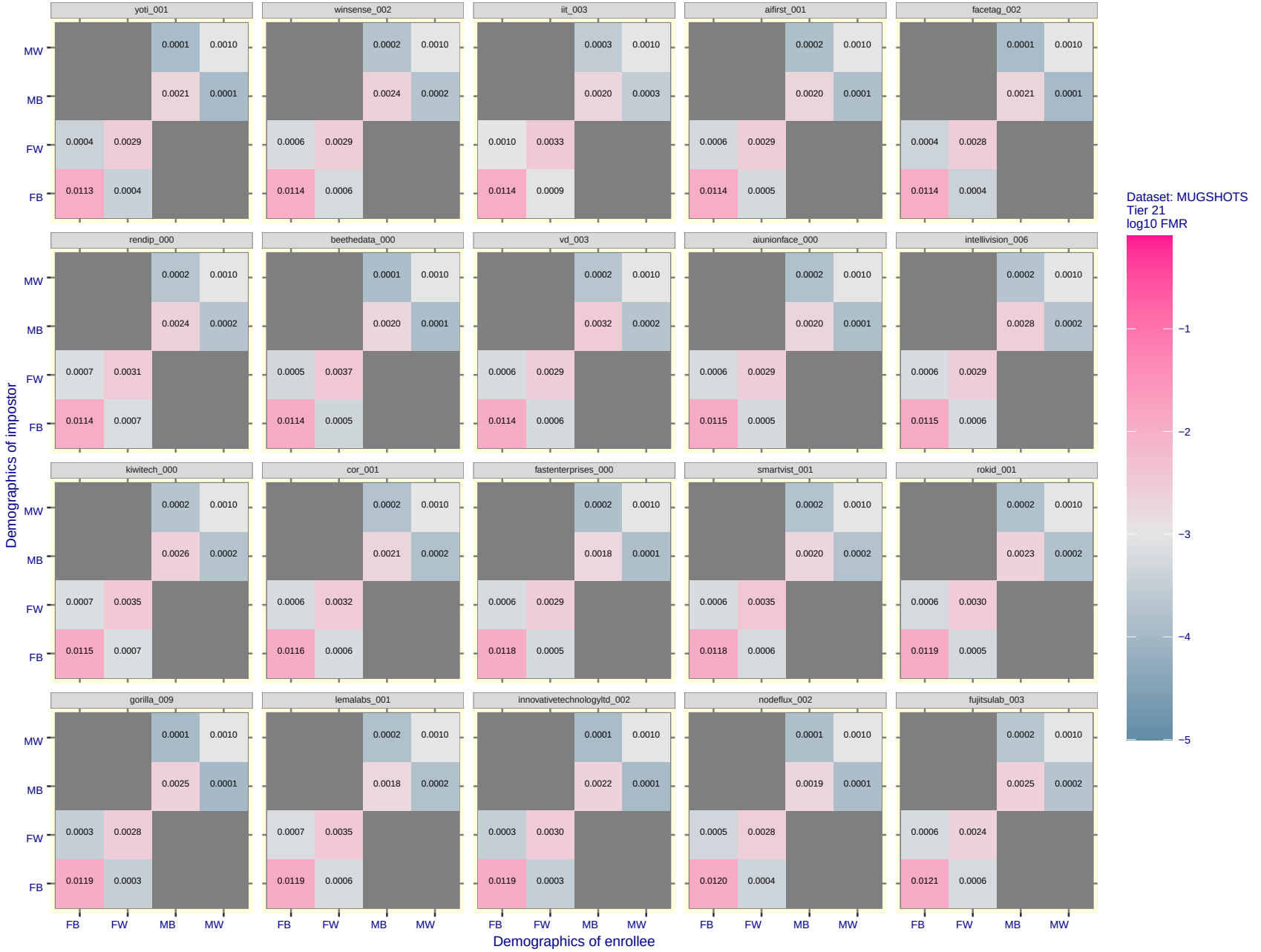

Figure 173: For the mugshot images, FMR *for same-sex impostor pairs of images annotated with codes for black female, black male, white female, white male. The threshold is set for each algorithm to give* FMR *= 0.001 for white males which is the demographic that usually gives the lowest* FMR*. This means the top right box is the same color in all panels. The panels are sorted over multiple pages in order of* FMR *on black females, which is the demographc that usually gives the highest* FMR*.*

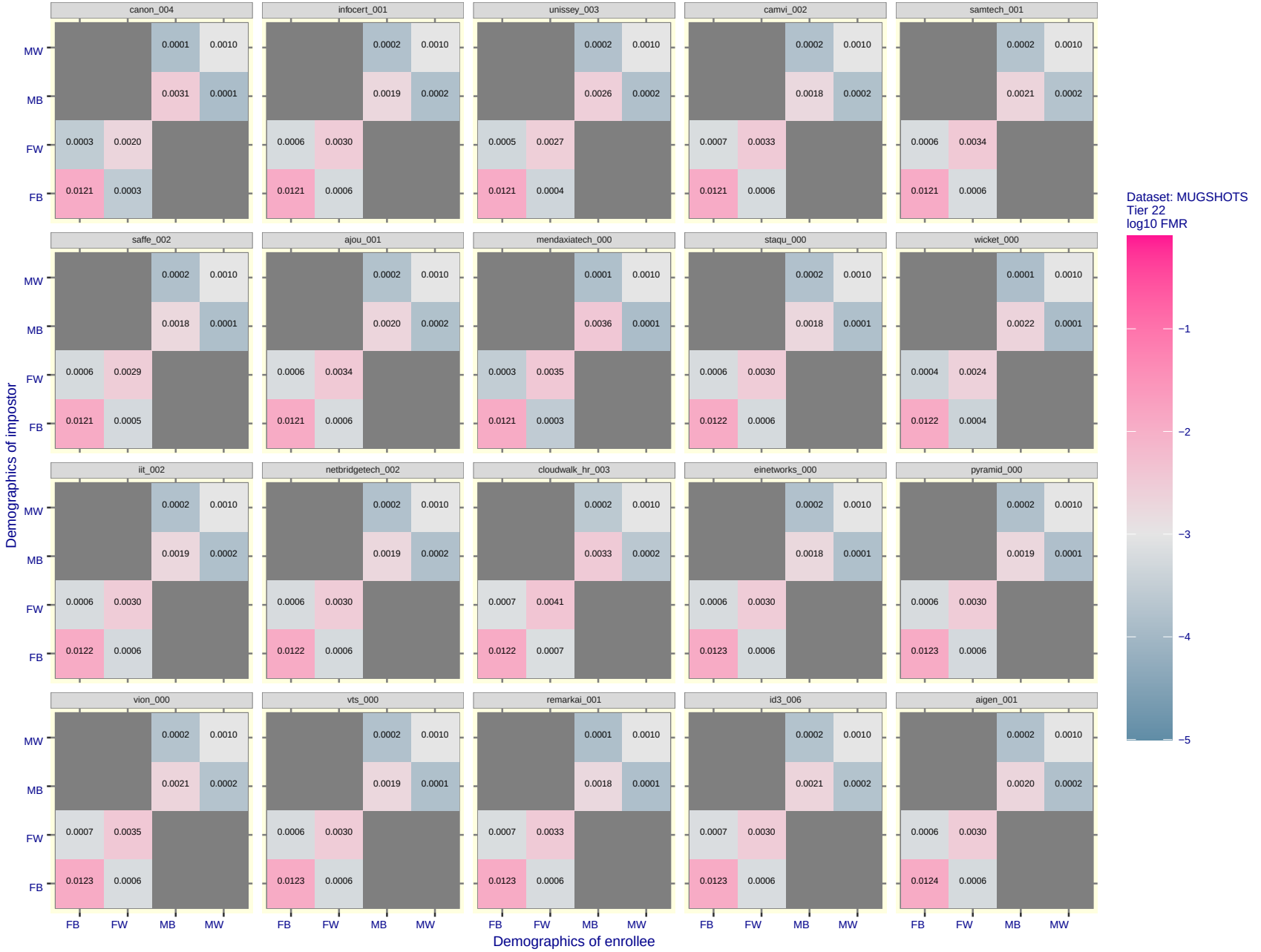

Figure 174: For the mugshot images, FMR *for same-sex impostor pairs of images annotated with codes for black female, black male, white female, white male. The threshold is set for each algorithm to give* FMR *= 0.001 for white males which is the demographic that usually gives the lowest* FMR*. This means the top right box is the same color in all panels. The panels are sorted over multiple pages in order of* FMR *on black females, which is the demographc that usually gives the highest* FMR*.*

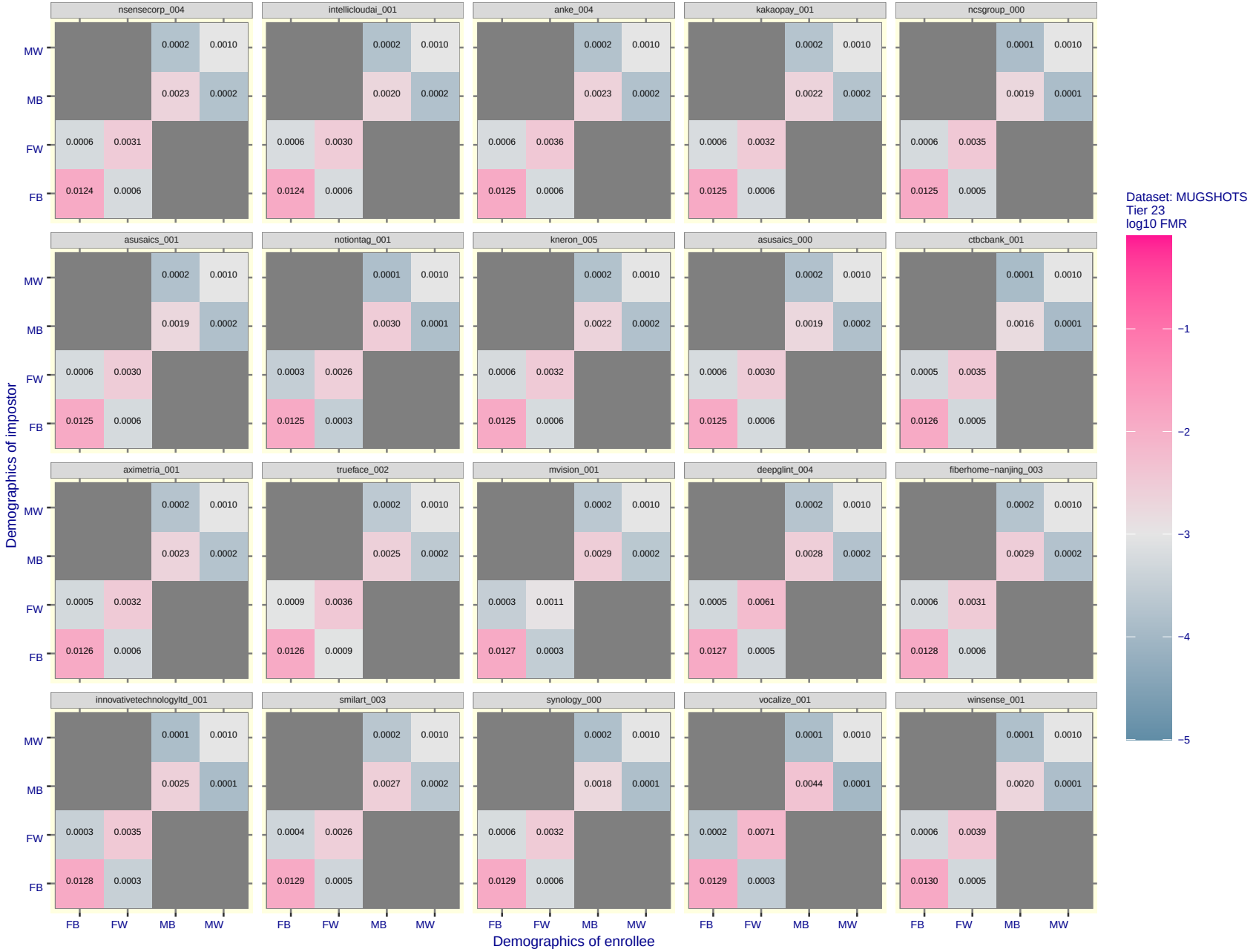

Figure 175: For the mugshot images, FMR *for same-sex impostor pairs of images annotated with codes for black female, black male, white female, white male. The threshold is set for each algorithm to give* FMR *= 0.001 for white males which is the demographic that usually gives the lowest* FMR*. This means the top right box is the same color in all panels. The panels are sorted over multiple pages in order of* FMR *on black females, which is the demographc that usually gives the highest* FMR*.*

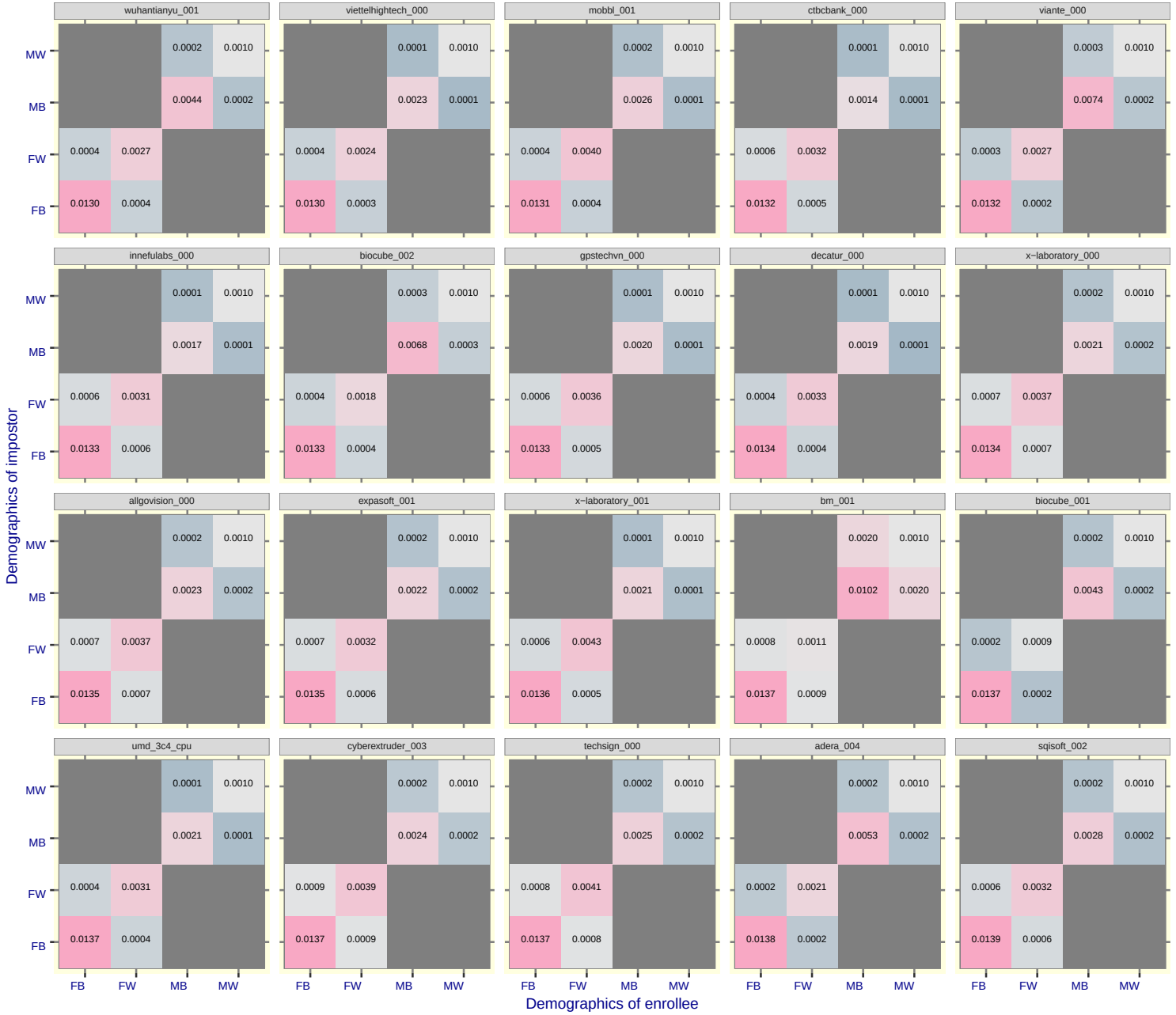

Figure 176: For the mugshot images, FMR *for same-sex impostor pairs of images annotated with codes for black female, black male, white female, white male. The threshold is set for each algorithm to give* FMR *= 0.001 for white males which is the demographic that usually gives the lowest* FMR*. This means the top right box is the same color in all panels. The panels are sorted over multiple pages in order of* FMR *on black females, which is the demographc that usually gives the highest* FMR*.*

2024/04/17 08:45:50
FNMR(T) "False non-match rate"
FMR(T) "False match rate"

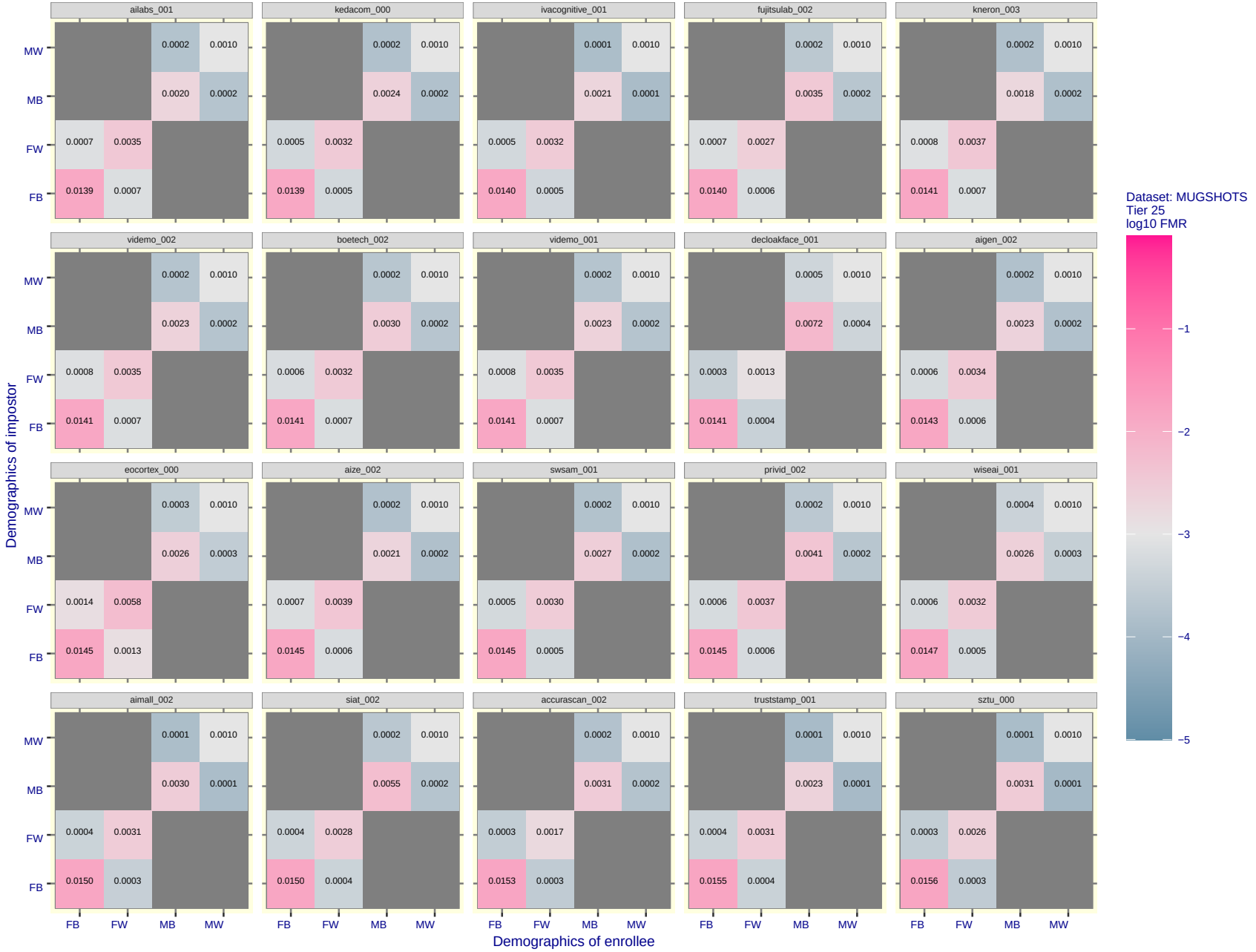

Figure 177: For the mugshot images, FMR *for same-sex impostor pairs of images annotated with codes for black female, black male, white female, white male. The threshold is set for each algorithm to give* FMR *= 0.001 for white males which is the demographic that usually gives the lowest* FMR*. This means the top right box is the same color in all panels. The panels are sorted over multiple pages in order of* FMR *on black females, which is the demographc that usually gives the highest* FMR*.*

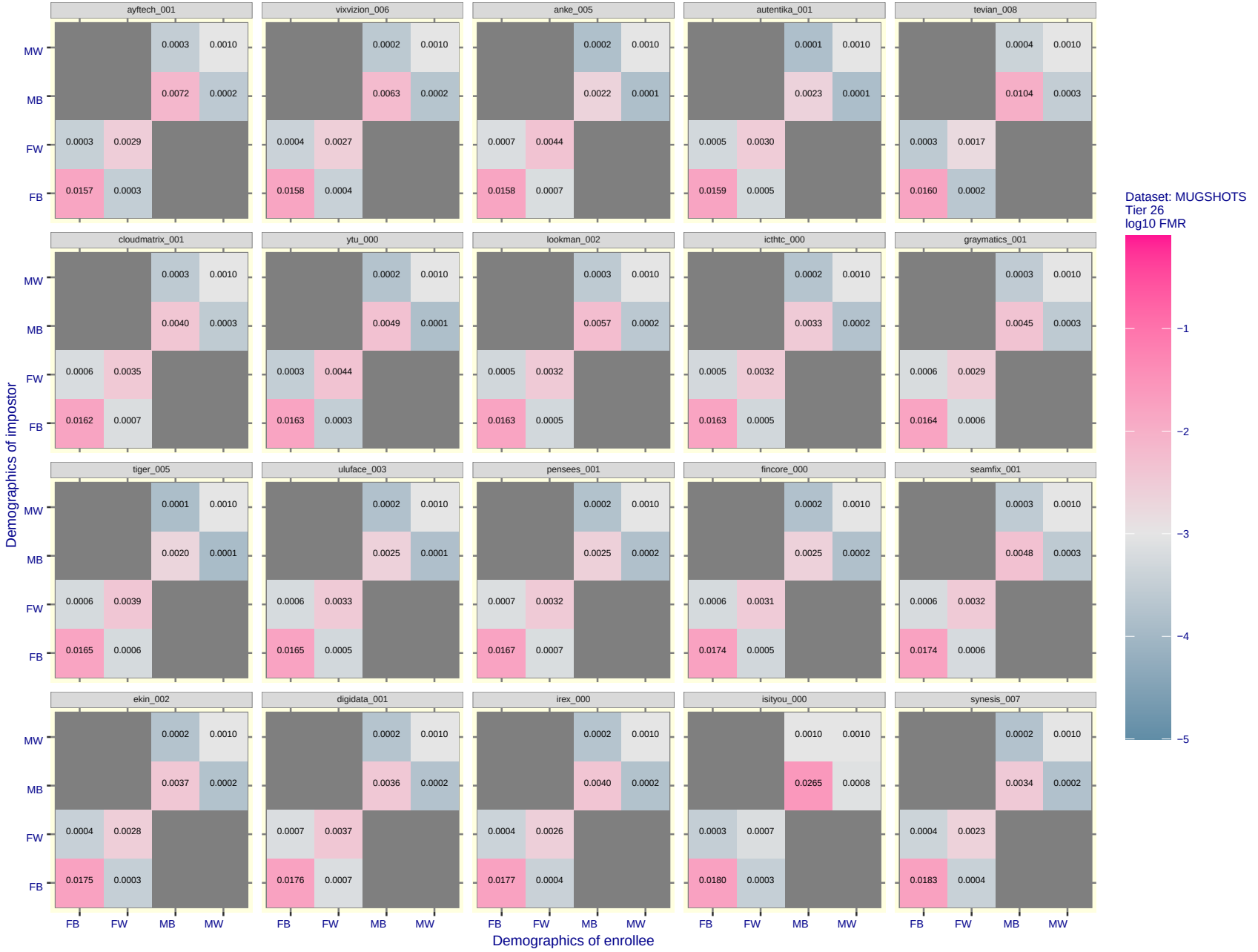

Figure 178: For the mugshot images, FMR *for same-sex impostor pairs of images annotated with codes for black female, black male, white female, white male. The threshold is set for each algorithm to give* FMR *= 0.001 for white males which is the demographic that usually gives the lowest* FMR*. This means the top right box is the same color in all panels. The panels are sorted over multiple pages in order of* FMR *on black females, which is the demographc that usually gives the highest* FMR*.*

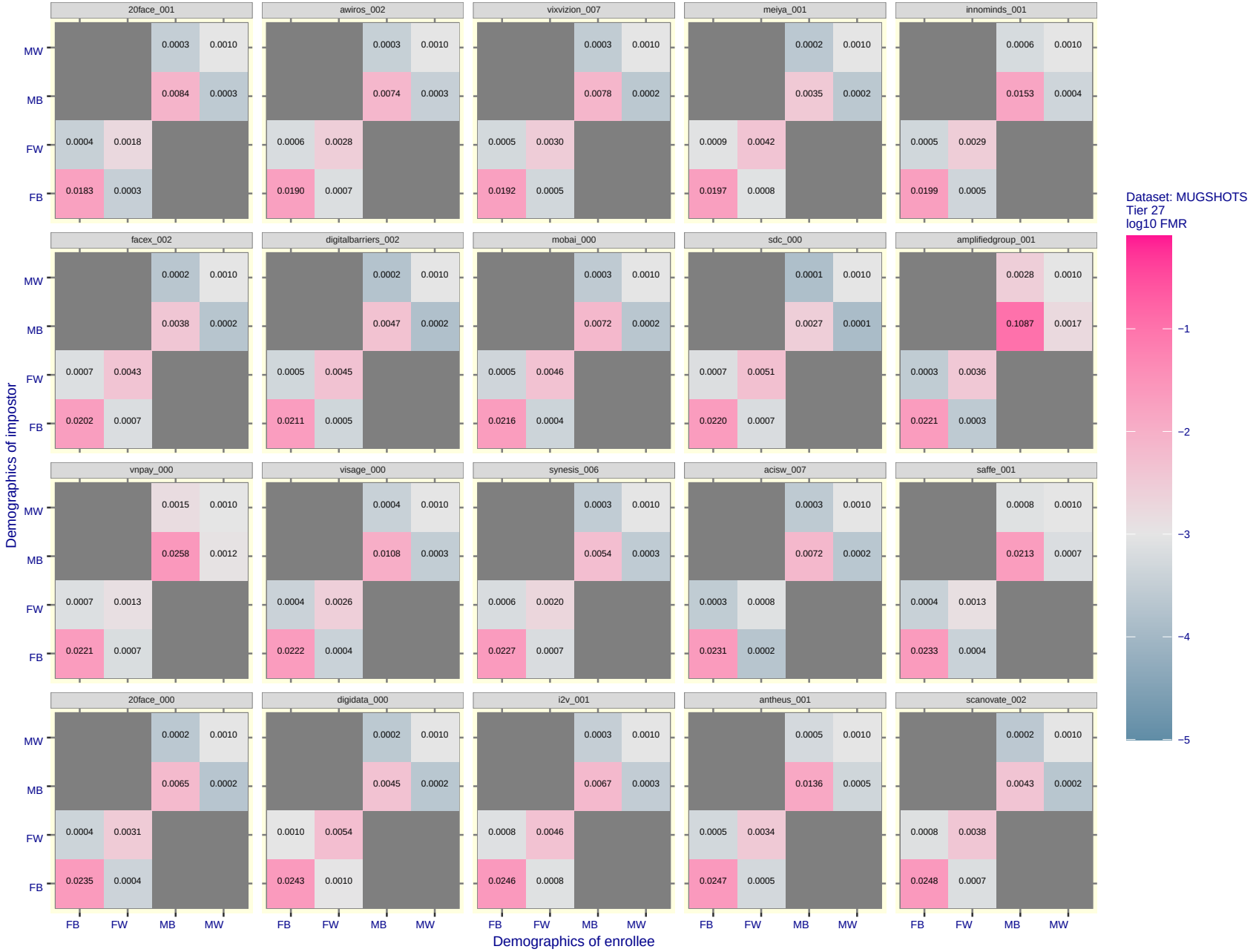

Figure 179: For the mugshot images, FMR *for same-sex impostor pairs of images annotated with codes for black female, black male, white female, white male. The threshold is set for each algorithm to give* FMR *= 0.001 for white males which is the demographic that usually gives the lowest* FMR*. This means the top right box is the same color in all panels. The panels are sorted over multiple pages in order of* FMR *on black females, which is the demographc that usually gives the highest* FMR*.*

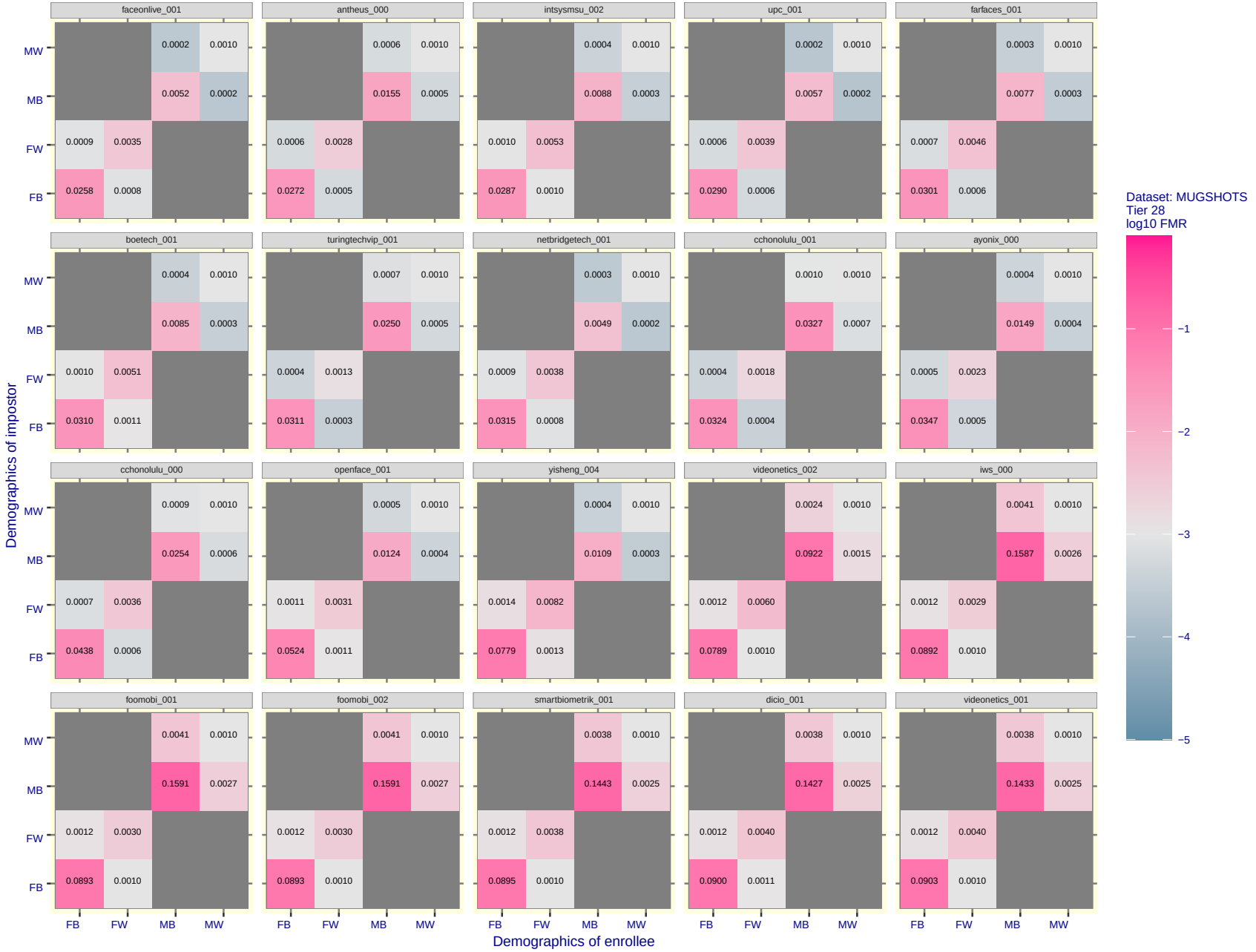

Figure 180: For the mugshot images, FMR *for same-sex impostor pairs of images annotated with codes for black female, black male, white female, white male. The threshold is set for each algorithm to give* FMR *= 0.001 for white males which is the demographic that usually gives the lowest* FMR*. This means the top right box is the same color in all panels. The panels are sorted over multiple pages in order of* FMR *on black females, which is the demographc that usually gives the highest* FMR*.*

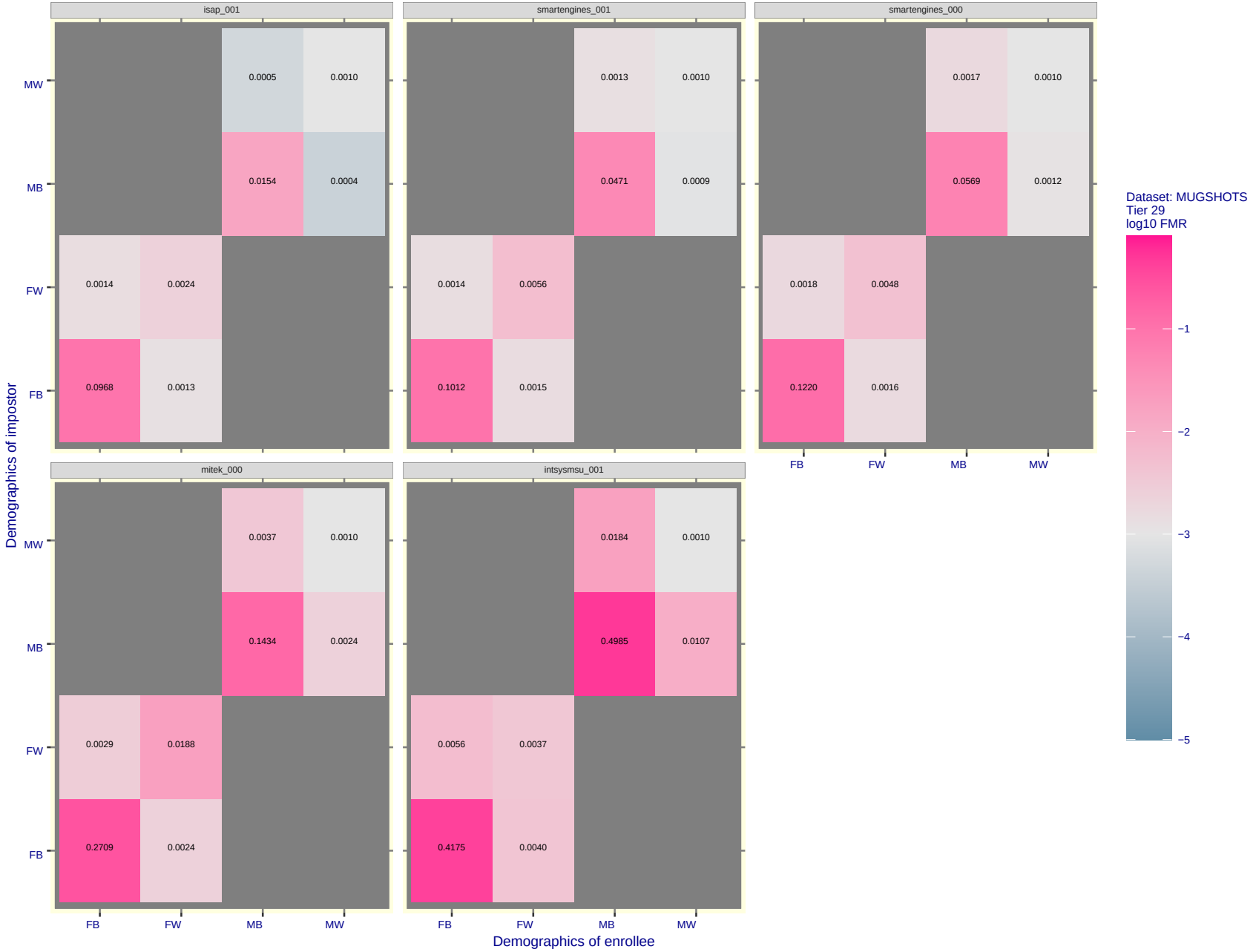

Figure 181: For the mugshot images, FMR *for same-sex impostor pairs of images annotated with codes for black female, black male, white female, white male. The threshold is set for each algorithm to give* FMR *= 0.001 for white males which is the demographic that usually gives the lowest* FMR*. This means the top right box is the same color in all panels. The panels are sorted over multiple pages in order of* FMR *on black females, which is the demographc that usually gives the highest* FMR*.*

FNMR(T) "False non-match rate"
FMR(T) "False match rate"

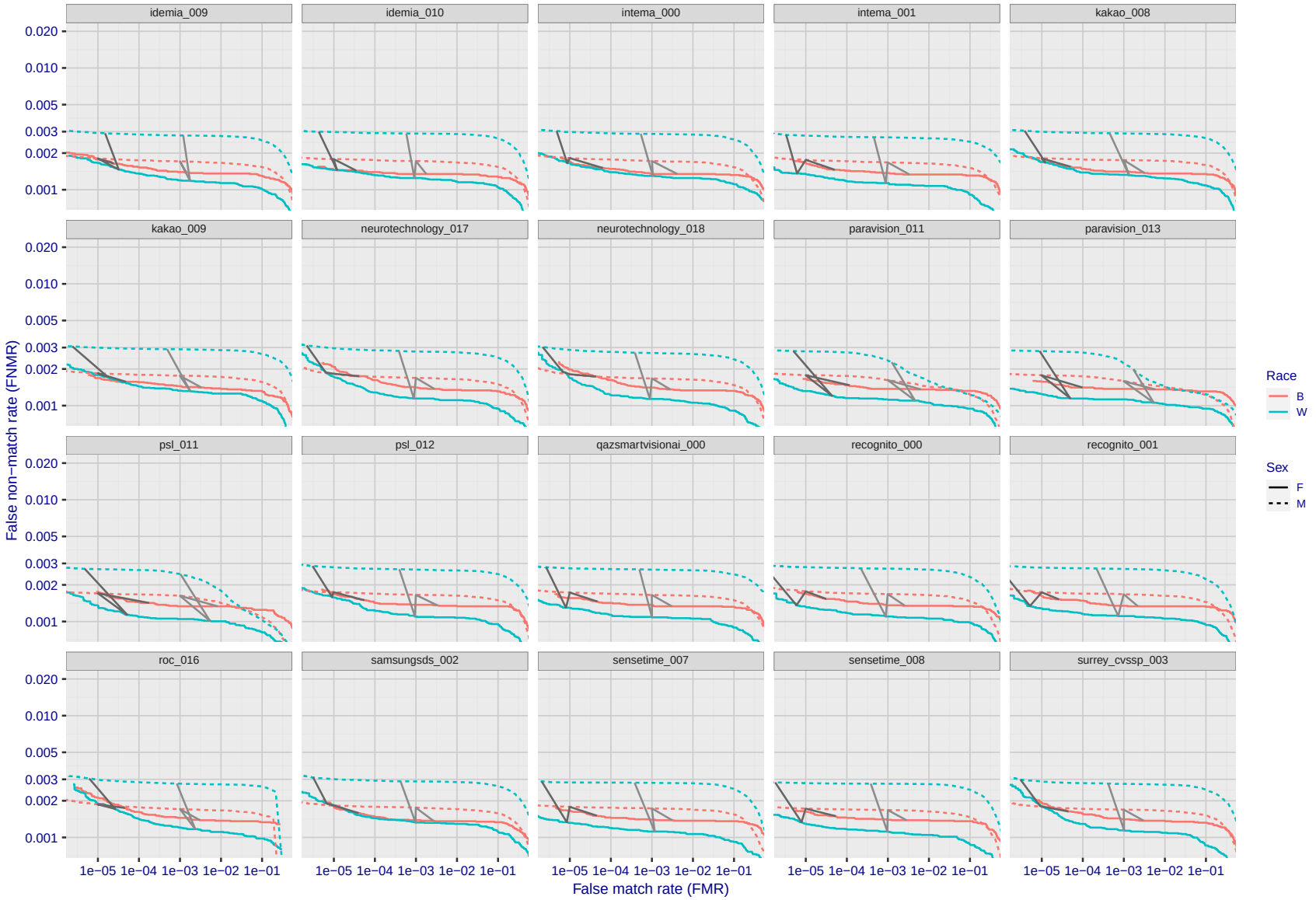

Figure 182: For the mugshot images, error tradeoff characteristics for white females, black females, black males and white males. The Z-shaped grey lines correspond to fixed thresholds, showing both *FNMR and FMR vary at one T value. Note: Many of the plots will naively be read as saying women gives worse error rates than men because the solid traces lie above the dotted ones. However, this is misleading and incomplete: The grey lines show the traces reveal horizontal shifts. Thus for the cogent-003 algorithm FNMR for men is* higher *than for women* at a fixed threshold *but, at the same time, FMR is higher for women - see Figure 284. As access control systems almost always operate at a fixed threshold, the naive interpretation is incorrect.*

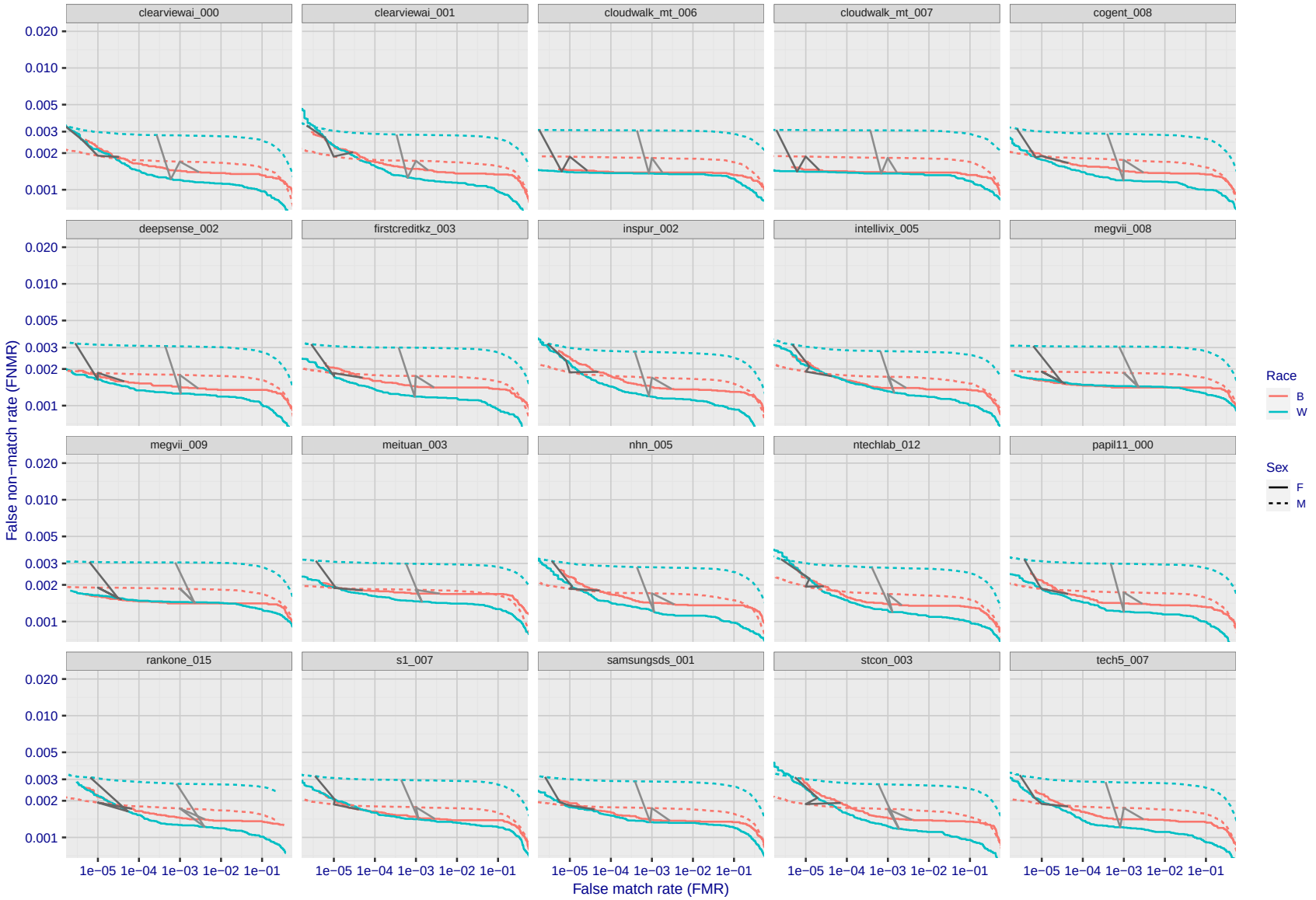

Figure 183: For the mugshot images, error tradeoff characteristics for white females, black females, black males and white males. The Z-shaped grey lines correspond to fixed thresholds, showing both *FNMR and FMR vary at one T value. Note: Many of the plots will naively be read as saying women gives worse error rates than men because the solid traces lie above the dotted ones. However, this is misleading and incomplete: The grey lines show the traces reveal horizontal shifts. Thus for the cogent-003 algorithm FNMR for men is* higher *than for women* at a fixed threshold *but, at the same time, FMR is higher for women - see Figure 284. As access control systems almost always operate at a fixed threshold, the naive interpretation is incorrect.*

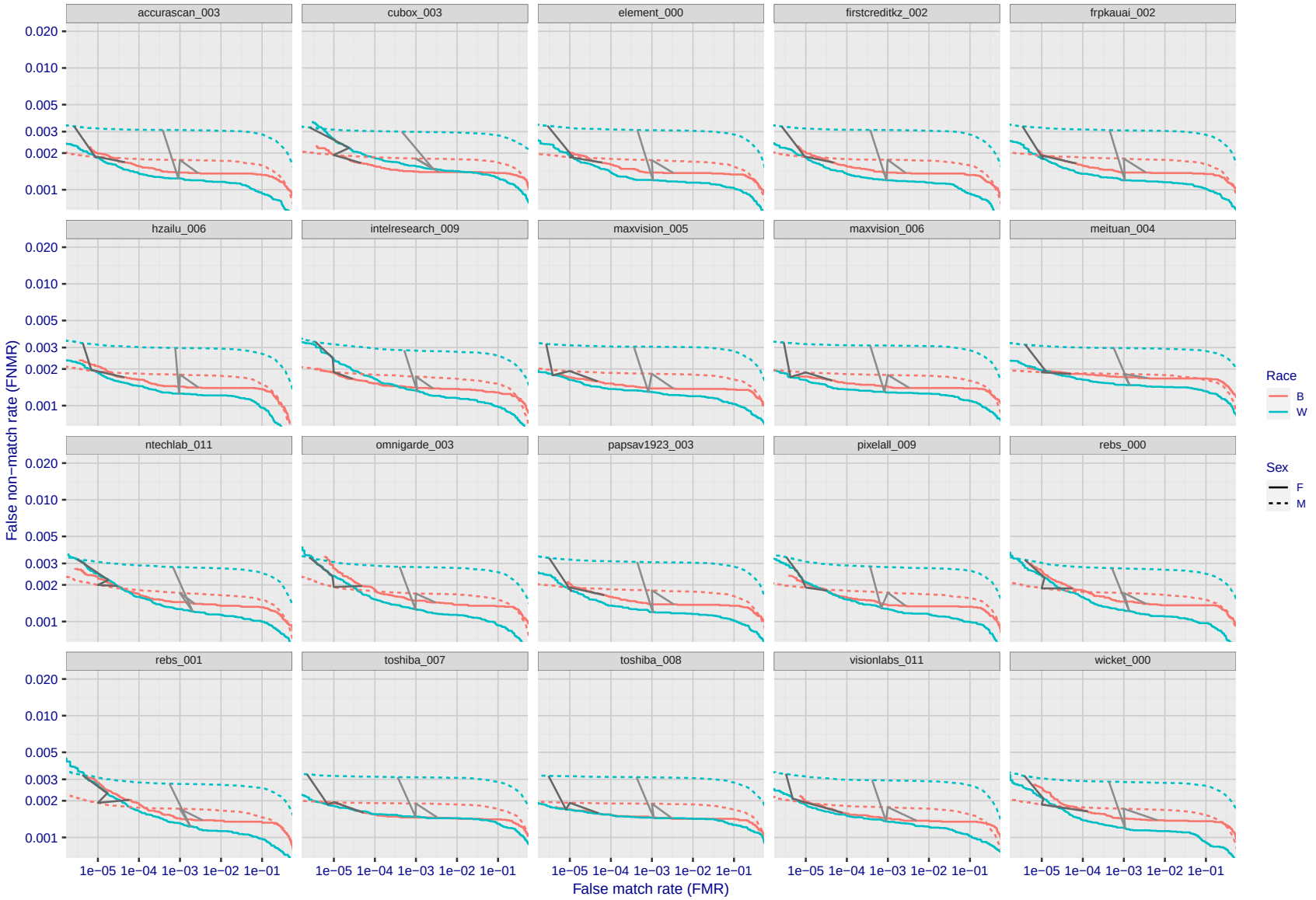

Figure 184: For the mugshot images, error tradeoff characteristics for white females, black females, black males and white males. The Z-shaped grey lines correspond to fixed thresholds, showing both *FNMR and FMR vary at one T value. Note: Many of the plots will naively be read as saying women gives worse error rates than men because the solid traces lie above the dotted ones. However, this is misleading and incomplete: The grey lines show the traces reveal horizontal shifts. Thus for the cogent-003 algorithm FNMR for men is* higher *than for women* at a fixed threshold *but, at the same time, FMR is higher for women - see Figure 284. As access control systems almost always operate at a fixed threshold, the naive interpretation is incorrect.*

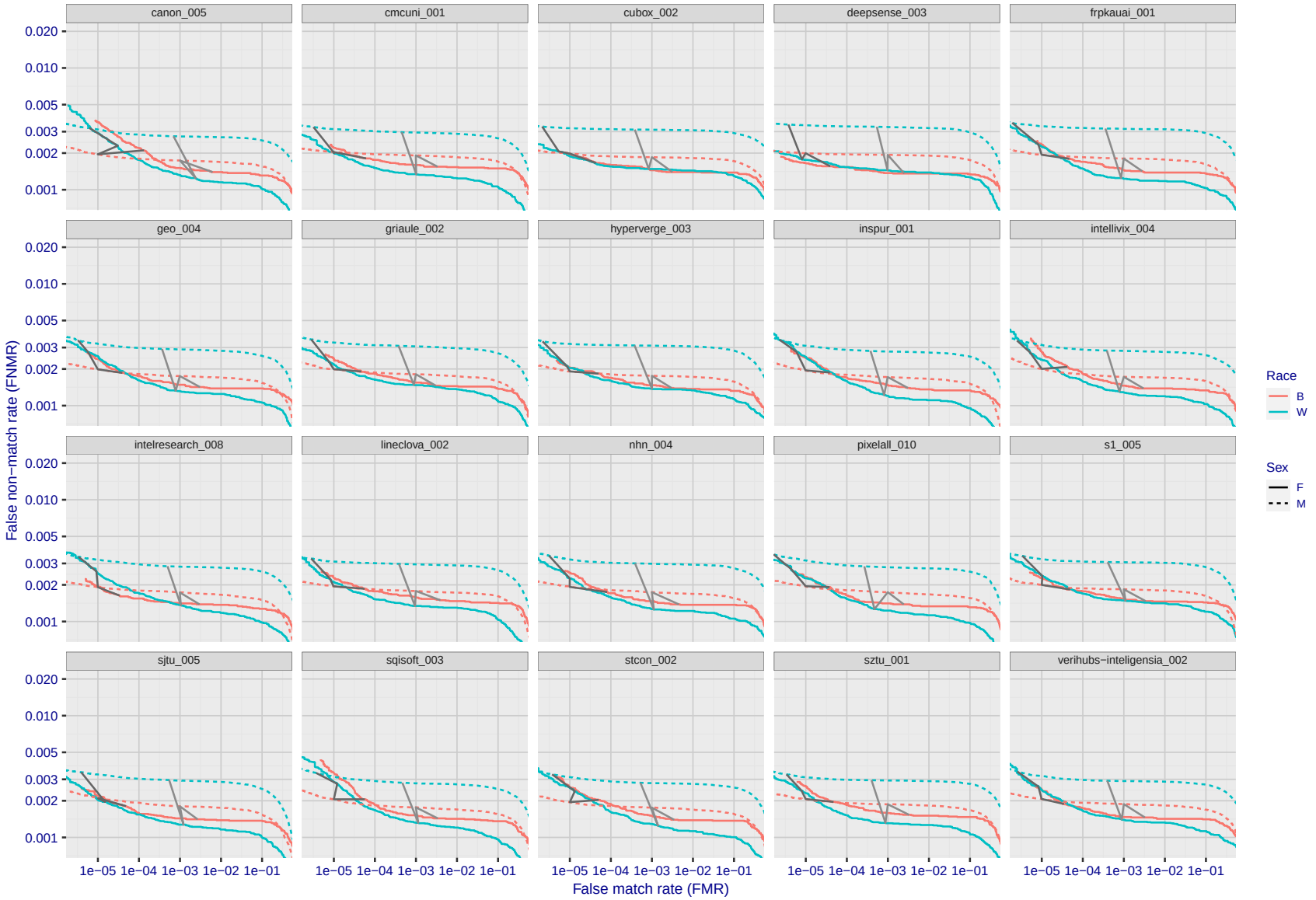

Figure 185: For the mugshot images, error tradeoff characteristics for white females, black females, black males and white males. The Z-shaped grey lines correspond to fixed thresholds, showing both *FNMR and FMR vary at one T value. Note: Many of the plots will naively be read as saying women gives worse error rates than men because the solid traces lie above the dotted ones. However, this is misleading and incomplete: The grey lines show the traces reveal horizontal shifts. Thus for the cogent-003 algorithm FNMR for men is* higher *than for women* at a fixed threshold *but, at the same time, FMR is higher for women - see Figure 284. As access control systems almost always operate at a fixed threshold, the naive interpretation is incorrect.*

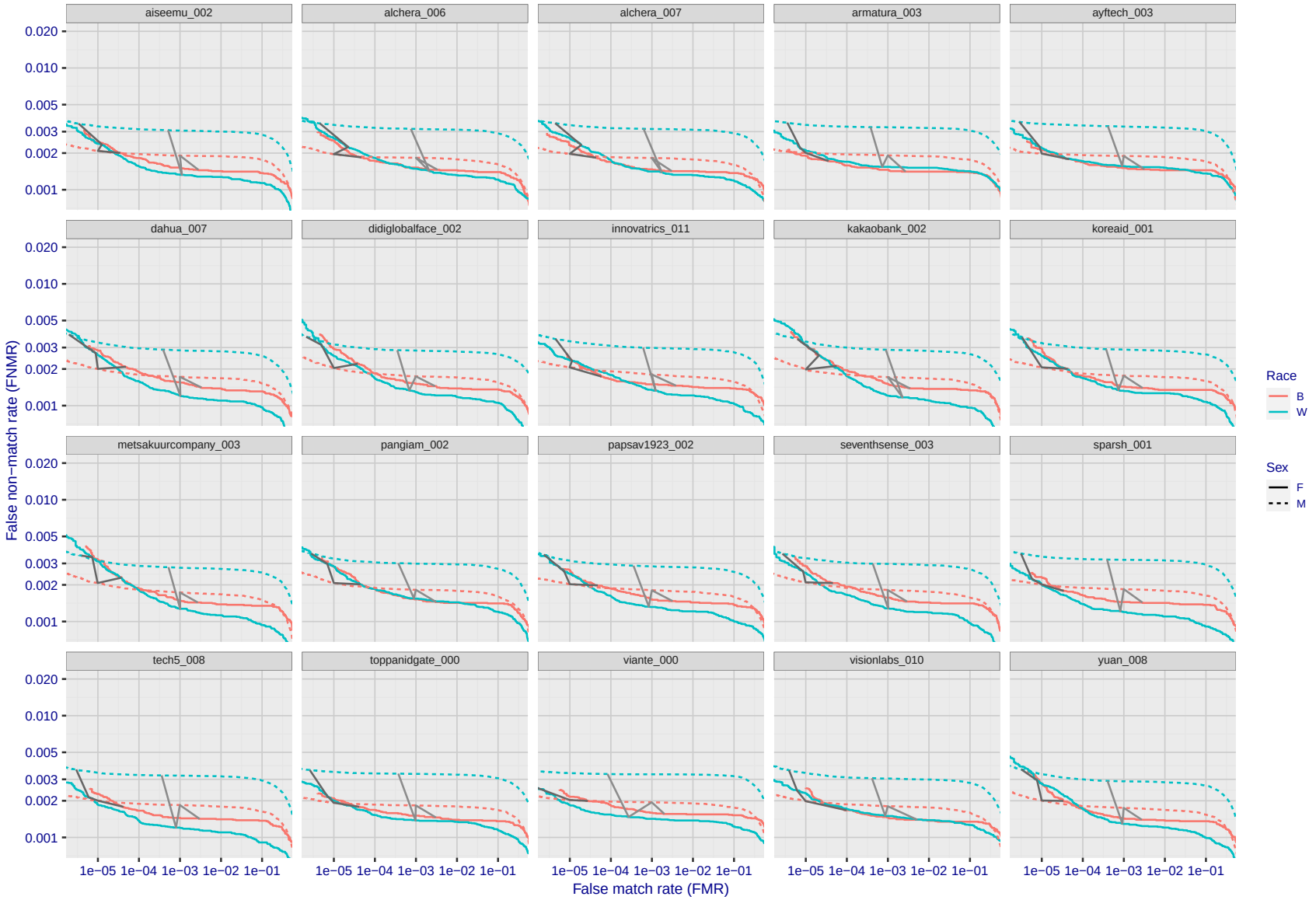

Figure 186: For the mugshot images, error tradeoff characteristics for white females, black females, black males and white males. The Z-shaped grey lines correspond to fixed thresholds, showing both *FNMR and FMR vary at one T value. Note: Many of the plots will naively be read as saying women gives worse error rates than men because the solid traces lie above the dotted ones. However, this is misleading and incomplete: The grey lines show the traces reveal horizontal shifts. Thus for the cogent-003 algorithm FNMR for men is* higher *than for women* at a fixed threshold *but, at the same time, FMR is higher for women - see Figure 284. As access control systems almost always operate at a fixed threshold, the naive interpretation is incorrect.*

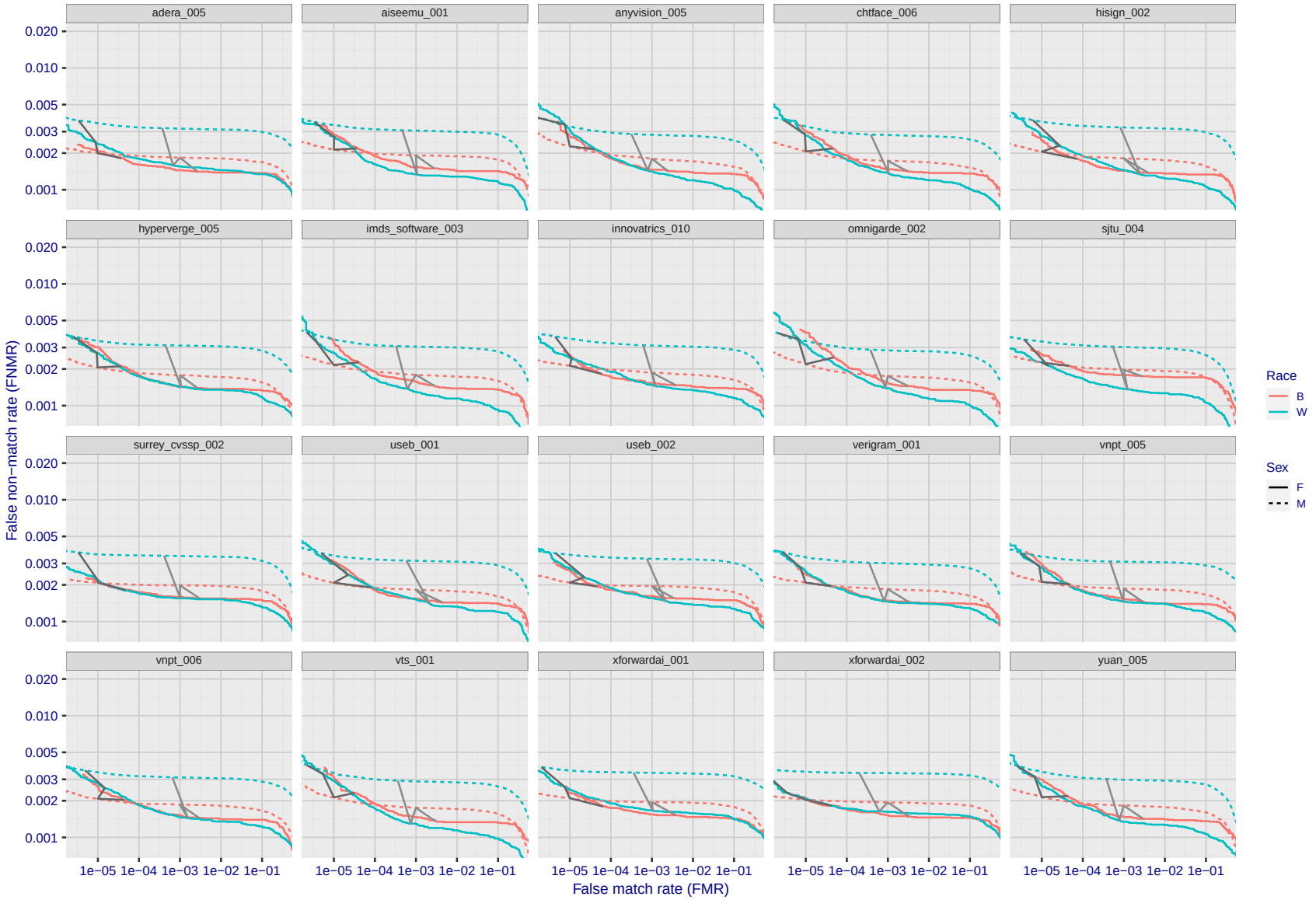

Figure 187: For the mugshot images, error tradeoff characteristics for white females, black females, black males and white males. The Z-shaped grey lines correspond to fixed thresholds, showing both *FNMR and FMR vary at one T value. Note: Many of the plots will naively be read as saying women gives worse error rates than men because the solid traces lie above the dotted ones. However, this is misleading and incomplete: The grey lines show the traces reveal horizontal shifts. Thus for the cogent-003 algorithm FNMR for men is* higher *than for women* at a fixed threshold *but, at the same time, FMR is higher for women - see Figure 284. As access control systems almost always operate at a fixed threshold, the naive interpretation is incorrect.*

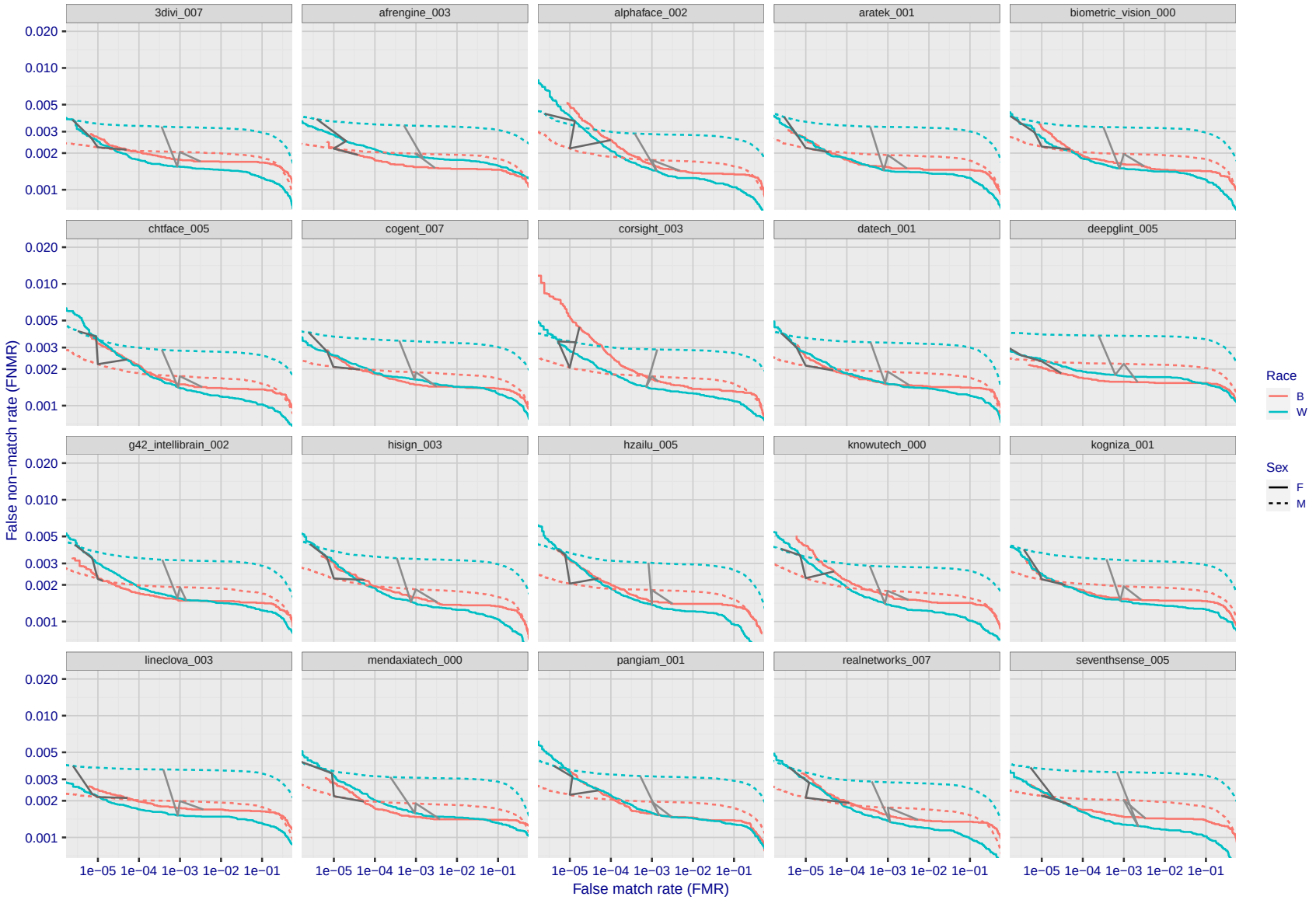

Figure 188: For the mugshot images, error tradeoff characteristics for white females, black females, black males and white males. The Z-shaped grey lines correspond to fixed thresholds, showing both *FNMR and FMR vary at one T value. Note: Many of the plots will naively be read as saying women gives worse error rates than men because the solid traces lie above the dotted ones. However, this is misleading and incomplete: The grey lines show the traces reveal horizontal shifts. Thus for the cogent-003 algorithm FNMR for men is* higher *than for women* at a fixed threshold *but, at the same time, FMR is higher for women - see Figure 284. As access control systems almost always operate at a fixed threshold, the naive interpretation is incorrect.*

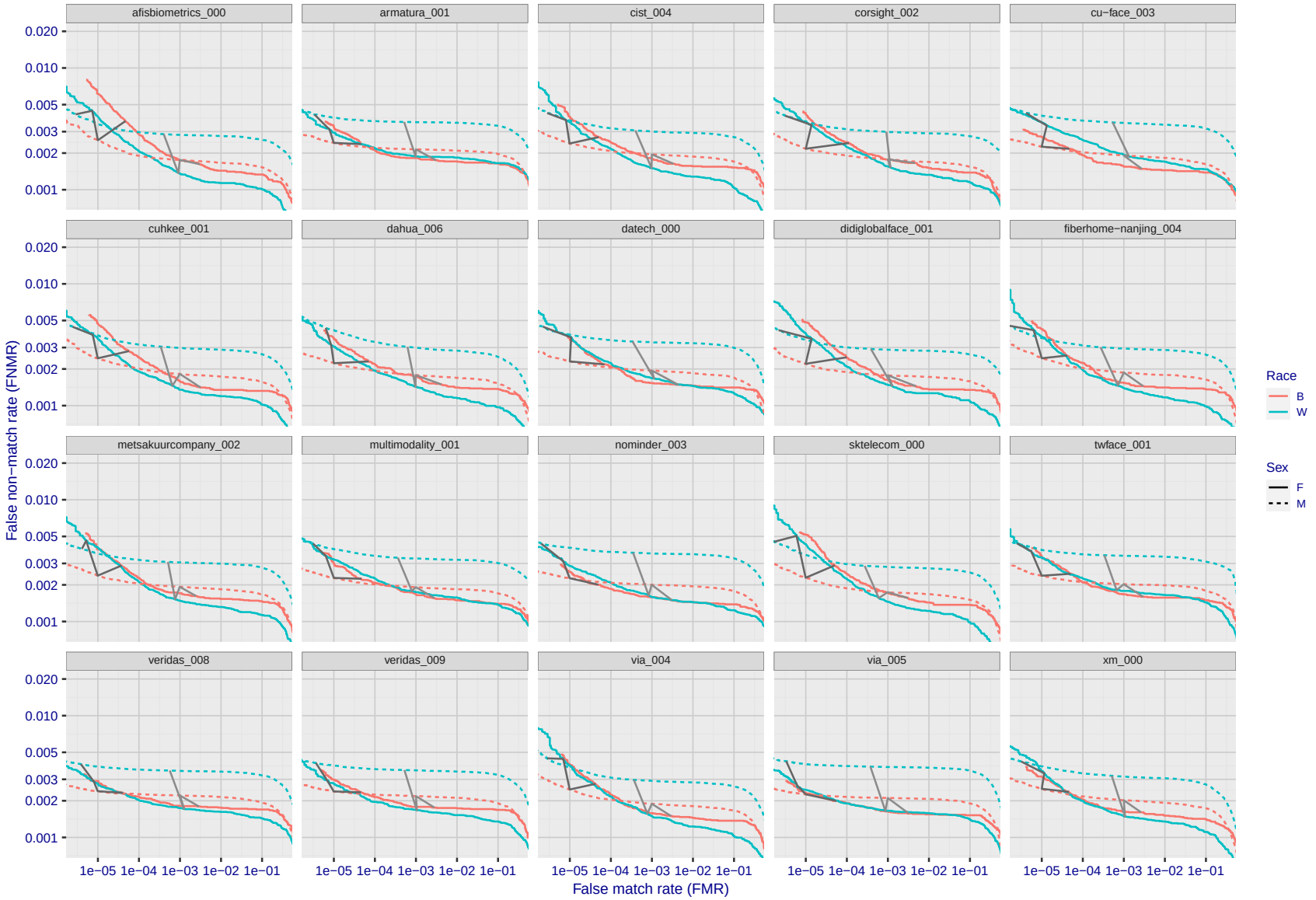

Figure 189: For the mugshot images, error tradeoff characteristics for white females, black females, black males and white males. The Z-shaped grey lines correspond to fixed thresholds, showing both *FNMR and FMR vary at one T value. Note: Many of the plots will naively be read as saying women gives worse error rates than men because the solid traces lie above the dotted ones. However, this is misleading and incomplete: The grey lines show the traces reveal horizontal shifts. Thus for the cogent-003 algorithm FNMR for men is* higher *than for women* at a fixed threshold *but, at the same time, FMR is higher for women - see Figure 284. As access control systems almost always operate at a fixed threshold, the naive interpretation is incorrect.*

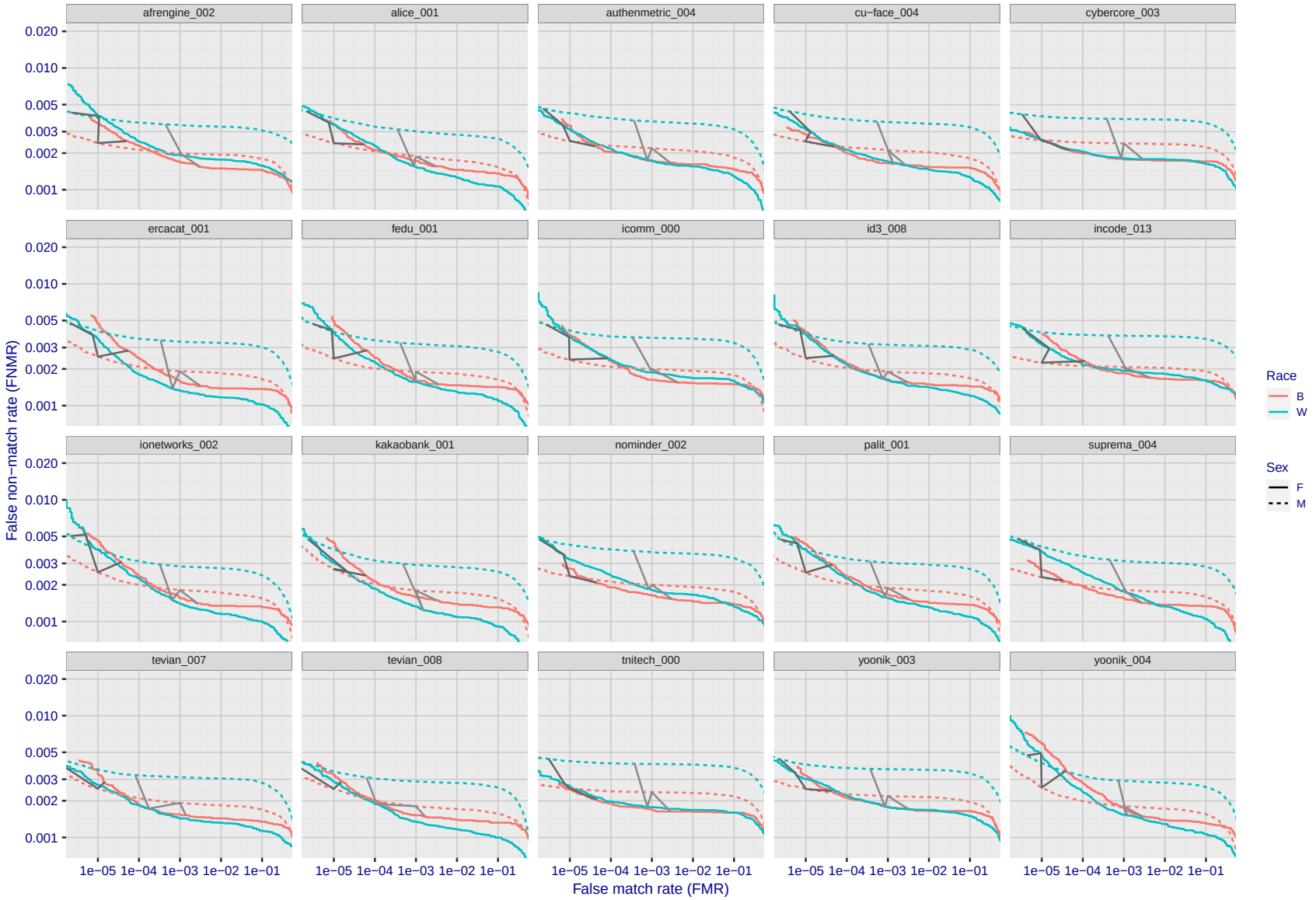

Figure 190: For the mugshot images, error tradeoff characteristics for white females, black females, black males and white males. The Z-shaped grey lines correspond to fixed thresholds, showing both *FNMR and FMR vary at one T value. Note: Many of the plots will naively be read as saying women gives worse error rates than men because the solid traces lie above the dotted ones. However, this is misleading and incomplete: The grey lines show the traces reveal horizontal shifts. Thus for the cogent-003 algorithm FNMR for men is* higher *than for women* at a fixed threshold *but, at the same time, FMR is higher for women - see Figure 284. As access control systems almost always operate at a fixed threshold, the naive interpretation is incorrect.*

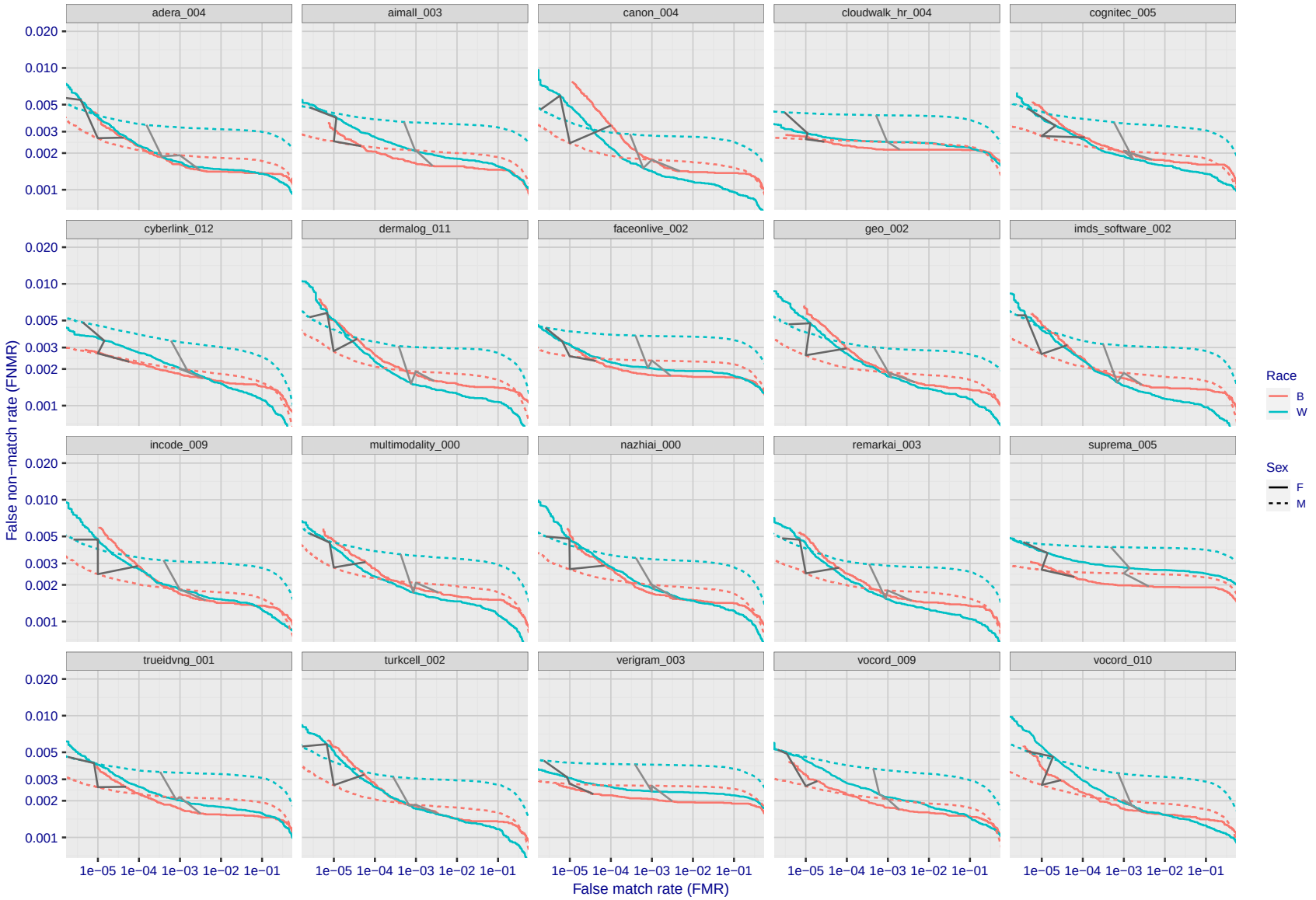

Figure 191: For the mugshot images, error tradeoff characteristics for white females, black females, black males and white males. The Z-shaped grey lines correspond to fixed thresholds, showing both *FNMR and FMR vary at one T value. Note: Many of the plots will naively be read as saying women gives worse error rates than men because the solid traces lie above the dotted ones. However, this is misleading and incomplete: The grey lines show the traces reveal horizontal shifts. Thus for the cogent-003 algorithm FNMR for men is* higher *than for women* at a fixed threshold *but, at the same time, FMR is higher for women - see Figure 284. As access control systems almost always operate at a fixed threshold, the naive interpretation is incorrect.*

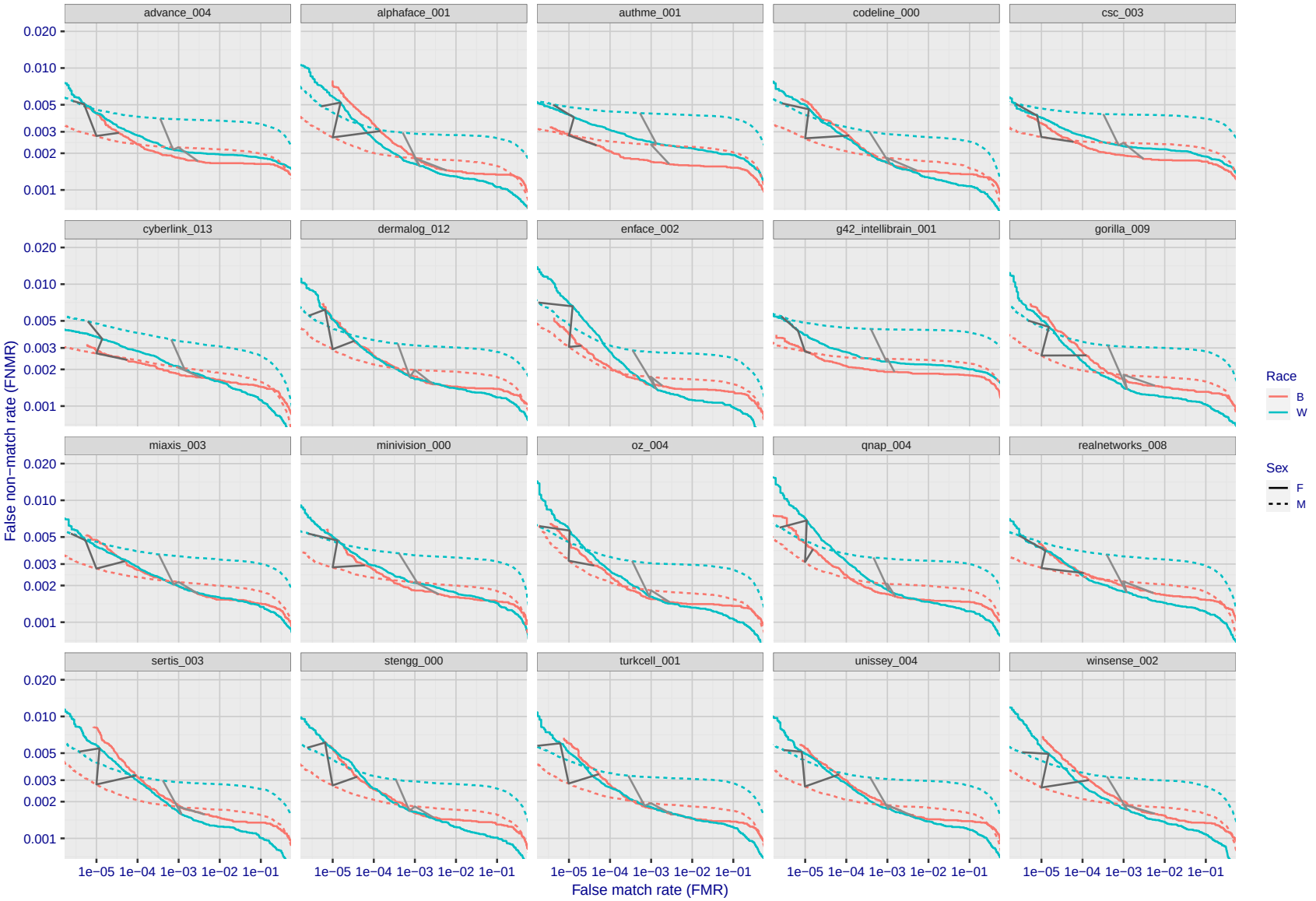

Figure 192: For the mugshot images, error tradeoff characteristics for white females, black females, black males and white males. The Z-shaped grey lines correspond to fixed thresholds, showing both *FNMR and FMR vary at one T value. Note: Many of the plots will naively be read as saying women gives worse error rates than men because the solid traces lie above the dotted ones. However, this is misleading and incomplete: The grey lines show the traces reveal horizontal shifts. Thus for the cogent-003 algorithm FNMR for men is* higher *than for women* at a fixed threshold *but, at the same time, FMR is higher for women - see Figure 284. As access control systems almost always operate at a fixed threshold, the naive interpretation is incorrect.*

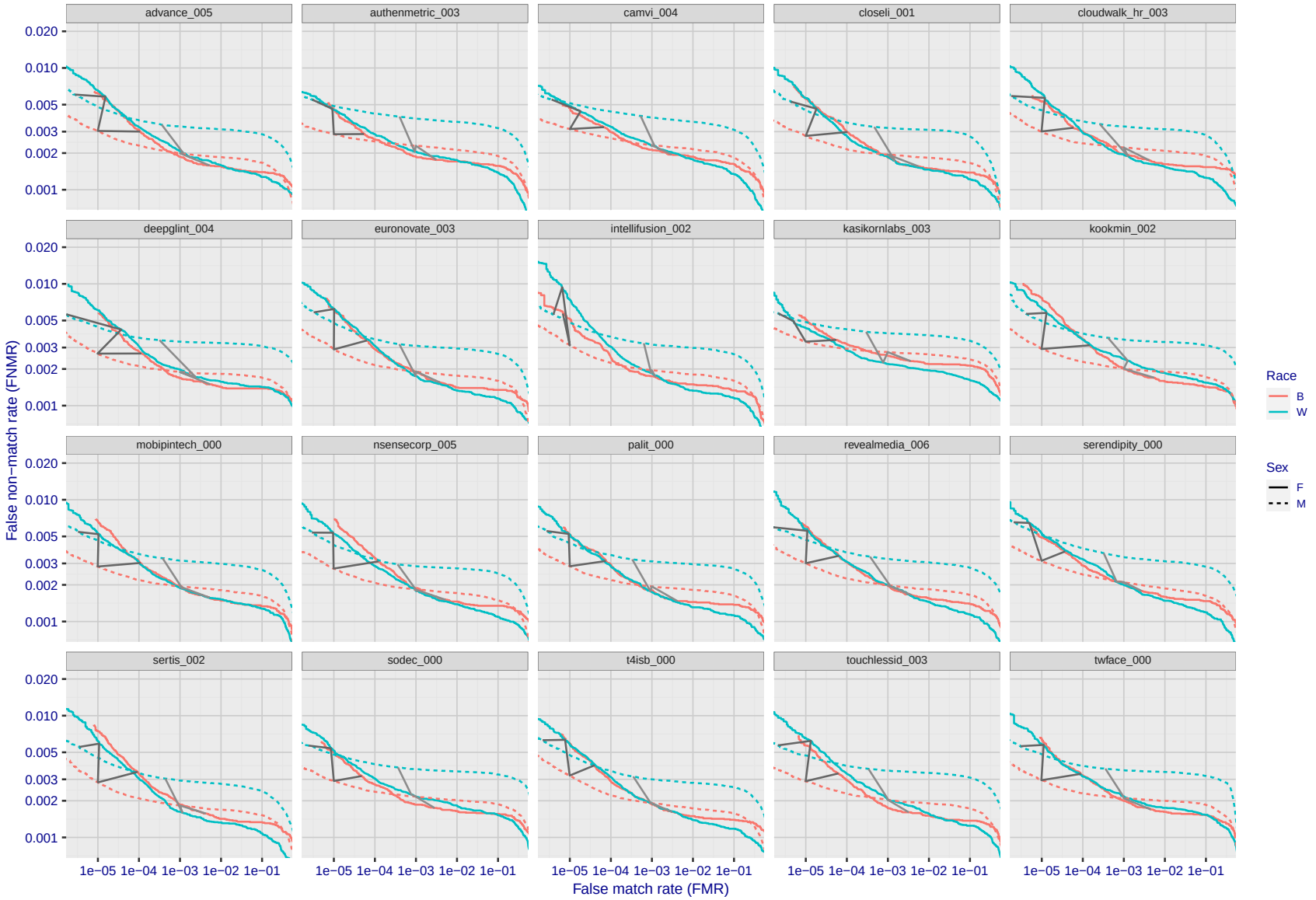

Figure 193: For the mugshot images, error tradeoff characteristics for white females, black females, black males and white males. The Z-shaped grey lines correspond to fixed thresholds, showing both *FNMR and FMR vary at one T value. Note: Many of the plots will naively be read as saying women gives worse error rates than men because the solid traces lie above the dotted ones. However, this is misleading and incomplete: The grey lines show the traces reveal horizontal shifts. Thus for the cogent-003 algorithm FNMR for men is* higher *than for women* at a fixed threshold *but, at the same time, FMR is higher for women - see Figure 284. As access control systems almost always operate at a fixed threshold, the naive interpretation is incorrect.*

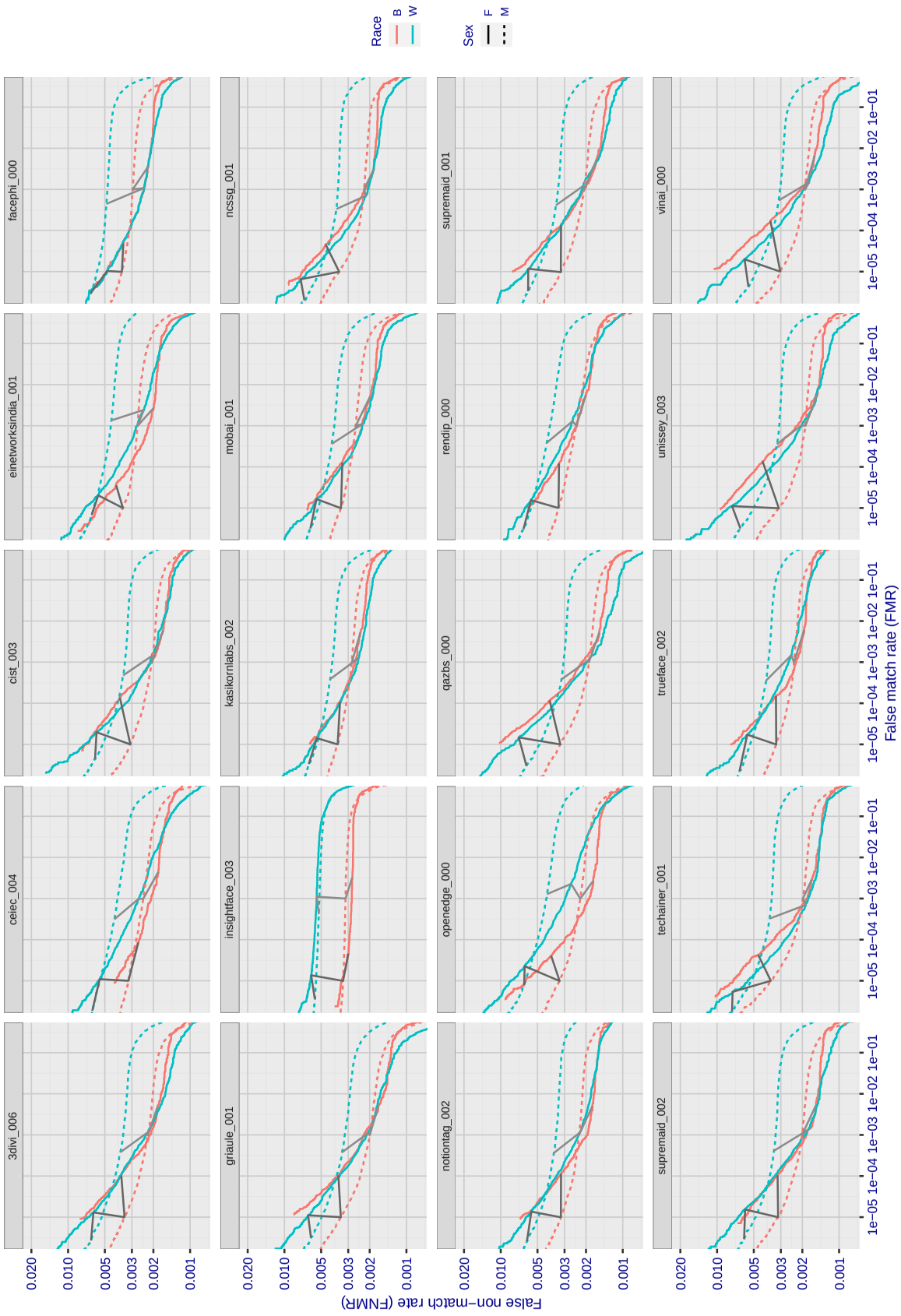

Figure 194: For the mugshot images, error tradeoff characteristics for white females, black females, black males and white males. The Z-shaped grey lines correspond to fixed thresholds, showing both FNMR and FMR vary at one T value. Note: Many of the plots will naively be read as saying women gives worse error rates than men because the solid traces lie above the dotted ones. However, this is misleading and incomplete: The grey lines show the traces reveal horizontal shifts. Thus for the cogent-003 algorithm FNMR for men is higher than for women at a fixed threshold but, at the same time, FMR is higher for women - see Figure 284. As access control systems almost always operate at a fixed threshold, the naive interpretation is incorrect.

FNMR(T) "False non-match rate"
FMR(T) "False match rate"

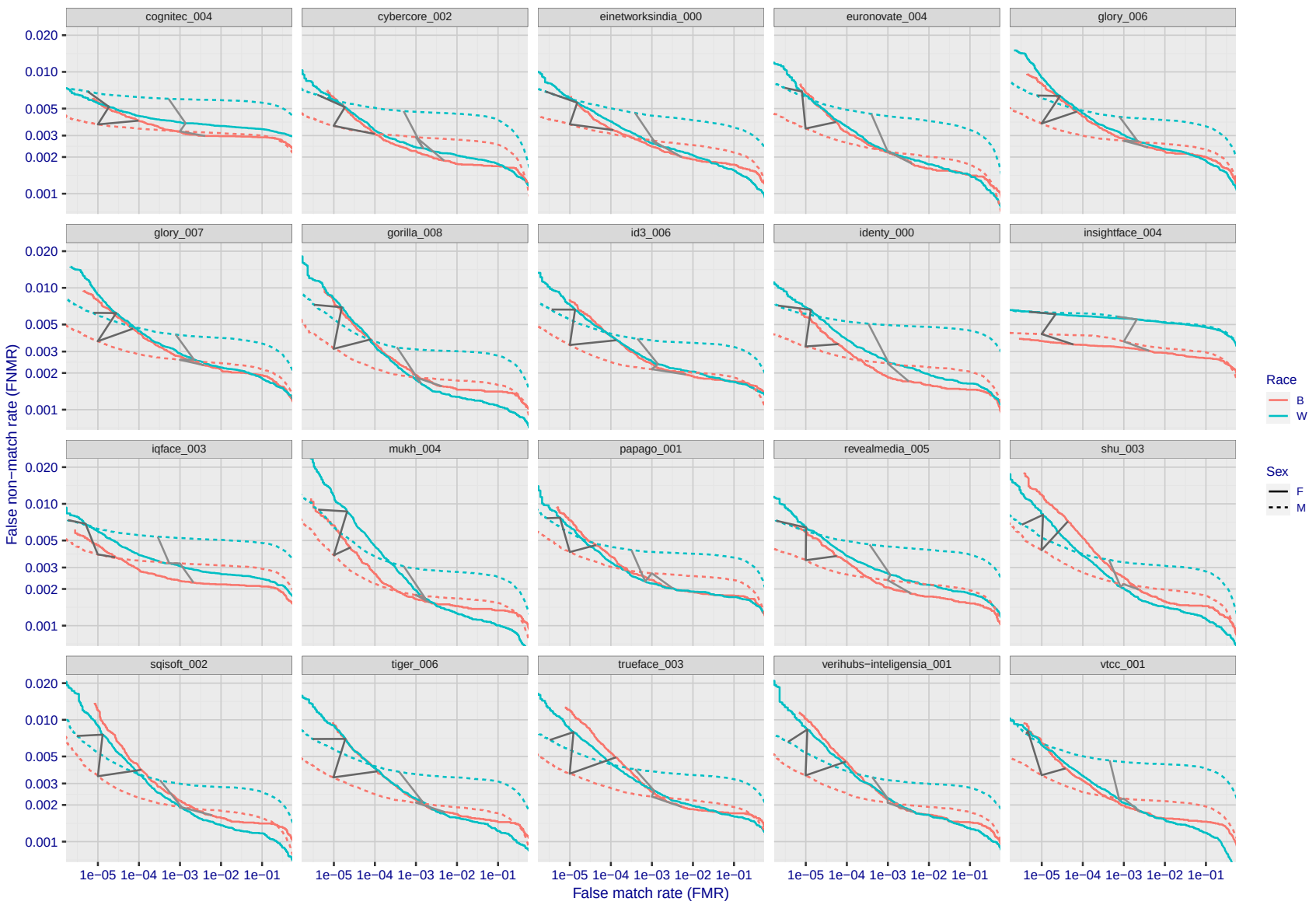

Figure 195: For the mugshot images, error tradeoff characteristics for white females, black females, black males and white males. The Z-shaped grey lines correspond to fixed thresholds, showing both *FNMR and FMR vary at one T value. Note: Many of the plots will naively be read as saying women gives worse error rates than men because the solid traces lie above the dotted ones. However, this is misleading and incomplete: The grey lines show the traces reveal horizontal shifts. Thus for the cogent-003 algorithm FNMR for men is* higher *than for women* at a fixed threshold *but, at the same time, FMR is higher for women - see Figure 284. As access control systems almost always operate at a fixed threshold, the naive interpretation is incorrect.*

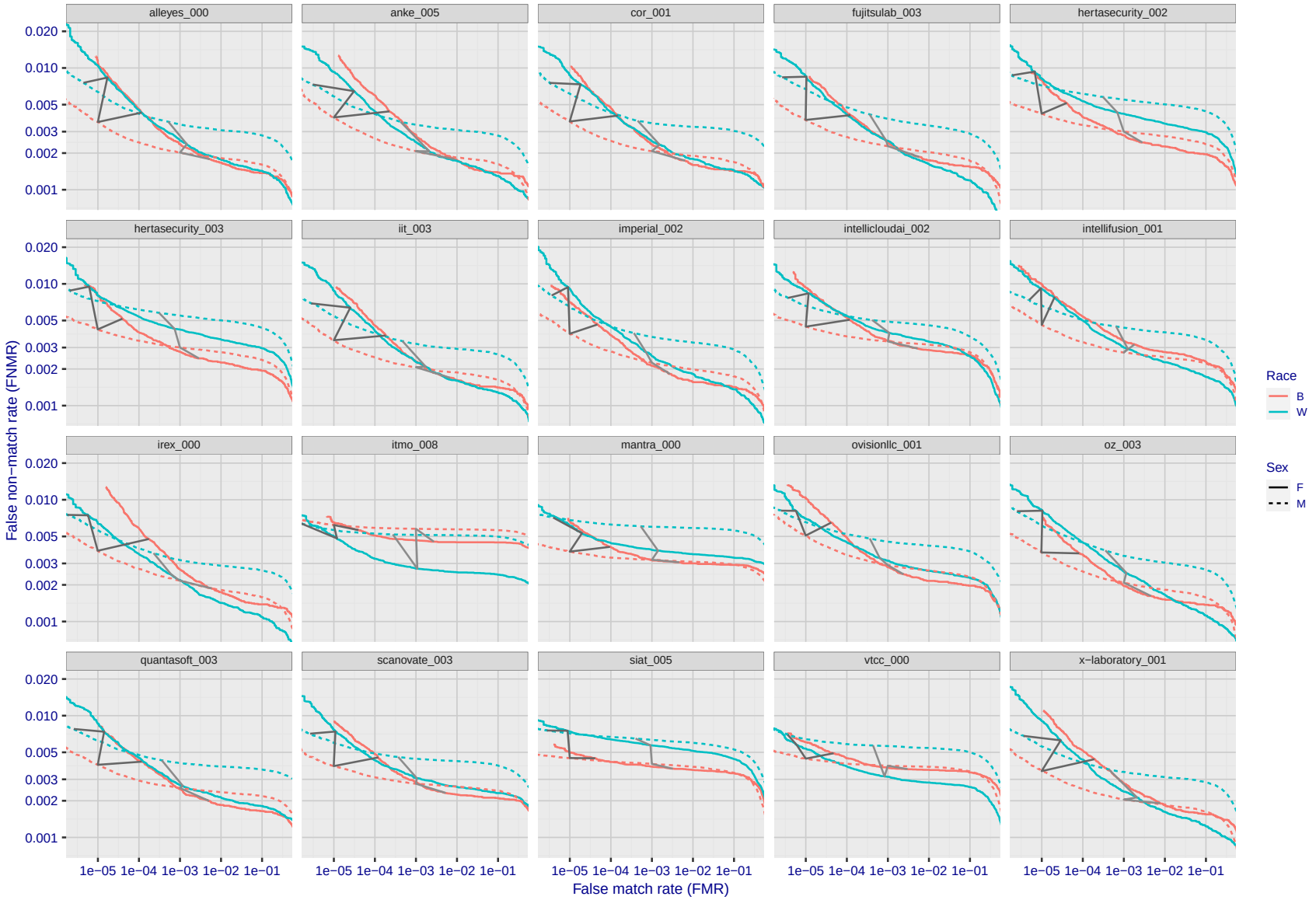

Figure 196: For the mugshot images, error tradeoff characteristics for white females, black females, black males and white males. The Z-shaped grey lines correspond to fixed thresholds, showing both *FNMR and FMR vary at one T value. Note: Many of the plots will naively be read as saying women gives worse error rates than men because the solid traces lie above the dotted ones. However, this is misleading and incomplete: The grey lines show the traces reveal horizontal shifts. Thus for the cogent-003 algorithm FNMR for men is* higher *than for women* at a fixed threshold *but, at the same time, FMR is higher for women - see Figure 284. As access control systems almost always operate at a fixed threshold, the naive interpretation is incorrect.*

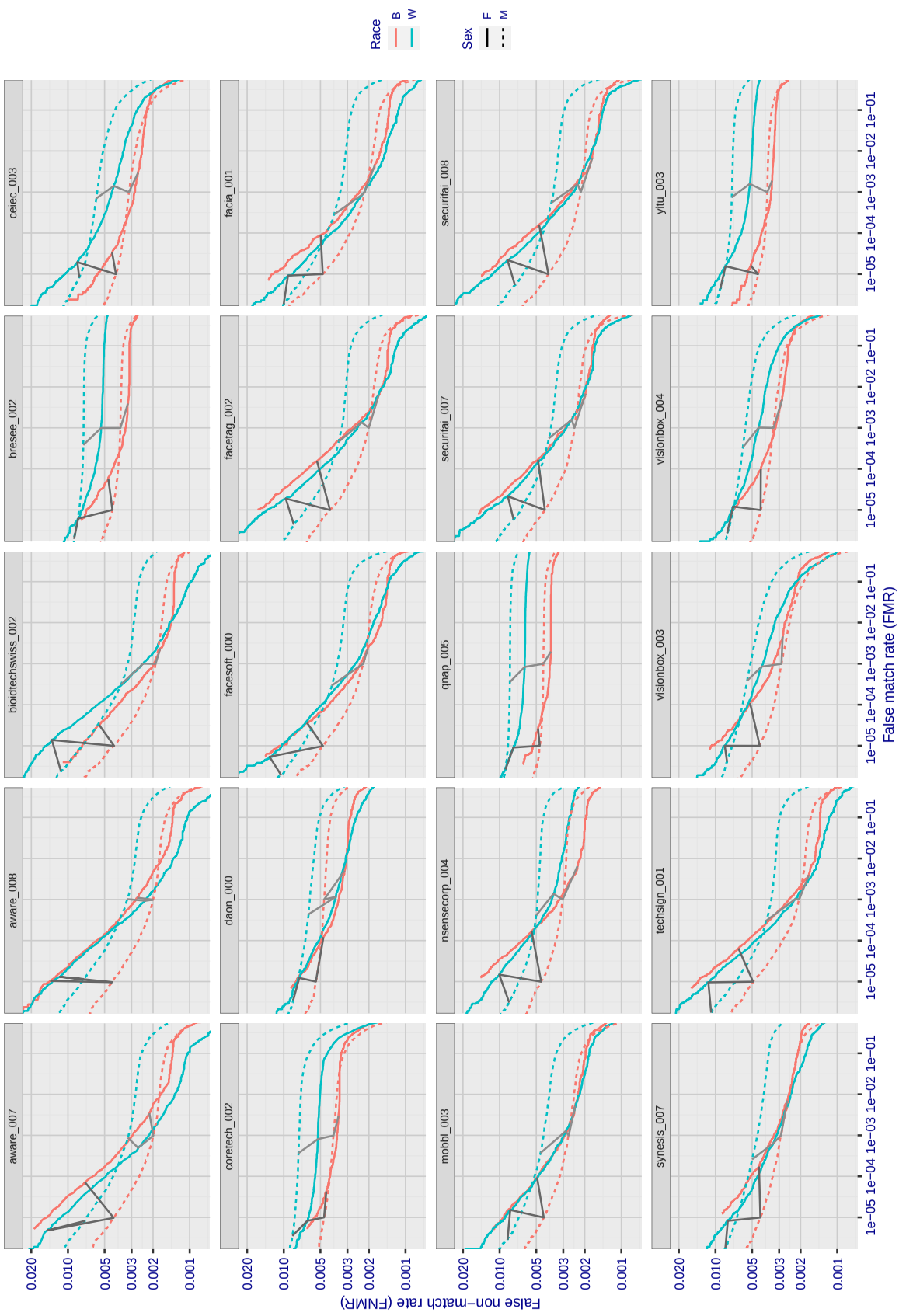

Figure 197: For the mugshot images, error tradeoff characteristics for white females, black females, black males and white males. The Z-shaped grey lines correspond to fixed thresholds, showing both FNMR and FMR vary at one T value. Note: Many of the plots will naively be read as saying women gives worse error rates than men because the solid traces lie above the dotted ones. However, this is misleading and incomplete: The grey lines show the traces reveal horizontal shifts. Thus for the cogent-003 algorithm FNMR for men is higher than for women at a fixed threshold but, at the same time, FMR is higher for women - see Figure 284. As access control systems almost always operate at a fixed threshold, the naive interpretation is incorrect.

FNMR(T) "False non-match rate"
FMR(T) "False match rate"

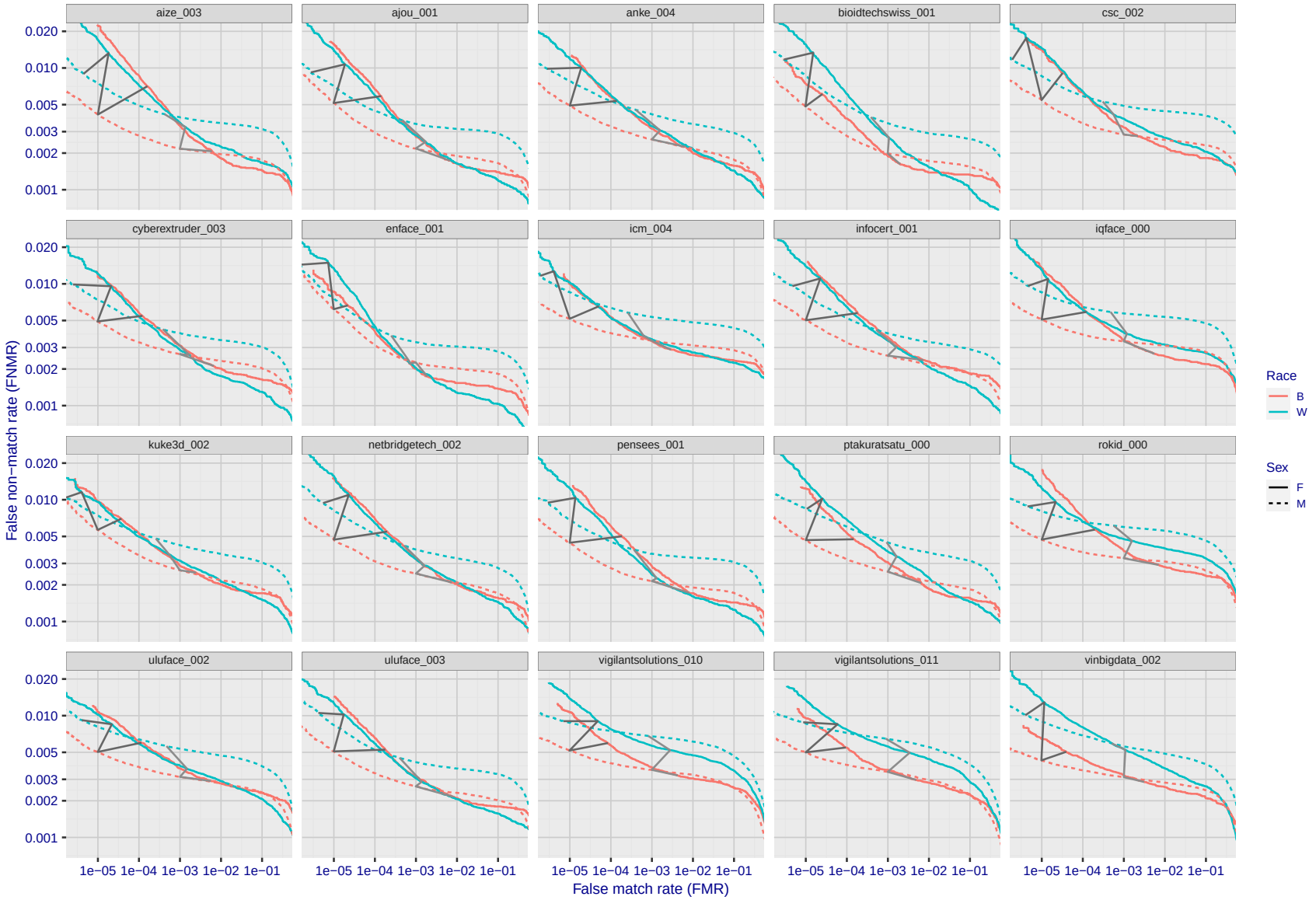

Figure 198: For the mugshot images, error tradeoff characteristics for white females, black females, black males and white males. The Z-shaped grey lines correspond to fixed thresholds, showing both *FNMR and FMR vary at one T value. Note: Many of the plots will naively be read as saying women gives worse error rates than men because the solid traces lie above the dotted ones. However, this is misleading and incomplete: The grey lines show the traces reveal horizontal shifts. Thus for the cogent-003 algorithm FNMR for men is* higher *than for women* at a fixed threshold *but, at the same time, FMR is higher for women - see Figure 284. As access control systems almost always operate at a fixed threshold, the naive interpretation is incorrect.*

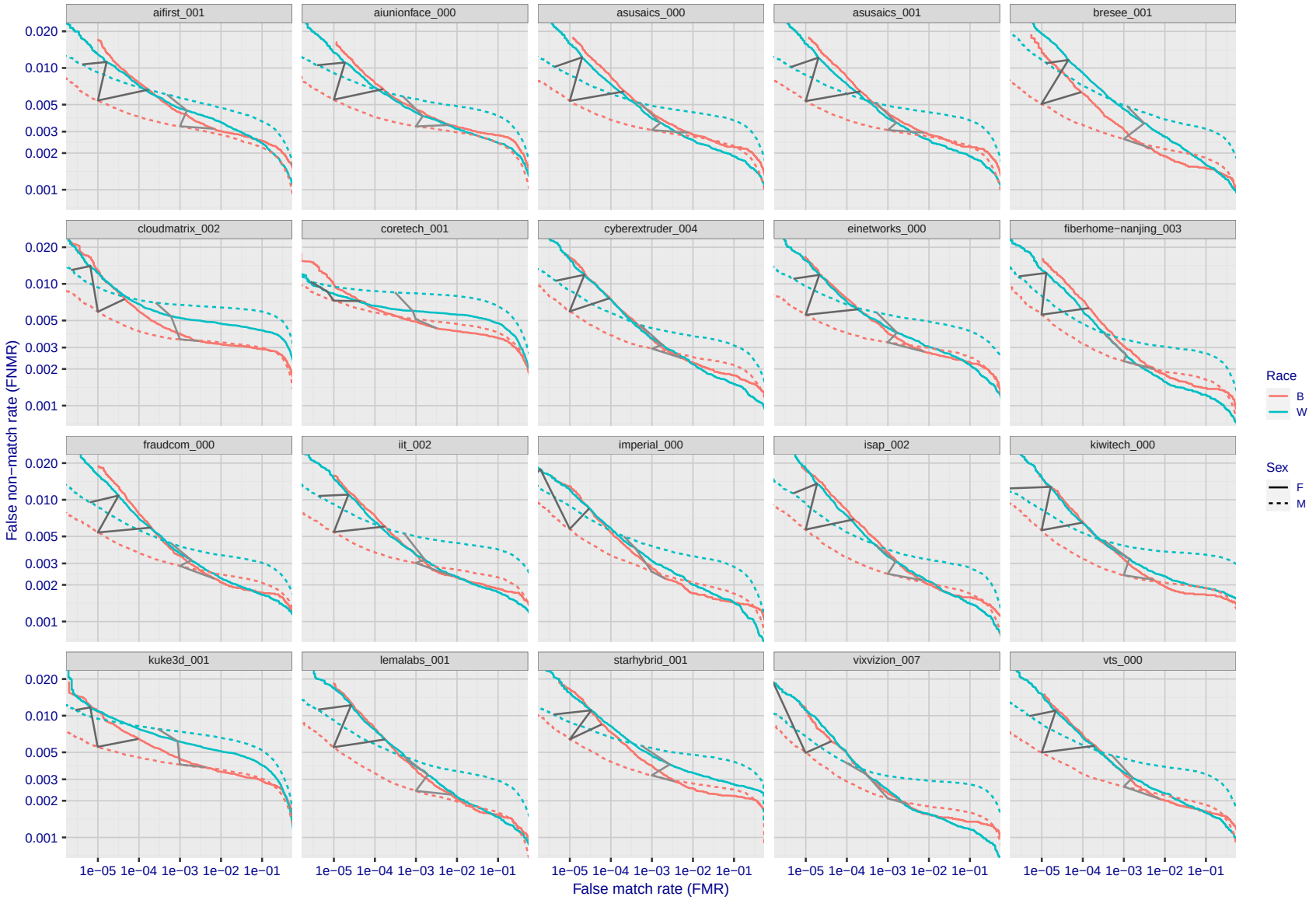

Figure 199: For the mugshot images, error tradeoff characteristics for white females, black females, black males and white males. The Z-shaped grey lines correspond to fixed thresholds, showing both *FNMR and FMR vary at one T value. Note: Many of the plots will naively be read as saying women gives worse error rates than men because the solid traces lie above the dotted ones. However, this is misleading and incomplete: The grey lines show the traces reveal horizontal shifts. Thus for the cogent-003 algorithm FNMR for men is* higher *than for women* at a fixed threshold *but, at the same time, FMR is higher for women - see Figure 284. As access control systems almost always operate at a fixed threshold, the naive interpretation is incorrect.*

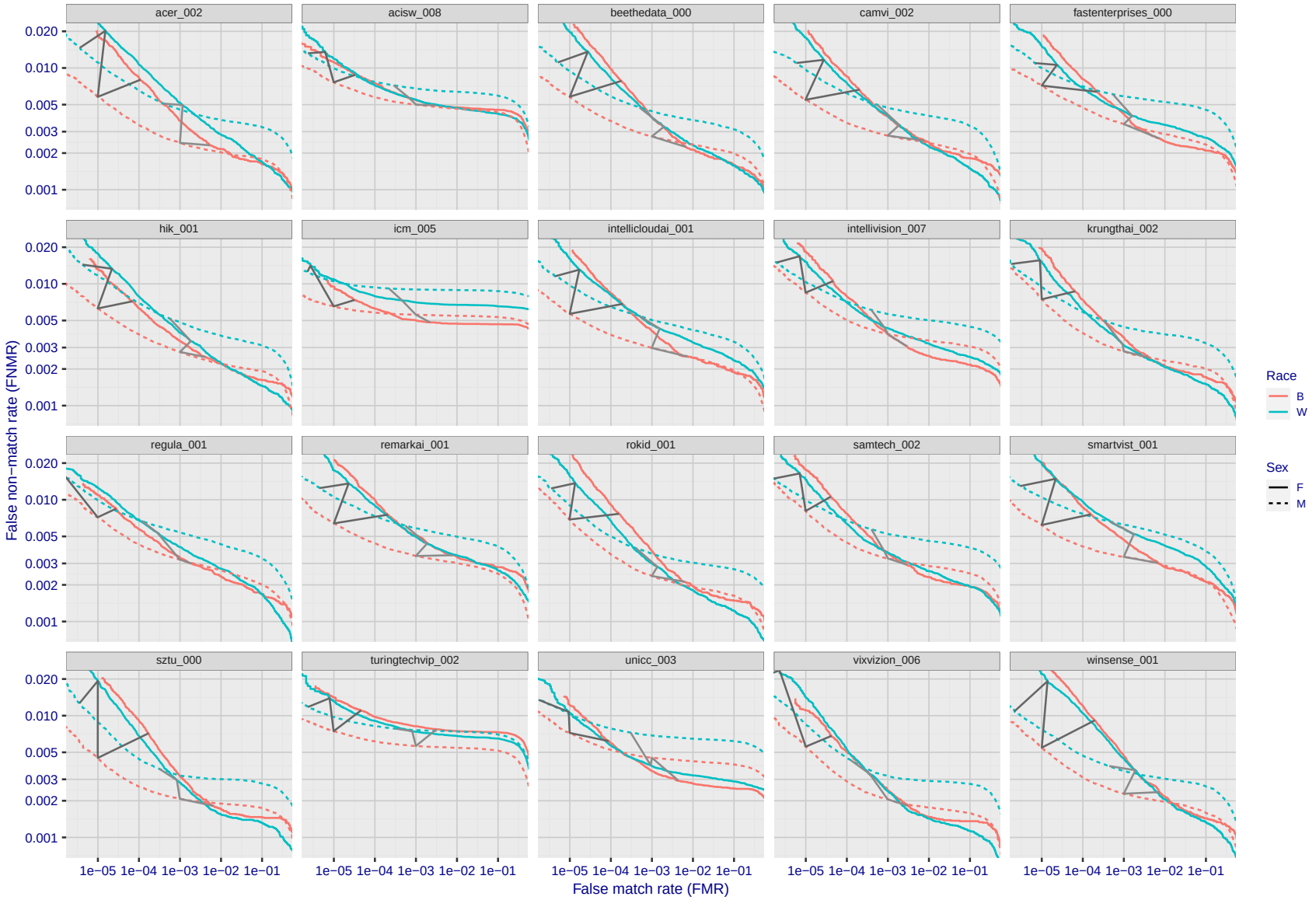

Figure 200: For the mugshot images, error tradeoff characteristics for white females, black females, black males and white males. The Z-shaped grey lines correspond to fixed thresholds, showing both *FNMR and FMR vary at one T value. Note: Many of the plots will naively be read as saying women gives worse error rates than men because the solid traces lie above the dotted ones. However, this is misleading and incomplete: The grey lines show the traces reveal horizontal shifts. Thus for the cogent-003 algorithm FNMR for men is* higher *than for women* at a fixed threshold *but, at the same time, FMR is higher for women - see Figure 284. As access control systems almost always operate at a fixed threshold, the naive interpretation is incorrect.*

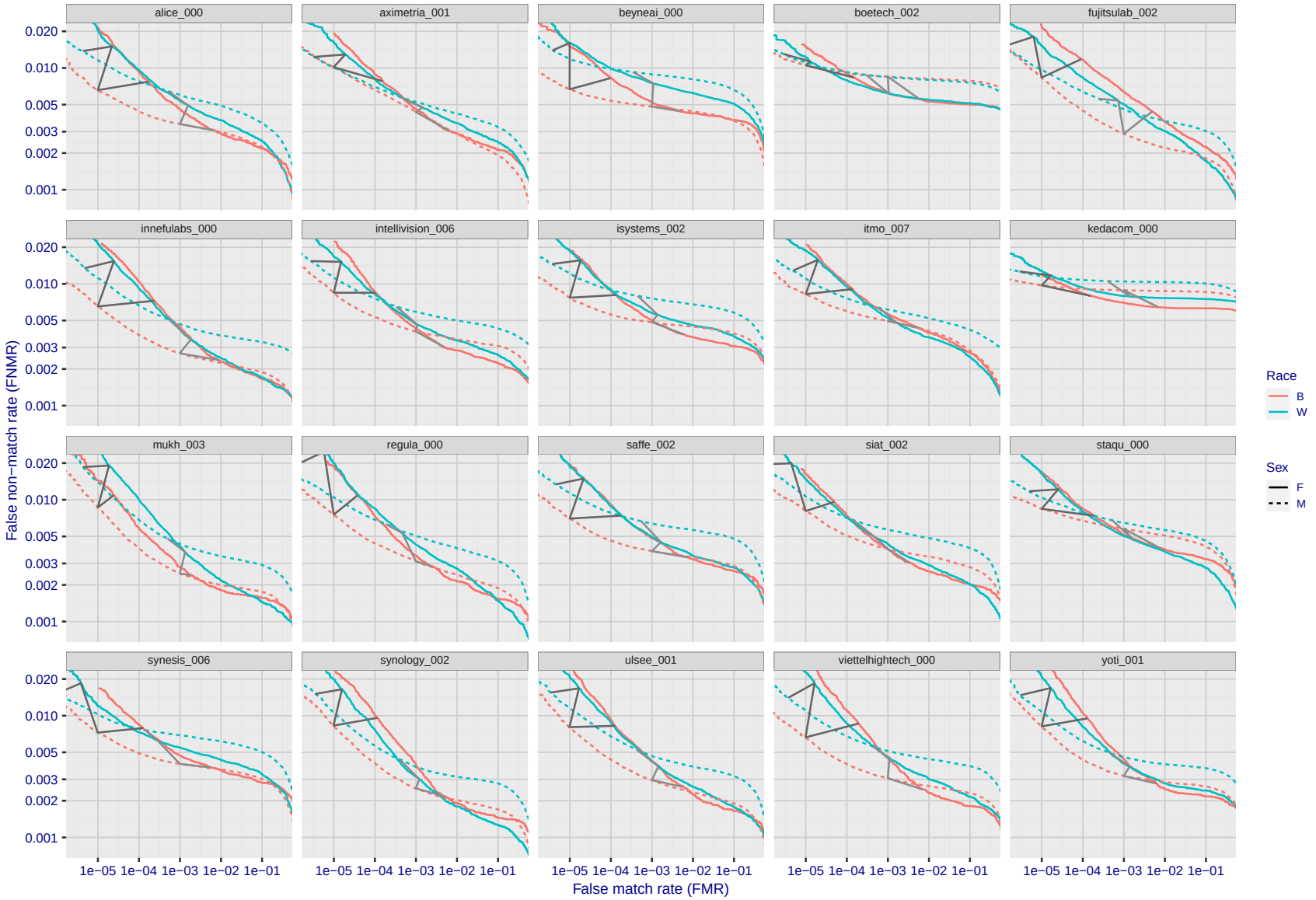

Figure 201: For the mugshot images, error tradeoff characteristics for white females, black females, black males and white males. The Z-shaped grey lines correspond to fixed thresholds, showing both *FNMR and FMR vary at one T value. Note: Many of the plots will naively be read as saying women gives worse error rates than men because the solid traces lie above the dotted ones. However, this is misleading and incomplete: The grey lines show the traces reveal horizontal shifts. Thus for the cogent-003 algorithm FNMR for men is* higher *than for women* at a fixed threshold *but, at the same time, FMR is higher for women - see Figure 284. As access control systems almost always operate at a fixed threshold, the naive interpretation is incorrect.*

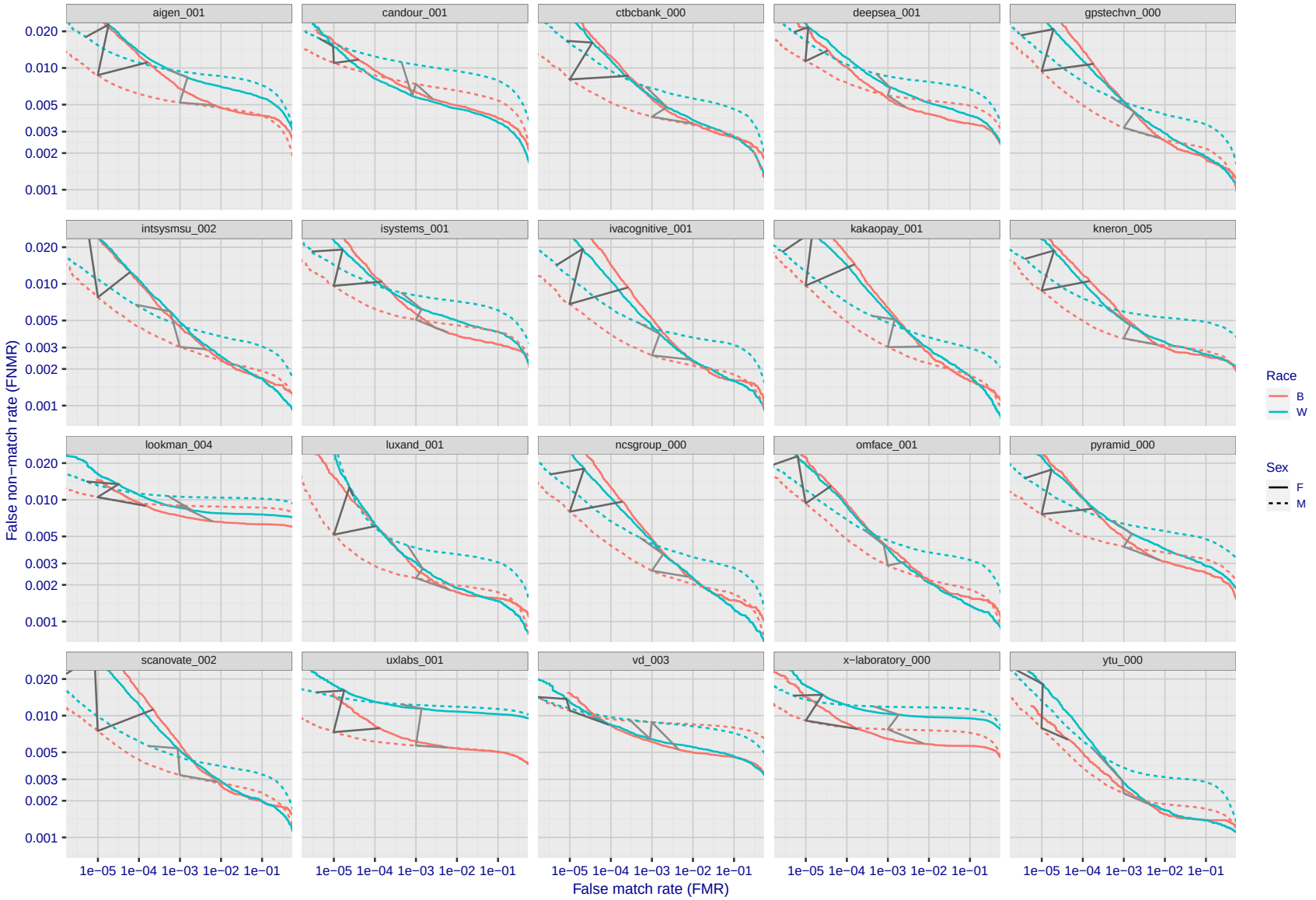

Figure 202: For the mugshot images, error tradeoff characteristics for white females, black females, black males and white males. The Z-shaped grey lines correspond to fixed thresholds, showing both *FNMR and FMR vary at one T value. Note: Many of the plots will naively be read as saying women gives worse error rates than men because the solid traces lie above the dotted ones. However, this is misleading and incomplete: The grey lines show the traces reveal horizontal shifts. Thus for the cogent-003 algorithm FNMR for men is* higher *than for women* at a fixed threshold *but, at the same time, FMR is higher for women - see Figure 284. As access control systems almost always operate at a fixed threshold, the naive interpretation is incorrect.*

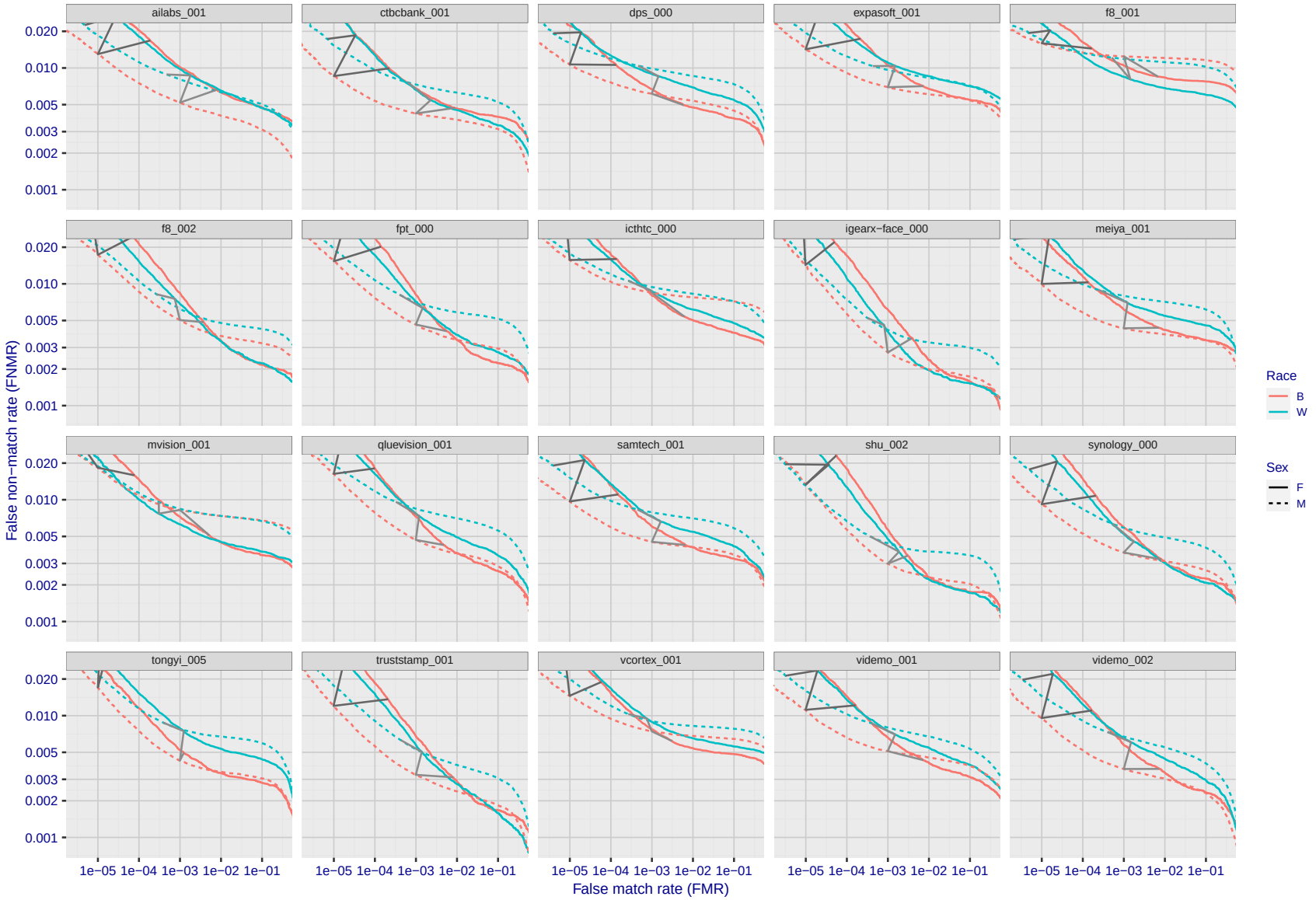

Figure 203: For the mugshot images, error tradeoff characteristics for white females, black females, black males and white males. The Z-shaped grey lines correspond to fixed thresholds, showing both *FNMR and FMR vary at one T value. Note: Many of the plots will naively be read as saying women gives worse error rates than men because the solid traces lie above the dotted ones. However, this is misleading and incomplete: The grey lines show the traces reveal horizontal shifts. Thus for the cogent-003 algorithm FNMR for men is* higher *than for women* at a fixed threshold *but, at the same time, FMR is higher for women - see Figure 284. As access control systems almost always operate at a fixed threshold, the naive interpretation is incorrect.*

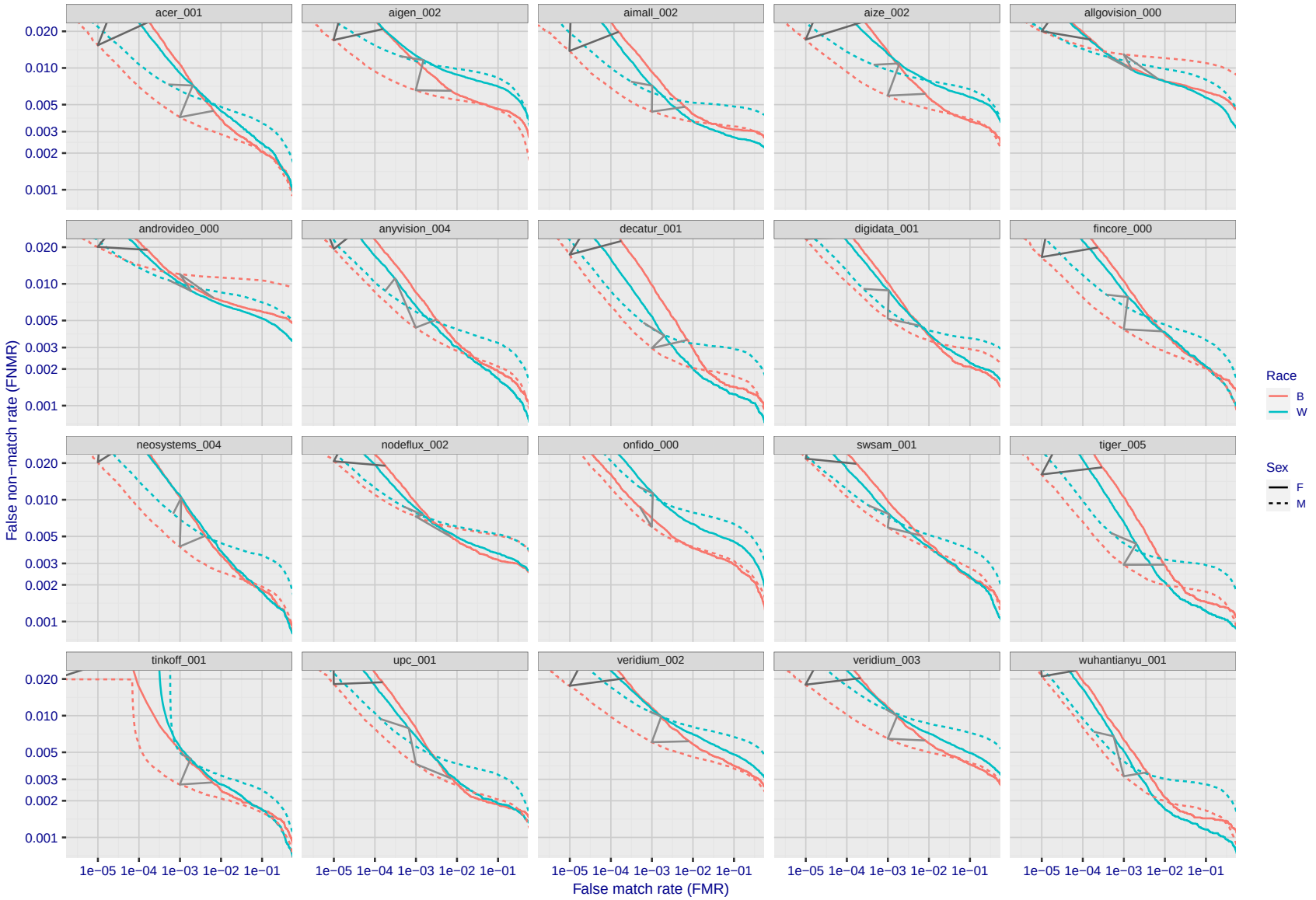

Figure 204: For the mugshot images, error tradeoff characteristics for white females, black females, black males and white males. The Z-shaped grey lines correspond to fixed thresholds, showing both *FNMR and FMR vary at one T value. Note: Many of the plots will naively be read as saying women gives worse error rates than men because the solid traces lie above the dotted ones. However, this is misleading and incomplete: The grey lines show the traces reveal horizontal shifts. Thus for the cogent-003 algorithm FNMR for men is* higher *than for women* at a fixed threshold *but, at the same time, FMR is higher for women - see Figure 284. As access control systems almost always operate at a fixed threshold, the naive interpretation is incorrect.*

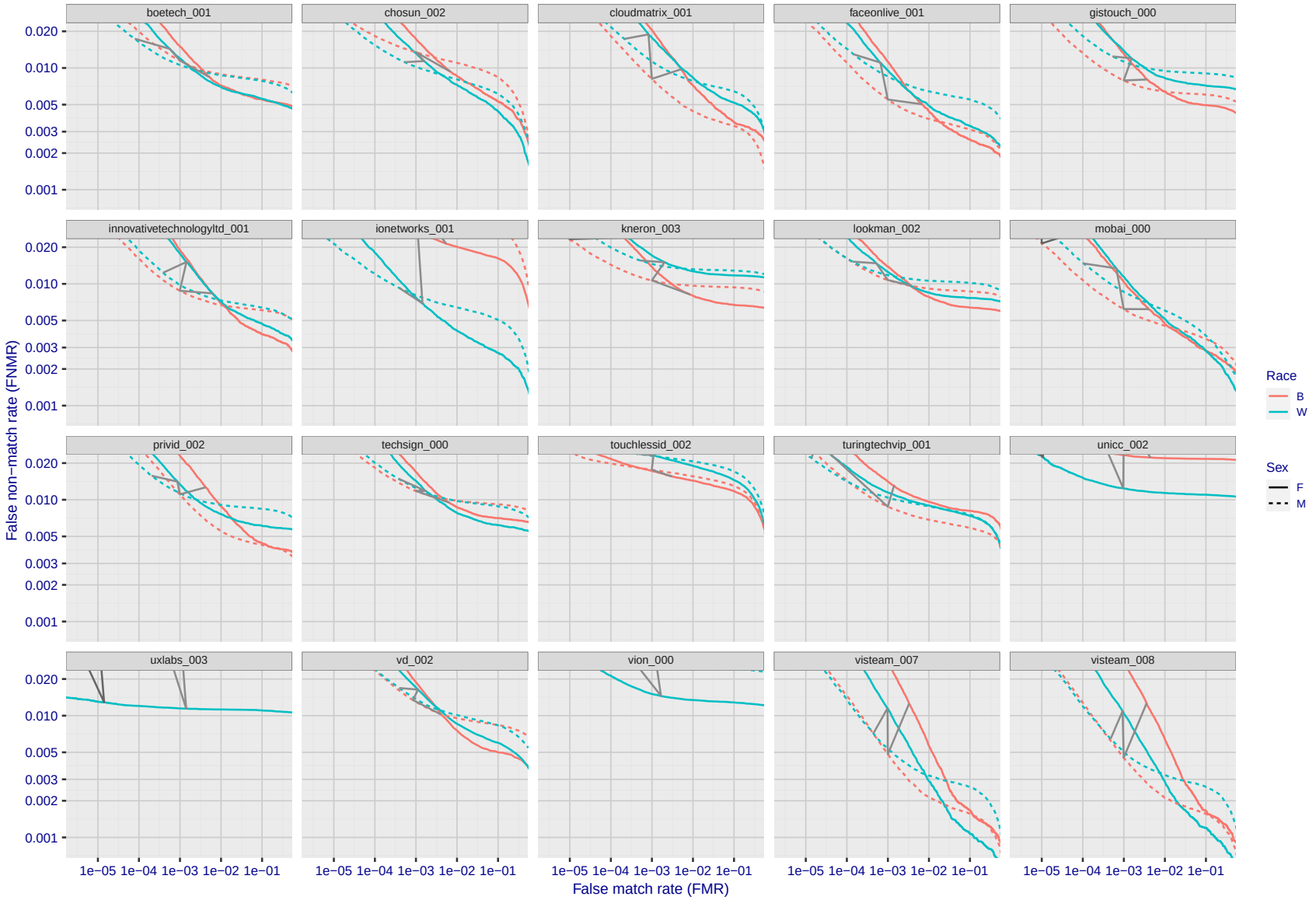

Figure 205: For the mugshot images, error tradeoff characteristics for white females, black females, black males and white males. The Z-shaped grey lines correspond to fixed thresholds, showing both *FNMR and FMR vary at one T value. Note: Many of the plots will naively be read as saying women gives worse error rates than men because the solid traces lie above the dotted ones. However, this is misleading and incomplete: The grey lines show the traces reveal horizontal shifts. Thus for the cogent-003 algorithm FNMR for men is* higher *than for women* at a fixed threshold *but, at the same time, FMR is higher for women - see Figure 284. As access control systems almost always operate at a fixed threshold, the naive interpretation is incorrect.*

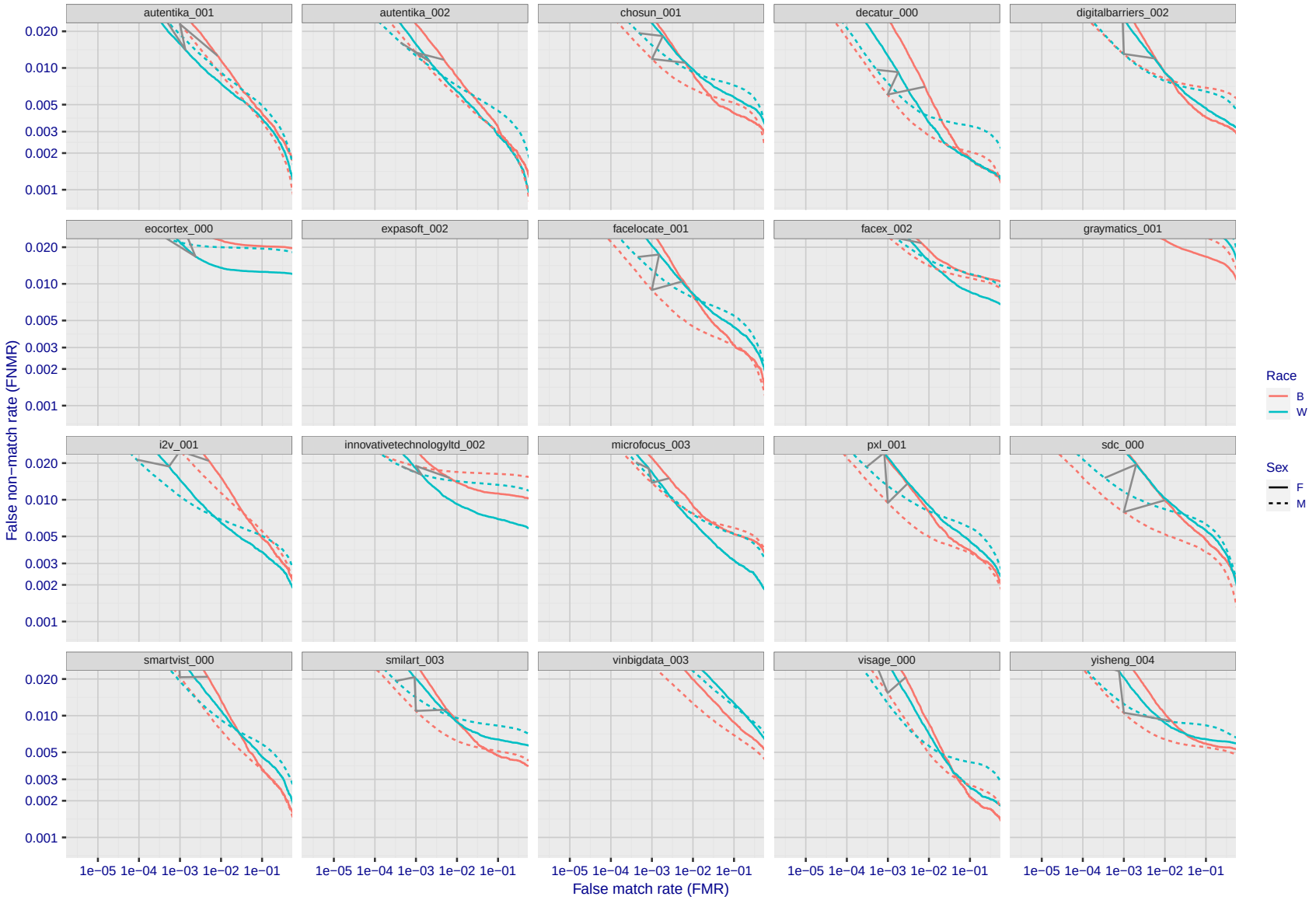

Figure 206: For the mugshot images, error tradeoff characteristics for white females, black females, black males and white males. The Z-shaped grey lines correspond to fixed thresholds, showing both *FNMR and FMR vary at one T value. Note: Many of the plots will naively be read as saying women gives worse error rates than men because the solid traces lie above the dotted ones. However, this is misleading and incomplete: The grey lines show the traces reveal horizontal shifts. Thus for the cogent-003 algorithm FNMR for men is* higher *than for women* at a fixed threshold *but, at the same time, FMR is higher for women - see Figure 284. As access control systems almost always operate at a fixed threshold, the naive interpretation is incorrect.*

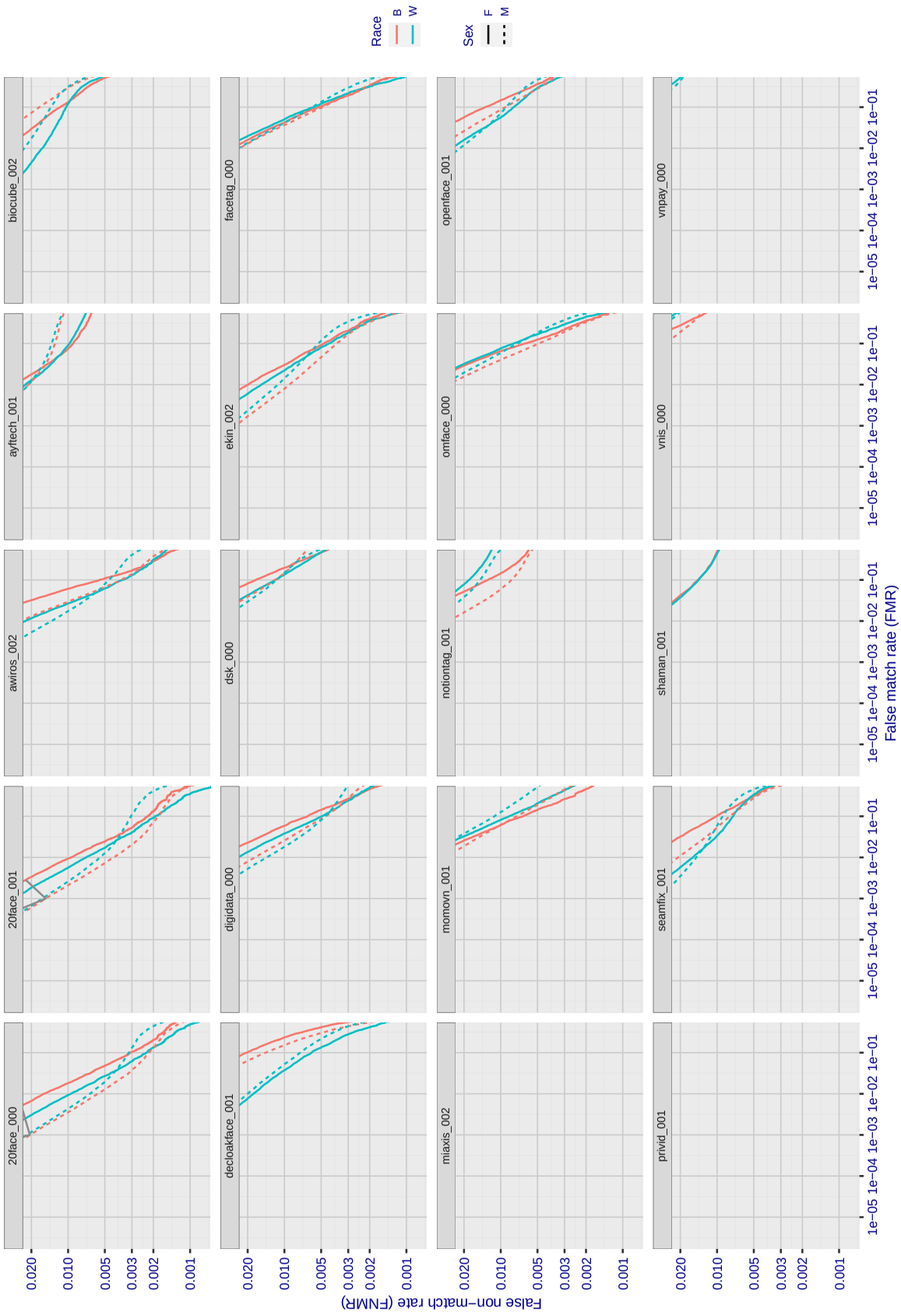

Figure 207: For the mugshot images, error tradeoff characteristics for white females, black females, black males and white males. The Z-shaped grey lines correspond to fixed thresholds, showing both FNMR and FMR vary at one T value. Note: Many of the plots will naively be read as saying women gives worse error rates than men because the solid traces lie above the dotted ones. However, this is misleading and incomplete: The grey lines show the traces reveal horizontal shifts. Thus for the cogent-003 algorithm FNMR for men is higher than for women at a fixed threshold but, at the same time, FMR is higher for women - see Figure 284. As access control systems almost always operate at a fixed threshold, the naive interpretation is incorrect.

FNMR(T) "False non-match rate"
FMR(T) "False match rate"

Figure 208: For the mugshot images, error tradeoff characteristics for white females, black females, black males and white males. The Z-shaped grey lines correspond to fixed thresholds, showing both *FNMR and FMR vary at one T value. Note: Many of the plots will naively be read as saying women gives worse error rates than men because the solid traces lie above the dotted ones. However, this is misleading and incomplete: The grey lines show the traces reveal horizontal shifts. Thus for the cogent-003 algorithm FNMR for men is* higher *than for women* at a fixed threshold *but, at the same time, FMR is higher for women - see Figure 284. As access control systems almost always operate at a fixed threshold, the naive interpretation is incorrect.*

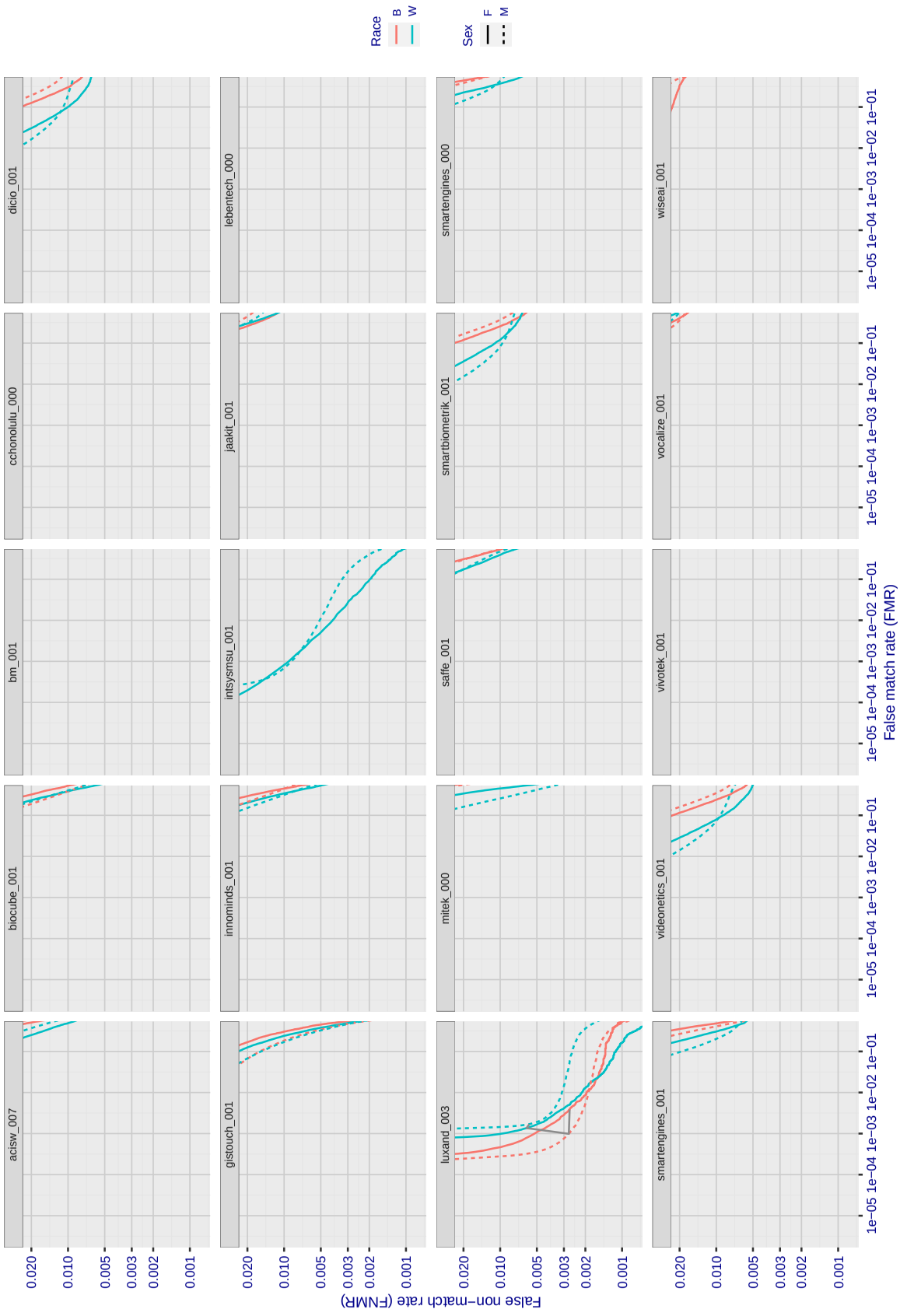

Figure 209: For the mugshot images, error tradeoff characteristics for white females, black females, black males and white males. The Z-shaped grey lines correspond to fixed thresholds, showing both FNMR and FMR vary at one T value. Note: Many of the plots will naively be read as saying women gives worse error rates than men because the solid traces lie above the dotted ones. However, this is misleading and incomplete: The grey lines show the traces reveal horizontal shifts. Thus for the cogent-003 algorithm FNMR for men is higher than for women at a fixed threshold but, at the same time, FMR is higher for women - see Figure 284. As access control systems almost always operate at a fixed threshold, the naive interpretation is incorrect.

FNMR(T) "False non-match rate"
FMR(T) "False match rate"

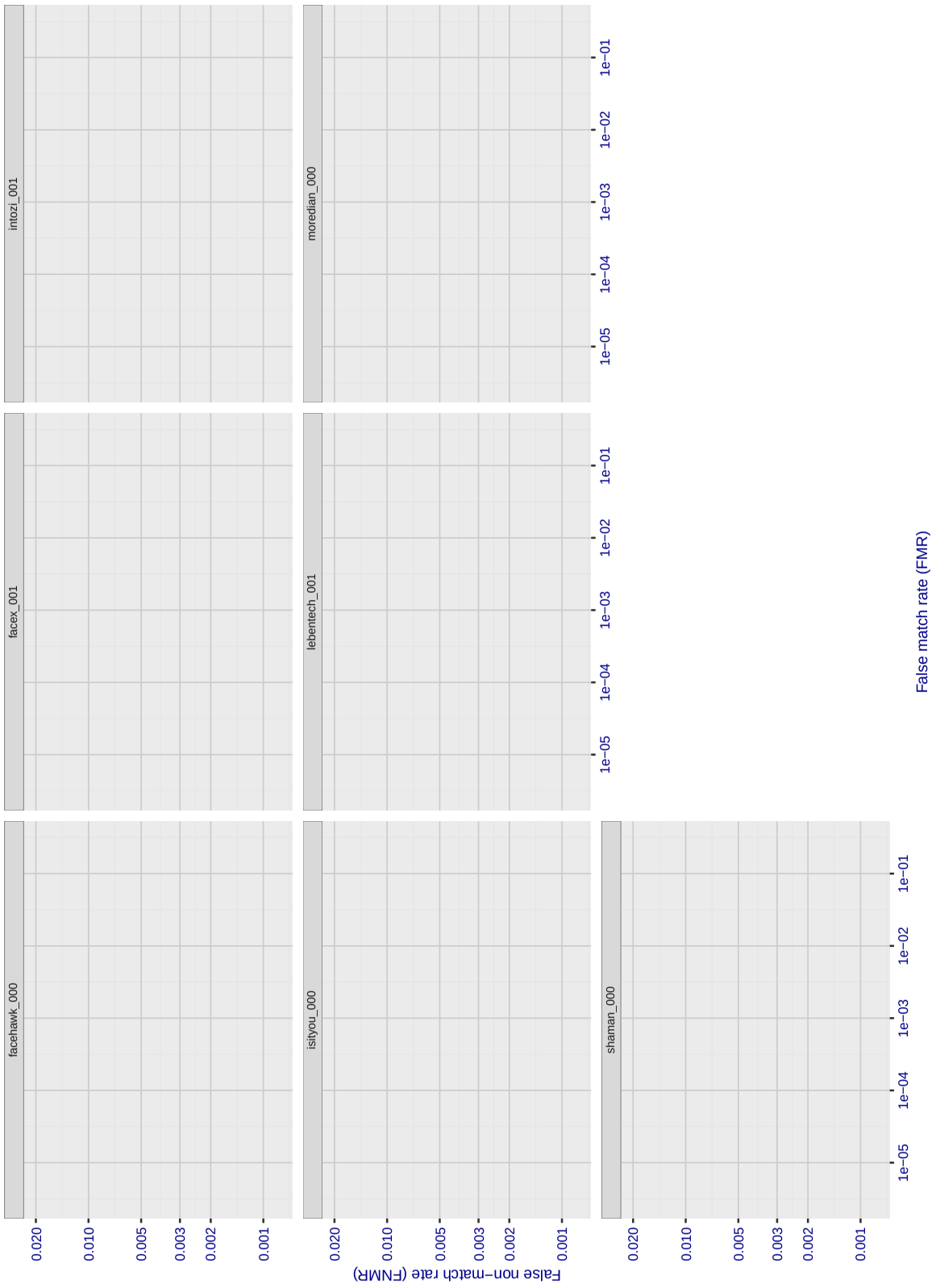

Figure 210: For the mugshot images, error tradeoff characteristics for white females, black females, black males and white males. The Z-shaped grey lines correspond to fixed thresholds, showing both *FNMR and FMR vary at one T value. Note: Many of the plots will naively be read as saying women gives worse error rates than men because the solid traces lie above the dotted ones. However, this is misleading and incomplete: The grey lines show the traces reveal horizontal shifts. Thus for the cogent-003 algorithm FNMR for men is* higher *than for women at a fixed threshold but, at the same time, FMR is higher for women - see Figure 284. As access control systems almost always operate at a fixed threshold, the naive interpretation is incorrect.*

FNMR(T) "False non-match rate"
FMR(T) "False match rate"

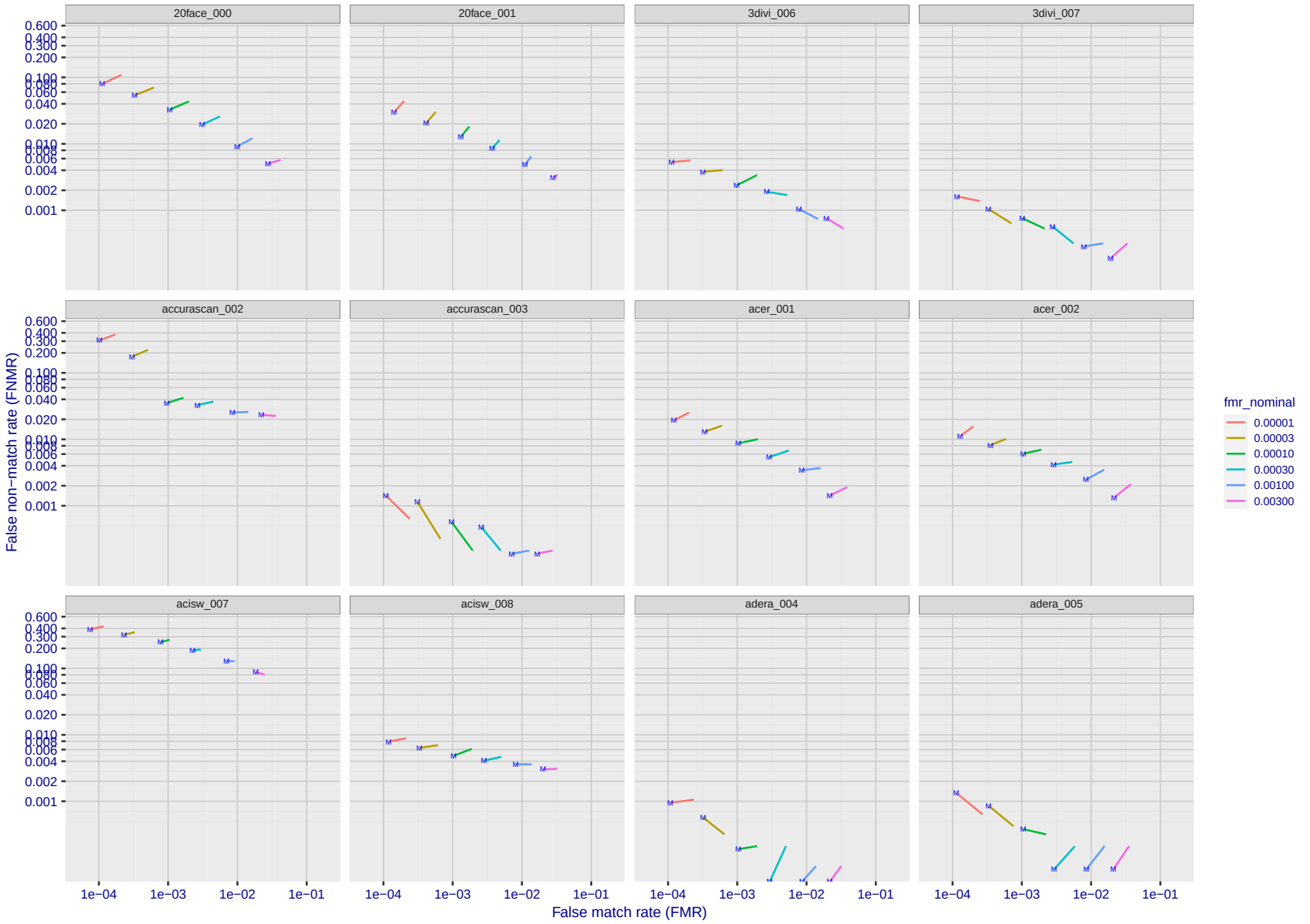

Figure 211: For the visa images, FNMR and FMR at six operating points along the DET characteristic. At each point a line is drawn between (FMR,FNMR)$_{\text{MALE}}$ and (FMR,FNMR)$_{\text{FEMALE}}$ showing how which sex has lower FMR and/or FNMR. The "M" label denotes male, the other end of the line corresponds to female. The six operating thresholds are selected to give the nominal false match rates given in the legend, and are computed over all impostor pairs regardless of age, sex, and place of birth. The plotted FMR values are broadly an order of magnitude larger than the nominal rates because FMR is computed over demographically-matched impostor pairs i.e individuals of the same sex, from the same geographic region (see section 3.6.1), and the same age group (see section 3.6.2).

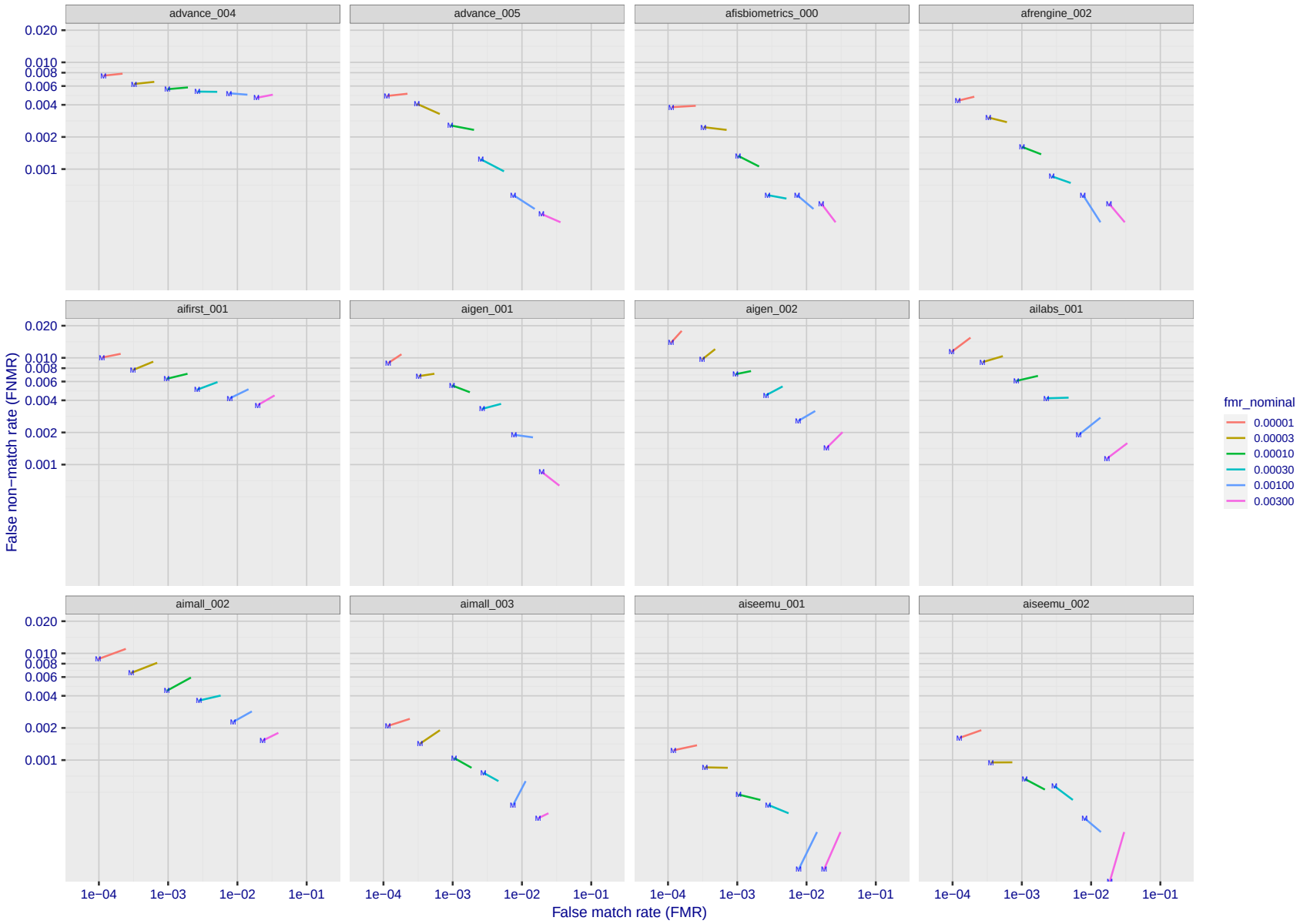

Figure 212: For the visa images, FNMR and FMR at six operating points along the DET characteristic. At each point a line is drawn between (FMR,FNMR)$_{\text{MALE}}$ and (FMR,FNMR)$_{\text{FEMALE}}$ showing how which sex has lower FMR and/or FNMR. The "M" label denotes male, the other end of the line corresponds to female. The six operating thresholds are selected to give the nominal false match rates given in the legend, and are computed over all impostor pairs regardless of age, sex, and place of birth. The plotted FMR values are broadly an order of magnitude larger than the nominal rates because FMR is computed over demographically-matched impostor pairs i.e individuals of the same sex, from the same geographic region (see section 3.6.1), and the same age group (see section 3.6.2).

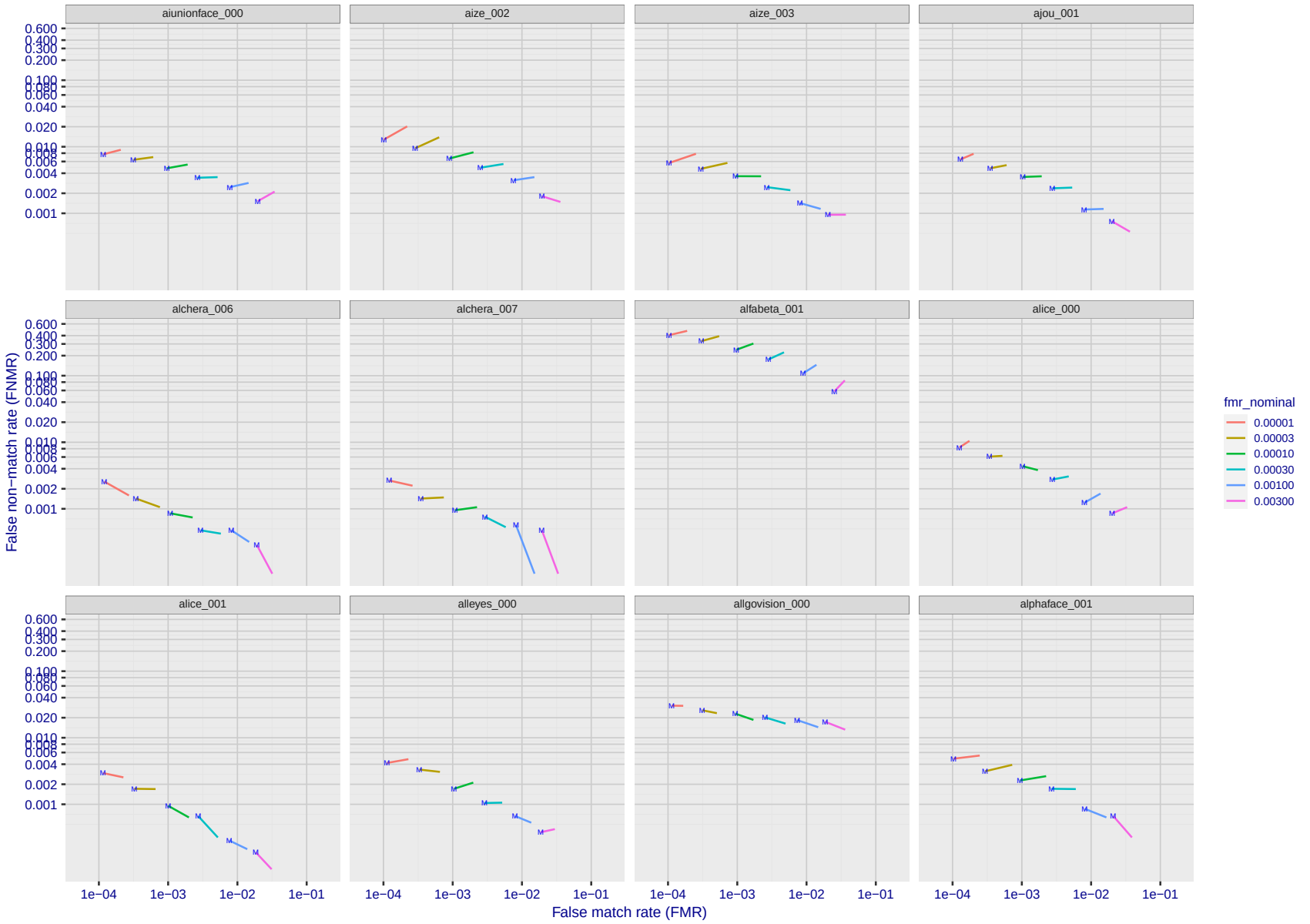

Figure 213: For the visa images, FNMR and FMR at six operating points along the DET characteristic. At each point a line is drawn between (FMR,FNMR)$_{\text{MALE}}$ and (FMR,FNMR)$_{\text{FEMALE}}$ showing how which sex has lower FMR and/or FNMR. The "M" label denotes male, the other end of the line corresponds to female. The six operating thresholds are selected to give the nominal false match rates given in the legend, and are computed over all impostor pairs regardless of age, sex, and place of birth. The plotted FMR values are broadly an order of magnitude larger than the nominal rates because FMR is computed over demographically-matched impostor pairs i.e individuals of the same sex, from the same geographic region (see section 3.6.1), and the same age group (see section 3.6.2).

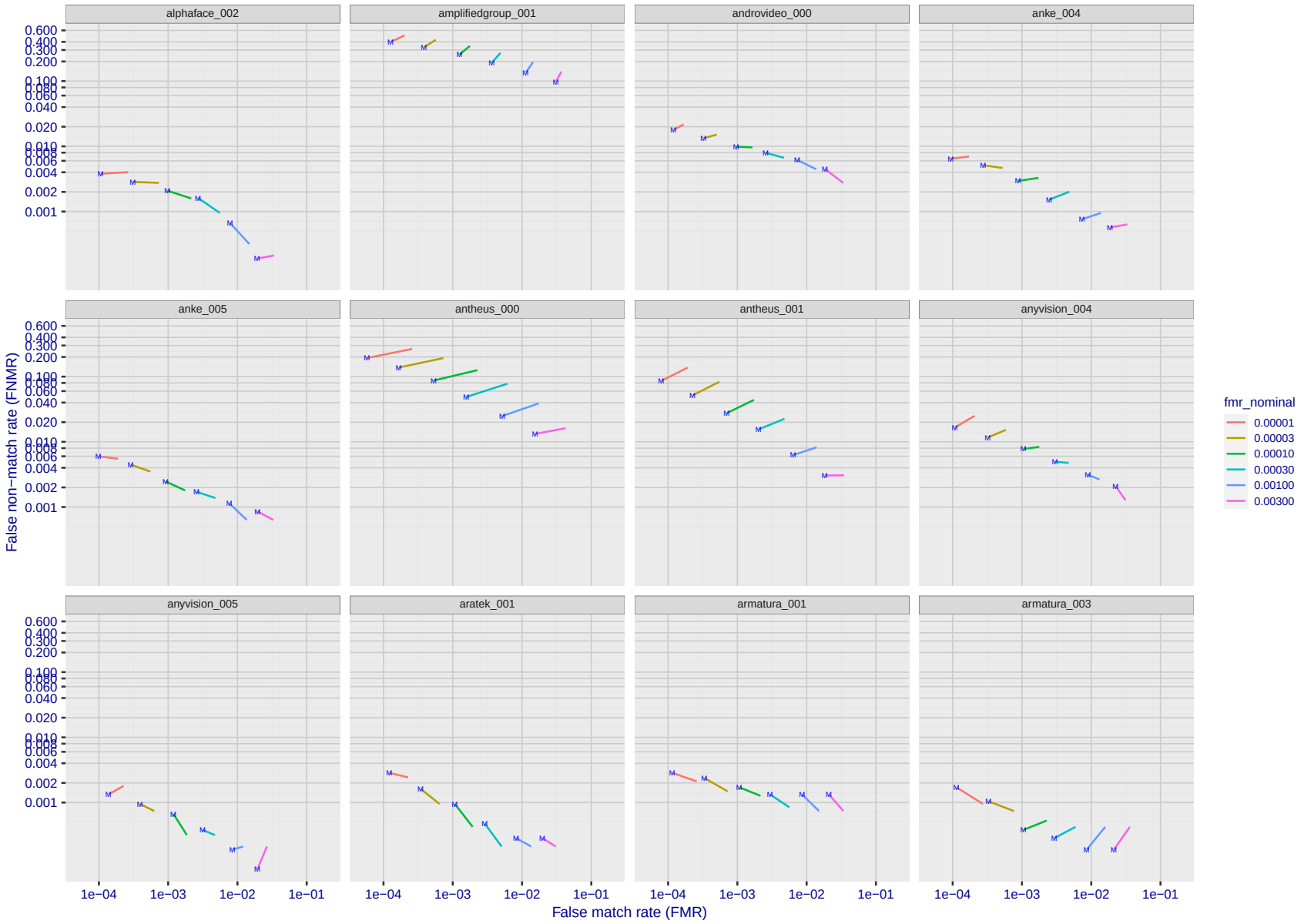

Figure 214: For the visa images, FNMR and FMR at six operating points along the DET characteristic. At each point a line is drawn between (FMR,FNMR)$_{\text{MALE}}$ and (FMR,FNMR)$_{\text{FEMALE}}$ showing how which sex has lower FMR and/or FNMR. The "M" label denotes male, the other end of the line corresponds to female. The six operating thresholds are selected to give the nominal false match rates given in the legend, and are computed over all impostor pairs regardless of age, sex, and place of birth. The plotted FMR values are broadly an order of magnitude larger than the nominal rates because FMR is computed over demographically-matched impostor pairs i.e individuals of the same sex, from the same geographic region (see section 3.6.1), and the same age group (see section 3.6.2).

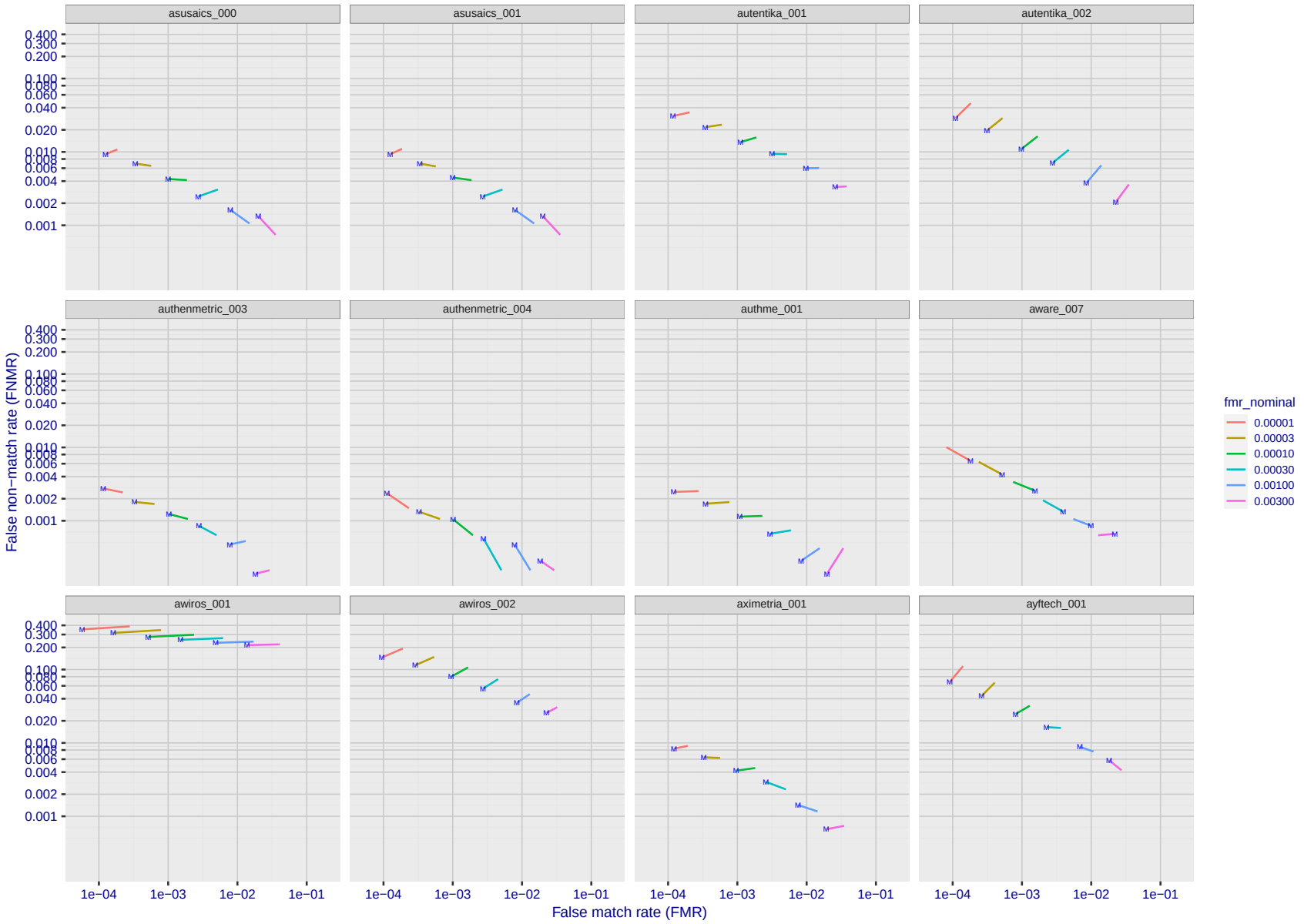

Figure 215: For the visa images, FNMR and FMR at six operating points along the DET characteristic. At each point a line is drawn between (FMR,FNMR)$_{\text{MALE}}$ and (FMR,FNMR)$_{\text{FEMALE}}$ showing how which sex has lower FMR and/or FNMR. The "M" label denotes male, the other end of the line corresponds to female. The six operating thresholds are selected to give the nominal false match rates given in the legend, and are computed over all impostor pairs regardless of age, sex, and place of birth. The plotted FMR values are broadly an order of magnitude larger than the nominal rates because FMR is computed over demographically-matched impostor pairs i.e individuals of the same sex, from the same geographic region (see section 3.6.1), and the same age group (see section 3.6.2).

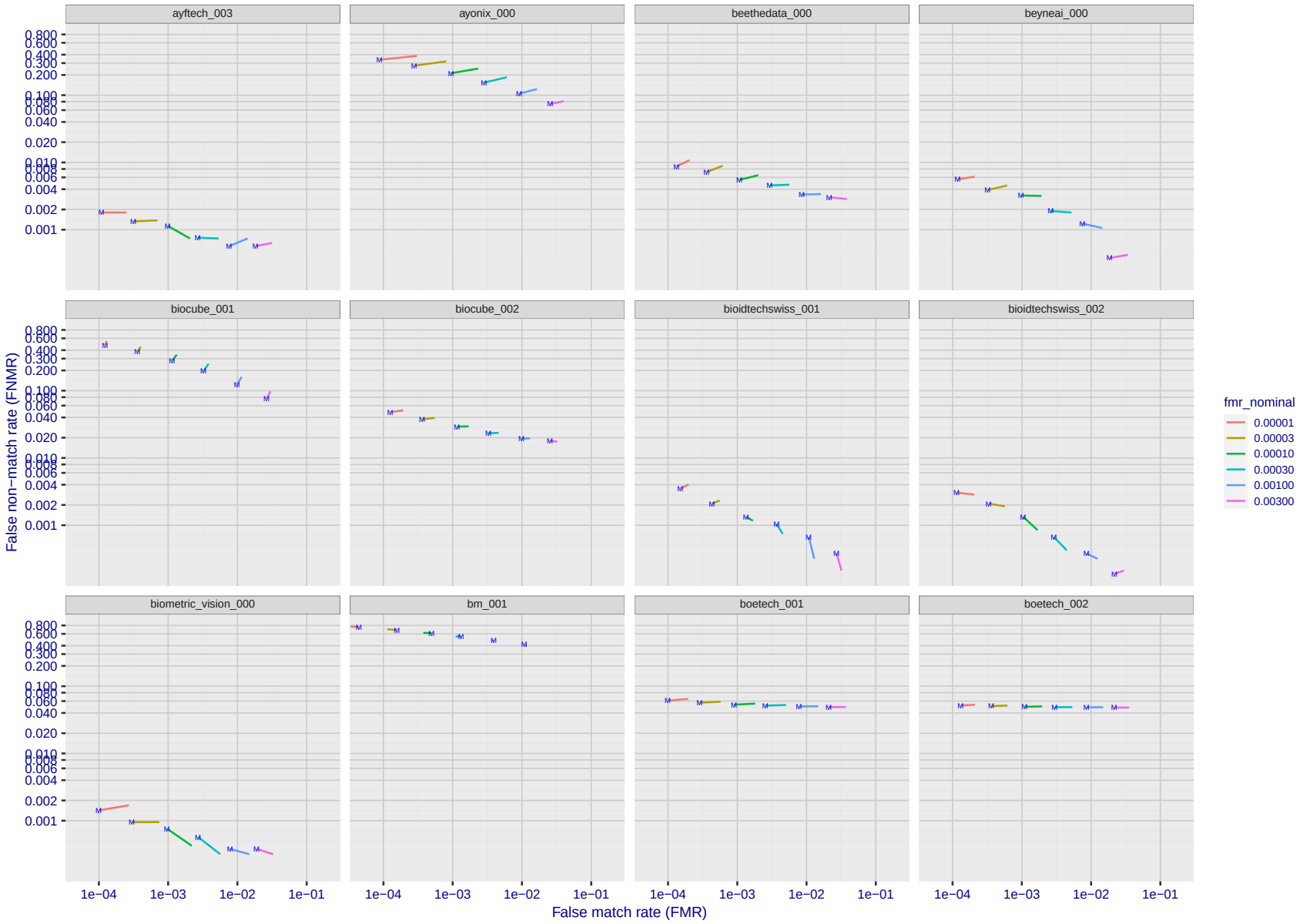

Figure 216: For the visa images, FNMR and FMR at six operating points along the DET characteristic. At each point a line is drawn between (FMR,FNMR)$_{\text{MALE}}$ and (FMR,FNMR)$_{\text{FEMALE}}$ showing how which sex has lower FMR and/or FNMR. The "M" label denotes male, the other end of the line corresponds to female. The six operating thresholds are selected to give the nominal false match rates given in the legend, and are computed over all impostor pairs regardless of age, sex, and place of birth. The plotted FMR values are broadly an order of magnitude larger than the nominal rates because FMR is computed over demographically-matched impostor pairs i.e individuals of the same sex, from the same geographic region (see section 3.6.1), and the same age group (see section 3.6.2).

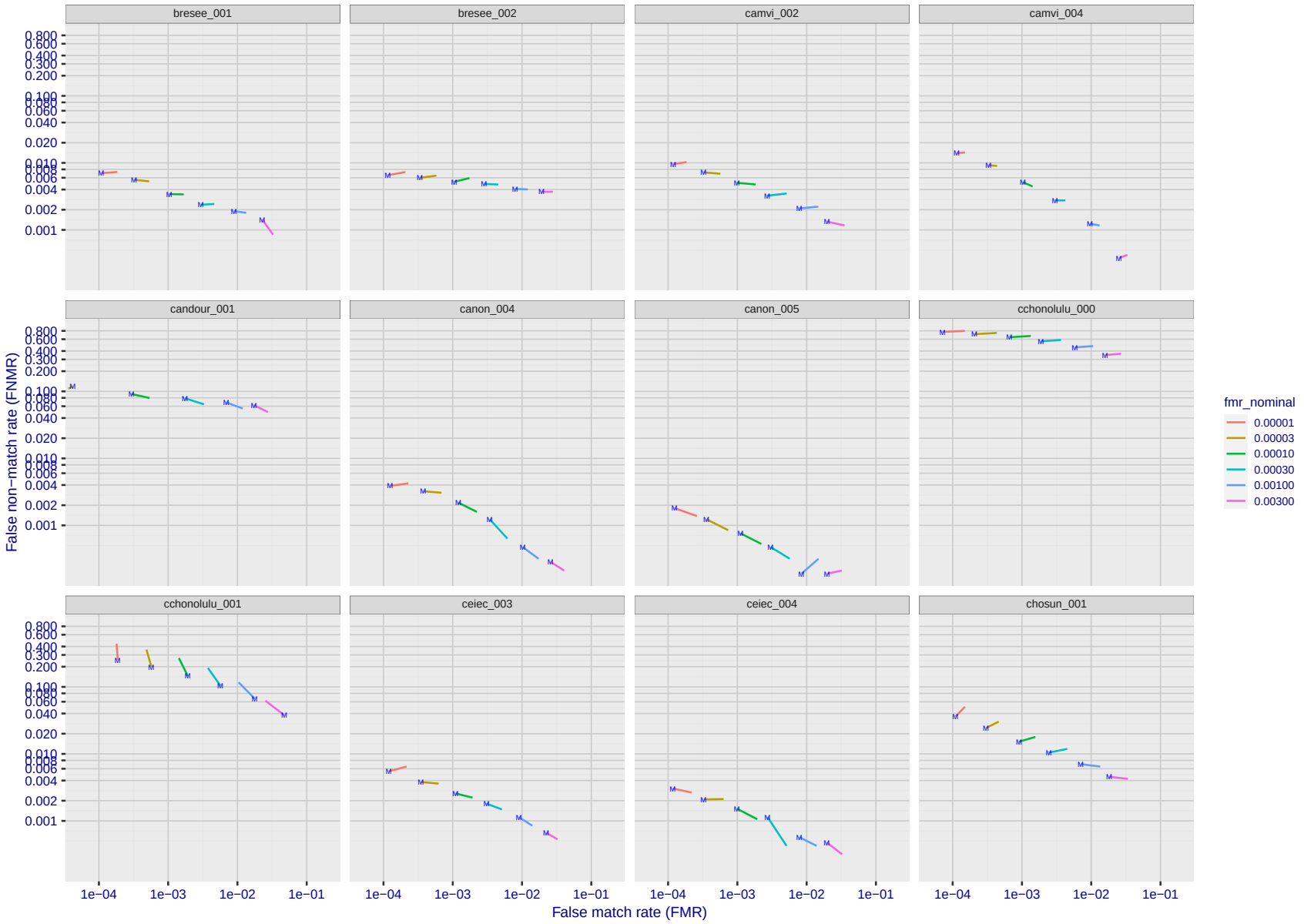

Figure 217: For the visa images, FNMR and FMR at six operating points along the DET characteristic. At each point a line is drawn between (FMR,FNMR)$_{\text{MALE}}$ and (FMR,FNMR)$_{\text{FEMALE}}$ showing how which sex has lower FMR and/or FNMR. The "M" label denotes male, the other end of the line corresponds to female. The six operating thresholds are selected to give the nominal false match rates given in the legend, and are computed over all impostor pairs regardless of age, sex, and place of birth. The plotted FMR values are broadly an order of magnitude larger than the nominal rates because FMR is computed over demographically-matched impostor pairs i.e individuals of the same sex, from the same geographic region (see section 3.6.1), and the same age group (see section 3.6.2).

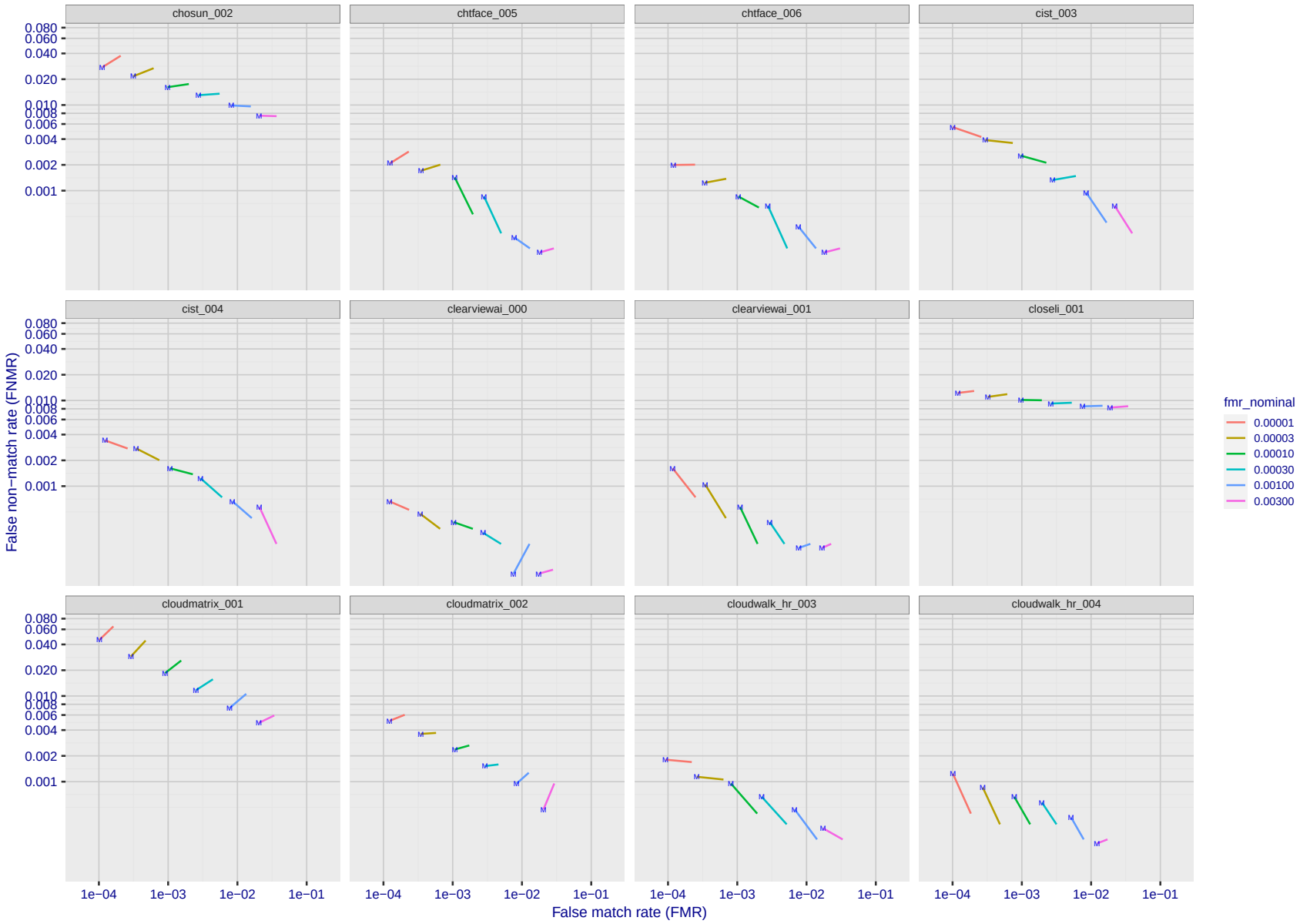

Figure 218: For the visa images, FNMR and FMR at six operating points along the DET characteristic. At each point a line is drawn between (FMR,FNMR)$_{\text{MALE}}$ and (FMR,FNMR)$_{\text{FEMALE}}$ showing how which sex has lower FMR and/or FNMR. The "M" label denotes male, the other end of the line corresponds to female. The six operating thresholds are selected to give the nominal false match rates given in the legend, and are computed over all impostor pairs regardless of age, sex, and place of birth. The plotted FMR values are broadly an order of magnitude larger than the nominal rates because FMR is computed over demographically-matched impostor pairs i.e individuals of the same sex, from the same geographic region (see section 3.6.1), and the same age group (see section 3.6.2).

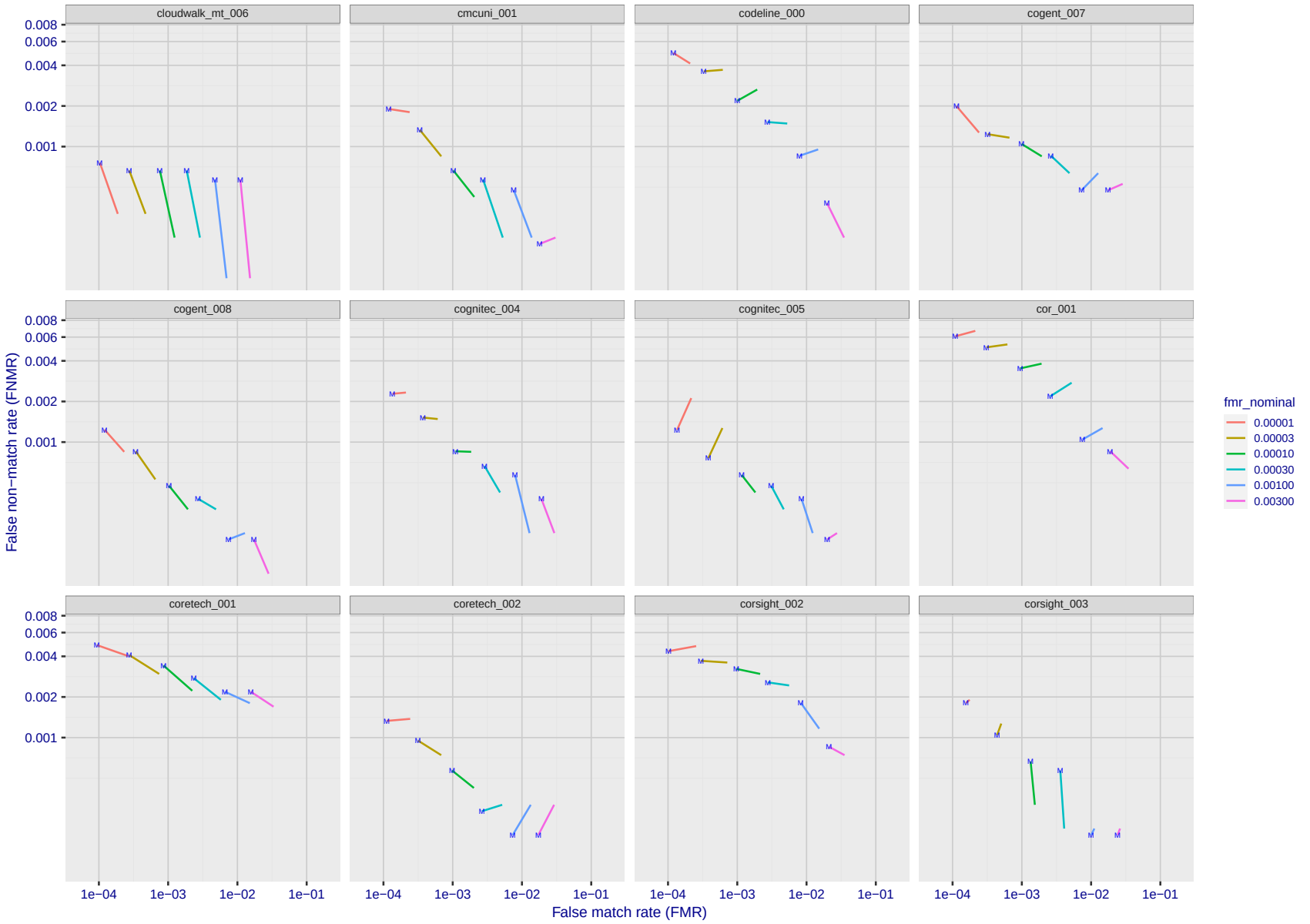

Figure 219: For the visa images, FNMR and FMR at six operating points along the DET characteristic. At each point a line is drawn between (FMR,FNMR)$_{\text{MALE}}$ and (FMR,FNMR)$_{\text{FEMALE}}$ showing how which sex has lower FMR and/or FNMR. The "M" label denotes male, the other end of the line corresponds to female. The six operating thresholds are selected to give the nominal false match rates given in the legend, and are computed over all impostor pairs regardless of age, sex, and place of birth. The plotted FMR values are broadly an order of magnitude larger than the nominal rates because FMR is computed over demographically-matched impostor pairs i.e individuals of the same sex, from the same geographic region (see section 3.6.1), and the same age group (see section 3.6.2).

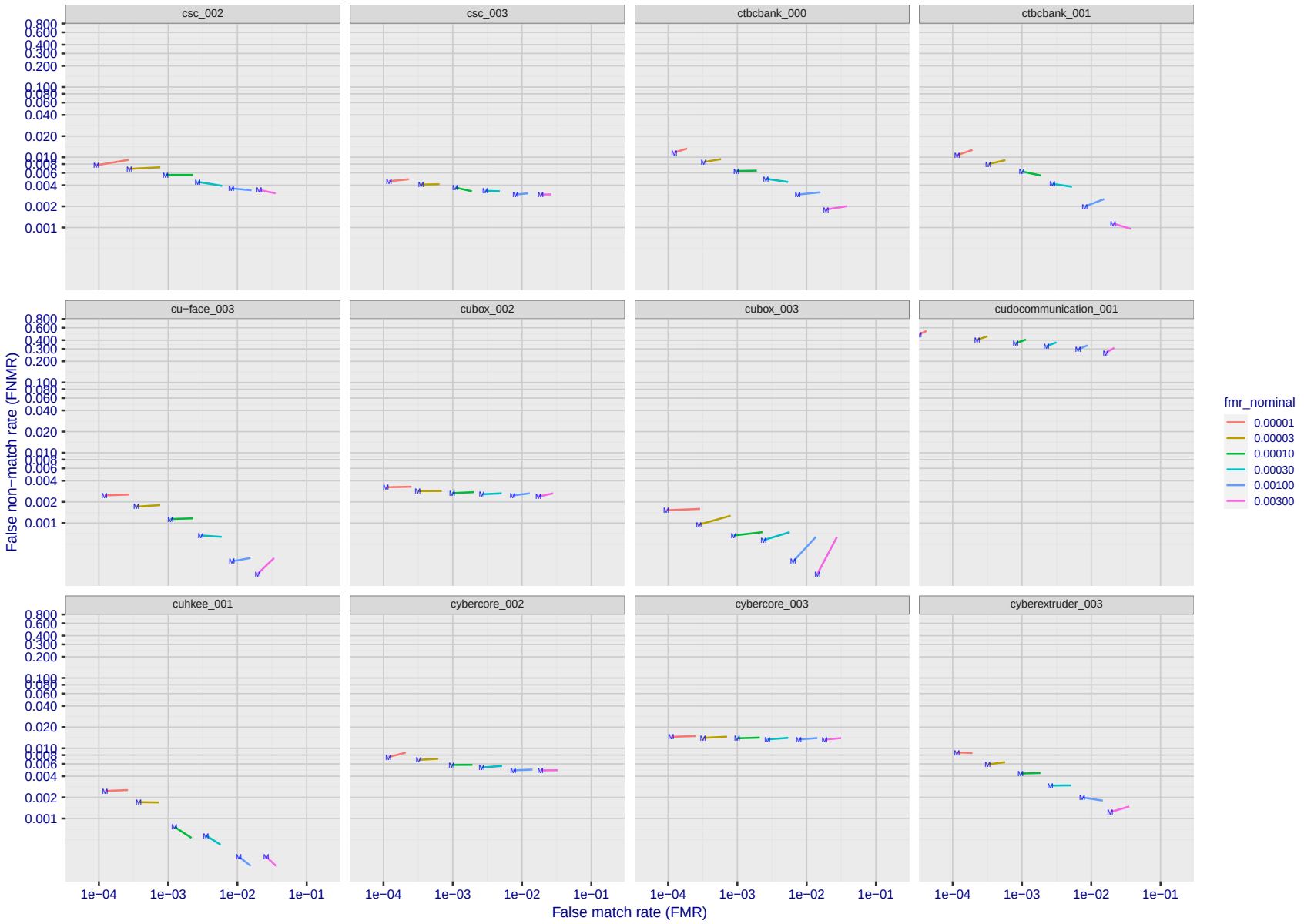

Figure 220: For the visa images, FNMR and FMR at six operating points along the DET characteristic. At each point a line is drawn between (FMR,FNMR)$_{\text{MALE}}$ and (FMR,FNMR)$_{\text{FEMALE}}$ showing how which sex has lower FMR and/or FNMR. The "M" label denotes male, the other end of the line corresponds to female. The six operating thresholds are selected to give the nominal false match rates given in the legend, and are computed over all impostor pairs regardless of age, sex, and place of birth. The plotted FMR values are broadly an order of magnitude larger than the nominal rates because FMR is computed over demographically-matched impostor pairs i.e individuals of the same sex, from the same geographic region (see section 3.6.1), and the same age group (see section 3.6.2).

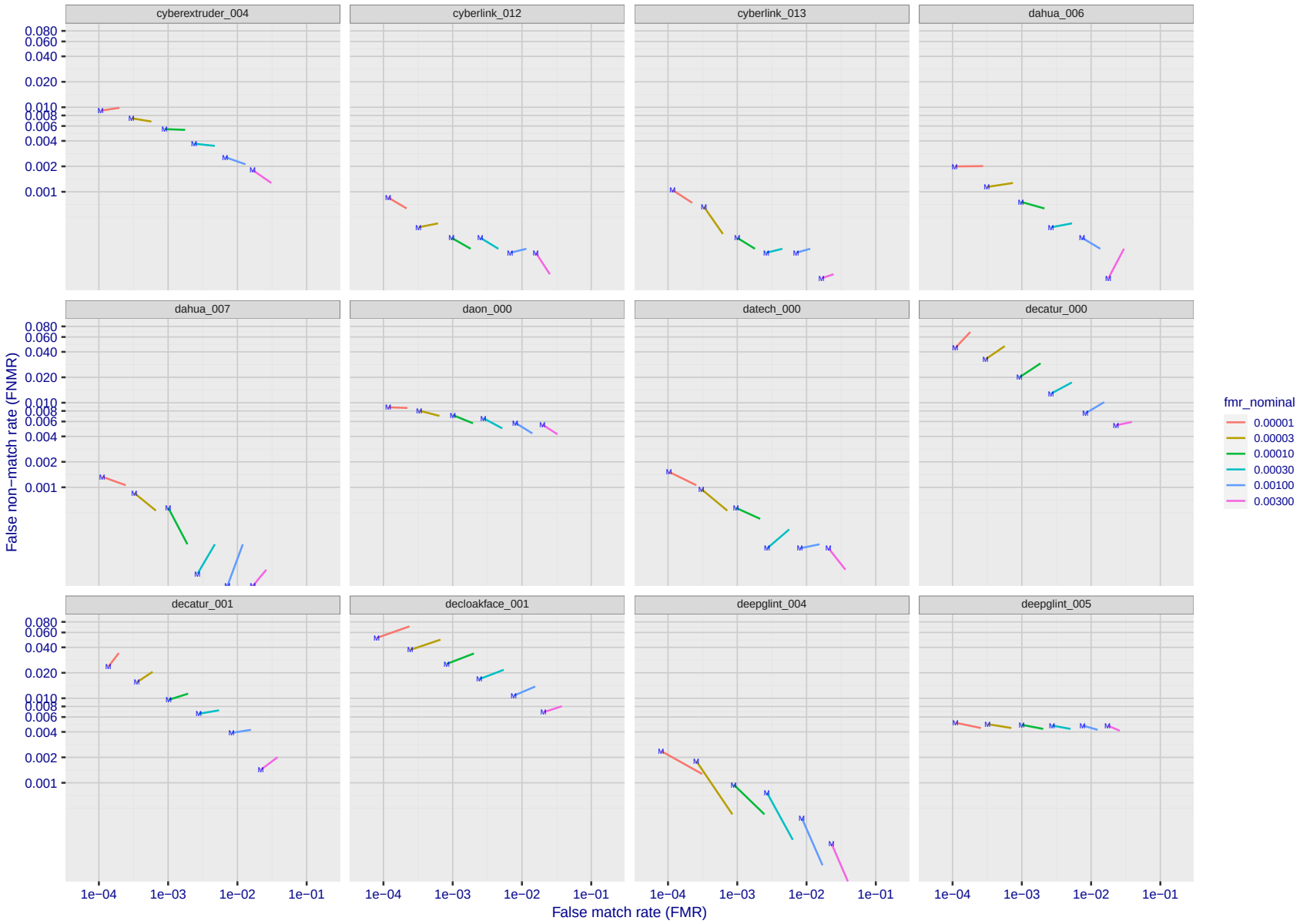

Figure 221: For the visa images, FNMR and FMR at six operating points along the DET characteristic. At each point a line is drawn between (FMR,FNMR)$_{\text{MALE}}$ and (FMR,FNMR)$_{\text{FEMALE}}$ showing how which sex has lower FMR and/or FNMR. The "M" label denotes male, the other end of the line corresponds to female. The six operating thresholds are selected to give the nominal false match rates given in the legend, and are computed over all impostor pairs regardless of age, sex, and place of birth. The plotted FMR values are broadly an order of magnitude larger than the nominal rates because FMR is computed over demographically-matched impostor pairs i.e individuals of the same sex, from the same geographic region (see section 3.6.1), and the same age group (see section 3.6.2).

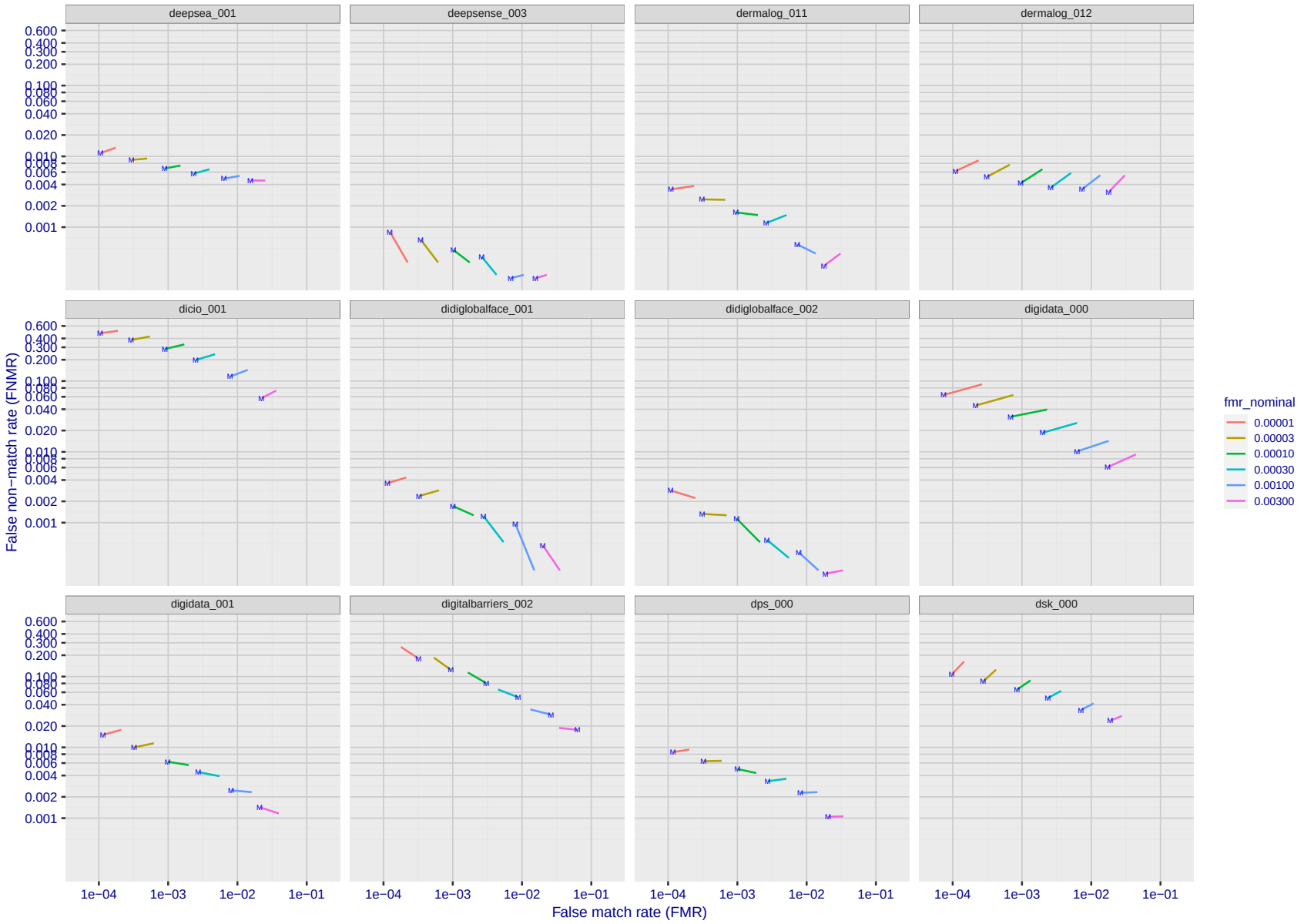

Figure 222: For the visa images, FNMR and FMR at six operating points along the DET characteristic. At each point a line is drawn between (FMR,FNMR)$_{\text{MALE}}$ and (FMR,FNMR)$_{\text{FEMALE}}$ showing how which sex has lower FMR and/or FNMR. The "M" label denotes male, the other end of the line corresponds to female. The six operating thresholds are selected to give the nominal false match rates given in the legend, and are computed over all impostor pairs regardless of age, sex, and place of birth. The plotted FMR values are broadly an order of magnitude larger than the nominal rates because FMR is computed over demographically-matched impostor pairs i.e individuals of the same sex, from the same geographic region (see section 3.6.1), and the same age group (see section 3.6.2).

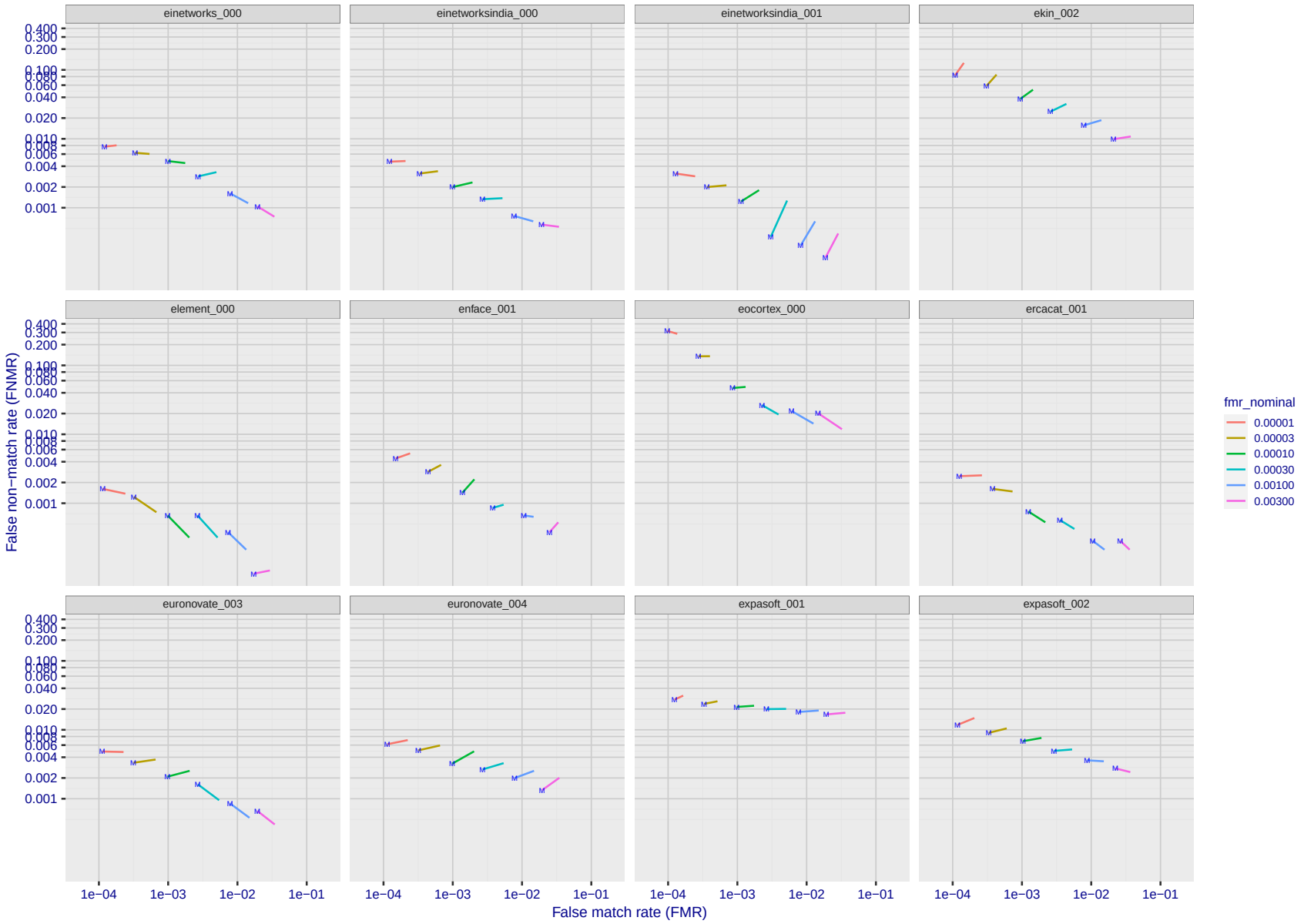

Figure 223: For the visa images, FNMR and FMR at six operating points along the DET characteristic. At each point a line is drawn between (FMR,FNMR)$_{\text{MALE}}$ and (FMR,FNMR)$_{\text{FEMALE}}$ showing how which sex has lower FMR and/or FNMR. The "M" label denotes male, the other end of the line corresponds to female. The six operating thresholds are selected to give the nominal false match rates given in the legend, and are computed over all impostor pairs regardless of age, sex, and place of birth. The plotted FMR values are broadly an order of magnitude larger than the nominal rates because FMR is computed over demographically-matched impostor pairs i.e individuals of the same sex, from the same geographic region (see section 3.6.1), and the same age group (see section 3.6.2).

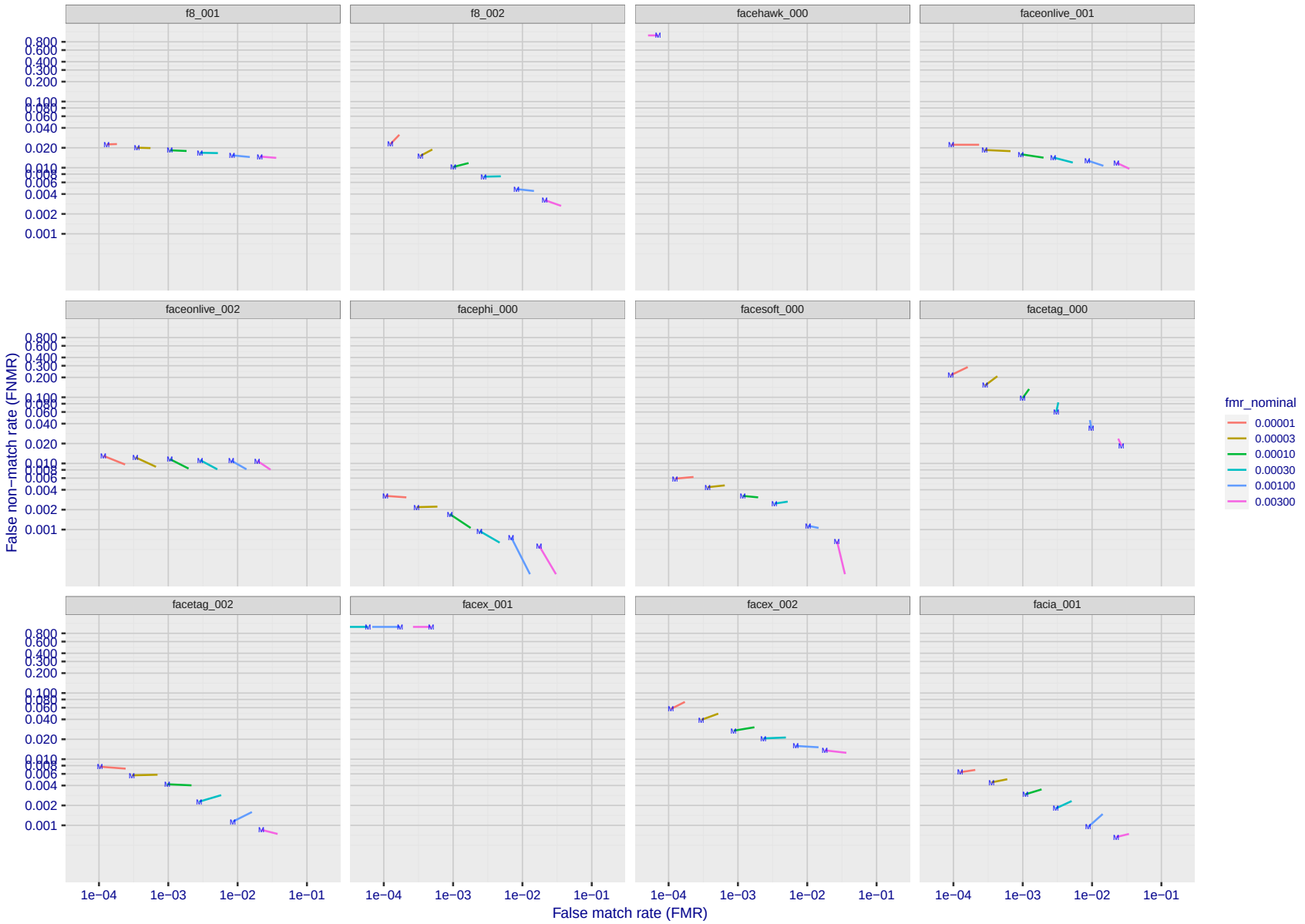

Figure 224: For the visa images, FNMR and FMR at six operating points along the DET characteristic. At each point a line is drawn between (FMR,FNMR)$_{\text{MALE}}$ and (FMR,FNMR)$_{\text{FEMALE}}$ showing how which sex has lower FMR and/or FNMR. The "M" label denotes male, the other end of the line corresponds to female. The six operating thresholds are selected to give the nominal false match rates given in the legend, and are computed over all impostor pairs regardless of age, sex, and place of birth. The plotted FMR values are broadly an order of magnitude larger than the nominal rates because FMR is computed over demographically-matched impostor pairs i.e individuals of the same sex, from the same geographic region (see section 3.6.1), and the same age group (see section 3.6.2).

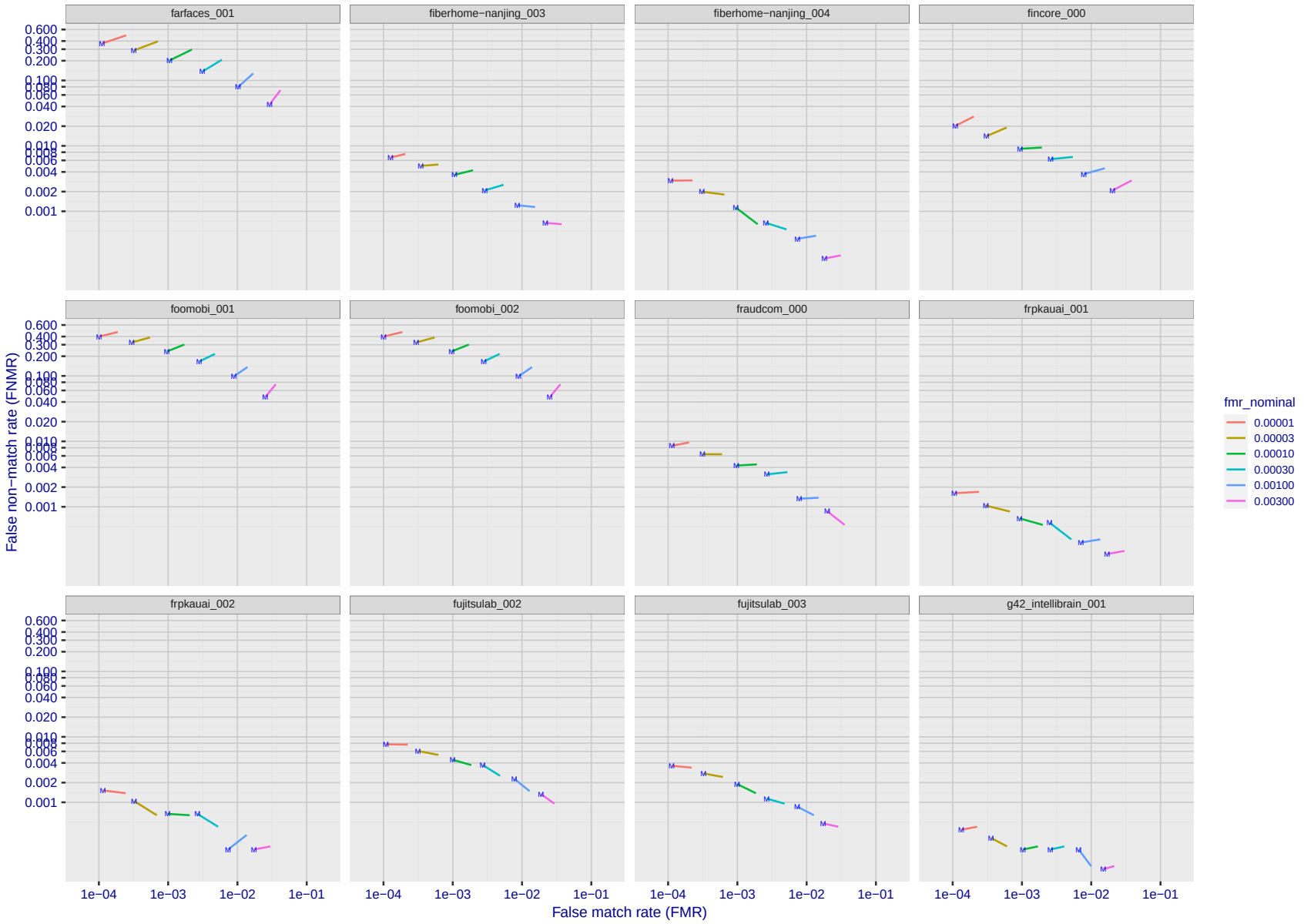

Figure 225: For the visa images, FNMR and FMR at six operating points along the DET characteristic. At each point a line is drawn between (FMR,FNMR)$_{\text{MALE}}$ and (FMR,FNMR)$_{\text{FEMALE}}$ showing how which sex has lower FMR and/or FNMR. The "M" label denotes male, the other end of the line corresponds to female. The six operating thresholds are selected to give the nominal false match rates given in the legend, and are computed over all impostor pairs regardless of age, sex, and place of birth. The plotted FMR values are broadly an order of magnitude larger than the nominal rates because FMR is computed over demographically-matched impostor pairs i.e individuals of the same sex, from the same geographic region (see section 3.6.1), and the same age group (see section 3.6.2).

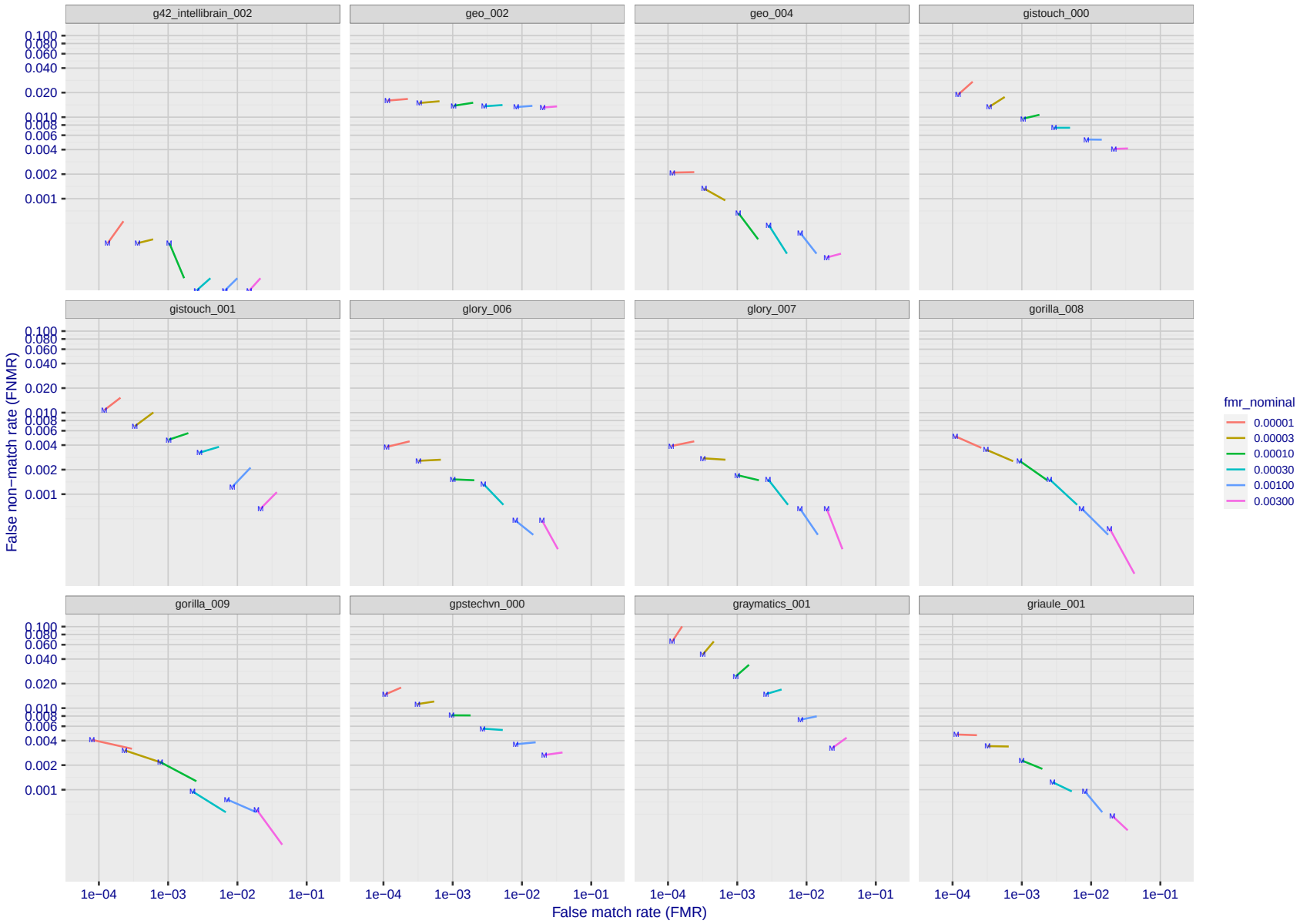

Figure 226: For the visa images, FNMR and FMR at six operating points along the DET characteristic. At each point a line is drawn between (FMR,FNMR)$_{\text{MALE}}$ and (FMR,FNMR)$_{\text{FEMALE}}$ showing how which sex has lower FMR and/or FNMR. The "M" label denotes male, the other end of the line corresponds to female. The six operating thresholds are selected to give the nominal false match rates given in the legend, and are computed over all impostor pairs regardless of age, sex, and place of birth. The plotted FMR values are broadly an order of magnitude larger than the nominal rates because FMR is computed over demographically-matched impostor pairs i.e individuals of the same sex, from the same geographic region (see section 3.6.1), and the same age group (see section 3.6.2).

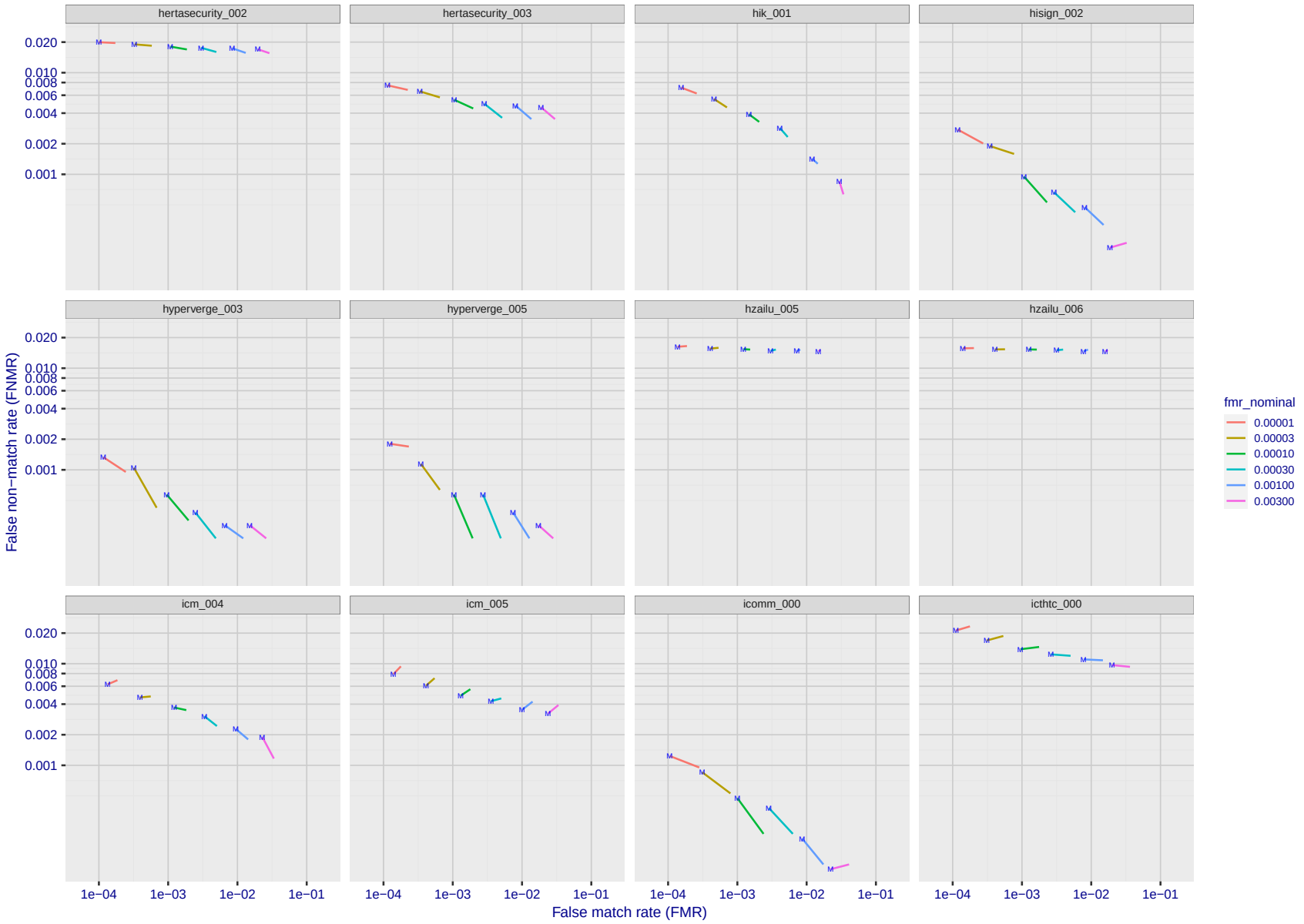

Figure 227: For the visa images, FNMR and FMR at six operating points along the DET characteristic. At each point a line is drawn between (FMR,FNMR)$_{\text{MALE}}$ and (FMR,FNMR)$_{\text{FEMALE}}$ showing how which sex has lower FMR and/or FNMR. The "M" label denotes male, the other end of the line corresponds to female. The six operating thresholds are selected to give the nominal false match rates given in the legend, and are computed over all impostor pairs regardless of age, sex, and place of birth. The plotted FMR values are broadly an order of magnitude larger than the nominal rates because FMR is computed over demographically-matched impostor pairs i.e individuals of the same sex, from the same geographic region (see section 3.6.1), and the same age group (see section 3.6.2).

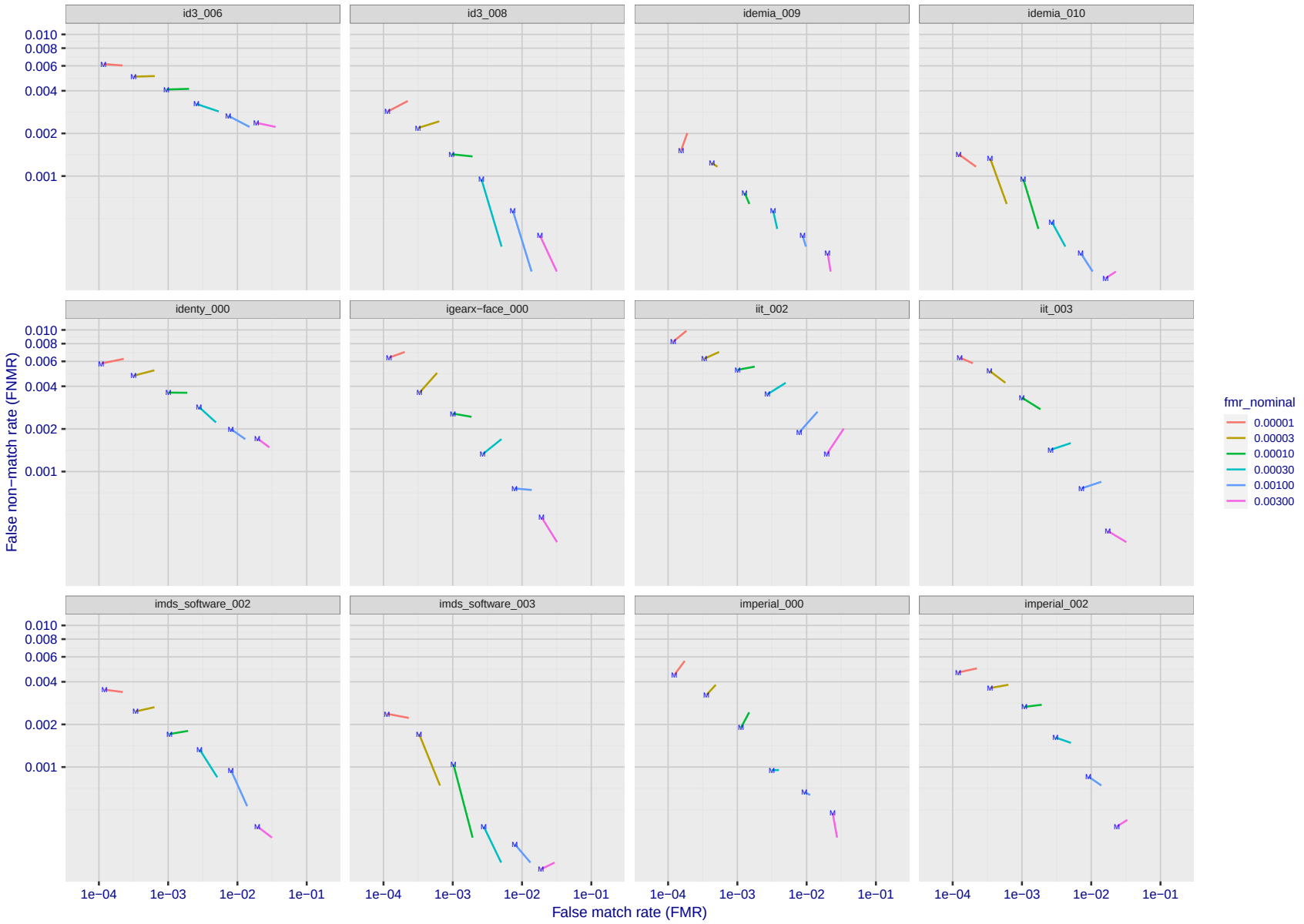

Figure 228: For the visa images, FNMR and FMR at six operating points along the DET characteristic. At each point a line is drawn between (FMR,FNMR)$_{\text{MALE}}$ and (FMR,FNMR)$_{\text{FEMALE}}$ showing how which sex has lower FMR and/or FNMR. The "M" label denotes male, the other end of the line corresponds to female. The six operating thresholds are selected to give the nominal false match rates given in the legend, and are computed over all impostor pairs regardless of age, sex, and place of birth. The plotted FMR values are broadly an order of magnitude larger than the nominal rates because FMR is computed over demographically-matched impostor pairs i.e individuals of the same sex, from the same geographic region (see section 3.6.1), and the same age group (see section 3.6.2).

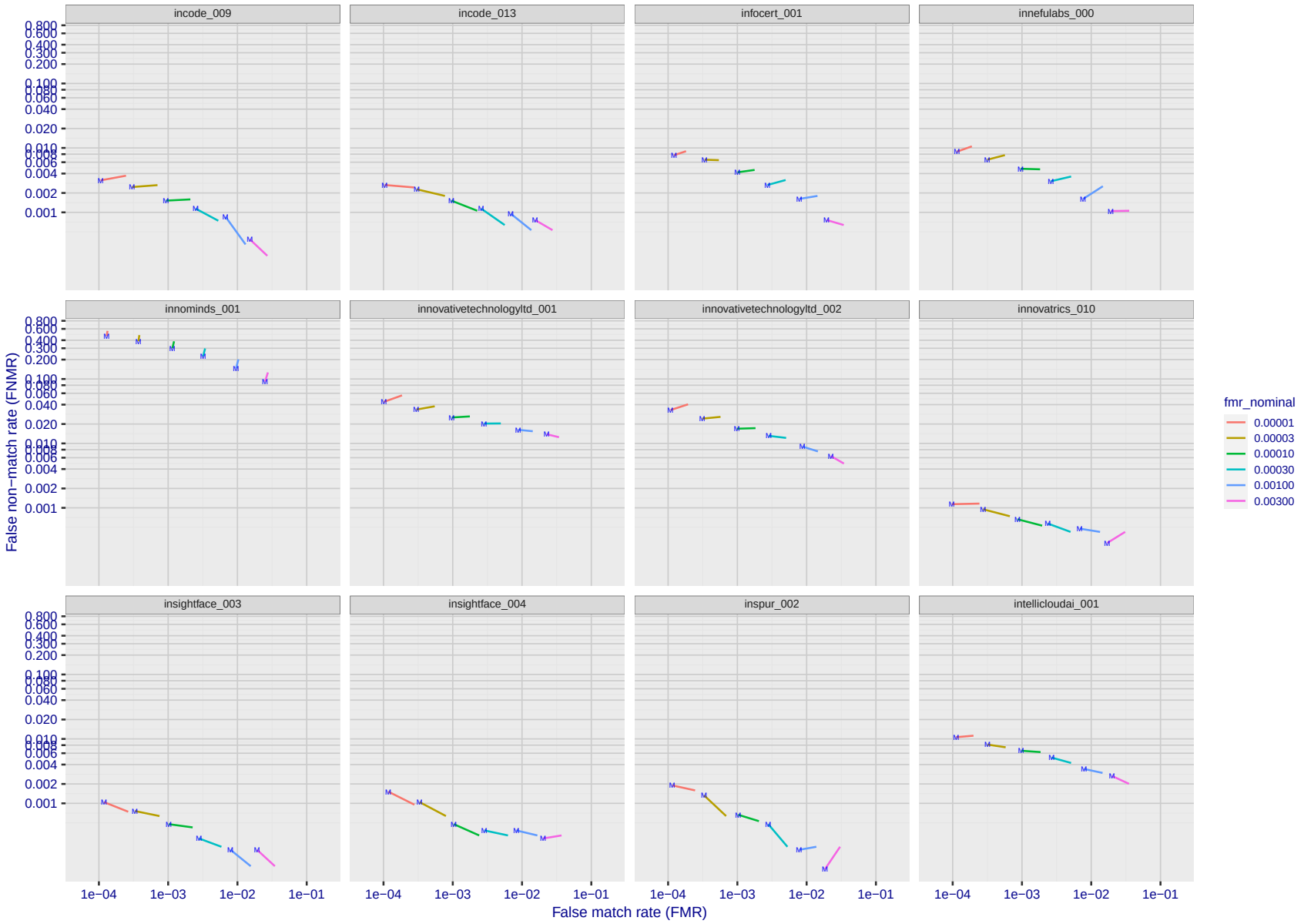

Figure 229: For the visa images, FNMR and FMR at six operating points along the DET characteristic. At each point a line is drawn between (FMR,FNMR)$_{\text{MALE}}$ and (FMR,FNMR)$_{\text{FEMALE}}$ showing how which sex has lower FMR and/or FNMR. The "M" label denotes male, the other end of the line corresponds to female. The six operating thresholds are selected to give the nominal false match rates given in the legend, and are computed over all impostor pairs regardless of age, sex, and place of birth. The plotted FMR values are broadly an order of magnitude larger than the nominal rates because FMR is computed over demographically-matched impostor pairs i.e individuals of the same sex, from the same geographic region (see section 3.6.1), and the same age group (see section 3.6.2).

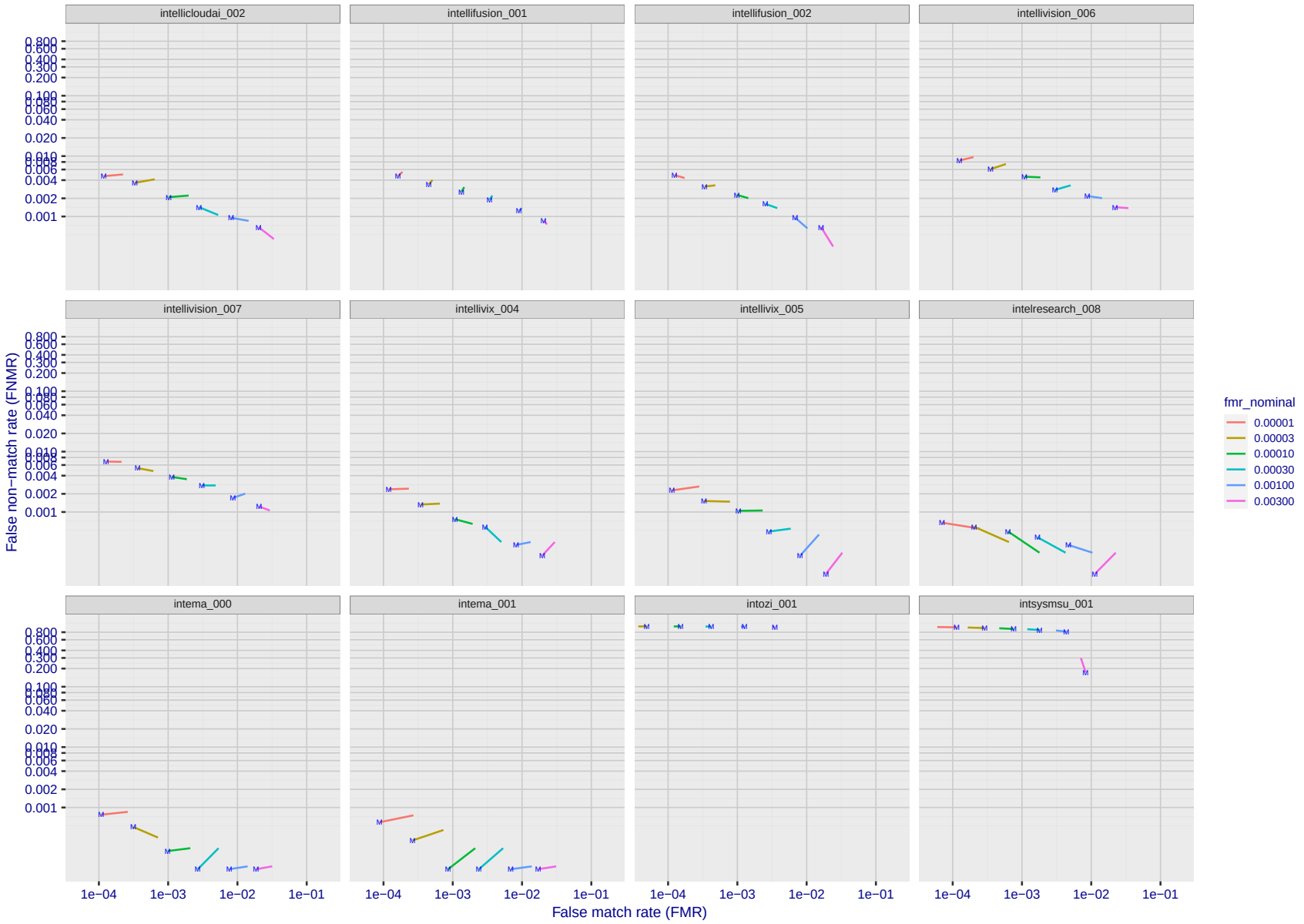

Figure 230: For the visa images, FNMR and FMR at six operating points along the DET characteristic. At each point a line is drawn between (FMR,FNMR)$_{\text{MALE}}$ and (FMR,FNMR)$_{\text{FEMALE}}$ showing how which sex has lower FMR and/or FNMR. The "M" label denotes male, the other end of the line corresponds to female. The six operating thresholds are selected to give the nominal false match rates given in the legend, and are computed over all impostor pairs regardless of age, sex, and place of birth. The plotted FMR values are broadly an order of magnitude larger than the nominal rates because FMR is computed over demographically-matched impostor pairs i.e individuals of the same sex, from the same geographic region (see section 3.6.1), and the same age group (see section 3.6.2).

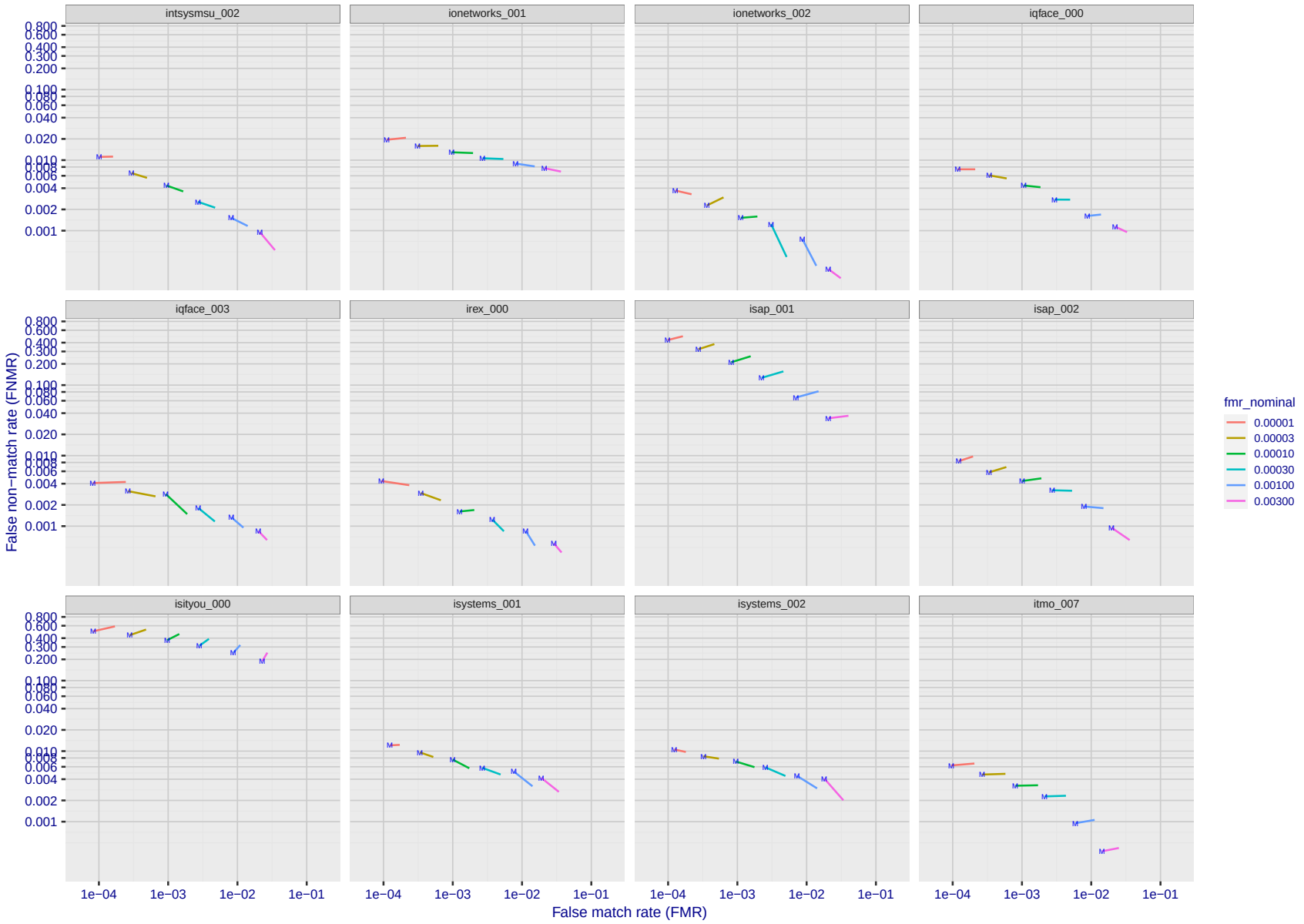

Figure 231: For the visa images, FNMR and FMR at six operating points along the DET characteristic. At each point a line is drawn between (FMR,FNMR)$_{\text{MALE}}$ and (FMR,FNMR)$_{\text{FEMALE}}$ showing how which sex has lower FMR and/or FNMR. The "M" label denotes male, the other end of the line corresponds to female. The six operating thresholds are selected to give the nominal false match rates given in the legend, and are computed over all impostor pairs regardless of age, sex, and place of birth. The plotted FMR values are broadly an order of magnitude larger than the nominal rates because FMR is computed over demographically-matched impostor pairs i.e individuals of the same sex, from the same geographic region (see section 3.6.1), and the same age group (see section 3.6.2).

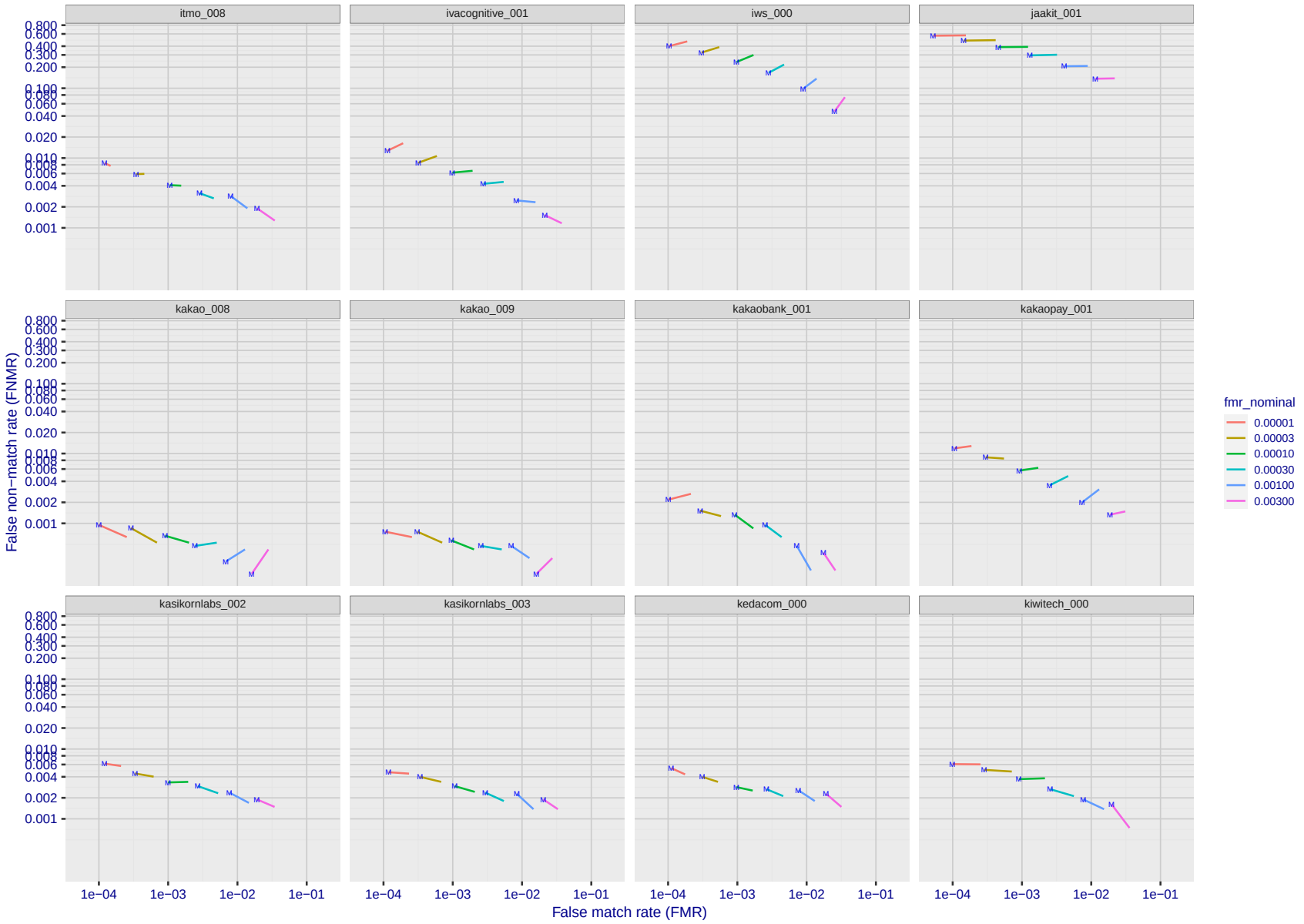

Figure 232: For the visa images, FNMR and FMR at six operating points along the DET characteristic. At each point a line is drawn between (FMR,FNMR)$_{\text{MALE}}$ and (FMR,FNMR)$_{\text{FEMALE}}$ showing how which sex has lower FMR and/or FNMR. The "M" label denotes male, the other end of the line corresponds to female. The six operating thresholds are selected to give the nominal false match rates given in the legend, and are computed over all impostor pairs regardless of age, sex, and place of birth. The plotted FMR values are broadly an order of magnitude larger than the nominal rates because FMR is computed over demographically-matched impostor pairs i.e individuals of the same sex, from the same geographic region (see section 3.6.1), and the same age group (see section 3.6.2).

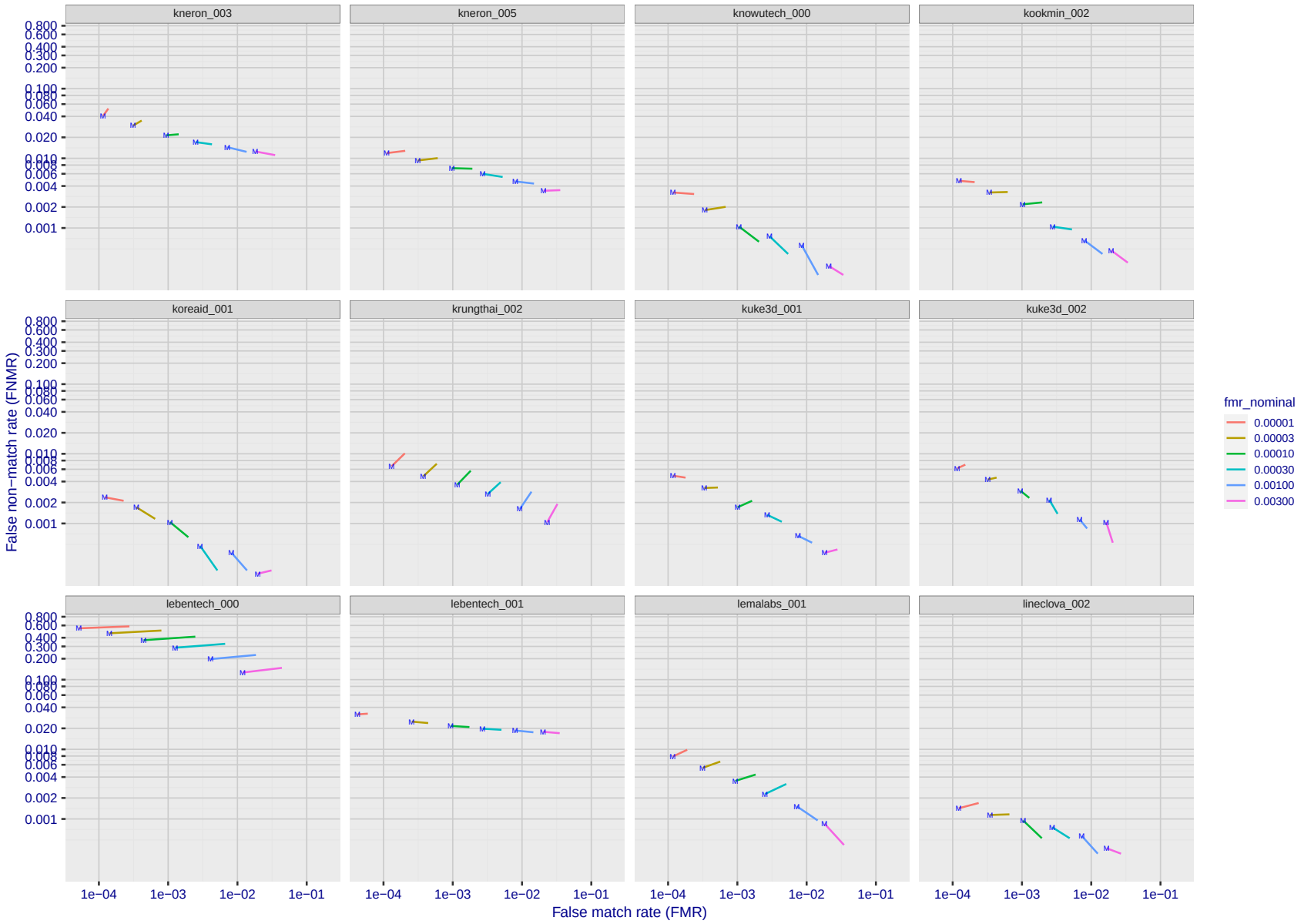

Figure 233: For the visa images, FNMR and FMR at six operating points along the DET characteristic. At each point a line is drawn between (FMR,FNMR)$_{\text{MALE}}$ and (FMR,FNMR)$_{\text{FEMALE}}$ showing how which sex has lower FMR and/or FNMR. The "M" label denotes male, the other end of the line corresponds to female. The six operating thresholds are selected to give the nominal false match rates given in the legend, and are computed over all impostor pairs regardless of age, sex, and place of birth. The plotted FMR values are broadly an order of magnitude larger than the nominal rates because FMR is computed over demographically-matched impostor pairs i.e individuals of the same sex, from the same geographic region (see section 3.6.1), and the same age group (see section 3.6.2).

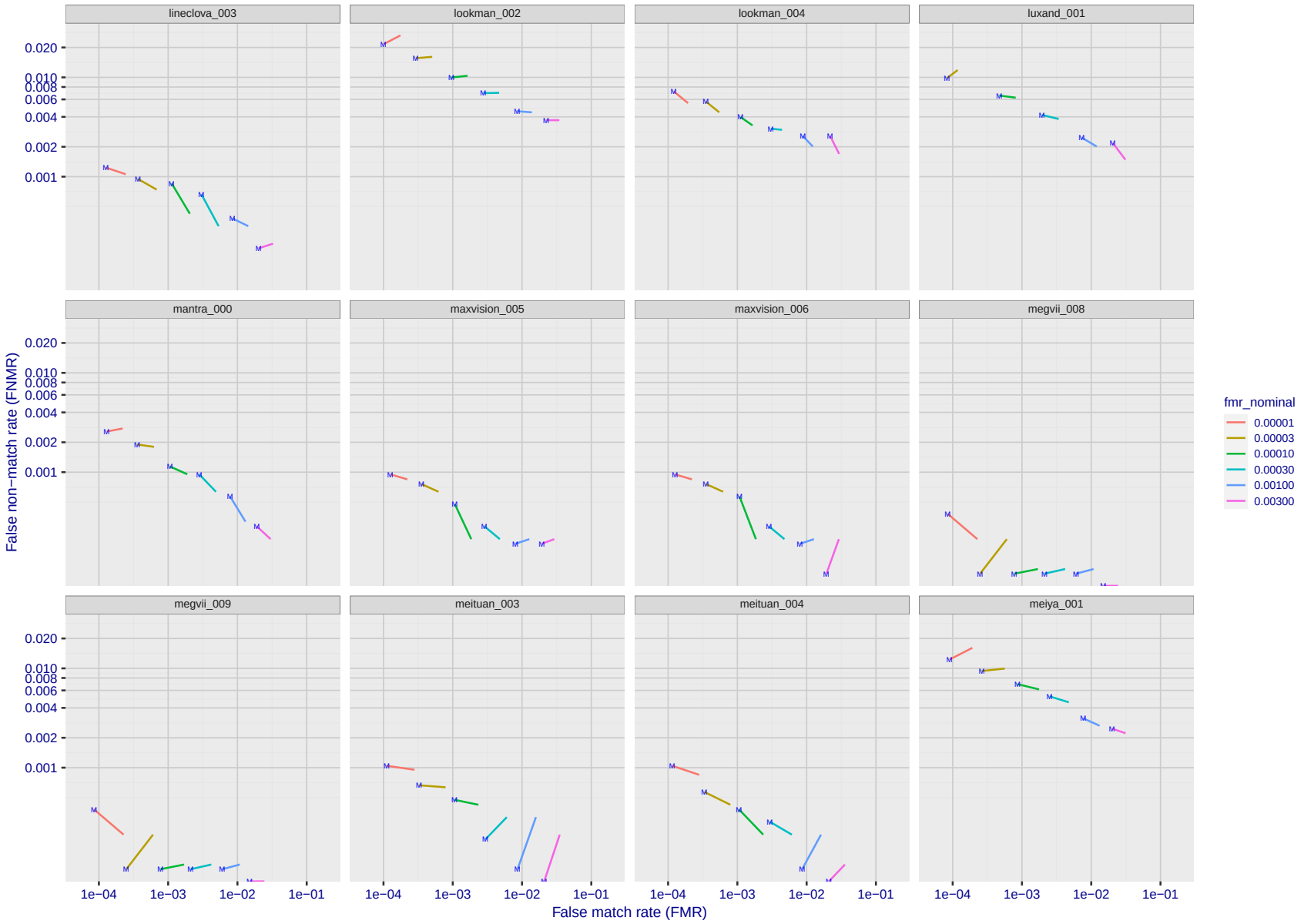

Figure 234: For the visa images, FNMR and FMR at six operating points along the DET characteristic. At each point a line is drawn between (FMR,FNMR)$_{\text{MALE}}$ and (FMR,FNMR)$_{\text{FEMALE}}$ showing how which sex has lower FMR and/or FNMR. The "M" label denotes male, the other end of the line corresponds to female. The six operating thresholds are selected to give the nominal false match rates given in the legend, and are computed over all impostor pairs regardless of age, sex, and place of birth. The plotted FMR values are broadly an order of magnitude larger than the nominal rates because FMR is computed over demographically-matched impostor pairs i.e individuals of the same sex, from the same geographic region (see section 3.6.1), and the same age group (see section 3.6.2).

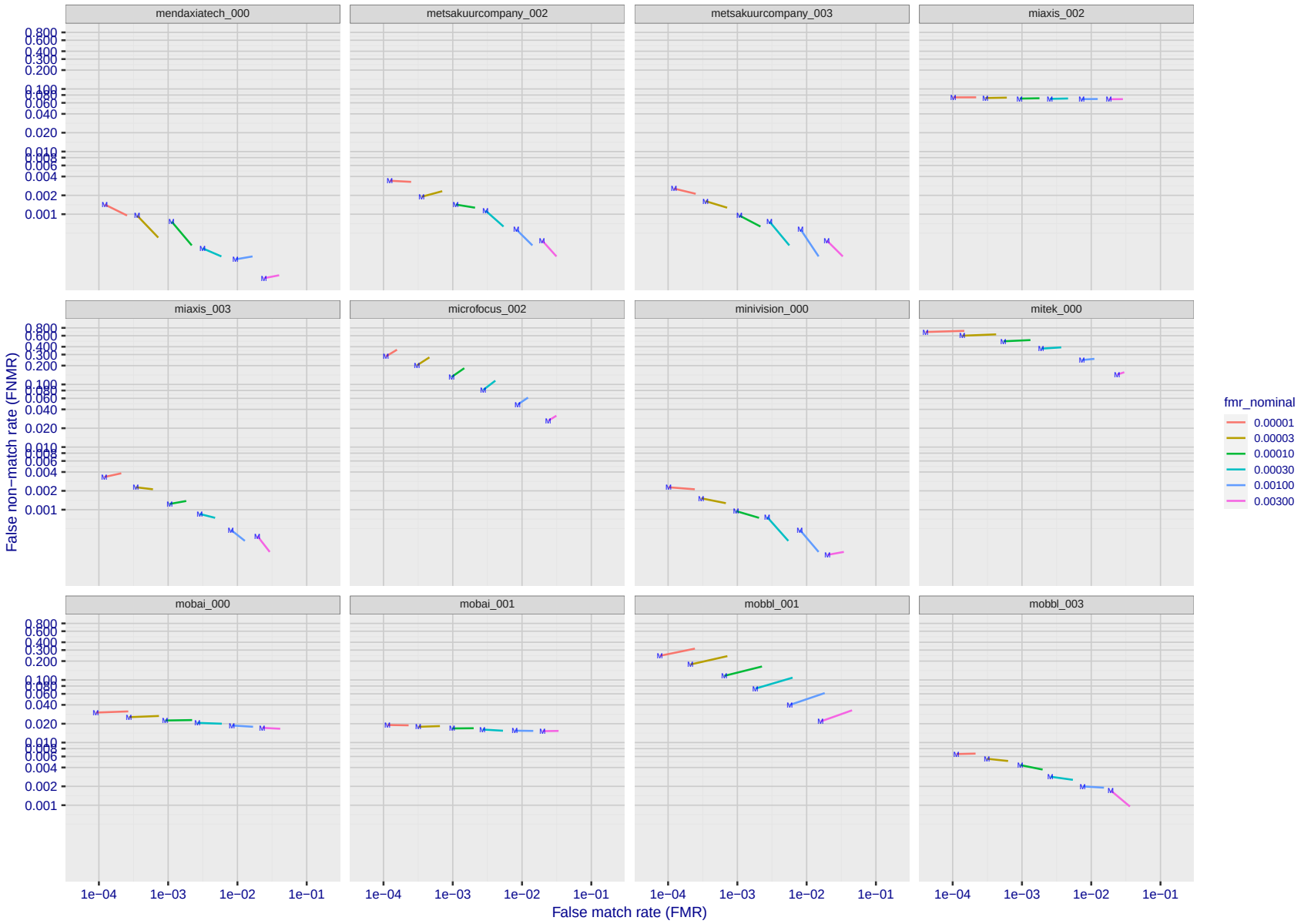

Figure 235: For the visa images, FNMR and FMR at six operating points along the DET characteristic. At each point a line is drawn between (FMR,FNMR)$_{\text{MALE}}$ and (FMR,FNMR)$_{\text{FEMALE}}$ showing how which sex has lower FMR and/or FNMR. The "M" label denotes male, the other end of the line corresponds to female. The six operating thresholds are selected to give the nominal false match rates given in the legend, and are computed over all impostor pairs regardless of age, sex, and place of birth. The plotted FMR values are broadly an order of magnitude larger than the nominal rates because FMR is computed over demographically-matched impostor pairs i.e individuals of the same sex, from the same geographic region (see section 3.6.1), and the same age group (see section 3.6.2).

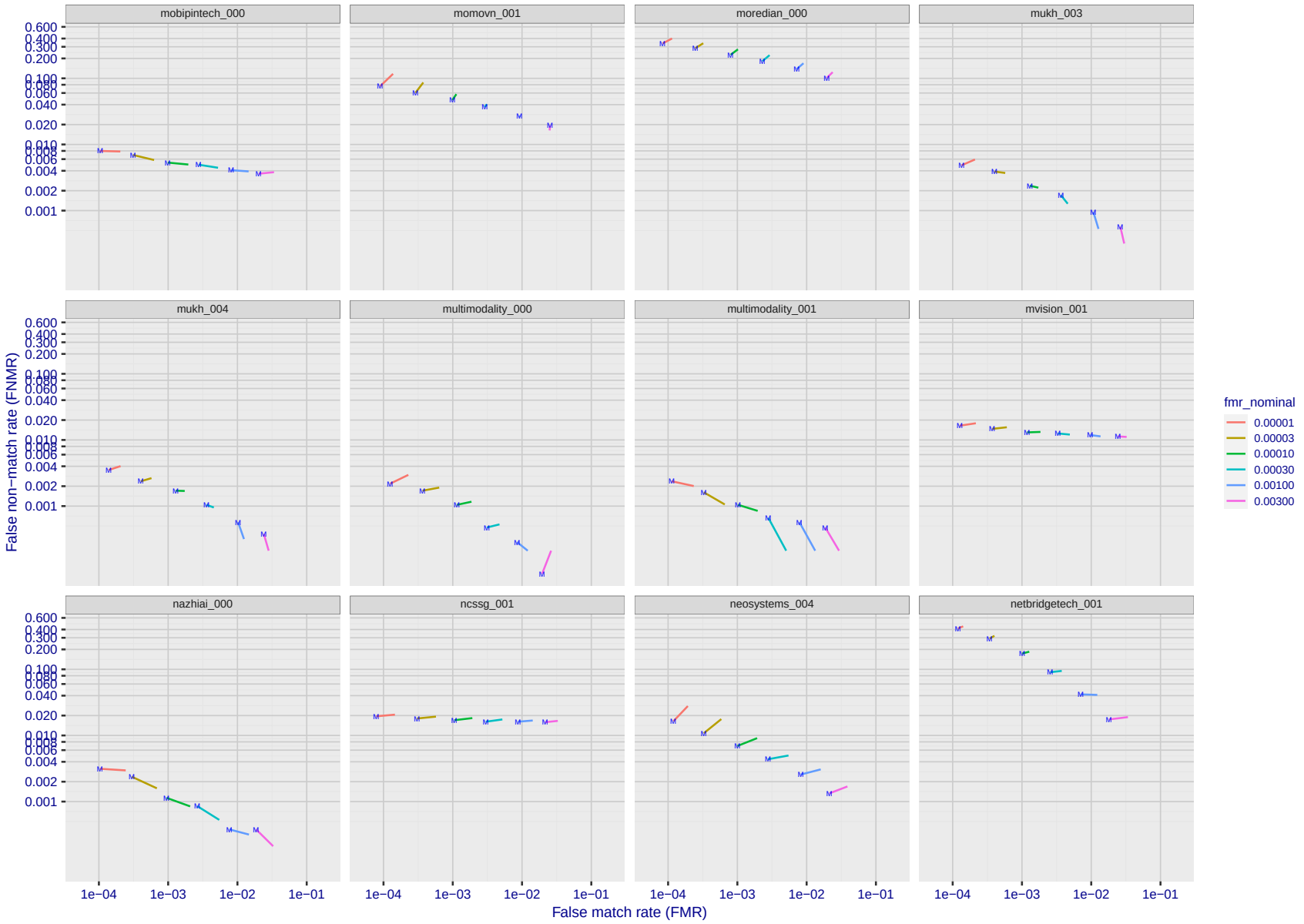

Figure 236: For the visa images, FNMR and FMR at six operating points along the DET characteristic. At each point a line is drawn between (FMR,FNMR)$_{\text{MALE}}$ and (FMR,FNMR)$_{\text{FEMALE}}$ showing how which sex has lower FMR and/or FNMR. The "M" label denotes male, the other end of the line corresponds to female. The six operating thresholds are selected to give the nominal false match rates given in the legend, and are computed over all impostor pairs regardless of age, sex, and place of birth. The plotted FMR values are broadly an order of magnitude larger than the nominal rates because FMR is computed over demographically-matched impostor pairs i.e individuals of the same sex, from the same geographic region (see section 3.6.1), and the same age group (see section 3.6.2).

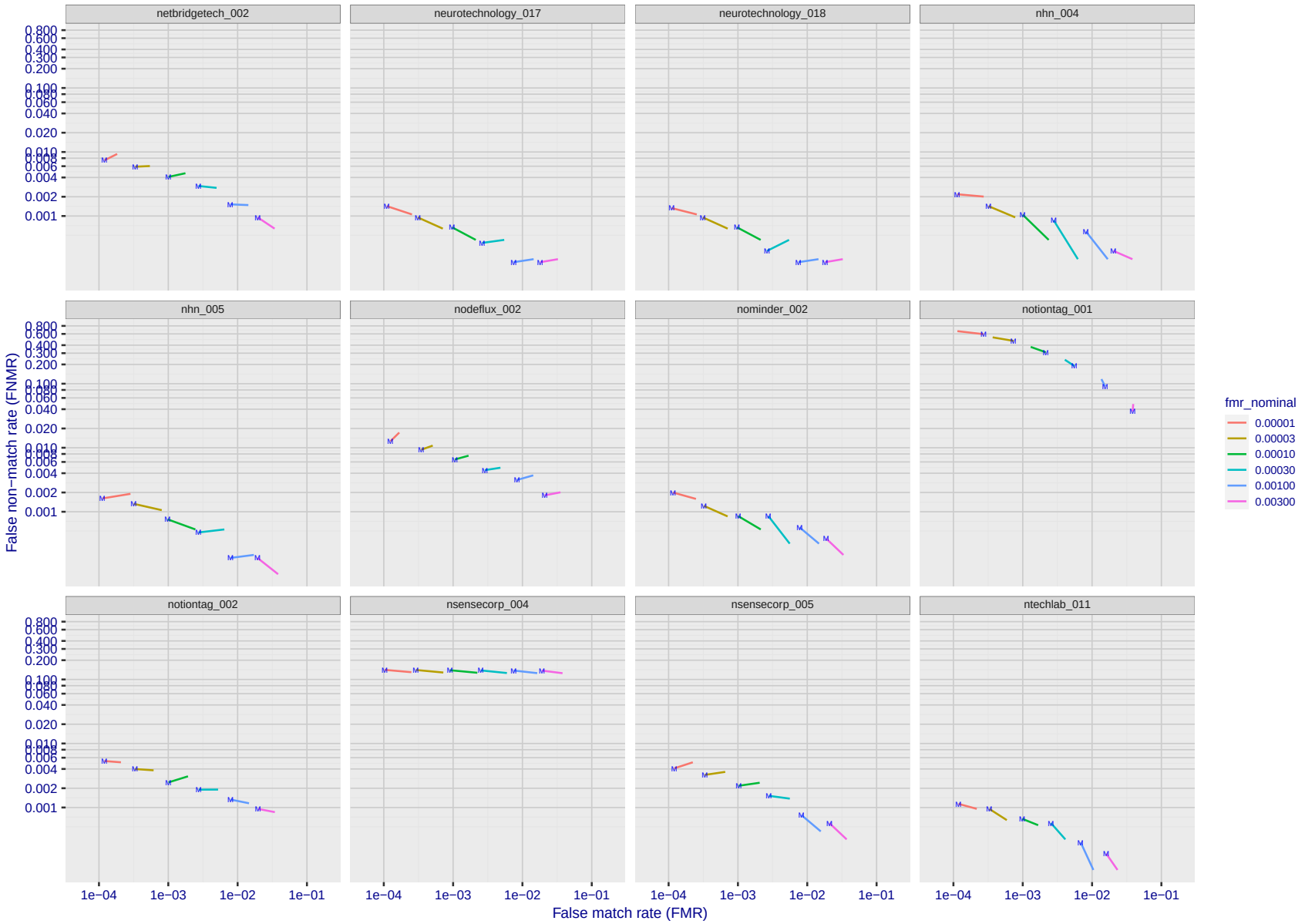

Figure 237: For the visa images, FNMR and FMR at six operating points along the DET characteristic. At each point a line is drawn between (FMR,FNMR)$_{\text{MALE}}$ and (FMR,FNMR)$_{\text{FEMALE}}$ showing how which sex has lower FMR and/or FNMR. The "M" label denotes male, the other end of the line corresponds to female. The six operating thresholds are selected to give the nominal false match rates given in the legend, and are computed over all impostor pairs regardless of age, sex, and place of birth. The plotted FMR values are broadly an order of magnitude larger than the nominal rates because FMR is computed over demographically-matched impostor pairs i.e individuals of the same sex, from the same geographic region (see section 3.6.1), and the same age group (see section 3.6.2).

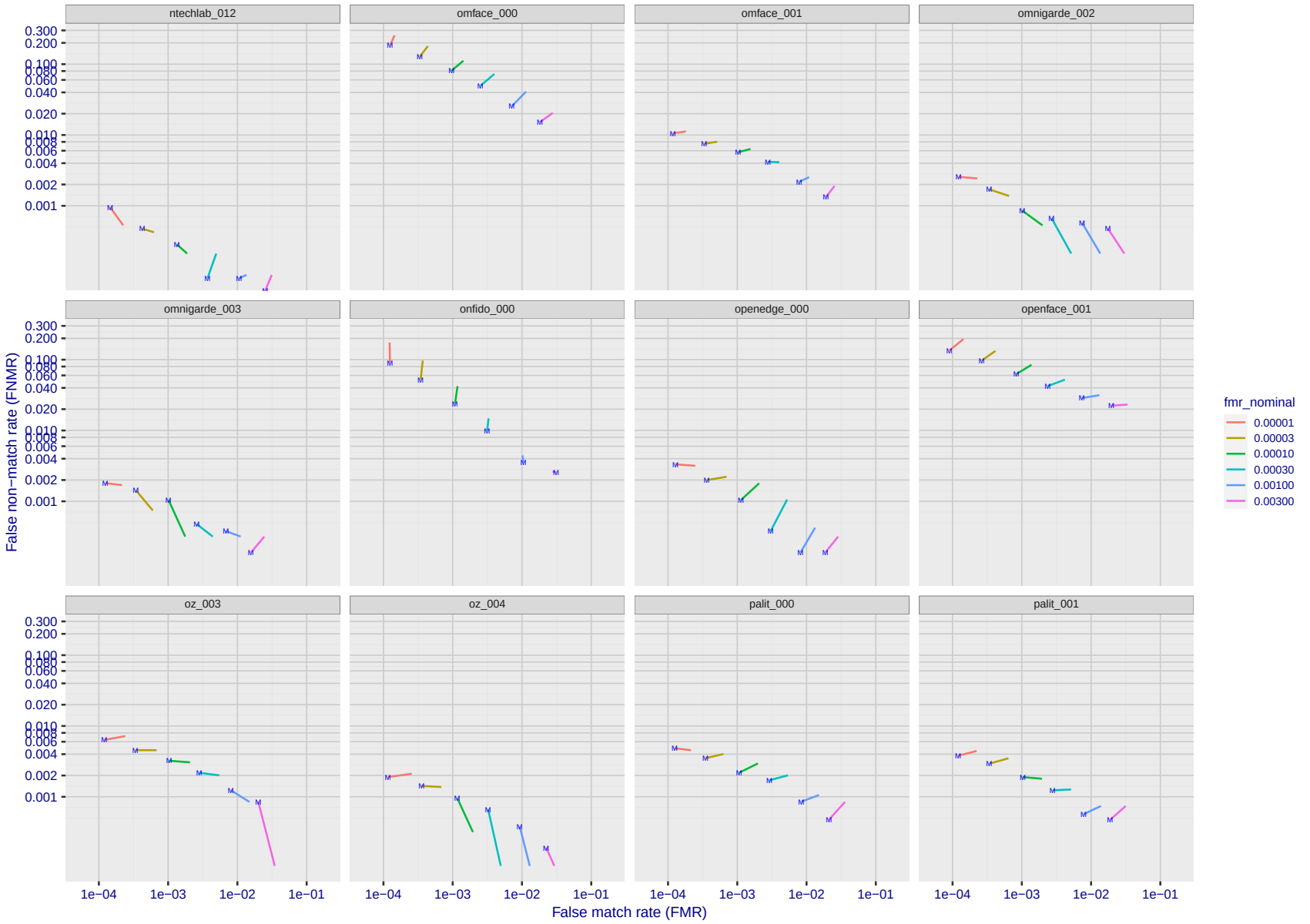

Figure 238: For the visa images, FNMR and FMR at six operating points along the DET characteristic. At each point a line is drawn between (FMR,FNMR)$_{\text{MALE}}$ and (FMR,FNMR)$_{\text{FEMALE}}$ showing how which sex has lower FMR and/or FNMR. The "M" label denotes male, the other end of the line corresponds to female. The six operating thresholds are selected to give the nominal false match rates given in the legend, and are computed over all impostor pairs regardless of age, sex, and place of birth. The plotted FMR values are broadly an order of magnitude larger than the nominal rates because FMR is computed over demographically-matched impostor pairs i.e individuals of the same sex, from the same geographic region (see section 3.6.1), and the same age group (see section 3.6.2).

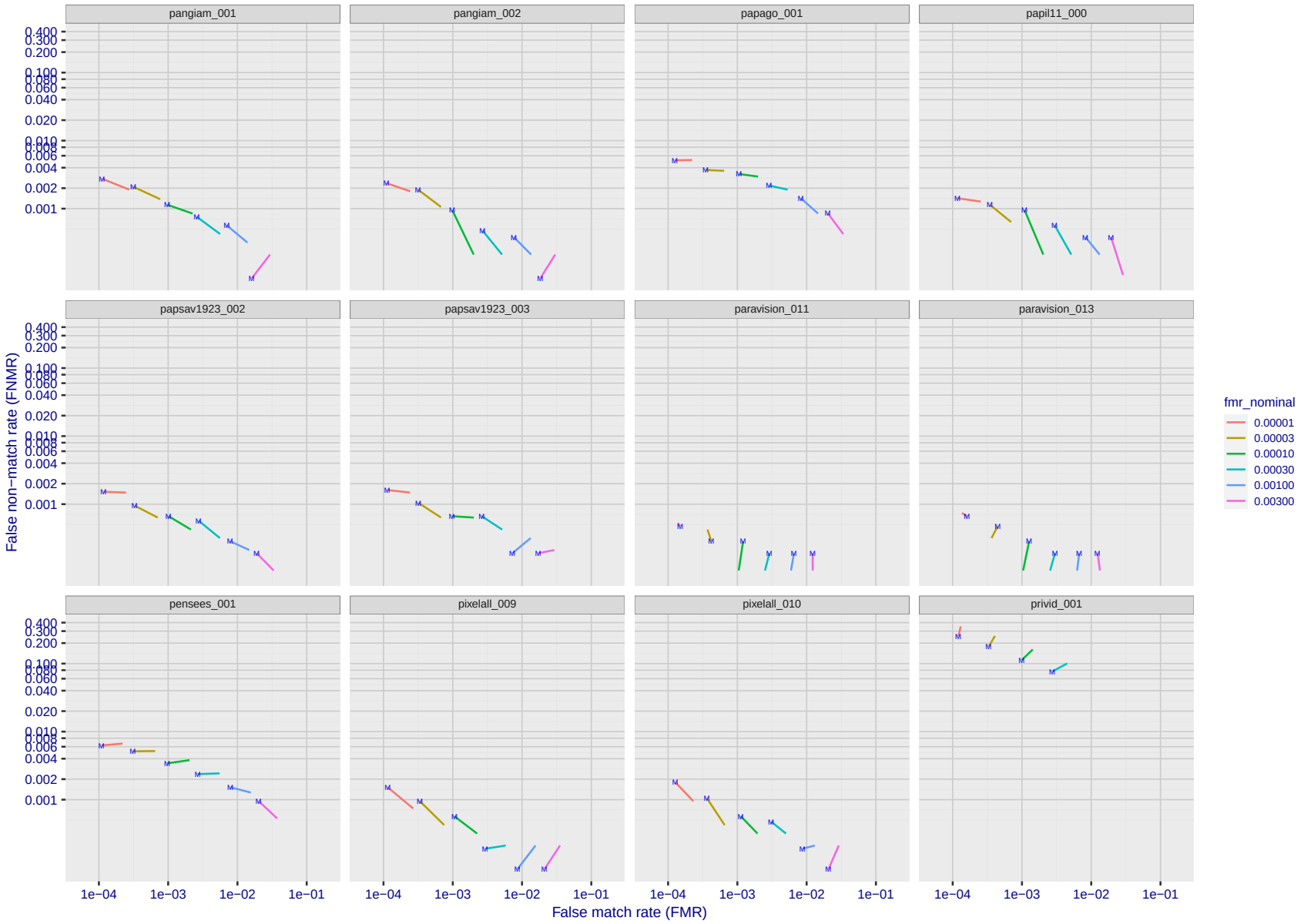

Figure 239: For the visa images, FNMR and FMR at six operating points along the DET characteristic. At each point a line is drawn between (FMR,FNMR)$_{\text{MALE}}$ and (FMR,FNMR)$_{\text{FEMALE}}$ showing how which sex has lower FMR and/or FNMR. The "M" label denotes male, the other end of the line corresponds to female. The six operating thresholds are selected to give the nominal false match rates given in the legend, and are computed over all impostor pairs regardless of age, sex, and place of birth. The plotted FMR values are broadly an order of magnitude larger than the nominal rates because FMR is computed over demographically-matched impostor pairs i.e individuals of the same sex, from the same geographic region (see section 3.6.1), and the same age group (see section 3.6.2).

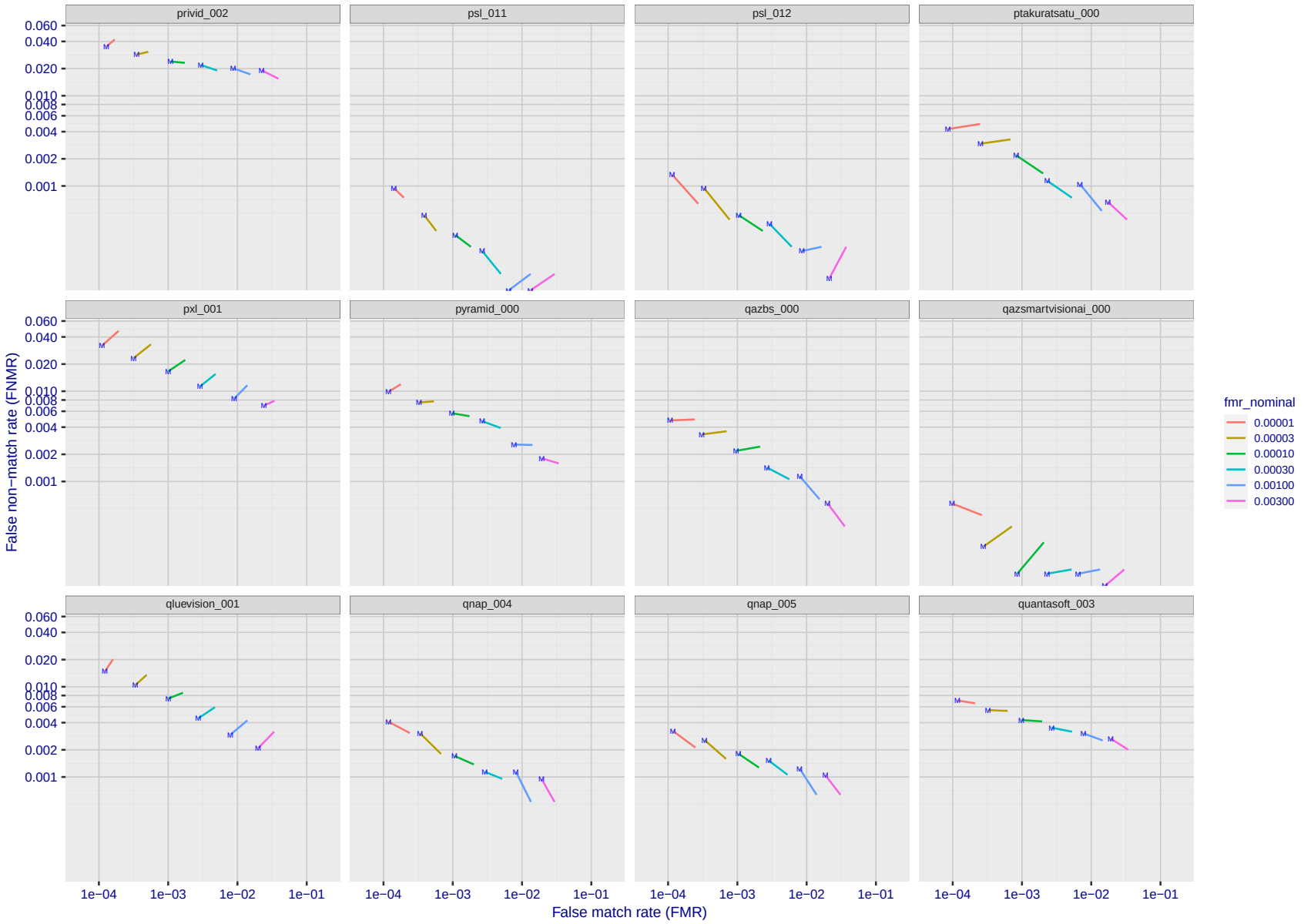

Figure 240: For the visa images, FNMR and FMR at six operating points along the DET characteristic. At each point a line is drawn between (FMR,FNMR)$_{\text{MALE}}$ and (FMR,FNMR)$_{\text{FEMALE}}$ showing how which sex has lower FMR and/or FNMR. The "M" label denotes male, the other end of the line corresponds to female. The six operating thresholds are selected to give the nominal false match rates given in the legend, and are computed over all impostor pairs regardless of age, sex, and place of birth. The plotted FMR values are broadly an order of magnitude larger than the nominal rates because FMR is computed over demographically-matched impostor pairs i.e individuals of the same sex, from the same geographic region (see section 3.6.1), and the same age group (see section 3.6.2).

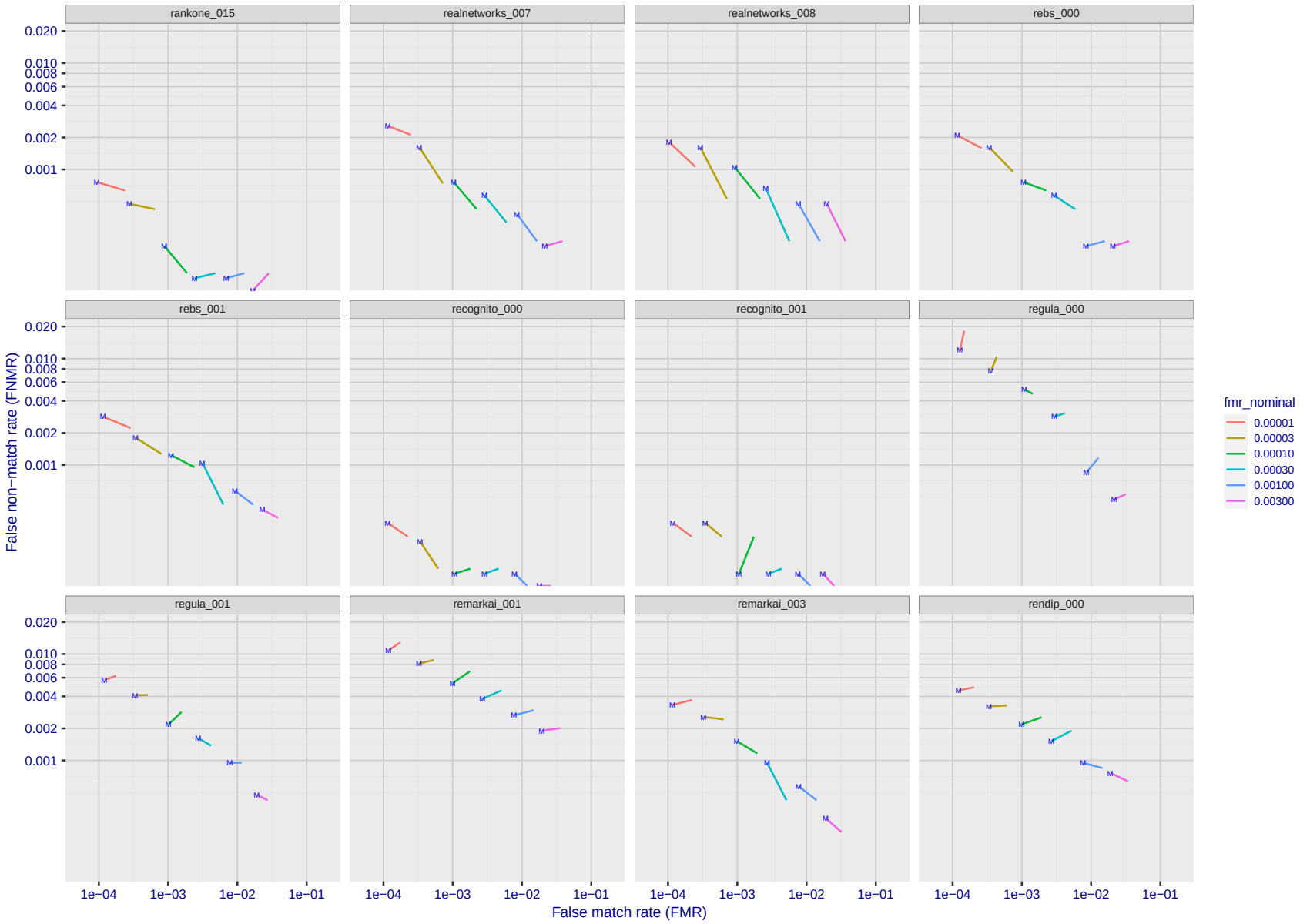

Figure 241: For the visa images, FNMR and FMR at six operating points along the DET characteristic. At each point a line is drawn between (FMR,FNMR)$_{\text{MALE}}$ and (FMR,FNMR)$_{\text{FEMALE}}$ showing how which sex has lower FMR and/or FNMR. The "M" label denotes male, the other end of the line corresponds to female. The six operating thresholds are selected to give the nominal false match rates given in the legend, and are computed over all impostor pairs regardless of age, sex, and place of birth. The plotted FMR values are broadly an order of magnitude larger than the nominal rates because FMR is computed over demographically-matched impostor pairs i.e individuals of the same sex, from the same geographic region (see section 3.6.1), and the same age group (see section 3.6.2).

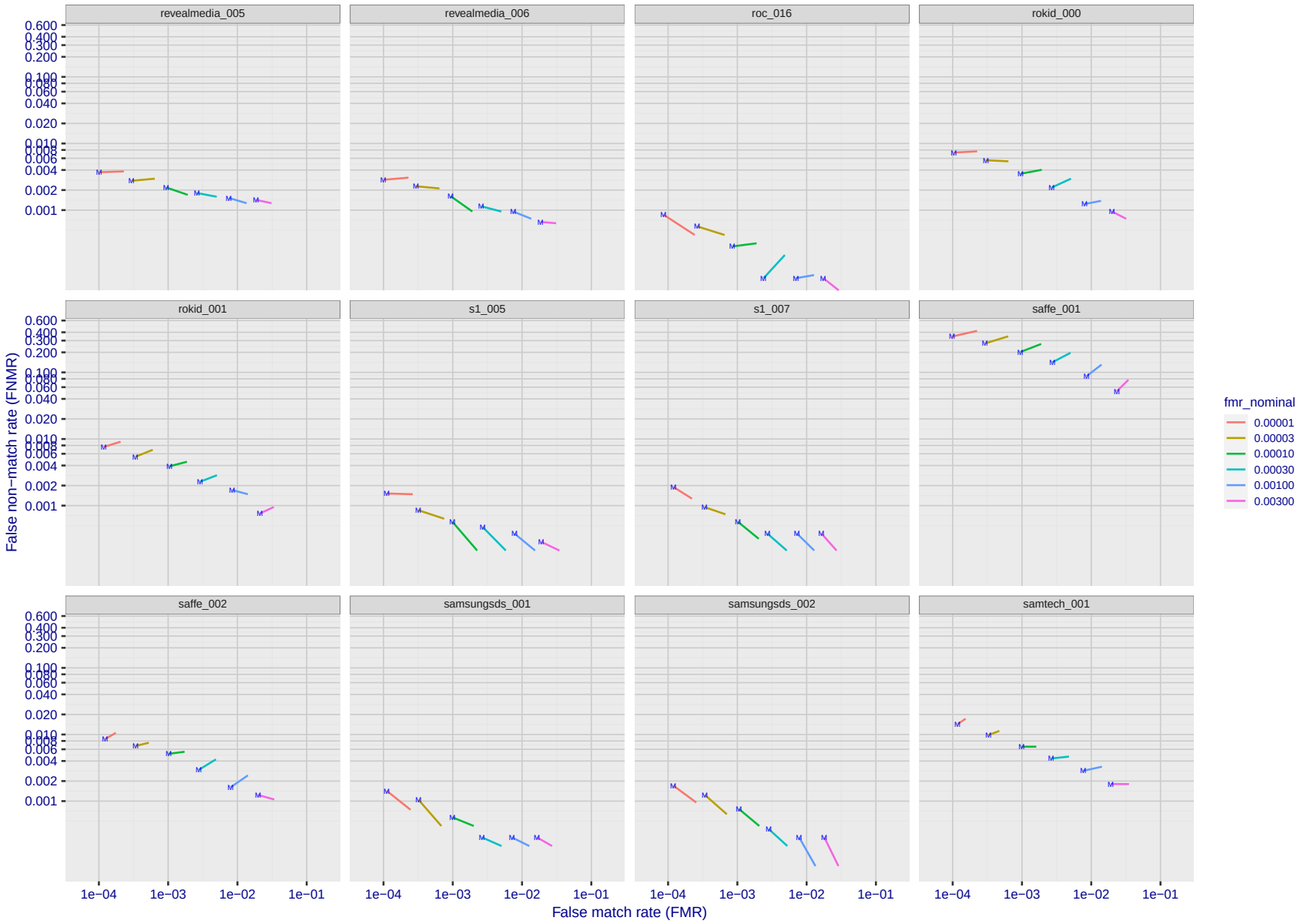

Figure 242: For the visa images, FNMR and FMR at six operating points along the DET characteristic. At each point a line is drawn between (FMR,FNMR)$_{\text{MALE}}$ and (FMR,FNMR)$_{\text{FEMALE}}$ showing how which sex has lower FMR and/or FNMR. The "M" label denotes male, the other end of the line corresponds to female. The six operating thresholds are selected to give the nominal false match rates given in the legend, and are computed over all impostor pairs regardless of age, sex, and place of birth. The plotted FMR values are broadly an order of magnitude larger than the nominal rates because FMR is computed over demographically-matched impostor pairs i.e individuals of the same sex, from the same geographic region (see section 3.6.1), and the same age group (see section 3.6.2).

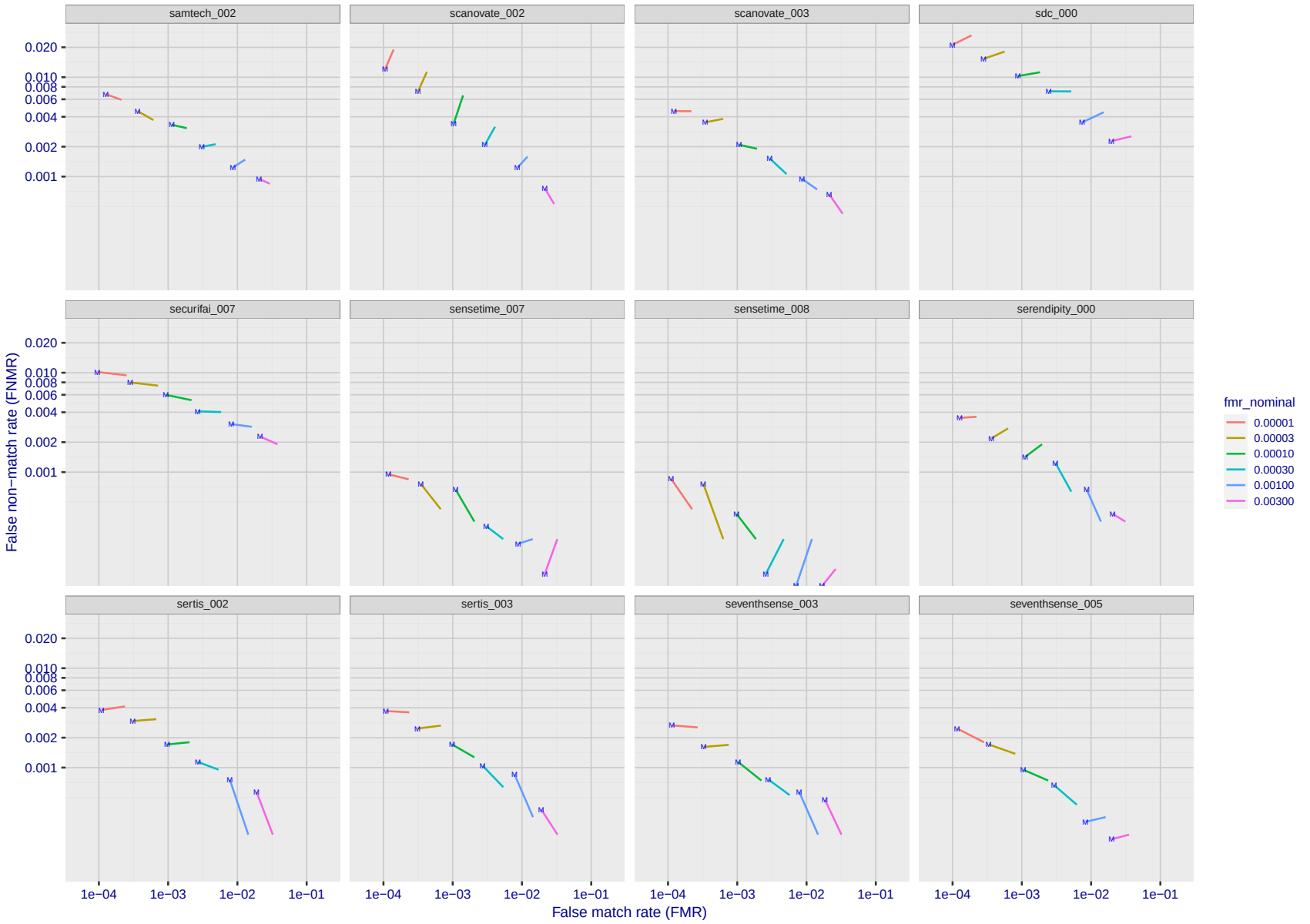

Figure 243: For the visa images, FNMR and FMR at six operating points along the DET characteristic. At each point a line is drawn between (FMR,FNMR)$_{\text{MALE}}$ and (FMR,FNMR)$_{\text{FEMALE}}$ showing how which sex has lower FMR and/or FNMR. The "M" label denotes male, the other end of the line corresponds to female. The six operating thresholds are selected to give the nominal false match rates given in the legend, and are computed over all impostor pairs regardless of age, sex, and place of birth. The plotted FMR values are broadly an order of magnitude larger than the nominal rates because FMR is computed over demographically-matched impostor pairs i.e individuals of the same sex, from the same geographic region (see section 3.6.1), and the same age group (see section 3.6.2).

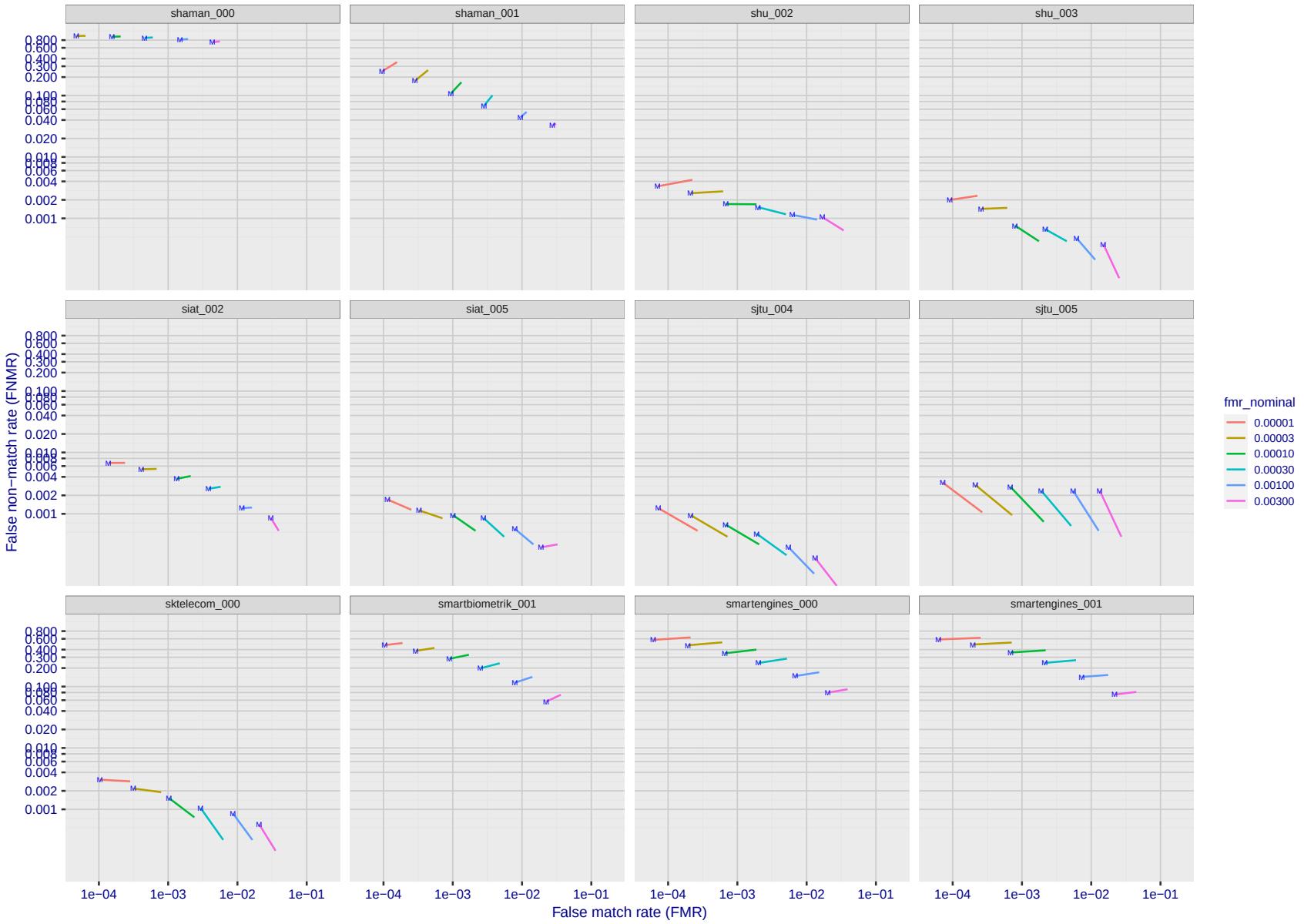

Figure 244: For the visa images, FNMR and FMR at six operating points along the DET characteristic. At each point a line is drawn between (FMR,FNMR)$_{\text{MALE}}$ and (FMR,FNMR)$_{\text{FEMALE}}$ showing how which sex has lower FMR and/or FNMR. The "M" label denotes male, the other end of the line corresponds to female. The six operating thresholds are selected to give the nominal false match rates given in the legend, and are computed over all impostor pairs regardless of age, sex, and place of birth. The plotted FMR values are broadly an order of magnitude larger than the nominal rates because FMR is computed over demographically-matched impostor pairs i.e individuals of the same sex, from the same geographic region (see section 3.6.1), and the same age group (see section 3.6.2).

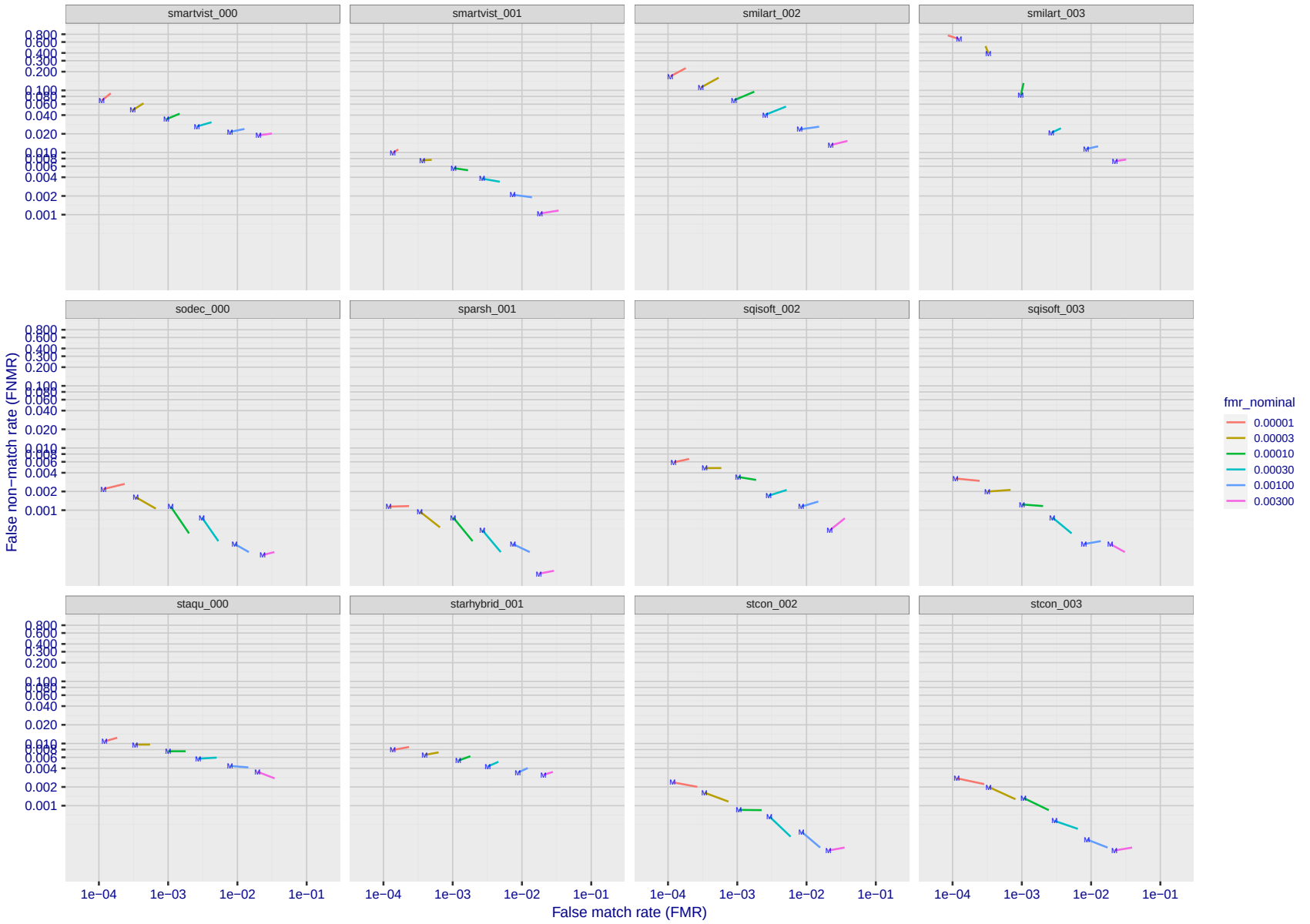

Figure 245: For the visa images, FNMR and FMR at six operating points along the DET characteristic. At each point a line is drawn between (FMR,FNMR)$_{\text{MALE}}$ and (FMR,FNMR)$_{\text{FEMALE}}$ showing how which sex has lower FMR and/or FNMR. The "M" label denotes male, the other end of the line corresponds to female. The six operating thresholds are selected to give the nominal false match rates given in the legend, and are computed over all impostor pairs regardless of age, sex, and place of birth. The plotted FMR values are broadly an order of magnitude larger than the nominal rates because FMR is computed over demographically-matched impostor pairs i.e individuals of the same sex, from the same geographic region (see section 3.6.1), and the same age group (see section 3.6.2).

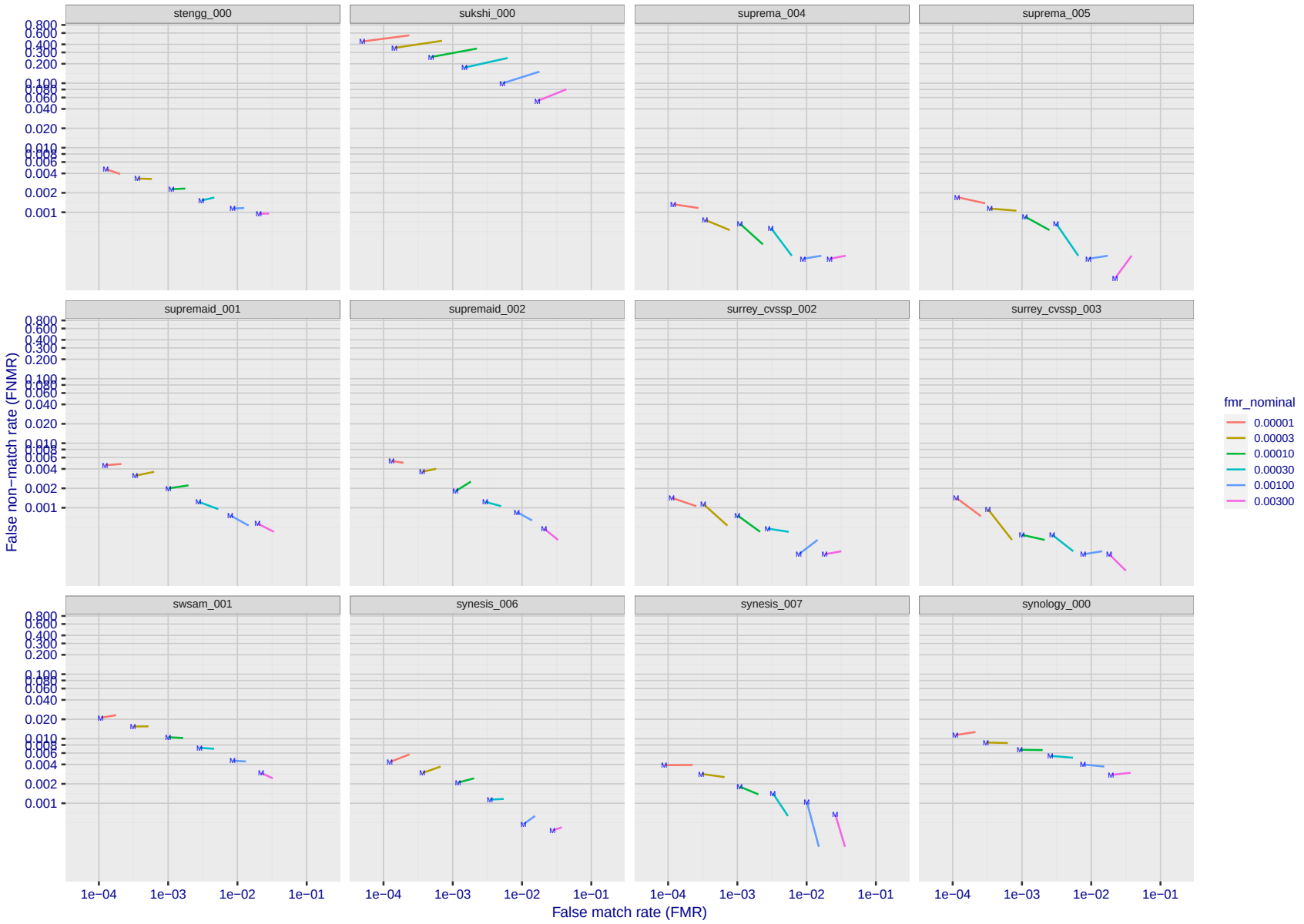

Figure 246: For the visa images, FNMR and FMR at six operating points along the DET characteristic. At each point a line is drawn between (FMR,FNMR)$_{\text{MALE}}$ and (FMR,FNMR)$_{\text{FEMALE}}$ showing how which sex has lower FMR and/or FNMR. The "M" label denotes male, the other end of the line corresponds to female. The six operating thresholds are selected to give the nominal false match rates given in the legend, and are computed over all impostor pairs regardless of age, sex, and place of birth. The plotted FMR values are broadly an order of magnitude larger than the nominal rates because FMR is computed over demographically-matched impostor pairs i.e individuals of the same sex, from the same geographic region (see section 3.6.1), and the same age group (see section 3.6.2).

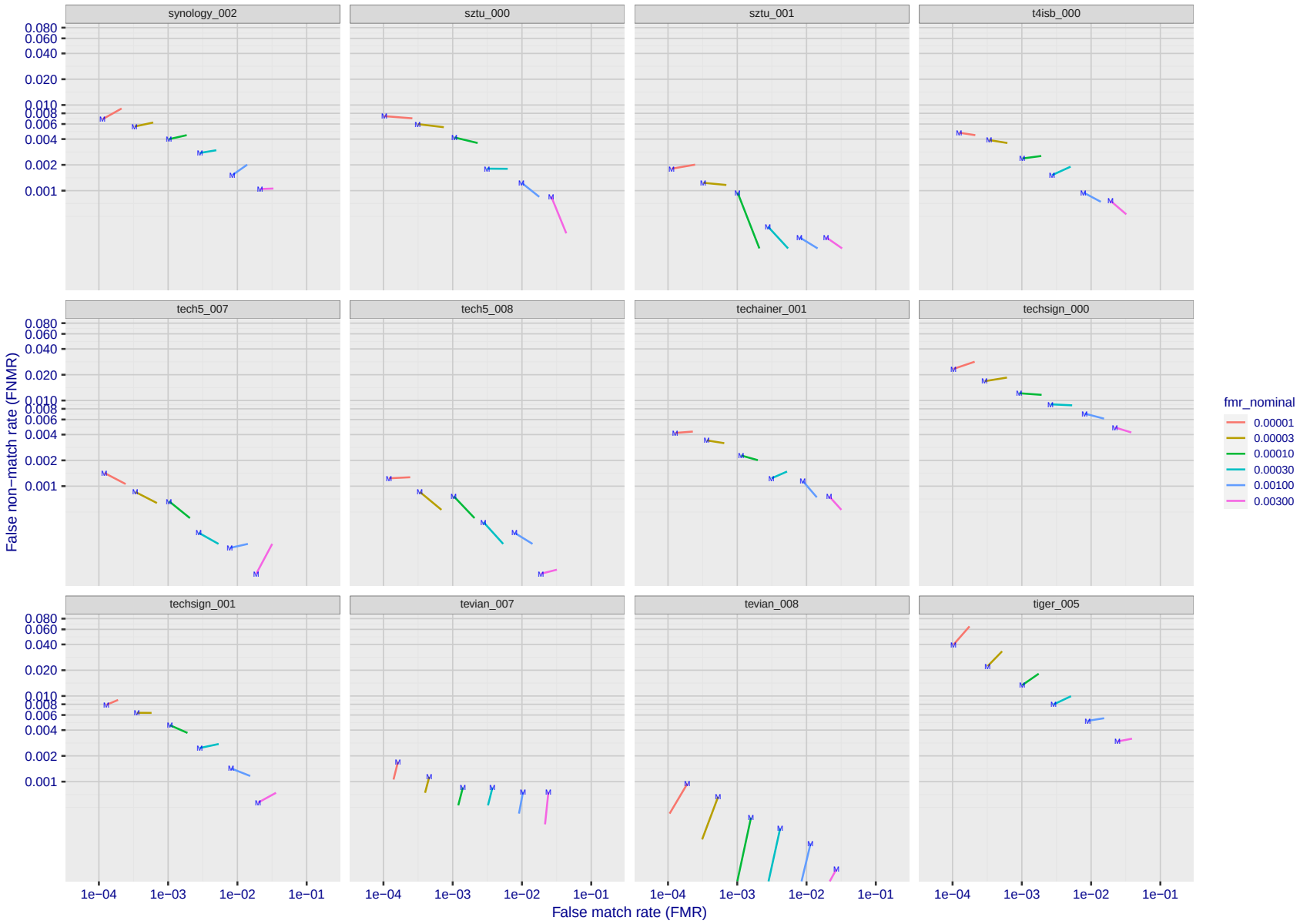

Figure 247: For the visa images, FNMR and FMR at six operating points along the DET characteristic. At each point a line is drawn between (FMR,FNMR)$_{\text{MALE}}$ and (FMR,FNMR)$_{\text{FEMALE}}$ showing how which sex has lower FMR and/or FNMR. The "M" label denotes male, the other end of the line corresponds to female. The six operating thresholds are selected to give the nominal false match rates given in the legend, and are computed over all impostor pairs regardless of age, sex, and place of birth. The plotted FMR values are broadly an order of magnitude larger than the nominal rates because FMR is computed over demographically-matched impostor pairs i.e individuals of the same sex, from the same geographic region (see section 3.6.1), and the same age group (see section 3.6.2).

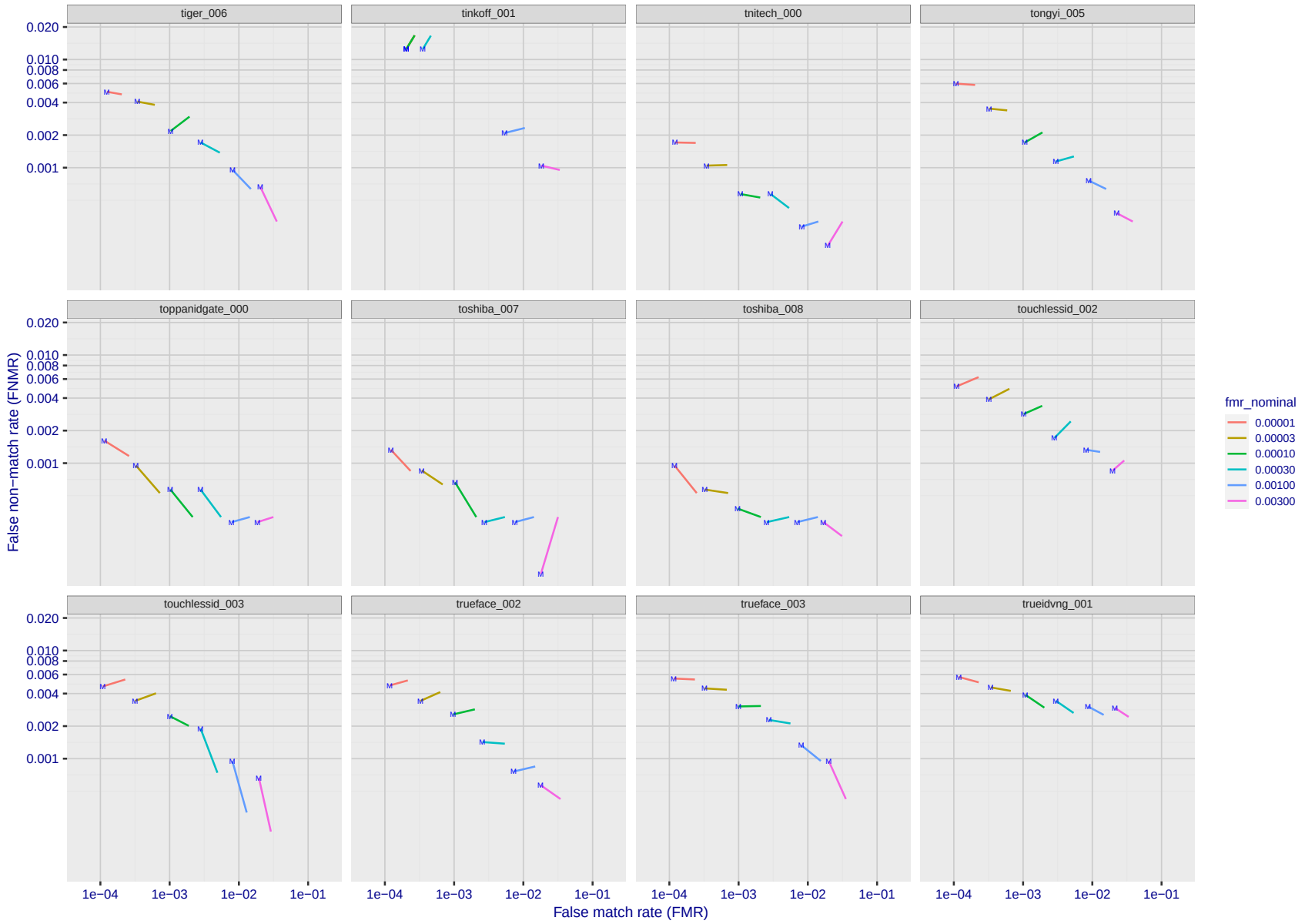

Figure 248: For the visa images, FNMR and FMR at six operating points along the DET characteristic. At each point a line is drawn between (FMR,FNMR)$_{\text{MALE}}$ and (FMR,FNMR)$_{\text{FEMALE}}$ showing how which sex has lower FMR and/or FNMR. The "M" label denotes male, the other end of the line corresponds to female. The six operating thresholds are selected to give the nominal false match rates given in the legend, and are computed over all impostor pairs regardless of age, sex, and place of birth. The plotted FMR values are broadly an order of magnitude larger than the nominal rates because FMR is computed over demographically-matched impostor pairs i.e individuals of the same sex, from the same geographic region (see section 3.6.1), and the same age group (see section 3.6.2).

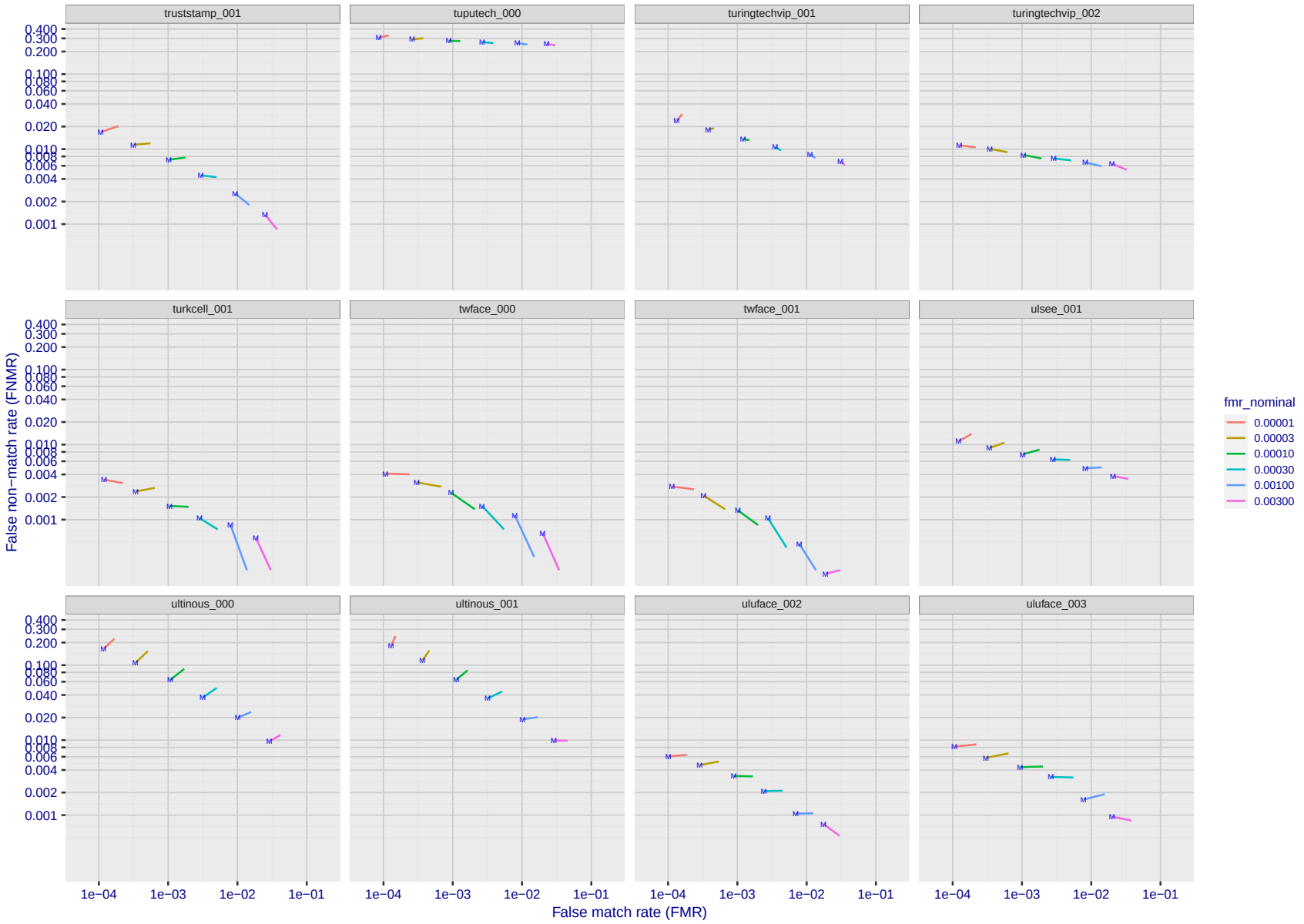

Figure 249: For the visa images, FNMR and FMR at six operating points along the DET characteristic. At each point a line is drawn between (FMR,FNMR)$_{\text{MALE}}$ and (FMR,FNMR)$_{\text{FEMALE}}$ showing how which sex has lower FMR and/or FNMR. The "M" label denotes male, the other end of the line corresponds to female. The six operating thresholds are selected to give the nominal false match rates given in the legend, and are computed over all impostor pairs regardless of age, sex, and place of birth. The plotted FMR values are broadly an order of magnitude larger than the nominal rates because FMR is computed over demographically-matched impostor pairs i.e individuals of the same sex, from the same geographic region (see section 3.6.1), and the same age group (see section 3.6.2).

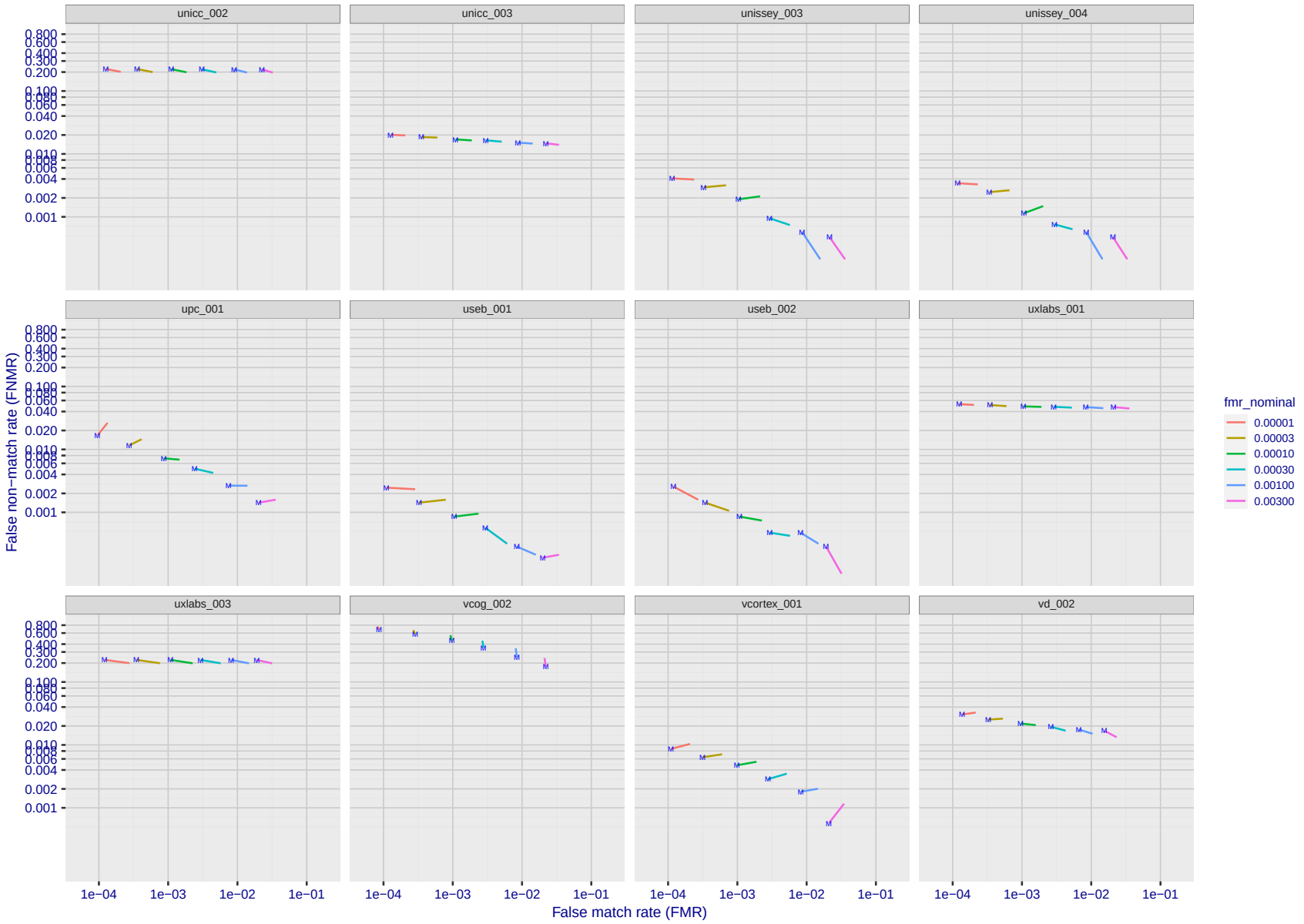

Figure 250: For the visa images, FNMR and FMR at six operating points along the DET characteristic. At each point a line is drawn between (FMR,FNMR)$_{\text{MALE}}$ and (FMR,FNMR)$_{\text{FEMALE}}$ showing how which sex has lower FMR and/or FNMR. The "M" label denotes male, the other end of the line corresponds to female. The six operating thresholds are selected to give the nominal false match rates given in the legend, and are computed over all impostor pairs regardless of age, sex, and place of birth. The plotted FMR values are broadly an order of magnitude larger than the nominal rates because FMR is computed over demographically-matched impostor pairs i.e individuals of the same sex, from the same geographic region (see section 3.6.1), and the same age group (see section 3.6.2).

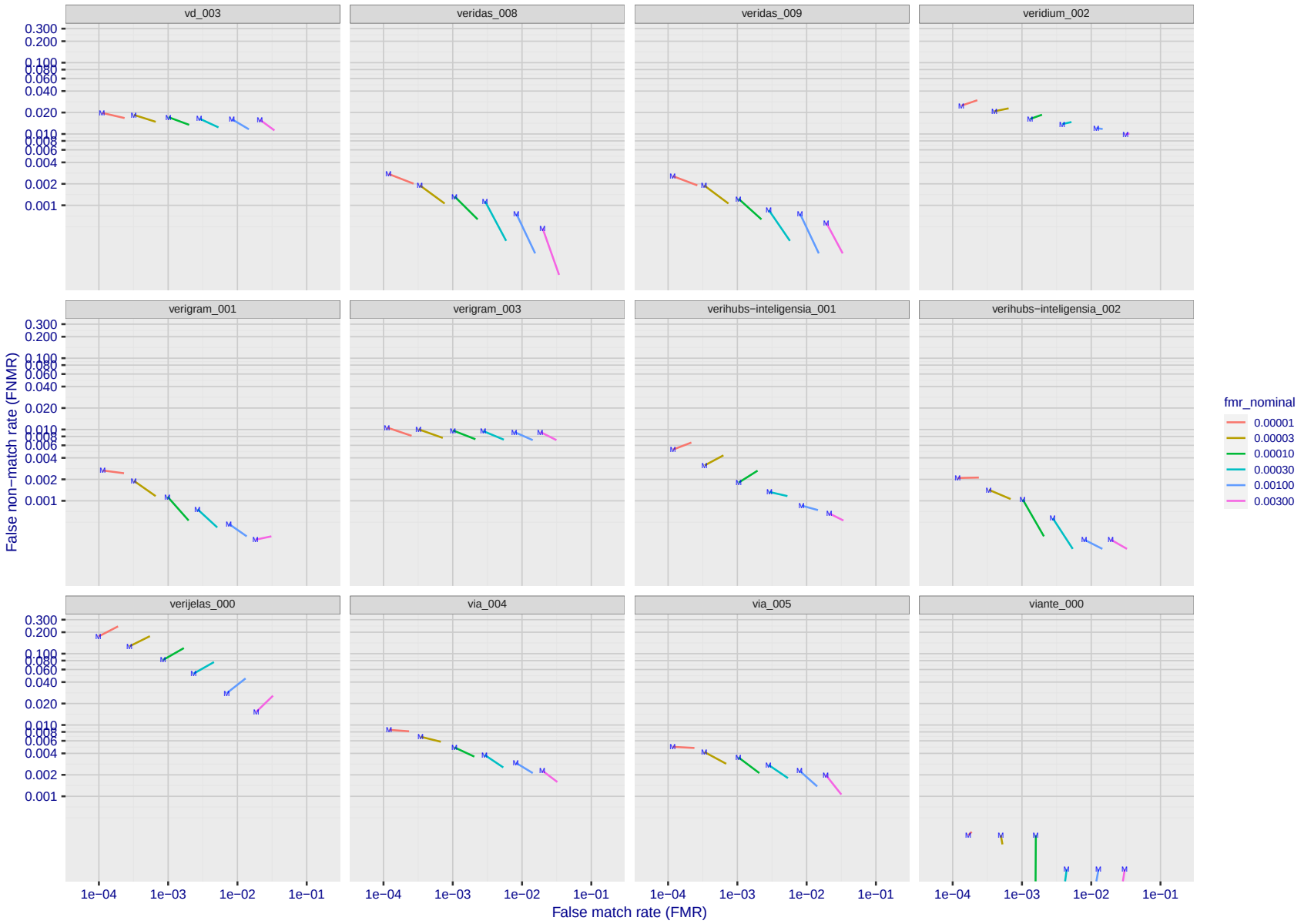

Figure 251: For the visa images, FNMR and FMR at six operating points along the DET characteristic. At each point a line is drawn between (FMR,FNMR)$_{\text{MALE}}$ and (FMR,FNMR)$_{\text{FEMALE}}$ showing how which sex has lower FMR and/or FNMR. The "M" label denotes male, the other end of the line corresponds to female. The six operating thresholds are selected to give the nominal false match rates given in the legend, and are computed over all impostor pairs regardless of age, sex, and place of birth. The plotted FMR values are broadly an order of magnitude larger than the nominal rates because FMR is computed over demographically-matched impostor pairs i.e individuals of the same sex, from the same geographic region (see section 3.6.1), and the same age group (see section 3.6.2).

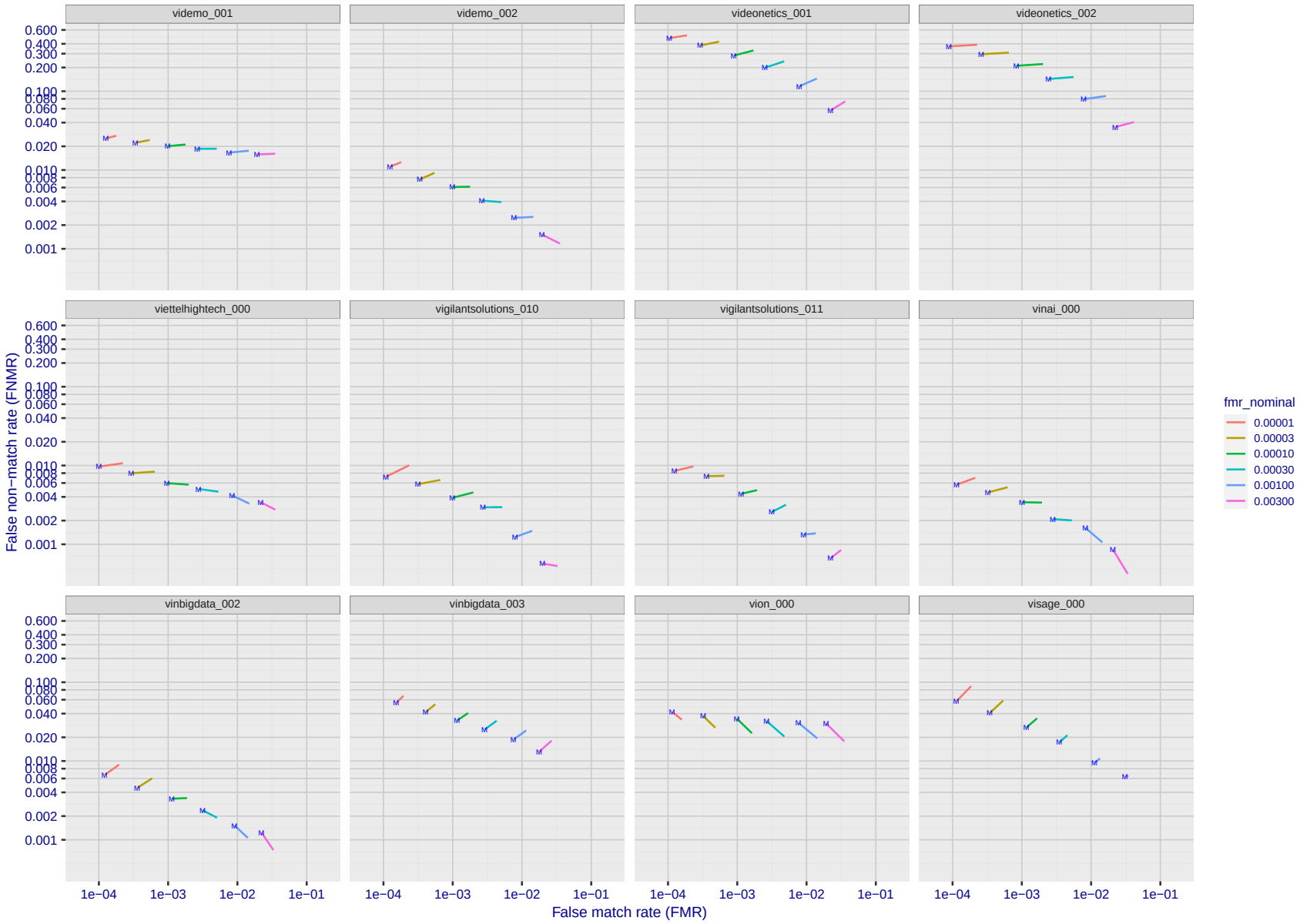

Figure 252: For the visa images, FNMR and FMR at six operating points along the DET characteristic. At each point a line is drawn between (FMR,FNMR)$_{\text{MALE}}$ and (FMR,FNMR)$_{\text{FEMALE}}$ showing how which sex has lower FMR and/or FNMR. The "M" label denotes male, the other end of the line corresponds to female. The six operating thresholds are selected to give the nominal false match rates given in the legend, and are computed over all impostor pairs regardless of age, sex, and place of birth. The plotted FMR values are broadly an order of magnitude larger than the nominal rates because FMR is computed over demographically-matched impostor pairs i.e individuals of the same sex, from the same geographic region (see section 3.6.1), and the same age group (see section 3.6.2).

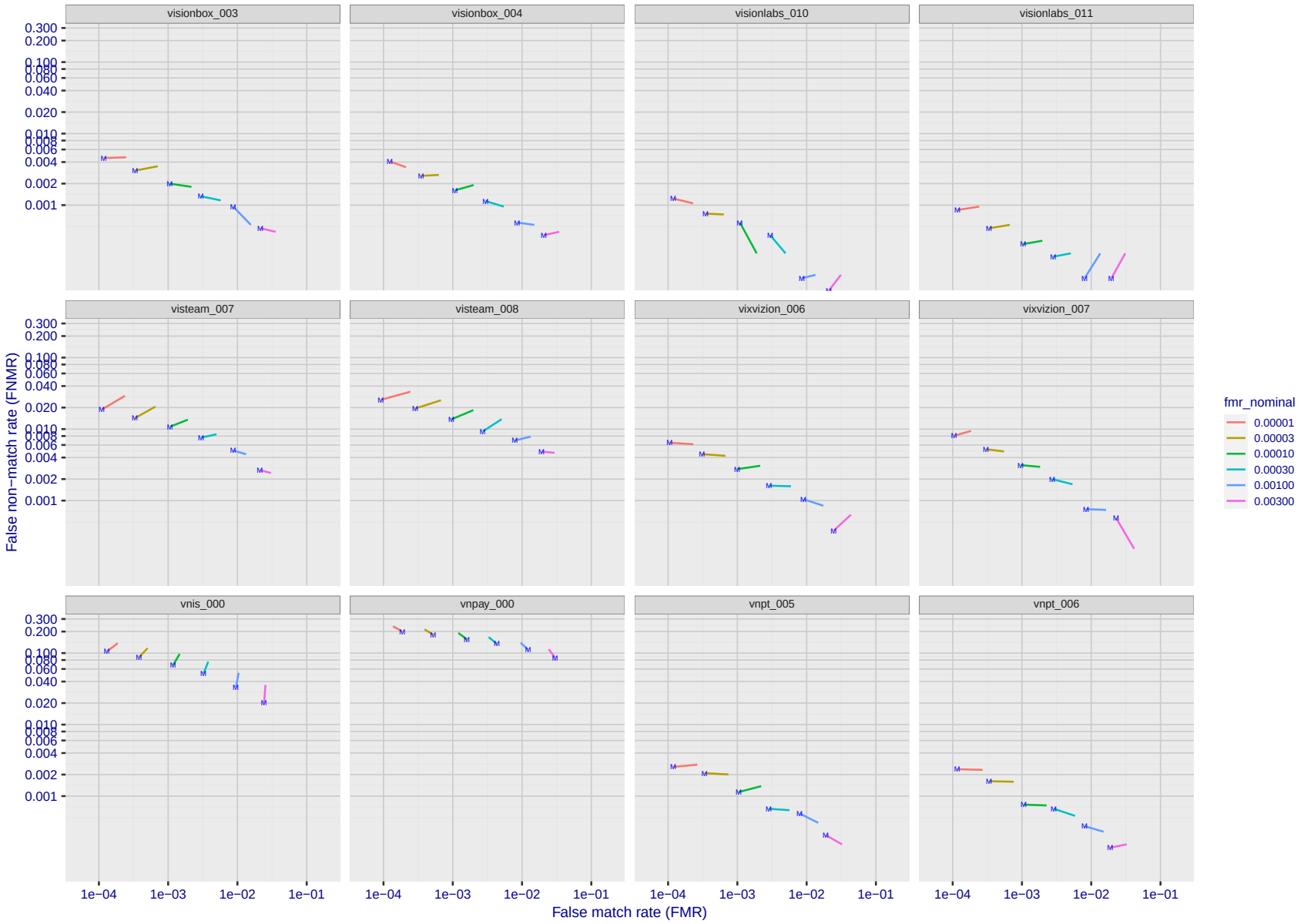

Figure 253: For the visa images, FNMR and FMR at six operating points along the DET characteristic. At each point a line is drawn between (FMR,FNMR)$_{\text{MALE}}$ and (FMR,FNMR)$_{\text{FEMALE}}$ showing how which sex has lower FMR and/or FNMR. The "M" label denotes male, the other end of the line corresponds to female. The six operating thresholds are selected to give the nominal false match rates given in the legend, and are computed over all impostor pairs regardless of age, sex, and place of birth. The plotted FMR values are broadly an order of magnitude larger than the nominal rates because FMR is computed over demographically-matched impostor pairs i.e individuals of the same sex, from the same geographic region (see section 3.6.1), and the same age group (see section 3.6.2).

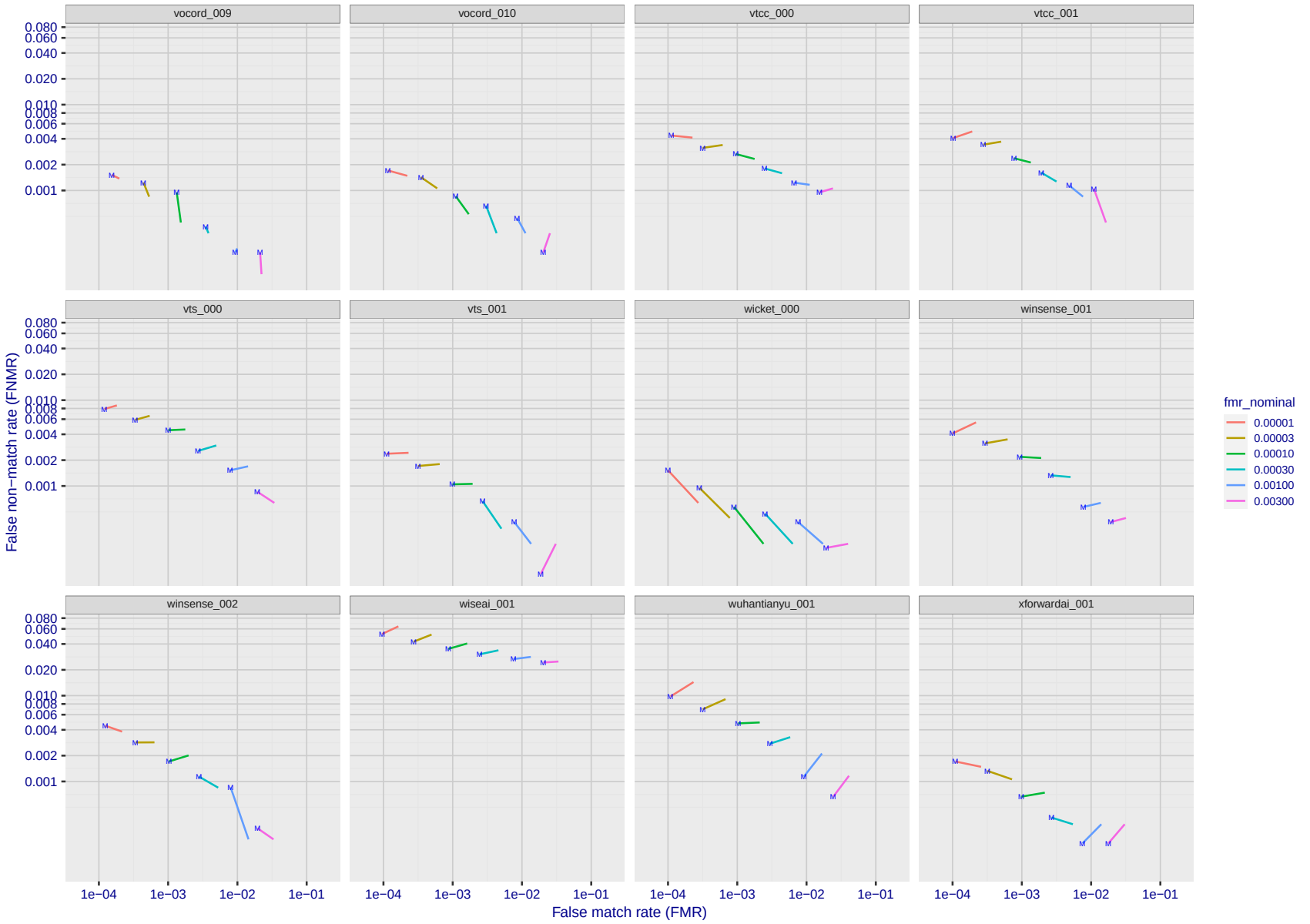

Figure 254: For the visa images, FNMR and FMR at six operating points along the DET characteristic. At each point a line is drawn between (FMR,FNMR)$_{\text{MALE}}$ and (FMR,FNMR)$_{\text{FEMALE}}$ showing how which sex has lower FMR and/or FNMR. The "M" label denotes male, the other end of the line corresponds to female. The six operating thresholds are selected to give the nominal false match rates given in the legend, and are computed over all impostor pairs regardless of age, sex, and place of birth. The plotted FMR values are broadly an order of magnitude larger than the nominal rates because FMR is computed over demographically-matched impostor pairs i.e individuals of the same sex, from the same geographic region (see section 3.6.1), and the same age group (see section 3.6.2).

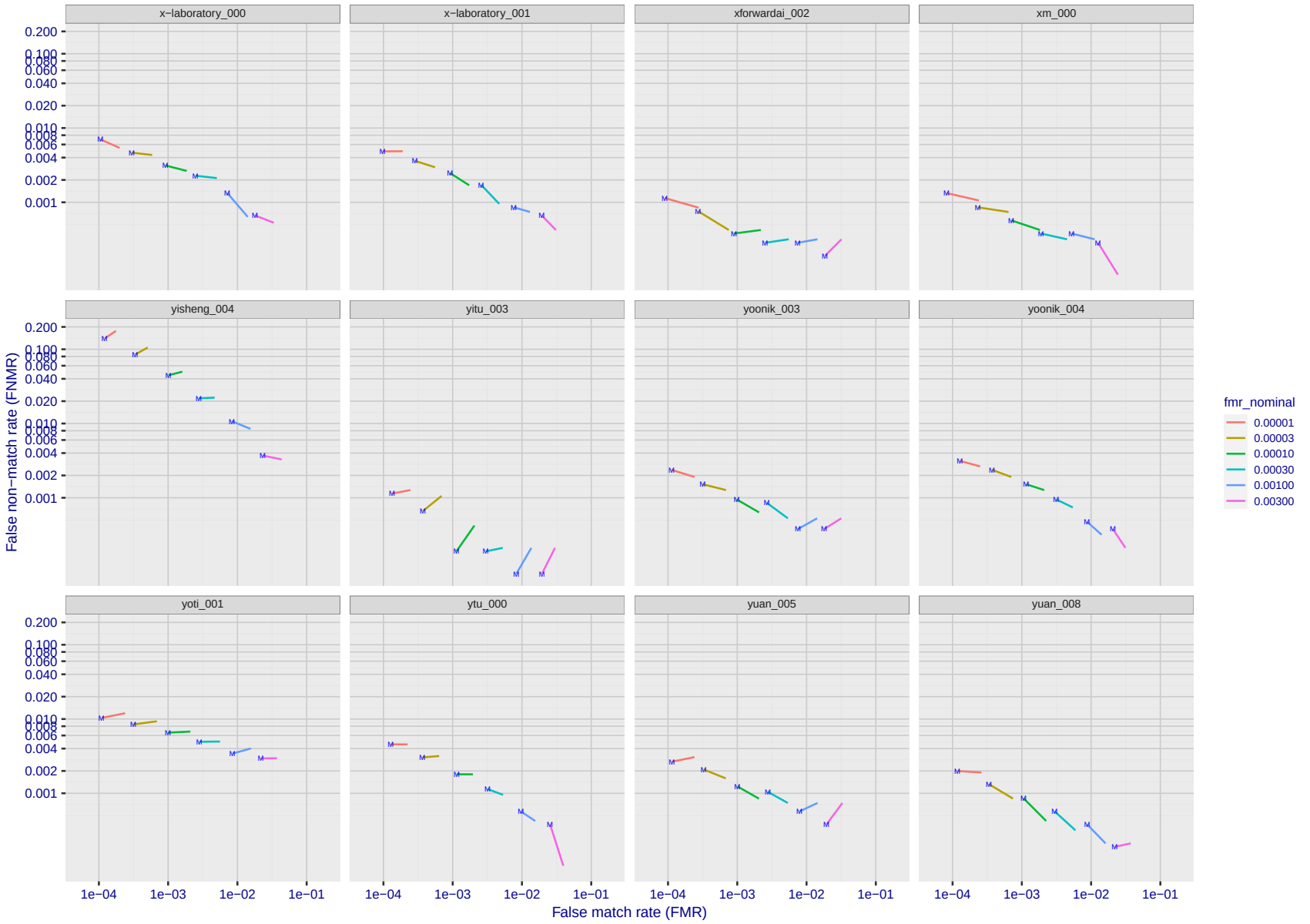

Figure 255: For the visa images, FNMR and FMR at six operating points along the DET characteristic. At each point a line is drawn between (FMR,FNMR)$_{\text{MALE}}$ and (FMR,FNMR)$_{\text{FEMALE}}$ showing how which sex has lower FMR and/or FNMR. The "M" label denotes male, the other end of the line corresponds to female. The six operating thresholds are selected to give the nominal false match rates given in the legend, and are computed over all impostor pairs regardless of age, sex, and place of birth. The plotted FMR values are broadly an order of magnitude larger than the nominal rates because FMR is computed over demographically-matched impostor pairs i.e individuals of the same sex, from the same geographic region (see section 3.6.1), and the same age group (see section 3.6.2).

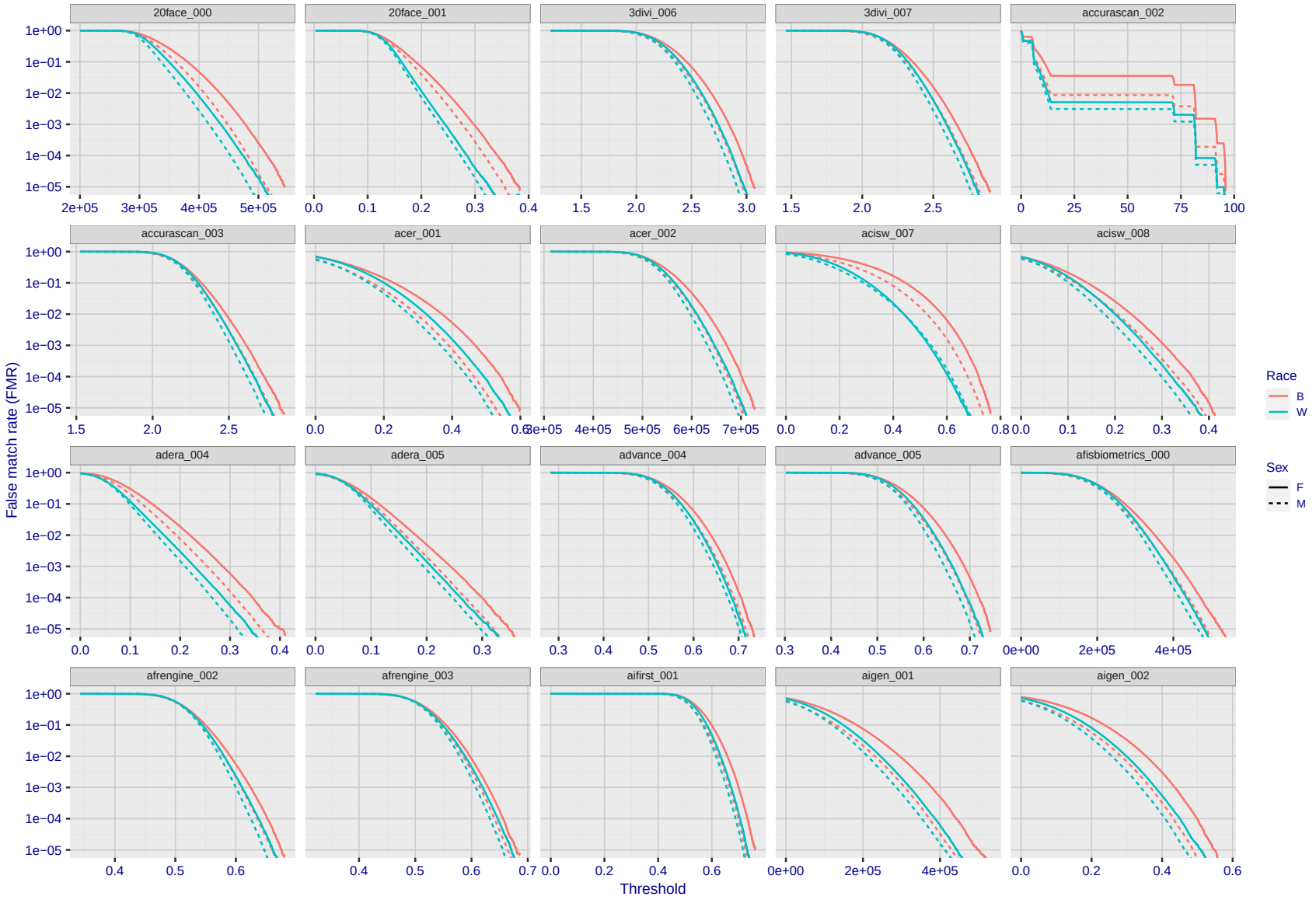

Figure 256: For the mugshot images, the false match calibration curves show false match rate vs. threshold. Separate curves appear for white females, black females, black males and white males.

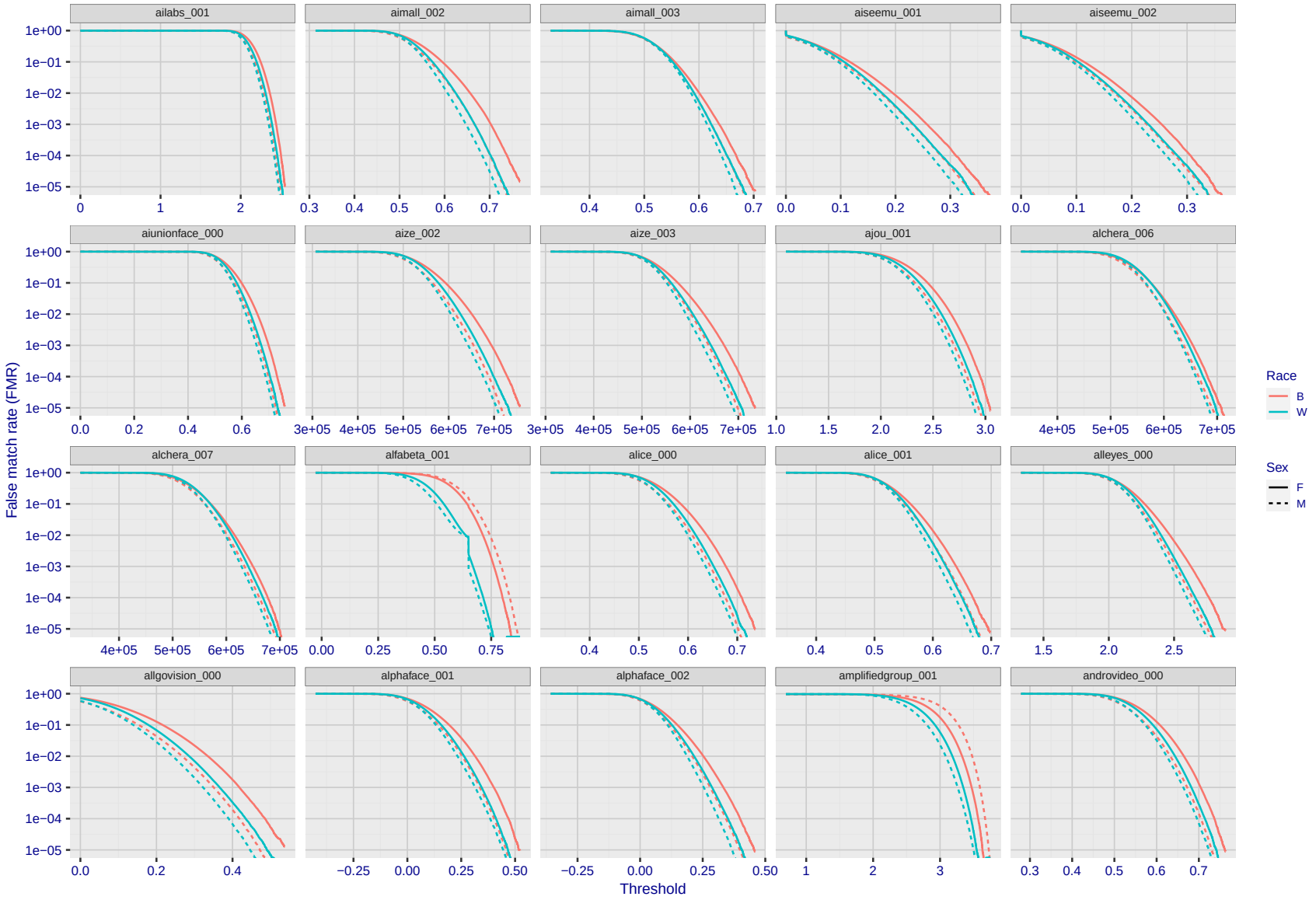

Figure 257: For the mugshot images, the false match calibration curves show false match rate vs. threshold. Separate curves appear for white females, black females, black males and white males.

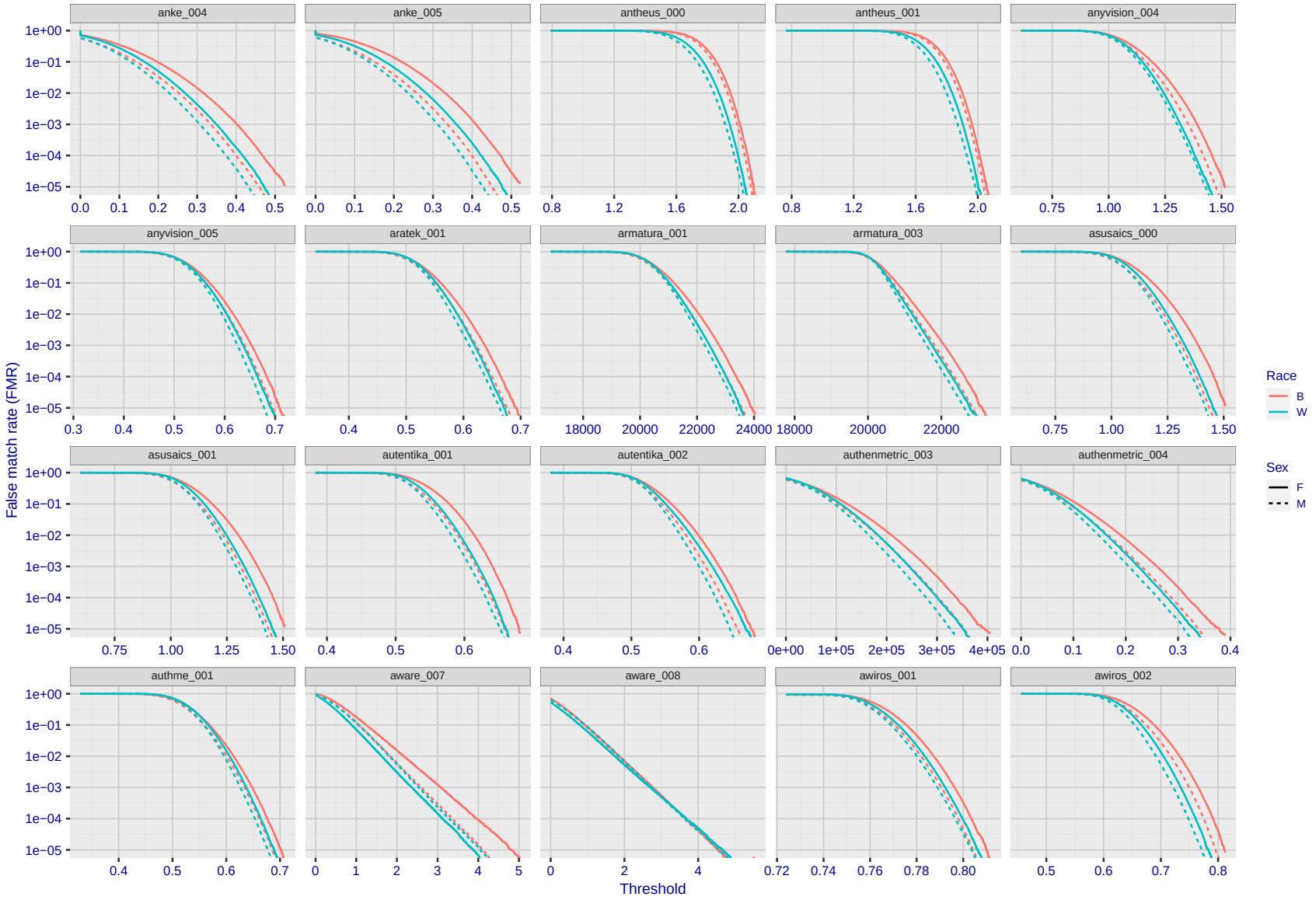

Figure 258: For the mugshot images, the false match calibration curves show false match rate vs. threshold. Separate curves appear for white females, black females, black males and white males.

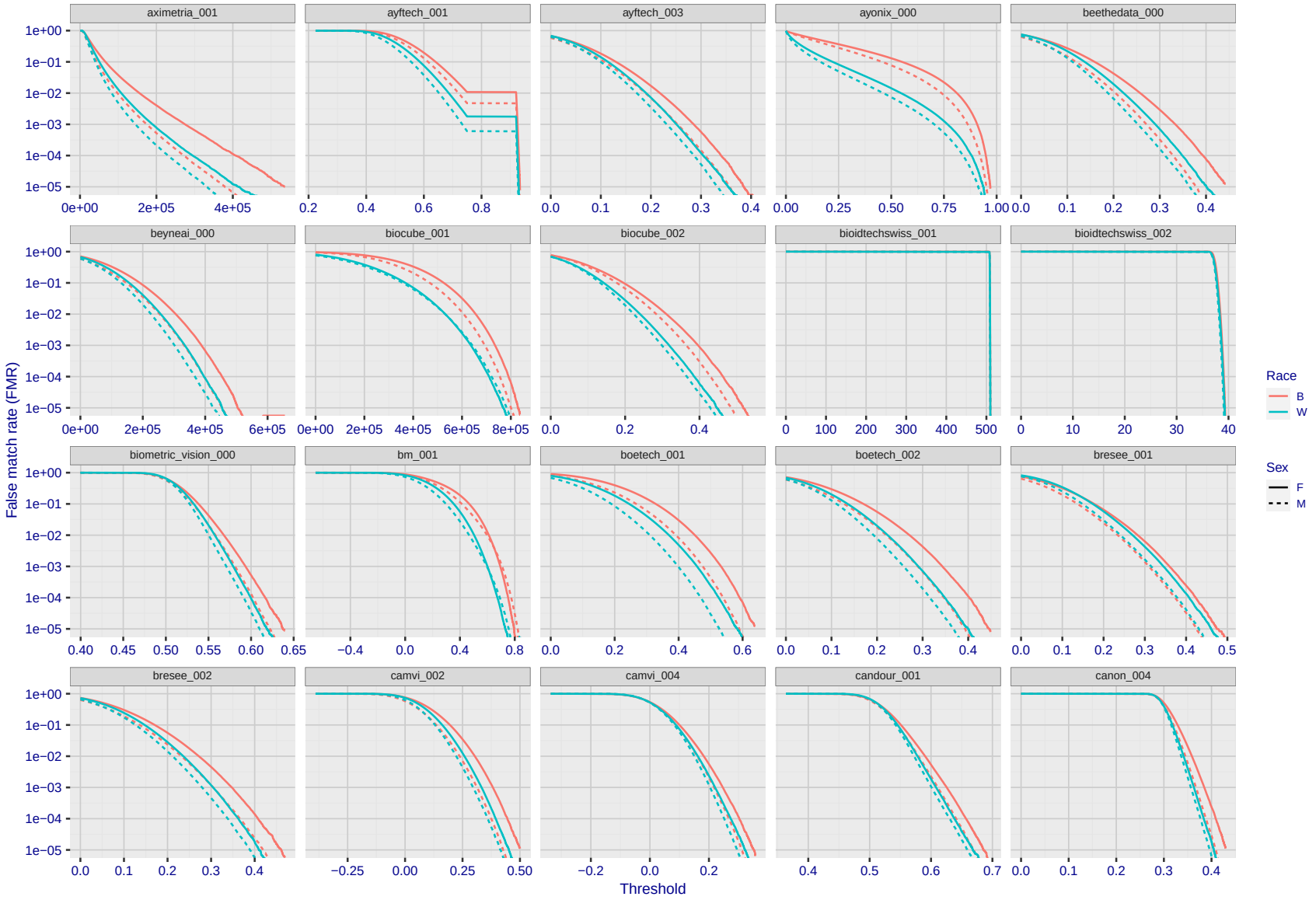

Figure 259: For the mugshot images, the false match calibration curves show false match rate vs. threshold. Separate curves appear for white females, black females, black males and white males.

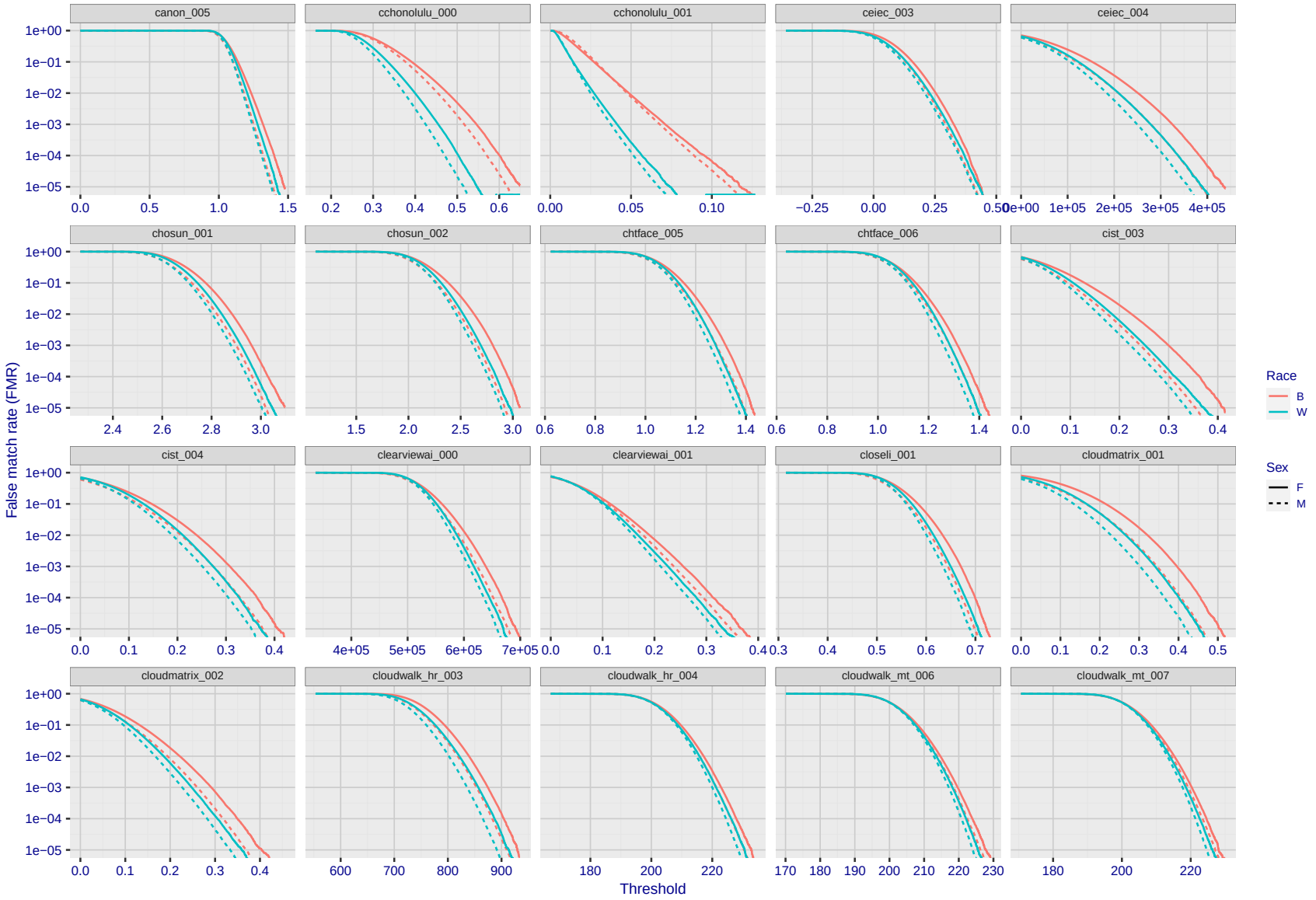

Figure 260: For the mugshot images, the false match calibration curves show false match rate vs. threshold. Separate curves appear for white females, black females, black males and white males.

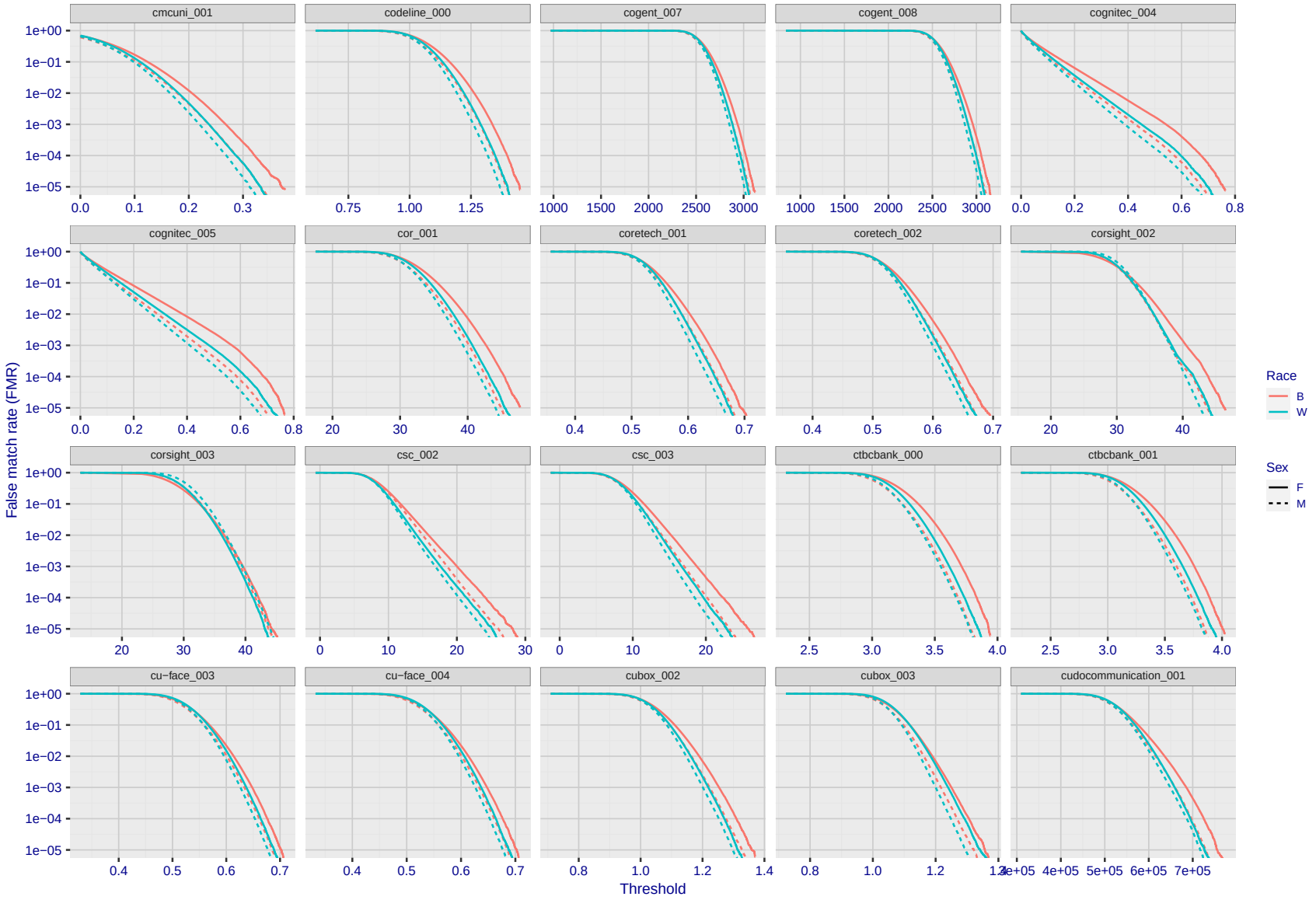

Figure 261: For the mugshot images, the false match calibration curves show false match rate vs. threshold. Separate curves appear for white females, black females, black males and white males.

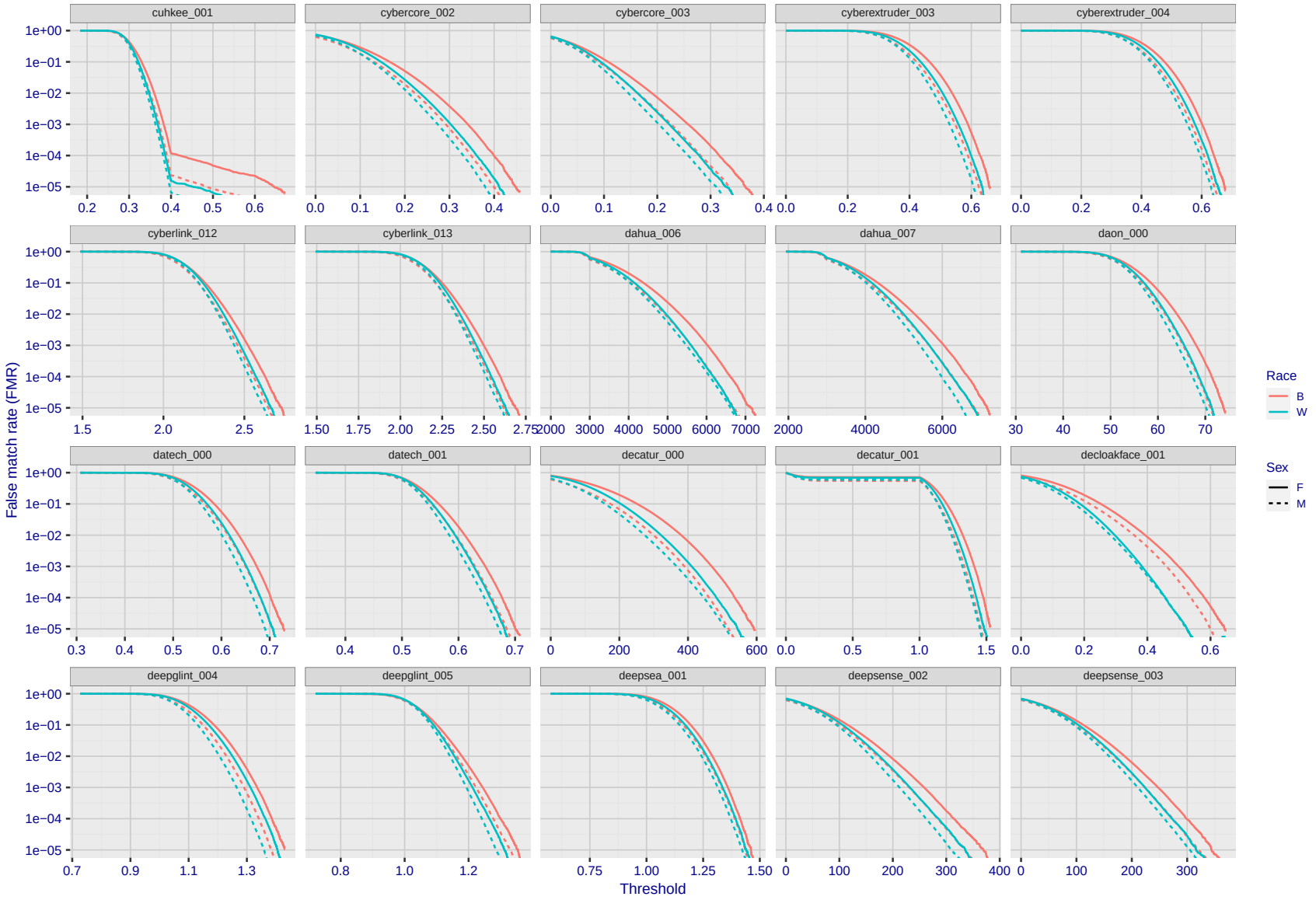

Figure 262: For the mugshot images, the false match calibration curves show false match rate vs. threshold. Separate curves appear for white females, black females, black males and white males.

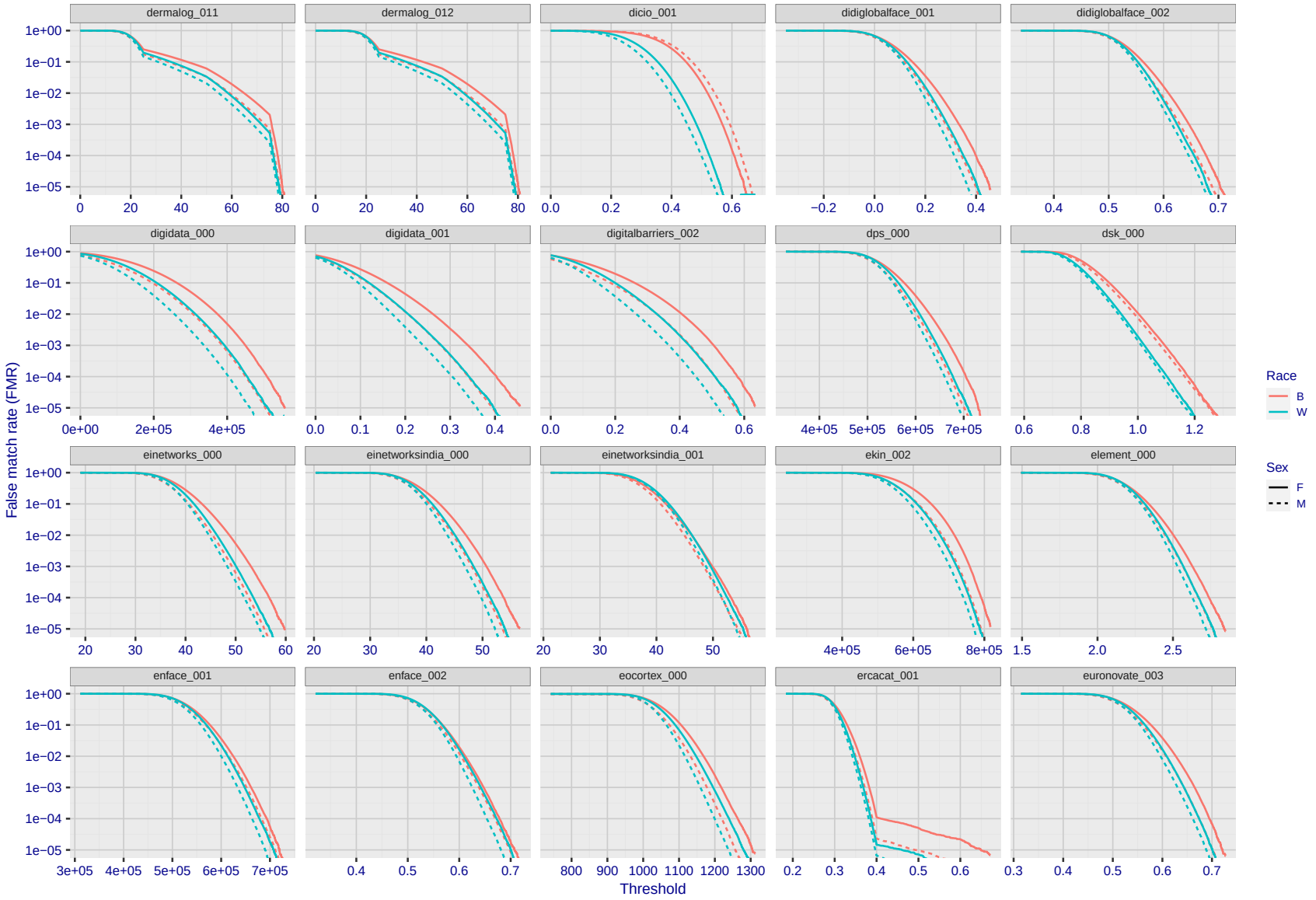

Figure 263: For the mugshot images, the false match calibration curves show false match rate vs. threshold. Separate curves appear for white females, black females, black males and white males.

2024/04/17 08:45:50
FNMR(T) "False non-match rate"
FMR(T) "False match rate"

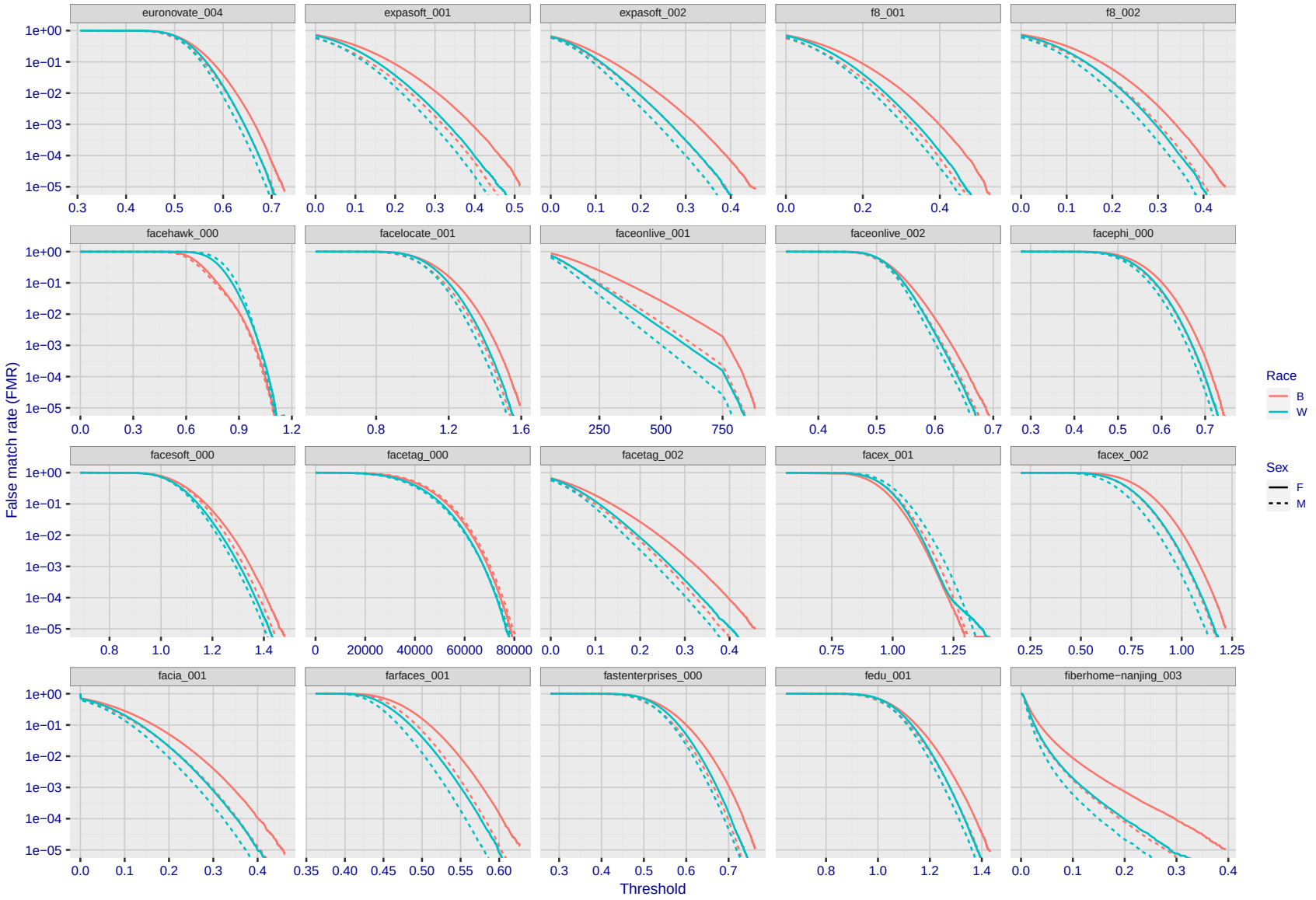

Figure 264: For the mugshot images, the false match calibration curves show false match rate vs. threshold. Separate curves appear for white females, black females, black males and white males.

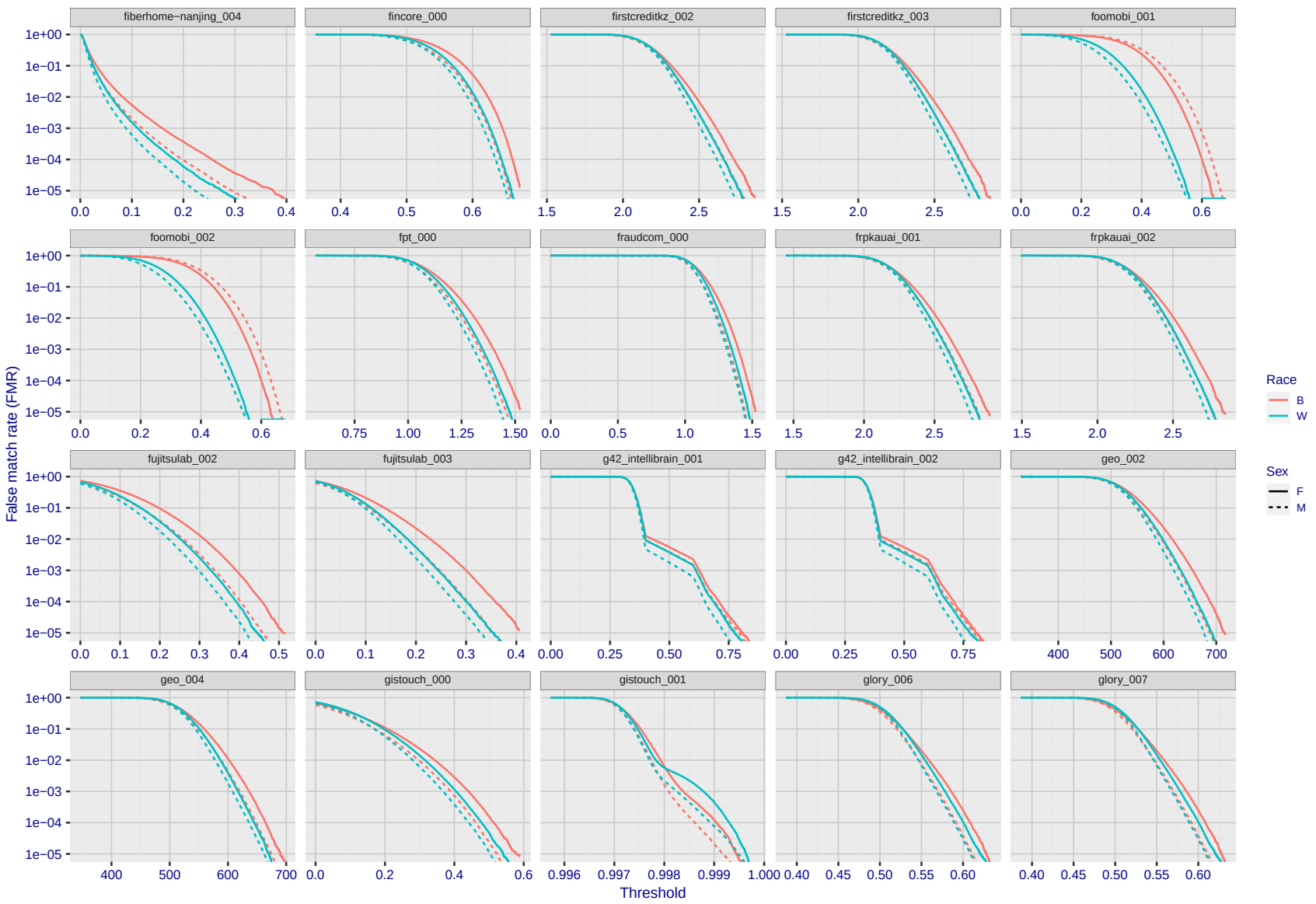

Figure 265: For the mugshot images, the false match calibration curves show false match rate vs. threshold. Separate curves appear for white females, black females, black males and white males.

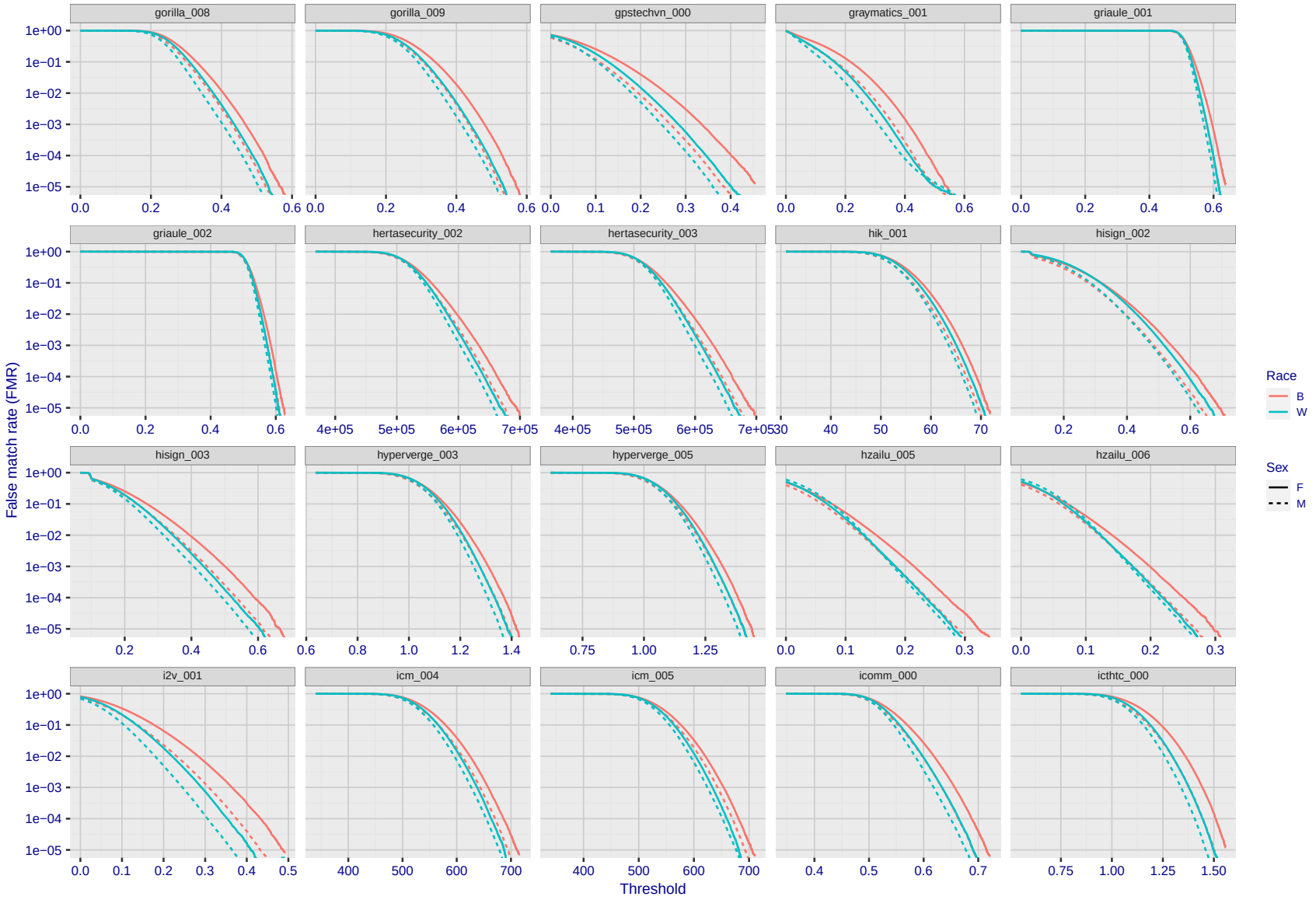

Figure 266: For the mugshot images, the false match calibration curves show false match rate vs. threshold. Separate curves appear for white females, black females, black males and white males.

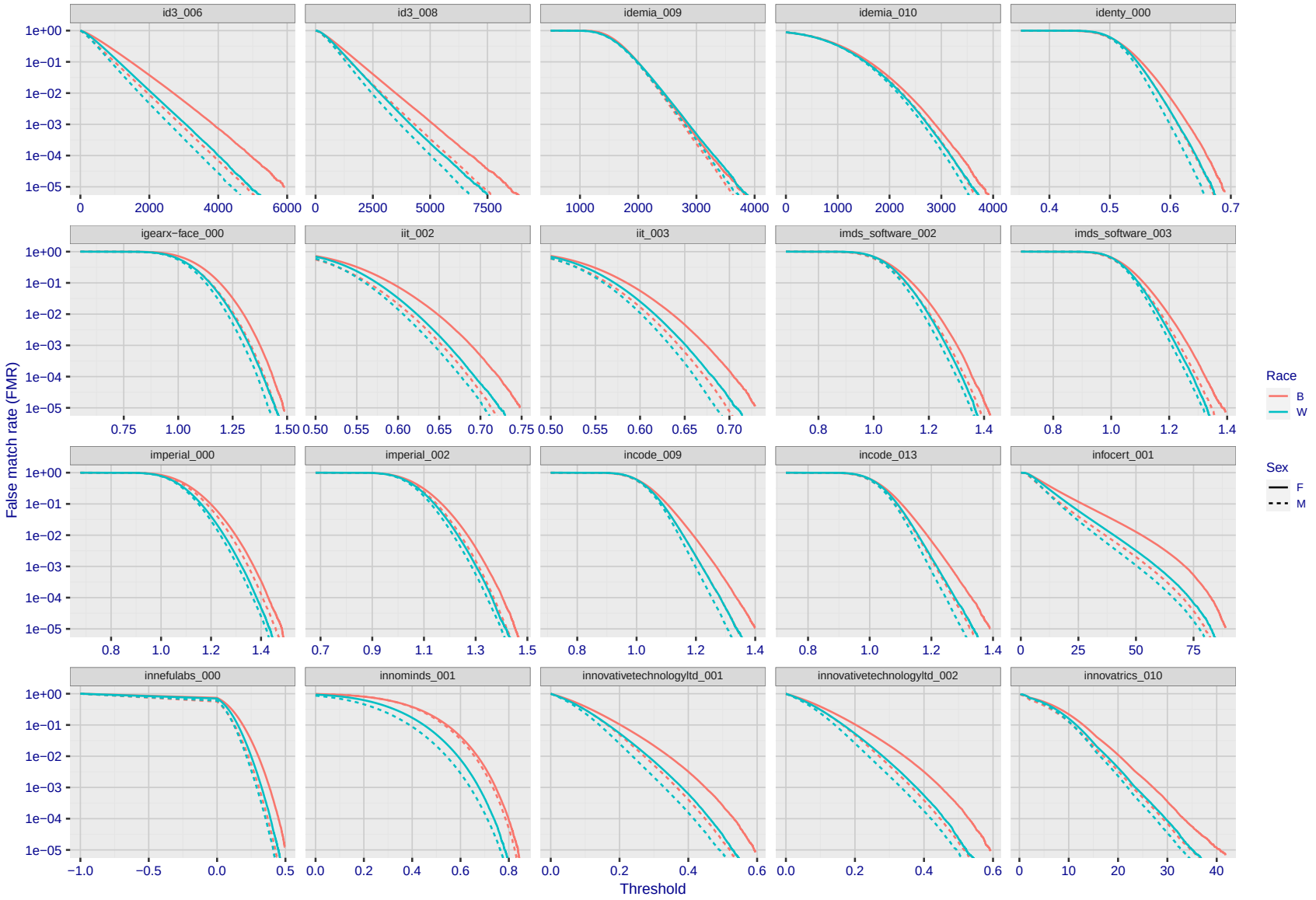

Figure 267: For the mugshot images, the false match calibration curves show false match rate vs. threshold. Separate curves appear for white females, black females, black males and white males.

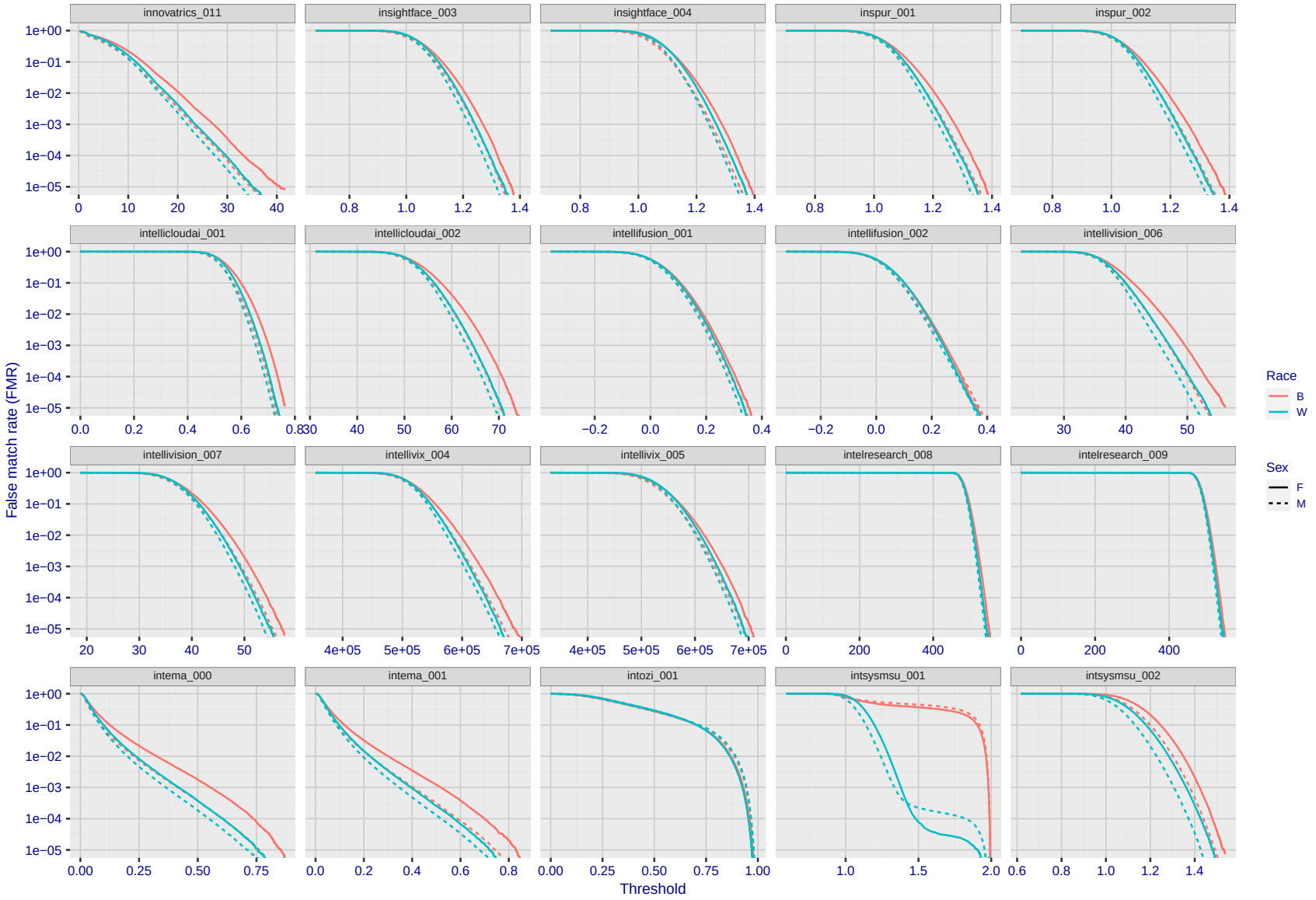

Figure 268: For the mugshot images, the false match calibration curves show false match rate vs. threshold. Separate curves appear for white females, black females, black males and white males.

2024/04/17 08:45:50
FNMR(T) "False non-match rate"
FMR(T) "False match rate"

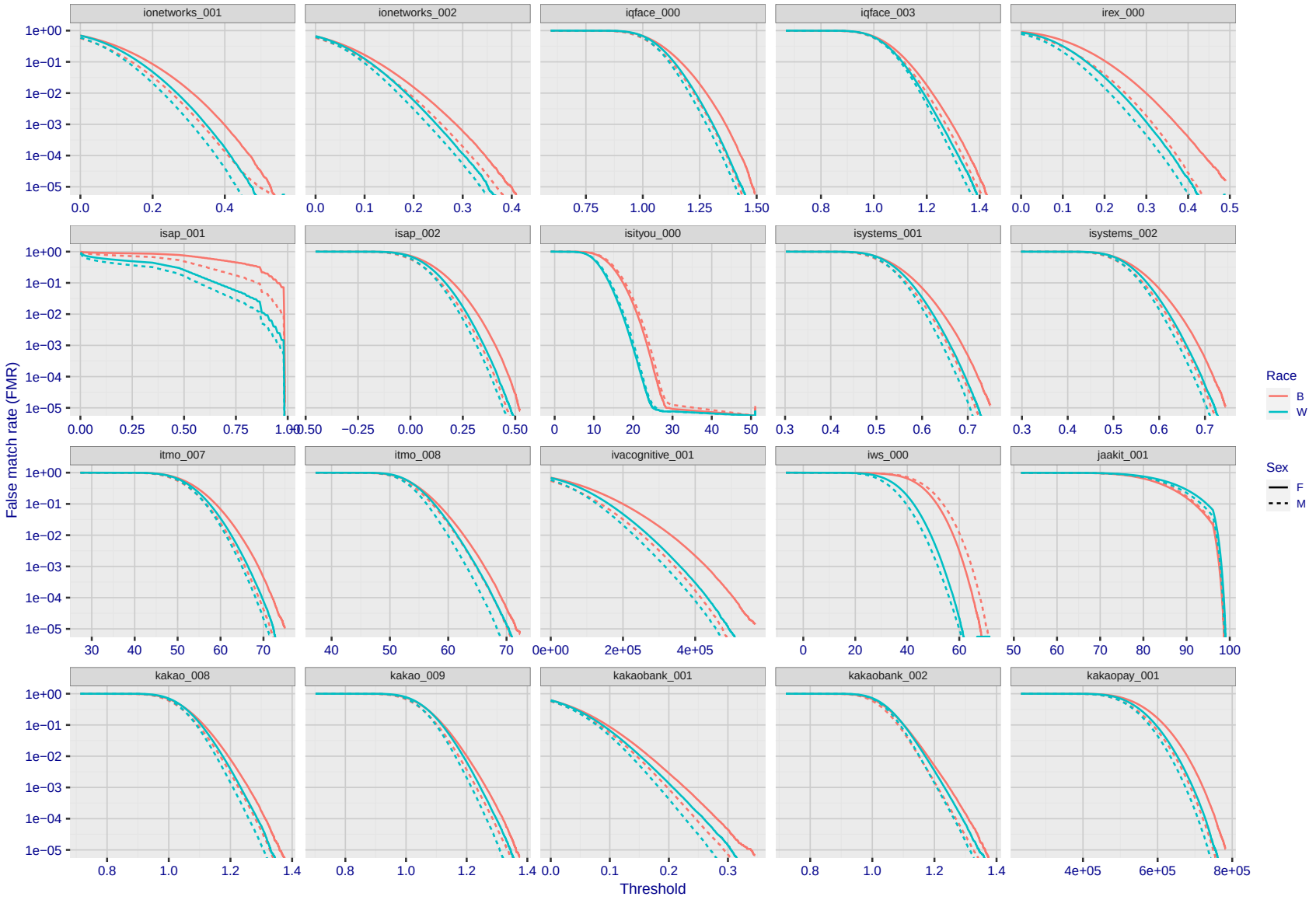

Figure 269: For the mugshot images, the false match calibration curves show false match rate vs. threshold. Separate curves appear for white females, black females, black males and white males.

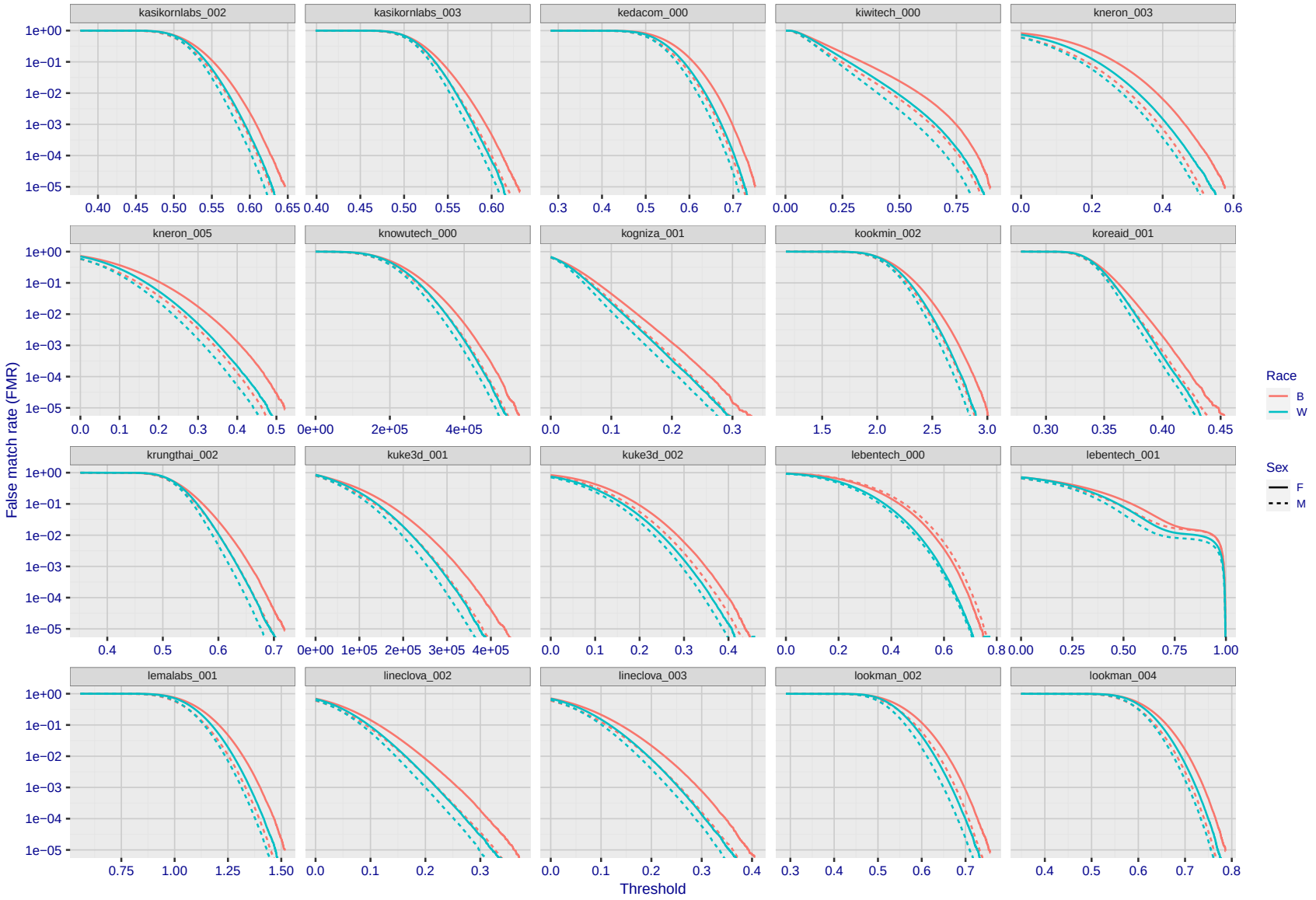

Figure 270: For the mugshot images, the false match calibration curves show false match rate vs. threshold. Separate curves appear for white females, black females, black males and white males.

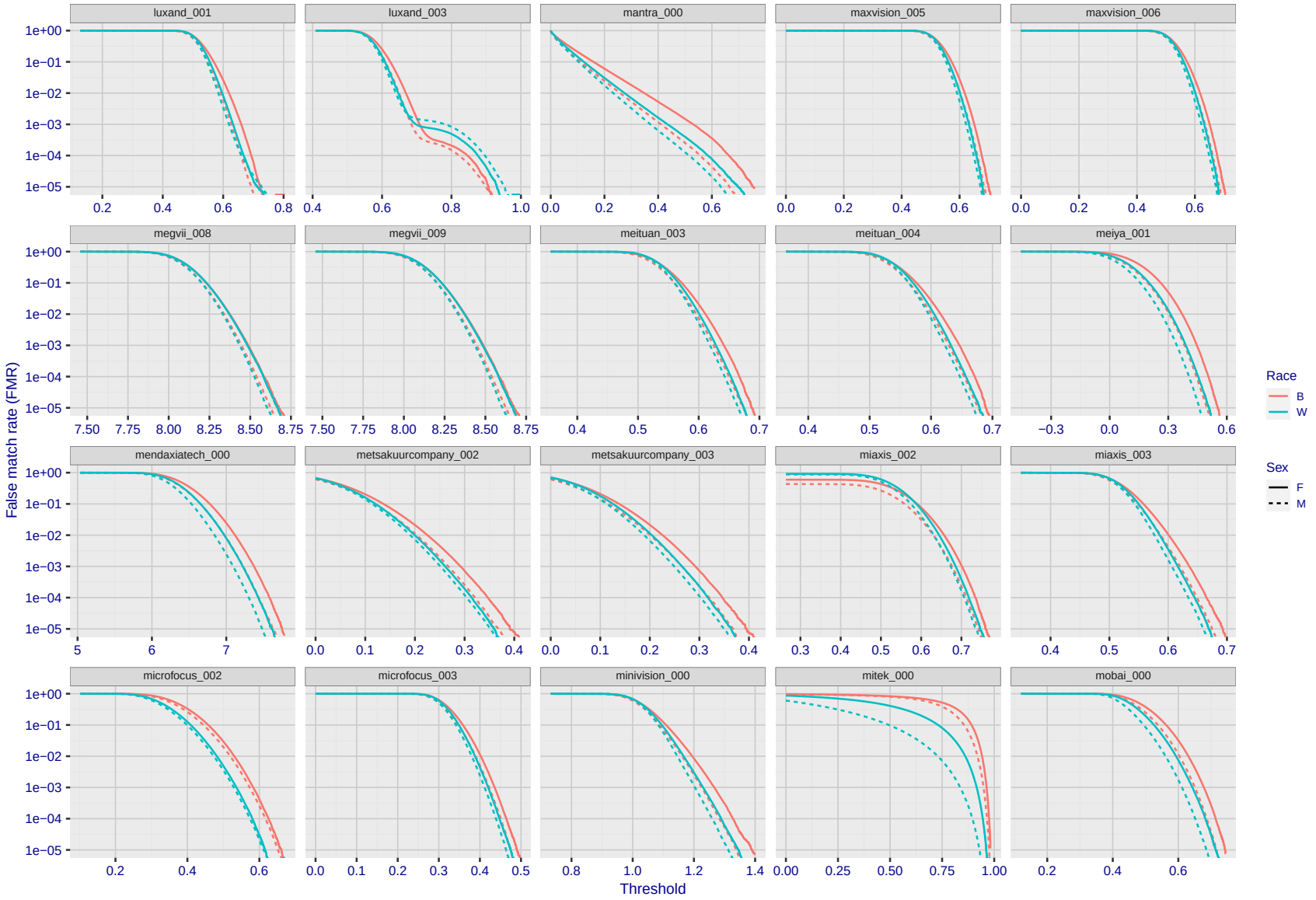

Figure 271: For the mugshot images, the false match calibration curves show false match rate vs. threshold. Separate curves appear for white females, black females, black males and white males.

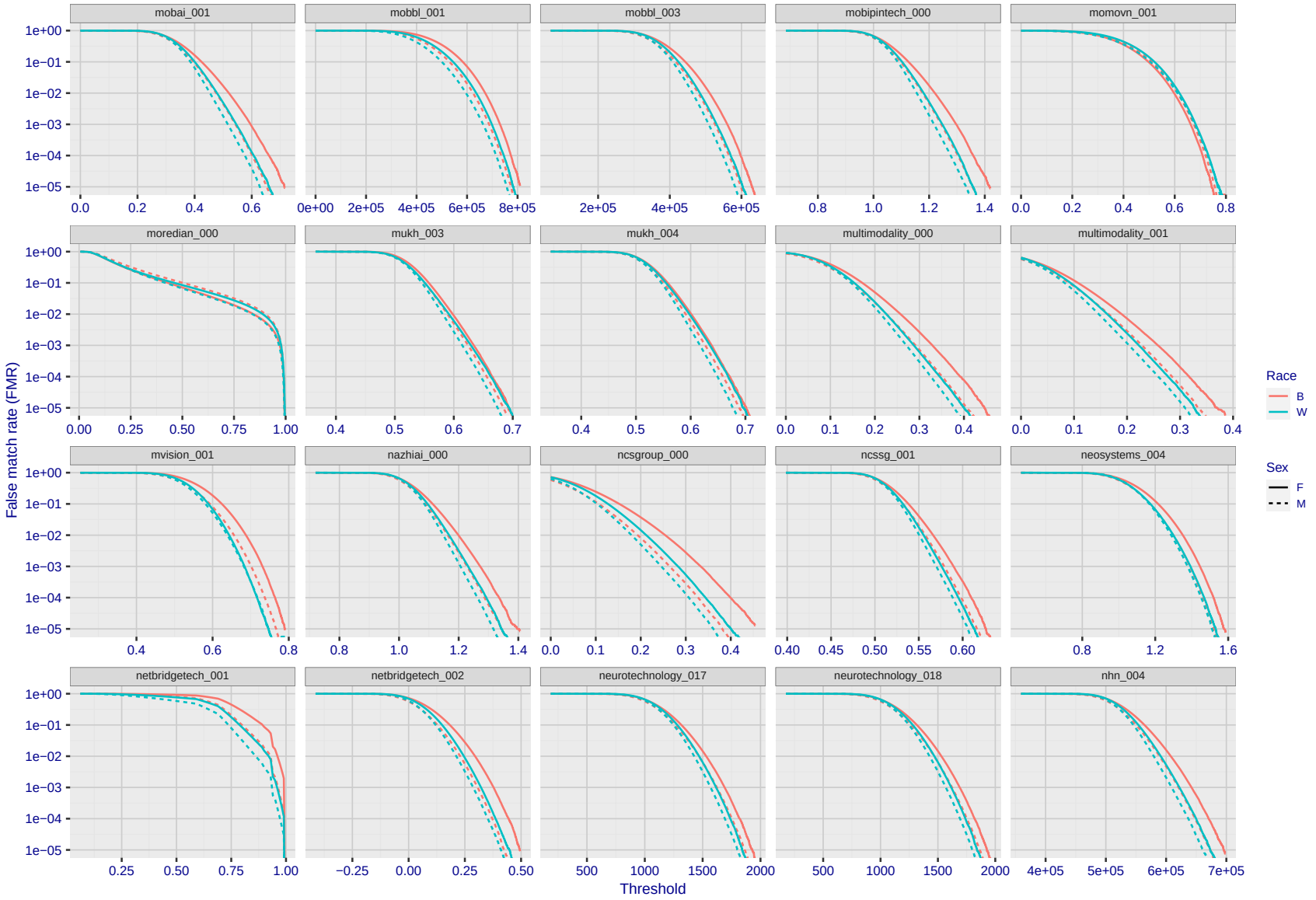

Figure 272: For the mugshot images, the false match calibration curves show false match rate vs. threshold. Separate curves appear for white females, black females, black males and white males.

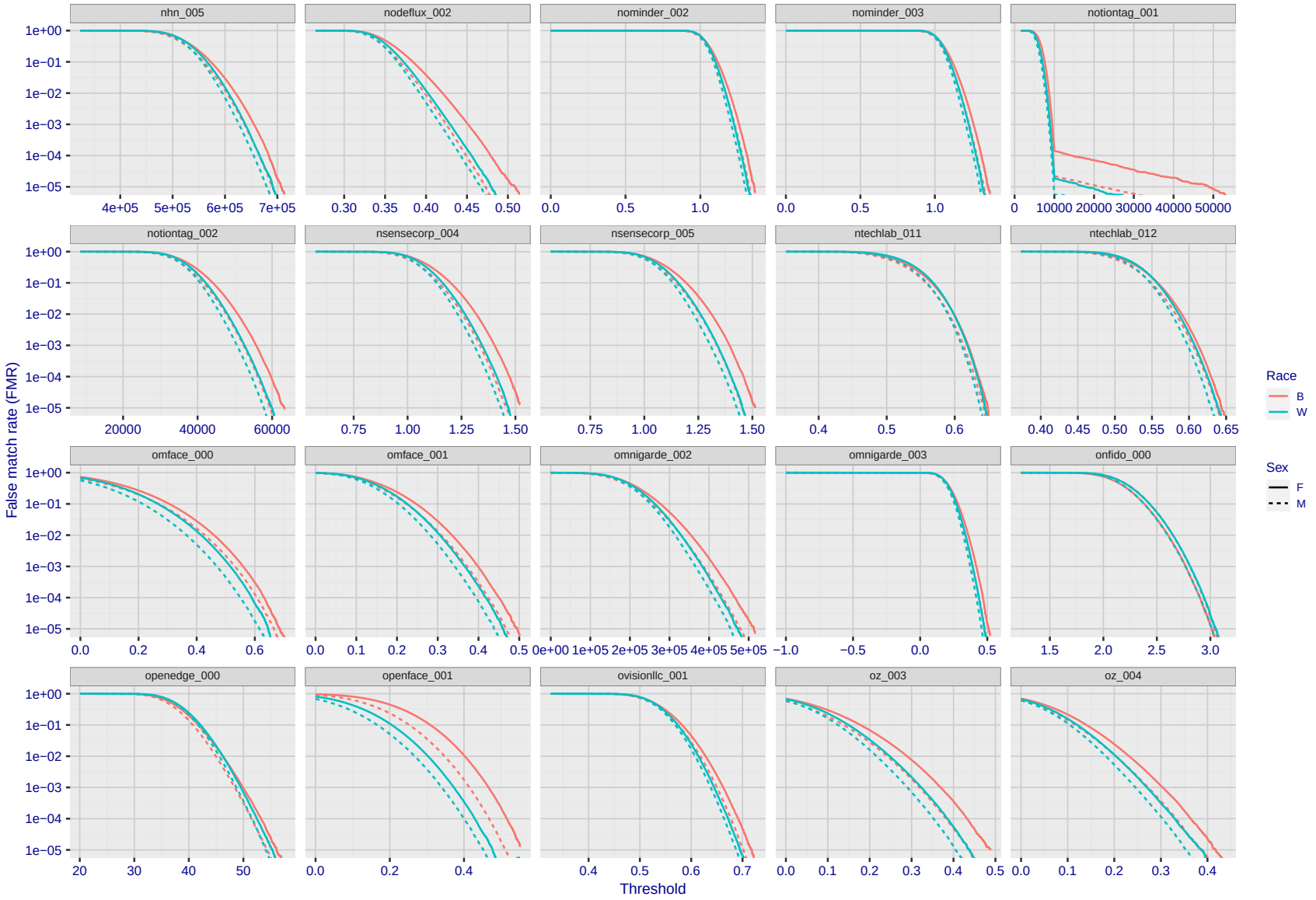

Figure 273: For the mugshot images, the false match calibration curves show false match rate vs. threshold. Separate curves appear for white females, black females, black males and white males.

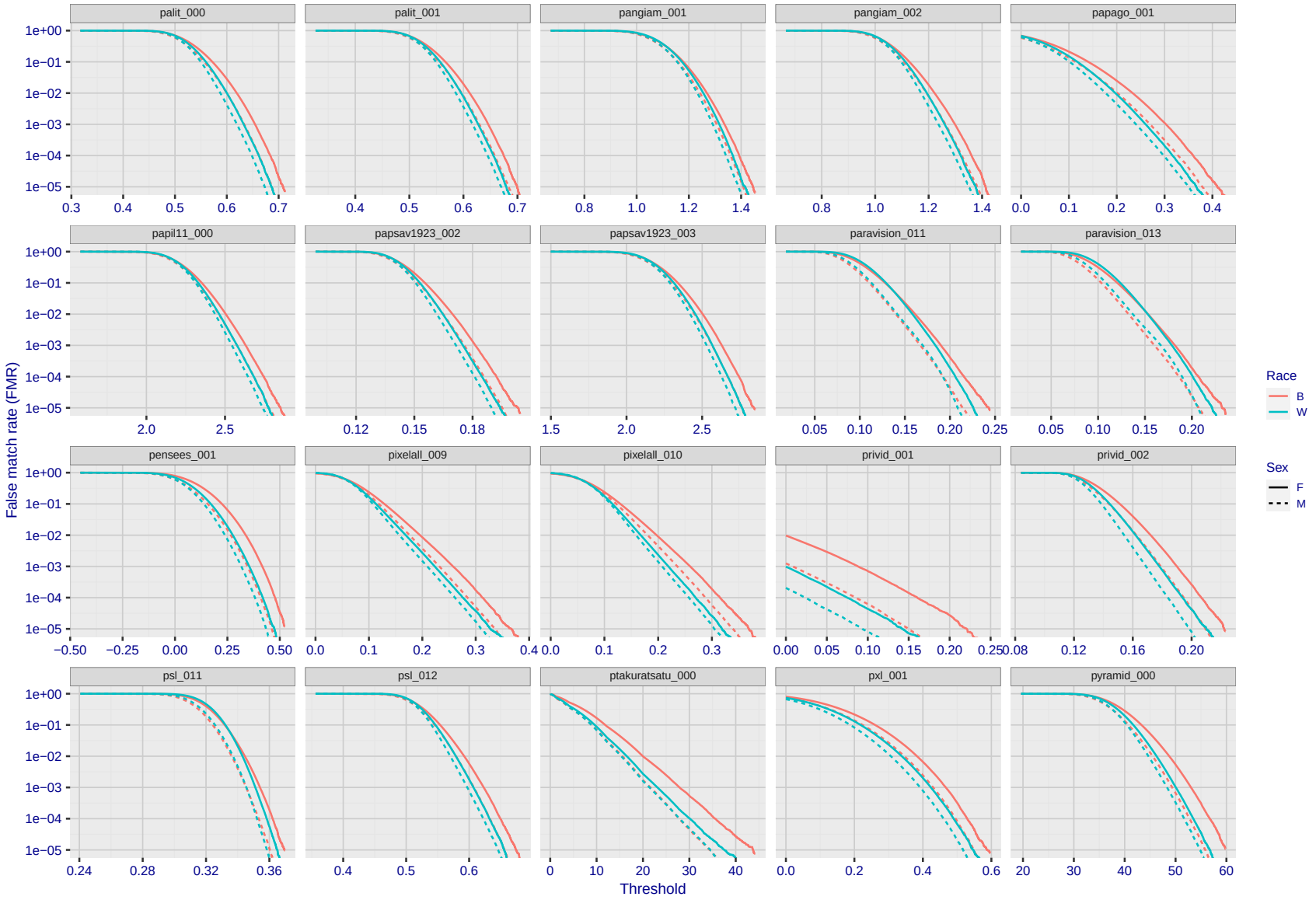

Figure 274: For the mugshot images, the false match calibration curves show false match rate vs. threshold. Separate curves appear for white females, black females, black males and white males.

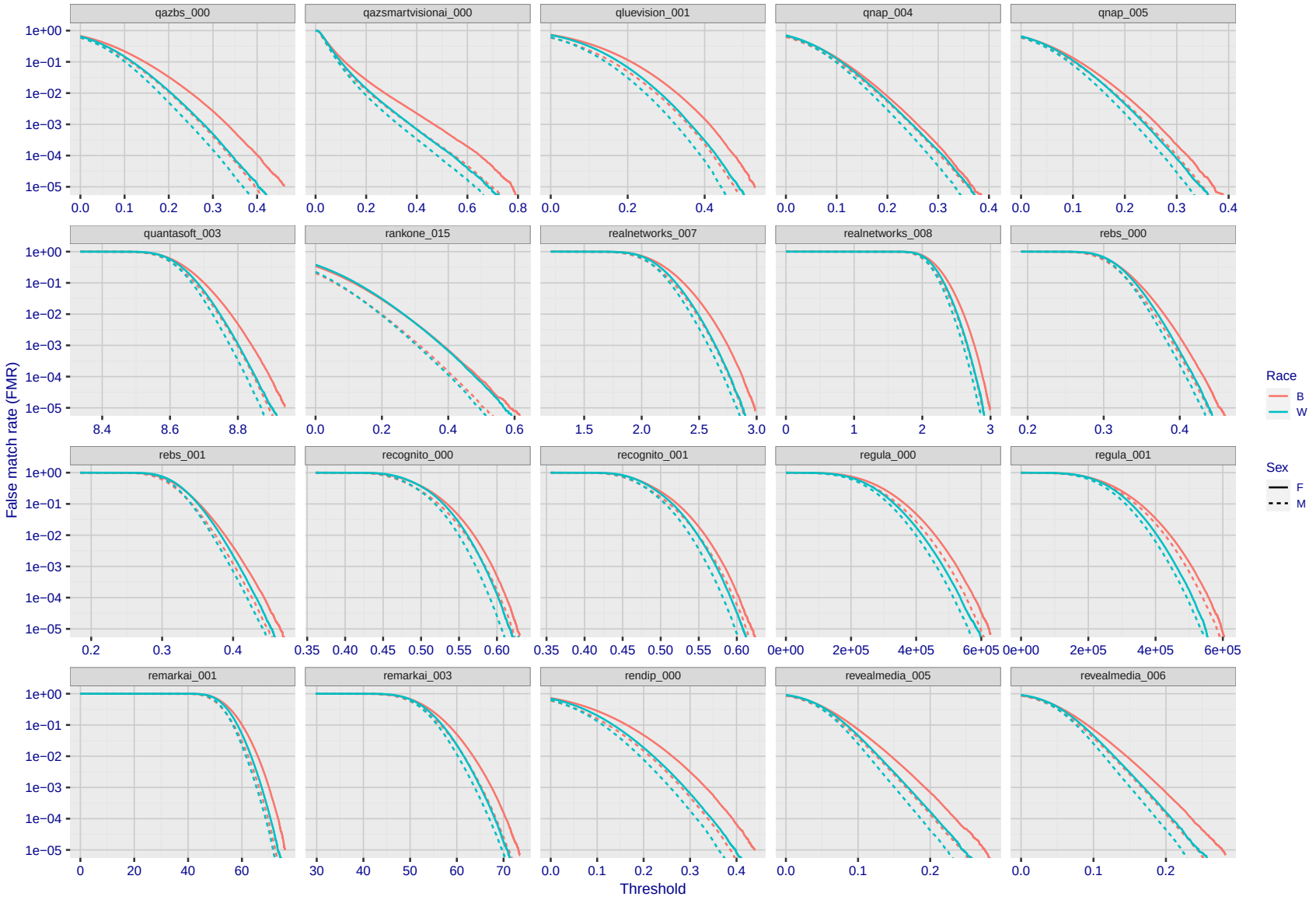

Figure 275: For the mugshot images, the false match calibration curves show false match rate vs. threshold. Separate curves appear for white females, black females, black males and white males.

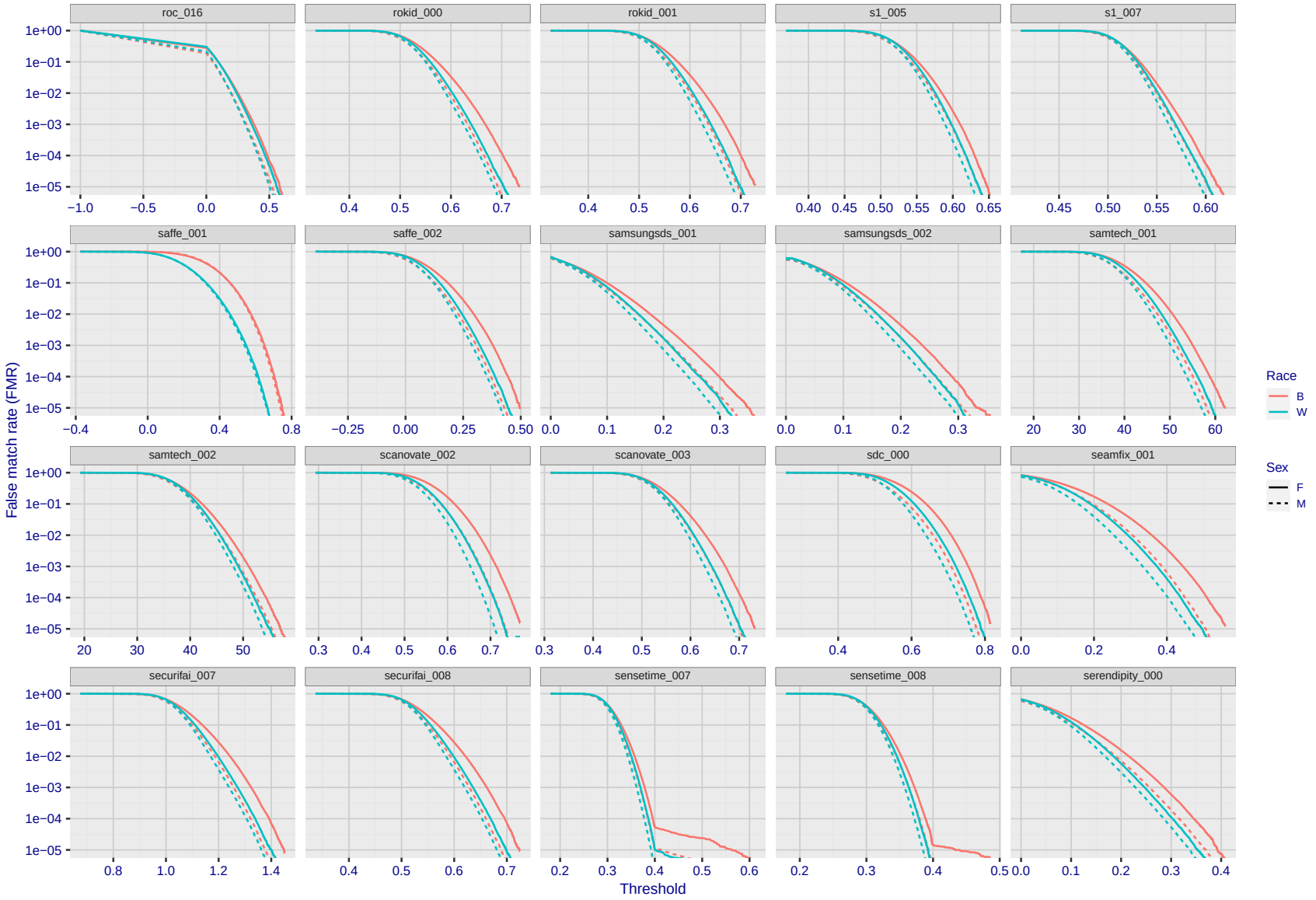

Figure 276: For the mugshot images, the false match calibration curves show false match rate vs. threshold. Separate curves appear for white females, black females, black males and white males.

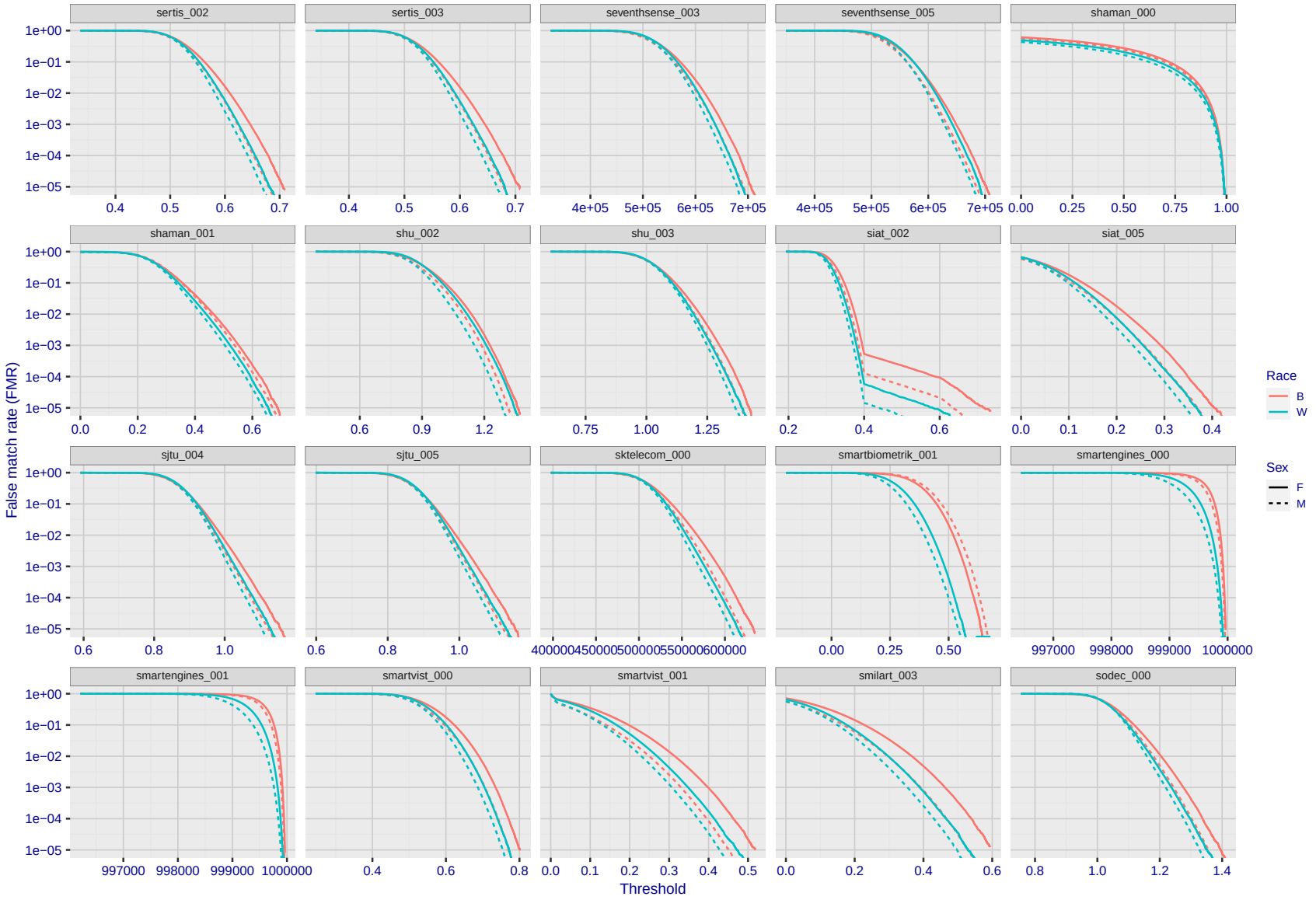

Figure 277: For the mugshot images, the false match calibration curves show false match rate vs. threshold. Separate curves appear for white females, black females, black males and white males.

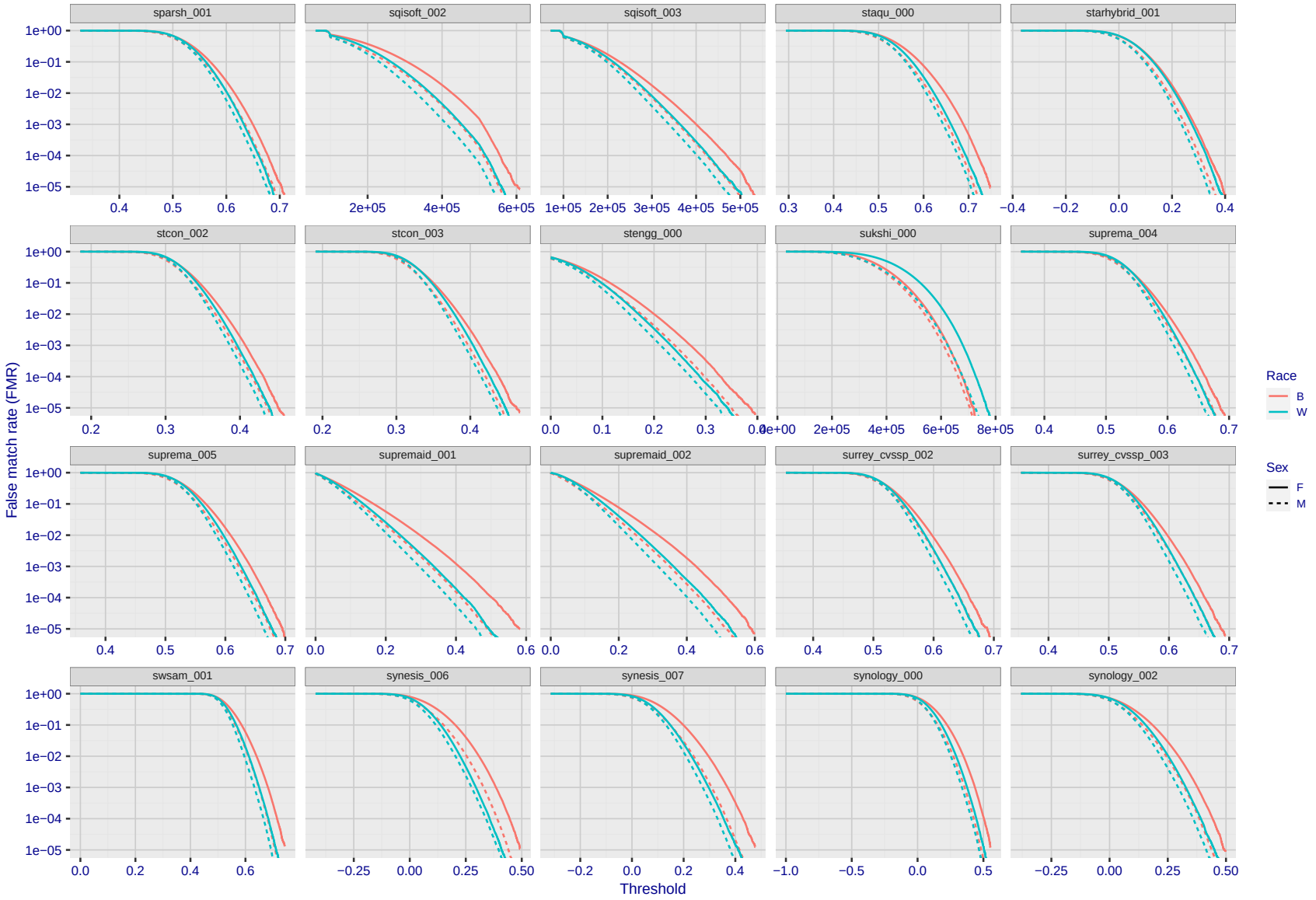

Figure 278: For the mugshot images, the false match calibration curves show false match rate vs. threshold. Separate curves appear for white females, black females, black males and white males.

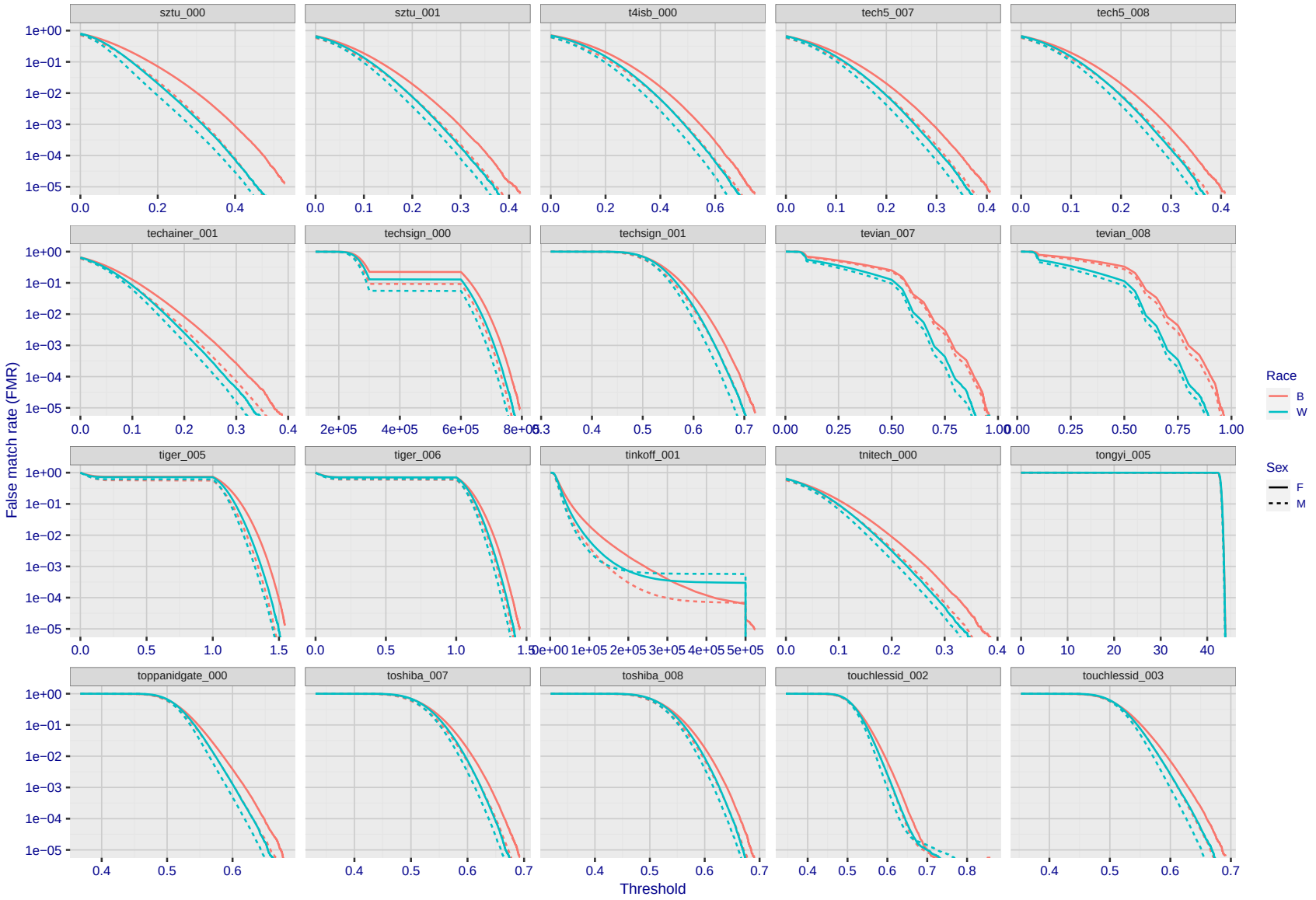

Figure 279: For the mugshot images, the false match calibration curves show false match rate vs. threshold. Separate curves appear for white females, black females, black males and white males.

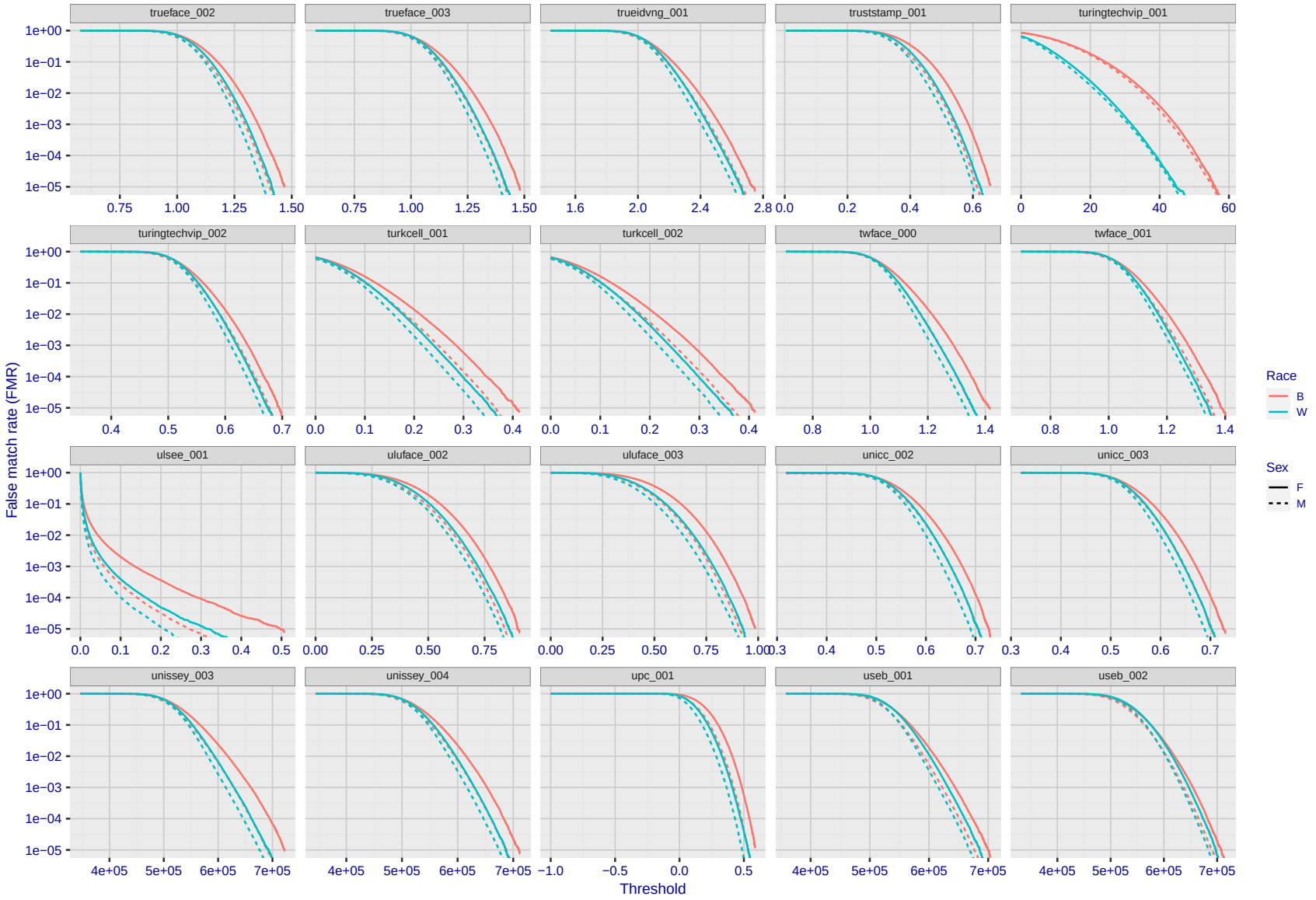

Figure 280: For the mugshot images, the false match calibration curves show false match rate vs. threshold. Separate curves appear for white females, black females, black males and white males.

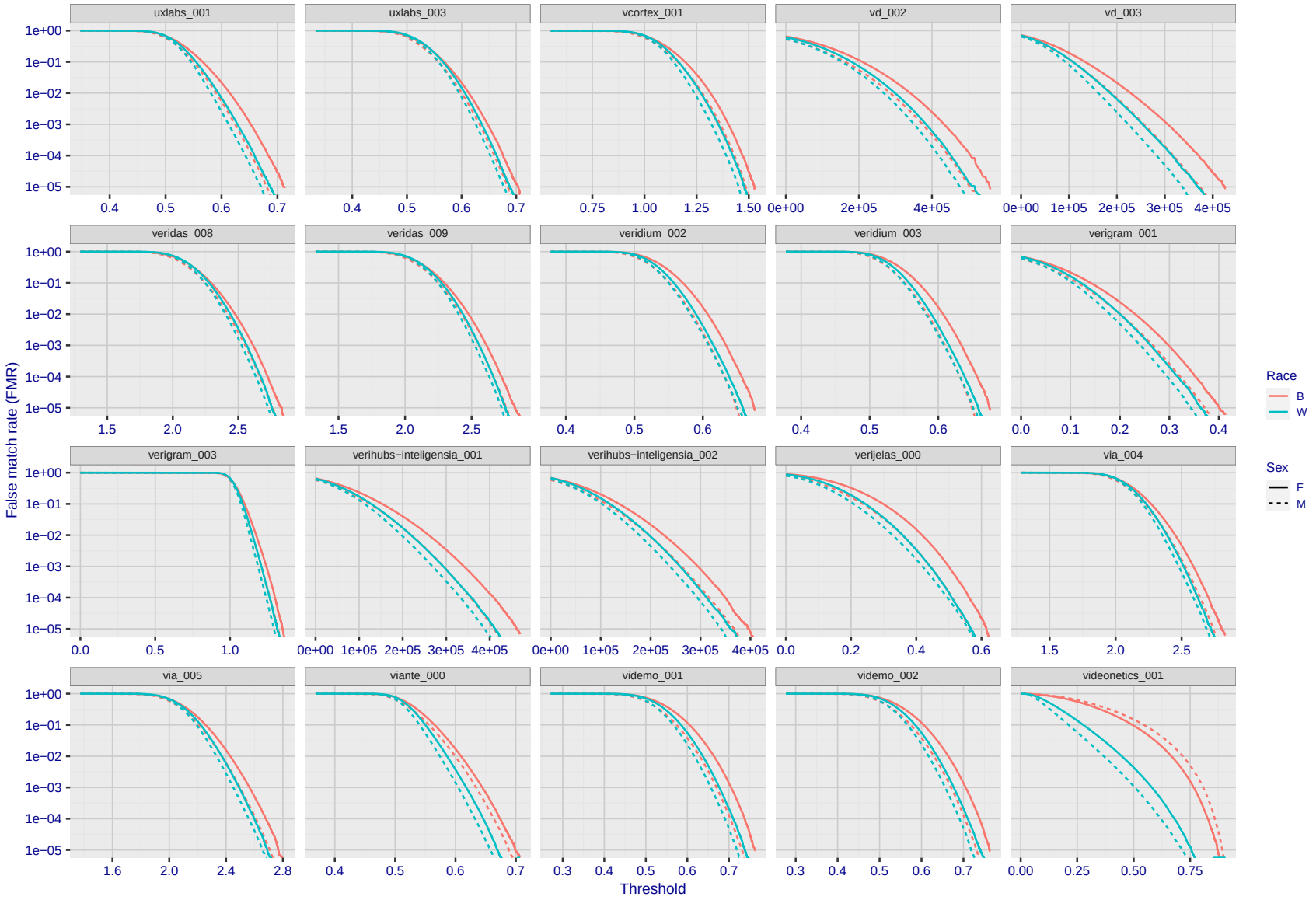

Figure 281: For the mugshot images, the false match calibration curves show false match rate vs. threshold. Separate curves appear for white females, black females, black males and white males.

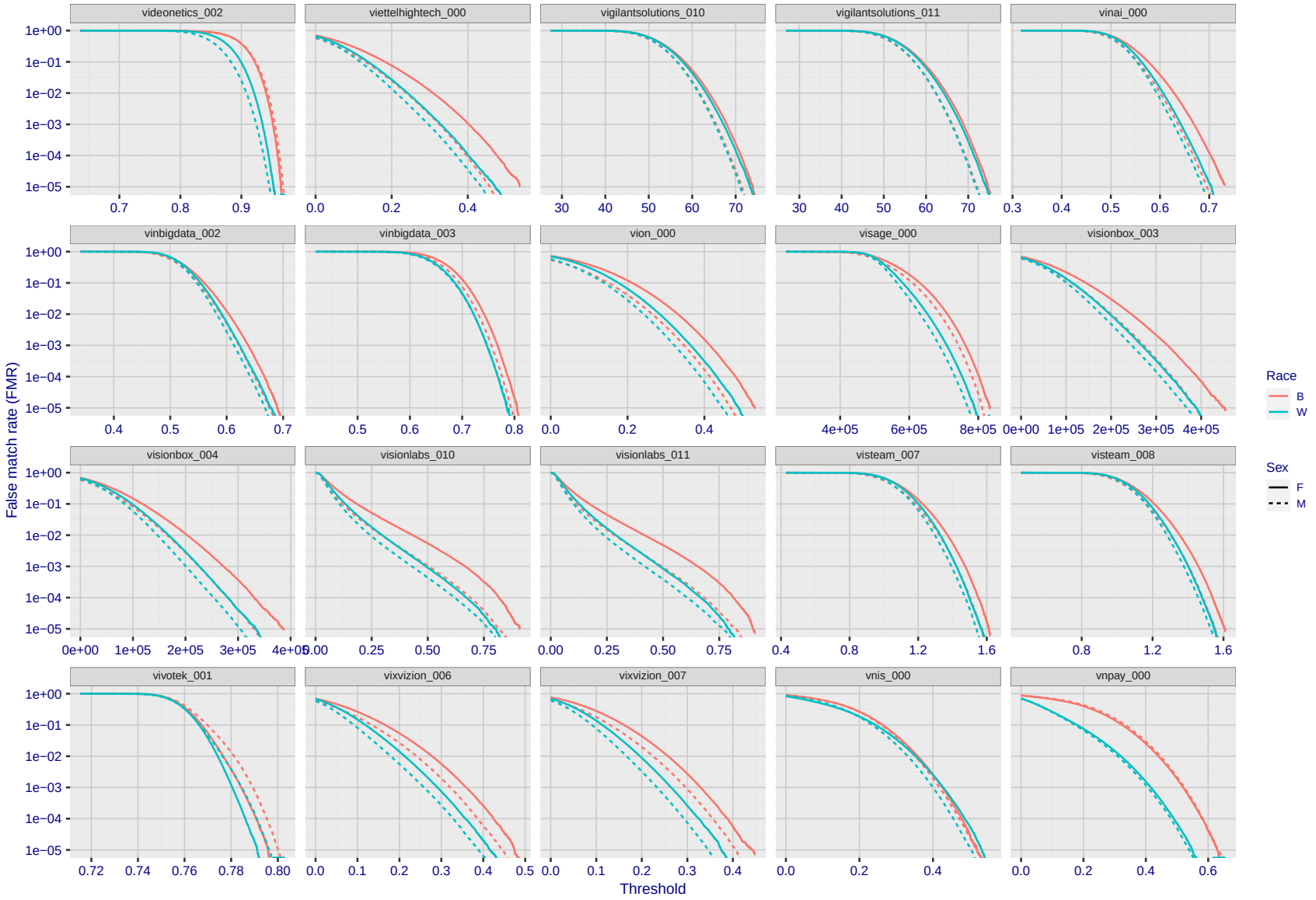

Figure 282: For the mugshot images, the false match calibration curves show false match rate vs. threshold. Separate curves appear for white females, black females, black males and white males.

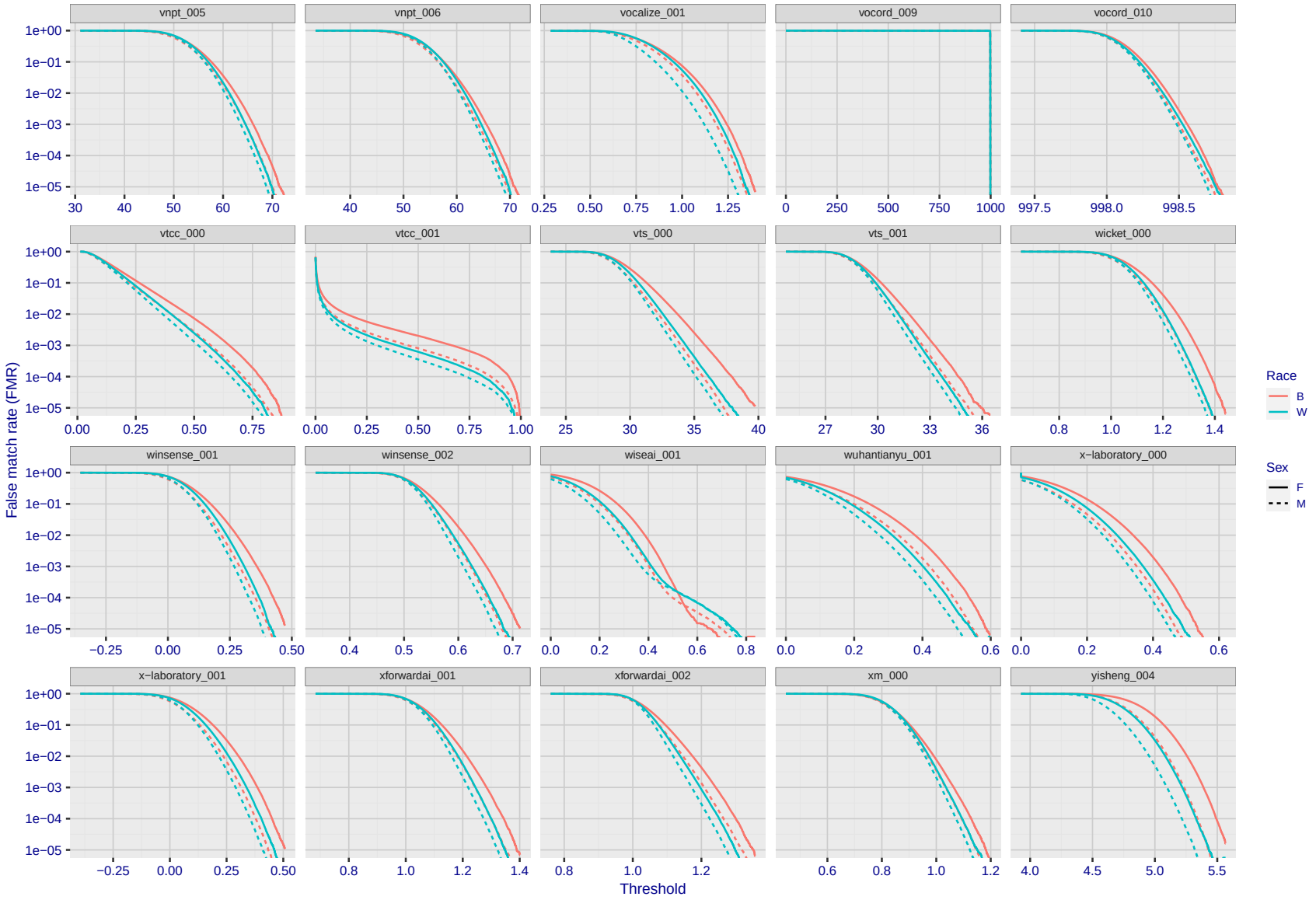

Figure 283: For the mugshot images, the false match calibration curves show false match rate vs. threshold. Separate curves appear for white females, black females, black males and white males.

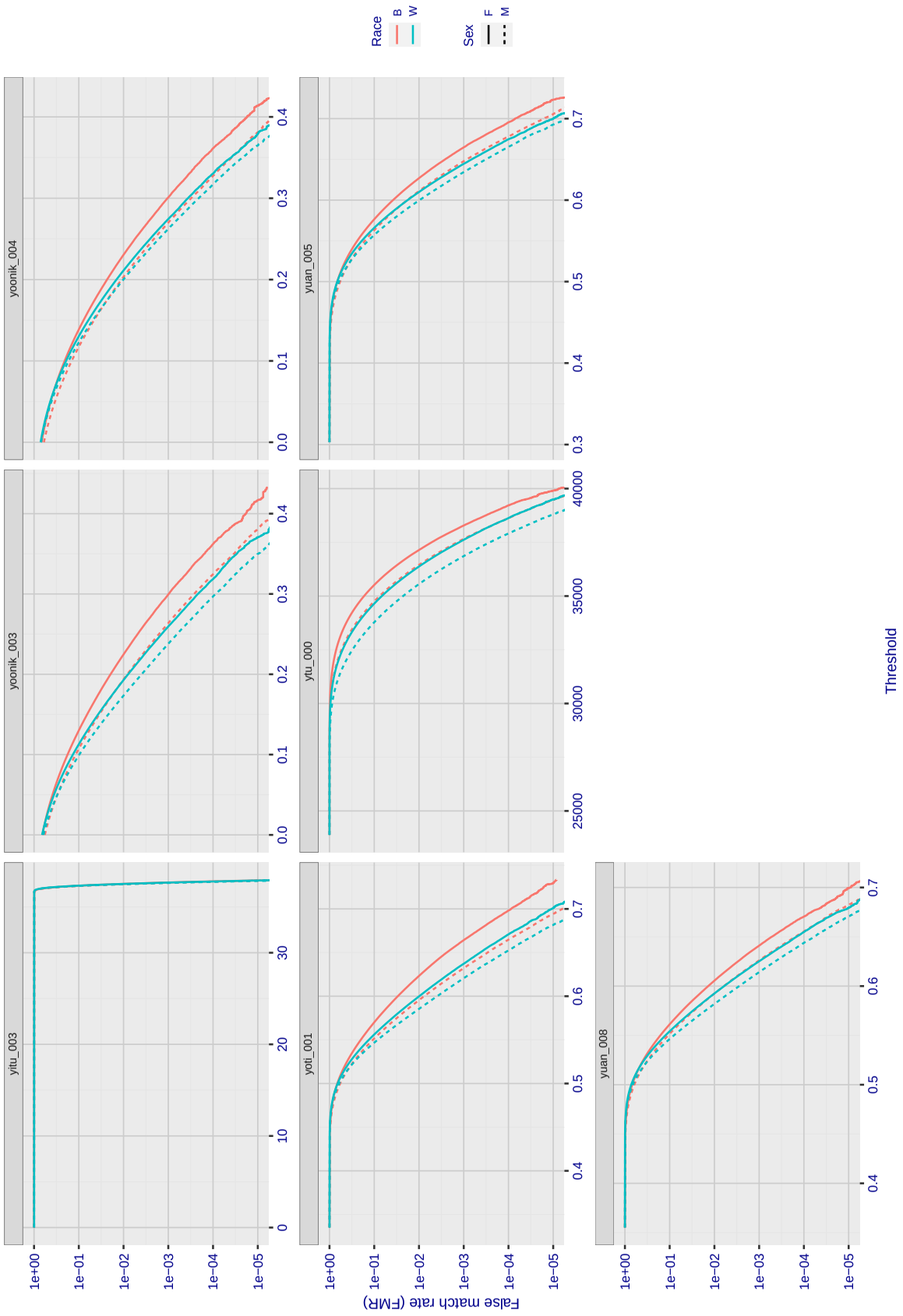

Figure 284: For the mugshot images, the false match calibration curves show false match rate vs. threshold. Separate curves appear for white females, black females, black males and white males.

FNMR(T) "False non-match rate"
FMR(T) "False match rate"

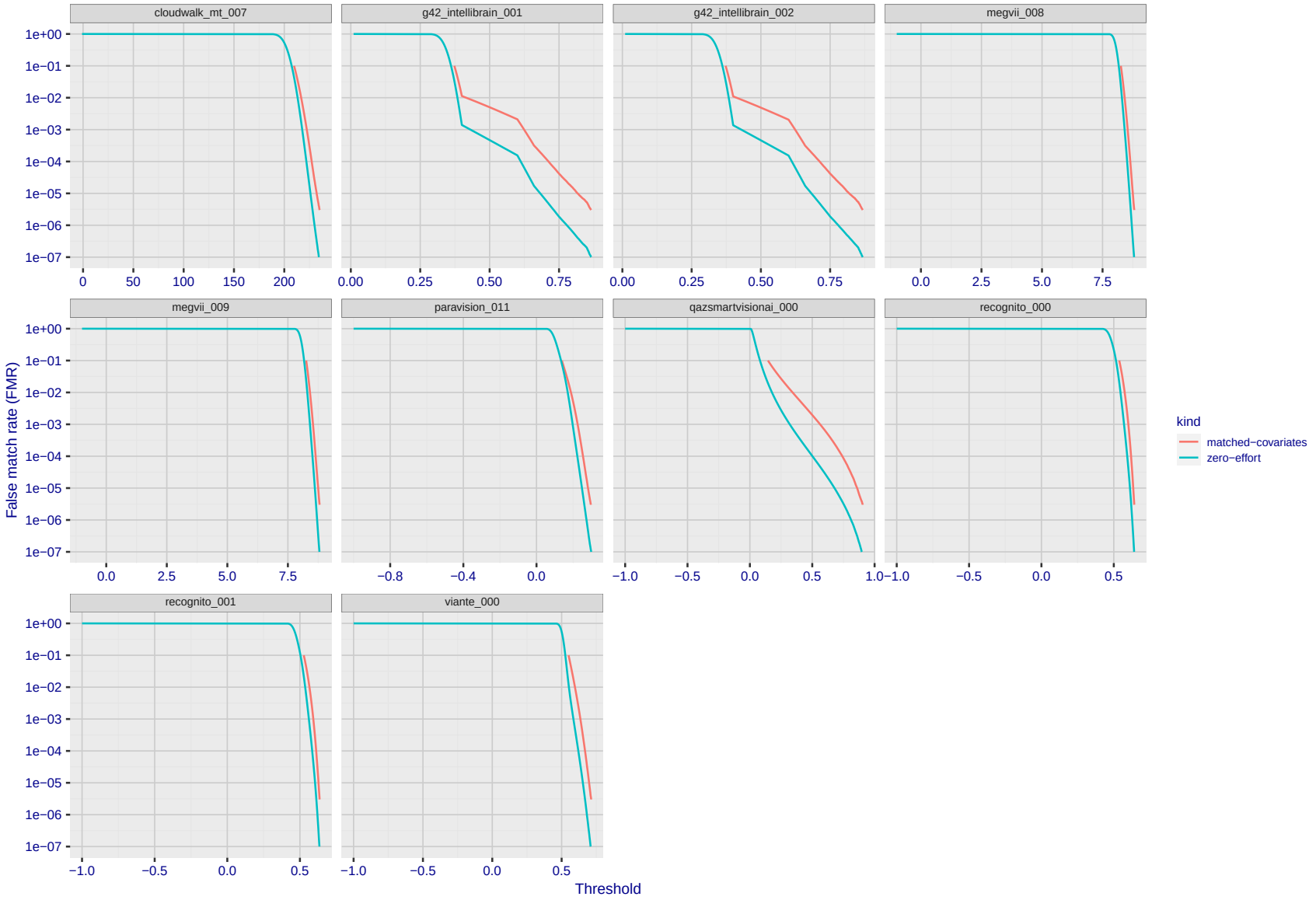

Figure 285: For the visa images, the false match calibration curves show FMR vs. threshold, T. The blue (lower) curves are for zero-effort impostors (i.e. comparing all images against all). The red (upper) curves are for persons of the same-sex, same-age, and same national-origin. This shows that FMR is underestimated (by a factor of 10 or more) by using a zero-effort impostor calculation to calibrate T. As shown later (sec. 3.6), FMR is higher for demographic-matched impostors.

3.5 Genuine distribution stability

3.5.1 Effect of birth place on the genuine distribution

Background: Both skin tone and bone structure vary geographically. Prior studies have reported variations in FNMR and FMR.

Goal: To measure false non-match rate (FNMR) variation with country of birth.

Methods: Thresholds are determined that give FMR = $\{0.001, 0.0001\}$ over the entire impostor set. Then FNMR is measured over 1000 bootstrap replications of the genuine scores. Only those countries with at least 140 individuals are included in the analysis.

Results: Figure 331 shows FNMR by country of birth for the two thresholds.

FNMR(T) "False non-match rate"
FMR(T) "False match rate"

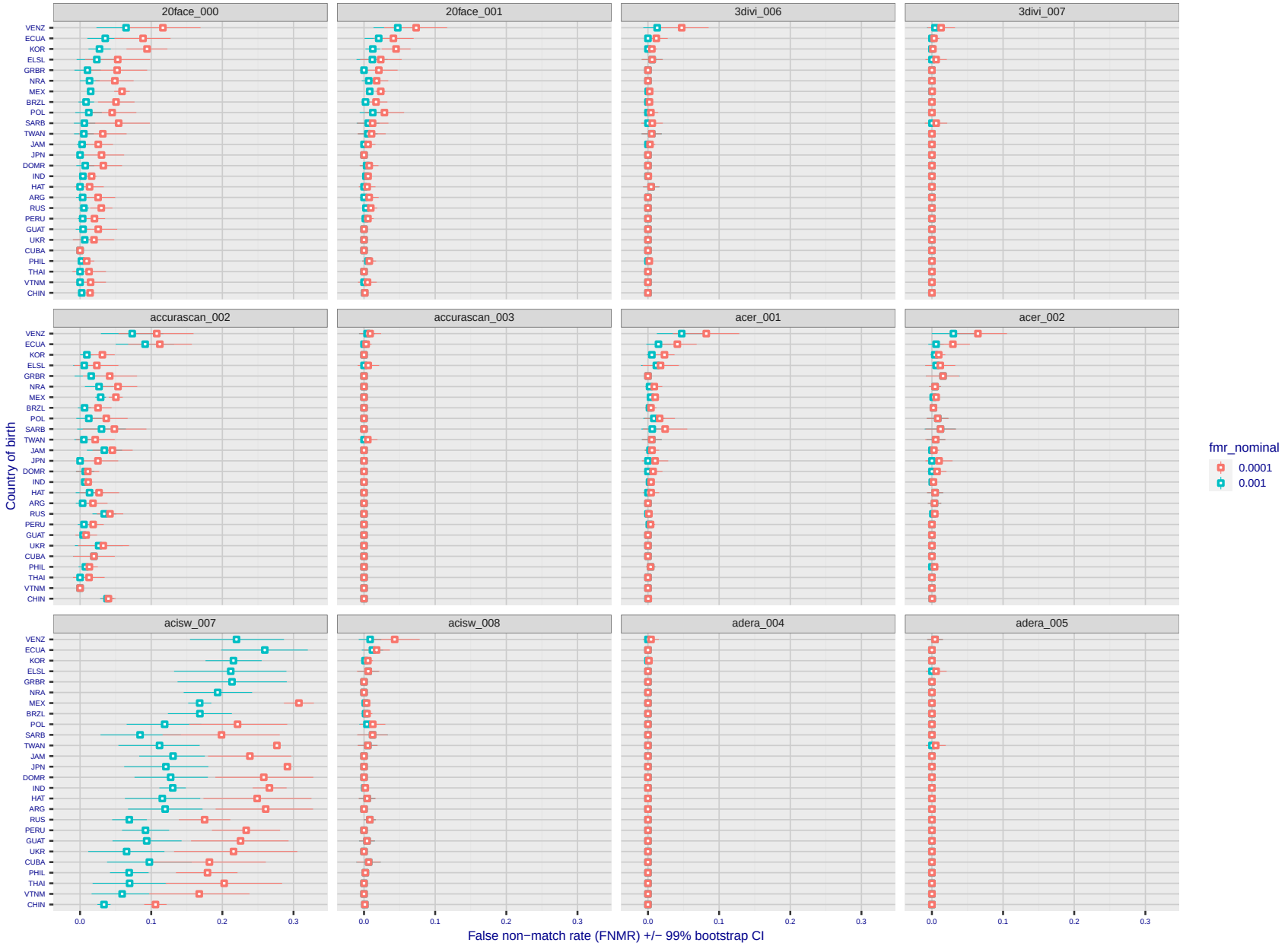

Figure 286: For the visa images, the dots show FNMR by country of birth for two globally set operating thresholds corresponding to FMR = $\{0.001, 0.0001\}$ computed over all on the order of 10^{10} impostor scores. The FMR in each bin will vary also - see subsequent impostor heatmaps in sec. 3.6.1. The figures shows an order of magnitude variation in FNMR across country of birth; these effects are likely due quality variations, then demographics like age and race. The error rates in some cases are zero, and in others the DET is flat so the error rates at the two thresholds are identical. The lines span 1% and 99% of boostrap replicated FNMR estimates.

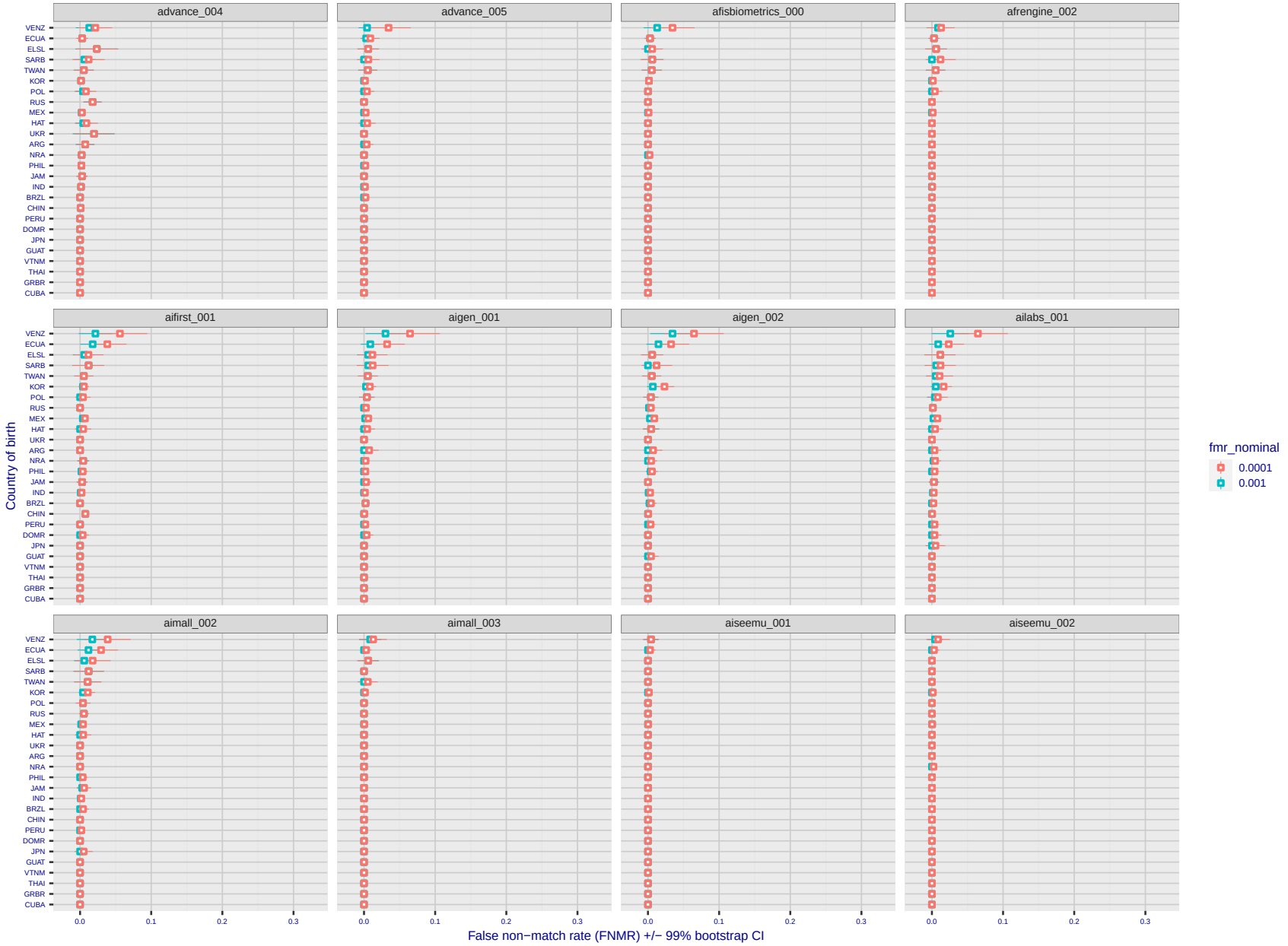

Figure 287: For the visa images, the dots show FNMR by country of birth for two globally set operating thresholds corresponding to FMR = $\{0.001, 0.0001\}$ computed over all on the order of 10^{10} impostor scores. The FMR in each bin will vary also - see subsequent impostor heatmaps in sec. 3.6.1. The figures shows an order of magnitude variation in FNMR across country of birth; these effects are likely due quality variations, then demographics like age and race. The error rates in some cases are zero, and in others the DET is flat so the error rates at the two thresholds are identical. The lines span 1% and 99% of boostrap replicated FNMR estimates.

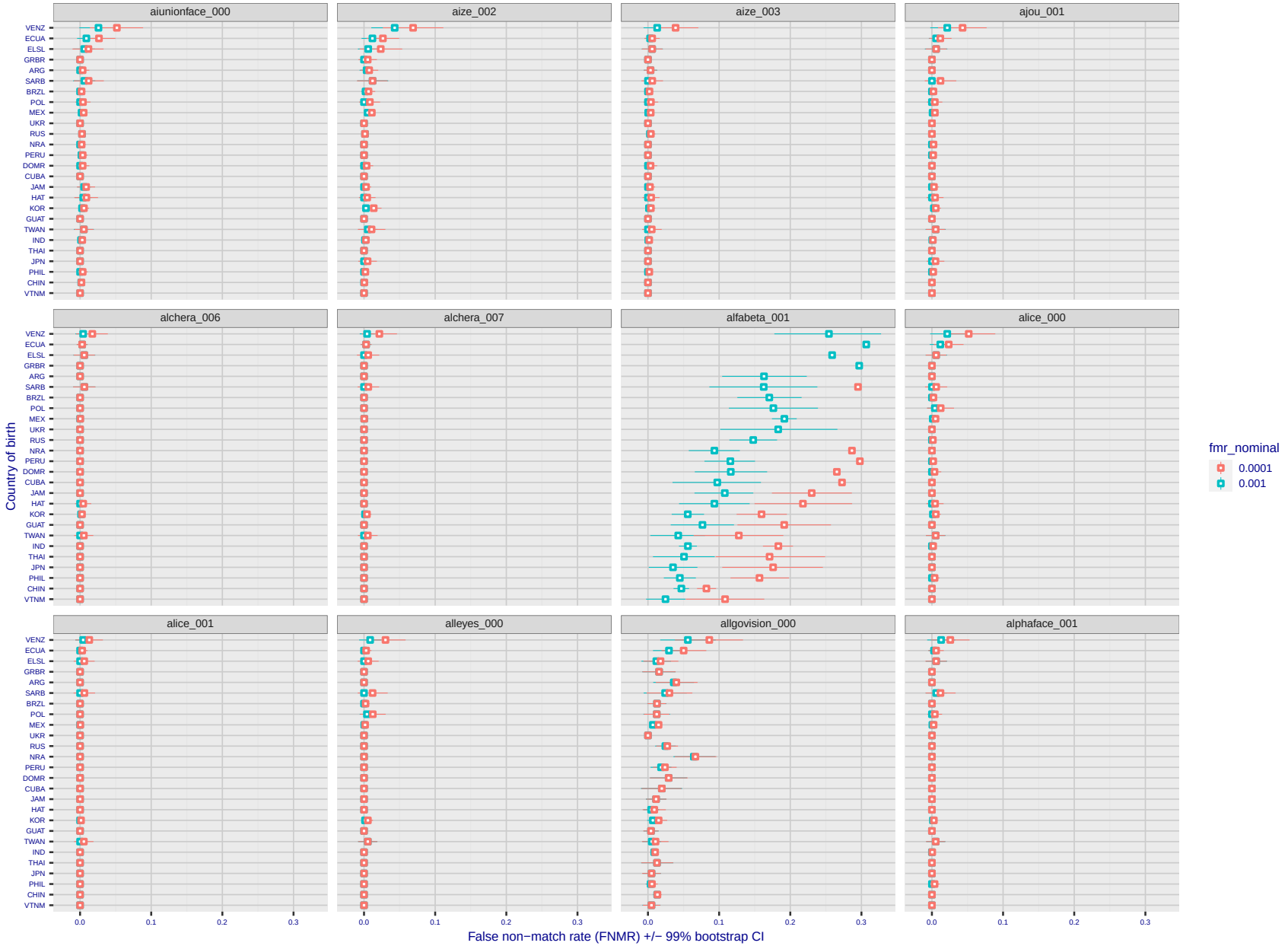

Figure 288: For the visa images, the dots show FNMR by country of birth for two globally set operating thresholds corresponding to FMR = $\{0.001, 0.0001\}$ computed over all on the order of 10^{10} impostor scores. The FMR in each bin will vary also - see subsequent impostor heatmaps in sec. 3.6.1. The figures shows an order of magnitude variation in FNMR across country of birth; these effects are likely due quality variations, then demographics like age and race. The error rates in some cases are zero, and in others the DET is flat so the error rates at the two thresholds are identical. The lines span 1% and 99% of boostrap replicated FNMR estimates.

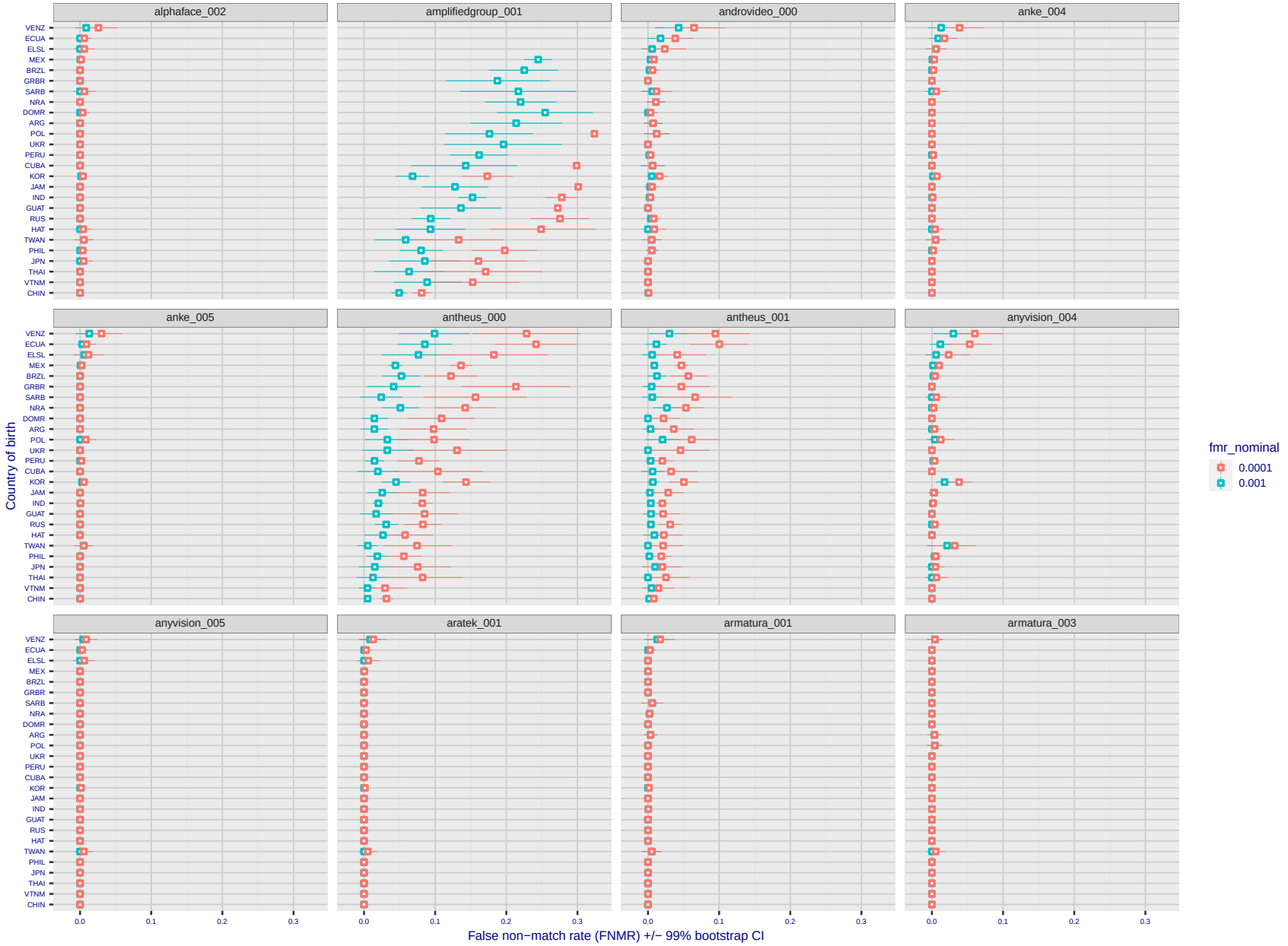

Figure 289: For the visa images, the dots show FNMR by country of birth for two globally set operating thresholds corresponding to FMR = $\{0.001, 0.0001\}$ computed over all on the order of 10^{10} impostor scores. The FMR in each bin will vary also - see subsequent impostor heatmaps in sec. 3.6.1. The figures shows an order of magnitude variation in FNMR across country of birth; these effects are likely due quality variations, then demographics like age and race. The error rates in some cases are zero, and in others the DET is flat so the error rates at the two thresholds are identical. The lines span 1% and 99% of boostrap replicated FNMR estimates.

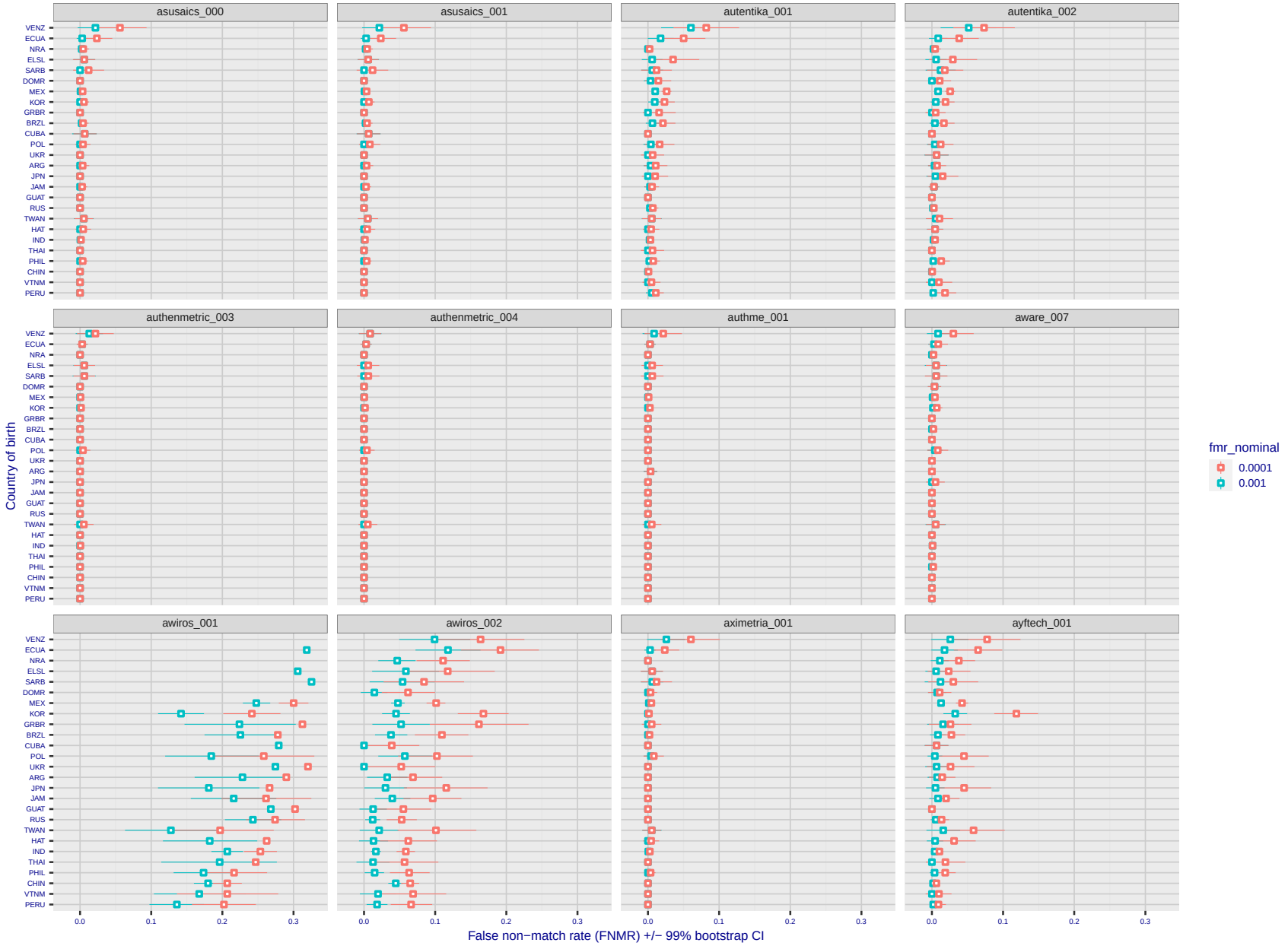

Figure 290: For the visa images, the dots show FNMR by country of birth for two globally set operating thresholds corresponding to FMR = $\{0.001, 0.0001\}$ computed over all on the order of 10^{10} impostor scores. The FMR in each bin will vary also - see subsequent impostor heatmaps in sec. 3.6.1. The figures shows an order of magnitude variation in FNMR across country of birth; these effects are likely due quality variations, then demographics like age and race. The error rates in some cases are zero, and in others the DET is flat so the error rates at the two thresholds are identical. The lines span 1% and 99% of boostrap replicated FNMR estimates.

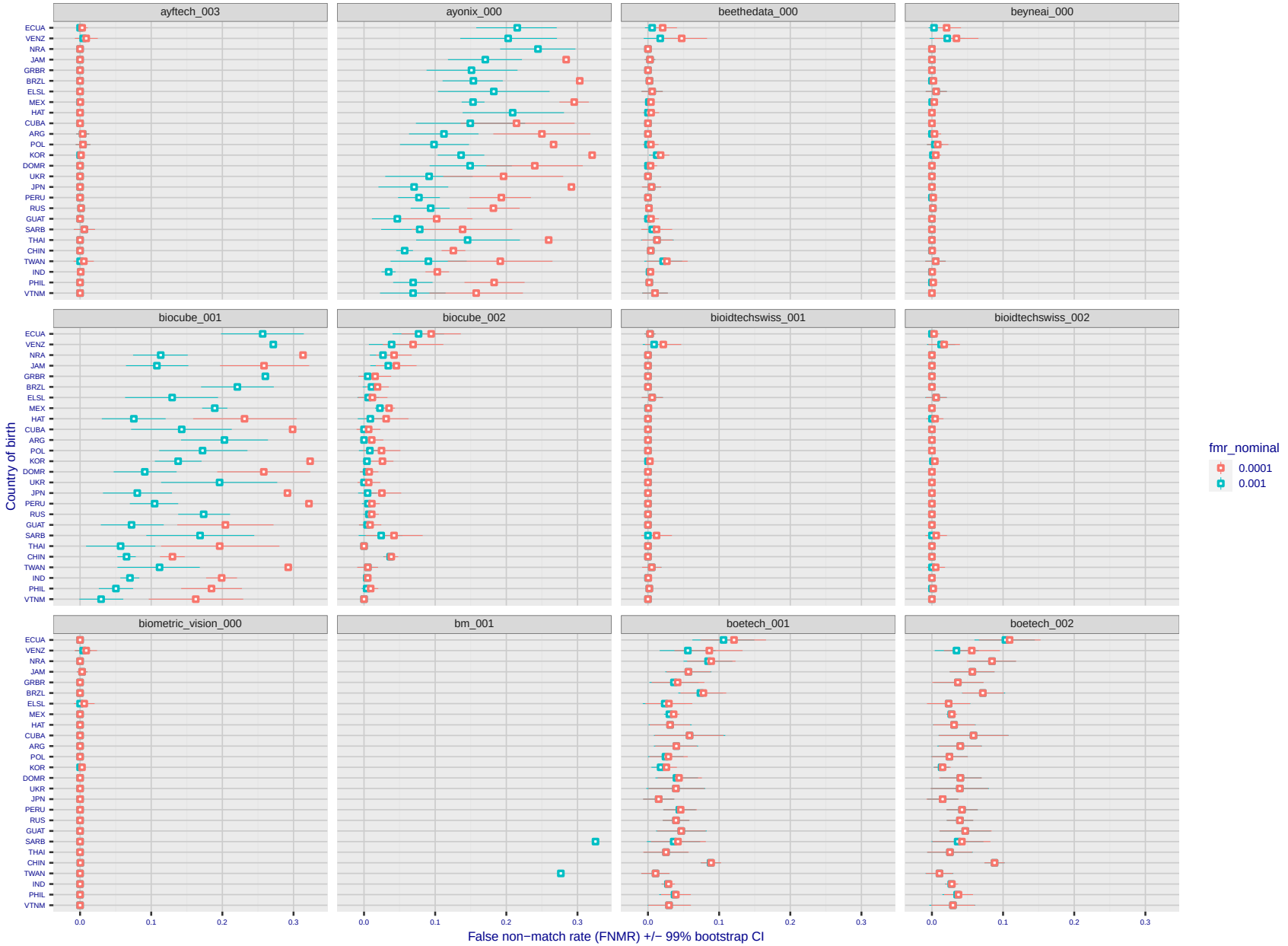

Figure 291: For the visa images, the dots show FNMR by country of birth for two globally set operating thresholds corresponding to FMR = $\{0.001, 0.0001\}$ computed over all on the order of 10^{10} impostor scores. The FMR in each bin will vary also - see subsequent impostor heatmaps in sec. 3.6.1. The figures shows an order of magnitude variation in FNMR across country of birth; these effects are likely due quality variations, then demographics like age and race. The error rates in some cases are zero, and in others the DET is flat so the error rates at the two thresholds are identical. The lines span 1% and 99% of boostrap replicated FNMR estimates.

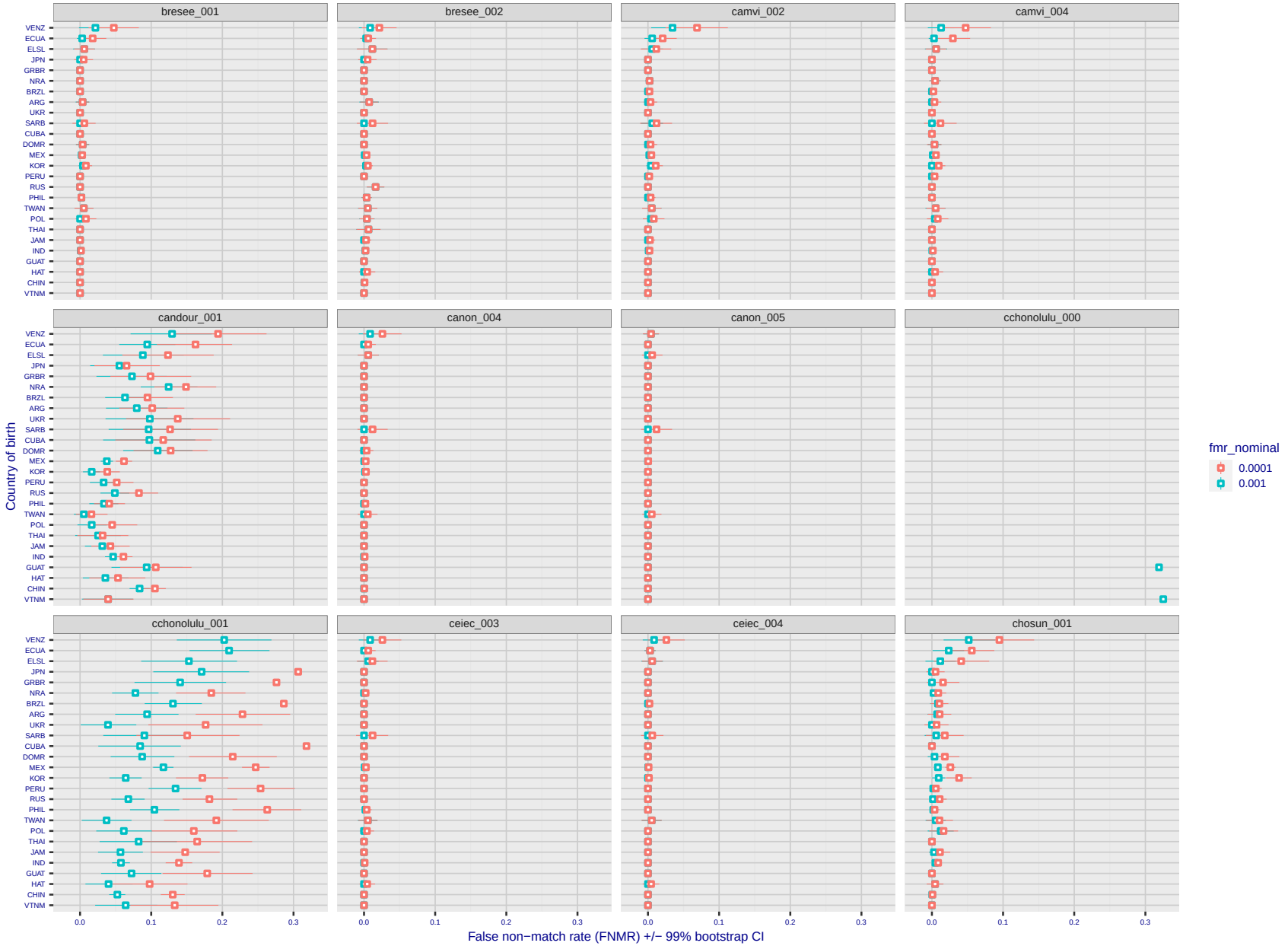

Figure 292: For the visa images, the dots show FNMR by country of birth for two globally set operating thresholds corresponding to FMR = $\{0.001, 0.0001\}$ computed over all on the order of 10^{10} impostor scores. The FMR in each bin will vary also - see subsequent impostor heatmaps in sec. 3.6.1. The figures shows an order of magnitude variation in FNMR across country of birth; these effects are likely due quality variations, then demographics like age and race. The error rates in some cases are zero, and in others the DET is flat so the error rates at the two thresholds are identical. The lines span 1% and 99% of boostrap replicated FNMR estimates.

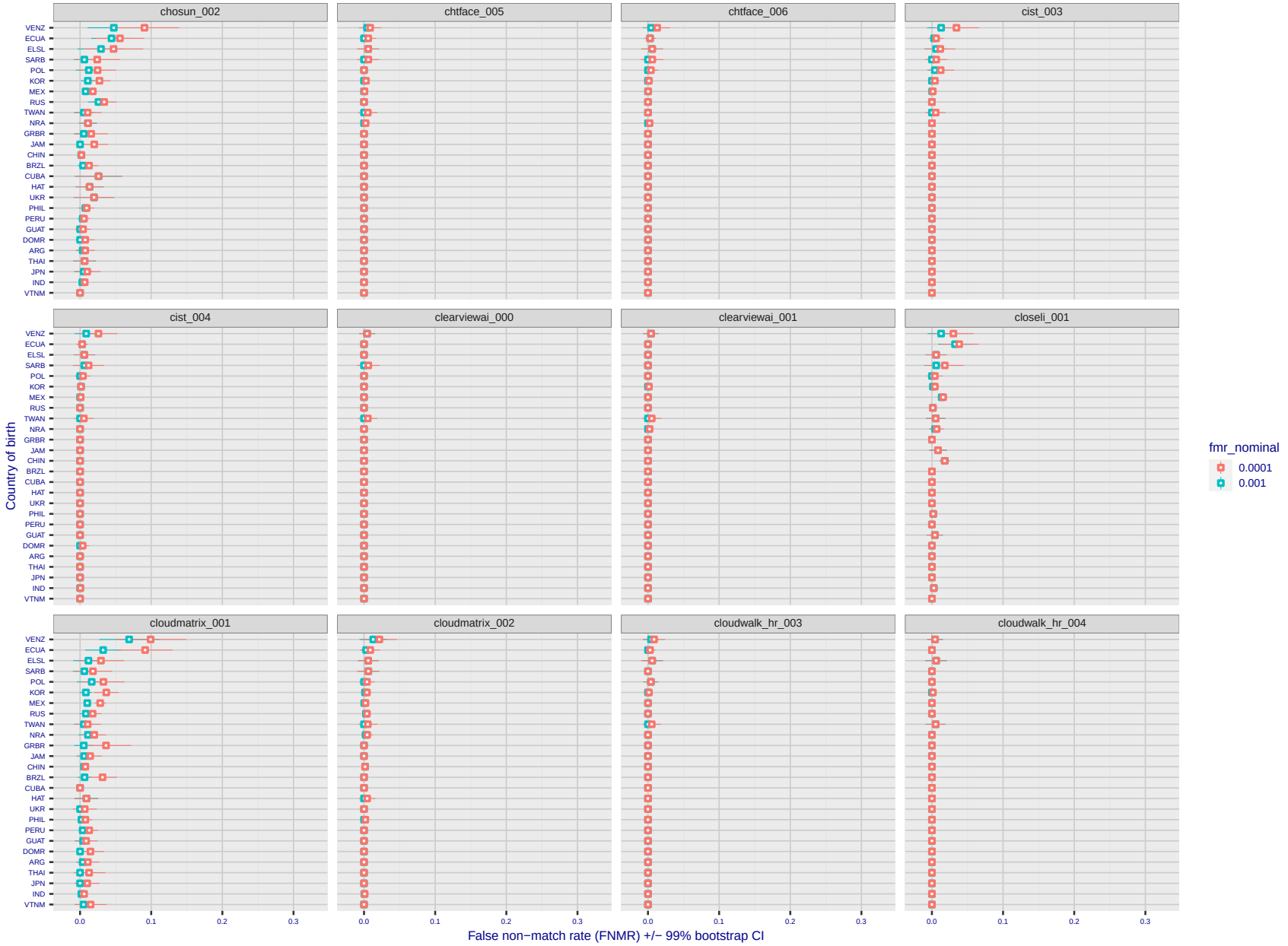

Figure 293: For the visa images, the dots show FNMR by country of birth for two globally set operating thresholds corresponding to FMR = $\{0.001, 0.0001\}$ computed over all on the order of 10^{10} impostor scores. The FMR in each bin will vary also - see subsequent impostor heatmaps in sec. 3.6.1. The figures shows an order of magnitude variation in FNMR across country of birth; these effects are likely due quality variations, then demographics like age and race. The error rates in some cases are zero, and in others the DET is flat so the error rates at the two thresholds are identical. The lines span 1% and 99% of boostrap replicated FNMR estimates.

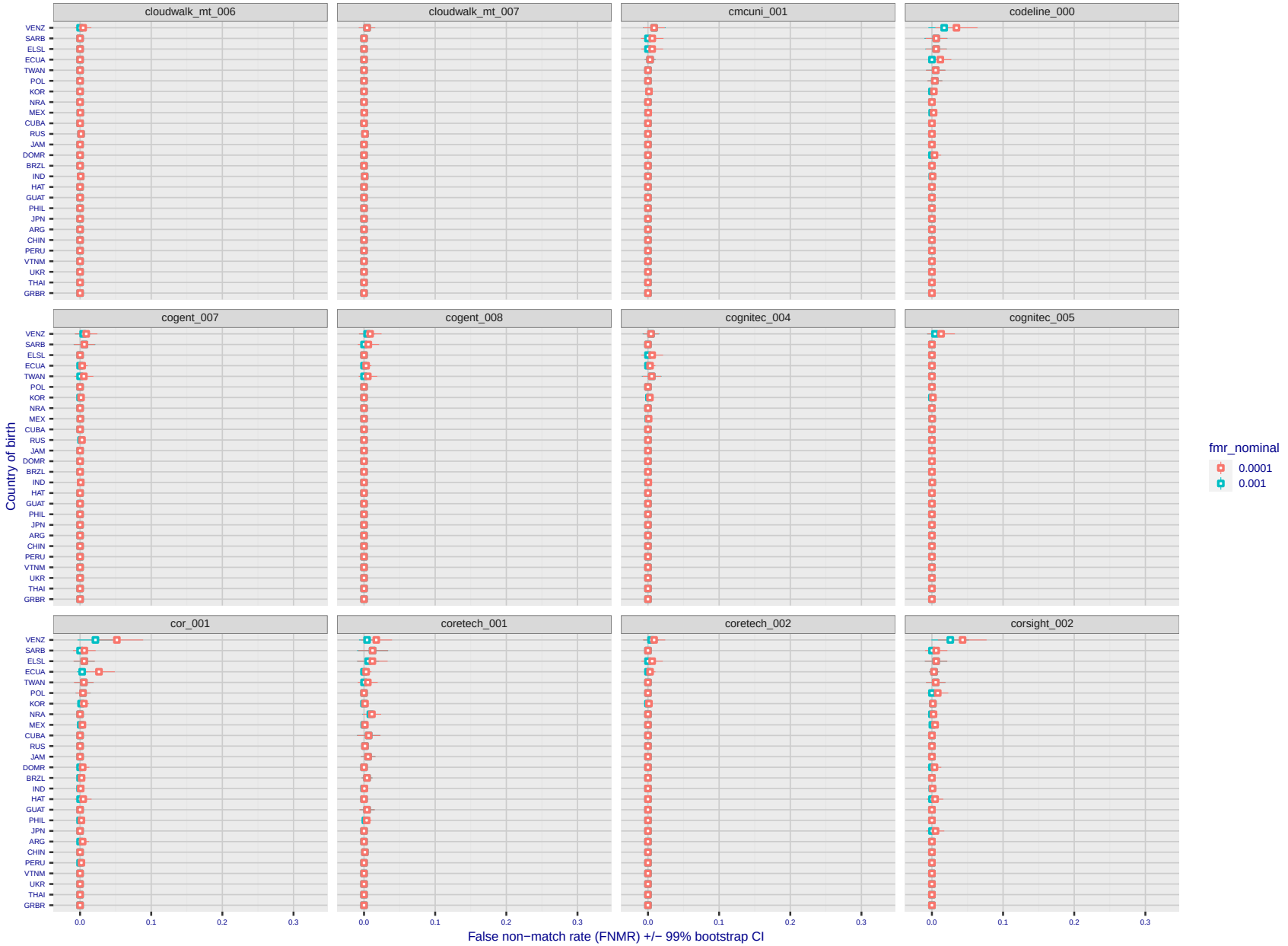

Figure 294: For the visa images, the dots show FNMR by country of birth for two globally set operating thresholds corresponding to FMR = $\{0.001, 0.0001\}$ computed over all on the order of 10^{10} impostor scores. The FMR in each bin will vary also - see subsequent impostor heatmaps in sec. 3.6.1. The figures shows an order of magnitude variation in FNMR across country of birth; these effects are likely due quality variations, then demographics like age and race. The error rates in some cases are zero, and in others the DET is flat so the error rates at the two thresholds are identical. The lines span 1% and 99% of boostrap replicated FNMR estimates.

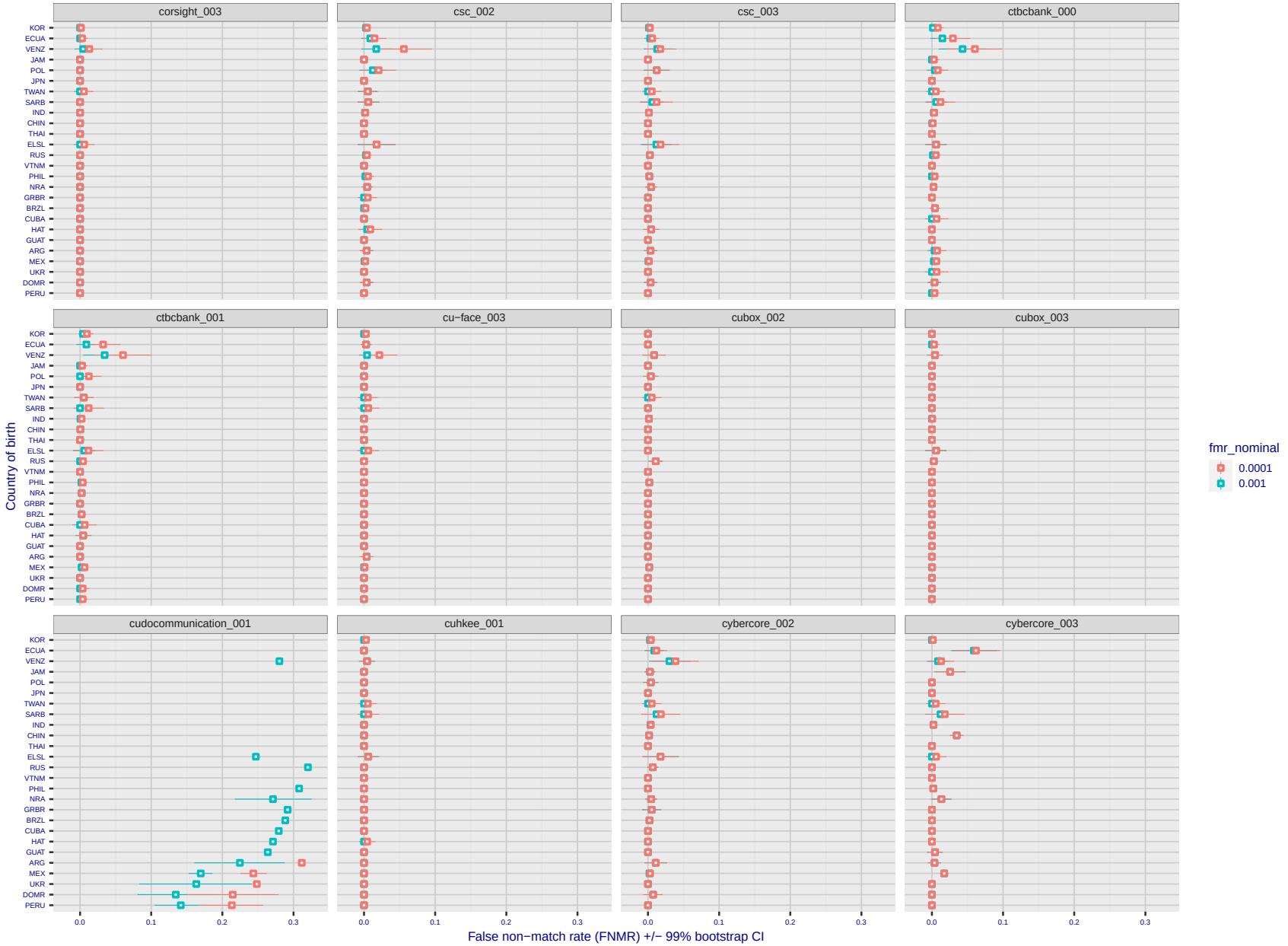

Figure 295: For the visa images, the dots show FNMR by country of birth for two globally set operating thresholds corresponding to FMR = $\{0.001, 0.0001\}$ computed over all on the order of 10^{10} impostor scores. The FMR in each bin will vary also - see subsequent impostor heatmaps in sec. 3.6.1. The figures shows an order of magnitude variation in FNMR across country of birth; these effects are likely due quality variations, then demographics like age and race. The error rates in some cases are zero, and in others the DET is flat so the error rates at the two thresholds are identical. The lines span 1% and 99% of boostrap replicated FNMR estimates.

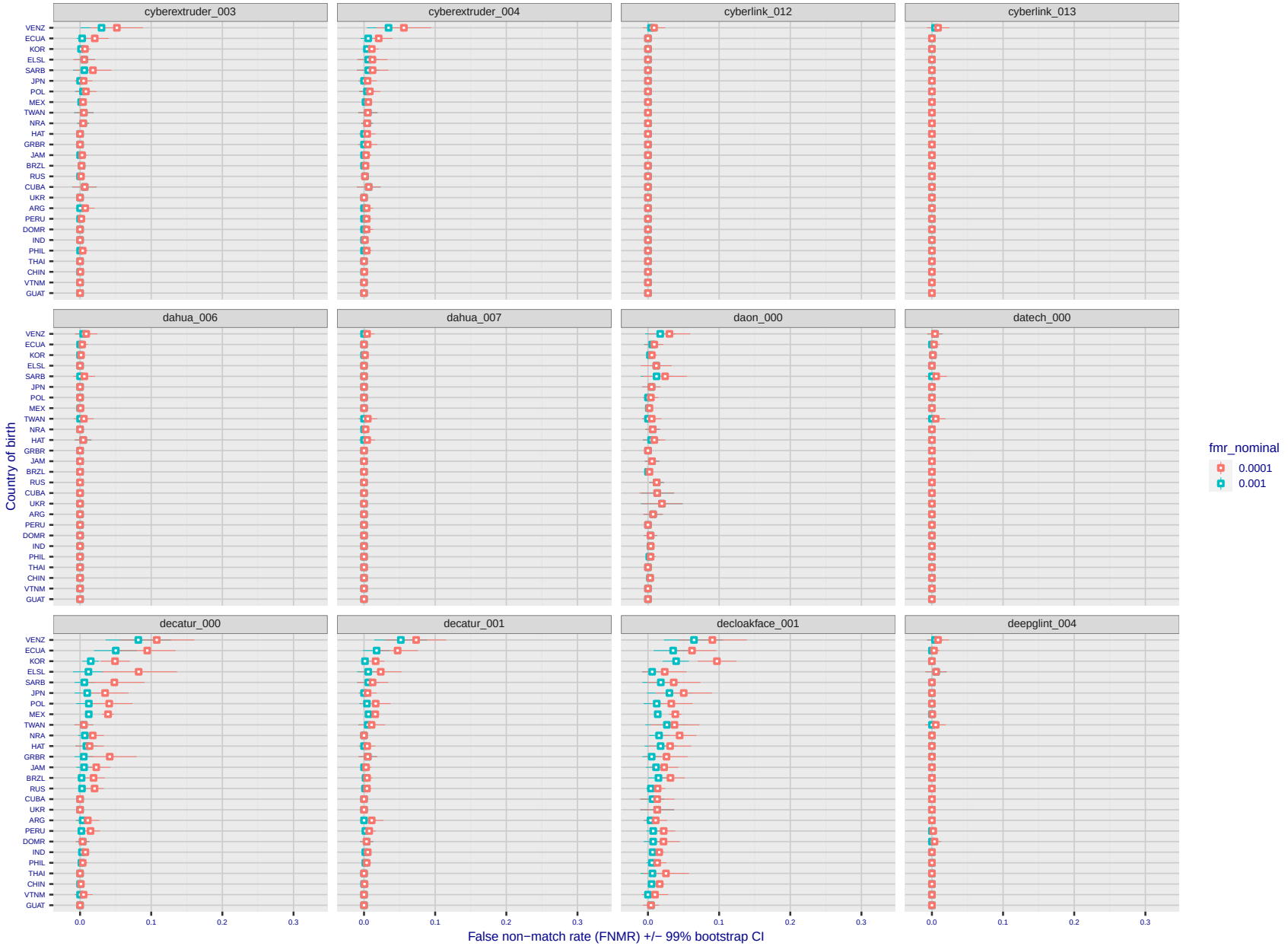

Figure 296: For the visa images, the dots show FNMR by country of birth for two globally set operating thresholds corresponding to FMR = $\{0.001, 0.0001\}$ computed over all on the order of 10^{10} impostor scores. The FMR in each bin will vary also - see subsequent impostor heatmaps in sec. 3.6.1. The figures shows an order of magnitude variation in FNMR across country of birth; these effects are likely due quality variations, then demographics like age and race. The error rates in some cases are zero, and in others the DET is flat so the error rates at the two thresholds are identical. The lines span 1% and 99% of boostrap replicated FNMR estimates.

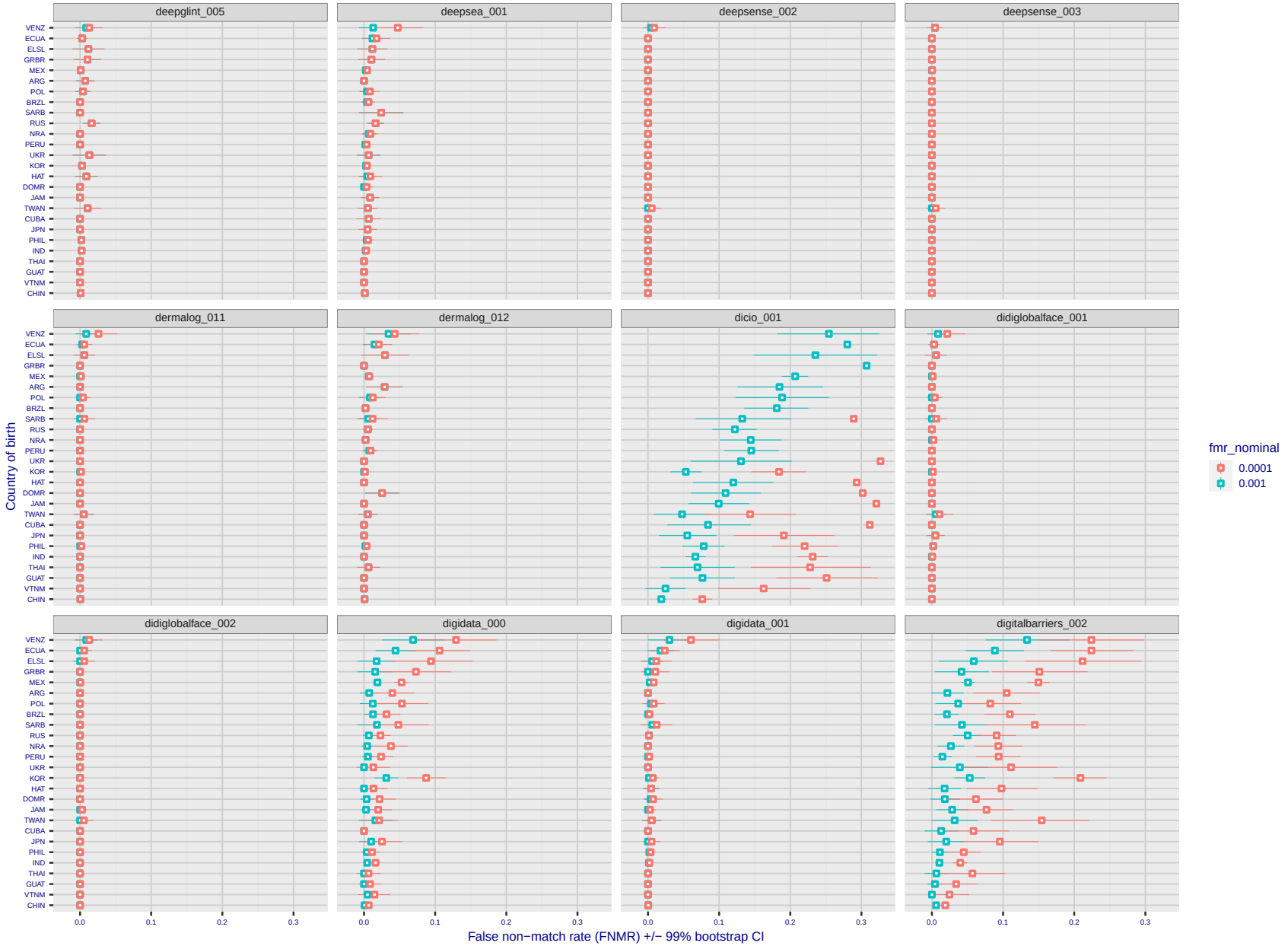

Figure 297: For the visa images, the dots show FNMR by country of birth for two globally set operating thresholds corresponding to FMR = $\{0.001, 0.0001\}$ computed over all on the order of 10^{10} impostor scores. The FMR in each bin will vary also - see subsequent impostor heatmaps in sec. 3.6.1. The figures shows an order of magnitude variation in FNMR across country of birth; these effects are likely due quality variations, then demographics like age and race. The error rates in some cases are zero, and in others the DET is flat so the error rates at the two thresholds are identical. The lines span 1% and 99% of boostrap replicated FNMR estimates.

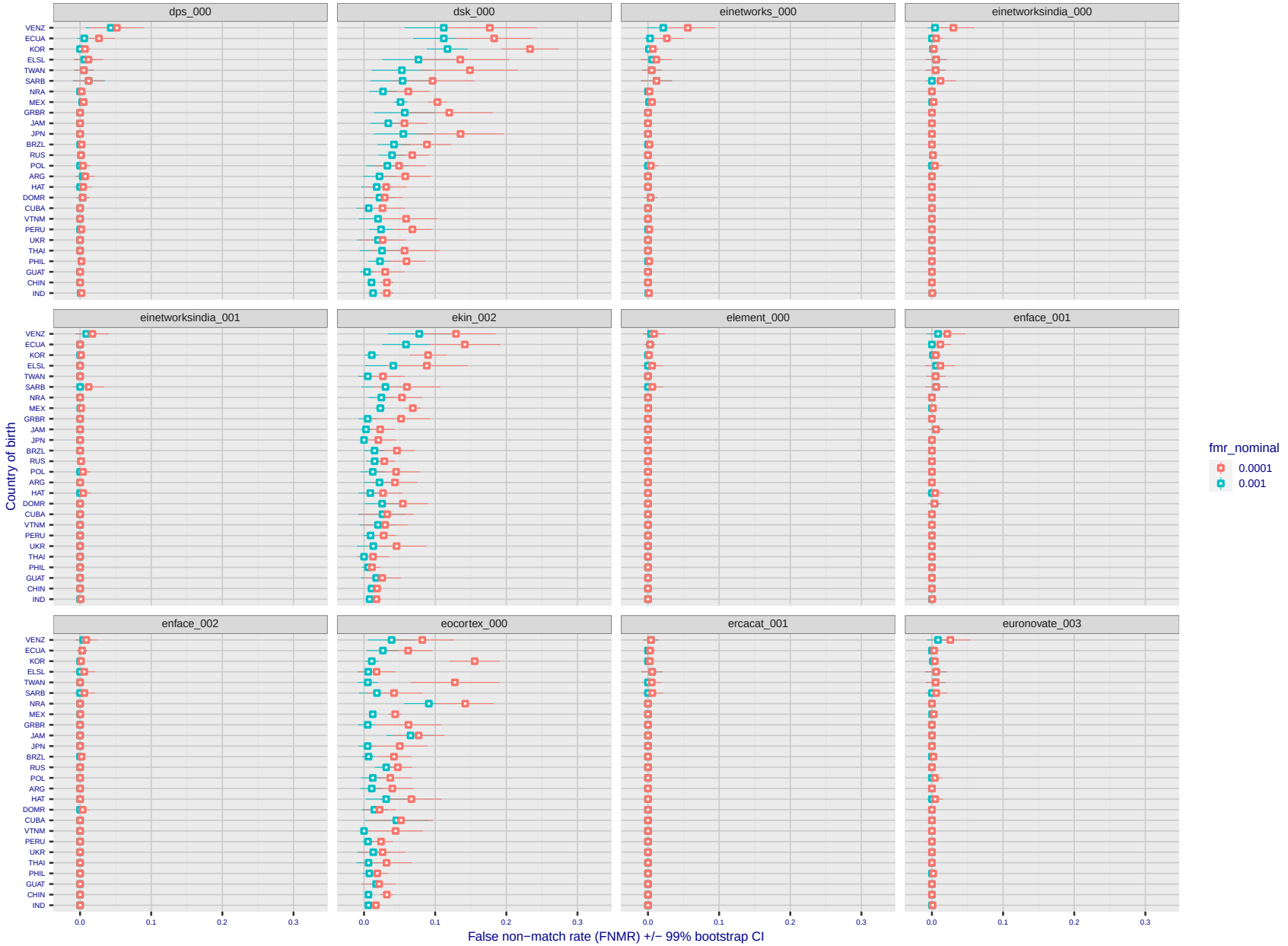

Figure 298: For the visa images, the dots show FNMR by country of birth for two globally set operating thresholds corresponding to FMR = $\{0.001, 0.0001\}$ computed over all on the order of 10^{10} impostor scores. The FMR in each bin will vary also - see subsequent impostor heatmaps in sec. 3.6.1. The figures shows an order of magnitude variation in FNMR across country of birth; these effects are likely due quality variations, then demographics like age and race. The error rates in some cases are zero, and in others the DET is flat so the error rates at the two thresholds are identical. The lines span 1% and 99% of boostrap replicated FNMR estimates.

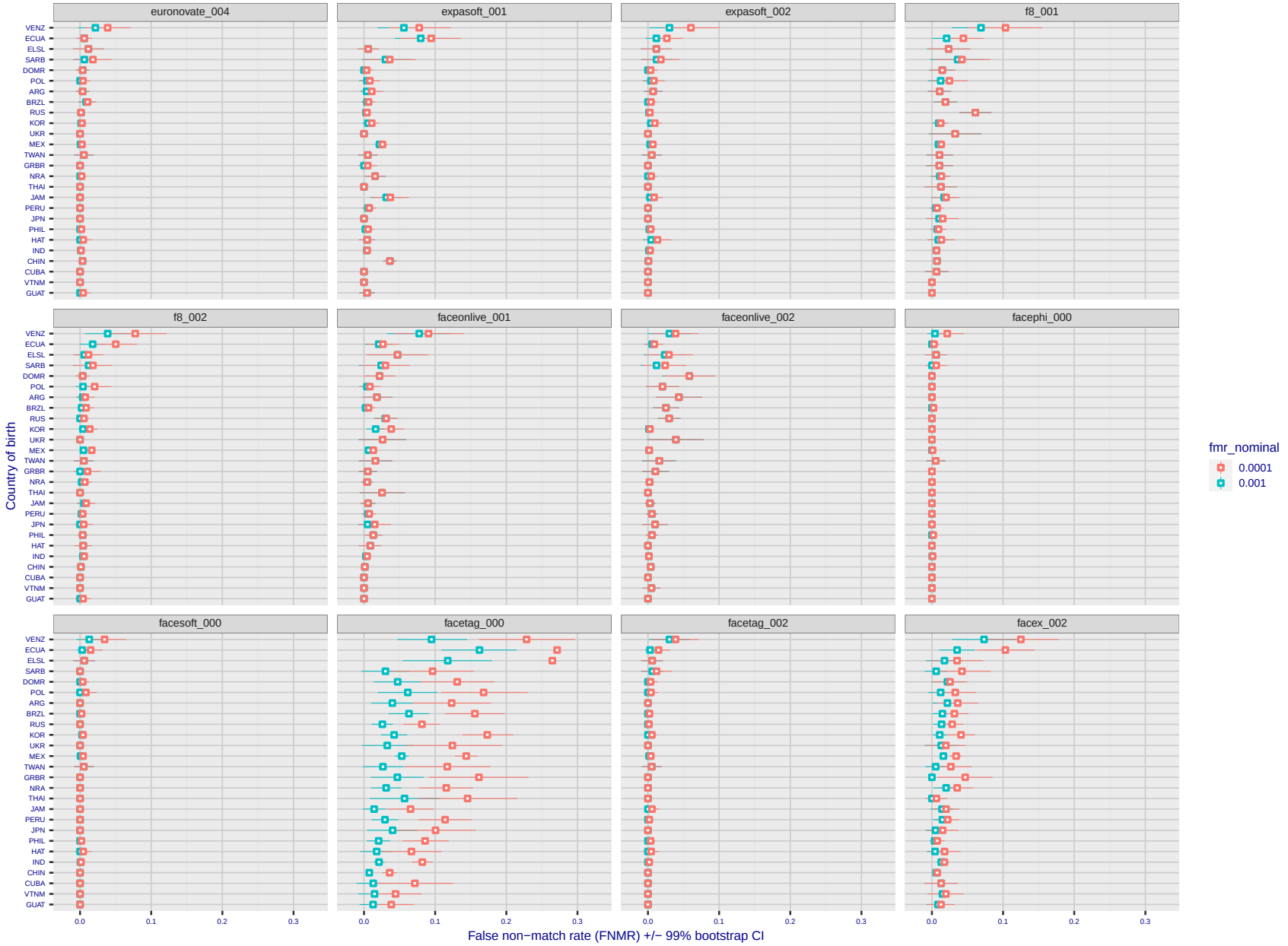

Figure 299: For the visa images, the dots show FNMR by country of birth for two globally set operating thresholds corresponding to FMR = $\{0.001, 0.0001\}$ computed over all on the order of 10^{10} impostor scores. The FMR in each bin will vary also - see subsequent impostor heatmaps in sec. 3.6.1. The figures shows an order of magnitude variation in FNMR across country of birth; these effects are likely due quality variations, then demographics like age and race. The error rates in some cases are zero, and in others the DET is flat so the error rates at the two thresholds are identical. The lines span 1% and 99% of boostrap replicated FNMR estimates.

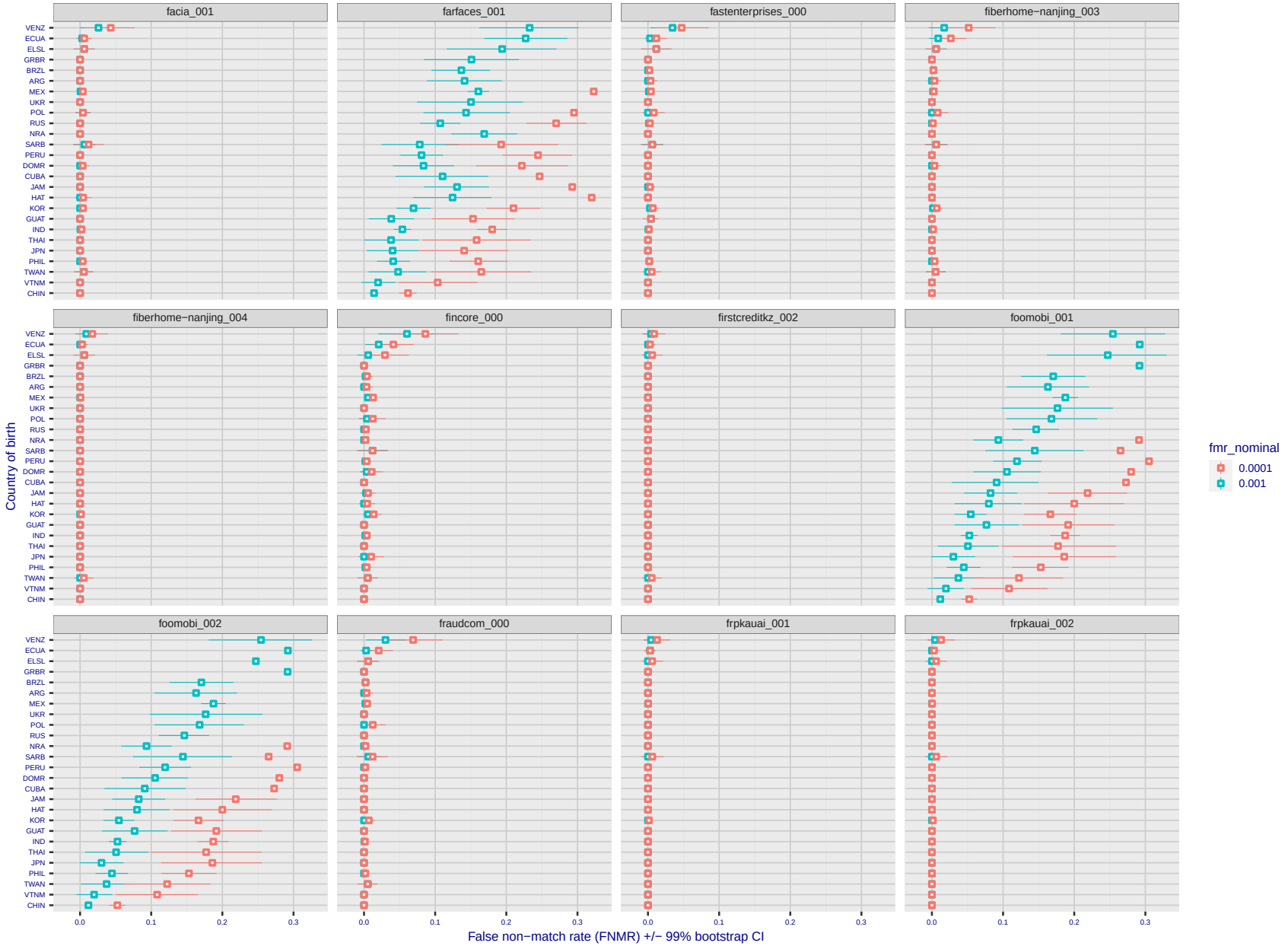

Figure 300: For the visa images, the dots show FNMR by country of birth for two globally set operating thresholds corresponding to FMR = $\{0.001, 0.0001\}$ computed over all on the order of 10^{10} impostor scores. The FMR in each bin will vary also - see subsequent impostor heatmaps in sec. 3.6.1. The figures shows an order of magnitude variation in FNMR across country of birth; these effects are likely due quality variations, then demographics like age and race. The error rates in some cases are zero, and in others the DET is flat so the error rates at the two thresholds are identical. The lines span 1% and 99% of boostrap replicated FNMR estimates.

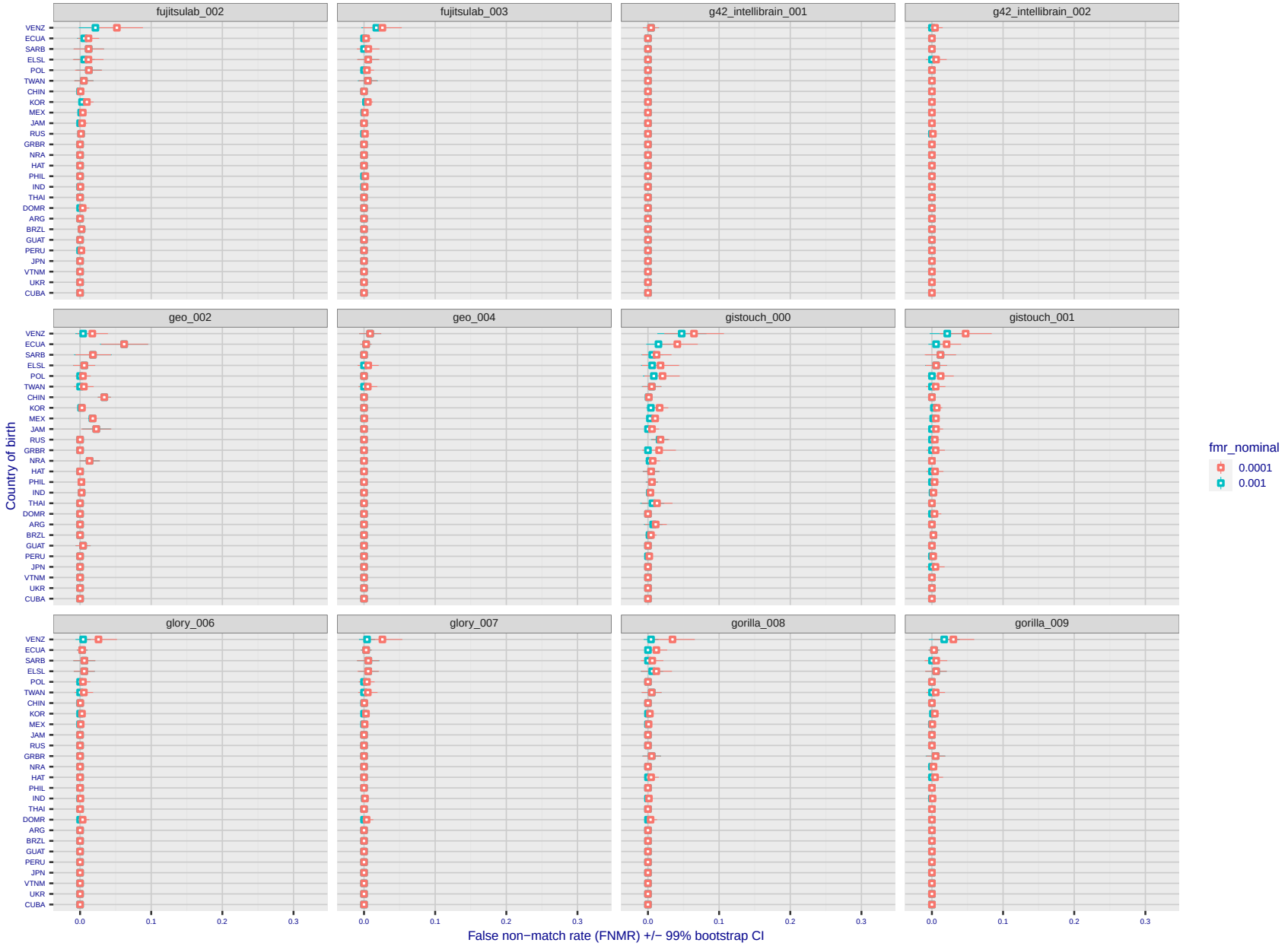

Figure 301: For the visa images, the dots show FNMR by country of birth for two globally set operating thresholds corresponding to FMR = $\{0.001, 0.0001\}$ computed over all on the order of 10^{10} impostor scores. The FMR in each bin will vary also - see subsequent impostor heatmaps in sec. 3.6.1. The figures shows an order of magnitude variation in FNMR across country of birth; these effects are likely due quality variations, then demographics like age and race. The error rates in some cases are zero, and in others the DET is flat so the error rates at the two thresholds are identical. The lines span 1% and 99% of boostrap replicated FNMR estimates.

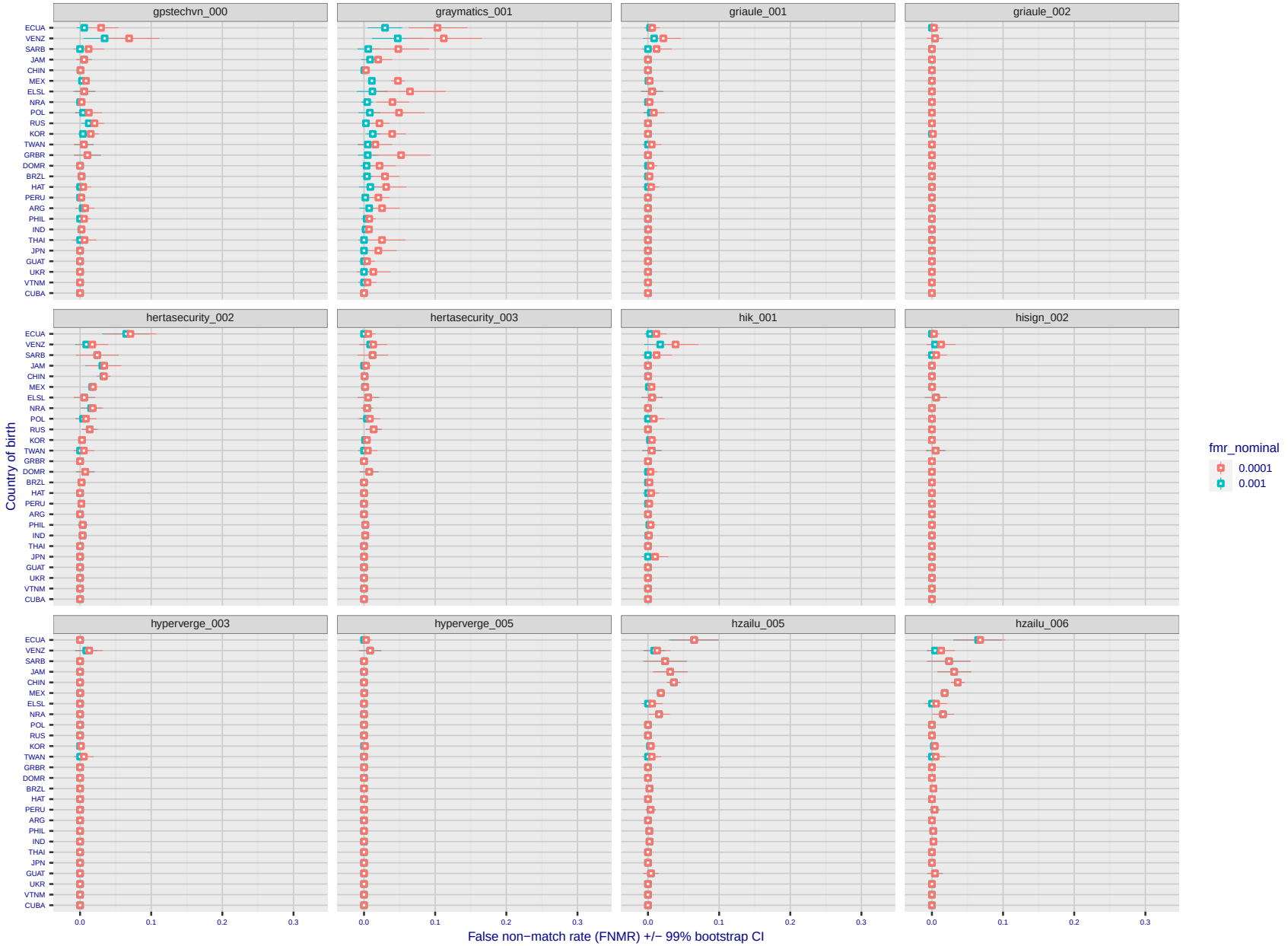

Figure 302: For the visa images, the dots show FNMR by country of birth for two globally set operating thresholds corresponding to FMR = $\{0.001, 0.0001\}$ computed over all on the order of 10^{10} impostor scores. The FMR in each bin will vary also - see subsequent impostor heatmaps in sec. 3.6.1. The figures shows an order of magnitude variation in FNMR across country of birth; these effects are likely due quality variations, then demographics like age and race. The error rates in some cases are zero, and in others the DET is flat so the error rates at the two thresholds are identical. The lines span 1% and 99% of boostrap replicated FNMR estimates.

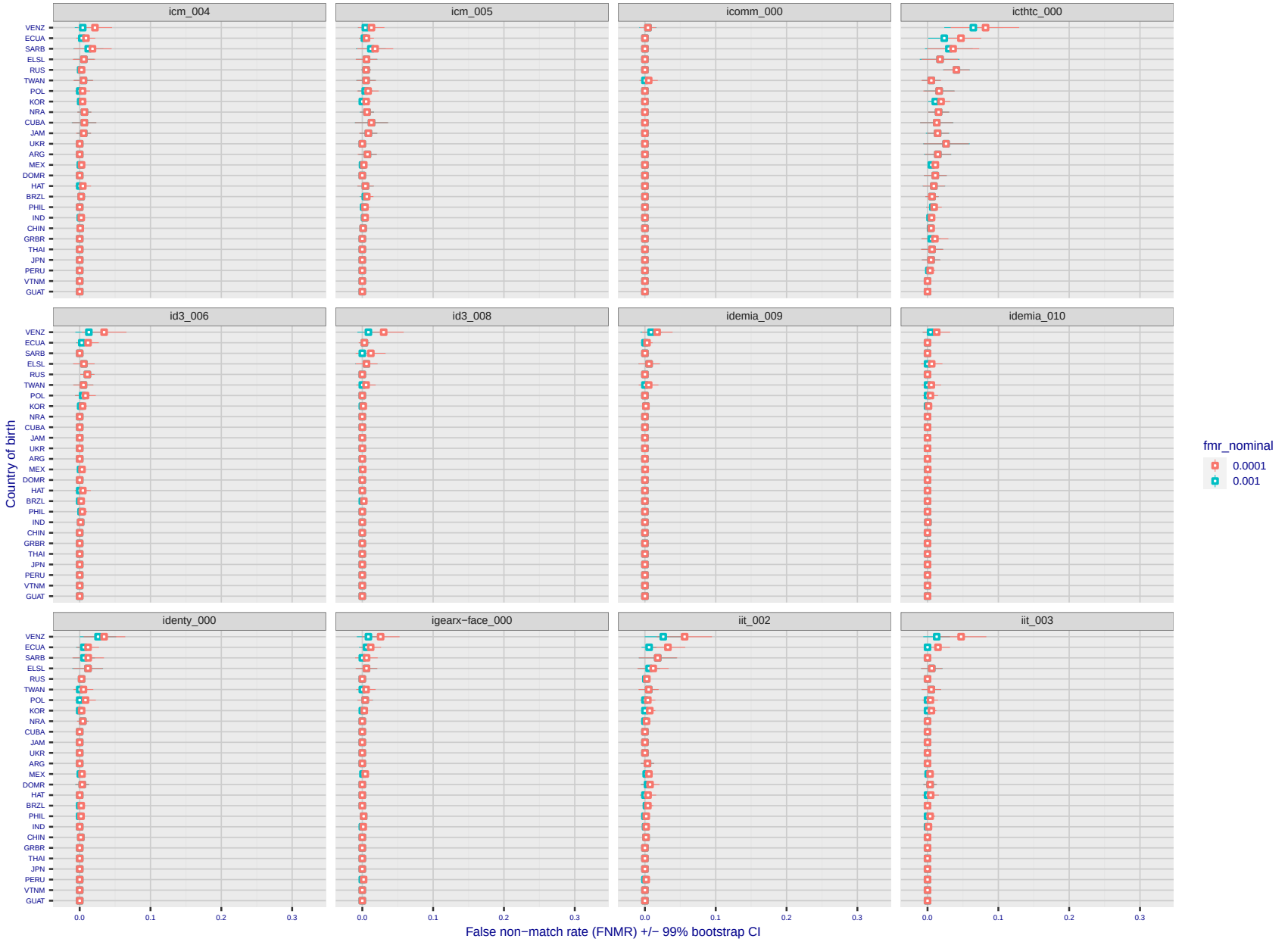

Figure 303: For the visa images, the dots show FNMR by country of birth for two globally set operating thresholds corresponding to FMR = $\{0.001, 0.0001\}$ computed over all on the order of 10^{10} impostor scores. The FMR in each bin will vary also - see subsequent impostor heatmaps in sec. 3.6.1. The figures shows an order of magnitude variation in FNMR across country of birth; these effects are likely due quality variations, then demographics like age and race. The error rates in some cases are zero, and in others the DET is flat so the error rates at the two thresholds are identical. The lines span 1% and 99% of boostrap replicated FNMR estimates.

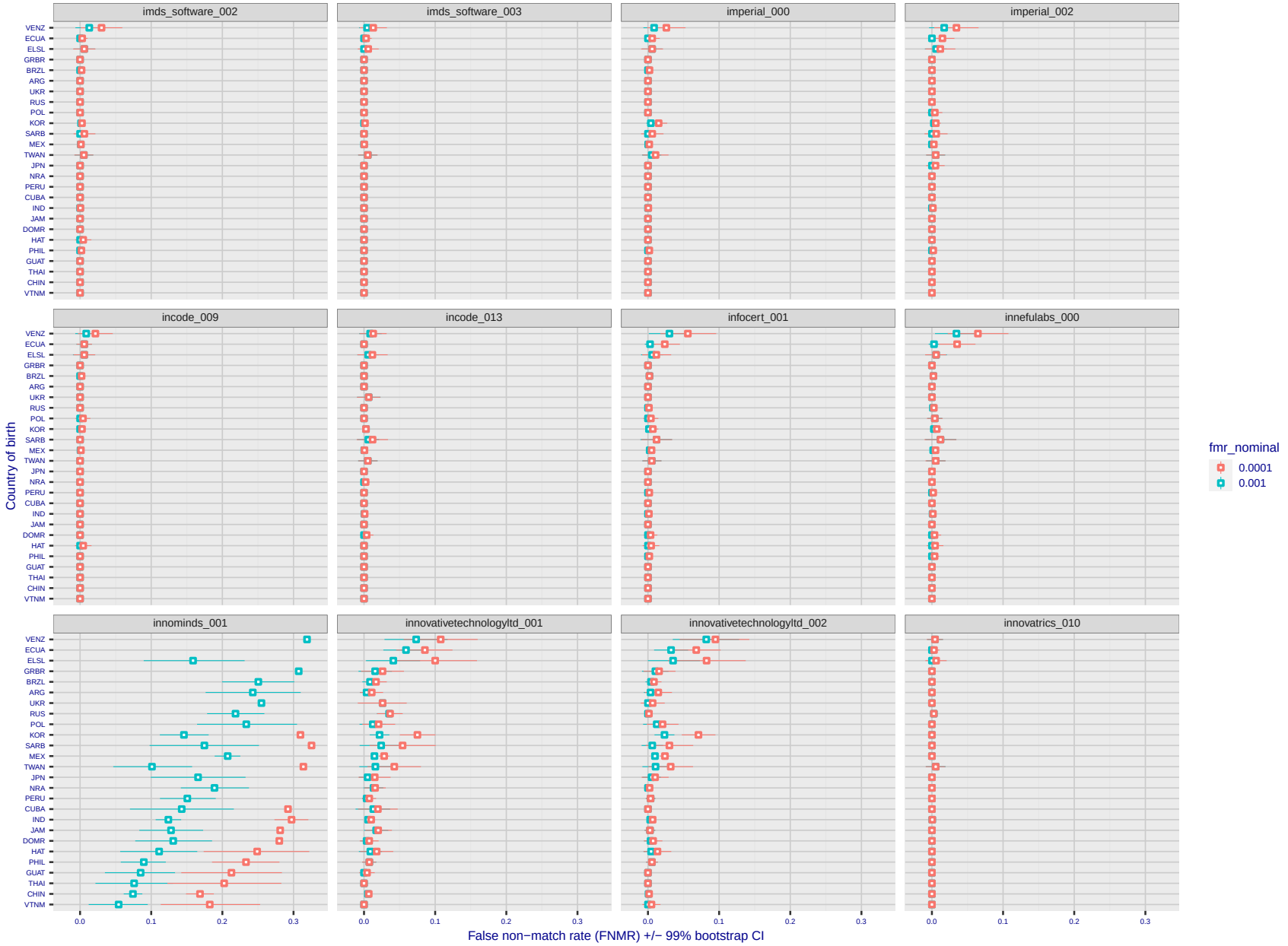

Figure 304: For the visa images, the dots show FNMR by country of birth for two globally set operating thresholds corresponding to FMR = $\{0.001, 0.0001\}$ computed over all on the order of 10^{10} impostor scores. The FMR in each bin will vary also - see subsequent impostor heatmaps in sec. 3.6.1. The figures shows an order of magnitude variation in FNMR across country of birth; these effects are likely due quality variations, then demographics like age and race. The error rates in some cases are zero, and in others the DET is flat so the error rates at the two thresholds are identical. The lines span 1% and 99% of boostrap replicated FNMR estimates.

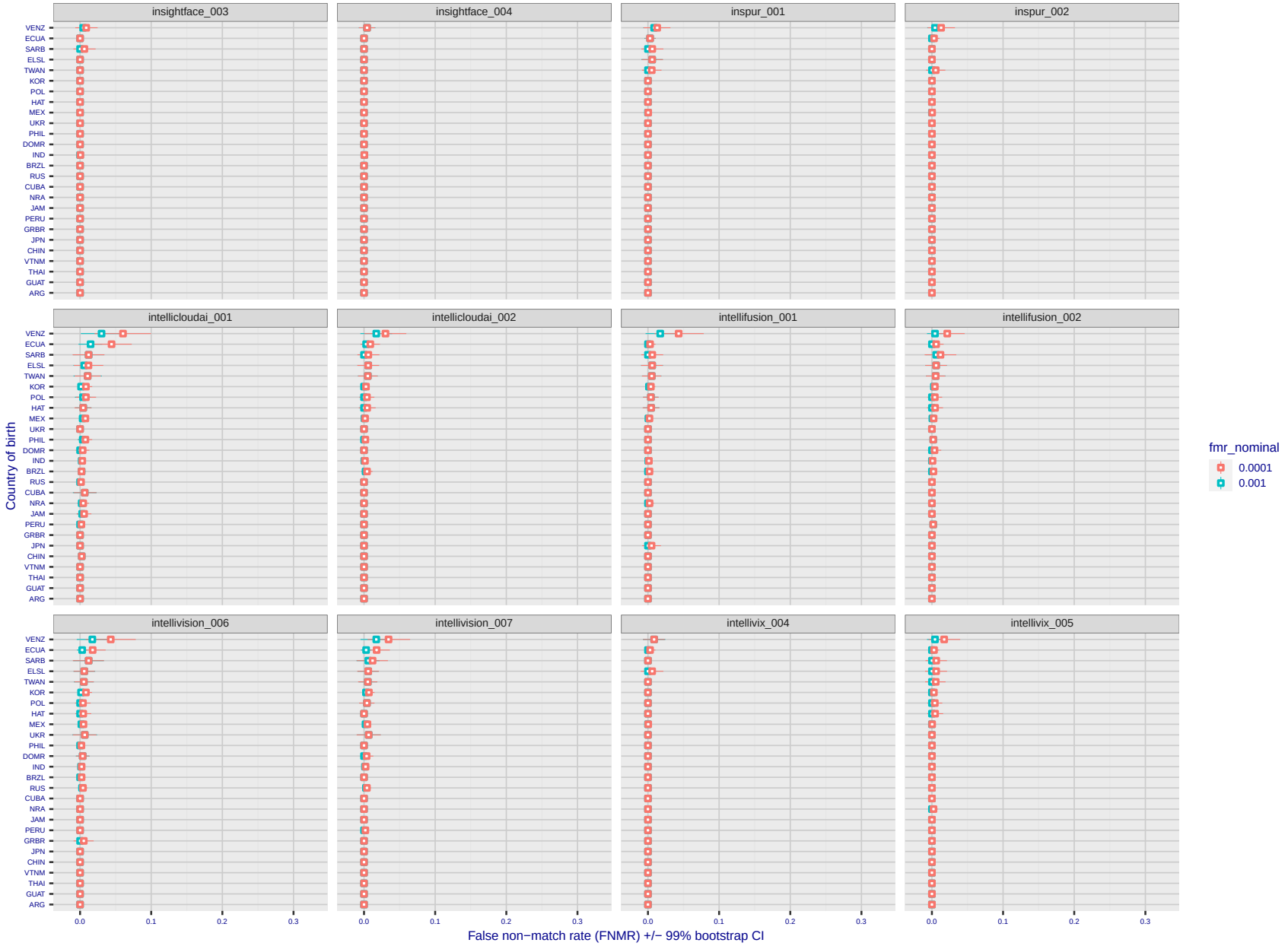

Figure 305: For the visa images, the dots show FNMR by country of birth for two globally set operating thresholds corresponding to FMR = $\{0.001, 0.0001\}$ computed over all on the order of 10^{10} impostor scores. The FMR in each bin will vary also - see subsequent impostor heatmaps in sec. 3.6.1. The figures shows an order of magnitude variation in FNMR across country of birth; these effects are likely due quality variations, then demographics like age and race. The error rates in some cases are zero, and in others the DET is flat so the error rates at the two thresholds are identical. The lines span 1% and 99% of boostrap replicated FNMR estimates.

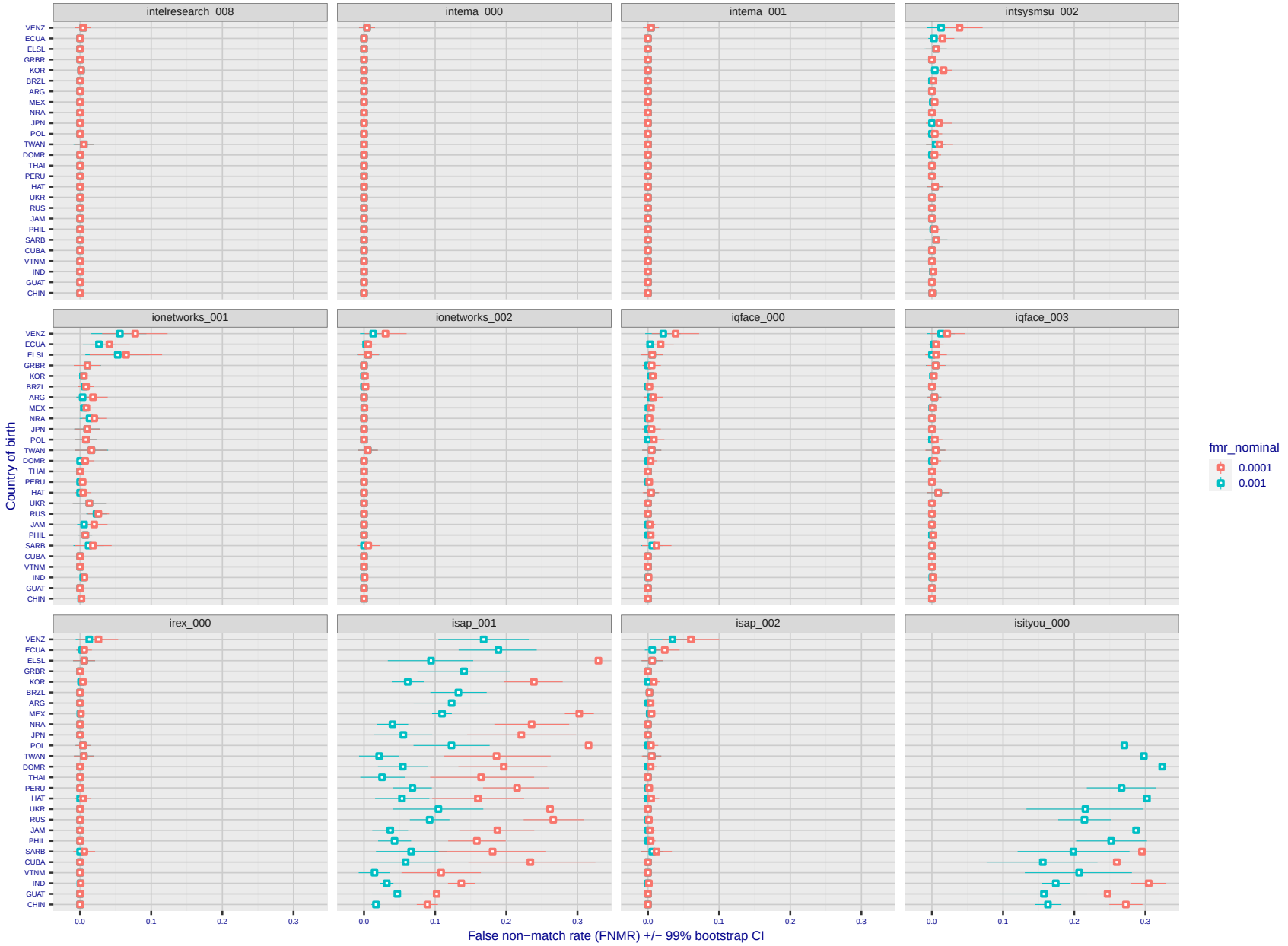

Figure 306: For the visa images, the dots show FNMR by country of birth for two globally set operating thresholds corresponding to FMR = $\{0.001, 0.0001\}$ computed over all on the order of 10^{10} impostor scores. The FMR in each bin will vary also - see subsequent impostor heatmaps in sec. 3.6.1. The figures shows an order of magnitude variation in FNMR across country of birth; these effects are likely due quality variations, then demographics like age and race. The error rates in some cases are zero, and in others the DET is flat so the error rates at the two thresholds are identical. The lines span 1% and 99% of boostrap replicated FNMR estimates.

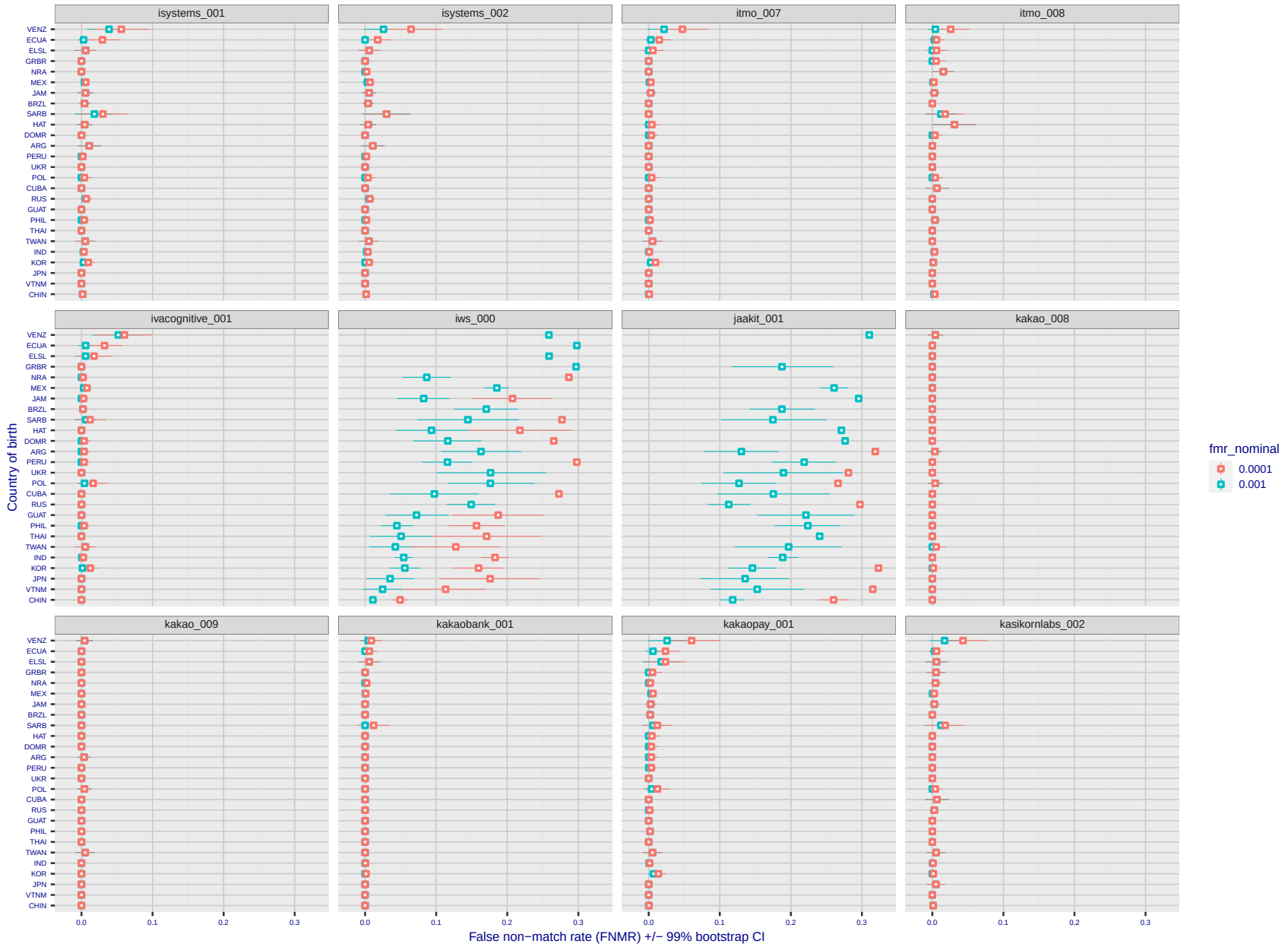

Figure 307: For the visa images, the dots show FNMR by country of birth for two globally set operating thresholds corresponding to FMR = $\{0.001, 0.0001\}$ computed over all on the order of 10^{10} impostor scores. The FMR in each bin will vary also - see subsequent impostor heatmaps in sec. 3.6.1. The figures shows an order of magnitude variation in FNMR across country of birth; these effects are likely due quality variations, then demographics like age and race. The error rates in some cases are zero, and in others the DET is flat so the error rates at the two thresholds are identical. The lines span 1% and 99% of boostrap replicated FNMR estimates.

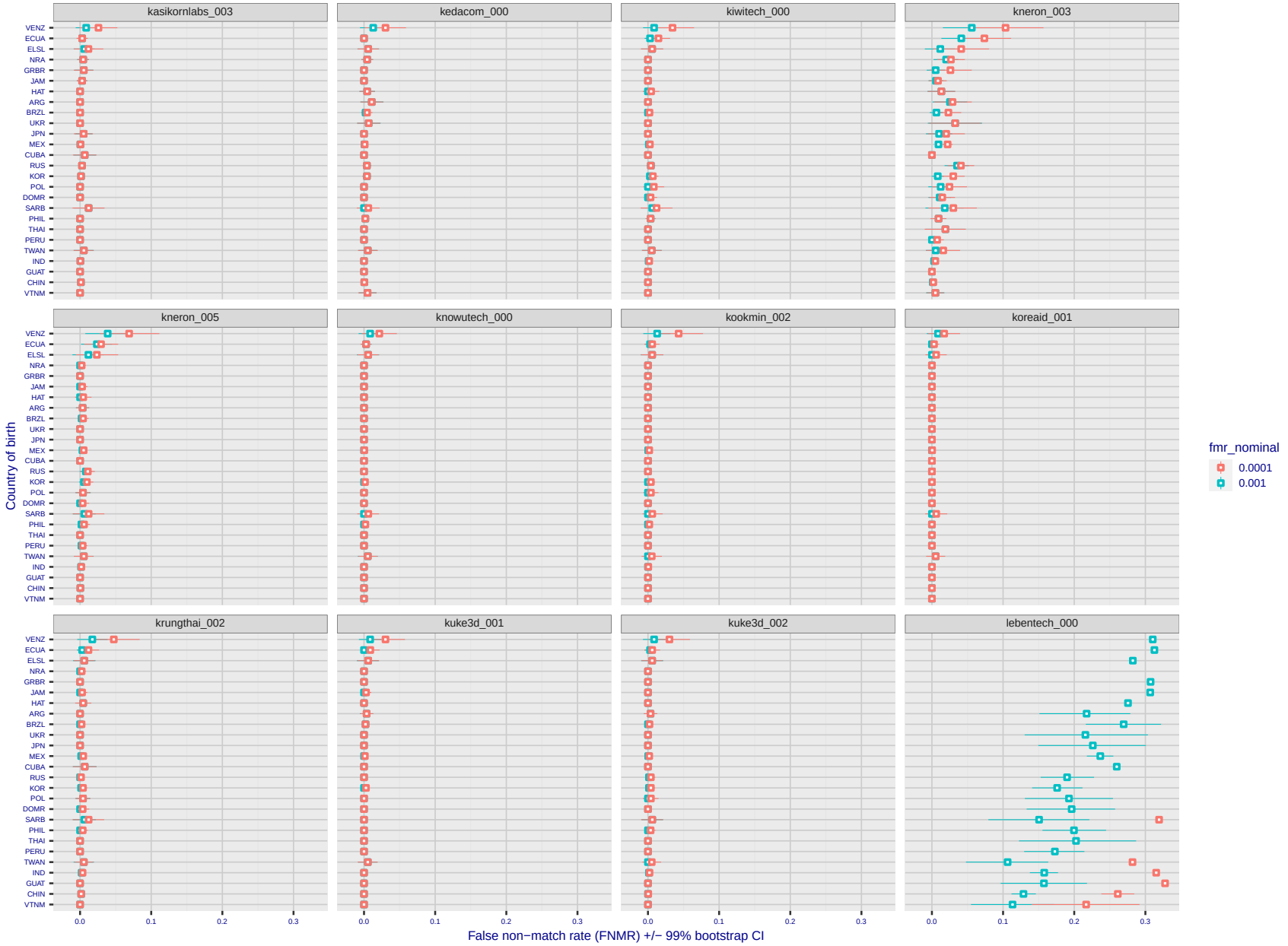

Figure 308: For the visa images, the dots show FNMR by country of birth for two globally set operating thresholds corresponding to FMR = $\{0.001, 0.0001\}$ computed over all on the order of 10^{10} impostor scores. The FMR in each bin will vary also - see subsequent impostor heatmaps in sec. 3.6.1. The figures shows an order of magnitude variation in FNMR across country of birth; these effects are likely due quality variations, then demographics like age and race. The error rates in some cases are zero, and in others the DET is flat so the error rates at the two thresholds are identical. The lines span 1% and 99% of boostrap replicated FNMR estimates.

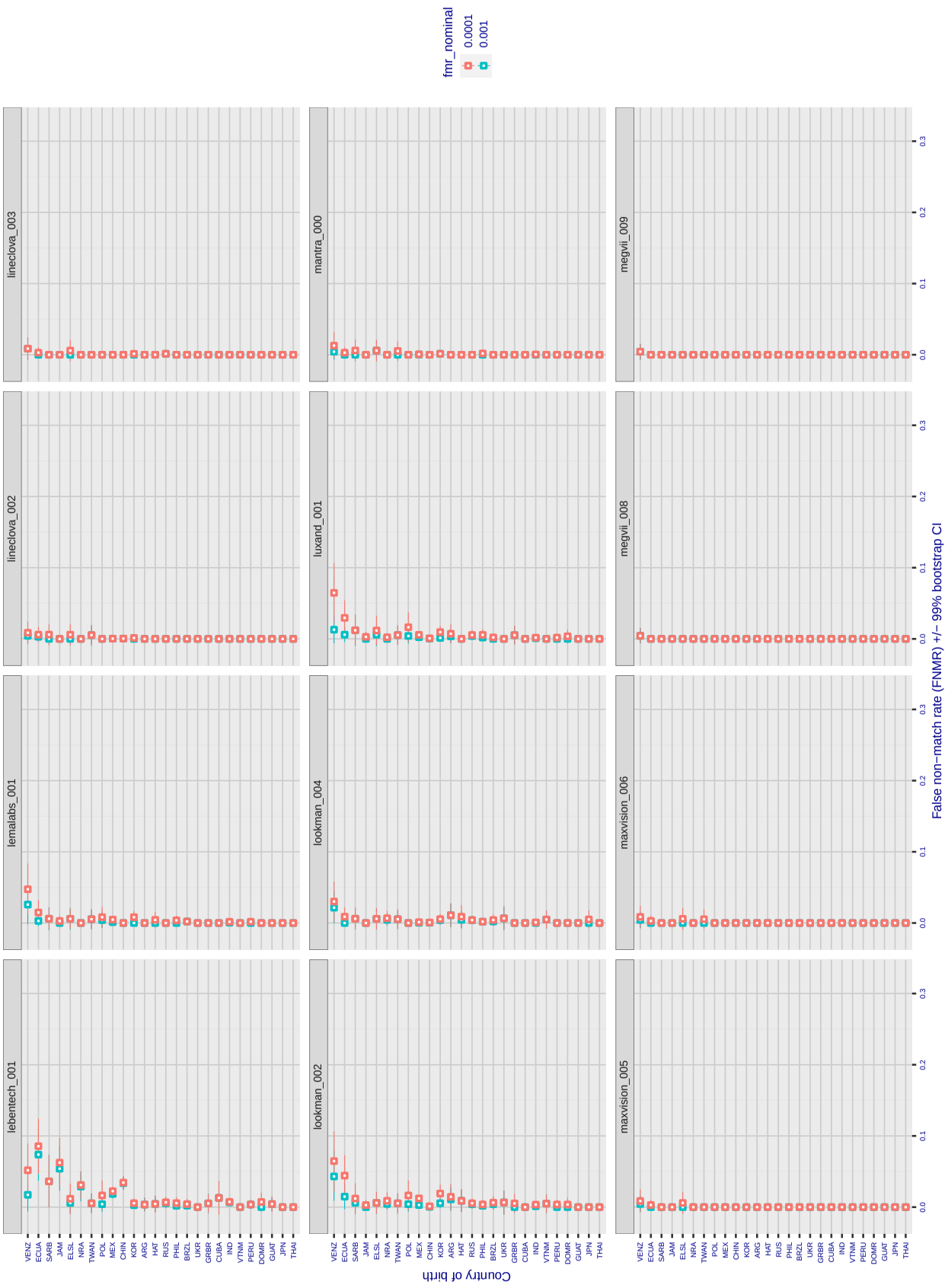

Figure 309: For the visa images, the dots show FNMR by country of birth for two globally set operating thresholds corresponding to FMR = $\{0.001, 0.0001\}$ computed over all on the order of 10^{10} impostor scores. The FMR in each bin will vary also - see subsequent impostor heatmaps in sec. 3.6.1. The figures shows an order of magnitude variation in FNMR across country of birth; these effects are likely due quality variations, then demographics like age and race. The error rates in some cases are zero, and in others the DET is flat so the error rates at the two thresholds are identical. The lines span 1% and 99% of boostrap replicated FNMR estimates.

FNMR(T) "False non-match rate"
FMR(T) "False match rate"

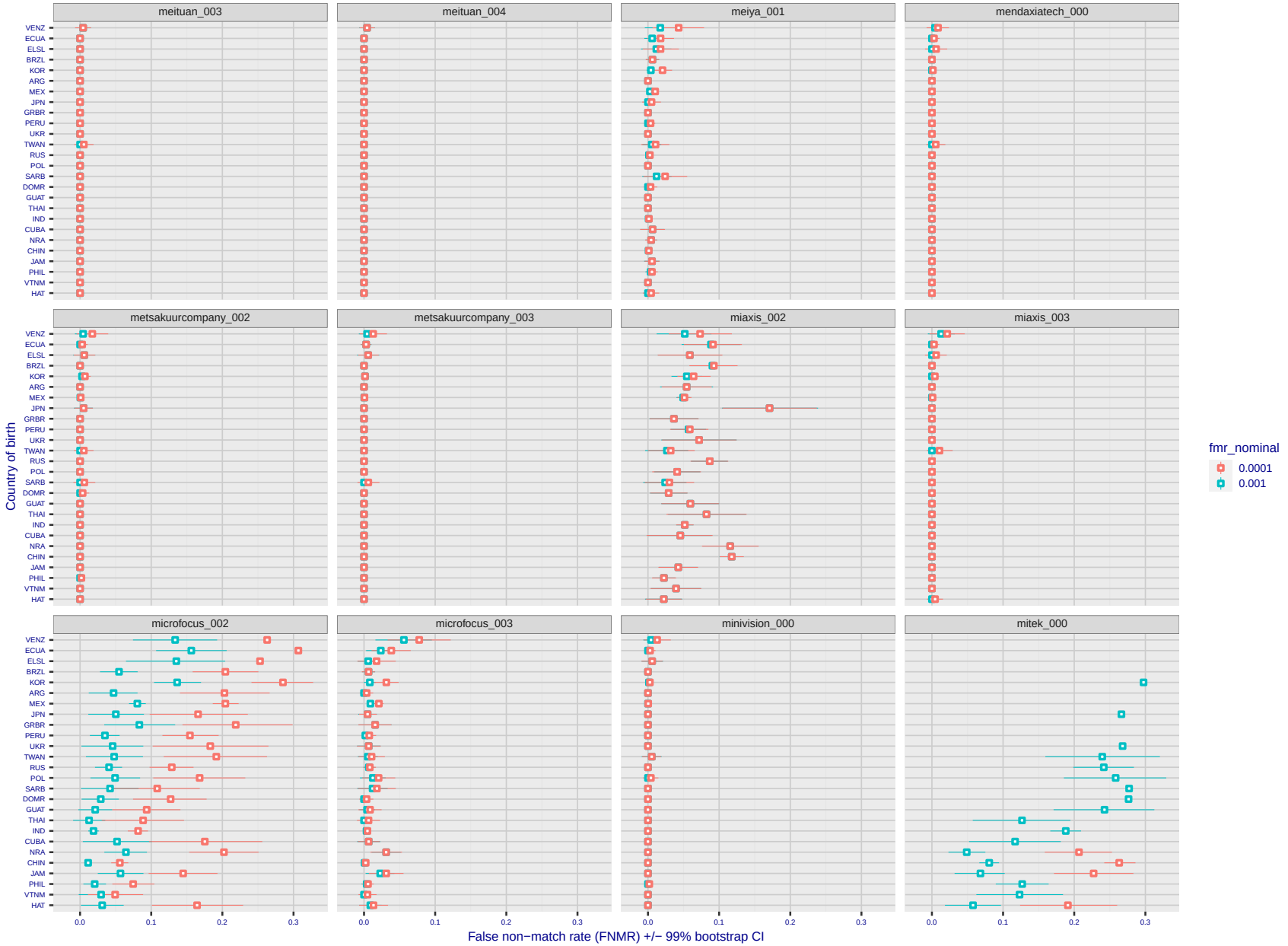

Figure 310: For the visa images, the dots show FNMR by country of birth for two globally set operating thresholds corresponding to FMR = $\{0.001, 0.0001\}$ computed over all on the order of 10^{10} impostor scores. The FMR in each bin will vary also - see subsequent impostor heatmaps in sec. 3.6.1. The figures shows an order of magnitude variation in FNMR across country of birth; these effects are likely due quality variations, then demographics like age and race. The error rates in some cases are zero, and in others the DET is flat so the error rates at the two thresholds are identical. The lines span 1% and 99% of boostrap replicated FNMR estimates.

Figure 311: For the visa images, the dots show FNMR by country of birth for two globally set operating thresholds corresponding to FMR = $\{0.001, 0.0001\}$ computed over all on the order of 10^{10} impostor scores. The FMR in each bin will vary also - see subsequent impostor heatmaps in sec. 3.6.1. The figures shows an order of magnitude variation in FNMR across country of birth; these effects are likely due quality variations, then demographics like age and race. The error rates in some cases are zero, and in others the DET is flat so the error rates at the two thresholds are identical. The lines span 1% and 99% of boostrap replicated FNMR estimates.

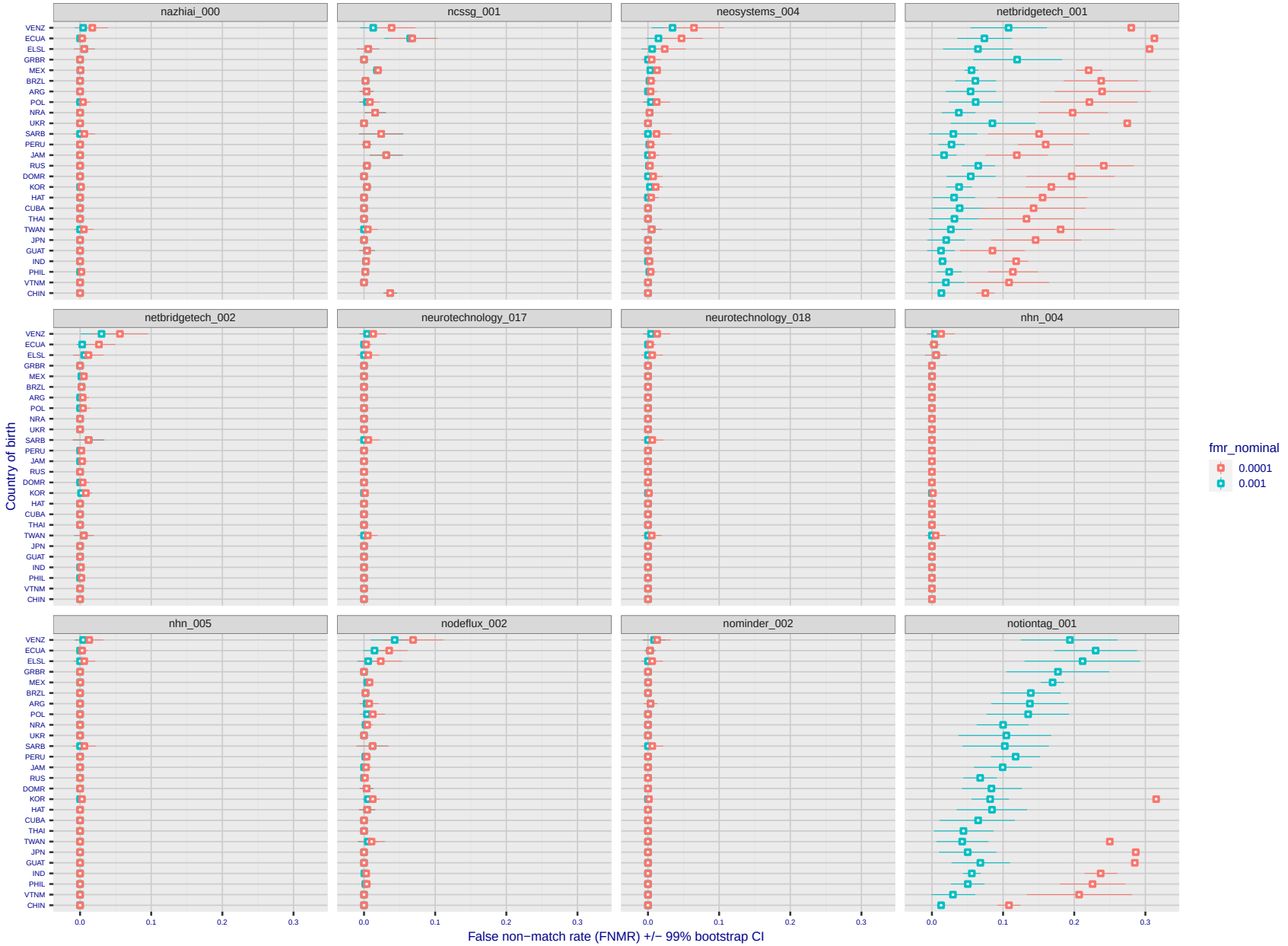

Figure 312: For the visa images, the dots show FNMR by country of birth for two globally set operating thresholds corresponding to FMR = $\{0.001, 0.0001\}$ computed over all on the order of 10^{10} impostor scores. The FMR in each bin will vary also - see subsequent impostor heatmaps in sec. 3.6.1. The figures shows an order of magnitude variation in FNMR across country of birth; these effects are likely due quality variations, then demographics like age and race. The error rates in some cases are zero, and in others the DET is flat so the error rates at the two thresholds are identical. The lines span 1% and 99% of boostrap replicated FNMR estimates.

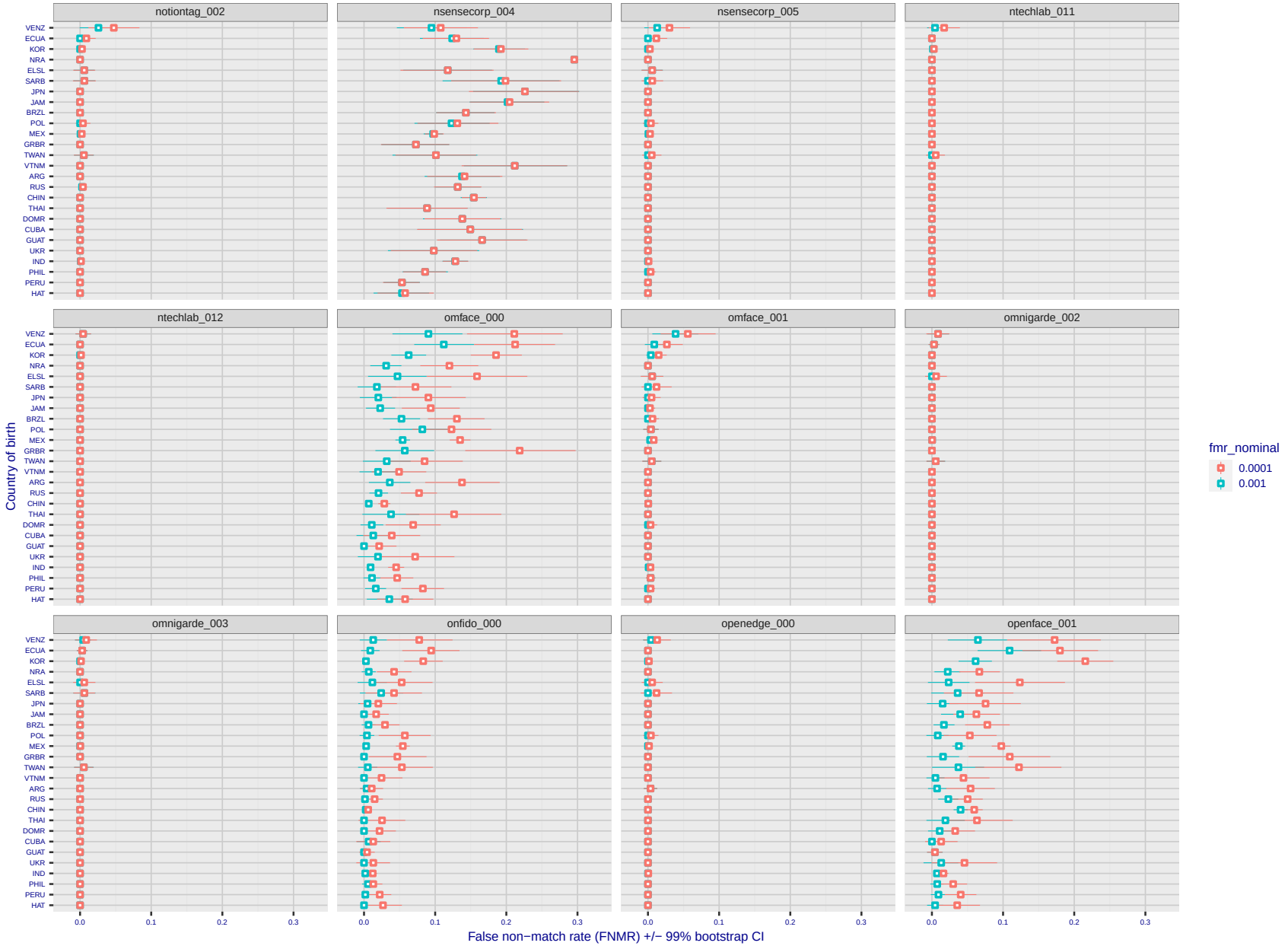

Figure 313: For the visa images, the dots show FNMR by country of birth for two globally set operating thresholds corresponding to FMR = $\{0.001, 0.0001\}$ computed over all on the order of 10^{10} impostor scores. The FMR in each bin will vary also - see subsequent impostor heatmaps in sec. 3.6.1. The figures shows an order of magnitude variation in FNMR across country of birth; these effects are likely due quality variations, then demographics like age and race. The error rates in some cases are zero, and in others the DET is flat so the error rates at the two thresholds are identical. The lines span 1% and 99% of boostrap replicated FNMR estimates.

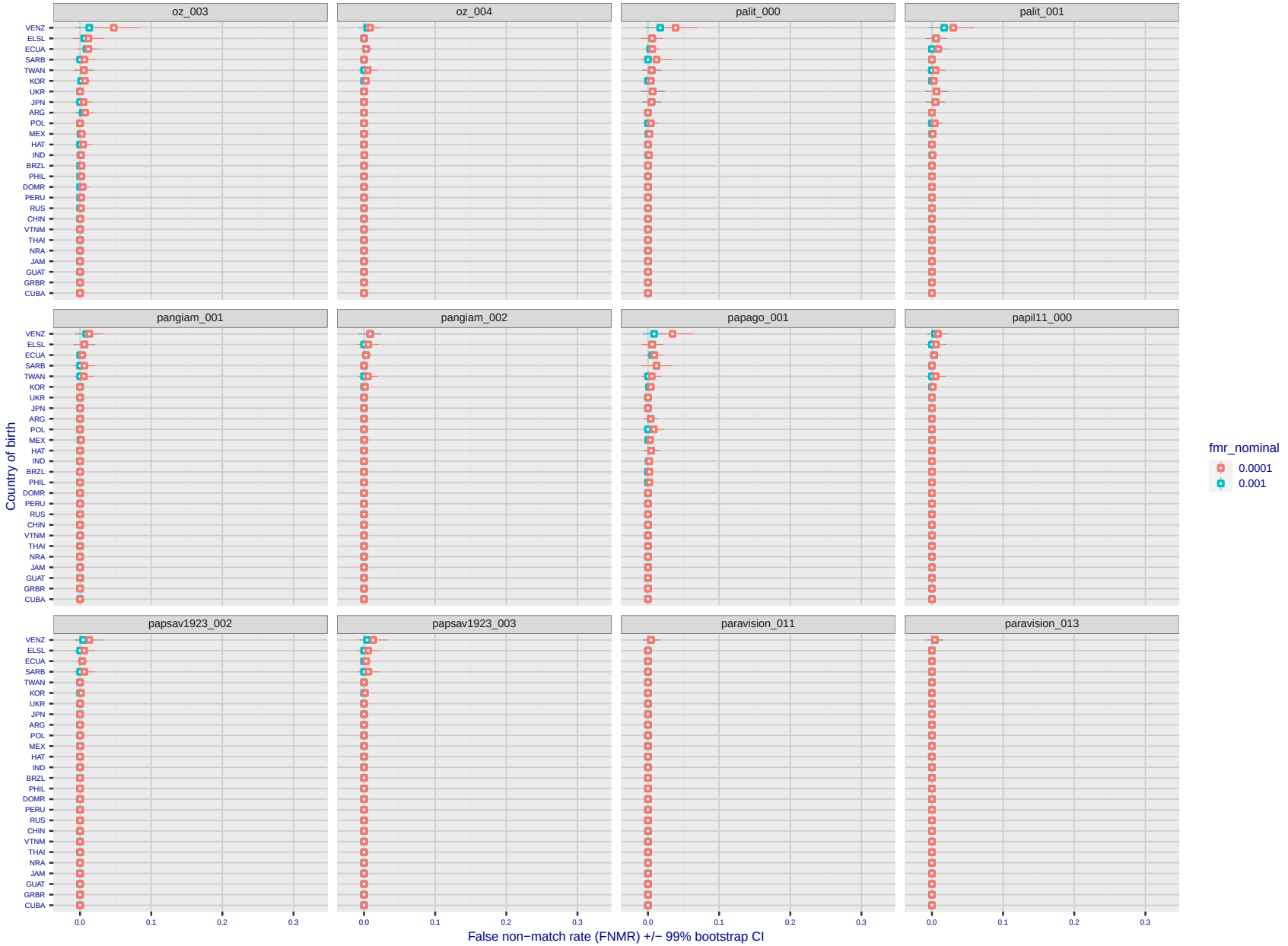

Figure 314: For the visa images, the dots show FNMR by country of birth for two globally set operating thresholds corresponding to FMR = $\{0.001, 0.0001\}$ computed over all on the order of 10^{10} impostor scores. The FMR in each bin will vary also - see subsequent impostor heatmaps in sec. 3.6.1. The figures shows an order of magnitude variation in FNMR across country of birth; these effects are likely due quality variations, then demographics like age and race. The error rates in some cases are zero, and in others the DET is flat so the error rates at the two thresholds are identical. The lines span 1% and 99% of boostrap replicated FNMR estimates.

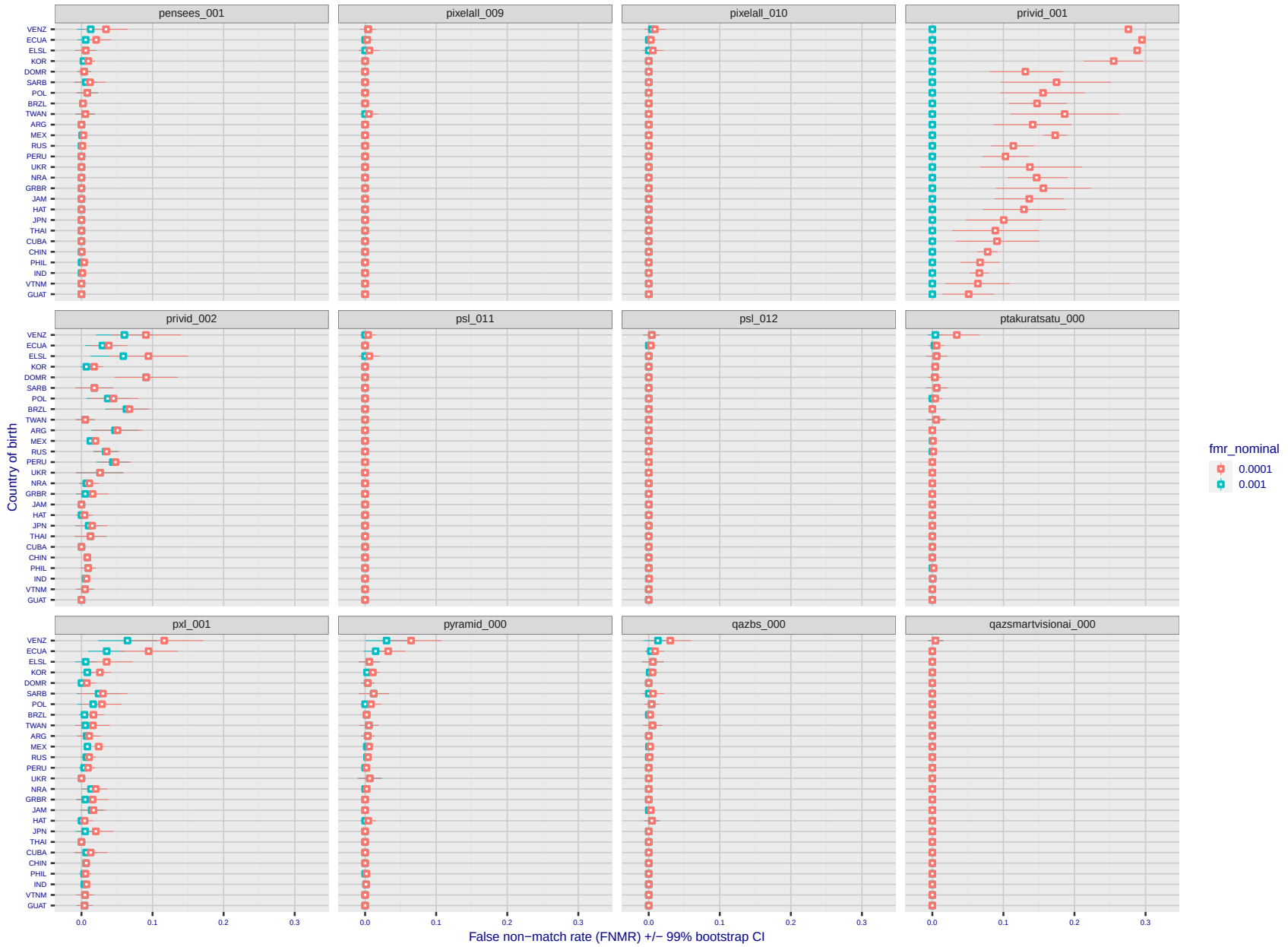

Figure 315: For the visa images, the dots show FNMR by country of birth for two globally set operating thresholds corresponding to FMR = $\{0.001, 0.0001\}$ computed over all on the order of 10^{10} impostor scores. The FMR in each bin will vary also - see subsequent impostor heatmaps in sec. 3.6.1. The figures shows an order of magnitude variation in FNMR across country of birth; these effects are likely due quality variations, then demographics like age and race. The error rates in some cases are zero, and in others the DET is flat so the error rates at the two thresholds are identical. The lines span 1% and 99% of boostrap replicated FNMR estimates.

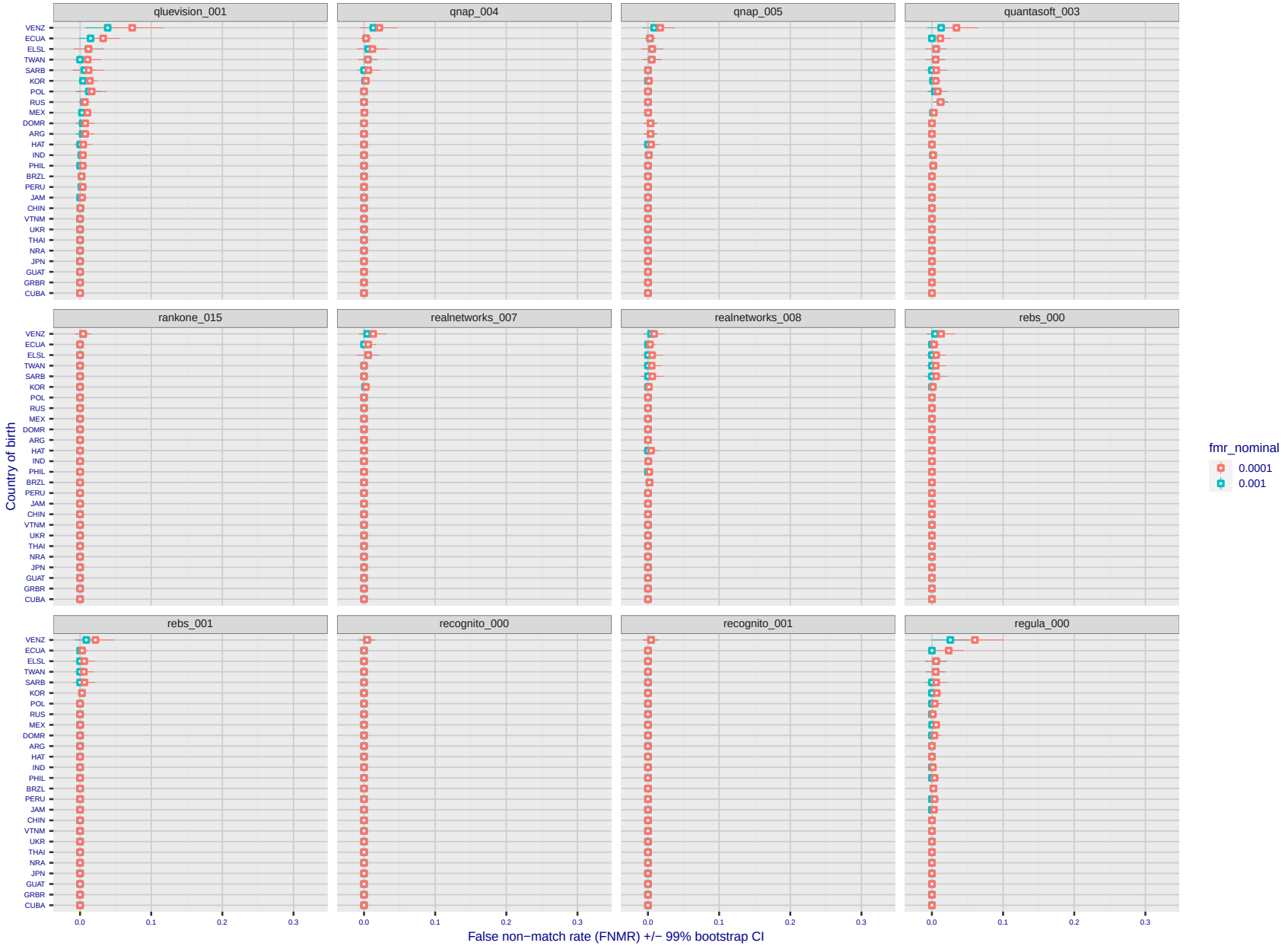

Figure 316: For the visa images, the dots show FNMR by country of birth for two globally set operating thresholds corresponding to FMR = $\{0.001, 0.0001\}$ computed over all on the order of 10^{10} impostor scores. The FMR in each bin will vary also - see subsequent impostor heatmaps in sec. 3.6.1. The figures shows an order of magnitude variation in FNMR across country of birth; these effects are likely due quality variations, then demographics like age and race. The error rates in some cases are zero, and in others the DET is flat so the error rates at the two thresholds are identical. The lines span 1% and 99% of boostrap replicated FNMR estimates.

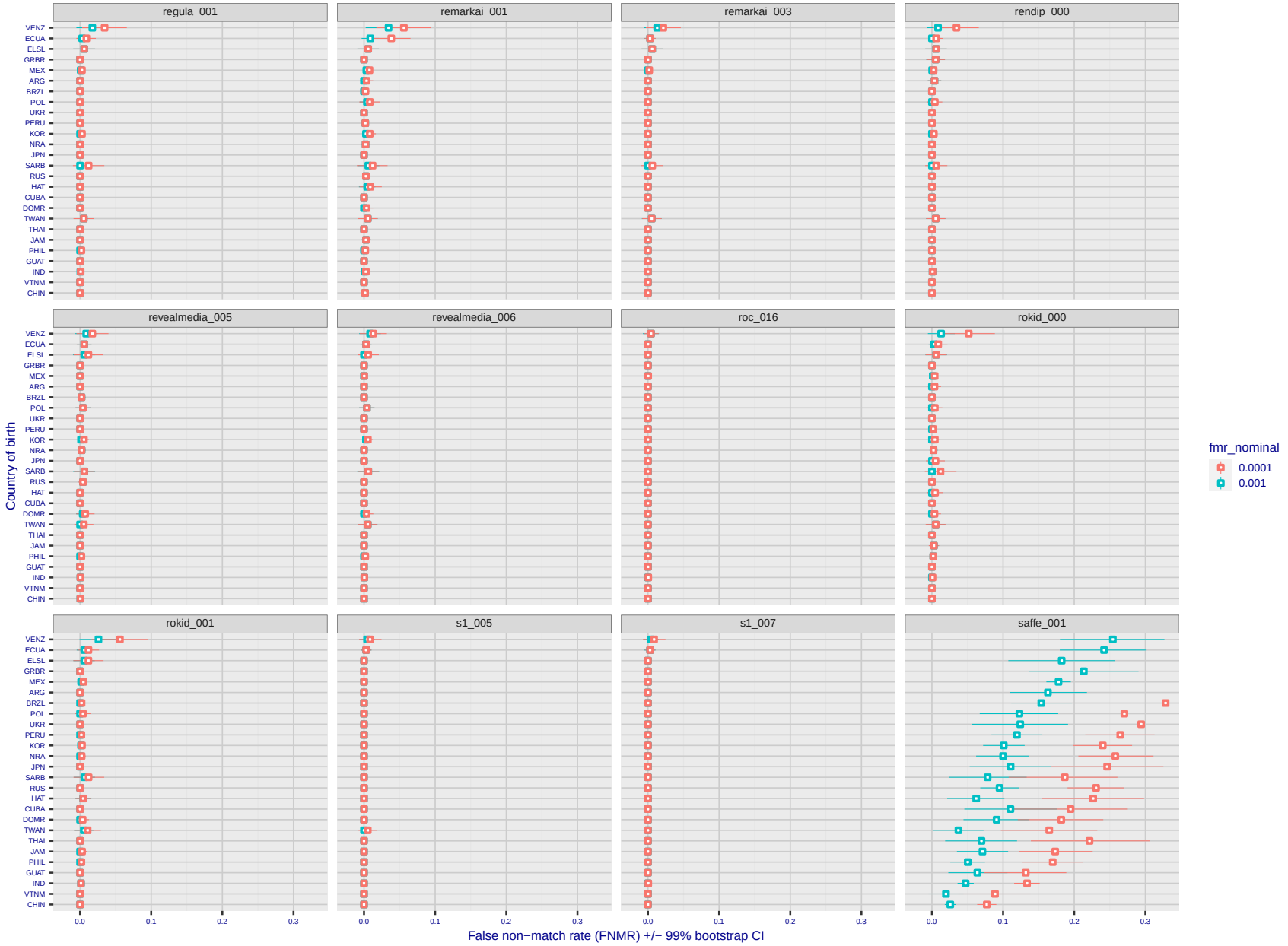

Figure 317: For the visa images, the dots show FNMR by country of birth for two globally set operating thresholds corresponding to FMR = $\{0.001, 0.0001\}$ computed over all on the order of 10^{10} impostor scores. The FMR in each bin will vary also - see subsequent impostor heatmaps in sec. 3.6.1. The figures shows an order of magnitude variation in FNMR across country of birth; these effects are likely due quality variations, then demographics like age and race. The error rates in some cases are zero, and in others the DET is flat so the error rates at the two thresholds are identical. The lines span 1% and 99% of boostrap replicated FNMR estimates.

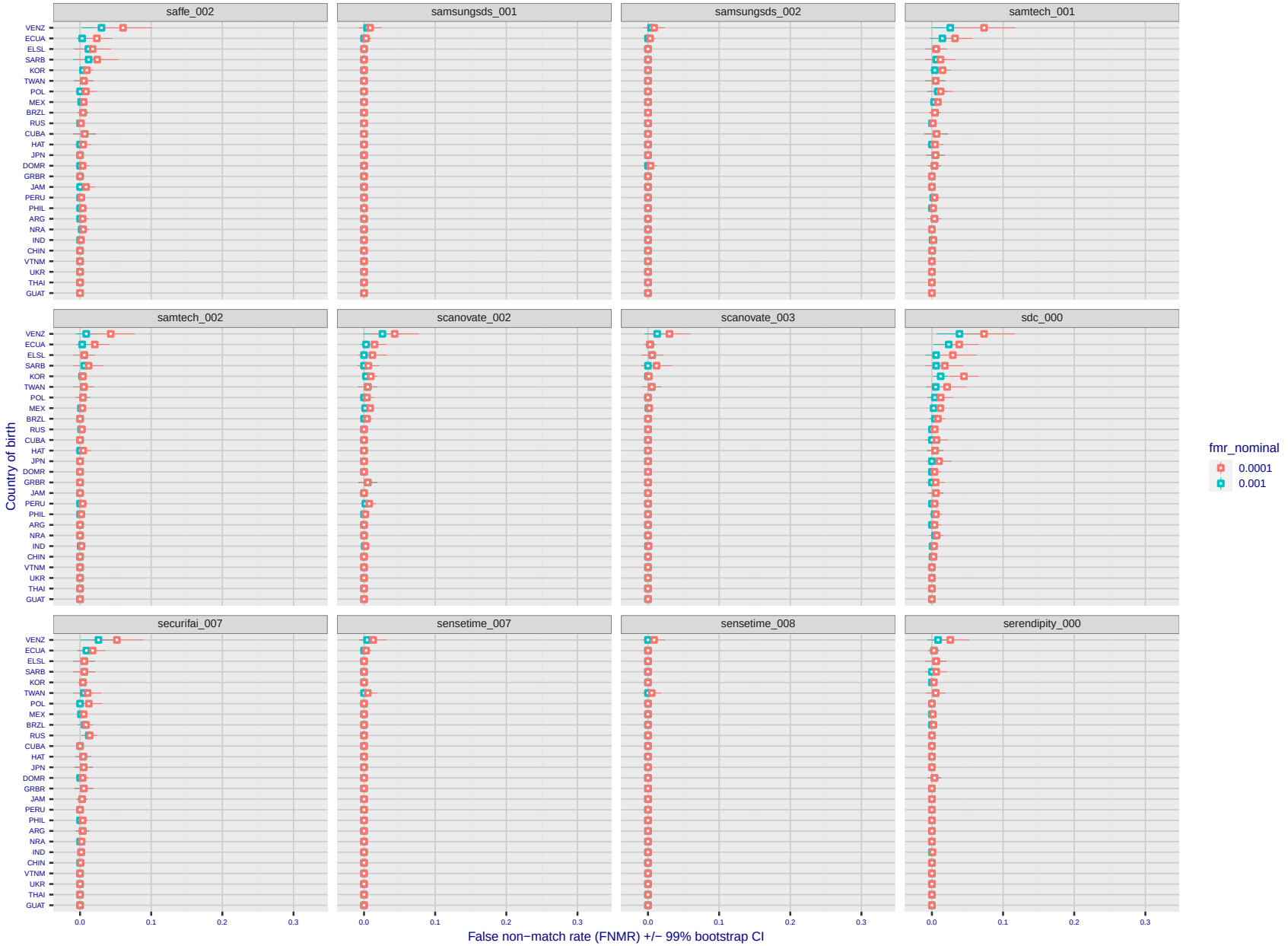

Figure 318: For the visa images, the dots show FNMR by country of birth for two globally set operating thresholds corresponding to FMR = $\{0.001, 0.0001\}$ computed over all on the order of 10^{10} impostor scores. The FMR in each bin will vary also - see subsequent impostor heatmaps in sec. 3.6.1. The figures shows an order of magnitude variation in FNMR across country of birth; these effects are likely due quality variations, then demographics like age and race. The error rates in some cases are zero, and in others the DET is flat so the error rates at the two thresholds are identical. The lines span 1% and 99% of boostrap replicated FNMR estimates.

FNMR(T) "False non-match rate"
FMR(T) "False match rate"

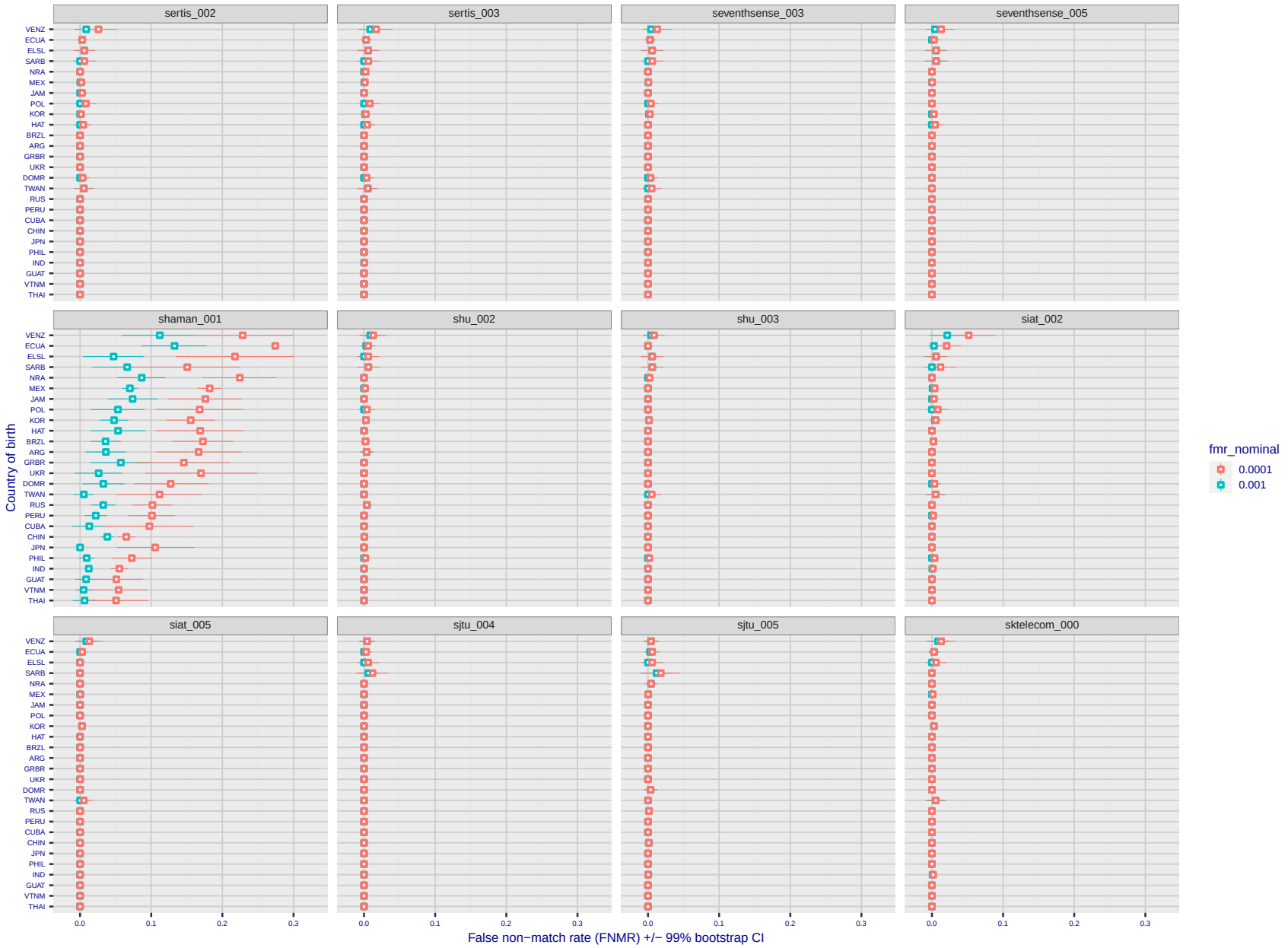

Figure 319: For the visa images, the dots show FNMR by country of birth for two globally set operating thresholds corresponding to FMR = $\{0.001, 0.0001\}$ computed over all on the order of 10^{10} impostor scores. The FMR in each bin will vary also - see subsequent impostor heatmaps in sec. 3.6.1. The figures shows an order of magnitude variation in FNMR across country of birth; these effects are likely due quality variations, then demographics like age and race. The error rates in some cases are zero, and in others the DET is flat so the error rates at the two thresholds are identical. The lines span 1% and 99% of boostrap replicated FNMR estimates.

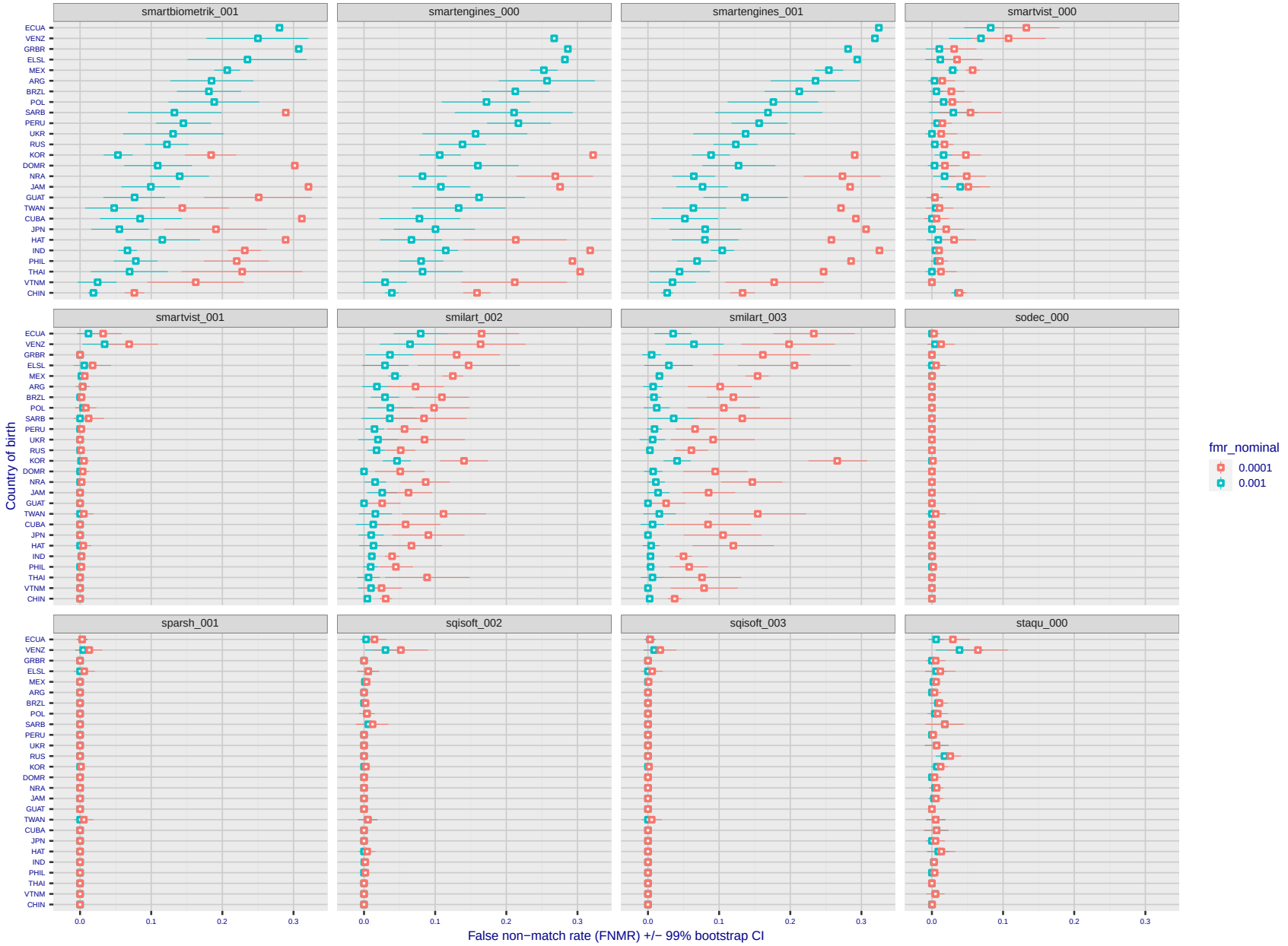

Figure 320: For the visa images, the dots show FNMR by country of birth for two globally set operating thresholds corresponding to FMR = $\{0.001, 0.0001\}$ computed over all on the order of 10^{10} impostor scores. The FMR in each bin will vary also - see subsequent impostor heatmaps in sec. 3.6.1. The figures shows an order of magnitude variation in FNMR across country of birth; these effects are likely due quality variations, then demographics like age and race. The error rates in some cases are zero, and in others the DET is flat so the error rates at the two thresholds are identical. The lines span 1% and 99% of boostrap replicated FNMR estimates.

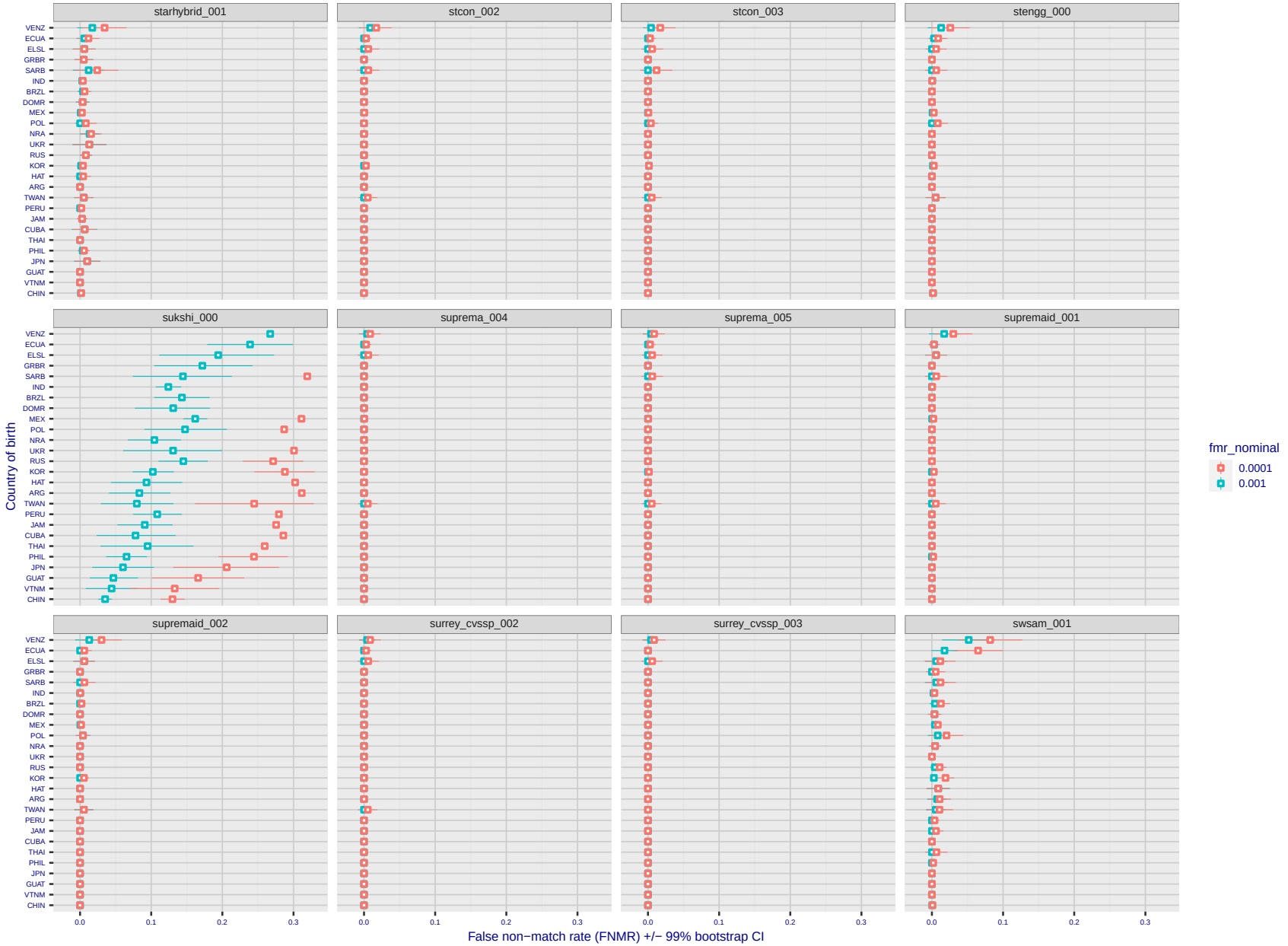

Figure 321: For the visa images, the dots show FNMR by country of birth for two globally set operating thresholds corresponding to FMR = $\{0.001, 0.0001\}$ computed over all on the order of 10^{10} impostor scores. The FMR in each bin will vary also - see subsequent impostor heatmaps in sec. 3.6.1. The figures shows an order of magnitude variation in FNMR across country of birth; these effects are likely due quality variations, then demographics like age and race. The error rates in some cases are zero, and in others the DET is flat so the error rates at the two thresholds are identical. The lines span 1% and 99% of boostrap replicated FNMR estimates.

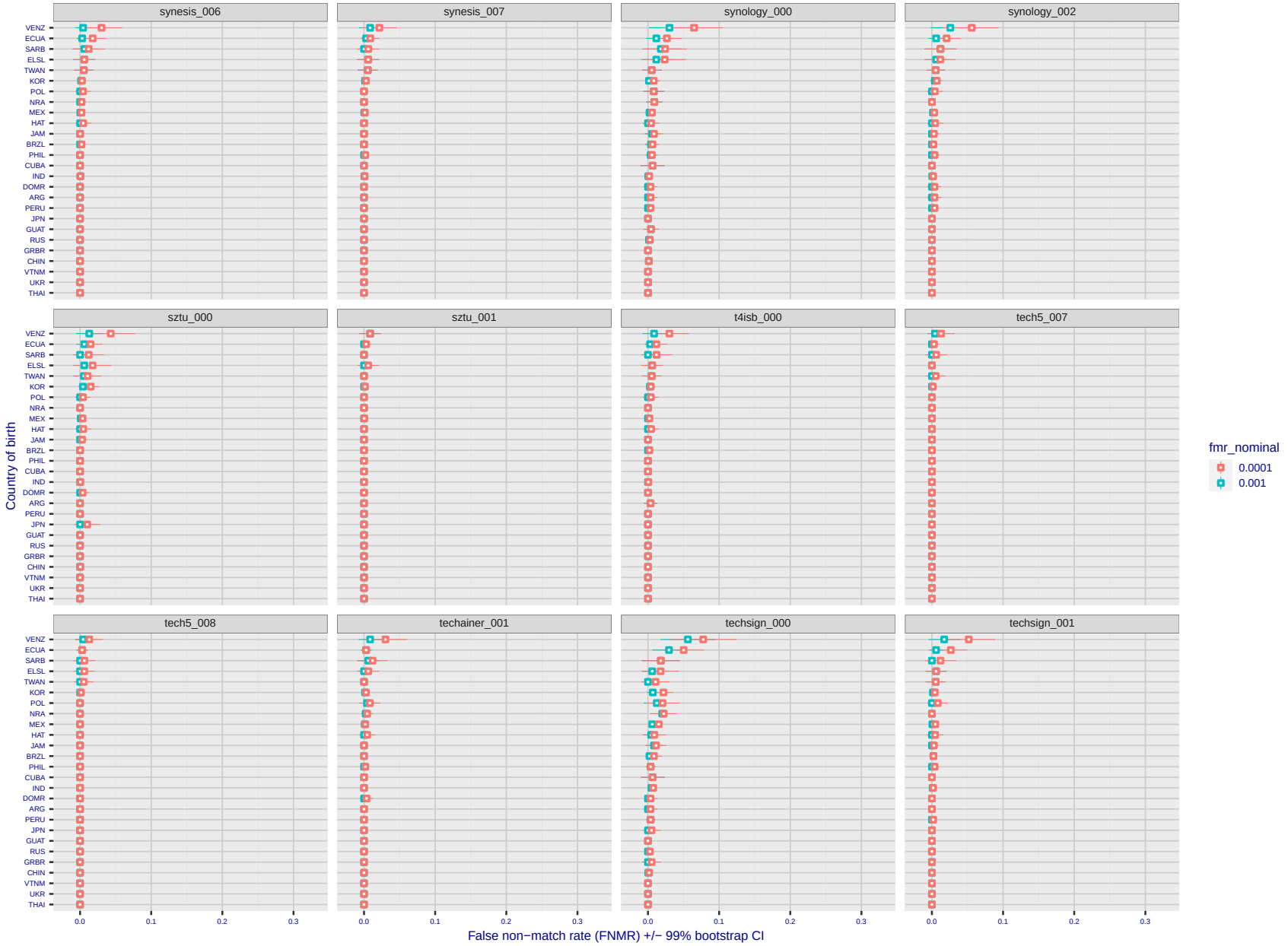

Figure 322: For the visa images, the dots show FNMR by country of birth for two globally set operating thresholds corresponding to FMR = $\{0.001, 0.0001\}$ computed over all on the order of 10^{10} impostor scores. The FMR in each bin will vary also - see subsequent impostor heatmaps in sec. 3.6.1. The figures shows an order of magnitude variation in FNMR across country of birth; these effects are likely due quality variations, then demographics like age and race. The error rates in some cases are zero, and in others the DET is flat so the error rates at the two thresholds are identical. The lines span 1% and 99% of boostrap replicated FNMR estimates.

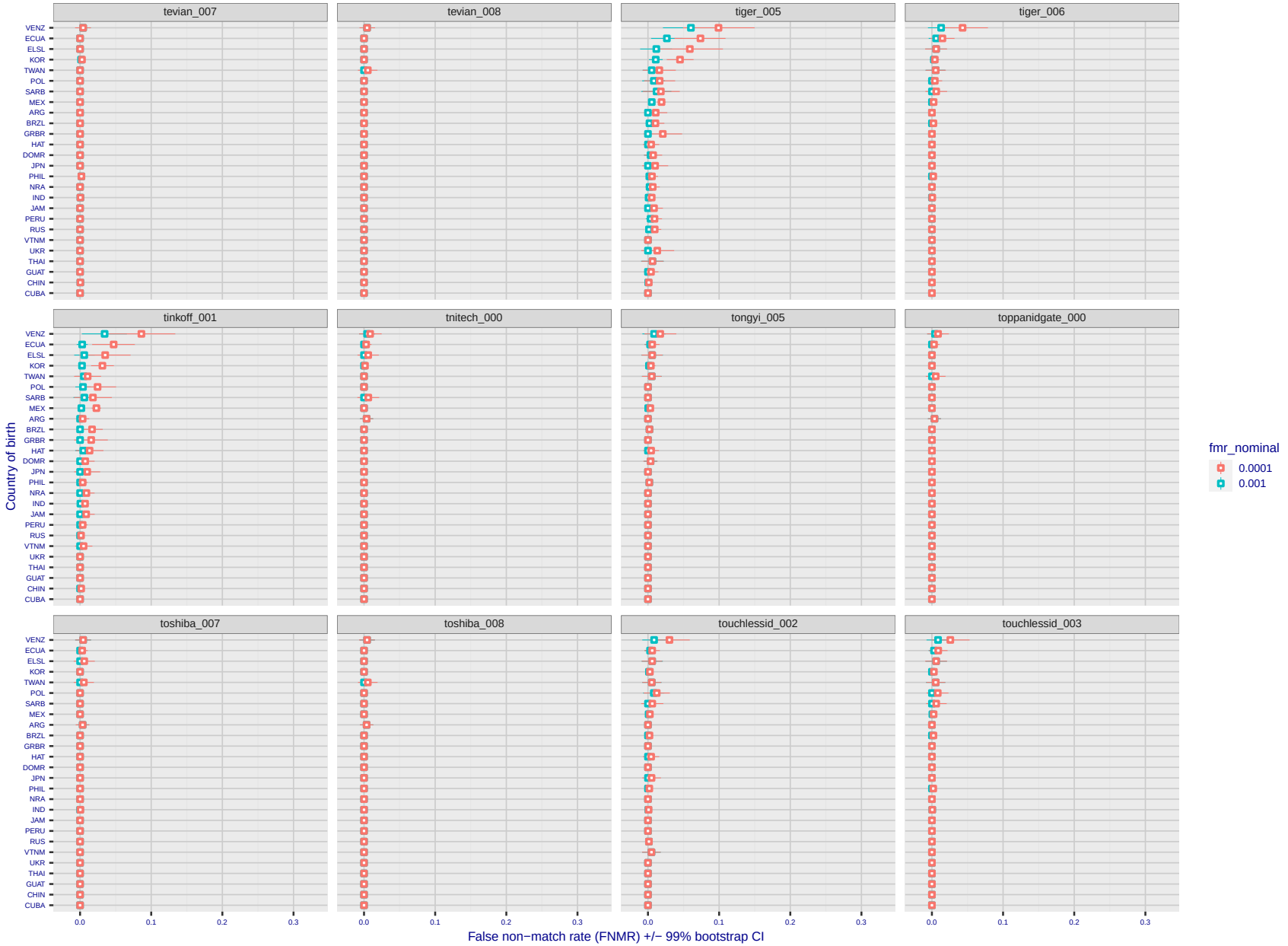

Figure 323: For the visa images, the dots show FNMR by country of birth for two globally set operating thresholds corresponding to FMR = $\{0.001, 0.0001\}$ computed over all on the order of 10^{10} impostor scores. The FMR in each bin will vary also - see subsequent impostor heatmaps in sec. 3.6.1. The figures shows an order of magnitude variation in FNMR across country of birth; these effects are likely due quality variations, then demographics like age and race. The error rates in some cases are zero, and in others the DET is flat so the error rates at the two thresholds are identical. The lines span 1% and 99% of boostrap replicated FNMR estimates.

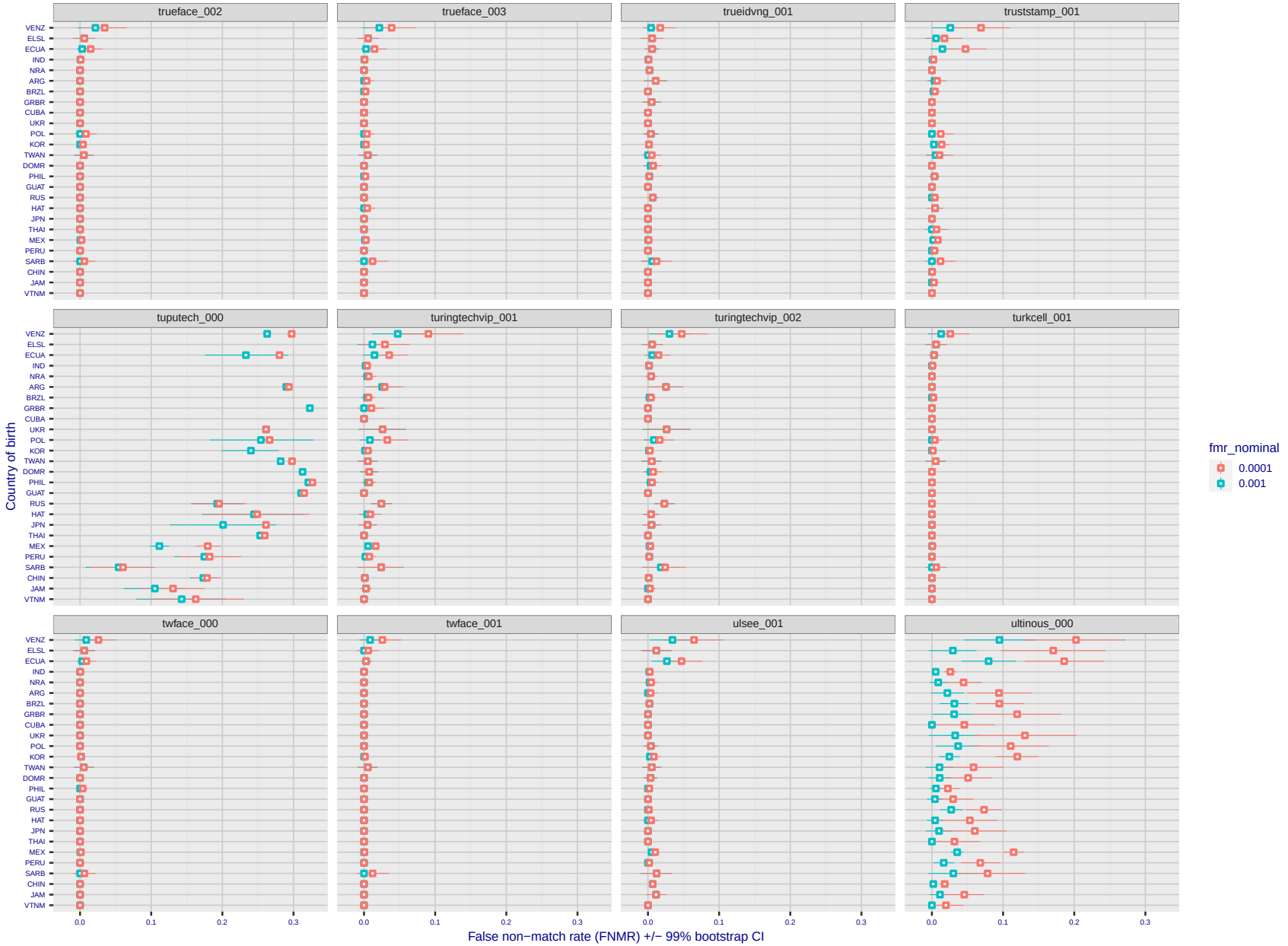

Figure 324: For the visa images, the dots show FNMR by country of birth for two globally set operating thresholds corresponding to FMR = $\{0.001, 0.0001\}$ computed over all on the order of 10^{10} impostor scores. The FMR in each bin will vary also - see subsequent impostor heatmaps in sec. 3.6.1. The figures shows an order of magnitude variation in FNMR across country of birth; these effects are likely due quality variations, then demographics like age and race. The error rates in some cases are zero, and in others the DET is flat so the error rates at the two thresholds are identical. The lines span 1% and 99% of boostrap replicated FNMR estimates.

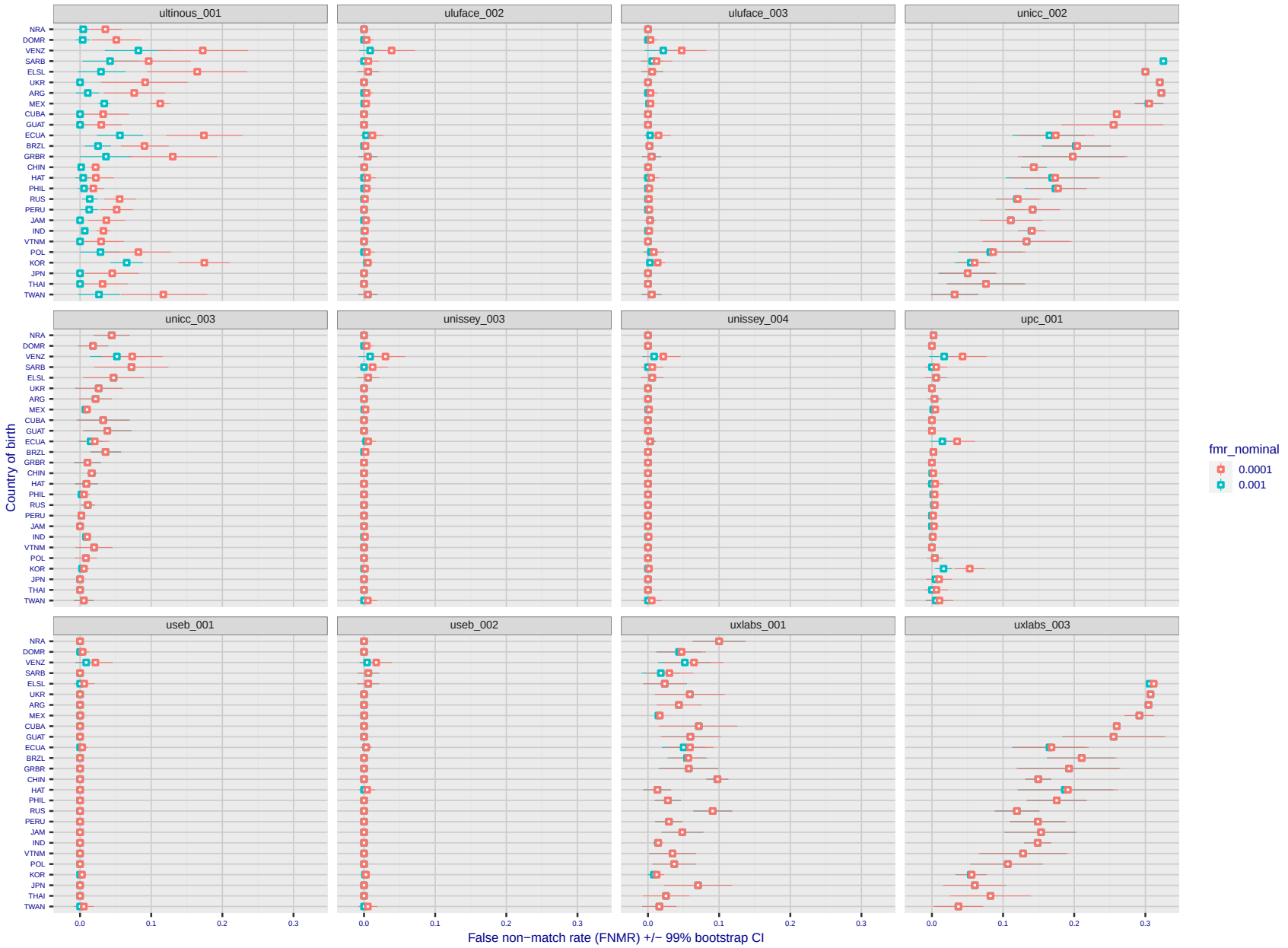

Figure 325: For the visa images, the dots show FNMR by country of birth for two globally set operating thresholds corresponding to FMR = $\{0.001, 0.0001\}$ computed over all on the order of 10^{10} impostor scores. The FMR in each bin will vary also - see subsequent impostor heatmaps in sec. 3.6.1. The figures shows an order of magnitude variation in FNMR across country of birth; these effects are likely due quality variations, then demographics like age and race. The error rates in some cases are zero, and in others the DET is flat so the error rates at the two thresholds are identical. The lines span 1% and 99% of boostrap replicated FNMR estimates.

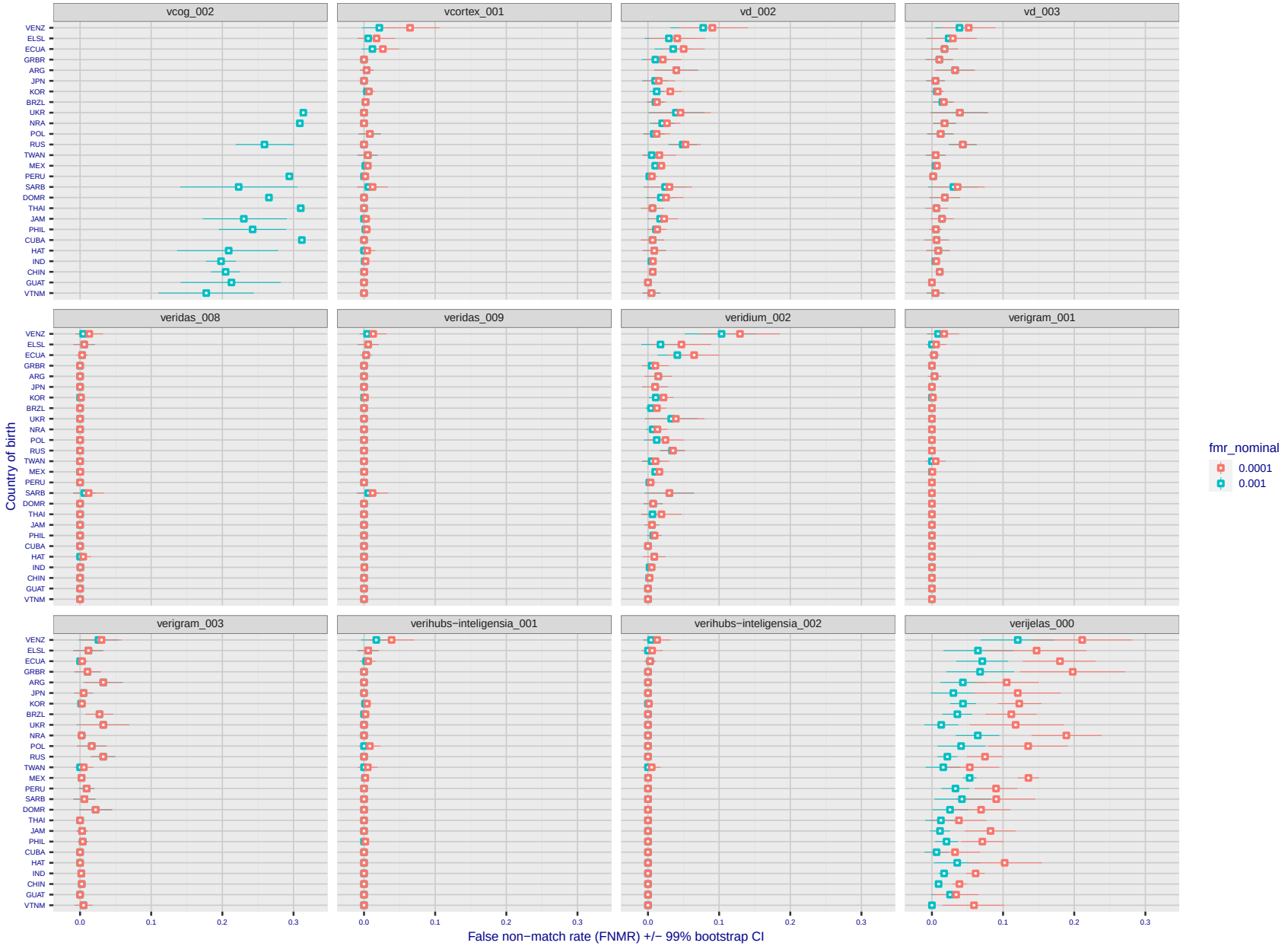

Figure 326: For the visa images, the dots show FNMR by country of birth for two globally set operating thresholds corresponding to FMR = $\{0.001, 0.0001\}$ computed over all on the order of 10^{10} impostor scores. The FMR in each bin will vary also - see subsequent impostor heatmaps in sec. 3.6.1. The figures shows an order of magnitude variation in FNMR across country of birth; these effects are likely due quality variations, then demographics like age and race. The error rates in some cases are zero, and in others the DET is flat so the error rates at the two thresholds are identical. The lines span 1% and 99% of boostrap replicated FNMR estimates.

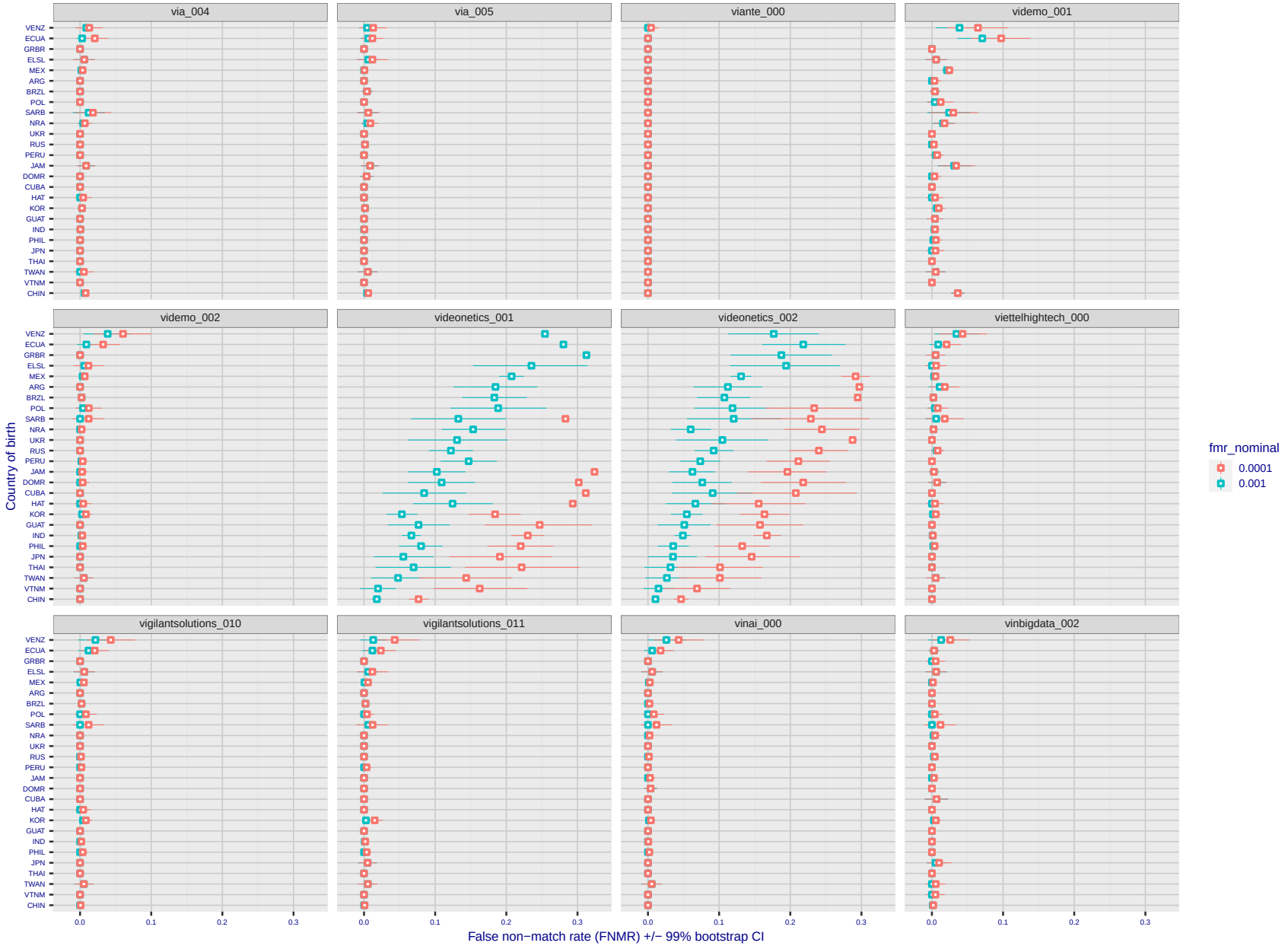

Figure 327: For the visa images, the dots show FNMR by country of birth for two globally set operating thresholds corresponding to FMR = $\{0.001, 0.0001\}$ computed over all on the order of 10^{10} impostor scores. The FMR in each bin will vary also - see subsequent impostor heatmaps in sec. 3.6.1. The figures shows an order of magnitude variation in FNMR across country of birth; these effects are likely due quality variations, then demographics like age and race. The error rates in some cases are zero, and in others the DET is flat so the error rates at the two thresholds are identical. The lines span 1% and 99% of boostrap replicated FNMR estimates.

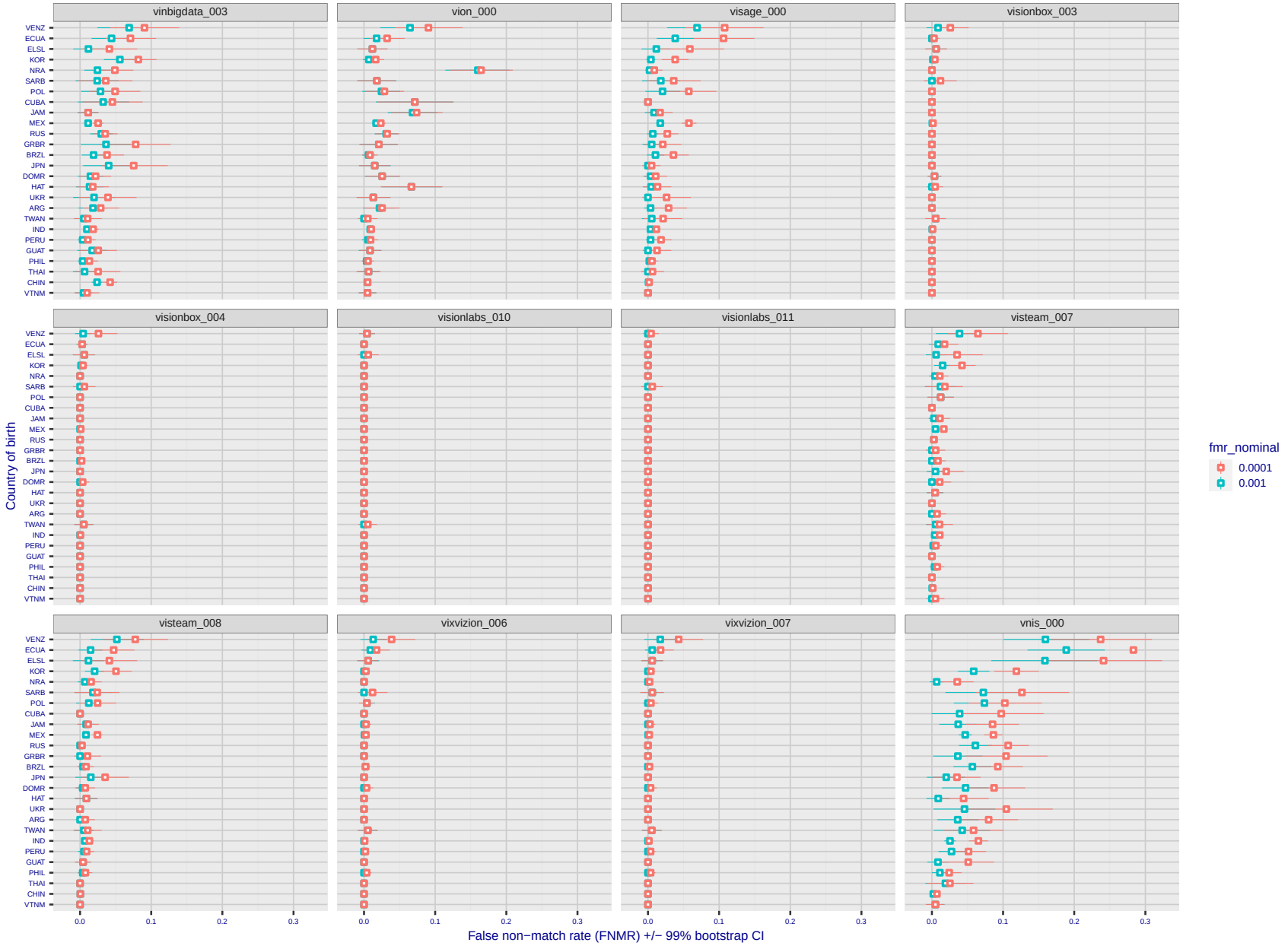

Figure 328: For the visa images, the dots show FNMR by country of birth for two globally set operating thresholds corresponding to FMR = $\{0.001, 0.0001\}$ computed over all on the order of 10^{10} impostor scores. The FMR in each bin will vary also - see subsequent impostor heatmaps in sec. 3.6.1. The figures shows an order of magnitude variation in FNMR across country of birth; these effects are likely due quality variations, then demographics like age and race. The error rates in some cases are zero, and in others the DET is flat so the error rates at the two thresholds are identical. The lines span 1% and 99% of boostrap replicated FNMR estimates.

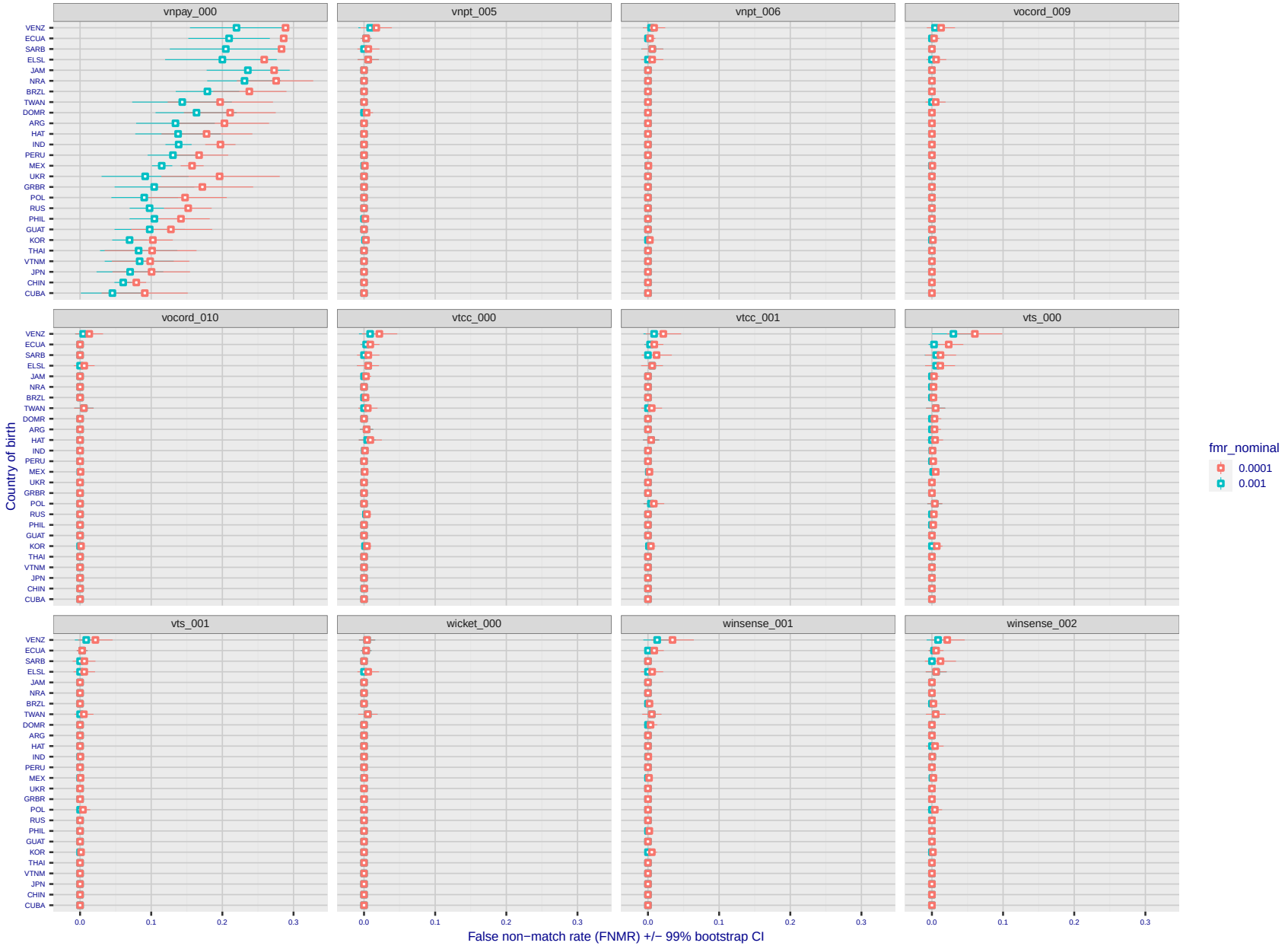

Figure 329: For the visa images, the dots show FNMR by country of birth for two globally set operating thresholds corresponding to FMR = $\{0.001, 0.0001\}$ computed over all on the order of 10^{10} impostor scores. The FMR in each bin will vary also - see subsequent impostor heatmaps in sec. 3.6.1. The figures shows an order of magnitude variation in FNMR across country of birth; these effects are likely due quality variations, then demographics like age and race. The error rates in some cases are zero, and in others the DET is flat so the error rates at the two thresholds are identical. The lines span 1% and 99% of boostrap replicated FNMR estimates.

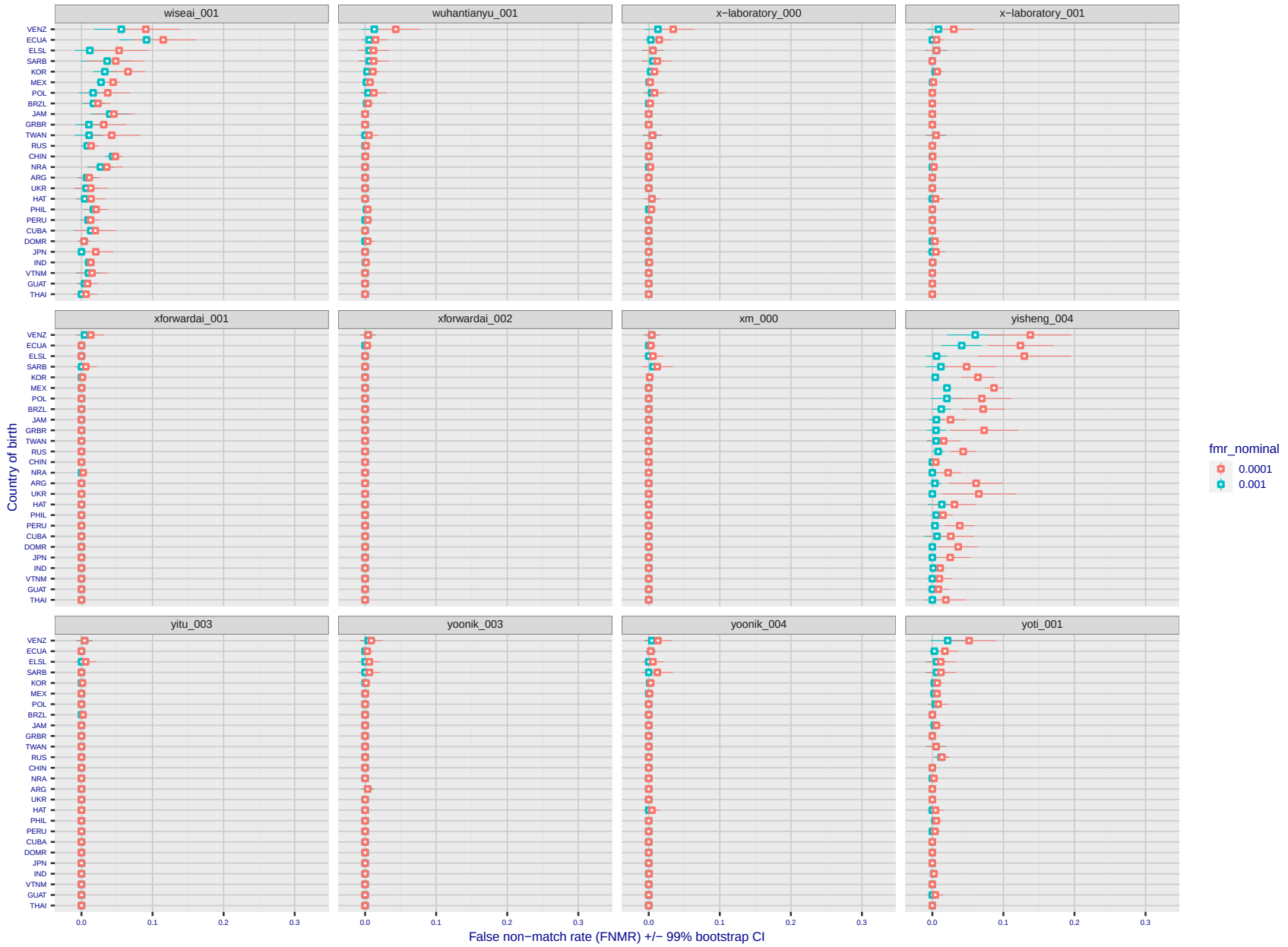

Figure 330: For the visa images, the dots show FNMR by country of birth for two globally set operating thresholds corresponding to FMR = $\{0.001, 0.0001\}$ computed over all on the order of 10^{10} impostor scores. The FMR in each bin will vary also - see subsequent impostor heatmaps in sec. 3.6.1. The figures shows an order of magnitude variation in FNMR across country of birth; these effects are likely due quality variations, then demographics like age and race. The error rates in some cases are zero, and in others the DET is flat so the error rates at the two thresholds are identical. The lines span 1% and 99% of boostrap replicated FNMR estimates.

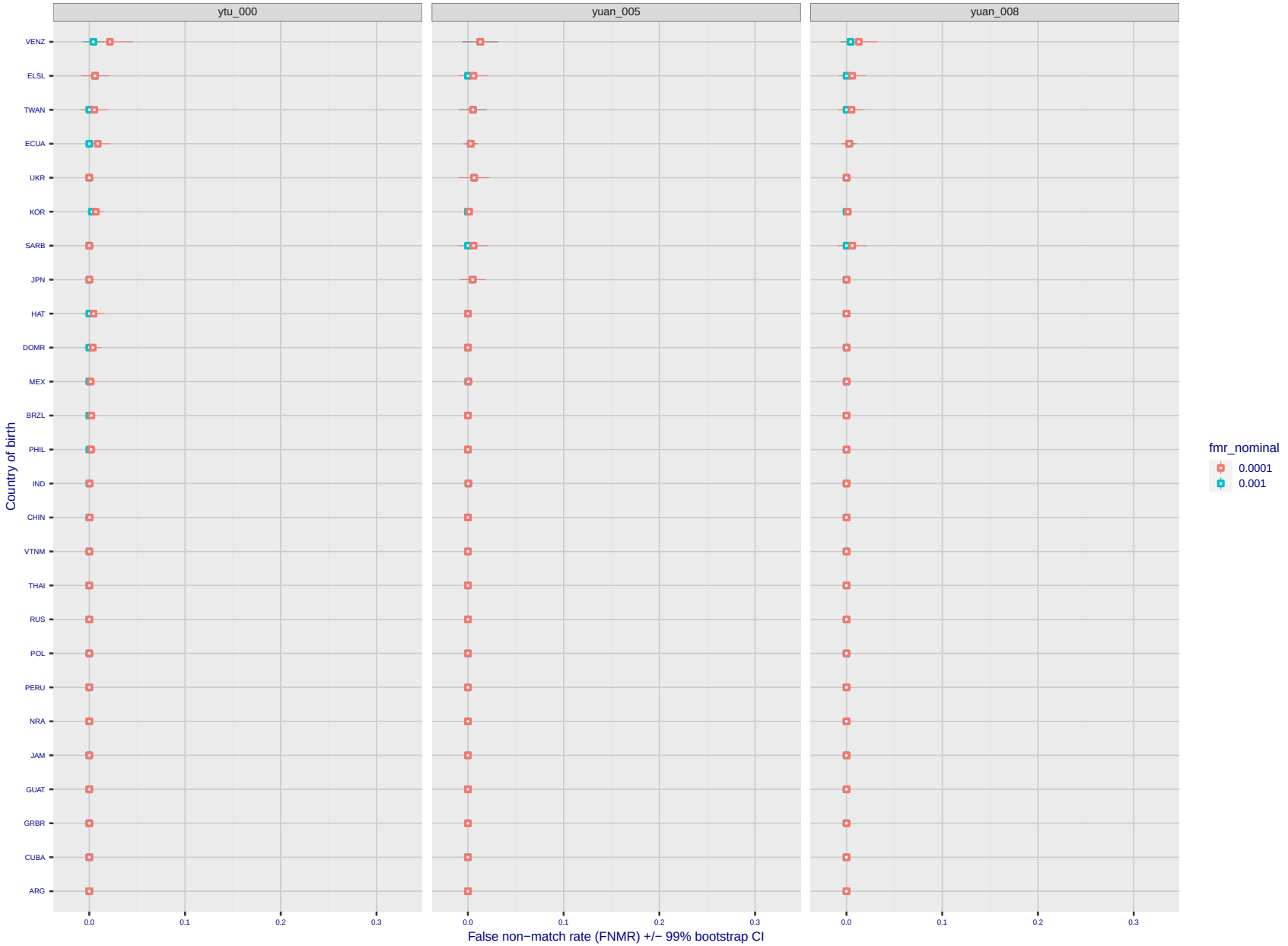

Figure 331: For the visa images, the dots show FNMR by country of birth for two globally set operating thresholds corresponding to FMR = $\{0.001, 0.0001\}$ computed over all on the order of 10^{10} impostor scores. The FMR in each bin will vary also - see subsequent impostor heatmaps in sec. 3.6.1. The figures shows an order of magnitude variation in FNMR across country of birth; these effects are likely due quality variations, then demographics like age and race. The error rates in some cases are zero, and in others the DET is flat so the error rates at the two thresholds are identical. The lines span 1% and 99% of boostrap replicated FNMR estimates.

Caveats: The results may not relate to subject-specific properties. Instead they could reflect image-specific quality differences, which could occur due to collection protocol or software processing variations.

3.5.2 Effect of ageing

Background: Faces change appearance throughout life. This change gradually reduces similarity of a new image to an earlier image. Face recognition algorithms give reduced similarity scores and more frequent false rejections.

Goal: To quantify false non-match rates (FNMR) as a function of elapsed time in an adult population.

Methods: Using the mugshot images, a threshold is set to give FMR = 0.00001 over the entire impostor set. Then FNMR is measured over 1000 bootstrap replications of the genuine scores.

Results: For the visa images, Figure 367 shows how false non-match rates for genuine users, as a function of age group.

FNMR(T) "False non-match rate"
FMR(T) "False match rate"

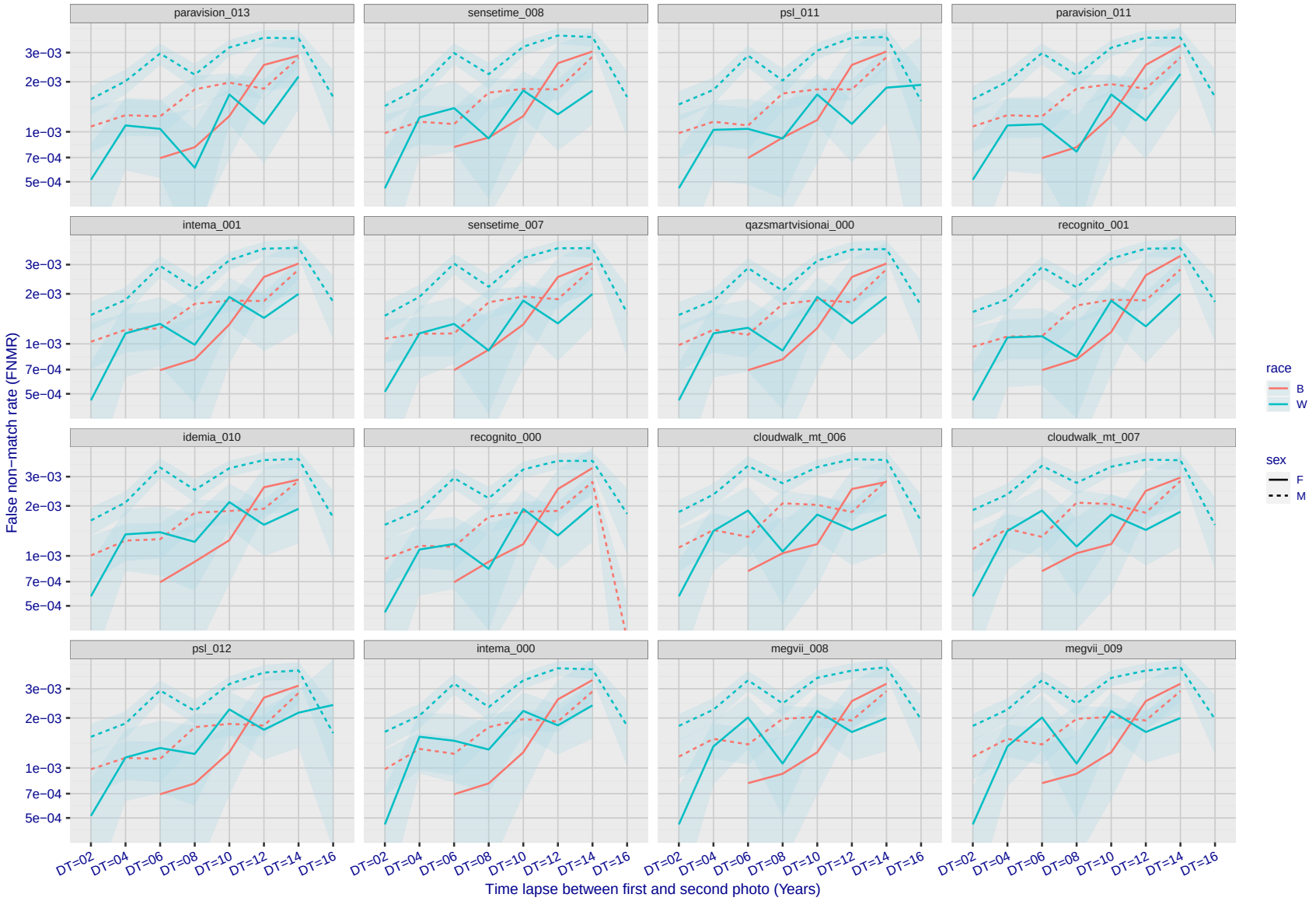

Figure 332: For the mugshot images, FNMR *as a function of elapsed time between initial enrollment and second verification images. The panels appear most accurate first, and vertical scale changes on each page. The four traces correspond to images annotated with codes for black female, black male, white female, white male. The threshold is fixed for each algorithm to give FMR = 0.00001 over all (10^8) impostor comparisons. For short time-lapses, the most accurate algorithms give very few errors (FNMR < 0.001) so that the uncertainty estimates are high.*

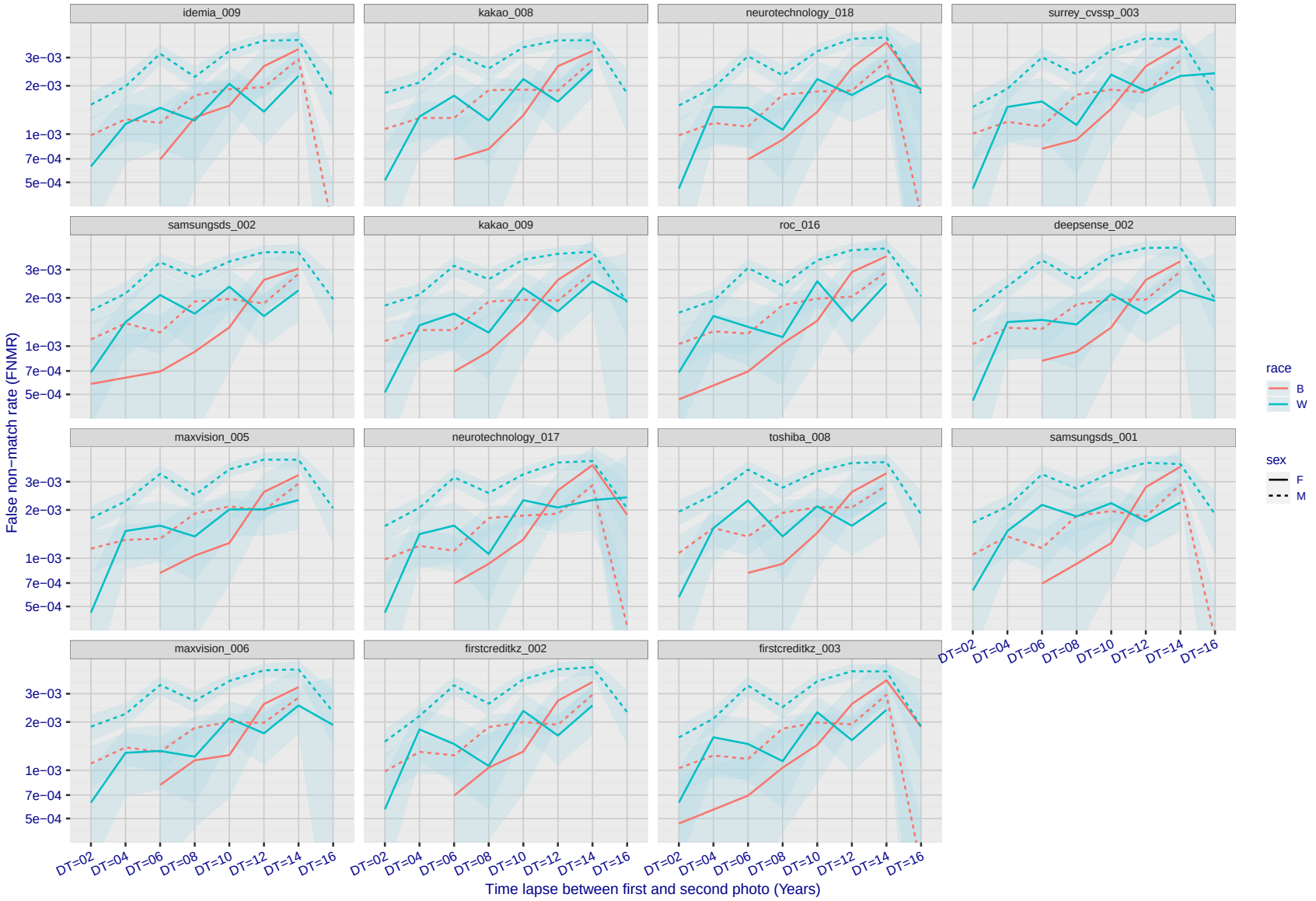

Figure 333: For the mugshot images, FNMR *as a function of elapsed time between initial enrollment and second verification images. The panels appear most accurate first, and vertical scale changes on each page. The four traces correspond to images annotated with codes for black female, black male, white female, white male. The threshold is fixed for each algorithm to give FMR = 0.00001 over all (10^8) impostor comparisons. For short time-lapses, the most accurate algorithms give very few errors (FNMR < 0.001) so that the uncertainty estimates are high.*

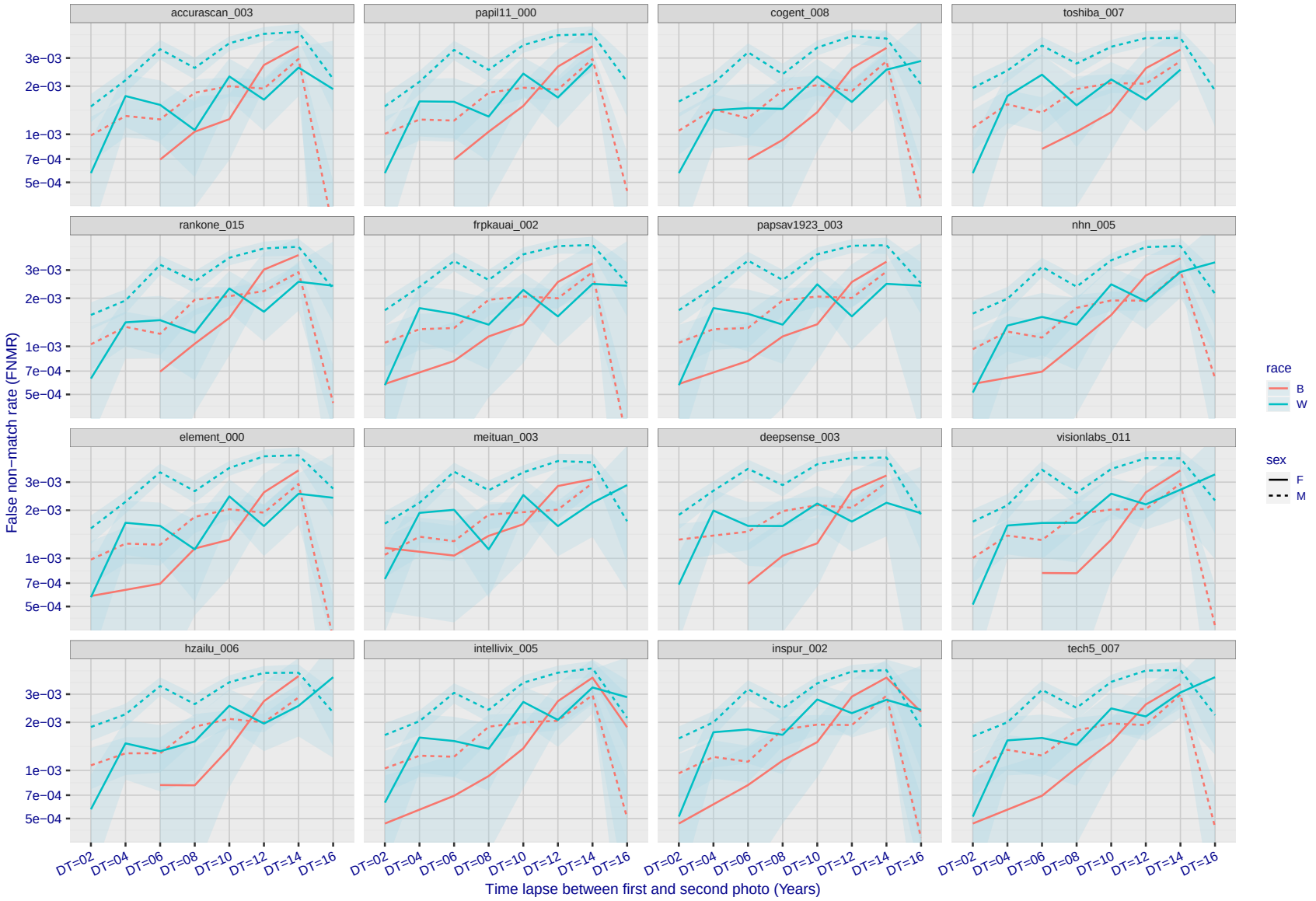

Figure 334: For the mugshot images, FNMR *as a function of elapsed time between initial enrollment and second verification images. The panels appear most accurate first, and vertical scale changes on each page. The four traces correspond to images annotated with codes for black female, black male, white female, white male. The threshold is fixed for each algorithm to give FMR = 0.00001 over all (10^8) impostor comparisons. For short time-lapses, the most accurate algorithms give very few errors (FNMR < 0.001) so that the uncertainty estimates are high.*

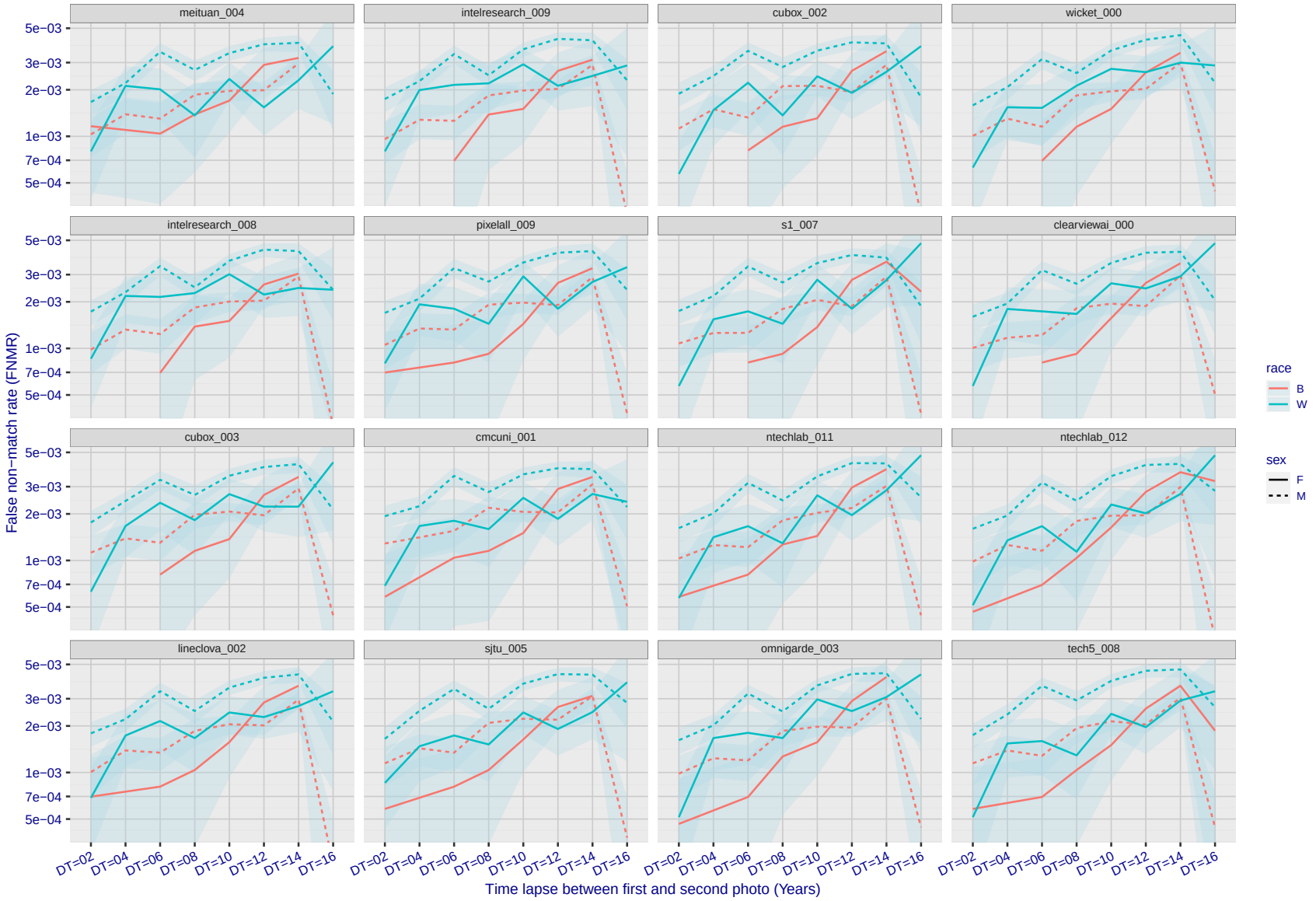

Figure 335: For the mugshot images, FNMR *as a function of elapsed time between initial enrollment and second verification images. The panels appear most accurate first, and vertical scale changes on each page. The four traces correspond to images annotated with codes for black female, black male, white female, white male. The threshold is fixed for each algorithm to give FMR = 0.00001 over all (10^8) impostor comparisons. For short time-lapses, the most accurate algorithms give very few errors (FNMR < 0.001) so that the uncertainty estimates are high.*

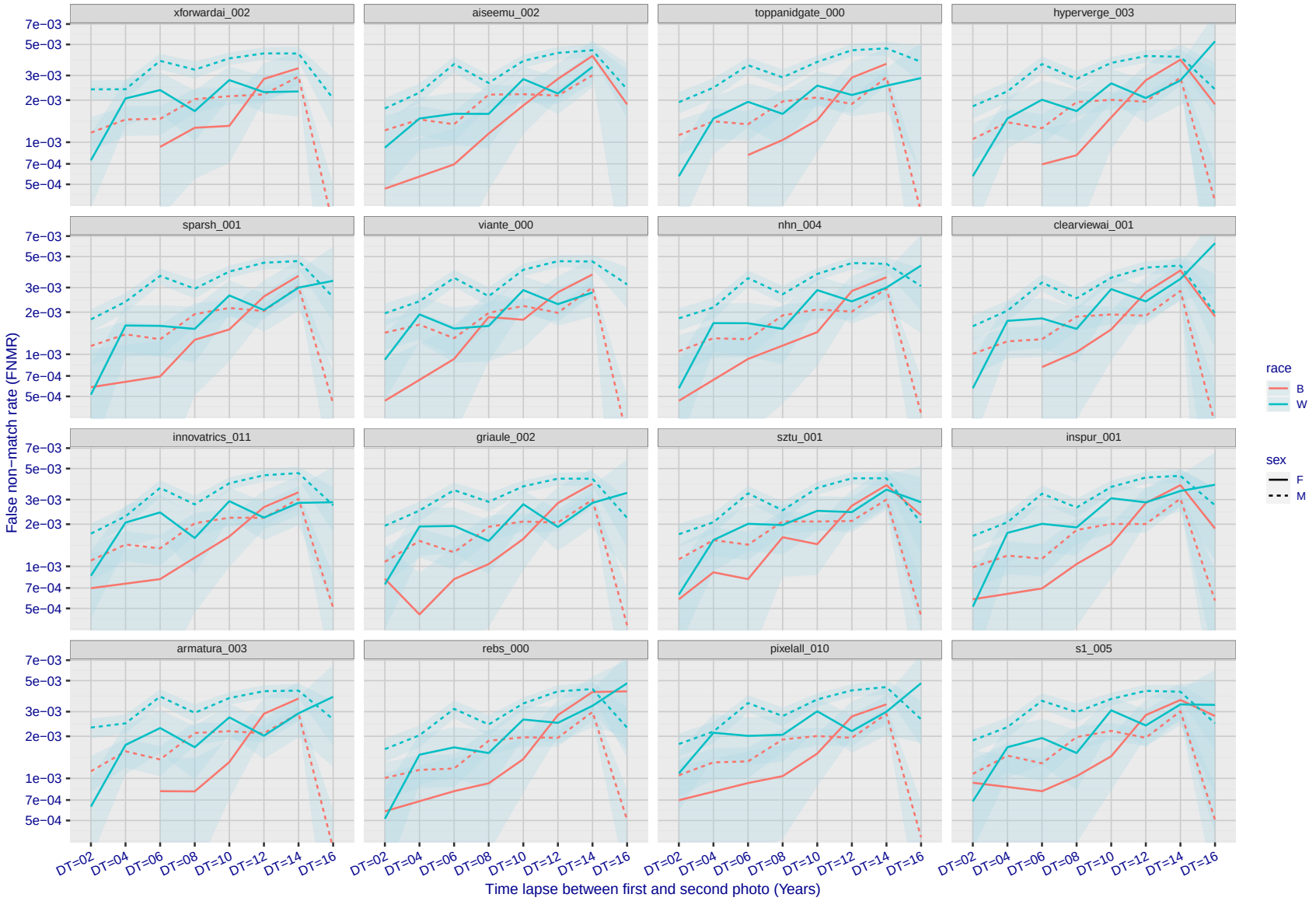

Figure 336: For the mugshot images, FNMR *as a function of elapsed time between initial enrollment and second verification images. The panels appear most accurate first, and vertical scale changes on each page. The four traces correspond to images annotated with codes for black female, black male, white female, white male. The threshold is fixed for each algorithm to give FMR = 0.00001 over all (10^8) impostor comparisons. For short time-lapses, the most accurate algorithms give very few errors (FNMR < 0.001) so that the uncertainty estimates are high.*

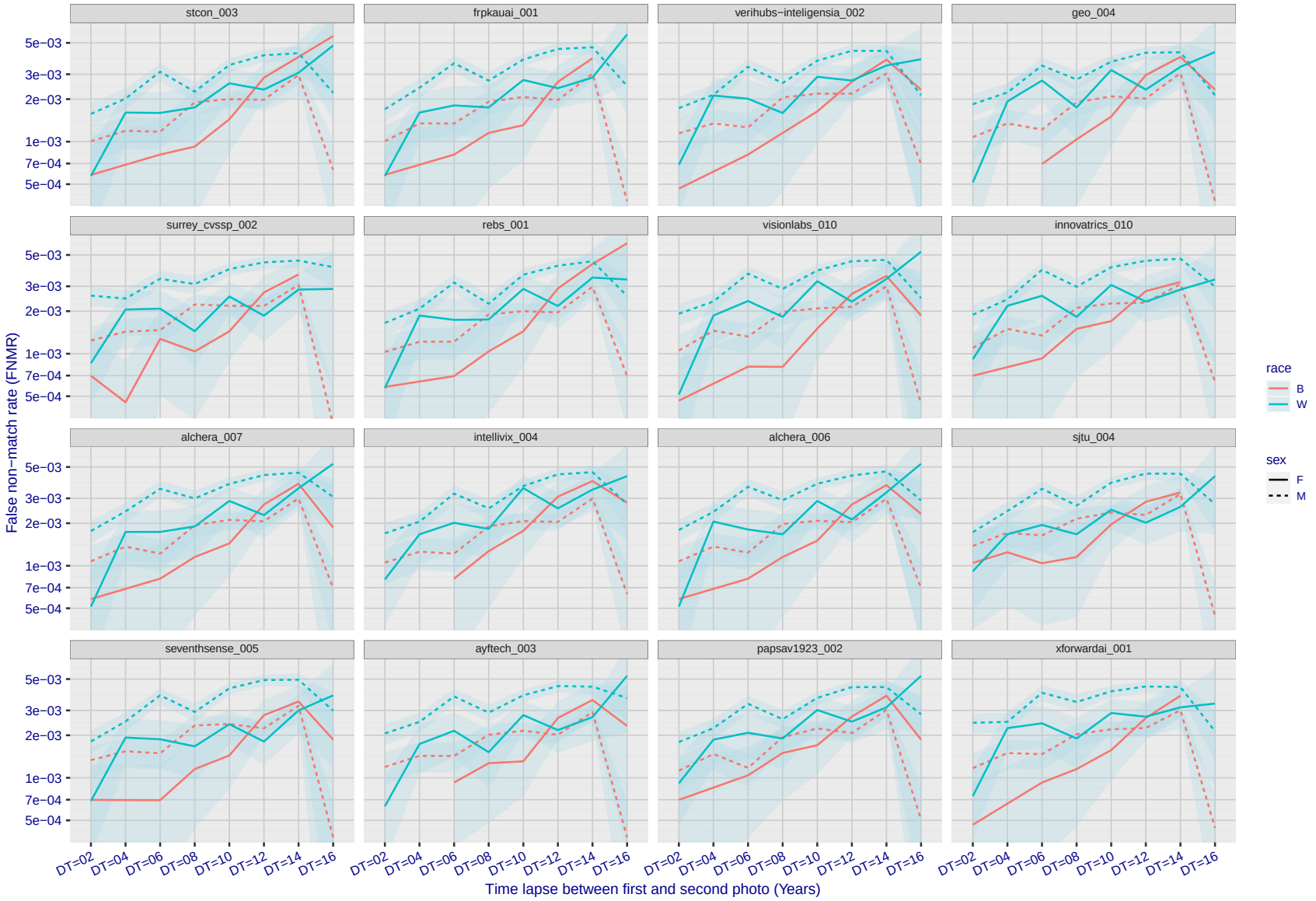

Figure 337: For the mugshot images, FNMR *as a function of elapsed time between initial enrollment and second verification images. The panels appear most accurate first, and vertical scale changes on each page. The four traces correspond to images annotated with codes for black female, black male, white female, white male. The threshold is fixed for each algorithm to give FMR = 0.00001 over all (10^8) impostor comparisons. For short time-lapses, the most accurate algorithms give very few errors (FNMR < 0.001) so that the uncertainty estimates are high.*

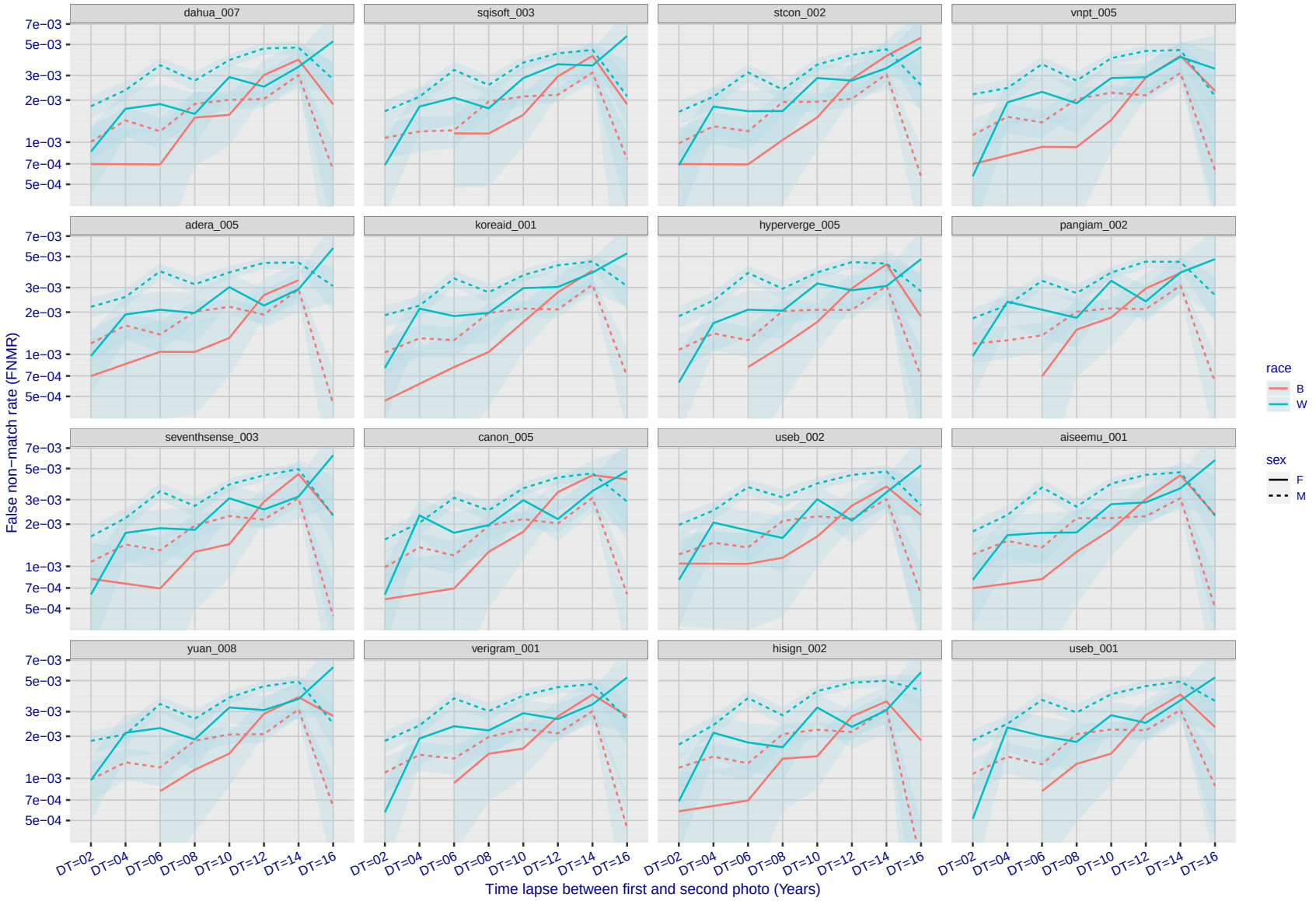

Figure 338: For the mugshot images, FNMR *as a function of elapsed time between initial enrollment and second verification images. The panels appear most accurate first, and vertical scale changes on each page. The four traces correspond to images annotated with codes for black female, black male, white female, white male. The threshold is fixed for each algorithm to give FMR = 0.00001 over all (10^8) impostor comparisons. For short time-lapses, the most accurate algorithms give very few errors (FNMR < 0.001) so that the uncertainty estimates are high.*

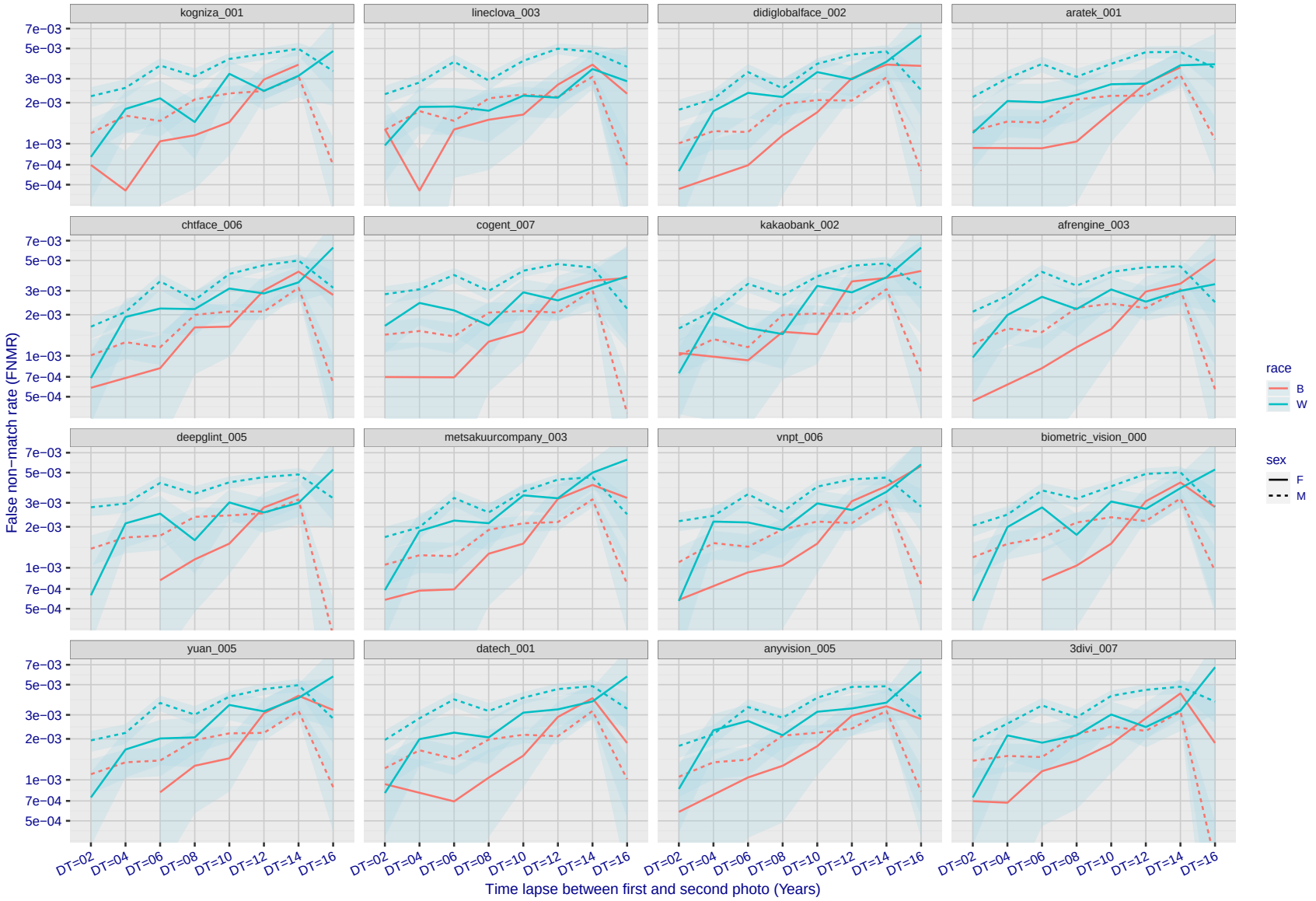

Figure 339: For the mugshot images, FNMR *as a function of elapsed time between initial enrollment and second verification images. The panels appear most accurate first, and vertical scale changes on each page. The four traces correspond to images annotated with codes for black female, black male, white female, white male. The threshold is fixed for each algorithm to give FMR = 0.00001 over all ($\tilde{10}^8$) impostor comparisons. For short time-lapses, the most accurate algorithms give very few errors (FNMR < 0.001) so that the uncertainty estimates are high.*

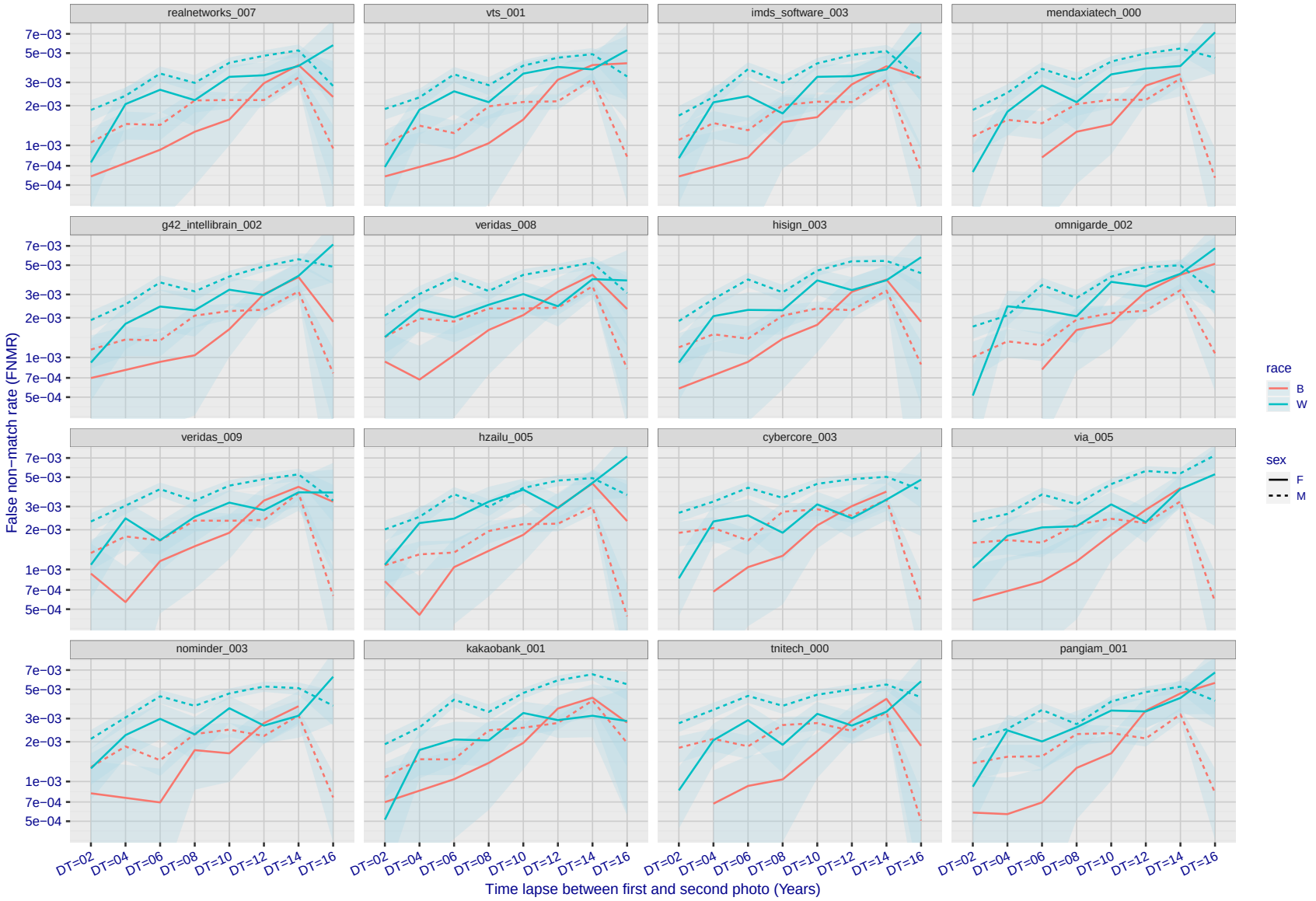

Figure 340: For the mugshot images, FNMR *as a function of elapsed time between initial enrollment and second verification images. The panels appear most accurate first, and vertical scale changes on each page. The four traces correspond to images annotated with codes for black female, black male, white female, white male. The threshold is fixed for each algorithm to give FMR = 0.00001 over all ($\tilde{10}^8$) impostor comparisons. For short time-lapses, the most accurate algorithms give very few errors (FNMR < 0.001) so that the uncertainty estimates are high.*

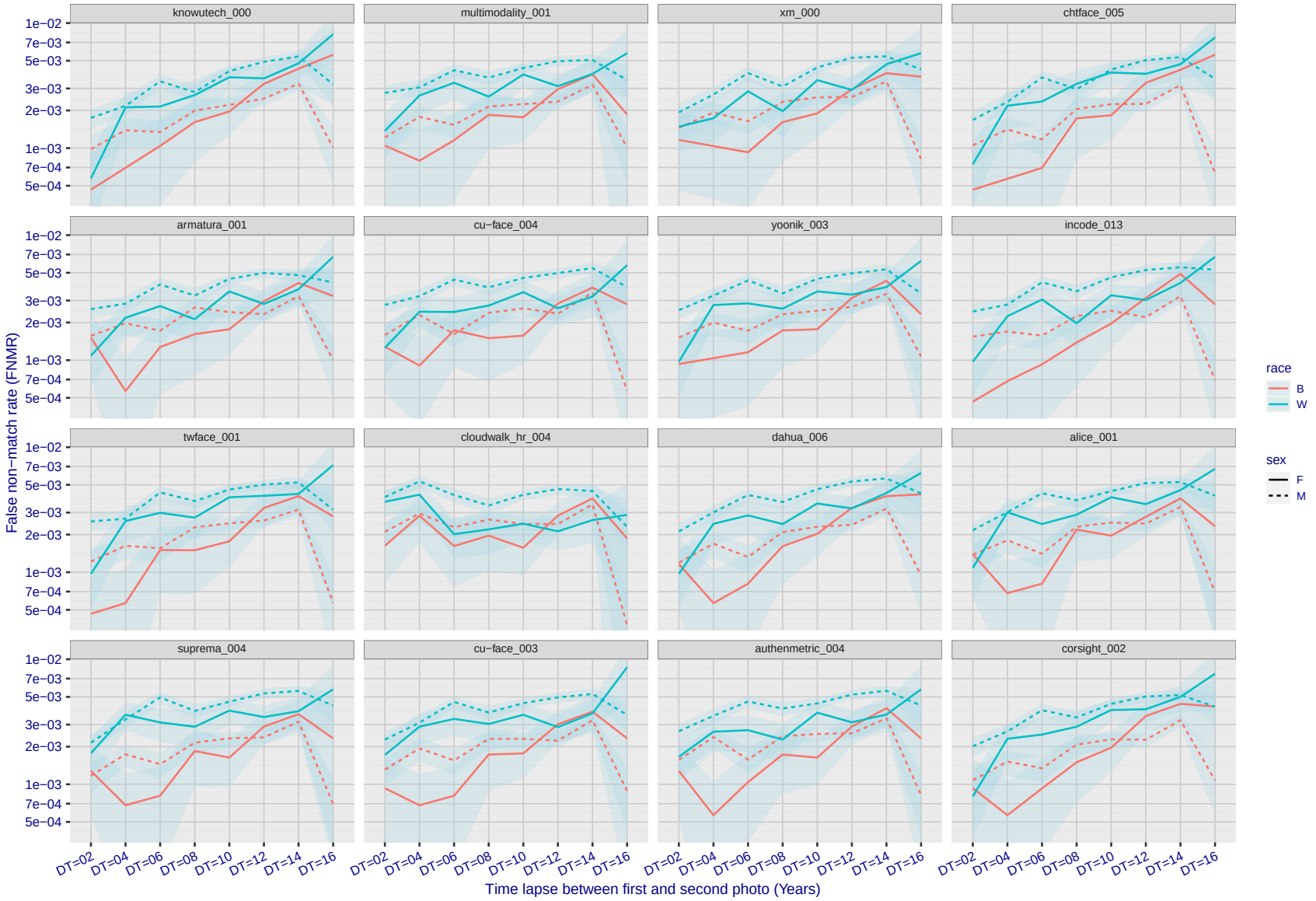

Figure 341: For the mugshot images, FNMR *as a function of elapsed time between initial enrollment and second verification images. The panels appear most accurate first, and vertical scale changes on each page. The four traces correspond to images annotated with codes for black female, black male, white female, white male. The threshold is fixed for each algorithm to give FMR = 0.00001 over all (10^8) impostor comparisons. For short time-lapses, the most accurate algorithms give very few errors (FNMR < 0.001) so that the uncertainty estimates are high.*

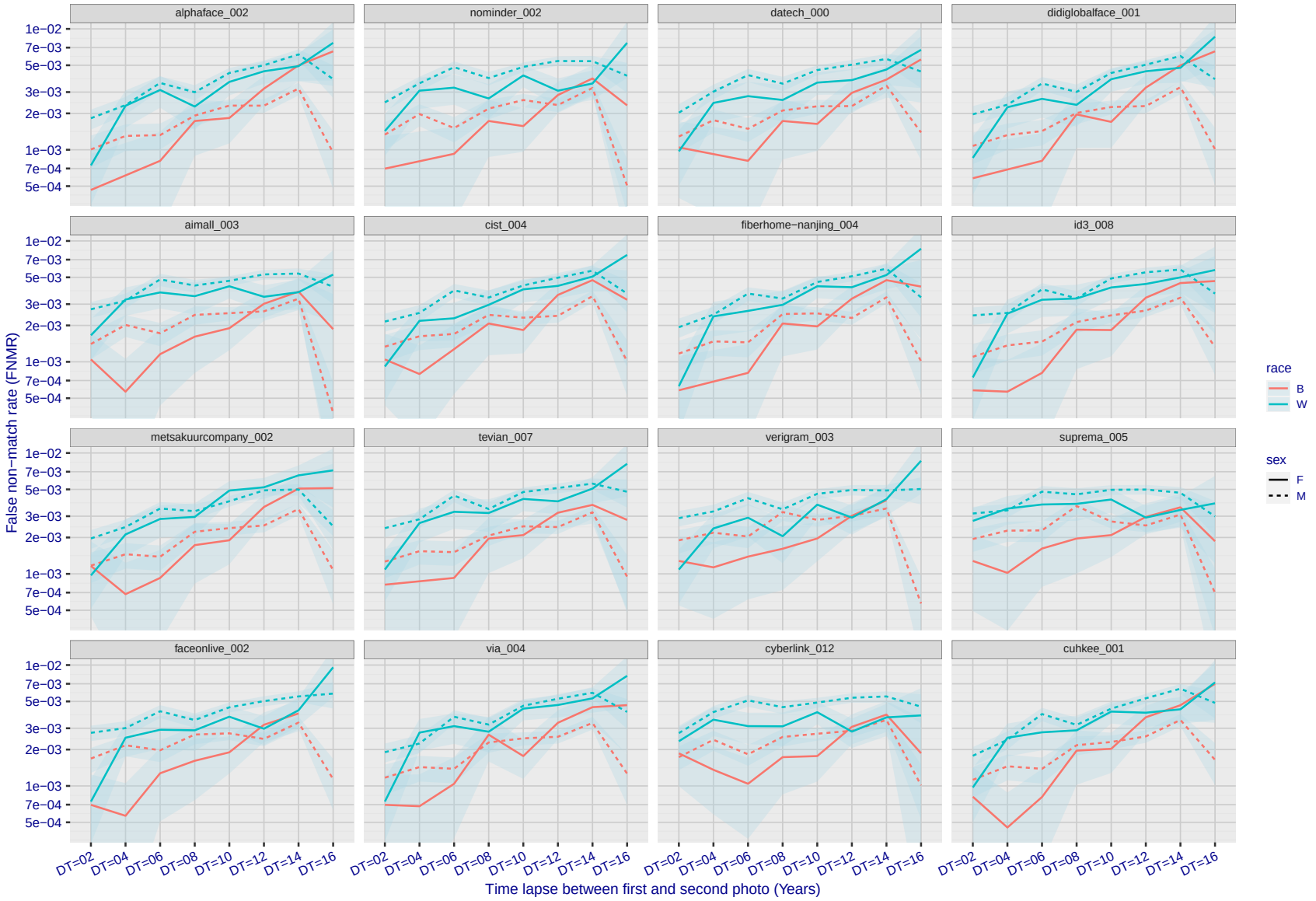

Figure 342: For the mugshot images, FNMR *as a function of elapsed time between initial enrollment and second verification images. The panels appear most accurate first, and vertical scale changes on each page. The four traces correspond to images annotated with codes for black female, black male, white female, white male. The threshold is fixed for each algorithm to give FMR = 0.00001 over all (10^8) impostor comparisons. For short time-lapses, the most accurate algorithms give very few errors (FNMR < 0.001) so that the uncertainty estimates are high.*

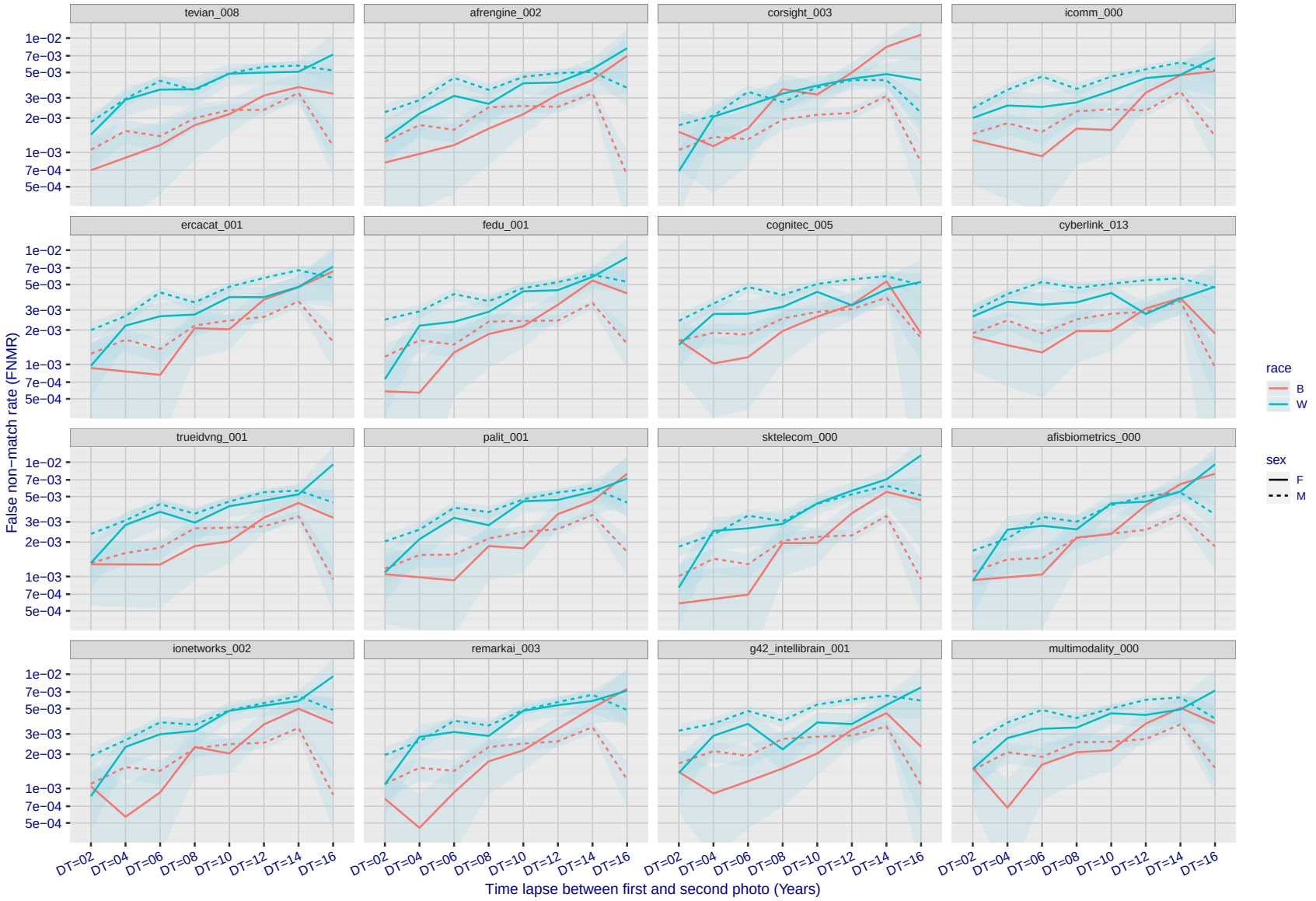

Figure 343: For the mugshot images, FNMR *as a function of elapsed time between initial enrollment and second verification images. The panels appear most accurate first, and vertical scale changes on each page. The four traces correspond to images annotated with codes for black female, black male, white female, white male. The threshold is fixed for each algorithm to give FMR = 0.00001 over all (10^8) impostor comparisons. For short time-lapses, the most accurate algorithms give very few errors (FNMR < 0.001) so that the uncertainty estimates are high.*

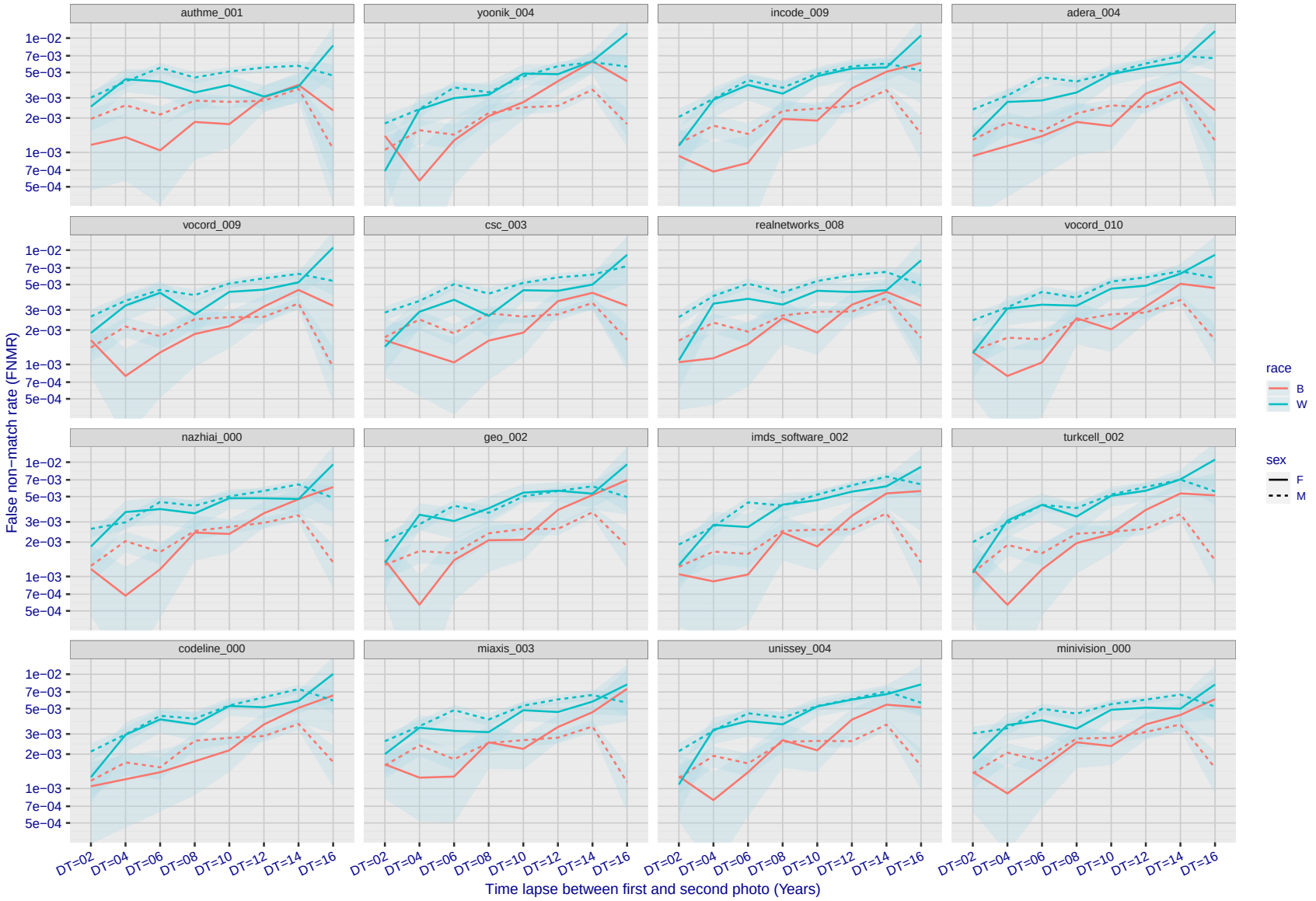

Figure 344: For the mugshot images, FNMR *as a function of elapsed time between initial enrollment and second verification images. The panels appear most accurate first, and vertical scale changes on each page. The four traces correspond to images annotated with codes for black female, black male, white female, white male. The threshold is fixed for each algorithm to give FMR = 0.00001 over all ($\widetilde{10}^8$) impostor comparisons. For short time-lapses, the most accurate algorithms give very few errors (FNMR < 0.001) so that the uncertainty estimates are high.*

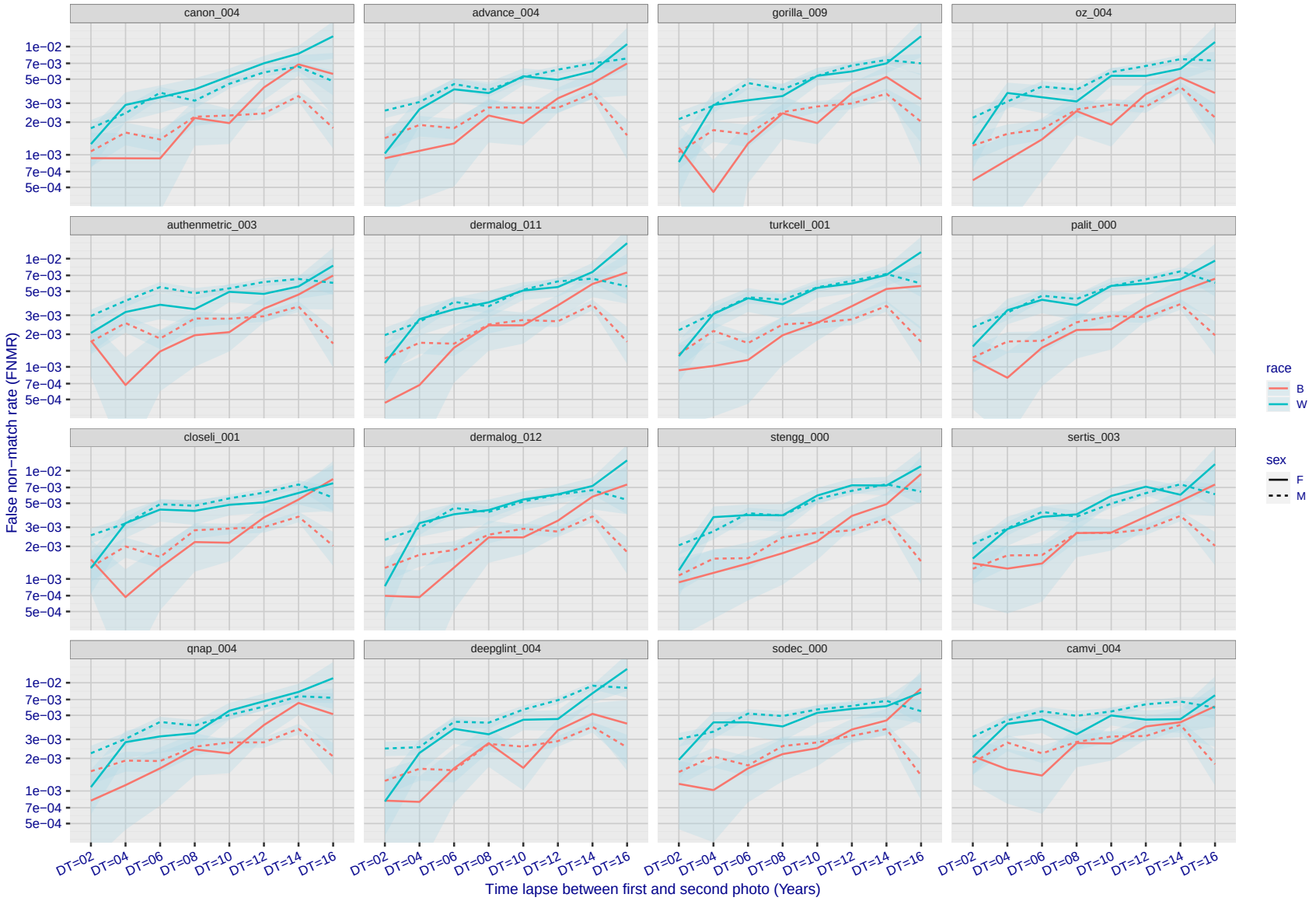

Figure 345: For the mugshot images, FNMR *as a function of elapsed time between initial enrollment and second verification images. The panels appear most accurate first, and vertical scale changes on each page. The four traces correspond to images annotated with codes for black female, black male, white female, white male. The threshold is fixed for each algorithm to give FMR = 0.00001 over all (10^8) impostor comparisons. For short time-lapses, the most accurate algorithms give very few errors (FNMR < 0.001) so that the uncertainty estimates are high.*

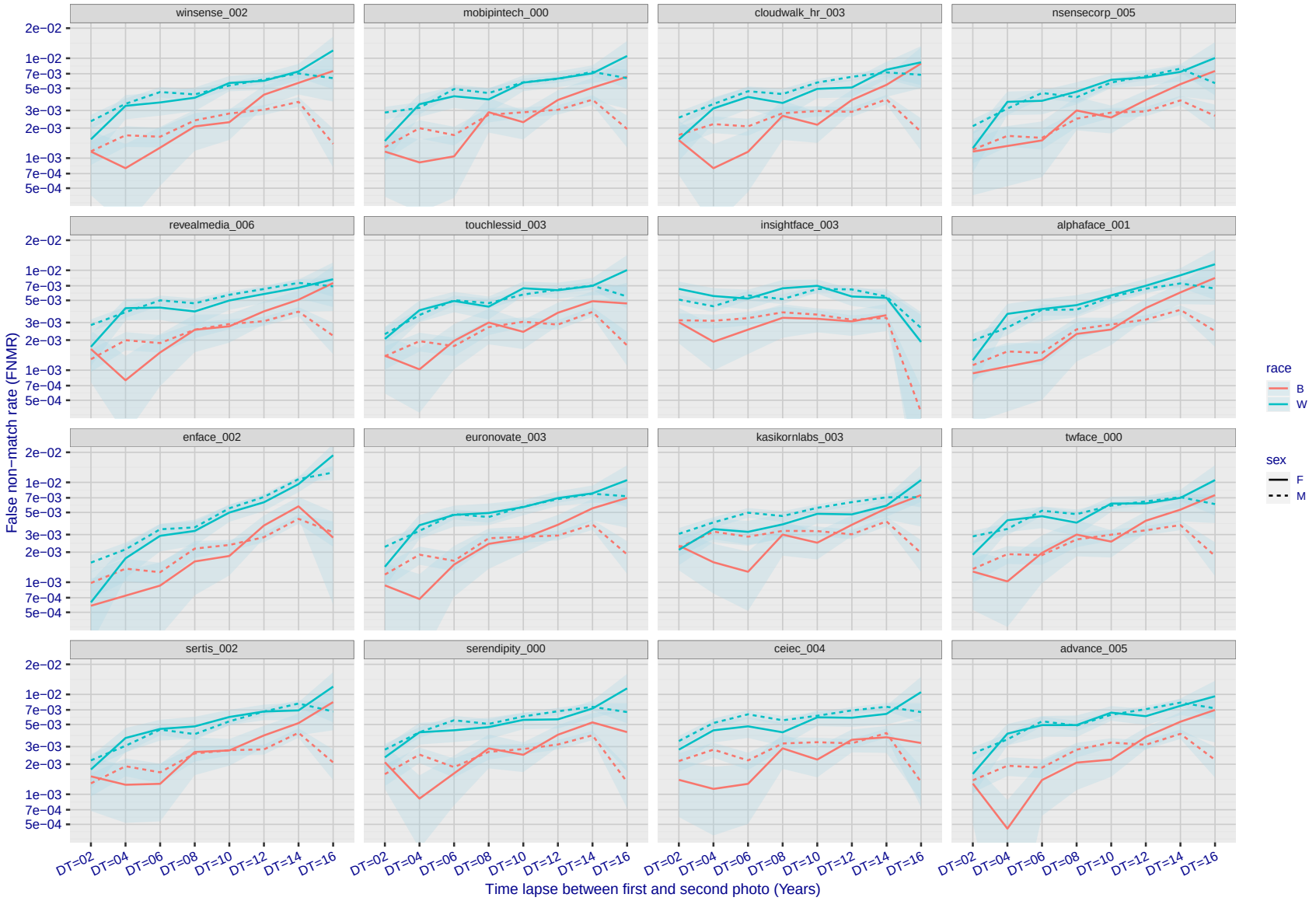

Figure 346: For the mugshot images, FNMR *as a function of elapsed time between initial enrollment and second verification images. The panels appear most accurate first, and vertical scale changes on each page. The four traces correspond to images annotated with codes for black female, black male, white female, white male. The threshold is fixed for each algorithm to give FMR = 0.00001 over all (10^8) impostor comparisons. For short time-lapses, the most accurate algorithms give very few errors (FNMR < 0.001) so that the uncertainty estimates are high.*

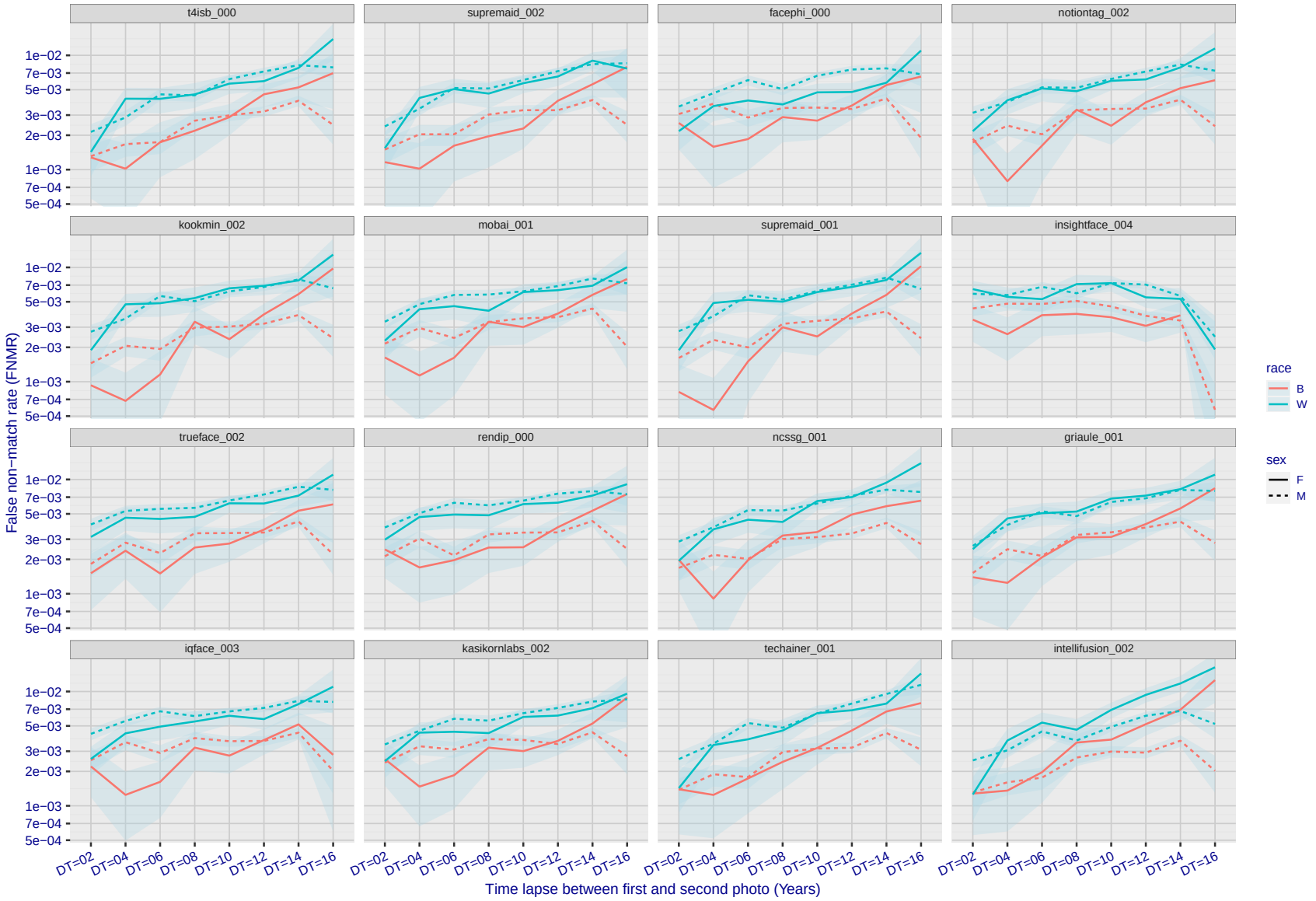

Figure 347: For the mugshot images, FNMR *as a function of elapsed time between initial enrollment and second verification images. The panels appear most accurate first, and vertical scale changes on each page. The four traces correspond to images annotated with codes for black female, black male, white female, white male. The threshold is fixed for each algorithm to give FMR = 0.00001 over all (10^8) impostor comparisons. For short time-lapses, the most accurate algorithms give very few errors (FNMR < 0.001) so that the uncertainty estimates are high.*

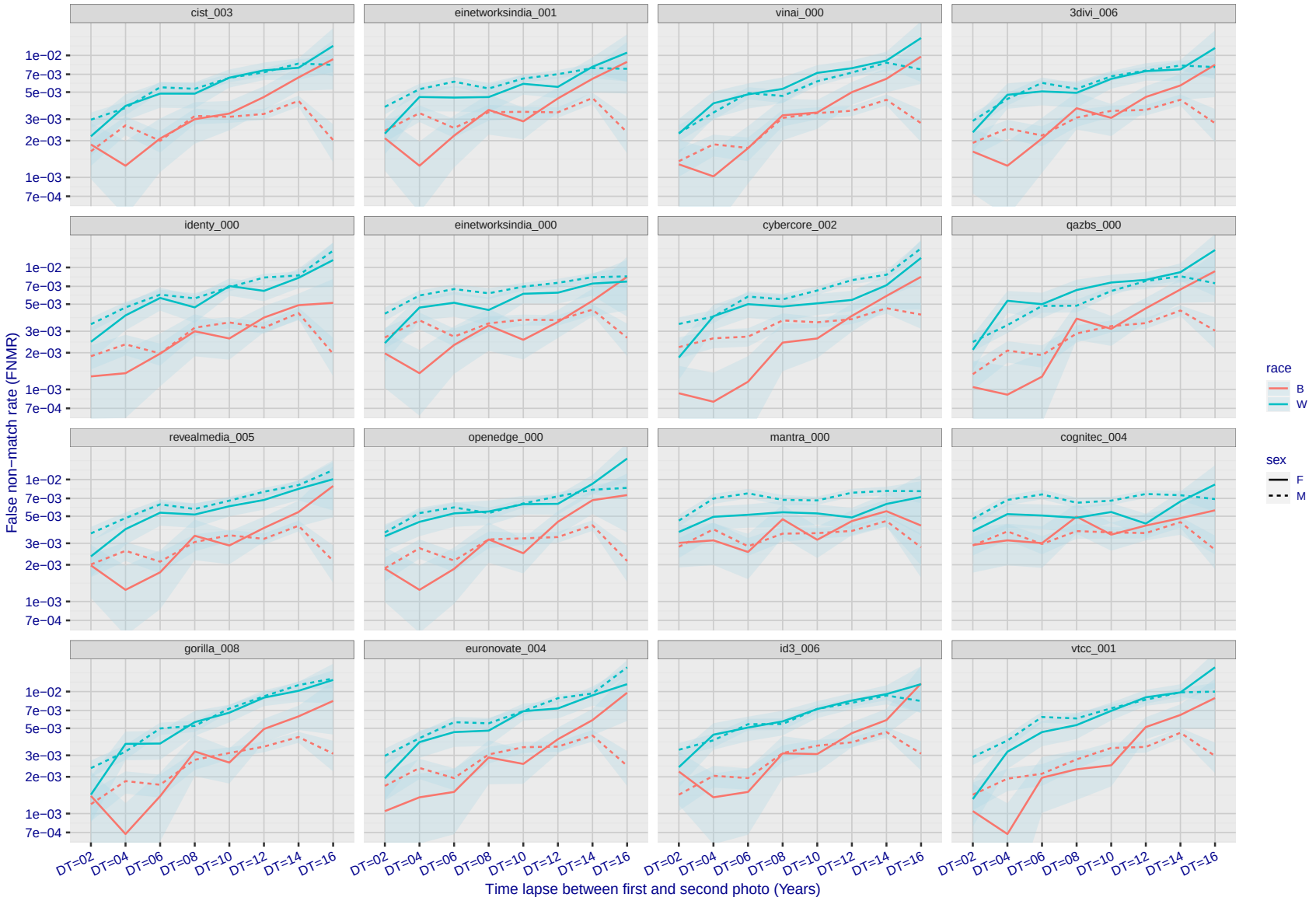

Figure 348: For the mugshot images, FNMR *as a function of elapsed time between initial enrollment and second verification images. The panels appear most accurate first, and vertical scale changes on each page. The four traces correspond to images annotated with codes for black female, black male, white female, white male. The threshold is fixed for each algorithm to give FMR = 0.00001 over all (10^8) impostor comparisons. For short time-lapses, the most accurate algorithms give very few errors (FNMR < 0.001) so that the uncertainty estimates are high.*

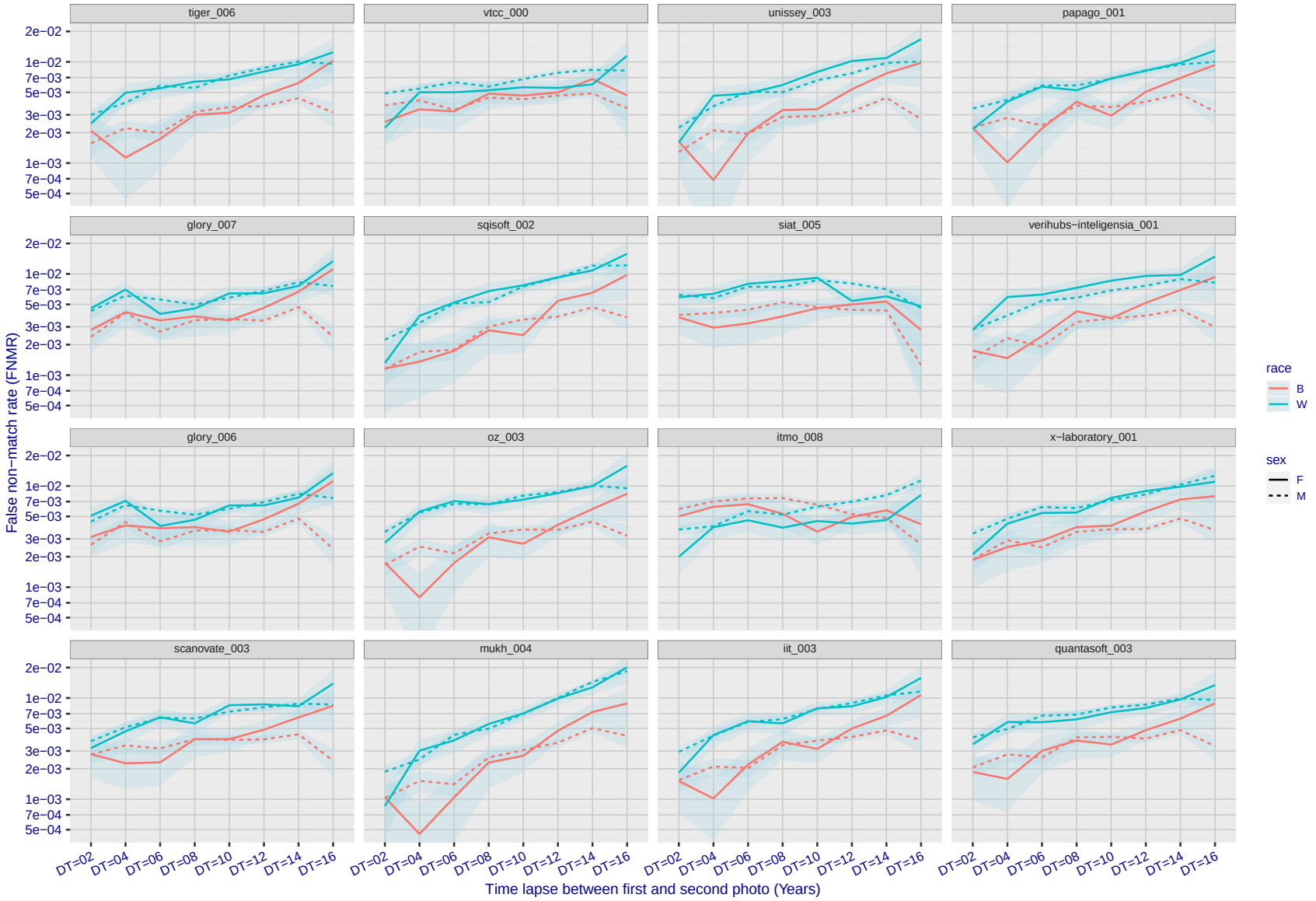

Figure 349: For the mugshot images, FNMR *as a function of elapsed time between initial enrollment and second verification images. The panels appear most accurate first, and vertical scale changes on each page. The four traces correspond to images annotated with codes for black female, black male, white female, white male. The threshold is fixed for each algorithm to give FMR = 0.00001 over all ($\tilde{10}^8$) impostor comparisons. For short time-lapses, the most accurate algorithms give very few errors (FNMR < 0.001) so that the uncertainty estimates are high.*

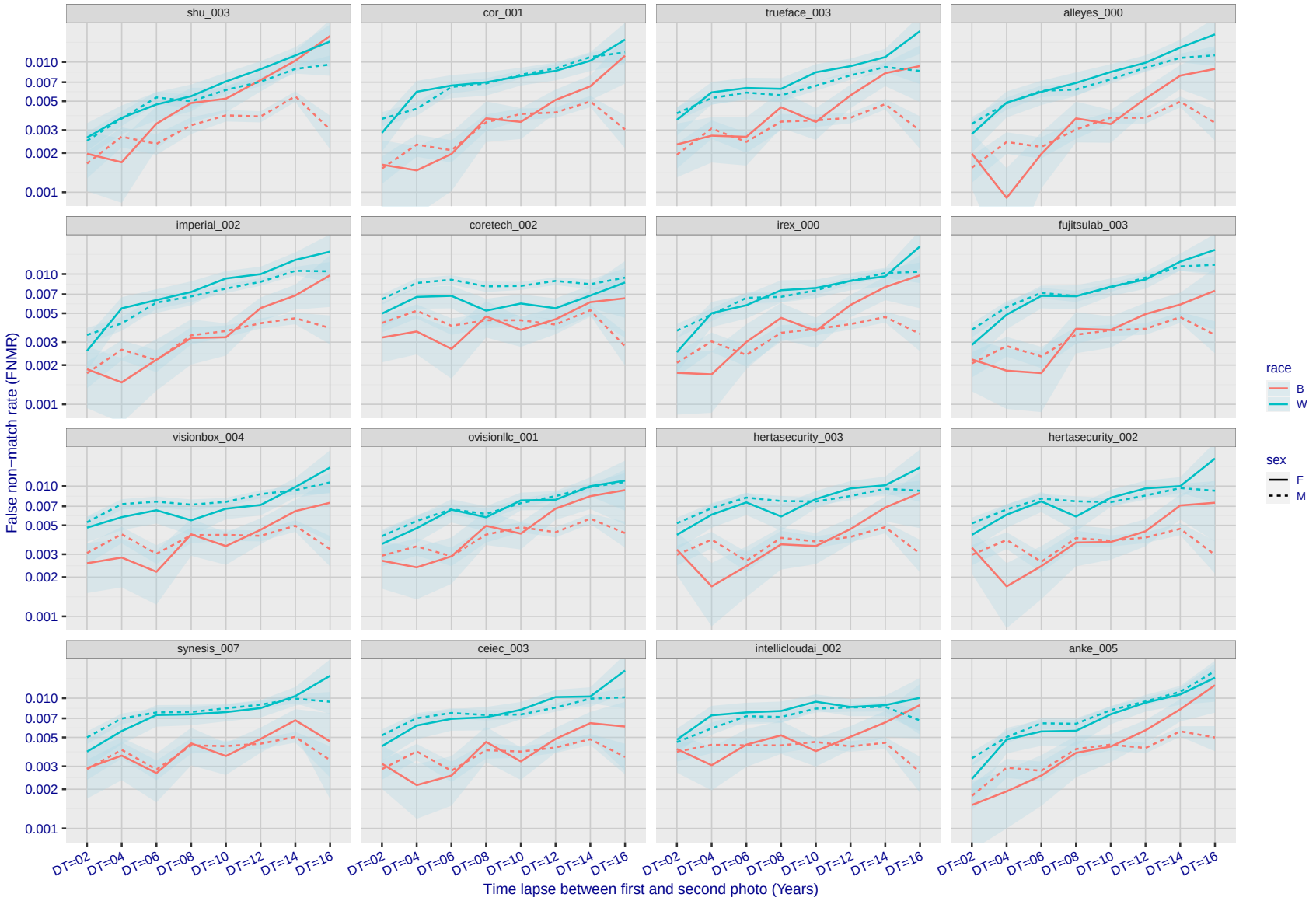

Figure 350: For the mugshot images, FNMR *as a function of elapsed time between initial enrollment and second verification images. The panels appear most accurate first, and vertical scale changes on each page. The four traces correspond to images annotated with codes for black female, black male, white female, white male. The threshold is fixed for each algorithm to give FMR = 0.00001 over all (10^8) impostor comparisons. For short time-lapses, the most accurate algorithms give very few errors (FNMR < 0.001) so that the uncertainty estimates are high.*

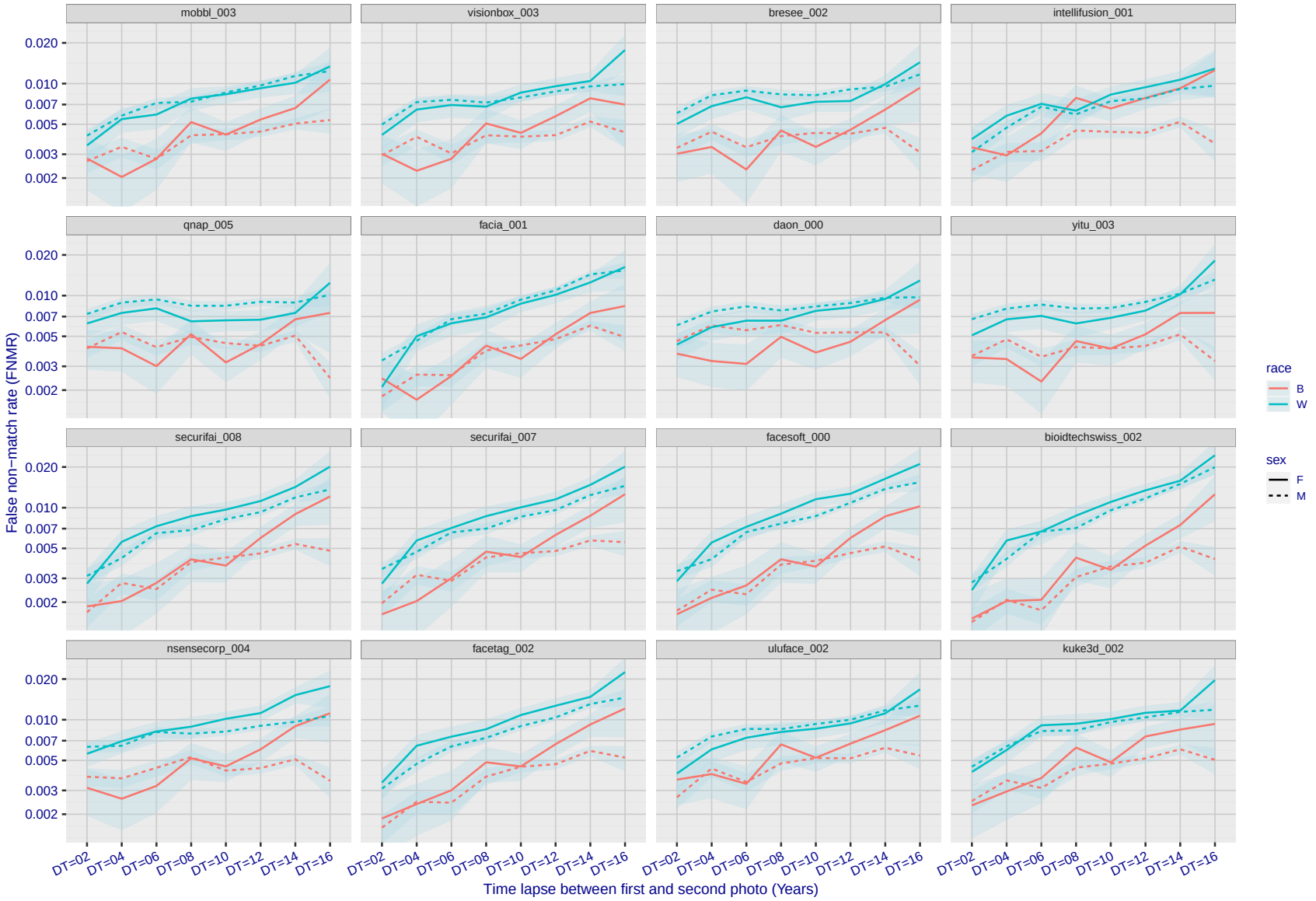

Figure 351: For the mugshot images, FNMR *as a function of elapsed time between initial enrollment and second verification images. The panels appear most accurate first, and vertical scale changes on each page. The four traces correspond to images annotated with codes for black female, black male, white female, white male. The threshold is fixed for each algorithm to give FMR = 0.00001 over all (10^8) impostor comparisons. For short time-lapses, the most accurate algorithms give very few errors (FNMR < 0.001) so that the uncertainty estimates are high.*

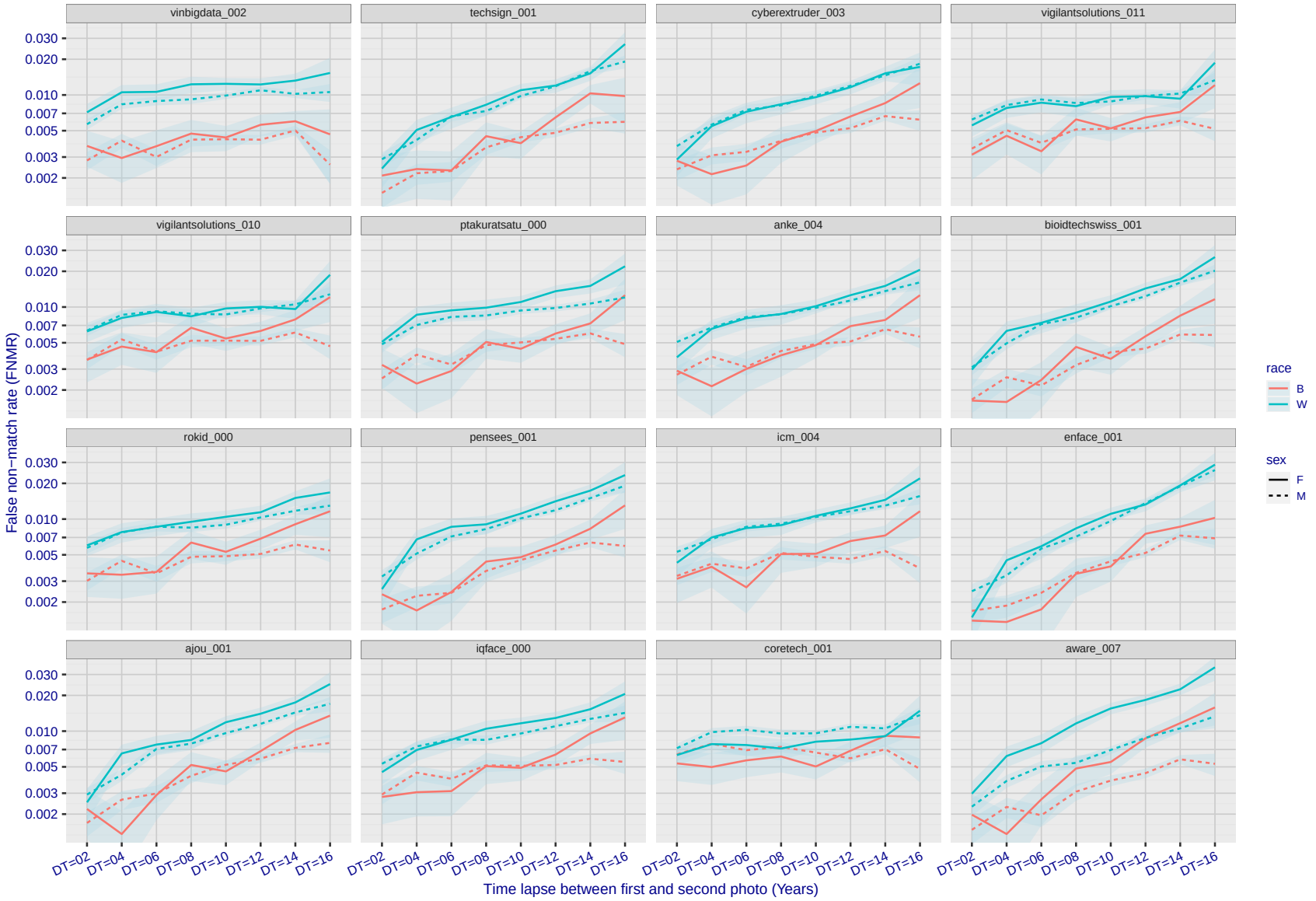

Figure 352: For the mugshot images, FNMR *as a function of elapsed time between initial enrollment and second verification images. The panels appear most accurate first, and vertical scale changes on each page. The four traces correspond to images annotated with codes for black female, black male, white female, white male. The threshold is fixed for each algorithm to give FMR = 0.00001 over all (10^8) impostor comparisons. For short time-lapses, the most accurate algorithms give very few errors (FNMR < 0.001) so that the uncertainty estimates are high.*

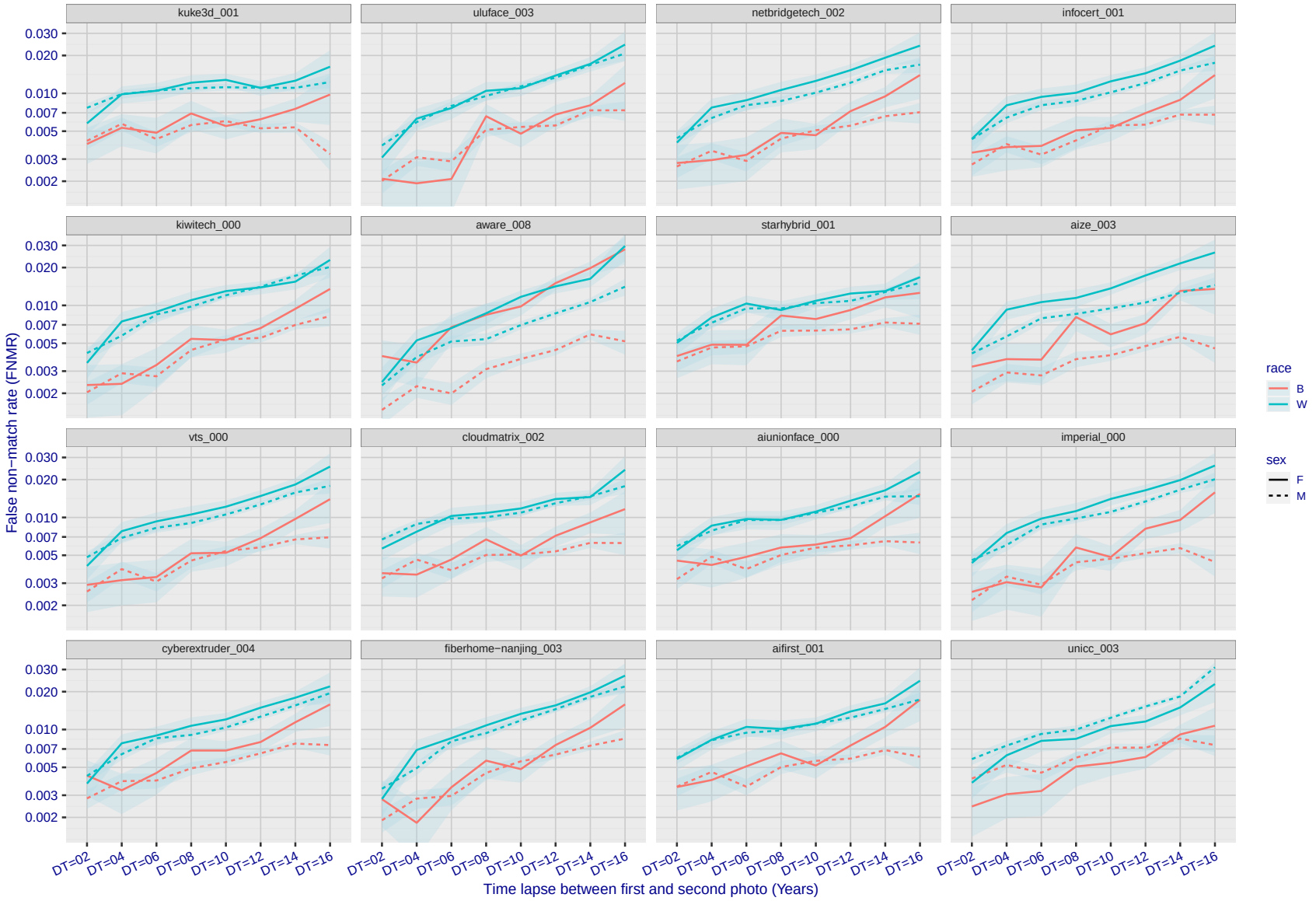

Figure 353: For the mugshot images, FNMR *as a function of elapsed time between initial enrollment and second verification images. The panels appear most accurate first, and vertical scale changes on each page. The four traces correspond to images annotated with codes for black female, black male, white female, white male. The threshold is fixed for each algorithm to give FMR = 0.00001 over all (10^8) impostor comparisons. For short time-lapses, the most accurate algorithms give very few errors (FNMR < 0.001) so that the uncertainty estimates are high.*

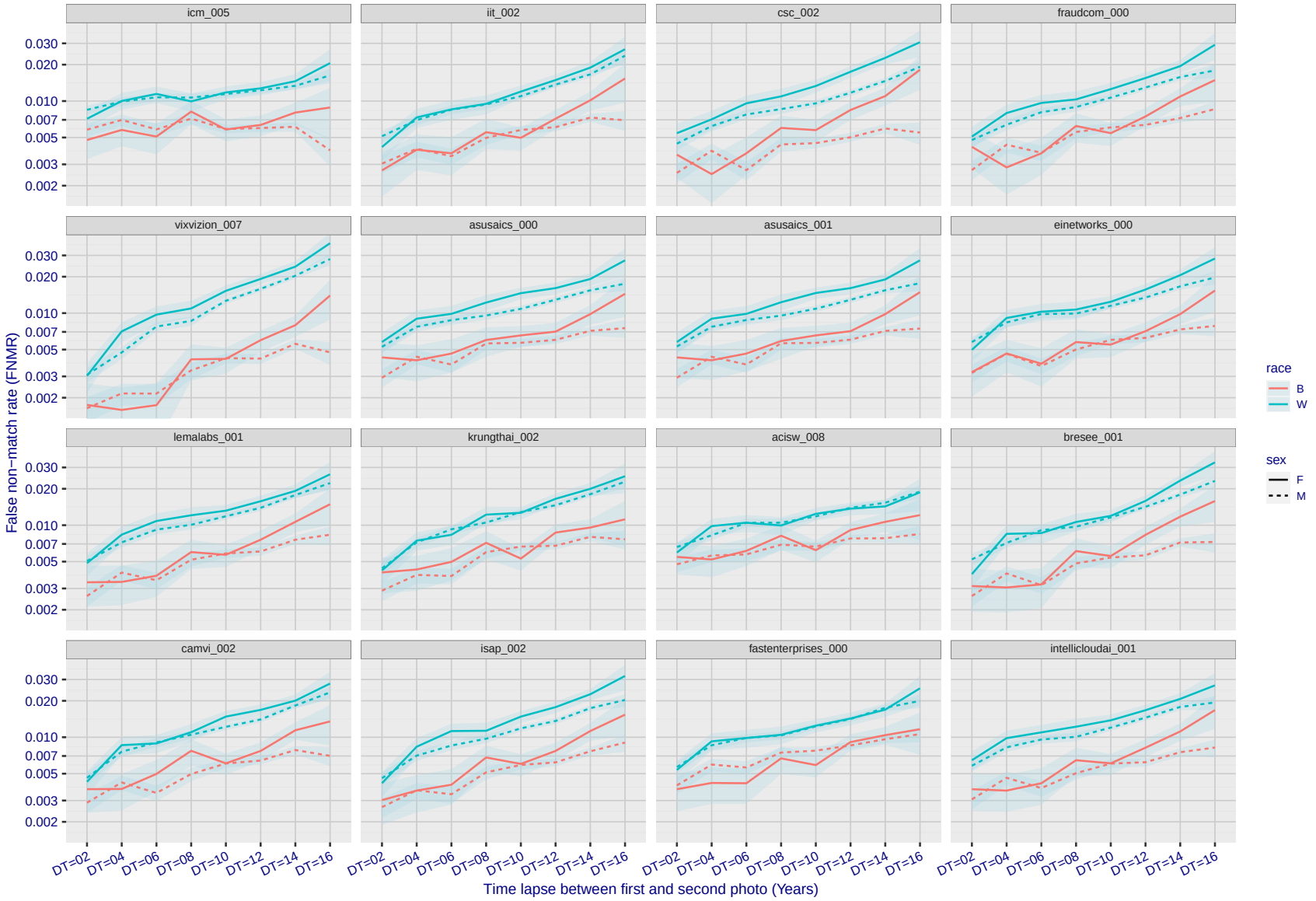

Figure 354: For the mugshot images, FNMR *as a function of elapsed time between initial enrollment and second verification images. The panels appear most accurate first, and vertical scale changes on each page. The four traces correspond to images annotated with codes for black female, black male, white female, white male. The threshold is fixed for each algorithm to give FMR = 0.00001 over all (10^8) impostor comparisons. For short time-lapses, the most accurate algorithms give very few errors (FNMR < 0.001) so that the uncertainty estimates are high.*

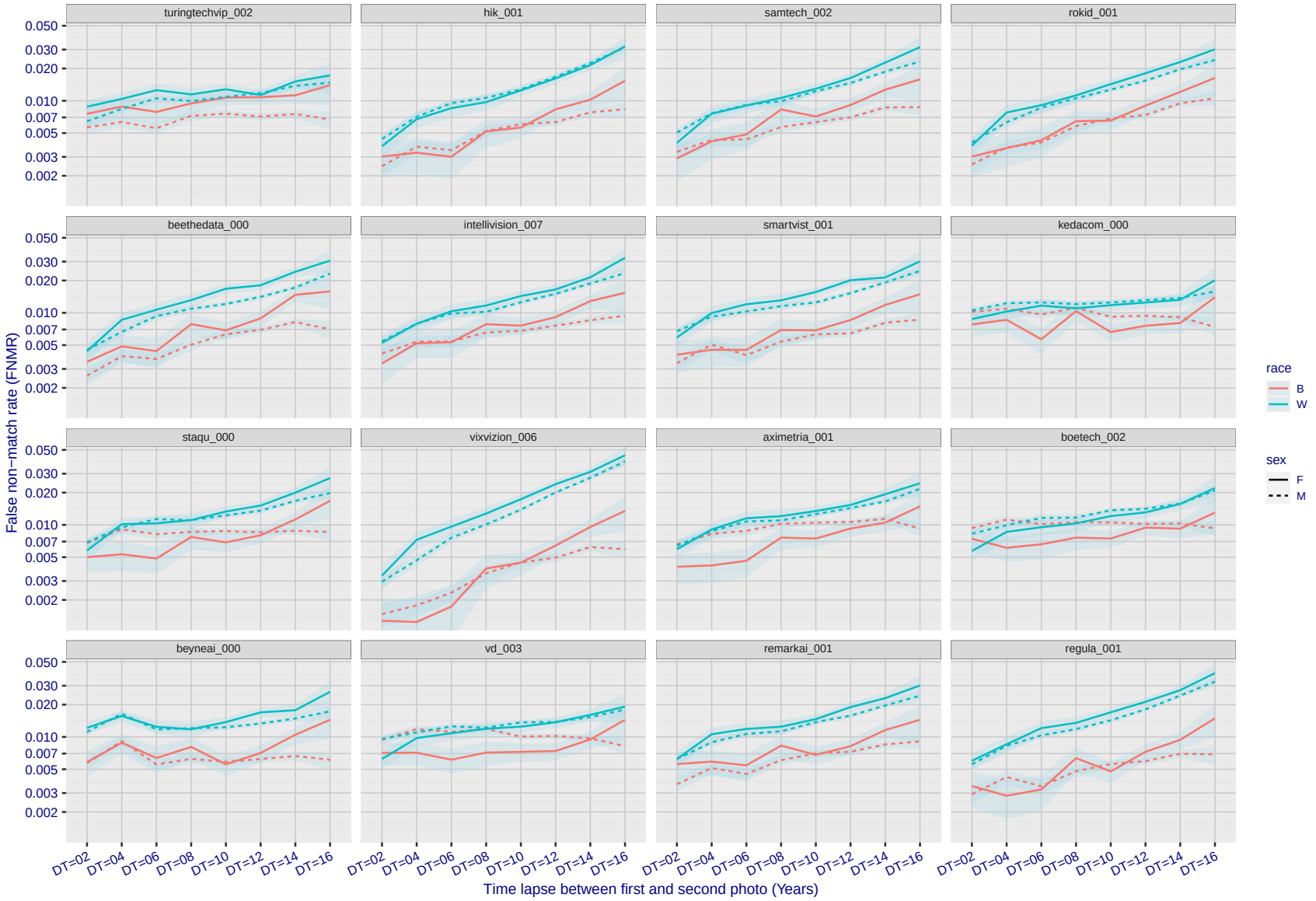

Figure 355: For the mugshot images, FNMR *as a function of elapsed time between initial enrollment and second verification images. The panels appear most accurate first, and vertical scale changes on each page. The four traces correspond to images annotated with codes for black female, black male, white female, white male. The threshold is fixed for each algorithm to give FMR = 0.00001 over all (10^8) impostor comparisons. For short time-lapses, the most accurate algorithms give very few errors (FNMR < 0.001) so that the uncertainty estimates are high.*

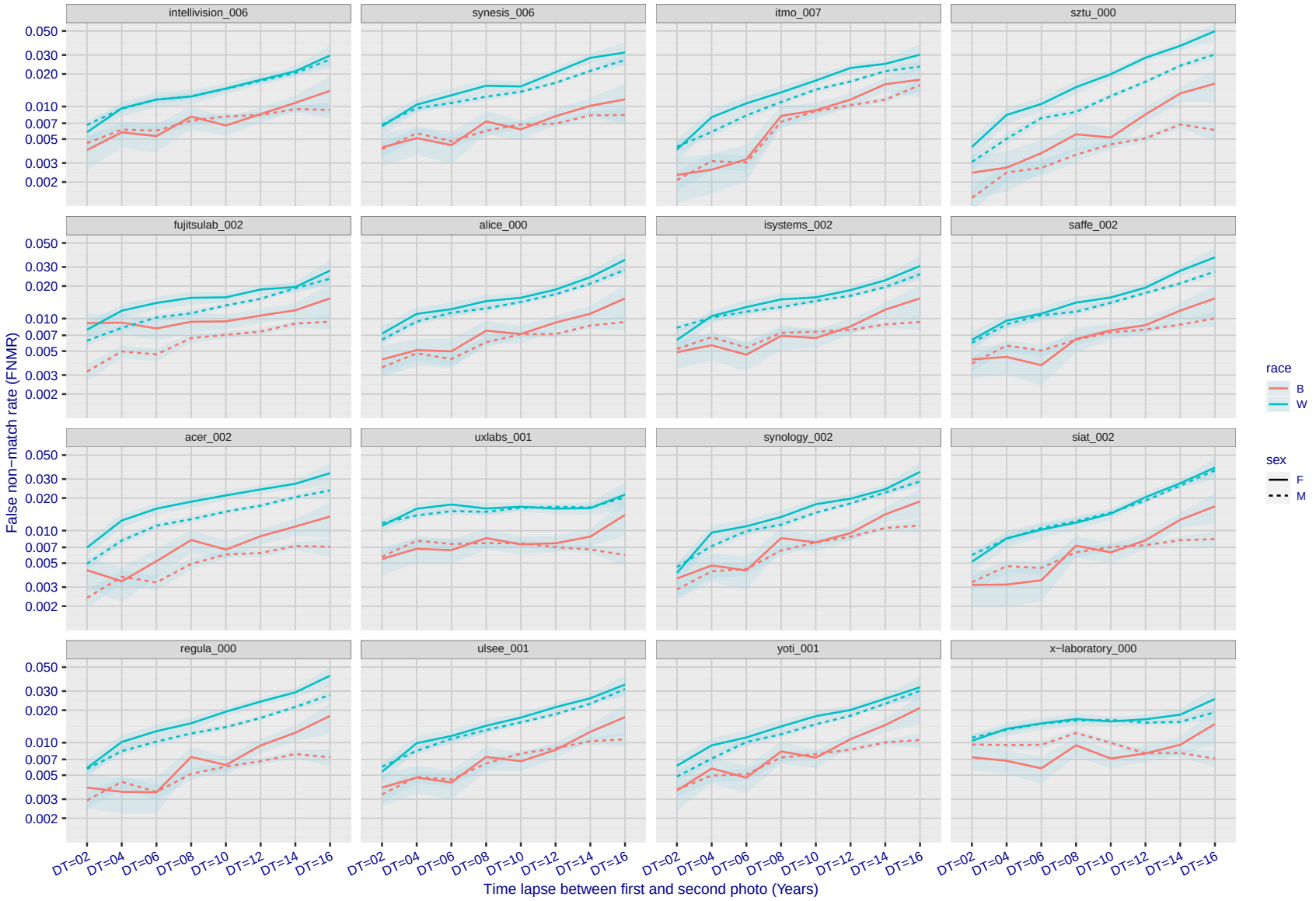

Figure 356: For the mugshot images, FNMR *as a function of elapsed time between initial enrollment and second verification images. The panels appear most accurate first, and vertical scale changes on each page. The four traces correspond to images annotated with codes for black female, black male, white female, white male. The threshold is fixed for each algorithm to give FMR = 0.00001 over all (10^8) impostor comparisons. For short time-lapses, the most accurate algorithms give very few errors (FNMR < 0.001) so that the uncertainty estimates are high.*

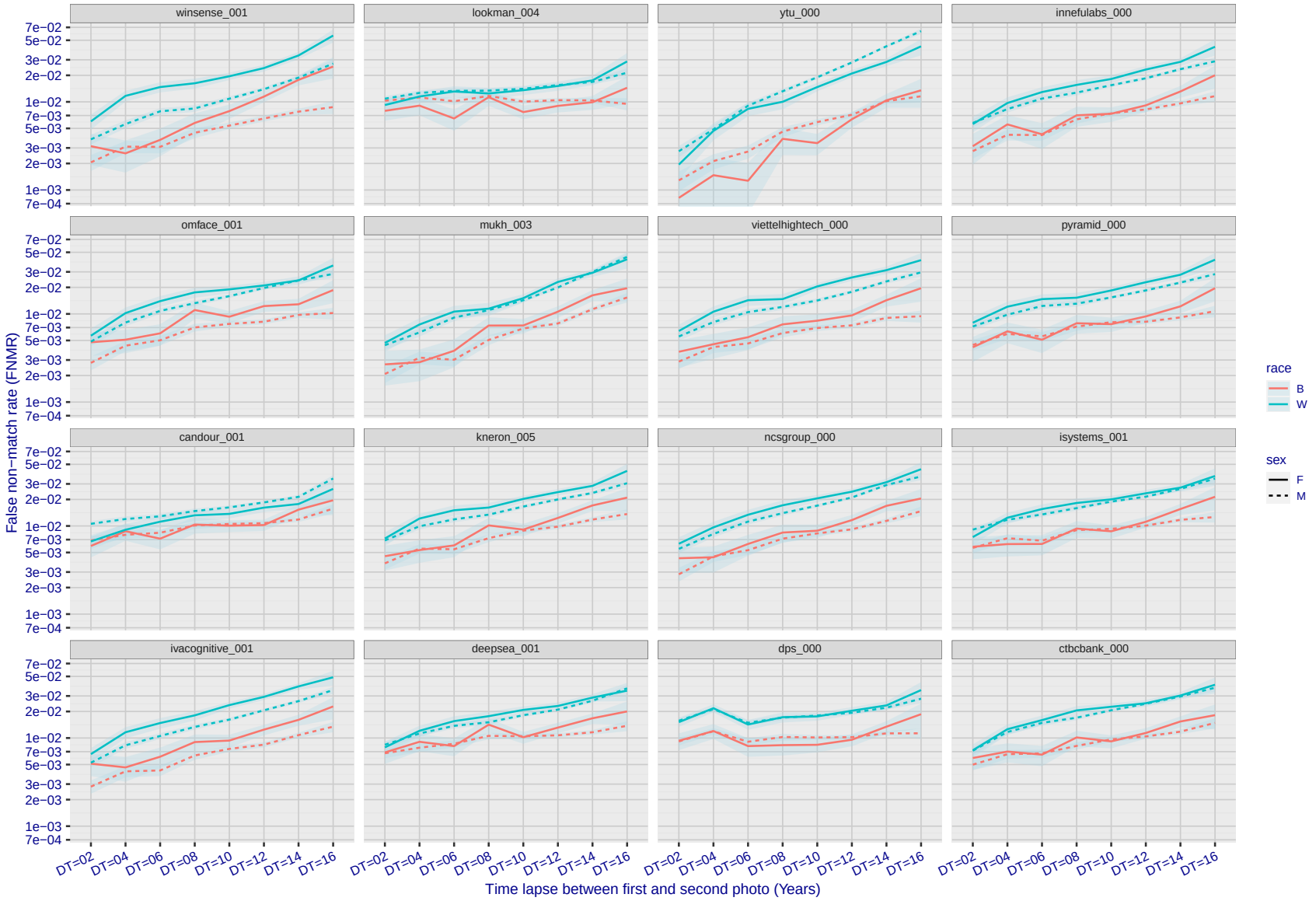

Figure 357: For the mugshot images, FNMR *as a function of elapsed time between initial enrollment and second verification images. The panels appear most accurate first, and vertical scale changes on each page. The four traces correspond to images annotated with codes for black female, black male, white female, white male. The threshold is fixed for each algorithm to give FMR = 0.00001 over all ($\tilde{10}^8$) impostor comparisons. For short time-lapses, the most accurate algorithms give very few errors (FNMR < 0.001) so that the uncertainty estimates are high.*

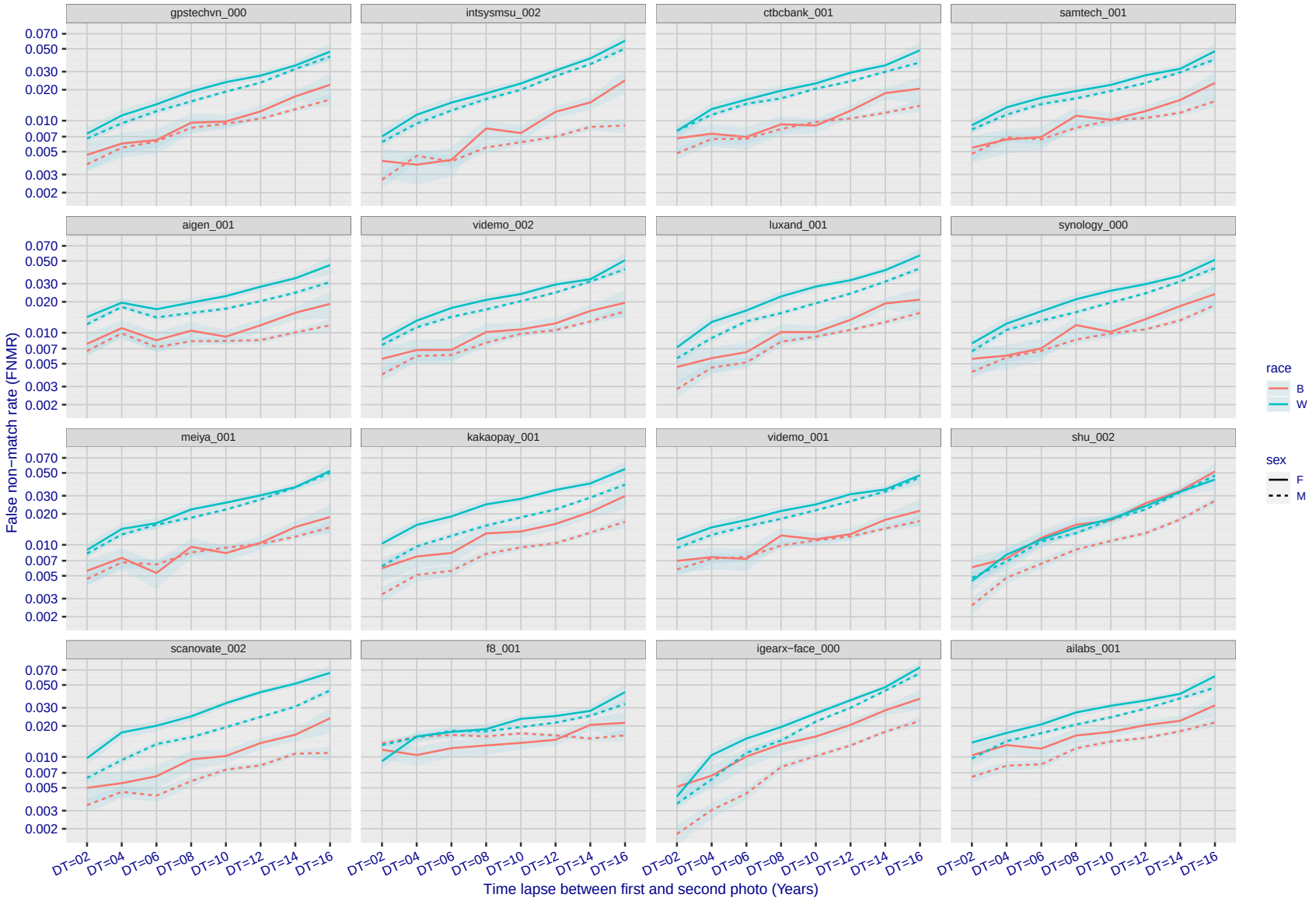

Figure 358: For the mugshot images, FNMR *as a function of elapsed time between initial enrollment and second verification images. The panels appear most accurate first, and vertical scale changes on each page. The four traces correspond to images annotated with codes for black female, black male, white female, white male. The threshold is fixed for each algorithm to give FMR = 0.00001 over all (10^8) impostor comparisons. For short time-lapses, the most accurate algorithms give very few errors (FNMR < 0.001) so that the uncertainty estimates are high.*

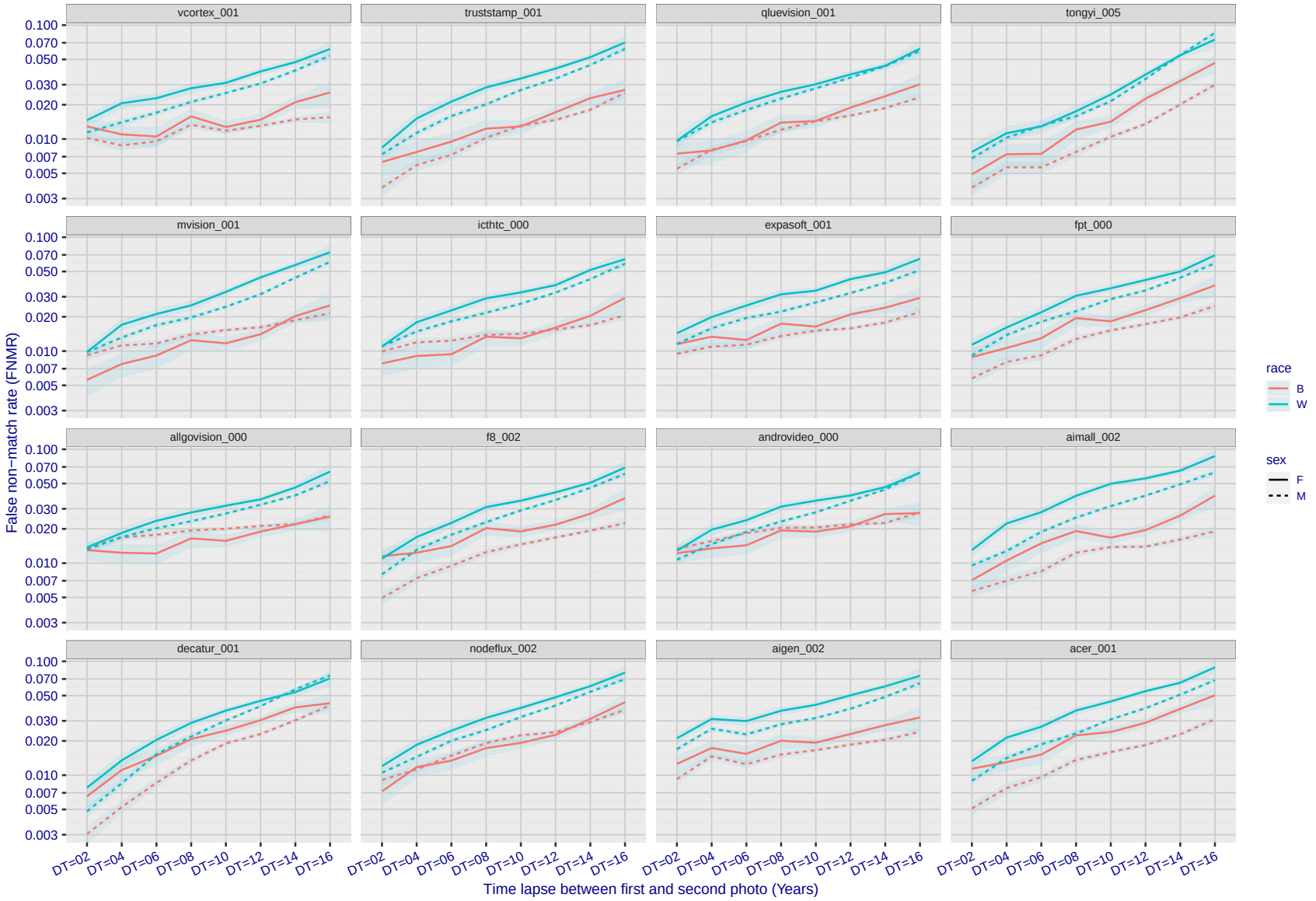

Figure 359: For the mugshot images, FNMR *as a function of elapsed time between initial enrollment and second verification images. The panels appear most accurate first, and vertical scale changes on each page. The four traces correspond to images annotated with codes for black female, black male, white female, white male. The threshold is fixed for each algorithm to give FMR = 0.00001 over all (10^8) impostor comparisons. For short time-lapses, the most accurate algorithms give very few errors (FNMR < 0.001) so that the uncertainty estimates are high.*

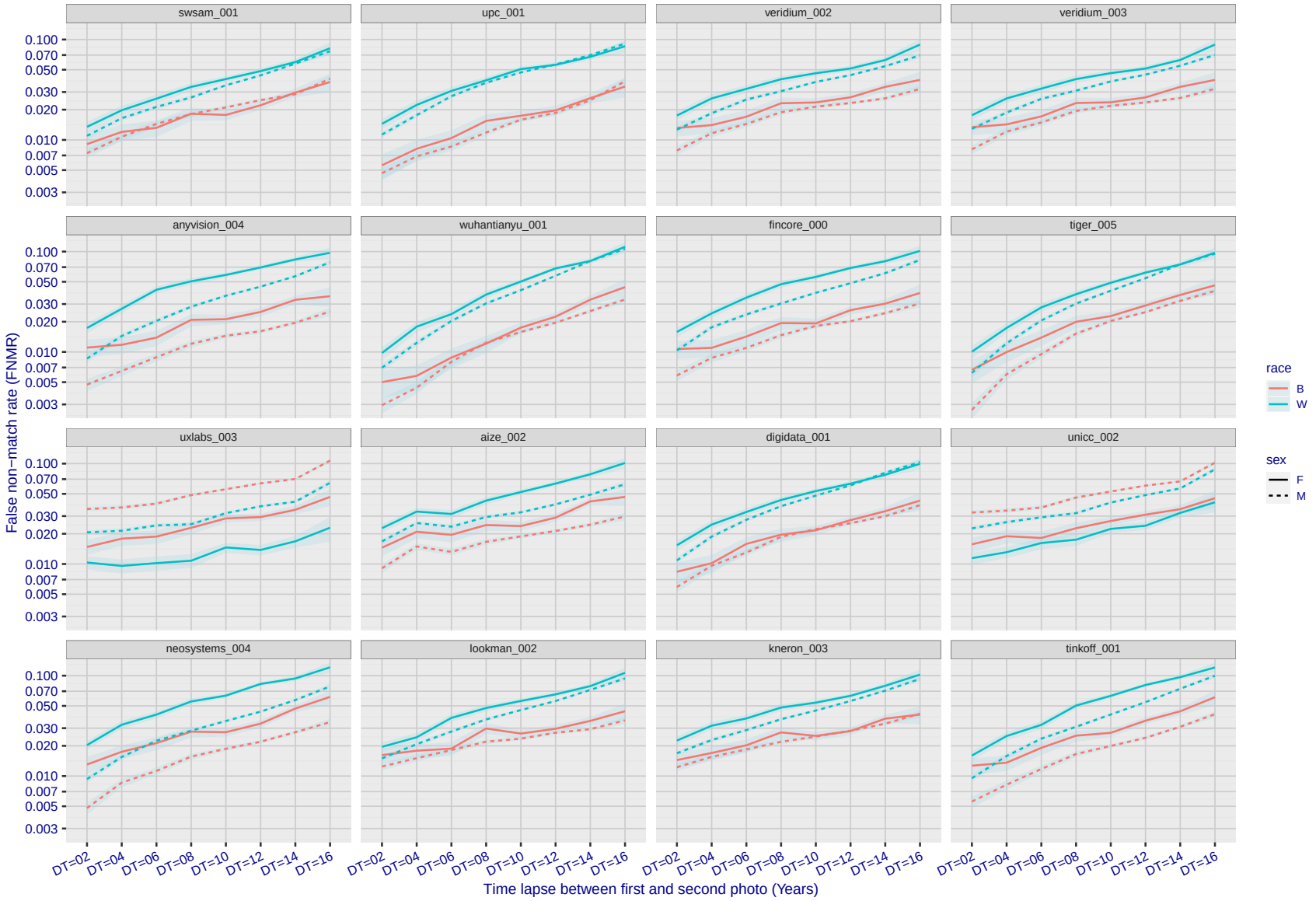

Figure 360: For the mugshot images, FNMR *as a function of elapsed time between initial enrollment and second verification images. The panels appear most accurate first, and vertical scale changes on each page. The four traces correspond to images annotated with codes for black female, black male, white female, white male. The threshold is fixed for each algorithm to give FMR = 0.00001 over all (10^8) impostor comparisons. For short time-lapses, the most accurate algorithms give very few errors (FNMR < 0.001) so that the uncertainty estimates are high.*

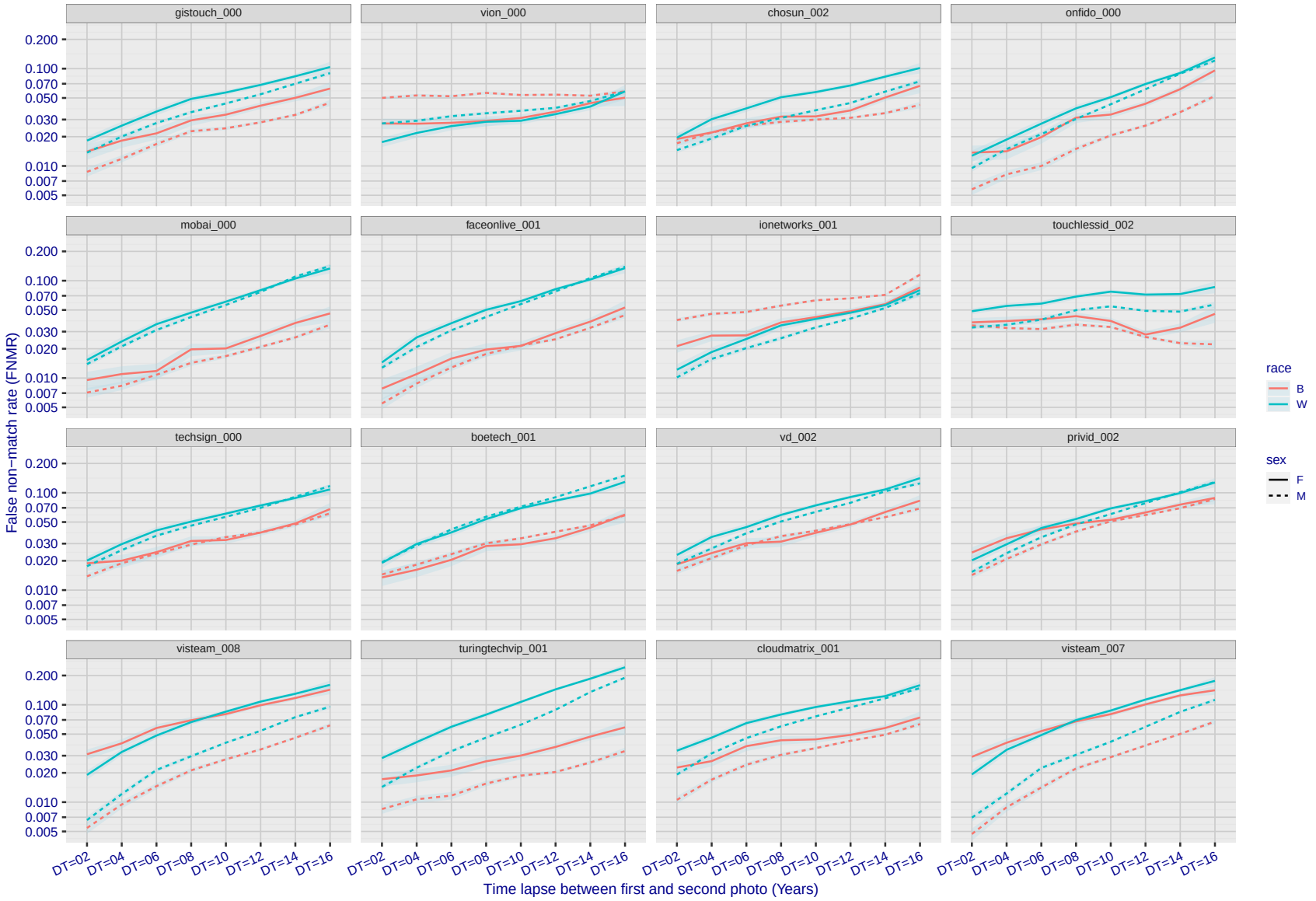

Figure 361: For the mugshot images, FNMR *as a function of elapsed time between initial enrollment and second verification images. The panels appear most accurate first, and vertical scale changes on each page. The four traces correspond to images annotated with codes for black female, black male, white female, white male. The threshold is fixed for each algorithm to give FMR = 0.00001 over all (10^8) impostor comparisons. For short time-lapses, the most accurate algorithms give very few errors (FNMR < 0.001) so that the uncertainty estimates are high.*

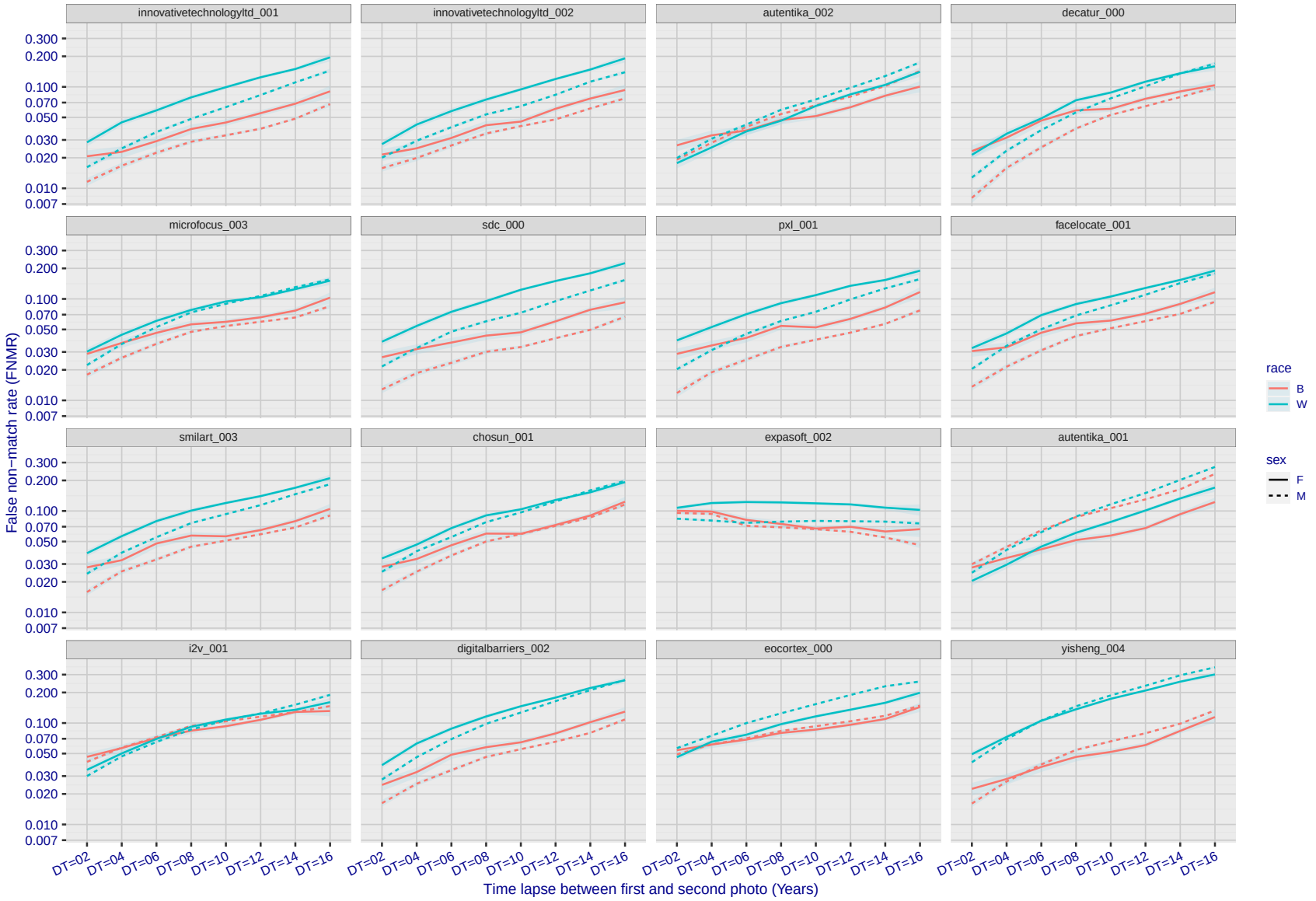

Figure 362: For the mugshot images, FNMR *as a function of elapsed time between initial enrollment and second verification images. The panels appear most accurate first, and vertical scale changes on each page. The four traces correspond to images annotated with codes for black female, black male, white female, white male. The threshold is fixed for each algorithm to give FMR = 0.00001 over all (10^8) impostor comparisons. For short time-lapses, the most accurate algorithms give very few errors (FNMR < 0.001) so that the uncertainty estimates are high.*

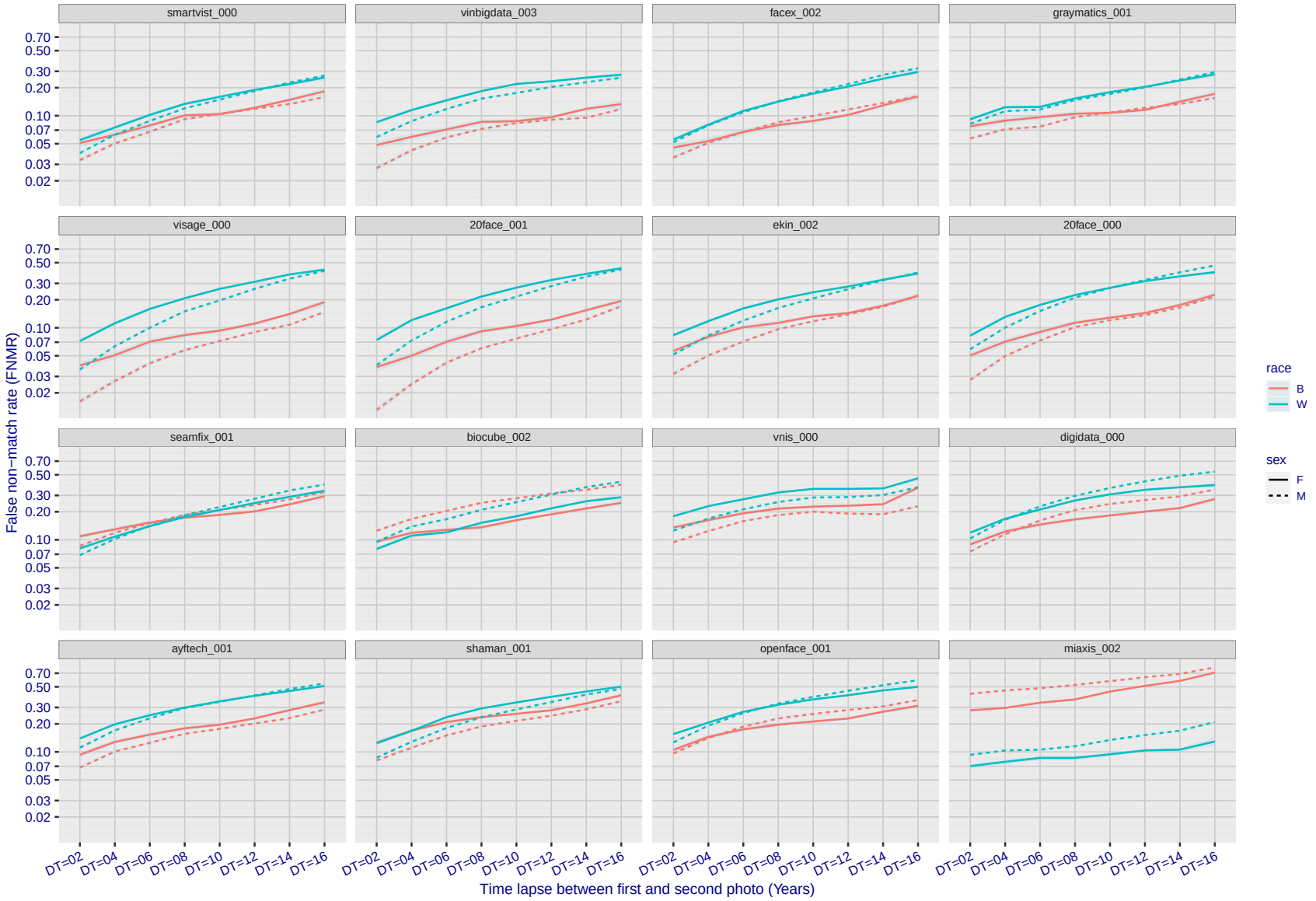

Figure 363: For the mugshot images, FNMR *as a function of elapsed time between initial enrollment and second verification images. The panels appear most accurate first, and vertical scale changes on each page. The four traces correspond to images annotated with codes for black female, black male, white female, white male. The threshold is fixed for each algorithm to give FMR = 0.00001 over all (10^8) impostor comparisons. For short time-lapses, the most accurate algorithms give very few errors (FNMR < 0.001) so that the uncertainty estimates are high.*

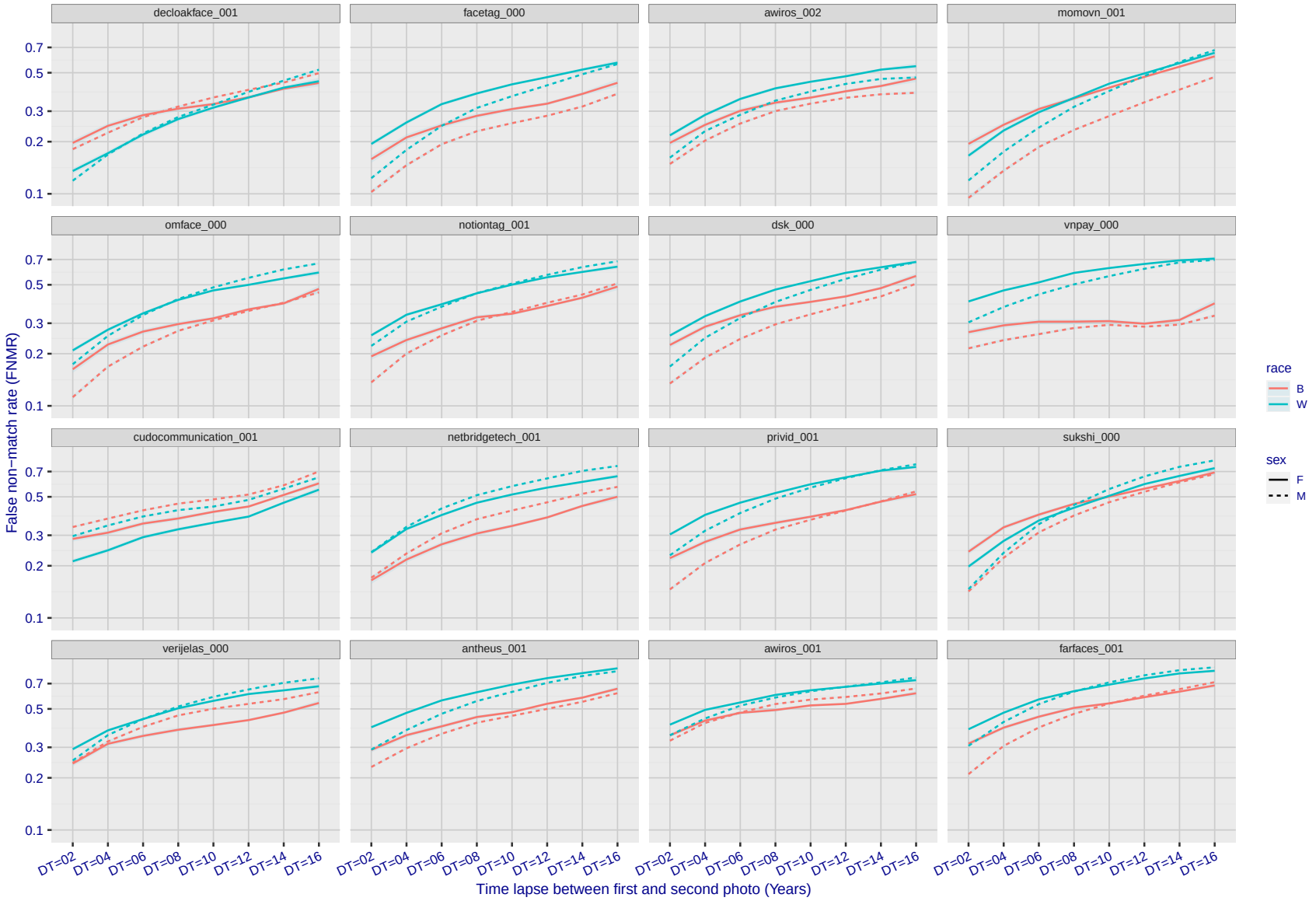

Figure 364: For the mugshot images, FNMR *as a function of elapsed time between initial enrollment and second verification images. The panels appear most accurate first, and vertical scale changes on each page. The four traces correspond to images annotated with codes for black female, black male, white female, white male. The threshold is fixed for each algorithm to give FMR = 0.00001 over all (10^8) impostor comparisons. For short time-lapses, the most accurate algorithms give very few errors (FNMR < 0.001) so that the uncertainty estimates are high.*

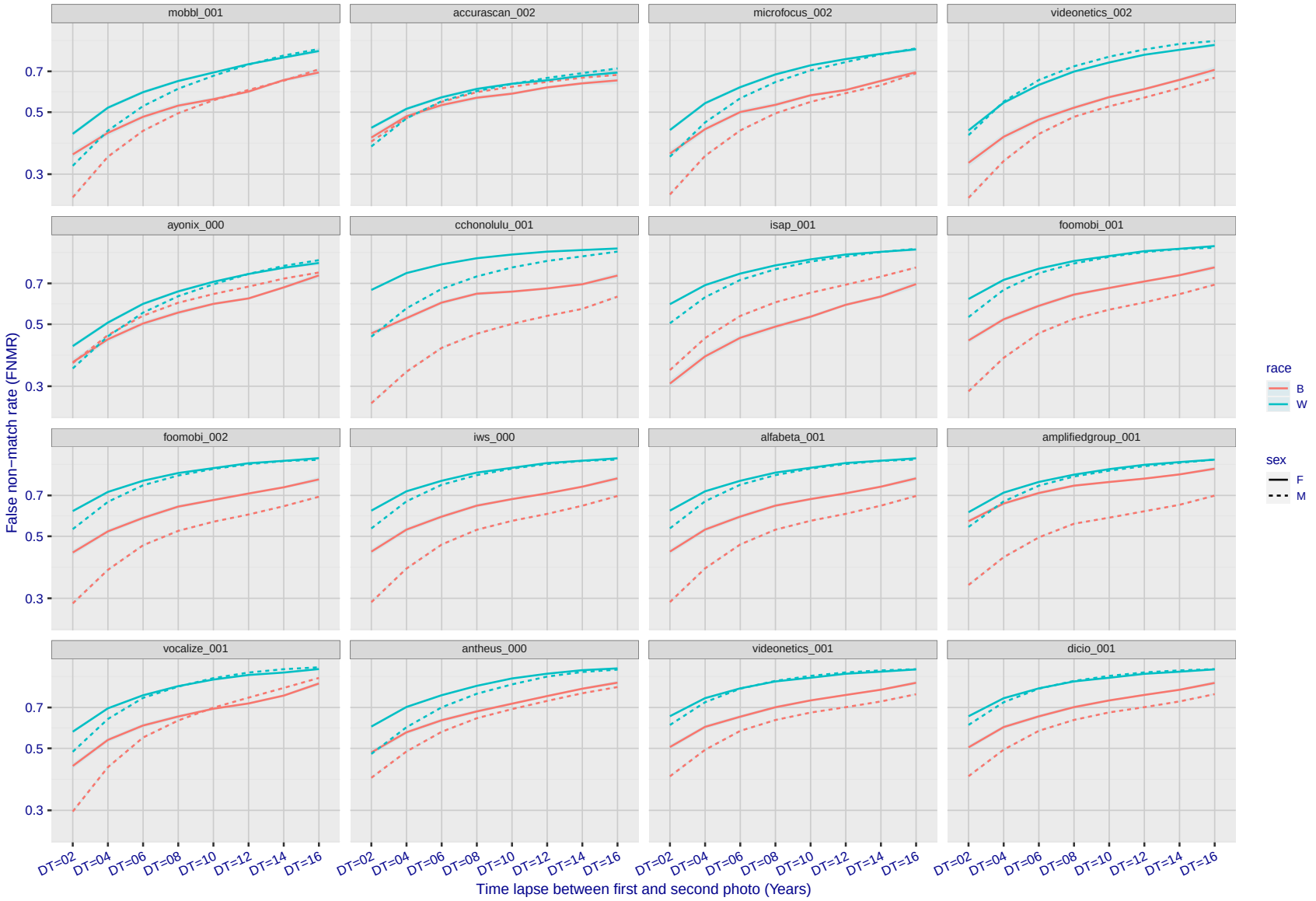

Figure 365: For the mugshot images, FNMR *as a function of elapsed time between initial enrollment and second verification images. The panels appear most accurate first, and vertical scale changes on each page. The four traces correspond to images annotated with codes for black female, black male, white female, white male. The threshold is fixed for each algorithm to give FMR = 0.00001 over all* (10^8) *impostor comparisons. For short time-lapses, the most accurate algorithms give very few errors (FNMR* < 0.001*) so that the uncertainty estimates are high.*

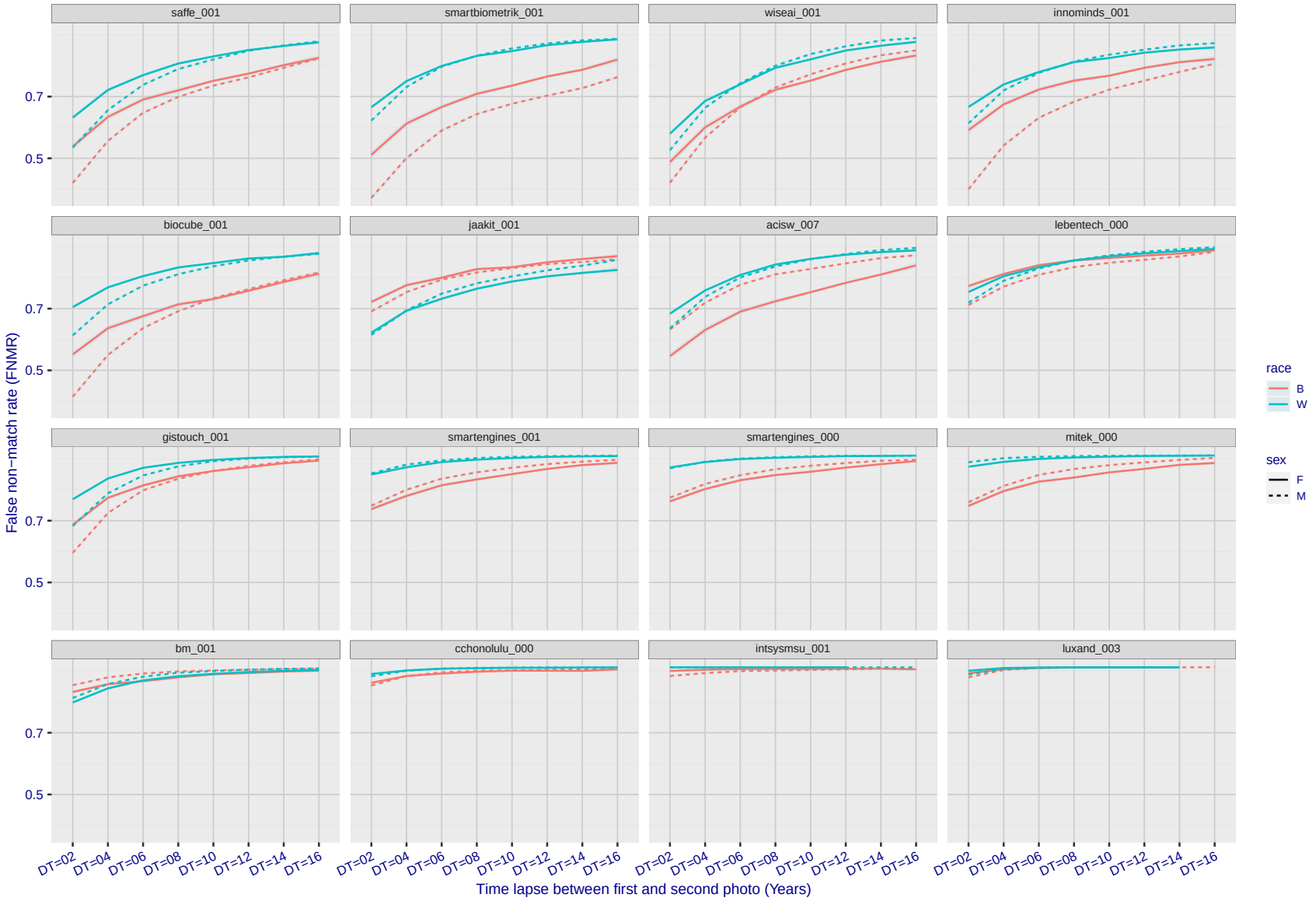

Figure 366: For the mugshot images, FNMR *as a function of elapsed time between initial enrollment and second verification images. The panels appear most accurate first, and vertical scale changes on each page. The four traces correspond to images annotated with codes for black female, black male, white female, white male. The threshold is fixed for each algorithm to give FMR = 0.00001 over all (10^8) impostor comparisons. For short time-lapses, the most accurate algorithms give very few errors (FNMR < 0.001) so that the uncertainty estimates are high.*

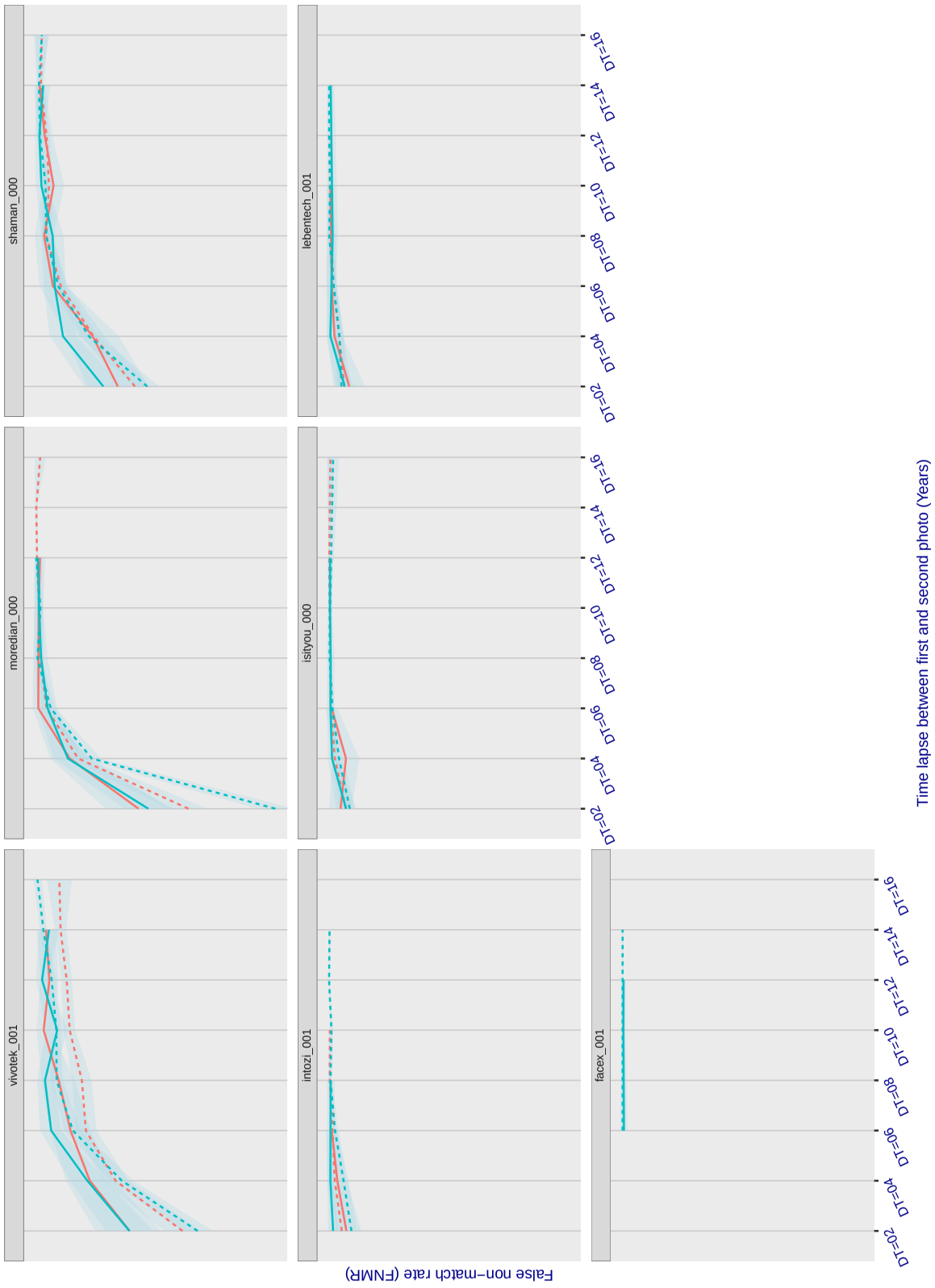

Figure 367: For the mugshot images, FNMR *as a function of elapsed time between initial enrollment and second verification images. The panels appear most accurate first, and vertical scale changes on each page. The four traces correspond to images annotated with codes for black female, black male, white female, white male. The threshold is fixed for each algorithm to give FMR = 0.00001 over all (10^8) impostor comparisons. For short time-lapses, the most accurate algorithms give very few errors (FNMR < 0.001) so that the uncertainty estimates are high.*

FNMR(T) "False non-match rate"
FMR(T) "False match rate"

3.5.3 Effect of age on genuine subjects

Background: Faces change appearance throughout life. Face recognition algorithms have previously beeen reported to give better accuracy on older individuals (See NIST IR 8009).

Goal: To quantify false non-match rates (FNMR) as a function of age, without an ageing component.

Methods: Using the visa images, which span fewer than five years, thresholds are determined that give FMR = 0.001 and 0.0001 over the entire impostor set. Then FNMR is measured over 1000 bootstrap replications of the genuine scores.

Results: For the visa images, Figure 413 shows how false non-match rates for genuine users, as a function of age group.

The notable aspects are:

- ▷ Younger subjects give considerably higher FNMR. This is likely due to rapid growth and change in facial appearance.
- ▷ FNMR trends down throughout life. The last bin, AGE $>$ 72, contains fewer than 140 mated pairs, and may be affected by small sample size.

FNMR(T) "False non-match rate"
FMR(T) "False match rate"

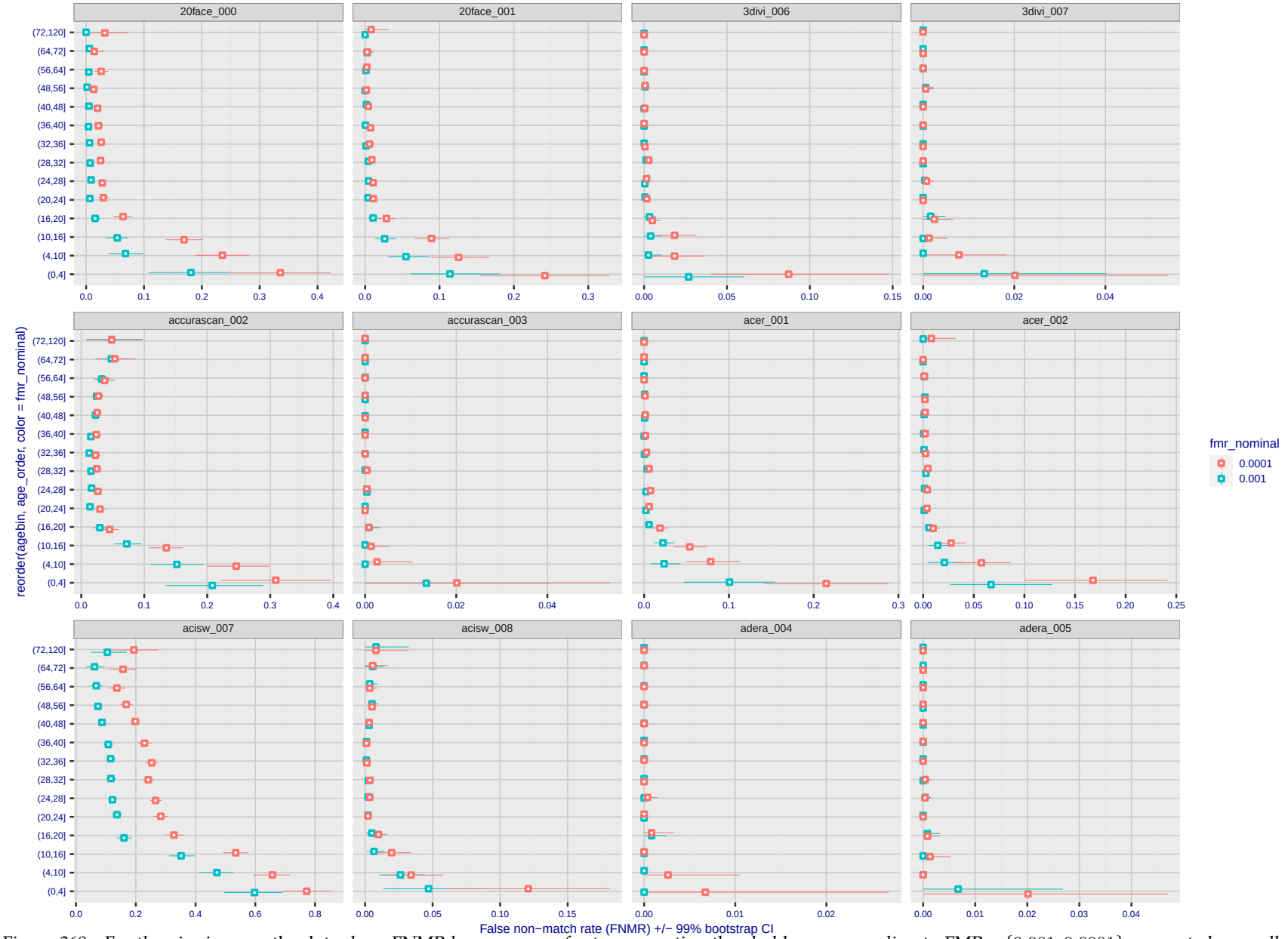

Figure 368: For the visa images, the dots show FNMR by age group for two operating thresholds corresponding to FMR = $\{0.001, 0.0001\}$ computed over all on the order of 10^{10} impostor scores. The FMR in each bin will vary also - see subsequent impostor heatmaps in sec. 3.6.2. Given a pair of face images taken at different times, we assign the comparison to the bin that is the arithmetic average of the subject's ages. This plot shows only the effect of age, not ageing. The number of comparisons in each bin is generally in the thousands, however the first and last bins are computed over 149 and 124 respectively. The error rates in some (adult) cases are zero, and in others the DET is flat so the error rates at the two thresholds are identical. The lines span 1% and 99% of boostrap replicated FNMR estimates.

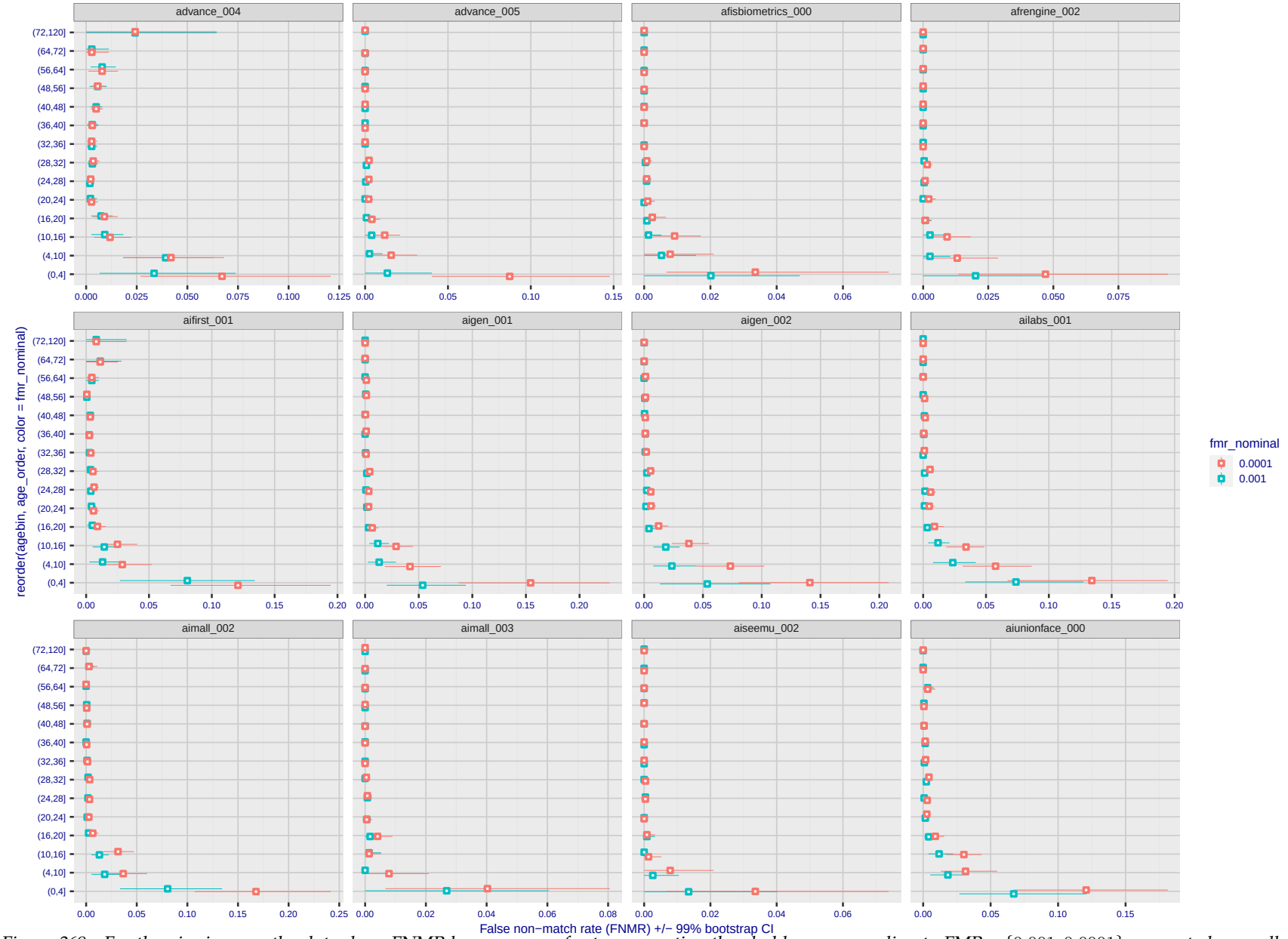

Figure 369: For the visa images, the dots show FNMR by age group for two operating thresholds corresponding to FMR = $\{0.001, 0.0001\}$ computed over all on the order of 10^{10} impostor scores. The FMR in each bin will vary also - see subsequent impostor heatmaps in sec. 3.6.2. Given a pair of face images taken at different times, we assign the comparison to the bin that is the arithmetic average of the subject's ages. This plot shows only the effect of age, not ageing. The number of comparisons in each bin is generally in the thousands, however the first and last bins are computed over 149 and 124 respectively. The error rates in some (adult) cases are zero, and in others the DET is flat so the error rates at the two thresholds are identical. The lines span 1% and 99% of boostrap replicated FNMR estimates.

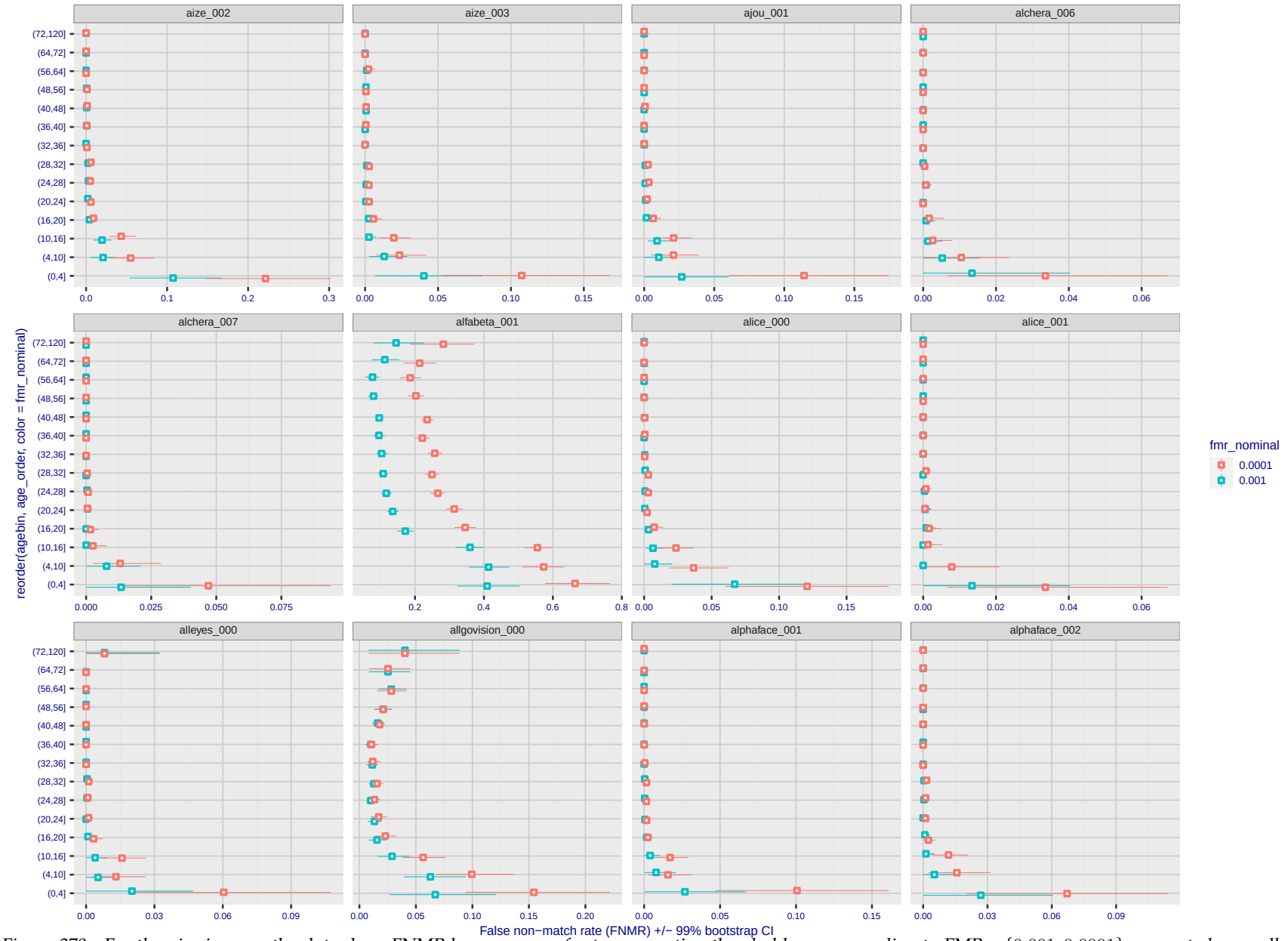

Figure 370: For the visa images, the dots show FNMR by age group for two operating thresholds corresponding to FMR = $\{0.001, 0.0001\}$ computed over all on the order of 10^{10} impostor scores. The FMR in each bin will vary also - see subsequent impostor heatmaps in sec. 3.6.2. Given a pair of face images taken at different times, we assign the comparison to the bin that is the arithmetic average of the subject's ages. This plot shows only the effect of age, not ageing. The number of comparisons in each bin is generally in the thousands, however the first and last bins are computed over 149 and 124 respectively. The error rates in some (adult) cases are zero, and in others the DET is flat so the error rates at the two thresholds are identical. The lines span 1% and 99% of boostrap replicated FNMR estimates.

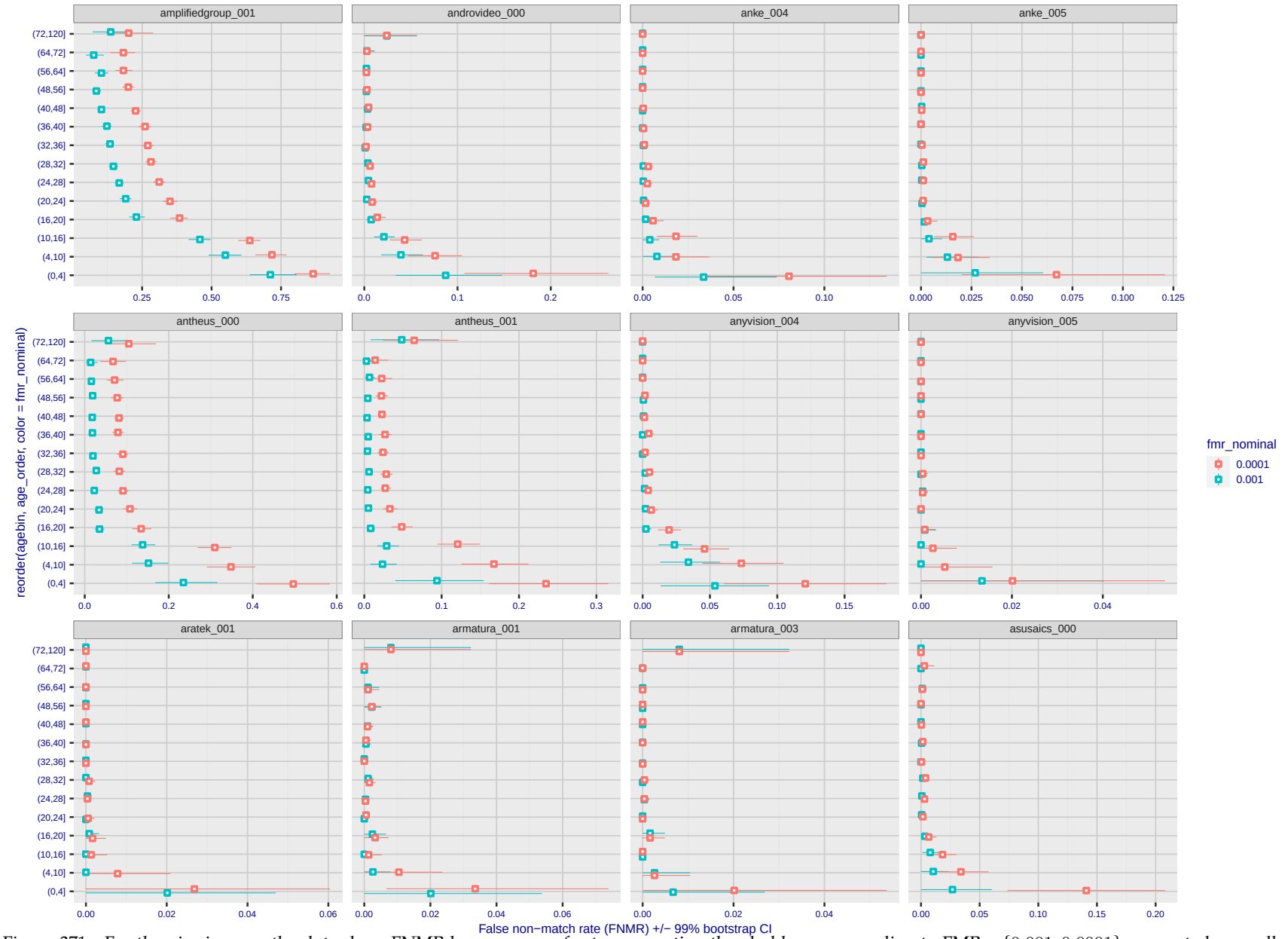

Figure 371: For the visa images, the dots show FNMR by age group for two operating thresholds corresponding to FMR = $\{0.001, 0.0001\}$ computed over all on the order of 10^{10} impostor scores. The FMR in each bin will vary also - see subsequent impostor heatmaps in sec. 3.6.2. Given a pair of face images taken at different times, we assign the comparison to the bin that is the arithmetic average of the subject's ages. This plot shows only the effect of age, not ageing. The number of comparisons in each bin is generally in the thousands, however the first and last bins are computed over 149 and 124 respectively. The error rates in some (adult) cases are zero, and in others the DET is flat so the error rates at the two thresholds are identical. The lines span 1% and 99% of boostrap replicated FNMR estimates.

Figure 372: For the visa images, the dots show FNMR by age group for two operating thresholds corresponding to FMR = $\{0.001, 0.0001\}$ computed over all on the order of 10^{10} impostor scores. The FMR in each bin will vary also - see subsequent impostor heatmaps in sec. 3.6.2. Given a pair of face images taken at different times, we assign the comparison to the bin that is the arithmetic average of the subject's ages. This plot shows only the effect of age, not ageing. The number of comparisons in each bin is generally in the thousands, however the first and last bins are computed over 149 and 124 respectively. The error rates in some (adult) cases are zero, and in others the DET is flat so the error rates at the two thresholds are identical. The lines span 1% and 99% of boostrap replicated FNMR estimates.

Figure 373: For the visa images, the dots show FNMR by age group for two operating thresholds corresponding to FMR = $\{0.001, 0.0001\}$ computed over all on the order of 10^{10} impostor scores. The FMR in each bin will vary also - see subsequent impostor heatmaps in sec. 3.6.2. Given a pair of face images taken at different times, we assign the comparison to the bin that is the arithmetic average of the subject's ages. This plot shows only the effect of age, not ageing. The number of comparisons in each bin is generally in the thousands, however the first and last bins are computed over 149 and 124 respectively. The error rates in some (adult) cases are zero, and in others the DET is flat so the error rates at the two thresholds are identical. The lines span 1% and 99% of boostrap replicated FNMR estimates.

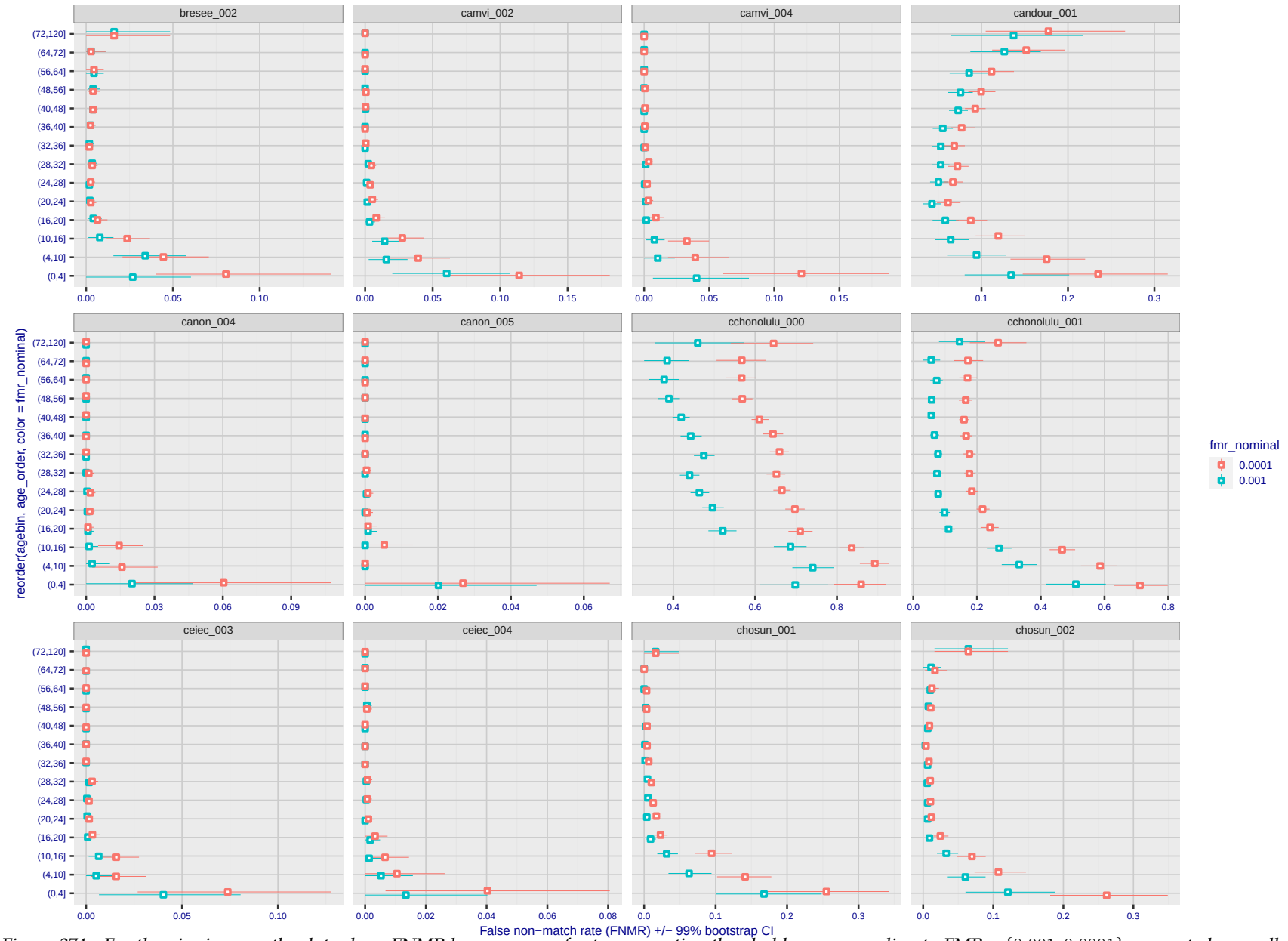

Figure 374: For the visa images, the dots show FNMR by age group for two operating thresholds corresponding to FMR = $\{0.001, 0.0001\}$ computed over all on the order of 10^{10} impostor scores. The FMR in each bin will vary also - see subsequent impostor heatmaps in sec. 3.6.2. Given a pair of face images taken at different times, we assign the comparison to the bin that is the arithmetic average of the subject's ages. This plot shows only the effect of age, not ageing. The number of comparisons in each bin is generally in the thousands, however the first and last bins are computed over 149 and 124 respectively. The error rates in some (adult) cases are zero, and in others the DET is flat so the error rates at the two thresholds are identical. The lines span 1% and 99% of boostrap replicated FNMR estimates.

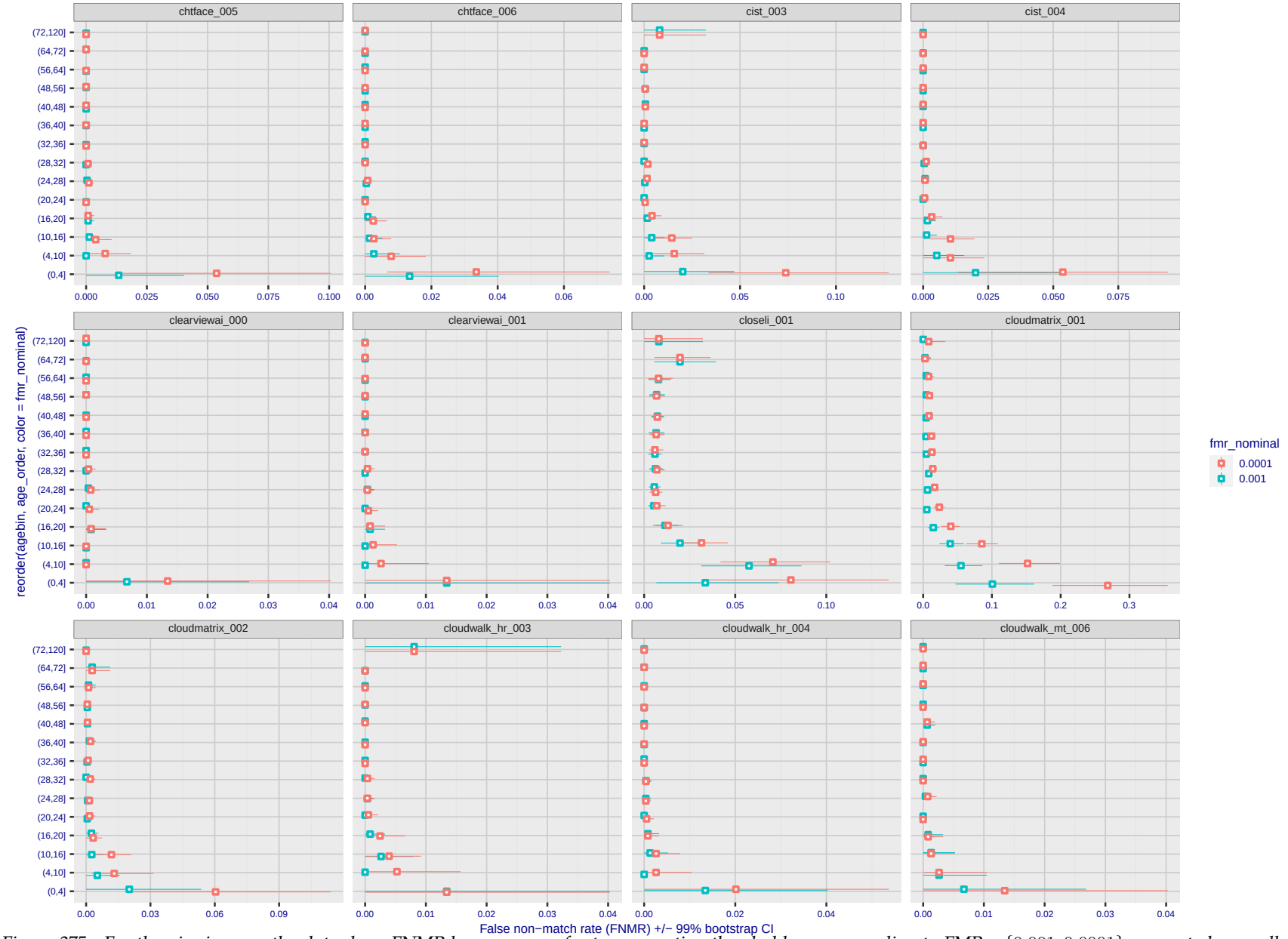

Figure 375: For the visa images, the dots show FNMR by age group for two operating thresholds corresponding to FMR = $\{0.001, 0.0001\}$ computed over all on the order of 10^{10} impostor scores. The FMR in each bin will vary also - see subsequent impostor heatmaps in sec. 3.6.2. Given a pair of face images taken at different times, we assign the comparison to the bin that is the arithmetic average of the subject's ages. This plot shows only the effect of age, not ageing. The number of comparisons in each bin is generally in the thousands, however the first and last bins are computed over 149 and 124 respectively. The error rates in some (adult) cases are zero, and in others the DET is flat so the error rates at the two thresholds are identical. The lines span 1% and 99% of boostrap replicated FNMR estimates.

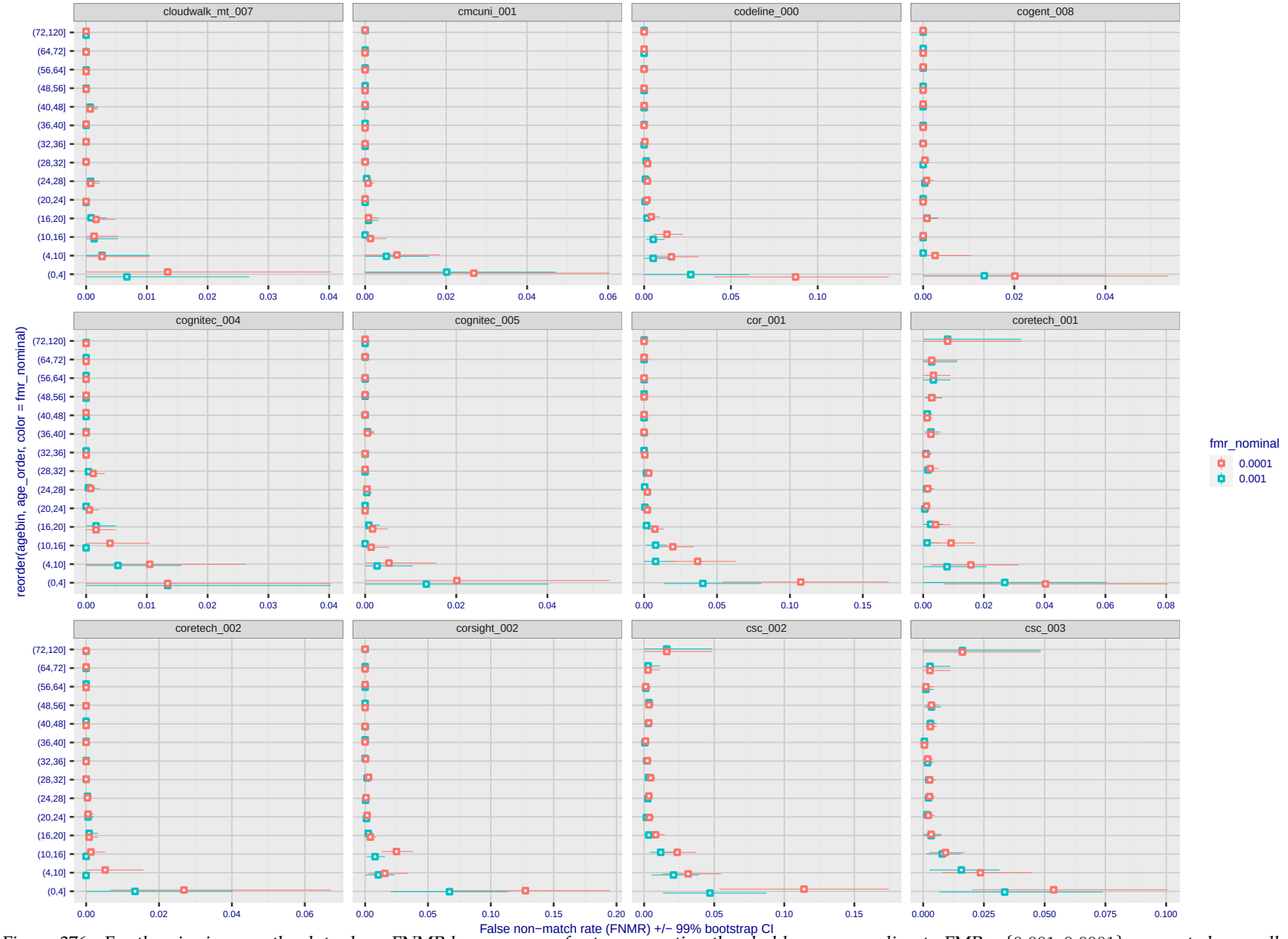

Figure 376: For the visa images, the dots show FNMR by age group for two operating thresholds corresponding to FMR = $\{0.001, 0.0001\}$ computed over all on the order of 10^{10} impostor scores. The FMR in each bin will vary also - see subsequent impostor heatmaps in sec. 3.6.2. Given a pair of face images taken at different times, we assign the comparison to the bin that is the arithmetic average of the subject's ages. This plot shows only the effect of age, not ageing. The number of comparisons in each bin is generally in the thousands, however the first and last bins are computed over 149 and 124 respectively. The error rates in some (adult) cases are zero, and in others the DET is flat so the error rates at the two thresholds are identical. The lines span 1% and 99% of boostrap replicated FNMR estimates.

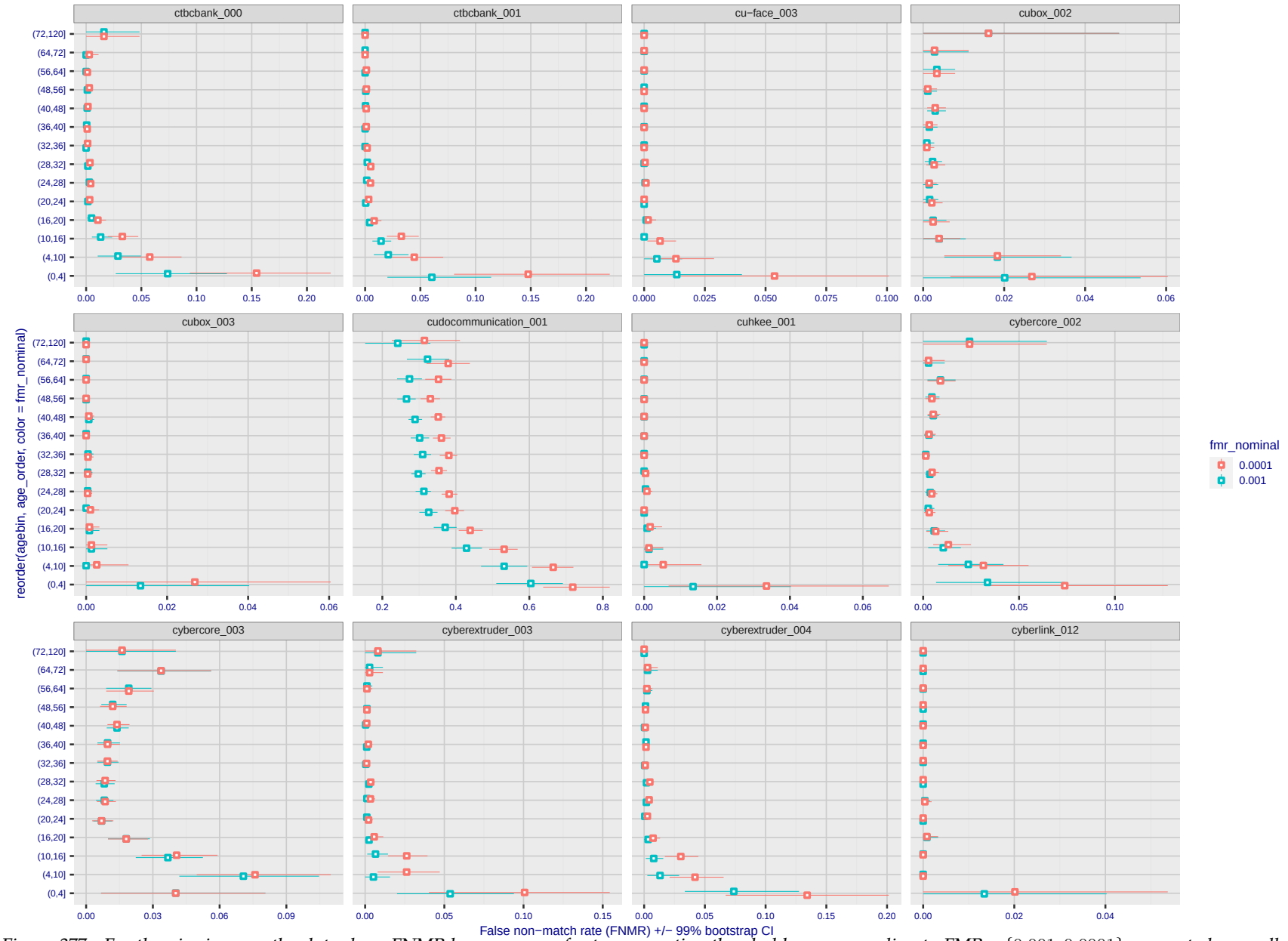

Figure 377: For the visa images, the dots show FNMR by age group for two operating thresholds corresponding to FMR = $\{0.001, 0.0001\}$ computed over all on the order of 10^{10} impostor scores. The FMR in each bin will vary also - see subsequent impostor heatmaps in sec. 3.6.2. Given a pair of face images taken at different times, we assign the comparison to the bin that is the arithmetic average of the subject's ages. This plot shows only the effect of age, not ageing. The number of comparisons in each bin is generally in the thousands, however the first and last bins are computed over 149 and 124 respectively. The error rates in some (adult) cases are zero, and in others the DET is flat so the error rates at the two thresholds are identical. The lines span 1% and 99% of boostrap replicated FNMR estimates.

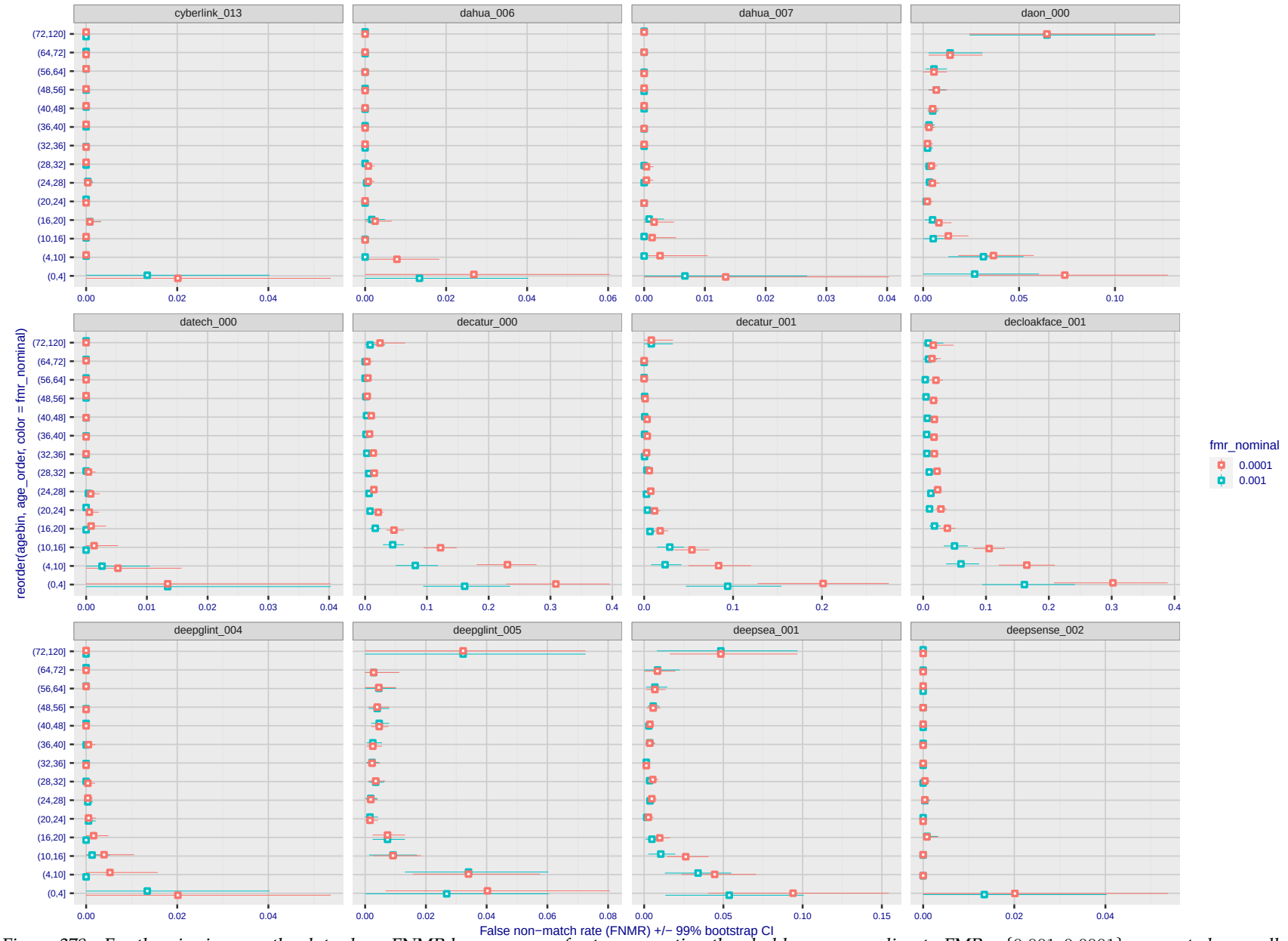

Figure 378: For the visa images, the dots show FNMR by age group for two operating thresholds corresponding to FMR = $\{0.001, 0.0001\}$ computed over all on the order of 10^{10} impostor scores. The FMR in each bin will vary also - see subsequent impostor heatmaps in sec. 3.6.2. Given a pair of face images taken at different times, we assign the comparison to the bin that is the arithmetic average of the subject's ages. This plot shows only the effect of age, not ageing. The number of comparisons in each bin is generally in the thousands, however the first and last bins are computed over 149 and 124 respectively. The error rates in some (adult) cases are zero, and in others the DET is flat so the error rates at the two thresholds are identical. The lines span 1% and 99% of boostrap replicated FNMR estimates.

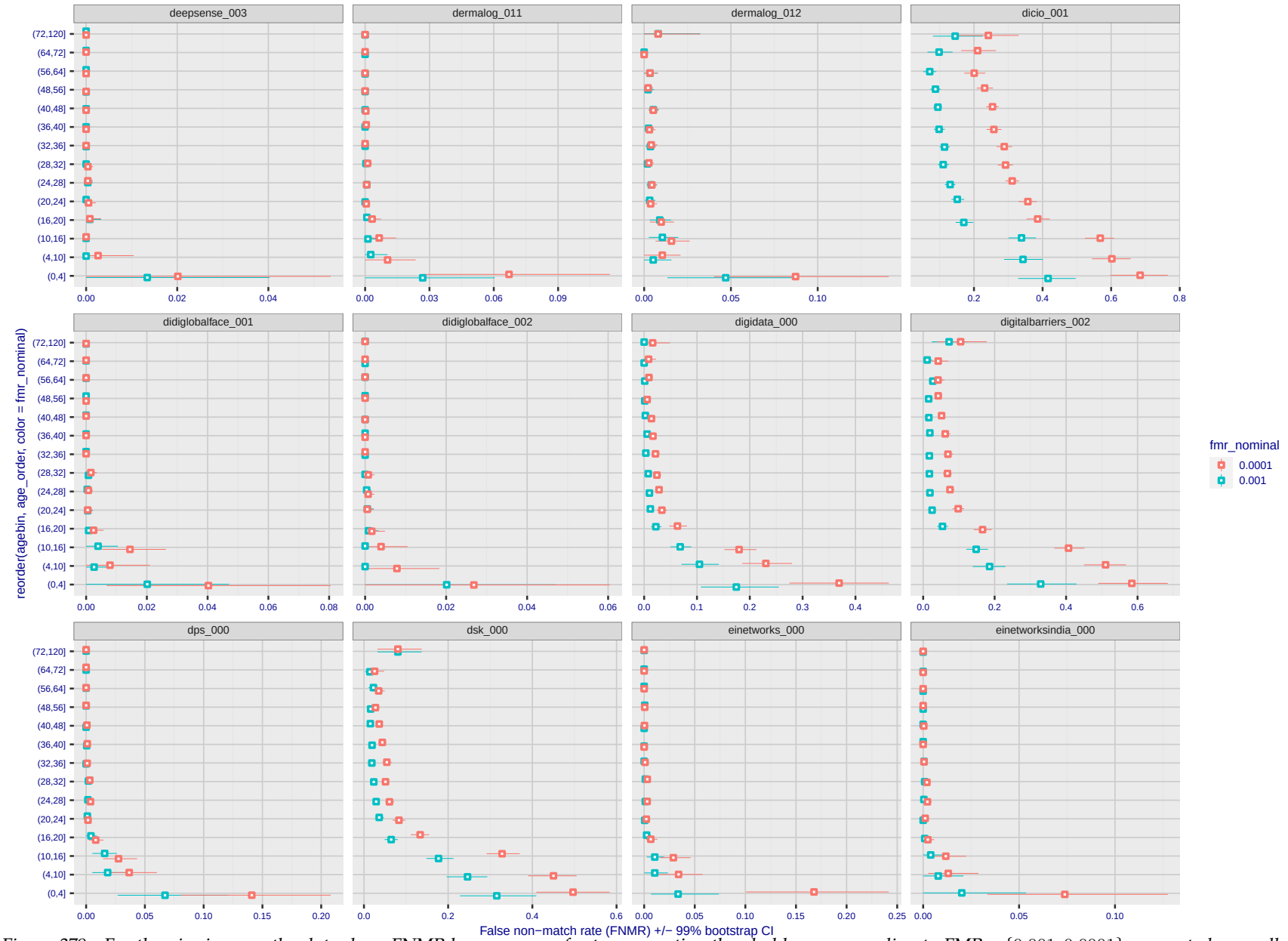

Figure 379: For the visa images, the dots show FNMR by age group for two operating thresholds corresponding to FMR = $\{0.001, 0.0001\}$ computed over all on the order of 10^{10} impostor scores. The FMR in each bin will vary also - see subsequent impostor heatmaps in sec. 3.6.2. Given a pair of face images taken at different times, we assign the comparison to the bin that is the arithmetic average of the subject's ages. This plot shows only the effect of age, not ageing. The number of comparisons in each bin is generally in the thousands, however the first and last bins are computed over 149 and 124 respectively. The error rates in some (adult) cases are zero, and in others the DET is flat so the error rates at the two thresholds are identical. The lines span 1% and 99% of boostrap replicated FNMR estimates.

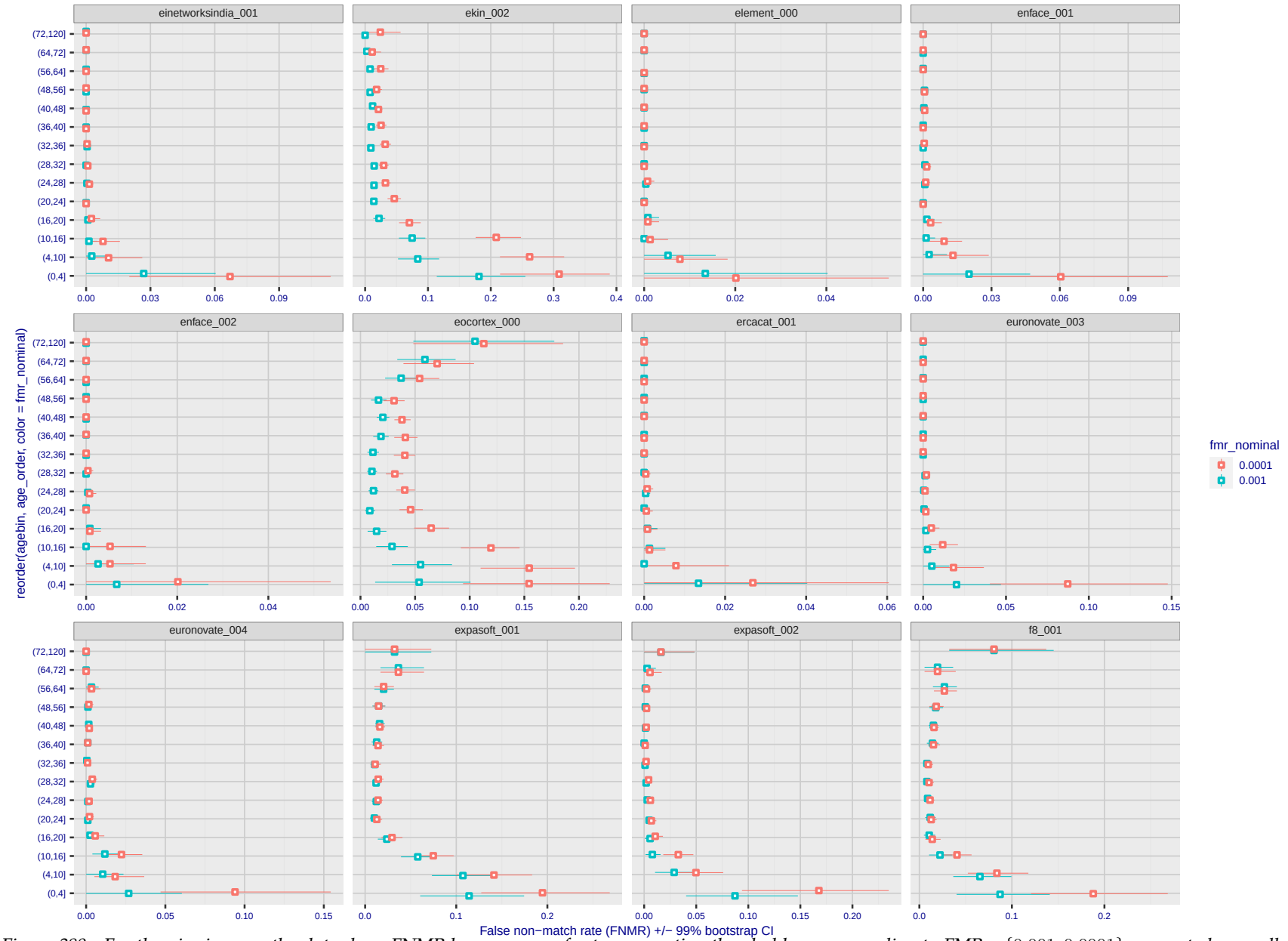

Figure 380: For the visa images, the dots show FNMR by age group for two operating thresholds corresponding to FMR = $\{0.001, 0.0001\}$ computed over all on the order of 10^{10} impostor scores. The FMR in each bin will vary also - see subsequent impostor heatmaps in sec. 3.6.2. Given a pair of face images taken at different times, we assign the comparison to the bin that is the arithmetic average of the subject's ages. This plot shows only the effect of age, not ageing. The number of comparisons in each bin is generally in the thousands, however the first and last bins are computed over 149 and 124 respectively. The error rates in some (adult) cases are zero, and in others the DET is flat so the error rates at the two thresholds are identical. The lines span 1% and 99% of boostrap replicated FNMR estimates.

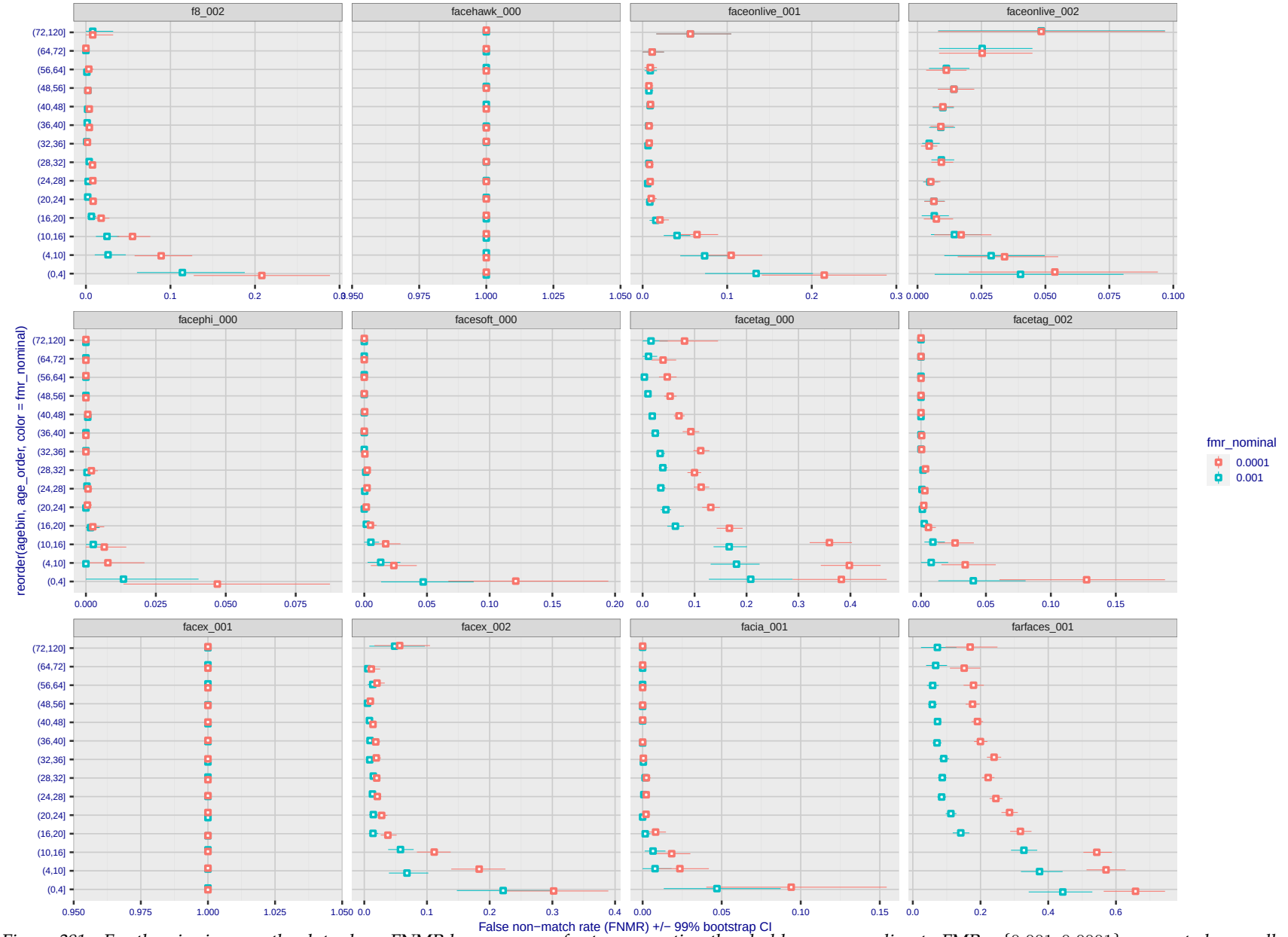

Figure 381: For the visa images, the dots show FNMR by age group for two operating thresholds corresponding to FMR = $\{0.001, 0.0001\}$ computed over all on the order of 10^{10} impostor scores. The FMR in each bin will vary also - see subsequent impostor heatmaps in sec. 3.6.2. Given a pair of face images taken at different times, we assign the comparison to the bin that is the arithmetic average of the subject's ages. This plot shows only the effect of age, not ageing. The number of comparisons in each bin is generally in the thousands, however the first and last bins are computed over 149 and 124 respectively. The error rates in some (adult) cases are zero, and in others the DET is flat so the error rates at the two thresholds are identical. The lines span 1% and 99% of boostrap replicated FNMR estimates.

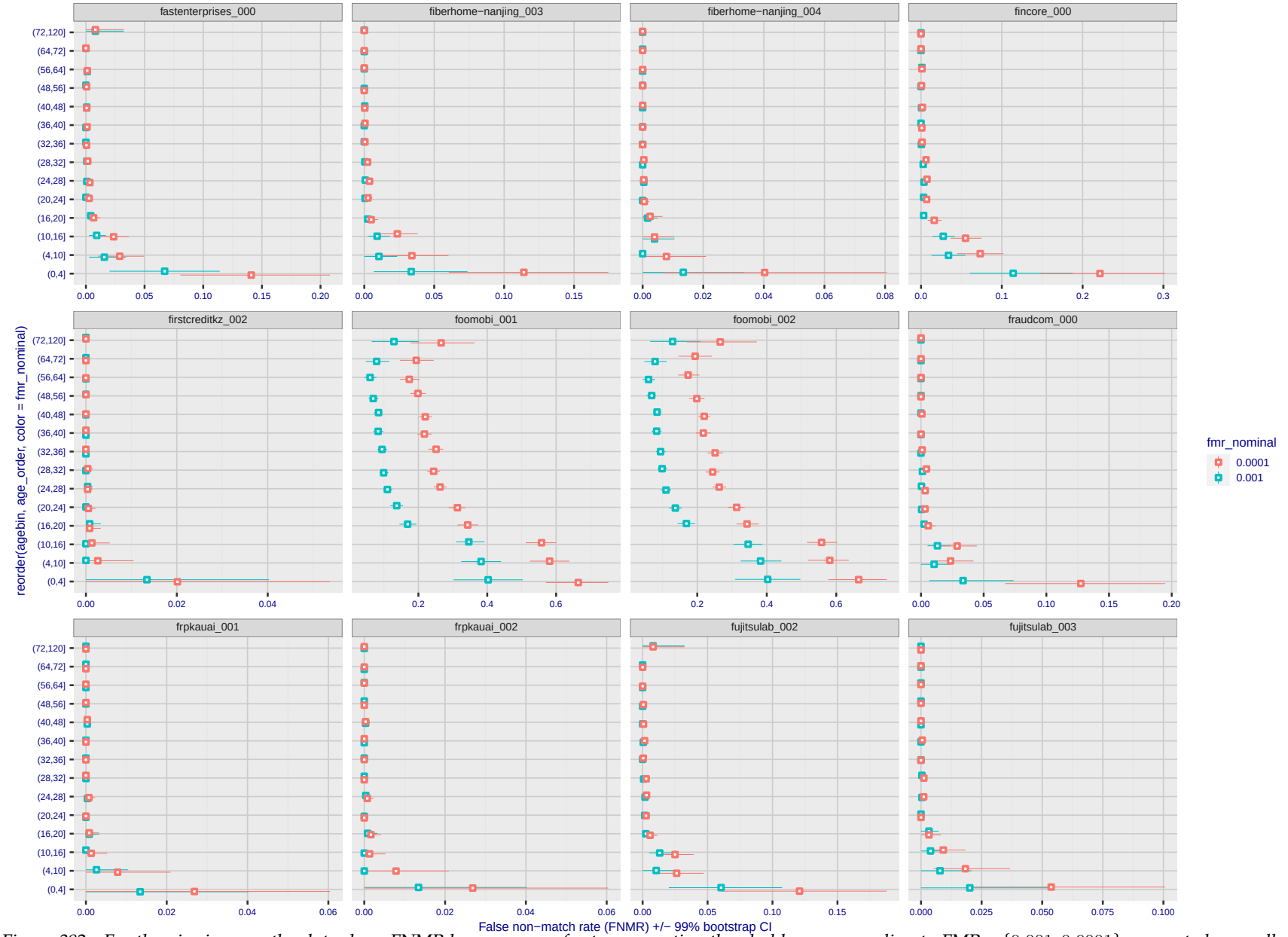

Figure 382: For the visa images, the dots show FNMR by age group for two operating thresholds corresponding to FMR = $\{0.001, 0.0001\}$ computed over all on the order of 10^{10} impostor scores. The FMR in each bin will vary also - see subsequent impostor heatmaps in sec. 3.6.2. Given a pair of face images taken at different times, we assign the comparison to the bin that is the arithmetic average of the subject's ages. This plot shows only the effect of age, not ageing. The number of comparisons in each bin is generally in the thousands, however the first and last bins are computed over 149 and 124 respectively. The error rates in some (adult) cases are zero, and in others the DET is flat so the error rates at the two thresholds are identical. The lines span 1% and 99% of boostrap replicated FNMR estimates.

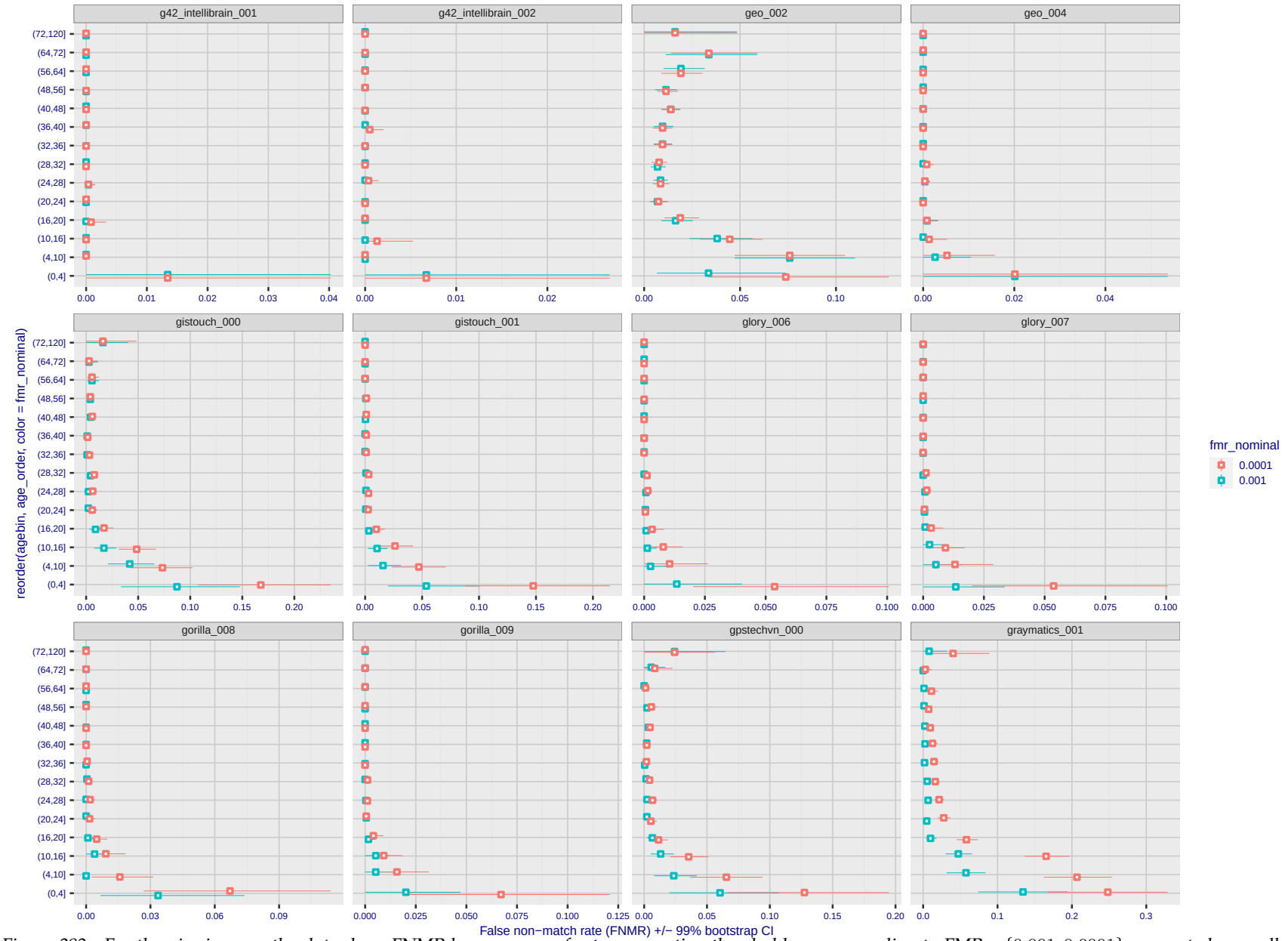

Figure 383: For the visa images, the dots show FNMR by age group for two operating thresholds corresponding to FMR = $\{0.001, 0.0001\}$ computed over all on the order of 10^{10} impostor scores. The FMR in each bin will vary also - see subsequent impostor heatmaps in sec. 3.6.2. Given a pair of face images taken at different times, we assign the comparison to the bin that is the arithmetic average of the subject's ages. This plot shows only the effect of age, not ageing. The number of comparisons in each bin is generally in the thousands, however the first and last bins are computed over 149 and 124 respectively. The error rates in some (adult) cases are zero, and in others the DET is flat so the error rates at the two thresholds are identical. The lines span 1% and 99% of boostrap replicated FNMR estimates.

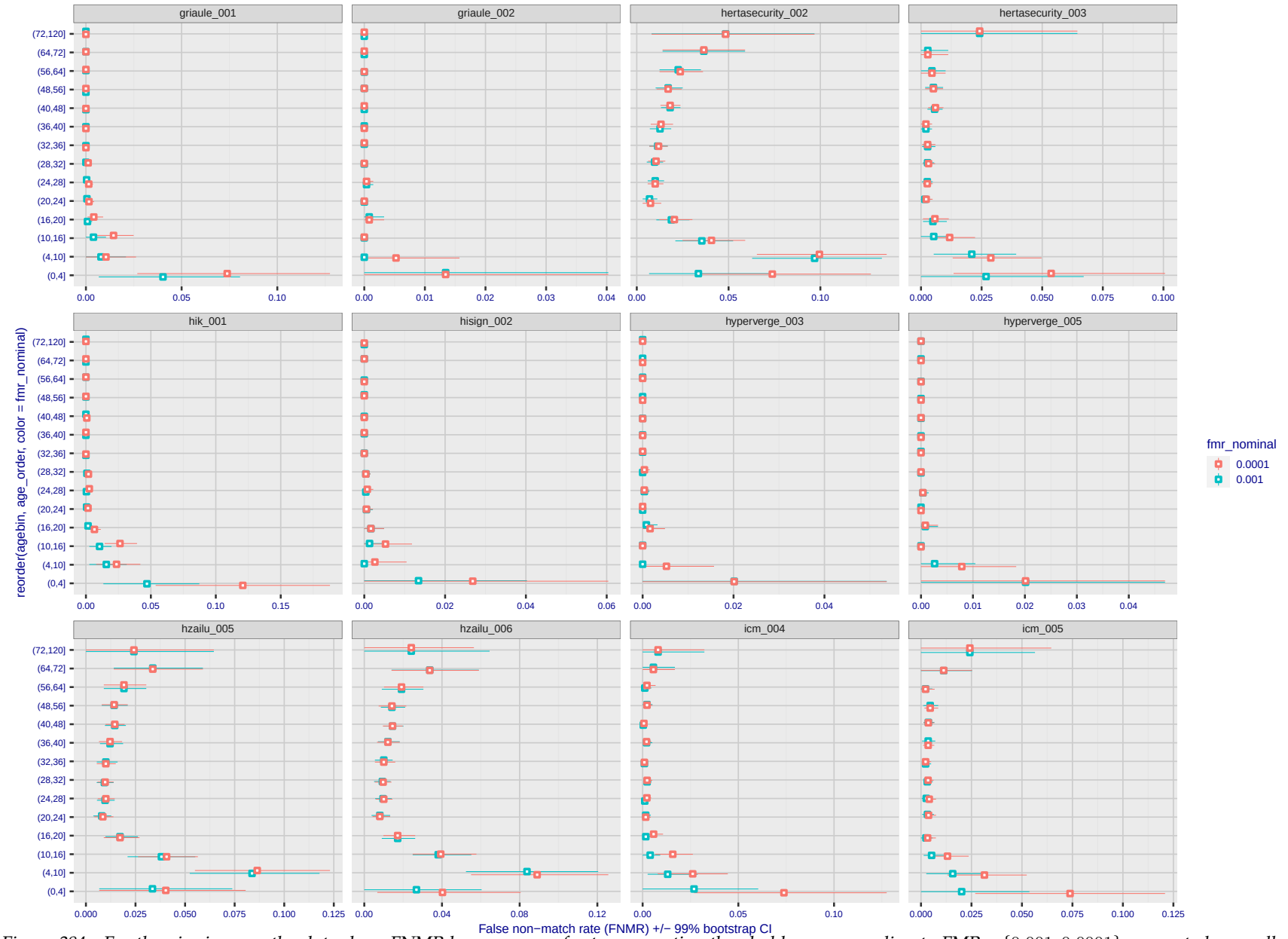

Figure 384: For the visa images, the dots show FNMR by age group for two operating thresholds corresponding to FMR = $\{0.001, 0.0001\}$ computed over all on the order of 10^{10} impostor scores. The FMR in each bin will vary also - see subsequent impostor heatmaps in sec. 3.6.2. Given a pair of face images taken at different times, we assign the comparison to the bin that is the arithmetic average of the subject's ages. This plot shows only the effect of age, not ageing. The number of comparisons in each bin is generally in the thousands, however the first and last bins are computed over 149 and 124 respectively. The error rates in some (adult) cases are zero, and in others the DET is flat so the error rates at the two thresholds are identical. The lines span 1% and 99% of boostrap replicated FNMR estimates.

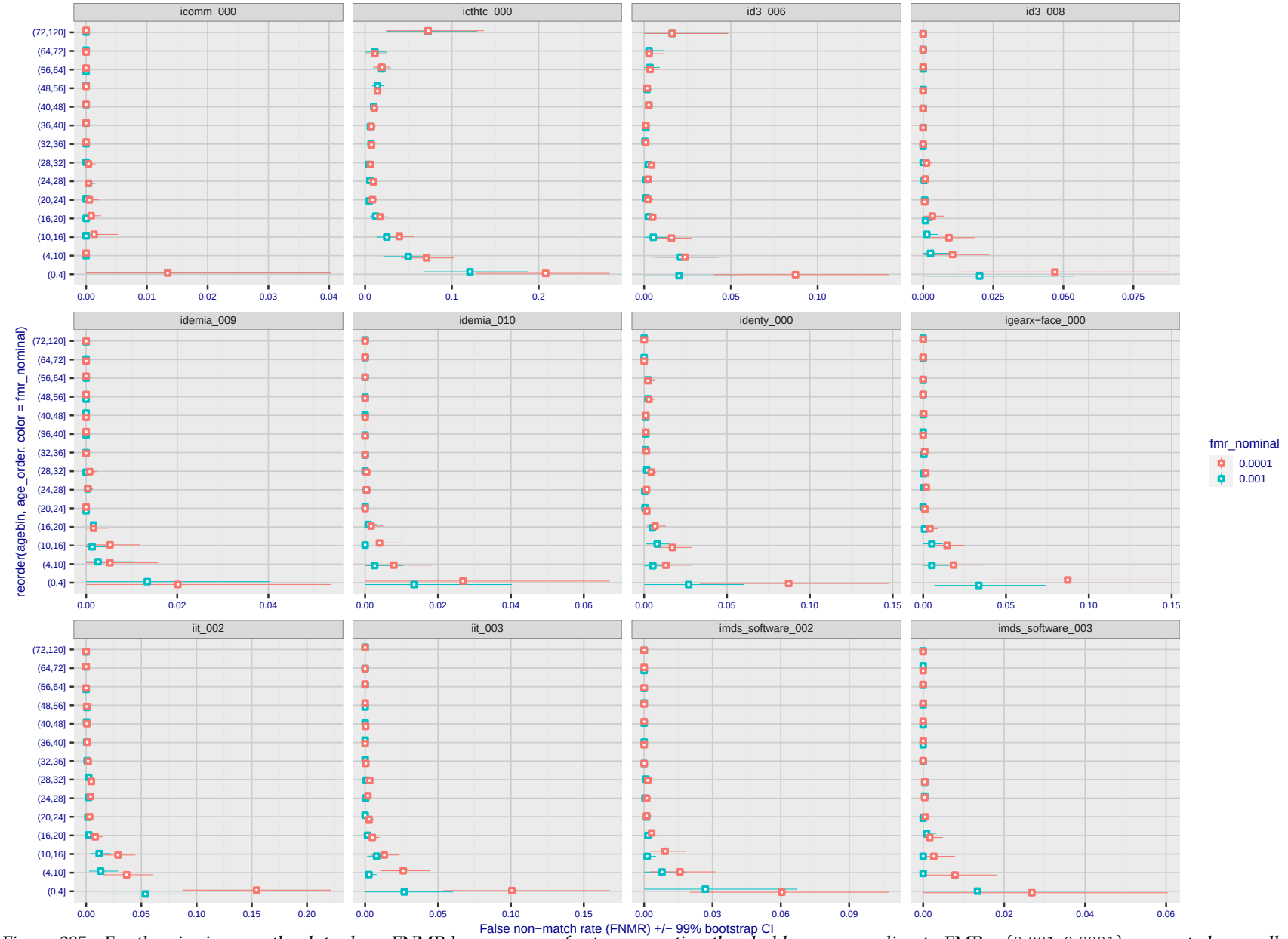

Figure 385: For the visa images, the dots show FNMR by age group for two operating thresholds corresponding to FMR = $\{0.001, 0.0001\}$ computed over all on the order of 10^{10} impostor scores. The FMR in each bin will vary also - see subsequent impostor heatmaps in sec. 3.6.2. Given a pair of face images taken at different times, we assign the comparison to the bin that is the arithmetic average of the subject's ages. This plot shows only the effect of age, not ageing. The number of comparisons in each bin is generally in the thousands, however the first and last bins are computed over 149 and 124 respectively. The error rates in some (adult) cases are zero, and in others the DET is flat so the error rates at the two thresholds are identical. The lines span 1% and 99% of boostrap replicated FNMR estimates.

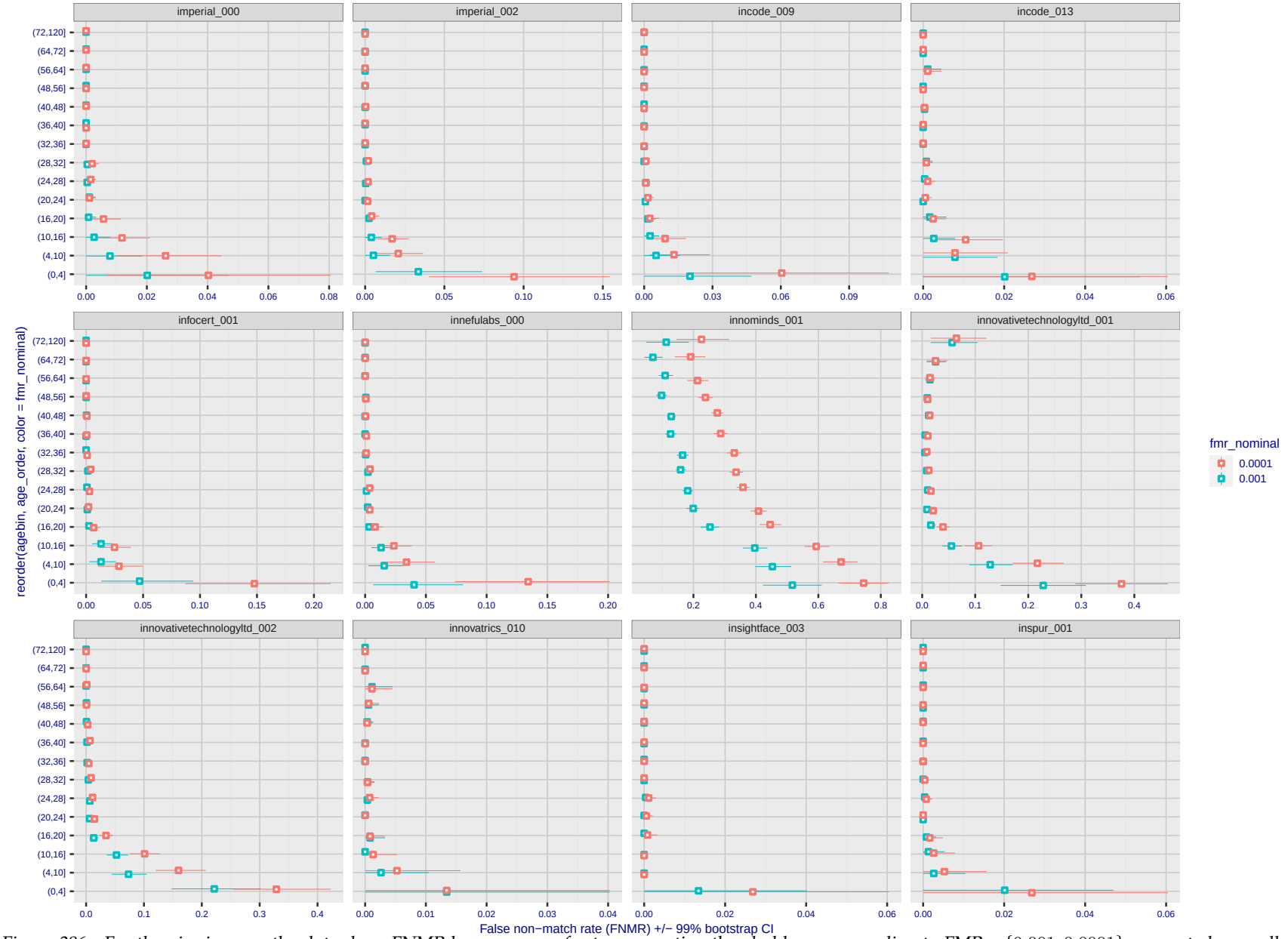

Figure 386: For the visa images, the dots show FNMR by age group for two operating thresholds corresponding to FMR = $\{0.001, 0.0001\}$ computed over all on the order of 10^{10} impostor scores. The FMR in each bin will vary also - see subsequent impostor heatmaps in sec. 3.6.2. Given a pair of face images taken at different times, we assign the comparison to the bin that is the arithmetic average of the subject's ages. This plot shows only the effect of age, not ageing. The number of comparisons in each bin is generally in the thousands, however the first and last bins are computed over 149 and 124 respectively. The error rates in some (adult) cases are zero, and in others the DET is flat so the error rates at the two thresholds are identical. The lines span 1% and 99% of boostrap replicated FNMR estimates.

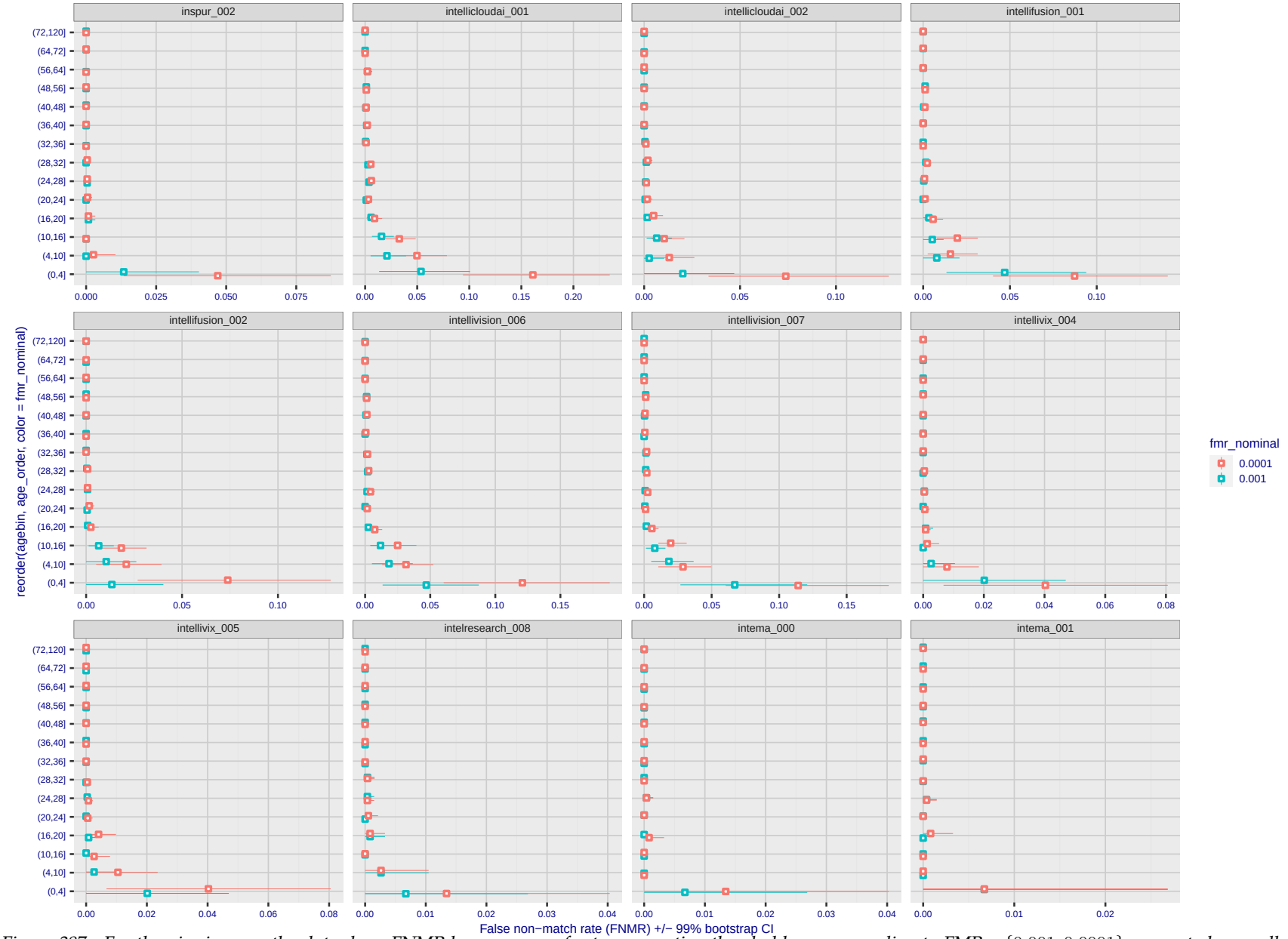

Figure 387: For the visa images, the dots show FNMR by age group for two operating thresholds corresponding to FMR = $\{0.001, 0.0001\}$ computed over all on the order of 10^{10} impostor scores. The FMR in each bin will vary also - see subsequent impostor heatmaps in sec. 3.6.2. Given a pair of face images taken at different times, we assign the comparison to the bin that is the arithmetic average of the subject's ages. This plot shows only the effect of age, not ageing. The number of comparisons in each bin is generally in the thousands, however the first and last bins are computed over 149 and 124 respectively. The error rates in some (adult) cases are zero, and in others the DET is flat so the error rates at the two thresholds are identical. The lines span 1% and 99% of boostrap replicated FNMR estimates.

Figure 388: For the visa images, the dots show FNMR by age group for two operating thresholds corresponding to FMR = $\{0.001, 0.0001\}$ computed over all on the order of 10^{10} impostor scores. The FMR in each bin will vary also - see subsequent impostor heatmaps in sec. 3.6.2. Given a pair of face images taken at different times, we assign the comparison to the bin that is the arithmetic average of the subject's ages. This plot shows only the effect of age, not ageing. The number of comparisons in each bin is generally in the thousands, however the first and last bins are computed over 149 and 124 respectively. The error rates in some (adult) cases are zero, and in others the DET is flat so the error rates at the two thresholds are identical. The lines span 1% and 99% of boostrap replicated FNMR estimates.

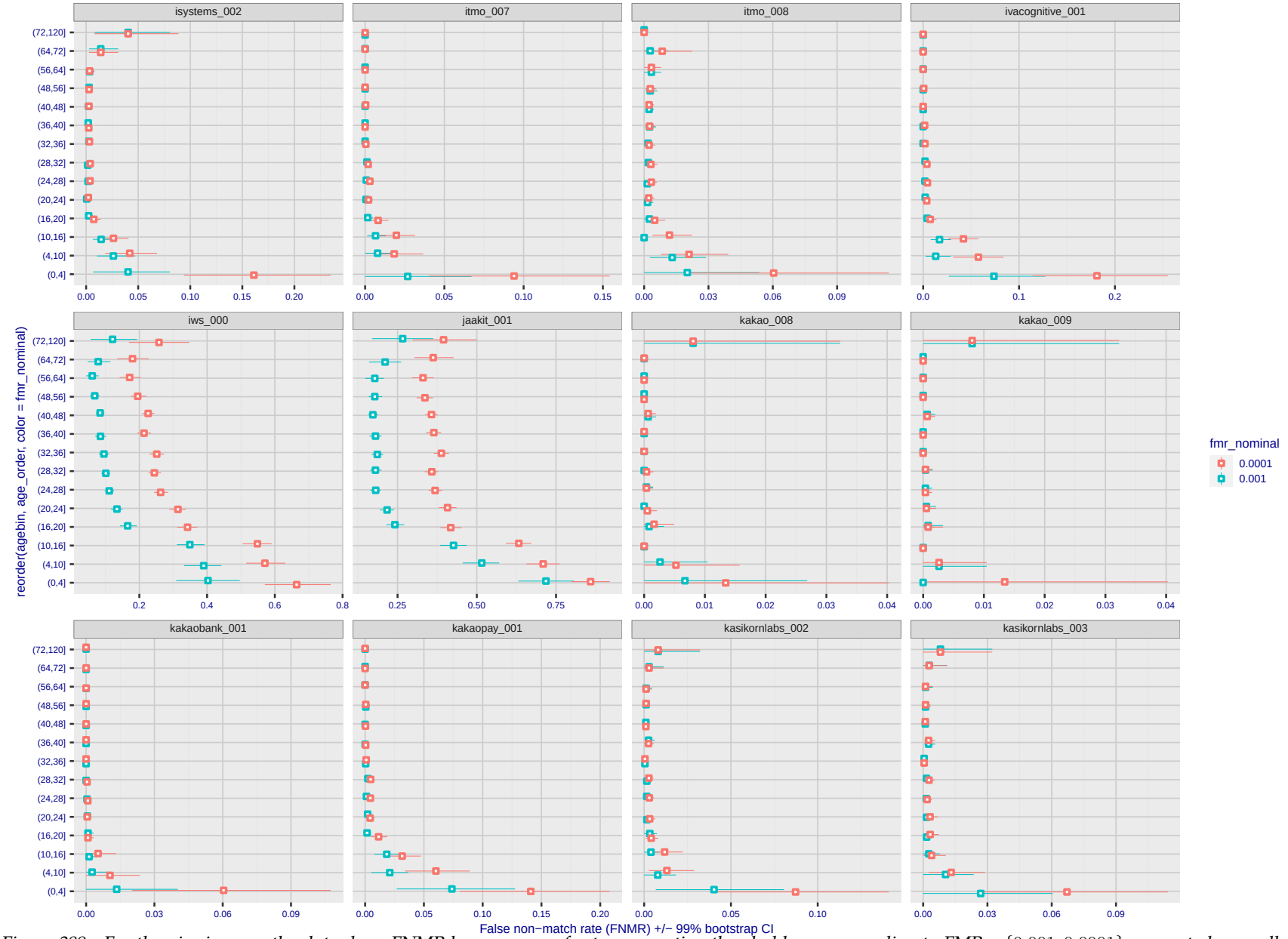

Figure 389: For the visa images, the dots show FNMR by age group for two operating thresholds corresponding to FMR = $\{0.001, 0.0001\}$ computed over all on the order of 10^{10} impostor scores. The FMR in each bin will vary also - see subsequent impostor heatmaps in sec. 3.6.2. Given a pair of face images taken at different times, we assign the comparison to the bin that is the arithmetic average of the subject's ages. This plot shows only the effect of age, not ageing. The number of comparisons in each bin is generally in the thousands, however the first and last bins are computed over 149 and 124 respectively. The error rates in some (adult) cases are zero, and in others the DET is flat so the error rates at the two thresholds are identical. The lines span 1% and 99% of boostrap replicated FNMR estimates.

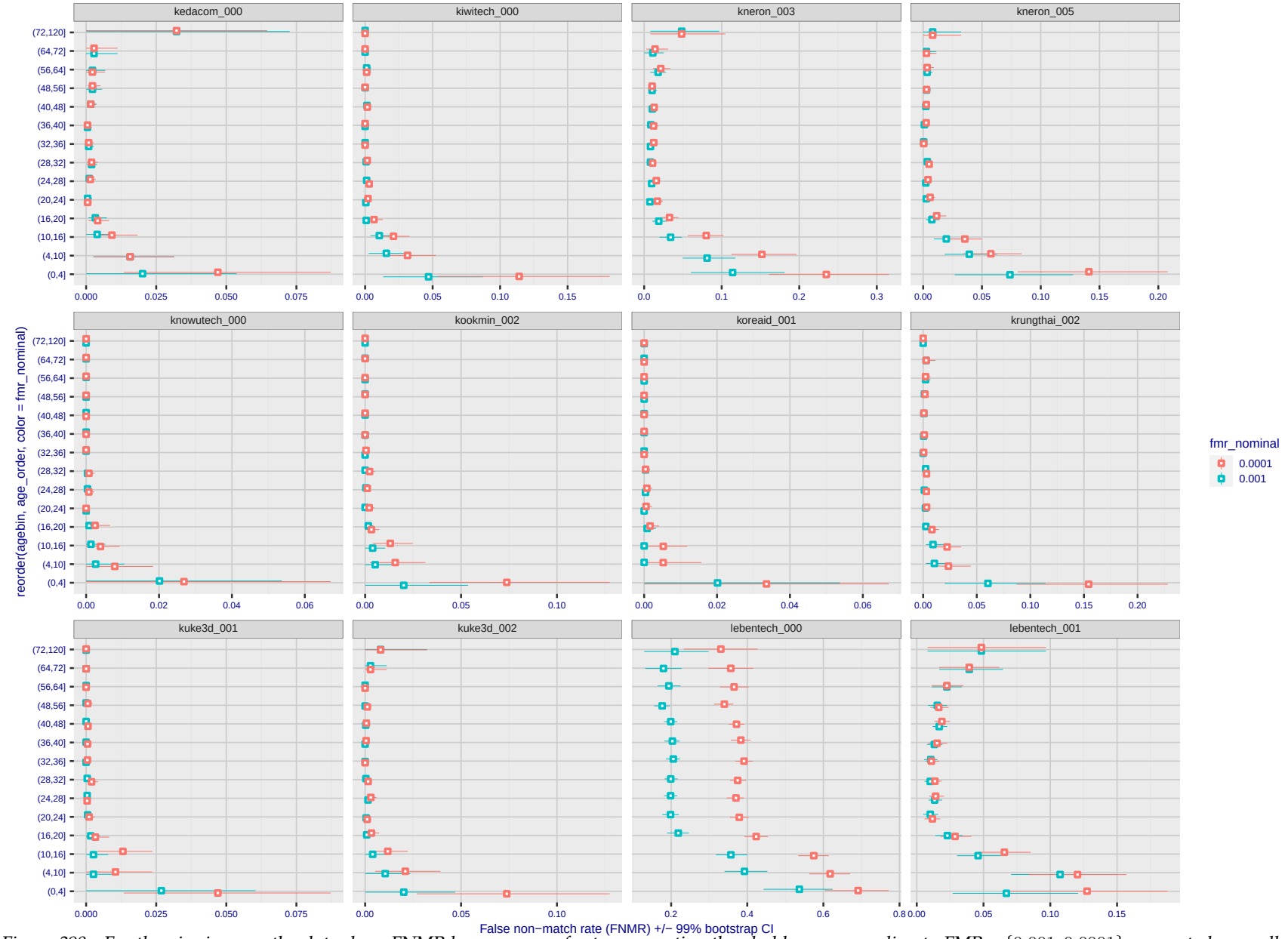

Figure 390: For the visa images, the dots show FNMR by age group for two operating thresholds corresponding to FMR = $\{0.001, 0.0001\}$ computed over all on the order of 10^{10} impostor scores. The FMR in each bin will vary also - see subsequent impostor heatmaps in sec. 3.6.2. Given a pair of face images taken at different times, we assign the comparison to the bin that is the arithmetic average of the subject's ages. This plot shows only the effect of age, not ageing. The number of comparisons in each bin is generally in the thousands, however the first and last bins are computed over 149 and 124 respectively. The error rates in some (adult) cases are zero, and in others the DET is flat so the error rates at the two thresholds are identical. The lines span 1% and 99% of boostrap replicated FNMR estimates.

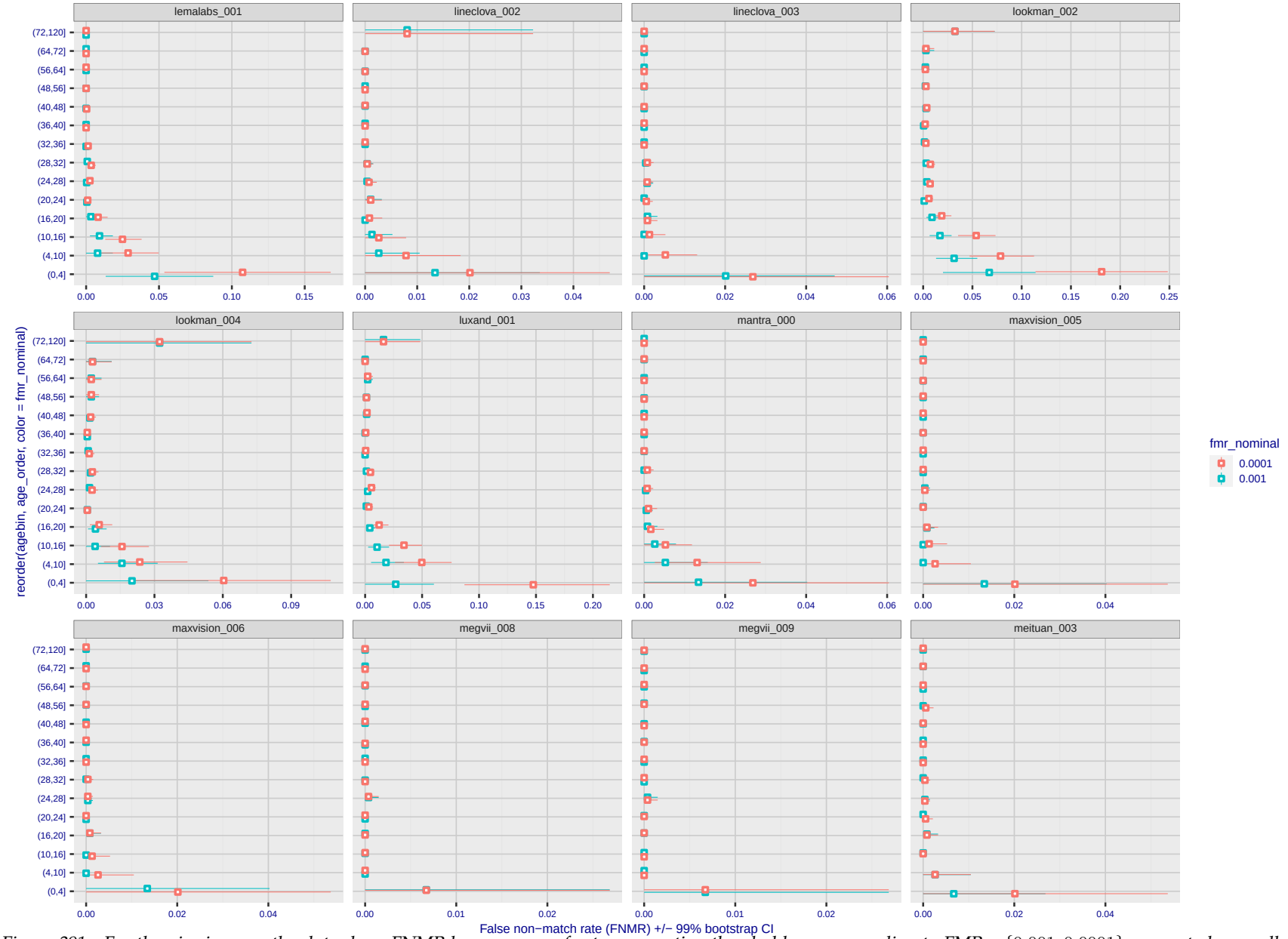

Figure 391: For the visa images, the dots show FNMR by age group for two operating thresholds corresponding to FMR = $\{0.001, 0.0001\}$ computed over all on the order of 10^{10} impostor scores. The FMR in each bin will vary also - see subsequent impostor heatmaps in sec. 3.6.2. Given a pair of face images taken at different times, we assign the comparison to the bin that is the arithmetic average of the subject's ages. This plot shows only the effect of age, not ageing. The number of comparisons in each bin is generally in the thousands, however the first and last bins are computed over 149 and 124 respectively. The error rates in some (adult) cases are zero, and in others the DET is flat so the error rates at the two thresholds are identical. The lines span 1% and 99% of boostrap replicated FNMR estimates.

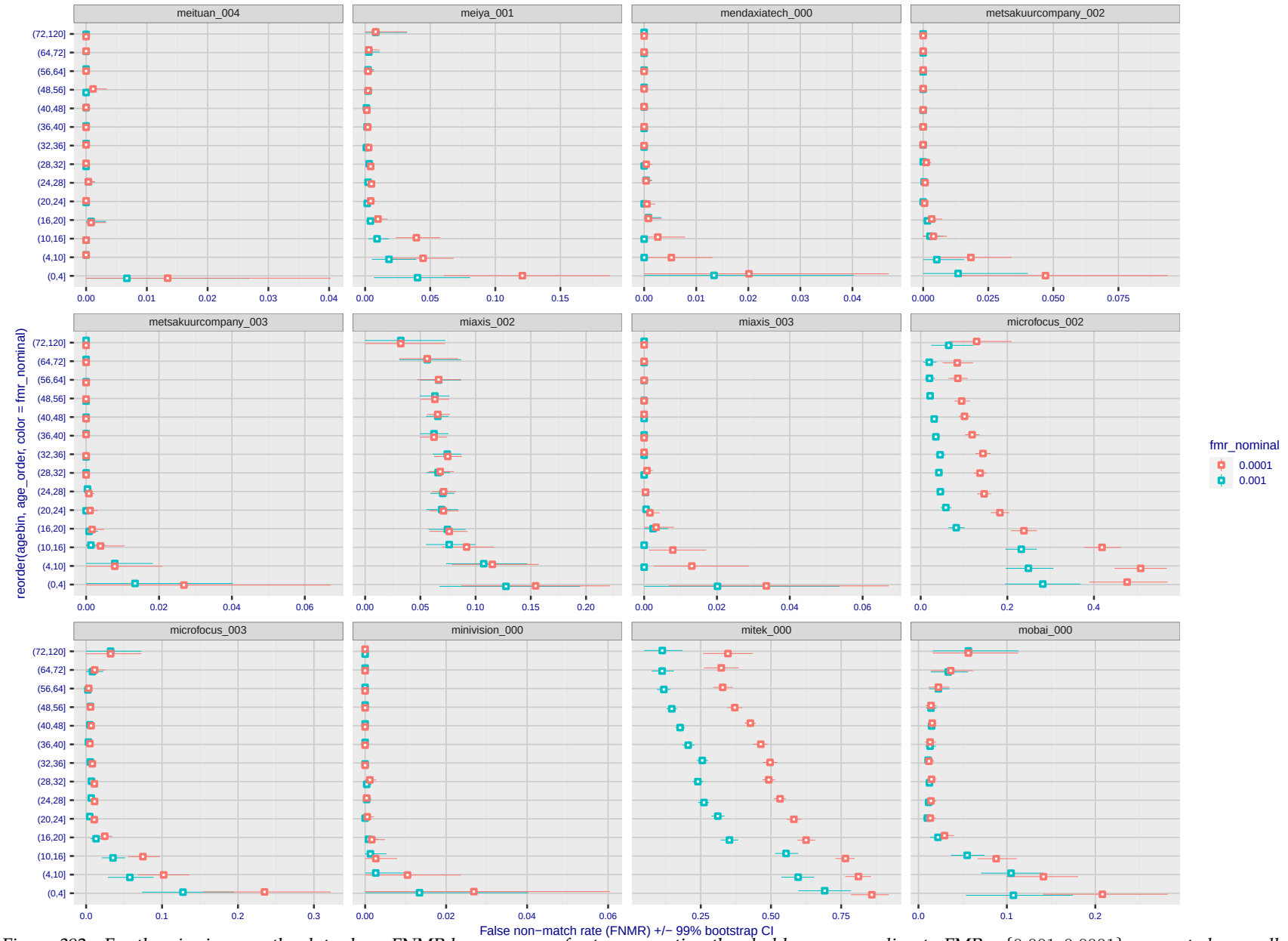

Figure 392: For the visa images, the dots show FNMR by age group for two operating thresholds corresponding to FMR = $\{0.001, 0.0001\}$ computed over all on the order of 10^{10} impostor scores. The FMR in each bin will vary also - see subsequent impostor heatmaps in sec. 3.6.2. Given a pair of face images taken at different times, we assign the comparison to the bin that is the arithmetic average of the subject's ages. This plot shows only the effect of age, not ageing. The number of comparisons in each bin is generally in the thousands, however the first and last bins are computed over 149 and 124 respectively. The error rates in some (adult) cases are zero, and in others the DET is flat so the error rates at the two thresholds are identical. The lines span 1% and 99% of boostrap replicated FNMR estimates.

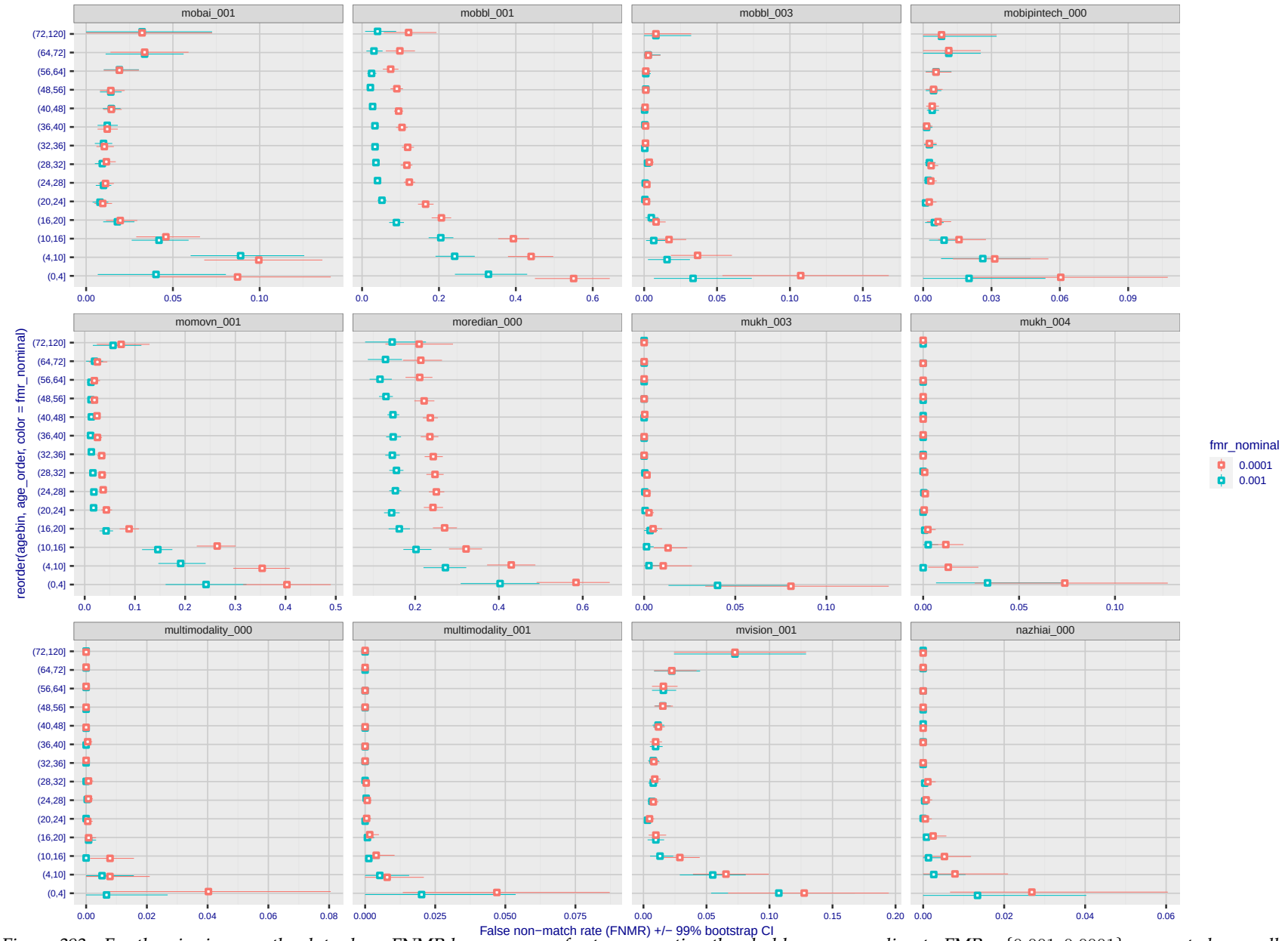

Figure 393: For the visa images, the dots show FNMR by age group for two operating thresholds corresponding to FMR = $\{0.001, 0.0001\}$ computed over all on the order of 10^{10} impostor scores. The FMR in each bin will vary also - see subsequent impostor heatmaps in sec. 3.6.2. Given a pair of face images taken at different times, we assign the comparison to the bin that is the arithmetic average of the subject's ages. This plot shows only the effect of age, not ageing. The number of comparisons in each bin is generally in the thousands, however the first and last bins are computed over 149 and 124 respectively. The error rates in some (adult) cases are zero, and in others the DET is flat so the error rates at the two thresholds are identical. The lines span 1% and 99% of boostrap replicated FNMR estimates.

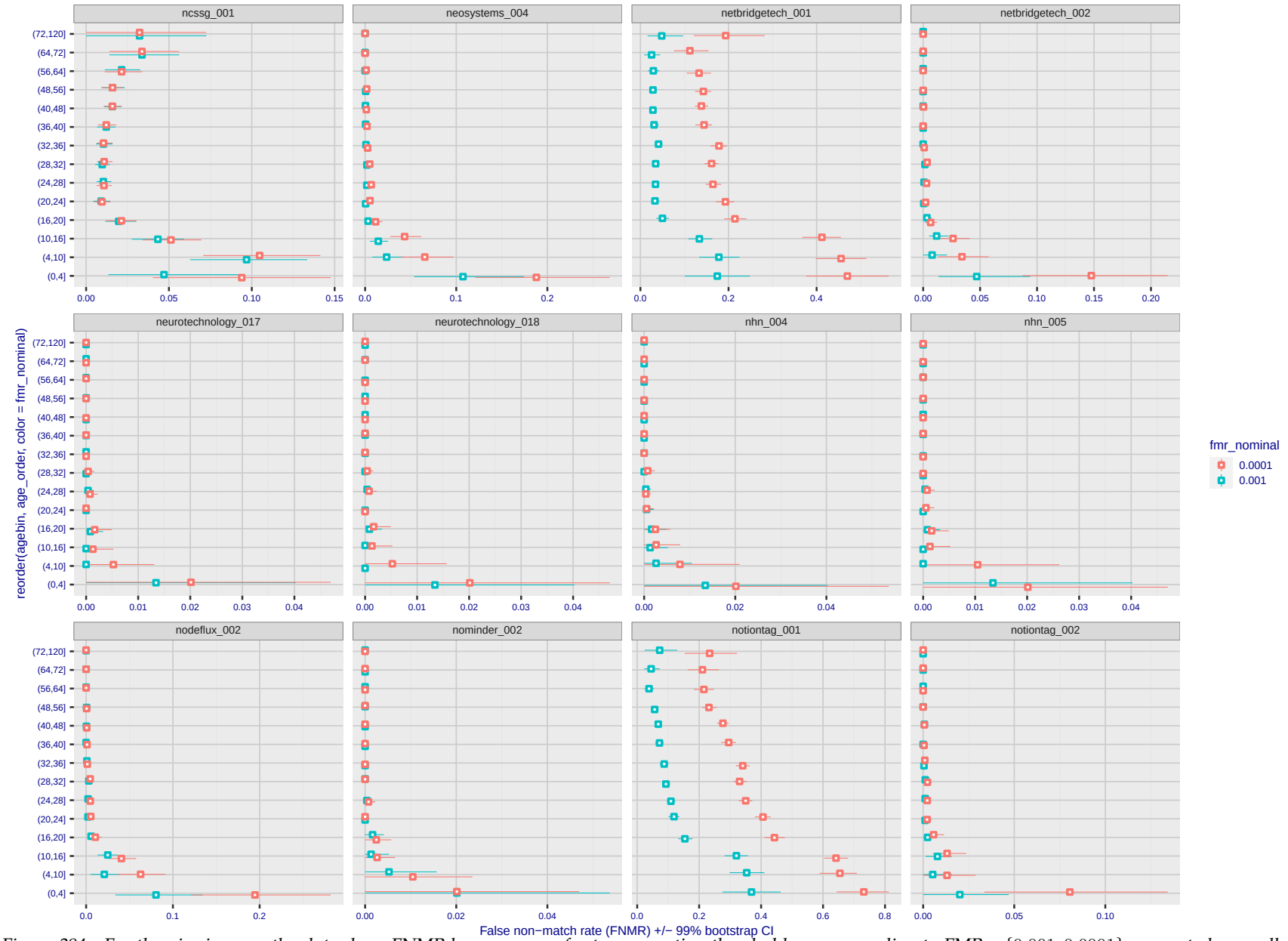

Figure 394: For the visa images, the dots show FNMR by age group for two operating thresholds corresponding to FMR = $\{0.001, 0.0001\}$ computed over all on the order of 10^{10} impostor scores. The FMR in each bin will vary also - see subsequent impostor heatmaps in sec. 3.6.2. Given a pair of face images taken at different times, we assign the comparison to the bin that is the arithmetic average of the subject's ages. This plot shows only the effect of age, not ageing. The number of comparisons in each bin is generally in the thousands, however the first and last bins are computed over 149 and 124 respectively. The error rates in some (adult) cases are zero, and in others the DET is flat so the error rates at the two thresholds are identical. The lines span 1% and 99% of boostrap replicated FNMR estimates.

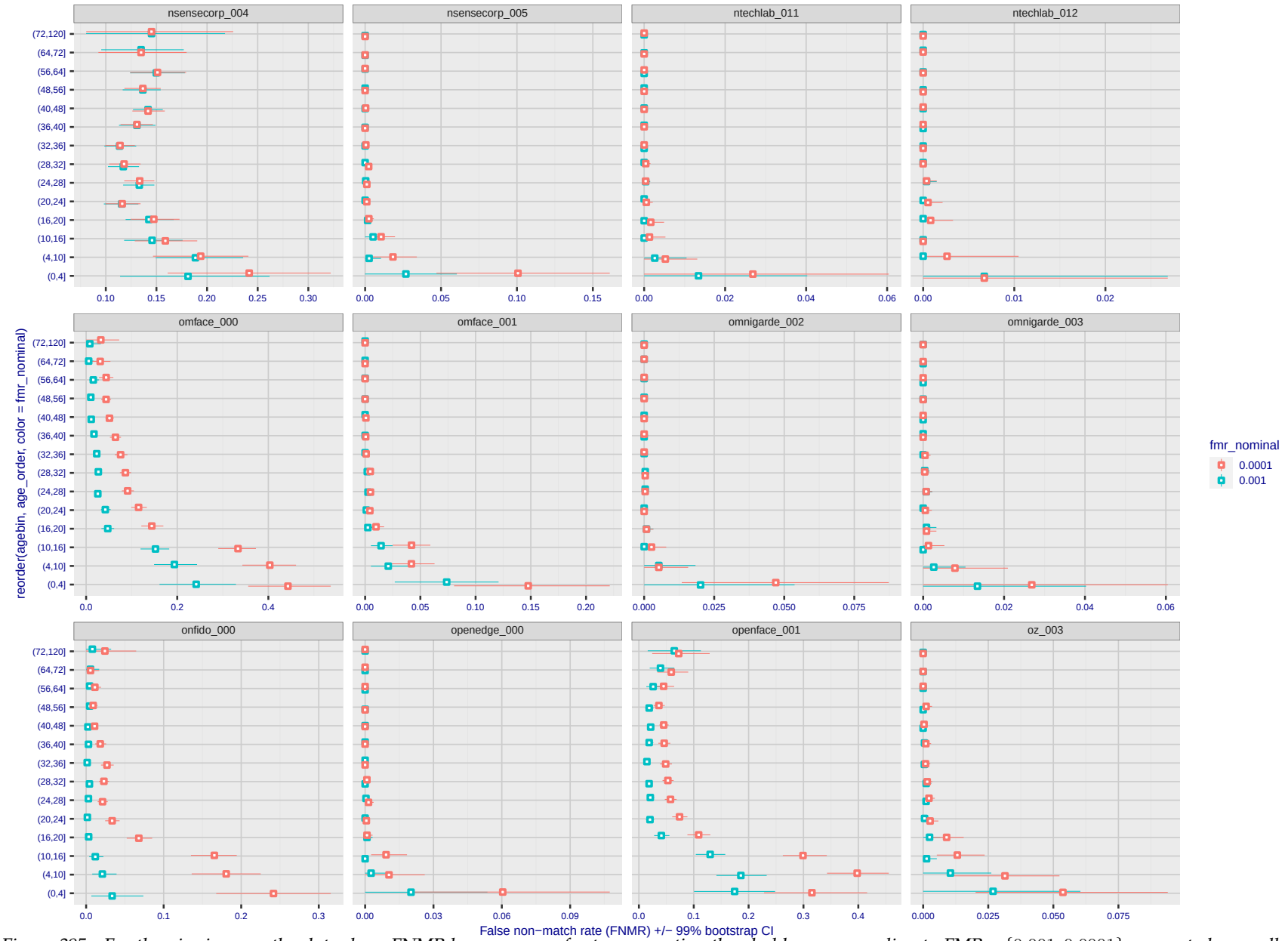

Figure 395: For the visa images, the dots show FNMR by age group for two operating thresholds corresponding to FMR = $\{0.001, 0.0001\}$ computed over all on the order of 10^{10} impostor scores. The FMR in each bin will vary also - see subsequent impostor heatmaps in sec. 3.6.2. Given a pair of face images taken at different times, we assign the comparison to the bin that is the arithmetic average of the subject's ages. This plot shows only the effect of age, not ageing. The number of comparisons in each bin is generally in the thousands, however the first and last bins are computed over 149 and 124 respectively. The error rates in some (adult) cases are zero, and in others the DET is flat so the error rates at the two thresholds are identical. The lines span 1% and 99% of boostrap replicated FNMR estimates.

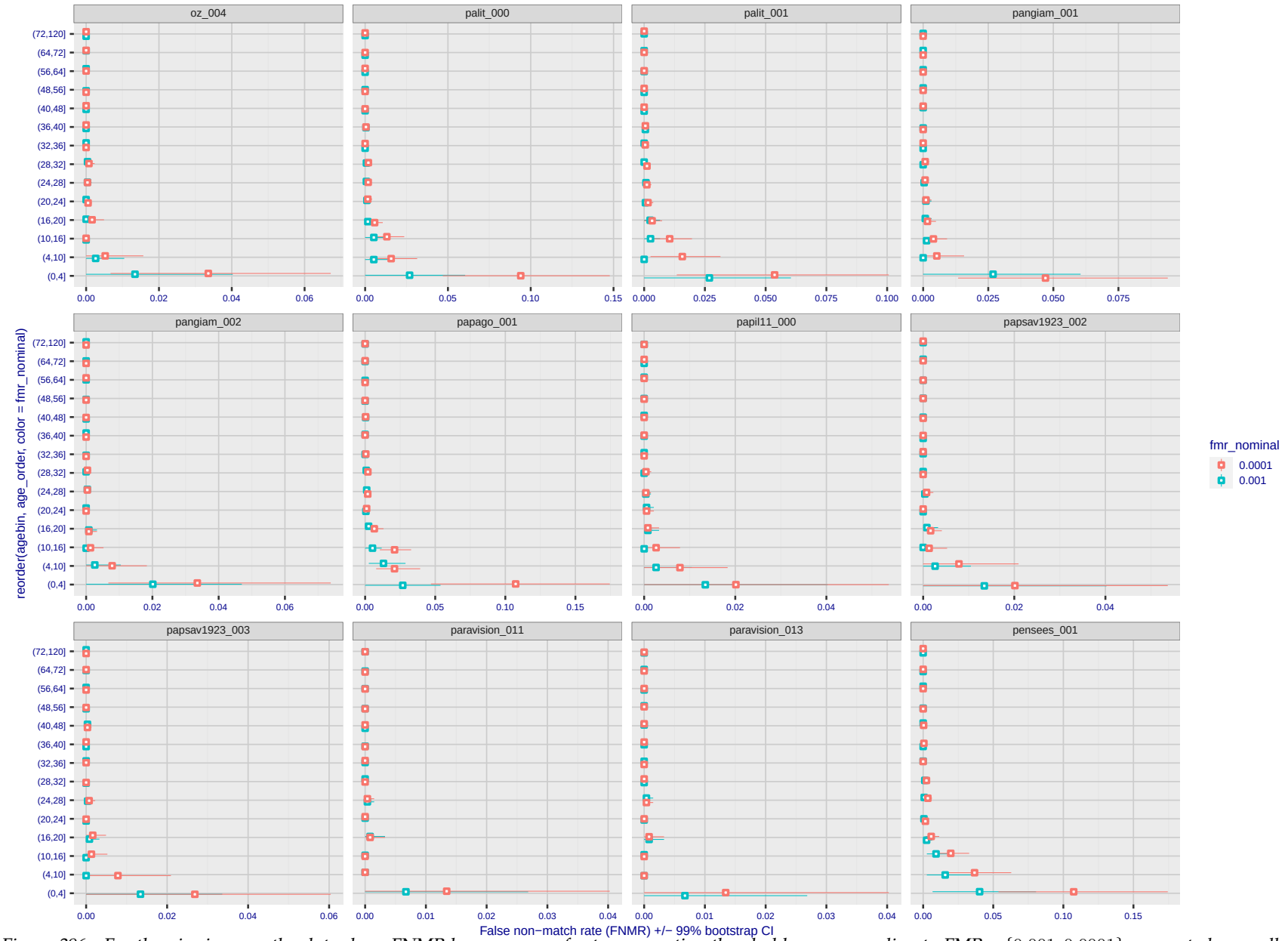

Figure 396: For the visa images, the dots show FNMR by age group for two operating thresholds corresponding to FMR = $\{0.001, 0.0001\}$ computed over all on the order of 10^{10} impostor scores. The FMR in each bin will vary also - see subsequent impostor heatmaps in sec. 3.6.2. Given a pair of face images taken at different times, we assign the comparison to the bin that is the arithmetic average of the subject's ages. This plot shows only the effect of age, not ageing. The number of comparisons in each bin is generally in the thousands, however the first and last bins are computed over 149 and 124 respectively. The error rates in some (adult) cases are zero, and in others the DET is flat so the error rates at the two thresholds are identical. The lines span 1% and 99% of boostrap replicated FNMR estimates.

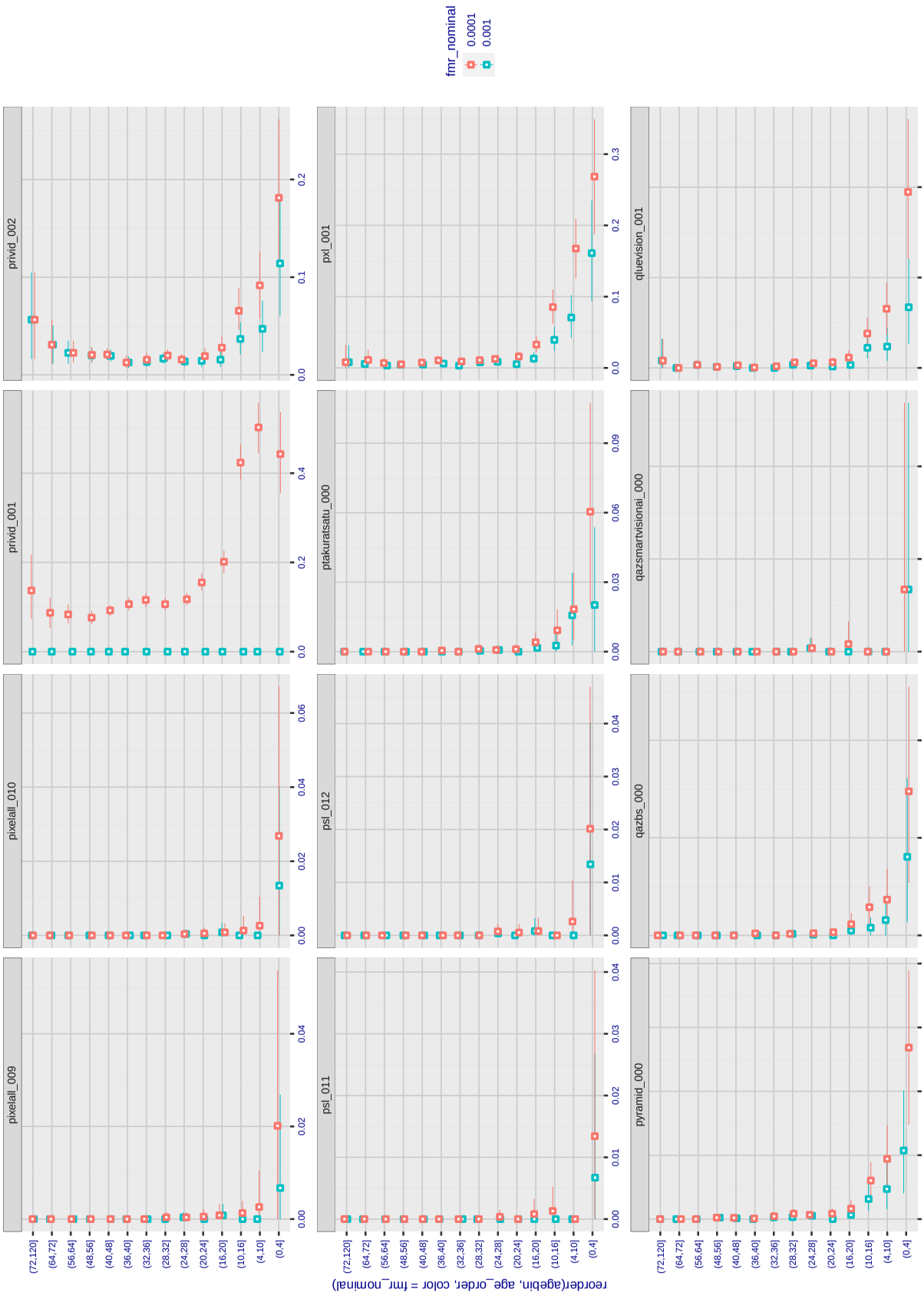

Figure 397: For the visa images, the dots show FNMR by age group for two operating thresholds corresponding to FMR = $\{0.001, 0.0001\}$ computed over all on the order of 10^{10} impostor scores. The FMR in each bin will vary also - see subsequent impostor heatmaps in sec. 3.6.2. Given a pair of face images taken at different times, we assign the comparison to the bin that is the arithmetic average of the subject's ages. This plot shows only the effect of age, not ageing. The number of comparisons in each bin is generally in the thousands, however the first and last bins are computed over 149 and 124 respectively. The error rates in some (adult) cases are zero, and in others the DET is flat so the error rates at the two thresholds are identical. The lines span 1% and 99% of boostrap replicated FNMR estimates.

FNMR(T) "False non-match rate"
FMR(T) "False match rate"

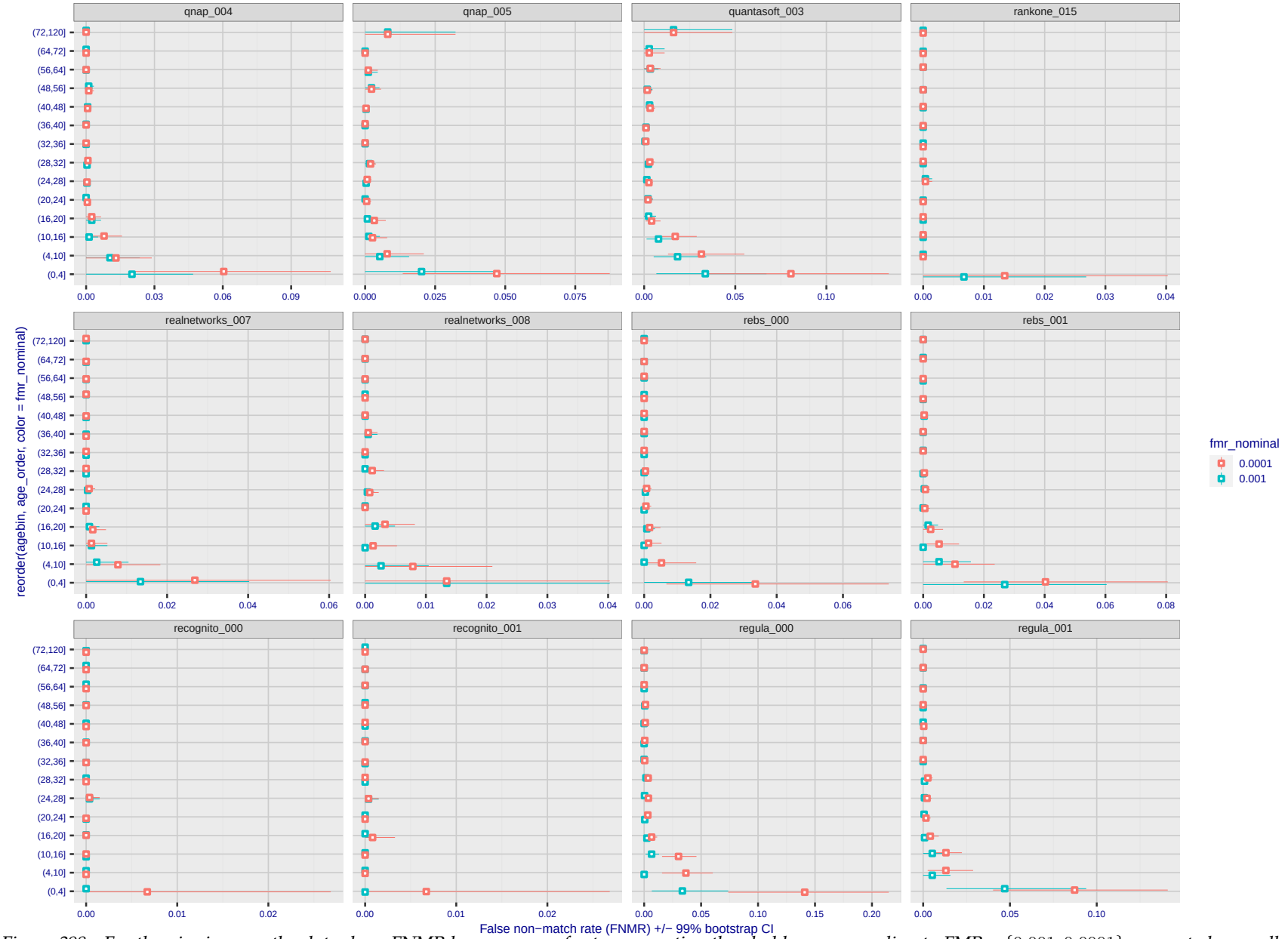

Figure 398: For the visa images, the dots show FNMR by age group for two operating thresholds corresponding to FMR = $\{0.001, 0.0001\}$ computed over all on the order of 10^{10} impostor scores. The FMR in each bin will vary also - see subsequent impostor heatmaps in sec. 3.6.2. Given a pair of face images taken at different times, we assign the comparison to the bin that is the arithmetic average of the subject's ages. This plot shows only the effect of age, not ageing. The number of comparisons in each bin is generally in the thousands, however the first and last bins are computed over 149 and 124 respectively. The error rates in some (adult) cases are zero, and in others the DET is flat so the error rates at the two thresholds are identical. The lines span 1% and 99% of boostrap replicated FNMR estimates.

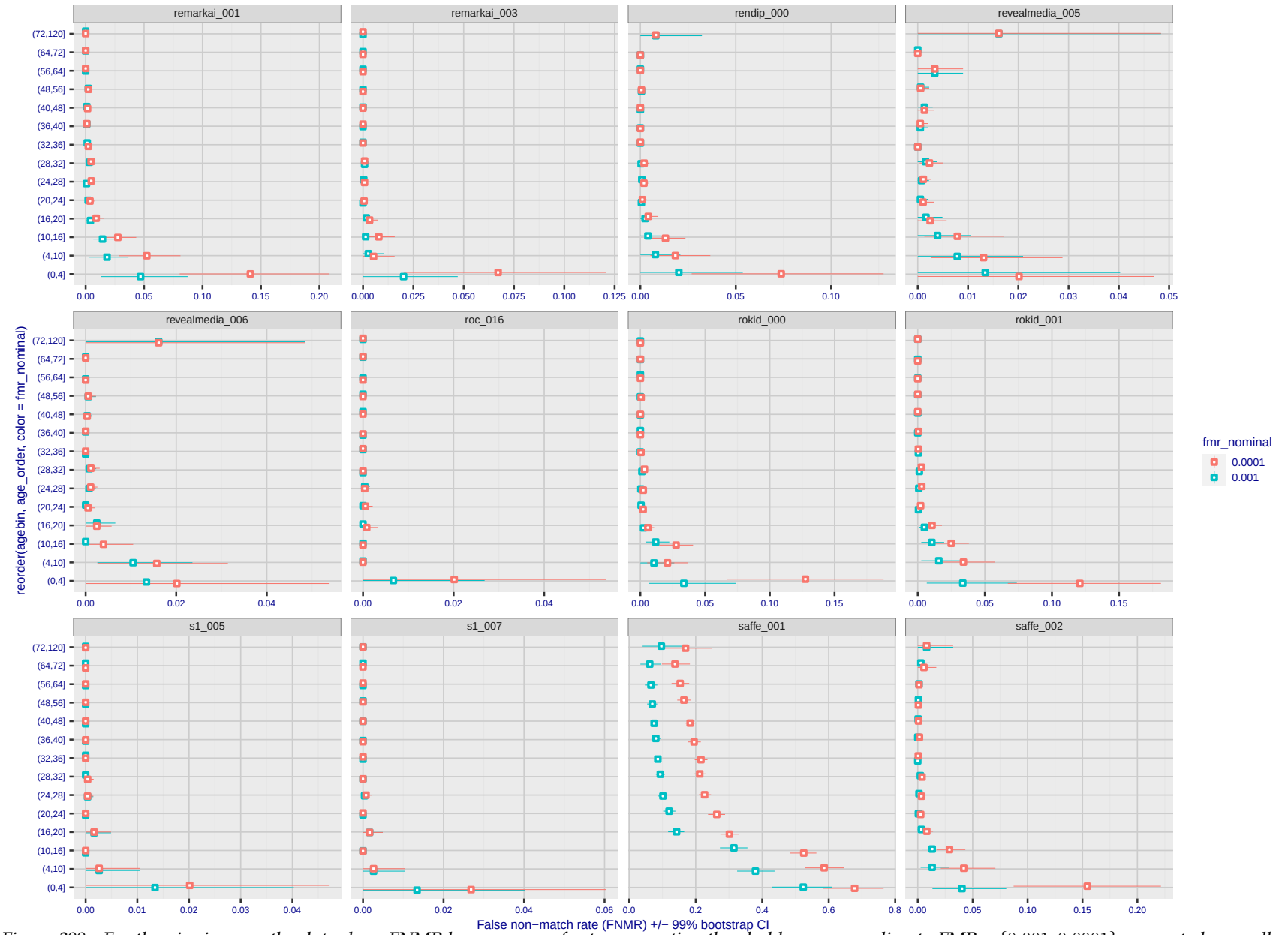

Figure 399: For the visa images, the dots show FNMR by age group for two operating thresholds corresponding to FMR = $\{0.001, 0.0001\}$ computed over all on the order of 10^{10} impostor scores. The FMR in each bin will vary also - see subsequent impostor heatmaps in sec. 3.6.2. Given a pair of face images taken at different times, we assign the comparison to the bin that is the arithmetic average of the subject's ages. This plot shows only the effect of age, not ageing. The number of comparisons in each bin is generally in the thousands, however the first and last bins are computed over 149 and 124 respectively. The error rates in some (adult) cases are zero, and in others the DET is flat so the error rates at the two thresholds are identical. The lines span 1% and 99% of boostrap replicated FNMR estimates.

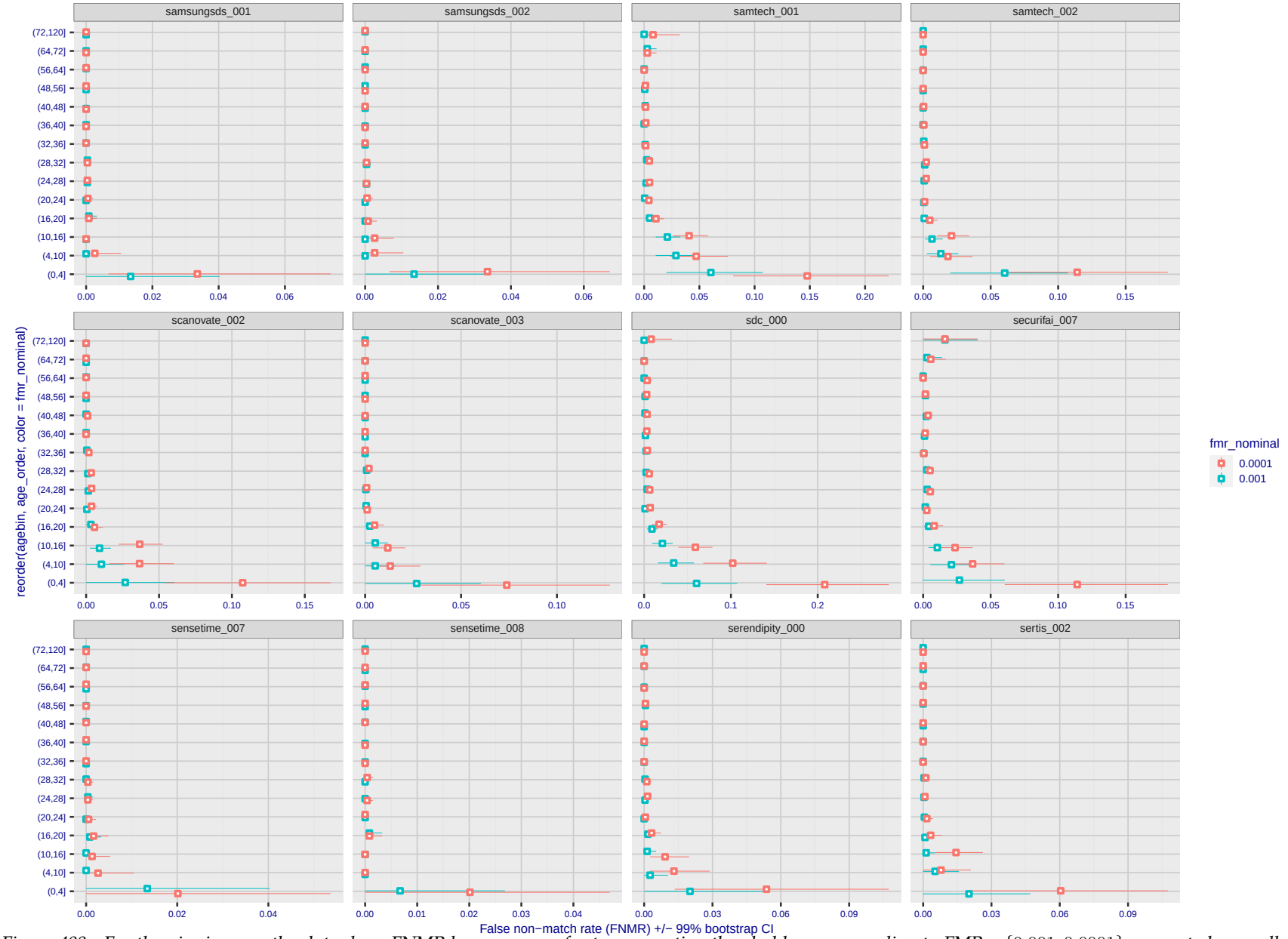

Figure 400: For the visa images, the dots show FNMR by age group for two operating thresholds corresponding to FMR = $\{0.001, 0.0001\}$ computed over all on the order of 10^{10} impostor scores. The FMR in each bin will vary also - see subsequent impostor heatmaps in sec. 3.6.2. Given a pair of face images taken at different times, we assign the comparison to the bin that is the arithmetic average of the subject's ages. This plot shows only the effect of age, not ageing. The number of comparisons in each bin is generally in the thousands, however the first and last bins are computed over 149 and 124 respectively. The error rates in some (adult) cases are zero, and in others the DET is flat so the error rates at the two thresholds are identical. The lines span 1% and 99% of boostrap replicated FNMR estimates.

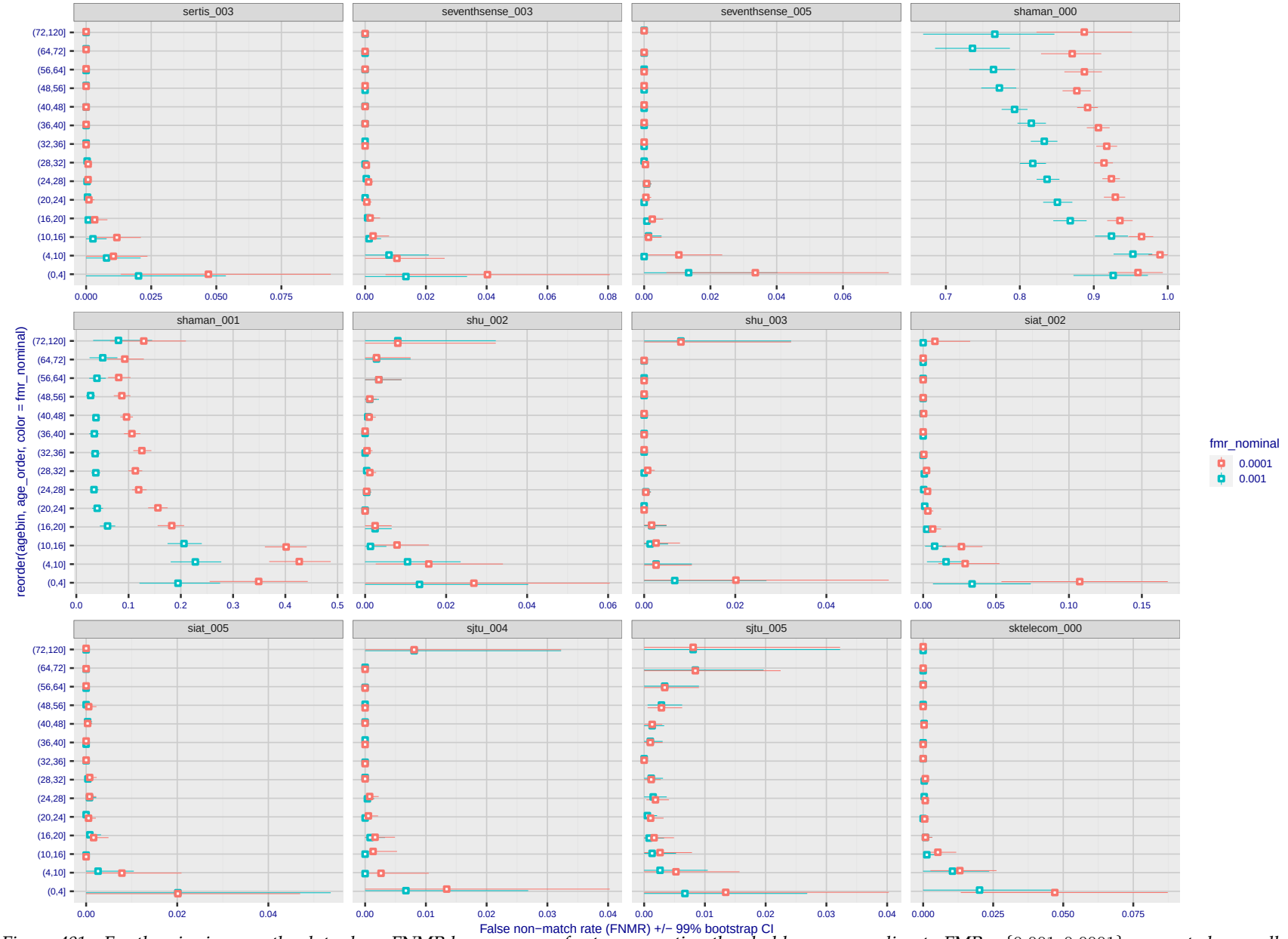

Figure 401: For the visa images, the dots show FNMR by age group for two operating thresholds corresponding to FMR = $\{0.001, 0.0001\}$ computed over all on the order of 10^{10} impostor scores. The FMR in each bin will vary also - see subsequent impostor heatmaps in sec. 3.6.2. Given a pair of face images taken at different times, we assign the comparison to the bin that is the arithmetic average of the subject's ages. This plot shows only the effect of age, not ageing. The number of comparisons in each bin is generally in the thousands, however the first and last bins are computed over 149 and 124 respectively. The error rates in some (adult) cases are zero, and in others the DET is flat so the error rates at the two thresholds are identical. The lines span 1% and 99% of boostrap replicated FNMR estimates.

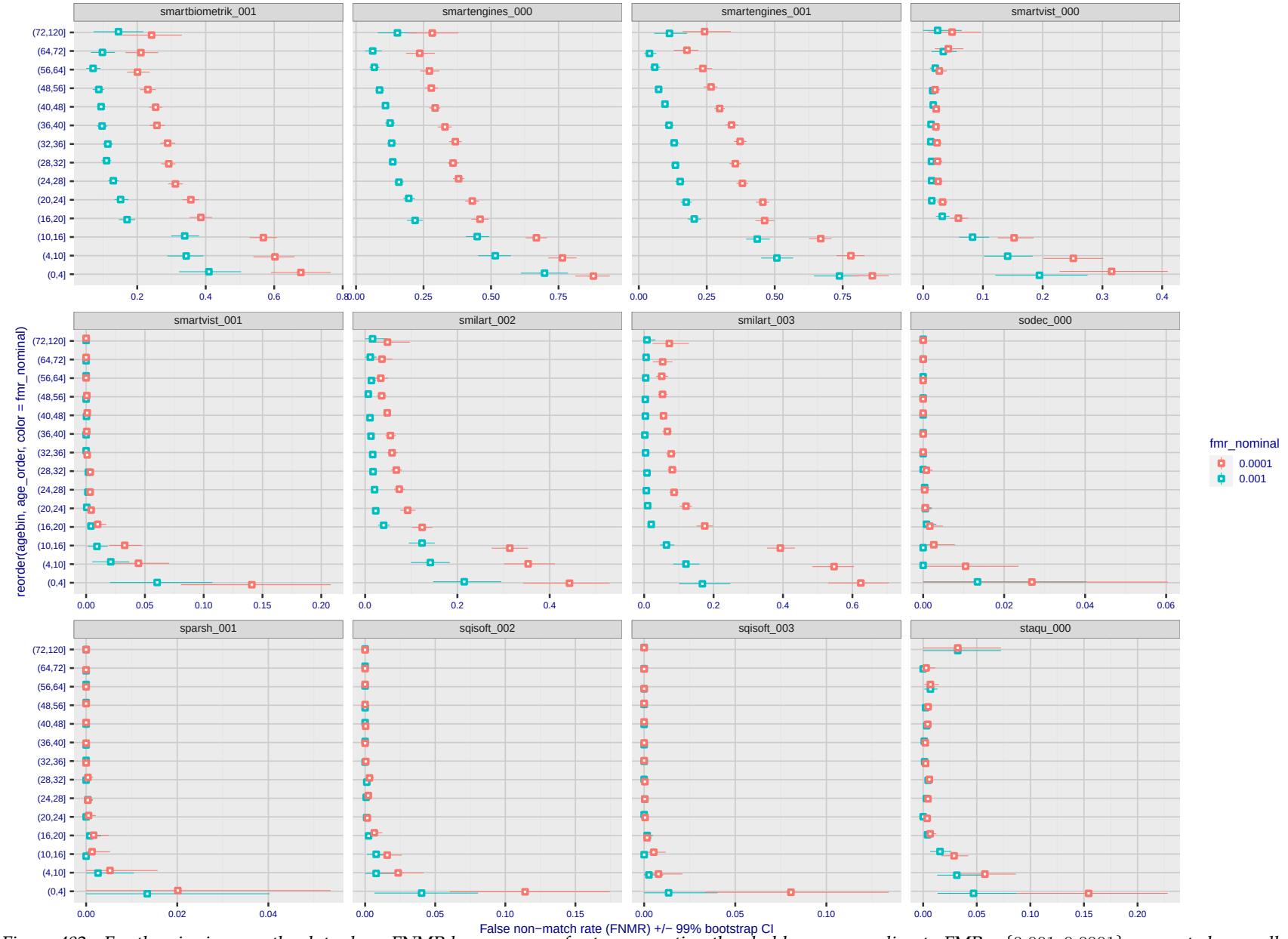

Figure 402: For the visa images, the dots show FNMR by age group for two operating thresholds corresponding to FMR = $\{0.001, 0.0001\}$ computed over all on the order of 10^{10} impostor scores. The FMR in each bin will vary also - see subsequent impostor heatmaps in sec. 3.6.2. Given a pair of face images taken at different times, we assign the comparison to the bin that is the arithmetic average of the subject's ages. This plot shows only the effect of age, not ageing. The number of comparisons in each bin is generally in the thousands, however the first and last bins are computed over 149 and 124 respectively. The error rates in some (adult) cases are zero, and in others the DET is flat so the error rates at the two thresholds are identical. The lines span 1% and 99% of boostrap replicated FNMR estimates.

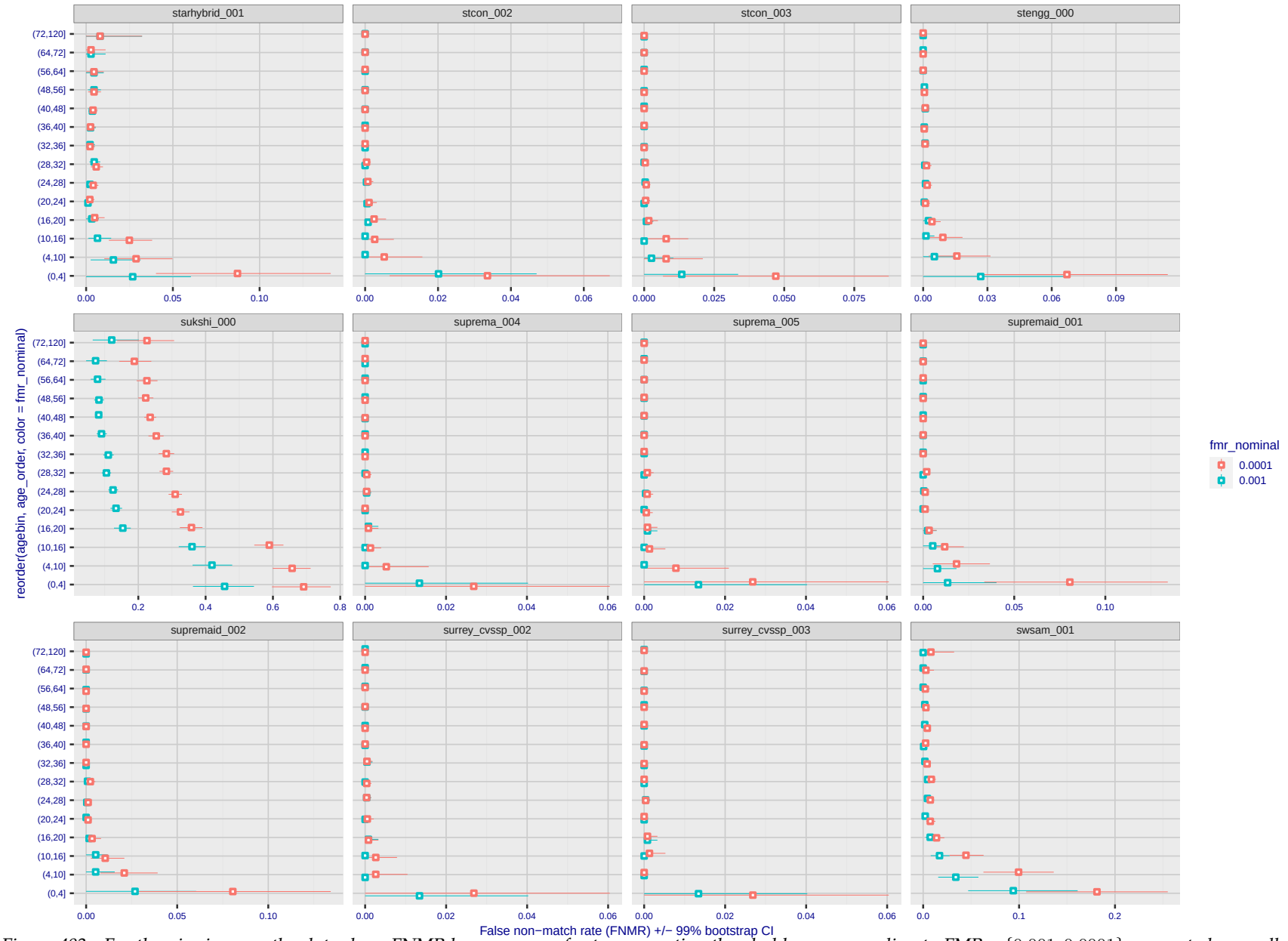

Figure 403: For the visa images, the dots show FNMR by age group for two operating thresholds corresponding to FMR = $\{0.001, 0.0001\}$ computed over all on the order of 10^{10} impostor scores. The FMR in each bin will vary also - see subsequent impostor heatmaps in sec. 3.6.2. Given a pair of face images taken at different times, we assign the comparison to the bin that is the arithmetic average of the subject's ages. This plot shows only the effect of age, not ageing. The number of comparisons in each bin is generally in the thousands, however the first and last bins are computed over 149 and 124 respectively. The error rates in some (adult) cases are zero, and in others the DET is flat so the error rates at the two thresholds are identical. The lines span 1% and 99% of boostrap replicated FNMR estimates.

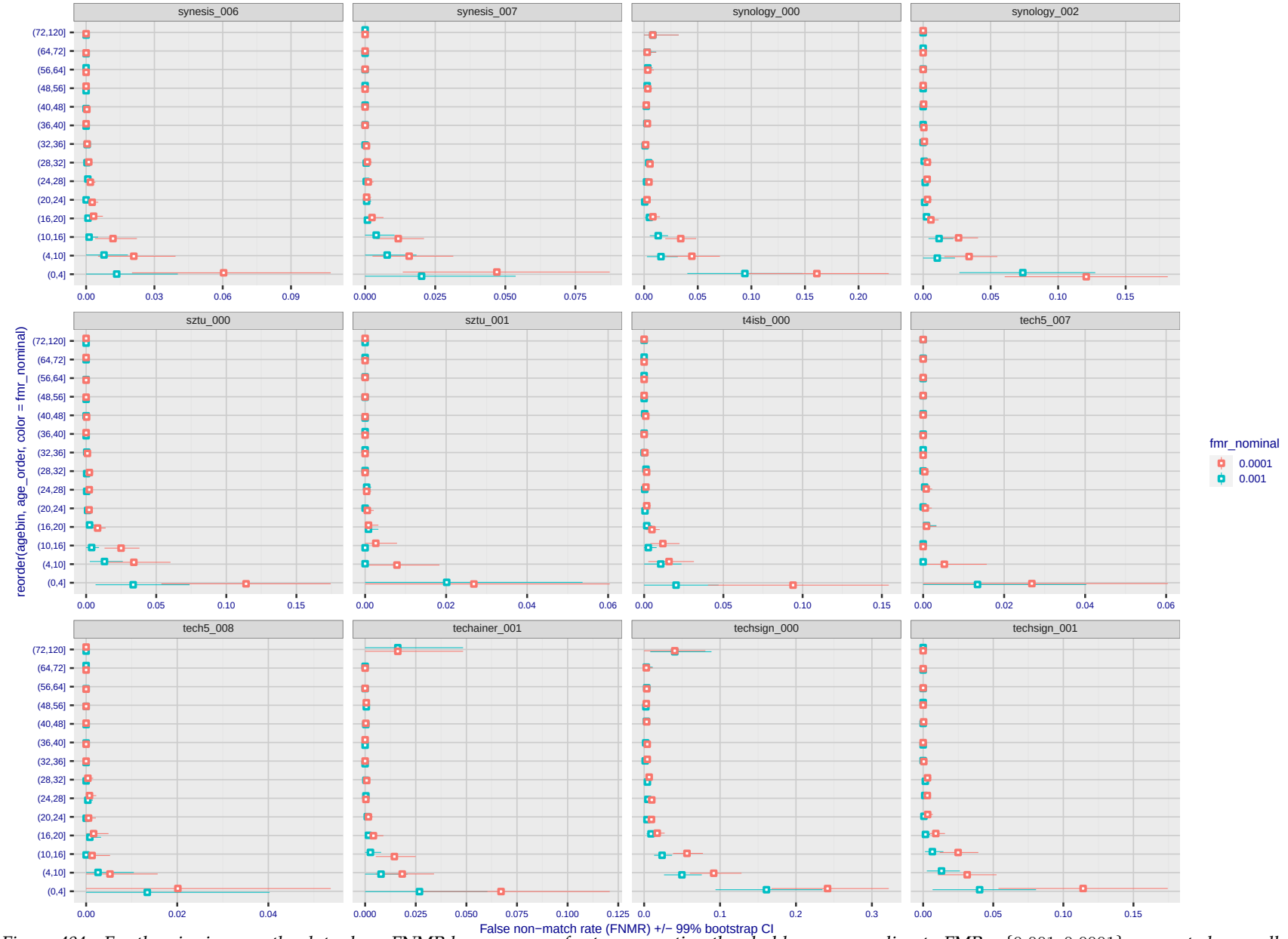

Figure 404: For the visa images, the dots show FNMR by age group for two operating thresholds corresponding to FMR = $\{0.001, 0.0001\}$ computed over all on the order of 10^{10} impostor scores. The FMR in each bin will vary also - see subsequent impostor heatmaps in sec. 3.6.2. Given a pair of face images taken at different times, we assign the comparison to the bin that is the arithmetic average of the subject's ages. This plot shows only the effect of age, not ageing. The number of comparisons in each bin is generally in the thousands, however the first and last bins are computed over 149 and 124 respectively. The error rates in some (adult) cases are zero, and in others the DET is flat so the error rates at the two thresholds are identical. The lines span 1% and 99% of boostrap replicated FNMR estimates.

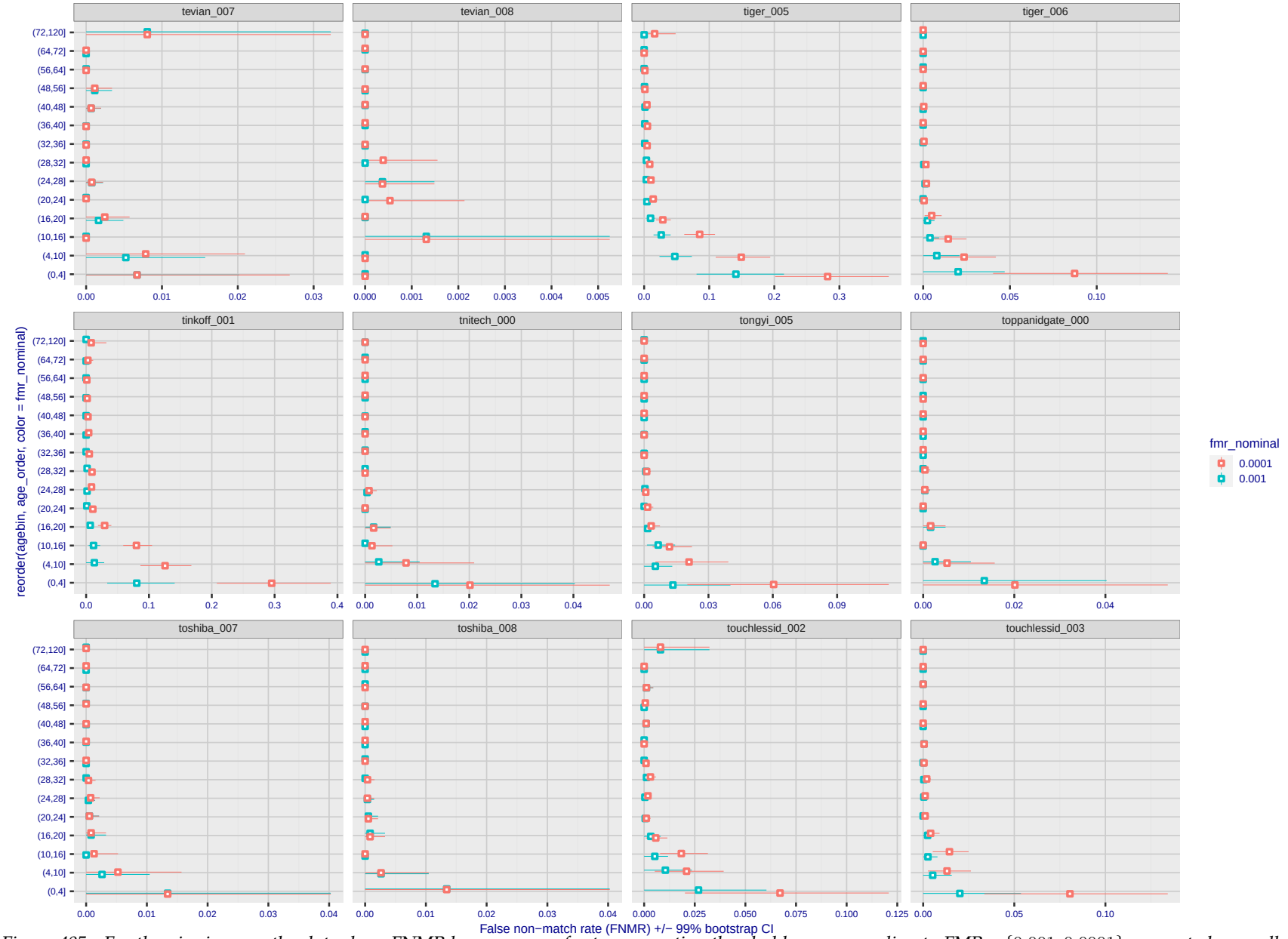

Figure 405: For the visa images, the dots show FNMR by age group for two operating thresholds corresponding to FMR = $\{0.001, 0.0001\}$ computed over all on the order of 10^{10} impostor scores. The FMR in each bin will vary also - see subsequent impostor heatmaps in sec. 3.6.2. Given a pair of face images taken at different times, we assign the comparison to the bin that is the arithmetic average of the subject's ages. This plot shows only the effect of age, not ageing. The number of comparisons in each bin is generally in the thousands, however the first and last bins are computed over 149 and 124 respectively. The error rates in some (adult) cases are zero, and in others the DET is flat so the error rates at the two thresholds are identical. The lines span 1% and 99% of boostrap replicated FNMR estimates.

Figure 406: For the visa images, the dots show FNMR by age group for two operating thresholds corresponding to FMR = $\{0.001, 0.0001\}$ computed over all on the order of 10^{10} impostor scores. The FMR in each bin will vary also - see subsequent impostor heatmaps in sec. 3.6.2. Given a pair of face images taken at different times, we assign the comparison to the bin that is the arithmetic average of the subject's ages. This plot shows only the effect of age, not ageing. The number of comparisons in each bin is generally in the thousands, however the first and last bins are computed over 149 and 124 respectively. The error rates in some (adult) cases are zero, and in others the DET is flat so the error rates at the two thresholds are identical. The lines span 1% and 99% of boostrap replicated FNMR estimates.

Figure 407: For the visa images, the dots show FNMR by age group for two operating thresholds corresponding to FMR = $\{0.001, 0.0001\}$ computed over all on the order of 10^{10} impostor scores. The FMR in each bin will vary also - see subsequent impostor heatmaps in sec. 3.6.2. Given a pair of face images taken at different times, we assign the comparison to the bin that is the arithmetic average of the subject's ages. This plot shows only the effect of age, not ageing. The number of comparisons in each bin is generally in the thousands, however the first and last bins are computed over 149 and 124 respectively. The error rates in some (adult) cases are zero, and in others the DET is flat so the error rates at the two thresholds are identical. The lines span 1% and 99% of boostrap replicated FNMR estimates.

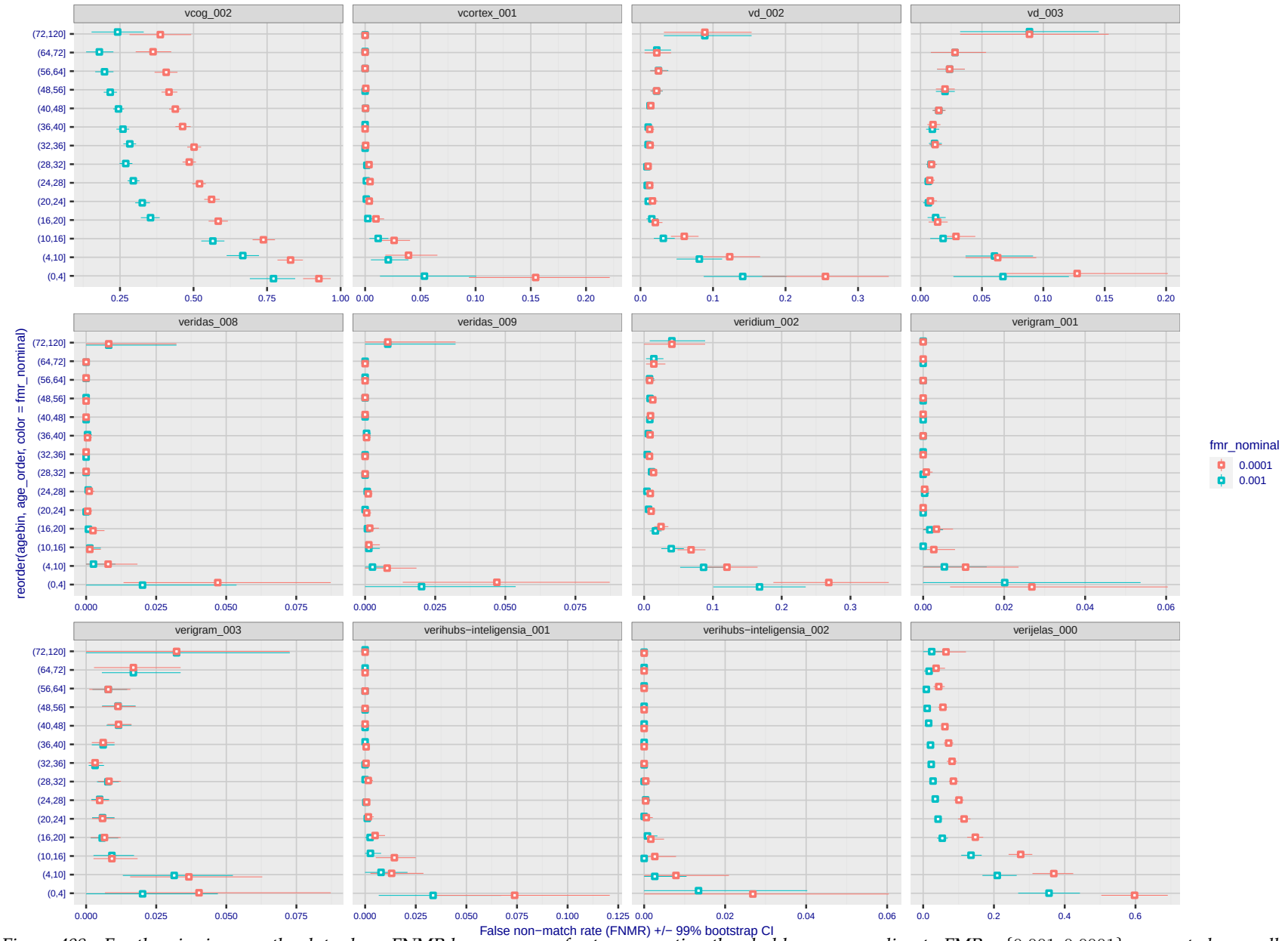

Figure 408: For the visa images, the dots show FNMR by age group for two operating thresholds corresponding to FMR = $\{0.001, 0.0001\}$ computed over all on the order of 10^{10} impostor scores. The FMR in each bin will vary also - see subsequent impostor heatmaps in sec. 3.6.2. Given a pair of face images taken at different times, we assign the comparison to the bin that is the arithmetic average of the subject's ages. This plot shows only the effect of age, not ageing. The number of comparisons in each bin is generally in the thousands, however the first and last bins are computed over 149 and 124 respectively. The error rates in some (adult) cases are zero, and in others the DET is flat so the error rates at the two thresholds are identical. The lines span 1% and 99% of boostrap replicated FNMR estimates.

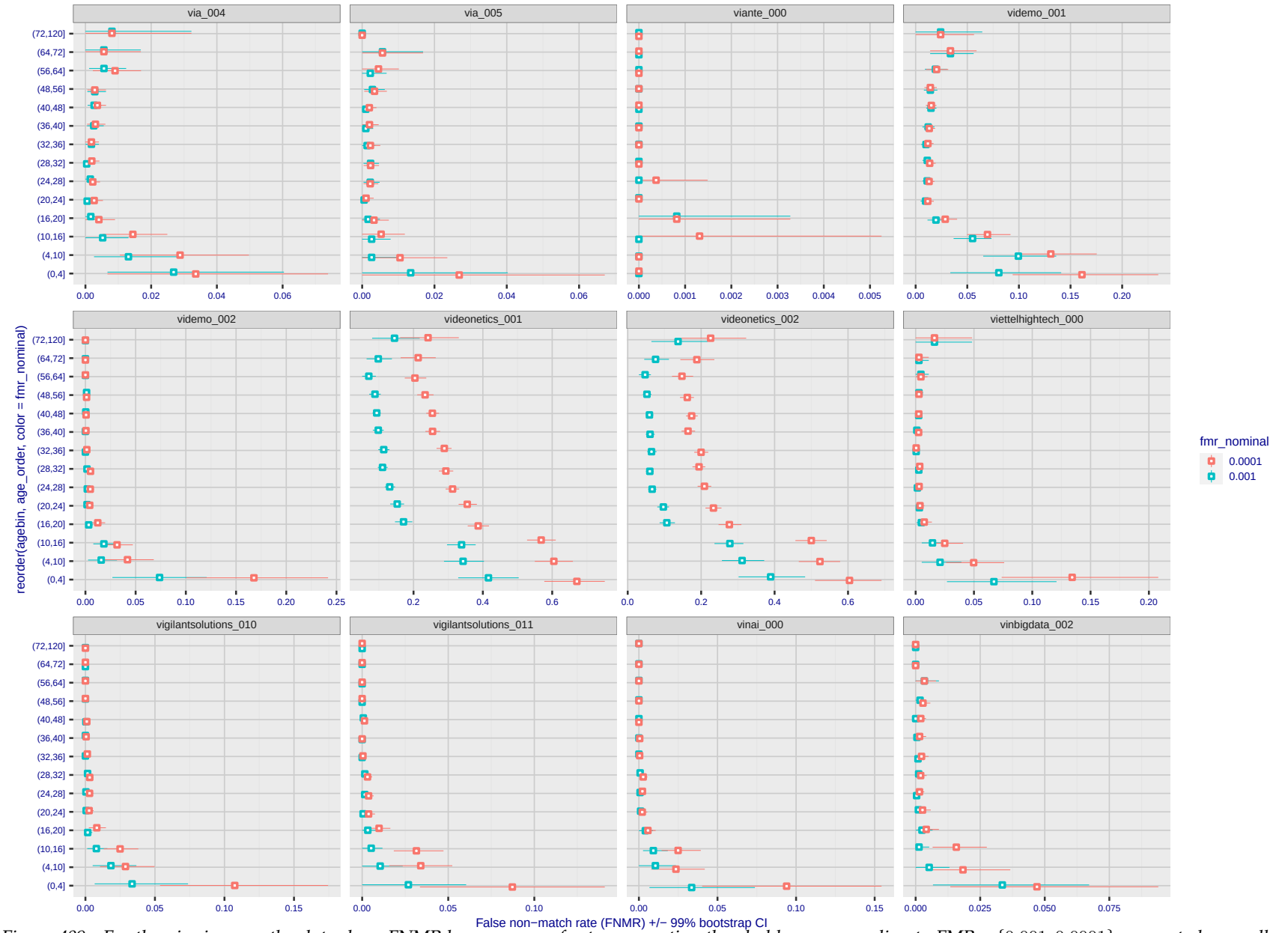

Figure 409: For the visa images, the dots show FNMR by age group for two operating thresholds corresponding to FMR = $\{0.001, 0.0001\}$ computed over all on the order of 10^{10} impostor scores. The FMR in each bin will vary also - see subsequent impostor heatmaps in sec. 3.6.2. Given a pair of face images taken at different times, we assign the comparison to the bin that is the arithmetic average of the subject's ages. This plot shows only the effect of age, not ageing. The number of comparisons in each bin is generally in the thousands, however the first and last bins are computed over 149 and 124 respectively. The error rates in some (adult) cases are zero, and in others the DET is flat so the error rates at the two thresholds are identical. The lines span 1% and 99% of boostrap replicated FNMR estimates.

Figure 410: For the visa images, the dots show FNMR by age group for two operating thresholds corresponding to FMR = $\{0.001, 0.0001\}$ computed over all on the order of 10^{10} impostor scores. The FMR in each bin will vary also - see subsequent impostor heatmaps in sec. 3.6.2. Given a pair of face images taken at different times, we assign the comparison to the bin that is the arithmetic average of the subject's ages. This plot shows only the effect of age, not ageing. The number of comparisons in each bin is generally in the thousands, however the first and last bins are computed over 149 and 124 respectively. The error rates in some (adult) cases are zero, and in others the DET is flat so the error rates at the two thresholds are identical. The lines span 1% and 99% of boostrap replicated FNMR estimates.

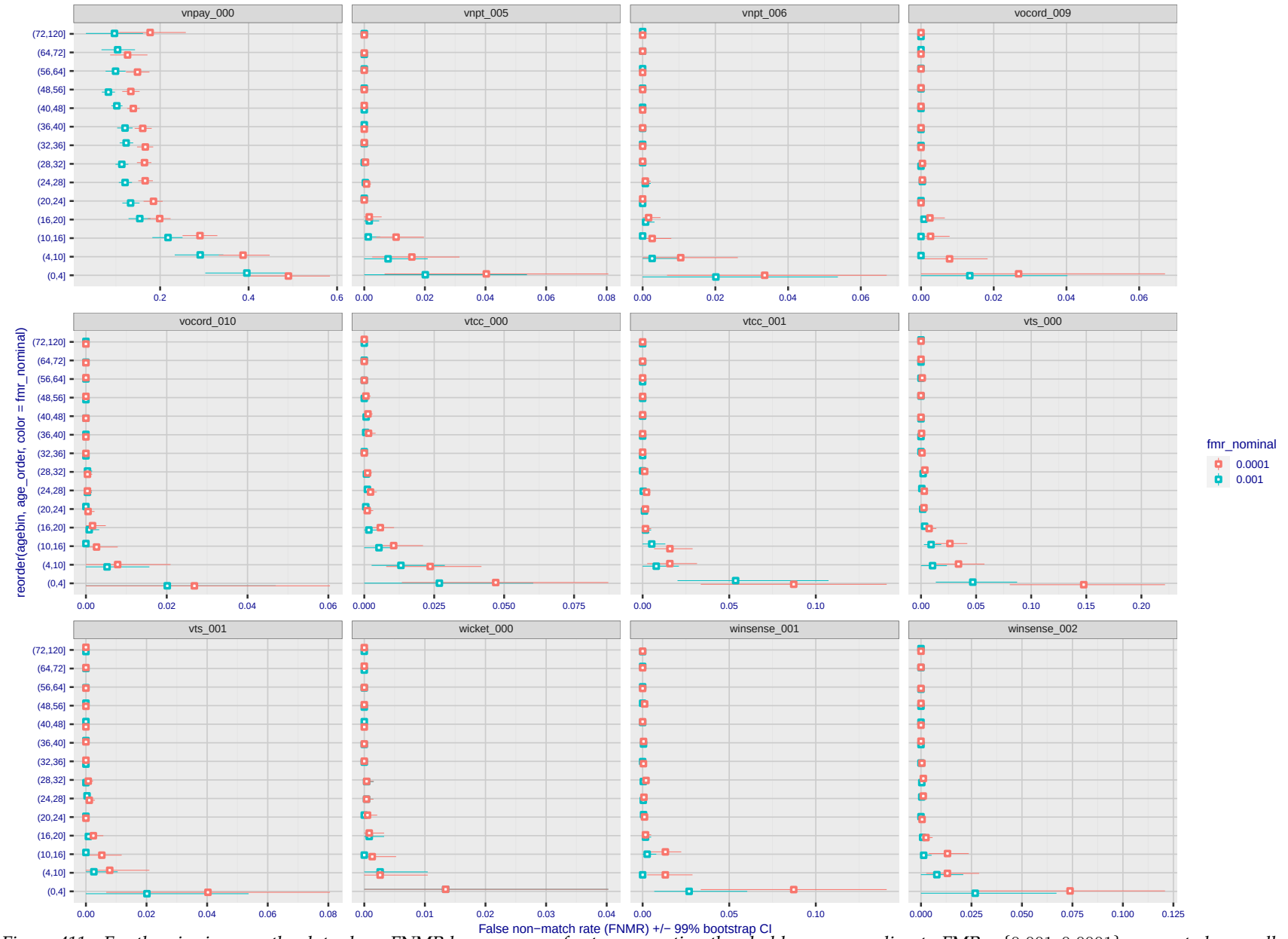

Figure 411: For the visa images, the dots show FNMR by age group for two operating thresholds corresponding to FMR = $\{0.001, 0.0001\}$ computed over all on the order of 10^{10} impostor scores. The FMR in each bin will vary also - see subsequent impostor heatmaps in sec. 3.6.2. Given a pair of face images taken at different times, we assign the comparison to the bin that is the arithmetic average of the subject's ages. This plot shows only the effect of age, not ageing. The number of comparisons in each bin is generally in the thousands, however the first and last bins are computed over 149 and 124 respectively. The error rates in some (adult) cases are zero, and in others the DET is flat so the error rates at the two thresholds are identical. The lines span 1% and 99% of boostrap replicated FNMR estimates.

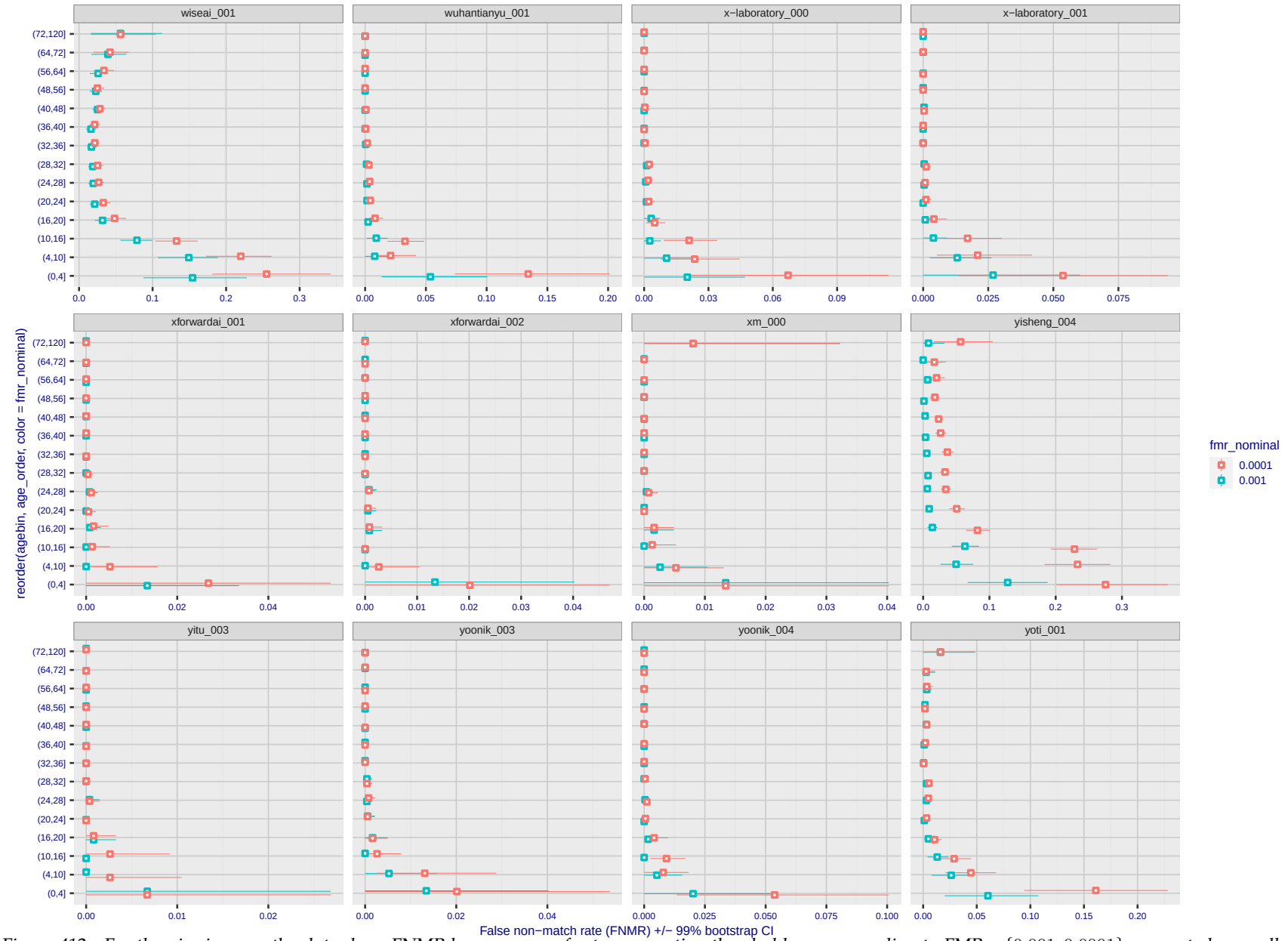

Figure 412: For the visa images, the dots show FNMR by age group for two operating thresholds corresponding to FMR = $\{0.001, 0.0001\}$ computed over all on the order of 10^{10} impostor scores. The FMR in each bin will vary also - see subsequent impostor heatmaps in sec. 3.6.2. Given a pair of face images taken at different times, we assign the comparison to the bin that is the arithmetic average of the subject's ages. This plot shows only the effect of age, not ageing. The number of comparisons in each bin is generally in the thousands, however the first and last bins are computed over 149 and 124 respectively. The error rates in some (adult) cases are zero, and in others the DET is flat so the error rates at the two thresholds are identical. The lines span 1% and 99% of boostrap replicated FNMR estimates.

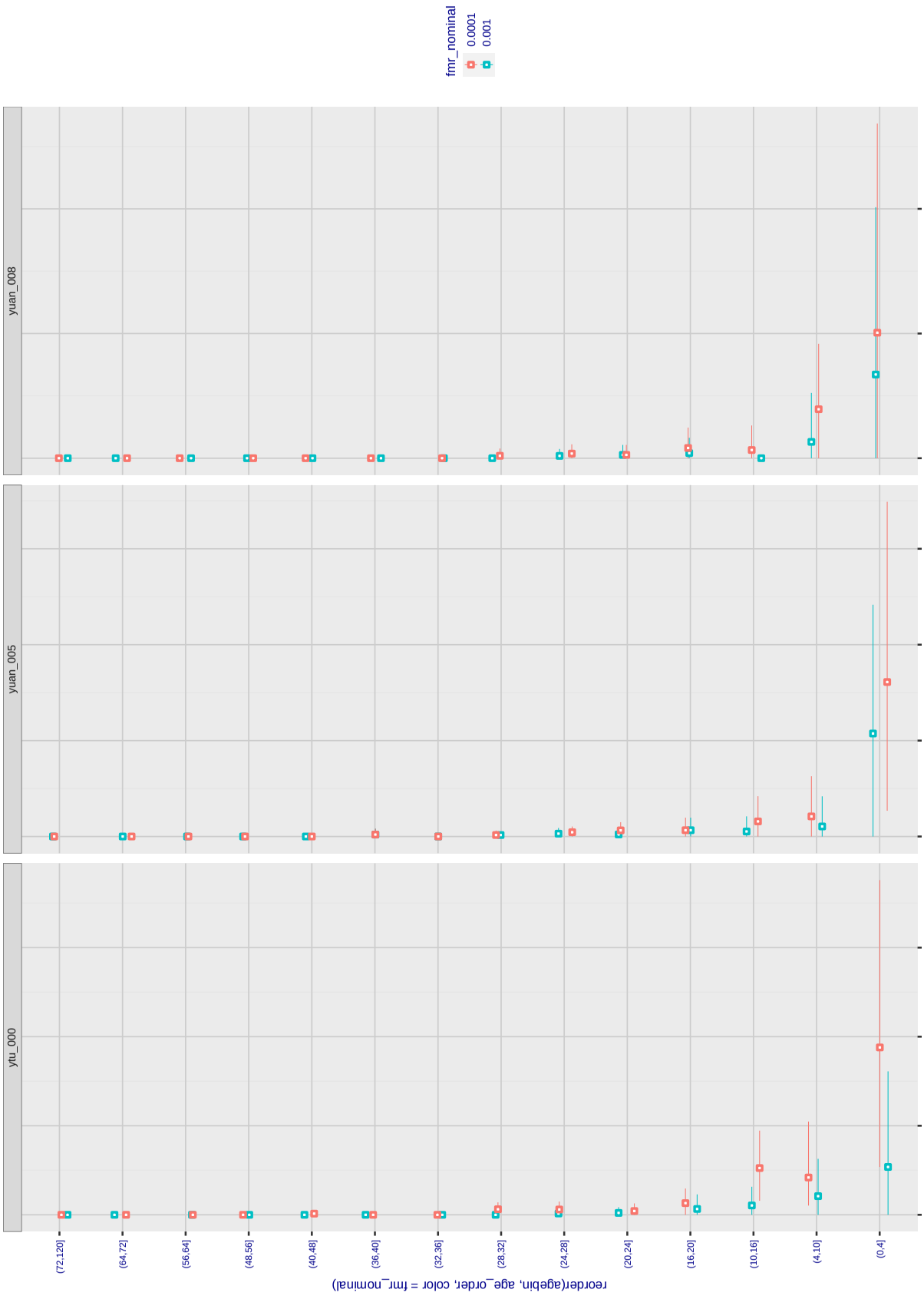

Figure 413: For the visa images, the dots show FNMR by age group for two operating thresholds corresponding to FMR = $\{0.001, 0.0001\}$ computed over all on the order of 10^{10} impostor scores. The FMR in each bin will vary also - see subsequent impostor heatmaps in sec. 3.6.2. Given a pair of face images taken at different times, we assign the comparison to the bin that is the arithmetic average of the subject's ages. This plot shows only the effect of age, not ageing. The number of comparisons in each bin is generally in the thousands, however the first and last bins are computed over 149 and 124 respectively. The error rates in some (adult) cases are zero, and in others the DET is flat so the error rates at the two thresholds are identical. The lines span 1% and 99% of boostrap replicated FNMR estimates.

FNMR(T) "False non-match rate"
FMR(T) "False match rate"

Caveats: None.

FNMR(T) "False non-match rate"
FMR(T) "False match rate"

3.6 Impostor distribution stability

3.6.1 Effect of birth place on the impostor distribution

Background: Facial appearance varies geographically, both in terms of skin tone, cranio-facial structure and size. This section addresses whether false match rates vary intra- and inter-regionally.

Goals:

- ▷ To show the effect of birth region of the impostor and enrollee on false match rates.
- ▷ To determine whether some algorithms give better impostor distribution stability.

Methods:

- ▷ For the visa images, NIST defined 10 regions: Sub-Saharan Africa, South Asia, Polynesia, North Africa, Middle East, Europe, East Asia, Central and South America, Central Asia, and the Caribbean.
- ▷ For the visa images, NIST mapped each country of birth to a region. There is some arbitrariness to this. For example, Egypt could reasonably be assigned to the Middle East instead of North Africa. An alternative methodology could, for example, assign the Philippines to *both* Polynesia and East Asia.
- ▷ FMR is computed for cases where all face images of impostors born in region r_2 are compared with enrolled face images of persons born in region r_1.

$$\text{FMR}(r_1, r_2, T) = \frac{\sum_{i=1}^{N_{r_1,r_2}} H(s_i - T)}{N_{r_1,r_2}} \tag{5}$$

  where the same threshold, T, is used in all cells, and H is the unit step function. The threshold is set to give FMR(T) = 0.001 over the entire set of visa image impostor comparisons.
- ▷ This analysis is then repeated by country-pair, but only for those country pairs where both have at least 1000 images available. The countries[1] appear in the axes of graphs that follow.
- ▷ The mean number of impostor scores in any cross-region bin is 33 million. The smallest number of impostor scores in any bin is 135000, for Central Asia - North Africa. While these counts are large enough to support reasonable significance, the number of individual faces is much smaller, on the order of $N^{0.5}$.
- ▷ The numbers of impostor scores in any cross-country bin is shown in Figure 414.

Results: Subsequent figures show heatmaps that use color to represent the base-10 logarithm of the false match rate. Red colors indicate high (bad) false match rates. Dark colors indicate benign false match rates. There are two series of graphs corresponding to aggregated geographical regions, and to countries. The notable observations are:

- ▷ The on-diagonal elements correspond to within-region impostors. FMR is generally above the nominal value of FMR = 0.001. Particularly there is usually higher FMR in, Sub-Saharan Africa, South Asia, and the Caribbean. Europe and Central Asia, on the other hand, usually give FMR closer to the nominal value.
- ▷ The off-diagonal elements correspond to across-region impostors. The highest FMR is produced between the Caribbean and Sub-Saharan Africa.
- ▷ Algorithms vary.

[1] These are Argentina, Australia, Brazil, Chile, China, Costa Rica, Cuba, Czech Republic, Dominican Republic, Ecuador, Egypt, El Salvador, Germany, Ghana, Great Britain, Greece, Guatamala, Haiti, Hong Kong, Honduras, Indonesia, India, Israel, Jamaica, Japan, Kenya, Korea, Lebanon, Mexico, Malaysia, Nepal, Nigeria, Peru, Philippines, Pakistan, Poland, Romania, Russia, South Africa, Saudi Arabia, Thailand, Trinidad, Turkey, Taiwan, Ukraine, Venezuela, and Vietnam.

▷ We computed the same quantities for a global FMR = 0.0001. The effects are similar.

Caveats:

▷ The effects of variable impostor rates on one-to-many identification systems may well differ from what's implied by these one-to-one verification results. Two reasons for this are a) the enrollment galleries are usually imbalanced across countries of birth, age and sex; b) one-to-many identification algorithms often implement techniques aimed at stabilizing the impostor distribution. Further research is necessary.

▷ In principle, the effects seen in this subsection could be due to differences in the image capture process. We consider this unlikely since the effects are maintained across geography - e.g. Caribbean vs. Africa, or Japan vs. China.

FNMR(T) "False non-match rate"
FMR(T) "False match rate"

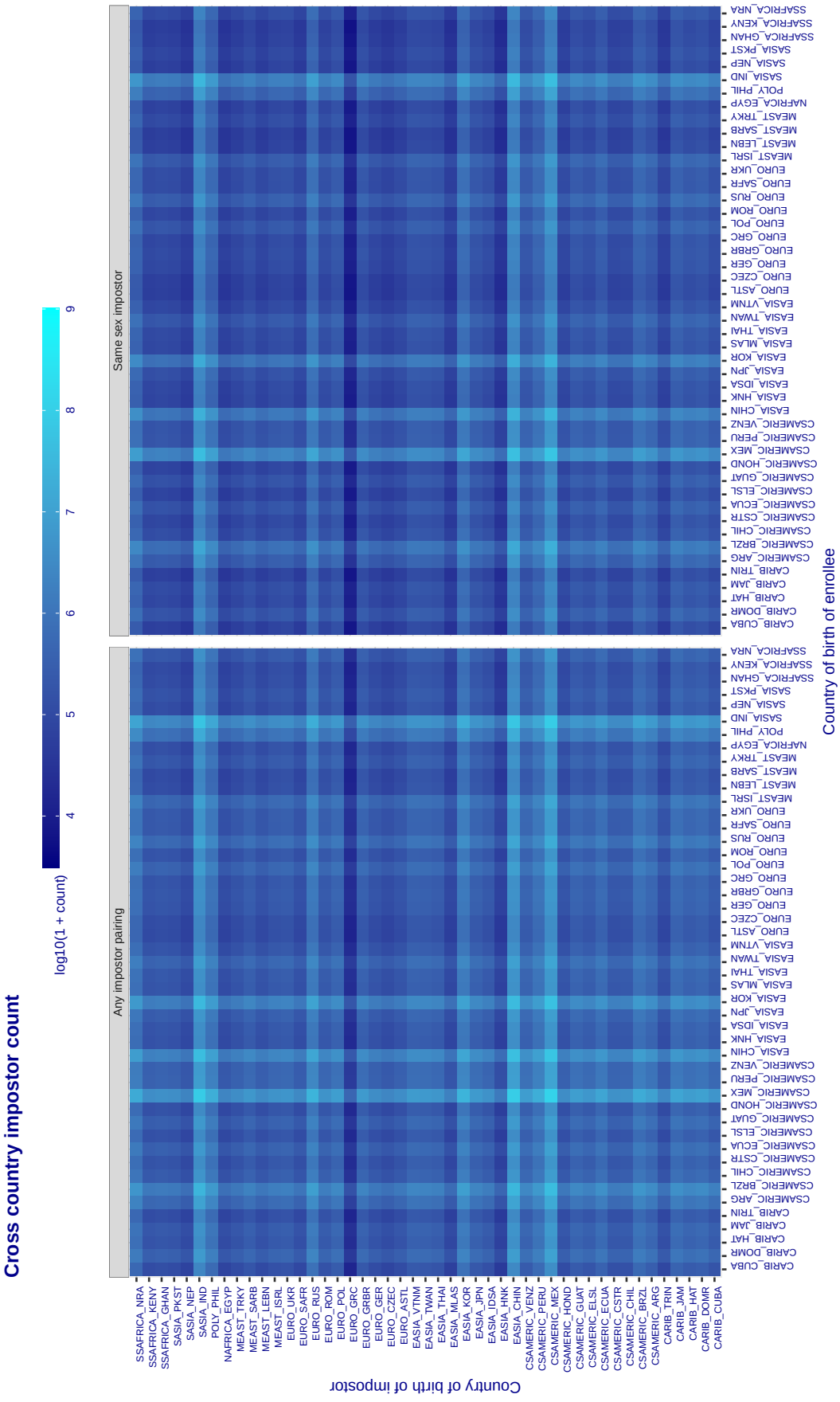

Figure 414: For visa images, the heatmap shows the count of impostor comparisons of faces from different individuals who were born in the given country pair. The FMR heatmaps themselves appear in the 1:1 report cards, for example, this one.

FNMR(T) "False non-match rate"
FMR(T) "False match rate"

3.6.2 Effect of age on impostors

Background: This section shows the effect of age on the impostor distribution. The ideal behaviour is that the age of the enrollee and the impostor would not affect impostor scores. This would support FMR stability over sub-populations.

Goals:

- ▷ To show the effect of relative ages of the impostor and enrollee on false match rates.
- ▷ To determine whether some algorithms have better impostor distribution stability.

Methods:

- ▷ Define 14 age group bins, spanning 0 to over 100 years old.
- ▷ Compute FMR over all impostor comparisons for which the subjects in the enrollee and impostor images have ages in two bins.
- ▷ Compute FMR over all impostor comparisons for which the subjects are additionally of the same sex, and born in the same geographic region.

Results:

The notable aspects are:

- ▷ Diagonal dominance: Impostors are more likely to be matched against their same age group.
- ▷ Same sex and same region impostors are more successful. On the diagonal, an impostor is more likely to succeed by posing as someone of the same sex. If $\Delta \log_{10}$ FMR $= 0.2$, then same-sex same-region FMR exceeds the all-pairs FMR by factor of $10^{0.2} = 1.6$.
- ▷ Young children impostors give elevated FMR against young children. Older adult impostor give elevated FMR against older adults. These effects are quite large, for example if $\Delta \log_{10}$ FMR $= 1.0$ larger than a 32 year old, then these groups have higher FMR by a factor of $10^1 = 10$. This would imply an FMR above 0.01 for a nominal (global) FMR = 0.001.
- ▷ Algorithms vary.
- ▷ We computed the same quantities for a global FMR = 0.0001. The effects are similar.

Note the calculations in this section include impostors paired across all countries of birth.

FNMR(T) "False non-match rate"
FMR(T) "False match rate"

Accuracy Terms + Definitions

In biometrics, Type II errors occur when two samples of one person do not match – this is called a **false negative**. Correspondingly, Type I errors occur when samples from two persons do match – this is called a **false positive**. Matches are declared by a biometric system when the native comparison score from the recognition algorithm meets some **threshold**. Comparison scores can be either **similarity scores**, in which case higher values indicate that the samples are more likely to come from the same person, or **dissimilarity scores**, in which case higher values indicate different people. Similarity scores are traditionally computed by **fingerprint** and **face** recognition algorithms, while dissimilarities are used in **iris recognition**. In some cases, the dissimilarity score is a distance; this applies only when **metric** properties are obeyed. In any case, scores can be either **mate** scores, coming from a comparison of one person's samples, or **nonmate** scores, coming from comparison of different persons' samples. The words **genuine** or **authentic** are synonyms for mate, and the word **impostor** is used a synonym for nonmate. The words mate and nonmate are traditionally used in identification applications (such as law enforcement search, or background checks) while genuine and impostor are used in verification applications (such as access control).

A **error tradeoff** characteristic represents the tradeoff between Type II and Type I classification errors. For verification this plots false non-match rate (FNMR) vs. false match rate (FMR) parametrically with T.

The error tradeoff plots are often called **detection error tradeoff (DET)** characteristics or **receiver operating characteristic** (ROC). These serve the same function but differ, for example, in plotting the complement of an error rate (e.g. TMR = 1 – FNMR) and in transforming the axes most commonly using logarithms, to show multiple decades of FMR. More rarely, the function might be the inverse Gaussian function.

More detail and generality is provided in formal biometrics testing standards, see the various parts of ISO/IEC 19795 Biometrics Testing and Reporting. More terms, including and beyond those to do with accuracy, see ISO/IEC 2382-37 Information technology -- Vocabulary -- Part 37: Harmonized biometric vocabulary

FNMR(T) "False non-match rate"
FMR(T) "False match rate"

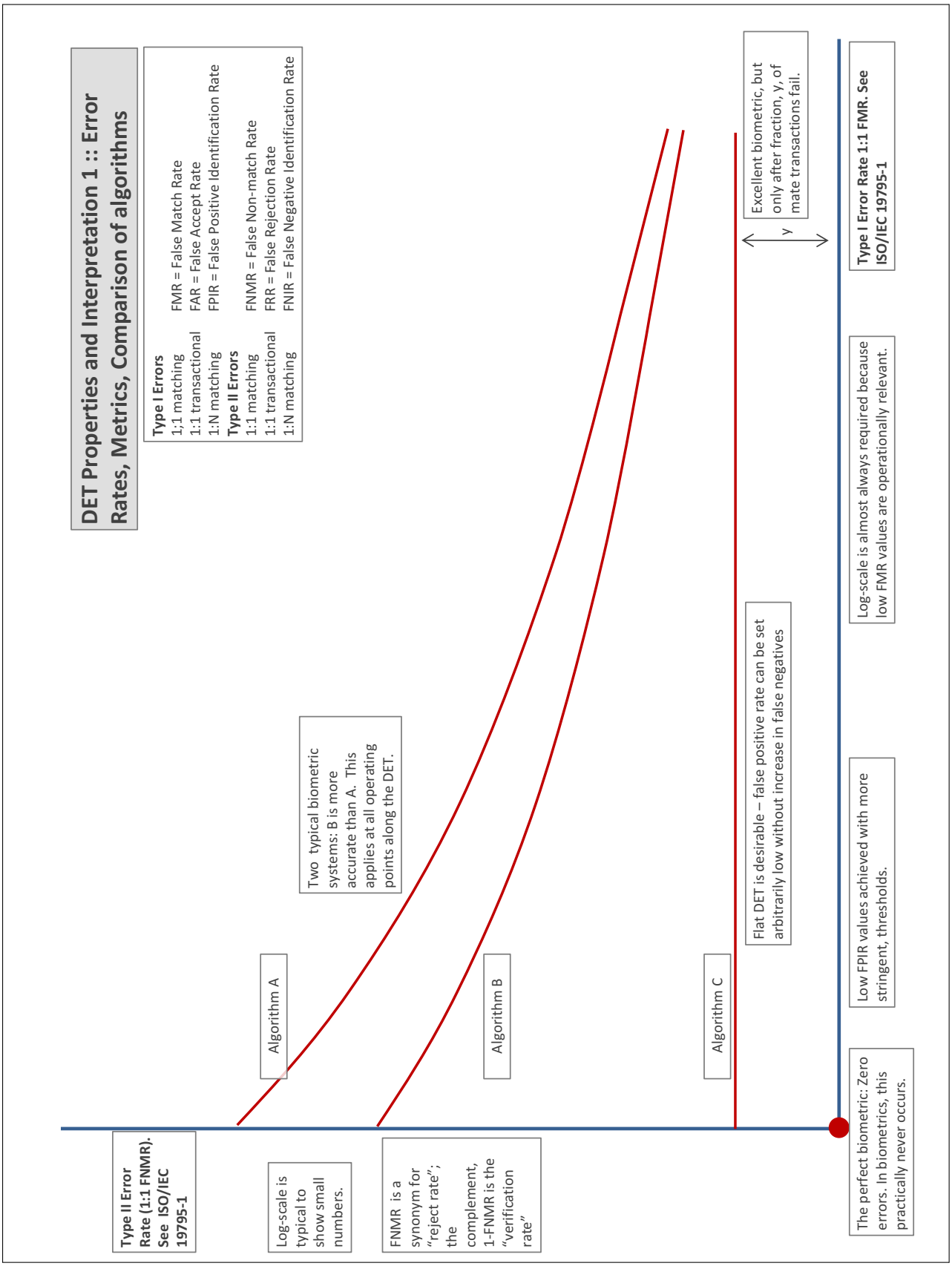

FNMR(T) "False non-match rate"
FMR(T) "False match rate"

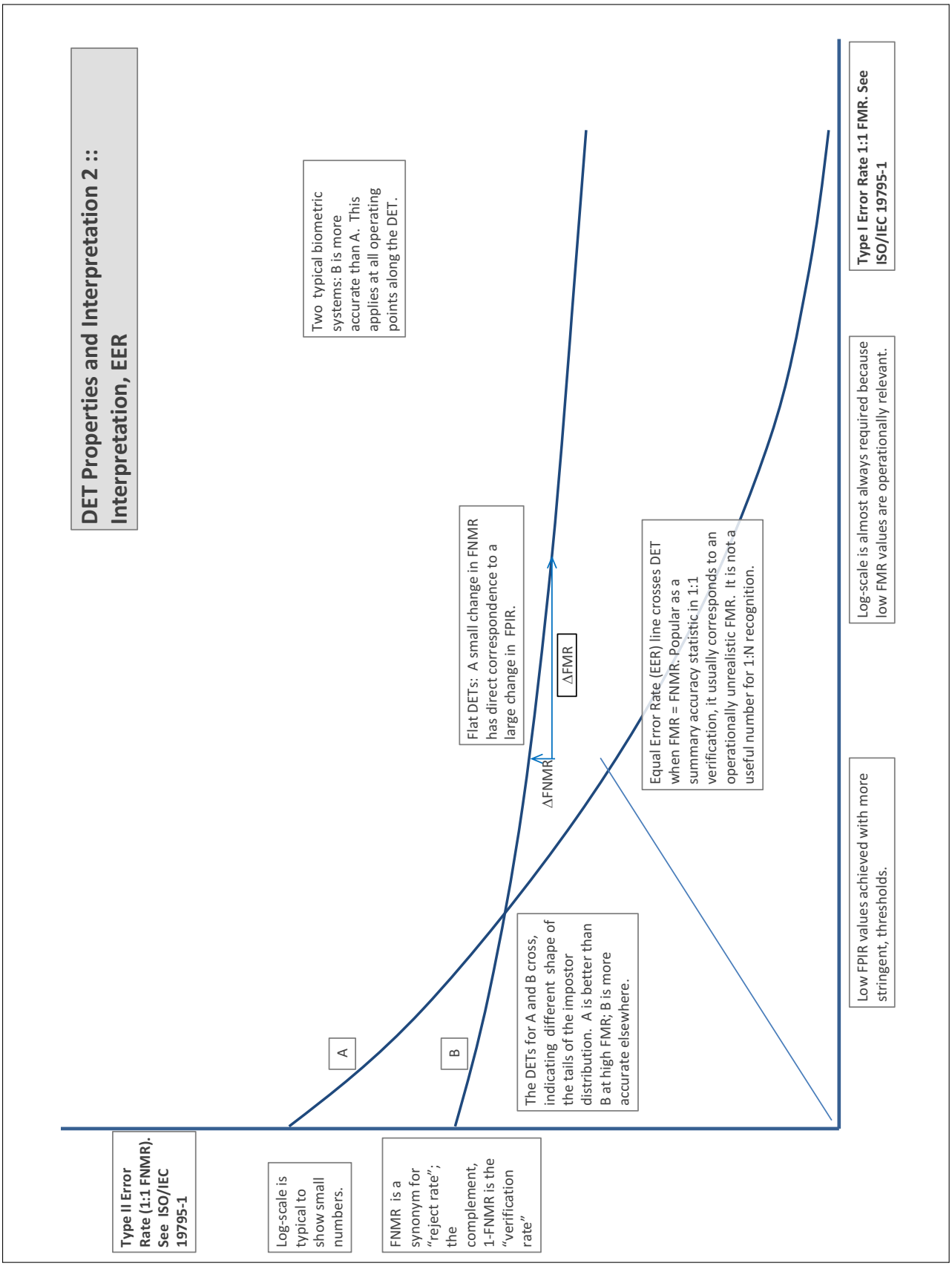

FNMR(T) "False non-match rate"
FMR(T) "False match rate"

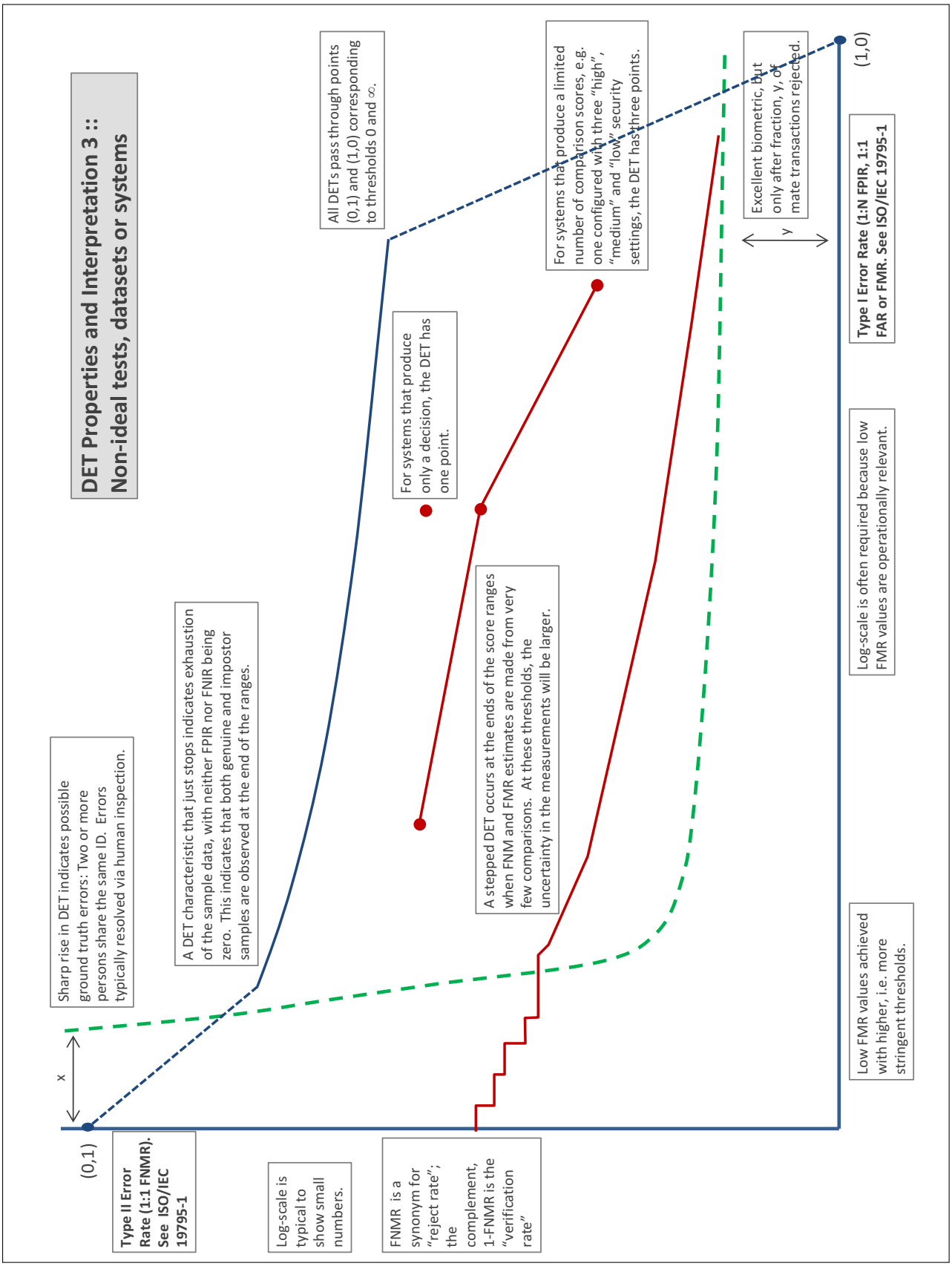

FNMR(T) "False non-match rate"
FMR(T) "False match rate"

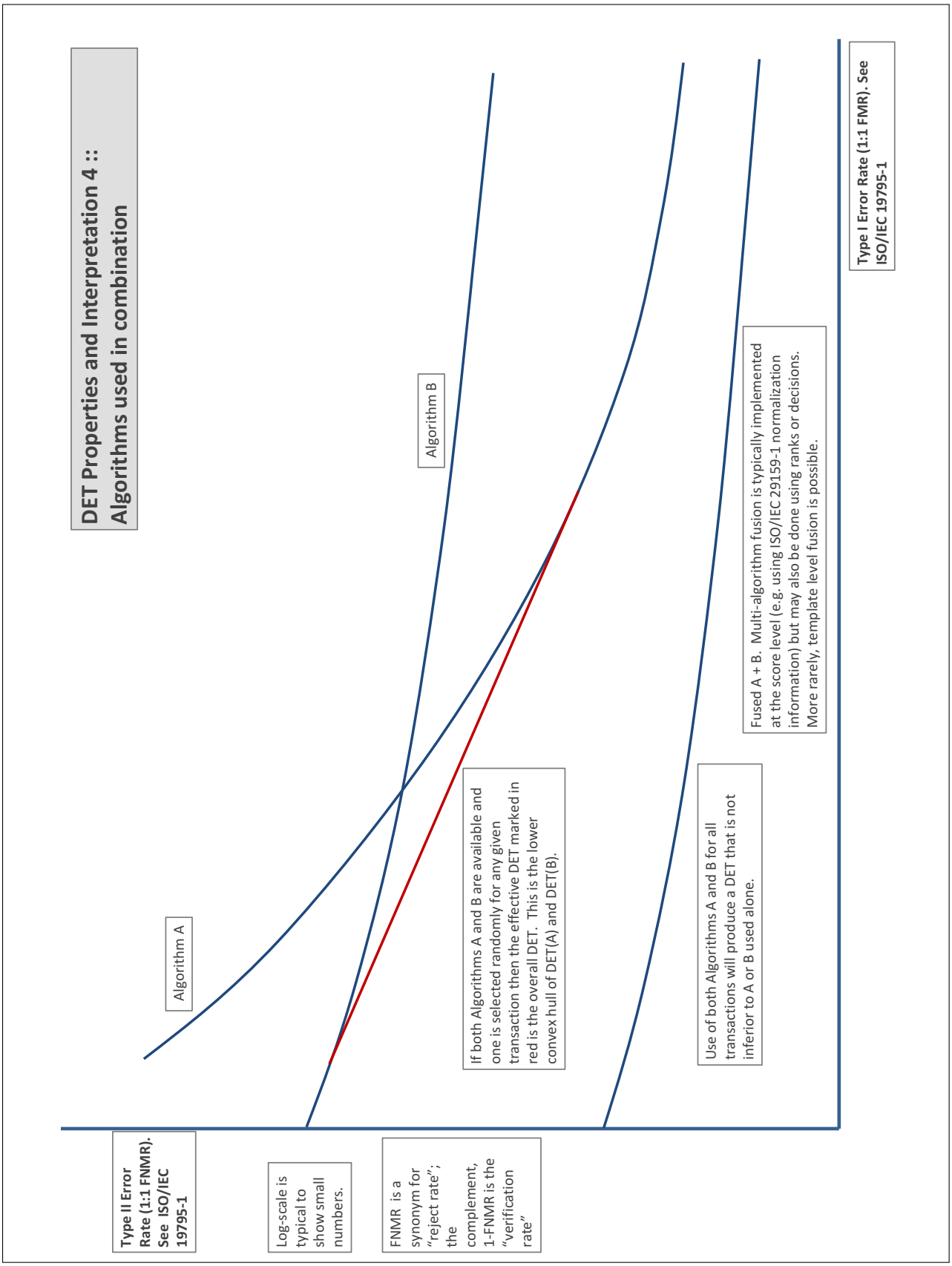

FNMR(T) "False non-match rate"
FMR(T) "False match rate"

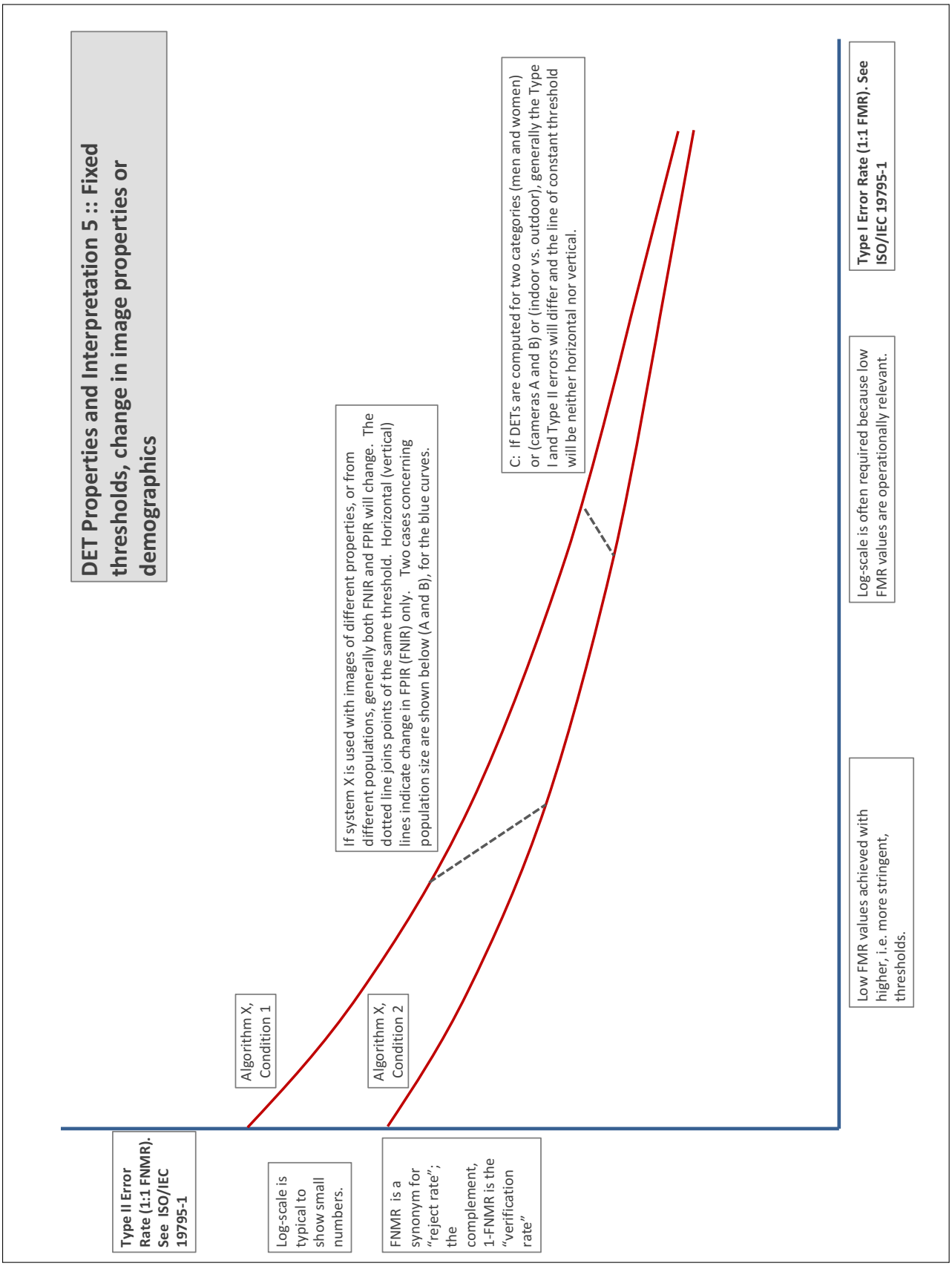

FNMR(T) "False non-match rate"
FMR(T) "False match rate"

References

[1] P. Jonathon Phillips, Amy N. Yates, Ying Hu, Carina A. Hahn, Eilidh Noyes, Kelsey Jackson, Jacqueline G. Cavazos, Géraldine Jeckeln, Rajeev Ranjan, Swami Sankaranarayanan, Jun-Cheng Chen, Carlos D. Castillo, Rama Chellappa, David White, and Alice J. O'Toole. Face recognition accuracy of forensic examiners, superrecognizers, and face recognition algorithms. *Proceedings of the National Academy of Sciences*, 115(24):6171–6176, 2018.

FNMR(T) "False non-match rate"
FMR(T) "False match rate"